

PB 292056



PROCEEDINGS OF THE NORTH AMERICAN MASONRY CONFERENCE

August 14, 15, 16, 1978

University of Colorado
Boulder, Colorado



REPRODUCED BY
**NATIONAL TECHNICAL
INFORMATION SERVICE**
U. S. DEPARTMENT OF COMMERCE
SPRINGFIELD, VA. 22161

Editors and
Conference Co-Chairmen:

James L. Noland
James E. Amrhein

The North American Masonry Conference was partially supported by the National Science Foundation under Grant No. PFR 77-27812, and by The Masonry Society.

Any opinions, findings, and conclusions or recommendations expressed in this publication are those of the authors and do not necessarily reflect the views of the National Science Foundation, The Masonry Society, nor the editors.

Printed in the United States of America

1978

REPORT DOCUMENTATION PAGE		1. REPORT NO. NSF/RA-780317	2.	3. Recipient's Accession No. PB292056
4. Title and Subtitle North American Masonry Conference, Proceedings (August 1978, University of Colorado)			5. Report Date 1978	6.
7. Author(s) J.L. Noland, J.E. Amrhein			8. Performing Organization Rept. No.	
9. Performing Organization Name and Address University of Colorado Boulder, Colorado 80302			10. Project/Task/Work Unit No.	
			11. Contract(C) or Grant(G) No. (C) (G) PFR7727812	
12. Sponsoring Organization Name and Address Applied Science and Research Applications (ASRA) National Science Foundation 1800 G Street, N.W. Washington, D.C. 20550			13. Type of Report & Period Covered	
15. Supplementary Notes			14.	
16. Abstract (Limit: 200 words) This conference was organized to convene people interested in masonry and to present the latest information concerning all facets of masonry. Experience and post-earthquake inspections have indicated a need for new analytical methods. Increased attention to education in masonry design is needed. National standards are necessary for the mechanical and physical properties of materials and for standard testing methods of units and components. The papers presented at this conference focus on the following: research and materials, codes and standards, evaluation and retrofit; lateral loads, construction, quality control, design, energy considerations, and papers of general interest.				
17. Document Analysis a. Descriptors				
Masonry	Construction	Concretes		
Bricks	Dynamic structural analysis	Ceramics		
Building stones	Earthquakes	Buildings		
b. Identifiers/Open-Ended Terms				
Masonry design Seismic loading				
c. COSATI Field/Group				
18. Availability Statement NTIS			19. Security Class (This Report)	21. No. of Pages
			20. Security Class (This Page)	22. Price 11MF A01

BIBLIOGRAPHIC INFORMATION

PB-292 056

Proceedings of the North American Masonry Conference Held at
Boulder, Colorado on August 14-16, 1978,

1978

James L. Noland, and James E. Amrhein.

PERFORMER: Colorado Univ., Boulder.
Grant NSF-PFR77-27812

SPONSOR: National Science Foundation, Washington, DC.
Applied Science and Research Applications.
NSF/RA780317

Sponsored in part by Masonry Society.

This conference was organized to convene people interested in masonry and to present the latest information concerning all facets of masonry. Experience and post-earthquake inspections have indicated a need for new analytical methods. Increased attention to education in masonry design is needed. National standards are necessary for the mechanical and physical properties of materials and for standard testing methods of units and components. The papers presented at this conference focus on the following: research and materials, codes and standards, evaluation and retrofit, lateral loads, construction, quality control, design, energy considerations, and papers of general interest.

KEYWORDS: *Construction materials, *Masonry, *Meetings.

Available from the National Technical Information Service,
Springfield, Va. 22161

PRICE CODE: PC A99/MF A01

|

|

|

|

|

|

|

|

|

|

|

|

|

|

|

|

|

|

|

|

|

|

|

|

|

|

|

|

|

|

|

|

|

|

ACKNOWLEDGEMENTS

The organizers of the North American Masonry Conference gratefully acknowledge the sponsorship of The Masonry Society, whose officers are:

George C. Hanson — President
William G. Temple — Vice President
J. Gregg Borchelt — Secretary-Treasurer

The encouragement and assistance given both by the Department of Civil, Environmental and Architectural Engineering and the Bureau of Conferences and Institutes, Division of Continuing Education at the University of Colorado, Boulder, was an extremely important factor in the success of the conference. Their consideration, advice and cooperation are very much appreciated.

The endorsement of the American Society of Civil Engineers — Colorado Section — and the Earthquake Engineering Research Institute was very important and was greatly appreciated as was the cooperation of the Colorado Masonry Institute, Western States Clay Products Association, Masonry Institute of America, Masonry Institute of Houston-Galveston, Brick Institute of America (Region 12), and Colorado Concrete Masonry Association.

Most important of all, however, was the work, expense, and time devoted by the many authors who prepared papers for the conference. Their work, presented at the conference and documented in the Proceedings, will help advance masonry technology for the benefit of society.

ORGANIZATION

NORTH AMERICAN MASONRY CONFERENCE

Chairmen

James L. Noland — Atkinson-Noland & Associates
 James E. Amrhein — Masonry Institute of America

Technical Program

James Chinn — University of Colorado

Publicity

Robert C. Sandoval — Colorado Masonry Institute

Conference Arrangements

Lawrence Christiansen — University of Colorado, Div. of Cont. Ed.

Exhibits and Films

Henry Bollman — Brick Institute of America (Region 12)

Spouses Program

Bonna J. Eatherton — Eatherton Masonry

Steering Committee

D. B. Anderson—Clalite Concrete Products, Inc., Denver, Colorado
 J. D. Berich—Dan Berich, Inc., Denver, Colorado
 Russell Brown—Clemson University, Clemson, South Carolina
 J. Gregg Borchelt—Masonry Institute of Houston-Galveston, Houston, Texas
 Walter L. Dickey—Higgins Brick Co., Los Angeles, California
 C. C. Feng—University of Colorado, Boulder, Colorado
 Richard Gensert—Gensert, Peller, Mancini & Assoc., Cleveland, Ohio
 George Hanson—Sallada, Hanson & Assoc., Denver, Colorado
 Gerald Harvey—Joint Apprenticeship Committee of Colorado, Denver, Co.
 Lewis Helbert—Helbert Masonry, Inc., Ft. Collins, Colorado
 Robert Helfrich—Colorado Masonry Institute, Denver, Colorado
 Emlyn Jessop—University of Calgary, Calgary, Alberta, Canada
 Dietz Lusk—Architect—AIA, Colorado Springs, Colorado
 Paul Maurenbrecher—National Research Council, Ottawa, Ontario, Canada
 C. B. Monk—Wiss, Janney and Elstner, Northbrook, Illinois
 Robert Norton—Valley Block Co., Loveland, Colorado
 Robert Rathburn—University of Colorado, Boulder, Colorado
 Donald Wakefield—Interstate Brick Co., West Jordan, Utah

PREFACE

The Masonry Society is pleased to sponsor the North American Masonry Conference as its first major activity offered for the benefit of the architects, engineers, contractors, craftsmen, building officials, construction inspectors, laboratory technicians, educators, researchers, manufacturers, and all interested in masonry.

The North American Masonry Conference was organized to bring together people interested in masonry and to have presented the latest information concerning all facets of masonry whether it be materials, construction, design, specifications, research, education, etc. It is hoped by the organizers that this conference will be viewed as a useful contribution to the development of masonry.

James L. Noland
James E. Amrhein
Co-Chairmen

TABLE OF CONTENTS

TITLE AND AUTHOR	Paper Number	TITLE AND AUTHOR	Paper Number
KEYNOTE ADDRESS		BEHAVIOR OF CONCRETE MASONRY STRUCTURES AND JOINT DETAILS USING SMALL SCALE DIRECT MODELS 10	
THE NEEDS OF MASONRY CONSTRUCTION 0 John B. Scalzi	0	Harry G. Harris, Ivan J. Becica	10
RESEARCH AND MATERIALS		EFFECT OF GROUTING ON THE STRENGTH CHARACTERISTICS OF CONCRETE BLOCK MASONRY 11	
BEHAVIOR OF CONCRETE MASONRY UNDER BIAXIAL STRESS 1 G. A. Hegemier, R. O. Nunn, S. K. Arya	1	Ahmad A. Hamid, Robert G. Drysdale, Arthur C. Heidebrecht	11
THE DEVELOPMENT OF A TECHNIQUE FOR INVESTIGATING THE DURA- BILITY OF REINFORCING STEEL IN REINFORCED CONCRETE BLOCKWORK 2 J. J. Roberts	2	ELASTIC AND CREEP PROPERTIES OF MASONRY 12	
GROUT — BLOCK BOND STRENGTH IN CONCRETE MASONRY 3 R. O. Nunn, M. E. Miller, G. A. Hegemier	3	E. L. Jessop, N. G. Shrive, G. L. England	
ON THE BEHAVIOR OF JOINTS IN CONCRETE MASONRY 4 G. A. Hegemier, S. K. Arya, G. Krishnamoorthy, W. Nachbar, R. Furgerson	4	THE PARAMETERS INFLUENCING SHEAR STRENGTH BETWEEN CLAY MASONRY UNITS AND MORTAR 13	
STRUCTURAL PROPERTIES OF BLOCK CONCRETE 5 Thomas A. Holm	5	Larry Nuss, J. L. Noland, James Chinn	
CURRENT MASONRY RESEARCH AT THE BRITISH CERAMIC RESEARCH ASSOCIATION 6 H. W. H. West	6	THE EFFECT OF SLENDERNESS AND END CONDITIONS ON THE STRENGTH OF CLAY UNIT PRISMS ... 14	
EFFECT OF CONSTITUENT PROPORTIONS ON UNIAXIAL COMPRESSIVE STRENGTH OF TWO-INCH CUBE SPECIMENS OF MASONRY MORTARS 7 Donald J. Frey, Robert J. Helfrich, Chuan C. Feng	7	J. L. Noland, K. T. Hanada, C. C. Feng	
SINTERED COAL REFUSE LIGHT- WEIGHT MASONRY AGGREGATE 8 J. G. Rose	8	THE INTERACTION OF MASONRY WALL PANELS AND A STEEL FRAME 15	
INHERENT COMPRESSIVE AND TENSILE STRENGTHS OF STRUCTURAL BRICK 9 P. F. Rad	9	James Colville, Richard Ramseur	
		THE EFFECT OF JOINT REINFORCEMENT ON VERTICAL LOAD CARRYING CAPACITY OF HOLLOW CONCRETE BLOCK MASONRY 16	
		M. Hatzinikolas, J. Longworth, J. Warwaruk	
		THE INFLUENCE OF FLAWS, COMPACTION, AND ADMIXTURE ON THE STRENGTH AND ELASTIC MODULI OF CONCRETE MASONRY 17	
		M. E. Miller, G. A. Hegemier, R. O. Nunn	
		PRISM TESTS FOR THE COM- PRESSIVE STRENGTH OF CONCRETE MASONRY 18	
		G. A. Hegemier, G. Krishnamoorthy, R. O. Nunn, T. V. Moorthy	

TITLE AND AUTHOR	Paper Number	TITLE AND AUTHOR	Paper Number
ON NONLINEAR RESPONSE PREDICTIONS OF CONCRETE MASONRY ASSEMBLIES	19	THE CENTER FOR EDUCATIONAL DEVELOPMENT — A MEDIUM SCALE SEISMIC UPGRADING	42
S. K. Arya, G. A. Hegemier		Harold A. Davis	
THE FLEXURAL BEHAVIOUR OF BRICKWORK	20	LATERAL LOADS	
S. J. Lawrence		LOW COST FACILITY FOR TESTING THE ULTIMATE EARTHQUAKE RESISTANCE OF MASONRY STRUCTURES	50
DEPENDENCE OF MASONRY PROPERTIES ON THE INTER- ACTION BETWEEN MASONRY UNITS AND MORTAR	21	W. O. Keightley	
T. Sneek		AN INVESTIGATION OF THE DYNAMIC RESPONSE OF THE PARK LANE TOWERS TO EARTHQUAKE LOADINGS	51
STRAIN GRADIENT EFFECTS IN MASONRY	22	Kenneth Medearis	
Carl J. Turkstra, Gareth R. Thomas		THE EFFECT OF FLOOR AND WIND LOADS APPLIED SEPARATELY OR SIMULTANEOUSLY TO TWO-STORY HIGH WALLS	52
THE EFFECT OF STRENGTH AND GEOMETRY ON THE ELASTIC AND CREEP PROPERTIES OF MASONRY MEMBERS	23	H. R. Hodgkinson	
D. Lenczner		SEISMIC RESEARCH ON MULTISTORY MASONRY BUILDINGS	53
REINFORCED BRICKWORK LINTEL SHEAR STUDY UTILIZING SMALL SCALE BRICKS	24	R. L. Mayes, R. W. Clough, P. A. Hidalgo, H. D. McNiven	
G. T. Suter, H. Keller		AN EXPERIMENTAL INVESTIGATION ON THE SEISMIC BEHAVIOR OF SINGLE-STORY MASONRY HOUSES ..	54
COMPRESSION TESTS OF CLAY-UNIT STACKBOND PRISMS	25	P. Gulkan, R. L. Mayes, R. W. Clough, R. Hendrickson	
John Baur, J. L. Noland, James Chinn		STABILITY UNDER SEISMIC LOADING OF BUILDINGS WITH FULLY CRACKED WALL-FLOOR JOINTS	55
CODES AND STANDARDS		W. Nachbar, R. Furgerson	
A DESIGN GUIDE FOR REINFORCED AND PRESTRESSED BRICKWORK	30	HIGH RISE BUILDING VIBRATION PROPERTIES: AN UNEXPECTED BEHAVIOR MECHANISM	56
B. A. Haseltine		Irving J. Oppenheim	
MASONRY IN BUILDING CODES	31	INTERACTION BETWEEN UNREIN- FORCED MASONRY STRUCTURES AND THEIR ROOF DIAPHRAGMS DURING EARTHQUAKES	57
Walter L. Dickey		S. A. Adham, R. D. Ewing	
A STRUCTURAL ENGINEER'S RATIONALIZATION OF THE MASONRY BUILDING CODE	32	CONSTRUCTION	
Don T. Pyle, Donald C. Weber		COAL ASH UTILIZATION IN MASONRY CONSTRUCTION	60
EVALUATION AND RETROFIT		John H. Faber	
A SIMPLE TECHNIQUE FOR DETERMINING STRENGTH OF BRICK.	40		
Parviz F. Rad			
RESTORATION OF THE PINE STREET INN TOWER	41		
John M. Looney			

TITLE AND AUTHOR	Paper Number	TITLE AND AUTHOR	Paper Number
CONSTRUCTION AND QUALITY CONTROL OF HIGH LIFT GROUTED REINFORCED MASONRY ..	61	AUTOMATED DESIGN OF MULTISTORY MASONRY SHEAR WALL STRUCTURES	83
Robert W. Harrington		Louis A. Hill, Jr., Richard H. Chasey, Jr.	
HOW THE HIGH LIFT GROUTING SYSTEM WAS DEVELOPED	62	MASONRY BUILDINGS: CONSTRUCTION ON SUBSIDENCE SITES	84
Oscar F. Person		Harold Clifford Hall	
THE USE OF CONCRETE UNIT MASONRY IN NUCLEAR POWER PLANTS	63	A CONTRIBUTION TOWARDS THE DESIGN OF HEAVILY LOADED WALLS ON REINFORCED CONCRETE BEAMS	85
J. M. Grant, A. Y. Wu		B. Stafford Smith, Luigi Pradolin	
USES OF CHEMICALLY RESISTANT MASONRY IN LINING AIR AND WATER POLLUTION CONTROL EQUIPMENT	64	SOME FUNDAMENTAL FACTORS IN THE STRUCTURAL DESIGN OF MASONRY BUILDINGS	86
Harry Clyburn, Walter L. Sheppard		A. W. Hendry	
SURFACE BONDING CEMENT: A NEW TECHNOLOGY FOR MASONRY	65	BUCKLING OF PLAIN MASONRY WALLS WITH INITIAL DOUBLE CURVATURE	87
Richard D. Klausmeier		M. Hatzinikolas, J. Longworth, J. Warwaruk	
QUALITY CONTROL		AN AUTOMATED DESK METHOD FOR ANALYZING LOAD BEARING MASONRY STRUCTURES	88
A SIMPLIFIED FLEXURAL BOND TEST FOR CLAY BRICK MASONRY	70	Jack M. Van Pelt	
A. Huizer, M. A. Ward		DIMENSIONAL CHANGE AND ITS CONTROL IN CLAY MASONRY CONSTRUCTION	89
QUALITY CONTROL OF LOAD BEARING CONCRETE BLOCK WALLS .	71	K. J. Wyatt	
E. J. Elnicky		RATIONAL ANALYSIS OF MASONRY STRUCTURES	90
TEST METHODS FOR MASONRY MORTARS	72	James Colville, Donald Vannoy	
E. L. Jessop, B. W. Langan		USE OF THE PRISM TEST TO DETERMINE COMPRESSIVE STRENGTH OF MASONRY	91
NON-DESTRUCTIVE TESTING TECHNIQUES TO EVALUATE EXISTING MASONRY CONSTRUCTION	73	A. H. P. Maurenbrecher	
Luke M. Snell		THE BENEFITS OF HIGH-STRENGTH MASONRY	92
DESIGN		Dean D. Froerer	
AN APPLICATION OF THIN WALL MASONRY	80	BASIC PRINCIPLES OF STRUCTURAL MECHANICS OF TALL MASONRY BUILDINGS	93
Don T. Pyle		P. T. Mikluchin	
CASE STUDY — COMPUTERIZED DESIGN FOR LOAD BEARING MASONRY	81	PROGRESSIVE COLLAPSE OF MASONRY STRUCTURES	94
D. Vannoy, H. E. Harvey, J. Colville		James E. Amrhein	
TWO-STORY MASONRY BUILDING SUPPORTED ON A 24-FOOT DEPOSIT OF ORGANIC FILL	82		
Donald R. Heil			

TITLE AND AUTHOR
Paper Number

TITLE AND AUTHOR
Paper Number

ENERGY CONSIDERATIONS

ENERGY SAVINGS WITH CONCRETE
MASONRY CONSTRUCTION 100
E. G. Eastman

AVERAGE VS. PEAK THERMAL
CHARACTERISTICS OF BUILDING
SHELL ELEMENTS 101
M. Dexter, L. Bickle, J. McNamara,
W. van der Meer

ENERGY CONSERVATION IN THE
MANUFACTURE AND USE OF BRICKS. 102
H. W. H. West, R. W. Ford

EXPERIMENTAL AND THEORETICAL
STUDY OF ENERGY CONSUMPTION
IN BUILDINGS 103
Jay L. McGrew, George P. Yeagle,
David P. McGrew

EXTERNALLY INSULATED MASONRY
CONSTRUCTION CASE STUDY 104
William C. Dries, Lawrence A. Soltis

THE LOW-ENERGY FULL-BRICK
HOUSE 105
S. Cumming, T. McNeilly

DEVELOPMENT OF SAND-LIME UNITS
WITH HIGH THERMAL INSULATION . 106
K. Wesche, P. Schubert

GENERAL INTEREST

MODERN LOADBEARING MASONRY
CONSTRUCTION IN THE
WESTERN UNITED STATES 110
John R. Mock

A NONFERROUS REINFORCED
CONCRETE MASONRY STRUCTURE .. 111
Allan W. Flandro

RELATIVE ECONOMIC PERFORMANCE

OF BRICK MASONRY AND
GLASS OFFICE BUILDINGS 112
Clayford T. Grimm

PROBLEMS IN MASONRY WALLS —
A CASE HISTORY 113
K. E. Fricke, W. D. Jones, J. E. Beavers

MASONRY PANELS: REVIEW,
PRESENT USE AND DESIGN 114
J. Gregg Borchelt

EFFECT OF MORTAR ON WATER
PERMEANCE OF MASONRY 115
Russell H. Brown

MEASURED STRESSES IN A CERAMIC
VENEER ON CONCRETE COLUMNS .. 116
W. G. Plewes

EDUCATION AND SCHOOLING —
REINFORCED MASONRY DESIGN
AND CONSTRUCTION 117
Robert R. Schneider, Walter L. Dickey

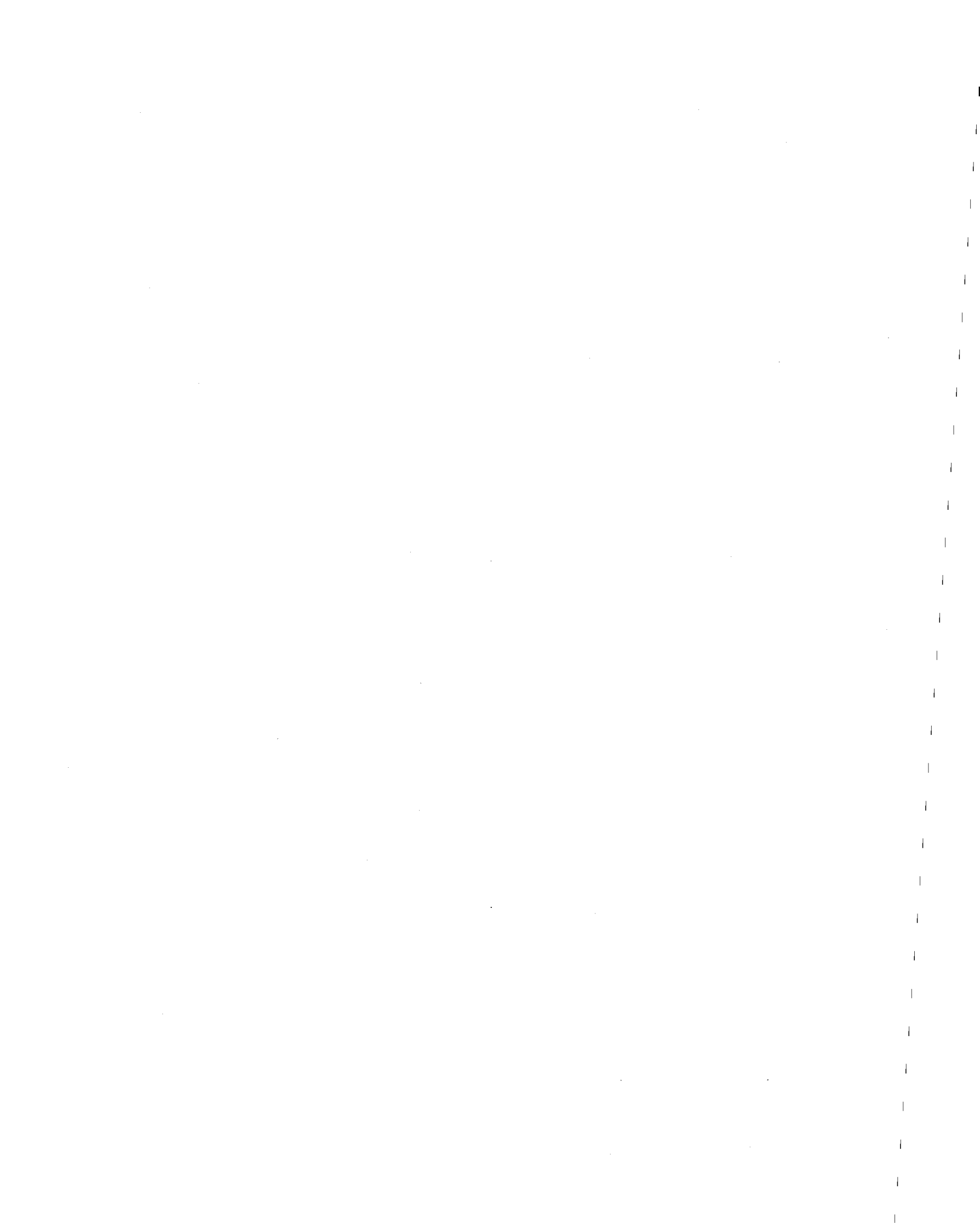
EFFECT OF SAND ON WATER
PERMEANCE OF MASONRY 118
Kenneth Gillam

TECHNIQUES FOR EDUCATING THE
STUDENT, INSPECTOR, ENGINEER
AND ARCHITECT IN THE DESIGN
AND CONSTRUCTION OF
MASONRY STRUCTURES 119
James E. Amrhein

AUTHOR INDEX Appendix I
CONVERSION OF MEASUREMENT
SYSTEMS Appendix II



PROCEEDINGS
OF THE
NORTH AMERICAN
MASONRY CONFERENCE



AUTHOR INDEX

APPENDIX I

AUTHOR	Paper Number
Adham, S. A.	57
Amrhein, J. E.	94, 119
Arya, S. K.	1, 4, 19
Baur, John	25
Beavers, J. E.	113
Becica, I.	10
Bickle, L.	101
Borchelt, J. G.	114
Brown, R. H.	115
Chasey, Jr., R. H.	83
Chinn, James	13, 25
Clough, R. W.	53, 54
Clyburn, H.	64
Colville, J.	15, 81, 90
Cumming, S.	105
Davis, H. A.	42
Dexter, M.	101
Dickey, W. L.	31, 117
Dries, W. C.	104
Drysdale, R. G.	11
Eastman, E. G.	100
Elnicky, E. J.	71
England, G. L.	12
Ewing, R. D.	57
Faber, J. H.	60
Feng, C. C.	7, 14
Flandro, A. W.	111
Ford, R. W.	102
Frey, D. J.	7
Fricke, K. E.	113
Froerer, D. D.	92
Furgerson, R.	4, 55
Gillam, K.	118
Grant, J. M.	63
Grimm, C. T.	112
Gulkan, P.	54
Hall, H. C.	84
Hamid, A. H.	11
Hanada, K. T.	14
Harrington, R. W.	61
Harris, H.	10
Harvey, H. E.	81
Haseltine, B. A.	30
Hatzinikolas, M.	16, 87
Hegemier, G. A.	1, 3, 4, 17, 18, 19
Heidebrecht, A. C.	11
Heil, D. R.	82
Helfrich, R. J.	7
Hendrickson, R.	54
Hendry, A. W.	86
Hidalgo, P. A.	53
Hill, Jr., Louis A.	83
Hodgkinson, H. R.	52
Holm, T. A.	5
Huizer, A.	70
Jessop, E. L.	12, 72
Jones, W. D.	113

AUTHOR	Paper Number
Keightley, W. O.	50
Keller, H.	24
Klausmeier, R. D.	65
Krishnamoorthy, G.	4, 18
Langan, B. W.	72
Lawrence, S. J.	20
Lenczner	23
Longworth, J.	16, 87
Looney, J. M.	41
Maurenbrecher, A. H. P.	91
Mayes, R. L.	53, 54
McGrew, D. P.	103
McGrew, J. L.	103
McNamara, J.	101
McNeilly, T.	105
McNiven, H. D.	53
Medearis, K.	51
Mikluchin, P. T.	93
Miller, M. E.	3, 17
Mock, J. R.	110
Moorthy, T. V.	18
Nachbar, W.	4, 55
Noland, J. L.	13, 14, 25
Nunn, R. O.	1, 3, 17, 18
Nuss, L.	13
Person, O. F.	62
Plewes, W. G.	116
Oppenheim, I. J.	56
Pradolin, L.	85
Pyle, D. T.	32, 80
Rad, P. F.	9, 40
Ramscur, R.	15
Roberts, J. J.	2
Rose, J. G.	8
Scalzi, J. B.	0
Schneider, R. R.	117
Schubert, P.	106
Sheppard, W. L.	64
Shrive, N. G.	12
Smith, B. S.	85
Sneck, T.	21
Snell, L. K.	73
Soltis, L. A.	104
Suter, G.	24
Thomas, G. R.	22
Turkstra, C. J.	22
van der Meer, W.	101
Vannoy, D.	81, 90
Van Pelt, J. M.	88
Ward, M. A.	70
Warwaruk, J.	16, 87
Weber, D. C.	32
Wesche, K.	106
West, H. W. H.	6, 102
Wu, A. Y.	63
Wyatt, K. J.	89
Yeagle, G. P.	103

SYSTEME INTERNATIONALE d' UNITES (METRIC)

By JAMES E. AMRHEIN, S.E.*

*Director of Engineering, Masonry Institute of America

CONVERSION OF MEASUREMENT SYSTEMS					
English Measurement to S. I. (Metric) Measurement			S. I. (Metric) Measurement to English Measurement		
Unit	Exact Conversion	Approximate Conversion	Unit	Exact Conversion	Approximate Conversion
Length			Length		
1 mile	1.609 344 kilometres	1.6 km or 1 1/2 km.	1 kilometre	0.621,4 miles	5/8 miles or 0.6 miles
1 yard	0.914 4 metres	0.9 m or 1 metre	1 metre	3.280,8 feet or 39-3/8 inches	3 ft. 3 in. or 3 ft.+
1 foot	0.304 8 metres	0.3 m or 1/3 metre	1 centimetre	0.393,7 inches	0.4 inches or 16/100 inches
1 inch	25.40 millimetres	25 mm or 1/40 metre	1 millimetre	0.039,4 inches	1/32 inch
Speed			Speed		
1 mile per hour	1.609 344 kilometres per hour	1.6 km/h or 1 1/2 km/h	1 kilometre per hr.	0.621,4 miles per hour	5/8 mph or 0.6 mph
1 foot per second	0.304 8 metres per second	0.3 m/s or 1/3 m/s	1 metre per second	3.280,8 feet per second or 39.375 inches per sec.	3 ft/s or 1 yd/s
Area			Area		
1 acre	4 046.856 square metres	4 000 m ²	1 square kilometre	0.386,1 square miles or 247.1 acres	1/3 mile ² or 250 acres
1 square foot	0.092 9 square metres	1/10 m ² or 1 000 cm ²	1 square metre	1.196 square yards or 10.764 square feet	1.2 yd ² or 10 ft. ²
1 square inch	6.452 square millimetres	6 cm ² or 650 mm ²	1 square centim.	0.155 square inches	1/6 inch ²
Weight or Mass			Weight or Mass		
1 ounce (avdp)	28.35 grams	30 g	1 gram	0.035,27 ounces (Avdp)	1/30 ounce
1 pound	0.453 59 kilo grams or 435.59 grams	1/2 kg or 500 g	1 kilogram	2.205 pounds	2 1/4 pounds or 2 pounds
1 kip	453.59 kilo grams	500 kg or 0.5 Mg	1 mega gram	2.205 kips or 2,205 pounds	2 kips or 2,000 pounds
1 Ton (short)	907.18 kilo grams or 907 mega grams	1 Mg	1 giga gram	1,102 Ton or 2,205,000 lbs.	1000 Tons or 2 million lbs
Volume			Volume		
1 cubic yard	0.764 6 cubic metres or 764.56 litres	3/4 m ³ or 750 litres	1 cubic metre	35.315 cubic feet or 264.17 gallons	35 ft ³ or 265 gal
1 cubic foot	0.028 3 cubic metres or 28.217 litres	1/35 m ³ or 30 litres	1 litre	0.035,3 cubic feet or 0.264,2 gal or 61.024 cubic inches	1/4 gal or 1 qt or 60 in ³
1 cubic inch	16.387 cubic centimetres	16 cm ³ or 16 000 mm ³	1 cubic centimetre	0.061 cubic inches	1/16 in ³
1 gallon	3 785.4 cubic centimetres or 3.785 litres	4 000 cm ³ or 4 litres			
1 quart	946.35 cubic centimetres or .94 635 litres	1 000 cm ³ or 1 litre			
Density			Density		
1 pound/cubic foot	0.016 02 grams/cubic metre or 16.018 kilograms/cubic metre or (grams/litre)	16 kg/m ³ or 16 g/litre	1 gram/cubic centimetre	8.345 lb/gal or 62.428 lb/cubic feet	8 1/2 lbs/gal or 62 lb/ft ³
1 pound/gallon	0.119 8 grams/cubic metre or 119.83 kilograms/cubic metre or (grams/litre)	120 kg/m ³ or 1/10 g/cm ³	1 kg/cubic metre	0.008,354 lb/gal or 0.062,428 lb cubic ft.	1/8 oz/gal or 1/16 lb/ft ³
Force			Force		
1 pound force	4.448 newtons	4 1/2 N	1 newton	0.224,8 pound force	1/4 pound force
1 kip force	4.448 kilo newtons	4 500 N	1 kilo newton	224.8 pound force	225 pound force
Pressure			Pressure		
1 pound/square inch	6 894.8 pascals	7 000 Pa	1 pascal	0.000,145 pounds/square inch	
1 kip/square inch	6.895 mega pascals	7 M Pa	1 kilo pascal	0.145 pounds/square inch	1/7 psi
			1 mega pascal	145 pounds/square inch	150 psi
Energy			Energy		
1 BTU	1 054.35 joule or 1.054 kilo joule	1 kj	1 joule	0.000,948 45 BTU	1/1000 BTU
			1000 joule	0.948,45 BTU	1 BTU
Temperature			Temperature		
°Fahrenheit	[(°F - 32)/5/9]	°Celsius	°Celsius	[(1.8 °C)+32]	°Fahrenheit

PROCEEDINGS
of the
NORTH AMERICAN
MASONRY CONFERENCE

ERRATA NO. 1

Paper No. 12.

Page 12-11: TABLE 2, Col. 4 (UNIT/(Vert)): Change 285 ± 61 to 182 ± 37
Change 182 ± 37 to 285 ± 61

Page 12-12: TABLE 6, Col. 5 (Small rptg unit (ii)): Change 10.7 in last
line to 11.7.

Paper No. 71.

Page 71-2: Change "CLOCK" in title to "BLOCK".

Pages 71-4 through 71-7: Replacement pages enclosed reflecting additional test data.

Paper No. 82.

Page 82-1: Remove "AIA" after author's name.

Paper No. 84.

Page 84-12: Add under FIGURE 1: Note: Sufficient reinforcing steel area (bottom bars) to resist ground stretching should be added.

Paper No. 105.

Page 105-2: Change (iii) to read: by determining the energy and plant requirements needed in the house of one construction to achieve the same level of comfort as prevails in the unconditioned house of the other construction.

Page 105-4: Starting with line 5, change to read:

Roof: terra-cotta tiles with reflective foil sarking except where otherwise noted.

Ceiling: 12 mm plasterboard with 50 mm bulk insulation except where otherwise noted.

Page 105-4: Under "Internal Walls", change "approximate" to "appropriate".

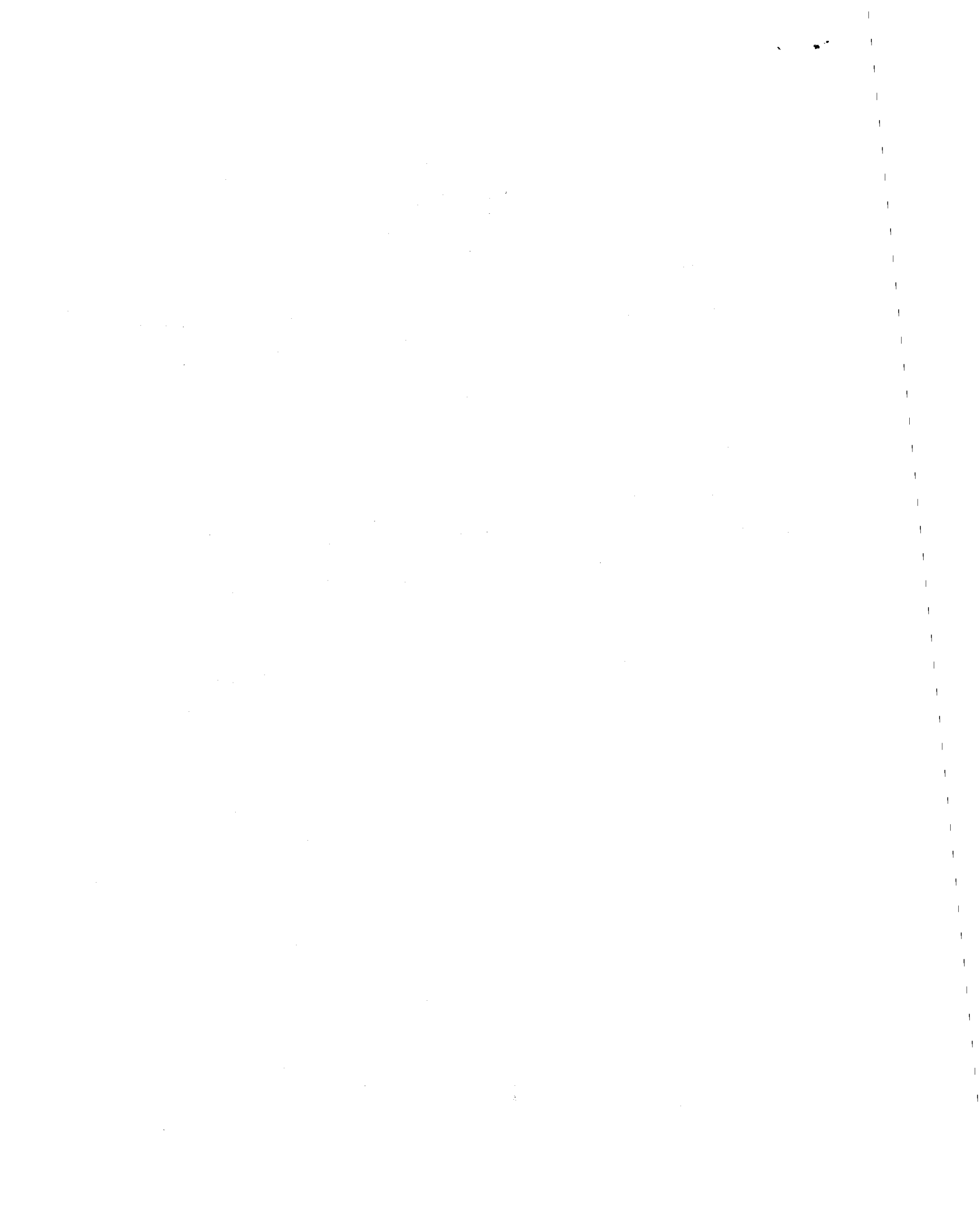
Paper No. 113.

Page 113-4: Under "Rapid Wall Movement", change "1966" to "1976".

Third paragraph of "Rapid Wall Movement", sixth line, change "actural" to "actual".

Page 113-7: Second complete paragraph, line 4, change "axis" to "axes".

Page 113-9: Fifth line, change "papapet" to "parapet".



The mason supervisor built all the prisms using block and mortar that was currently being used in the construction of the load bearing walls. The initial prisms were constructed with the job superintendent, block representative, and other representatives on hand. Prisms were constructed adjacent to the job trailer on level sheets of 3/4" x 4' x 8' plywood.

PRISM HANDLING AND CURING

Prisms were cured on the job site for 48 hours then banded with 3/4-inch plywood placed on the top and the bottom of the prism. They were then transported to the laboratory for five more days of curing, then taken to the Indiana University-Purdue University regional campus at Fort Wayne for testing.

PRISM CAPPING AND TESTING

The purpose of capping is to provide a smooth bearing surface for the load to be transmitted evenly throughout the prism. Prisms were first thoroughly examined for possible damage in transport before removing bands and plywood. The bearing surfaces were then rubbed with a carborundum stone to provide a surface free from any rough spots. Prisms were not capped with either sulfur mortar or high-strength gypsum plaster because of the difficulty in handling the prisms. Instead corrugated fiber board was placed on both bearing surfaces to transmit the load throughout the prism. Testing was done by using a Tinius Olsen Standard Super "L" universal testing machine with a capacity of 400,000 pounds. Prisms had a height to thickness (H/d) ratio of 2.0; therefore, a correction factor of 1.00 was applied to the ultimate compressive strength of the specimens (2).

BLOCK AND MORTAR TESTS

Individual block tests were performed by an independent testing firm, and the block exceeded the requirements of A.S.T.M. C-90, Grade NI and NIT. Cube mortar tests were performed on the Type S mortar used and exceeded the specified compressive strength of 1800 psi in 28 days.

STATISTICAL ANALYSIS

MEAN AND STANDARD DEVIATION

Statistical quality control implies the use of numbers and mathematical relationships to determine if a material, quantity or process meets job specifications. Using a sample size of 15 from the data given in Appendix III, a mean f'_m value of 2200 psi was calculated with a standard deviation of 284 psi for the foundation block. Figure 1 shows the relationship between the mean f'_m (sample size 3) and each foundation block set. While Figure 2 illustrates this same relationship for the 4-flute block. A sample size of 45 was used to compute a mean f'_m value of 3890 psi with a standard deviation of 434 psi for the 4-flute block.

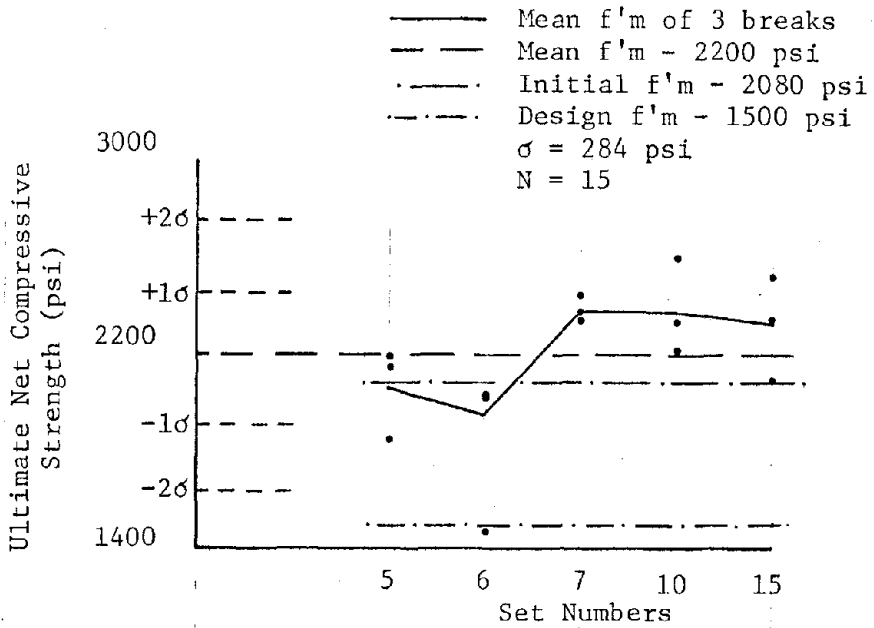


FIG. 1 - SET NUMBERS (FOUNDATION BLOCK) VERSUS ULTIMATE COMPRESSIVE STRENGTH (PSI)

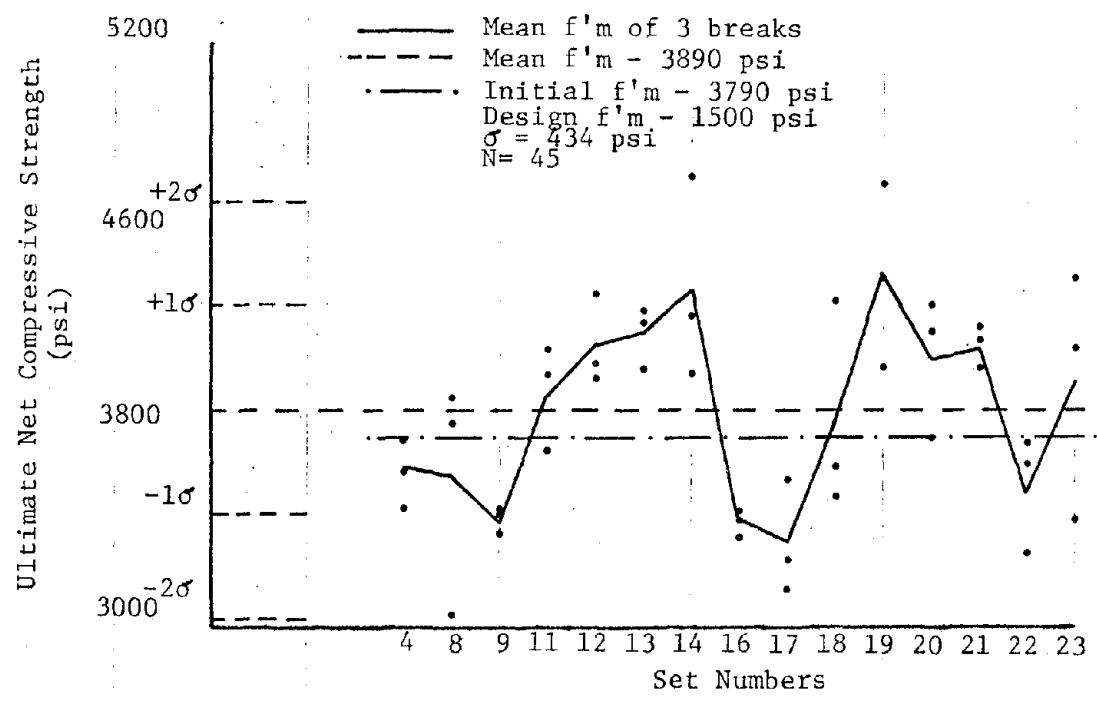


FIG. 2 - SET NUMBERS (4-FLUTE BLOCK) VERSUS ULTIMATE NET COMPRESSIVE STRENGTH (PSI)

From Figures 1 and 2, it is noted that there are three low prism breaks. One in Set 6 (foundation block) and the other two in Sets 8 and 17 (4-flute block). Upon examining the prisms in Set 6, a damaged corner was discovered. This could account for the low test break. There is no apparent reason for the low test break in Sets 8 and 17.

The relationship between the mean $f'm$ value for each building is given in Figures 3 and 4. Figure 3 shows this relationship for the foundation block while Figure 4 illustrates this same relationship for the 4-flute block. In both Figure 3 and 4, the mean $f'm$ value is greater than the initial and the design $f'm$ values. This indicates that the block being placed in the building is meeting specifications.

RANGE

The range is another measure of the dispersion or degree of scatter among test results. Table 1 lists the range for both the foundation and 4-flute block for all three buildings and the overall range for the prism breaks.

TABLE 1 - $f'm$ RANGE

Building	Foundation Block psi	4-Flute Block psi
A	700	890
B	390	1770
C	410	1520
ABC	1120	1810

SUMMARY

Quality control is vital on any construction project and is necessary for the safety and proper performance of any structure. The Edsall House Project was one where prism tests were used to establish and control the ultimate compressive strength ($f'm$) of the concrete masonry load bearing block walls. By having a method of control (prism tests) the architect, contractor and owner had assurance of the performance of the load bearing walls.

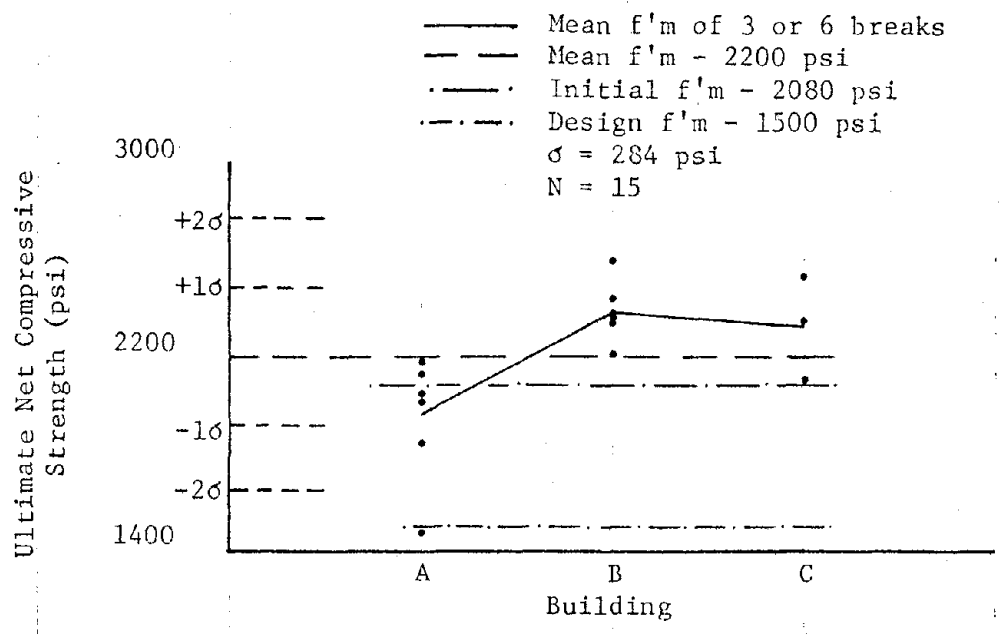


FIG. 3 - BUILDING (FOUNDATION BLOCK)
VERSUS ULTIMATE NET COMPRESSIVE
STRENGTH (PSI)

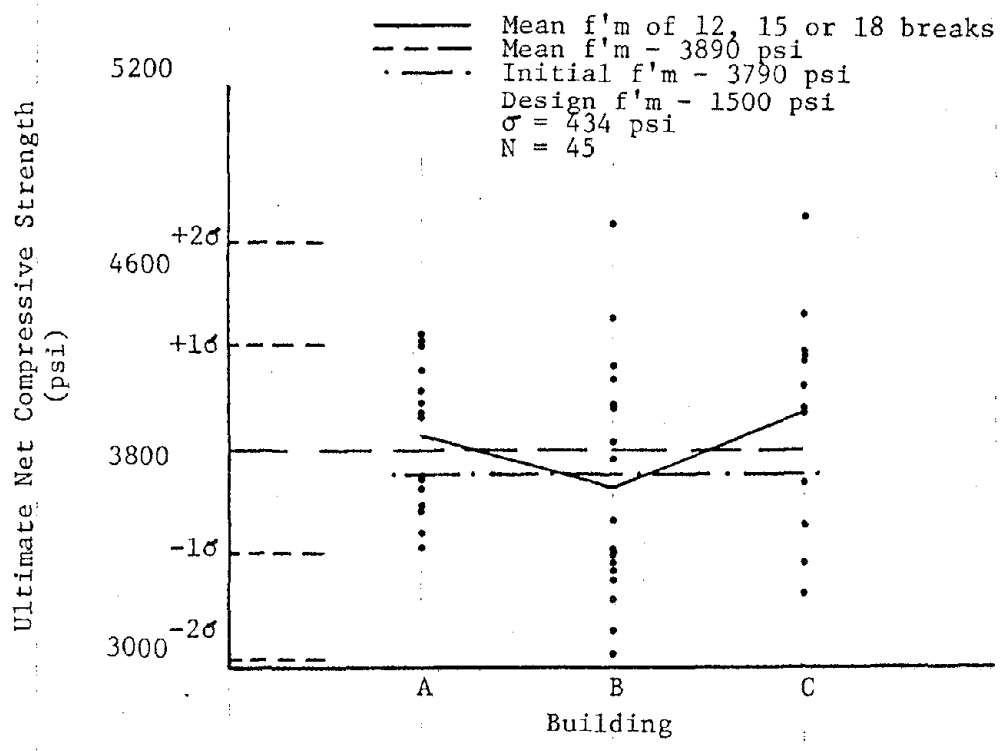


FIG. 4 - BUILDING (4-FLUTE BLOCK)
VERSUS ULTIMATE NET
COMPRESSIVE STRENGTH (PSI)



THE NEEDS OF MASONRY CONSTRUCTION¹By John B. Scalzi²

ABSTRACT: Masonry construction, one of the oldest of methods, is perhaps the least understood. In spite of a lack of sound information, engineers have been designing an increasing number of high-rise buildings in high to moderate seismic regions as well as in other areas.

Experience and post-earthquake inspections have indicated a need for new analytical methods. Increased attention to education in masonry design is needed. National standards are necessary for the mechanical and physical properties of materials and for standard testing methods of units and components.

Basic research in masonry is an emerging field. The National Science Foundation has funded a number of studies. However, additional work is necessary by more researchers. Professionals must become active in the development of design criteria and code provisions. The Masonry Society portends to be the guardian of research and practice information and dissemination to professionals and to be the coordinating vehicle for masonry information and activity to accomplish the required and essential tasks which be ahead.

¹Keynote address - North American Masonry Conference

²National Science Foundation, Washington, D.C.

THE NEEDS OF MASONRY CONSTRUCTION¹Dr. John B. Scalzi²

It is indeed a great honor and privilege to address you today as you begin the activities of this conference concerned wholly with masonry construction. I believe this is the first such conference in the United States and the organizers are to be congratulated for their efforts in generating the idea and developing the plans to implement it. It is no small task to arrange a meeting of this type in the face of limited funds and unknown bequests, contributions, and registration fees. Nevertheless, here we are today to discuss for the first time under one roof, the complete range of problems, questions and possible solutions involving masonry design and construction. The Steering Committee has planned carefully and the full range of papers attest to that fact.

Today, more than ever, knowledge on the behavior of masonry structures is needed because of the increased applications in high rise buildings throughout the country and especially in regions which are prone to earthquake actions.

The seismologists have been diligent in their pursuits of the movement of the earth's crust and have developed an understanding of seismic events to such an extent that all regions of the country have been classified with respect to an expected severity and probable risk.

As a result, design and construction of all types of buildings using various types of structural materials, such as steel, reinforced concrete, wood, and masonry are in a rebirth of research activity.

New data and information is needed for all structural materials, construction systems and details in order to design structures economically to resist not only the gravity and wind forces, but the seismic ground forces as well.

Until now, the professionals were content with the knowledge gained from elastic analyses and static tests. However, experience and post-earthquake inspections in various parts of the world as well as in California, Alaska and Hawaii have strongly indicated a great need for new analytical methods to include the inelastic behavior of structures and additional tests for material properties, strength of structural components and total structural systems.

¹Keynote address - North American Masonry Conference

²National Science Foundation, Washington, D.C.

Static tests are being replaced with pseudo-dynamic loadings and final verification tests on earthquake simulators such as shake table, which can produce earthquake effects.

Mathematical techniques which are under development are considering the limit state of behavior of materials and structural systems including such long neglected factors of torsional effects and soil structure interactions.

These recent advances into a better understanding of the behavior of materials and structural systems subjected to dynamic and/or seismic forces is of paramount interest to the Federal and local governments because of the impending inevitable consequences of a major earthquake in some regions of the United States in the not too distant future. For that reason, I am gratified to be a part of this Conference and to encourage all of you to apply your energies and talents to build better buildings to mitigate the losses caused by the disruption produced by a major earthquake.

Masonry construction is one of the oldest methods of building structures and yet, I believe, it is one of the least understood materials. Basic research activity in brick, and concrete block is a relatively new field of research emerging in the face of possible building failures as a result of seismic disturbances. These new research activities are extremely encouraging because the greatest danger from an earthquake will come from the existing inventory of masonry construction throughout the country, which was built prior to seismic codes and most of which is unreinforced masonry.

In spite of the dearth of sound research information on masonry construction engineers have been designing an increasing number of high rise buildings throughout the country in high to moderate seismic regions as well as those areas designated by seismologists as low probability risks.

With this increase in the number of buildings constructed of masonry units, it is prudent to encourage more basic and applied research in analysis techniques and experimental verification of these techniques in order to build structures which are not overly conservative but economical and safe for general occupancy.

As in many other areas of structural analysis and design, the practicing professional engineers who are faced with economic considerations of materials and labor have progressed far beyond the knowledge developed by the academic researchers. It is, therefore, heartening to learn of the new interest in basic research on masonry construction.

As a result, perhaps an increased number of researchers, faculty and consultants, will be encouraged to incorporate the principles of masonry analysis and design in their courses and professional practice in structural analysis and design.

The broadening interest in a seismic design for buildings constructed of all types of materials is stirring a review of all aspects of masonry construction.

For example, are the failure modes of unreinforced and reinforced masonry construction known to such an extent that engineers can design economical and safe buildings with confidence? Can ductility be calculated by elastic analysis techniques plus a judgement factor for the amount of ductility required or are the inelastic theories which are available sufficient for design use?

The profession has a right to ask for background information to support the concepts and theories which are currently in use by practitioners.

Masonry construction is a composite of four materials: a masonry unit, mortar, grout and steel reinforcement. The physical and mechanical properties of each by themselves should be known for application in structures which are dynamically excited. Based on this knowledge, the composite behavior should be known for the analytical solutions to be applied for design. Constants and parameters must be established for analysis purposes.

National standards are necessary for the mechanical and physical properties of materials and for standard testing methods of units and components. These standards are rapidly becoming a necessity because of the legal implications involved, in the design specifications for a project.

The types of masonry construction permitted in different regions of the country vary because of local building code requirements and the personal preference of engineers. Additional research information is needed on these systems, such as:

Unreinforced masonry

Reinforced masonry

Structural shear walls with or without openings

Veneer construction

Connections of all types, including interlocking units at corners and at interior to exterior wall joints, attachment of various types of floor and roof systems, infill panels in a reinforced concrete frame, and other combinations conceived by the architect-engineer teams.

Fortunately, a few research projects funded by the National Science Foundation establishing the static and dynamic behavior of a few of

the systems noted above are currently in progress in several universities. However, additional work is necessary by more researchers in order to determine the required data in a reasonably brief period of time for immediate application.

If we believe the earthquake predictions, then this increased research activity assumes the resemblance of a "crash program".

There are innumerable parameters and factors which require identification and evaluation that many more researchers can be absorbed easily into the total research activity and still not produce all the data required for a long time to come.

Workmanship of construction has been cited as an analysis variable which is difficult to evaluate with confidence, and, therefore, analyses must be overly conservative.

As engineers responsible for design analyses and project specifications, it behooves the profession to take a more active role in the training of construction workers to instill within them the necessity for good quality workmanship. Members of a unified team usually produce the expected desired results.

In order to achieve the final desired objective of sound, economical and safe masonry construction, there are several individual and collective actions which may be taken by professionals, by industry, and by regulatory agencies.

These actions will be briefly discussed for the single purpose of stimulating action by those groups who are in a position to assume the responsibility for the necessary action.

Research in all aspects of masonry analysis, design, and construction is needed to provide the necessary information to decision-makers at all levels of the construction process.

Research dissemination is becoming one of the most important phases of research. Without it, the research results will become obsolete while sitting on the bookshelf.

Educators must become a part of the dissemination process by including the latest results in their course material and develop new courses wherever required. They should understand that to do otherwise is an injustice to the student who expects and deserves the latest developments and information in all fields of engineering. Continuing education short courses are one of the best methods to disseminate information on specialized subjects such as masonry construction.

A close parallel to the short course is the specialized conference such as this one on masonry construction.

The rate of research publications has increased tremendously in the last decade and promises to increase further. Therefore, it is extremely important that designers have a single source of reference on a particular subject. A technical journal or newsletter is a convenient method to disseminate information economically and rapidly. A reference library should be established to provide a source for research material. Any organization interested in this library activity should have a facility to house the material and a staff to manage it.

Professionals must become active in the development of design criteria, and building code provisions which should be applicable throughout the country, with due consideration for local differences.

Professionals use the building codes, and, therefore, should have a voice in their development, adoption, and enforcement.

A building code does not substitute for good design but establishes minimums for the safety of occupants. It is advisable to specify reasonable minimums of design and to upgrade the minimums as new information is presented.

The combined efforts of professionals and industry may be required in this endeavor.

Special reports on the behavior of building systems and materials following an earthquake or other disaster is essential to the learning process. It can be said that an earthquake is "an experiment out of control" but from which much can be learned. Prompt reporting of the lessons is imperative to rapid inclusion of the results into practice and code requirement provisions.

As new concepts are technically and experimentally verified economic studies become essential in order to test the viability of the concept for practical application in the design and construction of buildings. These economic studies are a part of the implementation of the results.

In summary, I have indicated that masonry research has long been neglected by the researchers, omitted from the curricula in design at engineering and architectural schools, and omitted from the general education of the undergraduate and graduate student.

We have seen the professionals extending the application of masonry construction to higher buildings, and to all regions of the country whether seismically prone or not.

The time has arrived to resolve all the unknown parameters and factors which influence masonry construction in order to design and build economical and safe structures in all parts of the United States.

The recently established organization of "The Masonry Society" portends to be the guardian of research and practice information and dissemination to the professionals. It can become the coordinating vehicle for masonry information and activity to accomplish the required and essential tasks which lie ahead.

With the help of the professionals in cooperation with the industry, great benefits can be realized to the mutual advantage of all interested participants. We can all look forward to great achievements and accomplishments in the field of masonry construction.

BEHAVIOR OF CONCRETE MASONRY UNDER BIAXIAL STRESSES¹

by

G. A. Hegemier², R. O. Nunn³, S. K. Arya⁴

ABSTRACT

Biaxial tests of full-scale concrete masonry panels under monotonic and cyclic stress histories are described. The experimental results presented concern planar material behavior and are related to the formulation of constitutive relations for concrete masonry in both linear and nonlinear ranges of deformation. Topics discussed include: 1) the initial macrocracking or yield surface in stress space; 2) macrocracking and isotropy; 3) prediction of the initial macrocracking surface, and post-macrocracking behavior from component data; 4) influence of reinforcing steel on initial and post-macrocracking behavior; 5) elastic moduli and anisotropy; 6) elastic moduli and strength; 7) damping or energy absorption; and 8) strain-rate effects. Analytical models for certain of the above items are proposed.

The foregoing tests are part of an extensive University of California, San Diego research effort on the seismic response of concrete masonry structures; they constitute the first biaxial experiments on masonry. A brief description of the associated test setup, which is unique in size and sophistication, is provided.

¹Research was sponsored by the National Science Foundation under Grant NSF ENV 74-14818.

²Professor, Dept. Appl. Mech. & Engr. Sci., University of California, San Diego, La Jolla, California, 92093.

³Graduate Student, Dept. Appl. Mech. & Engr. Sci., University of Calif., San Diego, La Jolla, California, 92093.

⁴Principal Development Engineer, Dept. Appl. Mech. & Engr. Sci., University of California, San Diego, La Jolla, California, 92093.

BEHAVIOR OF CONCRETE MASONRY UNDER BIAXIAL STRESSES¹

by

G. A. Hegemier, R. O. Nunn, S. K. Arya²

INTRODUCTION TO UCSD MASONRY PROGRAM

General Remarks

Examination of recent surveys (2,8) relevant to the mechanics of concrete masonry systems reveals that, although a measurable amount of research on concrete masonry has been conducted over the past forty to fifty years, there has been little correlation among the various studies conducted by governmental, university, and promotional research organizations. Each study has, of economic necessity and/or impatience, been constrained within narrow bounds and primarily to specific structural configurations rather than to fundamental material research. In addition, most studies have not been sustained for a time interval sufficient to generate results of wide utility and integrity. As a consequence, a virtual vacuum exists concerning the material properties of concrete masonry, and the behavior of typical connections used in concrete masonry structures.

In the absence of reliable data, subjective judgement must be substituted for rational design and analysis. The ramifications of such a substitution are obvious and clearly undesirable from the standpoint of all parties involved - the public, the masonry industry, and the structural engineering community.

In response to the need for fundamental information, an extensive experimental, analytical, and numerical research program (6) was initiated at the San Diego campus of the University of California (UCSD). The objective of this program is the development of a basis for a rational earthquake response and damage analysis of concrete masonry structures. The study is sponsored by the National Science

¹Research was sponsored by the National Science Foundation under Grant NSF ENV 74-14818.

²Professor, Graduate Student, Principal Development Engineer, respectively, Dept. Appl. Mech. & Engr. Sci., Univ. of Calif., San Diego, La Jolla, 92093.

Foundation under project RANN (Research Appplied to National Needs). Contributions have also been received from the masonry industry.

It is noted that a related program, covering a number of masonry materials in addition to concrete masonry, exists at the Berkeley campus of the University of California. A valuable interchange of information between these programs has been effected, as will become evident later.

With respect to the San Diego program, the experimental effort is intended to define material behavior, and the behavior of typical connections used in concrete masonry structures. The analytical phase involves the translation of observed experimental data into viable mathematical models. The numerical effort concerns the conversion of mathematical models into numerical form and the construction of digital computer programs to simulate structural response and damage accumulation resulting from earthquake ground motion.

Methodology

The key word here is synthesis. The UCSD Masonry Program represents the first comprehensive effort to describe the material properties of concrete masonry, and to synthesize the behavior of complex structural elements from elementary component data, i. e., data on block, mortar, grout, and steel.

The approach selected to achieve the project objectives involves a sequence of increasingly complex levels of concurrent experimentation, analysis, and numerical simulation. This sequence begins with elementary experiments on the basic constituents of concrete masonry and their interactions, e. g., by fracture and slip across interfaces. It proceeds to homogeneous and nonhomogeneous biaxial tests of full-scale panels under both monotonic and cyclic load histories. The above is complemented by tests on typical connections. The sequence culminates with case studies of major structural elements and/or buildings. The ability to extrapolate from conceptually simple laboratory-scale experiments to a wide variety of structural configurations, including simulation of full-scale building response to earthquake ground motion, is one of the most significant aspects of the project.

The program partitions naturally into two main categories: 1) small-scale or microelement tests and micromodeling involving specimens of several unit (block) dimensions, and 2) large-scale or macroelement tests and macromodeling involving specimens of sufficient size to mirror full-scale masonry; the planar dimensions of the latter are approximately one order of magnitude larger than the

largest microdimension (block size).

The objective of the small-scale tests and the associated micro-modeling is to synthesize the behavior of masonry assemblies or macroelements from simple but universal experiments - experiments that can be conducted in a standard laboratory.

The large-scale or macroelement tests constitute a necessary check on the micromodeling process and, perhaps more important, constitute the starting point for the construction of a continuum or macromodel of concrete masonry. The latter, it is anticipated, may be used to efficiently synthesize the behavior of complex structures, in combination with appropriate connection data (7), through the use of explicit analytical and numerical techniques. The numerical method in use is the finite element method. The evolution of the program is depicted in Fig. 1.

Items Under Study

The basic experimental items under study concern planar material behavior and are related to the formulation of constitutive relations for concrete masonry in both linear and nonlinear ranges of deformation. Included are:

- . Strength and damage accumulation under combined plane-stress states
- . Stiffness parameters
- . Energy absorption and damping

In each of the above areas, studies will determine the influence of:

- . Anisotropy
- . Strain-rate
- . Reinforcing steel volume and configuration
- . Grout compaction
- . Grout admixtures
- . Flaws
- . Constituent properties on assembly properties
- . Scale effects
- . Cyclic load histories

Materials and Fabrication

Two nominal masonry types are currently under study: 1) "normal strength" - grade N normal weight hollow core concrete block (ASTM C90), type S mortar (ASTM C270), 2,000 psi coarse (pump

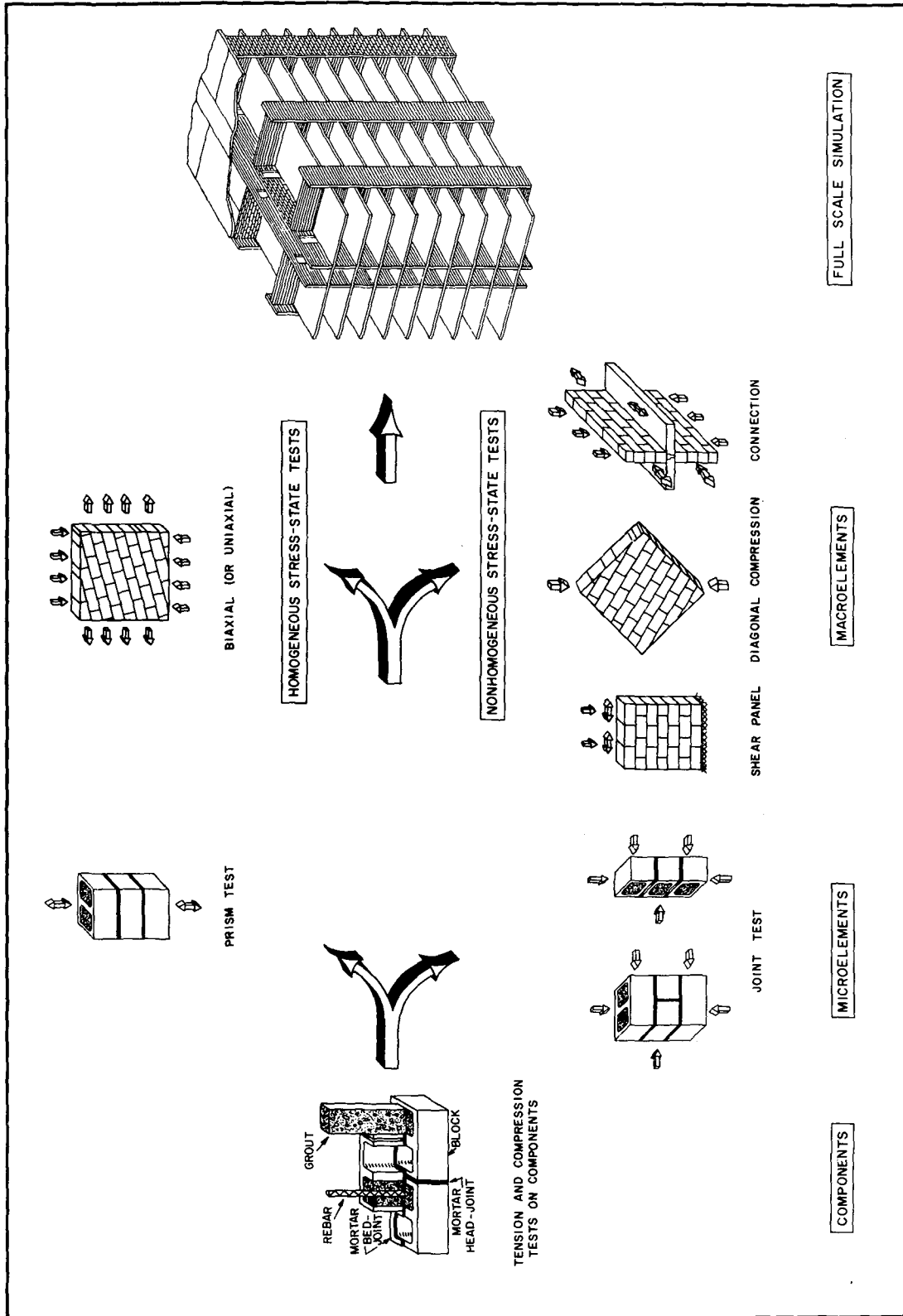


Fig. 1. Evolution of Research Program

mix, 8-10 inch slump) grout (ASTM C476); 2) "high strength" - light weight hollow core concrete block ($f'_c \geq 3750$ psi), type M mortar (ASTM C270), 3750 psi coarse (pump mix, 8-10 inch slump) grout (ASTM C476). Precise details concerning constituent properties are provided in conjunction with discussions of each test series.

Most specimens consist of fully grouted masonry (8-foot lifts on full scale specimens) with running bond and face-shell thickness mortar bedding. Both closed and open-end units are utilized, although focus is currently on the former. Standard 8-inch high, 8-inch wide block geometries (2) are used.

It is emphasized that all specimen fabrication is conducted by professional masons using conventional field practice. In particular, no effort has been made to achieve optimum "laboratory" conditions. All specimens are field cured.

Utilization

Information from this program may be extracted from different areas and at various levels of sophistication. Some experiments will provide a valuable guide for improved masonry through modified or standardized fabrication techniques. Others will provide a necessary data base for the designer and the engineer. A numerical program will allow case studies by researchers and analysis by the cognizant engineer. Distillation of data from experiments and case studies should provide a rational basis for meaningful building code modifications.

Selected Results

Selected portions of the materials properties segment of the aforementioned program are presented and discussed at this conference via a collection of companion papers. The first of these papers concerns the behavior of concrete masonry under biaxial stresses; this subject is discussed herein.

DESCRIPTION OF STATIC AND DYNAMIC BIAXIAL PANEL TESTS

Homogeneous Stress States

These tests, which represent a critical step in the continuum modeling process, are unique in that the panels (macroelements) are laid in running bond, but are saw-cut such that the bonds run at oblique incidence or layup to the edges of the finished panel. The rationale: any combination of homogeneous shear and normal stresses on the critical bed and head joint planes can be induced by application

of direct (principal) stresses (compression or tension) to panel edges, and the selection of a proper layup angle. The ability to apply direct tensile stresses which exceed the tensile strength of the assembly, and direct compressive stresses with negligible induced shear, follows from the use of a unique polysulfide bonding agent with a low shear modulus (≈ 150 psi) between the specimen and the load distribution fixtures. In the case of uniform load application to each panel edge, the resulting panel stress distribution is globally homogeneous, and hence statically determinate. Thus, in contrast to conventional test methods (8), the determination of material properties is not prejudiced by boundary constraints; further, in contrast to indirect methods (2), extraction of biaxial failure data does not necessitate a conjecture of isotropic, linear elastic material behavior prior to macrocracking.

Figure 2 illustrates the basic concept of oblique layup testing. If the x_1, x_2 - axes are principal stress directions, then the stress resultants¹ $N'_{11}, N'_{22}, N'_{12}$ associated with axes x'_1, x'_2 along the bed and head joint directions are related to the principal stress resultants N_{11}, N_{22} through

$$\begin{aligned} N'_{11}, N'_{22} &= \frac{N_{11} + N_{22}}{2} \pm \frac{N_{11} - N_{22}}{2} \cos 2\theta \\ N'_{12} &= \frac{N_{22} - N_{11}}{2} \sin 2\theta \end{aligned} \quad (1)$$

Equations (1) imply that any homogeneous stress state ($N'_{11}, N'_{22}, N'_{12}$) in a panel with surfaces oriented parallel to the head and bed joints can be obtained by selecting an appropriate layup angle θ and direct stress resultants N_{11}, N_{22} . In particular, given a desired stress state ($N'_{11}, N'_{22}, N'_{12}$), the combination (N'_{11}, N'_{22}, θ) is selected according to

$$\begin{aligned} \tan 2\theta &= \frac{-2N'_{12}}{N'_{11} - N'_{22}} \\ N_{11}, N_{22} &= \frac{N'_{11} + N'_{22}}{2} \pm \frac{N'_{11} - N'_{22}}{2} \cos 2\theta \mp N'_{12} \sin 2\theta \end{aligned} \quad (2)$$

The panels in the homogeneous stress-state test series are 64-by-64 inches in planar dimension, and are precision cut from

¹Stress resultants are related to stress by $\sigma_{ij} = N_{ij}/t$, where t is the panel thickness.

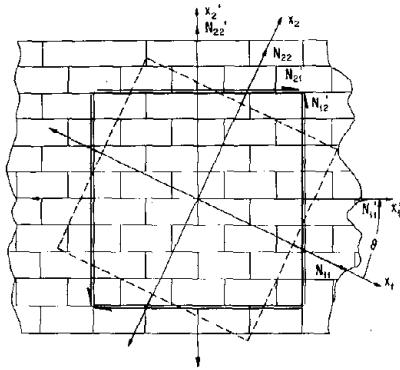


Fig. 2. Stress Transformation

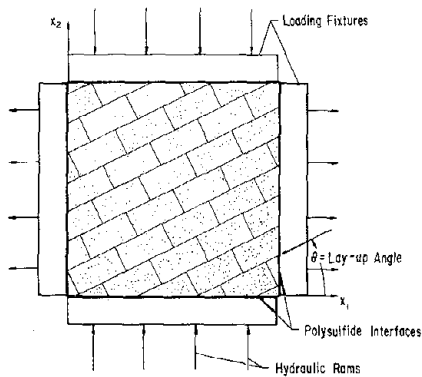


Fig. 3. Loading Schematic

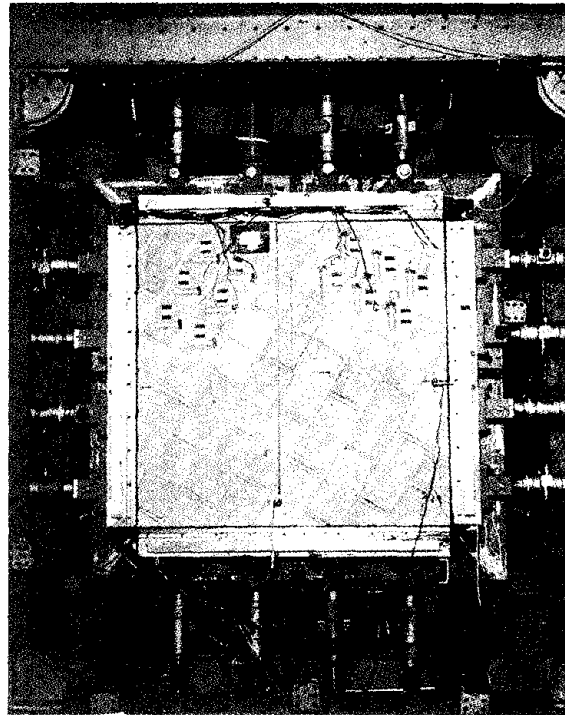


Fig. 4. Biaxial Fixture

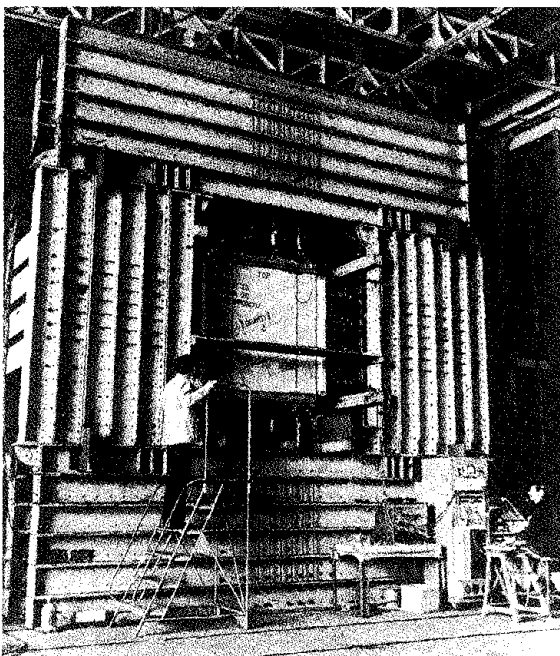


Fig. 5. Test Frame

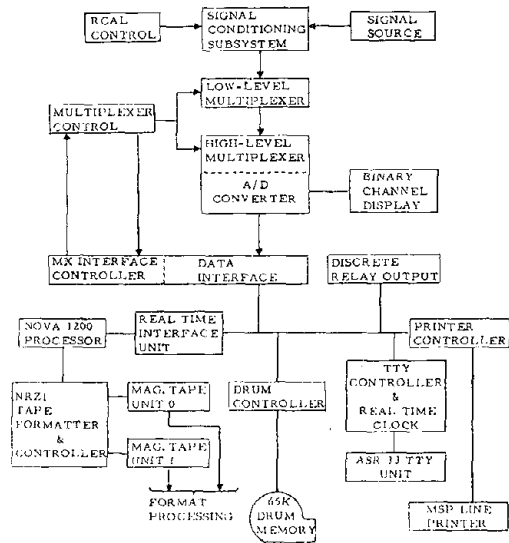


Fig. 6. Data Acquisition

8-by-8 foot fully grouted unreinforced or reinforced concrete masonry walls. Cutting is accomplished by use of a dynamically balanced, 30-inch-diameter, diamond-edge saw on an air-driven turbine attached to fixed rails.

A schematic of the biaxial test procedure is shown in Fig. 3. The actual setup is illustrated in Fig. 4. The load conditions include quasi-static monotonic, quasi-static cyclic, and dynamic cyclic (.05 to 5Hz). The system is capable of load, displacement, or combined load-displacement control. This is accomplished with a mini-computer-controlled, closed-loop-hydraulic-servo system utilizing four active actuators on each panel side connected to load distribution fixtures. This test system is housed in a massive dual test frame, Fig. 5. A high-speed digital data acquisition system (14 bits absolute value plus sign, 300 samples/sec/channel or 12,000 samples/sec total), Fig. 6, monitors 40 channels of signals from loadcells, linear variable differential transformers (LVDT's), and strain gages.

Rheological aspects of singular interest include: 1) elastic properties; 2) degree of anisotropy of elastic properties; 3) damping or stress-strain hysteresis in the "elastic" regime; 4) strain-rate sensitivity of item 3 in the .05 to 5Hz range; 5) initial "yield" or macrofracture surface in stress-space; 6) degree of anisotropy of item 5; 7) ultimate strength; 8) influence of load history on the degradation of stiffness and ultimate strength; 9) hysteresis in the highly nonlinear range; 10) role of reinforcing steel geometry and volume in the control of macrocracking; and 11) flaw sensitivity.

Nonhomogeneous Stress States

These tests constitute an advanced step in the micromodeling process and a first evaluation of the limits of applicability of the homogeneous stress-state data and/or an associated continuum model. Two basic test-types are utilized: 1) diagonal compression and 2) simple shear deformation.

The diagonal compression test is designed to evaluate the predictive accuracy of the failure (initial macrocracking) theory, developed from homogeneous stress-state data, in a nonhomogeneous stress field. Theoretically, the use of homogeneous stress-state data is based upon an assumption that the dominant characteristic length associated with variations in the stress field is "large" in comparison to the largest masonry microdimensions - 8 to 16 inches (the block size). From a practical standpoint, it is expected that such data may be utilized when "large" is only several microdimensions.

The diagonal compression test is illustrated schematically in Fig. 7. Under concentrated diagonal compressive loads, the central region of the test specimen is subjected to a biaxial stress-state, Fig. 8, which is reasonably uniform over a centered circular area of diameter equal to approximately 20-25 percent of the diagonal. For the 64-by-64 inch specimen utilized, this diameter is roughly 1 to $1\frac{1}{2}$ times the largest microdimension. Hence, this is a severe test of the limits of applicability of the homogeneous data. The mode of comparison is measured vs. predicted failure loads, P_d ; the latter is based upon the initial macrofracture surface as determined from the homogeneous tests. Data from an array of LVDT's, strain gages and a load cell is obtained with the aid of the high speed digital data acquisition system mentioned previously.

The "simple shear deformation" test is a shear-wall test wherein the top and bottom planes of the specimen are constrained to remain essentially parallel. This test-type serves to calibrate all modeling in a region of primary interest. The rheological items of interest here are similar to those listed in the discussion of homogeneous stress states.

The biaxial test system described previously is capable (with modifications) of producing simple shear deformation under ideal conditions as far as control is concerned. However, in view of an existing shear wall test program at U. C. Berkeley, it was decided to attempt to extract the necessary data for this case from this program. The Berkeley test setup is illustrated schematically in Fig. 9. It is a structural test and was not specifically designed for the purpose of furnishing fundamental material - behavioral information. The complexity of this test necessitated a considerable effort on the part of the U. C. San Diego research team with respect to the installation of a vast array of probes, data acquisition (the high speed U. C. San Diego digital data acquisition system was used), and extensive data reduction (conducted at U. C. San Diego).

SELECTED RESULTS PANELS UNDER HOMOGENEOUS STRESS STATES

A complete description of the biaxial tests (3, 4, 5) is beyond the scope of this presentation. For simplicity, attention is focused below on sample results obtained to date under this program. Brief discussions are presented concerning the homogeneous stress-state tests and the following associated items: 1) the initial macrocracking surface; 2) macrocracking or failure and isotropy; 3) prediction of the initial macrocracking surface from component data; 4) influence of reinforcing steel

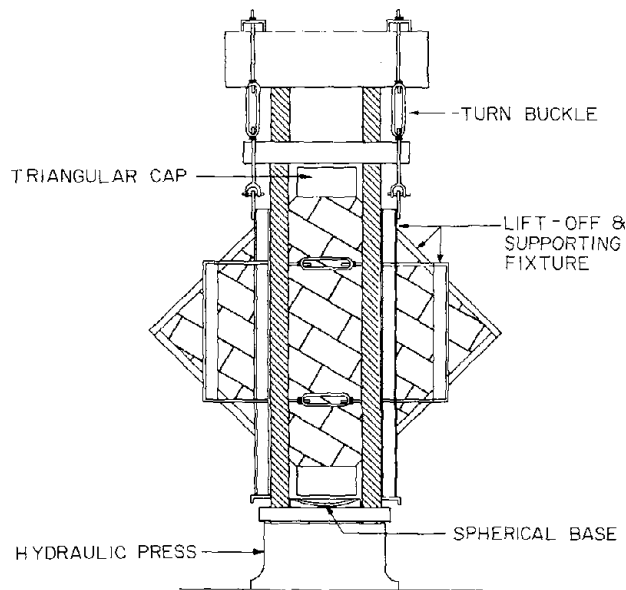


Fig. 7. Diagonal Compression Test

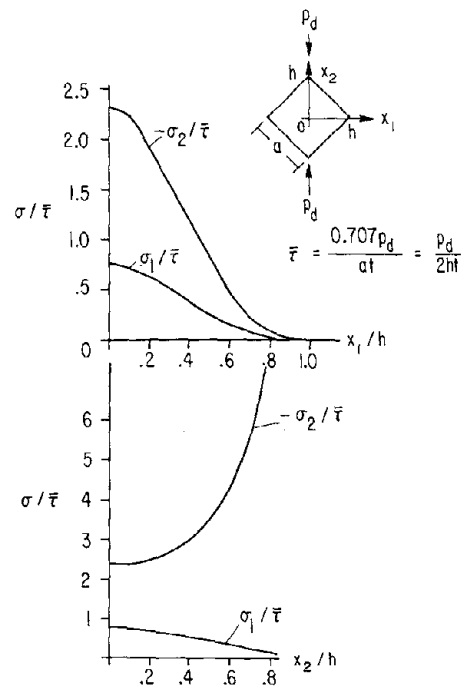


Fig. 8. Stress Distribution on the Planes $x_2=0$, $x_1=0$

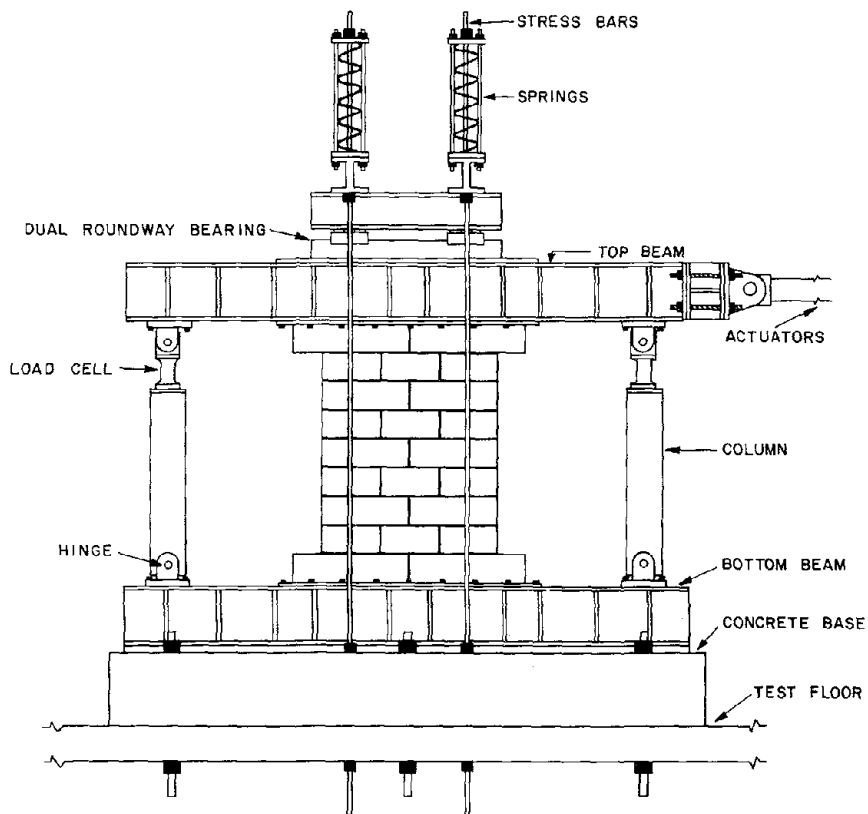


Fig. 9. Schematic of the Berkeley Shear Wall Test

on initial and post-macrocracking behavior; 5) elastic moduli and anisotropy; 6) elastic moduli and strength; and 7) damping and strain-rate effects in the linear range.

Initial Macrocracking Surface

From both design and analysis standpoints, this represents one of the most important aspects of material behavior. For unreinforced specimens, the initial macrocracking surface in stress space is that set of stress points at which failure occurs. For reinforced specimens, and under normal reinforcing volumes, the initial macrocracking surface represents the set of stress points at which major cracking occurs together with a primary load transfer from masonry to steel; the latter is usually accompanied by a substantial drop in stress under monotonically increasing strain, reflecting the reduction in the load carrying capacity of the element over a certain interval.

Complete mapping of the initial macrocracking surface in the stress space (N'_{11} , N'_{22} , N'_{12}), or the principal stress vs. θ -space (N_{11} , N_{22} , θ), is a major undertaking. This problem is, however, alleviated by two factors; 1) extensive calculations concerning shear walls and other complex structures reveal that, in most applications, the normal stress on head joint planes is small when compared with normal and shear stresses on bed joint planes, i. e.

$$N'_{11} \ll N'_{22}, N'_{12} \quad (3)$$

and 2) experimental data reveals a weak dependence of strength on the layup angle θ , i. e., the masonry under consideration is approximately isotropic - a point to be discussed later.

A typical intersection of the initial macrocracking surface with the plane $N'_{11} = 0$ is illustrated in Fig. 10 for fully grouted specimens, the component properties of which are given in Table 1 for one specimen set ("batch 6"). The rays in this figure represent the layup angles and the corresponding proportional loading which results from the condition $N'_{11} = 0$ in equations (1) and (2); this furnishes the proportional loading relation

$$N_{11} = -N_{22} \tan^2 \theta \quad (4)$$

Data points, which represent statistical means of repeated tests, are denoted by circles and triangles for unreinforced specimens and open squares for reinforced specimens. Stresses shown are based upon net cross-sectional areas. Steel volumes utilized in the reinforced masonry are discussed in a subsequent section. The data indicates,

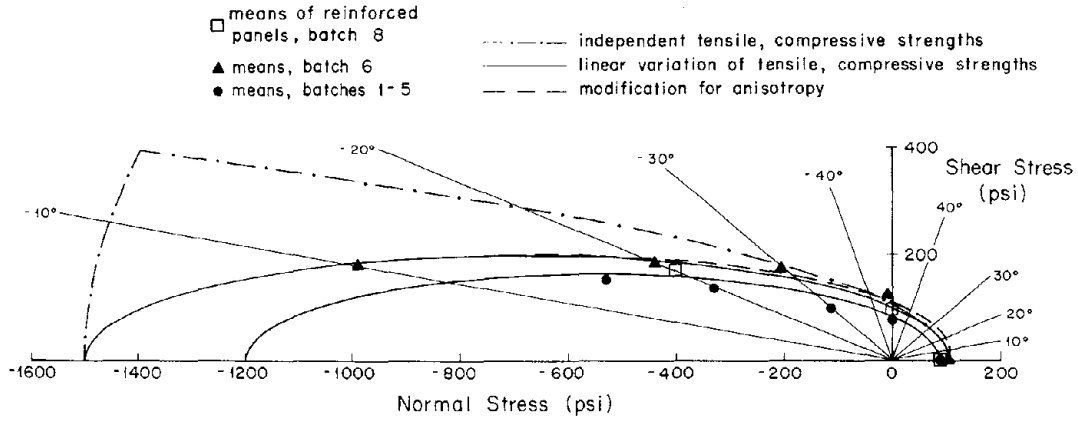


Fig. 10. Failure Envelope for Zero Head Joint Normal Stress

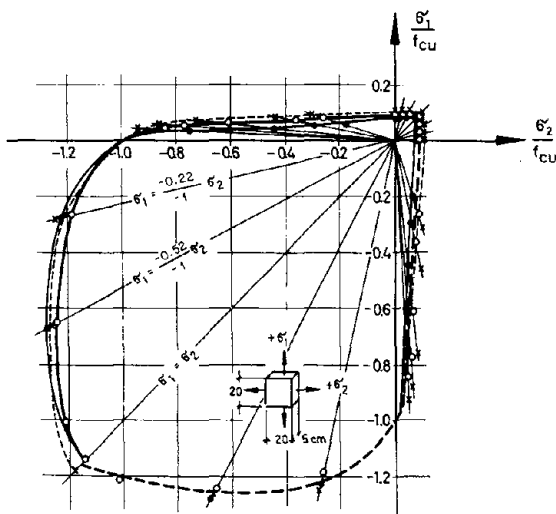
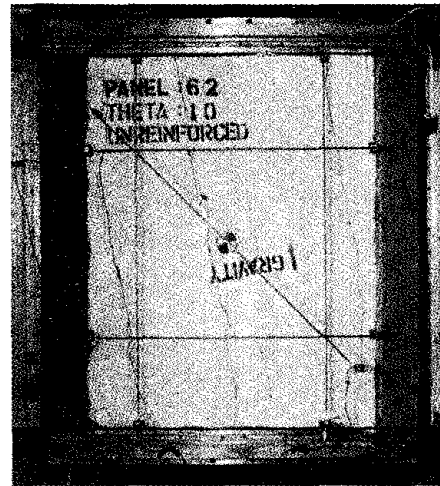
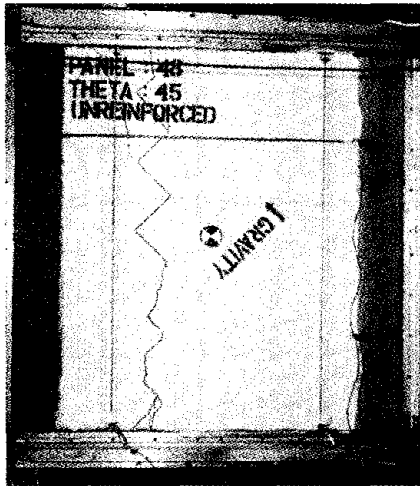


Fig. 12. Biaxial Strength of Concrete

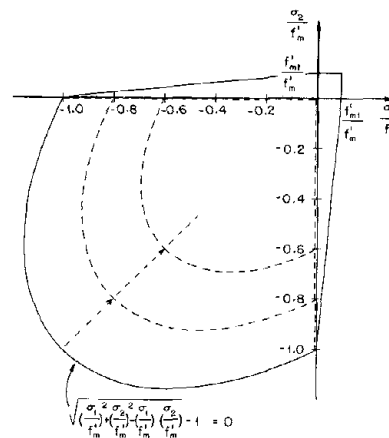


Fig. 13. Initial Macrocracking Envelope for Masonry

as should be expected, that the initial macrocracking surface is not appreciably influenced by reinforcement for practical ranges of steel volumes.

For unreinforced specimens, two basic failure modes were observed. In the tension zone (see Fig. 10), and in the compression zone for $|\theta| > 15$ deg., a brittle failure with a single crack was frequently observed, as illustrated in Fig. 11 (a) ($\theta = -45$ deg.). In the compression zone for $|\theta| < 15$ deg., failure consisted of multiple cracks, as shown in Fig. 11 (b) for $\theta = -10$ deg. For reinforced specimens, multiple cracking was most frequently observed (this point will be discussed subsequently).

The curves in Fig. 10 represent several macroscopic, analytical failure models considered to date. The dotted curve, shown for "batch 6," is based upon the premise that failure occurs when a principal stress reaches either the tensile strength or the compressive strength associated with a uniaxial, 0 deg. layup test. The solid curves result from the premise that the failure envelope in principal stress-space is linear in the tension-compression zone, as illustrated in Fig. 12 for plain concrete under biaxial stress states. The resulting model is seen to provide a more accurate description of material behavior. The solid curves in Fig. 10 correspond to estimated (from prism tests) compressive strengths, and measured (from 0 deg. layup panels) uniaxial tensile strengths for two groups of specimens. Note that only two tests are necessary for construction of this failure model: 1) the uniaxial tensile strength and 2) the uniaxial compressive strength. The dashed curve in Fig. 10 represents a modification of the solid curve for "batch 6," to account for anisotropy; this was accomplished by allowing the uniaxial tensile strength to vary with θ ; this variation is discussed below. As can be observed, the correction is small. For such cases, the initial macrocracking model depicted by Fig. 13 is proposed (the compression-compression quadrant will be treated later). The premise of linearity of the failure envelope in the tension-compression zone of principal stress is substantiated by biaxial data, Fig. 14, on unreinforced macroelements.

Macrocracking or Failure and Isotropy

Data on unreinforced macroelement tensile failure indicates a slight increase in strength for layup angles near 45 deg., as shown in Fig. 15, but the premise of material isotropy can be seen to hold within normal data-scatter for brittle materials of the type under consideration. For a layup angle of 0 deg., tension is applied to the bed joints. Each curve in Fig. 15 represents a fit to the data of a second degree polynomial.

Table 1. Component Properties for Batch 6

	Strengths (psi)				Young's Mod. (10 ⁶ psi)		Poisson's Ratio
	compressive		tensile		cmpr.	tnsl.	
	mean	std. dev.	mean	std. dev.			
Block	3300	370	329	40	2.5	-	0.16
Mortar	2420	410	215	47	-	-	-
Grout	3870	350	266	39	2.6	2.3	0.16

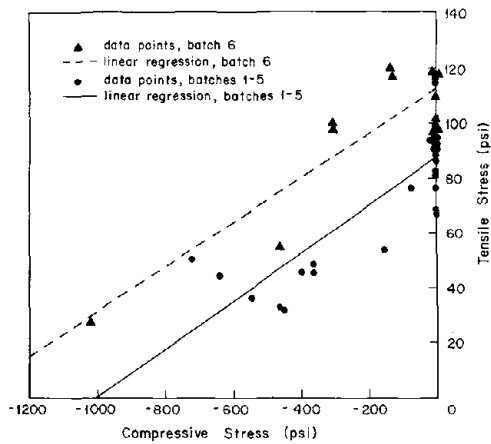


Fig. 14. Panel Tensile Strength vs. Compressive Stress

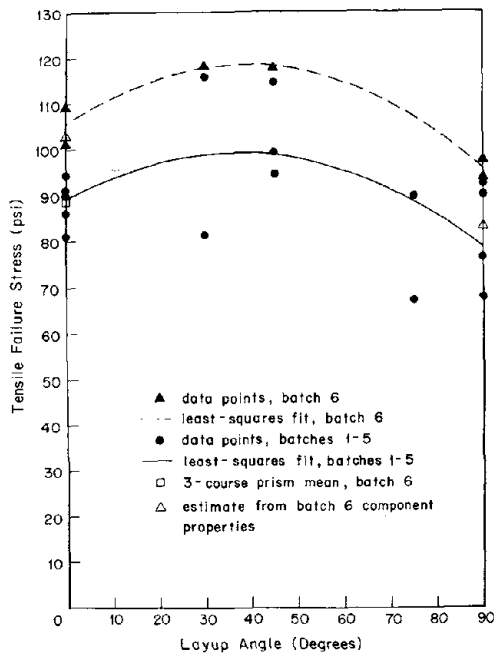


Fig. 15. Panel Tensile Strength Anisotropy

Table 2. Tensile Strength Predictions

	STD	STD VIBR
Grout Area		
Panel Area	0.54	0.54
Grout Tensile Strength		
Panel Tensile Strength	0.34	0.50
Prism Tensile Strength		
Panel Tensile Strength	1.06	0.99

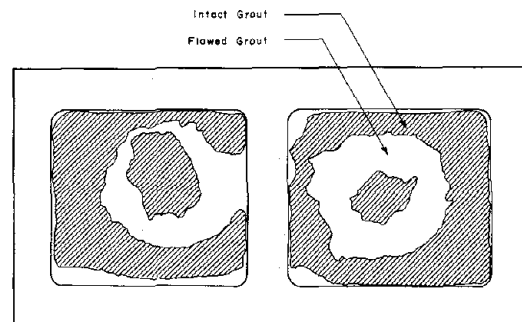


Fig. 16. Grout Flaws at Bed-Joint Plane

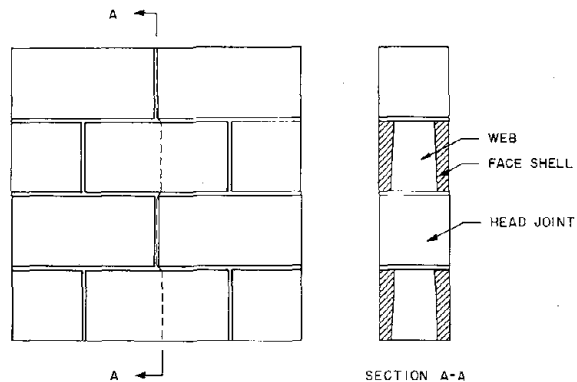


Fig. 17. Tensile Failure Pattern for 90 deg. Layup

It should be noted that material anisotropy for a macroelement is a direct function of block and grout strengths. The strength combinations under study, by accident, led to an essentially isotropic material. The latter can be destroyed by a nonjudicious selection of block and grout strengths. Estimation of material anisotropy from component properties is discussed below.

Prediction of Initial Macrocracking from Component Data

From both design and analysis viewpoints, it is highly desirable that one be able to predict macroelement properties from component properties and geometries. Extensive testing has revealed that this is indeed possible. The degree of success and complexity of the model involved, however, is a strong function of the number (distribution) and type of flaws in the masonry. Several examples concerning the initial macrocracking surface are given below to illustrate this point.

Consider once again the initial macrocracking theories represented by the solid or dashed curves of Fig. 10. Recall that the solid curves require material isotropy and two data points: the uniaxial tensile strength and the uniaxial compressive strength. Correction for anisotropy (dashed curve) requires an estimate of the variation of uniaxial tensile strength with the layup angle θ .

Let us consider the problem of predicting the necessary tensile strengths associated with the above models. For this purpose reference is made to Fig. 15 and the open triangles. The open triangle for "batch 6" at 0 deg. layup is based upon the premise that (in the absence of bond beams), the 0 deg. tensile strength is determined solely by the grout tensile strength and area; little or no tensile strength is attributed to the mortar bond - a fact which has been substantiated by joint tests. The resulting strength estimate is seen to be excellent. The reason? The "batch 6" specimens contained relatively few flaws. Based upon the grout core/panel area ratio, the correlation between component and panel 0 deg. tensile strength is observed to be excellent for the STD VIB specimens and poor for the STD specimens.

The bridge from component data to masonry strength in the presence of significant flaws necessitates a statistical analysis in conjunction with a considerable number of tests. Although this topic is extremely important, it is beyond the scope of this discussion. An explicit, dramatic flaw influence on strength, and the fact that one can predict strength if the flaw type and distribution are known, is worth noting at this point, however. Upon examination of the failure surface associated with a direct tensile test of a puddled prism with no admixture, the cross-hatched area of Fig. 16 was deduced to be free from

flaws, i. e., the remaining area represented a flaw in which no bond existed across the plane of failure. Based upon the measured tensile strength of the grout, and the measured area of integrity, the tensile strength of the prism was predicted within a few percent accuracy. The ratio of the area of flaw-free grout to the total grout area was 0.67. Thus, there can be no doubt that flaws significantly influence strength.

The strength of a 90 deg. layup specimen in uniaxial tension is primarily a function of block strength. A typical failure pattern is illustrated in Fig. 17. The head joints contribute little to overall strength of a macroelement, and inspection of failed specimens revealed that most grout cores separated cleanly from the webs. Addition of the area of web that adhered to the grout core to the area of the face shells provides the estimate of macroelement strength at 90 deg. shown as the open triangle in Fig. 15. The estimate is seen to be reasonable, and should not be significantly influenced by flaws. Block strength here was determined by direct tensile testing of coupons saw cut from full-blocks.

The prediction of macroelement compressive strength from component properties is not straightforward and this subject is currently under study.

Finally, the problem associated with flaw influence on 0 deg. uniaxial tensile or compressive strengths can be alleviated considerably by careful use of prism tests. In the case of tensile strength, three course prisms, fabricated and cured in the field using techniques that mirror (as close as is feasible) those of the full-scale masonry have been found to provide good to excellent correlation with macroelement data; examples are included in Table 2 and Fig. 15 (the open square). The use of prism tests for compressive strength requires extreme care; discussion of this subject is contained in a separate paper.

Influence of Reinforcing Steel on Initial and Post Macrocracking Behavior

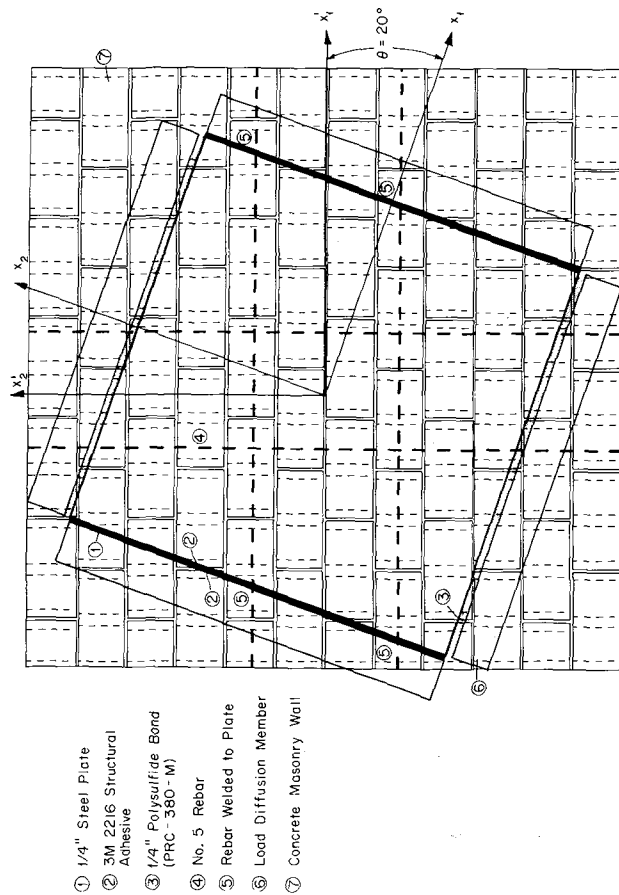
The influence of reinforcing steel on the extent of macrocracking, and on the nonlinear post-macrocracking response, is of major concern in our studies. Current reinforced specimens are fully grouted with two number five bars (grade 60) at approximately 32 inches on center—both vertically and horizontally. The steel area in each direction is 0.6 in^2 , whereas the net cross-sectional panel area is 487 in^2 ; this gives a steel/masonry area ratio of .00126 in each direction, which exceeds minimum UBC requirements.

Tests of reinforced specimens required a more complex fixture design than that associated with the unreinforced tests (see Fig. 3); a schematic for a typical 20 deg. layup is shown in Fig. 18. Note that the steel is welded to a steel plate on the "tensile" edge of the biaxial test; the plate is, in turn, hard bonded to the load distribution fixture; a soft bond is utilized on the "compression" edge. Specimen fixturing was designed to provide a uniform (tensile) strain field in both steel and masonry prior to macrocracking. Displacement (or strain) control was employed on the "tensile" edge via the use of LVDT's; loads on the "compressive" edge were adjusted for proportional loading by measurement of average tensile loads using load cells and appropriately modifying the signals to the compression actuators (servo valves).

Several important aspects of the reinforced tests are noted here. First, as was previously indicated, the initial macrocracking stress surface is not significantly influenced by steel/masonry area ratios of .00126 or less. Thus, failure envelopes, Fig. 10, as determined from unreinforced tests should predict the onset of major cracking. A typical comparison of reinforced and unreinforced results is given in Table 3.

Second, while the above steel/masonry area ratios do not influence the onset of cracking, they most certainly have a dramatic influence on crack distribution and on the individual crack size (opening). Whereas single cracks were observed in unreinforced specimens for $|\theta| > 15$ deg., multiple or distributed cracks were observed in all reinforced tests. Comparative examples of reinforced vs. unreinforced fracture modes may be found in Figs. 19-22. The domain of cracking was found to increase with an increase in the magnitude of the principal compressive stress, i. e., as $|\theta|$ decreased in the proportional loading tests.

Third, steel/masonry area ratios on the order of .00126 or less are not sufficient to prevent an unstable branch of the stress-strain curve associated with the principal stress direction perpendicular to the crack(s) plane(s). Typical such curves are shown for 0 deg. and 20 deg. specimens in Figs. 23 a, b and 24 a, b respectively, for both monotonically increasing and cyclic (tensile) strains. The associated macroelement tensile stress drop is observed to be dramatic for the uniaxial case (0 deg.) and the materials used; the magnitude of this drop, given the above steel area, will increase with an increase in grout tensile strength. The magnitude of the drop is less for specimens in the 15 to 20 deg. range since the compressive principal stress lowers the tensile principal stress at initial macrocracking (see Fig. 14). The strain interval over which the slope of the stress



- ① 1/4" Steel Plate
- ② 3M 2216 Structural Adhesive
- ③ 1/4" Polyulfide Bond (PRC-380-M)
- ④ No. 5 Rebar
- ⑤ Rebar Welded to Plate
- ⑥ Load Diffusion Member
- ⑦ Concrete Masonry Wall

Fig. 18. Fixture Details for Reinforced Specimens

Table 3. Panel Failure Stresses (psi) for $\sigma'_{11}=0$

θ	Unreinforced		Reinforced	
	σ'_{12}	σ'_{22}	σ'_{12}	σ'_{22}
0	0	77.5	0	88.3
	0	66.4	0	91.1
mean	0	72.0	0	89.7
20	130	-310	162	-382
	144	-343	175	-419
mean	137	-327	169	-401

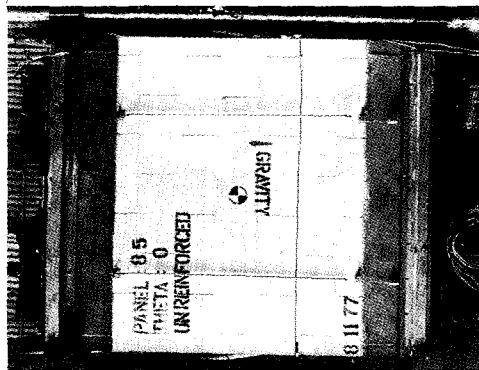


Fig. 19. 0° Unreinforced

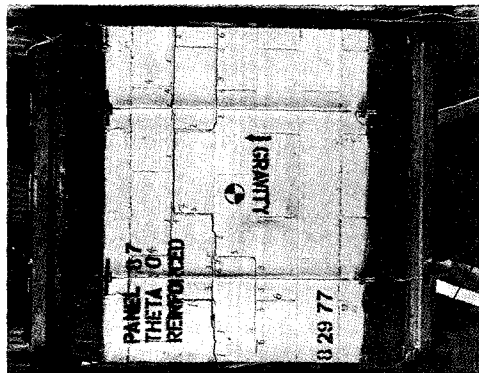


Fig. 20. 0° Reinforced



Fig. 21. 20° Unreinforced

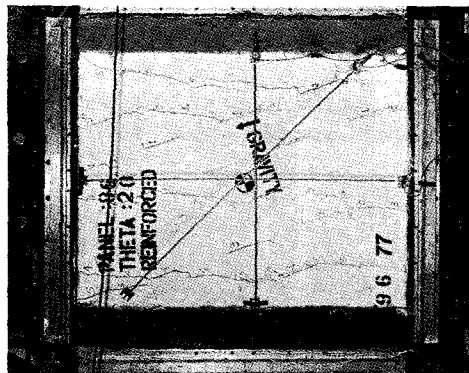


Fig. 22. 20° Reinforced

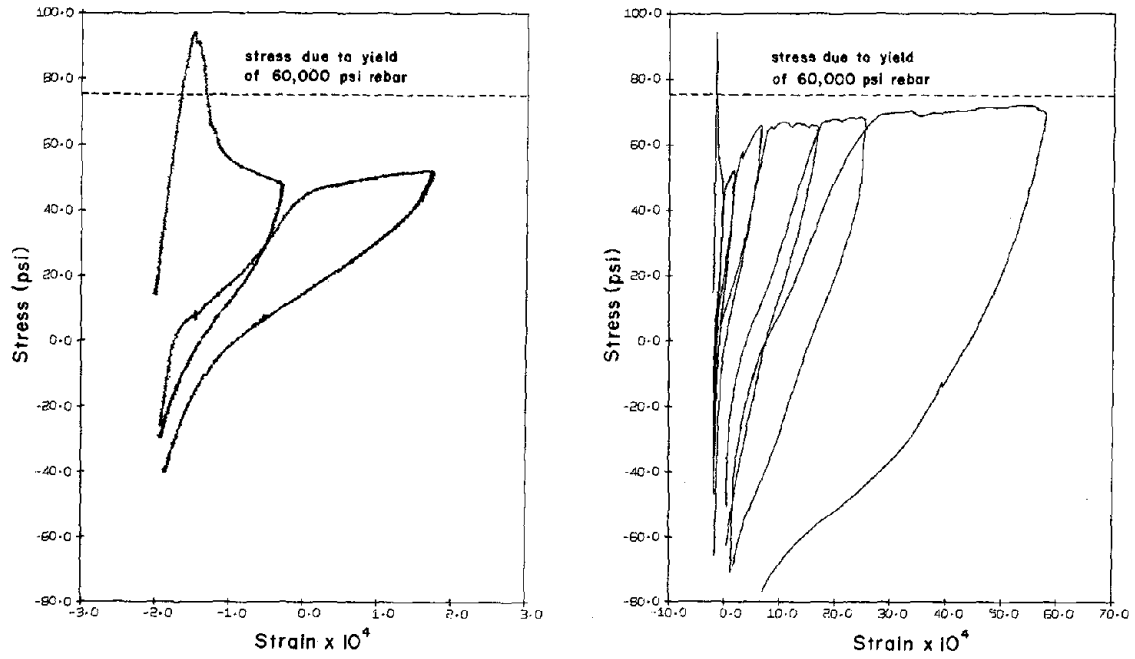


Fig. 23. 0° Reinforced Stress-Strain Curves

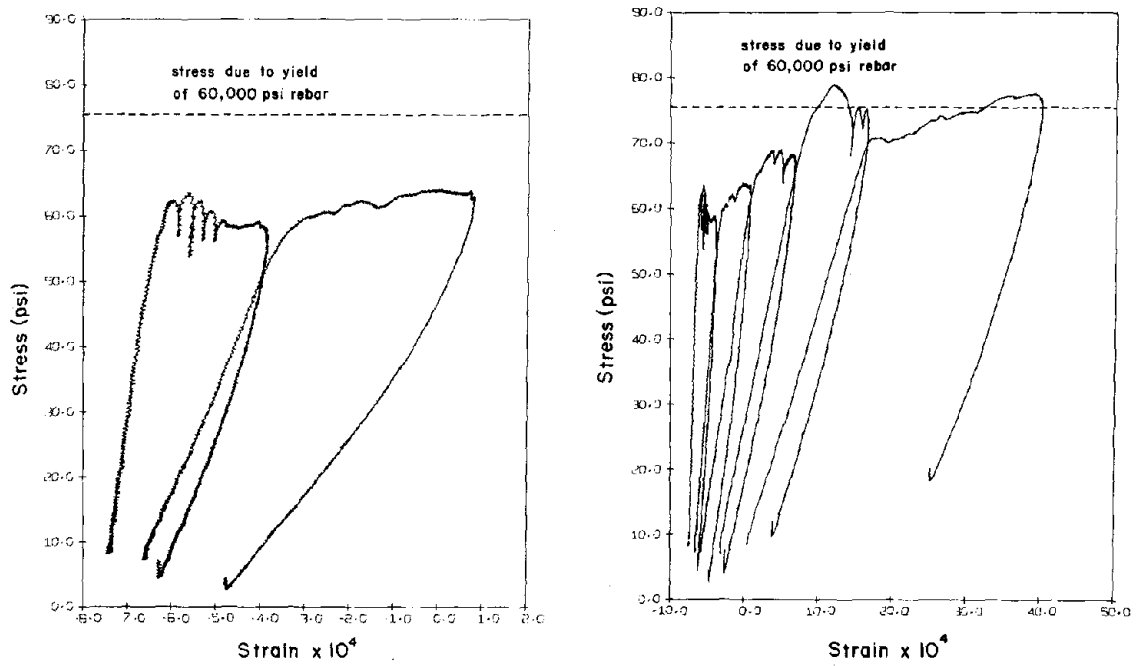


Fig. 24. 20° Reinforced Stress-Strain Curves

strain curve is negative (approximately .01 percent) represents a decrease in load carrying capability of the element. This reduction is attributed to 1) a load transfer from masonry to steel and 2) the fact that the steel area is not sufficient to maintain the original load without considerable extension.

Fourth, upon continued monotonic straining of the specimen, reloading is observed, the slope of which is less than that of the masonry but larger than that of the steel alone. This slope is monotonically decreasing. The stress level at initial macrofracture may or may not be reached again depending upon the steel area, the steel yield stress, and the biaxial stress-state at initial macrofracture.

Finally, upon cyclic straining from zero to a tensile strain, stiffness degradation can be observed, Figs. 23 a, b, 24 a, b. This degradation is accompanied by an increase in crack density and crack domain for each cycle.

Elastic Moduli and Anisotropy

Data on stiffness parameters is essential to both design and analysis of concrete masonry systems. Several important items in this area concern the elastic moduli at low stress levels, the degree of anisotropy of the above, and the ratio of Young's modulus to f'_m .

Typical variations of Young's modulus and Poisson's ratio with θ for the material discussed above are illustrated in Figs. 25, 26. This data was obtained by uniaxial compression tests in the range 0-300 psi. A linear regression analysis of the data reveals a trend in which both moduli decrease from $\theta = 0$ deg. (compression across bed joint planes) to $\theta = 90$ deg. (compression across head joint planes). Since most specimens provide two data points (by reversing the roles of the principal stresses), one may observe this trend in the absence of data scatter by following the same specimen number in Fig. 25. Compare, for example, $\theta = 15$ deg. with $\theta = 75$ deg. for specimens 19, 20, or 22 in Fig. 25, or compare $\theta = 30$ deg. with $\theta = 60$ deg. for specimen 32. Note that, while the data exhibits anisotropy, the materials under discussion may be approximated as isotropic within the data scatter observed.

Elastic Moduli and Compressive Strength

Typical data (means of multiple tests) concerning the ratio of Young's modulus to f'_m is shown in Table 4. The elastic modulus was computed from panel data in the 20 to 145 psi compressive stress range, and is in good agreement with data from five course prisms

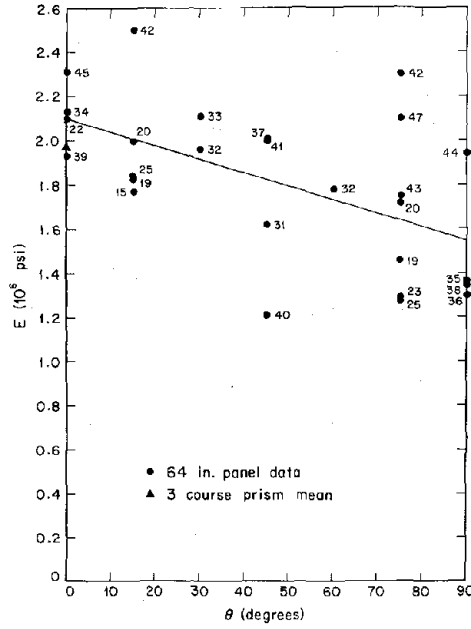


Fig. 25. Young's Modulus

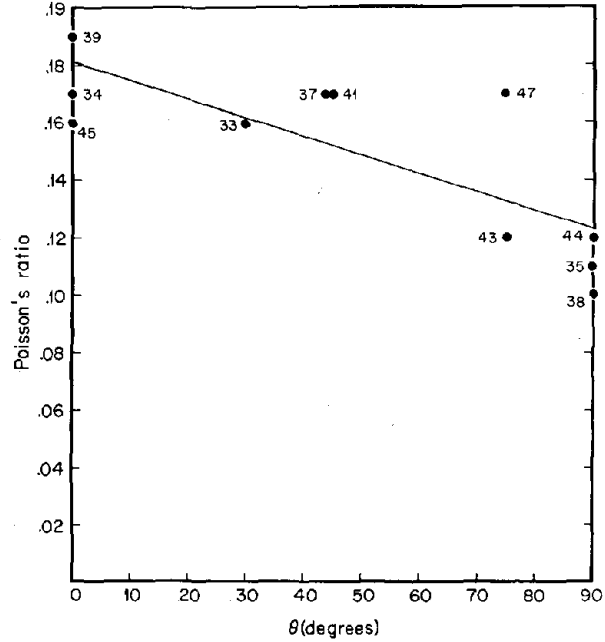


Fig. 26. Poisson's Ratio

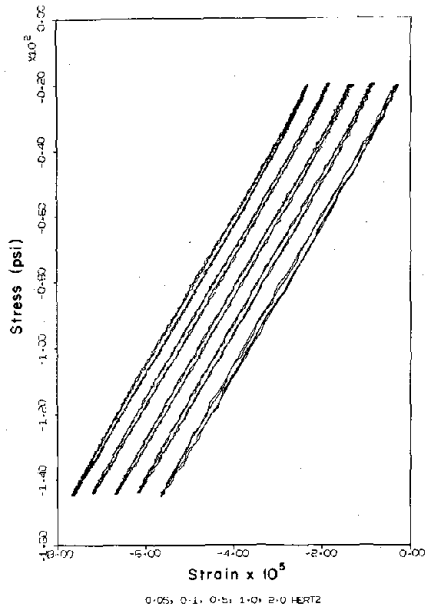


Fig. 27. Panel Compressive Cyclic Data

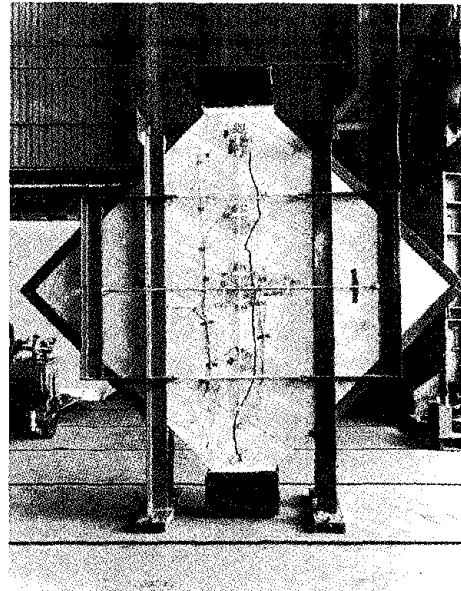


Fig. 28. Diagonal Compression Test Specimen

Table 4. Ratio of Young's Modulus to Strength

	STD	STD VIB	ADM	ADM VIB
Elastic Modulus	1129	1081	1192	1028
f'_m				
standard deviation	241	102	126	93

Table 5. Diagonal Compression Test Results

Predicted Values	105.9	78.2
Test Results	107.3	83.4
		89.7

in a similar stress regime. The values of f'_m employed were obtained from five course prisms laid in stack bond. The ratio of modulus to f'_m is in good agreement with the UBC (Table No. 24-H, 1967 version; inspection column) in which the number 1000 is assumed.

Damping and Strain-Rate Effects

Figure 27 shows typical compressive cyclic stress-strain data (same specimen) ranging from a slight prestress to approximately 250 psi for five strain rates from .05Hz to 2.0 Hz. Each figure depicts two cycles. Several extremely important observations regarding material behavior can be extracted from this data, which is typical.

First, the data clearly exhibits little or no strain-rate dependence over frequencies extending from essentially quasi-static to typical expected mode frequencies for full-scale structures. Both slopes and hysteresis loops remain invariant with frequency in the above range.

Second, the hysteresis loops provide a measure of energy absorption or damping in the "linear elastic" regime. The fact that the areas of these loops are not a function of frequency implies that material damping should not be modeled as viscous damping.

The implications of the above observations may be considerable. For example the current earthquake response spectrum approach (9) to the seismic design of buildings is based upon the premise that the damping involved is of the viscous type. If the damping associated with a complete structure is primarily the result of material behavior, then this premise is suspect in view of our findings. This potential problem is compounded by the fact that the response spectrum is highly sensitive to the damping assumed.

One may argue here that the first mode (or the first few modes) of a building performs as a narrow-band filter, and hence that one may approximate the structural damping mechanism as viscous wherein the damping factor is determined from data (logarithmic decrement) in the neighborhood of the modal frequency of interest. This approximation may suffice if conducted properly. Unfortunately, it does not appear that this has been the case in practice.

Consider, for example, the percent critical damping factors claimed in some masonry promotional literature(1). Values ranging from 8 to 10 percent have been proposed for some masonry materials. Such information has evolved from the measurement of the rate of decay (logarithmic decrement) of material response to a transient

blow from a hammer (in-plane), a steel-ball-pendulum impact (1) (out-of-plane), etc. Two things are wrong here. First, the response frequencies associated with such tests are too high - by several orders of magnitude in some cases; this results in artificially high damping coefficients (damping is certain to be frequency dependent for sufficiently large frequencies). Second, and more important, the concept of critical damping has been incorrectly used. The latter is based upon the response of a single degree of freedom oscillator; the percent critical damping calculation necessitates a knowledge of the mass and frequency of this oscillator. If the oscillator is to be associated, e. g., with the first mode of vibration of a building, then the effective mass and frequency must correspond to this mode. That is, the percent critical damping is a function of the assumed mass and the modal frequency.

It is of interest to estimate how far off the above mentioned 8 to 10 percent critical damping factors are, based upon the assumption that such numbers originate from the concrete masonry and not from connections or non-structural elements. Consider Fig. 27. If the damping is sufficiently small, the transient response to an initial value problem will be nearly harmonic. Suppose, as the data indicates, that material damping is independent of frequency. As in the case for viscous damping, the rate of decay curve is exponential and the decrement is a constant. The decrement for a macroelement can be calculated from Fig. 27 by measuring the areas representing hysteresis and strain energy, and by computing the loss of strain energy per cycle. If this quantity does not depend on stress amplitude, then the decrement for a macroelement is the same as the decrement for a full-scale structure composed of the same material, i. e., the energies of the subcomponents can be summed to yield the energy of the structure. Thus, one may now speak of a structural mode of vibration. The result? Critical damping factors of less than 2 percent are observed when the measured decrement is applied to an "equivalent" viscous model. Thus, if 8-10 percent critical damping factors are to be employed in practice for concrete masonry structures, such high values must be the result of connection behavior, or some other aspect of the structure.

The foregoing discussion concerned low stress amplitudes, e. g., material response in the essentially linearly elastic range. Energy absorption and strain-rate dependence in the high stress range is also under study, but will not be discussed herein.

SELECTED RESULTS PANELS UNDER NONHOMOGENEOUS STRESS STATES

Brief discussions of several salient results and important features of the nonhomogeneous stress-state test series are presented below. Primary emphasis is placed on the use of data from the homogeneous stress-state tests to predict 1) the failure load associated with the diagonal compression tests and 2) the nonlinear response of shear walls under both monotonic and cyclic loading.

Diagonal Compression

The diagonal compression test is conducted on square, 64x64 inch unreinforced but fully grouted masonry specimens, to which compressive loads are applied at two opposite corners (see Fig. 7, 8). The loads are applied through steel caps which extend along the panel edges approximately 10 inches from the corners. A layer of hydrocal is employed between the caps and the panel. The displacement of the cap is increased until fracture occurs. A typical failed specimen is shown in Fig. 28.

The diagonal compression test closely approximates a plane stress boundary value problem for which an analytical solution is available (2) (see Fig. 8) for the stress field. Here the loads are taken as point loads and the material is assumed to be homogeneous, isotropic, and linearly elastic; the resulting stress field is independent of the material elastic constants. Examination of this solution reveals that fracture will occur at the panel center. The analytically predicted principal stresses at this point are

$$\sigma_1 = 733.6 \bar{\tau} , \quad \sigma_2 = -2380 \bar{\tau} , \quad \bar{\tau} = 0.707 P_d / at \quad (5)$$

where a , t , P_d denote panel edge length, panel thickness and applied diagonal load, respectively. Corrections to this stress field for the actual test boundary conditions were determined via a finite element analysis; it was found that

$$\sigma_1 = 633 \bar{\tau} , \quad \sigma_2 = -2186 \bar{\tau} \quad (6)$$

at the panel center.

In order to predict, from homogeneous biaxial tests, the load P_d at which fracture occurs in the diagonal compression test, one needs the results of a test for which the principal stresses are in the same ratio as those of (6), namely -3.45. Since homogeneous data

was available for a ratio of -3.00 and a layup angle of 30 deg. relative to the principal stresses, a layup angle of 30 deg. was selected for the diagonal compression tests; the specimen(s) were of the same "batch" as the homogeneous tests. The load P_d was predicted by correcting the principal stress ratio by application of the model discussed previously, in which there is a linear decrease in tensile strength (σ_1) with an increase in compressive stress (σ_2) (see Fig. 13).

Three diagonal compression tests were conducted. The last two specimens were from a different batch than the first specimen, and for this batch strengths were generally lower, and some data scatter was observed. For each batch two homogeneous biaxial tests with a ratio of -3.00 were conducted. The predicted values and results of the tests are given in Table 5. The agreement is good, and it indicates that the biaxial data may be applicable even for cases in which the characteristic length associated with a nonhomogeneous stress field is of the same order as the block dimensions.

Simple Shear Deformation

The purpose of the experimental vs. theoretical comparisons presented below is twofold: 1) to illustrate the ability of our micro-modeling procedure to simulate the basic features of a highly complex process associated with shear wall deformations in the nonlinear regime of material response and 2) to ascertain the ability of an elementary macromodel to predict the initiation of macrocracking in shear walls. The former will be discussed in a companion paper; the latter is noted below.

Data for the experimental portion of the comparisons was obtained from the U. C. Berkeley shear wall/pier test program. The specimens selected for study were 48 inches wide and 56 inches high, with top and bottom bond beams (64 inches high including bond beams). A schematic of the test setup is given in Fig. 9. Initial vertical pre-load is applied to the specimen by springs; horizontal loads or displacements are applied by dual actuators which, in turn, are part of a MTS closed loop hydraulic servo system. The top and bottom surfaces of the bond beams are "rigidly" attached to steel beams by means of connectors embedded in the bond beams. The (passive) vertical columns serve to prevent relative rotation of the top surface with respect to the floor-plane.

Three test-types were selected for discussion. They include: 1) monotonic loading of an unreinforced specimen; 2) monotonic loading of a reinforced specimen; and 3) cyclic loading of a reinforced specimen. The reinforced shear wall had two No. 5 bars (grade 60) placed vertically in the end grout cores. Both unreinforced and reinforced

specimens were fully grouted; mortar bedding was face shell only.

Based upon 1) a linear finite element analysis, 2) the initial macrocracking envelope (obtained from homogeneous tests or component properties) and 3) the premise that macrocracking initiates in the central element, one can predict the ultimate load of a given shear wall within ten to fifteen percent accuracy. Such a simple approach does not, of course, reveal damage accumulation, the resulting stiffness degradation, and the proper hysteretic behavior. A macromodel capable of reflecting these items is under development.

SUMMARY

Data from biaxial tests show that the tensile strength of concrete masonry decreases with compressive stress, and that a linear relation between these two variables predicts accurately the initial macrocracking stresses for an arbitrary combination of bed joint normal and shear stresses. Results from uniaxial tests are used to modify slightly the macrocracking law to account for anisotropy. It is found that masonry tensile strength can be predicted from component strengths if the grout flaw distribution is known. Reinforcing steel in normal amounts has little effect on the initial macrocracking stresses, and allows reloading after a drop in stresses due to initial cracking. Some anisotropy in elastic moduli is observed, and damping is seen to be independent of strain rate. Finally, the results from homogeneous macroelement tests are used to predict with good accuracy the failure loads for two tests with complex nonhomogeneous stress states.

APPENDIX I.—REFERENCES

1. Dickey, W. L., and R. W. Harrington, "The Shear Truth about Brick Walls," Report for Western Clay Products Assoc., Inc., San Francisco, California, 1970.
2. Hegemier, G. A., "Mechanics of Reinforced Concrete Masonry: A Literature Survey," Report No. AMES-NSF TR-75-5-S, University of California, San Diego, 1975.
3. Hegemier, G. A., G. Krishnamoorthy, and R. O. Nunn, "An Experimental Study of Concrete Masonry Under Seismic-Type Loading," Proceedings of Workshop on Earthquake Resistant Masonry Construction, National Bureau of Standards, September 13-17, 1976.
4. Hegemier, G. A., M. E. Miller, and R. O. Nunn, "On the Influence of Flaws, Vibration Compaction, and Admixtures on the Strength and Elastic Moduli of Concrete Masonry," Report No. AMES-NSF TR-77-4, University of California, San Diego, 1977.

5. Hegemier, G. A., et al., "On the Behavior of Concrete Masonry Under Static and Dynamic Biaxial Stress-States," Report No. AMES-NSF TR-77-3, University of California, San Diego, 1977.
6. Hegemier, G. A., et al., "A Major Study of Concrete Masonry Under Seismic-Type Loading," Report No. UCSD/AMES/TR-77/002, University of California, San Diego, 1978.
7. Isenberg, J., G. A. Hegemier, and A. Anvar, "An Experimental Study of Connections in Reinforced Concrete Masonry Structures Under Seismic Loading," Proceedings of Workshop on Earthquake Resistant Masonry Construction, National Bureau of Standards, September 13-17, 1976.
8. Mayes, R. L., and R. W. Clough, "A Literature Survey-Compressive, Tensile, Bond and Shear Strength of Masonry," Report No. EERC 75-15, University of California, Berkeley, 1975.
9. An Evaluation of Response Spectrum Approach to Seismic Design of Buildings, A Study Report for Building Technology, Institute of Applied Technology, National Bureau of Standards, Washington, D. C. 20234, by Applied Technology Council (ATC-2), San Francisco, California, September 1974.

APPENDIX II.—NOTATION

The following symbols are used in this paper:

- a = length of edge of diagonal compression panel
- f'_c = masonry unit compressive strength
- f'_m = masonry compressive strength
- N_{11}, N_{22} = principal stress resultants
- $N'_{11}, N'_{22}, N'_{12}$ = stress resultants for layup coordinates
- P_d = failure load for diagonal compression test
- t = masonry wall thickness, 7.63 in.
- x_1, x_2 = coordinates in principal stress directions
- x'_1, x'_2 = coordinates in layup directions
- θ = layup angle
- σ_1, σ_2 = principal stresses at center of diagonal compression panel
- $\bar{\tau} = 0.707 P_d/at$

THE DEVELOPMENT OF A TECHNIQUE FOR INVESTIGATING THE DURABILITY OF
REINFORCING STEEL IN REINFORCED CONCRETE BLOCKWORK

By Roberts, J.J., Cement and Concrete Association

ABSTRACT: As part of a programme of research into the behaviour of reinforced concrete blockwork retaining walls it was considered necessary to investigate the durability of the reinforcing steel.

An electrical resistance technique has been used to determine the amount of corrosion that might take place on the steel contained in reinforced masonry. This test procedure can be applied to the practical conditions of site exposure and finished structures, is fairly simple, but is, nevertheless, suitable for laboratory use for accelerated tests.

This paper summarizes the work that has been carried out over the last four years and presents preliminary results from some of the exposure sites, which indicate conditions under which the steel might corrode.

THE DEVELOPMENT OF A TECHNIQUE FOR INVESTIGATING
THE DURABILITY OF REINFORCING STEEL IN
REINFORCED CONCRETE BLOCKWORK

By John J. Roberts,¹ BSc(Eng) PhD CEng MICE

INTRODUCTION

Reinforced concrete blockwork has not been widely used in the United Kingdom because there has been a lack of design information on this topic in the Code of Practice. Furthermore, seismic problems are not encountered as they are in North America, and, traditionally, little serious attempt was made to tie the components of a building together. Six years ago, it was decided to investigate the behaviour of reinforced blockwork walls subjected to flexural loading only, because it was felt that more use could be made of reinforced masonry retaining walls if realistic design information was made available. Subsequently, increased emphasis on lateral wind loadings, changes in stability requirements, and more fundamental construction changes resulting from the necessity to produce walls with better thermal performance will probably result in the increased use of reinforced masonry.

An important part of the Cement and Concrete Association's research programme on this topic is the investigation of the durability of the reinforcing steel embedded in the blockwork. An electrical resistance technique has been used to determine the extent to which the steel might corrode. This test procedure can be applied to the practical conditions of site exposure and finished structures, is fairly simple, but is, nevertheless, suitable for laboratory use for accelerated tests.

This paper summarizes the work that has been carried out over the last four years and presents preliminary results from some of the exposure sites which indicate conditions under which the steel might corrode.

¹ Section Head, Construction Research Department, Cement and Concrete Association, Wexham Springs, Slough, Berks, England.

SELECTION OF A SUITABLE TEST METHOD

Although a considerable amount of work has been carried out over many years into various aspects of the corrosion of reinforcing steel in concrete, little research has been carried out into the durability of the steel in reinforced blockwork or brickwork. A literature study was carried out to establish the extent of current knowledge and this has been published elsewhere (1). The review of the literature included many papers dealing with reinforced concrete which contained information on testing techniques which could be applied to reinforced masonry. The recommendations of various authorities on the minimum cover to the steel were also reviewed.

In considering a test to assess the durability of reinforcement in concrete blockwork the following requirements were considered desirable:

1. The test should be capable of application in the practical conditions of site exposure and to finished structures.
2. The equipment and test procedure should be simple to facilitate its use on site.
3. The test method should be suitable for laboratory use for accelerated tests.

It was thought worthwhile to employ a test that may be used under realistic service conditions because the results of site tests would be readily acceptable to engineers and others involved in the specification of blockwork. The disadvantage of site testing for corrosion is that, because of the nature of the process, a considerable time period is usually involved in the assessment of the performance of the structure.

Seven techniques were considered:

1. Visual inspection of the degree of corrosion.
2. Destructive testing to establish loss of strength of reinforcing steel.
3. Electrode potential.
4. Galvanokinetic polarization.
5. Constant anodic current polarization.
6. Polarization resistance.
7. Electrical resistance technique.

After careful consideration of the advantages and disadvantages of each method, it was decided to use an electrical resistance technique. This method of test has several advantages for blockwork:

1. It is essentially simple.
2. Examination of the corrosion gauge may enable the position of the corroded area to be determined, e.g. near a mortar joint.
3. The rate of corrosion may be monitored.
4. It is equally applicable to site and laboratory investigations.
5. Readings may be taken remote from the gauge.

The major disadvantage is the information is only obtained about locations at which gauges have been placed.

THE ELECTRICAL RESISTANCE TECHNIQUE

The basic concept of the test is that a thin section of steel, when corroded, will undergo a large change in electrical resistance because the corrosion products do not conduct electricity. The electrical resistance corrosion gauges were made from proprietary mild steel shim and the ultimate tensile stress for the gauges was $640-800 \text{ N/mm}^2$, increasing with decreasing thicknesses of the shim. Three thicknesses of gauge were employed, 0.05, 0.10 and 0.15 mm, the width of each gauge being 6 mm. The length of the gauges varied according to the type of installation required, from 100 mm up to about 1 m in length. Lengths beyond 1 m would be very difficult to handle and install in wall elements.

The resistance of the gauges was measured by a Kelvin double bridge, which is designed for the accurate measurement of low resistances. By using a four lead arrangement, the effect of lead resistance was minimized. Power for the bridge was provided by a stabilized power supply of variable output. A solid-state null detector was employed which, although similar to a mirror galvanometer in its accuracy and sensitivity, was sufficiently robust for site use. In the laboratory readings could generally be repeated to within $0.2 \text{ m}\Omega$.

The effect of temperature on gauge resistance was determined over the range -5°C to 40°C for each thickness of gauge (0.05, 0.10 and 0.15 mm) by tests carried out in a temperature-controlled cabinet. The results, corrected for the effect of lead resistance, are expressed in terms of $\frac{\Delta R}{R_0}$ * against temperature (related to a datum temperature of

* where ΔR is the change in resistance from time of commencement of test until time T, i.e. $\Delta R = R - R_0$.

0°C for R_0). All readings taken on the site or in the laboratory are corrected for temperature.

The effect of the moisture content of the masonry on gauge resistance was also investigated in the laboratory but the largest differences in moisture content gave only a 1% difference in the indicated resistance and it was therefore considered unnecessary to make a correction for this effect.

The composition of the steel used to fabricate the corrosion gauges was, because of the method of manufacture, different from that of the reinforcing steel. Tests were therefore carried out in order to be able to correlate the results of tests using the corrosion gauges with the behaviour of steel reinforcement. Tensile strength tests were also carried out on the gauges to establish the way in which corrosion affects them. The programme involved maintaining gauges and steel under known aggressive conditions, weight loss and tensile strength being recorded at set intervals.

It is important to note that these tests are being continued over a period of years and that interim results only are presented in this paper. The specimens were maintained in concentrated salt solution to produce severe corrosion. Preliminary results of $\log \frac{R}{R_0}$ against time are presented as Figure 1 for three gauge thicknesses. All results apply to gauge resistance only, lead resistances have been eliminated and all the results have been corrected for temperature.

The relationship between $\frac{R}{R_0}$ and $\frac{\sigma}{\sigma_0}$ (failure stress at time T over original failure stress) for the specimens are presented in Figure 2. Also plotted is the hyperbola which, if corrosion occurred completely uniformly over the surface of the specimen at a constant rate, would be the curve of $\frac{R}{R_0}$ against $\frac{\sigma}{\sigma_0}$. It is apparent that corrosion occurs in a more localized form such that the resistance changes more rapidly than the indicated tensile strength. The shape of the measured and theoretical curves are similar with the thinnest gauge giving the best correlation. This may possibly be explained by the fact that the difference in effect between pitting and general corrosion is less significant in a very thin section because the steel is quickly corroded through.

The measurements of weight loss were used to evaluate the proportion of reinforcement remaining in the dimensionless form $\frac{W}{W_0}$. This parameter was thought to be of more use in making an assessment of the effect of corrosion on the structural performance of the masonry than the loss of weight because the engineer is able to make directly a notional calculation for the effect of the reduction in the area of reinforcing steel. The relationship between $\frac{W}{W_0}$ for the 6 mm diameter mild steel bars is related to $\log \frac{R}{R_0}$ for the three thicknesses of corrosion gauge in Figure 3.

There was a wide scatter in the results, as might be expected in conjunction with the weight loss method, and the best fit curves are shown in the Figure. These interim results are sufficiently accurate to indicate the relationship between the electrical resistance gauge readings and the weight loss for a mild steel bar. The weight loss results for other diameters of reinforcement were not as consistent as those for the 6 mm diameter reinforcement. Some preliminary results for various specimen sizes are provided in Table 1, although more extensive longer term results will be available in due course. The more variable results from 10 mm and 16 mm bars are related to the more consistent 6 mm results by expressing the weight loss as a proportion of the perimeter and, hence, of the diameter of the reinforcement. This is verified very well for the 10 mm diameter mild steel bar and quite well for the 16 mm mild steel bar. Inevitably, there will be considerable variation in any experiment of this kind. The weight loss for the high-yield steel is markedly less than for the corresponding mild steel.

By considering the weight loss in terms of volume of the steel and, hence, determining the change in area (assuming completely uniform corrosion) the reduction in indicated strength, expressed as a function of the original strength for the 6 mm diameter reinforcement, is 0.007; the measured value from the tensile strength tests was 0.011. For the 16 mm diameter mild steel reinforcement, the measured value of tensile strength after the 28-week period, expressed in terms of the original strength, was 0.992.

SITE TRIALS

A number of trial sections of walling or, alternatively, small wall panels have been constructed containing electrical resistance corrosion gauges. The oldest walls are now some four years old.

Details of each installation vary from site to site, some factors being changed to provide additional variables. Typically, 390 x 190 x 190 mm dense-aggregate hollow concrete blocks were employed, each containing two vertical cores. A 1:¹/₄:3 by volume cement:lime:sand mortar was usually used to lay the blocks. Usually, the cores were filled with a 1:3:2 by weight mix of cement:sand:10 mm maximum size aggregate.

For convenience, the ends of the corrosion gauges were cast in small cylinders of concrete. This concrete not only protected the potting compound covering the electrical connections but also made the positioning of the gauges in vertical cores easier. Using this technique, gauges up to 1 m long have been positioned, although some care is required to retain them in position whilst the cores are filled. Gauges for positioning in horizontal joints to simulate bed joint reinforcement needed to be positioned as construction proceeded.

A summary of the exposure sites currently in operation is provided in Table 2.

Half-block specimens containing corrosion gauges were usually filled on site using the same materials as were used in the main wall. These control specimens were returned to the protected environment of the laboratory and the resistances were monitored periodically.

RESULT OF EXPOSURE TRIALS

The idealized behaviour of reinforced blockwork walls in practice is shown in Figure 4. There is an initial period of time, t_0 , during which no corrosion occurs because of the protection and passivity offered by the concrete and masonry to the steel. Due to the effects of carbonation, the ingress of chloride ions etc., this passivity is reduced until suitable conditions are brought about for the onset of corrosion. The period t_1 then represents the time until the corrosion reaches an unacceptable level with respect to loss of structural performance and disruption of the masonry. Clearly the period $t_0 + t_1$ represents the limit state of corrosion in terms of design life.

In the case of the laboratory trials using solutions containing chloride ions, t_0 is extremely small compared to t_1 and in the case of some of the exposure specimens deliberately given inadequate cover corrosion clearly started shortly after construction of the walling was completed.

The oldest exposure walls were those constructed at Lowestoft, as described in Table 1. One of the two exposure panels at this site is shown as Figure 5. The results from these walls are presented as graphs of $\log \frac{R}{R_0}$. The results for the gauges in the inner harbour wall, wall 1, are steady over the 700-day period after indicating a small change in gauge resistance over the first 300 days. The gauge with the least cover indicates a slightly higher resistance than the gauge located in the centre of the core.

For the very exposed sea wall, wall 2, both gauges corroded completely. In the case of the gauge with the least cover the corrosion occurred at a faster rate and the curve crosses the line $\log \frac{R}{R_0} = 2$ at 200 days. The curve for the gauge at the centre of the core crosses the line $\log \frac{R}{R_0} = 2$ at 500 days.

Both walls were broken open after 700 days and the shims and reinforcing steel examined. The reinforcement in both walls had a cover of infill concrete which varied from about 6 mm to around 20 mm depending upon the taper of the blocks. At the points where the infill concrete cover was at a minimum the concrete block cover was, of course, at a maximum.

The three reinforcing bars taken from wall 1 did not exhibit more than the superficial corrosion present on the reinforcing steel when the walls were built, although some discoloration was noted at the mortar joints.

For wall 2, in which the gauges indicated appreciable corrosion, the three specimens of reinforcing steel were examined and in places the bars were quite deeply pitted. It was apparent that more corrosion had taken place towards the bottom of the wall and at points which corresponded with the mortar joints in the wall.

To examine the infill concrete, some sections of the reinforcement were removed complete with core concrete. The compaction of this concrete was not quite as good as was achieved in the laboratory with wall specimens used for structural tests and was probably attributable to the use of a lower water content than for the laboratory wall sections.

Care was taken when removing the corrosion gauges. However, because the gauges were only 0.05 mm thick, it was impossible to examine in detail the gauges to determine where corrosion was occurring. It was found, however, that for the gauge in wall 2 with the least cover that corrosion appeared to have occurred at the mortar joint in at least one place.

The half-block specimens made at Lowestoft at the same time as the walls and stored in the laboratory did not exhibit any change in resistance of the embedded corrosion gauges. This result was anticipated because of the very sheltered laboratory environment, but does help to confirm the validity of the test procedure.

The results for the section of walling instrumented at Nant-y-Geifr are presented in Figure 7. Gauge 1 indicates that severe corrosion was taking place and the curve crosses the line $\log \frac{R}{R_0} = 2$ at 120 days. This gauge was situated against the face of the block with little or no concrete cover. However, the other gauges located at the same position, and the two gauges embedded in the cores of blocks, do not indicate that serious corrosion was taking place after a period of four years. This anomaly is possibly explained by the degree of compaction of the infill concrete. The mix for filling the core around gauge 1 was too stiff to be efficiently compacted with a tamping rod. More water was, therefore, added to the mix and this modified mix was used to fill the cores surrounding gauges 2, 3 and 4. Although by increasing the water/cement ratio of the mix the porosity of the hardened concrete would tend to be increased, it is apparent that it is more important to be able to compact the concrete well to provide the appropriate cover to the reinforcement. Although gauge 3 did not superficially have any cover from the infill concrete, the tamping of the flowing infill mix probably gave the gauge a coating of cement grout which provided some cover in addition to the concrete block. It was not possible to examine the condition of the gauges visually because they were contained in a retaining wall rather than a trial wall.

For the two pairs of walls at Wexham Springs, no significant change has been noted in gauge resistance over a period of three years. Small differences in readings from week to week are accounted for by small errors in the temperature correction applied. Air temperatures were used to obtain the correction factor whereas the temperature within the

blockwork, depending upon depth from the outer face, could be significantly higher or lower because the wall has a high thermal capacity. Thermo-couples have been located in the more recent silage retaining walls constructed at Hurley along with the electrical resistance corrosion gauges. This enables a more accurate correction to be made.

For the Allington exposure walls, no significant change in resistance has yet occurred after periods of exposure of two years.

SUMMARY

The electrical resistance corrosion gauges may be employed to indicate whether corrosion would take place on reinforcing steel exposed to the same conditions. It is possible to quantify the rate and amount of corrosion taking place under practical conditions by first calibrating similar gauges with the behaviour of reinforcing steel under laboratory conditions.

In three cases, the corrosion gauges indicated that severe corrosion would take place on reinforcing steel exposed to the same conditions at the exposure sites. Two of these gauges were located in a wall in a position of severe exposure to the sea in an area where a very high quality concrete was required for adequate performance in sea defence structures. It was, therefore, anticipated that the gauge with no infill concrete cover would corrode. The gauge, located in the centre of the core, had a total cover of 95 mm and a minimum cover of infill concrete of about 50 mm. It is apparent that, for this severe exposure condition, the protection was inadequate. Although the compaction of the concrete was not as good as could be achieved, it is probably representative of that which might occur in practice. It is, therefore, essential to achieve better workmanship in areas of severe exposure. This might be achieved by the use of a superplasticizer.

The corrosion of the gauge in the Nant-y-Geifr water-course seems to have been directly attributable to a poorly compacted infill concrete.

In all other cases, the durability of the reinforcement seems to be assured to date under the conditions of exposure to which they have been subjected. This tends to suggest that the protection afforded to the reinforcing steel by the blockwork can partially contribute to the overall cover to the reinforcement, although it is suggested that, even in fairly well protected locations, the reinforcing steel should have a cover of infill concrete of at least 6 mm, as indicated by American and Canadian Codes (2, 3). It is not possible to attach too much significance to the few results obtained to date; now that it has been established that the test procedure is effective, the results of the other more recently instrumented exposure sites should be of considerable value in due course. Inevitably, this type of information takes a considerable period of time to collect.

It is not possible to quantitatively relate the gauge change in resistance to the corrosion of the reinforcement but significant corrosion and pitting were present on the three bars removed from wall 2 at 700 days which confirmed the corrosion predicted by the corrosion gauges.

APPENDIX I - REFERENCES

1. Roberts, J.J. Aspects of the Strength and Durability of Reinforced Concrete Blockwork. Thesis submitted to the University of London for the degree of Doctor of Philosophy, December 1975.
2. ACI Committee 531. Concrete Masonry Structures - design and construction. Proceedings of the American Concrete Institute. Vol.67, No.5. May 1970. pp.380-430.
3. National Building Code of Canada. Section 4.4. Plain, Reinforced and Grouted Masonry. Ottawa, National Research Council. pp.29.

APPENDIX II - NOTATION

The following symbols are used in this paper:

- R_o = resistance of corrosion gauge at commencement of test
- R = resistance of corrosion gauge after a given time
- t_o = time to onset of corrosion
- t_1 = time from onset of corrosion until limit of acceptable corrosion
- W_o = original weight of reinforcing steel
- W = weight of reinforcing steel after a given time period
- T = time from the commencement of the test
- σ_o = original failure stress of specimen
- σ = failure stress after a given time period
- $\Delta R = R - R_o$

TABLE 1. - Total Weight Loss over 28-Week Period for Various Specimens of Reinforcing Steel

(1) Diameter of reinforcement (mm)	(2) Weight loss over 28 weeks (g)	(3) Ratio $\frac{(2)}{(1)}$ (g/mm)
6 M.S. ^a	0.27	0.045
10 M.S.	0.45	0.045
16 M.S.	0.67	0.042
16 H.Y. ^b	0.54	-

^a M.S. = Mild steel

^b H.Y. = High yield steel

TABLE 2. - Summary of Parameters under Investigation at the Exposure Sites

Site		Description of location	Variables
Lowestoft	Wall 1	Tide level of inner harbour	Depths of cover gauges at centre of core as against exposed face of blocks.
	Wall 2	On sea wall	
Nant-y-Geifr		Part of watercourse retaining wall	Depths of cover - gauges at centre of core or against exposed face of blocks.
Wexham Springs	Wall 1	Test panels in protected environment	Depths of cover 95, 85, 75, 65 and 55 mm to gauges.
	Wall 2		Gauges at centre or side of blocks. Three designs of infill mix.
	Wall 3		As wall 1 but soaked twice weekly with salt solution.
	Wall 4		As wall 2 but soaked twice weekly with salt solution.
Hurley		Part of silage retaining wall	Gauges at sides or centre of vertical cores. Horizontal gauges in bed joints. Thermo-couples used to monitor temperatures.
Allington	Wall 1	Near sluice in River Medway	Depths of cover 50, 55, 60, 65, 70, 80, 95. Type and size of block. 1: $\frac{1}{4}$:3 and 1:1:6 mortar. 0.05 and 0.15 mm thick gauges. Specimens of reinforcing steel with same range of covers as gauges.
	Wall 2		
	Wall 3		
	Wall 4		

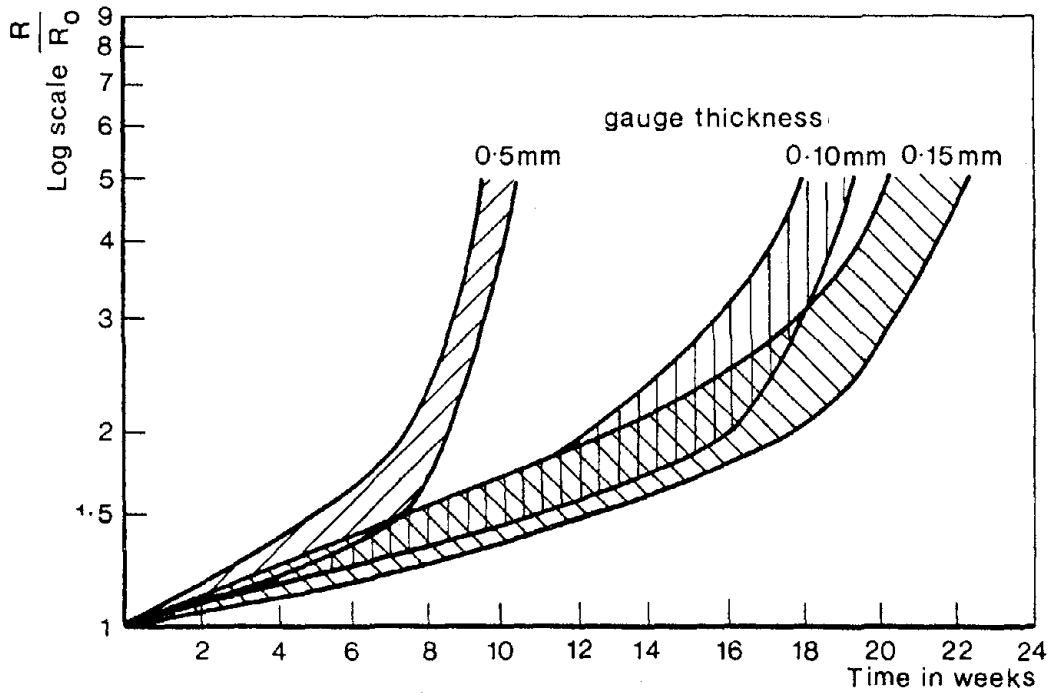


FIGURE 1: GRAPHS OF $\log \frac{R}{R_0}$ AGAINST TIME FOR GAUGES SUBJECTED TO CONCENTRATED SALT SOLUTION

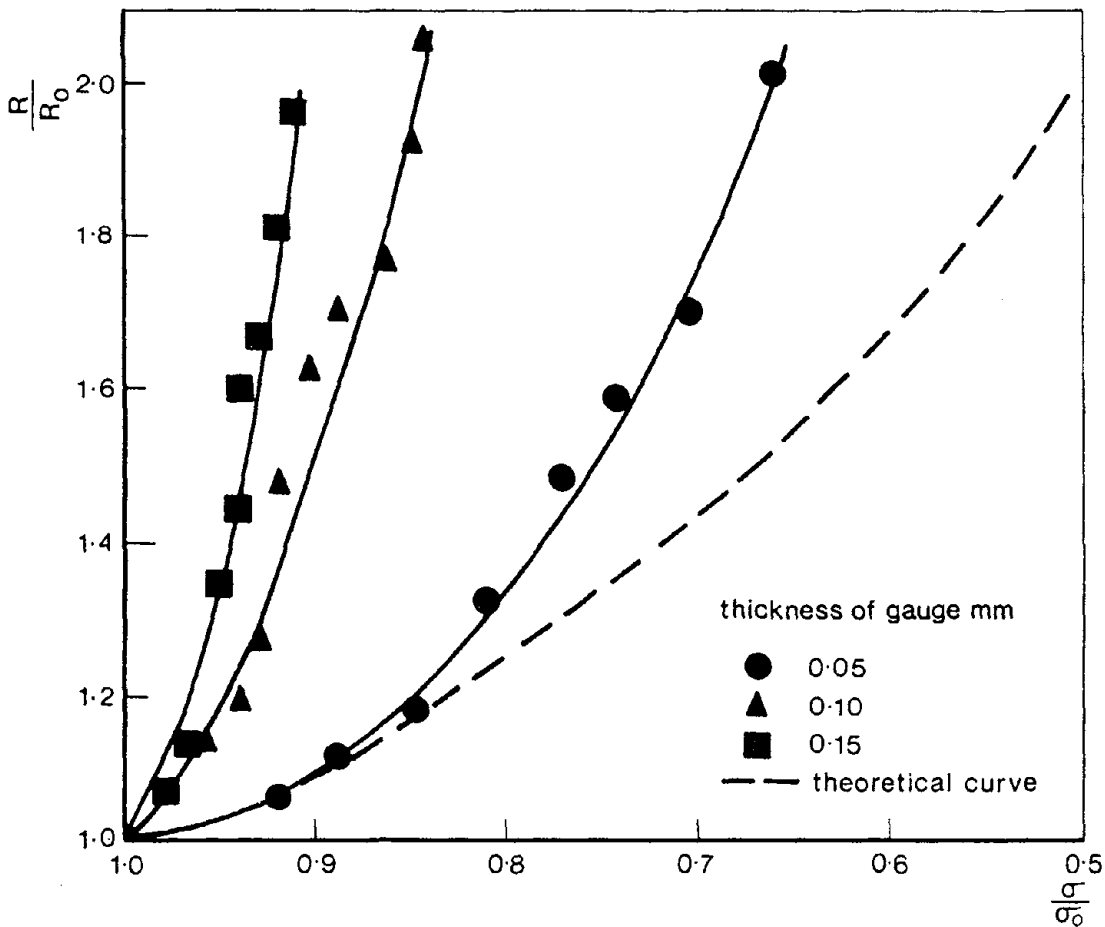


FIGURE 2: CHANGE IN ELECTRICAL RESISTANCE AGAINST GAUGE FAILURE STRESS

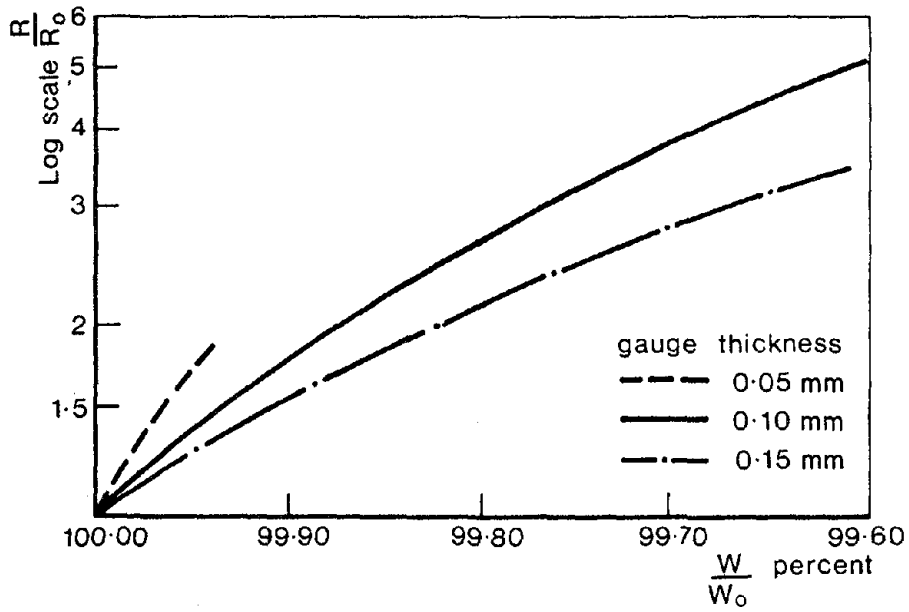


FIGURE 3: LOG $\frac{R}{R_0}$ AGAINST $\frac{W}{W_0}$ FOR 6mm BARS

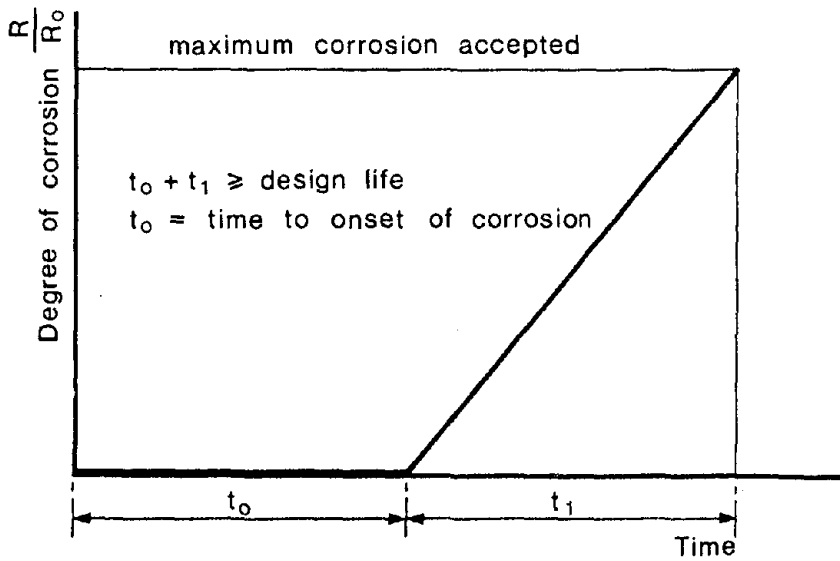


FIGURE 4: IDEALIZED BEHAVIOUR OF REINFORCED BLOCKWORK WALLS IN PRACTICE

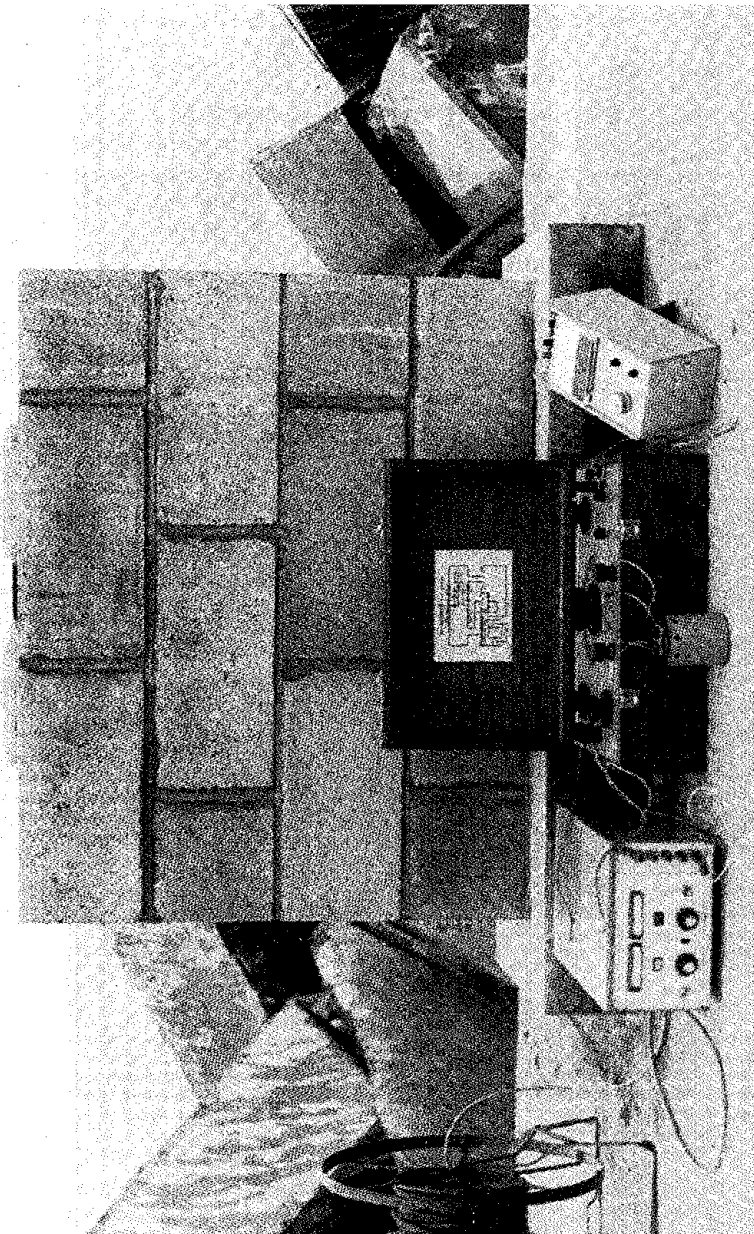


Figure 5 : Seaward facing wall 2 at Lowestoft

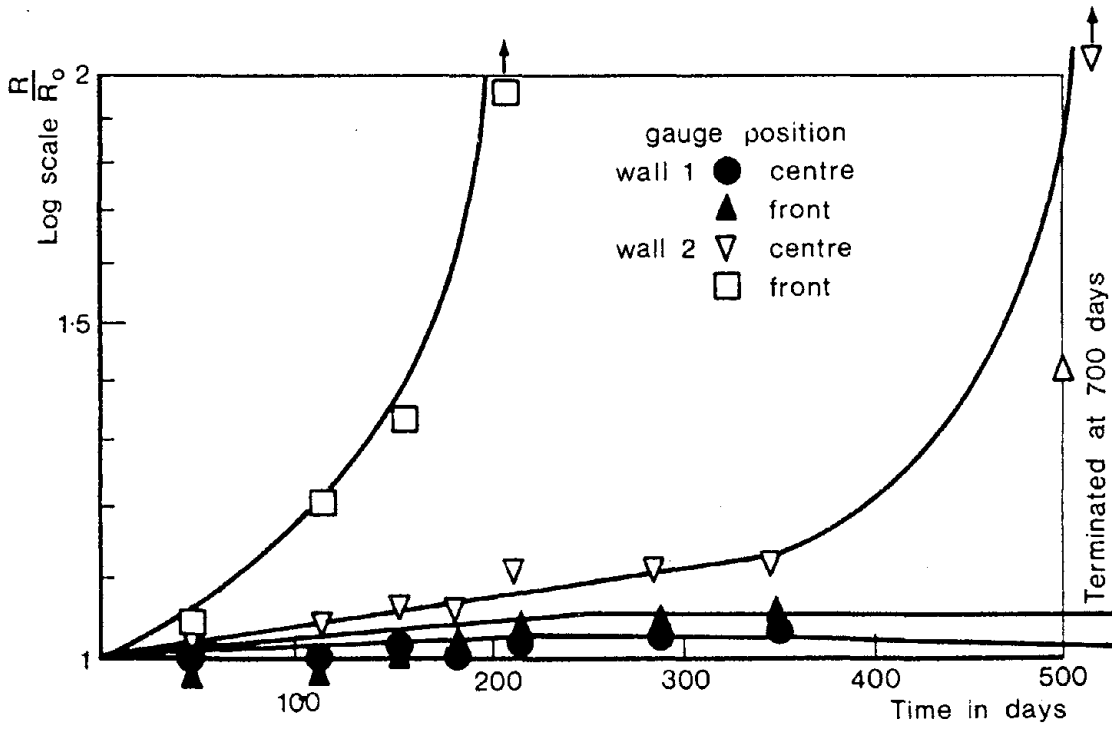


FIGURE 6: RESULTS FROM LOWESTOFT WALLS

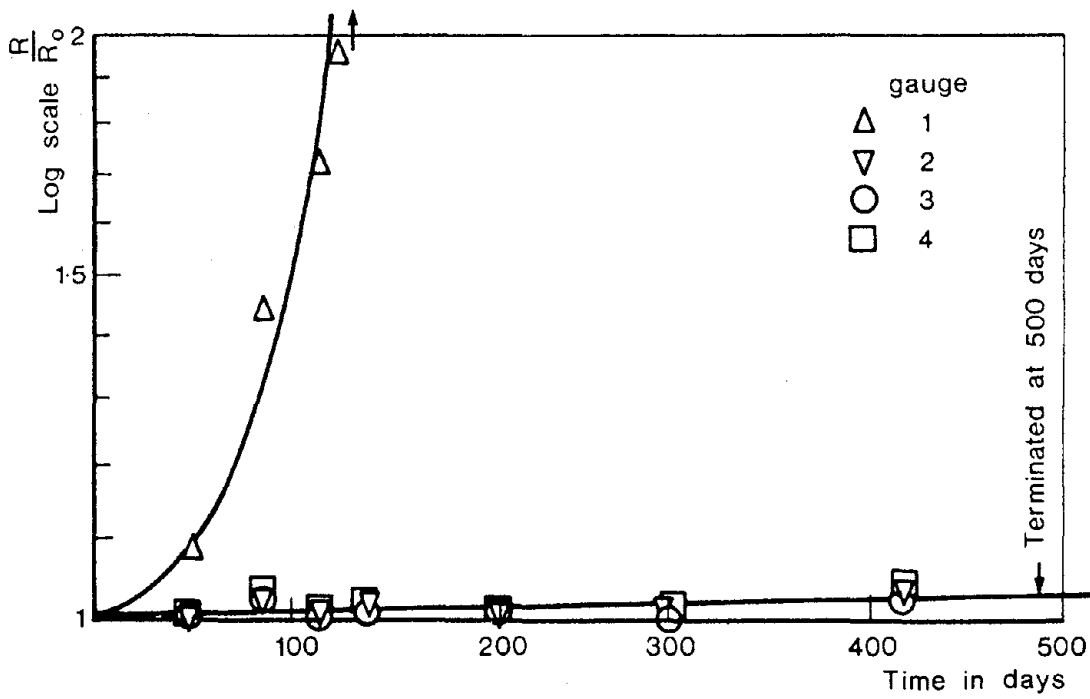


FIGURE 7: RESULTS FROM NANT - Y - GEIFR WALL

GROUT-BLOCK BOND STRENGTH IN CONCRETE MASONRY¹

by

R. O. Nunn², M. E. Miller³, G. A. Hegemier⁴

ABSTRACT

Results of a series of shear tests on cores taken from masonry walls are presented. The influences of wall height, grout admixture, and vibration compaction are discussed. It is found that standard puddled grout produces a large proportion of zero strength bonds, and that this problem is nearly eliminated through the use of admixture and vibration. Photographs illustrating grout-block separation and face shell spallation are included.

¹Research was sponsored by the National Science Foundation under Grant NSF ENV 74-14818.

²Graduate Student, Dept. Appl. Mech. & Engr. Sci., Univ. of Calif., San Diego, La Jolla, Calif., 92093.

³Associate Development Engineer, Dept. Appl. Mech. & Engr. Sci. Univ. of Calif., San Diego, La Jolla, Calif., 92093.

⁴Professor, Dept. Appl. Mech. & Engr. Sci., Univ. Of Calif., San Diego, La Jolla, Calif., 92093.

GROUT-BLOCK BOND STRENGTH IN CONCRETE MASONRY¹

by

R. O. Nunn, M. E. Miller, G. A. Hegemier²

INTRODUCTION

The grout and block of concrete masonry are often assumed to be perfectly bonded by analysts, who treat masonry as a homogeneous material similar to concrete. While this practice may be convenient, inspection of laboratory and field specimens indicates that it constitutes a poor approximation under some loading conditions.

An opportunity to examine in detail the grout-block bond was recently afforded by saw-cutting of concrete masonry walls as part of a research program being conducted at the University of California, San Diego (1). Separation of grout cores from face shells was frequently observed, as shown in Fig. 1. Further indication of low bond strength is provided by masonry walls whose face shells break away from the grout cores (spallation) under loading. Such was the behavior of prisms (Fig. 2) tested at the University of California, San Diego (2), shear walls (Fig. 3) tested at the University of California, Berkeley (3), and of load bearing elements of the juvenile facility and other structures (Figs. 4a, b), which were damaged in the San Fernando earthquake of 1971. The variability in geographical location, block type, grout mix, grout lift height, and grout consolidation methods employed in these example cases clearly indicates that the problem is widespread and not simply a local phenomenon (4).

Eliminating grout-block separation due to grout shrinkage and increasing the strength of the grout-block bond, while holding constant other variables such as flaw distribution and grout compressive strength, can be expected to lead to a masonry assemblage of greater structural integrity. In an effort to obtain some estimate of the magnitude of the effect of bond strength on masonry behavior, calculations

¹Research was sponsored by the National Science Foundation under Grant NSF ENV 74-14818.

²Graduate Student, Associate Development Engineer, Professor, respectively, Dept. Appl. Mech. & Engr. Sci., Univ. of Calif., San Diego, La Jolla, 92093.

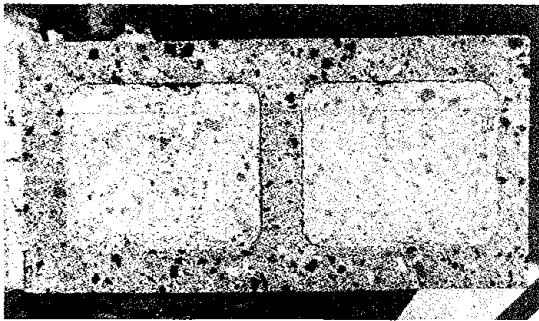


Fig. 1. Grout - Block Separation

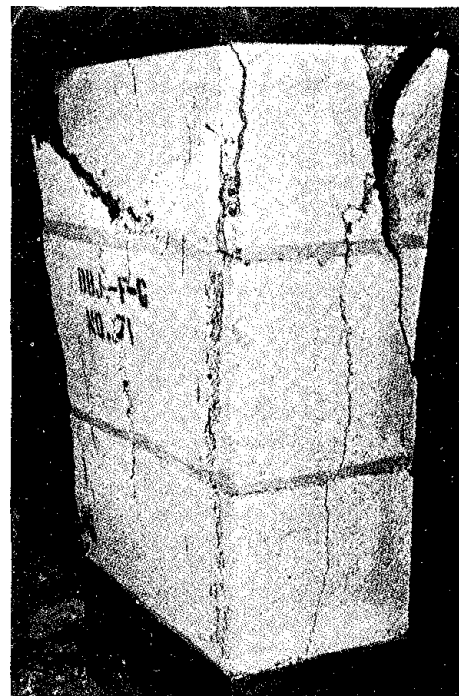
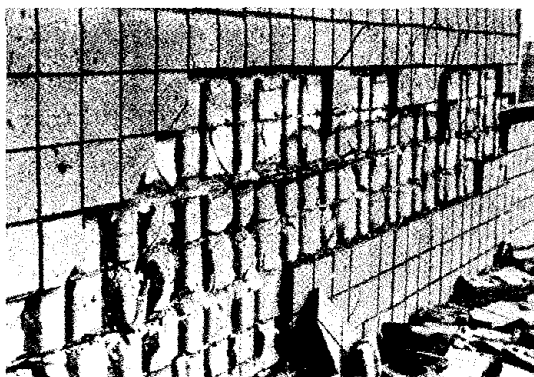


Fig. 2. Spallation in Prism Test



Fig. 3. Spallation in Shear Wall Test



Figs. 4a, b. Spallation in Earthquake Damaged Structures

of strength in bending were made based upon several simplifying assumptions concerning component interaction (5). These assumptions ranged from a perfect grout-block bond to zero bond strength. Out-of-plane bending, as occurs in a retaining wall for example, was selected for analysis since grout-block bond strength plays a significant role in such problems and the shear stress between the grout and the face shell can readily be seen to develop. In each case, as a measure of strength, the bending moment per unit length at which the maximum tensile stress reached 100 psi was computed. The calculations were done for unreinforced masonry. Our experience indicates that steel reinforcing in normal amounts has little influence on masonry behavior before major cracking; hence these results should predict the onset of major cracking.

A comparison of the above cases indicates that bond strength may have a large effect on assemblage strength. It was found that a partial grout-block bond would produce an assemblage strength nearly 50 percent less than that of a perfect bond.

It is evident at this point that a quantitative measure of grout-block bond strength is needed in order to select a rational analysis procedure. For this purpose two tests were considered. One was to pull the face shell from the grout core in direct tension; the other was to shear off the face shell. While a tension test results in a more elementary state of stress and is relevant to walls loaded in-plane, a shear test is easier to perform and is of considerable importance with respect to out-of-plane bending. There is probably a strong correlation between the two test types, as there would be if the materials followed a Mohr-Coulomb interface law of failure and sliding. For this investigation, we chose to base the measure of grout-block interface strength on cores tested in single shear (the two face shell disks being sheared off one at a time). The results of this study constitute the main body of this paper.

SPECIMEN AND TEST DESCRIPTIONS

The specimens tested were cylindrical cores cut from three levels of 96-inch square field prepared walls as shown in Fig. 5. The dashed line square is the outline of the specimens cut for the tests described in Reference (1), while the dashed line circles mark the locations of cores A, B, and C. Coring was performed by using a 5-inch o. d. cutter, which produced a core of 4-9/16 inch diameter.

Four types of specimens were tested: 1) STD: standard 6-sack coarse grout (no admixture), consolidation by puddling; 2) STD VIBR: standard grout, consolidation by vibration with a WACO 5000 rpm head vibrator; 3) ADM: admixture grout with puddling; and 4) ADM VIBR:

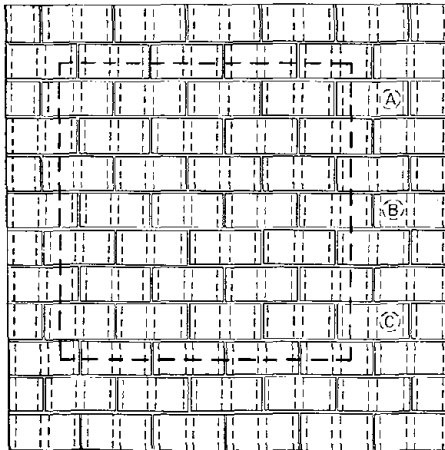


Fig. 5. Core Locations

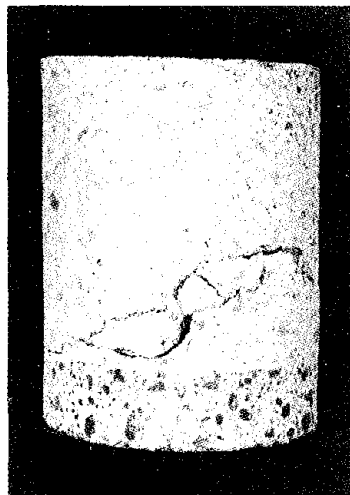


Fig. 7. Fracture Along a Grout Flaw

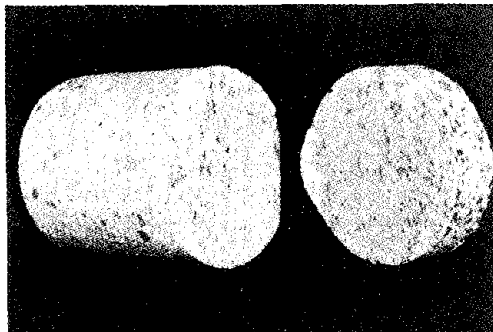


Fig. 8. Mottled Surfaces

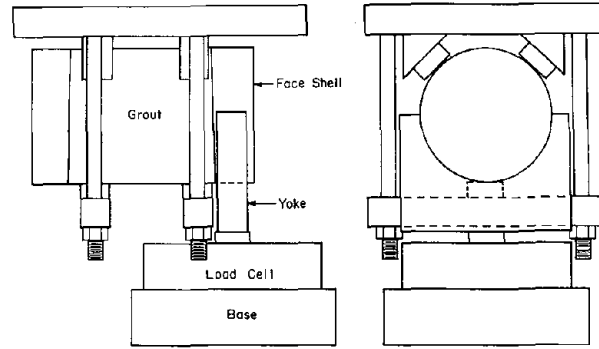


Fig. 6. Test Fixture

Table 1a. Component Descriptions

Block: 8x8x16-inch Grade N Normal Weight (ASTM C90)
 Grout: 2000 psi Pump, 6-sack Coarse Grout (ASTM C476)
 Mortar: Type S, 3/8-inch thick (ASTM C270)
 Admixture: Sika Grout Aid

Table 1b. Component Strengths (psi)

Component	Tension	Compression
Block	373	3580
Mortar	108	1987
Standard Grout	230	2490
Admixture Grout	327	3180

Table 2. Peak Shear Stresses (psi)

STANDARD			ADMIXTURE		
Panel	Front	Back	Panel	Front	Back
68 A	6	251*	67 A	136	51
B	26	grout failure	B	132	44
C	89	0	C	162	118
72 A	213	0	71 A	76	164
B	187	0	B	0	292
C	0	145	C	165	81
STD. VIBRATION			ADM. VIBRATION		
Panel	Front	Back	Panel	Front	Back
65 A	76	0	66 A	118	208
B	216	141*	B	321	275
C	0	81	C	grout failure	
70 A	31	21	69 A	142	242
B	265	99*	B	286	51
C	61	148	C	118	63
74 A	158*	0	73 A	0	138
B	283*	0	B	130	84
C	145	67	C	156	145

*For these tests the grout and block did not separate cleanly.

admixture grout with vibration. All grouting was performed in 8-foot lifts. The block, mortar, grout, and admixture are described in Tables 1a, b.

The tests were performed with a single shear fixture, illustrated in Fig. 6, which was attached to the fixed crosshead of an 80 kip Tinius-Olsen hydraulic test machine. The shear load was applied to the face shell and measured with the load cell-yoke fixture also shown in Fig. 6. The loading rate was roughly 100 lb./sec. The load cell (Interface Model 1220-AF) signal was amplified and recorded versus time on a Hewlett-Packard Model 7045A X-Y Recorder. The shear load was applied parallel to the vertical direction of the original wall, which was marked on each specimen before the coring operation.

RESULTS

Most loading records show a smooth climb to a peak, followed by a sudden drop to zero. Table 2 lists the peak shear stresses for the entire test series. The stress is based on an area of 16.35 sq. in., from a core diameter of 4.56 in.

Grout flaws caused some difficulties in conducting the tests. The results marked with an asterisk in Table 2 represent tests for which the face shell did not separate cleanly. For these tests a segment of grout remained attached to the face shell as the fracture penetrated the grout. Where this occurred, there was usually a flaw visible close to the interface, as in the specimen shown in Fig. 7.

Examination of the interfaces after testing revealed several types of surfaces. Fig. 8, core 66 B front, is an example of a mottled surface. Those interfaces with mottled appearance generally had high strengths, usually over 200 psi. Fig. 9, core 72 C front, illustrates a surface on which a powder appears to have been deposited. All such surfaces had low or zero strength bonds. The powder may be from the lubricating wash used during the coring operation.

Several surfaces had regions that appeared to be unbonded. A difference in texture and color suggested that the grout in those regions had been air cured. In Fig. 10, core 67 C back, for example, only the central vertical strip seems to have been bonded, and the failure stress was about 30 percent less than the failure stress of the front side of the core, which appears to have been completely bonded.

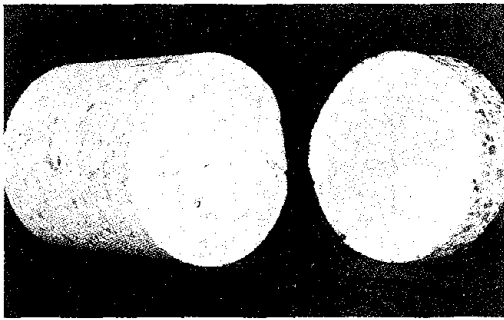


Fig. 9. Powder Deposit

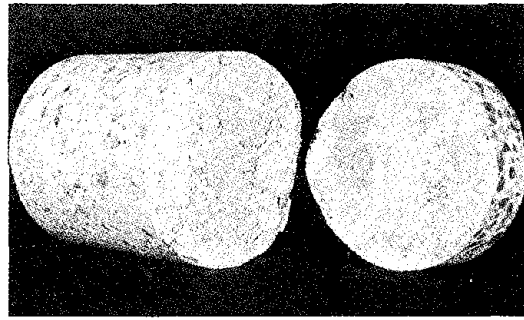


Fig. 10. Partially Bonded Interface

Table 3. Bond Strength vs. Core Location

	<u>A</u>	<u>B</u>	<u>C</u>
No. Less Than 10 psi	5	3	3
Mean (psi)	102	149	97
Standard Deviation (psi)	87	113	57

Table 4. Bond Strength vs. Grout Type

	<u>STD</u>	<u>STD VIBR</u>	<u>ADM</u>	<u>ADM VIBR</u>
Mean (psi)	83	100	118	155
Std. Dev. (psi)	98	90	76	90

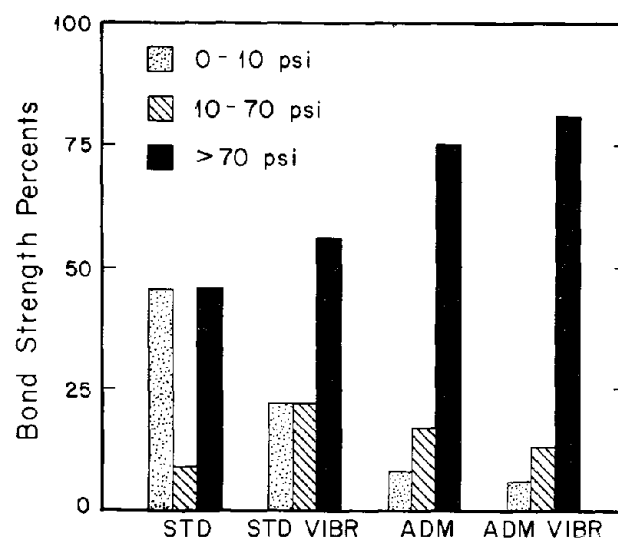


Fig. 11. Bond Strength vs. Grout Type

DISCUSSION

An examination of the test results in Table 2 reveals a large data scatter. Stresses are fairly uniformly distributed from 0 to 300 psi. Items of interest include variation of strength with core location and panel side, and the effects of grout admixture and vibration compaction.

Table 3 indicates the variation of bond strength with core location (Fig. 5). The middle (B) cores were significantly stronger than the top (A) cores or the bottom (C) cores. The number of zero strength bonds was slightly greater at the top of the walls. Though hydrostatic pressure might be expected to increase bond strength at the bottom of the walls, such an effect is not evident, and an explanation of the higher strengths at the middle of the walls has not been formulated.

There was no significant difference in the number of zero strength bonds occurring on the front and back sides of the walls. Thus the coring operation does not seem more inclined to detach poorly bonded face shells on the front of the walls.

To assist in the analysis of the effects of grout admixture and vibration compaction, the bond strengths for each grout type were placed in one of three groups: 1) zero strength: 0-10 psi; 2) low strength: 10-70 psi, and 3) high strength: greater than 70 psi. These groups are somewhat arbitrary, but were chosen to correspond to patterns in the data. In Fig. 11 the bond strengths are given as a percentage of the number of bonds in each group. Table 4 lists the mean strength for each grout type.

A result of major importance is that nearly half of the standard grout bonds are in the zero strength group. Table 2 shows that nearly every core had one bond below 10 psi. This represents a serious problem, but the data shows that both vibration compaction and admixture help to eliminate it. First consider the effects of admixture.

From Fig. 11 one can see that the number of zero strength bonds of puddled grout is greatly reduced by the use of admixture, and for vibrated grout there is also a noticeable reduction. Further, there is a significant increase in the number of high strength bonds for both cases. This shift from the zero strength group to the high strength group shows up clearly in the increased mean strengths in Table 4.

The effect of vibration compaction is similar to that of admixture, though the increase in strength is not as great. The salient results are the decrease in number of zero strength bonds of standard grout, and the increase in mean strength of admixture grout.

It is clear that the combination of vibration compaction and grout admixture produces bonds far superior to those of standard puddled grout, with the zero strength problem almost eliminated.

SUMMARY AND CONCLUSIONS

Grout-block separation and face shell spallation are frequently observed in laboratory tests and in earthquake damaged structures. This indication of low grout-block bond strength was confirmed by the shear tests conducted in this investigation. Because of the large data scatter observed, further tests should be conducted to better determine strength distributions.

Nearly half of the cores from walls with puddled grout and no admixture had zero strength bonds. Until a fabrication procedure can be effected to remedy this situation, a zero bond strength should be assumed for analysis purposes. Grout admixture greatly reduced the number of zero strength bonds, and increased the mean bond strength, while vibration compaction had a similar effect, and its use with admixture produced the strongest bonds.

REFERENCES

1. Hegemier, G. A., et al., "A Major Study of Concrete Masonry Under Seismic-Type Loading," Report No. UCSD/AMES/TR-77/002, University of California, San Diego, January, 1978.
2. Hegemier, G. A., G. Krishnamoorthy, R. O. Nunn, and T. V. Moorthy, "Prism Tests for the Compressive Strength of Concrete Masonry," Report No. AMES-NSF TR-77-1, University of California, San Diego, November, 1977.
3. Mayes, R. L., R. W. Clough, and Y. Omote, "Seismic Research on Masonry," U. S. National Bureau of Standards Building Science Series 106, 1977.
4. Meehan, J. F., "Suggested Researchable Items Relating to Masonry Construction," U. S. National Bureau of Standards Building Science Series 106, 1977.
5. Nunn, R. O., M. E. Miller, G. A. Hegemier, "Grout-Block Bond Strength in Concrete Masonry," Report No. UCSD/AMES/TR-78/001, University of California, San Diego, March, 1978.

ON THE BEHAVIOR OF JOINTS IN CONCRETE MASONRY¹

by

G. A. Hegemier², S. K. Arya², G. Krishnamoorthy³, W. Nachbar⁴ and
R. Furgerson⁴

ABSTRACT

Joints or interfaces in concrete masonry assemblies constitute planes of weakness and a major source of stiffness degradation and damping. Failures frequently initiate in joints, and subsequent deformation and energy absorption may occur by relative slip across joint planes. Thus, data on joint fracture and post-fracture behavior is a prerequisite to a basic understanding of failure processes in concrete masonry.

This paper presents selected results from a test program on joints in concrete masonry. Joint types selected for study include ungrouted bed joints, grouted bed joints, and head joints. Test specimens consist primarily of triplets (three blocks, two interfaces). Joint planes are subjected to constant levels of normal stress and both monotonic and cyclic shear stress. In each test the initial and post-fracture shear stress versus normal stress envelopes, and deformation histories are determined. Experimental results are supplemented by analytical and numerical studies.

¹ Research was sponsored by the National Science Foundation under Grant NSF ENV 74-14818.

² Professor and Principal Development Engineer, respectively, Dept. of Appl. Mech. & Engr. Sci., University of California, San Diego, La Jolla, California, 92093

³ Professor, Dept. of Civil Engr., San Diego State University, San Diego, California, 92182

⁴ Professor and Research Assistant, respectively, Dept. of Appl. Mech. & Engr. Sci., University of California, San Diego, La Jolla, California, 92093.

ON THE BEHAVIOR OF JOINTS IN CONCRETE MASONRY¹

by

G. A. Hegemier², S.K. Arya², G. Krishnamoorthy³, W. Nachbar⁴
and R. Furgerson⁴

INTRODUCTION

Joints in concrete masonry constitute both planes of weakness and a source of material damping. Failures frequently initiate in joints, and subsequent deformation and energy absorption may occur by relative slip across joint planes. Consequently, data on joint fracture and post-fracture behavior is a prerequisite to a basic understanding of failure processes, and is necessary for modeling on both the macro- and microscales.

In an effort to supplement the existing literature (2,4) on joint behavior, experimental studies were initiated in conjunction with the masonry program (3) at the San Diego campus of the University of California. In these studies joint planes were subjected to constant levels of (average) normal stress and "static" or "dynamic" (average) shear stress. In each test the initial and post-fracture shear stress vs. normal stress envelopes, and deformation histories were determined.

In addition to joint tests, concurrent analytical and numerical studies were conducted. These included statistical analyses of data, the construction of global analytical joint models, and detailed finite element simulations of joint behavior. Selected portions of these studies are presented herein.

¹Research was sponsored by the National Science Foundation under Grant NSF ENV 74-14818.

²Professor and Principal Development Engineer, respectively, Dept. of App. Mech. & Engr. Sci., University of California, San Diego, La Jolla, California, 92093

³Professor, Dept. of Civil Engr., San Diego State University, San Diego, California, 92182

⁴Professor and Research Assistant, respectively, Dept. of Appl. Mech. & Engr. Sci., University of California, San Diego, La Jolla, California 92093.

SOME OBSERVATIONS ON JOINT BEHAVIOR

In the previous section it was noted that failures in concrete masonry frequently initiate along joint planes. This point is worth emphasizing at this juncture.

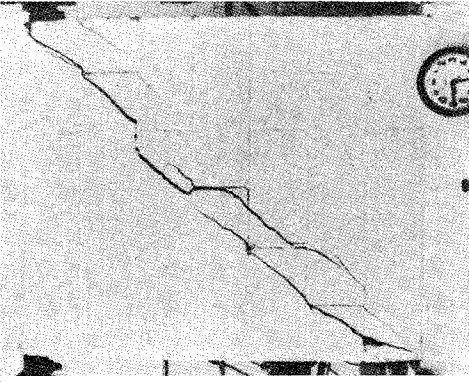
Failure initiation in joints is sometimes obvious by observation of the final failure modes in laboratory (Fig. 1a) and field (Fig. 1b) specimens. More often, however, the final failure mode is complex (Fig. 1c) and one cannot deduce the evolution of failure by simply viewing the failed specimen. In most cases, therefore, it is necessary to observe the evolution of failure in the laboratory.

An example of a complex failure evolution process is furnished in Figs. 1d-f. The specimen shown was tested as part of the University of California, Berkeley, shear wall/pier program (5). This particular element was subjected to oscillatory simple shear deformation. The test was conducted by specifying a sequence of monotonically increasing peak deformation amplitudes and running for three cycles at one Hz for each peak amplitude. The failure sequence is typical. Initial cracking occurs in the head joints, Fig. 1d. As the peak amplitude is increased, bed joint cracking is observed, Fig. 1e, together with additional head joint fractures. As the peak amplitude continues to increase, face shell cracking commences, yielding a complex overall crack pattern (Fig. 1f).

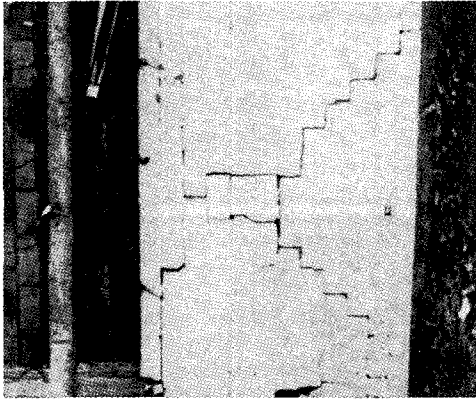
MATERIALS AND METHODS

Test Specimens

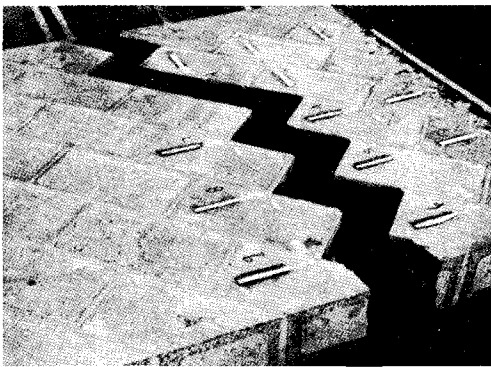
Test specimens in the joint test series consisted of triplets, i. e., three blocks and two interfaces. Both full and half-blocks were used in the monotonic deformation tests. Cyclic deformation was confined to half-blocks due to the complexity of the necessary test fixture. Typical specimens are illustrated schematically in Figs. 2, 3. The complete test series included: 1) ungrouted bed joints; 2) grouted bed joints; 3) grouted bed joints with steel; 4) head joints; and 5) combination of head and bed joints with and without steel. Mortar geometries included both full and face-shell thickness bedding. The component materials consisted of Grade N-1 normal weight concrete block (ASTM C 90), Type S mortar (ASTM C 270), coarse grout (ASTM C 476) with $f'_c \approx 2,000$ psi. All test specimens were fabricated by professional masons using current construction practices and were field cured. In addition to the test specimens, components were tested as controls. These included 2 x 4 - inch cylindrical mortar specimens, sampled, cured, and tested according to ASTM C 780-74; 3 x 3 x 6 - inch grout prisms, constructed, cured, and



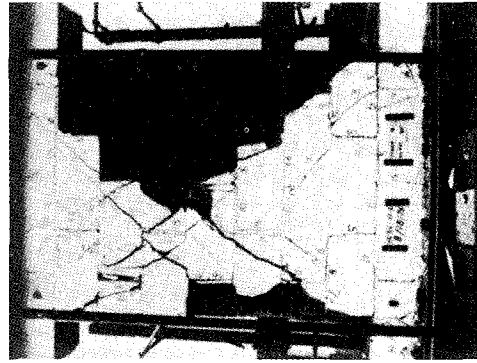
c.



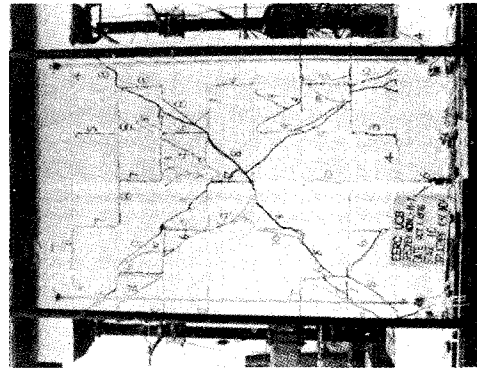
b.



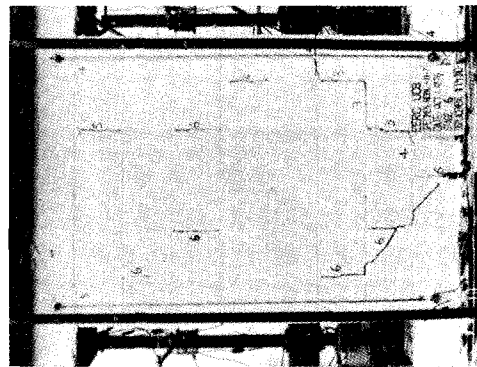
a.



f.



e.



d.

Fig. 1. Typical Laboratory and Field Joint Failures

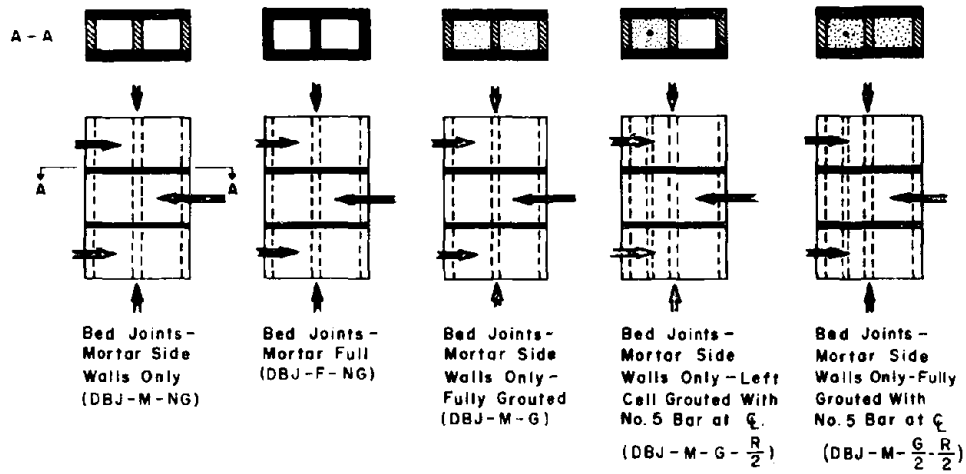


Fig. 2. Bed Joint Triplet Tests - Full-Blocks (8x8x16-in.)

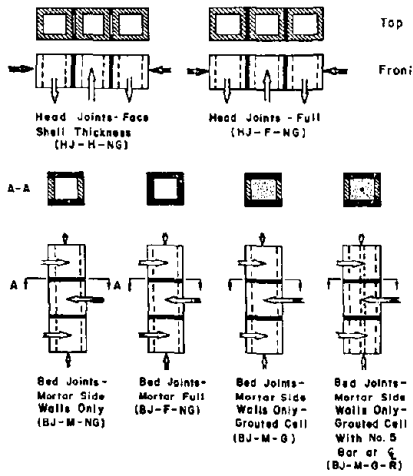


Fig. 3. Head and Bed Joint Triplet Tests - Half-Blocks (8x8x8-in.)

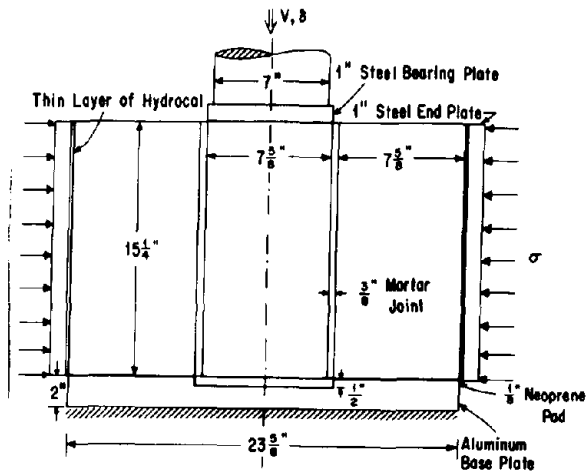


Fig. 4. Schematic of the Monotonic Deformation Test Fixture

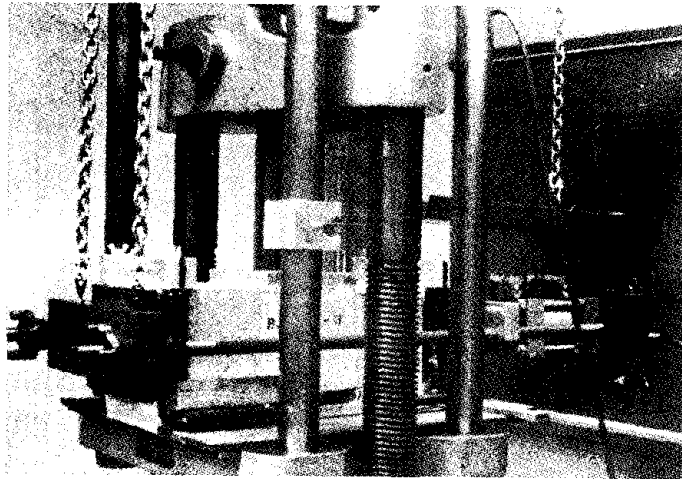


Fig. 5a. Half-Block Test Specimen and Normal Stress Fixture

tested according to UBC Standard No. 24-23; and compression tests (ASTM C 140), direct tension tests, and initial rate of absorption (IRA) tests (ASTM C 67) on individual half-blocks.

Test Fixtures and Loading Devices

A schematic of the monotonic deformation test fixture is provided in Fig. 4. The normal stress σ across the joint planes was generated by use of Miller Power Company 4-inch diameter hydraulic cylinder with a 2-inch stroke. To maintain a constant normal stress in the presence of axial deformation due to mortar degradation, an accumulator was plumbed into the hydraulic system. By pre-charging the 30-cubic inch accumulator with dry nitrogen gas to approximately 90 percent of the hydraulic pressure required for a given normal stress, the variability of the normal stress was reduced to approximately 10 percent for a 0.25-inch change in specimen length. Actual measured changes in specimen length during most tests were less than 0.080 inch. Thus, the normal stress was held constant to within 3 percent. The complete normal stress loading system, including reaction rods and plates, is shown in Figs. 5a, b for half-blocks and in Figs. 6a, b for full-blocks. This system includes swivel connections for overall stability. The necessary shear force V in Fig. 4 was generated by use of a modified Tinius Olsen test machine (200 kip, constant flow hydraulic unit) in the case of half-blocks and a modified Riehle test machine (300 kip, screw-actuated, force-balance unit) in the case of full-blocks. All loading surfaces were capped with a high strength gypsum plaster (Ultra-Cal-30) in order to provide smooth aligned surfaces to mate with test fixtures and test machine load platens.

Design requirements for cyclic deformation were severe in comparison to the fixtures used in the monotonic tests. Cyclic testing requires that both ends of the three-block assembly be firmly gripped and held quite rigid while the center block is firmly gripped and displaced in a vertical direction. The methods of gripping must not in any way impede the horizontal motion due, for example, to mortar degradation. Specially lubricated surfaces were provided at both top and bottom to permit this horizontal translation. An exploded isometric view of the test fixture is shown in Fig. 7. Installation of the test fixture, a specimen, and the normal stress loading device in a closed-loop servo-controlled MTS machine (50 kip) is illustrated in Fig. 8; the latter was used to generate the necessary shear force V and a shear displacement δ . The capping and bedding process in the cyclic tests necessitated treatment of four of the six external sides of the test specimen; Ultra-Cal-30 was again used for this purpose.

In addition to combined normal stress (compression) and shear stress tests, joints were subjected to uniaxial tension. This was

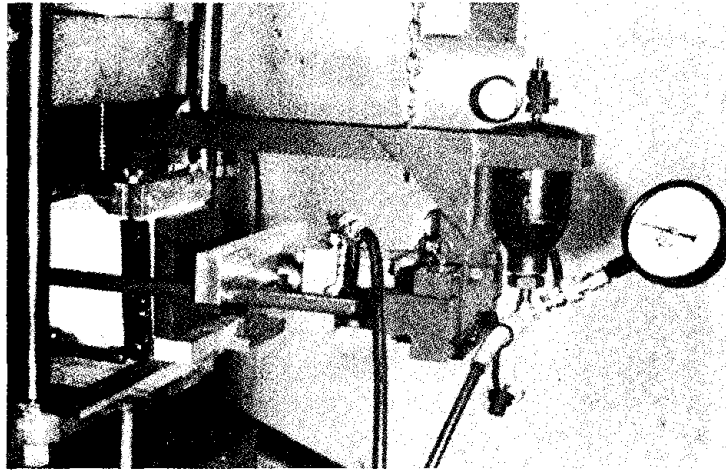


Fig. 5b. Hydraulic Actuator End of Normal Stress Fixture

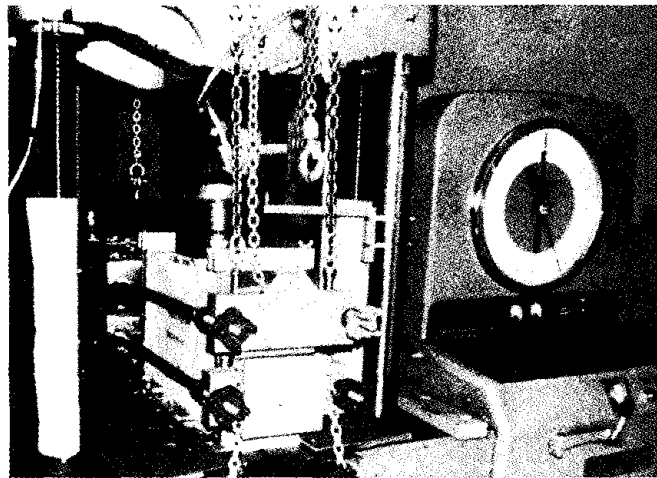


Fig. 6a. Full-Block Triplet Specimen in Riehle Testing Machine (300 kip)

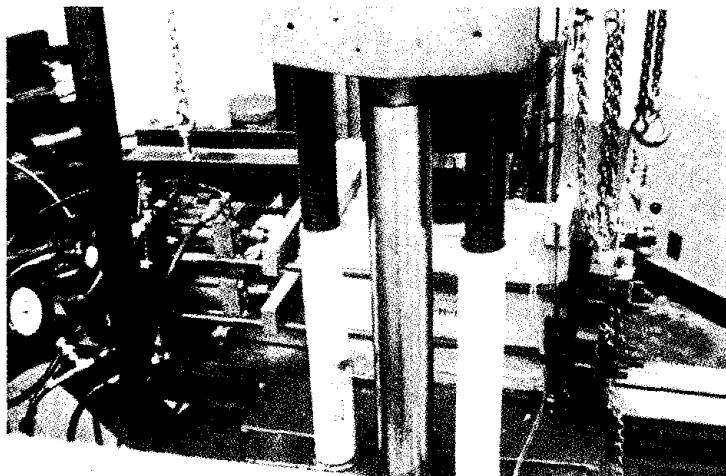


Fig. 6b. Side View of Fig. 6a.

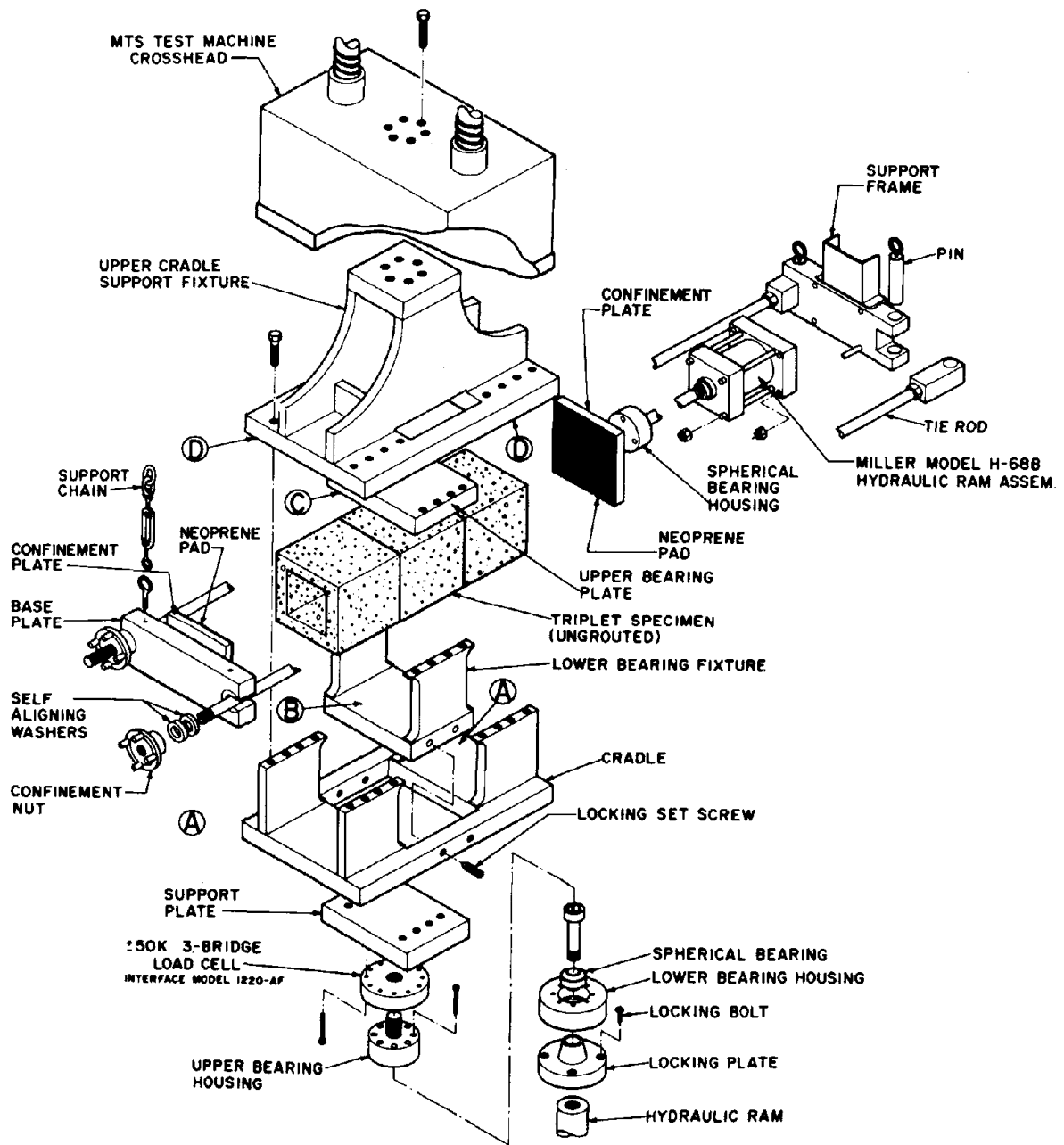


Fig. 7. Exploded Isometric View of the Cyclic Triplet - Test Fixture

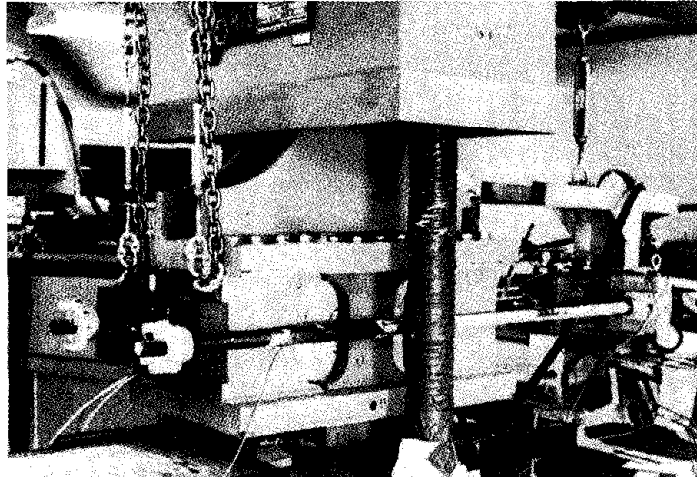


Fig. 8. Cyclic Triplet - Test Fixture and Specimen in MTS Machine

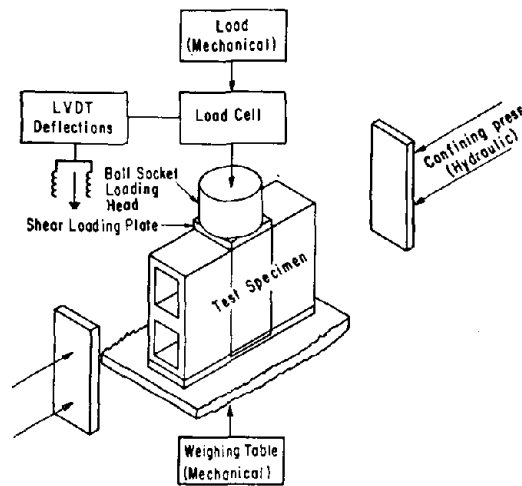


Fig. 9. Mechanical Schematic - Monotonic Triplet Test

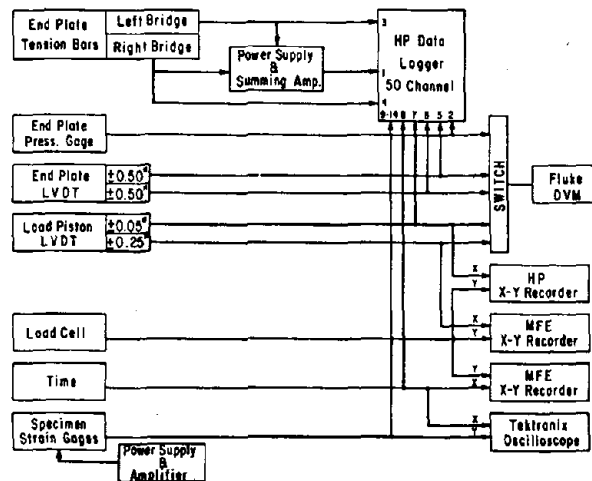


Fig. 10. Electrical Schematic - Cyclic Triplet Test

accomplished by use of a 10 kip Instron test machine.

Data Acquisition Systems

The mechanical and electrical schematics which constitute the data acquisition systems for monotonic and cyclic deformation tests are shown in Figs. 9-11. The basic components include: 1) an HP 50 channel data logger; 2) two MFE X-Y recorders; 3) an HP X-Y recorder; 4) a load cell (strain-gage type) in series with the testing machine ram; 5) a tektronix oscilloscope; 6) a pressure transducer mounted in the normal stress device accumulator system; 7) a time-base generator; and 8) power supplies, amplifiers, and bridges for strain-gage measurements on the specimen and a selection of Linear Variable Differential Transducers (LVDT's). A complete test setup for the dynamic experiments is illustrated in Fig. 12.

Test Conduct

All tests were conducted by first applying the (constant) normal stress σ (or normal force P) across the joint planes, and then by driving the center block under displacement (δ) control. Monotonic deformation tests were conducted at 0.012 in./sec. in the Tinius Olsen and Riehle machines, and from 0.012 in./sec. to 0.500 in./sec. in the MTS machine. Cyclic displacement tests were conducted in the MTS machine using a sinusoidal displacement-time history at frequencies ranging from 0.05 Hz to 0.5 Hz. Displacement cycles were continued at fixed frequency until a stable shear force level was reached, usually within three to five cycles. End-block rotations were initially measured and concluded to be negligible.

RESULTS AND DISCUSSION

Selected Experimental Results

The discussion to follow is confined to head and bed joints in the absence of steel reinforcement.

Figures 13-18 exemplify typical behavior of head joints and grouted and ungrouted bed joints. The following basic characteristics of such joints are noted: 1) joint fracture strength increases monotonically with precompression up to a block-failure transition (the maximum shear stress vs. normal stress is shown in Figs. 13 a, b); 2) under precompression exceeding or equal to 100 psi, post-fracture load decreases with displacement (Figs. 14-16) in a relatively smooth manner to a limiting value which, in time, depends upon the level of precompression; 3) no discernible displacement rate dependence is evident in the range

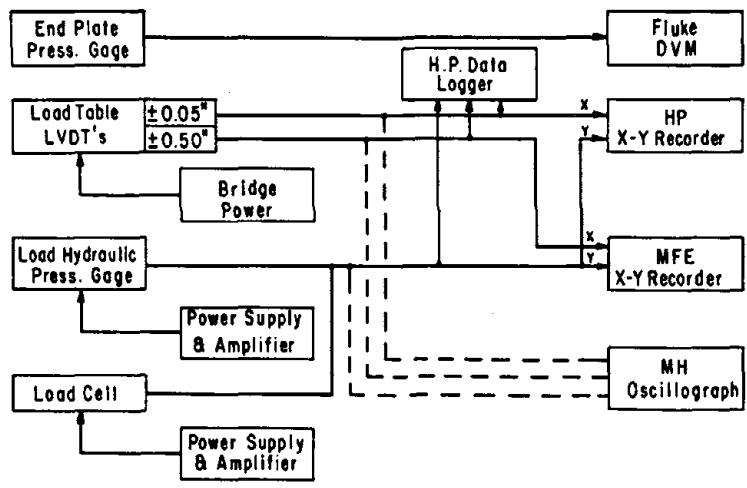


Fig. 11. Electrical Schematic - Monotonic Triplet Test

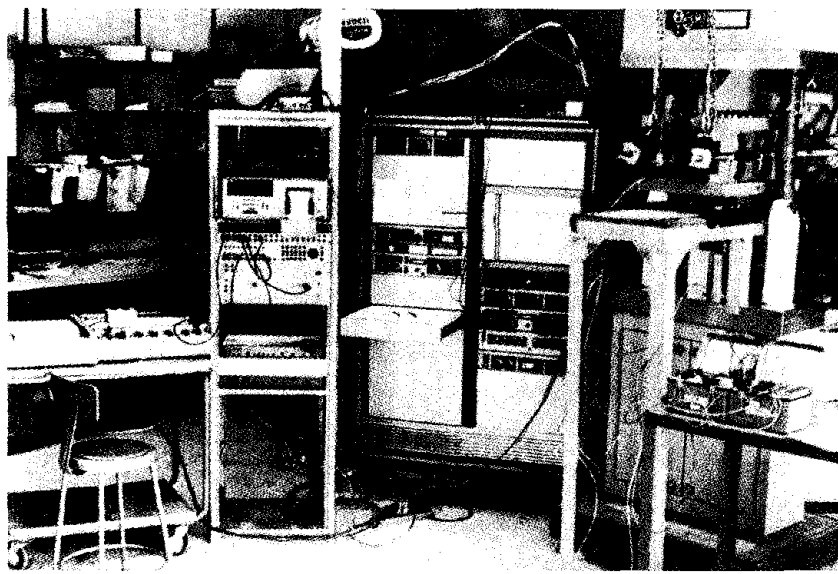


Fig. 12. Cyclic Test Setup

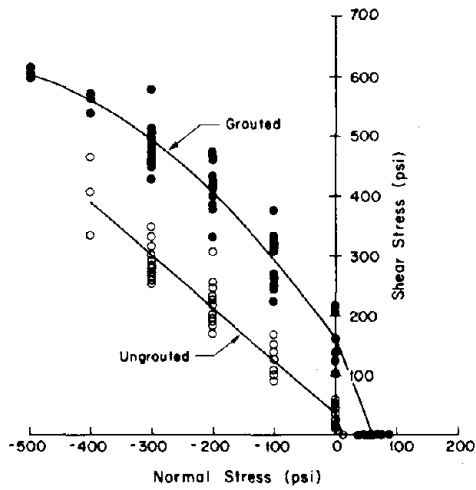


Fig. 13a. Failure Envelope for Bed Joints - Half-Block Triplets

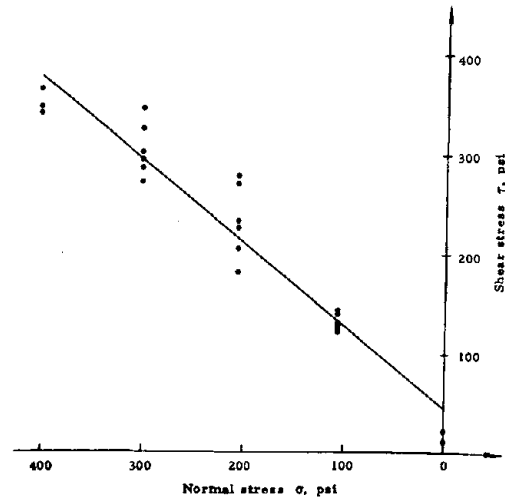


Fig. 13b. Failure Envelope for Head Joints - Half-Block Triplets

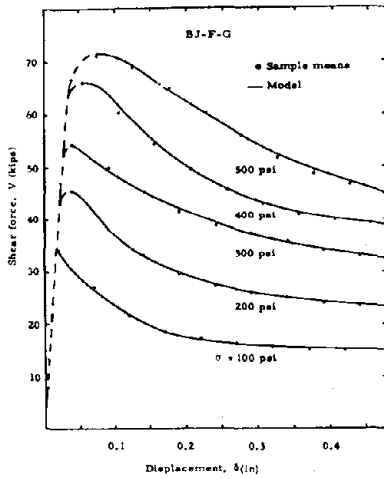


Fig. 14. Comparison of Exp. & Analyt. Data - Grouted Bed Joints

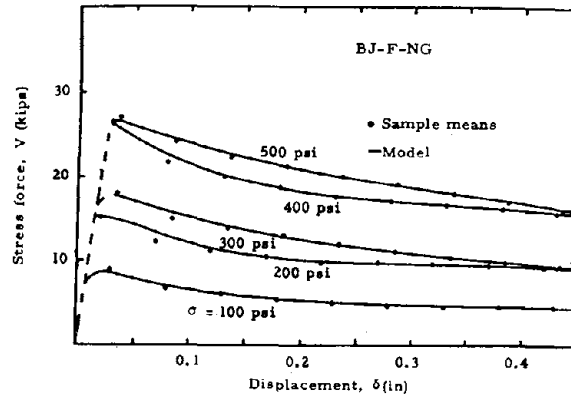


Fig. 15. Comparison of Exp. & Analyt. Data - Ungouted Bed Joints

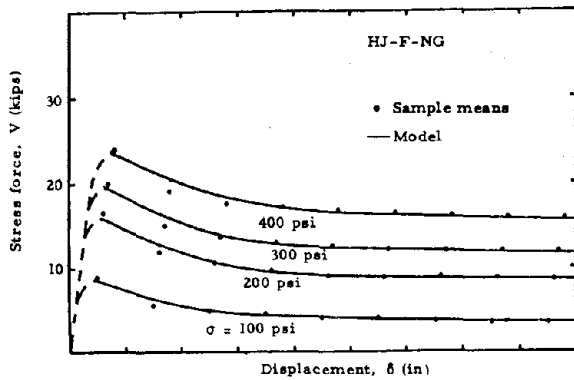


Fig. 16. Comparison of Exp. & Analyt. Data - Head Joints

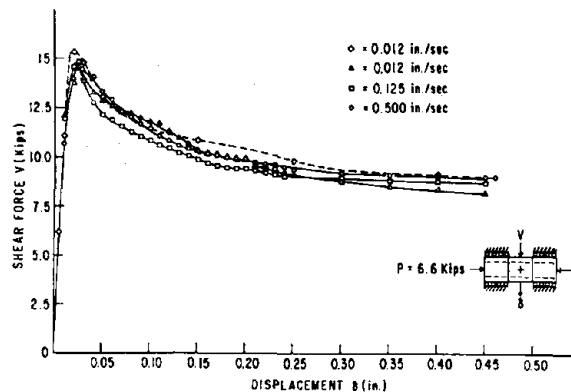


Fig. 17. Displacement Rate Dependence - Ungouted Bed Joints

0.01 to 0.50 in./sec. under monotonic displacement (see Fig. 17) and in the range 0.05 to 0.50 Hz under cyclic loading; 4) cyclic experiments (Fig. 18) indicate that, following the first load reversal, load-displacement history is a function only of total displacement-path length and is not direction-sensitive; 5) ultimate strengths of head joints, and ungrouted bed joints are considerably less than associated grouted bed joints; 6) in the absence of precompression, joint behavior is brittle - ungrouted bed joints and head joints exhibit extremely low (see Figs. 13a,b) shear and tensile strengths as well as extremely large data-scatter. For all practical purposes, head joint strength is zero; this is evidently the result of lack of weighting of the mortar joint during hardening (see (2)). Finally, although the data presented in graphical form concerns half-block specimens, it is noted that similar results were obtained from full-block tests.

Selected Analytical Results - Fracture Criteria

The points in Figs. 13a,b represent the fracture stress states for individual specimens. Using a linear function, a least-squares fit of this data for ungrouted joints gives

$$\tau = \rho + \mu\sigma \quad (\tau, \rho, \sigma \text{ in psi}) \quad (1)$$

where τ , σ denote average (based upon net mortar area) shear and normal stresses, respectively, σ is algebraically positive in compression, and the constants ρ , μ represent coefficients of adhesion and friction, respectively. For bed joints $\rho = 36$ psi, $\mu = 0.89$ in the range $0 \leq \sigma \leq 400$ psi while for head joints $\rho = 45$ psi, $\mu = 0.84$ in the range $50 \leq \sigma \leq 400$ psi. Equation (1) is illustrated as solid lines in Figs. 13a,b for the above constants. For head joints in the range $0 \leq \sigma \leq 50$ psi it appears appropriate to use $\rho = 15$ psi, $\mu = 1.44$; this bilinear relation reflects the low bond strengths of head joints in the absence of precompression.

It is instructive to compare the above results with existing data on both brick and block. For "normal quality" brick masonry Haller (2) found $\rho = 50$ psi, $\mu = 0.88$ for $0 \leq \sigma \leq 200$ psi. Benjamin and Williams (2) proposed $\rho = 220$ psi, $\mu = 1.1$ for $100 \leq \sigma \leq 600$ psi in the case of brick and three mortar compositions: 1: 1/4 :3, 1: 1/2 : 4 1/2 and 1:1:6. Meli and Reyes (2,4) proposed $\rho = 26$ psi, $\mu = 0.80$ for concrete blocks and three different types of mortar ranging from 610 psi to 2150 psi. Self and Balachandran (2), who studied bed joints in 8-inch hollow concrete masonry and type M mortar with two compositions, found $\rho = 34$ psi, $\mu = 0.61$ for 1:1:6 mortar and $\rho = 54$ psi, $\mu = 0.64$ for 1:1:4 1/2 mortar with $0 \leq \sigma \leq 300$ psi. It is of interest to note here that, with the exception of the later case, and with use of $\mu = 0.90$ as a norm, the values of μ from all tests lie within a 22 percent scatter band (the significant difference in μ in the case of Self and Balachandran may be

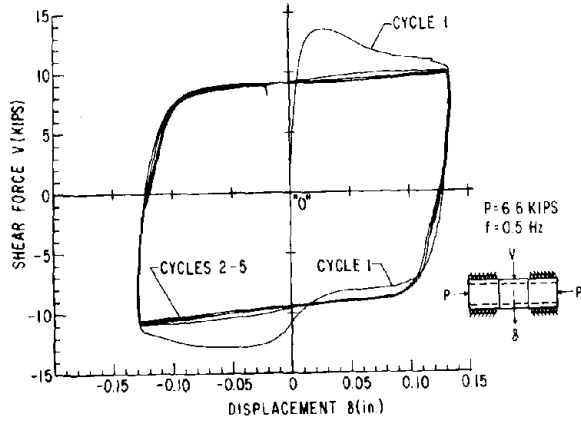


Fig. 18. Typical Cyclic Behavior of UngROUTed Bed Joints

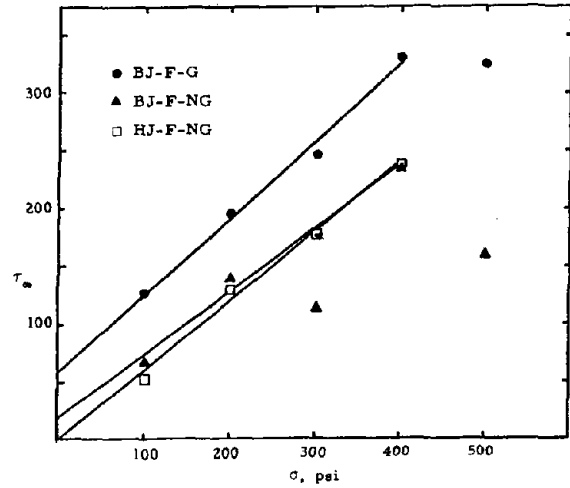


Fig. 19. Limit Values of Shear Stress τ_{∞} vs. Normal Stress σ

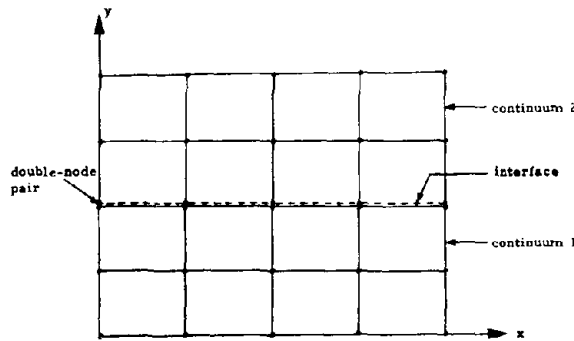


Fig. 20a. Finite Element Model of a Horizontal Interface

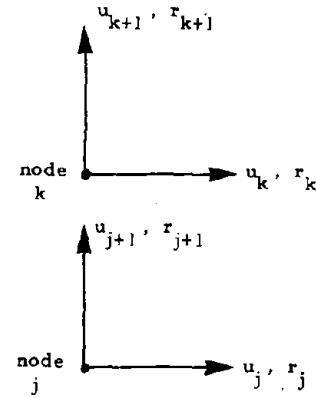


Fig. 20b. Displacements and Slip Forces at a Double-Node Pair

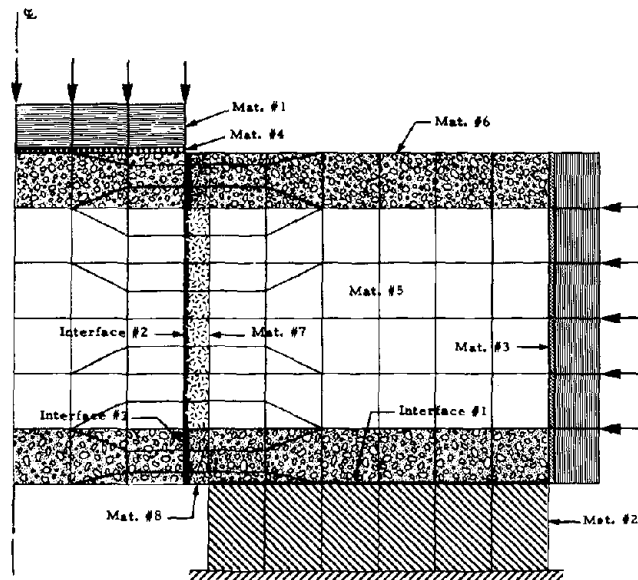


Fig. 21. Finite Element Model of Triplet Specimen

due to the indirect test technique utilized which relies heavily upon the applicability of beam theory for integrity of results.) The observed scatter for the coefficient of adhesion is to be expected and clearly indicates the erratic nature of mortar adhesion.

For grouted bed joints, the solid curve shown in Fig. 13a represents a parabolic, least-squares fit of the data for $\sigma \geq 0$, and a linear fit for $\sigma \leq 0$. Accordingly, one obtains (units are psi)

$$\begin{aligned} \tau &= 162 + 1.46\sigma - .00114 \sigma^2 & (\sigma \geq 0), \\ \tau &= 162 (1 + \sigma/45.6) & (\sigma < 0). \end{aligned} \quad (2)$$

Data on grouted joints is not available in the literature for comparative purposes.

Selected Analytical Results - Post-fracture Regime

The behavior of the data on shear force V vs. displacement δ in the triplet tests suggested that the post-fracture regime could be represented by solutions of the differential equation

$$\frac{d}{d\delta} V(\delta) = -c [V(\delta) - V_{\infty}]. \quad (3)$$

Here V_{∞} is the constant shear force approached at "infinite" displacement, while c has the dimension and role of a reciprocal decay length over which the fractured joint is smoothed. Theoretical arguments suggested that c might depend upon the work $W(\delta)$ done by interface friction up to the displacement δ , viz.,

$$W(\delta) = \int_{\delta_1}^{\delta} V(\delta') d\delta' . \quad (4)$$

For a single test, experimental values V_i are obtained at displacements δ_i , where i ranges from $i = 1$ at the displacement corresponding to maximum V , to $i = n$ (usually 9) at a displacement of 0.40 inches. This data is fitted by least-squares to the following solution of Eq. 3:

$$\frac{V(\delta) - V_{\infty}}{V_1 - V_{\infty}} = \exp \left[- \left\{ \bar{c} \int_0^{\delta} [W(\delta')]^{\beta} d\delta' + b \right\} \right] \quad (5)$$

In this fit, β is taken to be either zero or else a theoretically plausible value of $1/3$, and the constants \bar{c} , b and V_{∞} are regression parameters determined by an extremum procedure. The scale for δ is shifted in Eq. 5 and in the following, so that $\delta_1 = 0$; i. e., δ is measured from the displacement corresponding to the maximum shear force V_1 .

A procedure for iterative determination of regression parameters is described as follows; First, the parameters \bar{c} and b are determined for the test data by minimizing a quadratic form $M(\bar{c}, b, V_{\infty})$ which is

defined by the following set of equations for $i = 1, \dots, n$:

$$\xi_i \equiv \int_0^{\delta_i} W(\delta') d\delta' \quad , \quad (6a)$$

$$\eta_i \equiv \ln \left[\frac{V_i - V_\infty}{V_i - V_\infty} \right] \quad , \quad (6b)$$

$$\bar{\eta}_i \equiv \bar{c} \xi_i + b \quad (6c)$$

$$M(\bar{c}, b, V_\infty) = \sum_{i=1}^n (V_i - V_\infty)^\alpha (\eta_i - \bar{\eta}_i)^2 \quad . \quad (6d)$$

The values used for V_i are the mean values over the several runs (or samples) of the same test. The value of α is chosen to be either zero or 2, depending upon whether the estimated sample standard deviation of V as a function of δ did not or did, respectively, vary with the sample mean. In either case, standard methods for the linear regression of η on ξ enable \bar{c} and b to be obtained explicitly as functions of V_∞ through solution of the pair of equations

$$\frac{\partial M}{\partial \bar{c}} = 0; \quad \frac{\partial M}{\partial b} = 0 \quad . \quad (7)$$

These expressions for \bar{c} and b in terms of V_∞ permit the residual sum of squares divided by n , a quantity called f_m ,

$$f_m \equiv \frac{1}{n} \sum_{i=1}^n [V_i - V(\delta_i)]^2 \quad , \quad (8)$$

to be expressed as a function in which the only remaining unknown is the regression parameter V_∞ which minimizes f_m . This is determined by computer computation of f_m as a function of V_∞ for the values of V_∞ less than V_n .

Because several samples of triplets were tested under the same conditions for each test, the fitting procedure was applied only to the mean value of V_i (the sample mean) for each δ_i . An estimate of the accuracy of this procedure was obtained from the analysis of one series of tests in which seven sample runs were made under nominally identical conditions, and confidence intervals on the mean and variance of V_∞ were obtained for this series. This data can be found in (6). The values of V_∞ for each run were also compared with the V_∞ calculated for the sample mean. This statistical analysis indicated that the estimates of V_∞ based on sample mean values of V_i are acceptable.

Three types of tests were fitted to this model, and results of $V(\delta)$ vs. δ for various confining pressures are shown in Figs. 14-16. Full lines in these figures indicate values of $V(\delta)$ in its regime of applicability to post-bond-fracture. The dotted lines indicate the trend of experimental data at displacements prior to bond fracture. The fit is seen to be excellent in all cases. However, the crucial test of the model is the behavior of V_∞ vs. confining pressure; this behavior is shown for all three types of tests in Fig. 19.

In order to be able to use the test data as a point relation between shearing stress and confining pressure, V_∞ is divided in each instance by the appropriate bearing area A_b to show τ_∞ on the ordinate of Fig. 19,

$$\tau_\infty \equiv V_\infty / A_b \quad (9)$$

The data fits well the form of Coulomb's or Amonton's Law for sliding friction

$$\tau_\infty = \mu_\infty \cdot \sigma \quad (10)$$

for constant coefficient of friction μ_∞ . There are two explainable exceptions. At 500 psi, the concrete blocks themselves were observed to fracture and spall, and the plane interface sliding theory that underlies Eq. 3 above is no longer valid. These two points were therefore omitted for calculation of μ_∞ . For the ungrouted bed joints, some deformation and buckling of the inner walls was observed at 300 psi, and this suggested a cause for the pathological value of V_∞ at this pressure. This point was omitted in the linear regression to calculate μ_∞ . Test data for further tests at this pressure have shown V_∞ lying very close to this linear regression line, however.

The values of μ_∞ , from the linear regression lines shown in Fig. 19, are; 0.55 for ungrouted bed joints (BJ-F-NG), 0.60 for head joints (HJ-F-NG), and 0.66 for grouted bed joints (BJ-F-G).

Selected Numerical Results

A local finite element interface-slip model for both pre- and post- fracture behavior of joints is essential for micro-scale modeling of concrete masonry assemblies. The model (1) developed in this study employs a direct approach in representing the initial fracture or debonding, separation, recontact, and slip characteristics of an interface. It does not represent an interface by a two-dimensional finite element, thus avoiding difficulties due to pseudo thickness and fictitious material properties. Instead, an interface discontinuity is represented by a series of double-node pairs, as illustrated in Fig. 20. It is assumed that

the magnitude of slip at the interface is small compared to a typical element dimension. The equilibrium equations of the discretized structure are first assembled by assuming that the double nodes are free to move. These equations are then modified to simulate the actual state of each double-node pair. The details of the modification process are given in (1).

The status of each double-node pair is determined by knowing the nodal forces and displacements at each pair. When the nodal forces at a double-node pair are less than the strength of the pair, there is no separation or sliding of the nodal points, and the pair is treated as a continuum. When the normal force at a nodal pair exceeds the tensile strength of the pair, or when the tangential force exceeds the shear strength of the pair, nodal point separation occurs; the nodal displacements are independent of each other and no force is transmitted by such a nodal pair. When the normal force at a nodal pair is compressive and the tangential force exceeds the shear strength of the pair, sliding starts; the shear force transmitted by the nodes is equal to the shear strength of the pair, and the tangential displacements are independent of each other. In the normal direction, compatibility of displacements is enforced.

The computation of the strength of a double-node pair depends on the material properties of the interface in tension and shear. The interface is assumed to obey a Coulomb-type friction law:

$$\tau^* = \rho + \mu\sigma \quad (11)$$

where τ^* = allowable shear stress, σ = normal stress (algebraically positive in compression), and ρ, μ = cohesion, coefficient of friction. Both ρ and μ are assumed to be nonlinear functions of the relative tangential displacement as follows:

$$\rho = \rho_0 - \frac{2(\rho_0 - \rho_1)}{x_\rho} x + \frac{(\rho_0 - \rho_1)}{x_\rho^2} x^2 \quad 0 \leq x \leq x_\rho \quad (12a)$$

$$\mu = \mu_0 - \frac{2(\mu_0 - \mu_1)}{x_\mu} x + \frac{(\mu_0 - \mu_1)}{x_\mu^2} x^2 \quad 0 \leq x \leq x_\mu \quad (12b)$$

$$\rho = \rho_1, \quad x > x_\rho; \quad \mu = \mu_1, \quad x > x_\mu, \quad (12c)$$

where x = sum of tangential displacements (absolute values), ρ_0 = cohesion before cracking, ρ_1 = minimum cohesion after cracking, x_ρ = maximum x at which ρ_1 is attained, μ_0 = coefficient of friction before

cracking, μ_1 = minimum coefficient of friction after cracking, and x_μ = maximum x at which μ_1 is attained.

Finite element simulations of the joint tests, described above, were performed to determine the quantities for the coefficients ρ_0 , ρ_1 , etc. The triplet tests for finite element simulations included both grouted and ungrouted bed joints (in half-blocks) under monotonic loading. From economic consideration only three cases of axial confining pressure (100, 300, and 500 psi) were considered for numerical simulation.

The two-dimensional finite element model of the right half of the triplet specimen, as shown in Fig. 21, had 8 element groups of different materials (linear isotropic) which are described in Table 1. The elastic moduli for the materials 5 and 7 were obtained by assuming that the axial rigidity of a composite element is equal to the sum of the axial rigidities of its components.

Referring to Fig. 21, two interfaces were considered at the inside face of the mortar joint. The interface between the base plate and the end-block was also included in the model.

The finite element analyses were performed by prescribing vertical displacements at the top of the central bearing plate while holding the axial confining pressure constant. This procedure enabled the falling branch of the load-deflection relationship to be calculated for comparison with experimental data.

Typical results of the finite element simulation are shown in Figs. 22, 23, in which the analyses and the experiments are compared. The agreement is seen to be good. The interface properties are given in Table 2, and they appear to be reasonable.

CONCLUDING REMARKS

Experimental data obtained in the course of this study reveals that joint fracture strength increases monotonically with precompression up to a block-failure transition. This is consistent with available data on both block and brick masonry in the literature. For ungrouted joints, a Mohr-Coulomb failure criterion appears to suffice for engineering purposes and has been generally adopted by masonry researchers. Collection of all available test data from the literature indicates a scatter in the associated coefficient of friction ranging from 0.61 to 1.1 for brick and concrete masonry, and from 0.61 to 0.88 for concrete masonry alone. Scatter in the coefficient of adhesion for ungrouted concrete masonry alone ranges from 26 psi to 54 psi. A nonlinear failure criterion is required for grouted joints.

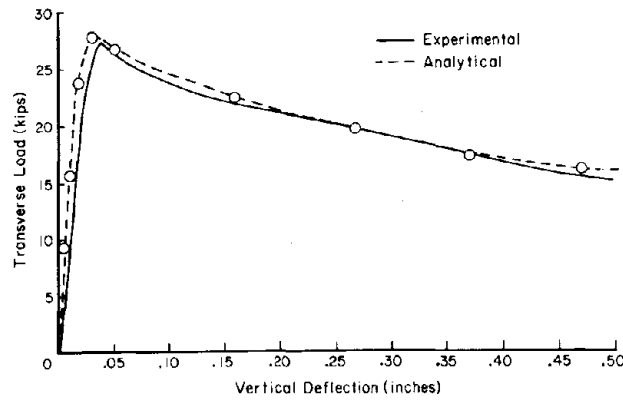


Fig. 22. Force-deflection Curves for UngROUTED Specimen - Normal Stress = 500 psi

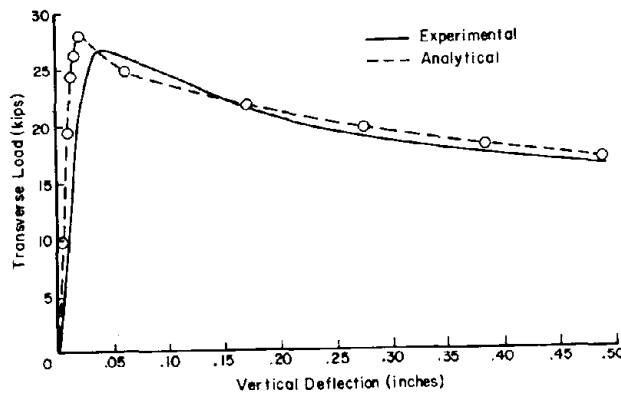


Fig. 23. Force-deflection Curves for Grouted Specimen - Normal Stress = 300 psi

Table 1. Elastic Moduli and Poisson's Ratios of Materials Used.

Material Identification	Description	Young's Modulus (E), psi	Poisson's Ratio
1	Steel	2.970×10^7	.29
2	Aluminum	1.050×10^7	.33
3	Neoprene	1.000×10^4	.40
4	Very soft artificial material	1.000×10^3	.40
5	Composite material 1†		
	UngROUTED specimen	0.200×10^6	.25
	Grouted specimen	1.190×10^6	.25
6	Concrete block	$*0.600 \times 10^6$.25
7	Composite material 2‡		
	UngROUTED specimen	0.292×10^6	.25
	Grouted specimen	1.290×10^6	.25
8	Mortar	$*0.877 \times 10^6$.25
None	Grout	$*1.500 \times 10^6$.25

* Quantities determined experimentally.

† Equivalent material representing the core and the block side walls.

‡ Equivalent material representing the core and the mortar side walls.

Table 2. Interface Properties Used in the Analysis

Coefficient	Units	Interface Type		Description
		Block-mortar	Grout-grout	
p_0	psi	100	475	Cohesion before cracking
p_1	psi	30	150	Minimum cohesion after cracking
x_p	inch	1	1	Maximum x at which p is attained
μ_0		.7	1.15	Coefficient of friction before cracking
		.4	.98	
μ_1		.4	.98	Minimum coefficient of friction after cracking
		.5	1.00	
x_μ	inch	.5	1.00	Maximum x at which μ is attained
σ_n^*	psi	60	240	Tensile strength

Note: x = sum of the absolute values of the relative incremental displacements in the tangential direction.

In the absence of precompression, joint behavior is brittle. For such cases, and for the material combinations studied, ungrouted joints exhibited relatively low (5-70 psi) shear strengths with large data scatter. For all practical purposes head joints possess zero shear strength in the absence of precompression; this is most likely due to a lack of weighting of the mortar during the curing process.

The proposed analytic model of the post-fracture behavior of joints provides excellent correlation with the experimental force vs. deflection data.

The interface-slip model provides a good representation for both pre- and post-fracture behavior of joints.

APPENDIX I. - REFERENCES

1. Arya, S. K., "A Method for Incorporating Interface Discontinuities in Finite Element Analysis with Application to Concrete Masonry Rheology," Report No. R-7522, prepared for University of California, San Diego, by Weidlinger Associates, Menlo Park, California, 1975.
2. Hegemier, G. A., "Mechanics of Reinforced Concrete Masonry: A Literature Survey," Report No. AMES-NSF-TR-75-5, University of California, San Diego, 1975.
3. Hegemier, G. A., S. K. Arya, R. O. Nunn, M. E. Miller, A. Anvar, and G. Krishnamoorthy, "A Major Study of Concrete Masonry under Seismic-type Loading," Report No. UCSD/AMES/TR-77-2, University of California, San Diego, 1978.
4. Mayes R. L., and R. W. Clough, "A Literature Survey - Compressive, Tensile, Bond and Shear Strength of Masonry," Report No. EERC 75-15, University of California, Berkeley, 1975.
5. Mayes, R. L., Y. Omote, and R. W. Clough, "Cyclic Shear Tests of Masonry Piers, Volume 1 - Test Results," Report No. EERC 76-8, University of California, Berkeley, 1976.
6. Nachbar, W., and R. Furgerson, "Friction Law for Grouted Concrete Blocks Following Interface Shear Failure," Report No. AMES-NSF-TR-75-4, University of California, San Diego, 1975.

APPENDIX II. - NOTATION

The following symbols are used in this paper:

- A_b = bearing area;
- c, b = regression parameters;
- P = normal force;
- V = shear force;

W = work done by interface friction;
 δ = displacement;
 σ = normal stress;
 τ = shear stress;
 σ_n^*, τ^* = allowable normal and shear stress, respectively;
 τ_∞ = shear stress at infinity;
 η, ξ = regression parameters;
 ρ, μ = cohesion, coefficient of friction, respectively;
 μ_∞ = coefficient of friction at infinity;
 $\rho_0, \rho_1, \text{etc.}$ = coefficients of nonlinear cohesion law;
 $\mu_0, \mu_1, \text{etc.}$ = coefficients of nonlinear coefficient of friction law.

STRUCTURAL PROPERTIES OF BLOCK CONCRETE

By Thomas A. Holm, P.E.*

ABSTRACT: Engineers have considered concrete block as a special type of concrete and not sufficient concern has been given to its properties. This paper outlines the various characteristics of the material, including tensile strength, elastic modulus, the influence of mix proportions, degree of compaction, and the shape design of the concrete masonry unit. This paper discusses the influence of these various properties on the strength of the masonry unit. By use of a modified Hilsdorf equation, the strength of masonry walls may be calculated.

*Director of Engineering, Solite Corporation, West New York, N.J.

STRUCTURAL PROPERTIES OF BLOCK CONCRETE

By Thomas A. Holm, P.E.*

Design professionals frequently express disappointment with the state-of-the-art of masonry structural design. This concern is entirely justified and is principally due to difficult to understand empirical design procedures that have roots in the mists of traditions as well as less than comprehensive testing methods. The remarkable renaissance of engineered masonry is rapidly providing a remedy to both of these deficiencies.

The first breakthrough in clarity is the identification of block concrete as a structural material to which much of the accumulated cast-in-place structural concrete design experience may be applied. (Suitably adjusted to reflect the high void content of a zero slump concrete mix.) Consistency with this approach would immediately require all reports and calculations to be based upon net area of units and walls. ACI Committee 531 "Concrete Masonry Structures" has recently adopted this approach and hopefully, other professional societies and independent testing laboratories would follow this progressive example. This would eliminate the general confusion regarding block shape influence on net area, as well as the widely held notion that masonry unit undergoes a mysterious transformation of physical properties when it reaches 75% solid content. Net area considerations will automatically develop precision of analysis and ultimately eliminate misleading trade jargon (solid, semi-solid hollow etc.).

Application of structural analysis will also lead to increasingly accurate testing of the tensile strength and strain characteristics of block concrete that to a decisive degree determine the performance of concrete masonry. The compressive strength of concrete is approximately ten times the tensile strength. This relationship is not unusual among building materials: stone, cast iron, mortar, and clay masonry have a similar high ratio of compressive strength to tensile strength. It is curious that the compressive strength of concrete masonry is considered the sole criterion of quality while tensile strength has been generally ignored.

Whether or not the origin of the forces are due to restrained volume change (moisture loss, carbonation, temperature drop), handling or manufacturing implications (culls, chipped corners), or frame movements (structural frame deflections, foundation settlement), the limitation is almost always imposed by an available tensile capacity. In most instances even the maximum compressive capacity in laboratory testing of units or prisms and especially high strength block is also limited by shear (diagonal tension) strength.

*Director of Engineering, Solite Corporation, West New York, N.J.

Tensile Strength

In 1963 the American Concrete Institute Committee 318 revised the building code and introduced the use of the ASTM Test for Splitting Tensile Strength of Cylindrical Concrete Specimens (C 496-71) to adequately document the shear (diagonal tension) strength of structural lightweight concrete. The method of loading a structural concrete cylinder is shown in Fig. 1. This code change spurred the lightweight aggregate producers into extensive testing programs to determine the factors that influenced this property. Through concerted individual and industry-wide work, the data were collected and has now become an ordinary, creditable structural design factor that engineers use daily with confidence. A similar documentation effort must now be conducted for the masonry industry with regard to tensile strength of block concrete.

ASTM Test C 496-71 can be adapted to the tensile testing of 100% solid lightweight concrete masonry units (Fig. 2). The theoretical applicability of testing a rectilinear unit as opposed to a cylindrical specimen has been verified by Nilsson [1] and Davies and Bose [2]. While the strength levels of concrete masonry may start somewhat lower than structural concretes (2000 psi as opposed to 3000 psi or 14 MPa versus 21 MPa), the results of indirect splitting tests on 100% solid lightweight concrete units of all ages and cures from twelve block plants are shown in Table 1. The relationship between tensile and compressive strengths, despite wide variations in age, is remarkably uniform and bears a close relationship to the data on structural lightweight concrete. In general, the ratio of tensile to compressive strength (f_t' / f_c') is lowered when compressive strengths are increased.

A unique and convenient portable device that allows the direct measurement of tensile strength has been developed and has been in practical use for several years. The device, developed by the author, [3] and called the "Blockbuster", has provided information on the two factors basic to a concrete masonry unit: maximum tensile strength and strain characteristics. As Fig. 3 demonstrates, the steel core used in molding the cores of a concrete masonry unit have been machined into a loading arrangement that is powered by a hand jack and measured by a conventional hydraulic gage. Block may be broken in tension simply by inserting the self-aligning rig within the core of a standard two-core 8 by 8 by 16 in. (203 by 203 by 406-mm) block, jacking the ram until failure occurs, and then reading the gage. The device is portable, no capping is required, and the test is completed within 1 or 2 min (after plant curing or at the job site or in a laboratory) at any age. The device could be used for acceptance testing and experimental work (such as optimizing aggregate gradations, compactive effort, and cementitious requirements). It may also be used for in-plant quality control applications (changing cement type or quantity as cold weather approaches).

The original structural analysis of the stresses developed by the Blockbuster was conducted using hand calculations and the results were later compared to an extensive computer solution where the general theoretical approach was corroborated. The analytic results were then verified in a carefully instrumented series of tests conducted at Lehigh

University where the shape of the distorted elastic curve was documented by bonded wire strain gages. While the derivation and analysis are rather complex, the tensile strength is simply read on the large dial. The dial reading is adjusted by a coefficient that is determined for the particular 8 by 8 by 16-in. (203 by 203 by 406 mm) two core block configuration.

A correlation experiment to determine the reliability of tensile testing of two-core hollow 8 by 8 by 16-in. units by the Blockbuster method against the results of the indirect tensile splitting of 100% solid units was conducted and the results are shown graphically in Fig. 4. The mix design, ingredients, curing, and machine cycles were identical for both hollow and solid units run in the same plant on the same machine within two days. Despite the fact that the difference in mold width would cause variation in filling and compacting, the results are remarkably uniform and, furthermore, reveal the early development of tensile strength so essential to avoid handling, curing and storage problems. Figure 5 graphically demonstrates the fact that the tensile strength of block concrete conforms to the well-documented American Concrete Institute (ACI) Building Code equations regarding tensile to compressive strength relationships of cast-in-place structural concrete. Each point shown, in most cases, represents at least five test specimen.

Elastic Modulus

Rigid materials have a high range of elastic modulus (steel, 30,000 ksi or 206 840 MPa; aluminum, 10,000 ksi or 68 950 MPa) and easily deformable materials have low moduli (wood, 15,000 ksi or 10 340 MPa). Hardened concretes have moduli that for design purposes have been approximated by the formula (from ACI Code 318-71).

$$E_c = 33 W^{1.5} \sqrt{f'_c}$$

Where E_c is the modulus of elasticity in compression (psi), W is the air-dry density (lb/ft³), and f'_c is the compressive strength (psi).

The Blockbuster has been extensively used as a loading rig in determining the moduli of elasticity of block concrete. The output from electrical wire strain gages bonded in the correct location on a concrete masonry unit (Fig. 6) is measured in a strain gage indicator to a reading of one microstrain (one millionth of an inch per inch of gage length) while the corresponding tensile stress is computed from the calibrated hydraulic gage reading. After plotting the stress-strain data the tensile modulus of elasticity may be computed and compared to compressive modulus data obtained by the usual compressive loading arrangement using large (greater than 30,000 lb or 1.3 MN) commercial testing machines. Figure 7 demonstrates the tensile modulus for two units of widely different strength and compaction. The wire strain gage can be adequately bonded by an adhesive (curing time, 4 to 24 h) and the modulus test may be completed on a desk top within an hour-again without capping or heavy laboratory equipment.

Based on the data developed by numerous tests, an equivalent formula for the elastic modulus for block concrete has been obtained:

$$E_c = 22 W^{1.5} \sqrt{f'_c}$$

Where W is the oven-dry density (lb/ft³) and f'_c is the compressive strength (net) (psi).

The difference in coefficient (33 for cast-in-place and 22 for block concrete) is due to the high void content of machine molded, zero-slump concrete. This result is predictable from theoretical studies that incorporate the effect of variable degree of compaction.

Under usual testing techniques the failure of brittle materials is sudden. Careful experimental techniques have, however, allowed the development of a reasonably complete stress-strain curve. Following the recommendations of Hedstrom [4], the extensibility of the concrete may be defined as the strain at 90% of the maximum strength achieved. This avoids the extreme difficulty of measuring a fracture strain and in most cases is still on a reasonably linear stress-strain relationship (Fig. 8). Strain characteristics coupled with maximum tensile strength will in time provide the tools for a fundamental insight into the properties and the performance of concrete masonry units, alone and within the wall.

Mix Proportioning

While most mix designs are developed through a trial and error process, it is possible to approach molded unit mix designs through absolute volume calculations that incorporate the specific gravity values associated with the binder and the aggregates. Through this technique, the interstitial void content (Fig. 9) may be computed and the interstitial porosity (interstitial void volume/total volume) determined. The effect of this interstitial void content on strength, stiffness, water permeability, and sound transmission is enormous.

The interstitial void system produced by the molding of zero-slump concrete masonry units is the principal difference between block and cast-in-place concretes. This difference is really one of degree, as all cast-in-place concretes contain entrapped air ($\pm 2\%$) and concretes exposed to the weather generally contain deliberately entrained air (4 to 8%). The influence of paste and aggregate porosity may also be evaluated but will not be considered in this paper.

Degree of Compaction

The concrete masonry producer has an opportunity to manipulate the physical properties of the unit through machine adjustments of feed, finish, and delay times as well as by optimizing the mix proportion and ingredients. The degree of compaction may be defined as $(1 - \text{porosity}) \times 100$. Commercial lightweight concrete masonry units manufactured in accordance with ASTM Specifications for Hollow Load Bearing Concrete Masonry Units (C 90-75) have interstitial porosities of about 15%, whereas highly compacted, high strength units may approach a porosity of only 15% (95% degree of compaction). As an example, note the increased efficiency in strength potential through the increase in compactive effort (feed and finish time) demonstrated in Fig. 10. Packing well-graded aggregates and filling the void system with efficient cementi-

tious materials will greatly improve the compressive and tensile strengths as well as the modulus of elasticity but will produce a corresponding increase in the density of the concrete. The interrelationship of strength, stiffness and extensibility may be evaluated for any particular combination of mix proportions and compaction by the stress-strain formula. Experiments with masonry units have validated the fact that the 5% increase in strength for each 1% reduction in the interstitial void system is roughly paralleled over a limited range with block concrete [5]. With different aggregates and mix designs, this reduction factor may be as much as 8 to 10% per 1% reduction of the interstitial void content. In the development of high strength masonry units (3500 psi or 24 MPa or more), minimization of this void system is crucial.

Extensibility

Trade-off of physical properties becomes obvious by rearranging the stress-strain formula to $e = f/E$, where e is the unit strain.

Thus, to achieve greater strain capacity (extensibility or the ability to deform prior to fracture) it is possible to improve the ratio between ultimate tensile strength and the corresponding modulus of elasticity. To illustrate, compare a structural lightweight concrete masonry unit with a typical normal weight unit by means of the modified formulas for cast-in-place concrete (ACI Code 318 - 77).

Lightweight Concrete Masonry Unit (ASTM Specification C 90-75)

$$\begin{aligned} \text{Tensile strength} &= (0.75) (6.7) \sqrt{f'_c} = 0.75 \times 6.7 \times \sqrt{2000} = 225 \text{ psi} \\ \text{Modulus of elasticity} &= 22 W^{1.5} \sqrt{f'_c} = 22 \times 95^{1.5} \times \sqrt{2000} = 911\,000 \text{ psi} \end{aligned}$$

$$\begin{aligned} \text{Indicated extensibility} &= \text{unit stress/modulus of elasticity} = \\ &225/911\,000 = .000\,247 \text{ "/} \end{aligned}$$

Normalweight Concrete Masonry Unit (ASTM Specification C 90-75)

$$\begin{aligned} \text{Tensile Strength} &= 6.7 \sqrt{f'_c} = 6.7 \sqrt{2000} = 300 \text{ psi} \\ \text{Modulus of elasticity} &= 22 W^{1.5} \sqrt{f'_c} \times 135^{1.5} \times \sqrt{2000} = 1\,543\,000 \text{ psi} \end{aligned}$$

$$\begin{aligned} \text{Indicated extensibility} &= \text{unit stress/modulus of elasticity} = \\ &300/1\,543\,000 = 0.000\,194 \text{ in/in.} \end{aligned}$$

Shape Design of Concrete Masonry Units

Market conditions are always in flux, and the masonry industry must perceive the changes, evaluate the significance, and, when necessary, adapt to the new requirements. As a case in point, consider the spectacular growth of load-bearing masonry. The present ASTM requirement for minimum web thickness is inadequate for load-bearing units. Many laboratory investigations have demonstrated the fact that the webs are too thin to adequately transfer the unbalanced loads always present in the two face shells. Premature failures have frequently occurred shortly after visual cracking in the end webs of loaded units but particularly so when prisms are tested. Mold manufacturers can easily accommodate the demand for a unit of better structural efficiency.

Influence of Unit Properties on Masonry Strength

An incisive study by Hilsdorf [6] suggests a line of investigation that could ultimately provide a procedure for the calculation of masonry strength from the properties of the constituents. This method, proposed for brick, and modified by the author only to reflect the accumulation of lateral tension in the webs of concrete masonry units more closely approximates the results of field and lab tests than the conservative (f'_m vs f'_c) relationships generally espoused in masonry codes.

Substitution of the physical and geometric properties of the assemblage (compressive strength of the block concrete and mortar, tensile strength of the block concrete, shape of units and thickness of joints) in the modified Hilsdorf equation allows a computation of the masonry strength and an insight into the significance of the variables. Figure 11 and table 2 demonstrate that the Hilsdorf equation provides masonry strengths intermediate between code recommendations and results of field prism tests but overestimates the strength of walls composed of strong units in weak mortars, which is bad practice in any case and should not be permitted in modern codes. Modification of the formula to reflect the better performance of units that have thicker cross-webs is easily accomplished by the introduction of a coefficient ω that represents the fraction of web area to face area for cored concrete masonry units.

APPENDIX I - REFERENCESReferences

- [1] Nilsson, S., "The Tensile Strength of Concrete Determined by Splitting Tests on Cubes", Bulletin, Reunion Internationale des Laboratoires d'Essais et de Recherches sur les Matériaux et les Constructions (The International Union of Testing and Research Laboratories for Materials and Structures), Paris, No. 11, June 1961 pp. 63-67.
- [2] Davies, J.D. and Bose, D.K., "Stress Distribution in Splitting Tests"; Journal of the American Concrete Institute, Vol. 65, No. 8, Aug. 1968 pp. 662-669.
- [3] Holm, T.A. et al, U.S. Patent No. 3,792,608
- [4] Hedstrom, R.O., "Tensile Testing of Concrete Block and Wall Elements", Journal of the Portland Cement Association Research and Development Laboratories, May 1966 pp. 42-52.
- [5] Gaynor, R.D., "High Strength Air Entrained Concrete", National Ready Mixed Concrete Association Bulletin No. 127, March 1968.
- [6] Hilsdorf, H.K., "Investigation into the Failure Mechanism of Brick Masonry Loaded in Axial Compression", "Designing, Engineering and Constructing with Masonry Products" Johnson, F.B. Dr., Editor.

Fig. 1 - Test method to determine splitting strength of concrete cylinder.

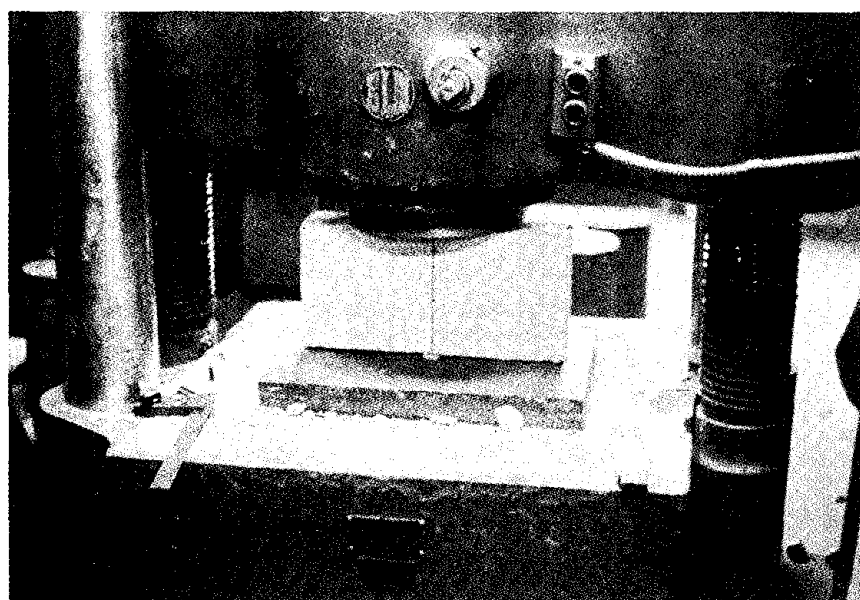
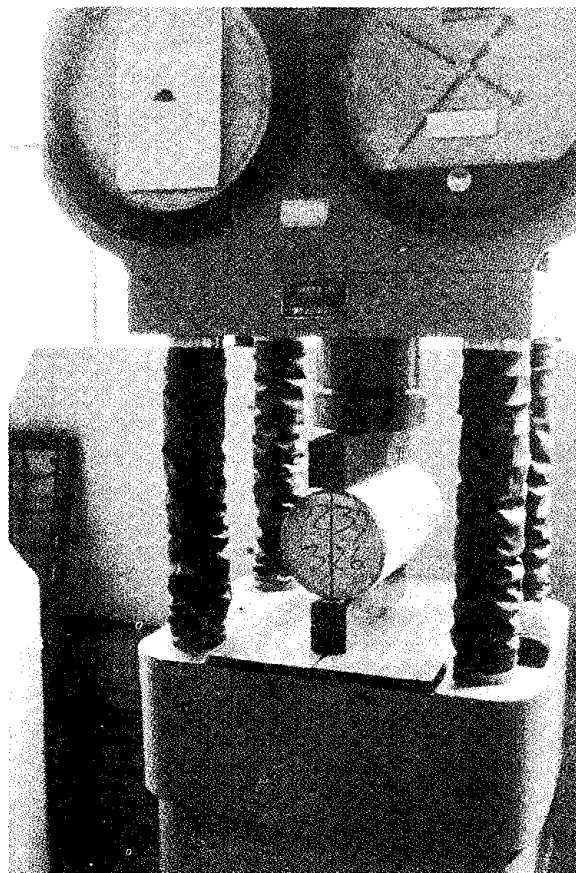


Fig. 2 - Test method to determine tensile splitting strength of concrete masonry unit.

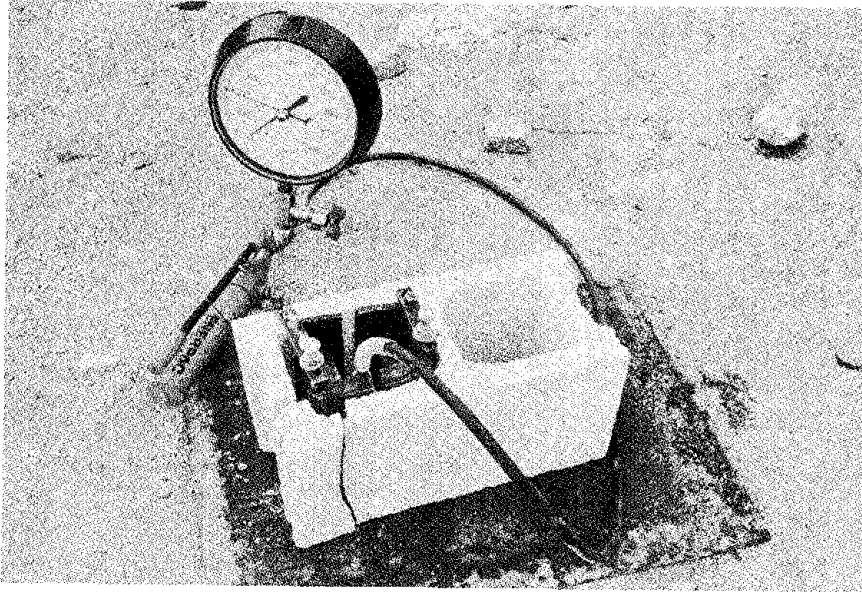


Fig. 3 - Tensile strength of masonry unit determined by blockbuster

TABLE I — Indirect tensile strength tests of 100% solid lightweight concrete masonry units of various ages randomly sampled from twelve concrete block plants.

Block Plant	Oven-Dry Concrete Density, lb/ft ³	Tensile Strength f_t , psi	Compressive Strength f_c , psi, Net Area	$\frac{f_t}{\sqrt{f_c}}$	$\frac{f_t}{f_c}$
1	89.0	302	2620	5.90	0.115
2	83.3	370	3350	6.39	0.110
3	84.0	285	2780	5.41	0.103
4	89.4	232	2000	5.19	0.116
5	86.7	279	2680	5.39	0.104
6	93.3	340	2530	6.76	0.134
7	91.6	288	2180	6.17	0.132
8	91.6	286	2590	5.62	0.110
9	93.1	321	2950	5.91	0.109
10	97.0	305	3280	5.33	0.093
11	97.4	390	2990	7.13	0.130
12	93.5	305	2320	6.33	0.131
Avg	90.8	309	2689	5.96	0.116

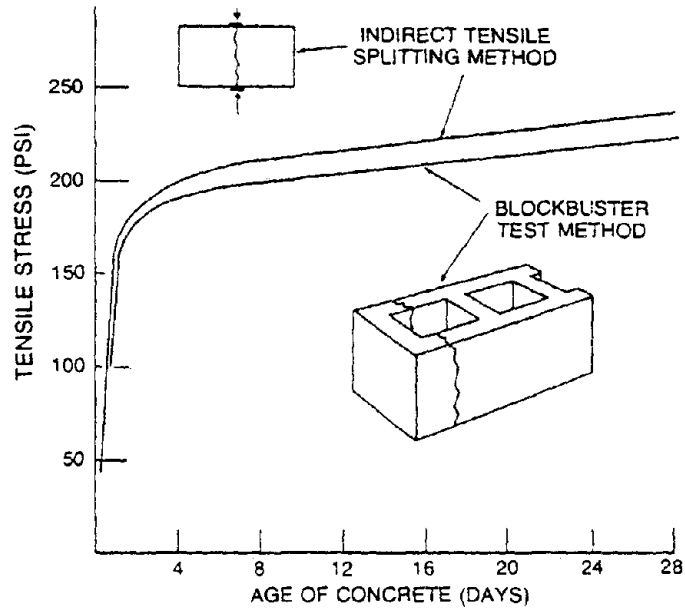


FIG. 4—Correlation of tensile strength of block concrete determined by the blockbuster and the indirect tensile splitting methods.

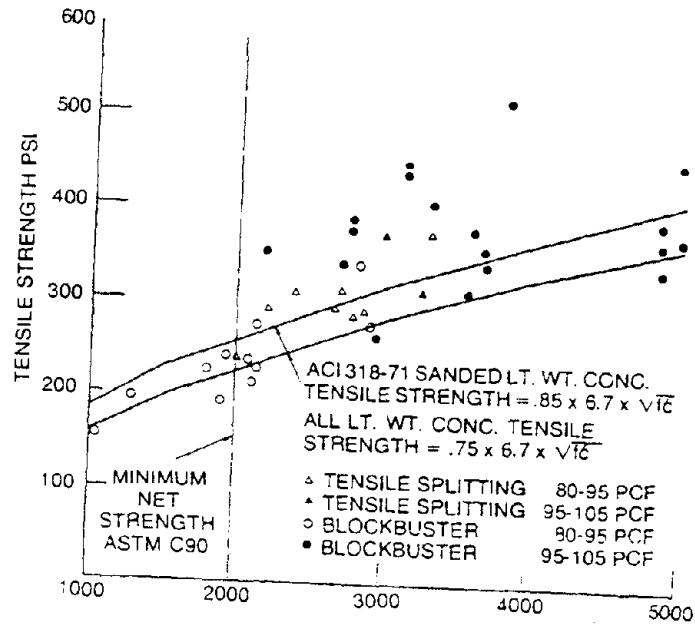


FIG. 5—Tensile strength versus compressive strength of light-weight concrete masonry units.

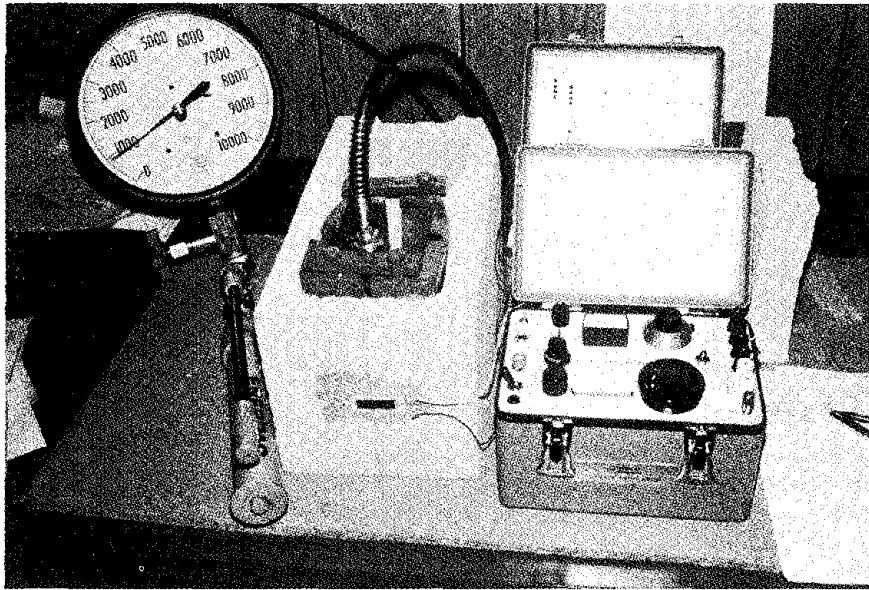


Fig. 6 - Determination of tensile modulus of elasticity of concrete masonry unit.

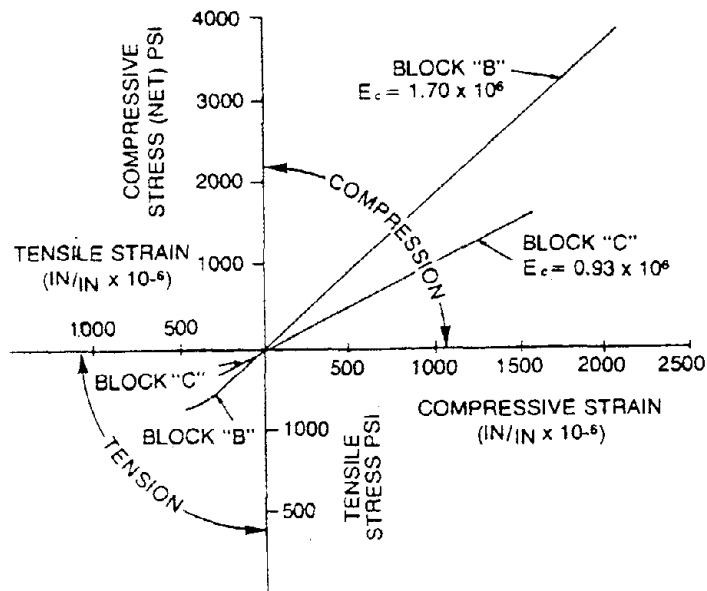


FIG 7—Modulus of elasticity in tension and compression for block concrete.

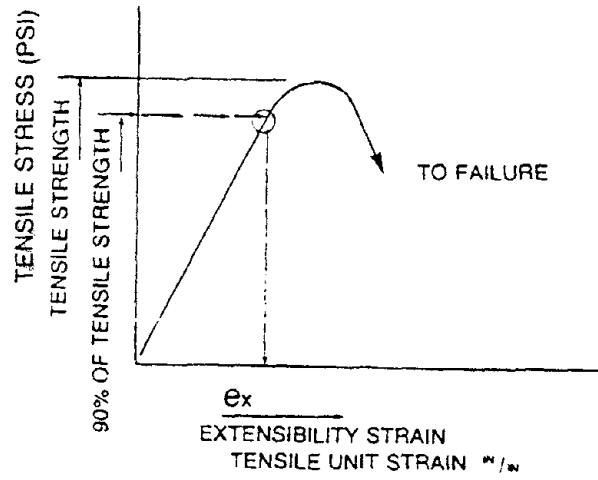


FIG. 8—Definition of extensibility strain.

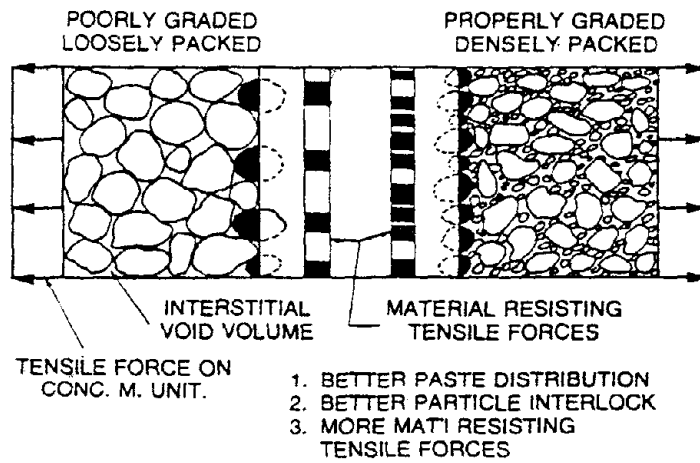


FIG. 9—Pictorial view of influence of gradation and compaction on tensile strength of block concrete.

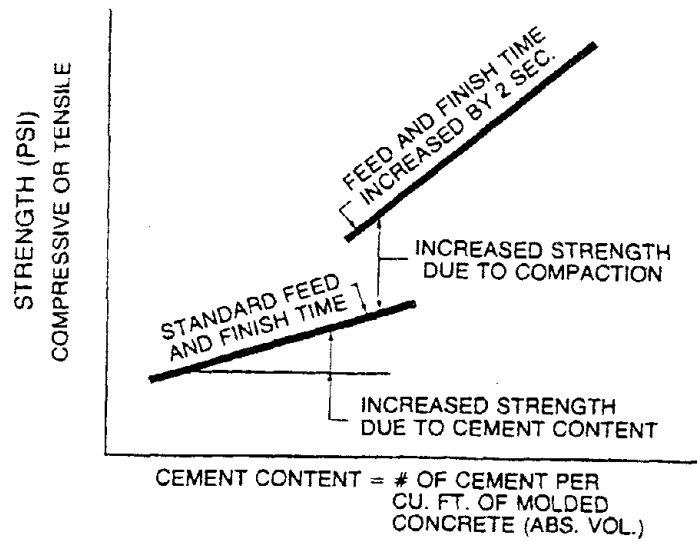


FIG. 10—Effect of compaction on strength.

TABLE 2. CALCULATION OF COMPRESSIVE STRENGTH OF MASONRY (f'_m) USING MODIFIED HILSDORF FORMULA

$$f'_m = \frac{f'_b}{U} \times \frac{(f'_{bt} + \alpha f'_j)}{(f'_{bt} + \alpha f'_b)}$$

(HILSDORF [6] FORMULA WITH α REPLACING GEOMETRIC FACTOR TO ALLOW FOR CORED MASONRY UNITS)

f'_m - CALCULATED COMPRESSIVE STRENGTH OF MASONRY (PSI)

f'_b - MEASURED COMPRESSIVE STRENGTH OF CONCRETE MASONRY UNIT (PSI) NET.

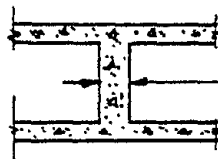
f'_j - MEASURED COMPRESSIVE STRENGTH OF MORTAR (PSI)

f'_{bt} - MEASURED TENSILE STRENGTH OF CONCRETE MASONRY UNIT (PSI)

U - WORKMANSHIP FACTOR (1.5 AFTER HILSDORF)

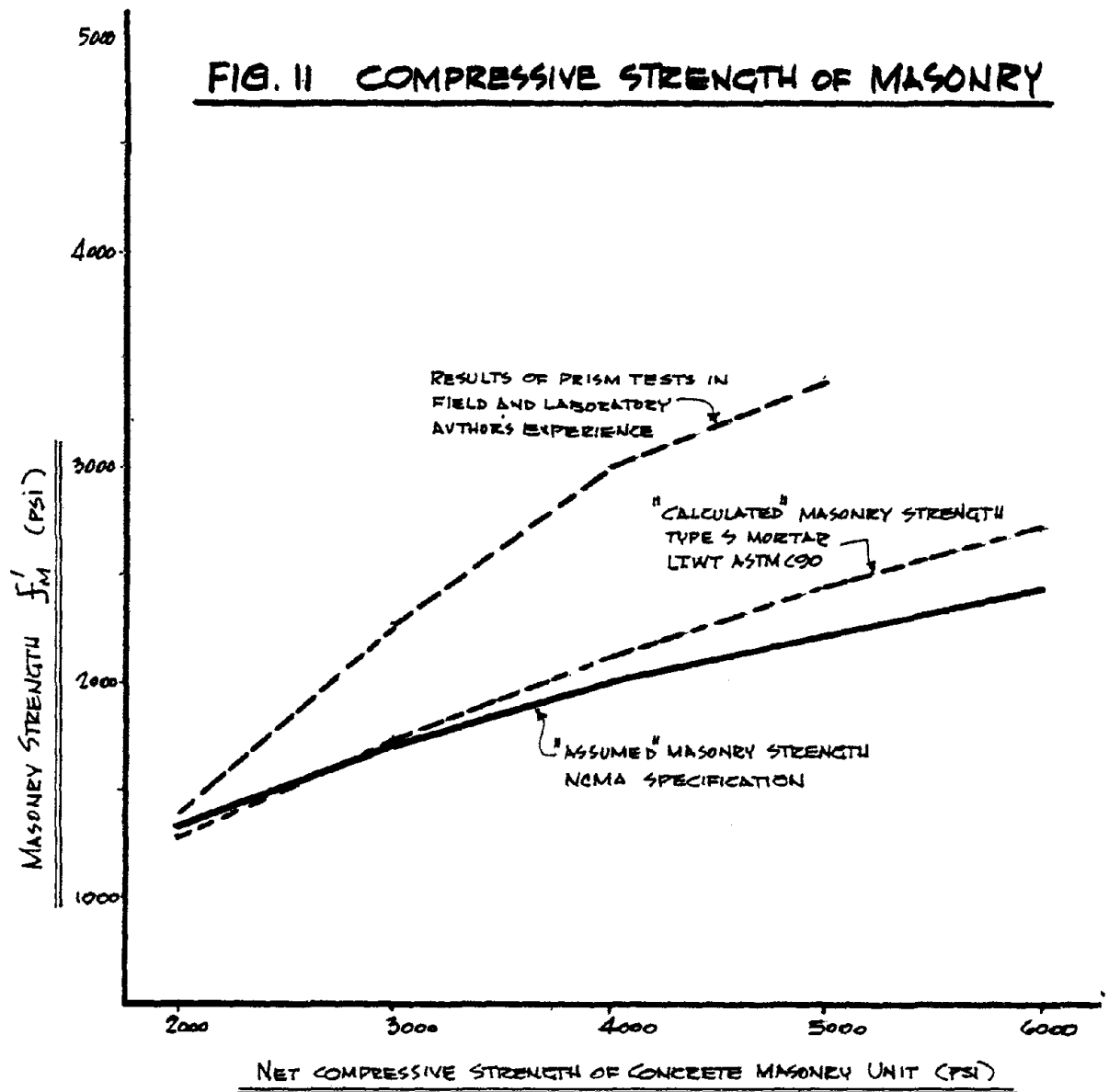
ω - FRACTION OF WEB AREA TO FACE AREA OF CONCRETE MASONRY UNIT
(.22 AVERAGE FOR ASTM C90 UNITS, .33 AVERAGE FOR ASTM C145 UNITS)

α - GEOMETRIC COEFFICIENT = $\frac{J}{4.1bw}$ WHERE J = HEIGHT OF MORTAR JOINT
b = HEIGHT OF MASONRY UNIT



ω (FRACTIONAL PART OF WEB AREA TO FACE AREA OF CONCRETE MASONRY UNIT .22 ASTM C90, .33 FOR ASTM C145)

f'_b COMPRESSIVE STRENGTH OF CONCRETE MASONRY UNIT (NET PSI)	f'_j COMPRESSIVE STRENGTH OF MORTAR (PSI)	f'_{bt} TENSILE STRENGTH OF CONCRETE MASONRY UNIT (PSI)		f'_m CALCULATED NET COMPRESSIVE STRENGTH OF CONCRETE MASONRY				f'_m ASSUMED VALUE FROM NCMA SPECIFICATION TABLE 3-1
		LT. WT ASTM C331	NOR. WT ASTM C33	LT. WT. CONCRETE DENSITY 120 PCF		NORMAL WT. CONCRETE DENSITY 135 PCF		
				$\omega = .22$ ASTM C90	$\omega = .33$ ASTM C145	$\omega = .22$ ASTM C90	$\omega = .33$ ASTM C145	
2000	M 2500	225	300	1400	1400	1400	1400	1350
2000	S 1800	225	300	1300	1300	1300	1300	1350
2000	N 700	225	300	1100	1100	1100	1200	
3000	M 2500	275	367	1900	1900	1900	1900	1700
3000	S 1800	275	367	1700	1800	1800	1800	1700
3500	M 2500	297	396	2100	2100	2100	2200	1850
3500	S 1800	297	396	1900	2000	2000	2100	1850
4000	M 2500	318	424	2300	2400	2300	2400	2000
4000	S 1800	318	424	2100	2200	2200	2300	2000
5000	M 2500	355	474	2600	2600	2700	2900	2200
5000	S 1800	355	474	2400	2400	2600	2700	2200
6000	M 2500	389	519	2900	3200	3100	3300	2400
6000	S 1800	389	519	2700	3000	2900	3200	2400



CURRENT MASONRY RESEARCH AT THE BRITISH CERAMIC RESEARCH ASSOCIATION

By WEST, H.W.H.

ABSTRACT: B.C.R.A. carries out research for the whole of the clay and calcium silicate brick industries in Great Britain, for members in other countries worldwide and for non-members, particularly the Building Research Establishment, on a sponsored basis. Current research includes major projects on the structural performance of masonry, including concrete blocks, particularly resistance to lateral forces when the walls have no precompression, the interaction of floors and walls, effects of openings and the contribution of straps and ties. Typical recent projects described include the compressive strength of calcium silicate brick walls under axial loading, the determination of the flexural strength of masonry in two orthogonal directions to establish the parameters to be used in design and confirmation of the design theory by tests of the lateral strength of full-sized walls.

CURRENT MASONRY RESEARCH AT THE
BRITISH CERAMIC RESEARCH ASSOCIATION

by

H.W.H. West*

1. INTRODUCTION

Masonry is a material of great antiquity originally built by instinct rather than design. Proper design rules in Great Britain start from the 1948 Code¹, which was based on some early experimental work at the Building Research Station² subsequently improved by the 1964 revision³ which took advantage of the Swiss experience made possible by Haller⁴. For the first time load-bearing brickwork high-rise buildings - entirely without reinforcement - could be erected more cheaply, and in many cases aesthetically more satisfactorily, than reinforced concrete framed ones. The result was not only many good buildings, but also the installation of full-size masonry testing capabilities at two brick companies, one University and the British Ceramic Research Association.

The early work⁵, establishing the relationship between brick strength and storey-height wall strength under both axial and eccentric loading, was important in demonstrating that cored bricks - then just becoming popular - behaved in the same way as solids. The Ronan Point disaster threw the lateral resistance of masonry into prominence because although this was a concrete pre-cast panel system, building legislation was made to apply to all materials. B.C.R.A. showed that brickwork under precompression behaved in the manner of a three-pin arch and also, by carrying out real gas explosions in real brick buildings that brickwork did not fail in such a manner as to cause progressive collapse⁶.

It then became evident that the new wind Code⁷, which enhanced the loads to be designed for, would cause difficulties since there was no economical method of designing an infill panel with a compressible joint in a frame building nor indeed for a free-standing wall. Since small forces are involved, the interaction of returns, floors and roofs may be important and the area of investigation has been extended to include tests on parts of buildings up to two-storeys which are described by Hodgkinson in another paper in these proceedings.

* Head of the Heavy Clay Division and Officer-in-Charge of the Mellor-Green Laboratory.

The nature of the ties between the horizontal and vertical planes is imperfectly known, but a start has been made by the publication of a guide to current methods of strapping and tying⁸.

This paper describes experiments to establish the usefulness of the characteristic flexural strength of masonry in the design of walls with no pre-load leading to design rules embodied in the new draft limit state Code. Work to confirm the equivalence of calcium silicate and clay bricks under compressive loading is also described.

2. LATERAL LOAD RESISTANCE

2.1 Experimental

The standard small wall specimens for BS bricks (face 215 x 65mm) are ten courses high and two bricks long to determine the flexural strength parallel to the bed joint (A in Figure 1) and four courses high and four bricks long for the flexural strength at right angles to the bed joint (B in Figure 1). For concrete blocks 450 x 215mm a larger format is required.

All the wallettes were tested under four point loading in a vertical aspect with hydraulic bolsters to spread the load over surface irregularities. One of each pair of bolsters was pivoted at its mid-point to permit alignment of wallettes which are not plane. The specimens were cured for 28 days and set on two layers of ptfе to obviate frictional restraint during testing. The load was applied by hydraulic jack at a uniform rate of 2.5 kN/min. Five replicates were tested in each format and the mean recorded.

In all 61 batches of clay bricks were tested from all over Great Britain covering the range of compressive strength from 22.3 to 117.6N/mm², water absorption from 2.1 to 29.4 per cent and suction rate from 0.07 to 3.87 kg/m².min. The processes of manufacture include semi-dry pressed, stiff plastic pressed with one and two frogs, soft and stiff extrusion both solid and with cores of 3, 5, 11, 14, 16 and 23 holes, and repressed extruded bricks; blues, blue brindles and smooth, rustic and sanded surfaces are included. Most are BS size but 190 x 90 x 65 mm and 290 x 90 x 90 mm and 290 x 90 x 65 mm have been included.

Walls and wallettes were constructed according to the requirements of SP 56 "Model Specification for Load-bearing Clay Brickwork"⁹ and clay bricks with an I.R.S. of more than 2 kg/m²/min were immersed in water for a short time before use. Most of the clay bricks have been laid in 1 : $\frac{1}{4}$: 3 cement : lime : sand mortar but a representative selection have also been laid in 1 : 1 : 6 and 1 : 2 : 9 mortar.

2.2 Determination of design values

Multiple regression analysis shows that the clay brick property which has the most significant relation to the flexural strength is the water absorption. Surprisingly the suction rate does not give

such a good relationship. No such distinction can be made with calcium silicate bricks, and concrete block flexural strengths are related to the block type though some distinction on density or compressive strength is possible.

In Figures 2 and 3 the curvilinear relationships for clay bricks are shown typically by 1 : $\frac{1}{4}$: 3 mortar results with the broken curved lines showing the calculated 95 per cent limit for the ultimate flexural strengths. These lines have been used to provide the stepped dotted lines which are the proposed characteristic flexural strengths for inclusion in the draft Code.

There are fewer different types of calcium silicate bricks available so it has not been possible to adopt the same statistical procedure. However, the results have been plotted as histograms, Figures 4 and 5 and show the Code values adopted for 1 : 1 : 6 (the most frequently used mortar with these bricks) and 1 : 2 : 9 mortars. 1 : $\frac{1}{4}$: 3 mortar is used so rarely that values for this are not considered necessary.

For concrete blocks a larger programme was carried out for the Building Research Establishment. The blocks have been supplied by 16 different manufacturers and each has been tested in 1:1:6 and 1:2:9 mortars. This programme is not complete, since 100, 150 and 215 mm thick blocks have to be tested both as solids and with holes and slots. Sufficient has been done already, however, to enable the industry to propose values for 100 mm blocks for the draft Code. In Table 1 all the values proposed for the Code are shown.

Table 1
Characteristic flexural strength of masonry (f_{kx}) in N/mm^2

Mortar grade	Plane of failure parallel to bed joints			Plane of failure perpendicular to bed joints		
	1:1:3	1: $\frac{1}{4}$:4 $\frac{1}{2}$ & 1:1:6	1:2:9	1:1:3	1: $\frac{1}{4}$:4 $\frac{1}{2}$ & 1:1:6	1:2:9
Clay bricks having a water absorption less than 7%	0.7	0.5	0.4	2.0	1.5	1.2
between 7% and 12%	0.5	0.4	0.35	1.5	1.1	1.0
over 12%	0.4	0.3	0.25	1.1	0.9	0.8
Calcium silicate bricks		0.3	0.2		0.9	0.6
Concrete blocks of compressive strength:						
2.8		0.25	0.2		0.4	0.4
3.5		0.25	0.2		0.45	0.4
7.0		0.25	0.2		0.6	0.5
10.5		0.25	0.2		0.75	0.6
14.0 and over		0.25	0.2		0.9	0.7

The ratio of the flexural strength in the perpendicular direction to that in the parallel direction is known as the orthogonal ratio. The two values of tensile resistance in the present Code, 0.07 and 0.14 N/mm² give an orthogonal ratio (1/μ) of 2.0. The overall range of the ratios of the strength in the perpendicular direction to that in the parallel direction found in the present work is 1.2 to 6.2.

The mean of all the values of flexural strength and orthogonal ratios for all the small walls are given in Table 2.

Table 2

Mean values of flexural strength and orthogonal ratio

Mortar		Flexural strength				
Mix proportions	Mean compressive strength N/mm ²	Normal		Parallel		Mean of orthogonal Ratios
		N/mm ²	% of 1 : $\frac{1}{4}$: 3	N/mm ²	% of 1 : $\frac{1}{4}$: 3	
1: $\frac{1}{4}$:3	17.69	2.10	100	0.73	100	3.13
1:1:6	5.98	2.14	101	0.71	97	3.23
1:2:9	2.44	1.86	89	0.57	78	3.30

Statistical analysis shows that there is no difference between 1: $\frac{1}{4}$:3 and 1:1:6 mortars. Between 1:1:6 and 1:2:9 it approaches significance in the normal direction and is significant in the parallel direction. While the orthogonal ratio is generally around 3.0 it becomes greater as the mortar becomes weaker, although the differences are not significant. Thus with the weaker mortars it is clearly the strength in the parallel direction that affects the orthogonal ratio since it falls away more quickly. The effect might be lessened by the use of high tensile strength mortars.

During the period when Sarabond was available experimentally in the United Kingdom some tests to verify this were carried out on three bricks with the results shown in Table 3.

Table 3
Effect of modifying 1: $\frac{1}{4}$:3 mortar

	Brick Number		
	6	18	31/52
Water absorption %	22.2	5.3	6.7
<u>Standard mortar</u>			
Compressive strength N/mm ²	17.79	16.27	19.43
Flexural strength (normal) N/mm ²	1.80	2.24	3.46
Flexural strength (parallel) N/mm ²	0.61	0.87	1.07
Orthogonal ratio	3.0	2.6	3.2
<u>Sarabond mortar</u>			
Compressive strength N/mm ²	32.99	33.3	35.23
Flexural strength (normal) N/mm ²	2.52	3.59	3.37
Flexural strength (parallel) N/mm ²	1.94	1.64	1.87
Orthogonal ratio	1.3	2.2	1.8
<u>Wanlip sand</u>			
Compressive strength N/mm ²	29.39	33.23	29.13
Flexural strength (normal) N/mm ²	2.20	3.04	3.19
Flexural strength (parallel) N/mm ²	0.65	0.86	1.26
Orthogonal ratio	3.4	3.5	2.5

The bond strength represented by the flexural strength in the parallel direction has increased considerably and this is reflected in the lower orthogonal ratio which averages less than 2.0 for these three bricks.

Also shown are some tests carried out with a sand of coarser particle size distribution than the one normally used for wall building.

Although the compressive strength of the mortar is higher, clearly the bond strength is very little changed and any improvement in the critical parallel direction is small.

2.3 Full sized tests and simplified design method

The walls have been mainly storey height (2.6m) with some 1.3m and some 3.6m high, of various lengths up to 5.5m and either single wythe walls (102.5mm thick) or conventional cavity walls (two 102.5m wythes with a 50mm gap between). The method of testing has been described¹⁰ and typical failure patterns are shown in Figure 6. Most of the tests have been done on two bricks, A which is a high strength perforated wirecut facing and B which is a semi-dry pressed deep frog common brick. X is 1:1:3 mortar and Y is 1:1:6.

Figure 7 shows that the failing pressure is proportional to the reciprocal of some power of the length and the curves drawn are of the general form

$$p = \frac{k}{L^n}$$

where p is the lateral load

L is the length

and k varies with the brick and mortar.

This can be extended to encompass height by introducing "effective length" (Figure 8)

$$L_E = L^h/h_0$$

where L_E is the effective length

L is the actual length

h is the actual height

h_0 is the storey height (2.6m)

By combining these two equations k can be replaced by a function of the flexural strength f_x and Figure 9 shows the result when the experimental failing pressure adjusted for height is plotted against $\frac{f_x}{L^2}$. The best straight line is given by

$$p = \frac{2.6}{h} (1.8 + 12.7 \frac{f_x}{L^2}) \text{ kN/m}^2$$

where p is the failing pressure in kN/m^2

L is the length in m

h is the height in m

f_x is the flexural strength in N/mm^2

The intercept on the ordinate can be explained as the contribution of in-plane forces. Other configurations of walls will need to be tested before this simplified approach can be used, but it would be very useful to pursue as a semi-empirical method in which only the height, length and flexural strength would need to be used for any given shape of wall.

In the meantime the modified yield line method, originally proposed by Haseltine in 1975¹¹ is recommended for design. It is recognised that yield-line theory cannot strictly apply to brickwork and in a recent discussion Hendry proposed the use of the term "fracture line" as being more representative.

2.4 Cavity Walls

It was originally considered that vertical twist steel ties were necessary to ensure that the full resistance was achieved from load from one wythe to the other. However, more recent tests sponsored by the Building Research Establishment (Table 4) have shown that with vertical twist strip ties the moment of resistance of the cavity wall may be taken as the sum of the moments of resistance of the two leaves.

The first butterfly wire tie tested (wall 800) turned out to be below the wire thickness permitted in BS 1243 : 1972¹² and subsequent tests with ties near the upper limit of wire thickness gave markedly different results. Thus it is also appropriate to take the sum of the leaves for the stiffer butterfly ties.

From the results of one wall (No. 1057) it seems that halving the spacing of ties both vertically and horizontally gives increased resistance.

3. COMPRESSIVE STRENGTH OF CALCIUM SILICATE BRICKWORK

A very considerable body of data is available on clay bricks but, surprisingly, very little work on calcium silicate bricks has been reported in the literature. A series of tests have therefore been carried out on a variety of bricks representative of different types and the range of strengths currently being manufactured in order to establish the relationship between brick strength and wall strength and to compare this with both the results for clay bricks and the requirements of the Code.

The bricks were from five manufacturers, both sand lime and flint lime, solid and frogged, built from three mortars, 1:¼:3, 1:1:6 and 1:2:9 cement:lime:sand. The wall specimens were 1.37m long, single wythe (nominal brick width, 102.5mm), storey height (nominal 2.6m) thirty four courses built within a jig on a concrete plinth set in a steel channel. The steel channel facilitated loading into the 1000t wall testing machine. The walls were covered with polythene sheets at the end of the day and remained covered until prepared for testing by casting grano-

TABLE 4
Storey-height cavity walls

Units/ Mortar	Wall No.	Length m	Type of Tie	Lateral Load at Failure kN/m ²	Mean Lateral Load kN/m ²	Single Leaf Equivalents kN/m ²	Ratio Load sum of leaves	Comments
A-A 1:1/4:3	788	5.5	T	5.72	5.84	3.18/3.18	0.90	
	790	5.5	T	5.93			0.93	
	792	5.5	T	5.86			0.92	
B-B 1:1:6	1041	5.5	T	4.59		2.02/2.02	1.14	
	1022	5.5	T	4.0			0.91	
A-B 1:1:6	1057	5.5	T	6.4		2.37/2.02	1.46	Quadruple ties
	1118	5.5	B	5.0			1.14	
	1053	5.5	T	3.85			1.20	
A-C 1:1:6	1087	5.5	T	3.85	3.85	2.37/0.83	1.20	
	810	5.5	T	4.76			1.27	
A-F 1:1:6	800	5.5	B	2.41		2.37/1.38	0.64	Different failure pattern in each leaf
	1049	5.5	T	3.38			1.19	
B-C 1:1:6	1084	5.5	T	3.15	3.27	2.02/0.83	1.11	
	1112	5.5	B	3.20			1.12	
	1113	4.5	B	3.50			n.d.	
	1115	3.6	B	3.80			n.d.	
	1068	5.5	T	4.85			1.18	
B-D 1:1:6	1093	5.5	T	5.35	5.10	2.02/2.1	1.30	
	1058	5.5	T	3.65			1.10	

B = Butterfly tie

T = Vertical twist steel tie

F = Breeze Block

C = Aerated concrete block

L = LWA concrete block

D = Dense aggregate block n.d. = not determined

fondue cappings onto the top of the walls on the day prior to testing with the spreader beam of the testing machine allowed to rest on top of the wet capping. The loading was axial, and the load applied at the rate of 690kN/m².min.

The detailed testing programme and results have been described¹³. In Figures 10 and 11 regression lines have been inserted on graphs of mean wall strength against brick strength for the three different mortars. Although little accuracy can be claimed for lines based on such a small number of points for the X and Z mortars, the results are consistent, with roughly linear relationships that are steeper for mortar X than for mortars Y and Z. The lines are valid only within the range of measurements and should not be extrapolated.

More results are available for mortar Y and Figure 11 shows a moderate degree of correlation between wall strength (y) and brick strength (x). The calculated linear regression equation is

$$y = 9.137 + 0.09035x$$

and the correlation coefficient is 0.619.

Equivalent equations calculated with a common intercept for solid and perforated clay bricks¹³ are

$$\text{Solid} \quad y = 8.88 + 0.116x$$

$$\text{Perforated} \quad y = 8.88 + 0.059x$$

These equations show relationships in the same region as that for calcium silicate bricks.

In Table 10 of CP 111 : 1970¹⁴ by interpolation a load factor of 8 is stipulated for these conditions of wall testing. In Figure 12 a to c the wall strengths are divided by the load factor 8 and the lines are the values of permissible stress determined according to the Code of Practice. It will be seen that all the points lie above the line indicating that calcium silicate bricks perform satisfactorily and that under axial compressive loading calcium silicate brickwork behaves at least as well as clay brickwork.

4. SUMMARY AND CONCLUSIONS

The work of a national research organisation on the behaviour of masonry in use will inevitably be concerned, often to a considerable extent, with areas of ignorance revealed by the revision of design codes. The original work on axial and eccentric loading of masonry composed of solid or cored bricks confirmed that the latter could be safely used.

The work on gas explosions was necessary to make government rethink the panic measures taken after the Ronan Point disaster and the current work on lateral loading is a response to a revised wind code which many regard as impossibly severe and at variance with observed practice. The compressive resistance of calcium silicate brickwork, however, was determined to satisfy the manufacturers that their product could indeed stand comparison with clay brickwork.

Besides these programmes for member industries BCRA carries out sponsored work for companies and consultants world wide. The results are confidential to the sponsors, but include work on d.p.c. materials, mortar additives, special ties, fixings and anchors, new masonry units, flooring systems, prefabricated masonry panels and portions of complete structures. All the research demonstrates that load-bearing masonry is a most efficient, economical, structural material with which engineers and architects should be more conversant in order to maintain and enlarge the attractive human environment that it provides.

ACKNOWLEDGEMENTS

The author thanks Mr. A. Dinsdale, O.B.E., Director, British Ceramic Research Association, for permission to publish this paper.

All the work reported has been carried out by the construction and testing team under the divisional Chief Engineer, Mr. H.R. Hodgkinson, who regularly performs the impossible and to whom no thanks can be too great.

Since January 1977 the research on lateral load resistance has been funded by the Building Research Establishment.

APPENDIX I

1. BRITISH STANDARDS INSTITUTION, Structural Recommendations for Load-bearing Walls, CP 111:1948.
2. DAVEY, N. and THOMAS, F.G., The Structural Uses of Brickwork, Institute of Civil Eng. Struct. and Building Paper No. 24, 1950.
3. BRITISH STANDARDS INSTITUTION, CP 111:1964 (revised edition).
4. HALLER, P., The Properties of Load-bearing Brickwork in Perforated Fired Bricks for Multi-storey Buildings. Schweiz. Bauztg., 76, (28), 1958.
5. WEST, H.W.H., HODGKINSON, H.R., BEECH, D.G. and DAVENPORT, S.T.E., The Performance of Walls Built of Wirecut Bricks with and without Perforations. Proc. Brit. Ceram. Soc., 17, 1970.
6. ASTBURY, N.F., WEST, H.W.H., HODGKINSON, H.R., CUBBAGE, P.A., and CLARE, R., Experiments to Determine the Resistance of Brick Buildings to Gas Explosions. Proceedings Second International Brick Masonry Conference. Edited by H.W.H. West and K.H. Speed, Stoke-on-Trent, B. Ceram. R.A., 1971.
7. BRITISH STANDARDS INSTITUTION, Code of Basic Data for the Design of Buildings Chapter V Loading: Part 2 Wind Loads, C.P.3, Chap. V, Part 2:1972.
8. BRITISH CERAMIC RESEARCH ASSOCIATION, Design Guide for Strapping and Tying of Load-bearing Brickwork in Low-rise Construction, B.Ceram.R.A., Spec. Publ. 93, Stoke-on-Trent, 1977.
9. BRITISH CERAMIC RESEARCH ASSOCIATION, Model Specification for Load-bearing Clay Brickwork, Revised (1975) Edition, B.Ceram.R.A., Spec. Publ.56, Stoke-on-Trent, 1975.
10. WEST, H.W.H., HODGKINSON, H.R., and HASELTINE, B.A., The Resistance of Brickwork to Lateral Loading, Part I: Experimental Methods and Results of Tests on Small Specimens and Full-sized Walls. The Structural Engineer Vol.55, No.10, 411-421, 1977.
11. HASELTINE, B.A., WEST, H.W.H., and TUTT, J.N., The Resistance of Brickwork to Lateral Loading, Part 2: Design of Walls to Resist Lateral Loads. The Structural Engineer, Vol.55, No. 10, 422-430, 1977.
12. BRITISH STANDARDS INSTITUTION, Metal Ties for Cavity Wall Construction, B.S. 1243:1972.
13. WEST, H.W.H., HODGKINSON, H.R., BEECH, D.G., and GOODWIN, J.F., The Compressive Strength of Calcium Silicate Brick Walls under Axial Loading, B.Ceram.R.A. T.N. 262, 1976.
14. BRITISH STANDARDS INSTITUTION, Structural Recommendations for Load-bearing Walls, CP 111:Part 2, 1970.

LIST OF FIGURES

1. Waillette format
2. Flexural strength/water absorption $1:\frac{1}{4}:3$ normal
3. Flexural strength/water absorption $1:\frac{1}{4}:3$ parallel
4. Flexural strength of calcium silicate wailettes 1:1:6
5. Flexural strength of calcium silicate wailettes 1:2:9
6. Typical failure patterns of walls
7. Relationship of failing pressure to length
8. Walls of varying height reduced to effective length
9. Relation of failing pressure to ratio of flexural strength to $(\text{length})^2$
for 102.5 mm walls
10. Calcium silicate bricks: wall strength/brick strength $1:\frac{1}{4}:3$ and 1:2:9
mortars
11. Calcium silicate bricks: wall strength/brick strength 1:1:6 mortar
12. Mean wall strength divided by 8 compared with permissible stress:
(a) $1:\frac{1}{4}:3$ (b) 1:1:6 (c) 1:2:9 mortar

EFFECT OF CONSTITUENT PROPORTIONS ON UNIAXIAL
COMPRESSIVE STRENGTH OF TWO-INCH CUBE SPECIMENS OF
MASONRY MORTARS

By Donald J. Frey¹, Robert J. Helfrich², and Chuan C. Feng³

ABSTRACT: Relationship between the constituent proportions of masonry mortar, consisting of portland cement, hydrated lime, masonry sand, and water and the compressive strength of two-inch cubes are developed. These include charts for designing mortar to have a required compressive strength and for determining compressive strength from known constituent proportions. Also developed are functional graphs and algebraic equations which have been fitted to data and express compressive strength in terms of cement-water ratio.

Data was collected from 435 cube specimens loaded to failure in a compression testing machine at an age of either seven days, twenty-eight days, or six months. All test procedures were as prescribed by the American Society for Testing and Materials.

On the charts which were established from the data, constituent proportions are displayed along with compressive strength. Mathematical formulas for points along the abscissa and ordinate of the charts involve constituent proportions in terms of either weight or volume. Values of strength are conveyed with contour lines. Individual charts for each of the three test specimen ages are presented.

The functional graphs fit to the cement-water ration versus compressive strength data are divided into two regions. For low values of the cement-water ration these are curved and become linear for higher cement-water ration values. Graphs for each of the three test specimen ages are developed.

1 Engineer, Crowther Architects Group, Denver, Colorado
(Formerly Graduate Student, University of Colo. Boulder, Colo.)

2 Technical Director, Colo. Masonry Institute, Denver, Colo.

3 Prof. of Civil Engrg., Univ. of Colo. Boulder, Colorado

EFFECT OF CONSTITUENT PROPORTIONS ON
UNIAXIAL COMPRESSIVE STRENGTH OF TWO-INCH
CUBE SPECIMENS OF MASONRY MORTARS

By Donald J. Frey¹, Robert J. Helfrich², and Chuan C. Feng³

INTRODUCTION

Modern mortar is called upon to perform a number of functions. It is primarily a bonding agent connecting discrete masonry units to form a continuous material. It must also be resistant to water penetration, because it is often used as an environmental barrier. It must be durable to withstand the forces of the environment for the lifespan of a structure. And, mortar must be strong. It must pass loads from one masonry unit to another.

All of the above properties are dependent upon a number of parameters. One of these is the proportion of the constituents with which the mortar is made. The study reported herein was an examination of the effect that the constituent proportions have on the compressive strength of mortar.

Test specimens for this investigation consisted of two inch cubes of portland cement-lime mortar made in precision molds. These specimens were tested for compressive strength in a universal testing machine. The age of the specimens at the time of testing was either seven days, twenty-eight days, or six months. The term "portland cement-lime mortar" as used in this report is a mixture of portland cement, hydrated lime, sand and water.

OBJECTIVE

The standard test, as established by the American Society for Testing and Materials (ASTM) for determining mortar compressive strength, f_c , consists of crushing two inch cubes of mortar in a

¹Engineer, Crowther Architects Group, Denver, Colorado
(Formerly Graduate Student, University of Colorado, Boulder, Colo.)

²Technical Director, Colo. Masonry Institute, Denver, Colo.

³Prof. of Civil Engrg., Univ. of Colo. Boulder, Colorado.

compression testing machine. Most specifications stipulate the compressive strength in pounds per square inch (psi) at an age of twenty-eight days after molding. It is often useful to know the strength at seven days as well. This value can be used to indicate strength at twenty-eight days.

The objective of this research was to determine the effect that constituent proportions have on the compressive strength of two inch cubical mortar specimens at seven days and twenty-eight days after molding, and to present this information to designers in a usable form. Testing cubical specimens in compression is an easy test to perform and is simply a standard test commonly run as measure of the quality of the mortar. This formulation is intended as a first step in correlating strength with the strength of masonry units to determine strength of the assemblage.

TEST PROCEDURES

Procedures for mixing, molding, storing, and testing specimens as well as specifications for equipment were all in accordance with the appropriate ASTM recommendations. (1)² The compression testing machine was fitted with a large swivel head as is usually used for concrete cylinders and the bed fitted with a small 3-¼ inch diameter swivel base to eliminate as much as possible any flexural loading.

TEST RESULTS

The constituents of portland cement-lime mortar are portland cement, hydrated lime, and masonry sand. Water is added to these three ingredients to produce a fluid mix with a flow in the range of 110±5. This study is limited to 44 different mix proportions. The proportions used are shown in Figure 1, entitled "Portland Cement-Lime Mortar Proportions by Volume". In the masonry industry, mortar mix proportions are normally specified by volume and the ingredients are expressed in a standard order.

²Numerals in parentheses refer to corresponding items in the Appendix I - References

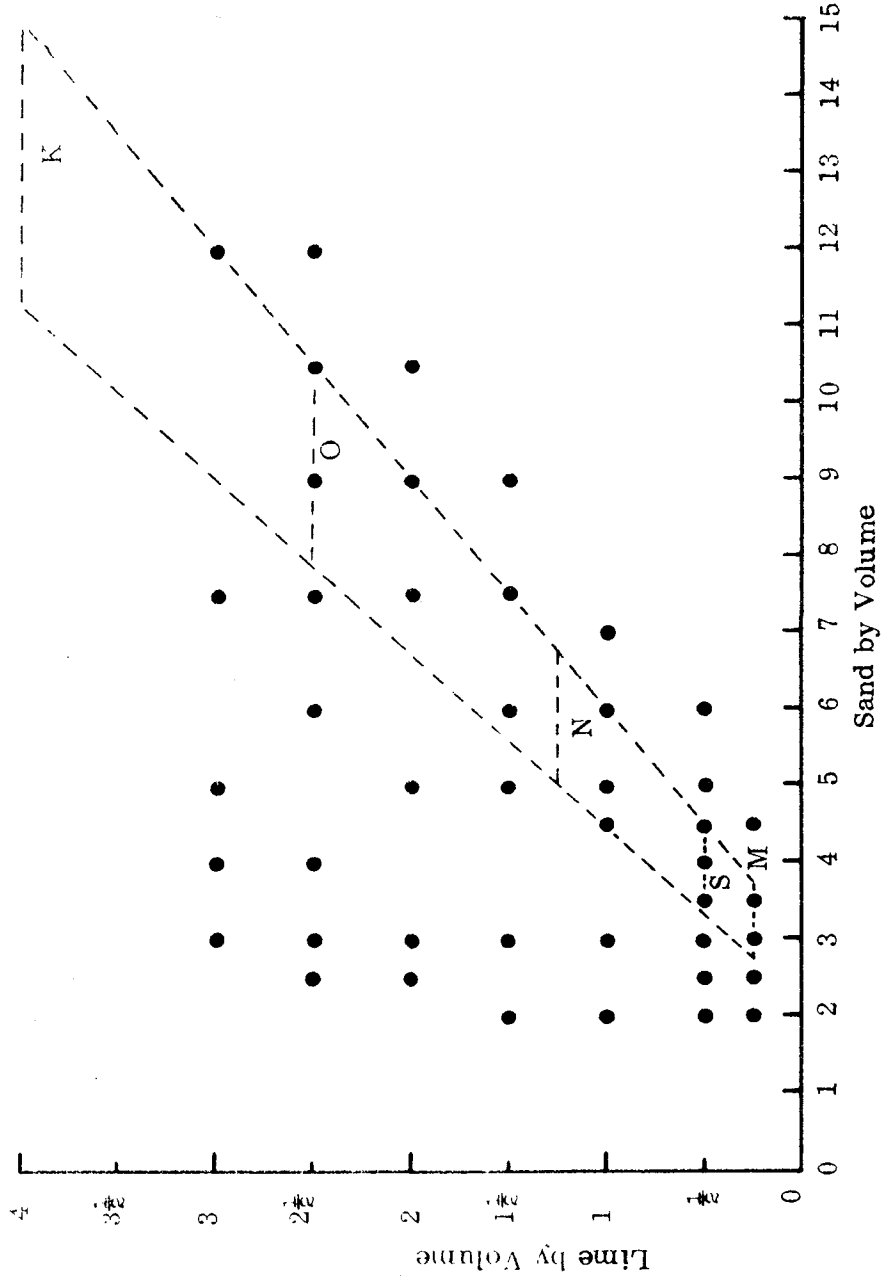


Fig. 1 - Portland Cement - Lime Mortar Proportions by Volume with Portland Cement Normalized to Unity

The number of parts of portland cement is first, followed by the number of parts of lime, and last the number of parts of sand. The amount of water is not specified because it is understood that the mortar will be mixed to a workable consistency. Also, if the mortar dries out on the mortar board it will be retempered to return it to proper consistency. A mix which is specified as a $1 : \frac{1}{2} : 4\frac{1}{2}$ will contain 1 part portland cement, $\frac{1}{2}$ part lime, and $4\frac{1}{2}$ parts sand on a volume basis.

For convenience, the mix proportions are divided by the first term, cement, such that the leading number of the proportions is indicated by unity; mathematically defined as a normalized expression. All expressions in Figure 1 have been normalized in this way so that the abscissa expresses parts of sand by volume and the ordinate expresses parts of lime by volume. The dots are the mixes which were used in this study. The areas which are bounded by lines represent the proportions which are recommended by the ASTM Specifications C 270-71, "Mortar for Unit Masonry." The recommended proportions are designated in C270-71 as type M, S, N, O, and K, and are shown in Fig. 1. In Table 1 the portland cement-lime mortar proportions by volume are shown which constitute the five different types. This table was adapted from Table II in C 270-71.

435 test specimens were molded to represent the portland cement-lime mortars. Of these, 183 were tested for compressive strength at seven days, 183 were tested at twenty-eight days, and 69 were tested after six months. Specimens consisting of standard type mixes only were tested at six months.

At seven days and twenty-eight days the 44 portland cement-lime mixes are represented by 183 test specimens. Either 6 cubes or 3 cubes were tested for each mix. Initially, 6 cubes were tested for each mix. As the testing program progressed, time became a factor, and it became important to have data on a large number of mix proportions rather than to have a small number of mix proportions, each represented by a large number of cubes. Therefore, the number of cubes representing each mix was reduced from 6 to 3.

TABLE I

PORTLAND CEMENT-LIME MORTAR
PROPORTIONS BY VOLUME

Mortar Type	Parts of Portland Cement	Parts of Hydrated Lime	Parts of Aggregate
M....	1	$\frac{1}{4}$	Not less than $2\frac{1}{4}$ and not more than 3 times the sum of the volumes of the cement and lime used.
S....	1	over $\frac{1}{4}$ to $\frac{1}{2}$	
N....	1	over $\frac{1}{2}$ to $1\frac{1}{4}$	
O....	1	over $1\frac{1}{4}$ to $2\frac{1}{2}$	
K....	1	over $2\frac{1}{2}$ to 4	

TABLE II

COMPRESSIVE STRENGTH, f_c , OF CUBES
MADE FROM THE DIFFERENT TYPES OF MORTAR

Mortar Type	Minimum Average Compressive Strength, f_c at 28 Days (psi.)
M.....	2500
S.....	1800
N.....	750
O.....	350
K.....	75

Design Charts

A synthesis of information concerning all the constituent parameters, compressive strength and age was necessary. A design chart to provide this information which could easily be used by professionals was desirable. For clarity a design chart for seven day strength and another chart for twenty-eight day strength was devised.

The design charts developed may be used by engineers, architects, and materials testing personnel. For this reason the charts can be entered either by volume or by weight. The architect and engineer work with mix proportions specified by volume in the order recognized by the mason. The materials testing person works both with volume and with weight.

Figure 2 is the design chart for portland cement-lime mortar cube strength at twenty-eight days after molding, as based on 183 cube samples. This chart incorporates all the features which have been mentioned. The determination of compressive strength can be made once the mix proportions by volume or by weight are known.

To use the chart with weight, the values of the abscissa and the ordinate must be calculated. The abscissa scale on the chart is labeled "Percent Sand $S/(C+S) \times 100$ ". To calculate the abscissa value, the weight of sand is divided by the sum of the weights of the portland cement and sand and the quotient is multiplied by 100 as indicated by the formula. The ordinate, labeled "Percent Lime of Cementitious Materials $L/(L+C) \times 100$ ", is calculated by dividing the weight of lime by the sum of the weight of lime plus cement and then multiplying the quotient by 100. The twenty-eight day strength is then found by locating the unique point described by the intersection of the abscissa and ordinate values, and finding the strength value at that point by interpolating between lines of constant strength. This procedure is similar to determining elevation on a topographic map.

To use the chart by volume, the volumetric mix ratio must first be normalized to a cement value of unity as previously described. Cement has a value of unity everywhere on the chart. The

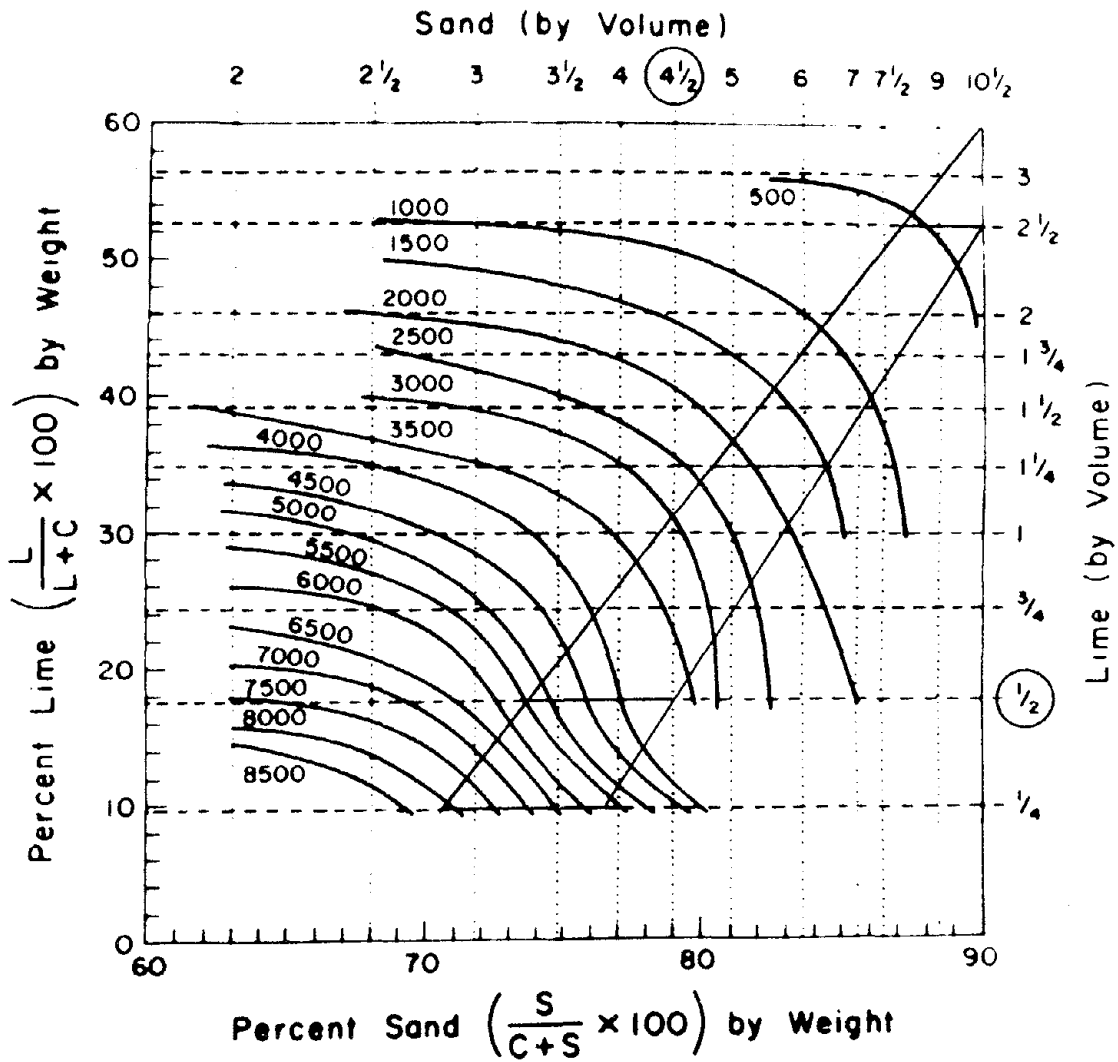


Fig. 2 Portland Cement-Lime Mortar Strength, f_c , at 28 Days Versus Constituent Proportions by Weight and Volume

dashed horizontal lines are lines of constant volumetric lime. They start at $\frac{1}{4}$ part lime and increase to three parts lime as shown by the labels at the right. The dotted vertical lines are for constant volumetric sand. They start at two and increase to the right to a value of ten and one-half. Volumetric mix proportions locate unique points on the chart. The strength value at any point is again determined by interpolating between lines of constant strength.

This type of design chart has a number of desirable features. The primary feature is that it can be used both by weight and by volume. One of the most confusing concepts is working with volumes and also with weights when designing a mix. The chart eliminates this confusion by displaying volume and weight simultaneously.

The abscissa and ordinate in these charts each play a dual role because the charts can be entered with constituent proportions by weight or by volume. The abscissa and ordinate corresponding to proportions by weight were chosen after investigation of alternative forms. The two main criteria for the selection of the axes are that each mix have a unique point in the plane and that constant strength lines be sufficiently widely spaced to be meaningful. In the form selected for these axes, one axis specifies sand content, the other specifies lime content, and the need for an axis for cement is eliminated by making each of the other two axes involved cement. The equation established for the ordinate is:

$$\text{Ordinate} = L/(L+C) \times 100 \quad (1)$$

and is labeled "Percent Lime." This equation uniquely specifies the lime content and also allows lines of constant lime by volume to be horizontal. The equation established for the abscissa is:

$$\text{Abscissa} = S/(C + S) \times 100 \quad (2)$$

and is labeled "Percent Sand." This equation uniquely specifies the sand content and also allows lines of constant sand by volume to be vertical. In the above equations "S" equals the weight of

sand, "C" equals the weight of cement, and "L" equals the weight of lime. Once these axes were determined, values had to be placed on the axes for lime and sand by volume. This was done using the unit weights of cement, lime, and sand and the equations for the abscissa and ordinate given above. The normalization procedure previously explained was used to force the value of cement by volume to unity everywhere in the plane. Calculations for values on the axes, expressing lime and sand by volume, were done next. The value of strength in this chart is expressed in terms of iso-lines or lines of constant strength. In this way the values of cement, lime, sand and strength are expressed on one chart in both volumetric and weight form.

The design chart discussed above does not contain any information about water. Water is the fourth ingredient in portland cement-lime mortar and a complete understanding of its behavior requires knowing something about strength versus water content. A functional graph of cement to water ratio versus strength is shown in Fig. 3. This graph is derived from the same data used to produce Fig. 2. For a cement - water ratio less than .85, the data follow a curved line, and for values greater than .85, they follow a straight line. All of the cement-water ratios produce flow values in the range 110 ± 5 . It is interesting that this plot contains no information about lime or sand. These two materials do require water, so their influence is seen in the term for water. No corrections were made on the values of water for absorption by sand or lime. The two types of plots which have been presented can be used together. The term which relates one to the other is the strength.

Charts of the type shown in Fig. 3 can be helpful in two different ways. One way is to predict how much water is required to produce a flow of 110 ± 5 for a test mix. The other way is to predict the strength of a mix when its cement-water ratio is known. When preparing a mix in the laboratory, the amount of water to use has to be estimated. The volumetric proportions of the mix are known and from these proportions the strength can be found using Fig. 2. With the value of strength known the cement-water ratio is found in Fig. 3 from which the amount of water to use is calculated.

Discussion of Twenty-Eight Day Charts

Figure 2 is the chart which relates cube strength at twenty-eight

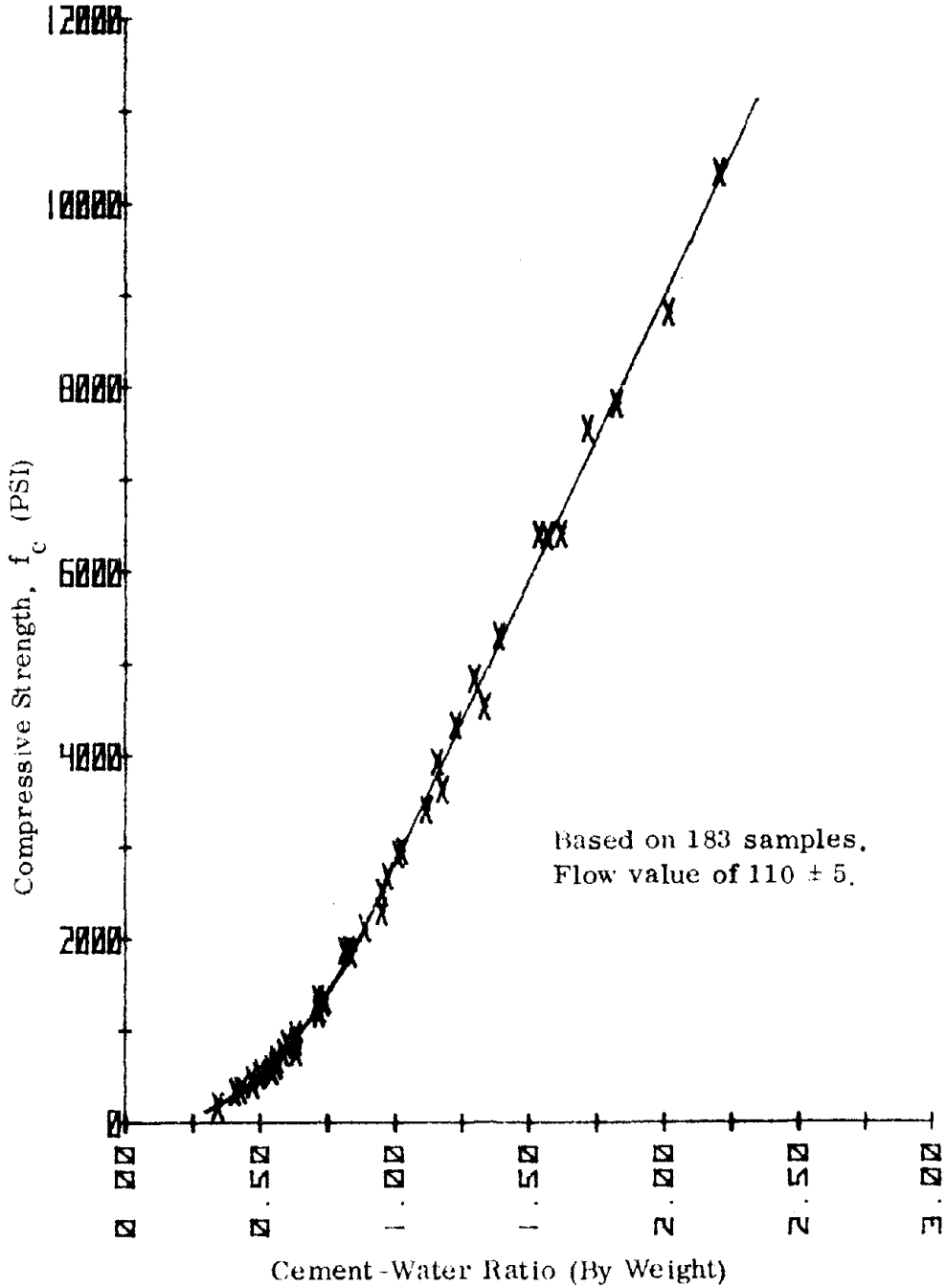


Fig. 3 - Cement-Water Ratio Versus Compressive Strength for Portland Cement - Lime Mortar at 28 Days.

days to mix proportions. A tabulation of the data used to make this chart is found in Table III. The first column in the table gives the volumetric mix ratio in the order portland cement, lime, then sand. All of the ratios in this column have values of cement equal to one and also have lime values greater than or equal to $\frac{1}{4}$. These are limitations placed upon the portland cement-lime mixes. The results that follow are valid only for mixes conforming to these limitations. The weights in grams of each of the ingredients used to prepare each of the mixes are given in columns two through four. Column five contains the cement-water ratio used. Columns six and seven contain the seven days and twenty-eight days strengths, respectively. The strengths shown are the average strengths in each case. This tabulation used in conjunction with the chart shown in Fig. 2 will yield the most accurate estimation of strength.

In this chart the strength curves start at 500 psi and increase to 8500 psi in increments of 500 psi. The lowest strength tabulated is 190 psi, and the highest strength is 10,317 psi. These are the lower and upper bounds of strength which can be found using the chart. The lowest values are at the upper right portion of the chart while the highest values are at the lower left portion. The trapezoidal zones of the standard mortar types, M, S, N, O, and K, are indicated with dark outlines. They are defined by volumetric proportions as shown in Table I. Type M mortar has strength ranging from 5750 psi to 8000 psi. Type S strength ranges from 3625 psi to 8000 psi. Type N strength ranges from 1400 psi to 5500 psi. Type O strength ranges from 365 psi to 2200 psi. Type K strength starts at 590 psi and decreases to 190 psi. Table II is a reprint of Table I in ASTM Specification C270-71. It defines a minimum average compressive strength for each type of mortar at twenty-eight days. There is poor correlation between the values presented in this table and the actual strength values presented above for each type of mortar. It is wrong to assume that if a mix can be categorized as one of the type in Table I it will have a strength similar to the value shown in Table II.

The chart, Fig. 2, has the property of reverse design. That is, given a particular mix, the strength can be determined or for a

desired strength the mix ratio can be designed. For example, for a volumetric mix ratio of 1 : 1 : 5 the strength can be determined as 2500 psi. To design a type S mortar with a strength of 4000 psi, the chart gives the mix ratio 1:½:4.

To determine the amount of water needed to produce a flow of 110 ± 5 in the laboratory, Fig. 3 is used. This is again the chart of cement-water ratio versus compressive strength, f_c . For a cement-water ratio less than .85, the curve follows the parabolic equation:

$$f_c = 111.6 - 1038.4 (C/W) + 3664.3 (C/W)^2 \quad (3)$$

For cement-water ratio values greater than .85, the curve follows the linear equation:

$$f_c = -3347.6 + 6146.8 (C/W) \quad (4)$$

For a mix ratio of 1 : 1 : 5 with a compressive strength of 2500 psi, a cement-water ratio of .951 is required.

Discussion of Seven Days Charts

Cube strength at seven days is related to mix proportions in Fig. 4. The data used to make this chart are also tabulated in Table III. The seven days strength data are found in the sixth column of this table. This tabulation of data should be used in conjunction with the figure to produce the most accurate estimation of strength.

The strength curves in the seven days strength chart start at 500 psi. and increase to 7000 psi. in increments of 500psi. The lowest strength tabulated is 139 psi., and the highest strength is 8112 psi. These are the lower and upper bounds of strength which can be found using this chart. The smallest values are at the upper right hand portion of the chart and the largest values are at the lower left hand portion. The trapezoidal zones of the standard mortar types, M, S, N, O, and K, are indicated with dark outlines. Type M mortar has strength ranging from 4440 psi to 6700 psi. Type S mortar strength ranges from 2400 psi. to 6700 psi. Type N mortar strength ranges from 1000 psi

TABLE III
PORTLAND CEMENT - LIME MIX DATA

Volumetric Mix Ratio C : L : S (a)	Portland Cement (Grams)	Hydrated Lime (Grams)	Masonry Sand (Grams)	C/W ^(b)	Average 7-Day Strength (psi)	Average 28 Day Strength (psi)
1: ¼:2	706	75	1202	2.21	8112	10317
1: ½:2	655	139	1114	1.72	5604	7542
1:1 :2	571	243	972	1.39	4115	5298
1:1½:2	506	323	861	1.12	2619	3406
1: ¼:2½	626	67	1331	2.02	7400	8800
1: ½:2½	585	124	1244	1.54	4687	6396
1:2 :2½	420	357	893	.89	1592	2123
1:2½:2½	384	408	816	.724	931	1243
1: ¼:3	841	90	2151	1.83	6400	7817
1: ½:3	465	99	1188	1.57	4711	6388
1:1 :3	425	181	1088	1.23	3048	4333
1:1½:3	426	272	1088	1.015	2060	2925
1:2 :3	390	332	995	0.814	1235	1873
1:2½:3	358	381	915	0.716	933	1355
1:3 :3	332	423	847	0.604	578	866
1: ¼:3½	763	81	2275	1.623	5056	6406
1: ½:3½	482	102	1435	1.30	3276	4834
1: ¾:4	443	94	1507	1.16	2579	3929
1:2½:4	317	337	1079	.634	728	896
1:3 :4	296	378	1007	.548	421	574
1: ¼:4½	429	46	1644	1.34	3194	4529
1: ½:4½	410	87	1569	1.18	2407	3625
1:1 :4½	562	240	2155	1.03	2198	2962
1: ¾:5	381	81	1622	.976	1722	2685
1:1 :5	526	223	2241	.956	1769	2512
1:1½:5	325	208	1385	.833	1348	1887
1:2 :5	303	258	1291	.721	928	1196
1:3 :5	267	341	1136	.562	475	634
1: ½:6	334	71	1708	.954	1703	2308
1:1 :6	311	132	1589	.840	1193	1847
1:1½:6	436	279	2227	.739	990	1317
1:2½:6	257	274	1314	.590	552	771
1:1 :7	279	119	1664	.744	1025	1346
1:1½:7½	251	160	1601	.635	642	970
1:2 :7½	354	303	2274	.638	589	777
1:2½:7½	225	240	1439	.542	453	606
1:3 :7½	215	274	1370	.477	320	429
1:1½:9	220	141	1689	.564	506	698
1:2 :9	210	179	1609	.506	377	541
1:2½:9	301	319	2305	.501	372	527
1:2 :10½	188	160	1684	.470	341	472
1:2½:10½	181	192	1615	.431	234	364
1:2½:12	164	175	1680	.410	239	344
1:3 :12	159	202	1620	.346	139	190

(a) C = Portland Cement, L = Lime, and S = Sand

(b) C/W = Cement - water ratio by weight

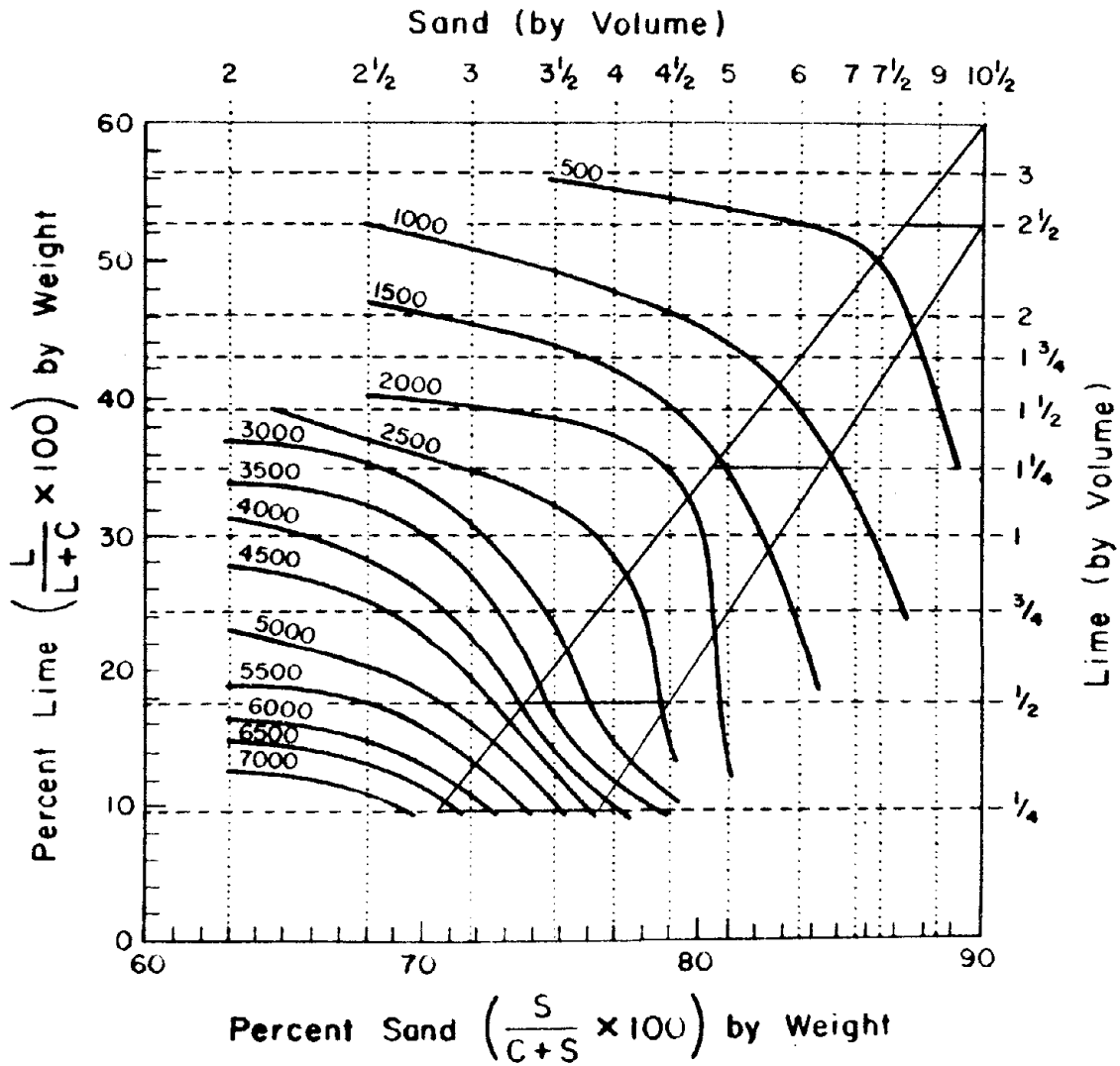


Fig. 4 Portland Cement-Lime Mortar Strength, f_c , at 7 Days Versus Constituent Proportions by Weight and Volume

to 3850 psi. The type O mortar strength ranges from 234 psi to 1500 psi. Type K strength starts at 425 psi and decreases to 139 psi. The ASTM specifications do not put a limit on the strength at seven days. They put a minimum only on twenty-eight days strength.

This design chart is similar in construction to the twenty-eight days chart. The only difference is that the lines of constant strength have shifted position. It, too, allows strength to be determined from a known mix ratio, as well as, allowing the mix ratio to be determined for a desired strength.

Figure 5 is used to determine the amount of water needed to produce a flow of 110 ± 5 in the laboratory. This figure is a plot of cement-water ratio versus compressive strength, f_c . For a cement-water ratio less than 1.35, the curve follows the parabolic equation:

$$f_c = -173.1 + 76.2 (C/W) + 2014.2 (C/W)^2 \quad (5)$$

For values of cement-water ratio greater than 1.35, the curve follows the linear equation:

$$f_c = -3846.6 + 5502.1 (C/W) \quad (6)$$

For mixes prepared in the laboratory and having a flow of 110 ± 5 the cement-water ratio is known. Figure 5 eliminates the need for testing specimens at seven days. Figure 2 eliminates the need for testing specimens at twenty-eight days.

Six months Results

Table IV shows the 15 mix proportions which were included in the six month tests. All of these mixes are standard types as defined in Table I. The strengths ranged from 208 psi. for a mix ratio of 1 : 3 : 12, which is a type K, to 9312 psi. for a mix ratio of 1 : $\frac{1}{4}$: 3, which is a type M. The increases in strength over the 28 day values range from nine percent for a mix ratio of 1 : $2\frac{1}{2}$: $10\frac{1}{2}$ to twenty-seven percent for a mix ratio of 1 : 2 : $7\frac{1}{2}$.

Figure 6 is a plot of cement-water ratio versus strength at six

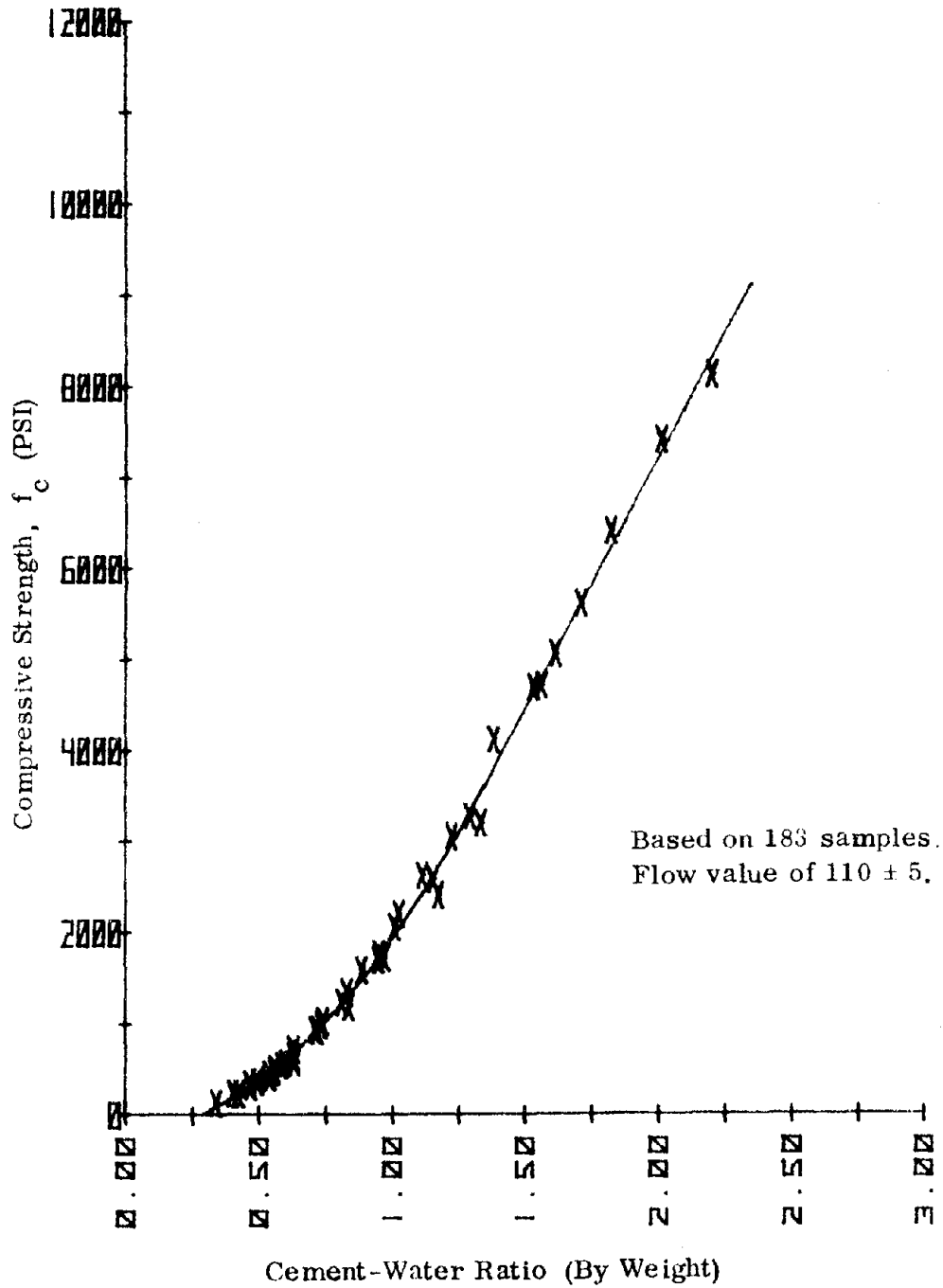


Fig. 5 - Cement-Water Ratio Versus Compressive Strength for Portland Cement-Lime Mortar at 7 Days.

TABLE IV
 PORTLAND CEMENT - LIME MIX DATA
 FOR SIX MONTHS

Volumetric Mix Ratio C:L:S ^(a)	Portland Cement (Grams)	Hydrated Lime (Grams)	Masonry Sand (Grams)	C/W ^(b)	Average 6 Month Strength (psi.)	% Increase Over 28 Day Strength
1: $\frac{1}{4}$:3	841	90	2151	1.83	9312	19.1
1: $\frac{1}{4}$:3 $\frac{1}{2}$	763	81	2275	1.623	7846	22.5
1: $\frac{1}{2}$:3 $\frac{1}{2}$	482	102	1435	1.30	5573	15.3
1: $\frac{1}{2}$:4	443	94	1507	1.16	4562	16.1
1: $\frac{1}{2}$:4 $\frac{1}{2}$	410	87	1569	1.18	4206	16.0
1: 1 :4 $\frac{1}{2}$	562	240	2155	1.03	3669	23.9
1: 1:5	526	223	2241	.956	3071	22.2
1: 1:6	311	132	1589	.840	2112	15.8
1: 1 $\frac{1}{2}$:6	436	279	2227	.739	1617	22.8
1: 1 $\frac{1}{2}$:7 $\frac{1}{2}$	251	160	1601	.635	1057	8.9
1: 2: 7 $\frac{1}{2}$	354	303	2274	.638	990	27.4
1: 2: 9	210	179	1609	.506	604	11.6
1: 2 $\frac{1}{2}$:9	301	319	2305	.501	635	20.5
1: 2 $\frac{1}{2}$:10 $\frac{1}{2}$	181	192	1615	.431	397	9.1
1: 3 :12	159	202	1620	.346	208	9.5

(a) C = Portland Cement, L = Lime, and S = Sand

(b) C/W = Cement - Water ratio by weight

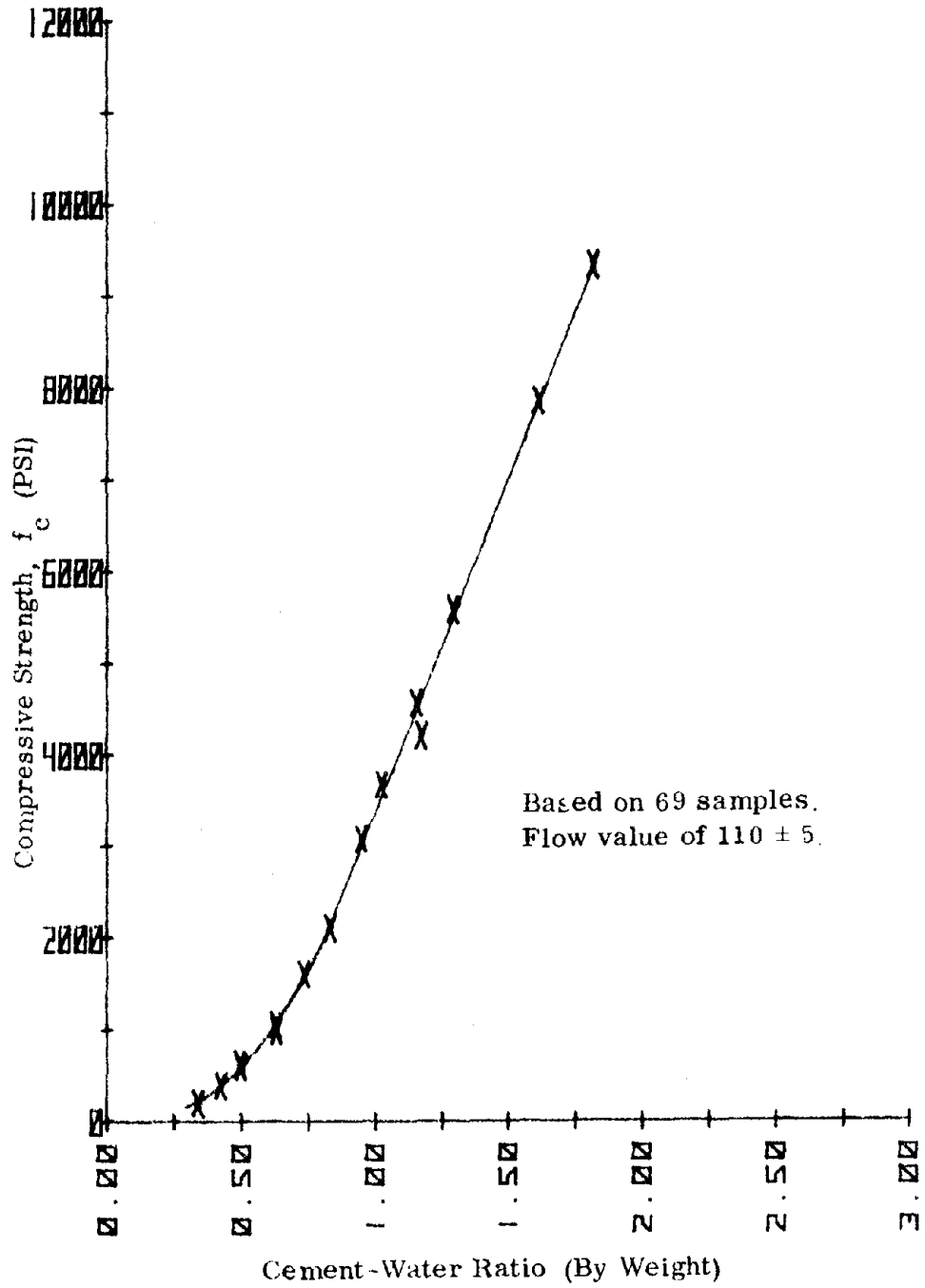


Fig. 6 - Cement-Water Ratio Versus Compressive Strength for Portland Cement-Lime Mortar at Six Months

months. This plot is based on 69 cubes from 15 different mix ratios. This graph allows six months strength to be predicted from a known cement-water ratio producing a flow of 110 ± 5 , when the chart in Fig. 6 is used in conjunction with the charts in Fig. 2 and Fig. 3, the twenty-eight days strength and six months strength can be designed. Also, using these three plots, the six months and twenty-eight days strength of a mix can be found from its volumetric proportions. To illustrate this last procedure, a type M mix with a volumetric mix ratio of $1 : \frac{1}{4} : 3\frac{1}{2}$ will be used. From Fig. 2 this mix will have a twenty-eight days strength of 6400psi. Figure 3 is now entered with a strength of 6400 psi. The cement-water ratio is found to be 1.58. Figure 6 is then entered with the cement-water ratio of 1.58 and gives a six months strength of 7500 psi. The actual value measured in the laboratory is 7846 psi. Using the three charts gave an error of only five percent. The equation indicated with each graph should be used to give the most accurate results.

The curve in Fig. 6 is broken into two regions. The first portion of the curve, for a cement water ratio less than .816 is curved.

In this region the parabolic equation,

$$f_c = 217.1 - 1550.9 (C/W) + 4547.9 (C/W)^2 \quad (7)$$

fits the data well. The second portion of the curve, for a cement-water ratio greater than or equal to .816, is well approximated by the linear equation,

$$f_c = -3919.3 + 7229.1 (C/W). \quad (8)$$

SUMMARY

The relationships between the compressive strength of 2 - inch cubes of portland cement-lime mortar and constituent proportions has been thoroughly investigated in the present study. These are presented in design charts and plots of cement-water ratio versus compressive strength, f_c . The design charts can be used to determine compressive strength from knowledge of constituent proportions either by volume or by weight. Charts were prepared for strength at seven days and at twenty-eight days. The plots of cement-water ratio versus compressive strength are also established for strength at seven days and twenty-eight days. These relationships have been determined using only ASTM procedures. Therefore, flow values were maintained in the range 110 ± 5 and the temperature throughout kept at approximately 72°F .

CONCLUSIONS

The objective of this research, as previously stated, was "to determine the effect that constituent proportions have on compressive strength of two inch cubical mortar specimens at seven days and twenty-eight days after molding, and to present this information to designers in a usable form." This objective has been reached and a number of conclusions have been made for the mortars tested.

The conclusions are:

1. Laboratory standardization of tests has been established. Using these procedures, tests results are repeatable.
2. Regardless of the mix ratio, the strength at twenty-eight days exceeds the strength at seven days. And, the strength at six months exceeds the strength at twenty-eight days.
3. Compressive strength can be predicted for the materials used in this study from constituent proportions using design charts (Fig. 1, Fig. 3.)
4. The design charts contain regions which correspond to mortar types M, S, N, O, and K as defined by Table II in ASTM Specification C 270-71. (Fig. 1, Fig. 3.)

5. Compressive strength, f_c , can be predicted for the materials used in this study from the cement-water ratio.

(Fig. 2, Fig. 4, Fig. 5)

6. A portion of the cement-water ratio versus compressive strength, f_c , data is curved while the other portion is linear. Algebraic expressions have been written for each portion, and the region to which each pertains has been defined.

(Fig. 2, Fig. 4, Fig. 5)

7. For the mortars tested, the compressive strength f_c , decreases as the amount of lime increases while sand and portland cement content are held constant.

8. For the mortars tested, the compressive strength, f_c , decreases as the amount of sand increases while lime and portland cement content are held constant.

9. For the mortars tested the compressive strength, f_c , increases as the amount of portland cement increases while lime and sand content are held constant.

10. All mortar mixes in this study were made with Colorado-produced materials and have compressive strengths which exceed the minimum values established by Table I in ASTM Specification C 270-71.

11. It was found that it is possible to express the mix ratios by volume of portland cement-lime mortar on a plot of "sand by volume" versus "lime by volume," if the portland cement value is normalized to unity (Fig. 1).

APPENDIX I
REFERENCES

1. Annual Book of ASTM Standards, American Society for Testing and Materials, Philadelphia, Pa., 1973, Specifications for C 91-71, Masonry Cement, Part 9; C 109-73, Compressive Strength of Hydraulic Cement Mortars, (Using 2-in. (50-mm.) Cube Specimens), Part 9; C 144-70, Aggregate for Masonry Mortar, Part 12; C150-73a, Standard Specifications for Portland Cement, Part 9; C 207-49 (Reapproved 1968), Hydrated Lime for Masonry Purposes, Part 9; C 230-68, Flow Table for Use in Tests of Hydraulic Cement, Part 9; C270-71, Mortar for Unit Masonry, Part 12; C 305-65 (Reapproved 1970), Mechanical Mixing of Hydraulic Cement Pastes and Mortars of Plastic Consistency, Part 9.

SINTERED COAL REFUSE LIGHTWEIGHT MASONRY AGGREGATE

By Rose, J. G., Assoc. Prof. of Civ. Engrg, Univ. of Kentucky

ABSTRACT: The availability of economical, quality aggregates for use in many varied construction applications is an important requisite for the construction industry of this country. This paper describes the development and evaluation of a synthetic lightweight aggregate, having particular application to the concrete masonry industry.

Bituminous coal refuse, a waste product obtained from five coal preparation plants in Kentucky, was successfully sintered on a traveling grate to produce lightweight construction aggregate. Brief discussions are presented on the origin of coal refuse and of the aggregate processing operation. Detailed descriptions are given of laboratory evaluations of the sintered aggregate to determine its suitability for use in manufactured concrete masonry products. Standard-size concrete blocks were fabricated using the sintered aggregate for purposes of ascertaining strength, durability, weight and heat conductivity properties. Results were compared with similarly-produced limestone control blocks. Test parameters were determined to be satisfactory.

Also described are advantages of lightweight aggregate and resultant benefits derivable from using coal refuse as a raw material for sintered lightweight aggregate production.

SINTERED COAL REFUSE LIGHTWEIGHT MASONRY AGGREGATE

By Jerry G. Rose¹

INTRODUCTION

The demands for quality aggregates for various construction applications have resulted in aggregate shortages in many parts of this country, with some areas experiencing a depletion of all quality natural aggregates (8,11).² Environmental constraints and urban sprawl have curtailed production in some areas where aggregate supplies are abundant. Although natural aggregate reserves are virtually inexhaustible in this country, geographic distribution and quality do not necessarily coincide with need, thus necessitating high costs for transporting the heavy, bulky commodity.

The manufacture of synthetic aggregates and the utilization of by-product (waste) materials represent means that are being used in order to provide locally available aggregates and/or aggregates having particular characteristics. Blast and steel furnace slag, power plant ash and various mine tailings, wastes, etc., represent by-product materials in current use. The most commonly manufactured synthetic aggregate is expanded lightweight shale (clay or slate), produced by heating the raw product to about 2000°F in a rotary kiln. At this elevated temperature, gasses are generated which expand (bloat) the material, while the high temperatures stabilize the material. A less commonly used method for producing synthetic lightweight aggregate is the continuous sintering grate process in which the raw material and an added fuel charge are placed on a traveling bed and ignited. As the product sinters (or burns) the particles fuse together and the carbon fuel burns, creating void spaces within the aggregate particles.

The Expanded Shale, Clay, and Slate Institute and the Lightweight Aggregate Producers Association promote the production and use of synthetic lightweight aggregates. All fuel requirements for rotary kiln processing are provided from an external fuel source, whereas the sintering operation requires only minimal external fuel with the bulk contained in the raw feed material.

During the past three years, the Department of Civil Engineering at the University of Kentucky has been involved in research studies to develop uses for bituminous coal refuse materials (2,5,6,12,13,14,15). Similar studies have been conducted in Great Britain, Pennsylvania, and

¹Assoc. Prof. of Civ. Engrg., Univ. of Kentucky, Lexington, Kentucky.

²Numerals in parentheses refer to corresponding items in Appendix I. - References.

elsewhere (7,10). The possibilities of converting the refuse into high-quality lightweight aggregate were examined. An evaluation was made of the technical competence of synthetic lightweight aggregate produced from the sintering of bituminous coal refuse. In order to accomplish this, a thorough laboratory evaluation was conducted on the sintered material. The basic goal of the research is to determine the capabilities of material for use as an aggregate for concrete building materials.

The purpose of this paper is to briefly discuss the origin of coal refuse and the production of sintered coal refuse lightweight aggregate, and to more fully describe laboratory studies which were conducted on the sintered aggregate to determine its suitability for use in manufacturing lightweight concrete masonry blocks.

COAL REFUSE

Coal refuse is a mixture of fragmented materials which are removed from the run-of-mine coal during the cleaning and preparation process so that the quality of the coal will be improved. Sources of refuse materials have been described (15) as follows:

Thin bands of shale and clay, and other impurities and minerals are inherent within the coal seam. Occasionally a coal seam will divide, or part vertically with an attendant thick layer of clay or shale filling the parting. With mechanized equipment it is easier and cheaper to extract a seam of coal with unwanted impurities than to try to mine only the pure coal. Contamination from overburden provides an additional source of impurities in strip mining operations. In underground mining it is sometimes necessary to mine a portion of the roof or floor in order to provide a satisfactory roof for clearance support or a hard, stable floor to work on. At selected locations the roof must be taken for overcasts and other ventilation structures. Many times the coal-seam thickness will decrease, thus requiring more roof and floor to be taken in order to provide clearances for mechanized mining and hauling equipment. Vertical cleates containing minerals are sometimes encountered. All these conditions provide sources for the refuse materials.

The processing is accomplished in preparation plants, some of which process as much as 20,000 tons of coal per day. Since coal has a lower specific gravity than the refuse materials, the coarser fractions are normally separated by heavy-media methods. Special frothing agents which attach to and float the coal are commonly utilized as a medium to separate the fine coal and refuse (5). The processes involved in the cleaning and preparation operations are depicted in Fig. 1.

Approximately 50 percent of the coal mined in this country is processed in preparation plants. The reject is about 25 percent of the 300 million tons of coal, or 75 million tons of refuse annually. Some 20

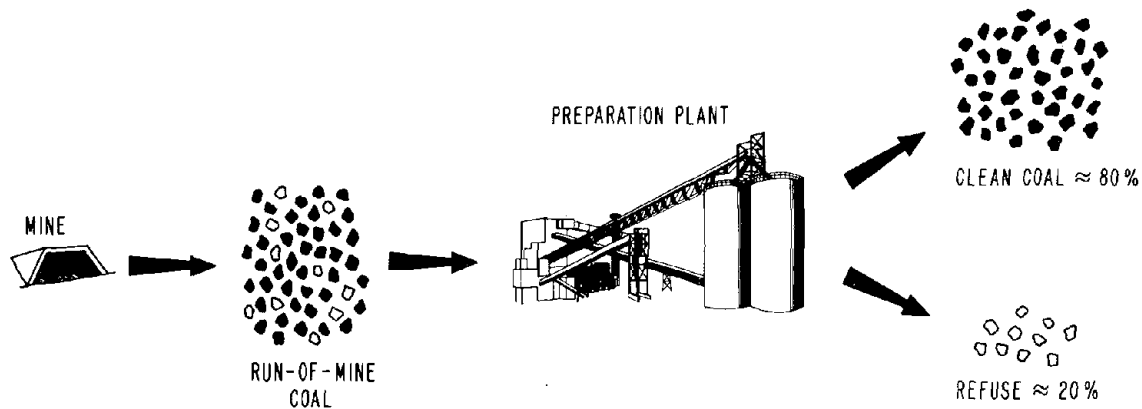


FIG. 1. - Generation of Coal Refuse

million tons of refuse are being produced yearly in Kentucky at present production rates (5,15). As the demand for coal increases during the coming years, it is anticipated that refuse production will increase at an even greater rate since a larger percentage of the coal will be processed. Environmental standards are demanding higher-quality, cleaner-burning coals which will require more intensive cleaning. This is particularly true in areas where lower-quality seams are now being mined since the higher-quality seams have previously been mined. Also, modern automated mines produce larger percentages of reject materials due to the lack of selected mining. In addition, cleaned and processed coal results in a constant quality product, a lower cost to transport since the nonburning fraction is removed at the mine site, and a market price increase of several dollars per ton over run-of-mine coal. The problem of how to dispose of the increasing quantity of refuse in an economical and environmentally acceptable manner is an issue currently facing the coal industry (4).

Conventional disposal practices involve either placing the refuse in large waste piles or pumping it behind retaining structures. It presently costs \$0.50 to \$1.00 per ton to dispose of the refuse, or an industry cost in this country of over \$50 million per year. The per-ton disposal costs are increasing due to higher costs associated with more stringent environmental controls (15). Obviously, if utilization of the coal refuse could be affected, it would eliminate the need for involved, permanent disposal facilities.

SINTERED AGGREGATE PROCESSING

PRELIMINARY PROCESSING

Preliminary pilot-scale rotary-kiln firings and bench-scale sinter

pot firings were conducted using small samples of the material (2).

Rotary-kiln tests at the Texas Transportation Institute Research Center indicated that bituminous coal refuse responded to rotary-kiln processing and a lightweight product could be produced, although some handling problems were encountered. However, no fuel benefit was obtained from the inherent carbon content in the refuse, since the generated heat exited through the stack and did not assist in further heating of the product. Environmental problems were also encountered because of the high sulfur content of the bituminous coal in the refuse.

Sinter pot firings using the bituminous coal refuse were made at McDowell-Wellman Engineering Company in Cleveland, Ohio. The test apparatus consisted of a balling disc and a sinter test pot to which the refuse responded favorably. Laboratory analyses of the small quantity of sintered aggregate produced indicated a high-quality, lightweight product. As expected, exhaust gasses from the batch sintering tests contained considerable smoke-sulfur emissions as particulates of carbon and condensable hydrocarbons from the bituminous coal inherent with the refuse. However, several tests performed with simulated recycle draft within designed time-temperature cycles indicated that the raw materials should respond to a multi-pass recycle draft sintering system.

PILOT PLANT PROCESSING

Following the favorable preliminary results, pilot plant tests were conducted using an improved sintering process to minimize exhaust draft quantities and to arrest combustibles in the draft stream through recycling and post-bed combustion. The intent of the pilot plant program was to demonstrate process feasibility on a practical scale and to provide tonnage samples of aggregate for large-scale product evaluation studies.

The sintering process has been basically described (3) as follows:

In principle, the sintering process consists of charging a bed of fine moistened materials, which are then subjected to heat developed by combustion of fuel within the bed while individual particles are kept in quiescent state. An air draft is induced through the bed, made porous for the operation, and this draft combined with an ignited solid fuel provides combustion. Through heat transfer the sintering process is completed. Usually mixing, igniting, burning, and cooling are the main phases of the generic term "sintering".

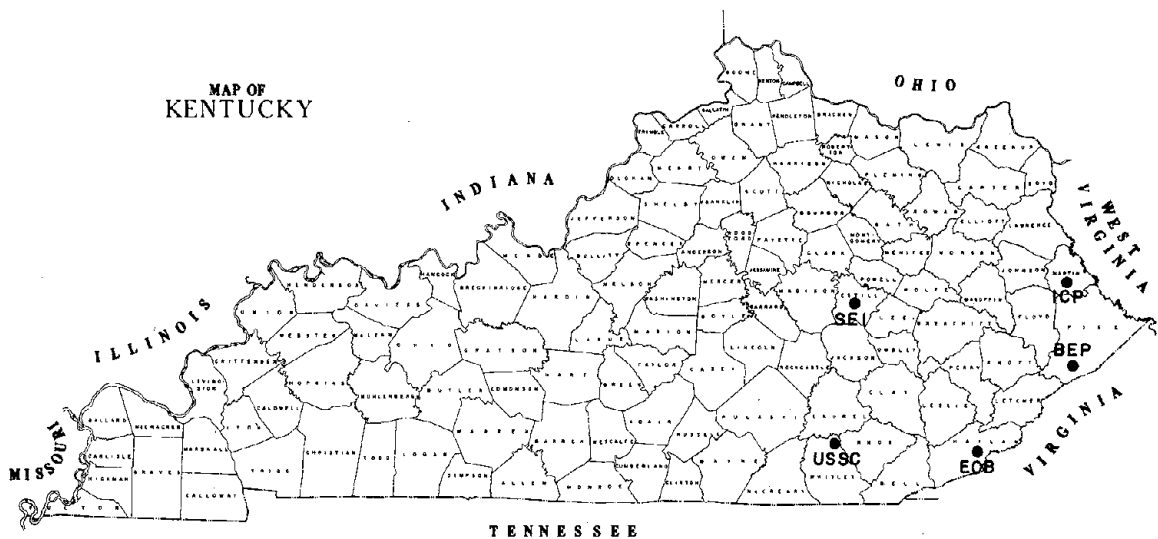
When first developed, the sintering process was performed in a large vessel, however in 1906 the continuous sintering process was invented by A. S. Dwight and R. L. Lloyd. Although primarily used for beneficiating metallic ores, the process has been used for other purposes including the processing of lightweight aggregate.

Refuse samples were obtained from five large coal preparation plants

in Eastern Kentucky, as noted in Fig. 2. They are typical of "total cleaning" plants in the Eastern Kentucky coal fields. A view of a typical refuse sample is shown in Fig. 3. The plus one-inch material was initially screened from the samples. Bulk density, moisture content and typical coal analyses of the raw refuse, as sampled, are given in Table 1. Prior to processing on the traveling grate, the refuse was permitted to dry to about 4.0 percent moisture content and hammermilled until more than 90 percent passed a 3/8-inch screen.

An extensive evaluation of processing conditions was made on the refuse obtained from the South-East Coal Company plant at Irvine (SEI). Fourteen material balance tests were conducted during the pilot plant program, not including a preliminary run. Sufficient data were acquired during the tests to establish a materials balance (optimum bed content of materials to be sintered), a draft flow circuit, and product analyses. Data collected were analyzed after each pilot plant test and this information was used to establish processing conditions for subsequent tests.

The operation of the pilot plant involved delivering the crushed raw refuse and a selected amount of return (partially sintered material from previous runs) to a nodulizing-balling disc. This consisted of an inclined rotary pan, and was used to blend and nodulize the raw feed, particularly fine material. The raw feed was discharged onto a two-foot



Legend:

- SEI - South-East Coal Co., Irvine Plant
- ICP - Island Creek Coal Co., Pevler Plant
- BEP - Beth-Elkhorn Corp., Pike Plant
- EOB - Eastover Mining Co., Brookside Plant
- USSC - U. S. Steel Corp., Corbin Plant

FIG. 2. - Preparation Plant Refuse Sampling Sites

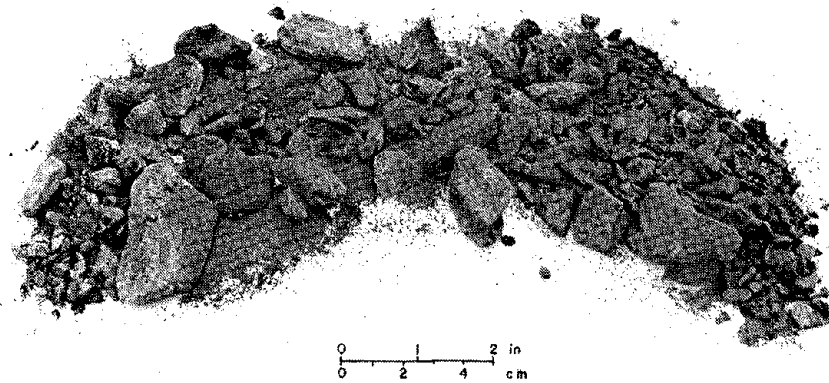


FIG. 3. - Raw Refuse as Sampled

TABLE 1. - As Sampled Raw Refuse Data

Plant	SEI	SEI-BC	ICP	BEP	EOB	USSC
Bulk Density, lb/ft ³	76.9	-	-	-	-	-
Moisture Content, %	8.1	10.6	12.5	-	9.1	11.6
Size, inch	-1.0	-3/8	-3/8	-3/8	-3/8	-3/8
Ash,* %	80.2	86.1	57.6	74.5	77.0	71.6
Volatile Matter,* %	12.0	8.4	19.3	13.5	13.8	14.2
Fixed Carbon,* %	7.8	5.5	22.8	12.0	8.7	14.2
Total Sulfur,* %	2.3	1.6	1.1	0.8	1.1	1.3
Heating Value,* Btu/lb	1380	970	4900	2500	2460	3430

*Moisture-Free Condition

wide by 18-foot long traveling grate machine positioned over active wind boxes, as illustrated in Fig. 4. Ignition of the nodulized feed was accomplished with natural gas ignition torches. Various feed rates, percentages of returns, bed depths, machine speeds, ignition times, and recycle and exhaust wind box flows were investigated. When the pilot plant was stabilized, as evidenced by relatively uniform conditions of

operation, the plus one-inch product (sinter cake) produced during the specific period was collected and saved for subsequent evaluations. The minus 3/8-inch size was used for returns, as was a portion of the minus one-inch to plus 3/8-inch size. The draft was incinerated in an after-burner, then exhausted to a scrubber and finally to a stack (1).

Less extensive evaluations were made on samples obtained from the other four plants and only small quantities of these were sintered. In addition, a sample consisting of 70 percent SEI refuse and 30 percent noncarbonaceous (blue) clay was also sintered. The blue clay was located adjacent to the plant. Its sample designation was SEI-BC.

It was concluded that the improved sintering process embodying strand cooling and draft recycle could be favorably applied to sintering of coal mine waste materials. Sinter quality appeared satisfactory and relatively low quantities of draft were available in a hot stream for final decomposition to produce a stack exhaust clear of visible emissions. The raw materials were relatively high in fuel content and possessed strong bloating characteristics. This necessitated use of high return levels and shallow beds as a means of controlling sinter operation and bed permeability. These raw material factors limited the full benefits of the improved sintering process because the high fuel content did not consistently enable complete strand cooling of the product. It was believed that the effect of these factors could be minimized through use of refuse containing a lower fuel value or a blend of some inert materials such as clay or sand within the sinter charge.

AGGREGATE PRODUCT EVALUATION

Bulk quantities of the sinter cake material were processed in the laboratory for use as graded aggregate in concrete blocks. The sinter

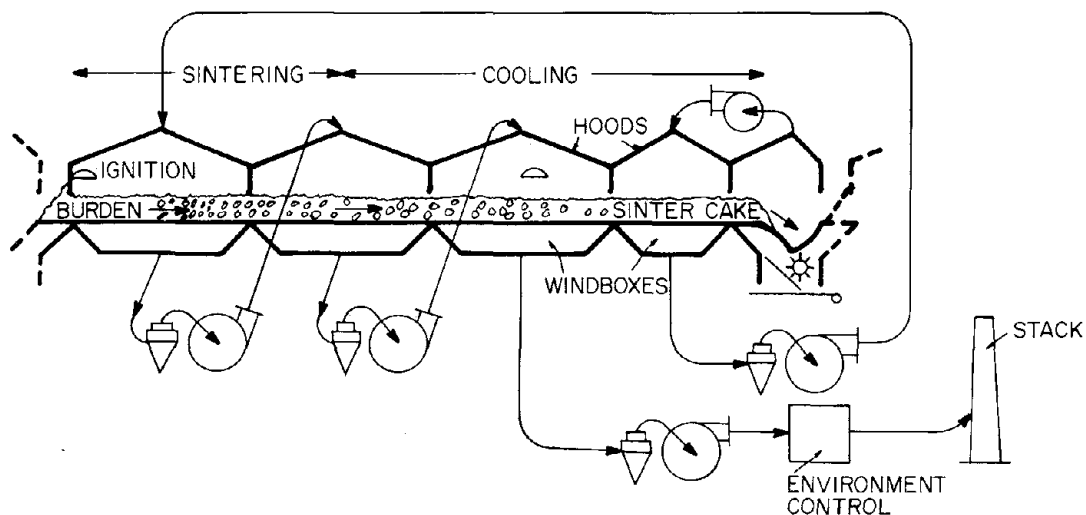


FIG. 4. - Traveling Grate Sintering Process

cake, Fig. 5, was crushed and screened to obtain the block grading shown in Table 2.

Laboratory tests were conducted on the discrete aggregate particles and comparisons of test values were made with those specified by the American Society for Testing and Materials (ASTM) designation C 331 "Lightweight Aggregates for Concrete Masonry Units" (18). Unit weight, deleterious substances and concrete-making properties were evaluated in accordance with the test procedures specified by ASTM C 331. In addition, bulk specific gravity and water absorption tests were conducted.

DRY-LOOSE UNIT WEIGHT

Unit weight was determined in accordance with ASTM C 29 (17) using the shoveling procedure. The net weight of dry-loose graded aggregate required to fill a one-half cubic foot measure was determined and the unit weight calculated.

ASTM C 331 specifies that the dry-loose unit weight of combined fine and coarse lightweight aggregate must be less than 65 lb/ft^3 . As noted in Table 3, all unit weights were much lower, ranging from 39 to 49 lb/ft^3 . The lower values are caused by a combination of low specific gravity of the sintered aggregate and rough surface texture which prevents a tight packing condition. Most rotary-kiln produced lightweight aggregates are slightly heavier and have smoother surface texture.

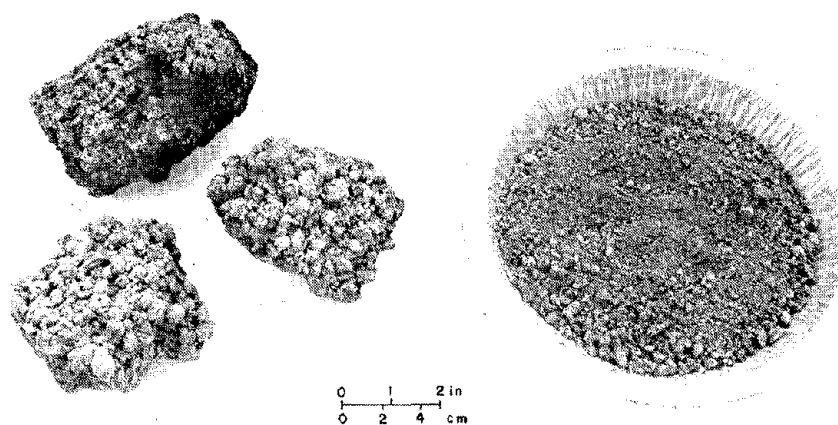


FIG. 5. - Sinter Cake and Crushed Block-Graded Material

TABLE 2. - Sintered Aggregate Block Grading

Sieve Size	Percent Passing By Weight *
1/2 in.	100
3/8 in.	90-100
No. 4	65-90
No. 8	35-65
No. 16	-
No. 50	10-25
No. 100	5-15

*Conforms to ASTM C 331 grading requirements for combined fine and coarse aggregate, 3/8-inch to 0 size.

DELETERIOUS SUBSTANCES

Organic Impurities

This test is used to detect the presence of materials in natural sands which might cause harmful effects in concrete products. The procedure followed was ASTM C 40 (17) (Alternate Procedure B) in which the material to be tested is soaked in a sodium hydroxide solution for 24 hours at which time the color of the supernatant liquid above the test sample is compared with a reference standard color. No organic impurities were indicated in any of the aggregate groups.

Staining Materials

This test is used to indicate the presence of iron compounds which produce staining in concrete products. The procedure, ASTM C 641 (17) involves material which is 3/8-inch by No. 30 sieve size. The aggregate is wrapped in a filter paper, saturated with water, and placed in a steam bath for 16 hours. The filter paper is then washed, dried, and compared to photographic reference standards. The average staining values were very light, light and moderate, as noted in Table 3. The ASTM specifications for lightweight blocks state that aggregate must be classified as lighter than heavy stain, thus all samples meet that criteria.

Clay Lumps

The test was conducted as outlined in ASTM C 142 (17) the determination of clay lumps and friable particles in natural aggregates. The procedure involved covering the No. 4 to No. 16 samples with water for 24 \pm 4 hours, rolling the particles between the fingers in order to

TABLE 3. - Unit Weight and Deleterious Materials Test Data

Plant	SEI	SEI-BC	ICP	BEP	EOB	USSC	ASTM C 331 Specifications
Dry-Loose Unit Weight, lb/ft ³	45.3	46.6	49.2	41.9	39.5	42.3	65 max
Organic Impurities	negative	negative	negative	negative	negative	negative	negative
Staining Materials, index	very light-light	light-moderate	light	very light-light	very light-light	light	less than "heavy stain"
Clay Lumps, %	1.5	1.8	1.4	1.1	1.8	1.4	2% max
Loss on Ignition, %	3.3	3.2	6.3	4.1	4.4	4.4	5% max

break any that contain clay lumps, and then wet sieving the material. The percent clay lumps and friable particles is calculated by dividing the weight of dry material passing the sieve on which it was originally retained by the original dry weight and multiplying by 100. The percent clay lumps values were all less than the two percent specification. Table 3 reports the test values.

Loss on Ignition

The loss on ignition test was performed in order to determine if the material had been completely fired during the sintering process. Values were determined in accordance with ASTM C 114 (16) (referee method). Samples were heated to 950°C and held until constant weight was obtained. The percent loss in weight was calculated.

As noted in Table 3, except for the ICP sample, the loss on ignition values were all less than the five percent maximum specification.

CONCRETE MAKING PROPERTIES

Drying Shrinkage

The determination of the length change of the hardened concrete was made in accordance with ASTM C 331 (18) and C 157 (17) using 100 percent sintered aggregate. The prism molds were filled in two layers, each rodded 33 times. After curing 23.5 ± 0.5 hours, they were removed from the molds and placed in saturated lime water at $73.4 \pm 3^\circ\text{F}$. At an age of seven days, the specimens were removed from the moist storage and an initial length measurement was made. The specimens were then stored at a temperature of $73.4 \pm 3^\circ\text{F}$ and relative humidity of 50 ± 2 percent. Subsequent measurements were made at 28 and 100 days. The percent change in length was calculated after both measurements as the change in corrected dial gage reading divided by the length of the specimen, 11.25 inches. The length change data, reported in Table 4, indicates that all the specimens were below the 0.10 percent maximum permitted shrinkage at 100 days.

Popouts

Specimens of 100 percent sintered aggregate were evaluated by the procedures described in ASTM C 331 (18) and ASTM C 151 (16). The mix was prepared in the proportions of one part of cement to six parts sintered aggregate, by dry loose volume. The mix was prepared with a two- to three-inch slump and was placed in a 3 x 3 x 11.5-inch prism mold in two layers, each rodded 33 times. The filled mold was then cured in a moist room for 24 ± 0.5 hours, at which time the specimen was removed from the mold and placed into an autoclave. The autoclave vessel was brought to a pressure of 295 psi and that condition was maintained for three hours, at which time a slow cooling period was begun. Upon removal from the autoclave, visual inspection of the entire specimen indicated no popouts had occurred.

TABLE 4. - Concrete-Making Properties Test Data

	SEI	SEI-BC	ICP	BEP	EOB	USSC	ASTM C 331 Specifications
Drying Shrinkage, %							-0.10, max
28 days	-0.023	-0.036	-0.036	-0.036	-0.036	-0.036	
100 days	-0.056	-0.062	-0.062	-0.058	-0.066	-0.058	
Popouts, autoclave	None	None	None	None	None	None	None
Freeze-Thaw Durability*	Excellent	Excellent	Excellent	Excellent	Excellent	Excellent	300 cycles +

*Test discontinued after 350 cycles. The durability factor was 100 percent for all specimens.

Freeze-Thaw Durability

The specimens for the freeze-thaw test were prepared as specified in ASTM C 331 (18), using air-entrained concrete. The determination of the resistance of the concrete to rapidly repeated cycles of freezing and thawing was completed in accordance with ASTM C 666 (17). The apparatus used followed Procedure B - freezing in air and thawing in water. The samples were made in prism molds measuring 4 x 3 x 16 inches, filled in two equal layers, and rodded 32 strokes per layer. After curing one day in the molds, the specimens were immersed in saturated lime water at $73.4 \pm 3^\circ\text{F}$ for 14 days. The specimens were then brought to a temperature of $42.5 \pm 5^\circ\text{F}$, immediately weighed, and tested for fundamental transverse frequency as described in ASTM C 215 (17). The prisms were then placed in the freeze-thaw chamber which subjects them to a 2.5-hour freeze/1.5-hour thaw cycle. The process of weighing and testing for fundamental frequency is repeated at various cycle intervals. The freeze-thaw cycling is continued until the specimen falls below 60 percent of its initial dynamic modulus of elasticity or withstands 300 cycles of freezing and thawing, whichever comes first. All specimens exhibited excellent freeze-thaw durability, as noted in Table 4.

BULK SPECIFIC GRAVITY AND WATER ABSORPTION

Since the absorption of sintered aggregate is higher and more variable than conventional aggregates, a select procedure standardized by the Texas Highway Department as Test Method Tex 433-A (9) was used. This method of testing is intended for use in determining the bulk specific gravity (both dry and saturated surface-dry), apparent specific gravity, absorption, and rate of absorption of both fine and coarse lightweight aggregates.

The procedure basically involves placing an oven-dry weight of a sample in a calibrated pycnometer jar and completely filling the jar with water, taking care to expel all air bubbles. Timing begins the instant the water is introduced into the jar. Combined weight of the pycnometer jar, sample, and sufficient water to fill the jar are taken after various time intervals. The weight increases with time because of extra water added to compensate for absorption. A curve of weight versus time, extended back to zero time, provides for an indirect calculation of the oven-dry bulk volume of the sample prior to water addition. The apparent volume of the sample and the amount of absorbed water at any time can also be calculated.

The percent absorption at any time is calculated by dividing the weight of the absorbed water at any time by the oven-dry weight of the sample. A plot of percent absorption versus time establishes the rate of absorption. The bulk specific gravity is calculated by dividing the oven-dry weight of the sample by the volume of the sample. The bulk specific gravity on a saturated, surface-dry basis at any time is calculated by dividing the sum of the oven-dry weight of the sample and the weight of the absorbed water at any time, by the bulk volume of the sample. The

apparent specific gravity at any time is calculated by dividing the oven-dry weight of the sample by the apparent volume at that time.

As noted in Table 5, average dry bulk specific gravities ranged from 1.53 to 1.68. After 100-minute and 24-hour soaks, the average bulk specific gravities ranged from 1.59 to 1.77 and 1.63 to 1.81, respectively. The average 100-minute absorptions ranged from 3.78 to 6.16 percent while increasing from 6.69 to 9.03 percent after 24 hours. Plots of absorption versus time for the various block-graded aggregates are given in Fig. 6. Specific gravities were slightly below average as compared to typical lightweight aggregates. Absorption values were average to slightly above average.

CONCRETE MASONRY BLOCKS

Concrete blocks of various sizes and shapes and containing many different material compositions have been used for numerous years. The current trend is to produce lightweight units with structural integrity permitting use throughout the broad scope of activities in which concrete blocks are applicable. Advantages of the synthetic aggregate lightweight blocks include light weight effects which lower dead loads with no loss in load bearing capacity while increasing construction productivity, and the combination of good thermal insulation and moisture resistance, low sound transmission, and high fire resistance due to the vesicular nature of the noncombustible aggregate.

Sintered coal refuse was evaluated as an aggregate in producing 6 x 8 x 16-inch lightweight blocks using a small commercial machine. The effects of varying cement and agricultural limestone (aglime) contents were studied. Limestone aggregate blocks were produced for control specimens and samples were also obtained from a local commercial manufacturing operation.

MANUFACTURING PROCESS

The experimental blocks were produced on a Fleming Model 180 block machine, shown in Fig. 7, located at the University of Kentucky research laboratory. The block mix is fed into the machine through the hopper at the top. A chamber moves forward to fill and compact the mix in the mold box (upside down in the picture), which then is inverted to release the block onto the steel pallet. After the blocks were made, they were air cured (in the closed steam room) for approximately two hours before being subjected to steam curing, thus permitting initial preset. The steam room was initially unheated. An approximate two-hour slow heating period brought the room temperature to 140-150°F and this temperature was maintained for 10 hours. A two-hour slow cooling period was allowed before the blocks were removed from the steam room. They were then stored at room temperature and humidity until the time of test, six days later. A sintered aggregate block is shown in Fig. 8.

TABLE 5. - Bulk Specific Gravity and Water Absorption Test Data

Plant	SEI	SEI-BC	ICP	BEP	EOB	USSC
Bulk Specific Gravity (O.D.)	1.61* (1.47-1.70)**	1.57 (1.55-1.59)	1.68 (1.66-1.69)	1.62 (1.58-1.65)	1.54 (1.54)	1.53 (1.51-1.55)
Bulk Specific Gravity @ 100 min (SSD)	1.68 (1.57-1.78)	1.67 (1.66-1.68)	1.77 (1.76-1.78)	1.68 (1.65-1.70)	1.62 (1.60-1.63)	1.59 (1.57-1.60)
Absorption @ 100 min, %	4.71 (2.91-9.38)	6.16 (5.18-7.32)	5.70 (5.09-6.30)	3.78 (2.93-4.63)	4.90 (4.49-5.31)	3.88 (3.38-4.37)
Bulk Specific Gravity @ 24 hr (SSD)	1.72 (1.63-1.82)	1.72 (1.71-1.72)	1.81 (1.80-1.81)	1.73 (1.70-1.75)	1.67 (1.65-1.68)	1.63 (1.62-1.64)
Absorption @ 24 hr, %	7.50 (5.77-12.40)	9.03 (7.89-10.23)	7.58 (6.82-8.34)	6.88 (6.27-7.48)	8.32 (7.58-9.06)	6.69 (5.96-7.42)

*Average of all test values.

**Range of all test values.

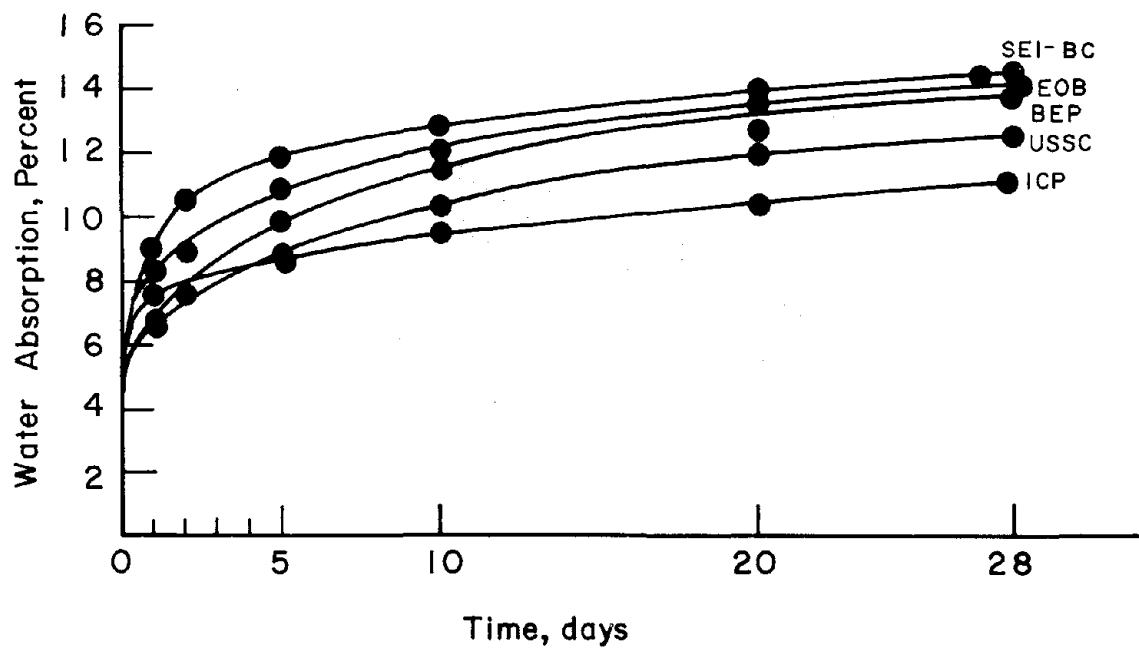
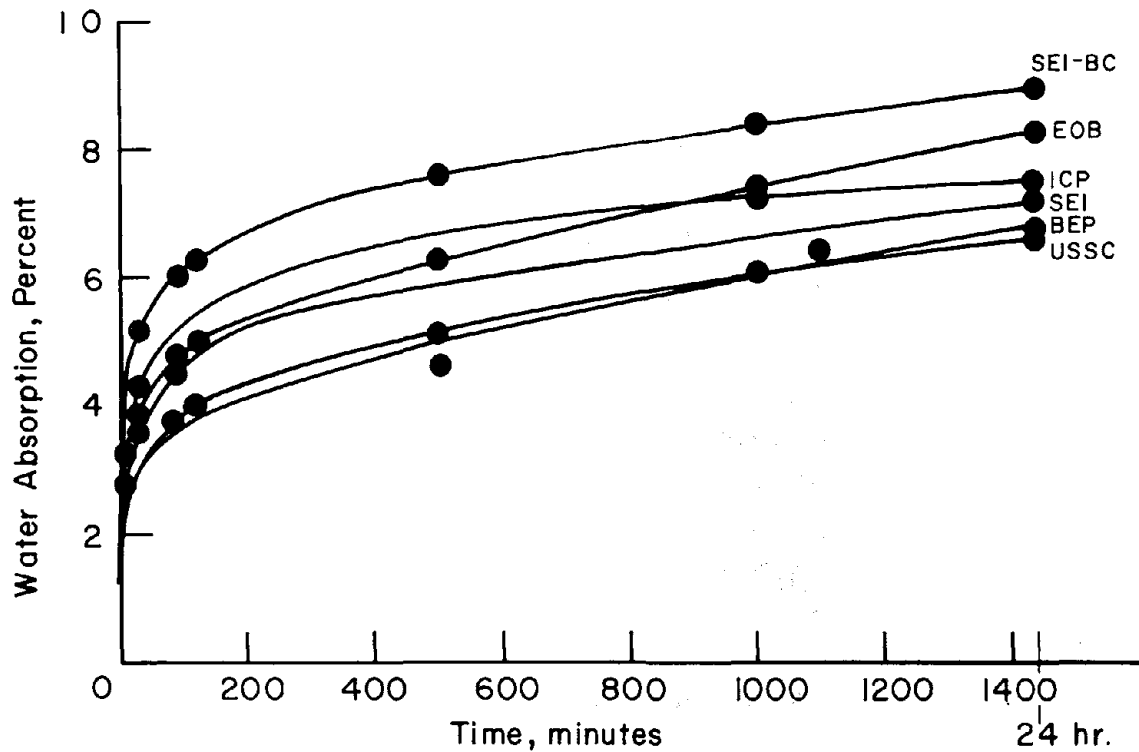


FIG. 6. - Long-Term Water Absorption Characteristics, Block-Graded Sintered Aggregate

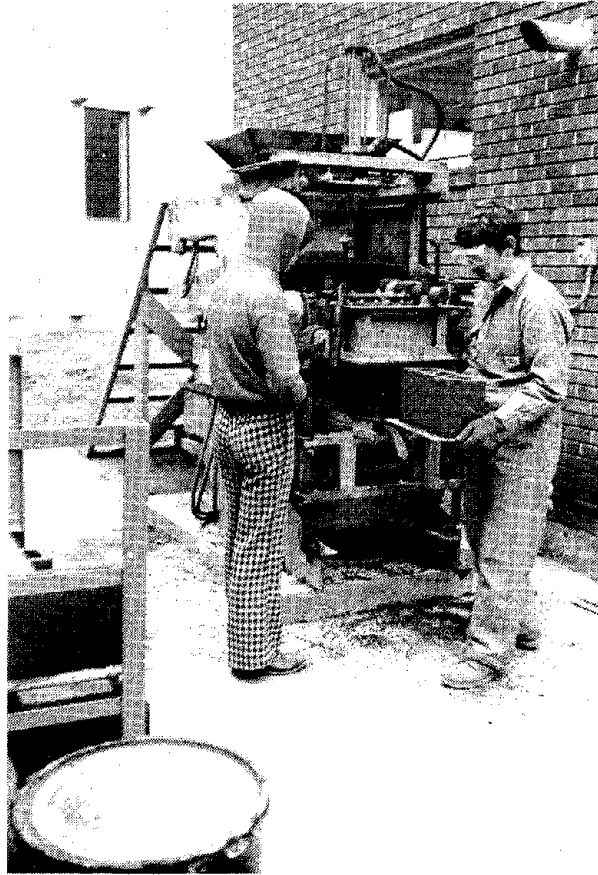


FIG. 7. - Block-Making Operation

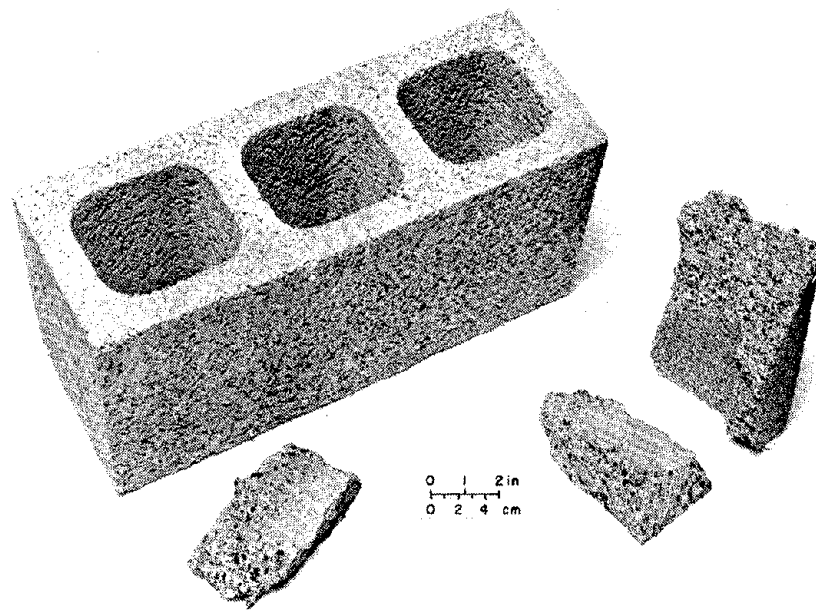


FIG. 8. - Sintered Aggregate Block

MIX DESIGNS AND DESCRIPTIONS

Unlike designing a concrete mix, concrete block proportioning is usually done by the trial and error method, utilizing past experience. The amount of water required is a subjective evaluation. It was decided to use a mix composition similar to that used in a local commercial operation - Lexington Concrete Products (LCP) - with adjustments made to compensate for the difference in specific gravity of the materials. Thus, knowing a typical commercial limestone block mix design, the sintered aggregate mix designs were derived by weight-volume relationships. This provided a check on the reliability of the block making procedure since the limestone blocks could be directly compared to those units produced by LCP. The mix design used by LCP was 3200.0 lb limestone block mix and 300.0 lb block cement. This was proportionately reduced to an amount (volume) that could be easily handled in the laboratory mixer: 250.0 lb of limestone block mix and 23.4 lb of block cement. Eight six-inch blocks could be made from each batch.

Since the specific gravity of the sintered aggregate is grossly different from that of the limestone block mix, it was necessary to adjust the weight of sintered aggregate used to replace the limestone material, in order to maintain the same batch volume and an equivalent volumetric cement factor. The same batch volume could be produced by using only 160.0 lb of sintered aggregate in place of 250.0 lb of limestone aggregate.

Several trial sintered mixes were made in an attempt to bracket the optimum design. The 100 percent sintered aggregate mix proved to have poor cohesion and low "green" strength and toughness, thus aglime was added to the sintered mixes to promote good consolidation. The specific gravity of the aglime is approximately that of the limestone block aggregate. The final mix design for the optimum sintered mix was 127.8 lb of sintered aggregate, 50.0 lb of aglime and 23.4 lb of block cement. Thus the batch volume and cement factor for the sintered mixes were the same as those for the limestone control mixes.

Preliminary strength testing of the sintered aggregate and limestone blocks (19) indicated that equivalent strengths could not be obtained at equal cement factors. Therefore the cement factor for the sintered mixes was increased by 30 percent. Design weights for the sintered aggregate mixes and the limestone control mixes are given in Table 6. The block aggregate data is present in Table 7.

LABORATORY TESTS

The concrete blocks were selectively tested for compressive strength, water absorption, and block weight. Yield and cement factors were also calculated. Eight units from each mix were used for testing purposes, five for compressive strength tests, and three for combined absorption and block weight calculations.

TABLE 6. - Block Mix Design Data

	Sintered Aggregate Mixes	Limestone Control Mixes (UK)	Limestone Control Mixes (LCP)
Sintered Aggregate, lb	127.8	-	-
Agricultural Limestone, lb	50.0	-	-
Cement,* lb	30.4**	23.4	23.4
Limestone Block Mix, lb	-	250.0	250.0
Water, lb	13.2	15.1	?

*"Speed" block cement.

**30 percent increase over control mixes.

TABLE 7. - Block Aggregate Data

Sieve Size	Individual Percent Retained		
	Sintered Aggregate	Agricultural Limestone	Limestone Block Mix
3/8-inch	0	0	0
No. 4	6.8	2.8	7.8
No. 8	36.5	39.7	41.5
No. 16	22.0	24.8	22.3
No. 50	19.2	17.4	13.9
No. 100	4.1	4.5	3.4
No. -100	11.4	10.8	11.1
Moisture content, %	variable	-	-
Bulk specific gravity (OD)	1.53-1.68	2.49	-
Bulk specific gravity (SSD)	1.59-1.77	2.59	-
Bulk specific gravity (prevailing)	-	-	2.50

Compressive Strength

The testing of compressive strength of concrete masonry units was done in accordance with ASTM Method C 140 (18). Having been cured in a steam room as previously described, the blocks were stored at room temperature for six additional days at which time they were capped and tested using a hydraulic testing machine. The compressive strength is calculated by dividing the maximum load in pounds by the gross cross-sectional area of the unit in square inches.

Compressive strength test results are given in Figure 9 and Table 8. The sintered aggregate blocks ranged in compressive strength from 1,210 psi to 1,520 psi. ASTM C 90 specifies that the minimum compressive strength for Grade N-Type I (general use, moisture controlled) blocks should be 1000 psi. All sintered units exceeded this requirement (18).

Limestone control blocks made with the small machine at UK compared favorably with those obtained from the commercial LCP plant. The limestone units made at UK averaged 1,605 psi, while the LCP blocks averaged 1,690 psi. Even though the sintered aggregate produces a quality block, it is inherently weaker than the limestone material.

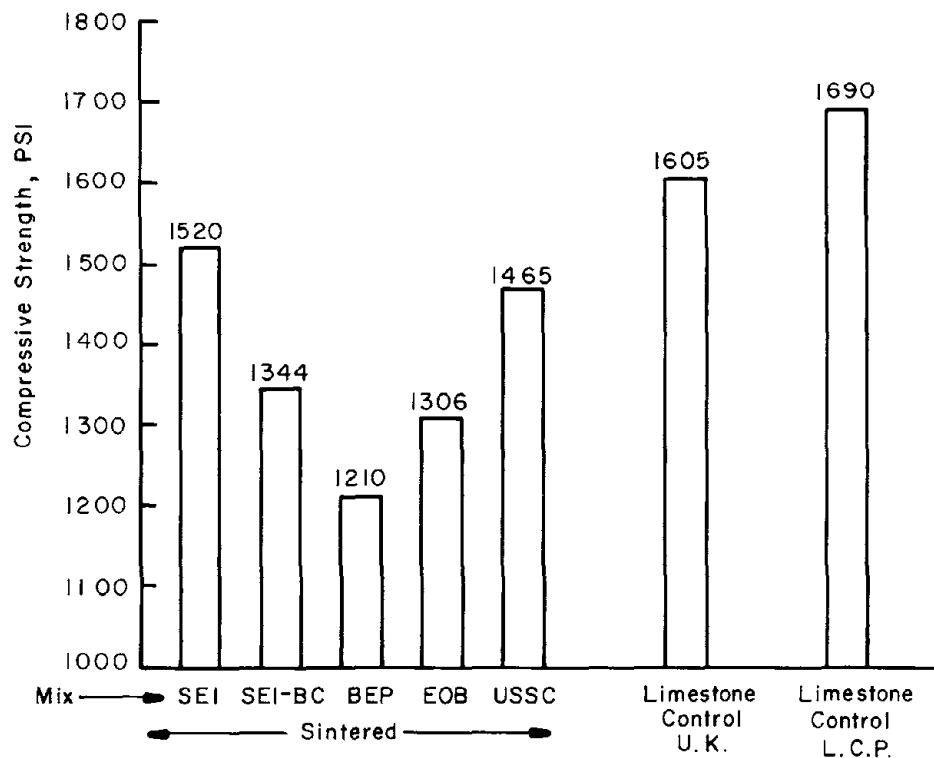


FIG. 9. - Block Compressive Strengths

TABLE 8. - Concrete Block Test Data

	SEI	SEI-BC	ICP	BEP	EOB	USSC	Control Limestone		ASTM
							U.K.	L.C.P.	
Compressive Strength, psi*	1520	1344		1210	1306	1465	1605	1690	1,000 min
Dry Block Weight, lbs**	20.7	20.9		19.6	20.4	21.0	29.5	29.8+	
Wet Block Weight, lbs**	23.6	24.8		22.6	23.7	24.6	31.9	32.0+	
Water Absorption, lb/ft ³ **	12.7	14.9		14.7	14.6	15.1	10.8	9.9	18 max
Yield, blocks/bag***	28.8	31.3		33.4	32.6	31.4	35.8	34.8++	

*Average of 5 units

**Average of 3 units

***Average of 8 units

+Converted to six-inch equivalent block size - actual dry weight = 36.27 lb; and actual wet weight = 38.99 lb for eight-inch block.

++Converted to 6 x 8 x 16-inch block equivalent.

Block Weight and Water Absorption

The weight and absorption of the concrete blocks were determined by ASTM C 140 (18). The specimens were immersed in water at room temperature for 24 hours, then weighed submerged. The unit was then removed from the water, allowed to drain for one minute while removing surface water with a cloth, and weighed to obtain the wet or saturated weight of the unit. The block was subsequently dried to a constant weight to obtain the dry weight of the unit.

The dry and saturated block weights are given in Table 8. Dry weights of the sintered units ranged from 19.6 to 21.0 pounds; the limestone control units averaged 29.5 pounds. In order to directly compare the UK blocks with the LCP units, a factor was applied to the eight-inch blocks to convert the data to six-inch equivalent block size. Saturated weights exhibited the same trends as the dry weights.

Table 8 contains absorption data for the various block units. Absorptions for the sintered units ranged from 12.7 to 15.1 lb/ft³. Absorptions for the limestone units were around 10 lb/ft³. ASTM C 90 specifies that the maximum water absorption of blocks with a dry density less than 105 lb/ft³ should be 18 lb/ft³ and that normal weight units which have a density of greater than 125 lb/ft³ should have an absorption of less than 13 lb/ft³. All units meet these specifications (18).

Yield and Cement Factor

The yield was calculated in terms of the number of blocks produced per bag of cement. This value can be easily obtained by monitoring the weight of constituents in the mix and weighing a fresh block as it is produced. (Actually, the first two blocks were weighed together to increase accuracy.) Dividing the total weight of the mix by the weight of a fresh block and dividing the weight of cement in the mix by that value, the weight of cement in each block (the cement factor) is attained. Finally, dividing the weight of cement per bag by the cement factor generates the yield.

The yield of the limestone control group was calculated by dividing the total weight of material in the mix by the saturated weight of the block, dividing that value by the weight of cement in the mix, and then multiplying by the weight of cement per bag. Table 8 presents the yield data for the units. The sintered units ranged from 28.8 to 33.4 blocks/bag. This compared to around 35 blocks/bag for the limestone units.

THERMAL ASPECTS

Materials to form parts of buildings and other containments of the future will necessarily be closely analyzed for their thermal resistance characteristics. Aside from the energy conservation aspects of construction, the overall economics of construction must be carefully analyzed

for establishing acceptable lifetime costs. The production of lightweight aggregate by sintering coal mine refuse dictates the determination of the energy conservation characteristics of construction components made from lightweight aggregate. Thus, materials generated were tested for thermal resistance in building block configurations. Although the results obtained were somewhat predictable they do give direction to optimum usage of the materials as made available to the construction market.

New energy conservation technology requires effective insulating materials in the field of building physics and economical usage of insulating materials requires increased knowledge of all types of solid materials. There must be an evaluation of the thermal conductivity, or inversely the thermal resistance, of materials in order to rate the effect on the loss of heat from a structure. Here, thermal resistance is regarded as a property of a particular body or assembly measured by the ratio of the difference between the average temperatures of two surfaces with steady state in effect, as noted in ASTM C 168 (19).

$$\text{Thermal Resistance} = \frac{\text{Heat Flow}}{\text{Temperature Difference}}$$

The specific mechanism employed in measuring heat flow through large sections or multiple material sections is the Guarded Hot Box. The basic procedure is fairly simple and is based on the steady state heat transfer between a hot (warm) and a cold plate (flat surface). Even though the mechanics of operations seem simple, comparison of results on given samples, as determined at different locations or at different times may vary. Points of contention seem to be the nonadiabatic (perfectly insulated) features of the test equipment and the nonadherence to taking measurements at steady state conditions (thermal).

Materials testing was done using test equipment designed, built, and utilized for the materials developed in this coal mine refuse utilization program. This was necessary since the desired test equipment was not otherwise available.

The test facility was built to accommodate concrete block wall sections. Sample components tested were made from both sintered aggregate and control limestone block. Structural details of the test facility are shown in Figure 10. The procedure for the test is contained in ASTM C 236 "Test for Thermal Conductance and Transmittance of Built-Up Sections by Means of the Guarded Hot Box" (19).

A summary of test results is given in Table 9. The overall heat transfer coefficient through the bounding surfaces of the wall decreased by 0.26 Btu/hr, Ft²/°F (45 percent) with the substitution of lightweight aggregate for the standard density limestone aggregate.

SUMMARY AND CONCLUSIONS

Synthetic lightweight aggregate was successfully produced from bituminous coal refuse using an improved sintering grate process. The improved process incorporates a sealed sintering facility with a multi-

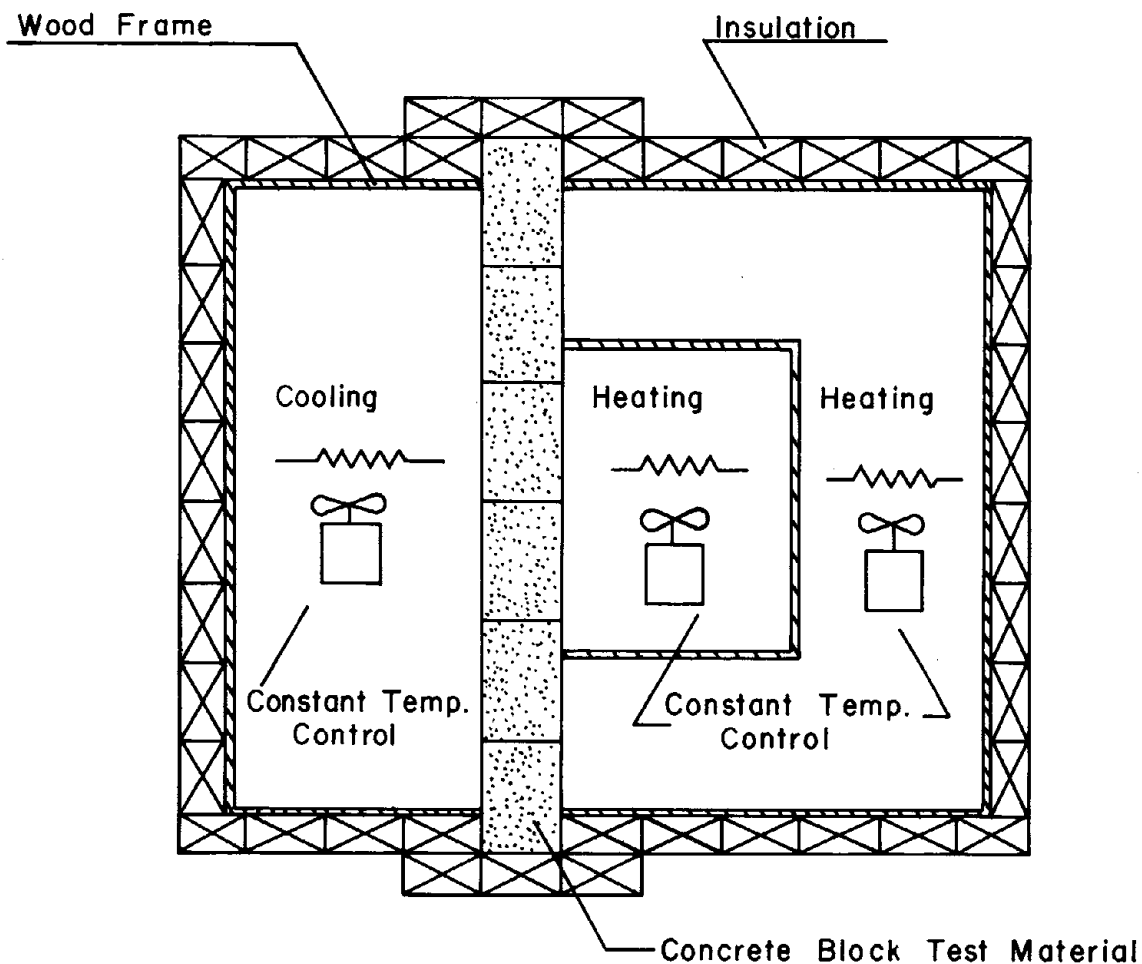


FIG. 10.- Apparatus for thermal conduction tests of blocks

TABLE 9. - Thermal Conductivity of Concrete Blocks
(6 x 8 x 16-inch, 3-Cavity - Empty)

Surface Temperatures (°F)		Material Density (lbs/Block)	Thermal Conductivity (U)* (Btu/hr, ft ² /°F)
Hot Side	Cold Side		
100	68	29.3 (Regular)	0.57
120	71	29.3	0.58 (0.58 avg)
135	72	29.3	0.60
102	70	20.7 (Lightweight)	0.30
125	72	20.7	0.32 (0.32 avg)
140	75	20.7	0.33

*Includes inside (0.17) and outside (0.68) coefficients

pass recycled draft and is particularly applicable to processing bituminous coal refuse since it alleviates some salient air-pollution problems and provides an environmentally acceptable process.

Several benefits could be derived from using coal refuse as a raw material for sintered lightweight aggregate. Coal refuse contains both the raw product and the necessary solid fuel for sintering, thus assuring a continued solid fuel supply, and an inherent energy savings that could contribute substantially to providing an economical end-product. Approximately three-fourths of the fuel requirement for sintering is provided by solid fuel in the raw feed. In conventional sintered aggregate operations this fuel is normally supplied by coke breeze, anthracite coal, or fly ash, and generally amounts to six to eight percent of the raw feed. In some instances these fuel supplies are uncertain and expensive, and several sintered aggregate plants have closed during recent years, reportedly due to these uncertainties and costs. Also, the coal refuse raw material is already mined and partially crushed, thus effecting certain additional economic benefits, as compared to conventional sintering plants requiring a considerable investment in equipment and expense for associated mining operations. Utilization of a waste fuel source and product are being simultaneously accomplished, with environmental benefits. Additional savings in disposal costs at the preparation plant would also be realized.

Concrete blocks produced using sintered aggregate met all quality requirements specified by the American Society for Testing and Materials for hollow load-bearing concrete masonry units. Compressive strengths were well in excess of the specifications and absorption levels were maintained below the maximum permitted. The addition of a quantity of aglime to the sintered aggregate was necessary to provide adequate toughness and "green" strength. Cement content was increased by about 30 percent in the sintered block in order to obtain strengths equivalent to limestone aggregate blocks. The increased cement resulted in an 11 percent decrease in yield, as compared to the limestone blocks. The typical mix design, by weight, for concrete blocks made with the sintered coal refuse aggregate was 62 percent sintered aggregate, 23 percent aglime, and 15 percent cement. The percent aglime and cement, by volume, were substantially less.

The dry sintered aggregate blocks weighed, on an average, 30 percent less than the control blocks. This represents a significant savings in handling and transportation costs. In addition, a 45 percent reduction in heat flow through the lightweight blocks was effected, as compared to the limestone units.

Although this research is based on aggregate produced by a pilot-scale operation and blocks manufactured on a small-scale commercial machine, extrapolations of data and findings to commercial size operations are believed justified.

Control of emissions during sintering the bituminous refuse on the traveling grate is of paramount concern; however, technology is available

to accomplish this. Complete combustion of the processing fuel must be attained during the sintering process. This requires an optimum percentage of solid fuel within the raw feed and a recycling of exhaust gasses through the bed of partially sintered material to complete the combustion process. Refuse containing a percentage of coal in excess of optimum would either have to be diluted with a noncarbonaceous shale or clay or preliminarily processed to remove a portion of the coal.

Bituminous coal refuse represents an essentially unlimited source of raw material for the production of lightweight, sintered aggregate in the coal producing areas of this country. A means is provided for utilizing a waste product while gaining an economic advantage during the processing of the inherent fuel value of the refuse. The lightweight properties and economical production costs of the synthetic aggregate will provide for relatively wide marketing areas. With the predicted high costs and scarcity of fuels in the future, the relatively low energy requirements of processing coal refuse will be even more attractive. In addition, the uncertainty of natural aggregate supplies in some areas and the desirability for better insulative building products are apparent.

ACKNOWLEDGMENTS

This research was sponsored by grants from the University of Kentucky Institute for Mining and Minerals Research and the Appalachian Regional Commission (Blue Grass Area Development District). Special mention is given to research assistants Dale S. Decker, Norman R. Simon, R. Kevin Floyd and Jeffery Lowe for their assistance in conducting the laboratory analyses.

APPENDIX I. - REFERENCES

1. Anon. "An Implementation Plan for Industrial Development Related to Coal Refuse Utilization in Estill County, Kentucky (tentative)," Research Report, Project ARC76-143/KY-4567-76, University of Kentucky Research Foundation and Blue Grass Area Development District, Inc., December, 1977 (in print).
2. Anon. "Feasibility Study of Utilization of Coal Mine Refuse in Estill County, Kentucky," Research Report, Project ARC 74-217/KY-3685, University of Kentucky Research Foundation and Blue Grass Area Development District, Inc., August, 1976, 305 pages.
3. Anon. "The Cake that Dwight and Lloyd Baked," McDowell-Wellman Engineering Company, Cleveland, Ohio, 1958, 16 pages.
4. Anon. "Underground Disposal of Coal Mine Wastes," Report to the National Science Foundation, National Academy of Science, Washington, D.C., 1975, 172 pages.
5. Bishop, C. S. and Rose, J. G., "Physical and Engineering Characteristics of Coal Preparation Plant Refuse," Proceedings, VII Ohio

- River Valley Soils Seminar, American Society of Civil Engineers, October, 1976, pp. 4.1-4.11.
6. Bryenton, D. L. and Rose, J. G., "Utilization of Coal Refuse as a Concrete Aggregate (Coal-Crete)," Proceedings, Fifth Mineral Waste Utilization Symposium, U. S. Bureau of Mines and IIT Research Institute, July, 1976, pp. 107-113.
 7. Charmbury, H. B., "Utilization of Pennsylvania Anthracite Refuse," Proceedings, First Kentucky Coal Refuse Disposal and Utilization Seminar, Office of Research and Engineering Service Report No. IMMR9-PD7-75, Institute for Mining and Minerals Research, University of Kentucky, Lexington, December, 1975, pp. 13-17.
 8. Ledbetter, W. B., "Introduction to Optimizing the Use of Materials and Energy in Transportation Construction," Special Report 166, Transportation Research Board, Washington, D.C., 1976, pp. 1-4.
 9. Ledbetter, W. B. and Buth, E., "Aggregate Absorption Factor as an Indicator of the Freeze-Thaw Durability of Structural Lightweight Concrete," Research Report 81-3, Texas Transportation Institute, Texas A&M University, College Station, February, 1967, pp. 11-15.
 10. Maneval, D. R., "Coal Refuse Utilization Prospects - An Update of Recent Work," Proceedings, Second Symposium on Coal Preparation, NCA/BCR Coal Conference and Expo III, Louisville, Kentucky, October, 1976, pp. 184-198.
 11. Miller, R. H. and Collins, R. J., "Waste Materials as Potential Replacements for Highway Aggregate," Report 166, National Cooperative Highway Research Program, Transportation Research Board, Washington, D. C., 1976, 94 pages.
 12. Robl, T. L., Bland, A. E. and Rose, J. G., "Kentucky Coal Refuse: An Assessment of its Potential as a Metal Source," Proceedings, Second Symposium on Coal Preparation, NCA/BCR Coal Conference and Expo III., Louisville, Kentucky, October, 1976, pp. 152-159.
 13. Rose, J. G., "Sintered Coal Refuse as a Construction Aggregate," Proceedings, Third Kentucky Coal Refuse Disposal and Utilization Seminar, Office of Research and Engineering Services Report No. IMMR32-M4-77, Institute for Mining and Minerals Research, University of Kentucky, Lexington, December, 1977, pp. 59-64.
 14. Rose, J. G. and Howell, R. C., "Proposed Coal Pillaring Procedure Using Concrete Containing Coal Refuse (Coal-Crete)," Preprint 77-F-102, Annual Meeting of the Society of Mining Engineers of AIME, March, 1977, 38 pages.
 15. Rose, J. G., Robl, T. L. and Bland, A. E., "Composition and Properties of Refuse from Kentucky Coal Preparation Plants," Proceedings, Fifth Mineral Waste Utilization Symposium, U. S. Bureau of Mines

and IIT Research Institute, July, 1976, pp. 122-131.

16. 1977 Annual Book of ASTM Standard, Part 13, Cement; Lime; Ceilings; and Walls (Including Manual of Concrete Testing), American Society for Testing and Materials, Philadelphia, 1977.
17. 1977 Annual Book of ASTM Standards, Part 14, Concrete and Mineral Aggregates (Including Manual of Concrete Testing), American Society for Testing and Materials, Philadelphia, 1977.
18. 1977 Annual Book of ASTM Standard, Part 16, Chemical-Resistant Non-metallic Materials; Vitrified Clay and Concrete Pipe and Tile; Masonry Mortars and Units; Asbestos-Cement Products, American Society for Testing and Materials, Philadelphia, 1977.
19. 1977 Annual Book of ASTM Standards, Part 18, Thermal and Cryogenic Insulating Materials; Building Seals and Sealants; Fire Tests; Building Constructions; Environmental Acoustics, American Society for Testing and Materials, Philadelphia, 1977.



INHERENT COMPRESSIVE AND TENSILE STRENGTHS OF STRUCTURAL BRICK

By Rad, P. F.

ABSTRACT: The structural brick is currently being reconsidered by the construction technologists as a load bearing material. Due to its high strength and pleasing decorative appearance, brick could be used as a structural material as well as a finishing material. Standard brick property tests apply varying constraint conditions to the brick and may thus result in different values for the same brick. In an attempt to infer the inherent strength of bricks, in this study tests were conducted on brick core samples to find the tensile and compressive strength of two different types of brick. These strength values were correlated to the values of the strength of the walls. The tensile strength and overall average compressive strength of the core samples are closely related to the compressive strength of the brick walls.

INHERENT COMPRESSIVE AND TENSILE STRENGTHS OF STRUCTURAL BRICK

By Parviz F. Rad¹

INTRODUCTION

The structural brick is currently being reconsidered by the construction technologists as a load bearing material. Due to its high strength and pleasing decorative appearance, brick could be used as a structural material as well as a finishing material.

The standard brick property test calls for applying compressive loads to the whole brick in the direction of extrusion. The results of this test are generally satisfactory for a first approximation of the brick material and hence the behavior of a brick prism. However, the restraint provided by the top and bottom steel platens influence the result to the extent that a brick nominally rated at 3629 psi may appear to have a compressive strength of 6776 psi if the platens are restrictive. If lateral expansion of the brick is facilitated by lubrication, a compressive strength of 3322 psi is achieved and if the restraint is minimized by using a one-half or one-eighth brick, compressive strengths of 3261 psi and 2241 psi is achieved, respectively.

The purpose of the work reported here is to determine the compressive and tensile strengths of bricks in all three directions using the cylindrical geometry commonly used for other construction materials such as concrete, mortar, and rocks. A successful attempt is made to correlate the inherent properties thus obtained to the strength of a brick prism.

EXPERIMENTAL PROCEDURE

Core samples were prepared by drilling a cylinder .667 in. in diameter and approximately 1.3 in. long from whole bricks. Forty five samples were prepared from each brick type, fifteen samples in each of three directions. The core samples were marked to show the direction of extrusion and the direction which they were drilled. Figure 1 shows the brick orientation and coordinate system. The compression tests were run by placing the core samples on end in a Universal Testing Machine and loading the samples axially. Five samples were tested for compressive strength for each of three directions, x, y, z. The compressive strength was obtained by dividing the ultimate load by the nominal cross section. The tension tests were run by placing the core

¹Associate Professor, Department of Civil Engineering, Clemson University, Clemson, S.C.

samples on the side and loading them perpendicular to the axis of rotation. Five samples were tested for each of six directions, xy, yz, zx, xz, zy, yx. The tensile strength was determined by calculating the term $2P/\pi LD$ where P, L and D are the ultimate load, length, and diameter of the cylindrical specimen, respectively.

RESULTS AND DISCUSSION

Table 1 shows the compressive strengths of the Richtex and Southern Bricks in each of the three orthogonal directions. The compressive strengths of both of these bricks are highest along the length of the brick; presumably due to shrinkage patterns after extrusion. The average compressive strength of the Richtex Brick in all three directions is 3560 psi. The average compressive strength of the Southern Brick is 4794 psi. Table 2 shows the strength of various prisms made with these two bricks and using standard N and M mortars as well as Sarabond-treated mortar. The average prism strength for Southern Brick is 5283 psi whereas that of Richtex Brick is 3406 psi. The average prism strength correlates closely to the overall average inherent compressive strength determined from the test cylinders. Their inherent compressive strength can be used as a good tool in estimating the average prism strength. A more accurate and systematic prism strength estimation would be possible if in addition to the compressive strength and bonding characteristics of the mortar the mortar's relative lateral displacement characteristics with respect to the brick are determined.

Table 3 shows tensile strength of the bricks determined for all the three directions by subjecting cylindrical specimens to diametrical compression. The overall average tensile strength for the Southern Brick and Richtex Brick is 1631 psi, and 1182 psi, respectively. Comparing the tensile and compressive strength of each axis separately it becomes apparent that the average ratio of compressive strength to tensile strength for the Richtex Brick is 2.25 in the x direction, 7.13 in the y direction, and 6.49 in the z direction. For the Southern Brick, these values are 1.94, 8.98, and 6.09, respectively.

Some further correlation can be sought between the average tensile strengths in the x and y directions and prism compressive strength which is measured in the z direction. The prism compressive strength is higher than the x-y average tensile strength by factors of 3.03 and 3.17 for the Richtex and Southern Brick, respectively.

SUMMARY AND CONCLUSIONS

The results of compressive and tensile strength tests on cylinders cored from the three directions of brick show that the direction of testing influences the results of tension or compression tests significantly. Therefore, brick's compressive and tensile strength data should always be used in the light of the test direction. Further, standard

brick property tests are susceptible to variations in end-constraints and thus cause different stress fields in the brick resulting in wide variations in results. It is debatable whether fully restrained, partially restrained, or fully lubricated specimens simulated field behavior of bricks accurately.

The values of inherent compressive and tensile strengths can be used to estimate the average prism strengths made with a brick; further refinement of the estimation can be conducted on the basis of mortar strength and behavior. Tensile strength of the bricks show very close correlation with prism strength; the latter being between 3.03-3.17 times the former. Further, the overall average compressive strength was nearly equal to average prism strength.

FIGURE 1
BRICK ORIENTATION AND
COORDINATE SYSTEM

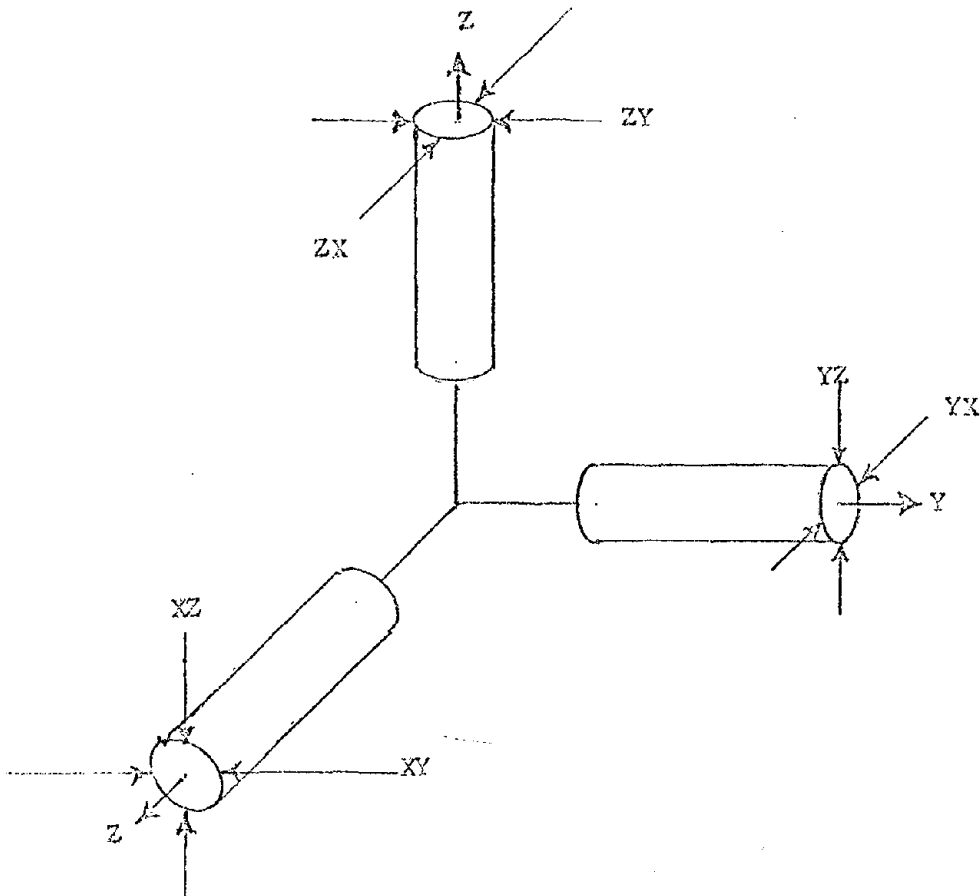
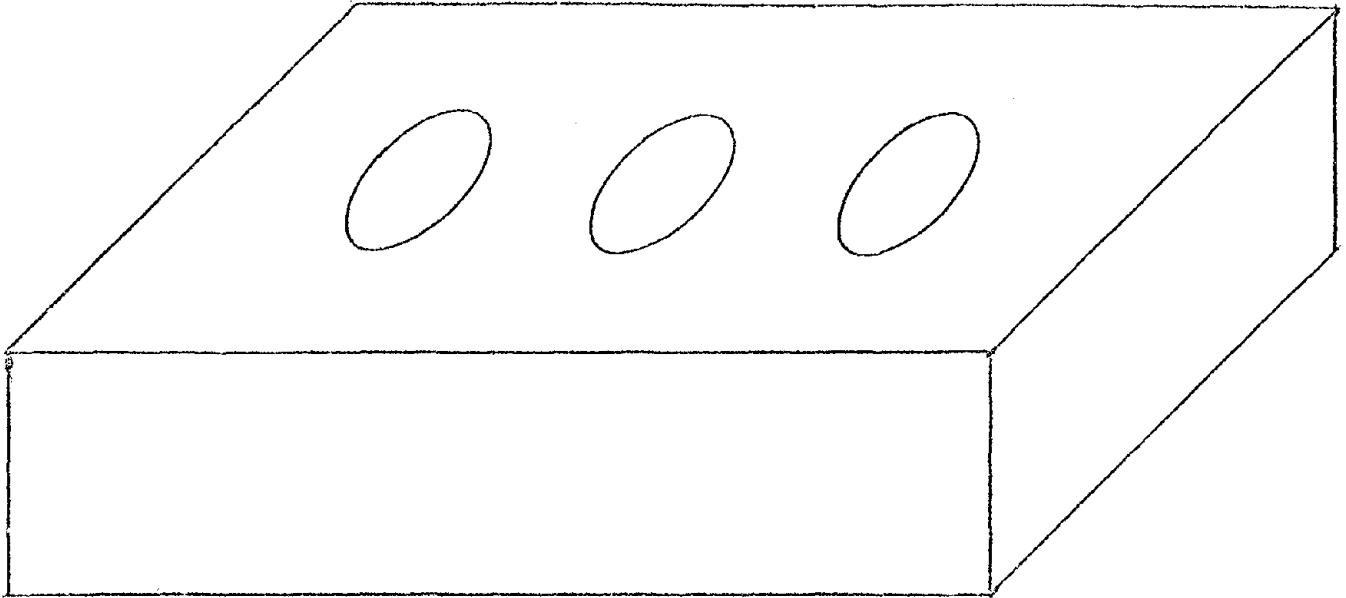


Table 1. Compressive Strength of the Bricks.

	Richtex Brick	Southern Brick
x, width of brick	3042 ± 610	3140 ± 710
y, length of brick	5162 ± 822	6154 ± 2584
z, direction of extrusion	2475 ± 467	5089 ± 1369

Table 2. Compressive Strength of Brick Prisms
Made With Various Mortar Types.

	Southern Brick Prisms, psi	Richtex Brick Prisms, psi
N mortar	4832	2842
M mortar	3732	3969
S mortar	7286	3711
Average	5283	3406

Table 3. Tensile Strength of the Bricks.

	Richtex Brick	Southern Brick
xy	1543 ± 297	1817 ± 131
yx	1048 ± 315	1301 ± 270
yz	794 ± 168	1415 ± 298
zy	600 ± 146	1091 ± 302
zx	685 ± 229	1411 ± 301
xz	2424 ± 184	2752 ± 284

BEHAVIOR OF CONCRETE MASONRY STRUCTURES AND
JOINT DETAILS USING SMALL SCALE DIRECT MODELSBy Harry G. Harris¹ and Ivan J. Becica²

ABSTRACT

The methodology of using small scale direct models of concrete masonry structures has been presented. The basic strength evaluation tests for compressive, flexural bond and shear strengths recommended for prototype structures have been also developed with minor modifications for the evaluation of model masonry strength. A systematic analysis of the parameters which affect the strength and stiffness of masonry under compressive, flexural and shear loadings has provided the means to compare model and prototype test results. Correlation of the model and prototype results ranged from excellent to good. For the case of masonry in compression, the testing of prisms has shown that the model masonry behavior is essentially the same as that reported for prototype tests. Model tests on larger compression components have also shown good correlation with prototype data. In the case of flexural bond and shear strength of masonry, proper considerations must be given to the tensile strength of the joint mortar including the effects of the stressed volume. This implies that very small size control specimens i.e. cubes or cylinders must be tested in order to be sure that the small volume of the model joint bears the same relation to its control specimen as the volume in the prototype mortar joint bears to its respective control specimen. When proper consideration of the above effects are made, the correlation of model and prototype masonry strength tests for evaluating flexural bond and shear are shown to be satisfactory.

Excellent correlation of the elastic modulus of concrete masonry in compression and shear was obtained from the model tests and the limited stress-strain data of prototype masonry reported in the literature. This work has produced a systematic approach to the direct modeling of concrete masonry structures. Extensions of this approach to the study of joint details between masonry bearing walls and pre-cast floor/roof systems has also been demonstrated. The versatility of this approach for studying the inelastic behavior of concrete masonry structures in a direct and relatively inexpensive manner has been indicated.

-
1. Assoc. Prof. of Civ. Engrg.; Dept. of Civil Engrg.,
Drexel Univ., Philadelphia, Pa.
 2. Graduate Assistant, Dept. of Civ. Engrg; Drexel Univ.,
Philadelphia, Pa.

BEHAVIOR OF CONCRETE MASONRY STRUCTURES AND
JOINT DETAILS USING SMALL SCALE DIRECT MODELSBy Harry G. Harris¹ and Ivan J. Becica²

INTRODUCTION

Recent advances in reinforced masonry structures and the widespread use of precast, prestressed hollow core floor slabs resting on masonry walls have necessitated a closer examination of the structural behavior of these components. One of the problems of prefabricated construction is the additional attention that must be paid by the designer to the details in the connection areas to insure that the various wall and floor elements have adequate structural continuity and can work together to accommodate the lateral as well as the gravity loadings. Such effects as abnormal loadings due to internal high pressure caused by accidental explosions, loss of members due to accidental impact and lateral loads imposed on the building by wind or ground motion resulting from earthquakes must be carefully evaluated with extensive experimental programs.

Due to the high cost of full scale testing a more economical method to study the complete structural behavior of masonry structures is needed. With this objective in view, the following effort was undertaken in the Structural Models Laboratory of Drexel University. A direct small scale modeling technique which has been successfully used in both reinforced and prestressed concrete structures^(7,8) is proposed as an economical alternative to full scale testing. Appropriately, a 1/4 scale was chosen as a first step in modeling the behavior of hollow core concrete masonry structures using carefully constructed 1/4 scale masonry blocks supplied by the National Concrete Masonry Association. Attention has been focused on the physical properties of the constituent materials and the necessary tests that must be performed to ascertain the basic strength characteristics of the masonry units and masonry components. To this effect, both the hollow core concrete masonry block and the mortar that is used to bind these units together to form masonry structures were studied in detail^(2,5). It is important to realize that units used in structural masonry components form a composite mechanical action system because the two materials, the masonry block and the masonry mortar, do not have identical mechanical characteristics. A full understanding of both components is therefore needed so that direct modeling will be achieved to a satisfactory level of confidence for the masonry composite to function under loading in the same manner as the prototype. Not only are we interested in elastic behavior of the composite system but also the behavior beyond cracking up to ultimate loading. It is this inelastic behavior requirement which complicates the modeling problem and forces one to

1. Assoc. Prof. of Civ. Engrg.; Dept. of Civil Engrg.,
Drexel Univ., Philadelphia, Pa.
2. Graduate Assistant, Dept. of Civ. Engrg.; Drexel Univ.,
Philadelphia, Pa.

adopt techniques in the modeling of masonry structures which parallel those used in the modeling of reinforced and prestressed concrete structures. (7,8) Additional difficulties arise, however, because the masonry model specimens (walls, prisms, etc.) are not cast but must be fabricated using techniques fully described in Ref. 2.

SIMILITUDE REQUIREMENTS

The most general and useful modeling techniques used in the design and analysis of masonry structures subjected to static and dynamic loads are those which can predict inelastic as well as elastic behavior and have the ability to study with confidence the mode of failure of the structure. These techniques are, however, very restrictive on the choice of model materials and their methods of fabrication. Under the assumption that there are no significant time dependent effects in the loading which influence the structural behavior, the pertinent parameters that enter the modeling process are listed in Table 1. For complete similarity of the structural behavior, including the inelastic effects of cracking and yielding, a dimensional analysis will give the prediction and design equations shown in Table 2. This assumes that the stresses caused by the self weight of the structure are not significant, as is usually the case in most masonry buildings. As can be seen from the prediction equations (Table 2(b)), the stress-strain curves of both model and prototype masonry must be the same, presenting a very difficult challenge to the model analyst. The approach taken in this study was to attempt to achieve the above requirements at the selected scale of 1/4 because of the availability of the model masonry blocks at this scale.

Table 1 Pertinent Variables for the Modeling of Reinforced Masonry Structures Under Static Loadings

Symbol	Definition	Basic Dimension
(a) Structural Parameters		
δ	Deflection at any point	L
ϵ	Strain at any point	-
ν	Poisson's ratio	-
f'_m	Compressive strength of masonry	FL ⁻²
f'_t	Tensile strength of masonry	FL ⁻²
f_y	Yield strength of the reinforcement	FL ⁻²
t	Wall thickness	L
A	Area of net section	L ²
E_m	Young's modulus of masonry	FL ⁻²
E_s	Young's modulus of reinforcement	FL ⁻²
M	Moment per unit length	F
P	Axial compression per unit length	FL ⁻¹
(b) Loading Parameters		
q	Pressure loading	FL ⁻²
w	Line load	FL ⁻¹
Q	Point load	F

Table 2 Prediction and Design Equations for Reinforced Masonry Under Static Loading

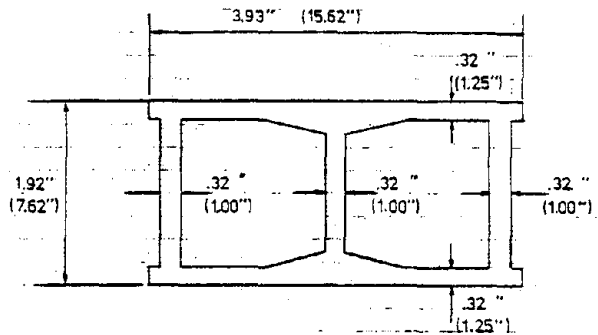
(a) Prediction Equations		(b) Design Equations	
$\epsilon_m = \epsilon_p$	Strain in model is same as in prototype	$t_m = \frac{t_p}{S_L}$	Thickness
$\delta_m = \frac{\delta_p}{S_L}$	Deflections; $S_L = \frac{L_p}{L_m}$ is the length scale	$A_m = \frac{A_p}{S_L^2}$	Areas
$M_m = \frac{M_p}{S_L^2}$	Bending moment per unit length	$E_m = E_p$	Young's moduli
$P_m = \frac{P_p}{S_L}$	Compression load per unit length	$(f'_m)_m = (f'_m)_p$	Compressive strength of masonry
		$(f'_t)_m = (f'_t)_p$	Tensile strength of masonry
		$(f_y)_m = (f_y)_p$	Yield strength of the reinforcement
		$\nu_m = \nu_p$	Poisson's ratio

STRENGTH OF MASONRY IN COMPRESSION, FLEXURAL BOND AND SHEAR

In order to evaluate the basic strength of masonry structures in compression, flexure and shear, tests are performed on representative elements of the masonry construction. The validation of direct modeling techniques applicable to concrete masonry structures focused, as a first step, in the performance of model control specimens whose strength and stiffness could be compared directly to available prototype data. Model tests were thus developed for evaluating the compressive, flexural bond and shear strength of 1/4 scale concrete masonry structures.

The configuration of the units used in this study (Fig. 1) resemble the double corner and regular stretcher type of 8" x 8" x 16" nominal size concrete masonry blocks. The quarter-scale units 2" x 2" x 4" nominal were manufactured using Ottawa sand and had two distinct compressive strengths, one in the range of 1100 psi and the other 315 psi on the gross area. These two types were easily distinguished. Data on the physical properties of both model and prototype units are given in Ref. 2 and their dimensions are shown in Fig. 1.

Because available test data on full scale hollow core masonry incorporates the use of ASTM type N masonry mortar, it was necessary to develop a similar type model mortar. Using the proportion specification as outlined in ASTM C190 as a guide, three mixes were tested in an attempt to match the reported 28 day strength of 750 psi on two inch cubes. The development of model masonry mortars⁽²⁾ must take into account the workability of the mix in selecting the aggregate gradation and mix proportions. In addition, the very small model joints exhibit material volume effects on the



MODEL DIMENSIONS
(PROTOTYPE DIMENSIONS)

FIGURE 1

strength determination which must be taken into account (2). Strength vs. age properties of the model masonry mortar used in the present study are shown in Fig. 2.

At the present time there is no firm standard for determining the compressive strength of concrete masonry prisms. The Portland Cement Association (PCA) and the National Concrete Masonry Association (NCMA) presently recommend a prism not less than sixteen inches

high with a height-to-thickness ratio of two. The ASTM E447-74⁽¹⁾ guidelines are more general, specifying prisms of height to thickness ratio from two to five with correction factors for slenderness effects. It is generally felt that end restraints have a large effect on the strength of two block prisms of full scale. At a reduced scale, such effects are easily amplified and require careful consideration. The majority of specimens used in this study, therefore, are three block stacked bond prisms as shown in Fig. 3. Also, much of the available data on prototype prisms are for the three block type and thus these serve as the compressive strengths used to correlate the model data.

All prisms were capped on both bearing surfaces with Hydrostone and tested on a Baldwin-Southwark 50 kip (222.5 kN) hydraulic testing machine. Load was applied thru a roller to a 3/8" top bearing platen. The loading rate varied depending on the specimen being tested with failure occurring in two to four minutes. The instrumented specimens were loaded at a slower rate to permit the recording of strain data. As shown in Fig. 3, both strain and deformation measurements were taken on some of the series tested in order to evaluate the consistency of the strain measurements. Two 4 inch SR-4 strain gages were bonded to the face shell of the prisms at the center line of the specimen and crossing both horizontal bond lines. The dial gages were attached to the face shells on stiff aluminum brackets using 5-minute epoxy. These recorded the deformation over an identical 4 inch gage length

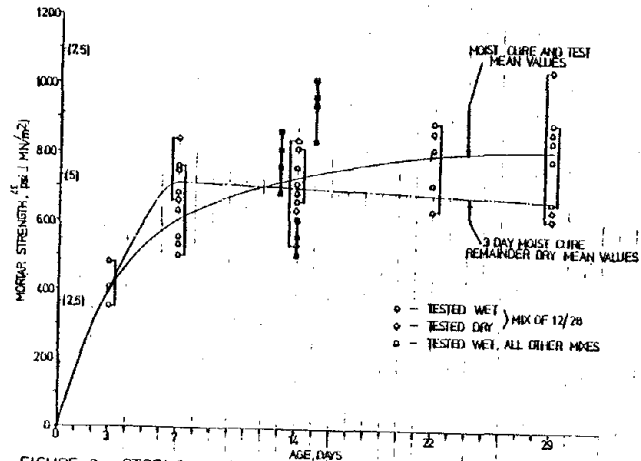


FIGURE 2 STRENGTH-AGE CURVES FOR 1x2' CYLINDERS OF MASONRY MORTAR 1:1:4 MIX

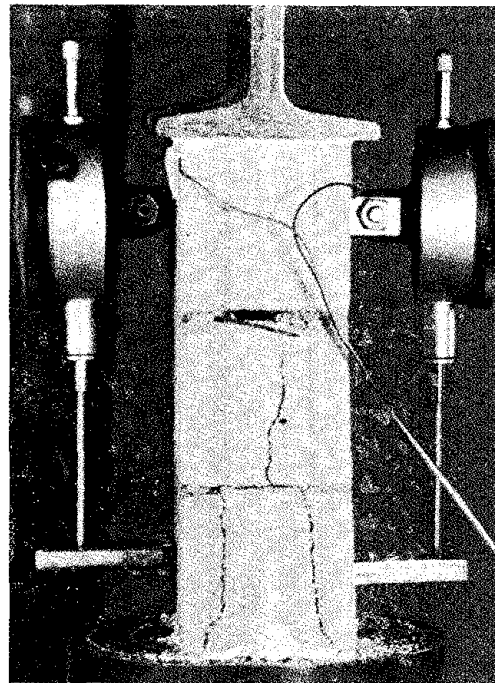


Figure 3 Compression Prism

on opposite faces of the prisms. The load vs. strain data is shown in Fig. 4 for two unreinforced and two "Durowall" reinforced three unit prisms. The results, shown in Fig. 4, indicate a consistency within each type of strain measurement i.e. strain gage and dial gage with the reinforced prisms having very similar initial moduli based on the two types of strains. The unreinforced prisms show more erratic behavior between the strain and dial gage readings. All compression prism specimens failed by end splitting (Fig. 5) as is normally observed in prototype masonry.

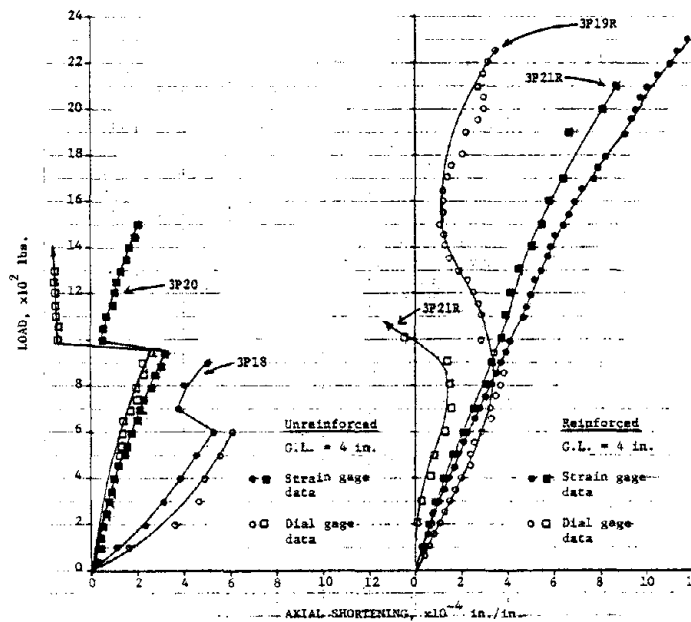


FIGURE 4 COMPRESSIVE LOAD STRAIN CURVES FOR MODEL MASONRY PRISMS

Since masonry strength is directly related to the mortar strength^(4,9,10), the adjusted model strengths are compared to the prototype data⁽¹⁰⁾ as shown in Fig. 6 in which the prism compressive strength on the gross area is related to the mortar strength. Comparison of six series of model compression prism data with prototype data obtained by Yokel et al.⁽¹⁰⁾ is shown in Fig. 6. Model data were obtained on the stronger hollow core units which had a compressive strength of 1100 psi. on the gross area. Some imperfections were noted in the scaling of the 1/4 scale masonry units used in this study. In particular, the oversized web structures (see Fig. 1) caused perhaps most of the deviation in the compressive strength of three course prism test specimens. To compensate for the increased tensile strength that these units could sustain in splitting due to their increased web

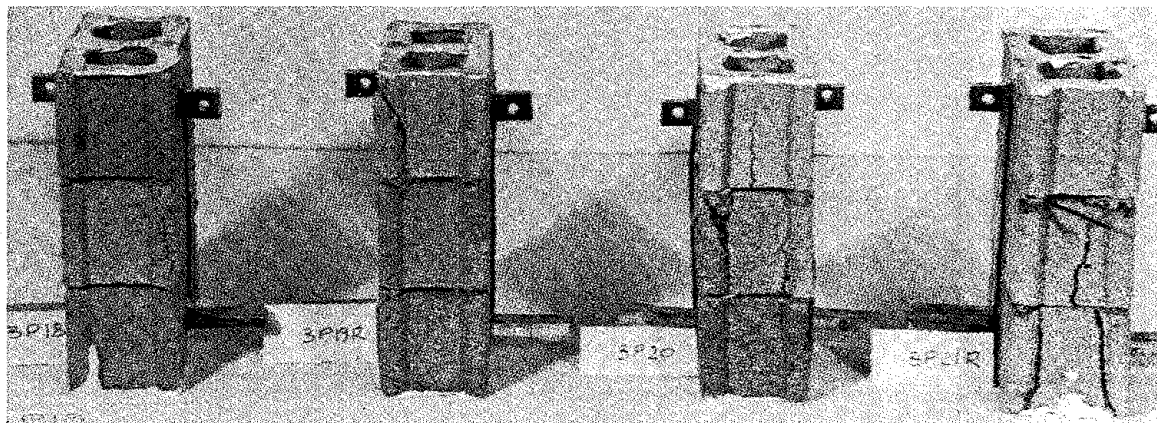


Figure 5 Failed Compression Prisms

area, a correction to the apparent strength was made. In addition, the effect of volume of mortar in the joints on the compressive strength was taken into account by empirically determining the effect of size of specimen on the unconfined compressive strength. The model data shown in Fig. 6 have been corrected for scale and geometry effects. Note the small deviation from the mean curve (shown dashed) suggesting that the modeling technique developed for prisms in compression is indeed feasible.

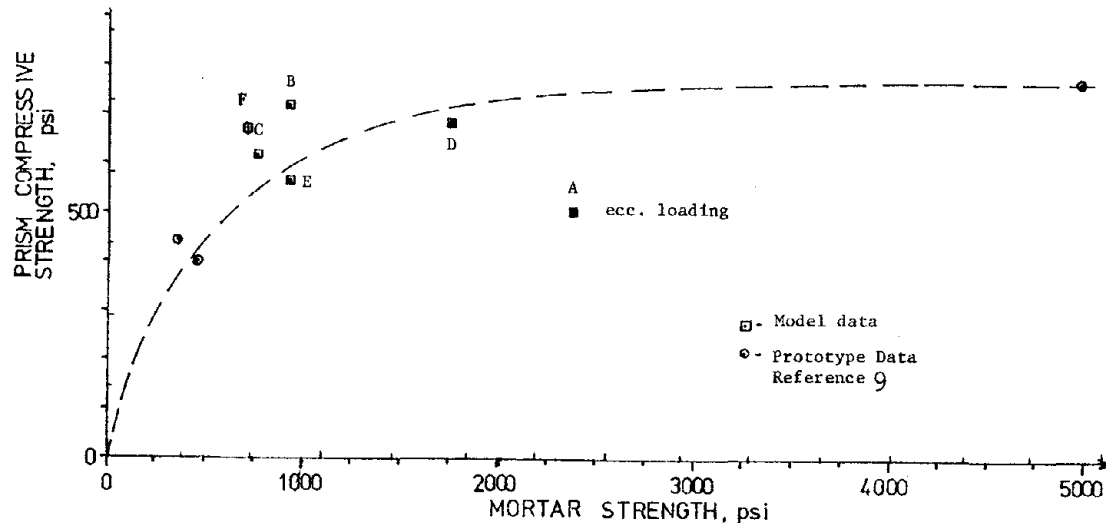


FIGURE 6 MASONRY PRISM STRENGTH VS. MORTAR STRENGTH SHOWING PROTOTYPE/MODEL CORRELATION

The flexural bond strength was determined by testing two-block high prisms that were clamped in metal frames at both the top and bottom of the prism and loaded eccentrically 4 inches from the centroid of the prism as in Fig. 7. This method was duplicated from tests conducted by Yokel et. al. (10) and as described in ASTM E149-66. The prisms were constructed of regular stretcher units with face-shell and end web bonding. The prototype specimens in tests by Yokel et. al. (10) were constructed of similar units with only face shell bonding. Because of the relatively weak bond developed between units the mortar ultimate loads were small and thus failure occurred within one minute of load application. The typical mode of failure was separation at the mortar-to-unit interface with one unit remaining free of mortar. The test results of two model series consisting of 6 specimens each are shown in Table 3 together with the results of 3 prototype specimens. It should be noted that series A prisms were cast using dry blocks while series B were cast using saturated surface dry units. The effect of de-watering the mortar via the high block adsorption is a probable contributor to the reported strength difference within the model study. The effects of end-web bonding and high mortar strength have also

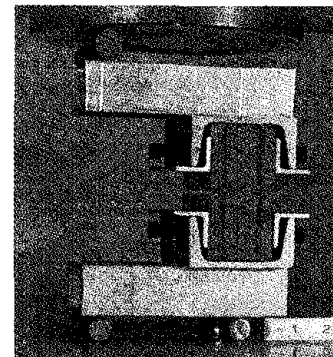


Figure 7 Flexural Bond Specimen

contributed significantly to the differences between prototype and model results.

TABLE 3 SUMMARY OF FLEXURAL TESTS ON MASONRY PRISMS

Specimen Designation	Mortar Compr. Strength 2" Cubes		Age at time of test days	Masonry Flexural Strength		No. of Specimens	Mode of Failure	Test Conditions
	psi	No. of specimens		Gross Area psi	Net Area psi			
1	2	3	4	5	6	7	8	9
Prototype: 2-Block High Prisms, 8-in Hollow Block Ref. 10	345	3	180	6	9	3	Separation at mortar-unit interface	Dry
1/4 Scale Model, 2-Block High Prisms A	882	6 ¹	15	42	50	6	-do-	S.S.D.*
B	588	6	14	48	58	6	-do-	S.S.D.*

*Saturated surface dry (S.S.D.)

Determination of masonry shear strength usually consist of testing square prisms by compression along one diagonal, with a resulting failure in diagonal tension⁽³⁾. Two model series of tests were designed after the work of Fishburn⁽⁴⁾ and the ASTM specification E519-74⁽¹⁾ for the determination of masonry shear (diagonal tension) strength. This procedure calls for the testing of small masonry walls with height to length ratio (H/L) of one in diagonal compression. The model specimen size was chosen to be two units long by four units high of the running bond pattern. After curing, the specimens were instrumented with SR-4 strain gages placed along the compressive and tension diagonals of both faces. These were wired in series to provide average strain readings. In lieu of the loading shoes recommended by the ASTM specification, a 3 inch structural tube with 1/4 inch wall was cut into lengths which fit at opposite ends of the specimen diagonal such that the resulting bearing area encompassed one unit height (2 inches). These were then placed on a level surface and filled with a stiff mix of Hydrostone capping material. Fig. 8 shows a typical shear specimen ready for testing. Fig. 9 shows the plots of shear stress versus shear strain for model series B and prototype tests. There exist some differences in the method used to measure the shear strains in model (strain gages) and prototype (deflection gages) tests but these are considered essentially the same in the lower load range prior to cracking.

The model shear specimens, which had sides only one third of the scaled prototype values for reasons of economy, showed an average shear strength of 38.5 psi in 6 specimens.

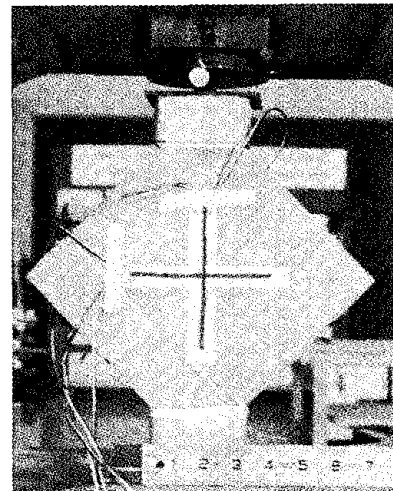


Figure 8 Shear Specimen

The prototype shear strength was found to be 18 psi. on an average of 3 specimens. In making a direct comparison of the model and prototype results, the assumption must be made that uniform tensile and compressive stresses exist all along the diagonal length of the specimen. Apart from the size difference mentioned above, however, the model mortar was 84% stronger than the prototype mortar based on 2 in. (5.08 cm.) cubes. This increase in strength, amplified by the volume of stressed material differences which exist between the 1/8 in. model joint and the 2 in. cube tested for strength determination, will result in a higher apparent shear strength in the model specimens. The influence of the higher mortar strengths of the model specimens are, however, harder to evaluate under a combined stress state condition. Combined compressive and tensile stresses exist all along the compressed diagonal of the shear specimen but the volume effects in such complex stress situations cannot be evaluated in the present comparison because no empirical data exist to relate the strength of different size specimens under these stress states as was the case of unconfined compression.

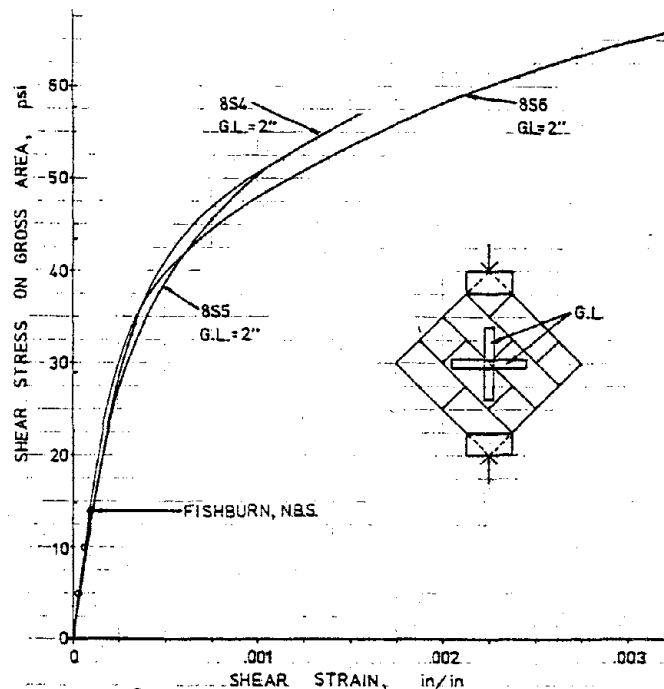


FIGURE 9 SHEAR STRESS STRAIN CURVES FOR SMALL MASONRY WALLS

MASONRY COMPONENTS AND JOINTS

Small wall specimens two blocks long by three blocks high were fabricated in running bond and tested in axial compression. The lower courses were laid in full mortar beds atop a 3/16" thick strip of aluminum. This allowed for transport of the specimens and eliminated the need for lower bearing surface capping. Another advantage of the full mortar bed is to simulate actual boundary conditions. The first series (Series A) consisting of 3 tests was used as a pilot study to determine typical small wall compressive strengths. The specimens of Series B were instrumented with 4" SR-4 strain gages. These were placed at midheight at the center on both faces of the walls and wired in series thus providing average readings. Series A specimens were capped and tested within one hour of their removal from the wet room. Series B specimens were removed from the wet room after 26 days and allowed to dry for 4 days to allow for instrumentation. The stress strain data collected for series B walls is plotted in Fig. 10. End splitting became visible for specimens 4P6 and 5P6 at 570 psi which

is 89% and 95% of f'_m for 4P6 and 5P6 respectively. First end splitting appeared at 500 psi or 85% of f'_m for specimen 6P6. The discontinuities which appear at 63% (400 psi), 70% (420 psi), 50% (300 psi) of f'_m for 4P6, 5P6, and 6P6 respectively is attributed to tension increments being recorded as a result of face shell buckling. These points, therefore, represent the failures of the interior web structures. In addition, cracking was audible at these load levels. The average secant modulus of elasticity at $0.5 f'_m$ was found to be 505,500 psi for the three model specimens.

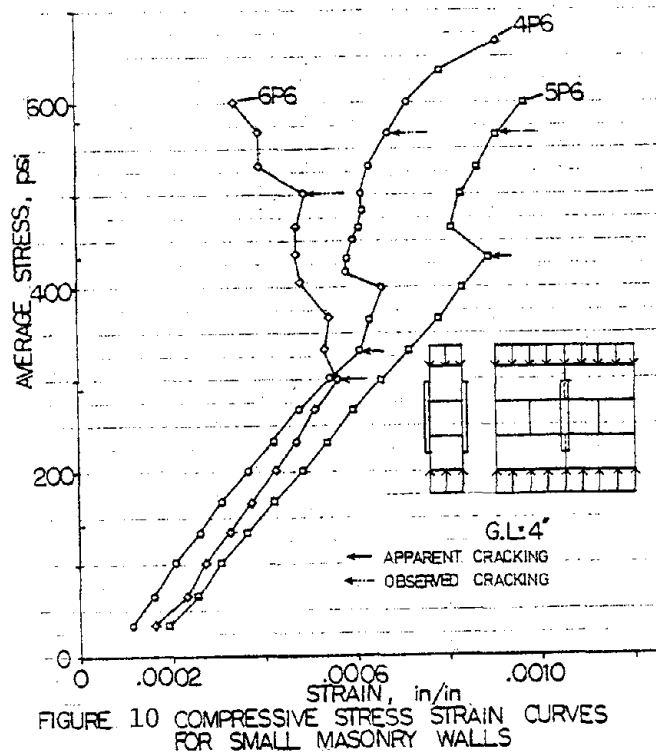
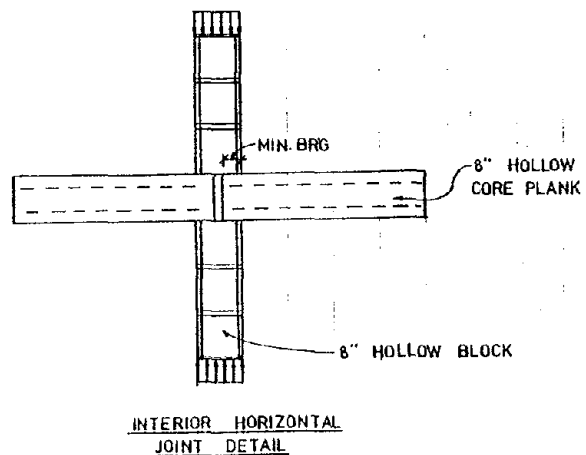


FIGURE 10 COMPRESSIVE STRESS STRAIN CURVES FOR SMALL MASONRY WALLS

In concrete masonry structures which utilize precast hollow core floor and roof slabs, the horizontal wall-to-floor joint plays a critical role. It must be able to accommodate the gravity and lateral loading without appreciable distress. An evaluation of horizontal wall-to-floor joint behavior under axially applied gravity loading is therefore the first step in developing model techniques for masonry with precast components. For this purpose the joint detail commonly found in low rise masonry construction (Fig. 11) was used in the present study. Two unreinforced and two "Durowall" reinforced joints were tested to determine the strength and joint shortening for the full range of loading. Hollow core precast slabs at 1/4 scale, developed in the Structural Models Laboratory, Drexel University, under a study sponsored by the U. S. Department of Housing and Urban Development (6) were used in these joints.

Joints M/PCP-J-1 and M/PCP-J-2 were unreinforced joints and also served as pilot studies for this program. The fabrication of the joints was very similar to the small wall specimens described above. Wall elements consisted of 3 units in height and 1-1/2 units in width, thus giving a nominal 6"x6" wall panel 2" thick. The hollow core floor units were 6" wide, 6" in length and 2" thick. A gage



INTERIOR HORIZONTAL JOINT DETAIL

FIGURE 11

length of 8" across the joint was used to determine the joint shortening. Load vs. joint shortening for the unreinforced joints is shown in Fig. 12. Joint M/PCP-J-2 appears to be stiffer and stronger than joint M/PCP-J-1. The mode of failure of both joints was by end splitting of either the top or the bottom masonry wall panel. Fig. 13 shows the crack pattern of joint M/PCP-J-2 which failed by splitting of the upper wall panel and Fig. 14 shows joint M/PCP-J-1 which failed by splitting of the lower wall panel. The results of the two unreinforced joints are summarized in Table 4. The compressive strength of the

1/4 scale masonry units used was 1100 psi. as shown in Col. 2 of Table 4. Col. 3 shows the compressive strength of the joint mortar and Col. 4 the compressive strength of two 3 block prisms cast with the joints. The ultimate joint load and joint strength on the gross area are given in Cols. 5 and 6 of Table 4 respectively. A compressive strength reduction of approximately 23% over the prism strength was shown by the average of

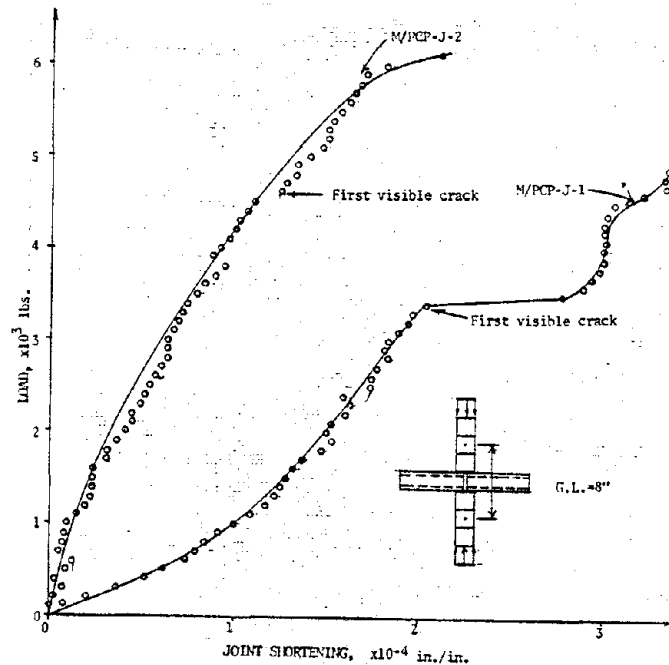


FIGURE 12 COMPRESSIVE LOAD SHORTENING CURVES FOR MODELS M/PCP-J-1 AND M/PCP-J-2

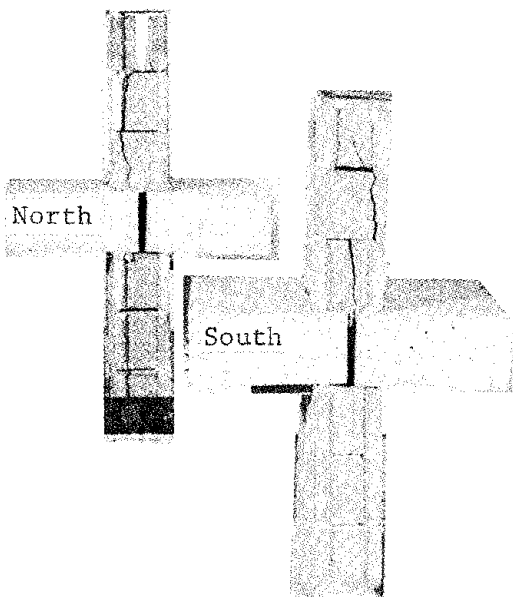


Figure 13 Joint M/PCP-J-2

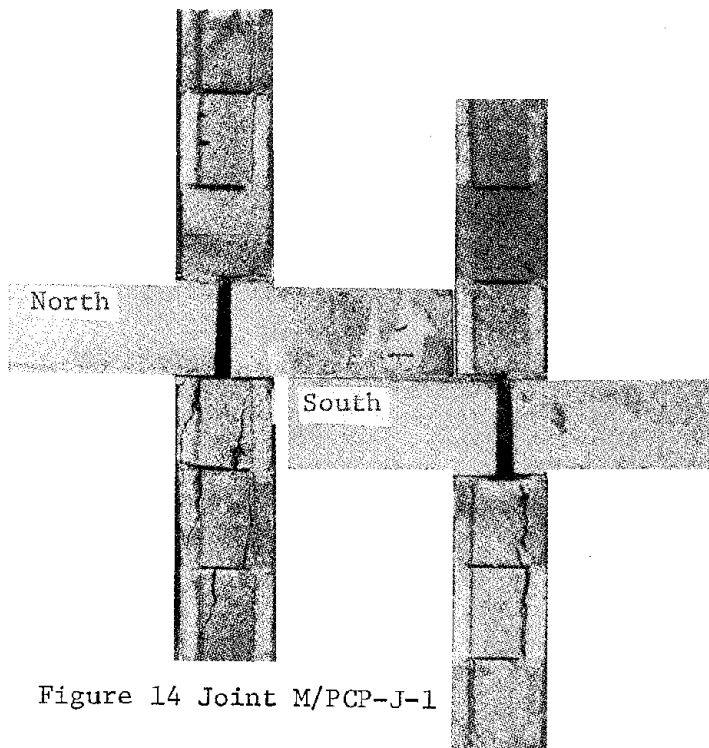


Figure 14 Joint M/PCP-J-1

Table 4 Summary of Horizontal Joint Test Results

Joint Designation	Compr.Streng. Unit Masonry Gross Area f' (psi)	Compr.Streng. Mortar 1"x2" f'_b (psi)	Comp.Streng. 3 Course Prism Gross Area f'_m (psi)	Ult. Joint Load P'_u (lbs)	Joint Strength Gross Area (psi)
1	2	3	4	5	6
M/PCP-J-1	1100	687	671	6140	560
M/PCP-J-2	1100	687	671	5260	479
			Ave.	5700	519
M/PCP-J-3R*	315	1310	191	2925	267
M/PCP-J-4R*	315	1310	292-R*	2200	201
			Ave.	2563	234

R* means wire reinforced as shown below:

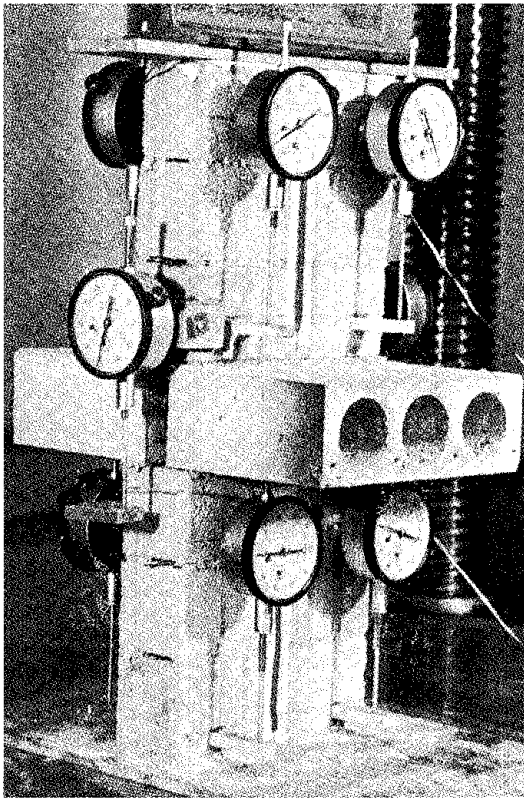
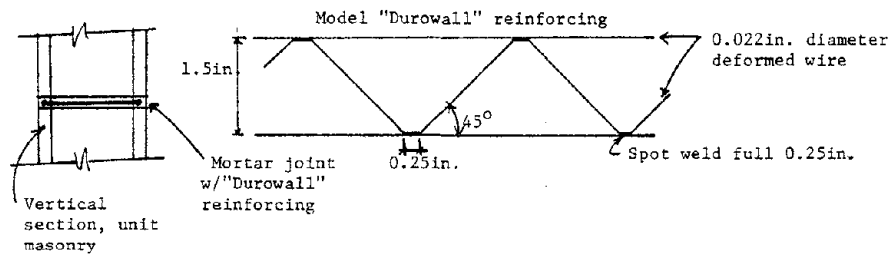


Figure 15 Horizontal Joint Test Set-up

the two unreinforced joints. This reduction was anticipated because the hollow core slabs provide only partial support to the upper masonry wall panel (see Fig. 11).

The second series of horizontal joints tested under the present effort were reinforced with model "Durowall" trusses having the configuration shown at the bottom of Table 4. The test set-up and instrumentation is shown in Fig. 15. Scaled model reinforcement was placed between the second and third courses of the bottom wall panel and between the first and second courses of the upper wall panel to simulate field construction procedures. Companion 3 block compression prisms with and without the "Durowall" reinforcement were also cast at the same time as the joints to determine the effect of the reinforcement in increasing the compressive strength. As can be seen from Fig. 15, the shortening of the upper and lower masonry wall panels was measured

by both dial gages and strain gages to allow comparison of the results. Four dial gages (two on each side), with an accuracy to 0.01 mm. were attached to each wall panel on stiff aluminum brackets over a 4 in. gage length as shown in Fig.15. In addition, 2 4 in. gage length SR-4 strain gages were symmetrically placed on each wall panel center line and wired together to read the average wall shortening. Two dial gages were attached, one on each end, across the joint (Fig. 15) to measure the joint shortening over a 4 in. gage length. The joints were loaded axially in 100 lb. increments allowing adequate time for the 10 dial gage and 4 strain gage readings to be made. The results of the load vs. axial shortening of the top and bottom wall panels of joints M/PCP-J-3R and M/PCP-J-4R is shown in Figs. 16 and 17 respectively. As can be seen from Fig. 16, the strain gage and dial gage values are very close for each wall with the bottom wall showing considerably higher stiffness.

The same general tendency of increased stiffness of the bottom wall is shown by the average readings of joint M/CPC-J-4R (Fig. 17) although in this case the strain and dial gage readings show considerable disagreement.

Load vs. axial shortening curves of the average dial gage readings of the top and bottom walls and across the joint are shown in Figs. 18 and 19 for joints M/PCP-J-3R and M/PCP-J-4R respectively. The bottom wall appears to be considerably stiffer in both joints. From these rather limited test results shown in Figs. 18 and 19, it appears that the top wall and the joint have comparable

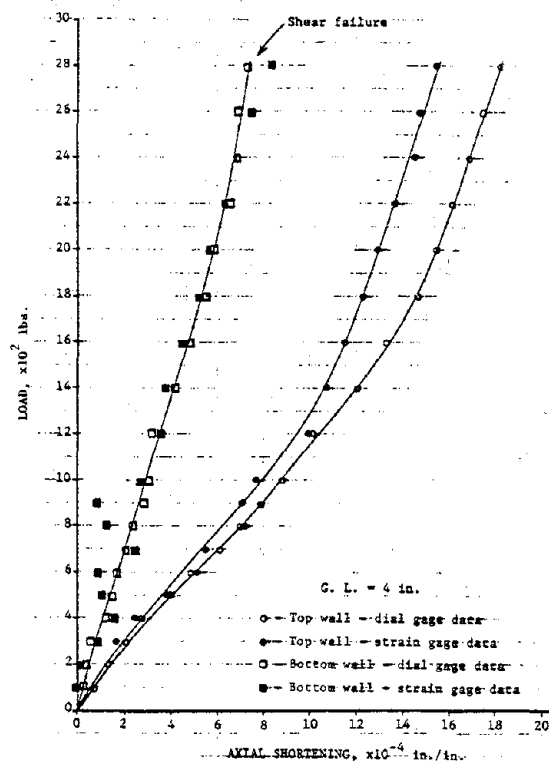


FIGURE 16 COMPARISON OF STRAIN AND DIAL GAGE DATA FOR JOINT M/PCP-J-3R

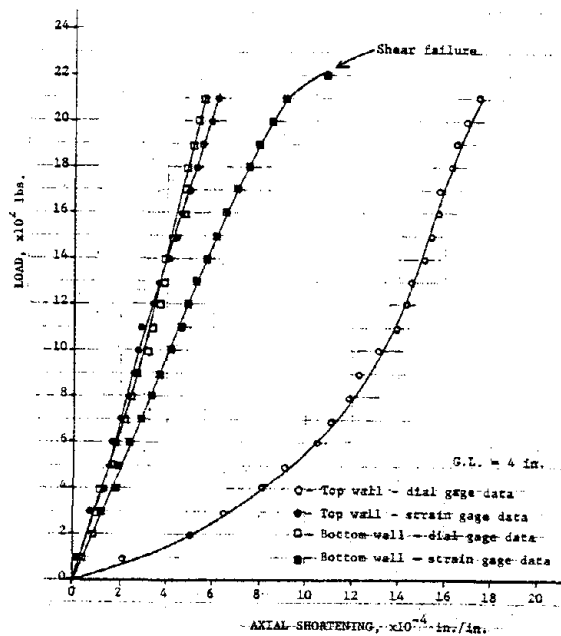


FIGURE 17 COMPARISON OF STRAIN AND DIAL GAGE DATA FOR JOINT M/PCP-J-4R

stiffnesses. The results of the two reinforced joints are summarized in Table 4. As can be seen from Table 4, the type of model masonry units used in the two reinforced joints were of the very weak kind with an average compressive strength of only 315 psi. in 6 specimens. The reason for this was the fact that all of the stronger units had been exhausted in previous phases of the program and the weaker units were the only ones available. Although, it was realized that no direct comparison could be made between the two unreinforced and the two reinforced joints because of the large differences in compressive strength of the masonry units, it was felt that a determination of the wall strength as influenced by the joint could still be made. Thus, using the results of the 3 course reinforced prisms (Col. 4, Table 4) of 292 psi. on the gross area, as a measure of the wall strength without joints, a strength reduction of approximately 20% was obtained from the average of the two joints tested (Col. 6, Table 4) which had a compressive strength of 234 psi. on the gross area. This compares favorably to the 23% reduction obtained in the unreinforced joints. Failure of both reinforced joints was sudden, with limited end splitting of the bottom wall in both cases turning into a massive shear failure across the full width of the bottom wall panel. The two end views of the failed specimen M/PCP-J-3R are shown in Fig. 20 and those of specimen M/PCP-J-4-R are shown in Fig. 21.

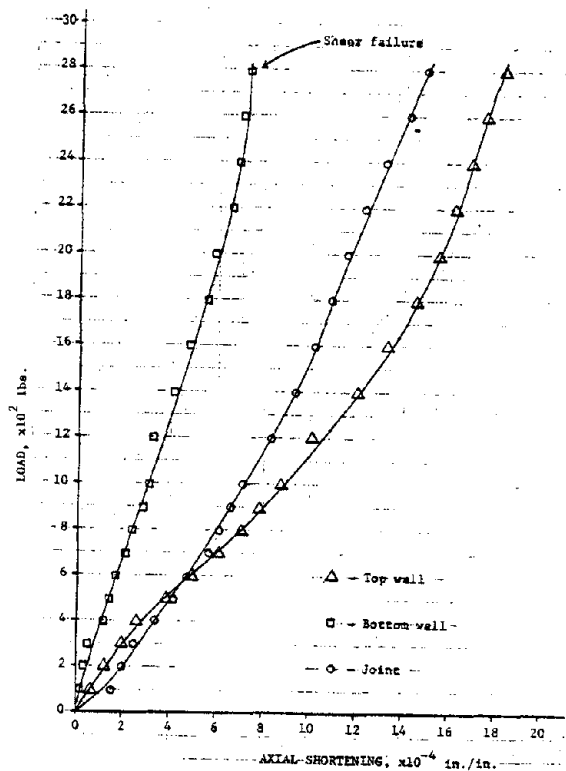


FIGURE 18 COMPRESSIVE LOAD SHORTENING CURVES FOR JOINT M/PCP-J-3R

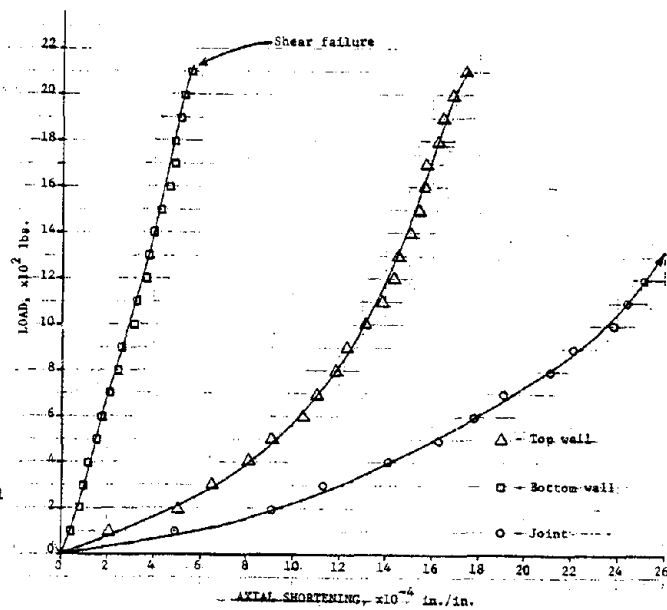


FIGURE 19 COMPRESSIVE LOAD SHORTENING CURVES FOR JOINT M/PCP-J-4-R

CONCLUSIONS

The methodology of using small scale direct models of concrete masonry structures has been presented. The basic strength evaluation tests for compressive flexural bond and shear strengths recommended for prototype structures have been also developed with minor modifications for the evaluation of model masonry strength. A systematic analysis of the parameters which affect the strength and stiffness of masonry under compressive, flexural and shear loadings has provided the means to compare model and prototype test results. Correlation of the model and prototype results ranged from excellent to good. For the case of masonry in compression, the testing of prisms has shown that the model masonry behavior is essentially the same as that reported for prototype tests. Model tests on larger compression components have also shown good correlation with prototype data. In the case of flexural bond and shear strength of masonry, proper considerations must be given to the tensile strength of the joint mortar including the effects of the stressed volume. This implies that very small size control specimens i.e. cubes or cylinders must be tested in order to be sure that the small volume of the model joint bears the same relation to its control specimen as the volume in the prototype mortar joint bears to its respective control specimen. When proper consideration of the above effects are made, the correlation of model and prototype masonry strength tests for evaluating flexural bond and shear are shown to be satisfactory. Excellent correlation of the elastic modulus of concrete masonry in compression and shear was obtained from the model tests and the limited stress-strain data of prototype masonry reported in the literature. This work has produced a systematic approach to the direct modeling of concrete masonry structures. Extensions of this approach to the study of joint details between masonry bearing walls and precast floor/roof systems has also been demonstrated. The versatility of this approach for studying the inelastic behavior of concrete masonry structures in a direct and relatively inexpensive manner has been indicated.

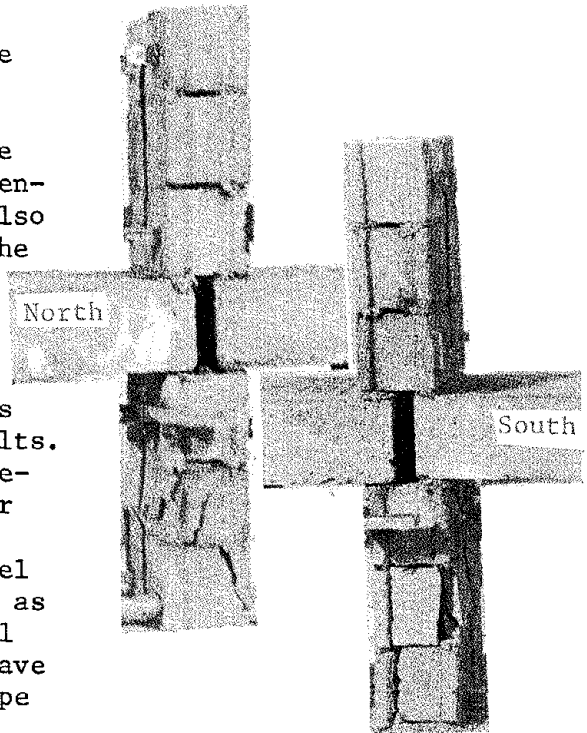


Figure 20 Joint M/PCP-J-3R

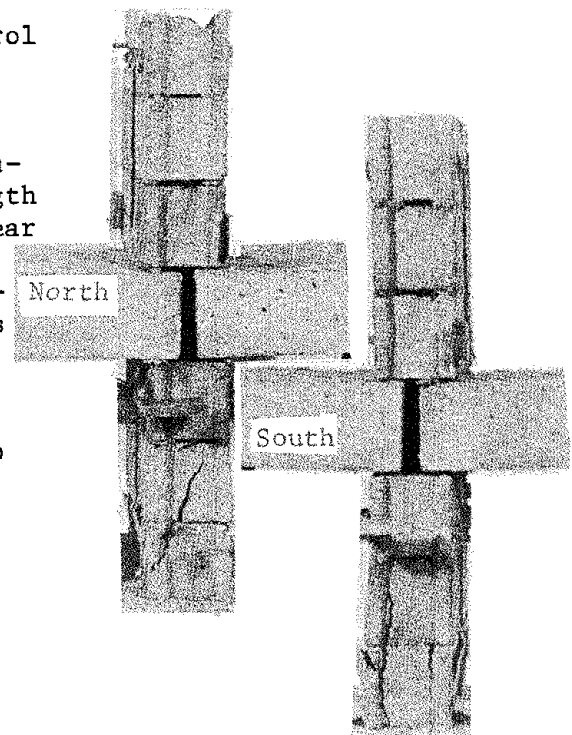


Figure 21 Joint M/PCP-J-4R

APPENDIX I - REFERENCES

1. ASTM Standard Specifications for Brick and Applicable Standard Testing Methods for Units and Masonry Assemblages, American Society for Testing and Materials, Philadelphia, Pa., May, 1975.
2. Becica, I. J. and Harris, H. G., "Evaluation of Techniques in the Direct Modeling of Concrete Masonry Structures", Structural Models Laboratory Report No. M77-1, Dept. of Civil Engineering, Drexel University, Philadelphia, Pa., June, 1977.
3. Fattal, S. G. and Cattaneo, L. E., "Evaluation of Structural Properties of Masonry in Existing Buildings," NBSIR 74-520, National Bureau of Standards, Washington, D. C., July, 1974.
4. Fishburn, Cyrus C., "Effect of Mortar Properties on Strength of Masonry," NBS Monograph 36, National Bureau of Standards, Washington, D. C., November 20, 1961.
5. Harris, H. G. and Becica, I. J. "Direct Small Scale Models of Concrete Masonry Structures" paper presented at the 2nd Annual ASCE Engineering Mechanics Division Specialty Conference, North Carolina State University, Raleigh, N. C., May 23-25, 1977, published in Advances in Civil Engineering Through Engineering Mechanics, ASCE, New York, N. Y., 1977.
6. Harris, H. G. and Muskivitch, J. C., "Report 1: Study of Joints and Sub-Assemblies - Validation of the Small Scale Direct Modeling Techniques", Nature and Mechanism of Progressive Collapse in Industrialized Buildings, Office of Policy Development and Research, Department of Housing and Urban Development, Washington, D. C., October 1977.
7. Harris, H. G., Sabnis, G. M. and White, R. N., "Small Scale Direct Models of Reinforced and Prestressed Concrete Structures," No. 326 Department of Civil Engineering, Cornell University, Ithaca, N. Y., Sept. 1966.
8. Harris, H. G., Schwindt, P. C., Taher, I., Werner, S., "Techniques and Materials in the Modeling of Reinforced Concrete Structures Under Dynamic Loads," NCEL-NBY-32228 (MIT Report No. R63-54), U. S. Naval Civil Engineering Laboratory, Port Hueneme, CA, December 1963.
9. Sahlin, S., Structural Masonry, 1st ed., Prentice-Hall, Inc., Englewood Cliffs, N. J., 1971.
10. Yokel, F. Y., Mathey, R. G., Dikkers, R. D., "Strength of Masonry Walls Under Compressive and Transverse Loads," Building Science Series 34, National Bureau of Standards, Washington, D.C., March, 1971.

APPENDIX II - NOTATION

A	=	Area of net section
A_m	=	Net area in model
A_p	=	Net area in prototype
E_m	=	Young's modulus of masonry, also of model material
E_p	=	Young's modulus of prototype material
E_s	=	Young's modulus of reinforcement, also secant modulus
f_y	=	Yield strength of reinforcement
f'	=	Compressive strength of concrete masonry unit
f'_b	=	Compressive strength of masonry mortar
f'_m	=	Compressive strength of masonry
$(f_y)_m$	=	Yield strength of model reinforcement
$(f_y)_p$	=	Yield strength of prototype reinforcement
$(f'_m)_m$	=	Compressive strength of model masonry
$(f'_m)_p$	=	Compressive strength of prototype masonry
$(f'_t)_m$	=	Tensile strength of model masonry
$(f'_t)_p$	=	Tensile strength of prototype masonry
G.L.	=	Gage Length
H	=	Height of compressive specimen
L	=	Length of compressive specimen
L_m	=	Length in model
L_p	=	Length in prototype
M	=	Moment per unit length
M_m	=	Bending moment per unit length in model
M_p	=	Bending moment per unit length in prototype
P	=	Axial compression per unit length
P_m	=	Compression load per unit length in model
P_p	=	Compression load per unit length in prototype
P'_u	=	Ultimate load
Q	=	Point load
q	=	Pressure loading
S_L	=	Scale of lengths, $\equiv L_p / L_m$
t	=	Wall thickness
t_m	=	Wall thickness in model
t_p	=	Wall thickness in prototype

w = Line loading

Greek Symbols

δ = Deflection at a point

δ_m = Deflection of model

δ_p = Deflection of prototype

ϵ = Strain at a point

ϵ_m = Strain in model

ϵ_p = Strain in prototype

ν = Poisson's ratio

ν_m = Poisson's ratio of model material

ν_p = Poisson's ratio of prototype material

ABSTRACTEFFECT OF GROUTING ON THE STRENGTH CHARACTERISTICS
OF CONCRETE BLOCK MASONRY

By Ahmad A. Hamid,¹ Robert G. Drysdale,²
and Arthur C. Heidebrecht³

In this paper the behavioural characteristics of plain and grouted concrete masonry under axial compression, shear, and splitting tension are discussed utilizing the results of an experimental program. Results for axial compression tests are reported for prisms composed of three half blocks, using different mortars and grouts. The prism test results indicate that the concept of matching the compressive strength of the grout and the masonry units is not sound and it is suggested that matching the deformational characteristics would be more efficient. It is shown that the concept of strength superposition highly overestimates the compression capacity of grouted masonry. Also, the compression results show that the mortar type is not the most significant parameter for grouted masonry whereas it is for plain masonry. Results for shear and tension tests are not presented but are referred to in order to comment on their respective behaviours. It is reported that the current Code provisions concerning allowable stresses for shear and tension for grouted masonry are very inconsistent in that they may either underestimate or overestimate the contribution of grouting for different situations.

¹Doctoral Candidate, ²Associate Professor, and ³Professor, Department of Civil Engineering and Engineering Mechanics, McMaster University, Hamilton, Ontario, Canada.

EFFECT OF GROUTING ON THE STRENGTH CHARACTERISTICS
OF CONCRETE BLOCK MASONRY

By Ahmad A. Hamid,¹ Robert G. Drysdale,²
and Arthur C. Heidebrecht³

INTRODUCTION

Design practice has more and more incorporated the feature of filling the cells in masonry with grout. This may simply be for the purpose of anchoring nominal reinforcing steel in the masonry to help develop a more ductile wall behaviour. Alternatively, the grout may be necessary to share the compression, shear or tension stresses in a wall. In this latter case, the recognized procedure embodied in North American masonry codes^{(1,2)*} is to base the analysis on the gross section which combines the area of grout and of the masonry units. They require that the grout be at least as strong as the masonry units and hence the compressive strength may be based on the strength associated with the ungrouted masonry assemblage.

It is the purpose of this paper to review the validity and adequacy of the above approach for grouted masonry. The main emphasis will be directed toward behaviour under axial compression stresses. Some comments will be made on comparable behaviour for shear and tension conditions. This discussion will be mainly based upon some of the experimental results from a research program⁽³⁾ at McMaster University.

¹Doctoral Candidate, ²Associate Professor, and ³Professor, Department of Civil Engineering and Engineering Mechanics, McMaster University, Hamilton, Ontario, Canada.

*Numerals in parentheses refer to corresponding items in Appendix I: References.

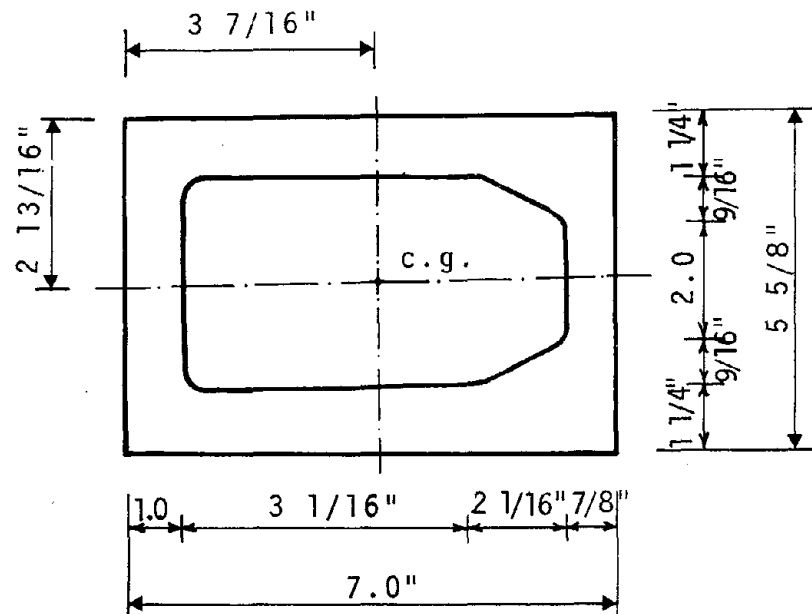
BEHAVIOUR OF PRISMS UNDER AXIAL COMPRESSION

MATERIALS

For the ensuing discussion, the ranges of parameters have been limited to one block size, a single strength of concrete block, two types of mortars and several types of grout. Specific properties are discussed below:

Concrete Blocks: The autoclaved concrete masonry units used in most of the test program⁽³⁾ were standard hollow 6 inch blocks having 2 cores. This gave a net to gross area per block of $52.1 \text{ in}^2/87.9 \text{ in}^2 = 0.59$. However, since half blocks were used for the axial compression prisms, they were obtained by cutting kerfed blocks which resulted in the cross section shown in Figure 1. Physical and mechanical properties of the half units, based on five test repetitions, are listed below.

Figure 1.
CROSS SECTION OF
HALF BLOCK UNIT



Physical Properties:

- gross area, A_g	39.4 in^2
- net solid area, A_n	24.5 in^2
- net to gross area ratio, n	0.62 in^2
- specific gravity	130 lb/ft^3
- initial rate of absorption	36.3 gm/30 sq.in/min

Mechanical Properties:

- compressive strength, gypsum-cement capping, tested flat-wise	2850 psi ($v = 4.3\%$)
- flexural tensile strength	440 psi ($v = 8.5\%$)
- splitting tensile strength	250 psi ($v = 11.5\%$)

Mortars: Types S and N mortars (ASTM 270-64T) were used. Two different mixes for type S were adopted. The properties of the three different mixes are listed in Table 1. The proportions were actually controlled by weight rather than by volume. Both measures are shown. The sand was sieved to meet the specifications in ASTM C 144-62. The water contents were established by the mason's requirements for suitable workability. This water-cement ratio was reproduced for a particular mortar type with only slight variations due to one possible retempering. The mortars were thrown out after half hour period to avoid variations resulting from excessive retempering. The control specimens were 2 inch cubes which were air cured in the laboratory under the same conditions and tested under axial compression at approximately the same age as the corresponding assemblages.

Table 1. MORTAR PROPERTIES

Mortar Type	Proportions by Volume (Weight)				Initial Flow (%)	Cube Strength (psi)	V ^c (%)
	cement	lime	sand	water			
S ₁	1	0.5 (0.21)	4.0 (4.24)	(0.9)	115	2100 ^a	7.5
S ₂	1	0.5 (0.21)	3.375 (3.58)	(0.73)	110	2640 ^b	5.9
N	1	1.25 (0.53)	6.75 (7.16)	(1.46)	118	830 ^b	4.5

^a-average of 6 batches, 3 cubes each

^b-average of 3 cubes

c-coefficient of variation

Grout: Since this investigation was mainly concerned with the influence of grout properties, an attempt was made to include a wide range of both strength and flexibility of the grout. The properties of the different types of grout are listed in Table 2. It should be noted that the weak grout, GW, and the strong grout, GS, do not satisfy the specifications of ASTM C 404-62. Batching was controlled by weight. The water-cement ratios were established to give about a 10 inch slump assuring a fluid grout which could be poured in the cores without separation of its components. Two types of control specimens were used; air cured 3 inch by 6 inch high cylinders, and block moulded prisms using paper towels as a porous separator so that water could pass through into the blocks. The prism dimensions were 2 1/2 in x 5 5/8 in x 7 5/8 in. which gives nearly the same surface area to volume ratio as the unit's cell. The control specimens were tested under axial compression at the time of testing

the corresponding assemblages. The compressive strength of the grout, converted to equivalent strength for cylinders of height to diameter ratio of two, was determined from the prism strength using the following empirical formula adopted for concrete⁽⁴⁾:

$$\frac{P_s}{P} = 0.85 \left(0.56 + 0.697 \frac{d}{\left(\frac{v}{6h} + h\right)} \right) \quad (1)$$

where

P_s = cylinder compressive strength
 P = prism compressive strength
 d = the maximum lateral dimension of the prism
 h = height of the prism
 v = volume of the prism

Table 2. GROUT PROPERTIES

Type of Grout	Proportions by Volume (Weight)					Cylinder Strength (psi)	V (%)
	cement	lime	sand	coarse aggregate	water		
GW	1		5 (5.95)		(1.11)	1100 ^a	8.0
GN ₁	1	0.1 (0.044)	3.3 (3.55)		(0.70)	1990 ^b	9.0
GN ₂	1	0.1 (0.044)	3.0 (3.22)		(0.66)	2550 ^a	3.8
GN ₃	1	0.1 (0.044)	2.475 (2.66)		(0.60)	3010 ^a	5.0
GS	1		1 (1.11)	1 (0.9)	(0.45)	5960 ^a	3.1

^a - average of 3 cylinders

^b - average of 6 cylinders

These results from the block moulded prisms are used in the discussion as being representative of the grout strength in the block. The test results of the cylinders cast in non-absorbent moulds are shown in Table 2 and are representative of the unmodified grout.

EXPERIMENTAL DETAILS AND TESTING PROCEDURE:

A total of 43 half block prisms were built in stack bond with flush-cut joints. After 24 hours, different grout

mixes were poured into the cells and puddled with a steel rod. At the age of 28 to 42 days, the prisms were capped using a gypsum-cement compound (ASTM C 140-56) and after 24 hours they were tested under axial compression. The load was applied at the centroid of the net area of the ungrouted prisms and at the centre of the gross area of the grouted prisms.

The adopted three course prism, shown in Figure 2(a), having a slenderness ratio of 4.2, was selected to eliminate the effect of the platen restraint which can cause an erroneously high compressive strength⁵¹. For this prism, the central block will be free from artificial confining effects.

Mechanical gauge points were mounted on both faces of the prisms using a 4 inch gauge length, so that the deformations in the vertical direction (across the top and bottom joints and on the middle block) and in the horizontal direction (along the height of the central block which is free from the confining lateral stresses produced from the platen restraint) could be measured. The arrangement of the gauge points is shown in Figure 2(a). Strain measurements were taken at regular load increments up to about 90% of the failure load.

DISCUSSION OF TEST RESULTS

The comprehensive strength of the tested prisms were calculated on the basis of the net area for the plain specimens, A_n , and on the basis of the gross area for the grouted specimens, A_g . The results of the tested prisms and their corresponding control specimens are listed in Table 3.

Figure 3 shows the results of grouted prism strengths in terms of the compressive strength of the grout (calculated from block moulded prism strength) for type S₁ mortar. The most striking feature to be noted is that the average compressive strengths of the grouted prisms are all less than the strength of the plain prism, f'_{mp} , which is also indicated in the Figure, even for grouts having higher strength than that of the block. Apparently, little increase in prism strength was achieved with a large increase in grout strength, thereby indicating that the strength superposition concept highly overestimates the compression capacity. In fact, if the individual strength of plain masonry, f'_{mp} , and the grout, σ_{cg} , are linearly combined as shown by the dashed line in Figure 3, the extent to which superposition is not valid is even more obvious. This finding contradicts the commonly held opinion that design strength values may be efficiently increased by increasing the grout strength.

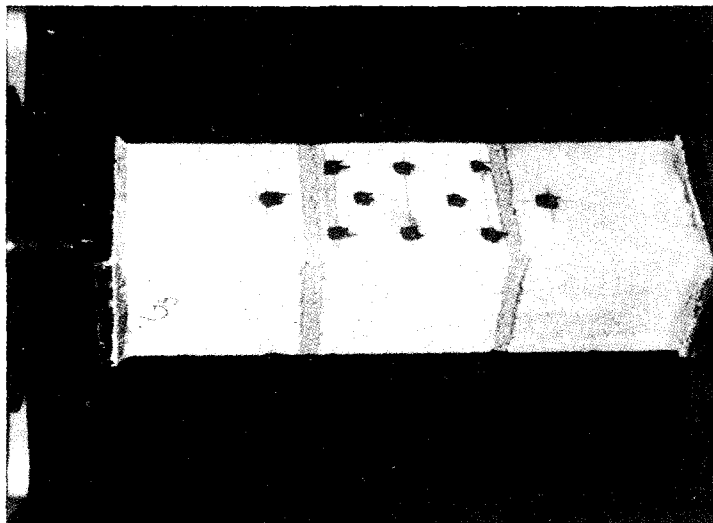


Figure 2(a)

Prior to Test

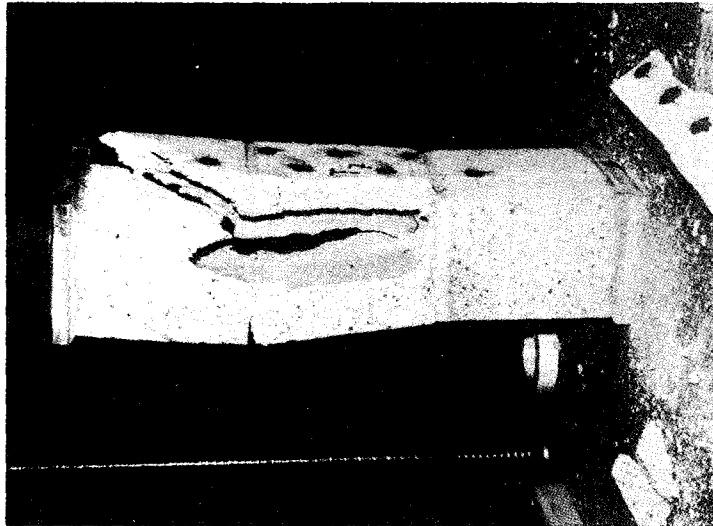


Figure 2(b)

Plain Prism

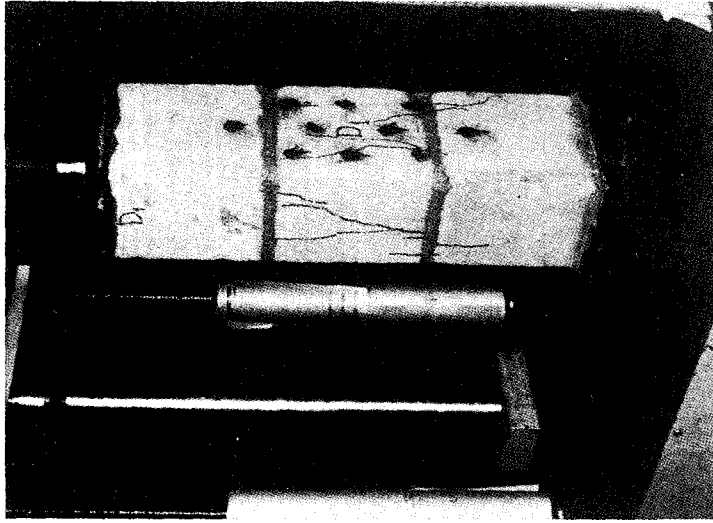


Figure 2(c)

Grouted Prism

Figure 2. PRISMS UNDER AXIAL COMPRESSION

Using a linear regression analysis, the compressive strength of the grouted prisms can be related to the strength of the corresponding grout and the plain prism strength as:

$$\frac{f'_{mg}}{f'_{mp}} = \eta + 0.143 \frac{\sigma_{cg}}{\sigma_{cb}} \quad (2)$$

The above relationship is shown in Figure 3 by the solid line. It should be noted that this empirical equation is obtained using one block size and a single strength of concrete block.

The stress-strain relationships for plain and grouted prisms are plotted in Figures 4(a) and (b) for both vertical and horizontal strains, respectively. It can be seen that grouted prisms have less axial stiffness and exhibit larger tension strains compared to the plain prism. This behaviour is especially noticeable at high stress levels. Since the loading conditions assures that uniform axial strains are imposed in both the outer shell and the grouted core, it would usually be considered that the compression load would be shared in proportion to their axial stiffnesses. Compared to the test results of the plain prism, the prism with weak grout, GW, ($\sigma_{cg} = 2040$ psi) exhibited large lateral strain at much lower stress levels. A large increase in the grout strength ($\sigma_{cg} = 5500$ psi) using the strong grout, GS, resulted in vertical stress-strain behaviour ($\sigma_y - \epsilon_y$) approaching that of the plain prism. Therefore, it might be assumed that axial strength of the outer shell is near to being developed and is the controlling factor. However when the corresponding lateral strains are reviewed, (Figure 4(b)) a different behaviour is very apparent. At stresses above approximately 40% of the strength of the plain prisms, the grouted prisms showed comparatively large lateral strains. Although it was usually difficult to differentiate between the failure modes for the plain and grouted prisms, these lateral strain measurements provide a key to understanding the failure mechanism.

It is suggested that at high stresses in the grout, the resulting inelastic deformations in the horizontal direction produce high bilateral tensile stresses in the outer shell as it tends to confine the grout. These stresses in combination with the vertical stresses cause a premature splitting failure of the block under a state of biaxial compression-tension stress⁽³⁾. This explanation indicates that it might be more appropriate to match the deformational characteristics of the grout to those of the block rather than matching the strength as codes^(1,2) suggest.

In Figure 2(b) a photograph of a typical failure of a plain prism is shown. The failure is similar to the behaviour of

Table 3. RESULTS OF COMPRESSION TESTS

Type of Prism	Mortar Strength ^a (psi)	Grout Strength ^b (psi)	Compressive Strength of Prisms		
			Individual psi	Mean psi	V(%)
plain, S ₁ mortar	2130		2310	2380	3.6
			2260		
			2430		
			2440		
			2440		
plain, S ₂ mortar	2640		2390	2360	3.3
			2290		
			2450		
			2290		
			2290		
plain, N mortar	830		2100	2230	5.5
			2250		
			2190		
			2390		
			2390		
Grouted, GN ₁ S ₁ mortar	2060	1790	1510	1640	13.6
			1550		
			2010		
			1450		
			1670		
Grouted, GN ₁ S ₂ mortar	2640	2050	1770	1750	3.0
			1780		
			1670		
			1780		
			1780		
Grouted, GN ₁ N mortar	830	2050	1500	1510	3.3
			1600		
			1430		
			1510		
			1510		
Grouted, GN ₂ S ₁ mortar	2290	2500	1820	1860	6.4
			1860		
			2060		
			1760		
			1780		
Grouted, GN ₃ S ₁ mortar	1960	3630	2110	1940	7.2
			1960		
			1780		
			1900		
			1900		
Grouted, GW S ₁ mortar	1960	2040	1770	1750	3.0
			1780		
			1670		
			1780		
			1780		
Grouted, GS S ₁ mortar	1970	5500	1980	2200	6.9
			2310		
			2280		
			2240		
			2240		

^a-compressive strength of mortar cubes

^b-compressive strength of grout as calculated from block moulded prisms

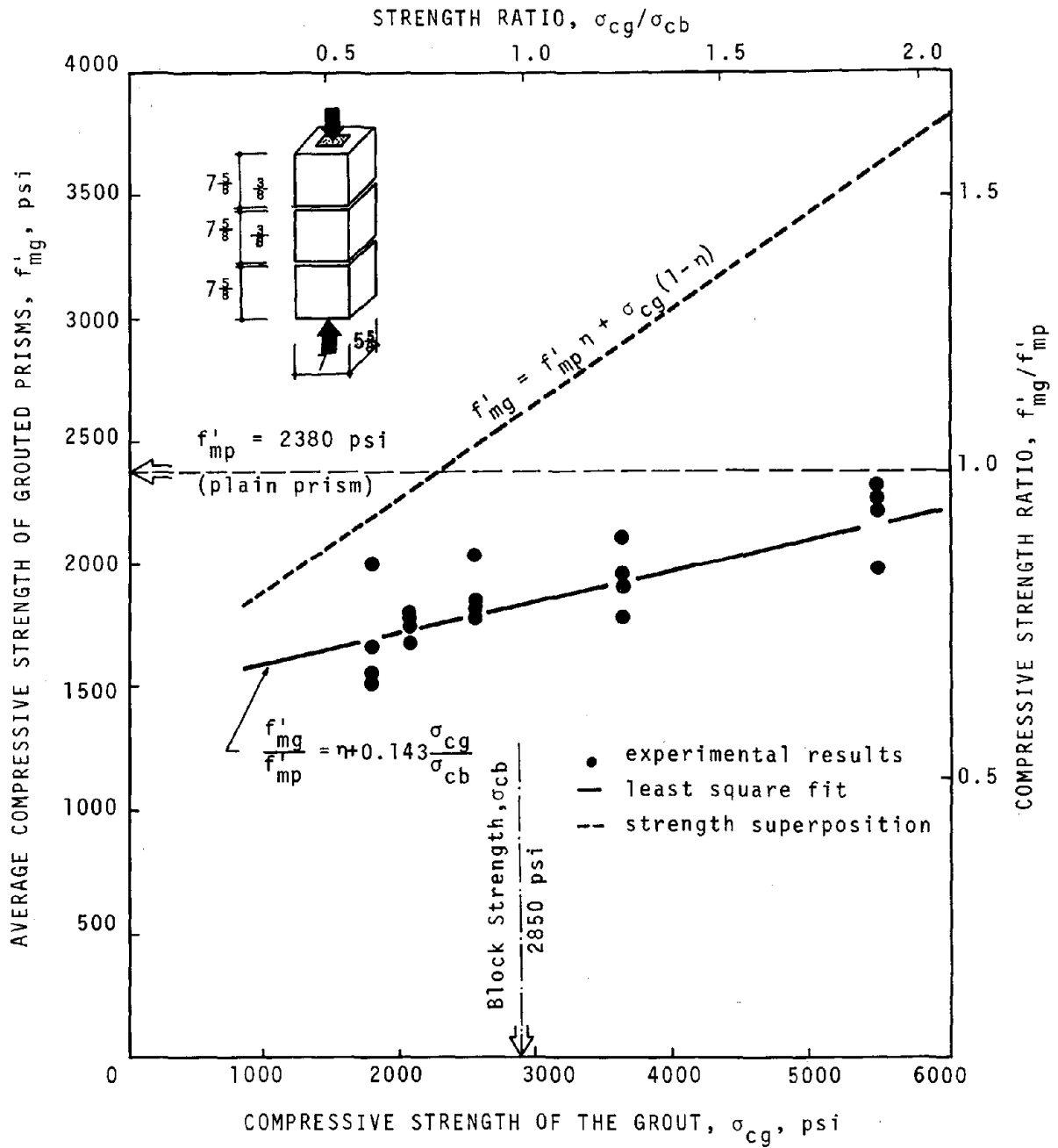


Figure 3. GROUTED PRISM STRENGTH VERSUS GROUT STRENGTH (type S1 mortar)

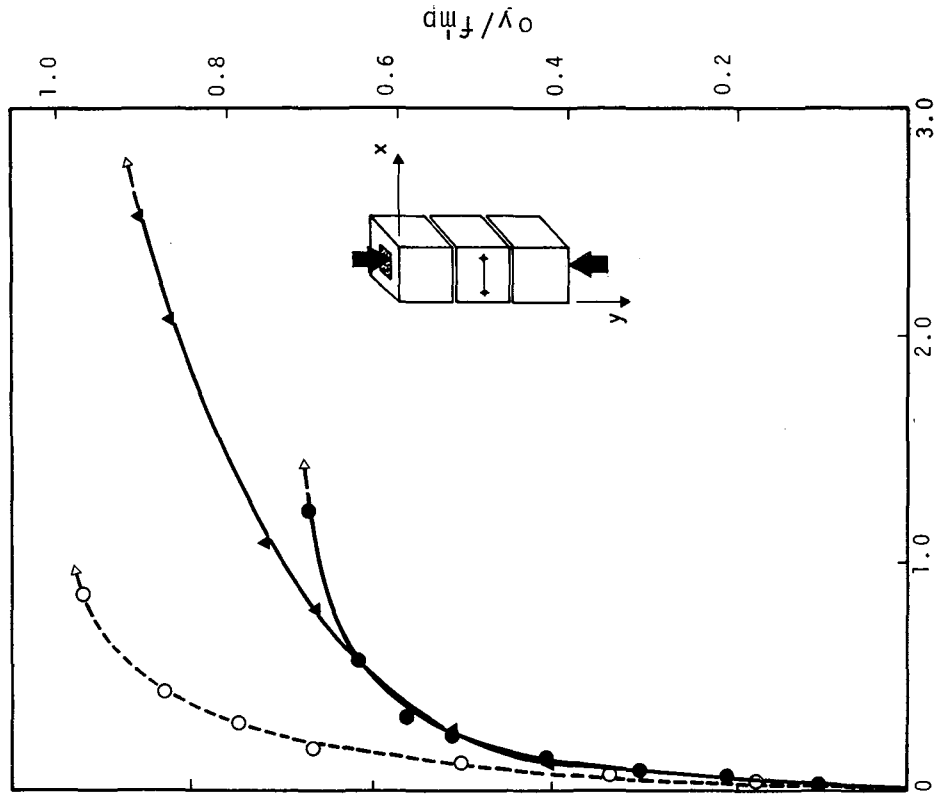


Figure 4(a)

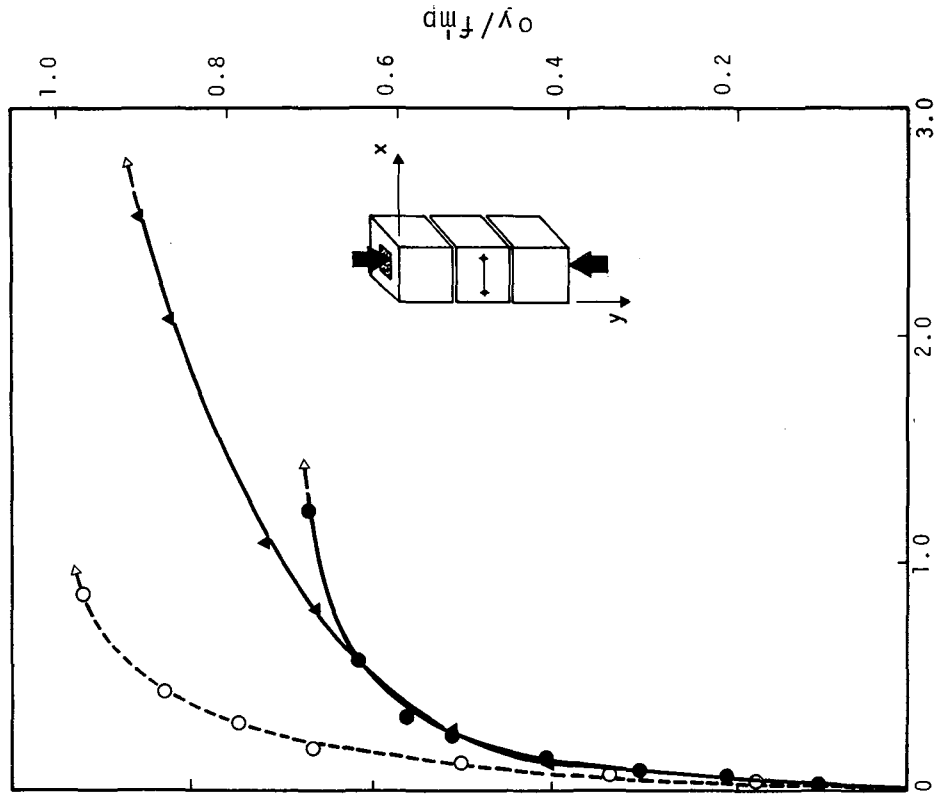


Figure 4(b)

Figure 4. STRESS STRAIN RELATIONSHIPS FOR PLAIN AND GROUTED PRISMS

solid brick masonry, where the differential deformational characteristics of the units and the mortar joints produces a splitting failure of the block. This is due to the tendency of the mortar joints to expand laterally more than the block, which then act to confine the mortar. These confining stresses are balanced by lateral tensile stresses in the block which upon failure usually results in splitting of the blocks on either side of the joint. A photograph of a typical failure of a grouted prism is shown in Figure 2(c). At failure, splitting of the prism as shown tended to originate in the central block away from the confining effect of the platen restraint. In many cases it was possible to recover the grout core intact after extensive splitting of the shell. In addition the grouted prisms showed a more gradual failure.

Figures 5, (a) and (b) show the different stress-strain relationships for deformations measured on the block compared to those measured across the joint for plain and grouted prisms for types S₁ and N mortars, respectively. For plain prisms, the vertical strains measured across the joint using a 4 inch gauge length are greater than corresponding strains taken within the height of the central block. For grouted prisms these strains are quite close. It would seem that the continuity provided by the grout reduces the significance of the characteristics of the mortar joint for axial compression loading. From a comparison of the results for the two mortar types, it can be seen that the same trend is evident. Figure 5 also indicates that the difference for deformation across the joint compared to on the block are higher for type N mortar than for type S₁ mortar. Design codes^(1,2) designate that the compressive strength, f'_m , for grouted masonry is considered to be equivalent to solid masonry where only the mortar type affects this value for a particular unit. The results in Figure 5 indicate that there may be some inaccuracy associated with such a simple approach. In fact, Figure 6 which shows the variation of the compressive strength of plain and grouted prisms for different compressive strength of the mortar cubes illustrates this more clearly. The results indicate that the mortar strength (within the range considered for types S and N) has little effect on the compressive strength of either plain or grouted prisms. Also this figure clearly indicates the strength reduction associated with grouted masonry compared to plain masonry and supports the conclusion that matching the block and the grout strengths may overestimate the strength capacity.

Figure 7 shows the variation of the modulus of elasticity compared to prism compressive strength for plain and grouted prisms, again for types S₁ and N mortar. The modulus of elasticity is based on the secant modulus at 50% of the strength. It is shown that there is no direct correlation

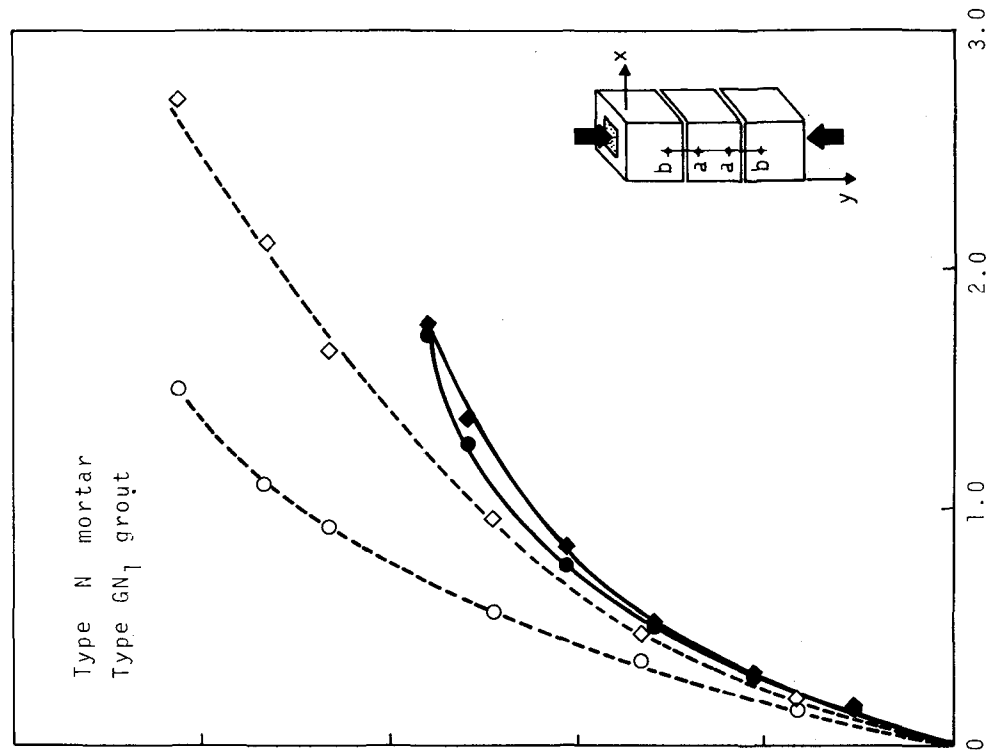
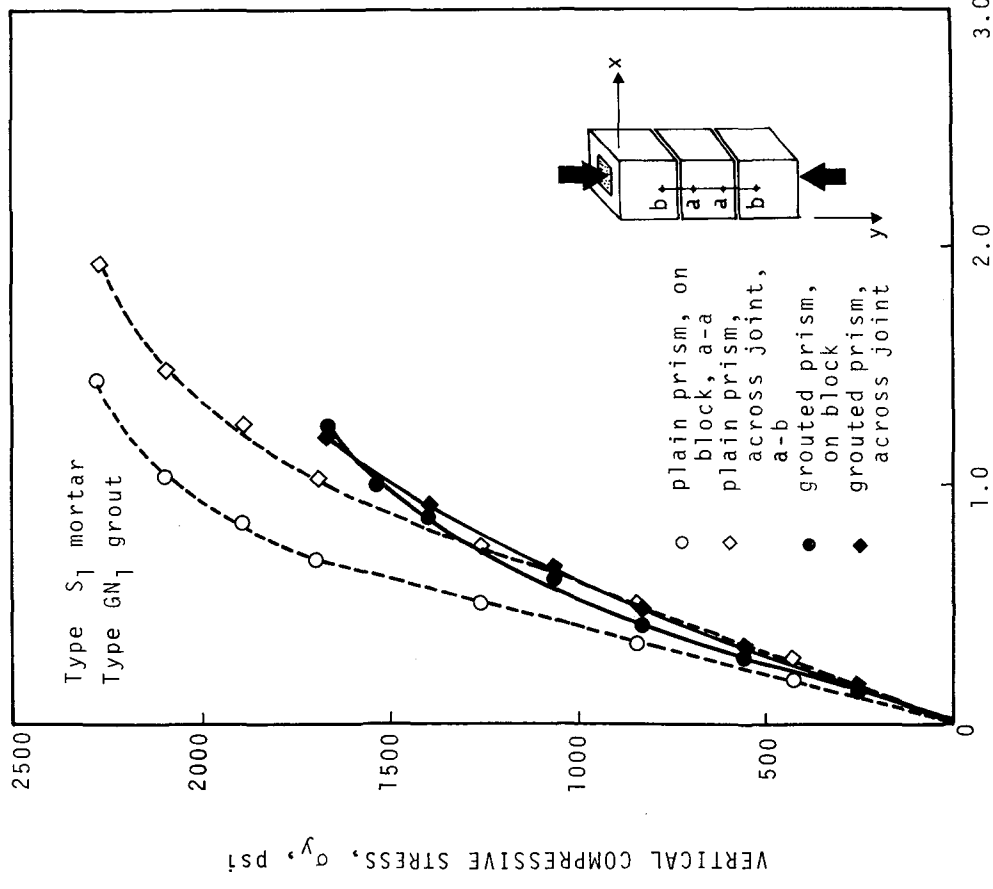


Figure 5(a)

Figure 5(b)

Figure 5. DEFORMATIONS ON BLOCKS AND ACROSS THE JOINTS OF PRISMS UNDER AXIAL COMPRESSION

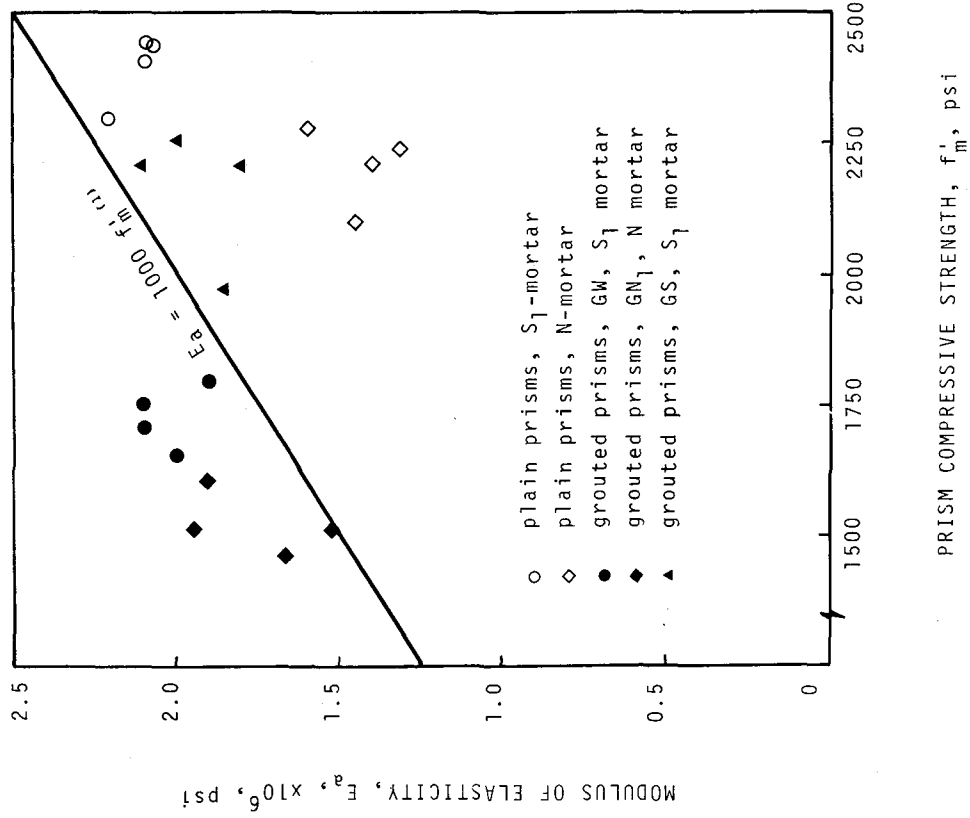


Figure 7. MODULUS OF ELASTICITY VERSUS COMPRESSIVE STRENGTH OF PRISMS

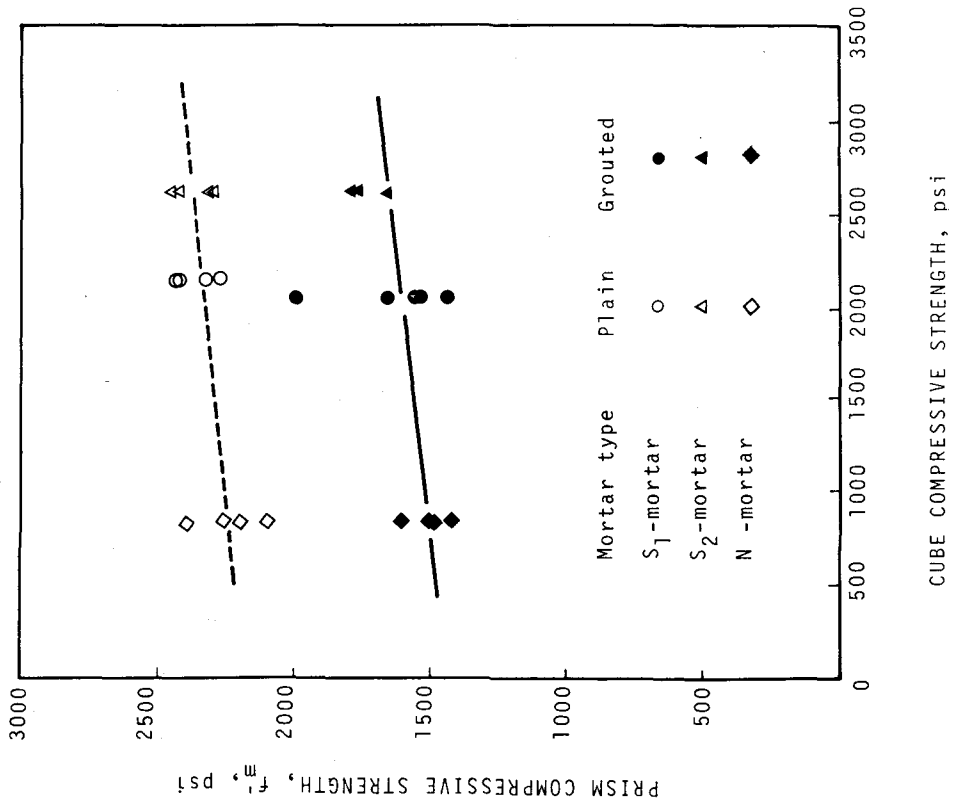


Figure 6. PRISM COMPRESSIVE STRENGTH VERSUS MORTAR STRENGTH

between the modulus of elasticity and the compressive strength as the parameters affecting these two characteristics are not the same. At failure the interaction of the different constituent materials (block, mortar and grout), due to the high inelastic deformations, creates in the components complex states of stresses which are different from those at early stage of loading. While it is possible to get a strong correlation between the strength and the stiffness for isotropic homogeneous material, it is rather difficult to achieve this correlation for an anisotropic nonhomogeneous material such as masonry, which has two or three materials of different inelastic deformation characteristics. Figure 7 shows, clearly, that the code⁽¹⁾ formula ($E_a = 1000 f_m'$) significantly overestimates the elastic modulus of plain masonry constructed with type N mortar. For type S₁ mortar the code formula seems to overestimate the stiffness for plain masonry and for grouted masonry of high strength grout, while it underestimates the stiffness for grouted masonry having low strength grout.

INDICATIONS OF BEHAVIOUR OF MASONRY ASSEMBLAGES UNDER SHEAR AND TENSION

Limitations of space preclude a full treatment of the results of tests⁽³⁾ concerning shear and tension capacities. However, a brief indication of the main trends will be presented.

Under shear parallel to bed joints, the mode of failure for both plain and grouted assemblages was that of a debonding failure at the block-mortar interface followed instantly by a shear-slip failure of the grout for the latter. The average shear stresses at failure were greatly increased by grouting the cores and were significantly influenced by increasing the strength of the grout. Providing precompression stresses increased the shear strength proportionally for plain and grouted specimens. A main conclusion was that grouting increases the resistance to debonding and thereby shows that the design provisions may underestimate the shear capacity of grouted masonry.

To establish the tensile strength at different orientations from the bed joint, plain and grouted masonry discs were tested under splitting loads. As expected for anisotropic material, the tensile strength varied with the orientation of the principal tensile stress. Grouting contributed most when the tension was normal to the bed joint, whereas there was no contribution for tension parallel to the bed joint. For the latter case the capacities of plain and grouted specimens were almost the same no matter what the grout

strength was. High tensile strengths of grout resulted in proportionally higher tensile capacities under tension normal to the bed joint. These results indicate that tensile strength parallel to the bed joint, based on gross area for grouted masonry, is smaller than for plain masonry based on net area. This contradicts the code provisions.

CONCLUSIONS

The compressive test results indicate that the concept of matching compressive strength of grout and masonry units is not sound and that matching deformational characteristics would be more efficient. Also for grouted masonry, the compression results show that the influence of mortar type is not the most significant parameter.

Although the test results for shear and tension were not presented here it has been mentioned that the current approaches by the codes^(1,2) for grouted masonry are very inconsistent in that they may underestimate or overestimate the contribution of grouting.

It is recommended that the development of a more rational basis for design of grouted masonry must include the study of the complex interactions which exist between the constituent materials (block, mortar and grout). This is particularly important for the development of an ultimate strength approach to design where the potential of masonry may be fully recognized.

ACKNOWLEDGEMENTS

This research was funded through Operating Grants from the National Research Council of Canada. The authors appreciate the contribution of mason's time and equipment made available through the Ontario Masonry Contractors Association and the Ontario Masonry Industry Promotion Fund and we also thank General Concrete Ltd. for providing the concrete blocks.

APPENDIX I - REFERENCES

1. CSA Standard S304-1977, "Masonry Design and Construction for Buildings," Canadian Standards Association, Rexdale, Ontario, 1977.
2. Recommended Practice for Engineering Brick Masonry, Structural Clay Products Institute, Virginia, 1969.
3. Hamid, A.A., "Behaviour Characteristics of Plain and Grouted Concrete Masonry Assemblages," Ph.D. Thesis, McMaster University, Hamilton, Canada (in preparation).
4. Neville, A.M., "General Relation for Strengths of Specimens," ACI JOURNAL, Proceedings, v. 63, No. 52, October, 1966, pp. 1095-1109.
5. Mayes, R.L. and Clough, R.W., "A Literature Survey. Compressive, Tensile, Bond and Shear Strength of Masonry," Report No. EERC 75-15, College of Engineering, University of California, Berkeley, Calif., June, 1975.

APPENDIX II - NOTATION

- η = net to gross area ratio of half block unit, A_n/A_g
- f'_{mp} = compressive strength of plain prisms
- f'_{mg} = compressive strength of grouted prisms
- f'_{mgw} = compressive strength of grouted prism, GW grout
- f'_{mgs} = compressive strength of grouted prism, GS grout
- σ_{cb} = compressive strength of half blocks
- σ_{cg} = compressive strength of grouts as calculated from block moulded prisms
- E_a = modulus of elasticity of prisms based on the secant modulus at 50% of the strength

ELASTIC AND CREEP PROPERTIES OF MASONRY

By E. L. Jessop¹, N. G. Shrive² and G. L. England³

ABSTRACT

At present there is a dearth of knowledge of the engineering properties of masonry assemblies, restricting improvement in masonry design techniques. A system of theoretical modelling is described by which elastic, creep and shrinkage properties of masonry assemblies may be predicted. Five stack-bonded prisms were tested in compression to failure with strains measured on an individual brick unit, a mortar joint and for a series of units and joints. Values of elastic modulus determined from the individual components are used to predict the overall modulus. Less than 20% error is observed between the predicted and measured values. There is some explanation of possible causes for the difference and it is thought that with better knowledge of *in situ* properties, the models may well be of engineering use to masonry designers.

¹ Associate Professor and ² Assistant Professor, Department of Civil Engineering, University of Calgary, Calgary, Alberta, Canada.

³ Reader of Mechanics, Department of Civil Engineering, King's College, University of London, London, England.

ELASTIC AND CREEP PROPERTIES OF MASONRY

By E. L. Jessop¹, N. G. Shrive² and G. L. England³

INTRODUCTION

Sophisticated procedures are employed in the design of concrete and steel structures; these design methods are continuously refined and improved. However, even though masonry has been used as a construction material for hundreds of years, there is a paucity of basic engineering data about the material. For example, the present Canadian Code (CSA S304, 1976) indicates that the modulus of elasticity for brickwork be calculated by taking 1000 times the compressive strength of a prism of the appropriate bricks and mortar. Considering the (statistical) variance of the strength of brickwork joints (1)*, and the scatter of data presented by Plowman (2), there is clearly an inherent inaccuracy in such a method of estimation.

If masonry design techniques are to be improved then basic engineering data for the material must be available or predictable. Compressive and flexural strength are important in design but knowledge of elastic, creep and shrinkage properties are essential for determining the initial distribution of stress in a structure under load, and how the stresses may be redistributed with time.

Lenczner (3) has broached the problem of creep, and some stress-strain data have been presented by others (4, 5, 6). Base and Baker (5) also used a simple theoretical model to predict the elastic modulus of prisms. To our knowledge however, there has been no concerted attempt to theoretically predict the elastic modulus, creep and shrinkage properties of masonry assemblies. In this paper, a system of theoretical modelling via which such properties might be predicted will be discussed, together with some of the problems associated with the experimental determination of the necessary input data.

THEORETICAL MODELLING

The objective of this theoretical modelling is to use relatively simple models to predict the elastic, creep and shrinkage properties of masonry assemblies with sufficient accuracy for engineering purposes. For reasons which are apparent later, we have been unable as yet to determine whether or not the proposed type of models satisfy the objective completely. It is therefore appropriate to discuss briefly the concept

¹ Associate Professor and ² Assistant Professor, Department of Civil Engineering, University of Calgary, Calgary, Alberta, Canada.

³ Reader of Mechanics, Department of Civil Engineering, King's College, University of London, London, England.

and derivation of a model, with associated results, before concentrating on the problems of experimental work.

The theoretical models are based on combinations of the series and parallel models for two-phase composite materials (see Figure 1). Actual properties of composite materials lie between the property values predicted by these two systems. It follows that an actual two-phase material is some combination of the two systems. Masonry, with its regular structure, can be easily broken down into different combinations of the series and parallel models. Consider, for an example, a single wythe wall. A side-elevation is shown in Figure 2. Two different repeating units are shown - the larger unit is repeated both vertically and horizontally, and the smaller unit is repeated horizontally but is displaced laterally in the vertical direction. The smaller repeating unit may be broken down into two different combinations of the series and parallel models as shown in Figure 3(a). The larger unit can be divided into the same combinations as the smaller unit and a further one (Figure 3(b)). Thus three different series and parallel combinations are obtained for the wall.

For an example analysis, the masonry unit and mortar are given dimensions $a \rightarrow f$ as in Figure 4. A vertical force, F , is applied and the apparent modulus of elasticity for the combination is determined.

Consider the first combination for the smaller repeating unit (Figure 3(a)). Equilibrium and compatibility conditions may be applied as follows:

(i) Equilibrium:

$$F = F_A = F_B \quad \text{in the vertical direction}$$

and within section (A),

$$\sigma_m A_m + \sigma_b A_b = F$$

where A_m , and A_b and σ_m , σ_b are the cross-sectional area and vertical stress in the mortar and brick or block respectively.

(ii) Compatibility:

$$\Delta_{(Total)} = \Delta_{(A)} + \Delta_{(B)} \quad \text{in the vertical direction;}$$

and within section (A),

$$\Delta_{(A)m} = \Delta_{(A)b}$$

where $\Delta_{(Total)}$ is the total decrease in length of the combination and $\Delta_{(A)}$, $\Delta_{(B)}$ are the decreases in length of sections (A) and (B). The subscripts m and b again refer to mortar and brick or block respectively.

If we assume that there is no interference between the materials from different Poisson effects, so that there are no lateral stresses, we can relate stress to strain in the vertical direction using Hooke's Law ($\sigma = E \epsilon$: $\sigma =$ stress, $\epsilon =$ strain, $E =$ modulus of elasticity).

The above conditions and assumption can be used to determine the apparent modulus of elasticity, E_{comb} of the repeating unit.

$$E_{\text{comb}} = \frac{(b+e)(a+d) f E_m (acE_b + dfeE_m)}{A_{\text{comb}} [(a+d)fbE_m + aceE_b + dfeE_m]}$$

where A_{comb} is the apparent cross-sectional area of the combination. A_{comb} may be determined by putting

$$E_b = E_m = E_{\text{comb}},$$

since if $E_b = E_m$, then the modulus of the combination should be no different. Thus

$$A_{\text{comb}} = \frac{(b+e)(a+d)(ac + de)f}{[(a+d)fb + ace + dfe]}$$

It should be noted that if a brick or block is cored - not solid as in this example analysis - then by varying the values of dimensions a , c , d and f , allowance can be made for the different cross-sectional areas of mortar and brick. If the core is not totally filled with mortar allowance could be made by introducing a third element, air, in the model but the need for this has not yet been demonstrated.

Further, if the dimensions f and c are the same, then A_{comb} reduces to

$$A_{\text{comb}} = f(a + d) = c(a + d)$$

as one might expect.

The remaining two combinations for the wall may be similarly analysed. By choosing values of the dimensions $a \rightarrow f$, the predictions of E_{comb} for different values of E_b and E_m may be compared for the three combinations. Figure 5 is a plot of E_{comb}/E_m vs E_b/E_m and it may be seen that all three combinations show similar trends.

To demonstrate how such models might be used to predict the effects of creep and shrinkage in different geometrical masonry assemblies, a very simple system was considered. The system is shown in Figure 6. If the area of grout A_g is zero then the model approximates to a wall with no vertical mortar joints: with $A_g = A_b$, a simple pier is approximated. The model may be analysed for elastic response to load as in the analysis

above. Creep and shrinkage effects may be introduced by using specific creep. The use and advantages of the concept of specific creep are described in detail elsewhere (7). Briefly, specific creep strains are the strains of the unit stress creep curve normalized with respect to temperature by a suitable function $\phi(T)$. Thus at a given time:

$$\text{creep strain} = \epsilon_{cr} = c \sigma \phi(T)$$

where c = specific creep, σ = stress and $\phi(T)$ is a function of temperature. The quantity c may be used as a pseudo-time parameter in creep analyses, with the advantage that calculations may be carried out in isolation of real time, and with greater ease than when the relationship between c and real time is incorporated in the analysis.

In the model analysed here, once the elastic response is determined, a step increase in specific creep of the mortar is allowed and the model re-analysed. Shrinkage strains have been assumed to be a direct multiple of the creep strains, and the properties of the grout a multiple of the properties of the mortar. This latter is not entirely true for cement paste (for which data is available) but is a reasonable approximation. No *in situ* data has been found for masonry mortars.

In the pier model, the non-shrinking core of grout will provide considerable restraint to shrinkage until it eventually begins to shrink itself. In this particular analysis the grout was assumed to creep but not shrink.

By assuming various values for the parameters involved, the creep and shrinkage effects in the pier may be compared with those for the wall. From Figure 7 it can be seen that the wall is subject to considerably more strain than the pier (with the assumed values). However in order that the calculations be realistic, the *in situ* properties of the mortar, grout and brick (or block) should be known - that is, the properties of these components when in a complete masonry assembly rather than as separate materials. The same requirement is true for the elastic property predictions. Hence, attempts were made to determine some of the *in situ* properties of the masonry components when in an assembly.

EXPERIMENTAL PROGRAMME

In order to determine values of elastic modulus (E) and Poisson's ratio (ν) for units and mortar *in situ*, five stack-bonded clay masonry prisms were constructed in the laboratory using a simple prism-jig. The prisms comprised of six units and five joints and care was taken both to fill the unit cores with mortar and to finish the mortar joints flush with the units. The prisms were tested in compression to failure.

Figures 8 and 9 show complete details of a typical prism. Strains from the gauges and load were recorded on a fourteen channel recorder and replayed later to obtain individual strain vs load curves. The LVDT (Linear Variable Differential Transducer) displacements were recorded

directly as functions of load. Suitable scale adjustment converted the displacement readings to strain.

In Table 1, measured strain data are presented for three different stress levels for the unit, mortar and prisms. In Table 2 average data are presented together with data on statistical variances.

Data was also obtained for the two mortar batches from which the prisms were constructed. 5.1 cm cubes were formed directly from the mortar and also after the mortar had been laid on fresh units for two minutes. Table 3 gives values of strain at similar stress levels to those used for the prisms; the cubes were compressed to failure and strains determined from the testing machine cross-head displacement. Mortar from batch 1 was used to construct prism 1 and batch 2 to construct prisms 2 to 5 inclusive.

DISCUSSION

We found, as did Beard (4), considerable difficulty in obtaining non-eccentric loading, and this may account for some of the variability in the results. Other factors will be the variability of the units, workmanship (even though one person constructed all five prisms) and the different mortar batch for prism 1.

Nevertheless, if a direct linear relationship between stress and strain is assumed for the units and mortar, that is $\sigma = E \epsilon$, values of the secant moduli of elasticity for the units, mortar and prism can be determined. The assumption of no lateral interference between brick and mortar due to Poisson's effect is clearly erroneous. As noted by others (8, 9) the mortar must be laterally constrained, otherwise failure of the prism would occur at lower stress levels than observed. It is of interest to note here, that although the average vertical strains in the unit and mortar are very different (Table 2, columns 4 and 5), the average lateral strains are the same (Table 2, columns 6 and 7). Results for individual prisms (Table 1) are not so clearly similar. The average data however would appear to confirm lateral restraint of the mortar. All measured strains therefore are not only dependent on the applied compressive stress but also on the lateral stresses which develop in the mortar and unit.

Although mortar in the gross sense may be isotropic it is improbable that pressed or extruded units are also isotropic. The bricks used in our tests were extruded in the direction of the cores - that is the vertical direction of the prisms. The modulus of elasticity in the vertical direction will therefore be different to the moduli in the lateral directions. Furthermore if any lamination occurs, the moduli in the two lateral directions will not be the same. Concomitant with different moduli will be different Poisson effects between strains in the various directions. We noted that failure of the prisms invariably occurred by vertical cracking down the short side of the units. If the moduli of elasticity, Poisson effects and failure stress were the same in the two lateral directions,

the chance of the five prisms failing as noted is 1 in 32. It would appear therefore that there are different properties in the two lateral directions, and that the bricks are triaxially anisotropic. Hence, analysis of the state of stress within prisms is more complex than previously suggested (8,9).

Since the intention of this work was to use simple models to predict overall behaviour from individual component behaviour, values of secant "elastic modulus" were calculated from strain values at given stress levels. The results are shown in Table 4. Values of secant modulus for the mortar cube tests were determined at 3 and 5 MPa together with tangent moduli at initial loading. These are shown in Table 5, and are lower than the values obtained for the mortar from the prism tests. The prism values will be overestimates of the actual magnitude of elastic modulus because of the triaxial compression of the mortar. This accounts for some of the discrepancy. Also there are differences between the cube and prism mortar due to the methods of curing and the loss of moisture from the mortar when the prisms were constructed. Spreading the mortar on fresh units for 2 minutes before casting cubes was an attempt to account for this water loss.

Using the values of moduli as determined from the prism tests, the models described previously can be used to predict the overall prism stiffness. These predicted stiffnesses are compared with the measured modulus of the prism and also with the prediction using the theoretical model proposed by Base and Baker (5). It can be seen from Table 6 that the predictions are higher than the experimentally determined values. As mentioned, lateral stresses in the prisms will induce an overestimate of the mortar stiffness: such stresses will also induce an underestimate in the brick stiffness. The overestimate of the mortar stiffness is probably larger than the underestimate of the brick stiffness due to the different magnitudes of lateral stress in the brick and mortar: this will contribute to the over-prediction by the models. However, the predictions using our models are on average within 20% of the measured values, which suggests that with a more accurate method of determining the *in situ* properties, the models may be of engineering use. However, greater knowledge of the properties of the brick units is first required.

In Table 6 some predictions are also shown for when secant or tangent moduli from the mortar cube tests are used. Although these predictions are somewhat closer to the experimental values, use of mortar data of this type is not recommended since different *in situ* properties of the mortar will result from use with different bricks, and the variability of spreading mortar on fresh units requires study.

SUMMARY & CONCLUSIONS

Theoretical models have been described which may be used to predict the behaviour of masonry assemblies under load. In trying to determine the engineering use of such models elastic behaviour was considered and the models predicted values within 20% of the experimentally determined elastic moduli. The problems of brick anisotropy and lateral constraint

are thought to contribute to the error. With greater knowledge of brick properties the models may well be of engineering use in predicting elastic properties. For creep and shrinkage, again brick properties are required and a method must be determined for measuring these properties for mortar *in situ*. An experimental method has not yet been found in which mortar can be reproduced as in its "*in situ*" state. Experiments of this type are required for the determination of mortar properties.

ACKNOWLEDGEMENT

The authors would like to express their gratitude to Mr. G. Natt for the preparation of the prisms and mortar cubes, and to Mr. E. Damson for his technical help with the preparation and running of data acquisition. The work was funded through the National Research Council of Canada.

REFERENCES

- (1) L. R. Baker, G. L. Franken: "Variability Aspects of the Flexural Strength of Brickwork". Proc. IV. Int. Brick Masonry Conf., Bruges, 1976.
- (2) J. M. Plowman: "The Modulus of Elasticity of Brickwork". Proc. British Ceramic Soc., 4, 37-48, 1965.
- (3) D. Lenczner, J. Salahuddin: "Creep and Moisture Movements in Masonry Walls and Piers". Proc. 1st Canadian Masonry Symposium, Calgary, 72-86, 1976.
- (4) R. Beard: "Measurements of Compressive Strains in Bricks and Brickwork of a 4½ in. Test Wall under Axial Loading". Proc. Brit. Ceramic Soc., No. 17, 137-154, 1970.
- (5) G. D. Base, L. R. Baker: "Fundamental Properties of Structural Brickwork". J. Austr. Ceram. Soc., 9, 1-6, 1973.
- (6) I. C. McDowall, T. H. McNeilly, W. G. Ryan: "The Strength of Brick Walls and Wallettes", Brick Development Research Institute, University of Melbourne, Special Report No. 1, Nov. 1966.
- (7) G. L. England: "Steady-State Stresses in Concrete Structures Subjected to Sustained Temperatures and Loads". Nuclear Engineering and Design, 3, 54-65, 1966.
- (8) H. K. Hilsdorf: "Investigation into the Failure Mechanism of Brick Masonry Loaded in Axial Compression". Proc. Int. Conf. on Masonry Structural Systems, Texas 1969: Gulf Publishing Coy, Houston, Texas, 1969.
- (9) A. J. Francis, C. B. Horman, L. E. Jerrems: "The Effect of Joint Thickness and other Factors on the Compressive Strength of Brickwork". Proc. 2nd Int. Brick Masonry Conf. Stoke-on-Trent, England, 1970.

Stress Level	Prism	* LVDT (ave.)	* UNIT (Vertical) Ave. Gauges 1:5	* UNIT (Vertical) Ave. Gauges 9:11	* MORTAR (Vertical) Ave. Gauges 3:7	* MORTAR (Vertical) Ave. Gauges 10:12	UNIT (Horizontal) Ave. Gauges 2:6	MORTAR (Horizontal) Gauges 4:8
3 MPa	1	150	127.5	132.5	185.0	195.0	** 40.0	** 32.5
	2	200	182.5	172.5	397.5	407.5	40.0	17.5
	3	425	130.0	160.0	-	270.0	22.5	32.5
	4	370	147.5	195.0	502.5	382.5	22.5	40.0
	5	170	280.0	185.0	425.0	357.5	40.0	32.5
5 MPa	1	240	222.5	220.0	340.0	345.0	** 57.5	** 44.0
	2	335	305.0	290.0	695.0	625.0	67.5	32.5
	3	725	220.0	267.5	-	457.5	37.5	50.0
	4	600	250.0	317.5	905.0	632.5	40.0	72.5
	5	275	447.5	310.0	715.0	595.0	67.5	55.0
16.5 MPa	1	1240	860.0	752.5	1572.5	1550.0	**222.5	**237.5
	2	1890	875.0	782.5	2975	-	387.5	340.0
	3	-	650.0	682.5	-	-	227.5	552.5
	4	3520	810.0	867.5	-	3262.5	240.0	332.5
	5	1687.5	1507.5	885.0	-	-	447.5	440.0

TABLE 1 Values of microstrain at three different stress levels for units, mortar and prisms. A dash means value unobtainable.

* Values are negative (compressive); others are positive (tensile)

** Lateral strains measured on long rather than short side of prism.

Stress	Prisms	LVDT	UNIT (Vert)	MORTAR (Vert)	UNIT (Lateral)	MORTAR (Lateral)
3 MPa	1 → 5	263 ± 126	171 ± 39	357 ± 111		
3 MPa	2 → 5	291 ± 125	285 ± 61	412 ± 27	31 ± 10	31 ± 9
5 MPa	1 → 5	435 ± 215	182 ± 37	607 ± 189		
5 MPa	2 → 5	484 ± 214	301 ± 57	695 ± 64	53 ± 17	52 ± 16

TABLE 2 Average strain readings ± standard deviation from prism data

Stress Level	Batch 1		Batch 2	
	A	B	A	B
3 MPa	960 ± 63	750 ± 124	968 ± 374	622 ± 172
5 MPa	-	2092 ± 356	-	1720 ± 534
Maximum Stress (MPa)	4.3 ± 0.04	5.2 ± 0.15	4.1 ± 0.32	5.4 ± 0.20

TABLE 3 Strains ± standard deviation (three tests) at different stress levels and maximum stress values for mortar cubes: type A were straight from the mixer and B were made after the mortar had been spread for two minutes on fresh units.

Stress Level MPa	Prisms	Overall E (GPa)	Unit E (GPa)	Mortar E (GPa)	Unit ν	Mortar ν
3	1 → 5	11.4	17.5	8.42		
3	2 → 5	10.3	16.5	7.3	.17	.075
5	1 → 5	11.5	17.5	8.24		
5	2 → 5	10.3	16.6	7.2	.17	.072
16.5	1 → 5	7.9	19.0	-		

TABLE 4 Values of "Secant Modulus" (E) and "Poisson's ratio", without accounting for lateral stresses

Batch	Secant Modulus in GPa at 3 MPa Compressive Stress	Secant Modulus in GPa at 5 MPa Compressive Stress	Tangent Modulus at zero MPa
1A	3.13 ± 0.20	-	4.49 ± 0.24
1B	4.07 ± 0.63	2.43 ± 0.39	5.39 ± 0.41
2A	3.37 ± 1.07	-	4.99 ± 1.22
2B	5.07 ± 1.36	3.08 ± 0.83	5.99 ± 1.03

TABLE 5 Average secant and tangent modulus values ± standard deviation (3 tests) for mortar cube tests.

Prisms	Mortar	Stress Level for Secant Modulus	Model				Experimental Value
			Small rptg unit (i)	Small rptg unit (ii)	Large rptg unit	Base & Baker	
1 → 5	N/A	N/A	13.8	13.6	13.2	15.1	11.4
2 → 5			12.7	12.5	12.1	14.0	10.3
2 → 5	2A	3 MPa	9.5	9.0	8.2	10.6	10.3
	2B	3 MPa	11.2	10.9	10.2	12.5	10.3
	2B	5 MPa	9.2	8.6	7.8	10.2	10.3
2 → 5	2A	Tangent	11.1	10.8	10.1	12.4	10.3
	2B	Moduli	11.9	10.7	11.1	13.2	10.3

TABLE 6 Predictions of elastic modulus (GPa) using theoretical models: comparison with experimental value

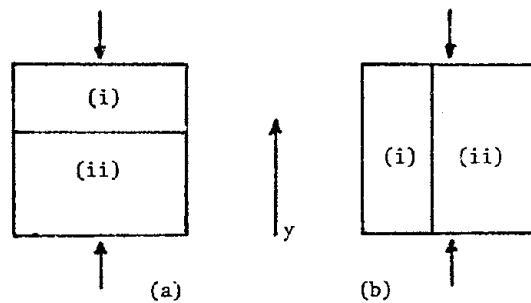


Figure 1 (a) Series and (b) parallel models for two phase material, (i) and (ii), in y-direction

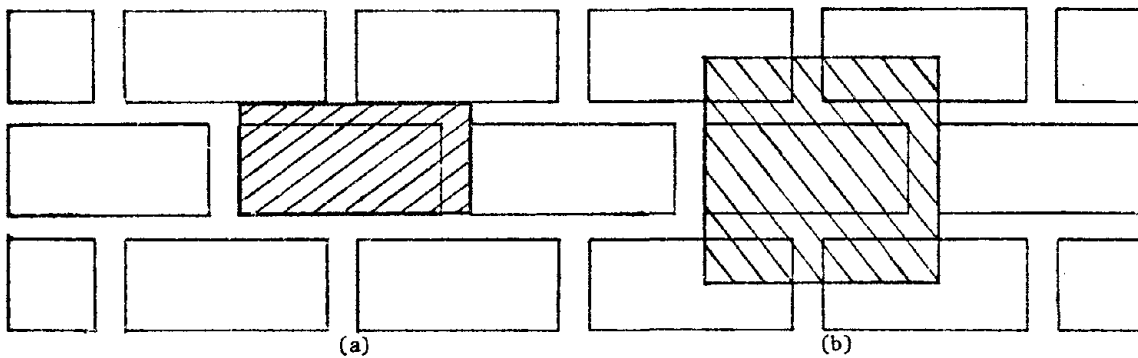


Figure 2 Repeating units in a single wythe wall.
(a) small unit (b) large unit.

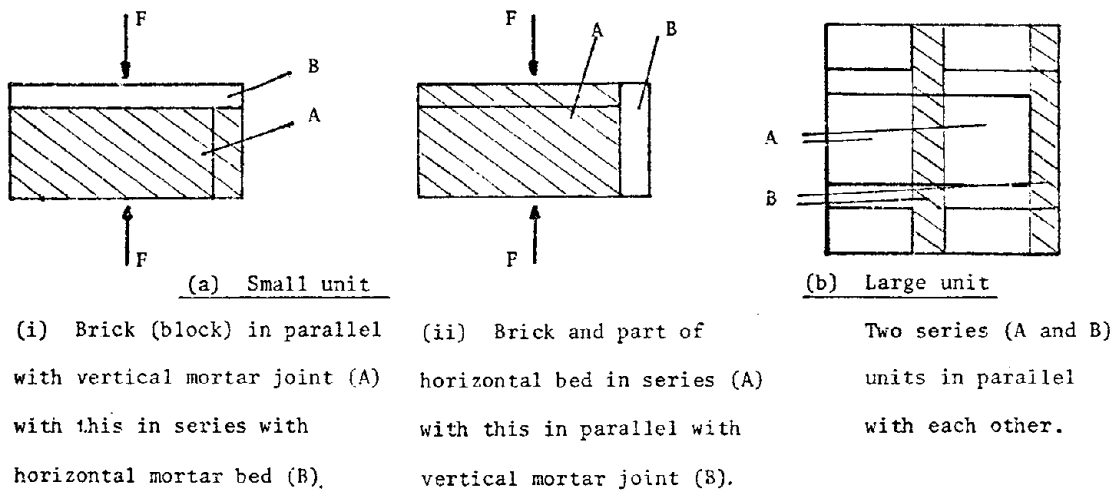


Figure 3: Breakdown of repeating units

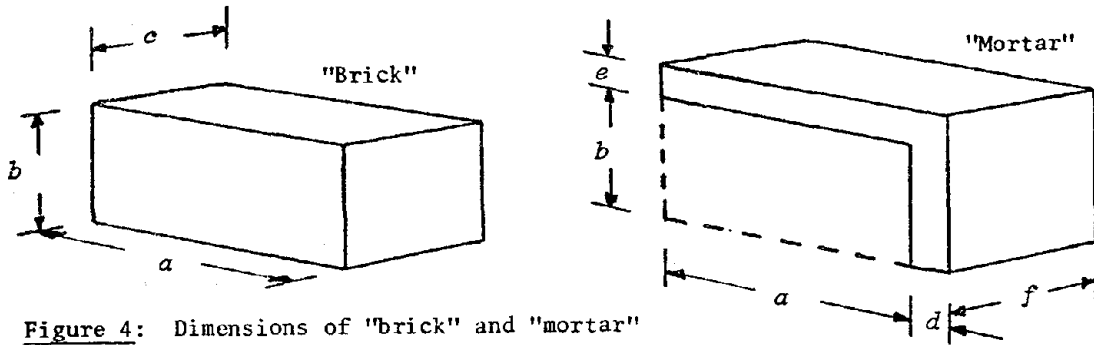


Figure 4: Dimensions of "brick" and "mortar"

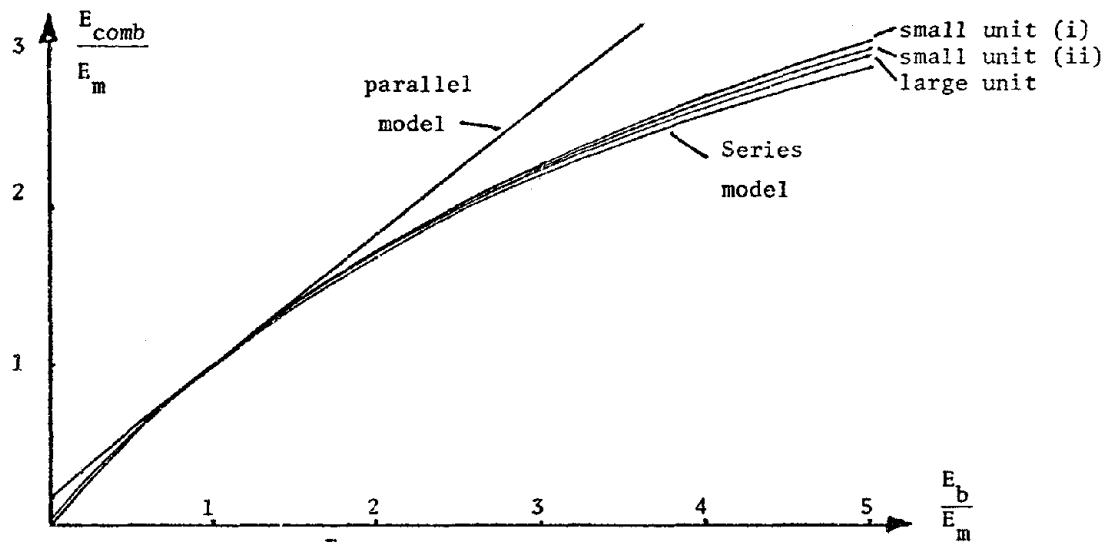


Figure 5: Predictions of $\frac{E_{comb}}{E_m}$ for different single-wythe wall models

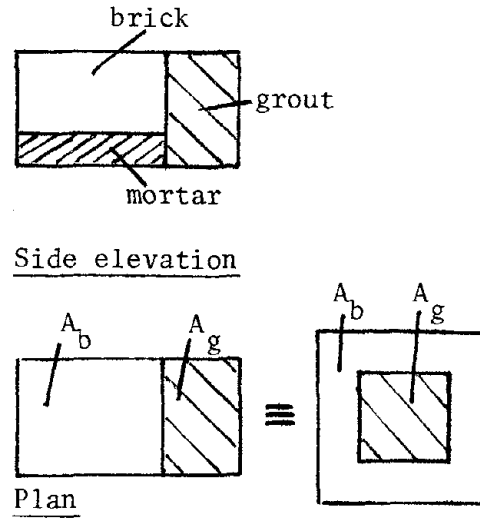


Figure 6: Simple model to demonstrate effects of geometry on creep & shrinkage

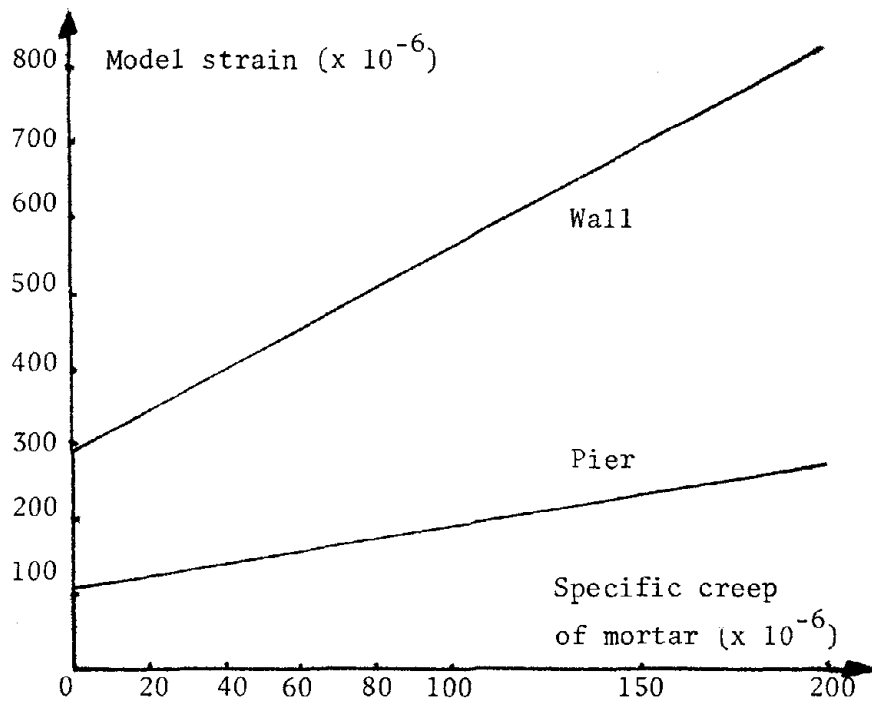


Figure 7: Comparison of wall and pier strains for stress of 1 MPa. Creep and shrinkage considered.

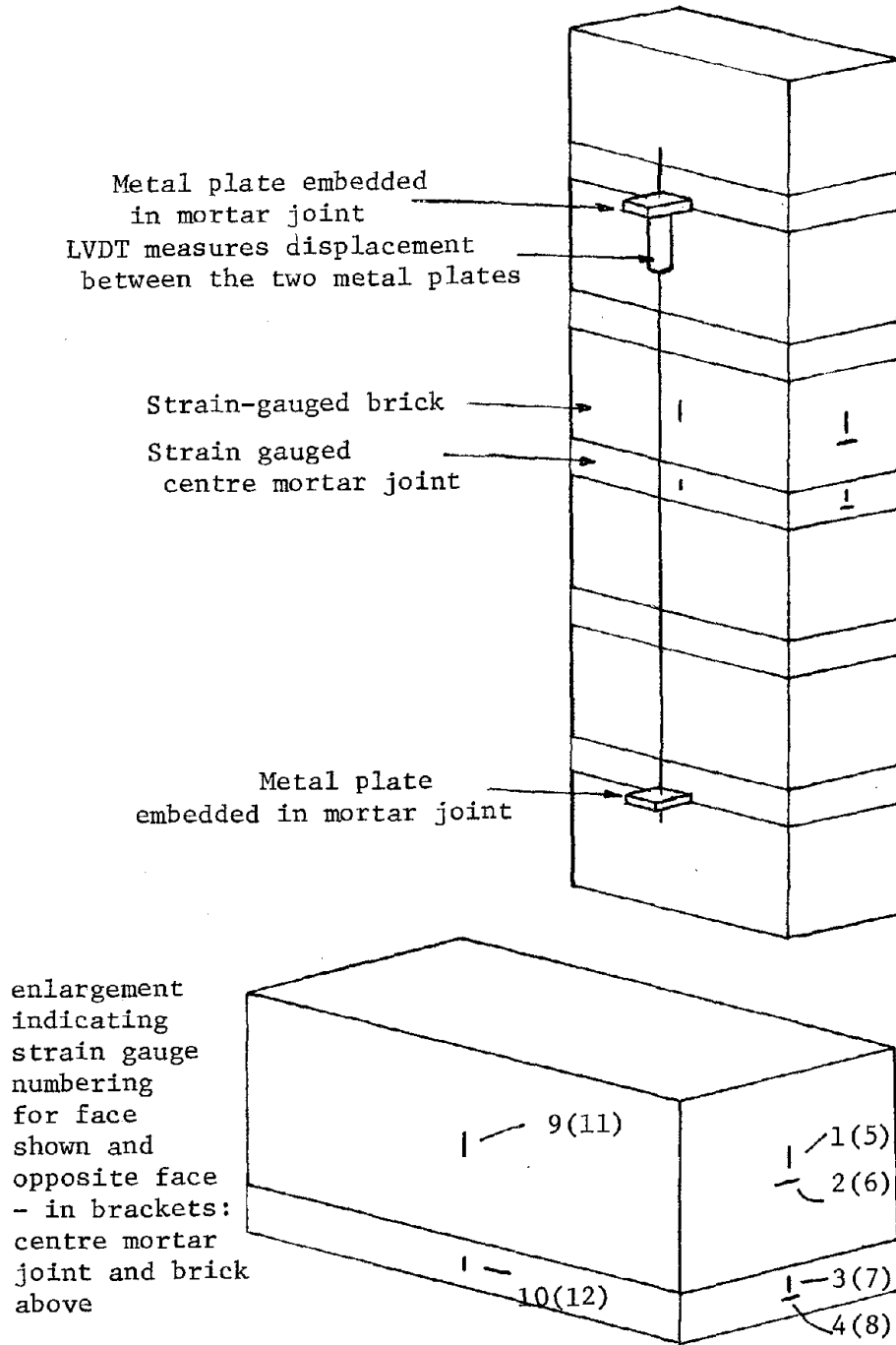


FIGURE 8: Schematics of prism and enlarged view of centre mortar joint and superior unit

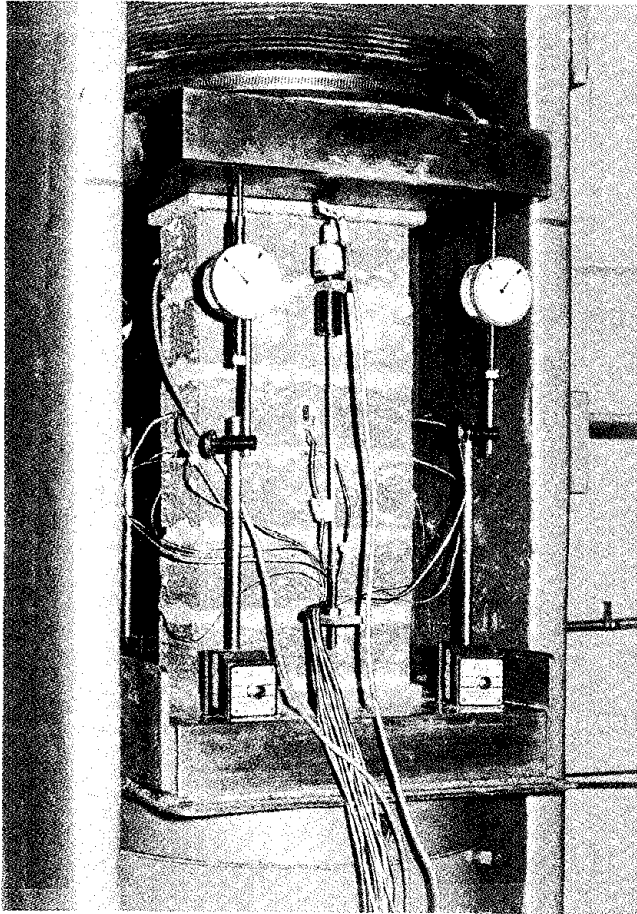


FIGURE 9: The plate shows a prism in the testing machine. The centre mortar joint and the unit above this joint are strain-gauged. The LVDT measured displacement over four bricks and joints. The dial gauges were used to determine the machine cross-head movement.

THE PARAMETERS INFLUENCING SHEAR STRENGTH
BETWEEN CLAY MASONRY UNITS AND MORTAR

Larry K. Nuss¹, J. L. Noland² and James Chinn³

ABSTRACT: An investigation of shear strength between clay masonry units and mortar is described in this paper. An effective, easily performed, joint shear test was developed from which shear strength of masonry joints could be determined. Quantitative results from the tests showed the influence of mortar strength, mortar water content, mortar mix proportions, and clay unit water suction rate on shear strength. Linear and quadratic polynomial equations relating shear strength to joint normal compressive stress were fitted to the test data. Multiple regression techniques were used in an attempt to relate shear strength to multiple masonry parameters in a single equation.

¹Civil Engineer, U.S. Bureau of Reclamation, Denver, Colorado

²Principal, Atkinson-Noland & Associates, Inc., Boulder, Colorado

³Professor, Department of Civil, Environmental & Architectural Engineering, University of Colorado, Boulder, Colorado

THE PARAMETERS INFLUENCING SHEAR STRENGTH
BETWEEN CLAY MASONRY UNITS AND MORTAR

Larry K. Nuss¹, J. L. Noland² and James Chinn³

INTRODUCTION

Brick masonry is being used more and more today in major buildings as a structural material. If, however, it is to be utilized to its optimum potential in resisting lateral forces, it is essential that better knowledge of the shear capacity of its joints be obtained. The present paper is a report on tests performed to obtain some of this knowledge.

TYPES OF SHEAR TESTS

Shear tests of joints in the past have generally fallen into two categories, couplet tests or racking tests. Couplets have consisted of two or three-unit-high assemblages, and attempts were made to produce uniform shear stress or a combination of uniform shear and uniform normal stress on the joint during testing. Racking tests have been on entire masonry wall panels, and they have been loaded parallel to the joints or along a diagonal.

In all the tests reported in the literature, some aspect of the test specimen or test procedure has the potential of producing nonuniform stresses on the joints.

DEVELOPMENT OF NEW TEST

For the tests from which results are reported herein, a new type of couplet test was developed. A four-brick-high prism was built with 3/8 in. thick joints. The middle joint contained the standard mortar being tested while the top and bottom joints were made with mortar strengthened with Sarabond* admixture. The test specimen was then cut from this prism at an angle to produce a smaller prism 3-9/16 in. wide by

* Sarabond is the trade name of a latex-base mortar admixture produced by Dow Chemical Company.

¹Civil Engineer, U.S. Bureau of Reclamation, Denver, Colorado

²Principal, Atkinson-Noland & Associates, Inc., Boulder, Colorado

³Professor, Department of Civil, Environmental & Architectural Engineering, University of Colorado, Boulder, Colorado

2-5/8 in. thick by 7-1/2 in. long, with joints at a preselected angle with the transverse direction. When this was loaded in the longitudinal direction, shear and compression were produced on the mortar joint faces.

DESCRIPTION OF SPECIMENS

All materials used in test specimens were donated by their manufacturer or supplier. Bricks were standard modular 2-2/3 x 4 x 8 in. solid clay units, extruded and side-wire-cut from Colorado Brick Company and Lakewood Brick Company. Compressive strengths of the bricks ranged from 10,000 to 14,000 psi, and the initial rates of absorption (IRA) ranged from 5 to 20 grams per minute (gpm). Sand was furnished by the Rio Grande Company of Denver, and it was sieved and blended to give a continuous grading meeting requirements of ASTM C144 Standard Specification for Aggregate for Masonry Mortar. Portland cement was Type I, manufactured by the Martin-Marietta Company. Lime was Type S, produced by the Flintkote Company to meet requirements of ASTM C207, Standard Specification for Hydrated Lime for Masonry Purposes.

Mortar was mixed in a Hobart dough mixer following ASTM C270, Standard Specification for Mortar for Unit Masonry, and procedures devised by D. J. Frey(7). Prisms were laid up by Mr. Judd Harvey, a journeyman mason with over thirty years of experience. Prisms were cured for seven days at 70°F in a 100% humidity room. They were then taken to a diamond-blade masonry saw where the smaller test specimens with the joints at the desired angles were cut from them. These were then air cured at 70°F until they were load tested.

A set of shear specimens, identical except for joint angles, was termed a "shear family." Joint angles used were nominally 45°, 50°, 55°, 60° and 65° (Photo 1). Not all angles were represented in all shear families, however.

Three series of tests were run in which mortar proportions, mortar flow and brick IRA were varied. In series I, the mortar proportions were the only variable. The mortar flow was 130 \pm 5%, and clay units had IRA of 5 to 10 gpm. Testing was done at age 14 or 28 days.

In series II, the mortar flow was varied. Three flows were used, 110, 120, and 140, \pm 5%. Two mortar types, 1:1/4:3 and 1:1:6 (cement:lime:sand by volume), were used. The clay units had IRA's in the range of 5 to 10 gpm. Tests were performed at 28 days after prism construction.

In series III, two different suction rates were used, an IRA of 10 to 15 gpm and one of 15 to 20 gpm. Three mortar types, 1:1/4:3, 1:1:6, and 1:2:9 were used. Mortar flow was held constant at 130 \pm 5%. Tests were performed 28 days after construction.

Each shear family of specimens was assigned a test designation number that identifies its mortar type, mortar flow, age at test, and clay unit IRA as explained in Table I.

COMPANION TESTS

Whenever prisms were made for shear specimens, companion four-brick-high prisms with 3/8 in. thick joints were made for testing to obtain prism compressive strength, f_m' . Two-inch mortar cubes were also made for testing to obtain mortar compressive strength, f_c' . Mortar flow was measured for every mortar made, and clay unit compressive strength, f_b' and IRA were determined on random samples. All tests were in accordance with the applicable ASTM standard methods of test.

TESTING PROCEDURE

Before testing, shear specimens were capped on both ends (Fig. 1) with Cylcap, a commercial sulphur-clay capping compound in the capping fixture shown in Photo 2. Measurements showed caps were parallel within 1° .

Specimens were tested in uniaxial compression in a 300,000 lb. capacity Baldwin-Southwark-Emery universal testing machine. Load was applied through a spherical bearing block at a constant rate of 20,000 lb/min until failure occurred. The nature of the failure was noted, and compressive and shear stresses on the joint at failure were calculated.

TEST RESULTS

Results from tests of 115 shear specimens, 87 mortar cubes, 48 mortar flow tests, 15 IRA tests, 10 clay unit compression tests, and 60 clay unit compression prism tests are presented in Tables II through XI. Tables II, III, IV and V contain test data for Series I, 28-day tests; Series I, 14-day tests; Series II tests and Series III tests, respectively. Test data for all mortars are listed in Tables VI and VII. Compressive strength and IRA for five randomly-selected clay units from each of three major clay unit groups are found in Table VIII. Tables IX, X, and XI contain compression prism test data and strengths for Series I, Series II and Series III tests, respectively.

All the shear specimens failed randomly in shear along one of three failure surfaces in the test joint. The failure surfaces were along the top interface between the mortar and clay unit, along the bottom interface between the mortar and clay unit, or a combination of the two with a crack running across the mortar bed connecting the two planes. Close examination of the failed surfaces revealed mortar particles on the clay unit face, but no clay unit particles in the mortar. Typical shear failures are shown in Photo 3. These specimens, made with 1:1/2:4-1/2 mortar having a flow of 130 and clay units having an IRA of 5 to 10 gpm, were tested on the 14th day after construction.

ANALYSIS OF TEST RESULTS

Applied longitudinal stress (σ_x), shear stress on the joint (τ), and normal stress on the joint were calculated for each specimen from the shear specimen test data in Tables II through V, using the equations:

$$\sigma_x = \frac{P}{A}$$

P = load of failure

$$\sigma_n = \sigma_x \cos^2 \theta$$

in which A = area of prism

$$\tau = \frac{\sigma_x}{2} \sin 2\theta$$

θ = angle between joint
and transverse plane

One of the main objectives of the test program was to investigate whether a general relationship existed relating shear stress (τ) and compressive stress (σ_n) in joints at joint failure. Failure stress values were plotted with τ^n as the ordinate and σ_n as the abscissa for each shear family as in Fig. 2. Test points always clustered about a straight line or a slightly curved line, both intersecting the τ axis at some positive value and both having positive slopes.

Least squares techniques were applied to fit linear and quadratic equations to the results of each shear family in the forms:

$$\tau = a_1 \sigma_n + \tau_0$$

and

$$\tau = a_2 \sigma_n^2 + a_1 \sigma_n + \tau_0 .$$

Typical linear and quadratic equations are given on Fig. 2(A) for a shear family made with 130 percent flow, 1:1/4:3 mortar and clay units having 5 to 10 gpm IRA, tested on the 28th day after construction.

Linear and quadratic least squares equations are grouped according to test series and plotted in Figs. 3 through 8. The lines on Fig. 3 show joint shear strengths when mortar mix proportions were varied. The lines on Fig. 4 show joint shear strengths when 1:1/4:3 mortar percent flows were varied. In Fig. 5, the lines show joint shear strengths when flows of 1:1:6 mortar were varied. The lines in Figs. 6, 7 and 8 show joint shear strengths when clay unit IRAs were varied for 1:1/4:3, 1:1:6, and 1:2:9 mortars, respectively.

The pure shear strength of a joint, (τ_0), is the shear capacity of the joint with no compressive stress acting normal to the joint bed. The ordinates of the least squares curves at σ_n equal to zero in Figs. 3 through 8 are the pure shear strengths of the joints. Relationships between τ_0 and other masonry properties were investigated. Average values of τ_0 , seven-day

mortar cube strength (f'_c), 28-day prism compressive strength (f'_m), clay unit compressive strength (f'_b), clay unit Initial Rate of Absorption (IRA), and water-to-cement ratio by weight (W/C) were included in the investigation as listed in Table XII.

Joint pure shear strength was not a function of prism compressive strength alone, nor of seven-day mortar cube compressive strength alone. Small changes in water-to-cement ratio (Fig. 9) and variation in clay unit IRA (Fig. 10) greatly influenced joint pure shear strength. It was influenced by many masonry parameters. Multiple regression techniques were therefore applied in an attempt to relate joint pure shear strength to several independent masonry variables in the forms

$$\tau_0 = a + bx + cy + dz$$

and

$$\tau_0 = ax^b y^c z^d$$

where a, b, c, and d are multiple regression coefficients; x, y, and z are independent masonry variables, and τ_0 is joint pure shear strength.

Masonry parameters that influenced, or when combined with other parameters might correlate with, joint pure shear strength, were used in the multiple regression analyses. Eight measurable masonry parameters were chosen: seven-day mortar cube strength, prism compressive strength, clay unit compressive strength, clay unit Initial Rate of Absorption, and four mortar water content ratios W/C, W/L, W/(C+L), and L/C, all by weight.

The results from the multiple regression analyses using the data in Table XII but excluding Series I, 14-day tests are listed in Table XIII. Each row contains regression coefficients calculated from one multiple regression analysis. The correlation coefficients in column 11 indicate that joint pure shear strength was more a function of f'_c , IRA, and some form of mortar water content than any other parameters.

When joint pure shear strength was expressed as a function of f'_c , IRA, and mortar water content, the calculated values for Series II tests showed less correlation with the test values than did the Series I and III calculated values. This is logical because mortar strength and joint pure shear strength are two independent quantities. Mortar strength is independent of the clay unit properties, and joint shear is dependent upon bond between clay unit and mortar as well as upon strength of the mortar as modified by clay unit suction. An increase in mortar water content produced a decrease in mortar cube strength but an increase in joint pure shear strength. It is believed, therefore, that joint pure shear strength can be more accurately related to mortar cube strength, IRA, and mortar water content if the mortar percent flow is relatively constant.

The multiple regression coefficients were therefore reevaluated, using the same independent variables in Table XII, but using only the data

from the 28-day shear tests of Series I and III. The results of these linear multiple regression analyses are listed in Table XIV.

Using multiple regression analyses, the following two equations were fitted to the strength data for mortar flow of 130 ± 5 percent:

$$\tau_0 = 8.0 \frac{f'_c (W/C)^{1.70}}{IRA^{1.50}}$$

and

$$\tau_0 = 18.0 \frac{f'_c \left[\frac{W}{C+L}\right]^{3.0}}{IRA^{1.55}}$$

For the 28-day Series I and III, the actual joint pure shear strengths are plotted against those calculated from these equations in Figs. 11 and 12.

GENERALIZED JOINT SHEAR EQUATION

The slopes of the straight lines fitted to the joint shear stress-compressive stress test data were relatively constant. An average of these slope values was 0.772 with a 95 percent confidence interval of ± 0.043 . Generalized expressions for the 28-day joint shear strength of a shear specimen while keeping the mortar flow constant at 130 ± 5 percent are then:

$$\tau = 0.772 \sigma_n + 8.0 \frac{f'_c (W/C)^{1.70}}{IRA^{1.50}}$$

or

$$\tau = 0.772 \sigma_n + 18.0 \frac{f'_c \left[\frac{W}{C+L}\right]^{3.0}}{IRA^{1.55}}$$

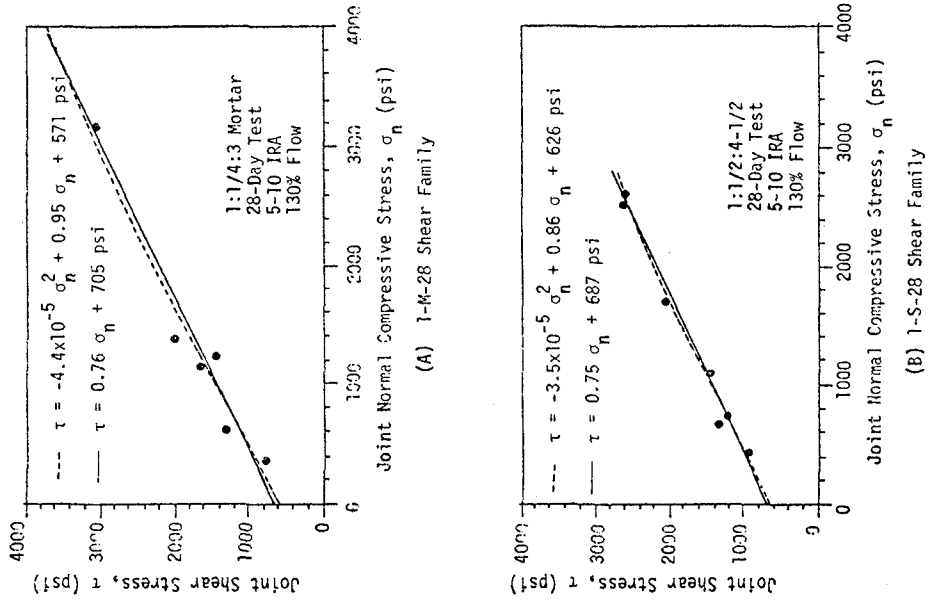
SUMMARY

The prime objective of the research reported herein was to study shear strength of joints in clay masonry. The specimen developed to test joint shear produced very satisfactory and consistent results when simple test procedures were followed diligently. The test was economical and easy to perform and could be run in any laboratory that has access to a compression testing machine, fog room, and masonry saw. Relationships between joint

pure shear strength and multiple masonry variables could be expressed in a single equation. These relationships showed strong correlations; however, they should not be used in design at this time. The authors believe that the shear specimen test can be used in future research studies to develop design equations.

ACKNOWLEDGEMENTS

The research reported herein was supported by a grant to the University of Colorado from the Colorado Masonry Institute and the Northern Colorado Masonry Guild. The project was monitored by Robert J. Helfrich, Technical Director, Colorado Masonry Institute. Project Director for the University of Colorado was Professor C.C. Feng.



Joint Stress-Variied Mortar Type

Figure 2

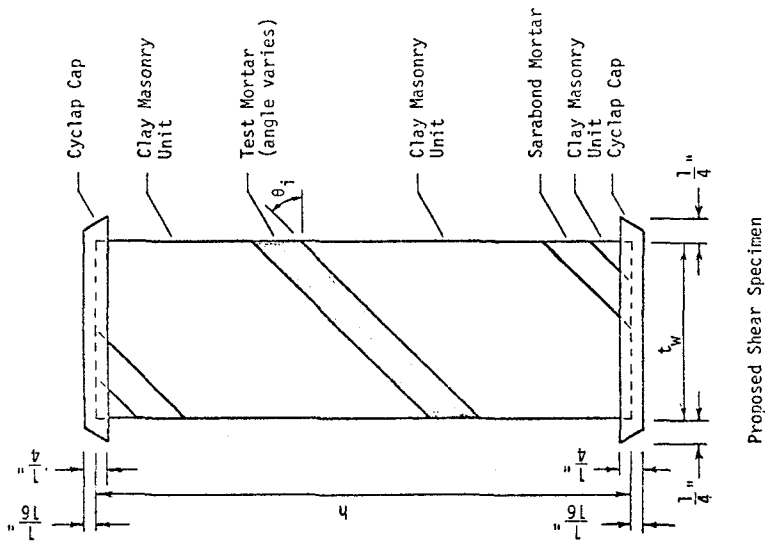
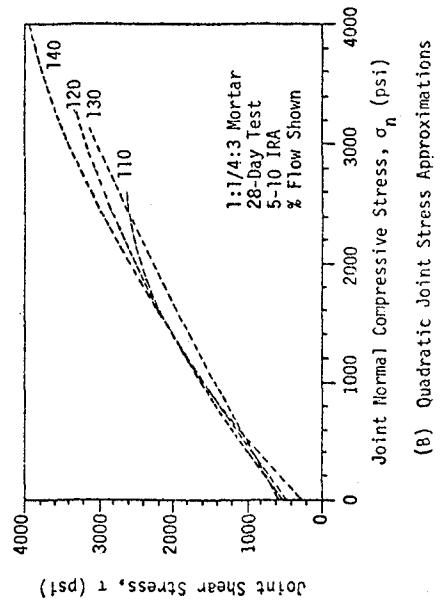
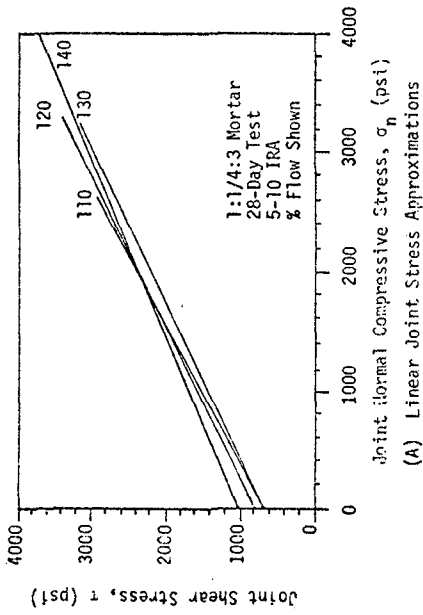
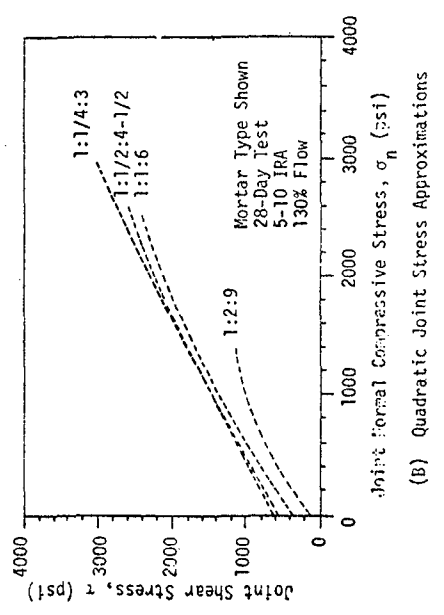
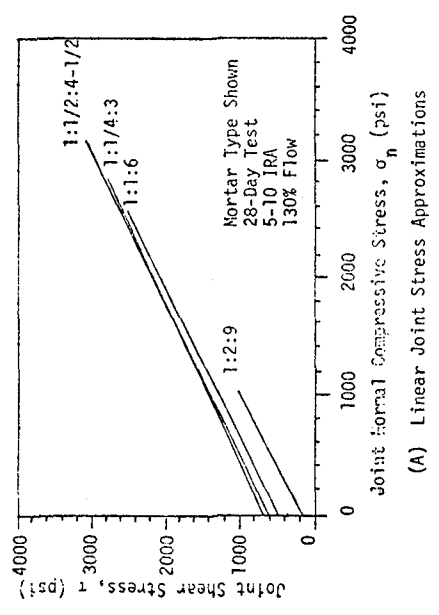


Figure 1



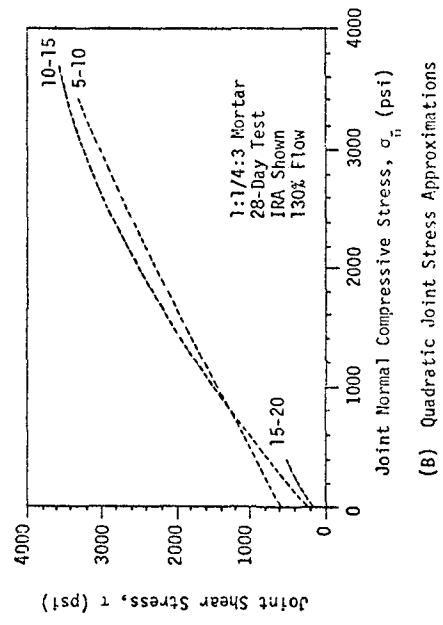
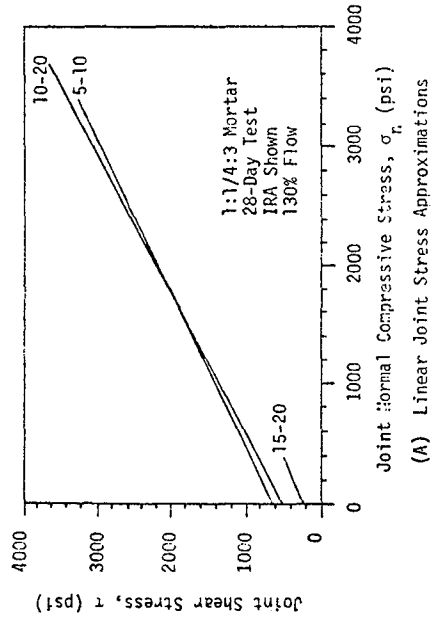
Joint Shear Stress Approximations-Variied 1:1/4:3 Mortar Water Content

Figure 4



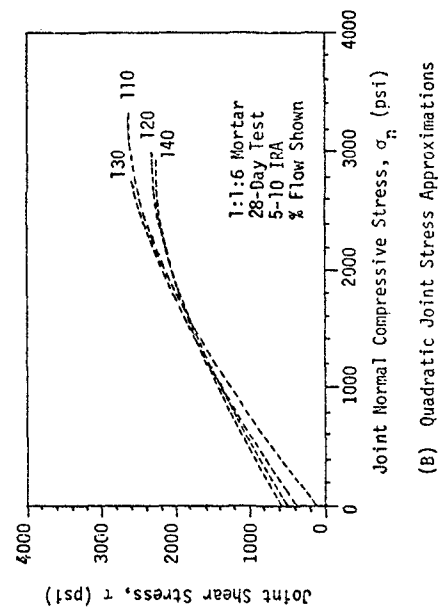
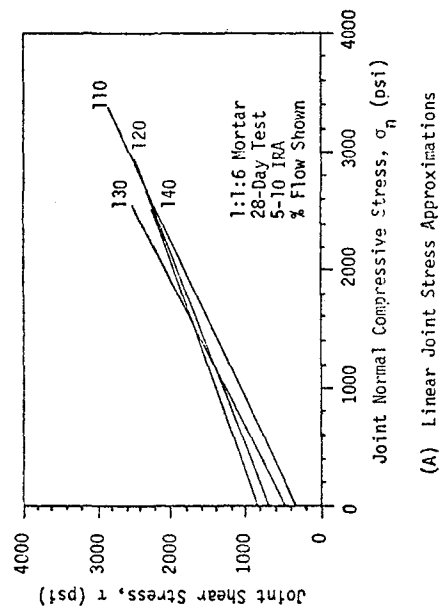
Joint Shear Stress Approximations-Variied Mortar Type

Figure 3



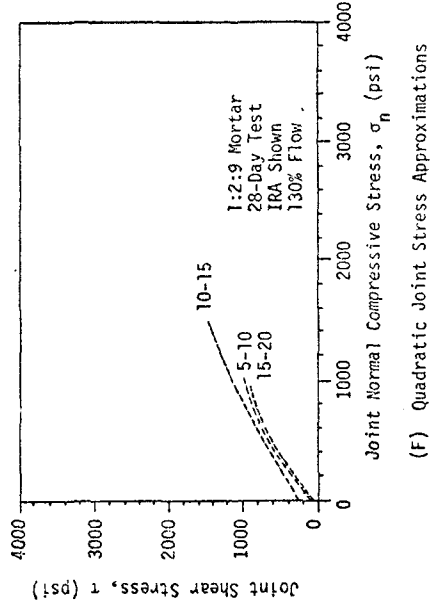
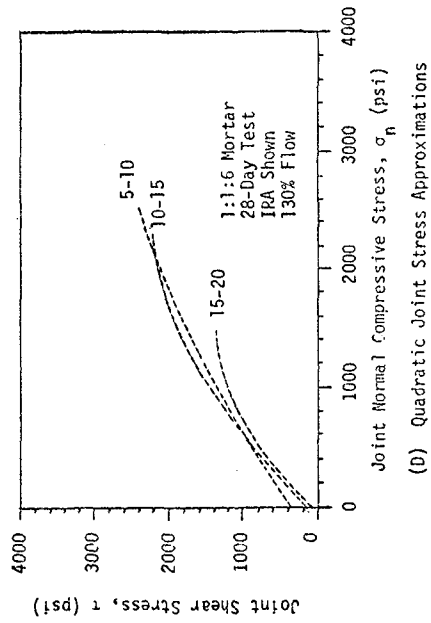
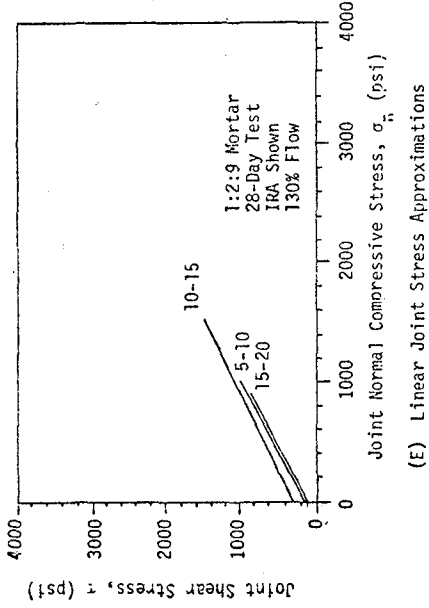
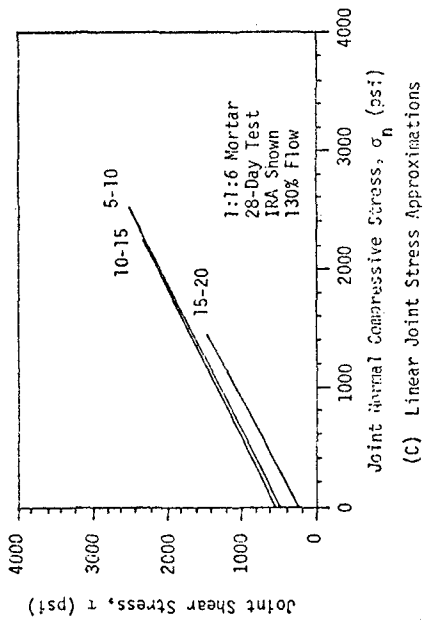
Joint Shear Stress Approximations - Varied Clay Unit IRA

Figure 6



Joint Shear Stress Approximations-Varied 1:1:6 Mortar Water Content

Figure 5



Joint Shear Stress Approximations - Varied Clay Unit
IRA (Continued)

Joint Shear Stress Approximations - Varied Clay Unit
IRA (Concluded)

Figure 7

Figure 8

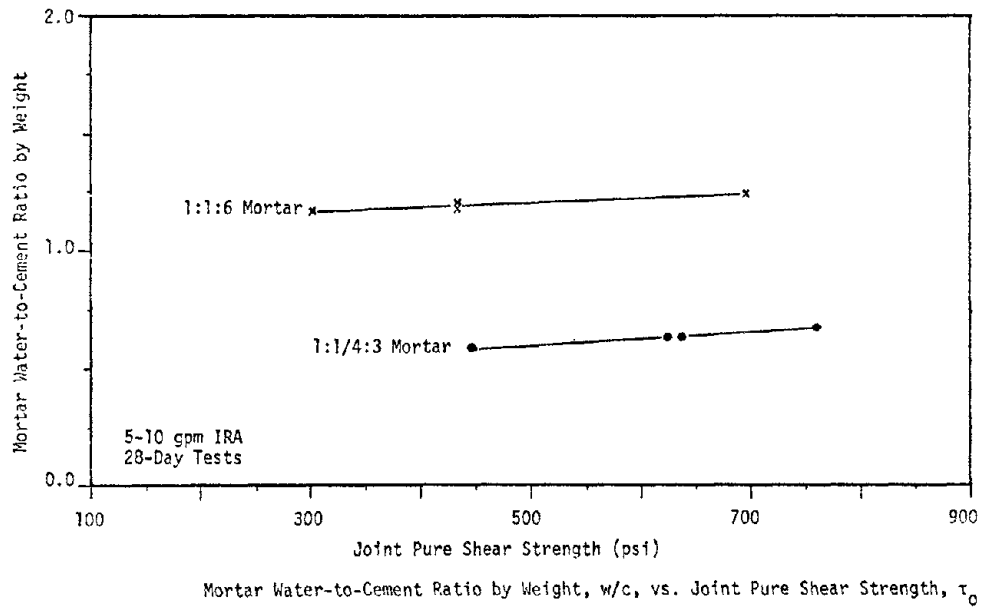


Figure 9

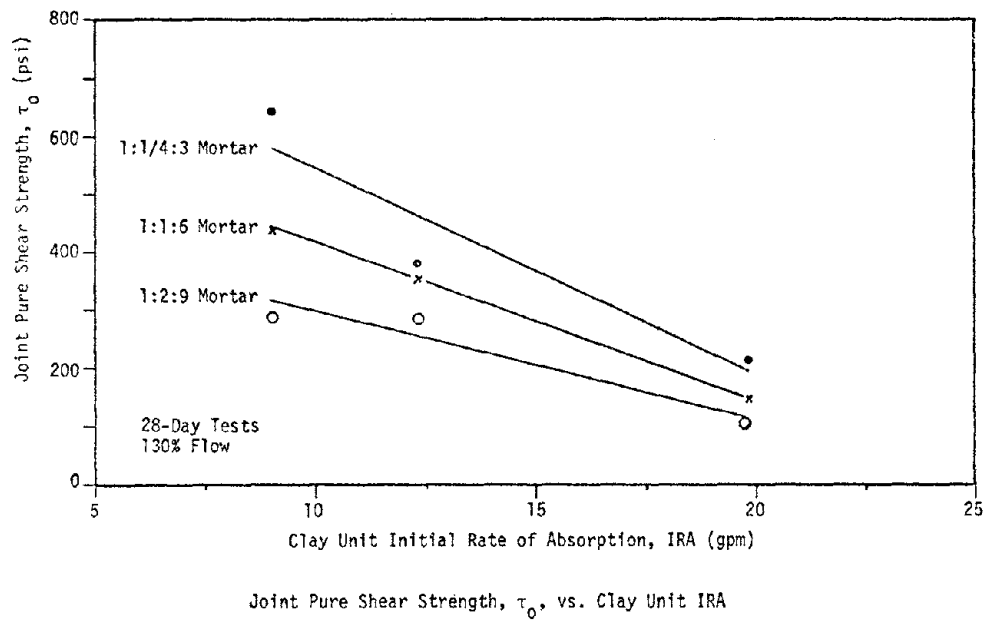


Figure 10

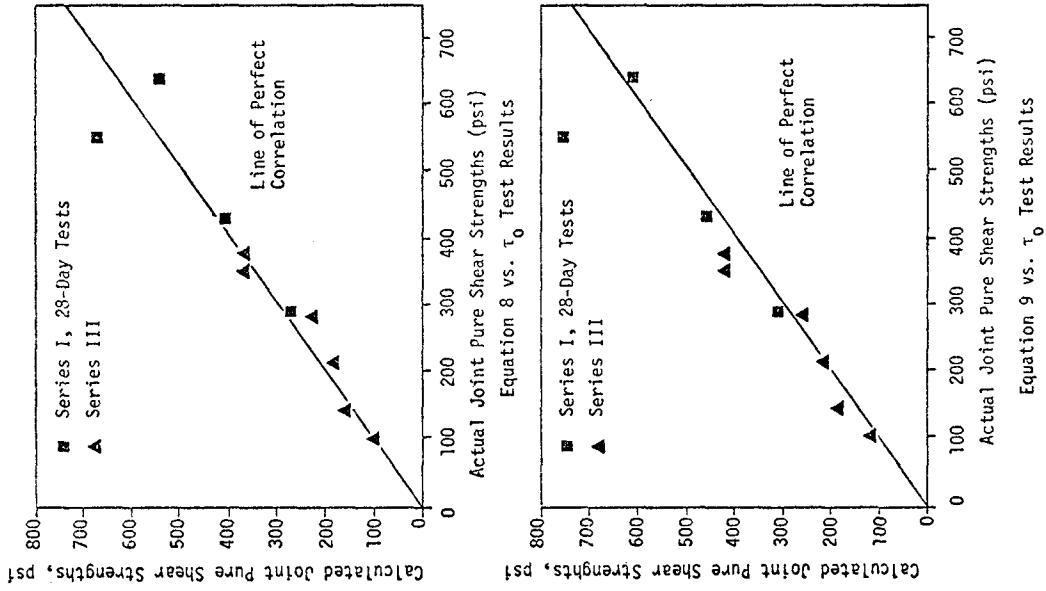


Figure 11

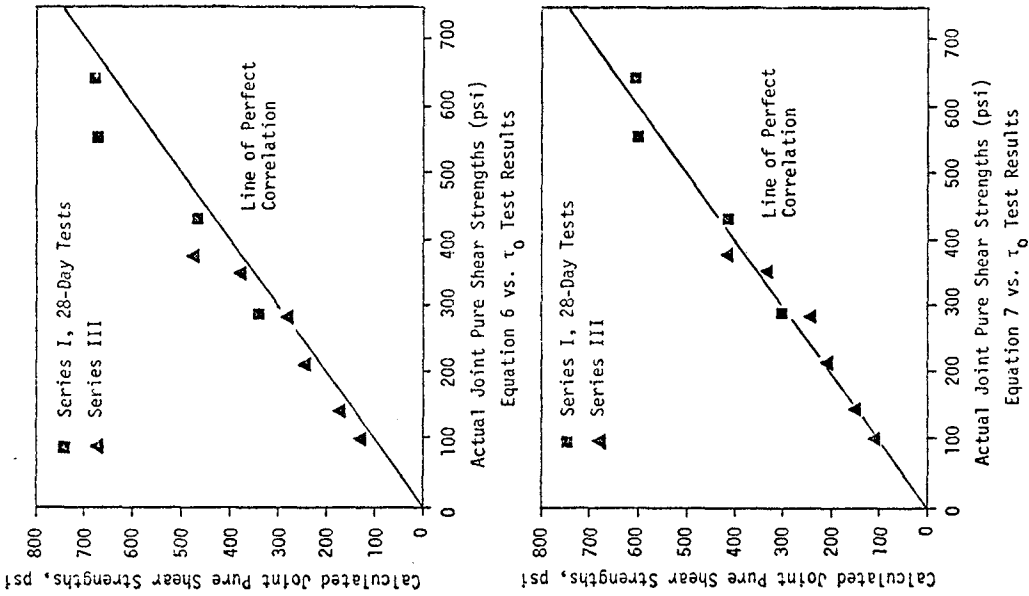


Figure 12

TABLE I
Proposed Masonry Joint Shear Test Series

Test		Proposed Masonry Properties			
Series (1)	Test ^a Design (2)	Mortar ^b Type (3)	Flow ^c % ±5% (4)	IRA ^d (5)	Test Day (6)
Series I	1-M-28	M(1:¼:3)	130	5-10	28
	1-S-28	S(1:½:4½)	"	"	"
	1-N-28	N(1:1:6)	"	"	"
	1-O-28	O(1:2:9)	"	"	"
	1-M-14	M(1:¼:3)	"	"	14
	1-S-14	S(1:½:4½)	"	"	"
	1-N-14	N(1:1:6)	"	"	"
	1-O-14	O(1:2:9)	"	"	"
Series II	M-140	M(1:¼:3)	140	5-10	28
	M-120	M(1:¼:3)	120	"	"
	M-110	M(1:¼:3)	110	"	"
	N-140	N(1:1:6)	140	"	"
	N-120	N(1:1:6)	120	"	"
	N-110	N(1:1:6)	110	"	"
Series III	M-Wet	M(1:¼:3)	130	10-15	28
	N-Wet	N(1:1:6)	"	"	"
	O-Wet	O(1:2:9)	"	"	"
	M-Dry	M(1:¼:3)	"	15-20	"
	N-Dry	N(1:1:6)	"	"	"
	O-Dry	O(1:2:9)	"	"	"

a) Test Designation

b) X(C:L:S)

X = ASTM C270 Designation
C = Part cement by volume
L = Part hydrated lime by volume
S = Part aggregate by volume

c) Percent Flow by ASTM C230 Test

d) Initial Rate of Absorption using ASTM C67 Test in gpm

TABLE II

SHEAR SPECIMEN TEST DATA
SERIES I, 28-DAY TESTS

Test ^a Design (1)	Test Data				
	p ^b (2)	θ^c (3)	t _w ^d (4)	t _d ^e (5)	
1-M-28	T1 ^f	69,000	43.0	2.44	3.56
		33,750	55.0	2.69	3.56
	T2 ^f	31,250	65.0	2.56	3.56
		57,500	44.0	2.63	3.56
		28,000	49.5	2.66	3.56
		39,750	55.0	2.63	3.56
18,000	64.5	2.50	3.56		
1-S-28	T1	47,500	45.0	2.56	3.56
		26,750	53.0	2.50	3.56
		27,750	64.0	2.31	3.56
	T2	50,000	46.0	2.69	3.56
		38,500	50.0	2.63	3.56
		24,500	58.0	2.56	3.56
20,750	65.0	2.38	3.56		
1-H-28	T1	35,750	45.0	2.56	3.56
		21,000	56.0	2.63	3.56
		15,400	65.0	2.56	3.56
	T2	44,750	45.0	2.50	3.56
		33,250	50.0	2.56	3.56
		27,250	59.0	2.50	3.56
16,250	64.0	2.50	3.56		
1-O-28	T1	15,450	45.0	2.38	3.56
		11,700	55.0	2.50	3.56
		6,050	66.0	2.69	3.56
	T2	19,000	45.0	2.63	3.56
		13,175	55.0	2.56	3.56
		7,000	60.0	2.63	3.56
5,500	64.5	2.56	3.56		

TABLE III

SHEAR SPECIMEN TEST DATA
SERIES I, 14-DAY TESTS

Test ^a Design (1)	Test Data				
	p ^b (2)	θ^c (3)	t _w ^d (4)	t _d ^e (5)	
1-M-14	T1 ^f	42,750	46.0	2.69	3.50
		21,750	55.0	2.50	3.56
	T2 ^f	16,250	63.0	2.56	3.56
		50,750	44.5	2.63	3.56
		26,000	50.0	2.63	3.56
		22,750	55.0	2.63	3.56
12,500	65.5	2.63	3.56		
1-S-14	T1	36,250	45.0	2.44	3.56
		24,750	55.0	2.56	3.56
		20,800	65.0	2.56	3.56
	T2	25,250	45.5	2.56	3.56
		35,000	50.0	2.56	3.56
		30,750	55.0	2.63	3.56
13,500	65.0	2.56	3.56		
1-N-14	T1	22,250	54.0	2.63	3.56
		12,125	64.0	2.56	3.56
		27,250	45.0	2.56	3.56
	T2	24,500	50.0	2.69	3.56
		16,225	53.5	2.69	3.56
		8,950	64.0	2.44	3.56
1-O-14		16,375	46.0	2.63	3.56
		10,050	50.0	2.56	3.56
		9,350	56.5	2.63	3.56
		8,050	60.0	2.53	3.56
		8,050	64.0	2.50	3.56

- a) Test designation legend in Table I
b) Failure load in pounds
c) Joint angle in degrees
d) Shear specimen width in inches
e) Shear specimen depth in inches
f) Two shear families tested

TABLE IV

SHEAR SPECIMEN TEST DATA
SERIES II

Test ^a Design (1)	Test Data				
	p^b (2)	θ^c (3)	t_w^d (4)	t_d^e (5)	
M-140	83,500	39.0	2.50	3.56	
	78,250	45.0	2.56	3.56	
	53,250	49.0	2.56	3.56	
	46,000	55.0	2.56	3.56	
	26,500	65.0	2.63	3.56	
M-120	63,750	46.0	2.63	3.56	
	-	50.0	-	-	
	32,500	55.0	2.56	3.56	
	37,000	59.0	2.44	3.56	
	25,000	65.0	2.56	3.56	
M-110	T1	50,250	46.0	2.63	3.56
		46,000	54.0	2.59	3.56
		35,000	65.0	2.63	3.56
	T2	41,000	52.0	2.69	3.56
		25,250	54.0	2.69	3.56
		43,250	59.0	2.69	3.56
		16,500	62.0	2.50	3.56
24,000	65.0	2.50	3.56		
N-140	41,000	40.0	2.44	3.56	
	37,000	45.0	2.44	3.56	
	31,500	51.0	2.56	3.56	
	27,000	54.0	2.47	3.56	
	26,700	60.0	2.63	3.56	
	24,025	64.0	2.56	3.56	
N-120	46,750	39.0	2.69	3.56	
	39,750	44.0	2.63	3.56	
	34,750	50.0	2.63	3.56	
	26,000	55.0	2.69	3.56	
	24,000	61.0	2.56	3.56	
	19,250	65.0	2.56	3.56	
N-110	49,250	39.0	2.50	3.56	
	56,750	44.0	2.69	3.56	
	34,500	49.5	2.63	3.56	
	33,750	54.0	2.69	3.56	
	17,500	59.5	2.75	3.56	
	6,575	64.0	2.56	3.56	

TABLE V

SHEAR SPECIMEN TEST DATA
SERIES III

Test ^a Design (1)	Test Data			
	p^b (2)	θ^c (3)	t_w^d (4)	t_d^e (5)
M-Wet	74,000	45.0	2.75	3.69
	37,000	55.0	2.56	3.69
	16,250	60.0	2.56	3.69
	21,750	64.0	2.50	3.69
	43,000	45.0	2.56	3.69
N-Wet	30,750	54.5	2.56	3.69
	24,250	59.0	2.63	3.69
	15,250	63.0	2.50	3.69
	29,000	45.0	2.63	3.69
O-Wet	13,000	55.0	2.63	3.69
	16,000	60.5	2.63	3.69
	11,300	64.5	2.56	3.69
M-Dry	8,250	51.0	2.56	3.69
	10,500	55.0	2.63	3.69
	6,000	60.0	2.50	3.69
	10,750	65.0	2.50	3.69
N-Dry	25,500	43.0	2.56	3.69
	17,750	50.0	2.50	3.69
	22,775	54.0	2.50	3.69
	10,875	60.0	2.56	3.69
	5,600	62.0	2.50	3.69
O-Dry	16,775	45.0	2.50	3.69
	6,025	51.0	2.50	3.69
	11,300	54.0	2.44	3.69
	4,425	60.0	2.56	3.69
	8,250	63.0	2.50	3.69

See Table II for notes.

TABLE VII
COMPRESSION PRISM MORTAR DATA

Test ^a Design (1)	Mortar Data			
	Cube Strengths ^b		%C Flow (4)	w/c ^d (5)
	No. 1 (2)	No. 2 (3)		
1-M-28	5981	5920	135	0.610
1-S-28	2763	-	132	0.920
1-N-28	1187	-	130	1.280
1-O-28	369	381	131	2.070
1-M-14	6040	5915	132	0.610
1-S-14	2600	-	132	0.920
1-N-14	1194	-	128	1.275
1-O-14	356	-	134	2.070
M-140	5438	4969	141	0.670
M-120	5100	5419	116	0.625
M-110	6545	6620	110	0.575
N-140	1075	1194	135	1.320
N-120	1350	1356	122	1.255
N-110	1450	1443	115	1.220
M-Wet	5400	5388	132	0.625
N-Wet	1163	-	130	1.335
O-Wet	375	381	131	2.120
M-Dry	5825	5863	135	0.625
N-Dry	1188	1194	132	1.300
O-Dry	375	388	130	2.120

- a) Test designation legend in Table I
- b) T1, T2 = test 1, test 2 as in Table II
- c) 7-day 2-inch mortar cube compressive strength, f'_c in psi
- d) Percentage increase in flow water-to-cement ratio, by weight

TABLE VI
SHEAR SPECIMEN FAMILY MORTAR DATA

Family ^a Test Design (1)	Mortar Data			
	Cube Strengths ^b		%C Flow (4)	w/c ^d (5)
	No. 1 (2)	No. 2 (3)		
1-M-28 T1	5075	5012	132	0.630
1-M-28 T2	5563	5475	131	0.625
1-S-28 T1	2620	-	132	0.920
1-S-28 T2	2731	2681	127	0.920
1-N-28 T1	1106	1131	132	1.275
1-N-28 T2	1200	1175	134	1.295
1-O-28 T1	319	344	131	2.070
1-O-28 T2	419	412	128	2.120
1-M-14 T1	5388	5463	130	0.625
1-M-14 T2	5381	5325	132	0.625
1-S-14 T1	2750	-	131	0.920
1-S-14 T2	2663	2650	127	0.925
1-N-14 T1	1213	1244	127	1.275
1-N-14 T2	1200	1219	128	1.300
1-O-14 -	413	-	133	2.095
M-140 -	4919	4925	142	0.670
M-120 -	5400	5269	117	0.625
M-110 T1	6025	5300	112	0.600
M-110 T2	6225	5863	110	1.246
N-140 -	1212	1200	140	1.320
N-120 -	1331	1381	121	1.255
N-110 -	1390	1380	114	1.245
M-Wet -	5369	5756	130	0.625
N-Wet -	1213	1263	132	1.335
O-Wet -	406	419	135	2.120
M-Dry -	5413	5581	132	0.625
N-Dry -	1263	1200	132	1.310
O-Dry -	356	393	133	2.140

TABLE VIII

CLAY MASONRY UNIT TEST DATA

Test Series (1)	Test No. ^b (2)	Water Suction Rate			Compressive Strength		
		IRA ^c (3)	t_w^e (4)	t_d^f (5)	f_b^d (6)	t_w^e (7)	t_d^f (8)
I and II	1	6.0	7.63	3.56	12,572	3.80	3.56
	2	7.2	7.63	3.56	15,622	3.75	3.56
	3	12.6	7.63	3.56	13,961	3.75	3.56
	4	11.7	7.63	3.56	12,521	3.80	3.56
	5	9.3	7.63	3.56	13,672	3.85	3.56
III (Dry)	1	18.7	7.73	3.70	8,940	3.50	3.70
	2	22.7	7.70	3.70	12,606	3.50	3.70
	3	16.2	7.70	3.75	9,274	3.65	3.70
	4	19.5	7.75	3.73	12,125	3.70	3.70
	5	22.0	7.73	3.70	12,553	3.80	3.70
III (Wet)	1	10.7	7.73	3.73	clay units III (dry) and III (wet) were from the same batch except units III (wet) were modified in the laboratory to have a lower IRA as explained in Chapter IV		
	2	11.2	7.70	3.73			
	3	13.6	7.73	3.70			
	4	12.7	7.75	3.73			
	5	13.1	7.70	3.75			

Note: 1 psi = 6.895 kN/m²; 1 inch = 25.4 mm

- a) Test series where units were used
- b) Five tests per clay unit group
- c) Initial Rate of Absorption in gpm
- d) Compressive stress in psi
- e) Width in inches
- f) Depth in inches

TABLE IX

COMPRESSION PRISM TEST DATA
SERIES I

Test ^a Design (1)	Compression Prism Test Data			
	p^b (2)	t_w^c (3)	t_d^d (4)	f_m^e (5)
1-M-28	343,000	7.625	3.625	12,410
	342,000	7.625	3.625	12,370
	345,000	7.625	3.625	12,480
1-S-28	238,000	7.625	3.563	8,760
	234,000	7.625	3.563	8,615
	247,750	7.625	3.563	8,750
1-N-28	185,500	7.625	3.563	6,830
	179,750	7.625	3.563	6,620
	184,250	7.625	3.563	6,780
1-O-28	124,000	7.625	3.563	4,565
	137,250	7.625	3.563	5,050
	137,500	7.625	3.563	5,060
1-M-14	332,000	7.625	3.625	12,010
	324,000	7.625	3.625	11,720
	357,000	7.625	3.625	12,920
1-S-14	209,250	7.625	3.563	7,700
	215,250	7.625	3.563	7,925
	213,500	7.625	3.563	7,860
1-N-14	175,500	7.625	3.563	6,460
	165,500	7.625	3.563	6,090
	166,000	7.625	3.563	6,110
1-O-14	110,500	7.625	3.563	4,070
	114,250	7.625	3.563	4,205
	118,750	7.625	3.563	4,370

Note: 1 lb = 0.453 kg; 1 in. = 25.4 mm;
1 psi = 6.895 kN/m²

- a) Test designation legend in Table I
b) Failure load in pounds
c) Prism width in inches
d) Prism depth in inches
e) Prism compressive strength in psi

TABLE X

COMPRESSION PRISM TEST DATA
SERIES II

Test ^a Design (1)	Compression Prism Test Data			
	P ^b (2)	t _w ^c (3)	t _d ^d (4)	f _m ^e (5)
M-140	353,000	7.759	3.563	12,770
	335,000	7.759	3.563	12,120
	342,000	7.759	3.563	12,370
M-120	366,000	7.759	3.563	13,240
	335,000	7.759	3.563	12,120
	399,000	7.759	3.563	14,435
M-110	363,000	7.759	3.563	13,130
	303,000	7.759	3.563	10,960
	336,000	7.759	3.563	12,160
N-140	170,000	7.625	3.563	6,260
	198,500	7.625	3.563	7,310
	201,500	7.625	3.563	7,420
N-120	203,000	7.625	3.563	7,475
	205,250	7.625	3.563	7,555
	197,750	7.625	3.563	7,280
N-110	203,500	7.625	3.563	7,490
	212,500	7.625	3.563	7,825
	220,500	7.625	3.563	8,120

TABLE XI

COMPRESSION PRISM TEST DATA
SERIES III

Test ^a Design (1)	Compression Prism Test Data			
	P ^b (2)	t _w ^c (3)	t _d ^d (4)	f _m ^e (5)
N-Wet	234,750	7.688	3.688	8,280
	210,000	7.688	3.688	7,410
	228,250	7.688	3.688	8,050
N-Wet	162,500	7.688	3.688	5,730
	176,500	7.688	3.688	6,225
	195,500	7.688	3.688	6,895
O-Wet	135,250	7.688	3.688	4,770
	140,750	7.688	3.688	4,965
	138,000	7.688	3.688	4,860
N-Dry	235,250	7.688	3.688	8,300
	232,500	7.688	3.688	8,200
	240,500	7.688	3.688	8,485
N-Dry	162,750	7.688	3.688	5,740
	160,500	7.688	3.688	5,660
	166,000	7.688	3.688	5,855
O-Dry	133,500	7.688	3.688	4,710
	133,750	7.688	3.688	4,720
	144,250	7.688	3.688	5,090

See Table IX for notes.

TABLE XII
AVERAGE MASONRY PROPERTY VALUES

Test ^a Design (1)	τ_0^b (2)	f_c^c (3)	f_m^d (4)	f_b^e (5)	IRA ^f (4)	w/c ^g (7)	w/L ^h (8)
1-M-28	638	5044	12,420	13,670	9.0	0.623	5.86
1-S-28	554	2620	8,710	13,670	9.0	0.917	4.31
1-N-28	433	1150	6,743	13,670	9.0	1.200	2.82
1-O-28	290	330	4,893	13,670	9.0	2.070	2.43
1-M-14	366	5390	11,730	13,670	9.0	0.623	5.86
1-S-14	423	2755	7,830	13,670	9.0	0.917	4.51
1-N-14	231	1225	6,220	13,670	9.0	1.196	2.81
1-O-14	215	415	4,215	13,670	9.0	2.119	2.49
M-140	758	4920	12,420	13,670	9.0	0.672	6.32
M-120	626	5323	13,265	13,670	9.0	0.623	5.86
M-110	450	5875	12,080	13,670	9.0	0.585	5.50
N-140	695	1206	6,995	13,670	9.0	1.242	2.92
N-120	433	1356	7,436	13,670	9.0	1.178	2.77
N-110	302	1385	7,810	13,670	9.0	1.171	2.75
M-Wet	380	5662	7,845	11,100	12.3	0.623	5.86
N-Wet	353	1233	6,285	11,100	12.3	1.334	3.13
O-Wet	285	413	4,865	11,100	12.3	2.119	2.49
M-Dry	215	5844	8,343	11,100	19.8	0.623	5.86
N-Dry	145	1193	5,753	11,100	19.8	1.299	3.05
O-Dry	103	389	4,839	11,100	19.8	2.119	2.49

- a) Test designation legend in Table I
b) Average joint pure shear strength in psi
c) Average 2-inch mortar cube strength in psi
d) Average compression prism strength in psi
e) Average clay unit compressive strength in psi
f) Average Initial Rate of Absorption in gpm
g) Water-cement ratio by weight
h) Water-to-lime ratio by weight

TABLE XIII
 MULTIPLE REGRESSION ANALYSES
 ALL 28-DAY SHEAR TESTS

Eq. No. (1)	r (2)	s (3)	t (4)	u (5)	v (6)	w (7)	x (8)	y (9)	z (10)	R ^b (11)
1	4.03	1.00	-	-	2.74	-1.58	-	-	-0.55	0.9781
2	16.83	1.00	-	-	-	-1.52	-	2.98	-	0.9769
3	5.66	1.00	-	-	1.94	-1.56	0.26	-	-	0.9761
4	13.48	1.00	-	-	0.62	-1.43	-	-	0.62	0.9654
5 ^c	1.00	1.37	-0.0002	-0.07	2.57	-1.59	-	-	-	0.9406
6	0.34	1.42	-0.08	-	2.66	-1.64	-	-	-	0.9403
7	0.41	1.41	-	-	2.68	-1.62	-	-	-	0.9402
8	9902.0	0.25	-1.76	-	-	-1.50	-	-	-	0.9251
9	2577.0	0.20	-	-	-	-1.44	-	-	-	0.9245
10	8938.0	-	0.03	-	-0.42	-1.41	-	-	-	0.9188
11 ^c	1.00	-	0.92	-	-	0.99	-	-	-	0.8988
12	0.0001	-0.30	1.93	-	-	-	-	-	-	0.7191
13 ^c	1.00	-	0.66	-	-	-	-	-	-	0.6298
14 ^c	1.00	0.70	-	-	-	0.25	-	-	-	0.0000
15 ^c	1.00	0.78	-	-	-	-	-	-	-	0.0000

a) $\tau_0 = r \cdot (f'_c)^s \cdot (f'_m)^t \cdot (f'_b)^u \cdot (w/c)^v \cdot (IRA)^w \cdot (w/L)^x \cdot (w/[C+L])^y \cdot (L/c)^z$

- τ_0 = Joint pure shear strength in psi
- r = Constant
- f'_c = Seven-day two-inch mortar cube strength in psi
- f'_m = Compression prism strength in psi
- f'_b = Clay unit compressive strength in psi
- IRA = Initial Rate of Absorption in gpm
- w, c, L = Water, cement, and lime ratios by weight
- b) Multiple correlation coefficient
- c) Regression forced through zero
- d) Equation number

TABLE XIV
 MULTIPLE REGRESSION ANALYSES
 SERIES I AND III, 28-DAY SHEAR TESTS

Eq. No. (1)	r (2)	s (3)	t (4)	u (5)	v (6)	w (7)	x (8)	y (9)	z (10)	R ^b (11)
1	10.40	1.00	-	-	1.56	-1.52	-0.25	-	-	0.9979
2	9.01	1.00	-	-	1.60	-1.56	-	-	0.07	0.9968
3	8.23	1.00	-	-	1.72	-1.56	-	-	-	0.9967
4	18.09	1.00	-	-	0.63	-1.53	-	-	0.63	0.9956
5	28.36	1.00	-	-	-	-1.51	-	-	1.45	0.9937
6	18.15	1.00	-	-	-	-1.54	-	2.95	-	0.9916
7 ^c	1.00	1.12	0.13	-	2.06	-1.55	-	-	-	0.9912
8	2.71	1.15	-	-	2.06	-1.58	-	-	-	0.9906
9	2095.0	0.23	-	-	-	-1.43	-	-	-	0.9776
10	1017.0	-	0.25	-	-0.35	-1.34	-	-	-	0.9716
11	4.63	-	0.82	-	-	-1.22	-	-	-	0.9652
12	80.32	1.00	-	-	-	-1.15	-2.47	-	-	0.9617
13	0.01	-	1.25	-	-	-	-	-	-	0.6725
14	51.70	0.24	-	-	-	-	-	-	-	0.4696

a) $\tau_0 = r \cdot (f'_c)^s \cdot (f'_m)^t \cdot (f'_b)^u \cdot (w/c)^v \cdot (IRA)^w \cdot (w/L)^x \cdot (w/[C+L])^y \cdot (L/c)^z$

τ_0 = Joint pure shear strength in psi

r = Constant

f'_c = Seven day two-inch mortar cube strength in psi

f'_m = Compression prism strength in psi

f'_b = Clay unit compressive strength in psi

IRA = Initial Rate of Absorption in gpm

w, c, L = Water, cement, and Lime ratios by weight

b) Multiple correlation coefficient

c) Regression forced through zero

d) Equation number

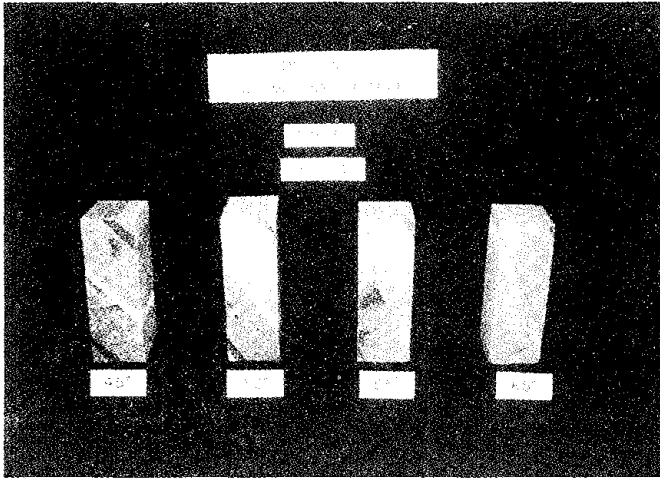


Photo 1. Family of Shear Specimens

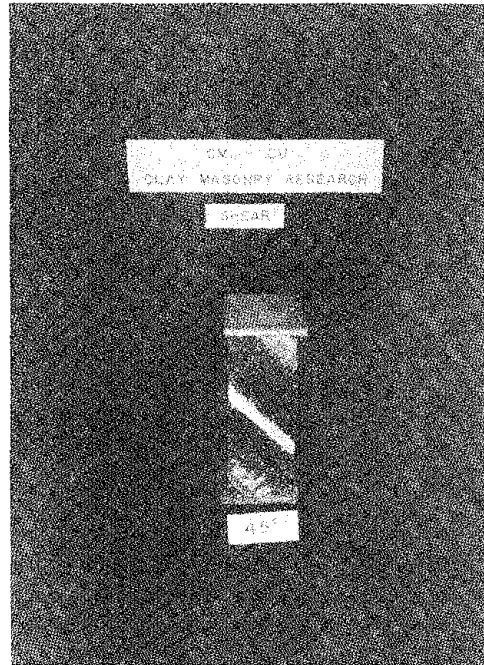


Photo 2. Capped Specimen

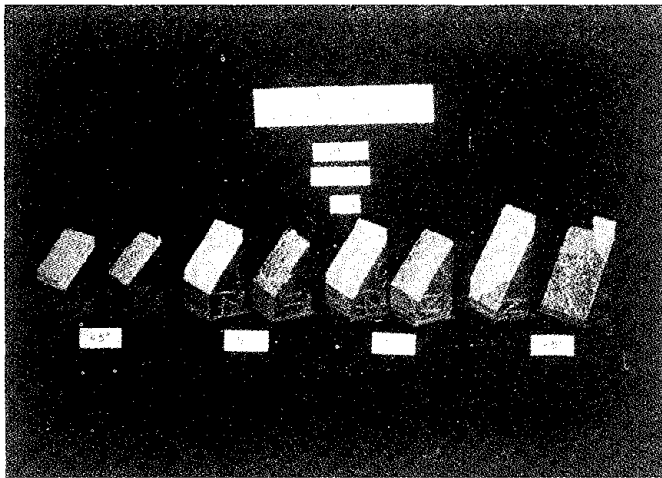


Photo 3. Typical Shear Failures

APPENDIX I - BIBLIOGRAPHY

1. American Society for Testing and Materials, Annual Book of ASTM Standards, Philadelphia, 1975.
2. Baur, J.C., "Compression and Tension Bond Strength of Small Scale Masonry Specimens," thesis presented to the University of Colorado at Boulder in 1977, in partial fulfillment of the requirements for the degree of Master of Science.
3. Benjamin, J.R., and Williams, H.A., "The Behavior of One-Story Brick Shear Walls," Journal of the Structural Division, ASCE, Vol. 84, No. 4, July 1958, Paper 1723, pp. 1-30.
4. Blume, J.A., and Prolux, J., "Shear in Grouted Brick Masonry Wall Elements," Western States Clay Products Association, San Francisco, Calif., Aug. 1968.
5. Brick Institute of America, Recommended Practice for Engineered Brick Masonry, 2nd Ed., Brick Institute of America, McLean, Va., 1967.
6. Fishburn, C.C., "Effect of Mortar Properties on Strength of Masonry," Monograph 36, National Bureau of Standards, United States Government Printing Office, Dec. 1961, pp. 1-45.
7. Frey, D.J., "Effect of Constituent Proportions on Uniaxial Compressive Strength of 2 Inch Cube Specimens of Masonry Mortars," thesis presented to the University of Colorado at Boulder in 1975, in partial fulfillment of the requirements for the degree of Master of Science.
8. Johnson, F.B., Designing, Engineering, and Constructing with Masonry Products, 1st Ed., Gulf Publishing Co., Texas, 1967, pp. 139-147.
9. Mayes, R.L., and Clough, R.W., "A Literature Survey - Compressive, Tensile, Bond and Shear Strength of Masonry," Report No. EERC 75-15, National Science Foundation, College of Engineering, University of California, Berkeley, California, pp. 50-51.
10. Sahlin, S., Structural Masonry, 1st Ed., Prentice-Hall, N.J., 1971.
11. Smith, B.S., and Carter, C., "Hypothesis for Shear Failure of Brickwork," Journal of the Structural Division, ASCE, Vol. 97, No. 4, April 1971, Paper 1056, pp. 1055-1066.
12. Yokel, F.Y., and Fattal, G., "A Failure Hypothesis for Masonry Shearwalls," Report No. NBSIR 75-703, National Bureau of Standards, Washington, D.C., May 1975.

APPENDIX II - NOTATION

- f'_b = compressive strength of a clay masonry unit determined using ASTM C67 test procedures.
- f'_c = compressive strength of seven-day, two-inch mortar cubes determined using ASTM C109 test procedures.
- f'_m = compressive strength of four-unit-high, clay, single-wythe stack-bond 3/8 inch joint prisms determined using ASTM E447 test procedures.
- P = failure load applied to a shear specimen or compression prism along the centroidal longitudinal axis.
- W/C = the water-cement ratio by weight of a given mortar.
- W/(C+L) = the water-to-(cement plus lime) ratio by weight of a given mortar.
- σ_n = the compressive stress normal to the mortar bed in a shear specimen.
- σ_x = the compressive stress applied to a shear specimen calculated by dividing the failure load, P, by the cross sectional area.
- θ = the acute angle of the joint bed of a shear specimen measured from a transverse plane.
- τ_0 = the pure shear strength of a joint of a shear specimen.
- τ = the shear strength of a joint of a shear specimen subjected to normal stress on the joint.



THE EFFECT OF SLENDERNESS AND END CONDITIONS ON
THE STRENGTH OF CLAY UNIT PRISMS

J. L. Noland¹, K. T. Hanada², C. C. Feng³

ABSTRACT: An experimental program was conducted to study the effect of slenderness and end conditions on the ultimate compressive strength of stackbond clay-unit prisms. The prisms were constructed using different mortar mixes to permit the influence of that factor to be observed. One type of solid clay unit was used and slenderness varied from $h/t = 1.44$ to 5.12 .

Two test series were done in parallel. One series involved prisms whose ends were directly in contact with the test machine surfaces. The other utilized lateral friction relief material at the machine-prism interface in order to be able to observe the effects of end lateral restraint. The prisms with no friction relief at the interface failed in various combinations of shear and lateral tensile splitting while those with friction relief failed by lateral tensile splitting alone.

Analyses of results revealed that: 1) the difference in ultimate compressive strength between prisms tested with restrained ends and unrestrained ends was much greater for prisms made with high strength mortar, 2) for the units used, ultimate prism strength was quite mortar dependent for all slenderness ratios, and 3) for the prisms tested with unrestrained ends (as is current practice), slenderness correction factors found in presently used codes in the U.S. are inaccurate.

A hypothesis was formulated that ultimate compressive strength of prisms with unrestrained ends could be related to the total lateral force exerted by the mortar joints. It was observed that (for prisms of 3 or more joints) a factor based upon the relative volume of mortar to units in prisms when multiplied by prism failing stress resulted in a constant value of ultimate compressive stress.

¹Principal, Atkinson-Noland & Associates, Boulder, Colorado.

²Formerly Graduate Student, University of Colorado, Boulder, Colorado.

³Professor of Civil, Environmental, & Architectural Engineering, University of Colorado, Boulder, Colorado.

THE EFFECT OF SLENDERNESS AND END CONDITIONS ON THE
STRENGTH OF CLAY UNIT PRISMSJ. L. Noland¹, K. T. Hanada², and C. C. Feng³

INTRODUCTION

The prism test⁴ is widely used as a means to establish the ultimate compressive design strength, f'_m , of masonry. Its importance is magnified because the value f'_m is used not only to establish design allowable compressive stress, but frequently design allowable flexural and shear stresses (1,12,17,18,24).

At the current time, there are inconsistencies due to the method of test and interpretation of results. Primary among these, in the authors' opinion, are those related to the effects of the interface between the prism and test machine (9,23,25,26,27), and the effects of slenderness.

The nature of the interface between a prism and a test machine affects the failure mode of the prism. It has been widely observed that the basic failure mechanism of full-scale masonry under centroidal axial compression is lateral splitting (3,7,10,23,14,15, 18-22). However, that failure mode is inhibited in a prism whose ends are placed directly in contact with the loading surfaces of a test machine; friction forces develop which tend to restrict lateral deformation of the prism (2,3). The restriction affects the end units of the prism the most, with the inner units experiencing varying degrees of combined shear and lateral tensile failure (2). The question then arises: How representative of full scale masonry strength is prism strength when the prisms are subjected to lateral friction restraining forces at the machine-prism interface?

One approach to a solution has been to make prism failure mode resemble full-scale masonry failure mode by basing design f'_m on a prism slenderness ratio of five (18). Prisms of that slenderness ratio fail primarily by lateral tensile splitting with shear failure confined to the end units and units adjacent to the end units.

¹Principal, Atkinson-Noland & Associates, Boulder, Colorado.

²Formerly Graduate Student, University of Colorado, Boulder, Colorado.

³Professor of Civil, Environmental, & Architectural Engineering, University of Colorado, Boulder, Colorado.

⁴A compressive test of a small masonry assemblage composed of two or more units laid in stack bond.

Another approach has been to base design f'_m on prism slenderness ratio of two (24). Apparently the governing philosophy here is that a value of design f'_m based on the short prism is representative of pure material strength without slenderness effects.

An intermediate position has been adopted in Australia where the bases for design f'_m is a slenderness ratio of three (17).

The result of all this is that the designer of clay unit masonry in the U.S. is confronted with two means of determining design f'_m based upon prism test. The results of the prism test are modified by "correction factors" which purport to convert the strength of a given prism with a particular slenderness ratio (expressed as height, h , divided by the least lateral dimension, t) to that of either a slenderness ratio of two (24) or five (18).

An analysis (3) of "correction factors" used in various standards in the U.S., Canada, Australia, and New Zealand concluded that (as of 1973) the correction factors apparently have a common source, i.e., Krefield's work (8) in 1938. The study reports that he delineated the limitations of his work which was based upon one solid clay unit and one mortar type, and that he observed that the effect of other factors e.g., unit strength and mortar strength required investigation. The report observes that the correction factors due to Krefield "...have apparently been accepted as being of general validity, not only for brick, but for concrete masonry as well".

OBJECTIVE

The primary objective of the research (6) was to study the influence of slenderness (h/t ratio), the nature of the machine-prism interface, and mortar upon the compressive strength of solid clay-unit masonry prisms. Specifically, the relationship between slenderness and compressive failure stress was studied for prisms with "restrained interfaces" and "unrestrained interfaces" for each of three mortar types.

SCOPE

The test series conducted was designed to observe only the effects mentioned earlier, hence a single type of solid clay unit was used throughout. The specimens built and tested are defined in Tables I and II.

Table I

Test Series I: Restrained Interface

Set	Mortar ¹ Type	Number of Units	Slenderness ² Ratio	Number of ³ Specimens
1	1:¼:3	2	1.44	3
		3	2.18	3
		4	2.91	2
		5	3.65	3
		6	4.39	3
		7	5.12	3
		2	1:1:6	2
3	2.18			3
4	2.91			3
5	3.65			3
6	4.39			3
7	5.12			3
3	1:2:9			2
		3	2.18	3
		4	2.91	3
		5	3.65	3
		6	4.39	3
		7	5.12	3

¹Refers to parts by volume of portland cement, lime, and aggregate.

²Based upon average measured dimensions of each group. Slenderness ratio equals the height divided by the least lateral dimension.

³The basic sample consisted of three prisms. If excessive scatter was observed in the first three, two more were built and tested. Occasionally, a prism was damaged. If the remaining two tested to nearly the same value, a third was not built. No results were omitted in the data analysis.

Table II

Test Series II: Unrestrained Interface¹

Set	Mortar Type	Number of Units	Slenderness Ratio	Number of Specimens
1	1:½:3	2	1.44	3
		3	2.18	5
		4	2.91	5
		5	3.65	3
		6	4.39	2
		7	5.12	3
		2	1:1:6	2
3	2.18			3
4	2.91			3
5	3.65			3
6	4.39			3
7	5.12			3
3	1:2:9			2
		3	2.18	3
		4	2.91	3
		5	3.65	3
		6	4.39	2
		7	5.12	3

¹See notes to Table I.

CONSTITUENTS

Clay Units. The solid clay units used were of a single clay mix using local clays. The units were manufactured by the stiff-mud extrusion process, were wire cut, and fired at 1990°F. The units conformed to the requirements of ASTM C216-75a, "Facing Brick". The final shape and dimensions of the clay unit are shown in Figure 1. Table III presents results of unit tests.

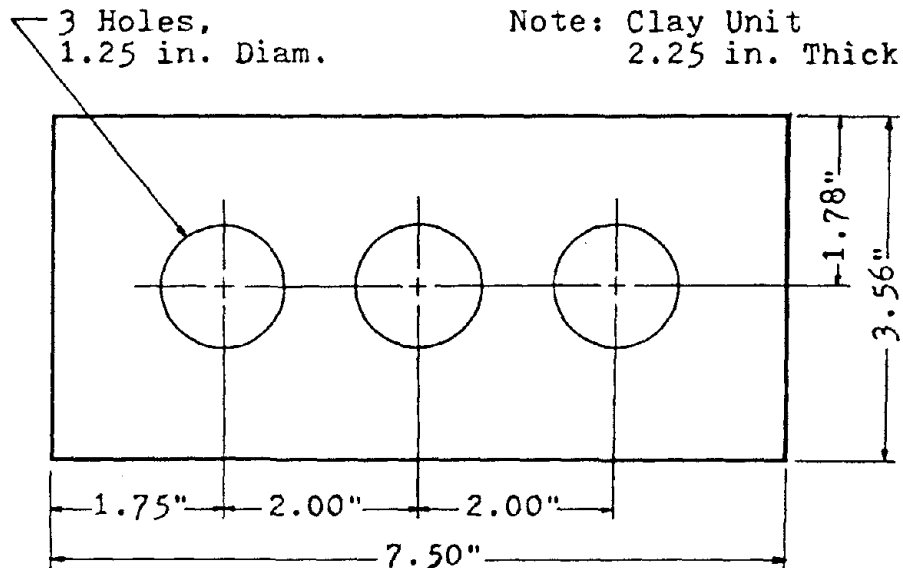


Figure 1. Dimensions of Clay Unit

The solid clay units were delivered to the laboratory in 500 unit "cubes". Units were selected randomly for use in constructing prisms with only those with obvious defects rejected.

Mortar. Mortar used was made from portland cement, lime, and sand ingredients. The amount of water used for each different mortar mix was that which produced a flow of 130 ±5% per ASTM C109-73. The proportions of the ingredients for each mix were controlled by weight measurements in order to maintain constant properties (2,4).

Mortar was mixed in accordance with ASTM C305-65. Cube compressive tests per ASTM C109 were performed periodically for quality assurance. The mixes used in the study were 1:¼:3, 1:1:6, and 1:2:9 proportions of cement:lime:sand by volume.

Only fresh Type I portland cement meeting the requirements of ASTM C150-73a manufactured by Martin-Marietta Corporation was used. The lime used was Type S meeting the requirements of ASTM C207-68 manufactured by the Flinkote Company.

Table III

Solid Clay Unit Properties

Test	Initial Rate ¹ of Absorption (g/30 in ² /min.)	Compressive Strength ² (psi)	
		Symmetrical Section	Unsymmetrical Section
1	6.64	11828	10798
2	9.64	11362	10996
3	13.67	12422	11630
4	10.29	12040	10872
5	11.46	11659	9670
Average	10.34	11862	10793

¹IRA was determined in accordance with ASTM C67-73.

²Flatwise compression tests per ASTM C67-73. The ASTM Standard requires that the specimen be of equal length and width with 1 in. variance permitted. The specimens termed "symmetrical sections" were essentially a half-unit cut from the center while the "unsymmetrical sections" were essentially formed by cutting a unit in half. The difference in compressive strength is believed to be due to eccentricity effects inherent in the unsymmetrical specimens.

A commercially available blended sand was used which satisfied the requirements of ASTM C144-70. The average fineness modulus was 2.26. Results of sieve analysis are presented in Figure 2.

PREPARATION OF PRISM SPECIMENS

The prisms were laid in stack bond with a 3/8 inch mortar joints which were given a concave finish. Bed joints were only lightly furrowed, if at all. Care was exercised to level each unit as it was placed. All prisms were constructed by a single, experienced mason.

Completed prisms remained in place for approximately four hours to allow some set to occur prior to placing in a fog room at 70°F and 100% humidity for seven days. Subsequently, the prisms were dry cured in laboratory air at 71° ±5 and a relative humidity between 20% and 50%.

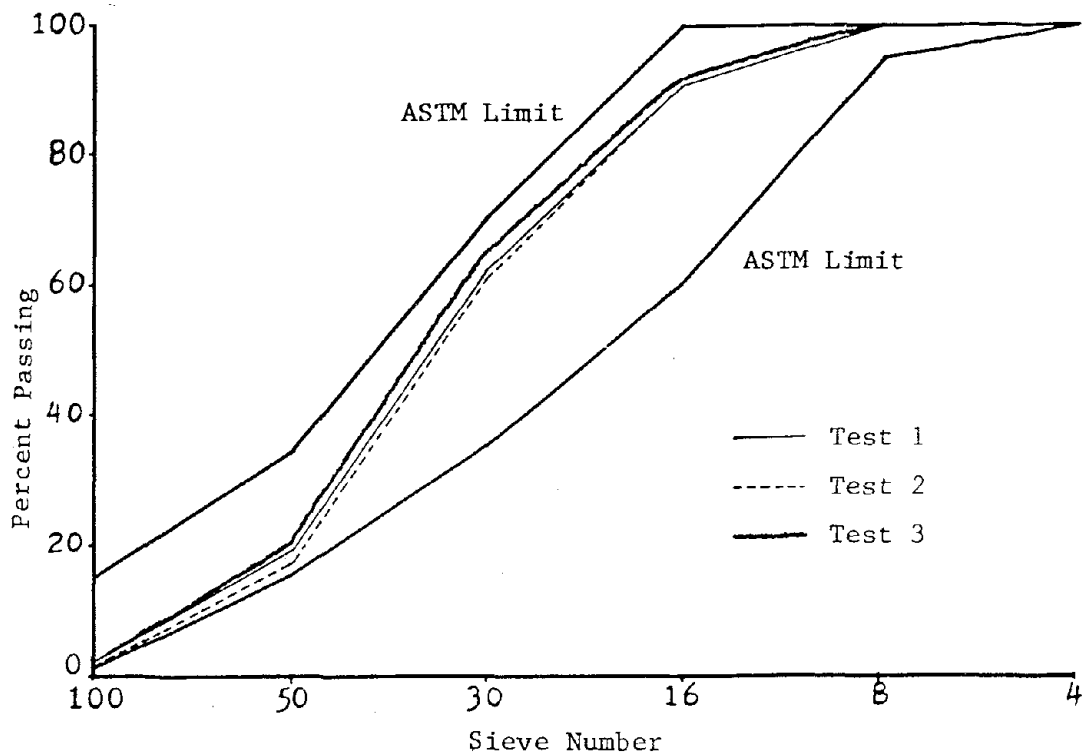


Figure 2. Comparison of Sample Sand with ASTM Specifications.

Approximately 2 days prior to testing, prisms were capped (1/8 in. thick) with a sulphur-clay compound marketed under the name Cylcap and manufactured by DFC Ceramics, Inc. The material satisfies the requirements of ASTM C617, Part 10. The results of a test series performed by Commercial Test Laboratory, Denver, Colorado are presented in Table IV.

Table IV

Compressive Strength Tests of Cylcap

Lot No.	Test Age (hr)	Compressive Strength (psi)			
		1	2	3	Average
020576	2	4980	4990	5060	5010
	6	5250	5460	5390	5360
	12	5440	5500	5470	5470
	24	5510	5600	5625	5580
	48	6160	6000	6050	6070
022376	2	5600	5710	5550	5620
	6	6040	5925	6025	5995
	12	5850	5825	5910	5860
	24	6210	6375	6250	6280
	48	6500	6785	6700	6660

A criterion for parallelism of the capped ends, about both lateral axes, of $\pm 0.5^\circ$ was used. The requirement was established during a previous program (2) in which it was determined that, within the accuracy limits of the equipment used, that amount of angular deviation had no appreciable effect upon results.

INTERFACE MATERIAL

The interface material used to eliminate lateral end restraint consisted of a 0.003 in. plastic sheet between two thin layers of grease¹. This was a departure from the material used in a pilot study by Baur (2) who used light lubricating oil between two thin sheets of teflon. The switch to plastic was for purposes of economy. Comparative prism tests revealed that both materials provide very nearly the same degree of friction relief and that in both cases, full lateral splitting failure is attained (6).

TEST PROCEDURE

Prisms were placed on the lower platen of the compression machine very carefully so that the centroidal axis of the prism and center of thrust of the machine were aligned. As the upper spherically seated platen was brought to bear on the prism it was rotated by hand to be parallel with the prism cap.

Load was applied in accordance with the requirements of ASTM E447-74, i.e., at any convenient rate up to about one-half the expected maximum and then adjusted to provide failure within 1 to 2 minutes.

TEST RESULTS

Compression Failure of Prisms with Restrained Interface. The end units in prisms with a restrained interface, i.e., the capping in direct contact with the platen, appear to serve as load-introduction for the inner units. Figure 3 depicts the post-test appearance of a 4-unit prism built with 1:2:9 mortar. Note that the end units are scarcely damaged. Prisms built with 1:2:9 mortar exhibited a relatively slow progressive cracking leading to failure while prism with high strength (1:½:3) mortar failed in a sudden, explosive manner. Results of Test Series I are presented in Table V.

¹Keystone Specialized Lubricant, mfg. by Keystone Lubricating Co.

Table V

Prism Compressive Strength - Restrained Interface

Mortar Mix	Height-to-Thickness, h/t	Prism Strength (psi)	Average (psi)	Standard Deviation
1:k:3 1:k:3 1:k:3	1.439 1.439 1.439	11,395 11,438 11,525	11,458	66
1:k:3 1:k:3 1:k:3	2.175 2.175 2.175	10,016 11,102 11,503	10,874	769
1:k:3 1:k:3	2.912 2.912	10,602 10,939	10,771	288
1:k:3 1:k:3 1:k:3	3.649 3.649 3.649	9,826 10,673 10,461	10,342	409
1:k:3 1:k:3 1:k:3	4.386 4.386 4.386	10,700 10,266 10,396	10,454	223
1:k:3 1:k:3 1:k:3	5.123 5.123 5.123	10,005 9,246 9,745	9,655	386
1:1:6 1:1:6 1:1:6	1.439 1.439 1.439	9,682 8,683 7,294	8,553	1199
1:1:6 1:1:6 1:1:6	2.175 2.175 2.175	7,511 7,250 7,250	7,337	151
1:1:6 1:1:6 1:1:6	2.912 2.912 2.912	7,381 7,587 6,708	7,225	460
1:1:6 1:1:6 1:1:6	3.649 3.649 3.649	6,838 7,120 6,425	6,749	350
1:1:6 1:1:6 1:1:6	4.386 4.386 4.386	7,315 6,664 7,272	7,084	364
1:1:6 1:1:6 1:1:6	5.123 5.123 5.123	6,653 6,838 6,295	6,595	276
1:2:9 1:2:9 1:2:9	1.439 1.439 1.439	5,947 6,077 5,578	5,867	259
1:2:9 1:2:9 1:2:9	2.175 2.175 2.175	4,536 5,535 5,252	5,108	515
1:2:9 1:2:9 1:2:9	2.912 2.912 2.912	4,862 4,883 4,818	4,854	33
1:2:9 1:2:9 1:2:9	3.649 3.649 3.649	3,994 4,471 4,927	4,464	467
1:2:9 1:2:9	4.386 4.386	4,363 4,384	4,374	15
1:2:9 1:2:9 1:2:9	5.123 5.123 5.123	4,308 4,254 3,972	4,178	180

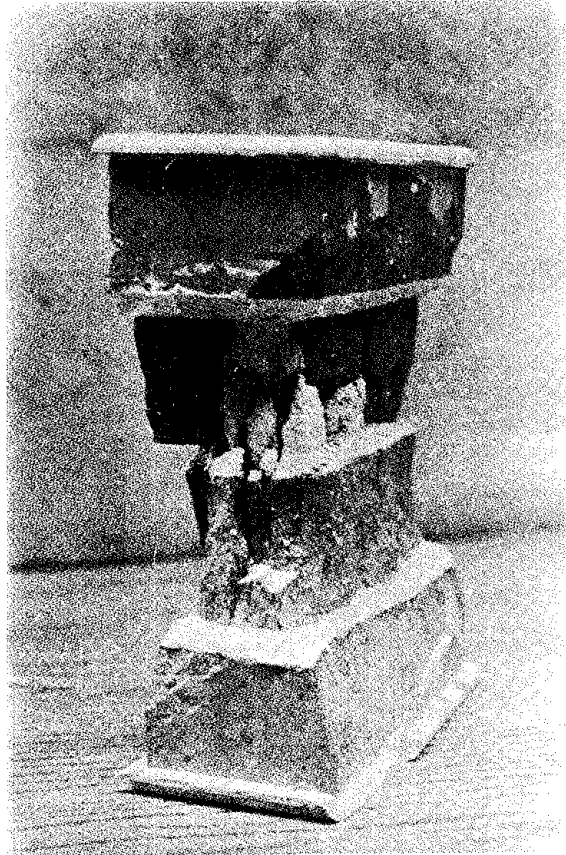


Figure 3. Prism Failure, 1:2:9 Mortar.

Compressive Failure of Prisms with Unrestrained Interface. The failure mode of the prisms with the grease-plastic interface was predominately lateral tensile splitting on the narrow side for the full height of the prism. Figure 4 presents photographs of 2, 3, 4, and 6 unit prisms after test. Prisms made with high strength mortar failed suddenly with a "popping" sound, while cracks would appear and slowly grow until ultimate load was reached in prisms made of low strength mortar.

Results of Test Series II are presented in Table VI.

ANALYSIS AND EVALUATION

Analysis Method. Bivariate regression analyses were done of the results of Test Series I and II with f'_{mt} as the dependent variable and slenderness (h/t) as the independent variable. Five bivariate models were used to determine the best curve fit for the data collected, i.e., linear, power, exponential, logarithmic, and quadratic. The basic forms of the resulting equations are:

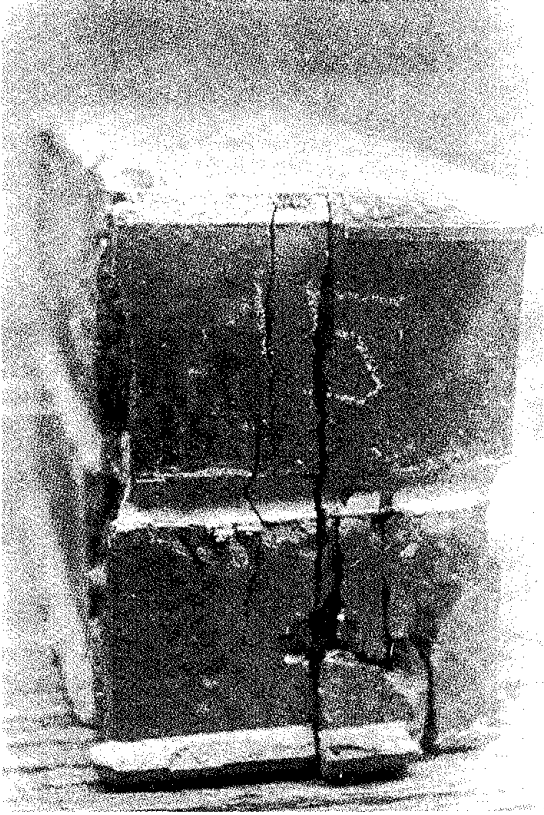


Figure 4a. Failure of Two-Unit Prism, Unrestrained Interface.

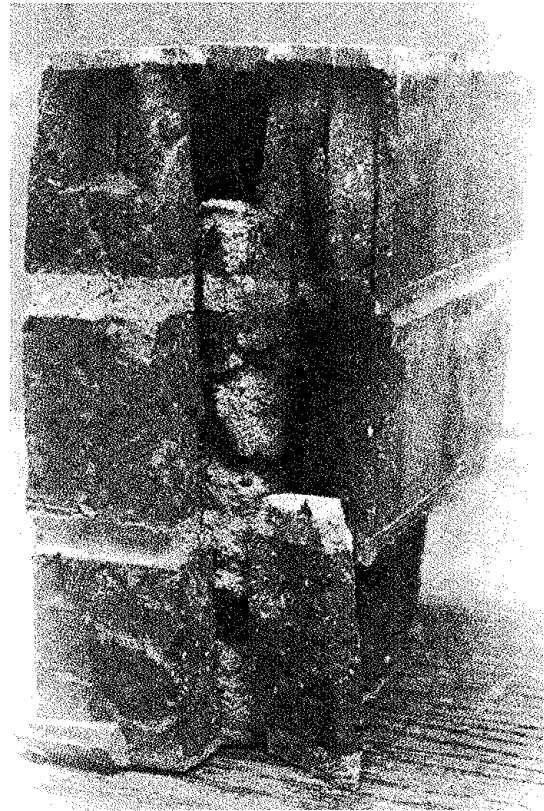


Figure 4b. Failure of Three-Unit Prism, Unrestrained Interface.



Figure 4c. Failure of Four-Unit Prism, Unrestrained Interface.

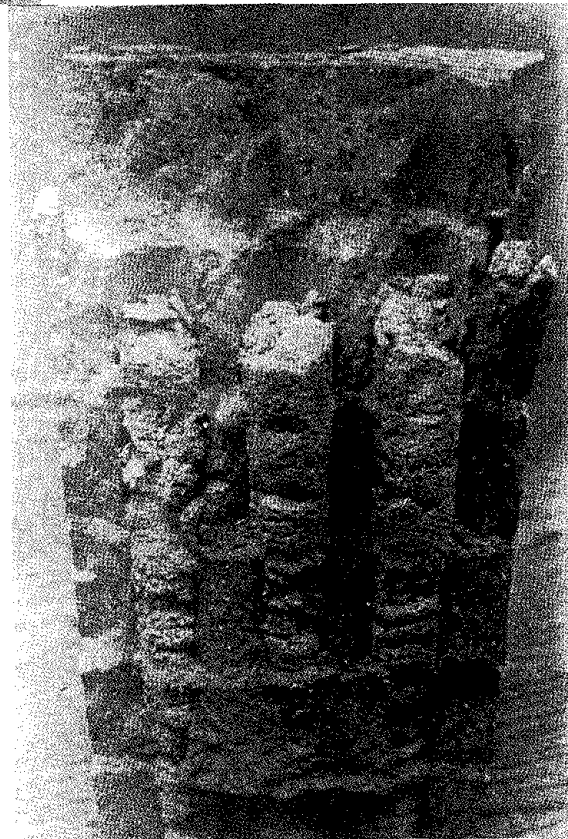


Figure 4d. Failure of Six-Unit Prism, Unrestrained Interface.

Table VI

Prism Compressive Strength - Unrestrained Interface

Mortar Mix	Height-to-Thickness, h/t	Prism Strength (psi)	Average (psi)	Standard Deviation
1:4:3 1:4:3 1:4:3	1.439 1.439 1.439	8410 8790 9517	8905	562
1:4:3 1:4:3 1:4:3 1:4:3 1:4:3	2.175 2.175 2.175 2.175 2.175	7510 9246 8486 7607 8682	8306	738
1:4:3 1:4:3 1:4:3 1:4:3 1:4:3	2.912 2.912 2.912 2.912 2.912	8486 8616 9799 7314 6945	8232	1137
1:4:3 1:4:3 1:4:3	3.649 3.649 3.649	7488 7922 7596	7669	226
1:4:3 1:4:3	4.386 4.386	7510 7162	7336	246
1:4:3 1:4:3 1:4:3	5.123 5.123 5.123	7227 6121 6958	6735	563
1:1:6 1:1:6 1:1:6	1.439 1.439 1.439	7543 7294 7706	7514	207
1:1:6 1:1:6 1:1:6	2.175 2.175 2.175	7359 6729 7120	7069	318
1:1:6 1:1:6 1:1:6	2.912 2.912 2.912	7270 6165 7142	6860	604
1:1:6 1:1:6 1:1:6	3.649 3.649 3.649	6708 6317 6360	6462	214
1:1:6 1:1:6 1:1:6	4.386 4.386 4.386	6773 6187 6534	6498	295
1:1:6 1:1:6 1:1:6	5.123 5.123 5.123	6491 6404 6143	6346	181
1:2:9 1:2:9 1:2:9	1.439 1.439 1.439	4905 5361 5426	5231	284
1:2:9 1:2:9 1:2:9	2.175 2.175 2.175	4384 4927 4536	4616	280
1:2:9 1:2:9 1:2:9	2.912 2.912 2.912	4601 4666 4590	4619	41
1:2:9 1:2:9 1:2:9	3.649 3.649 3.649	4297 4319 4276	4297	22
1:2:9 1:2:9	4.386 4.386	4363 4211	4287	107
1:2:9 1:2:9 1:2:9	5.123 5.123 5.123	4048 4145 4030	4091	49

$$\text{linear: } y' = A + Bx \quad (1)$$

$$\text{power: } y' = Ax^B \quad (2)$$

$$\text{logarithmic: } y' = A + B \ln x \quad (3)$$

$$\text{exponential: } y' = Ae^{Bx} \quad (4)$$

$$\text{quadratic: } y' = B_1 x^2 + Bx + A \quad (5)$$

in which: y' is the estimated value of f'_{mt} for slenderness values h/t , and A and B are constants determined during the curve fit process and x is h/t . A regression computer program was used to develop the best-fit expressions (13) and to determine the coefficient of determination (r^2) for each as a measure of goodness of fit. The resulting expressions were used to 1) evaluate currently used prism test "correction" factors, 2) assess the effects of interface frictional restraint, and 3) assess the effects of height (hence number of mortar joints), upon prism compressive strength for each mortar used.

Evaluation of Correction Factors. Best fit curves/equations for each of the five bivariate models previously discussed were developed for the results of Test Series I - Restrained Interface. The equations were then used to determine the "correction factors" which would convert the strength of the prisms tested to strength at slenderness ratios of two and five in order to permit a comparison with the correction factors contained in widely used codes.

The results of the regression analyses are presented in Table VII. Note that the coefficients of determination are generally high for all bivariate models for each individual mortar, but that when data for all mortars were processed, the coefficients were drastically lower. The power curve equations are plotted in Figure 5 for each mortar along with the average of test results for each mortar and slenderness ratio from Table V.

Correction factors, for the prisms tested, developed in terms of $h/t = 2$ and $h/t = 5$ are shown in Figures 6 and 7 respectively compared to those from currently used codes. One may observe from Figure 6 that for values of h/t exceeding 2, the Code correction factors are unconservative, and for h/t values less than 2, the factors are conservative. Note also that correction factors are mortar dependent for prisms made of the unit used in this study.

Examination of Figure 7 will reveal that with the exception of a small portion of the curve for prisms made with 1:2:9 mortar, the Code correction factors are conservative. Again, the correction factors for prisms made of the units used in this study are mortar dependent.

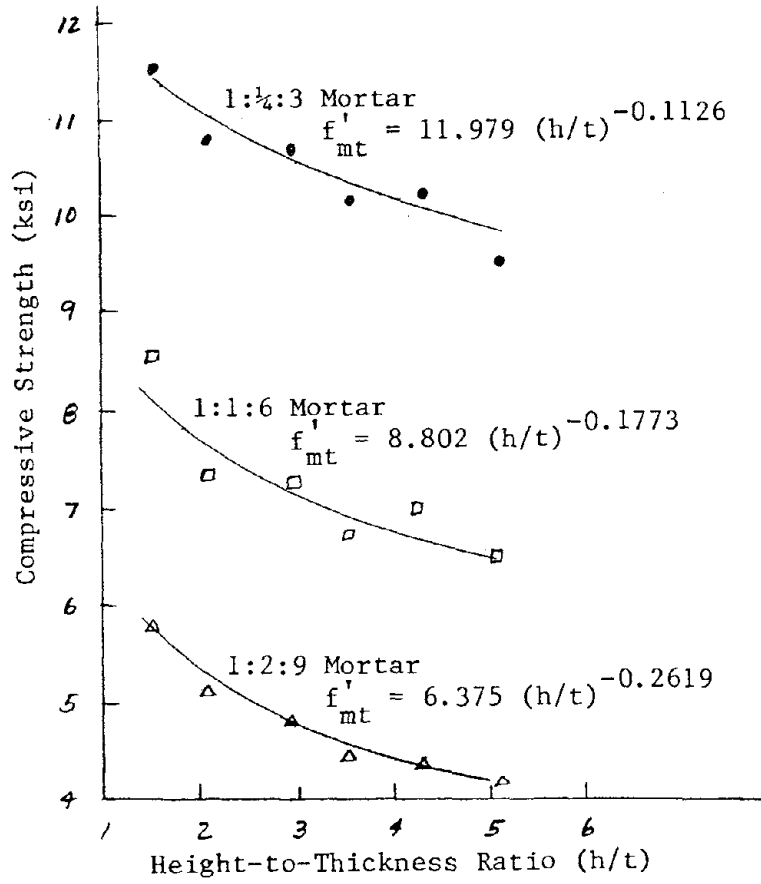


Figure 5. Bivariate Model for Restrained-Interface Prisms.

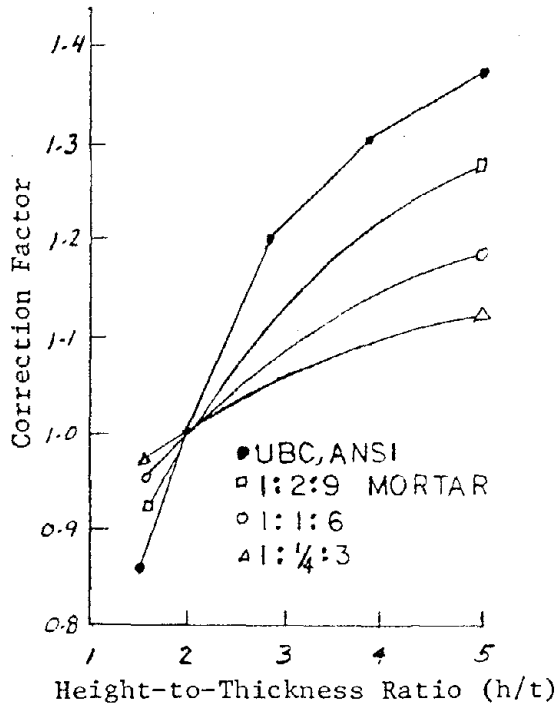


Figure 6. Comparison of Experimental Correction Factors with those from the UBC (24) and ANSI (1).

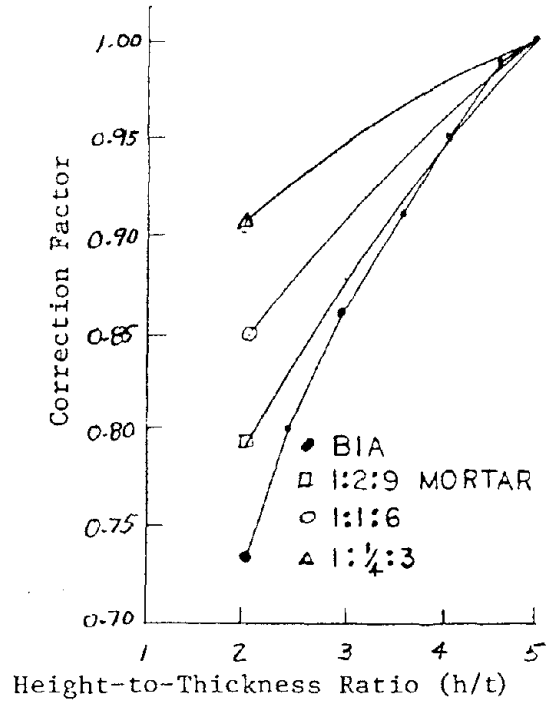


Figure 7. Comparison of Experimental Correction Factors with those from BIA (18).

Table VII

Regression Analyses - Restrained Interface Prism Tests

Mortar	Model	Equation ¹	Coefficient Determination
1:4:3	Linear	$f_{mt}^1 = -0.4131(h/t) + 11.949$	0.900
	Power	$f_{mt}^1 = 11.979(h/t)^{-0.1126}$	0.867
	Exponential	$f_{mt}^1 = 12.030e^{-0.0392(h/t)}$	0.895
	Logarithmic	$f_{mt}^1 = 11.912 - 1.1948 \ln(h/t)$	0.881
	Quadratic	$f_{mt}^1 = -0.00539(h/t)^2 - 0.3777(h/t) + 11.900$	0.900
1:1:6	Linear	$f_{mt}^1 = -0.4257(h/t) + 8.6612$	0.727
	Power	$f_{mt}^1 = 8.802(h/t)^{-0.1773}$	0.849
	Exponential	$f_{mt}^1 = 8.722e^{-0.0568(h/t)}$	0.746
	Logarithmic	$f_{mt}^1 = 8.79 - 1.337 \ln(h/t)$	0.839
	Quadratic	$f_{mt}^1 = 0.1725(h/t)^2 - 1.5575(h/t) + 10.245$	0.865
1:2:9	Linear	$f_{mt}^1 = -0.4279(h/t) + 6.2114$	0.908
	Power	$f_{mt}^1 = 6.375(h/t)^{-0.2619}$	0.987
	Exponential	$f_{mt}^1 = 6.356e^{-0.09711(h/t)}$	0.933
	Logarithmic	$f_{mt}^1 = 6.240 - 1.299 \ln(h/t)$	0.979
	Quadratic	$f_{mt}^1 = 0.1142(h/t)^2 - 1.1775(h/t) + 7.2601$	0.932
All	Linear	$f_{mt}^1 = -0.4222(h/t) + 8.941$	0.047
	Power	$f_{mt}^1 = 8.760(h/t)^{-0.1839}$	0.056
	Exponential	$f_{mt}^1 = 8.737e^{-0.0610(h/t)}$	0.052
	Logarithmic	$f_{mt}^1 = 8.963 - 1.277 \ln(h/t)$	0.051
	Quadratic	$f_{mt}^1 = 0.09378(h/t)^2 - 1.037(h/t) + 9.802$	0.016

¹ f_{mt}^1 is the predicted ultimate compressive strength for a prism with a given slenderness ratio, h/t . f_{mt} is in kips/in².

Evaluation of End Restraint. Bivariate regression analyses of the results of Test Series II - Unrestrained Interface, of the same kind done for the results of Test Series I, were performed to establish best fit curves/equations. The results are presented in Table VIII. Again, the coefficients of determination are quite high for all bivariate models for each mortar.

Table VIII

Result of Regression Analysis for Unrestrained Interface Prisms

Mortar	Model	Equation	Coefficient Determination
1:4:3	Linear	$f'_{m,t} = -0.5554(h/t) + 9.686$	0.975
	Power	$f'_{m,t} = 9.7018(h/t)^{-0.2017}$	0.907
	Exponential	$f'_{m,t} = 9.8967e^{-0.07134(h/t)}$	0.969
	Logarithmic	$f'_{m,t} = 9.6085 - 1.5821 \ln(h/t)$	0.927
	Quadratic	$f'_{m,t} = 0.03434(h/t)^2 - 0.3300(h/t) + 9.3705$	0.982
1:1:6	Linear	$f'_{m,t} = -0.3083(h/t) + 7.803$	0.906
	Power	$f'_{m,t} = 7.8677(h/t)^{-0.1350}$	0.959
	Exponential	$f'_{m,t} = 7.8546e^{-0.0449(h/t)}$	0.914
	Logarithmic	$f'_{m,t} = 7.8185 - 0.9313 \ln(h/t)$	0.968
	Quadratic	$f'_{m,t} = 0.0305(h/t)^2 - 0.8364(h/t) + 8.5417$	0.976
1:2:9	Linear	$f'_{m,t} = -0.2719(h/t) + 5.415$	0.864
	Power	$f'_{m,t} = 5.4868(h/t)^{-0.1780}$	0.939
	Exponential	$f'_{m,t} = 5.4731e^{-0.05905(h/t)}$	0.883
	Logarithmic	$f'_{m,t} = 5.4331 - 0.8249 \ln(h/t)$	0.932
	Quadratic	$f'_{m,t} = 0.06722(h/t)^2 - 0.71286(h/t) + 6.0322$	0.983

¹See footnote to Table VII.

For each mortar, the quadratic expression had the highest coefficient of determination. Figure 8 illustrates the quadratic curve equations plotted along with the average of test results for each mortar and slenderness ratio from Table VI.

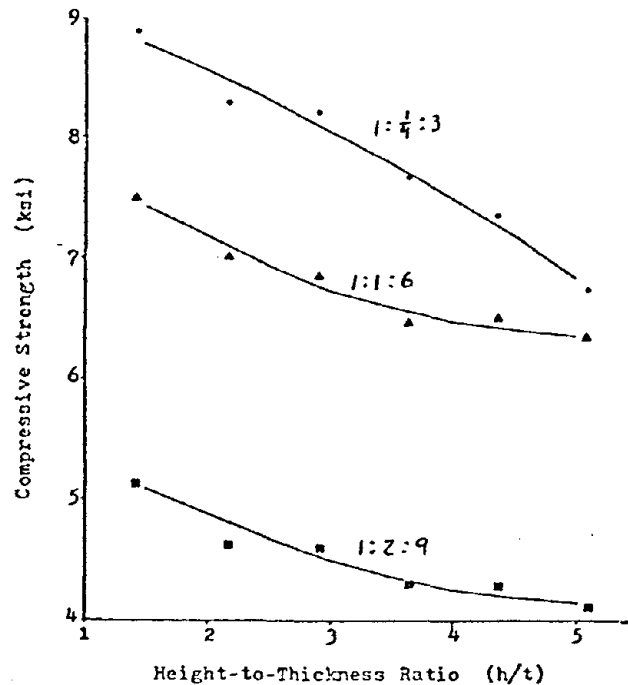


Figure 8. Quadratic Bivariate Equations, Unrestrained Interface Prisms

Additional analyses were performed which included two mortar parameters as well as h/t , i.e., the lime/water (L/W) ratio and the cement/water (C/W) ratio for the data of Test Series I and Test Series II for purposes of end restraint evaluation. A multivariate regression expression of the power form, i.e.,

$$f'_{mt} = A_0 \left(\frac{h}{t}\right) + A_1 \left(\frac{L}{W}\right)^{x_1} + A_2 \left(\frac{C}{W}\right)^{x_2} \quad (6)$$

proved in both cases to have the highest coefficient of determination.

The selection of L/W and C/W as parameters was the result of step-wise multiple regression methods which initially considered many parameters in addition to L/W and C/W. The parameters which were observed to have the strongest influence on f'_{mt} were those in Eq. (6) above.

Using both the bivariate expressions and the multivariate expressions, values of f'_{mt} were calculated at several values of h/t for both the case of the restrained interface and the case of the unrestrained interface. The effect of lateral restraint at the interface was evaluated by means of the following relationship:

$$\% \text{ restraint} = \frac{f'_{mt}(\text{restrained IF}) - f'_{mt}(\text{unrestrained IF})}{f'_{mt}(\text{restrained})} \quad (7)$$

The results are presented in Table IX.

It may be noted that for prisms built for a given mortar, the percent restraint, whether determined by bivariate or multivariate models was essentially the same for all values of h/t . Further, the effects of end restraint upon f'_{mt} are more pronounced for low-lime mortar than for higher-lime mortars.

Effects of Height on f'_{mt} . Present theory suggests that, for prisms tested with restrained interfaces, as prism slenderness increases, f'_{mt} will decrease towards a constant value as the influence of end restraint is progressively diminished (3,5,8,16,18), i.e., as most of the failure mode becomes lateral splitting.

Accepting this, one could conclude that if interface restraint were eliminated, then prisms of the same materials would fail at the same load regardless of slenderness (if general instability is not a factor). However, as observed in this study, prisms unrestrained (at least to the degree obtained in this study as presented in Table IX) at the test machine-prism interface do indeed reflect the influence of slenderness.

Table IX
Percent Constraint in Restrained Prisms

Restrained Prism Equation ¹	Unrestrained Prism Equation ¹	h/t	Percent Constraint							
			1.5	2.0	2.5	3.0	3.5	4.0	4.5	5.0
1:k:3 - Bivariate, Quadratic $f_{mz}^1 = -0.00539(\frac{h}{t})^2 - .3777(\frac{h}{t}) + 11.900$	1:k:3 - Bivariate, Quadratic $f_{mz}^1 = -0.03434(\frac{h}{t})^2 - 0.3300(\frac{h}{t}) + 9.371$	0.223	0.229	0.237	0.247	0.259	0.272	0.287	0.305	0.257
1:1:6 - Bivariate, Power $f_{mz}^1 = 8.802(\frac{h}{t}) - 0.1773$	1:1:6 - Bivariate, Quadratic $f_{mz}^1 = 0.0805(\frac{h}{t})^2 - 0.8364(\frac{h}{t}) + 8.542$	0.088	0.076	0.071	0.067	0.064	0.058	0.050	0.037	0.064
1:2:9 - Bivariate, Power $f_{mz}^1 = 6.375(\frac{h}{t}) - 0.2619$	1:2:9 - Bivariate, Quadratic $f_{mz}^1 = 0.06722(\frac{h}{t})^2 - 0.7128(\frac{h}{t}) + 6.032$	0.108	0.088	0.069	0.059	0.050	0.040	0.026	0.008	0.055
1:k:3 - Multiple Power $f_{mz}^1 = 37.997(\frac{h}{t}) - .1839(\frac{h}{t}) + 1.021(\frac{h}{t}) + 1.2878$	1:k:3 - Multiple Power $f_{mz}^1 = 93.858(\frac{h}{t}) - .1715(\frac{h}{t}) + 1.833(\frac{h}{t}) + 1.6194$	0.266	0.263	0.261	0.259	0.258	0.257	0.256	0.255	0.259
1:1:6 - Multiple Power $f_{mz}^1 = 37.997(\frac{h}{t}) - .1839(\frac{h}{t}) + 1.021(\frac{h}{t}) + 1.2878$	1:1:6 - Multiple Power $f_{mz}^1 = 93.858(\frac{h}{t}) - .1715(\frac{h}{t}) + 1.833(\frac{h}{t}) + 1.6194$	0.072	0.068	0.066	0.064	0.062	0.060	0.059	0.058	0.064
1:2:9 - Multiple Power $f_{mz}^1 = 37.997(\frac{h}{t}) - .1839(\frac{h}{t}) + 1.021(\frac{h}{t}) + 1.2878$	1:2:9 - Multiple Power $f_{mz}^1 = 93.858(\frac{h}{t}) - .1715(\frac{h}{t}) + 1.833(\frac{h}{t}) + 1.6194$	0.064	0.061	0.058	0.056	0.054	0.053	0.051	0.050	0.056

¹The expressions shown are those which produced the highest coefficient of determination (r^2) for the test results obtained in this study.

A popular explanation of lateral splitting failure (7, et al.) was reviewed, i.e., essentially that the lower poisson's ratio of mortar will induce lateral tension in the units as compressive load is applied to the prism. It had been noted that all prisms tested in this study with the unrestrained interface failed by lateral tensile splitting from top to bottom with no apparent general instability effects.

A hypothesis was formed that the total lateral force exerted by the mortar joints was directly related to the ultimate compressive load carried by a prism, and that total lateral force effects could be related to the relative volume of mortar in the prism as compared to the volume of the units.

Since all prisms tested in this study were built with 3/8 in. thick joints and all the units were the same size, the relative volume effects (hence total lateral force effects) may be measured in terms of number of joints and number of units. In those terms, the relative volume of a two-unit prism is 1/2, i.e., one joint/two units, that of a three-unit prism is 2/3, and so on. As prism height increases the relationship approaches one, i.e.,

$$\lim_{h \rightarrow \infty} \frac{\#J}{\#U} = 1 \quad (8)$$

in which: h = prism height

#J = number of joints

#U = number of units

and the total lateral force exerted by the mortar joints hypothetically approaches a constant value.

If the total lateral force is a direct influence affecting the ultimate prism compressive strength then the strength value attained by a given unrestrained interface prism may be "normalized" by a factor related to the total lateral force, i.e., the factor #J/#U. The normalized value would be f'_m - the constant value to which tall prisms tested with restrained interfaces appear to converge (5,8,11,16). This relationship may be expressed by:

$$f'_m = Kf'_{mt} \quad (9)$$

in which: f'_m = the basic ultimate compressive strength, i.e., the "constant" value.

f'_{mt} = the ultimate compressive strength of a given prism test or as predicted by experimentally developed relationships.

$$K = \#J/\#U, \text{ i.e., } \frac{\text{number of joints}}{\text{number of units}}$$

The experimentally determined bivariate equations which had the highest coefficient of determination for the case of unrestrained interface prisms were used to predict the failing stress, f'_{mt} , of prisms tested at h/t ratios corresponding to whole integer numbers of clay units from 2 to 7. The values obtained were then multiplied by the appropriate "K" value to obtain f'_m as defined by Eq. (9). The results are presented in Table X.

Note that for each set associated with a different mortar, the value of f'_m stabilizes for prisms of 4 or more units. The values for prisms of two and three units is less in each case; one could speculate that the capping used, having a total thickness of $\frac{1}{4}$ inch (1/8 in. each end), could have had the effect of another partial mortar layer thus reducing the f'_m value.

CONCLUSIONS

Since the test program was a modest one involving one type of solid clay unit, one brand of portland cement, one brand of Type S lime, and one type of sand, generalizations may not be made. However, the results and analyses revealed characteristics of a kind which, in the authors' opinion, have a strong likelihood of being found, in various degrees, for solid clay unit prisms of other constituents. These are summarized as follows:

1) For improved consistency, the flat-wise unit test standard possibly should be more specific with respect to preparation of the specimen. In the present study, unit compressive strengths were about 10% higher for symmetrical $\frac{1}{2}$ units cut from the center of the

Table X

Calculation of Constant-Value Prism Strength (f'_m)
for Unrestrained Interface Prisms

Equation ¹	No. of Units	K	h/t	$f'_m = Kxf'_{mt}$
1:¼:3 Mortar $f'_{mt} = -0.3434\left(\frac{h}{t}\right)^2 - 0.3300\left(\frac{h}{t}\right) + 9.371$	2	1/2	1.439	4.412
	3	2/3	2.175	5.662
	4	3/4	2.912	6.089
	5	4/5	3.649	6.167
	6	5/6	4.336	6.050
	7	6/7	5.123	5.810
	1:1:6 Mortar $f'_{mt} = 0.0805\left(\frac{h}{t}\right)^2 - 0.8364\left(\frac{h}{t}\right) + 8.542$	2	1/2	1.439
3		2/3	2.175	4.738
4		3/4	2.912	5.092
5		4/5	3.649	5.250
6		5/6	4.386	5.350
7		6/7	5.123	5.459
1:2:9 Mortar $f'_m = 0.06722\left(\frac{h}{t}\right)^2 - 0.71286\left(\frac{h}{t}\right) + 6.032$		2	1/2	1.439
	3	2/3	2.175	3.202
	4	3/4	2.912	3.395
	5	4/5	3.649	3.461
	6	5/6	4.386	3.498
	7	6/7	5.123	3.551

¹See Table VIII

f'_m and f'_{mt} are in kips/in²

unit than for unsymmetrical $\frac{1}{2}$ units prepared by cutting a unit through the center.

2) Prism test correction factors, found in most codes and standards, which are used to convert the test ultimate compressive stress, f'_{mt} , to design ultimate stress, f'_m , at a standard slenderness ratio may be quite inaccurate. Results of this study indicate that correction factors are mortar dependent, and that they are unconservative for a wide range of h/t values for factors based on a $h/t = 2$ standard and essentially all conservative for factors based on a $h/t = 5$ standard. Regression analyses indicated a very poor correlation between prism strength (restrained interface) and h/t if mortar type is not considered.

3) The use of thin plastic between thin layers of grease as an interface between a prism and the test platens reduced friction enough to permit a complete vertical splitting failure for prisms ranging from 2 units high to 7 units high.

4) For a given mortar, the percentage of lateral restraint of restrained prisms, for several values of h/t , as compared to interface unrestrained prisms was essentially constant.

5) The percentage restraint imposed upon interface restrained prisms increased with the strength of mortar used.

6) A constant or single value of design f'_m may be obtained from tests of prisms of 4 or more units and with unrestrained interfaces by modifying f'_{mt} , the test ultimate stress, by a factor based upon the relative volume of mortar and units in a given prism.

RECOMMENDATIONS

The results of the study reported herein suggest that the whole issue of prism testing to determine design f'_m needs to be evaluated. While the tests performed used only one type of clay unit, the results cause some concern over the validity of presently used "correction" factors.

Substantiating tests are needed, but indications are that some type of restraint-releasing interface material could be made a standard practice in prism testing in order to permit the constant value of f'_m to be determined.

ACKNOWLEDGEMENTS

The research was supported by a grant from the Colorado Masonry Institute and the Northern Colorado Masonry Guild and was monitored by Robert J. Helfrich, Technical Director, Colorado Masonry Institute. The authors are grateful to Dr. James Chinn for his valuable suggestions and to Rio Grande Supply, Lakewood Brick & Pipe, and Martin-Marietta Corp. for supplying the materials used.

APPENDIX I - REFERENCES

1. American National Standards Institute, "Building Code Requirements for Reinforced Masonry", ANSI A41.2, 1960 (R1970).
2. Baur, John C., Tension Bond and Compressive Strength of Small-Scale Masonry Specimens, M.S. Thesis, University of Colorado, Boulder, 1977.
3. Foster, P.K. and Bridgeman, D.O., "Prism Tests for the Design and Control of Brick Masonry", Technical Report No. 22, New Zealand Pottery and Ceramics Assoc. 1973, also Proceedings of the Inst. of Civil Engrs., London, March, 1973.
4. Frey, D., Effects of Constituent Proportions on Uniaxial Compressive Strength of 2-Inch Cube Specimens of Masonry Mortars, M.S. Thesis, University of Colorado, Boulder, 1975.
5. Francis, A.J., "The SAA Brickwork Code: The Research Background", Inst. Eng., Aust. Civil Eng. Trans. CE11, 1969.
6. Hanada, K.T., Effects of Height and End Lateral Restraints on Clay Unit Prisms, M.S. Thesis, University of Colorado, Boulder, 1977.
7. Hilsdorf, H.K., "Investigation into the Failure Mechanism of Brick Masonry Loaded in Axial Compression", Designing, Engineering and Constructing with Masonry Products, Gulf Publishing Co., Houston, 1969.
8. Krefield, W., "The Effects of Shape of Specimens on the Apparent Compressive Strength of Brick Masonry", Proc. ASTM, Vol. 38, Part I, 1938.
9. Lenczner, D., "Strength and Elastic Properties of the 9-In. Brickwork Cube", Trans. Br. Ceramic Soc., 63, 1966.
10. Mayes, R., Clough, R., A Literature Survey--Compressive, Tensile, Bond and Shear Strength of Masonry, Report No. EERC 75-15, College of Engineering, Univ. of California, Berkeley, 1975.
11. Monk, C.B., "Column Action of Clay Masonry Walls", Designing, Engineering, and Constructing with Masonry Products, Gulf Publishing Co., Houston, 1969.
12. National Building Code of Canada, Assoc. Committee on the National Bldg. Code, National Res. Council of Canada, Ottawa, 1975.
13. Nie, N., Hull, C., Jenkins, J., Steinbrenner, K. and Bent, D., Statistical Package for the Social Sciences, McGraw-Hill, 2nd Ed., 1975.

14. Plummer, H.C., Blume, J.A., Reinforced Brick Masonry and Lateral Load Design, Structural Clay Products Institute (now Brick Inst. of America), McLean, VA, 1953.
15. Sahlin, S., Structural Masonry, Prentice-Hall, New Jersey, 1971.
16. Sinha, B.P. and Hendry, A.W., "Further Tests on Model Brick Walls and Piers", Proc. Br. Ceramic Soc., 17, 1970.
17. Standard Association of Australia Brickwork Code, Standard Assoc. of Aus., Standards House, Sidney, N.S.W., 1974.
18. Structural Clay Products Institute, Recommended Practice for Engineered Brick Masonry, McLean, VA, 1969.
19. Structural Clay Products Research Foundation, "Compressive Flexural and Diagonal Tensile Testing of Small 4-Inch Brick Masonry Specimens", National Testing Program, Progress Report No. 1, Geneva, IL, 1964.
20. _____, "Compressive and Transverse Tests on Five-Inch Brick Walls", Research Report No. 8, Geneva, IL, 1965.
21. _____, "Compressive Transverse and Racking Strength Tests of Four-Inch Brick Walls", Research Report No. 9, Geneva, IL, 1965.
22. _____, "Compressive Transverse Tests on Eight-Inch Brick Walls", Research Report No. 10, Geneva, IL, 1966.
23. Scrivener, J.C., Williams, D., "Compressive Behavior of Masonry Prisms", Proc. 3rd Australian Conf. on the Mechanics of Structures and Materials, Auckland, New Zealand, 1971.
24. Uniform Building Code, ICBO, Whittier, California, 1976.
25. West, H.W.H., Everill, J.B., Beech, D.G., "The Testing of Bricks and Blocks for Load-Bearing Brickwork", Xth Int'l Ceramic Congress, The Congress, Stockholm, 1966.
26. West, H.W.H., Everill, J.B., Beech, D.G., "Development of a Standard Nine-Inch Cube Test for Brickwork", Trans. Br. Ceramic Soc., 65, 1966.
27. Yokel, F.Y., Mathey, R.G., Dijkers, R.D., "Strength of Masonry Walls under Compressive and Transverse Loads", Bldg. Sci. Series No. 34, U.S. Bureau of Stds, Washington, D.C., 1971.

APPENDIX II - NOTATION

- f'_m - the ultimate compressive strength of masonry used as a basis for design.
- f'_{mt} - the ultimate compressive strength of masonry prisms. f'_{mt} may be a predicted value or a measured value.
- h - prism height
- t - the least lateral dimension of a prism.
- L/W - lime to water ratio in mortar by weight.
- C/W - cement to water ratio in mortar by weight.
- #J - the number of mortar joints in a prism.
- #U - the number of units in a prism.
- K - #J/#U
- r^2 - coefficient of determination



THE INTERACTION OF MASONRY WALL PANELS AND A STEEL FRAME

By James Colville¹ and Richard Ramseur²

ABSTRACT: A series of tests of pre-fabricated brick masonry wall panels, constructed with a high-bond strength saran polymer mortar additive, and a single-story, single-bay steel frame, subjected to lateral racking forces were conducted in order to investigate the contribution of nonstructural cladding of curtain wall panels to the lateral load resistance of framed structures.

A total of nine load tests were performed and the major variables in the test program included the magnitude of lateral load and the number of connectors used to attach the wall panel to the frame.

The results indicated that a considerable amount of load transfer can exist and that between 30%-40% of the lateral load is transferred to the nonstructural wall panels.

¹Associate Professor of Civil Engineering, University of Maryland, College Park, Maryland 20742.

²Formerly Graduate Research Assistant, Department of Civil Engineering, University of Maryland, College Park, Maryland 20742.

THE INTERACTION OF MASONRY WALL
PANELS AND A STEEL FRAME

by

James Colville¹ and Richard Ramseur²

INTRODUCTION

This paper presents the results of an experimental study of the interaction of pre-fabricated brick masonry wall panels constructed with a high-bond strength saran polymer mortar additive and a single-story, single-bay steel frame, subjected to lateral racking forces. The brick panel is not an infill panel, but rather is located outside the plane of the frame and is attached to the frame by a series of special insert bolts and clip angles. The purpose of the study is to investigate the contribution of nonstructural cladding of curtain wall panels to the lateral load resistance of framed structures.

This contribution has been measured experimentally in a series of nine (9) load tests, using three separate wall panels and two different arrangements of connection bolts. Details of the test specimen along with pertinent test results and the significance of these results are given in the paper.

MATERIALS AND CONSTRUCTION

A typical single-story, single-bay test structure is shown in Figure 1. The same steel frame was used in all of the tests described below and three prefabricated brick wall panels were used in the test program. Each single wythe wall panel, laid in running bond, measured approximately 8'-4" square. Standard size Baltimore "Norvel" cored clay bricks, grade SW, in accordance with ASTM C62-69, "Standard Specifications for Building Brick (Solid Masonry Units Made From Clay or Shale)", were used throughout. The average compressive strength of the brick was 6800 psi with an average initial rate of absorption of 31 grams/minute/30 sq. inches as determined in accordance with ASTM C67-66, "Standard Methods of Sampling and Testing Brick".

The walls were constructed in the laboratory by experienced bricklayers and the work was considered to be of good quality workmanship. No special curing procedures were employed and the specimen were air-cured over a temperature range of approximately 60^o to 85^oF and a relative humidity of 65-75%.

The mortar mix utilized a high-bond liquid saran polymer called SARABOND (Dow Chemical Company Registered trademark) with Type I portland cement. A workability additive of pulverized ground limestone was used in the mix and the mortar was allowed to be retempered twice, as necessary, during construction of the wall panels. The following proportions were used in the

¹Associate Professor of Civil Engineering, University of Maryland, College Park, Maryland 20742.

²Formerly Graduate Research Assistant, Department of Civil Engineering, University of Maryland, College Park, Maryland, 20742.

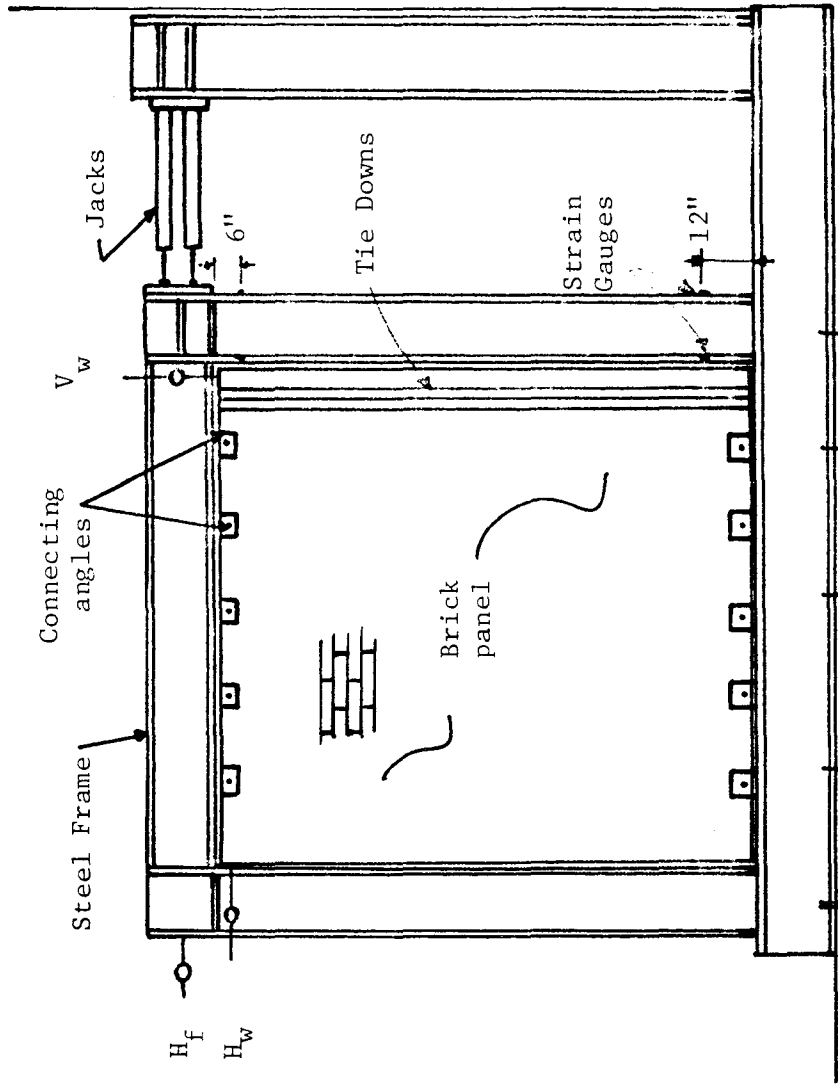


Figure 1 - Typical Test Structure

mortar mix:

Mason Sand	3¼ cu.ft.
Type I Portland Cement	1 bag (94 lbs)
Pulverized Limestone	1 bag (50 lbs)
SARABOND	4 gallons
Water ~ as required for workability to a maximum of 4 gallons.	

The results of tests at 35 days of 2 inch mortar cubes are given below in Table 1.

Table 1 Mortar Cube Strengths

No. of Specimen Tested	Average Comp. Strength in psi	Remarks
3	8940	Air cured, mortar retempered twice
6	6010	Moist cured, mortar retempered twice
3	12210	Air cured, mortar not retempered
6	8520	Moist cured, mortar not retempered

From Table 1, it is apparent that higher compressive strengths were obtained when air curing rather than moist curing was used. Also, retempering significantly reduced the mortar cube compression strength. Nevertheless, since the air cured specimen exhibited significantly higher strength than the brick strength, it was concluded that retempering would have no detrimental effect on the wall panel compressive strengths.

Fifteen (15) seven brick high flexural prisms were tested in accordance with ASTM C78, "Standard Method of Test for Flexural Strength of Concrete (Using Simple Beam with Third Point Loading)" as recommended by the Dow Chemical Company. The results of these tests were used to evaluate an approximate ultimate tensile strength of the high-bond mortar brick construction. While a considerable variation in the modulus of rupture, f_t , values was obtained in these tests, the average results indicated $f_t = 400$ psi for untempered mortar, and $f_t = 265$ psi for retempered mortar.

During construction of the walls, five (5) brick each in the second course from the bottom and the next to last top course were cut with a water-cooled diamond tipped masonry saw to accommodate placement of specially bent, 7/16" diameter, A36 steel insert bolts for attachment of the panels to the steel frame. The slots in a brick were ½" by 2¼", from one head joint end of the brick to one of the core holes. The specially bent bolt was then positioned in the slotted brick so that the threaded end projected from the panel at the intersection of a head and bed joint. Figure 2 shows the orientation of the connecting bolt in the slotted connector brick, along with details of the bolt shape. Slotted connector angles (½" thick) were welded to the steel frame at appropriate locations to accommodate the threaded ends of the connecting bolts which protruded from the prefabricated wall panels. A detail of this connection is shown in Figure 3.

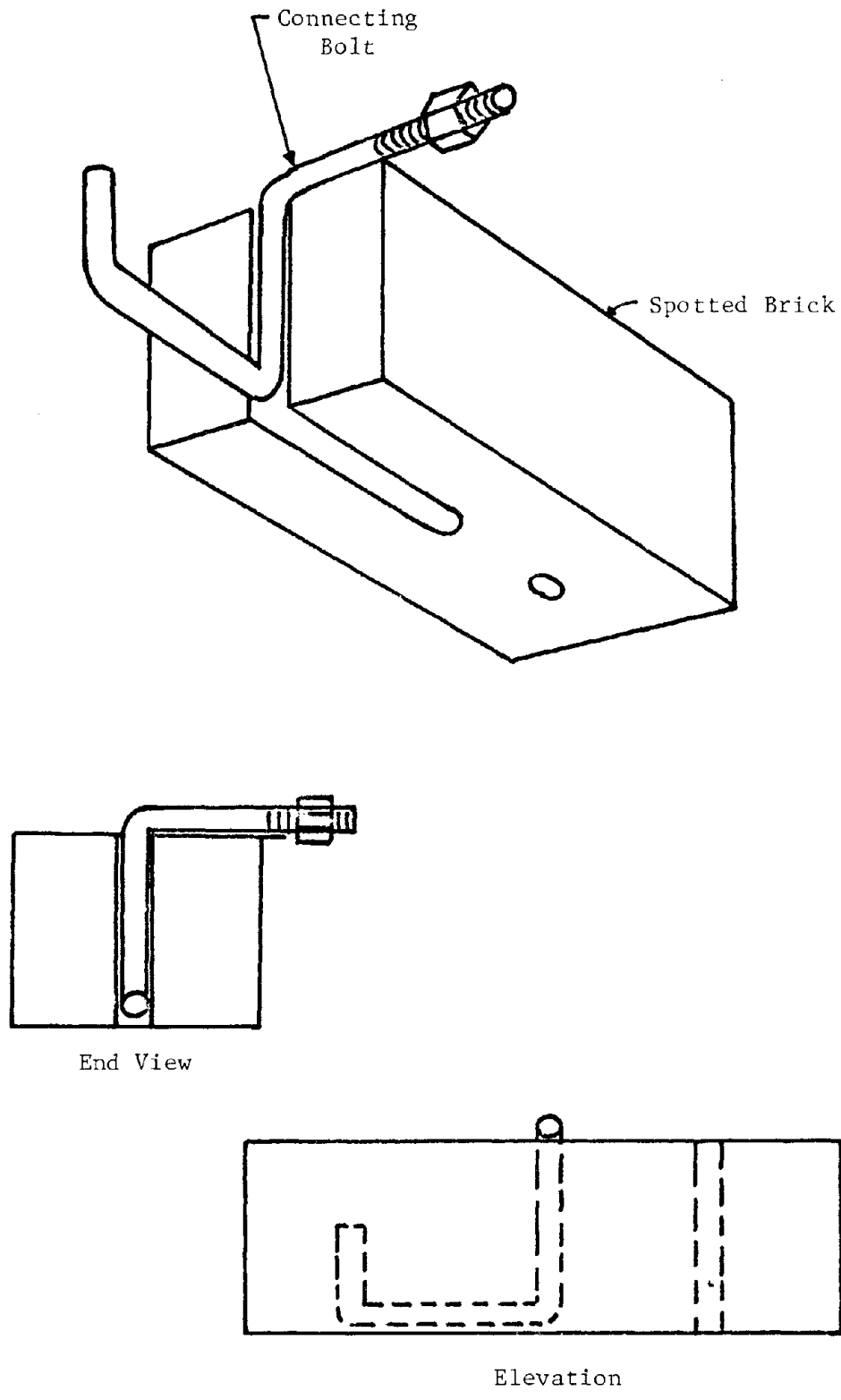


Figure 2 Details of Connecting Bolts

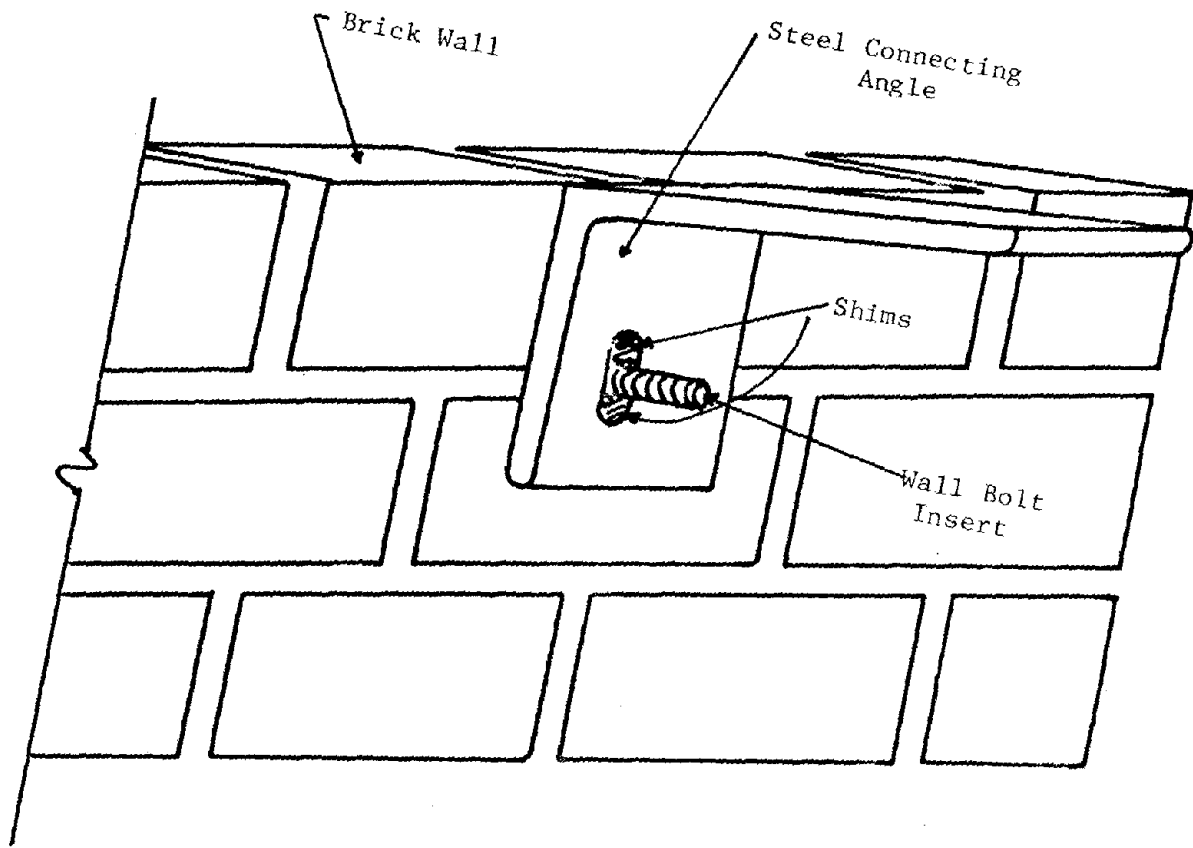


Figure 3 - Detail of Wall-Frame Connection

INSTRUMENTATION

Application of the horizontal load to the top of the steel frame was monitored by two strain indicator load cells, one for each of two jacks arranged in tandem to provide monotonically increasing loads. Horizontal displacements at the top of the frame, H_f , and the wall, H_w , were taken at the far end of the structure away from the point of load application. Vertical wall deflections, V_w , were recorded at the loaded end of the structure. All deflection measurements were made with 0.001 ins Ames dial gages.

Steel strains were recorded using SR-4 electrical resistance strain gages, and wall strains were measured with a hand-held mechanical Whittemore strain gage.

The locations of these strain gages and the displacement gages are indicated on Fig. 1.

TEST SEQUENCE

A total of nine (9) full scale load tests were conducted as described in Table 2. The major variables in the test programs included: magnitude of lateral load; number of connectors used to attach the wall panel to the frame; and the use of a tension tie-rod located near the loaded end of the assembly in order to minimize wall rotation (Fig. 1).

EXPERIMENTAL RESULTS

The most significant data recorded during the tests were the horizontal displacements of the wall and frame, and the vertical displacement of the wall adjacent to the point of application of the horizontal load.

Strain readings in the wall were not successfully recorded, due to the small magnitudes of these strains, and are, therefore, not included herein.

In the series of tests using wall panel 1, with 5 connectors top and bottom (Test 2), a considerable amount of wall rotation was observed due to the clearance in the vertically slotted holes in the connecting angles. Thus small shims were cut and wedged in place to minimize the possibility of slippage at the wall-frame connection. These shims were used in all subsequent tests.

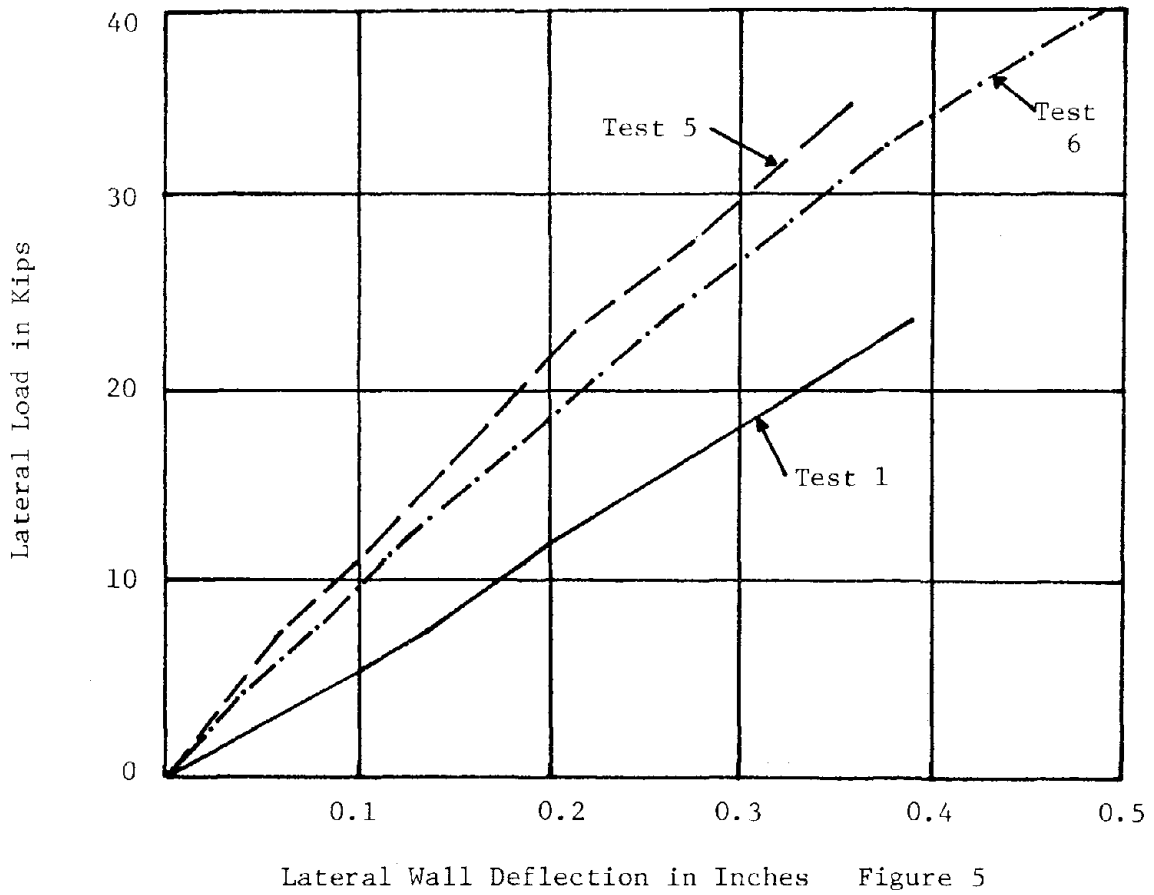
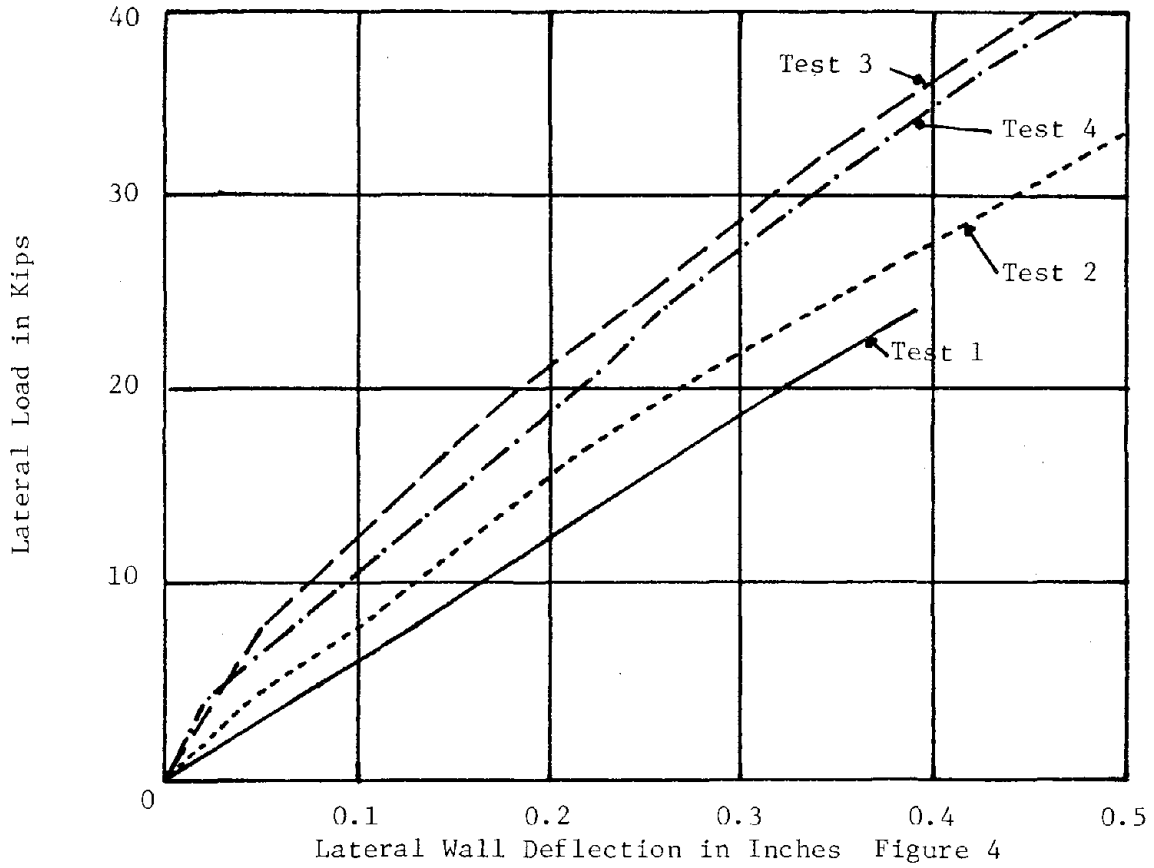
The maximum lateral load applied using wall panel 1 was 40 kips and the relationship between the frame horizontal deflection, H_f , and the lateral load, P , is given in Fig. 4 for Tests 1, 2, 3 and 4.

Tests 5 and 6 were conducted using wall panel 2 in order to provide a second set of data showing the influence of the number of connectors on the horizontal deflection of the frame. Relationships between H_f and P for these tests are compared to data obtained for the frame acting alone (Test 1) in Fig. 5.

Tests 7, 8 and 9 used the third wall panel and in each test, 5 connector bolts were used top and bottom. However, in an attempt to further investigate the significance of vertical slip in the slotted connection between

TABLE 2 DESCRIPTION OF TESTS

Test No.	Wall Panel No.	No. of Connectors	Max. Load (Kips)	Remarks
1	Frame Only		24 80	
2	1	5	40	No shims
3	1	5	40	Shims
4	1	3	40	Shims
5	2	5	36	Shims
6	2	3	40	Shims
7	3	5	80	Tie-down bolted
8	3	5	80	No tie-down
9	3	5	80	Welded tie-down



the wall panels and the frame, the nuts on the bolts protruding from the wall panels were welded to the angle attached to the frame. In addition, angle tie downs were installed adjacent to the loaded edge of the panel, in Test 7 and 9. The tie-down was bolted to a cross plate extending over the top of the wall in Test 7, and welded to a similar cross plate in Test 9. Relations between H_f and 8 for these tests are given in Fig. 6 along with corresponding results from Test 1.

The ratio between the vertical deflection of the wall panel, V_w , and the horizontal panel displacement, H_w , is given for all tests in Table 3.

DISCUSSION OF RESULTS

From the results given in Table 3, the average ratio of V_w/H_w for Test 2 was about 0.85, indicating a significant lifting of the wall near the loaded edge. This ratio decreased to an average of about 0.76 in Tests 3 and 4 due to the use of the shims described above. For wall panel 2, the average ratio of V_w/H_w was about 0.61. Thus although the shims did reduce the lifting of the panel there was still a significant amount of vertical displacement in comparison to the horizontal displacement.

Ratios of V_w/H_w for Tests 7 and 8 are essentially identical indicating that the bolted tie-down was not effective in reducing V_w . However, welding the nuts of the connecting bolts to the clip angles reduced the ratio of V_w/H_w to around 0.5 in Tests 7 and 8.

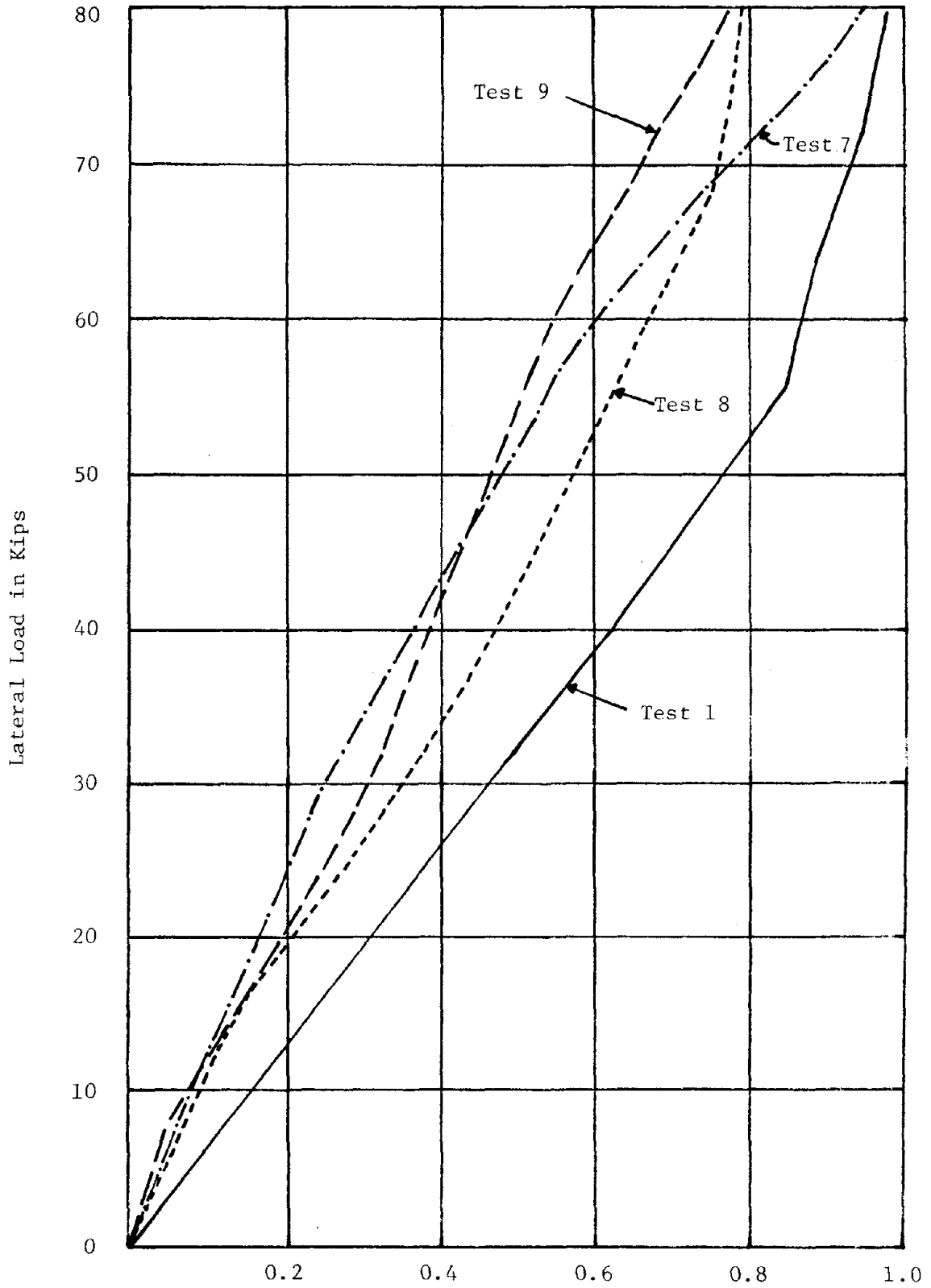
A significant reduction in V_w occurred in Test 9, where the tie-down was welded in place.

From a linear regression analysis of the deflection results given in Figs. 4, 5 and 6, the approximate linear stiffness values given in Table 4 were obtained for each of the nine tests.

TABLE 4 LINEAR STIFFNESS VALUES

Test No.	Stiffness Kips/Incl.	Percent Increase In Stiffness	Percent Load Carried by the Wall Panel
1	63.9	0.0	0.0
2	71.6	12.1	10.7
3	98.6	54.3	35.2
4	90.9	42.3	29.7
5	104.5	63.5	38.9
6	89.1	39.4	28.3
7	109.5*	71.4	41.6
8	94.1*	47.3	32.1
9	104.5*	63.5	38.9

*Values obtained for loads up to 56 kips.



Lateral Wall Deflection in Inches
Figure 6 - Load-Deflection Behavior

TABLE 3 RATIO OF H_v/H_w

Load in Kips	Wall Panel 1			Wall Panel 2		Wall Panel 3		
	Test 2	Test 3	Test 4	Test 5	Test 6	Test 7	Test 8	Test 9
4	.86	.87	.83	.63	.53	.45		
8	.89	.67	.74	.63	.56	.44	.32	.18
12	.87	.70	.78	.63	.60	.43		
16	.86	.71	.78	.62	.61	.41	.36	.15
20	.87	.73	.78	.61	.61	.41		
24		.73	.76	.61	.62	.43	.38	.13
28		.74	.76	.62	.62	.45		.13
32		.76	.77	.62	.63	.46	.41	.14
36		.76	.77	.62	.63	.48	.44	.15
40	.72	.76	.78		.64	.49	.46	.15
48						.51	.49	.16
56						.52	.50	.17
64						.52	.52	.17
72						.53	.54	.17
80						.54	.54	.16

As a result of the information presented in Table 4, the following observations are presented:

- 1) With the exception of Test 2, all results obtained using 5 connecting bolts (Test 3,5,7,8,9) give reasonably consistent values of the lateral stiffness of the composite structure.
- 2) With 5 connecting bolts installed along both the top and bottom edge of the wall, the average load carried by the wall is approximately equal to $3/8$ of the total load applied.
- 3) Results from Test 4 and 6 are in excellent agreement, and indicate that with 3 connecting bolts, about $3/10$ of the total load is transmitted to the wall.
- 4) Although the shims and tie-downs reduced the panel vertical displacements, they did not significantly affect the lateral load resistance of the wall-frame assembly.

SUMMARY

The results of an experimental study on the interaction of prefabricated brick masonry wall panels and a steel frame are presented. These results indicate that a considerable amount of load transfer can exist between these elements at service loads and that between 30%-40% of the lateral load is transferred to the nonstructural wall elements.

Of course, in practice the actual interaction between structural components is greatly affected by the rigidity of the interconnection between elements. However, it is significant that substantial load sharing was exhibited in the test described, herein, using relatively flexible bolted connections.

The implications of these results are of particular importance for existing and/or new construction requiring consideration of seismic loads in design, since in these cases it is necessary for proper design that the contribution of all parts of the structure to lateral load resistance be considered.

THE EFFECT OF JOINT REINFORCEMENT ON VERTICAL LOAD CARRYING CAPACITY
OF HOLLOW CONCRETE BLOCK MASONRY

By Hatzinikolas, M., Longworth, J., and Warwaruk, J.

ABSTRACT: The effectiveness of wire joint reinforcement in load bearing masonry is experimentally evaluated. Tests on prisms and full scale walls were conducted under axial and eccentric loads. #9 gauge, truss type wire reinforcement was used as joint reinforcement. It was used in two forms: as supplied (normal) and flattened to 60% of the original diameter.

All reinforced specimens failed at lower loads than the plain specimens. Those reinforced with normal reinforcement exhibited lower failure loads than those with flattened reinforcement. The reduction in capacity is attributed to stress concentrations produced by the joint reinforcement.

THE EFFECT OF JOINT REINFORCEMENT
ON VERTICAL LOAD CARRYING CAPACITY
OF HOLLOW CONCRETE BLOCK MASONRY

By M. Hatzinikolas¹, J. Longworth², and J. Warwaruk³

Most building codes specify a certain minimum amount of reinforcement to be placed in the horizontal joints of reinforced masonry walls. The Canadian Code⁽¹⁾ in article 4.6.8.1.1, specifies that reinforced masonry load-bearing and shear walls shall be reinforced horizontally and vertically with steel having a minimum area calculated in conformance with the following requirements:

$$A_v = 0.002 A_g \alpha \quad [1]$$

$$A_h = 0.002 A_g (1 - \alpha) \quad [2]$$

where A_v = area of vertical steel per unit of length of wall
 A_h = area of horizontal steel per unit length of wall
 A_g = gross section area per unit length of wall
 α = reinforcement distribution factor varying from 0.33 to 0.67 as determined by the designer.

The purpose of the horizontal reinforcement is to provide a certain amount of two way action for resisting lateral loads. Theoretically, there is no reason to expect that joint reinforcement will increase the load bearing capacity of concrete masonry walls, especially with the construction procedures commonly used in Canada. The actual effect on vertical load capacity is not well defined.

As a result of the substantial difference in the elastic properties of steel and mortar it can be assumed that the stress distribution in the mortar joint will be similar to the one for a plate with a rigid inclusion. Figure 1 shows the shape of the stress in a uniformly loaded reinforced mortar joint. This stress distribution has a peak of at least 1.56 W, where W is the uniformly distributed load acting on the joint. This distribution is based on the assumption that the steel is infinitely stiffer than the mortar. This is a realistic assumption considering that the ratio of modulus of elasticity of steel to that of mortar is of the order of 40. In reality the

¹ Graduate Student, The University of Alberta, Edmonton, Canada T6G 2G7

² Professor of Civil Engineering, University of Alberta, Edmonton, Canada T6G 2G7

³ Professor of Civil Engineering, University of Alberta, Edmonton, Canada T6G 2G7

stress distribution is more complex because of the presence of confinement stresses and inelastic action. Exact analytical evaluation of the stress distribution in anisotropic plates is complex and beyond the scope of this paper. Reference (1) gives a complete detailed account of stress patterns created in anisotropic plates under various loading conditions.

The purpose of this investigation is to experimentally examine the effect of joint reinforcement and its shape on the load carrying capacity of hollow concrete block masonry.

SPECIMEN MANUFACTURE

Walls and prisms were constructed of 8x8x16 in. (nominal) concrete blocks. The blocks were manufactured locally using 4 parts of light weight aggregate mixed to 1 part sand. The mean compressive strength of the block was 2350 psi. Type S mortar, proportioned by volume, was used. The mortar was mixed in an electrically driven mixer and the workability adjusted to the blocklayers requirements. The average water cement ratio of the mortar (w/c) was 1.2. The mean strength of 50 - 2x2x2" mortar cubes tested was 2500 psi. The horizontal joint reinforcement was #9 gauge truss type wire as shown in Figure 2. This reinforcement was used either as supplied or in a flattened form. The wire was flattened to 60% of its original diameter by passing it through a set of rollers. The diameter of the wire was reduced by about 40% in this process. Walls and prisms were constructed by a skilled blocklayer and were cured in laboratory environment at 72° F temperature and 42% relative humidity.

A total of 30 two-block prisms, as shown in Figure 3, were built. Twenty prisms had no joint reinforcement. Ten of these unreinforced prisms were fully bedded in mortar. All other prisms were constructed with face shell mortar bedding. Five of the prisms had "normal" truss-type joint reinforcement and five had "flattened" reinforcement.

A total of 30 short walls, as shown schematically in Figure 4, were constructed in running bond (blocks overlapping by 50%). Ten walls were plain and seven were horizontally reinforced at every second course, five with normal and two with flattened reinforcement.

In addition to the prisms and short walls, twelve full scale walls, 16 blocks high and 2 1/2 blocks wide, were built in running bond. Six were plain and six had normal #9 gauge wire joint reinforcement.

All specimens were tested at an age of at least 28 days.

TEST METHODS

All two-block prisms were tested in axial compression in a 1.6 million lb. hydraulic testing machine, with flat-end conditions. 1/4-inch plates were placed at the ends, and even bearing was achieved by capping the specimen with high strength plaster of Paris. The walls were tested with pin-ended conditions using a roller and channel arrangement shown in Plate 1. To avoid local failure in walls tested with eccentric loads, the top and bottom courses were fully grouted. The full scale walls were tested in double curvature using the same arrangement as shown in Plate 1.

TEST RESULTS

a) Prisms

Failure loads and resulting stresses for the axially loaded two block prisms are given in Table 1. Average stresses for each group of similar specimens are also listed.

The average failure stresses were 2090 psi for the fully bedded prisms, 2009 psi for the face shell bedded, 1895 psi for the prisms with flattened joint reinforcement and 1642 psi for those with normal #9 gauge wire joint reinforcement.

b) Short Walls

Table 2 summarizes the test results for axially loaded short walls and Table 3 summarizes results for eccentrically loaded walls.

The average failure stress for the axially loaded specimens was 2323 psi for the plain, 2129 psi for those with flattened joint reinforcement and 1856 psi for those with normal joint reinforcement.

c) Full Scale Walls

The results of tests on wall specimens subjected to double curvature are shown in Table 4. The stress at failure is calculated using linear stress distribution and the mortar bedded area. P- Δ effects are neglected in the stress computations. The average stress at failure for plain walls was 3662 psi and for walls containing joint reinforcement was 3215 psi.

DISCUSSION OF TEST RESULTS

a) Prisms

The average failure stresses for prisms with normal joint reinforcement was 18% lower than for plain prisms. For prisms with flattened joint reinforcement the reduction was 8%. The results for fully bedded prisms indicate that the load capacity is influenced directly by the area of block covered by mortar. Failure for fully bedded specimens occurred at an average stress of 2090 psi as compared to 2009 psi for prisms with face shell mortar. The average failure load was in the order of 35.5% higher for the fully bedded prisms.

Failures were caused by splitting of the block at the cross webs for plain specimens and splitting at the flanges for the reinforced ones. These types of failures are illustrated in Plate 2.

b) Short Walls

Axially loaded short walls failed in a similar manner to prisms. Failure modes are illustrated in Plate 3. Short walls with normal joint reinforcement failed at average stresses 20% less than plain ones, and specimens with flattened joint reinforcement at 8% less than plain specimens. Fully bedded specimens carried only 10% additional load than specimens with face shell mortar. Eccentrically loaded short wall specimens with normal joint reinforcement failed at an average stress 22% less than the plain specimens.

c) Full Scale Walls

The average stress at failure for full scale walls with normal joint reinforcing tested under axial and eccentric loads was 12% less than for the plain walls. However, for eccentricities larger than 3.0 inches there was no effect due to the presence of the joint reinforcement. If the results from tests with a 3.5" eccentricity are excluded, the average failure stress for walls with joint reinforcement was 16% less than plain walls.

The results indicate that the presence of joint reinforcement reduces the load carrying capacity of hollow concrete block masonry. It was observed that the mortar joint at failure, for prisms with joint reinforcement was completely crushed, whereas in the case of plain specimens, a ring of hard mortar remained on both blocks. Plate 4 shows this ring of hard mortar at the middle of the flanges and webs of a block after failure. This observation further strengthens the assumption of premature mortar failure at the location of the joint reinforcement.

CONCLUSIONS

On the basis of experimental evidence it is concluded that:

1. Joint reinforcement reduced the ultimate load bearing capacity of masonry walls as a result of a stress concentration created by the presence of the reinforcement.
2. The reduction in strength was less in the case of flattened reinforcement.

ACKNOWLEDGEMENTS

This study was performed in the Department of Civil Engineering at the University of Alberta. Financial assistance from the Canadian Masonry Institute, the Alberta Masonry Institute and the National Research Council of Canada is acknowledged.

REFERENCES

1. CSA Standard S304-M, Masonry Design and Construction, Canadian Standards Association, Rexdale, Ontario, Canada.
2. Lekhnitskii, S.G., "Anisotropic Plates", translated for the second edition by Tsai, S.W. and Cheron, T. Gordon and Breach Science Publishers, New York, London, Paris.
3. Mayes, R.L. and Clough, R.W., A Literature Survey, Compressive, Tensile, Bond and Shear Strength of Masonry, U.S. Department of Commerce, National Technical Information Service, P.B.-246-296.
4. Supplement No. 4 to the National Building Code of Canada, 1975. Issued by the Associate Committee on the National Building Code, National Research Council of Canada, Ottawa.

TABLE 1 - Results From Axially Loaded
Two Block Prisms

Prism	Mortar bedded Area in. ²	Joint Reinforc.	Load at Failure kips	Stress at Failure Based on Mortar Bedded Area	Stress based on Gross Area of psi in. ²
* 1	58.3	Plain	132.4	2271	1111
2	"		117.5	2015	986
3	"		112.9	1936	947
4	"		150.1	2574	1259
5	"		106.6	1828	894
6	"		127.9	2193	1073
7	"		129.8	2226	1089
8	"		136.0	2332	1141
9	"		90.0	1543	755
10	"		115.7	1984	971
		Average	121.9	2090	1023
11	39.1	Plain	75.7	1936	635
12	"		100.0	2557	839
13	"		68.9	1762	578
14	"		78.8	2015	661
15	"		94.3	2411	791
16	"		90.0	2301	755
17	"		60.0	1534	503
18	"		65.5	1675	549
19	"		87.5	2237	734
20	"		65.0	1662	545
		Average	78.57	2009	659
21	"	Flattened #9 Gauge Wire	90.0	2301	841
22	"		98.5	2519	826
23	"		60.4	1544	506
24	"		60.6	1549	508
25	"		50.8	1299	426
		Average	72.06	1842	621
26	"	#9 Gauge Wire	60.5	1547	507
27	"		45.8	1171	384
28	"		55.2	1411	463
29	"		60.1	1537	504
30	"		70.0	2790	841
		Average	58.32	1646	540

* Specimens 1 to 10 were fully bedded.

** For specimens 11 to 30 mortar was placed at the face shells only.

TABLE 2 - Results of Tests on Short Walls
Axially Loaded

Specimen	Mortar Bedded Area in. ²	Joint Reinforc.	Load at Failure kips	Stress at Failure Based on Mortar Bedded Area psi	Stress Based on Gross Area psi
* 1	152.5	plain	257.4	1687	553
2	152.5	plain	260.0	1704	558
Avg.			258.7	1696	555
** 3	100	plain	215.5	2155	706
4	100	plain	249.1	2491	816
Avg.			232.3	2323	761
5	100	Flattened	234.8	2348	769
6	100	#9 Gauge Wire	191.1	1911	626
Avg.			212.9	2129	698
7	100	#9 Gauge	200.0	2000	655
8	100	Wire	171.2	1712	561
Avg.			185.6	1856	608

* Specimens 1 and 2 were fully bedded in mortar.

** For Specimens 3 to 8 mortar was placed only at the face shell.

TABLE 3 - Results From Eccentrically Loaded
Short Wall Specimens

Specimen	Mortar Bedded Area in. ²	Joint Reinforc.	Eccen- tricity in.	Load at Failure kips	Moment at Failure k-in	Stress at Failure Based on Mortared Area (psi)
1	100	plain	t/6=1.27"	196.9	250.0	3537
2	"	"	t/6=1.27"	150.1	190.6	2696
3	"	"	t/3=2.54"	119.3	303.0	3094
4	"	"	t/3=2.54"	158.7	403.0	4115
Avg.						3360
5	"	#9 Gauge	t/6=1.27"	160.0	203.2	2875
6	"	Wire	t/6=1.27"	149.1	189.35	2679
7	"	"	t/3=2.54"	92.75	235.5	2405
8	"	"	t/3=2.54"	105.5	264.9	2717
9	"	"	t/3=2.54"	92.75	235.5	2405
Avg.						2616

TABLE 4 - Loading Conditions and Test Results
From Full-Scale Wall Segments

Wall	Joint Reinforc.	h/t	Eccentricity of top in.	Eccentricity at bottom in.	Failure Load kips	Maximum Stress at Failure Based on Mortared Area psi
D1	plain	19.97	0.00	0.00	218.3	2183
N1	"	"	+1.27	-1.27	191.3	3511
N2	"	"	+2.54	-2.54	158.6	4236
N3	"	"	+3.00	-3.00	154.9	4606
N4	"	"	+3.50	-3.50	123.3	4072
N5	"	"	+1.27	0.00	183.5	3368
Avg.						3662
F1	#9 Gauge	"	0.00	0.00	160.0	1600
F2	Wire	"	+1.27	-1.27	160.0	2936
F3	"	"	+2.54	-2.54	144.6	3862
F4	"	"	+3.00	-3.00	124.6	3705
F5	"	"	+3.50	-3.50	128.8	4253
G1	"	"	+1.27	0.00	160.0	2936
Avg.						3215

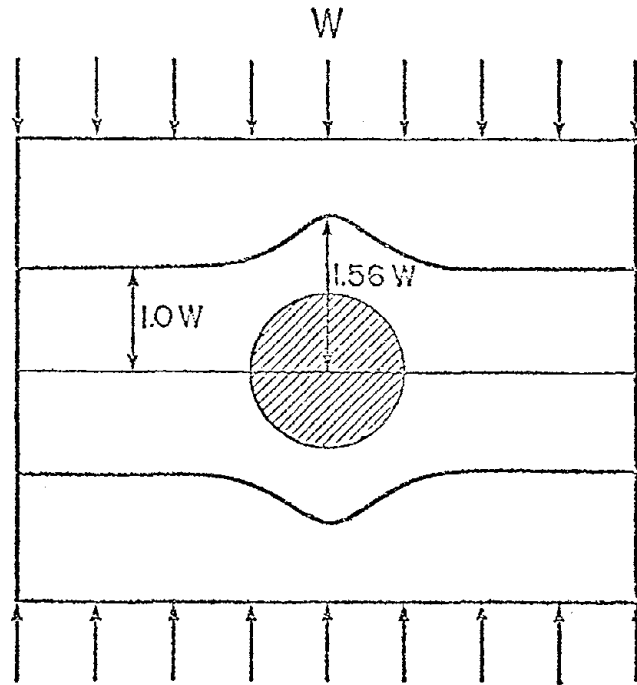


FIGURE 1 - Stress Distribution in a Plate With Rigid Inclusion

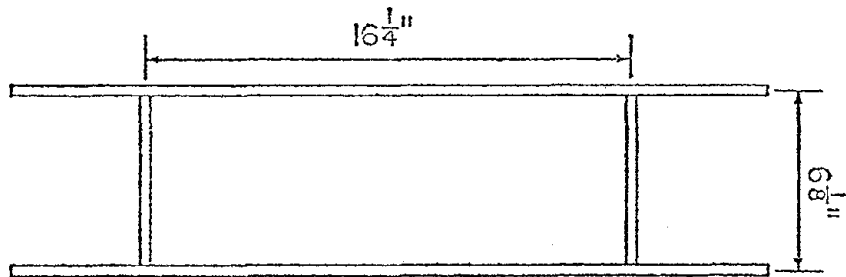


FIGURE 2 - #9 Gauge Wire Joint Reinforcement

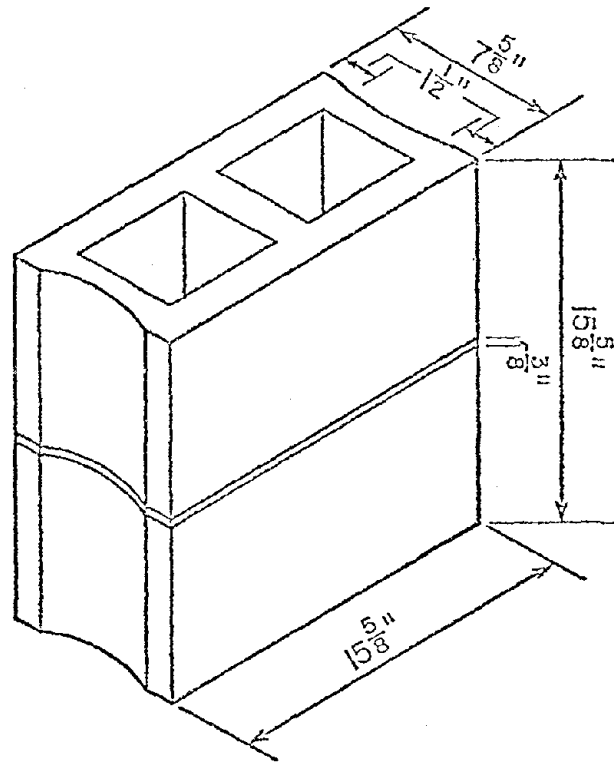


FIGURE 3 - Two Block Prism

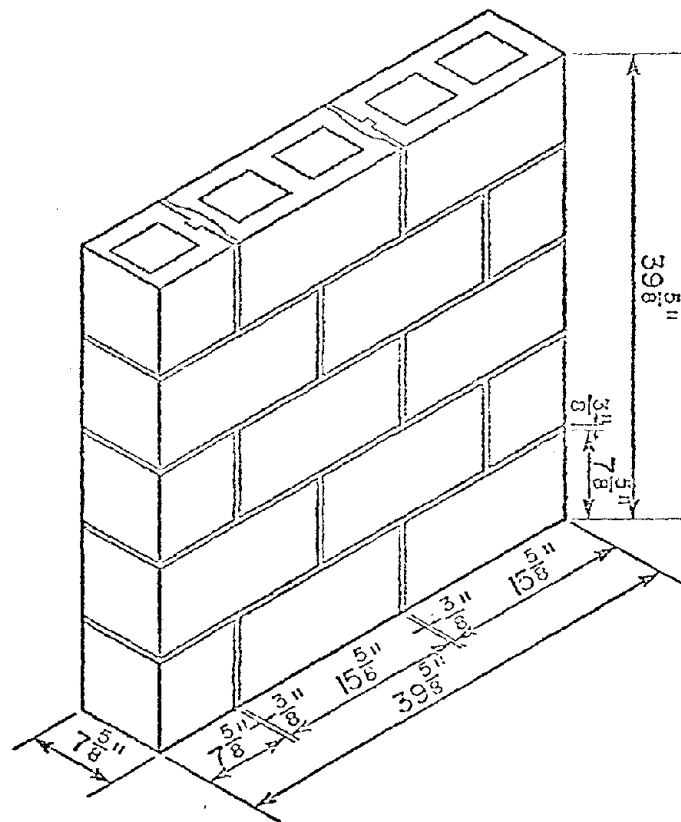


FIGURE 4 - Short Wall Specimen

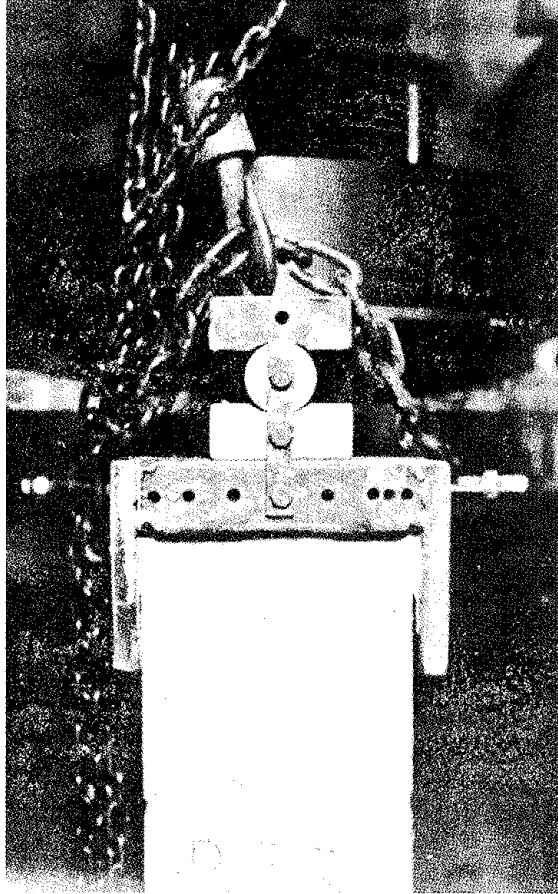


PLATE 1 - Loading Arrangement for Prism and Walls
Tested With Pin-Ended Conditions

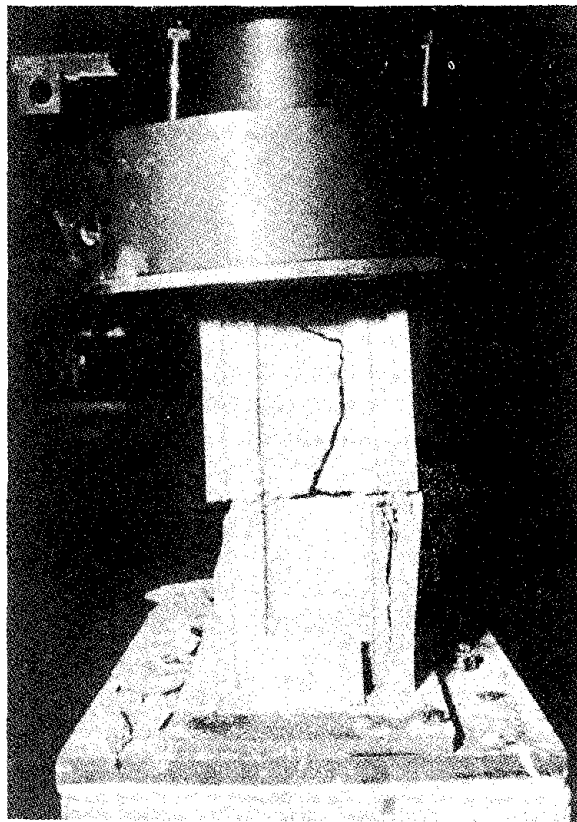
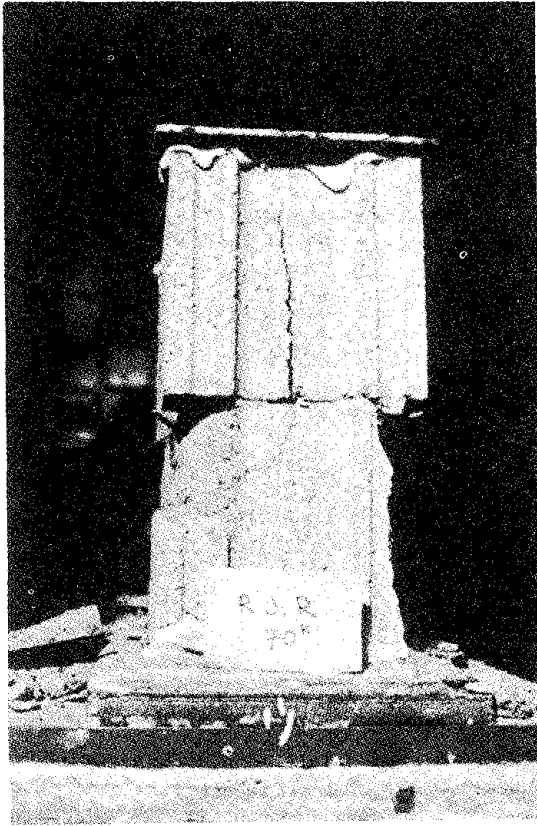


PLATE 2 - Typical Failures of Prisms With No. 9
Gauge Wire Joint Reinforcement

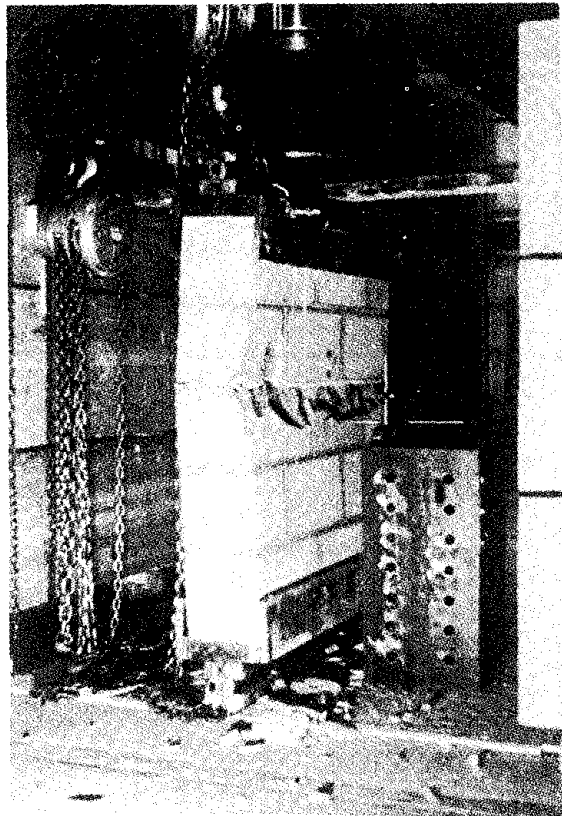
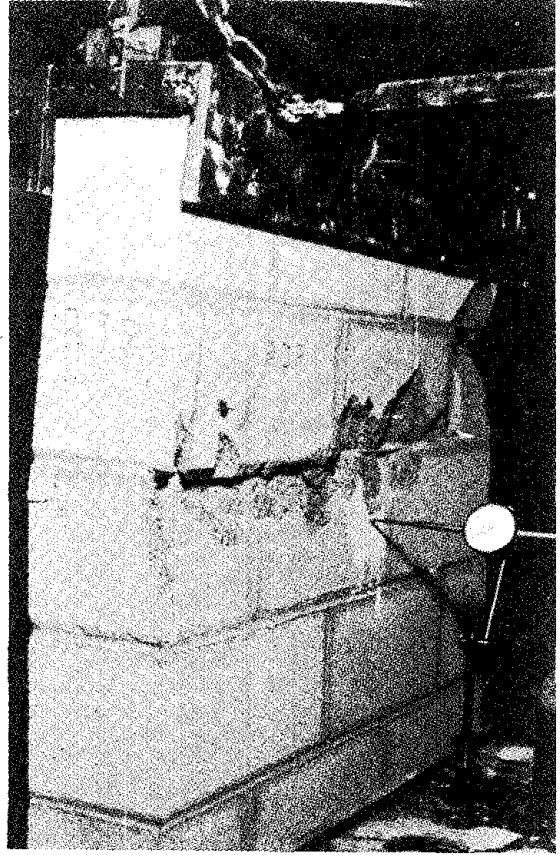
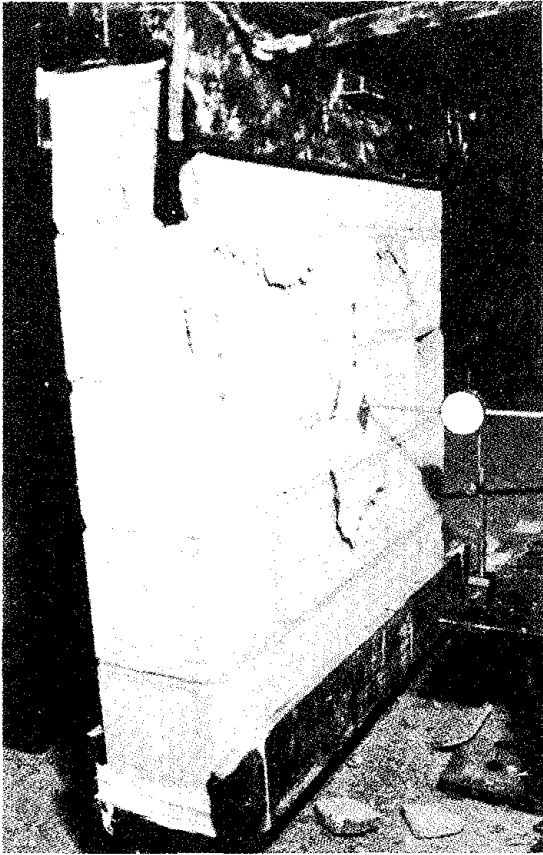


PLATE 3 - Short Wall Specimens With and Without Joint Reinforcement After Failure

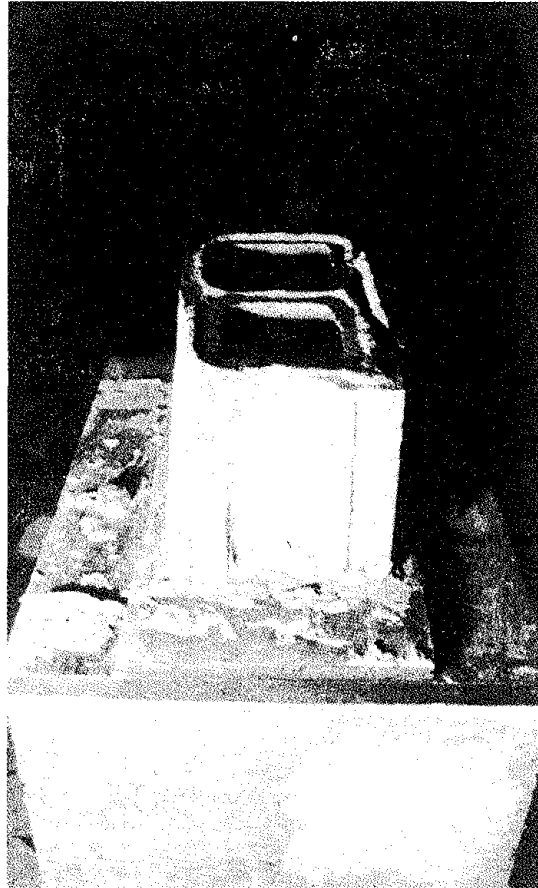


PLATE 4 - Ring of Hard Mortar on Fully
Bedded Prism After Failure

THE INFLUENCE OF
FLAWS, COMPACTION, AND ADMIXTURE
ON THE STRENGTH AND ELASTIC MODULI OF CONCRETE MASONRY¹

by

M. E. Miller², G. A. Hegemier², and R. O. Nunn²

ABSTRACT

This paper reports the results of tests conducted to determine the effects of admixed grout and vibration compaction on the strengths and elastic moduli of unreinforced concrete masonry under field and controlled slump conditions. Four specimen groups consisting of two grout types, standard and admixed; and two compaction types, puddled and vibrated, were fabricated and over ninety tests performed. Flaws in the form of grout bridges are shown to seriously degrade uniaxial strengths and elastic moduli based on prediction of assemblage properties from component data. Use of admixture and vibration under field conditions is discussed and recommendations are made based on test results.

¹ Research was sponsored by the National Science Foundation under Grant NSF ENV 74-14818.

² Associate Development Engineer, Professor, and Research Assistant, respectively; Department of Applied Mechanics and Engineering Sciences, University of California, San Diego; La Jolla, California 92093.

THE INFLUENCE OF
FLAWS, COMPACTION, AND ADMIXTURE
ON THE STRENGTH AND ELASTIC MODULI OF CONCRETE MASONRY¹

by

M. E. Miller², G. A. Hegemier², and R. O. Nunn²

INTRODUCTION

Flaws in concrete masonry adversely affect the strength and elastic moduli of an assemblage and render prediction of assemblage properties based on component data difficult and perhaps unreliable. Flaw mitigation is consequently an item of major importance.

Specimen sawcutting associated with the masonry research program at the University of California, San Diego (1), has afforded an excellent opportunity to observe flaws in concrete masonry. Test specimens are fabricated in 8 x 8 foot wall sections according to standard field practice and are subsequently precision sawcut to the desired test size of 64 x 64 inches. Approximately one hundred panels have been cut to date. The majority of these specimens have exhibited flaws in the form of grout-block separation, mortar-block separation, grout voids, and shrinkage cracks forming grout bridges. A typical vertical sawcut through a wall section is shown in Figure 1. The grout bridges (parabolic flaws adjacent to each bed joint or attendant mortar intrusion) are particularly evident in this example.

In addition to full-scale panels, three and four-course stack bond prisms are tested as controls. These specimens provide additional information concerning the influence of flaws. Figure 2 shows a 3-course stack bond prism failed in uniaxial tension. The domed grout cores appear to be air-cured grout and show little evidence of failed material. The shape of these grout domes corresponds closely to the parabolic shape of the cut section in Figure 1. A projected area analysis of the failure cross section, and use of grout material strength in tension, predicted the actual prism failure load to within a few percent. Figure 3 illustrates this method. The cross-hatched area was judged to be failed grout material

¹ Research sponsored by the National Science Foundation under Grant NSF ENV 74 14818.

² Assoc. Development Engineer, Professor, and Research Assistant, respectively, Dept. Applied Mech. And Engr. Sci., University of California at San Diego, La Jolla, California, 92093.

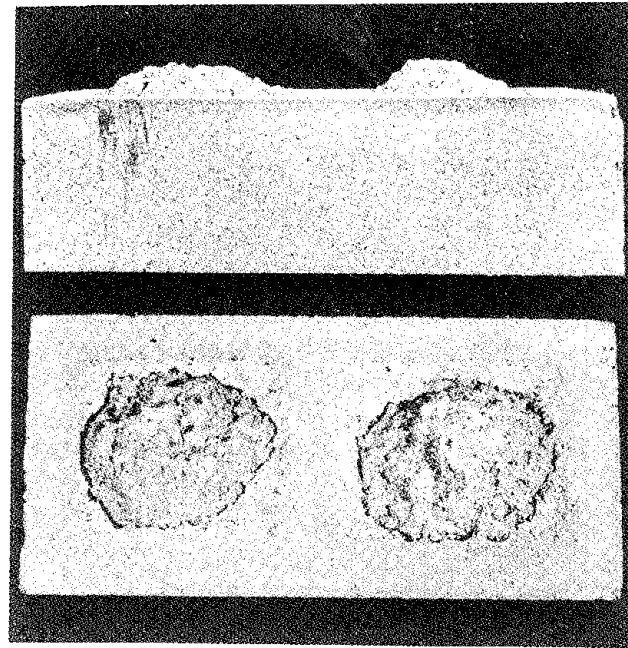
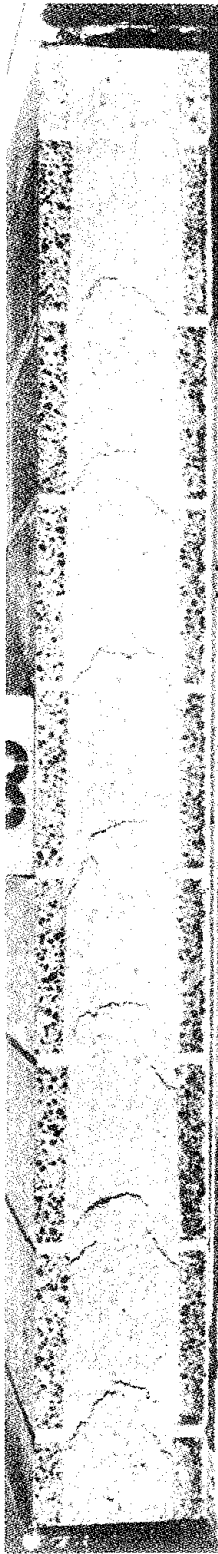


Fig. 2. Puddled Prism Failed in Tension

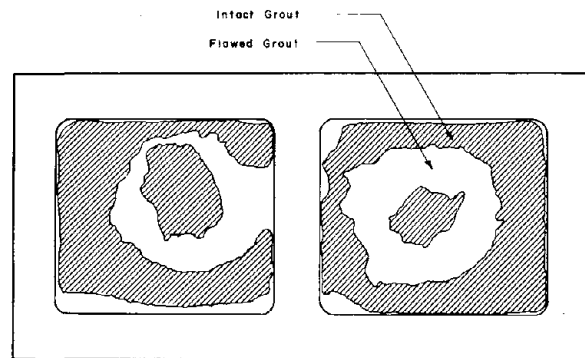


Fig. 3. Projected Area Analysis

Fig. 1. Vertical Sawcut Through Masonry Wall Section

while the remaining area represents a flaw where a bond was not evident. The tensile strength of the prism was found equal to the area of integrity times the grout strength in tension. This assumes the mortar-block bond strength to be negligible relative to the grout material strength. The fact that this load was only 66% of the total based on the full grout core area is alarming.

In view of the serious strength degradation resulting from the presence of grout flaws, and in cooperation with local masonry industry representatives, two series of tests were initiated to determine the effects a commercially available grout admixture and grout consolidation by vibration have on the strength and elastic moduli of fully grouted unreinforced masonry.

TEST PROGRAM

The two test series are shown in test matrix form in Tables 1 and 2. Table 1 is the test matrix for the field practice specimens; Table 2 is the matrix for the controlled group. The field practice prisms were constructed by journeyman masons according to accepted field practices while the controlled group of prisms and panels were constructed with emphasis on producing specimens of known origin. In the field practice group the grout was judged by the masons to be of workable consistency, as is field practice, while in the controlled group the grout slump was rigorously maintained at 10 inches, as measured by a 12 inch concrete slump cone (ASTM C143). Time intervals between grout placement, consolidation and reconsolidation were also carefully controlled. Temperature and humidity at the construction site during the cure period were recorded for additional information on variables possibly affecting the control group. The field practice prisms were constructed, grouted and consolidated with a minimum of controls to determine what results might be expected from the use of admixed grout and/or vibration at an actual job site, while the controlled series was an attempt to better understand the individual and combined effects of admixture and vibration under specified conditions.

Test Matrices

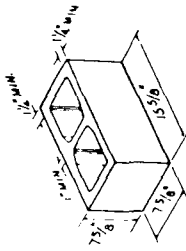
The two test series are subdivided into two grout types, STD and ADM, and two consolidation methods, puddled and vibrated. The standard grout (STD) was a 6-sack coarse grout of the same design mix used previously in approximately sixty panel tests. An admixture grout (ADM) was produced by adding Sika Grout Aid to the STD design mix at 6 lbs/cubic yard of grout, as supervised by a Sika Chemical representative.

Table 1. Field Practice Specimens - Test Matrix

Tension		Prisms		Compression	
	STD	ADM		STD	ADM
puddled	5	5	puddled	5	5
vibrated	5	5	vibrated	5	5

Table 3. Masonry Component Descriptions

Block: 8 x 8 x 16 inch Type N Normal Weight (ASTM C90)



Aggregate	Vol. %	Wt. /Cu. Ft.
Expanded shale	32	46 lbs.
Concrete sand	58	85 lbs.
Colton block cement	10	94 lbs.

Grout: 2000 psi Pump, 6-sack Coarse Grout (ASTM C476)

Aggregate	Vol. %	Wt. /Cu. Yd.
Coarse aggregate (3/8" x #4)	13	570 lbs.
Concrete sand	51.8	2259 lbs.
Water	24.6	415 lbs.
Riverside type II cement	10.6	564 lbs.

Mortar: Type S, 3/8-inch thick (ASTM C270)

Aggregate	Proportion by Volume
Masonry cement	1
Lime (type S)	1/2
Masonry sand	4

Admixture: Silka Grout Aid

Table 2. Controlled Slump Specimens - Test Matrix

Tension		Prisms		Compression	
	STD	ADM		STD	ADM
puddled	8	5	puddled	5	5
vibrated	5	5	vibrated	5	5

Panels		Tension	
	STD	ADM	
puddled	3	3	3
vibrated	3	3	3

Grout consolidation was by puddling with a 1 x 2 inch pine stick or by vibrating with a Waco 5000 RPM vibrator. The puddled specimens are listed by grout type alone, without a suffix denoting this method of consolidation. Thus, standard grout with puddling is listed as STD, while standard grout with vibration is listed as STD VIBR. Admixture grout is similarly ADM and ADM VIBR.

The prisms tested in tension were sawcut to 22 inches in length to accommodate the testing facility. This is approximately 3-courses. The prisms tested in compression were sawcut to 30 inches in length, or just under the original 4-course construction height. The panels constructed for the controlled group were precision sawcut to 64 inches square, oriented as shown in Figure 4. Cores were taken at three levels in each panel and the grout-block bond strength tested in single shear (2). Figure 4 also shows the core locations.

Fabrication

All test specimens were constructed adjacent to the structural test laboratory at the Harbor Drive Facility of General Dynamics, Convair Division, San Diego. Work was performed by journeyman masons in accordance with current field practices. The prisms were fabricated by leveling the first block of each prism in a bed of sand. Subsequent courses were aligned with a carpenter's level to minimize any load eccentricity due to prism geometry. One full day was allowed for complete cure of the mortar joints prior to grouting. The panels were fabricated on 12 in. x 12 in. x 10 ft. I-beams. The first course was bedded in mortar and struck level before additional courses were added. The twelve panels were initially laid to 6-courses or mid-height, and then completed to 12-courses. All specimens were constructed using the same block, mortar, and grout design mixes.

Materials

The specimens in both series were fabricated using 8 x 8 x 16 inch grade N, normal weight, two cell hollow concrete block (ASTM C90), type S 3/8 inch mortar joints (ASTM C270), and 6-sack coarse grout (ASTM C476). Aggregate proportions by volume are listed in Table 3.

Block material properties were tested using coupons 4 x 6 inches cut from full blocks. The coupons were tested in tension as well as compression and the results are listed in Table 4. Absorption tests were conducted to determine initial moisture content and the 24-hr. absorption percentage. These results are listed in Table 5.

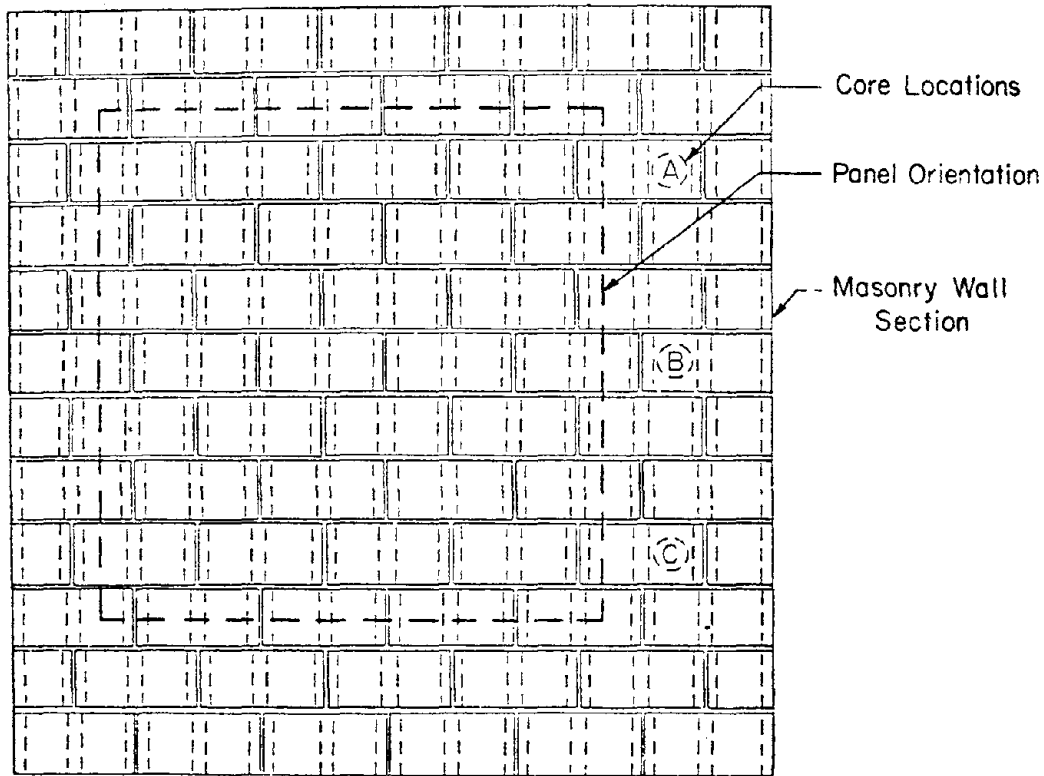


Fig. 4. Panel Orientation for Uniaxial Tests

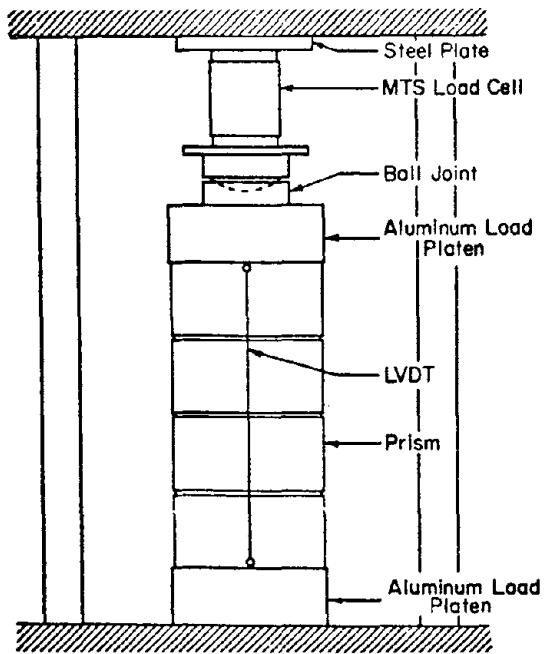


Fig. 5. Compression Test Set-Up

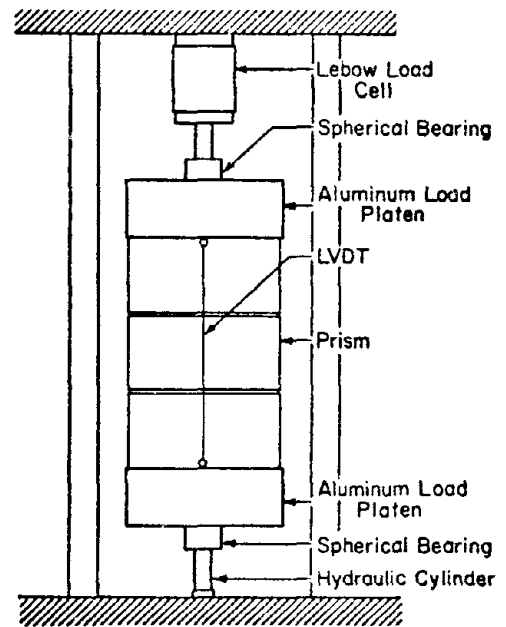


Fig. 6. Tension Test Set-Up

Table 4. Block Material Strength, Coupon Tests

Table 5. Block Absorption Tests

Field Practice Specimens		Controlled Slump Specimens
Compressive Strength	3.97	3.56
f_c (ksi)	2.97	3.12
	3.27	3.35
	2.95	3.54
	3.41	3.63
	3.16	3.80
	3.00	3.66
	3.68	3.98
mean	3.30	3.58
std. dev.	.37	.26
Tensile Strength	310	432
f_t (psi)	291	420
	373	331
	294	314
	297	368
	363	
	377	
mean	329	373
std. dev.	40	52

Field Practice Specimens

	S/N 1	S/N 2	S/N 3
24-Hr Absorption, %	7.7	7.7	6.7
Controlled Slump Specimens			
	S/N 1	S/N 2	S/N 3
24-Hr Absorption, %	11	10	11
Moisture Content as Rec'd as % of Total Absorption	31	21	34

Table 6. Mortar Compressive Strength

	Field Practice Specimens	Controlled Slump Specimens
Compressive Strength (kai)	2.42	2.40
	2.86	2.24
	2.39	1.96
	2.66	1.89
	2.83	1.50
	2.03	2.52
	1.77	1.41
mean	2.42	1.99
std. dev.	.41	.43

Mortar was mixed in accordance with ASTM standards and discarded 1 hour after initial mixing. Test cylinders 2 inches in diameter by 4 inches in length were manufactured and allowed to air cure with the prisms and panels for 28 days. Tests were conducted in compression with the results listed in Table 6.

Grout material properties for both STD and ADM grout were obtained from tension and compression tests performed on 3 x 3 x 8 inch rectangular prisms. The grout prisms were manufactured at the construction site and allowed to air cure with the prisms and panels for 28 days. Grout material properties are listed in Table 7.

Test Methods

Figure 5 illustrates the test set-up used to obtain the compressive failure loads and deflections for the 4-course prisms. A 300 kip MTS load cell was attached to the lead screw controlled cross-head. A 9 inch ball and socket and 6 x 8 x 16 inch aluminum load platens were seated above and below the test specimen. The ball and socket insured proper initial alignment and prevented application of moments prior to and during failure. The solid aluminum bearing platens diffused any load irregularities and produced a more uniform load distribution than that obtainable with the one and one-half inch steel plate prescribed by ASTM C140. Load was measured by a MTS load cell while displacements across a 28 inch gage length were measured by $\pm .050$ inch DC LVDTs (Linear Variable Differential Transformer) on both long sides of the prisms. The two LVDT signals were averaged and plotted versus the conditioned load signal on a HP 7045A X-Y plotter.

The prism tension tests were performed in a 50 kip MTS closed loop servo controlled testing frame illustrated in Figure 6. Specialized fixtures were required for testing the prisms. A 50 kip Lebow load cell is attached to the screw thread adjustable crosshead. An axially loaded spherical bearing connects the load cell to a 6 x 8 x 16 inch aluminum load platen. As in the compression test set-up, bearing platens were used above and below the prism to insure uniform load distribution at the specimen boundary. The hydraulic actuator was attached to the lower bearing platen with a spherical bearing identical to that used at the load cell. The aluminum load bearing platens were epoxy bonded to the prism and post-test removal was accomplished by heating the aluminum with cartridge heaters. Load was measured by the Lebow load cell while displacements across a 20 inch gage length were measured by $\pm .050$ inch DC LVDTs on both long sides of the prism. The signals were processed and recorded as described in the compression test set-up.

Table 7. Grout Material Strengths

	Field Practice Specimens		Controlled Slump Specimens	
	STD	ADM	STD	ADM
Compressive Strength (ksi)	4.03	4.34	2.90	3.49
	3.53	3.79	2.28	2.46
	3.51	3.41	2.53	3.49
	3.79	3.72	2.43	4.03
	4.15	3.66	2.33	2.42
	3.69			
	3.69			
	4.32			
	4.35			
	3.98			
	4.17			
	3.25			
mean	3.87	3.78	2.49	3.18
std. dev.	1.35	.34	.25	.71
Tensile Strength (psi)	247	284	219	284
	253	283	250	283
	324	283	223	283
	240	390	228	390
		397		397
mean	266	327	230	327
std. dev.	39	60	14	60

Table 8. Compressive Strength of 4-Course Field Practice Prisms

	STD	STD VIBR	ADM	ADM VIBR
Failure Stress f_c (psi)	1348	2274	2181	2004
	1449	2426	2350	2282
	1398	2089	2324	2173
	1887	2434	2308	2148
	1490	2358	2450	2468
mean	1524	2316	2323	2215
std. dev.	212	142	96	173

Table 9. Tensile Strength of 3-Course Field Practice Prisms

	STD	STD VIBR	ADM	ADM VIBR
Failure Stress f_t (psi)	69.7	116.3	92.5	94.8
	111.2	91.8	110.7	98.6
	111.2	127.3	118.3	116.3
	84.3	113.0	110.4	143.2
	69.9	89.9	95.8	107.4
mean	89.3	107.7	105.5	112.1
std. dev.	20.9	16.3	10.9	19.3

TEST RESULTS

Field Practice Specimens

Table 8 lists the compressive strengths for the 4-course field practice prisms. The stresses are based on a net area of 118.7 square inches. The STD VIBR, ADM, and ADM VIBR groups had mean strengths of 2316, 2323, and 2215 psi, respectively. These results are statistically identical and approximately 50% higher than the 1524 psi mean compressive strength of the STD group. This suggests that a similar compressive strength increase may be obtained by vibration compaction and admixed grout used individually or in combination.

Table 9 lists the tensile strengths for the 3-course field practice prisms. The STD, ADM, and ADM VIBR groups had mean tensile strengths of 107.7, 105.5 and 112.1 psi, respectively. These results are 21, 18 and 26% higher than the 89.3 psi mean tensile strength of the STD group. This suggests that vibration and admixture may produce approximately the same increase in strength when used individually, but the increase may be slightly higher when vibration and admixture are used in combination.

Controlled Specimens

Table 10 lists the compressive strengths for the controlled slump series of 4-course prisms. The mean strengths differ dramatically from those obtained from field practice prisms. The ADM group had the lowest strength with a mean of 1673 psi. The STD group had a mean of 1984 psi, or 19% above the ADM group. STD VIBR and ADM VIBR recorded mean compressive strengths of 2171 and 2566 psi, respectively. The increase in mean compressive strength obtained with vibration compaction was 9% for the STD grout and 53% for the ADM grout.

The 3-course tensile strengths are listed in Table 11. Again, the ADM group had the lowest strength with a mean of 83.9 psi. The STD group had a mean of 95.7 psi, or 14% above the ADM group. The STD VIBR and ADM VIBR groups recorded mean tensile strengths of 114.6 and 162.4 psi, respectively. Vibration compaction increased the mean tensile strength of the STD grout by 20% while the increase over the ADM grout was a surprising 94%.

The tensile strengths obtained from the panel tests are listed in Table 12. The STD and ADM groups had similar mean strengths of 89.6 and 92.0 psi, respectively. STD VIBR and ADM VIBR recorded means of 114.8 and 115.5 psi, respectively. The effect of admixture is statistically negligible while vibration compaction increased the mean tensile strength of the STD grout by 28% and of the ADM grout by 26%.

Table 10. Compressive Strength of 4-Course Controlled Slump Prisms

	STD	STD VIBR	ADM	ADM VIBR
	2140	2123	1685	2359
	1702	2140	1735	2584
Failure Stress f_c (psi)	2079	2241	1574	2595
	2072		1735	2746
	1928		1634	2544
mean	1984	2171	1673	2566
std. dev.	176	60.4	69.2	139

Table 11. Tensile Strength of 3-Course Controlled Slump Prisms

	STD	STD VIBR	ADM	ADM VIBR
	74.9	99.8	91.8	160.0
	82.1	93.8	81.1	150.0
Failure Stress f_t (psi)	105.0	114.8	92.4	161.0
	119.7	131.3	70.4	178.6
	88.2	133.4		
	95.4			
	107.1			
	93.5			
mean	95.7	114.6	83.9	162.4
std. dev.	14.5	17.9	10.4	11.9

Table 12. Tensile Strength of Panels

	STD	STD VIBR	ADM	ADM VIBR
	90.0	129.5	67.1	125.2
Tensile Strength (psi)	79.7	96.7	111.9	119.5
	99.1	118.3	97.1	101.8
mean	89.6	114.8	92.0	115.5
std. dev.	9.7	16.7	22.8	12.2

Table 13. Initial Compressive Tangent Modulus of Controlled Slump Prisms

	STD	STD VIBR	ADM	ADM VIBR
	2.36	2.36	1.87	2.32
	2.59	2.49	1.83	--
Young's Modulus, E_c (x 10^6 psi)	2.31	2.17	1.86	2.84
	2.17		2.14	2.52
	1.67		2.26	2.84
mean	2.22	2.33	1.99	2.63
std. dev.	.34	.16	.20	.26

The results of the core shear tests are discussed in reference (2) and are not presented here. The component tests are listed in Tables 4-7. The relationships between component and assembly strengths will be discussed in the next section.

DISCUSSION

Generalizations made about complex material and assemblage behavior based on a limited number of tests may be misleading if the number of tests is not sufficient to support statistical analysis. Mean values and standard deviations are statistical tools employed to characterize the behavior of a group of specimens with the minimum number of parameters. Increasing the number of test specimens will generally increase the confidence level associated with each mean value. Consequently, predictions of masonry assemblage behavior based on component properties and failure mode theories will be improved as the number of tests increases. The number of specimens in each of the previously discussed test groups was the minimum number necessary to establish statistical mean values and, consequently, the results of these tests are of preliminary importance.

Several conclusions are supported by the results listed in Tables 4-15. Two major effects are noted as well as several which can only be supported by further testing. As will be seen, masonry strengths and elastic moduli may be improved and perhaps predicted through the use of admixed grout and vibration compaction.

Inspection of the data in Table 8-12 immediately discloses that ADM VIBR consistently produced the strongest prisms and panels. This result is true in both tension and compression. In the Field Practice prisms, the increase in compressive strength over the STD group was 45% while the increase in tensile strength was 26%. In the Controlled Slump prisms the increases in compressive and tensile strengths were 29% and 70% respectively. These strength increases are very significant and easily recognizable through the use of Grout Aid and vibration compaction.

The second major effect, one that is perhaps more important than ultimate strength, is the predictable strengths obtained with vibration compaction. In all test groups, vibrated standard grout produced consistent mean strengths. The Field Practice and Controlled Slump compressive strengths were 2316 and 2171 psi, respectively, despite the fact that STD grout strengths were 1524 and 1984 psi. Vibration compaction of standard 6-sack coarse grout appears to yield consistent 2200-2300 psi prism compressive strength. The puddled standard grout strengths varied considerably and may

have been slump sensitive. Further testing might reveal vibration compaction to be an important factor in reducing the sensitivity of grout strength to grout slump, an important factor in field construction. The mean tensile strengths of the Controlled Slump STD VIBR prisms and panels, Tables 11 and 12, were statistically identical at 115 psi. This is extremely significant because prediction of full-size or macroelement behavior may be possible from knowledge of component strengths and failure mechanisms. Specifically, uniaxial tensile strength coincident with grout core axes appears to be dependent on grout material strength alone. Mortar - block bond strength in tension has little or no effect on assemblage strength. Table 7, Grout Material Strengths, lists the mean tensile strength of STD grout as 230 psi. Average grout core cross section in the hollow core blocks used in these tests is very nearly 50% of the gross block cross section. Assembly tensile strength based on grout core tensile strength is calculated by multiplying grout strength by the ratio of grout area to total area. Thus, vibration compaction allowed STD grout to develop full 115 psi mean tensile strength based on a simple failure model and mean grout strength. The puddled STD grout panels, at 90 psi tensile strength, were 22% below the predicted mean. Similarly, the ADM VIBR Controlled Slump prisms, Table 11, developed full assembly strength based on mean ADM grout tensile strength. The ADM prisms, at 84 psi tensile strength, were 48% below predicted mean tensile strength.

Predicting assemblage compressive strength based on component behavior is far more difficult and will require a complex failure model. Grout, block and mortar properties interact in three dimensions and several failure modes are possible. Additional component and assembly testing is required to develop a suitable compressive failure model.

The use of admixture grout with puddling produced conflicting results. The Field Practice ADM prisms showed significant strength increases over the STD group, but the Controlled Slump ADM prisms and panels were weaker or only as strong as the STD group. This suggests that puddled admixed grout may be sensitive to initial slump or water content, and may produce unpredictable results from job to job. Again, additional tests investigating the slump sensitivity of admixed grout are necessary to determine if controlled use will produce the desired strength increases and improve predictability.

The variation of elastic moduli with grout type and compaction was similar to the variation in mean strengths. Tables 13-15 list the mean initial tangent elastic moduli for the Controlled Slump series of specimens. The ADM VIBR specimens were by far the stiffest, while the ADM and STD specimens were consistently the most compliant. Vibration compaction increased the elastic moduli of both STD and ADM

Table 14. Initial Tensile Tangent Modulus
of Controlled Slump Prisms

	STD	STD VIBR	ADM	ADM VIBR
	1.72	2.03	2.01	2.24
	1.95	2.19	2.16	2.17
Young's Modulus, E_t	2.10	--	2.27	2.67
(x 10^6 psi)	2.47	2.47	2.25	2.55
	2.21	2.21		
	2.15			
	2.27			
	2.10			
mean	2.12	2.23	2.17	2.41
std. dev.	.22	.18	.12	.24

Table 15. Initial Tensile Tangent Modulus
of Controlled Slump Panels

	STD	STD VIBR	ADM	ADM VIBR
	2.36	2.51	2.18	2.57
Young's Modulus, E_t	2.11	2.23	2.55	2.88
(x 10^6 psi)	1.91	2.53	1.93	2.73
mean	2.13	2.42	2.22	2.73
std. dev.	.23	.17	.32	.16

Table 16. Ratio of Compressive Elastic Modulus
to Compressive Strength

	STD	STD VIBR	ADM	ADM VIBR
$\frac{E_c}{f_c}$				
mean	1130	1081	1193	1028
std. dev.	241	102	126	93.6

grout. Table 16 lists the ratio of elastic compressive modulus to compressive strength of the Controlled Slump 4-course stack bond prisms. The values of 1000-1200 are in the range assumed in the 1976 UBC (Table No. 24-H) and provide an indication of the relationship between f'_m and compressive modulus. The vibrated groups provided the best agreement with the UBC assumed values of 1000. The values of one standard deviation were smaller for the vibrated groups, indicating less data scatter or more reliable mean values. It is significant to note that the tensile elastic moduli of the panels, Table 15, are very similar to those obtained during the tensile prism tests listed in Table 14. Macroelement behavior based on small-scale laboratory tests appears to be reliably predicted.

SUMMARY

It has been shown that flaw formation in concrete masonry construction seriously degrades strength and elastic moduli preventing full strength design based on component properties. This paper has reported on a preliminary series of tests (3) initiated to determine if flaw mitigation and subsequent strength increases could be obtained through the use of admixed grout and vibration compaction. The most significant conclusions and recommendations formulated from the test results are:

- Vibration compaction produced specimens with fewer flaws, improved strength and predictability, and reduced data scatter than did puddling compaction. Consequently, vibration compaction is recommended over puddling for all concrete masonry construction.
- Puddling compaction, with and without admixed grout, produced specimens with extensive flaws in the form of grout bridges, voids, and shrinkage cracks at grout-block interfaces.
- Sika Grout Aid and vibration compaction produced specimens with the highest uniaxial strengths and elastic moduli. Strength variations from test series to test series indicates that further testing is needed to determine the effect of initial water content or grout slump on admixture grout.
- Vibration compaction produced specimens with the ratio of elastic compressive modulus to compressive strength closer to the UBC value of 1000 than did puddling compaction.

REFERENCES

1. G. A. Hegemier, S.K. Arya, R.O. Nunn, M.E. Miller, A. Anvar, G. Krishnamoorthy, A Major Study of Concrete Masonry Under Seismic-Type Loading, Report No. AMES/NSF/TR-77/002, University of California, San Diego, 1977.
2. R.O. Nunn, M.E. Miller, G. A. Hegemier, Grout-Block Bond Strength in Concrete Masonry, Report No. AMES/NSF/TR-78/001, University of California, San Diego, 1978.
3. G. A. Hegemier, M. E. Miller, R. O. Nunn, On the Influence of Flaws, Vibration Compaction, and Admixtures on the Strength and Elastic Moduli of Concrete Masonry, Report No. AMES/NSF/TR-78/002, University of California, San Diego, 1978.

PRISM TESTS FOR THE COMPRESSIVE STRENGTH
OF CONCRETE MASONRY¹

by

G. A. Hegemier², G. Krishnamoorthy³, R. O. Nunn⁴, T. V. Moorthy⁵

ABSTRACT

Results of an experimental program on concrete masonry prisms are presented. Current masonry industry testing procedures and potential problems, and the influence of prism height, capping, bond configuration, and bearing-plate thickness are discussed. Modifications of existing codes are recommended.

¹Research was sponsored by the National Science Foundation under Grant NSF ENV 74-14818.

²Professor, Dept. of Appl. Mech. & Engr. Sci., University of California, San Diego, La Jolla, California, 92093.

³Professor, Dept. of Civil Engr., San Diego State University, San Diego, California, 92182.

⁴Graduate Student, Dept. of Appl. Mech. & Engr. Sci., University of California, San Diego, La Jolla, California, 92093.

⁵Graduate Student, Dept. of Civil Engr., San Diego State University, San Diego, California, 92182.

PRISM TESTS FOR THE COMPRESSIVE STRENGTH OF CONCRETE MASONRY¹

by

G. A. Hegemier², G. Krishnamoorthy³, R. O. Nunn⁴, T. V. Moorthy⁵

INTRODUCTION

The Prism Test

Present working stress design methods are based upon a knowledge of the masonry compressive strength, f'_m . In practice, f'_m is usually determined by prism tests. The importance of proper prism-test procedures and data interpretation is thus evident.

The word "prism" is synonymous with small specimens of masonry; in the case of ungrouted prisms the limiting case is the single block unit. For the determination of compressive strength the prisms are capped at both bottom and top with a capping material (e. g., sulphur, gypsum plaster, mortar, fiberboard, plywood, etc). The failure load in uniaxial compression is divided by the net cross-sectional area of the block for ungrouted prisms, and the gross area for grouted prisms, to obtain the value of f'_m .

¹ Research was sponsored by the National Science Foundation under Grant NSF ENV 74-14818.

² Professor, Dept. of Appl. Mech. & Engr. Sci., University of California, San Diego, La Jolla, California, 92093.

³ Professor, Dept. of Civil Engr., San Diego State University, San Diego, California, 92182.

⁴ Graduate Student, Dept. of Appl. Mech. & Engr. Sci., University of California, San Diego, La Jolla, California, 92093.

⁵ Graduate Student, Dept. of Civil Engr., San Diego State University, San Diego, California, 92182.

Current Practice

It is standard practice to compute f'_m on the basis of 2-course prisms laid in stack bond and capped with a high-strength sulphur fly-ash compound or a high-strength gypsum plaster ("Hydrostone" or "Hydrocal White") according to ASTM C140. Compression test procedures correspond to ASTM E447.

In the United States, current masonry codes (9, 11) not only allow the foregoing practice, but encourage the same by adopting universal correction factors for prism geometry (see Sec. 2404. C. 2 of the Uniform Building Code (UBC) (9)). These correction factors, given in Table 1, purport to enable conversion of the strength of a prism of a particular geometry to that of a standard 2-course prism, (more precisely, $h/t = 2.0$ where h, t denote prism height and least lateral dimension, respectively) the correction factor for which is unity. This, and the manner in which the correction factors are used (f'_m is taken as the compressive strength of the specimen multiplied by the correction factor) implies that a strong correlation exists between $h/t = 2.0$ and full-scale masonry. In view of the handling problems associated with larger assemblages, as well as the limited clearance in the universal testing machines, it is natural for commercial laboratories to prefer a 2-course prism.

Potential Problems and the Present Study

An extensive literature review of prism testing (2) revealed that current test procedures on prisms and the use of prism data in practice are open to serious question in the case of ungrouted concrete masonry. Items of particular concern include: 1) the code(s) correction factors for prism geometry; 2) the influence of prism construction, geometry, bond configuration, curing process, and capping procedures on strength; 3) the influence of bearing-plate thickness; and 4) correlation of prism strength with full-scale wall strength.

As noted, the foregoing literature review concerns ungrouted masonry. Sufficient information to allow judgements on grouted masonry, which is more relevant to multistory, reinforced concrete masonry construction in seismic zones, is not available in the current published literature.

Consequently, an experimental study was initiated to complement the available literature via an investigation of grouted concrete masonry within the context of the foregoing items. The results of this study together with correlation of previous works are presented herein. The significant findings are discussed and recommendations pertinent to general practice, and to building codes, are made. The original stress-strain data is included in reference (3).

Table 1. Code Correction Factors Table 2. Component Properties

h/t* ratio	1.5	2.0	3.0	4.0	5.0
Correction Factor	0.86	1.00	1.20	1.30	1.37

* h = height of specimen
t = minimum dimension of specimen

	Block*	Mortar	Grout
mean	3711	1720	2649
std. dev.	399	312	615

*Tests conducted on coupons

Table 3. Comparison of Code Correction Factors

Source	"Code factor"	h/t =							
		1.5	2.0	2.5	3.0	4.0	5.0	6.0	
Krefeld	—	0.59	0.67	0.75	0.80	0.89	0.96	1.00	
New Zealand Standard	1.50	0.58	0.67	0.74	0.80	0.89	0.95	1.00	
Australian Standard	1.25	—	0.68	0.74	0.80	0.88	0.93	0.93	
Canadian Code (concrete)	1.50	0.57	0.67	0.74	0.80	—	—	—	
Canadian Code (brick)	0.93	—	0.68	0.74	0.80	0.89	0.93	—	
Uniform Building Code	1.50	0.57	0.67	0.74	0.80	—	—	—	
National Bureau of Standards	1.50	0.57	0.67	0.74	0.80	—	—	—	
Structural Clay Prods. Inst.	0.93	—	0.68	0.74	0.80	0.89	0.93	—	

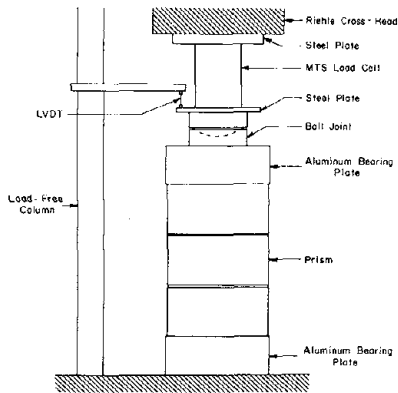


Fig. 1. Test Set-Up

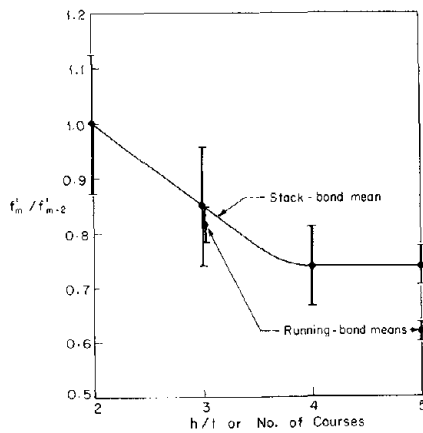


Fig. 2. Strength vs h/t

Table 4. Prism Strength vs h/t Ratio

Type of Prism	h/t ratio	Strength* (psi)	Type of Prism	h/t ratio	Strength* (psi)
cut, full mortar bed	2	2502	capped, full mortar bed	2	1791
		2160			2493
		<u>2562</u>			<u>2271</u>
		mean 2408			mean 2185
		std. dev. 217			std. dev. 359
cut, full mortar bed	3	1989	cut, face-shell mortar bed	3	1787
		1826			1939
		2405			<u>1883</u>
		1653			mean 1870
		1847			std. dev. 77
mean 1943	cut, full mortar bed	2	1690		
std. dev. 254				2170	
1989				<u>1736</u>	
1838				mean 1865	
1574				std. dev. 265	
cut, full mortar bed	4	1496	cut, capped full mortar bed	2	1616
		1625			1994
		1662			<u>1791</u>
		1699			mean 1800
		mean 1698			std. dev. 189
std. dev. 167	cut, full mortar bed	5	1426		
1699				1450	
1773				<u>1371</u>	
1607				mean 1416	
mean 1693				std. dev. 41	
std. dev. 83					

*Stress based on area of 119.1 in²

TEST PROGRAM

Objectives

The specific objectives and scope of this test program include the following:

- 1) Determine the source of the correction factors for prism geometry in the Uniform Building Code.
- 2) Determine the validity of the correction factors.
- 3) Investigate the effect of capping materials on prism compressive strength.
- 4) Investigate the effect of the h/t ratio and the number of courses on prism compressive strength for a given capping material.
- 5) Investigate the influence of bond configuration (running versus stack) on prism compressive strength.
- 6) Correlate prism strength with full-scale wall strength, where possible.
- 7) Recommend changes, if necessary, in prism construction/test procedures, and building code modifications, based upon the test results and literature review/evaluation.

Materials

Prisms were fabricated using 8 x 8 x 16-inch Grade N normal-weight two-cell concrete block (ASTM C90), with type S mortar 3/8 inch thick (ASTM C270), and grouted with a coarse 6-sack grout (ASTM C476) having an 8-10 inch slump (ASTM C143). Grout compaction was accomplished by puddling. One set of specimens was laid in stack bond with full mortar bedding; a second set was laid in stack bond with face shell mortar bedding; a third set was laid in running bond (using a combination of full and half blocks) with face shell mortar bedding. Prisms were constructed by professional masons using conventional field techniques in 2-, 3-, 4-, and 5- course sets¹; each set was field cured for at least 28 but not more than 40 days prior to testing.

In addition to prisms, component samples were tested as control variables. These included 3-inch square x 5-inch high grout prisms, 2-inch dia. x 4-inch high mortar cylinders, and 4 inch x 6 $\frac{1}{2}$ -inch high block coupons. Preparation and testing was conducted according to ASTM procedures with the exception that grout and mortar samples were field cured with the prisms. Component properties for the field cured prisms, determined as noted above, are given in Table 2.

¹Running bond specimens were fabricated only in 3- and 5- course sets to avoid a head joint adjacent to the load platen; the latter was thought to induce premature prism fracture.

Methods

In the main test series, precision cutting was utilized to obtain the desired h/t ratio and smooth parallel loading surfaces; cutting was conducted with a 30-inch diameter, dynamically balanced diamond-edge saw on an air-driven turbine attached to fixed rails; feed rates were sufficiently slow to prevent any specimen degradation. Cutting provided the capability of having one additional bed joint for the same h/t ratio, which permitted an examination of the effect of number of bed joints on the compressive strength of the prisms.

In another test series, specimens were cut and capped with a high strength gypsum plaster (Ultra-Cal-30, $f'_c \geq 6,000$ psi) according to ASTM C140. In other test series "soft" capping materials were investigated; these included a polysulfide (PRC-380 M, produced by the Products Research Corporation) and fiberboard, each of 1/4-inch thickness.

The test set-up is shown in Fig. 1. The bearing plates in each test consisted of solid 8 x 8 x 16-inch precisely machined aluminum blocks. A ball and socket joint was used between the top bearing plate and the test machine load platen in order to permit rotation at the top of the prisms and thus eliminate any artificial restraint-introducing moments.

Loads were applied by a 300 kip Riehle Machine and measured accurately by a 300 kip MTS load cell. All tests were conducted under displacement control at a rate of .012 in/sec.

The displacement was measured with a ± 0.50 inch LVDT (Linear Variable Differential Transformer), together with a $\pm .050$ inch LVDT for a more accurate record of the elastic portion of the curve. The load versus relative displacement curves were recorded on separate MFE x-y recorders. Prism failure or compressive strength was defined as the first peak in the load-displacement record.

RESULTS AND DISCUSSION

Literature

A representative cross section of the available literature on prism testing, and the correlation of prism data with wall data, is provided by the references.

The first reported research on representative specimens for concrete masonry wall strength was conducted on wallets by Richart (7) in 1932. The prism test concept evolved from an industrial need

for simpler and more economical methods for estimating the compressive strength f'_m .

Since the original work by Richart on wallets, an enormous number of compression tests on prisms have been conducted. One might suppose, therefore, that the obvious questions concerning a proper prism configuration (e. g., number of courses, stack or running bond, etc.), and a proper test procedure (e. g., capping material) for a quantitative measure of wall compressive strength have been answered with some degree of finality. Unfortunately, this is not the case.

The vast majority of prism tests have served as construction and manufacturing quality controls and the test results are not in the published literature. A substantial quantity of other prism data is evidently buried in the files of private laboratories, institutes, and associations. Consequently the published literature, in particular information pertaining to concrete masonry, is sparse and not well documented. It is sufficient, however, to reveal that considerable precautions are necessary to achieve a reliable estimate of the compressive strength of full-scale masonry.

Genesis of the Code Correction Factors

Code correction factors for prism geometry were noted previously. It is natural to question the origin of such universal factors. Foster and Bridgeman (1) addressed this question and uncovered an amazing fact: while different masonry codes may have a different "standard shape", i. e., a different value of h/t for which the correction factor is unity, the ratio of the conversion factors is constant - which suggests a common source. This source is almost certainly the preliminary and exploratory investigation by Krefeld (4) in 1936 on brick - as demonstrated by Table 3, which was reproduced from (1). Each set of correction factors has been divided by an appropriate "code factor" to yield a common value of 0.80 for $h/t = 3.0$, as was obtained experimentally by Krefeld. Krefeld fully delineated the limitations of his work which involved only one brick and one mortar type; and he concluded that other factors such as brick and mortar strength, bond configuration, and prism cross-sectional dimensions also require investigation. Table 3, however, shows that his results have been accepted as being of general validity, not only for brick, but for concrete masonry as well. This, as Foster and Bridgeman have emphasized, is patently unjustified.

Platen Restraint and Geometry

Test results on grouted prisms clearly indicate that high-strength capping materials, as used here and as specified in ASTM C140, lead to lateral restraint of the specimen at the bearing plates. Similar restraint was observed in the case of precision saw-cut specimens with no capping material. In particular, saw-cut surfaces yielded an estimate of compressive strength 10 percent greater than that for high-strength capped surfaces (see Table 4). In both cases bearing plate, or "platen" restraint is due to friction at the interface between the specimen and the platen.

Platen restraint can be observed by its effect on compressive strength, by its effect on failure mode, and by strain gage data.

1) Compressive Strength. The most sensitive measure of platen restraint is compressive strength. Test data indicates that prism compressive strength is significantly influenced by platen restraint and, in the absence of a soft capping material, is a strong function of the number of courses up to 4 courses, with strength invariance between 4 and 5 courses. A typical example is illustrated in Fig. 2; the data for this case was obtained from saw-cut stack-bond grouted specimens. The curve in Fig. 2 (the data was normalized using 2295 psi) represents the means of repeated tests at integer h/t ratios with interpolation between integer h/t ratios. Similar results were observed for precision saw-cut grouted specimens with running bond, for h/t = 3 and 5. For comparison purposes, results of the running-bond tests are included in Fig. 2; the data was again normalized on the 2-course stack-bond prism strength, 2295 psi. The test data is also presented in Table 4 for completeness.

As can be observed from Fig. 2, the 2-course estimate of f'_m in the presence of platen restraint is, based upon the 5-course prism data, approximately 36 percent high for grouted stack-bond masonry and 62 percent high for grouted running-bond masonry.

The prism test data revealed another important point. Based upon data from saw-cut specimens, prism compressive strength was observed to be primarily a function of the number of bed-joints in the specimen - not the h/t ratio. For example, prisms with 2 bed-joints saw-cut to h/t = 2.0 exhibited strengths similar to specimens with 2 bed-joints and h/t = 3.0 (see Table 4). Thus, interpolation for h/t between integer number of courses (uncut) or bed-joints is not a valid operation.

It must be emphasized at this point that the foregoing trends apply only to the material combination tested. In particular, one

should not attempt to construct correction factors based upon the data reported herein. The point, in fact, is just the opposite: since correction factors can be expected to be highly material dependent, they cannot be relied upon to furnish an adequate estimate of f'_m .

2) Failure Modes. Differentiation of failure modes in the case of full-block grouted prisms is difficult; thus, the failure mode(s) is not a good measure of platen restraint. This situation is quite different, however, for half-block prisms, and the latter is worth noting.

In the case of half-block grouted prisms (the component properties for which are given in Table 5), platen restraint in 2-course prisms generally produced shear-type failures, whereas the observed failure mode in walls is vertical tensile splitting; a typical shear failure mode is shown in Fig. 3. In prisms of 3 courses, the failure mode approaches the proper tensile splitting in the central unit; this is illustrated in Fig. 4. In 4-course and 5-course prisms, the failure mode more closely resembles a wall compression failure.

In the case of 2-course full-block grouted prisms, shear failures (Fig. 5) were usually observed. For prisms of more than 2 courses, the failure mode could frequently be characterized as tensile-splitting of the end face shells, and tensile splitting of the grout cores. A typical failure is shown in Fig. 6. The phenomenon of face-shell spallation away from the grout cores was observed frequently; the block and grout are clearly not functioning as an integral unit in these tests.

3) Strain-Gage Data. The influence of platen restraint can be clearly observed via strain gage measurements. Results of a test on a grouted 3-course prism are shown in Fig. 7.

Use of the polysulfide as a capping material yielded proper tensile splitting in 2-course prisms, Fig. 8, and strength invariance between 2 and 5 courses. This is the result of the polysulfide's low shear modulus (150 psi) which lubricates the interface between the specimen and the bearing block and essentially eliminates the platen restraint. Unfortunately, this material (and similar materials) is expensive and difficult to handle; improper use can lead to premature failure. Consequently, the polysulfide capping is judged to be impractical for conventional laboratory or field testing.

In contrast to tests on ungrouted prisms (10), fiberboard capping was observed to produce large data scatter and did not sufficiently relieve load platen restraint in grouted prisms. Further, fiberboard types and grades apparently differ considerably from region

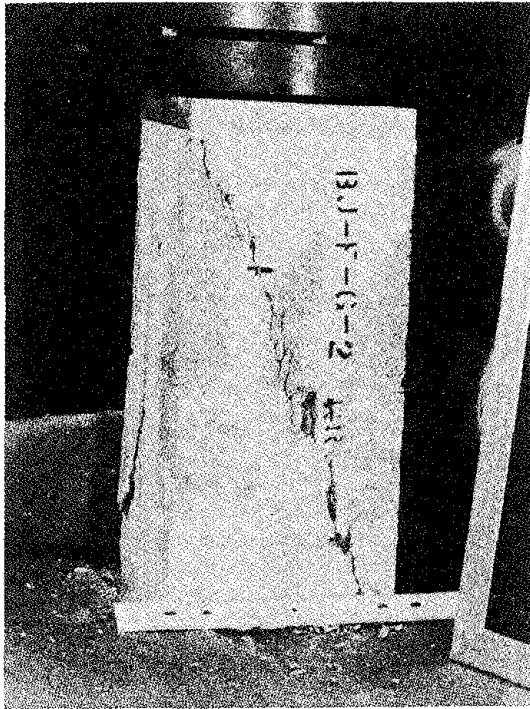


Fig. 3. Prism With "Hard" Cap



Fig. 4. Grout Core Splitting

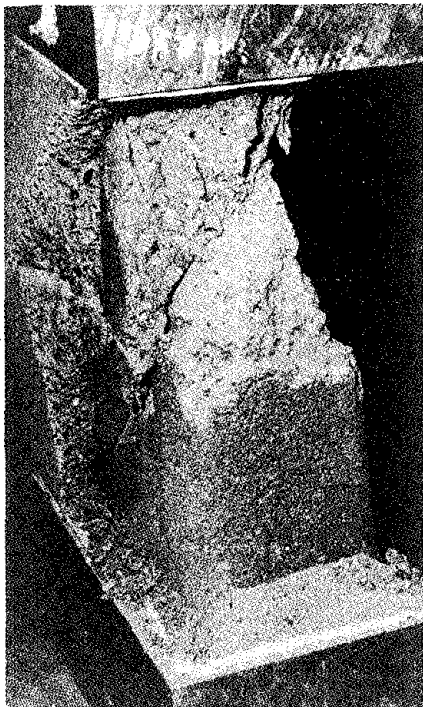


Fig. 5. Typical Shear Failure



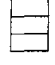
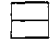


Fig. 6. Grout Core Tensile-Splitting

Table 5. Component Strengths

	Block*	Mortar	Grout
mean	2750	4100	5640
std. dev.	460	390	230
*Net area strength			

Table 6. Strength Comparison, Stack Bond vs. Running Bond

Type of Prism	Block Strength psi	Prism Strength psi	Efficiency Percent		Block Strength psi	Prism Strength psi	Efficiency Percent
	5100	2087	41	41	7400	2796	38
		1838	36			3246	44
		1845	36			2330	32
		2589	51			2934	40
	5100	2264	44	46	7400	3246	44
		2224	44			2883	39
		2380	47			3050	41
		2536	50			3262	44
	5100	4035	79	69	7400	4420	60
		3027	59			4811	65
		3136	61			4828	65
		3834	75			4485	61
	5100	3632	71	73	7400	4680	63
		3828	75			4542	61

Type S mortar with initial flow of 90%, 3300 psi at 28 days.
Capping material: fiberboard.

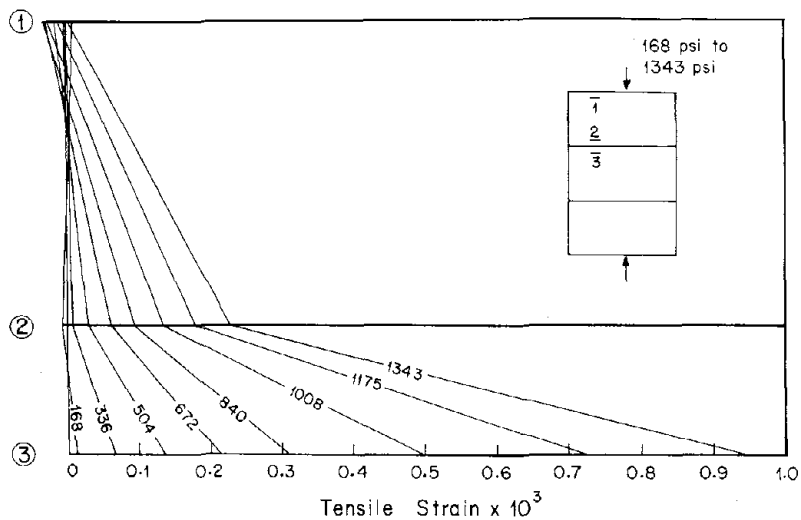


Fig. 7. Variation of Lateral Strain with Height



Fig. 8. Vertical Tensile Splitting

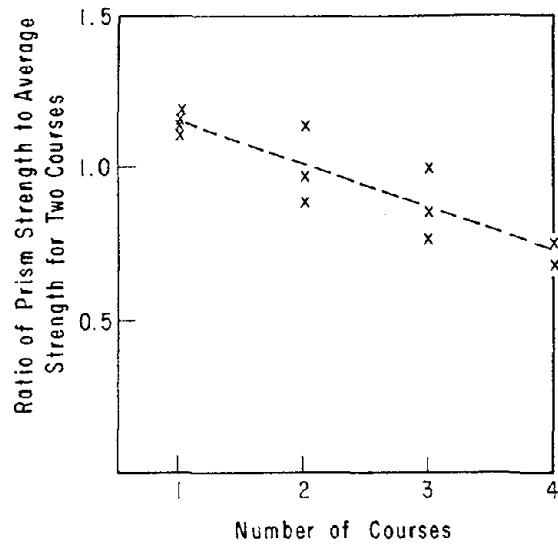


Fig. 9. Ratio of Strength to Number of Courses

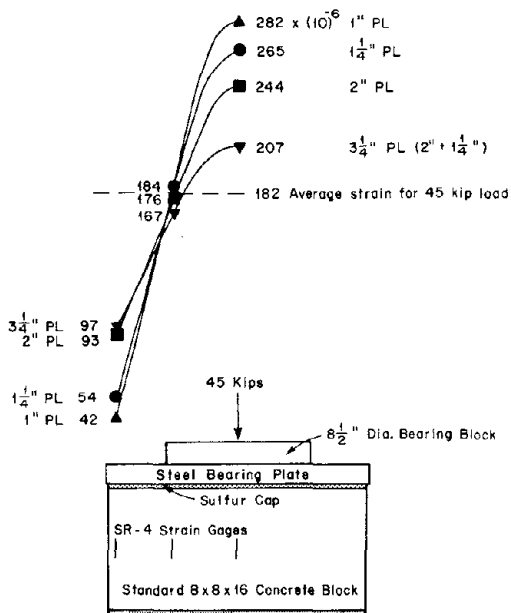


Fig. 10. Influence of Bearing Plate Thickness

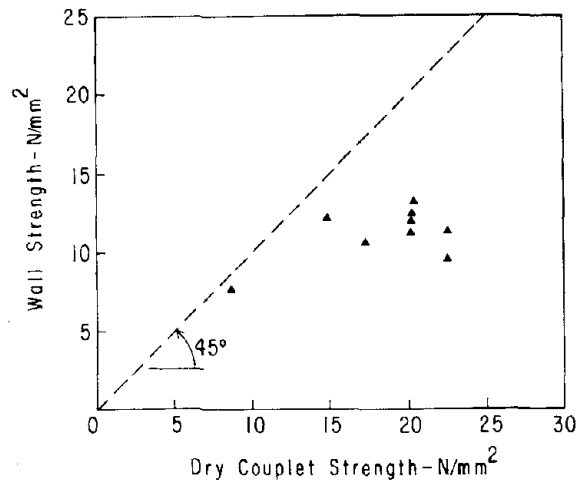


Fig. 11. Comparison of Couplet and Wall Strengths

to region. Consequently, fiberboard is not regarded as a suitable "standard" capping material for prisms.

The influence of platen restraint on compressive strength of ungrouted prism specimens is reported in the literature and is worth noting at this point.

The decrease in compressive strength with increasing number of courses, associated with the use of high strength capping materials, can be observed in the data of Foster and Bridgeman (1) on 4 x 8 x 16-inch hollow concrete block prisms. The latter is reproduced as Fig. 9. The data shows a decrease in strength at least up to 4 courses and $h/t = 8.7$.

It is clear that the undesirable effects of platen restraint are alleviated by increasing the number of prism courses. This can be observed via the strain gage data of Self (8) on 2- and 3-course ungrouted prisms.

Finally, data on ungrouted prisms supports the premise that reduced platen restraint, and a corresponding decrease in compressive strength, is achieved with soft capping materials. Yokel, Mathey and Dijkers (10), for example, report that the compressive strength of 3-course hollow 8-inch block prisms with high-bond mortar capped with fiberboard was 44 percent less than the same prisms capped with high-strength plaster.

As noted in the introduction, f'_m is taken as the strength of a prism multiplied by the h/t correction factor of Table 1. This procedure seems to imply the true strength of concrete masonry is that of a 2-course prism, while prisms of more than 2 courses are somehow weakened. But in fact 2-course prisms with hard caps are seen to be artificially strengthened, whereas prisms of 4 and 5 courses approach the true strength. While this artificial strengthening may now be compensated for in the safety factor of the allowable working stress, (equal to $.2 f'_m$ for walls) f'_m should be taken to be the strength of a 4 or 5 course prism, in which case the actual safety factor will be clearly evident.

Mortar Joint Geometry versus Strength

Foster and Bridgeman (1) have suggested that prism geometry, in particular mortar joint geometry, may influence prism strength; they in turn have concluded that bond configuration in the prism should simulate the bond configuration in the masonry structure as closely as possible. The experiments by Self (8) on bond pattern (stack or running)

in ungrouted prisms appear to support their premise. Table 6, from (8), exhibits considerable differences in compressive strength between stack-bond and running-bond ungrouted prisms. In ungrouted masonry this difference may be attributed to the following: in running bond the cross webs are not in vertical alignment and even if mortared may not effectively transmit compression through the joint. Self (8) concluded that, consequently, only the face shells (as contrasted to the net cross-sectional area) should be considered as effective bearing area in ungrouted running-bond masonry.

The current test program on grouted prisms has revealed a similar phenomenon: the compressive strength of prisms laid in running bond is significantly less than the compressive strength of prisms laid in stack bond. Table 4 shows typical results for 3- and 5-course prisms, the component properties of which are provided in Table 2. The specimens in this series were, again, precision saw-cut to the desired h/t ratio. In addition to the influence of bond type, Table 4 clearly reveals a decrease of prism compressive strength with increased number of courses for both stack-bond and running-bond masonry.

Influence of Bearing Plate Thickness

The bearing plates in the present tests were selected as solid 8 x 8 x 16-inch aluminum members, as previously noted. The reason for this selection is worth mentioning at this point.

ASTM C140 requires that steel bearing plates employed between the spherically seated head block and the test specimen shall have a thickness equal to at least one third the distance from the edge of the head block to the most distant corner of the specimen. For a typical 8-inch diameter round head block, and an 8 x 8 x 16-inch concrete block specimen, the required thickness of the bearing plate would be 1-1/2 inches.

Tests conducted by Self (8) on ungrouted prisms and Langpap (5) on grouted prisms reveal that a 1-1/2 inch bearing plate undergoes considerable bending and induces non-uniform strain distributions in blocks and/or prisms. Typical strain variations in single 8 x 8 x 16-inch two-cell hollow blocks versus plate thickness are shown in Fig. 10; this data was excerpted from (8).

The foregoing tests clearly indicate that ASTM C140 is inadequate and should be modified with respect to bearing plate thickness.

With respect to the present tests, aluminum was judged to be more acceptable than steel due to its low weight and cost, and an 8-inch thickness was, based upon independent calculations, considered a minimum thickness able to provide a reasonably uniform strain field.

Correlation with Wall Data

It was previously emphasized that 2-course prisms (couplets) laid in stack bond and capped according to ASTM C140 can lead to an over-estimate of f'_m for full-scale running-bond masonry. The magnitude of the error encountered in some cases can be observed in the data of Read and Clements (6). The walls tested in uniaxial compression were 2.6m high and 1.8m wide. Correlation between prism and wall data is illustrated in Fig. 11 for ungrouted walls. A running bond using a 1:4:3 mortar mix was employed.

SUMMARY AND CONCLUSIONS

Stack-bond prism compressive strength is seen to decrease, as much as 26 percent, with increasing number of courses. The reason for the decrease is that high strength capping materials lead to lateral restraint of the specimens at the bearing plates (platens). This restraint produces shear mode failures in 2-course prisms, while in 4- and 5-course prisms proper tensile splitting occurs in all units except possibly those adjacent to the platens.

Bond pattern (stack or running) also has a significant effect on prism compressive strength. For example, 5-course grouted prisms laid in running bond with face shell mortar bedding exhibited a strength 16 percent lower than 5-course grouted prisms laid in stack bond with full mortar bedding.

Due to the above two effects, the 2-course results were 62 percent high, based on data from 5-course prisms laid in running bond. Therefore the current wide-spread practice of evaluating f'_m from 2-course prisms laid in stack bond should be terminated.

Masonry code correction factors allow conversion of the strength of a prism of more than 2 courses to that of a standard 2-course prism. Virtually all such correction factors are based upon a common source: the preliminary and exploratory investigation by Krefeld in 1938 - on brick. The universal use of such data is clearly unjustified, and as discussed above, the strength of 2-course prisms is much higher than than of full-scale masonry. For these reasons correction factors for prism geometry should be deleted from all masonry codes.

It was found that platen restraint can be eliminated through use of a capping material having a sufficiently low shear modulus. However, the materials tested proved difficult to use, and are therefore judged not to be feasible for commercial applications. Further, it was found that compressive strength of prisms is primarily a function of the number of bed joints - not the h/t ratio. For example, grouted stack-bond prisms with 2 bed joints saw-cut to $h/t = 2.0$ exhibited strengths similar to specimens with 2 bed joints and $h/t = 3.0$ (i. e., 3 courses).

In view of the above findings, it is recommended that the compressive strength, f'_m , of concrete masonry be evaluated using prisms with not less than ^mthree nor more than four mortar bed joints. This may be accomplished with prisms of not less than four nor more than five courses. Grouted prisms may be precision saw-cut to a lower h/t ratio, commensurate with the above number of bed joints, in order to alleviate laboratory space problems. The mortar bond configuration (stack or running), the mortar bedding (face shell or full), and the grouting should, in so far as possible, be the same as is used in the structure. The ends of the prisms should be capped as set forth in ASTM C140 with the following exception: grouted prisms may be precision saw-cut, in lieu of capping, to provide smooth parallel surfaces.

APPENDIX I. -- REFERENCES

1. Foster, P.K., and D.O. Bridgeman, "Prism Tests for the Design and Control of Brick Masonry," The New Zealand Pottery and Ceramics Research Association (INC), Technical Report No. 22, 1973. (Also, see Proceedings: Institute of Civil Engineers, Part 2, Vol. 55, p. 292, March 1973).
2. Hegemier, G. A., "Mechanics of Reinforced Concrete Masonry: A Literature Survey," Report No. AMES-NSF TR-75-5, University of California, San Diego, 1975.
3. Hegemier, G. A., et al., "Prism Tests for the Compressive Strength of Concrete Masonry," Report No. AMES-NSF TR-77-1, University of California, San Diego, 1977.
4. Krefeld, W. J., "Effect of Shape of Specimen on the Apparent Compressive Strength of Brick Masonry," Proceedings: American Society for Testing Materials 38, pp. 363-369, 1938.
5. Langpap, T. V., "Concrete Masonry Prism Research Program," Technical Report M-9281, Southern California Testing Laboratory, Inc., October 1969.
6. Read, J. B., and S. W. Clements, "Strength of Concrete Block Walls, Phase II; Under Uniaxial Loading," Technical Report 42.473, Cement and Concrete Association, London, p. 17, 1972.

7. Richart, F. E., "Structural Performance of Concrete Masonry Walls," Journal of the American Concrete Institute, pp. 363-385, February 1932.
8. Self, M. W., "The Structural Properties of Load-Bearing Concrete Masonry," EIES Project D-622, Engineering and Industrial Experiment Station, University of Florida, March 1974.
9. Uniform Building Code, 1976 edition, published by the International Conference of Building Officials, 5360 So. Workman Mill Road, Whittier, California 90601.
10. Yokel, F. Y., R. G. Mathey, and R. D. Dikkers, "Strength of Masonry Walls under Compressive and Transverse Loads," U. S. National Bureau of Standards Building Science Series 34, 1971.
11. 1977 Masonry Codes and Specifications, printed and distributed by the Masonry Industry Advancement Committee, April 1977.

APPENDIX II. -- NOTATION

The following symbols are used in this paper:

- f' = gypsum plaster compressive strength
- f_m^c = masonry compressive strength
- h = prism height
- t = prism least lateral dimension

ON NONLINEAR RESPONSE PREDICTIONS OF CONCRETE
MASONRY ASSEMBLIES¹

by

S. K. Arya² and G. A. Hegemier²

ABSTRACT

Recent experimental investigations on concrete masonry indicate that the response of a masonry assemblage is nonlinear under both monotonic and cyclic loading conditions. This paper is concerned with the analytical prediction of such nonlinear response using the fundamental properties of the basic constituents of concrete masonry, which are derived from small-scale experiments on each constituent.

The finite element method is adopted as the basic analytical tool in this study, for it is the most versatile of the mathematical modeling techniques used in analyzing the behavior of structural systems. A finite element micromodel of reinforced concrete masonry is developed which has two main features; (1) a method for representing pre- and post-fracture behavior of joints or interfaces in a masonry assemblage, (2) a nonlinear material model which accounts for masonry cracking and the effects of reinforcing steel. The material model is based upon maximum tensile stress theory for cracking due to tension and the von Mises yield surface in conjunction with a strain softening, unconstrained flow rule for failure in compression. Reinforcing steel is assumed to be elastic-perfectly-plastic in both tension and compression.

The model has been implemented into an out-of-core version of the computer code NONSAP.

The effectiveness of the model is demonstrated by comparison of the predicted and experimental behavior of concrete masonry shear walls subjected to both monotonic and cyclic deformation histories. Excellent correlation between the experimental results and the analytical predictions is observed.

¹Research was sponsored by the National Science Foundation under Grant NSF ENV 74-14818.

²Principal Development Engineer and Professor, respectively; Dept. of Appl. Mech. & Engr. Sci., University of California, San Diego, La Jolla, California, 92093.

ON NONLINEAR RESPONSE PREDICTIONS OF CONCRETE
MASONRY ASSEMBLIES¹

by

S. K. Arya² and G. A. Hegemier²

INTRODUCTION

There are two basic approaches to the extremely difficult task of simulating the inelastic behavior of reinforced concrete masonry assemblages: 1) micro-level modeling, and 2) macro-level modeling. These methods serve different purposes, and both are currently under study as part of an extensive research program (8) on concrete masonry.

Micro-level modeling attempts to synthesize the behavior of a masonry assemblage from elementary component data. Hence, this is a fundamental and open-ended approach which commences at the constituent level and requires detailed knowledge of the properties of each constituent and constituent interface behavior under various stress states and histories. The necessary data can be extracted from small-scale laboratory tests.

Macro-level modeling is based upon a continuum representation of masonry. In contrast to micro-level modeling, the resulting theory is primarily phenomenological. Evaluation of the unknown parameters in such a model must be accomplished by experiments on assemblages of sufficient size to mirror full-scale masonry. These experiments may consist of actual laboratory tests, or micro-model simulations of such tests.

The micro-modeling approach is considered to be an excellent analysis tool in view of the degree of details that can be simulated in a masonry assemblage, and because it provides insight into the basic phenomena of masonry behavior. The primary function

¹Research was sponsored by the National Science Foundation under Grant NSF ENV 74-14818.

²Principal Development Engineer and Professor, respectively; Dept. of Appl. Mech. and Engr. Sci., University of California at San Diego, La Jolla, California, 92093

of this technique is the analysis of structural elements. For example, given a successful micromodel of reinforced concrete masonry, one can then study, in an orderly manner, the behavior of structural components such as shear walls, piers, spandrels, columns, etc. That is, one could replace costly experiments involving a vast array of different geometrical configurations of masonry and steel, as well as different boundary conditions, by direct numerical simulations.

It is not intended that the micro-level modeling process be used to analyze a full structure. This is the function of the less detailed, but more efficient macro-level modeling.

This paper is concerned with an exposition of the current micro-level modeling approach. The basic elements of this approach consist of 1) a nonlinear material model for the masonry-steel composite, 2) a nonlinear theory for the pre- and post-fracture behavior of joints or interfaces in a masonry system, 3) the finite element method, and 4) a modified version of the finite element program NONSAP (4). The material model employed (2) is two-dimensional and accounts for masonry cracking, masonry crushing, and the effects of reinforcing steel on the properties of an assemblage. The interface-slip model (3), which is based upon a double noding scheme, accounts for joint slip, separation and recontact.

In the following sections, which constitute a condensation of Refs. 2 and 3, important features of the micro-model are described. While the micro-model is applicable to any two-dimensional concrete masonry assemblage, its application has, to date, been confined to shear walls. In this paper, three numerical examples concerning the prediction of the inelastic response of a shear wall subjected to quasi-static monotonic and cyclic loading are presented.

It should be noted that this study represents the first attempt in developing a finite element micro-model of reinforced concrete masonry.

MATERIAL MODEL

In this section the constitutive relations for the pre- and post-fracture behavior of reinforced concrete masonry are developed. These relations are derived for subsequent use in a two-dimensional finite element analysis (tangent stiffness approach) under plane stress conditions. Time-dependent phenomena such as creep, and geometric nonlinearities are not considered.

Since the basic constituents of reinforced concrete masonry are essentially concrete (block, grout, mortar) and steel, it is quite appropriate to extract useful information from the literature on reinforced concrete.

Analytical studies of the response of reinforced concrete structures by means of the finite element method have received increasing attention from many investigators in the recent past. Different aspects of this approach have been reviewed by Argyris (1), Schnobrich (11), and Scordelis (12).

Several different approaches have been used in modeling the behavior of reinforced concrete structures. A popular approach (5, 9, 10) is to divide a reinforced concrete element into imaginary layers of concrete and steel (with zero shear stiffness). In this approach cracking and material nonlinearity are taken into account by altering progressively the constitutive equations of the material during the incremental solution procedure. Thus, in general, the tangent stiffness matrix and the residual force vector are reformulated at each step of the iterative process. The material model developed under this study is based upon a similar approach; only the details are different.

Basic Assumptions and Limitations

As mentioned earlier, the material model developed in this study is two-dimensional and is limited to plane stress conditions. Further, it is assumed that the analysis will be performed using an incremental procedure which is based on the instantaneous or tangent stiffness approach in which the incremental constitutive relations are written as

$$\{d\sigma\} = [D] \{d\epsilon\} \quad (1)$$

where $\{d\sigma\}$ = incremental stress vector, $\{d\epsilon\}$ = incremental strain vector, and $[D]$ = linear matrix of elastic coefficients.

Concrete Masonry

Concrete masonry is assumed elastic and brittle in tension, and elastic and strain-softening in compression. The von Mises yield criterion is used for failure in compression and the maximum tensile stress theory is adopted for cracking due to tension. The assumed yield or failure curve is shown in Fig. 1. This curve results from an intersection of the von Mises cylinder in principal stress space

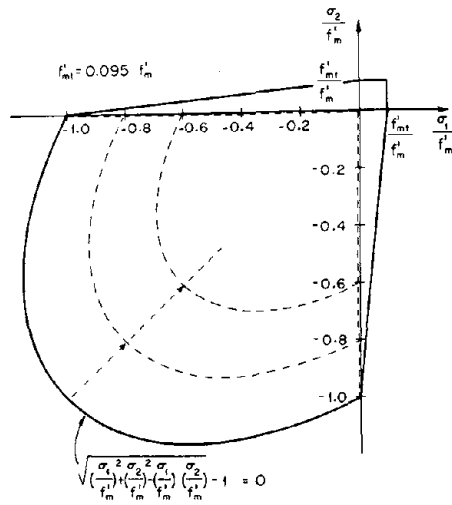


Fig. 1. Assumed Failure Curve for Concrete Masonry

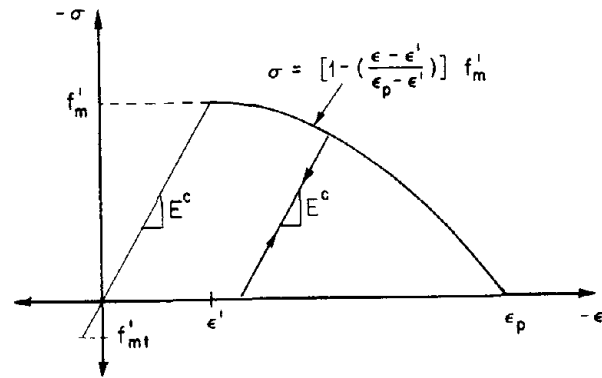


Fig. 2. Assumed Stress-Strain Behavior of Concrete Masonry

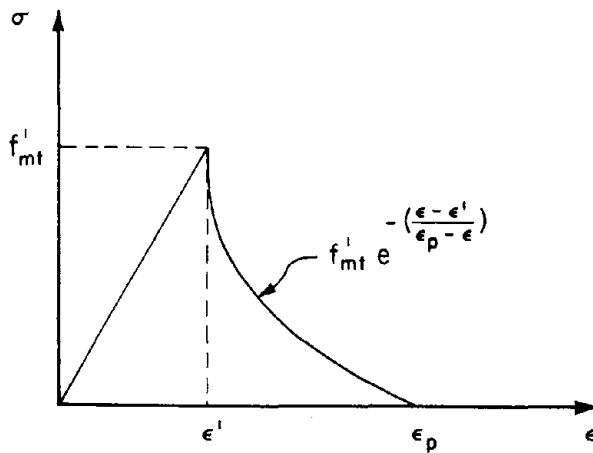


Fig. 3. Assumed Stress-Strain Behavior of Reinforced Concrete Masonry in Uniaxial Tension

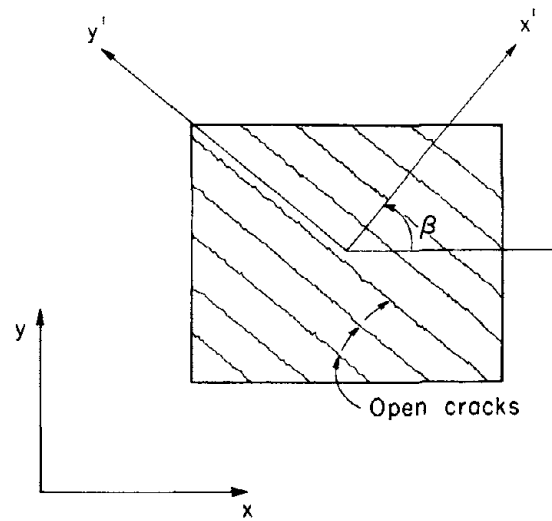


Fig. 4. A Cracked Element with One Set of Open Cracks

with σ_1, σ_2 principal stress plane. The material is assumed elastic and isotropic before the yield curve is reached. Thus, if unloading takes place interior to this curve, no permanent deformation occurs. Loading beyond the yield curve is assumed to follow another failure curve which gradually shrinks to the origin, thus exhibiting a strain-softening behavior. This curve is obtained by relating the octahedral shear stress to the octahedral shear strain and invoking radial unloading in stress space. Thus, the amount of shrinking is considered to be a function of the principal strains. The new strength of masonry after it has reached the yield curve is defined to be

$$f'_m = \left[1 - \left(\frac{\epsilon - \epsilon'}{\epsilon_p - \epsilon'} \right)^2 \right] f'_m ; \epsilon \geq \epsilon' \quad (2)$$

where f'_m = ultimate strength of masonry, ϵ_p = complete collapse strain in uniaxial compression test, ϵ = octahedral shear strain, ϵ' = value of ϵ at yield, and ϵ_1, ϵ_2 = principal strains.

A collapse curve is postulated to define the complete collapse or crushing of masonry at which it loses all its strength and stiffness. The collapse curve is defined as

$$\sqrt{\epsilon_1^2 + \epsilon_2^2 - \epsilon_1 \epsilon_2} - \epsilon_p = 0 \quad (3)$$

The assumed stress-strain relationship for masonry in uniaxial loading condition is shown in Fig. 2. Note that the unloading and reloading stiffness is the same as the initial elastic stiffness. Work is currently underway to make this stiffness a function of the strain history.

In tension cracking, the cracks are assumed "smeared" or distributed evenly across the element. The crack direction is normal to the major principal stress in masonry just prior to cracking. The cracked masonry is considered continuous, anisotropic, and capable of resisting only stresses parallel to the cracks. Further, the quantity f'_m is assumed to decrease with the opening cracks after reaching a certain normal strain ϵ_n^* . This assumption is based upon the observation that a cracked element with open cracks cannot sustain the full f'_m parallel to such cracks.

. Reinforcing Steel

It is assumed that the reinforcing steel is laid parallel to the coordinate axes. The reinforcement in each direction is replaced

by an equivalent layer of steel which is uniformly distributed and has stiffness only in the direction of reinforcement. The reinforcing steel is assumed to be elastic-perfectly-plastic in both tension and compression.

. Reinforced Concrete Masonry

Perfect compatibility of displacements is assumed between steel and masonry. This means the effect of bond slip is not considered in this model. However, the effect of bond on the strength of cracked masonry is included. Specifically, for a reinforced element the strength of masonry normal to the cracks is not dropped to zero immediately at the onset of cracking. Instead, as indicated in Fig. 3, it decays exponentially to zero when the reinforcing steel yields.

In a reinforced concrete masonry element, the principal stress directions and the principal strain directions differ due to the anisotropy of the element. Also, the masonry principal stress directions deviate from the total principal stress directions. In this model, it is assumed that masonry cracks when the masonry principal stresses satisfy the fracture criterion (Fig. 1).

Constitutive Relations

Consider a rectangular reinforced concrete masonry element in cartesian coordinates subject to plane stress conditions. Let r_x and r_y be the reinforcement area ratios in the x and y directions, respectively. Reinforcing area ratio is defined as the ratio of reinforcement area to the area of composite section.

The stresses in the composite element can be derived by superposing the stresses in the concrete masonry element and the steel layer element which has no shear stiffness:

$$\{\sigma\} = \{\sigma^c\} + \{\sigma^s\} \quad (4)$$

where the superscripts c and s designate concrete masonry and steel, respectively.

The incremental constitutive relations of Eq. 1 can now be written as

$$\begin{aligned} \{d\sigma\} &= \{d\sigma^c\} + \{d\sigma^s\} \\ &= [D^c] \{d\epsilon\} + [D^s] \{d\epsilon\} \\ &= [D] \{d\epsilon\} \end{aligned} \quad (5)$$

in which

$$[D] = [D^c] + [D^s] \quad (6)$$

It remains now to derive the constitutive tensors $[D^c]$ and $[D^s]$ for different states of the element.

. Uncracked Element

For the uncracked element both masonry and steel are assumed to be elastic, and masonry obeys Hooke's law for isotropic material in the plane stress condition. Thus,

$$[D^c] = \frac{E^c}{1 - \nu^2} \begin{bmatrix} 1 & \nu & 0 \\ \nu & 1 & 0 \\ 0 & 0 & (1-\nu)/2 \end{bmatrix} \quad (7)$$

and

$$[D^s] = E^s \begin{bmatrix} r_x & 0 & 0 \\ 0 & r_y & 0 \\ 0 & 0 & 0 \end{bmatrix} \quad (8)$$

in which E^c , E^s = elastic moduli for masonry and steel, respectively, and ν = Poisson's ratio for masonry.

. Cracked Element

Consider a cracked element as shown in Fig. 4 with one set of open cracks at an angle $(\beta + \pi/2)$ with the horizontal axis. The x' , y' system denotes the principal stress coordinate system for the element. In view of the assumption that the cracked element has no stiffness normal to the cracks, the constitutive tensor for masonry, $[D^c]'$, in the prime system is assumed as follows:

$$[D^c]' = \begin{bmatrix} 0 & 0 & 0 \\ 0 & E^c & 0 \\ 0 & 0 & \lambda G \end{bmatrix} \quad (9)$$

where G is the shear modulus for uncracked masonry, and $\lambda(\epsilon'_x)$ is a parameter which is used to estimate the effective shear modulus

(in the prime system) due to dowel action and aggregate interlock. The quantity λ decreases with opening of the cracks.

The incremental strains in the two coordinate systems are related by the equation

$$\{d\epsilon\}' = [T] \{d\epsilon\} \quad (10)$$

in which the transformation matrix $[T]$ is given by

$$[T] = \begin{bmatrix} \cos^2 \beta & \sin^2 \beta & \cos \beta \sin \beta \\ \sin^2 \beta & \cos^2 \beta & -\cos \beta \sin \beta \\ -2 \cos \beta \sin \beta & 2 \cos \beta \sin \beta & \cos^2 \beta - \sin^2 \beta \end{bmatrix} \quad (11)$$

The incremental constitutive relations for masonry in the two coordinate systems are

$$\{d\sigma^c\} = [D^c] \{d\epsilon\} \quad , \quad \text{and} \quad \{d\sigma^c\}' = [D^c]' \{d\epsilon\}' \quad (12)$$

It can readily be shown (2) that

$$[D^c] = [T]^T [D^c]' [T]. \quad (13)$$

The constitutive tensor $[D^s]$ is still given by Eq. 8 if the reinforcement in both the directions is elastic or the stresses in the reinforcement are below the yield stress of steel. When the reinforcement reaches its yield point, the corresponding stiffness is set equal to zero. Thus, $[D^s]$ becomes a null matrix if reinforcement in both the directions has reached the yield point.

It is evident from Eq. 9 that the constitutive tensor $[D^c]$ of Eq. 13 is singular. Consequently, a cracked element without reinforcement or where the reinforcement in both the directions has yielded, is unstable unless the displacements normal to the cracks are constrained. These displacements are normally constrained due to the stiffness of surrounding elements. However, if the surrounding elements have also cracked and the crack directions are the same, the element will be unstable. This situation is rare but can happen. To circumvent this difficulty a small artificial stiffness is assigned to those diagonal terms of the composite constitutive tensor $[D]$ which are theoretically zero.

A cracked element, in general, is considered to have two sets of cracks. The second set of cracks can form while the first set is either open or closed. If the first set is open, the second set will be normal to the first. If the first set is closed, then the orientation of the second set will depend on the orientation of the masonry principal stresses. From two sets of cracks, six different crack patterns or configurations are possible: first set open; first set closed; first set closed and second set open; both sets open; first set open and second set closed; and both sets closed.

The constitutive tensor $[D^c]$ of Eq. 13 is valid when there is one set of open cracks and the stress in masonry parallel to the cracks is less than the ultimate strength, f_m' . If both sets of cracks are open, $[D^c]$ becomes a null matrix. When both sets are closed, the element is considered to regain its elastic stiffness, except the shear stiffness term which is assumed to be λG , where a value of 0.8 is currently used for λ .

. Crushing of Masonry

This situation arises when masonry stresses satisfy the von Mises yield criterion. In the classical theory of plasticity for ductile metals, the associated or normality flow rule is usually assumed to derive the post-yielding constitutive relations. However, the inelasticity of masonry is caused by the cumulative effect of micro-cracking, instead of any actual plastic flow. Therefore, it is probably not appropriate to use the normality flow rule for masonry. Secondly, concrete masonry exhibits a strain-softening behavior after the ultimate strength is reached. Thus, the assumed stress-strain behavior for masonry, as shown in Fig. 2, has negative stiffness in the post-yielding region. Inclusion of negative stiffness terms in the constitutive tensor may cause numerical difficulties (stiffness matrix may not be positive definite) in the solution of equilibrium equations in the finite element procedure. Consequently, a null matrix is used for the constitutive tensor $[D^c]$ in the post-yielding region. Stresses in masonry, however, are governed by the assumed yield curve of Fig. 2, and therefore adjusted accordingly.

As shown in Fig. 2, the stiffness for unloading and reloading behavior of crushed masonry is assumed to be the initial elastic stiffness. Thus, the constitutive tensor $[D^c]$ will be the same as that of uncracked masonry, which is given by Eq. 7.

If a masonry element has reached the crushing state once, it is not permitted to carry any tension in the future. In case tensile

stresses develop, masonry is completely disrupted and from then on the element is considered as a void.

INTERFACE MODEL

Mortar joints and grout-block interfaces in concrete masonry assemblies constitute planes of weakness and a major source of stiffness degradation and damping. Failures frequently initiate in joints, and subsequent deformation and energy absorption may occur by relative slip across joint planes. Thus, an interface model is necessary for micro-scale modeling of concrete masonry assemblies.

Several investigators (6, 7, 13), with an objective of representing the joint behavior in rocks with a finite element, have developed so-called "slip or joint elements" and have apparently achieved moderate success in simulating the gross behavior of some physical problems. However, in using these slip elements for simulating interfaces or joints with thicknesses small in comparison to other typical problem dimensions, one encounters serious difficulties. First, one must assume a pseudo thickness for the element. To achieve acceptable numerical accuracy a small relative thickness is necessary. This, however, creates the well-known aspect ratio problem. Second, to maintain normal-displacement compatibility across the interface, one must assume a very large stiffness in this direction which, in addition to creating an ill-conditioned stiffness matrix, causes difficulty in simulating actual interface debonding.

In view of the above-mentioned drawbacks of the slip element approach there is an urgent need for a better understanding of the interface problem and development of methods which can simulate the physical behavior more accurately and with fewer difficulties. The method (3) developed in this study eliminates the need for constructing a two-dimensional element to represent an interface, thus avoiding the difficulties due to pseudo thickness and fictitious material properties. The method employs a direct approach in representing both the debonding and slip characteristics of an interface and is conceptually very simple. It is iterative in nature and can treat any non-linear material behavior including a velocity-dependent friction law without difficulty. A brief description of the method is given in the following sections; the details can be found in Ref. 3.

The Model

The physical behavior of an interface is nonlinear and, in general, non-conservative due to the presence of sliding friction. The main characteristics of the problem are; 1) no cracking, 2) debonding, and 3) recontact and/or sliding along the tangential direction.

Within the context of the finite element method an interface discontinuity is represented by a series of double nodes, one on each side of the interface but having the same coordinates. While a double-node pair may be in any one of the three cases mentioned above, the equilibrium equations for the whole structure are first assembled by assuming that the double nodes are free to move. These equations are then modified to simulate the actual state of each double-node pair.

. Case 1 - No Cracking

When the actual nodal forces at a double-node pair are less than the strength of the pair, there is no separation or sliding of the nodal points. Thus, the pair is treated as a continuum and both displacement compatibility and equilibrium conditions are satisfied in both tangential and normal directions. The computation of the strength of a double-node pair depends on the material properties of the interface in tension and shear. The interface is assumed to obey the following friction law:

$$\sigma_t^* = c - \mu \sigma_n \quad (14)$$

where σ_t^* = allowable shear stress, σ_n = normal stress, and c and μ represent the cohesion and the coefficient of friction, respectively. The coefficients c and μ are not constants. Instead, they are assumed to be functions of the relative tangential displacement at the interface, such that

$$c = c_0 - \frac{2(c_0 - c_1)}{x_c} \cdot x + \frac{(c_0 - c_1)}{x_c^2} \cdot x^2 \quad 0 \leq x \leq x_c, \quad (15a)$$

$$c = c_1 \quad x > x_c, \quad (15b)$$

$$\mu = \mu_0 - \frac{2(\mu_0 - \mu_1)}{x_\mu} \cdot x + \frac{(\mu_0 - \mu_1)}{x_\mu^2} \cdot x^2 \quad 0 \leq x \leq x_\mu, \quad (15c)$$

$$\mu = \mu_1 \quad x > x_\mu, \quad (15d)$$

where x = sum of tangential displacements (absolute values),
 c_0 = cohesion before cracking, c_1 = minimum cohesion after cracking,
 x_0 = maximum x at which minimum cohesion is attained, μ_0 = coef-
 ficient of friction before cracking, μ_1 = minimum coefficient of friction
 after cracking, and x_μ = maximum x at which minimum coefficient of
 friction is attained.

The quantities for the coefficients c_0 , c_1 , etc., and the allowable tensile stress (σ_n^*) are determined by simulating experimental data from joint or interface tests, and conducting parametric studies for several loading conditions.

• Case 2 - Debonding

If the normal force at a double-node pair is tensile, and if it exceeds the tensile strength of the pair or if the tangential force exceeds the shear strength of the pair, nodal point separation occurs. Thus, they are treated as free nodal points; i. e., the nodal displacements are independent of each other, and no force is transmitted by such a nodal pair.

• Case 3 - Recontract and/or Sliding

In this situation the normal force is compressive and there is a relative movement of nodal points in the tangential direction. The normal force is transmitted completely by the nodal pair, but the shear force between the nodes is less than or equal to the shear strength of the pair. This situation is treated by imposing compatibility of normal displacements and treating tangential displacements independently while still transmitting the shear force between the nodes.

FINITE ELEMENT PROCEDURE

As mentioned earlier, the micro-model developed in this study is based upon the tangent stiffness approach of the incremental finite element procedure for numerical integration of the equations of equilibrium of a discretized system; the model is implemented into an out-of-core version of NONSAP (2).

The incremental form (2) of the equations of equilibrium of a finite element model is

$$[\tilde{K}]_{i-1} \{\Delta u\}_i = \{\tilde{R}\}_{i-1} \quad (16)$$

where $[\tilde{K}]$ is the effective stiffness matrix, $\{\tilde{R}\}$ is the effective load vector, $\{\Delta u\}$ is the incremental displacement vector, and i represents the equilibrium iteration.

It is clear from the above discussion that, in general, the incremental finite element analysis of the response of a reinforced concrete masonry structure requires recomputation or updating of the effective stiffness matrix $[\tilde{K}]$ and the effective load vector $\{\tilde{R}\}$ of Eq. 16 at each iteration of the solution procedure. The updating of these matrices is necessitated by the progressive change in the stiffness and strength characteristics of the structure due to cracking and/or crushing of masonry, debonding, recontact and/or slipping at interfaces, and yielding of reinforcement.

Two criteria are used to establish convergence of the solution during equilibrium iterations: one based on displacements and the other upon nodal forces. The convergence criterion for displacements is given by

$$\frac{\|\{\Delta u\}_i\|}{\|\{u\}_{i-1}\|} \leq 10^{-6} \quad (17)$$

where $\|\ \|$ designates the Euclidean norm of a vector.

In the force criterion, the solution is assumed to be converged if

$$\frac{\|\{\tilde{R}\}_{i-1}\| - \|\{\tilde{R}\}_i\|}{\|\{\tilde{R}\}_{i-1}\|} \cong 10^{-10} \quad (18)$$

The equilibrium iterations are terminated if either of the above criteria is satisfied.

The computational procedure for each load increment of the incremental analysis of the response of a reinforced concrete masonry assemblage can be summarized as follows:

- (1) Assume a load increment and compute the load vector $\{R\}_{t+\Delta t}$.
- (2) Construct $[\tilde{K}]$ and $\{\tilde{R}\}$ using the constitutive tensor $[D]_t$ from the previous step, and solve Eq. 16 for $\{\Delta u\}$.
- (3) Compute the incremental stresses and strains in both the masonry and steel:

$$\{d\sigma^c\} = [D^c]_t \{d\epsilon\}$$

$$\{d\sigma^s\} = [D^s]_t \{d\epsilon\} .$$

- (4) Compute total stresses and strains in masonry and steel:

$$\{\sigma^c\}_{t+\Delta t} = \{\sigma^c\}_t + \{d\sigma^c\}$$

$$\{\sigma^s\}_{t+\Delta t} = \{\sigma^s\}_t + \{d\sigma^s\} .$$

- (5) Check for slipping, cracking, crushing, yielding, or any change in crack configurations and the status of slip-nodes. If nothing is changed, go to step (9).
- (6) Compute allowable stresses for each cracked element and set element stresses to these values.
- (7) Reconstruct $[\tilde{K}]$ and $\{\tilde{R}\}$ using appropriate constitutive tensors for masonry and steel; modify $[\tilde{K}]$ and $\{\tilde{R}\}$ for interface conditions; solve for $\{\Delta u\}$.
- (8) Go to step (3).
- (9) Check for solution convergence. If the desired convergence is not achieved, perform necessary equilibrium iterations, updating stresses and strains in each iteration. If the cracking status of any element changes during these iterations, go to step (6)
- (10) Print the solution vectors, if needed.
- (11) Go to step (1), if more load increments are needed; otherwise stop.

NUMERICAL EXAMPLES

In this section the results of three example problems are discussed where the micromodel developed in this study is used in predicting the response of a shear wall specimen subjected to monotonic and cyclic loading conditions. The experiments which were conducted at the Earthquake Engineering Research Center of the University of California, Berkeley, are described in a separate technical report which is under preparation.

The experimental setup of a shear wall specimen, as shown in Fig. 5, consists of top and bottom load beams, two side columns to prevent rotation of the top beam, a pair of hydraulic actuators for applying horizontal load or displacement, a mechanism for applying vertical compression, and a concrete base on which the specimen is constructed and bolted to the floor. The actuators are supported by heavily-braced reaction frames (not shown in the figure).

The specimens were constructed from 8 x 8 x 16-inch two-cell, type N hollow concrete blocks, and were fully grouted. The top and bottom spandrels were heavily reinforced to prevent any cracking in them. Each specimen had a height of 56 inches and a width of 48 inches, excluding the spandrels.

Example 1

In the first example, a reinforced specimen is considered in which the outermost cores of the specimen have a vertical reinforcement of one #5 re-bar. The specimen is subjected to a constant vertical confining pressure of 50 psi and a monotonically increasing shear deformation by controlling horizontal displacement of the actuators.

For the finite element analysis of the problem, the shear wall assembly is discretized into a system of two-dimensional plane stress elements for the masonry, spandrels, top beam, and truss elements for the side columns, as shown in Fig. 6. The discretized system has 5 element groups of different materials which are described in Tables 1 and 2. Materials 1 through 3 are assumed to be linear isotropic, and materials 4 and 5 are considered to obey the nonlinear model developed in this study. Referring to Fig. 6, the bottom spandrel of the specimen is not included in the analysis and the base is assumed fixed.

The finite element model also has three types of interfaces; head-joint interface, grout-web interface and an artificial interface representing the common point of the above two interfaces. The

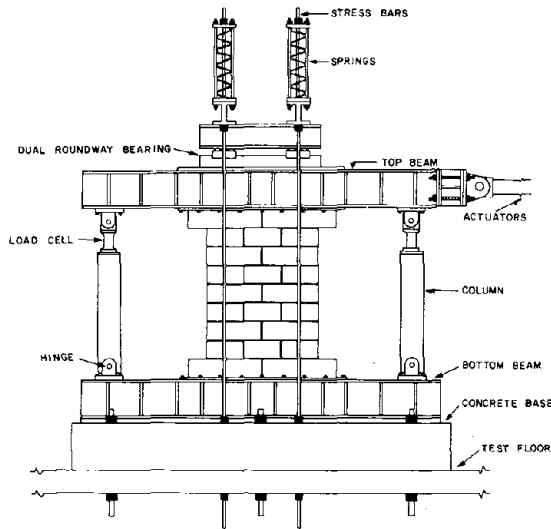


Fig. 5. Shear Wall Test Setup

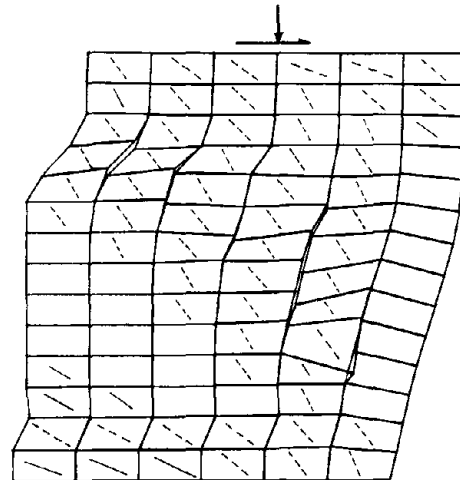


Fig. 8. Critical Def. Shape - Rein. Spec. - Mono. Load. - Scale Fac. =5

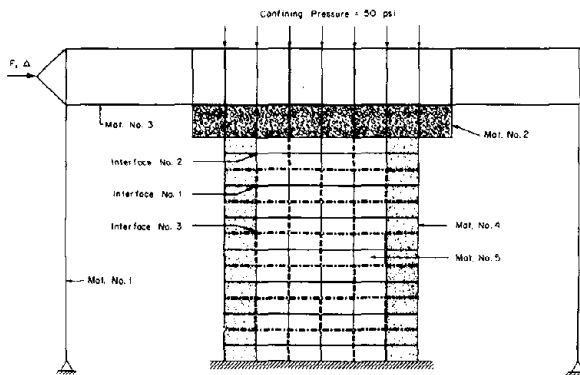


Fig. 6. Finite Element Model of the Shear Wall Specimen

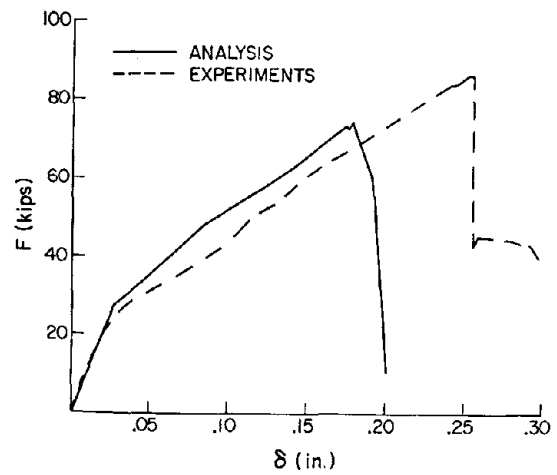


Fig. 9. F- δ Curves for the Unreinforced Specimen-Monotonic Loading

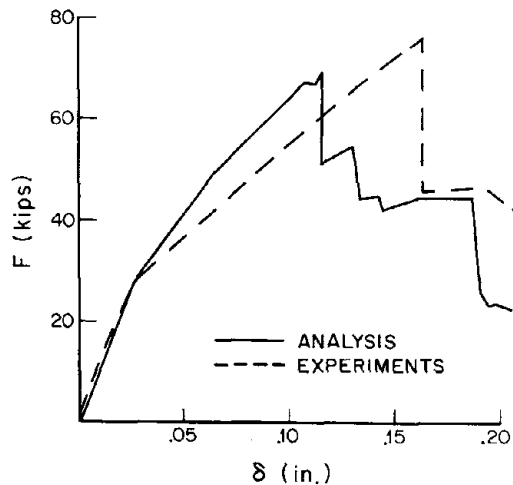


Fig. 7. F- δ Curves for the Reinforced Specimen-Monotonic Load.

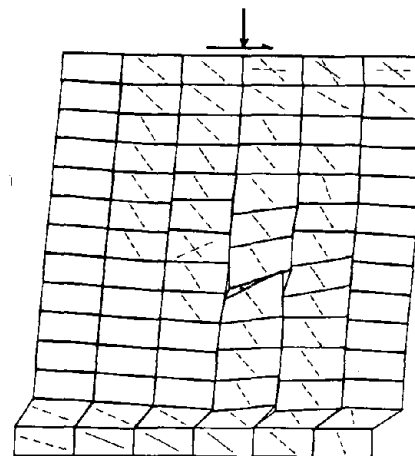


Fig. 10. Critical Def. Shape-Unrein. Spec. - Mono. Load. - Scale Fac. =3

Table 1. Material Properties Used for Linear Element Groups

Material Ident.	Description	Element Type	Young's Modulus (E), psi	Poisson's Ratio, ν	Cross-Sectional Area, in. ²
1	Steel	Truss	2.97×10^7	-	3.0*
2	Concrete	Plane Stress	3.00×10^6	0.20	-
3	Steel	Plane Stress	2.97×10^7	0.30	-

* Equivalent solid section having the stiffness of experimental column.

Table 2. Material Properties Used for Nonlinear Element Groups

Property #	Description	Quantity
1	Young's Modulus of Masonry (E^c)	8.00×10^5 psi
2	Young's Modulus of Steel (E^s)	2.97×10^7 psi
3	Compressive Strength of Masonry (f'_m)	2.50×10^3 psi
4	Yield Strength of Steel (f_y)	6.00×10^4 psi
5	Average Poisson's ratio (ν)	0.18
6	Tensile Strain Normal to a Crack at which Shear Modulus Become Zero (λ)	0.01
7	Maximum Stress Drop Allowed during One Iteration (σ_d)	2.00×10^2 psi
8	Minimum Young's Modulus Used	1.00×10^5 psi
9	Tolerance on Crack Closure (ϵ^*)	1.00×10^{-5}
10	Tensile Strain Normal to a Crack at which the Material Stiffness Parallel to the Crack Becomes Zero	2.50×10^{-3}
11	Complete Collapse Strain (ϵ_p)	8.00×10^{-3}

* Quantities determined experimentally.

Table 3. Interface Properties Used in the Analysis

Coeff.	Units	Interface Type			Description
		(1) Head-Joint	(2) Grout-Web	(3) Common Point	
c_0	psi	6.00×10^1	1.00×10^5	1.00×10^5	Cohesion Before Cracking.
c_1	psi	2.00×10^1	1.00×10^5	1.00×10^5	Minimum Cohesion After Cracking
x_c	inch	0.50	0.50	0.50	Maximum x at which c_1 is Attained
μ_0		0.70	0.80	0.75	Coeff. of Friction Before Cracking
μ_1		0.30	0.40	0.30	Minimum Coeff. of Friction After Cracking
x_μ	inch	0.50	0.50	0.50	Maximum x at which μ_1 is Attained
σ_n	psi	1.50×10^1	1.00×10^2	6.00×10^1	Tensile Strength

Note: x = sum of the absolute values of the relative incremental displacements in the tangential direction.

properties of these interfaces are given in Table 3. It should be noted that in the actual specimen the head-joint plane and the grout-web plane have an offset of about 1 inch, thus preventing any slipping at the grout-web interface. This effect is included in the finite element model by assigning large quantities to the cohesion of interfaces 2 and 3, as indicated in Table 3. In determining the tensile strength of the grout-web interface, it was assumed that the tensile force is primarily resisted by the face-shells. No interfaces are considered along the bed joints for two reasons: First, since the specimen is fully grouted there are no real interfaces in the grout cores; second, the inclusion of bed joint interfaces would increase the cost of analysis significantly.

The discretized system has 376 degrees of freedom with a bandwidth of 30. Referring to Fig. 6, at 7 nodal points of the top beam a vertical force corresponding to 50 psi confining pressure is prescribed, which remains constant for all load steps. The system is subjected to a monotonically increasing shear deformation by prescribing the horizontal displacement, Δ , at the center nodal point of the left edge of the top beam. The force, F , corresponding to the prescribed Δ is given by the horizontal component of the internal resisting force vector at the nodal point at the conclusion of equilibrium iterations.

The force, F , is graphed versus the horizontal displacement, δ , of the top left-hand corner of the masonry part of the specimen. Such a force-deflection curve is shown in Fig. 7 where it is compared with the corresponding curve obtained from the experiments. The correlation of the analytical and experimental results is good to excellent, depending upon the basis of comparison. For example, the predicted ultimate strength of the specimen is within 10% of the experimental value. Also, the analytical model correctly predicts the brittle behavior of masonry. In regard to the stiffness characteristics, considerable stiffness degradation is observed. The correlation is good, considering the complexity of the specimen and the test equipment. The contributing factors for the discrepancy between the analytical and experimental results are, possibly, the following: 1) Slipping of the specimen at the lower spandrel at higher loads; 2) Microcracking in the lower spandrel at higher loads; 3) Flaws in the specimen, particularly in grout cores.

The deformed shape of the specimen (masonry part only) immediately after the big diagonal crack is shown in Fig. 8. The corresponding cracking pattern in the specimen is also depicted in this figure. It is evident from Fig. 8 that the specimen undergoes a brittle failure, and at failure the major crack is the diagonal crack from the bottom-right to the top-left.

Example 2

This example is identical to the previous one except that the specimen is not reinforced. The analytical and experimental procedures used in this case are similar to those of the previous example and hence will not be repeated here.

The force-deflection curves for the unreinforced specimen under monotonic loading are shown in Fig. 9. Again, the correlation between the analytical and experimental results is good. Comparing Figs. 7 and 9, it appears that there is some discrepancy in the experimental results of this example, for it gives a much higher collapse load when compared to the reinforced specimen. It is possible that either the quality control of this specimen was much better than the previous one, or the material was of higher strength.

Fig. 10 shows the critical deformed shape of the specimen, including the cracking pattern. Referring to Figs. 8 and 10, the angle of the large diagonal crack at failure is slightly less in the unreinforced specimen compared to the reinforced case.

Example 3

In this example the reinforced specimen of Example 1 is subjected to a constant vertical confining pressure of 50 psi and a cyclic shear deformation. For the experimental specimen, the cyclic shear was applied in an increasing amplitude sequence of sinusoidal displacement cycles at 3 Hz, with three cycles of each amplitude. The amplitudes were (in inches): 0.02, 0.04, 0.08, 0.12, 0.14, 0.16, 0.20, 0.25, 0.30, 0.35, 0.40, 0.45, 0.50, and 0.55. Thus, in all, the specimen was subjected to 42 cycles.

In the finite element analysis, the specimen is subjected to only five cycles of quasi-static displacement input, in the interest of computational costs. The displacement amplitudes for the five cycles are (in inches): 0.05, 0.05, 0.10, 0.1225, and 0.1225. It should be noted that it is not the intent of this analysis to predict the system response corresponding to each experimental cycle. Instead, the objective here is to predict the failure envelope of the specimen under cyclic loading.

The analytical and a few selected experimental force-deflection curves for the reinforced specimen under cyclic loading are shown in Fig. 11. And, the corresponding failure envelopes are shown in Fig. 12. Both stiffness and strength degradation are evident.

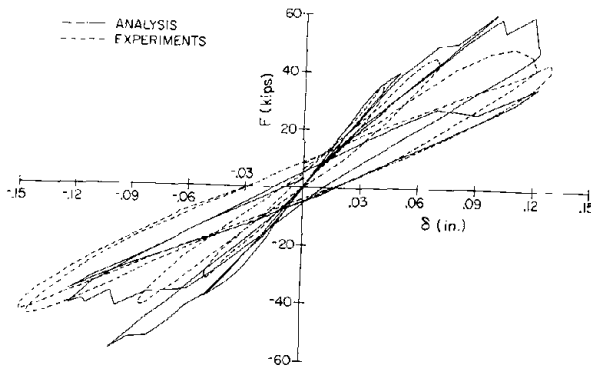


Fig. 11. F- δ Curves for the Reinforced Specimen-Cyclic Loading

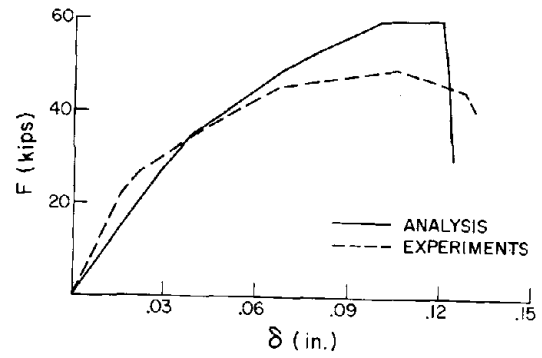
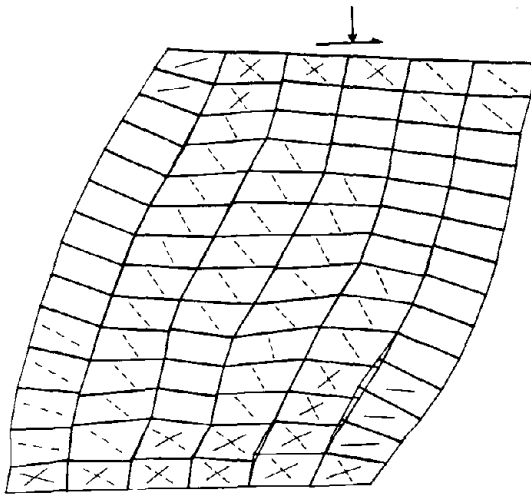
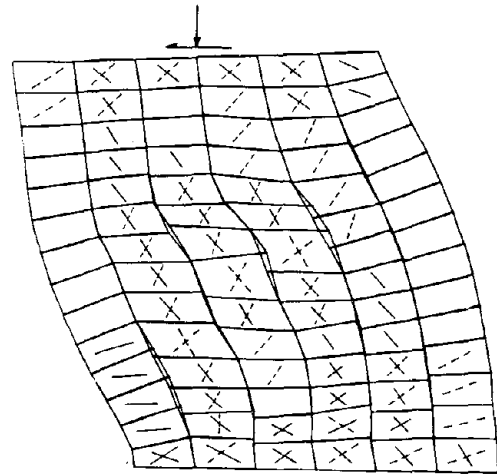


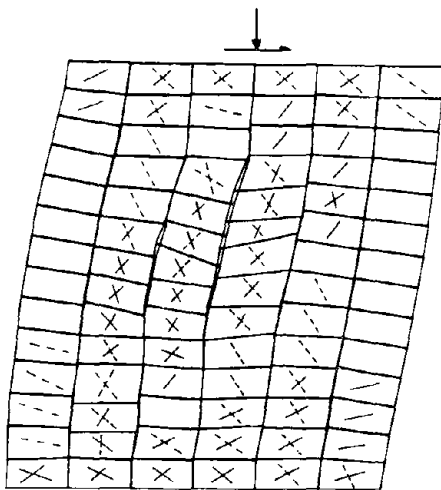
Fig. 12. Failure Envelopes of the Reinforced Specimen-Cyclic Load.



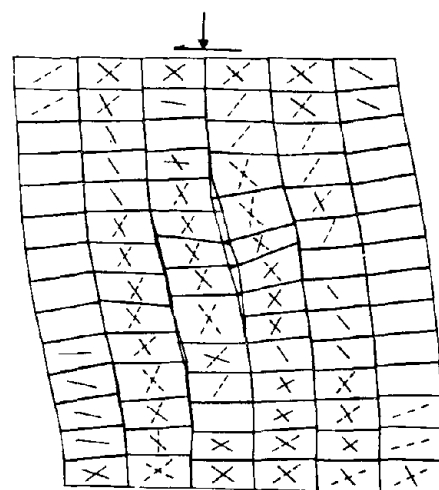
a. @ $\Delta = .1225$ in. (4th Cycle) - Scale Factor = 20



b. @ $\Delta = -.1225$ in. (4th Cycle) - Scale Factor = 15



c. @ $\Delta = .1225$ in. (5th Cycle) - Scale Factor = 7



d. @ $\Delta = -.1225$ in. (5th Cycle) - Scale Factor = 7

Fig. 13. Selected Deformed Shapes-Reinforced Specimen-Cyclic Load.

Overall there is a good correlation between the analytical and experimental results in spite of the fact that the analytical results do not include dynamic effects.

Figs. 13a through 13d depict selected deformed shapes of the specimen, including the cracking pattern. It is evident from these figures that the analytical model correctly predicts the dominant diagonal cracks.

SUMMARY

This paper represents the first attempt to develop a finite element micro-model of reinforced concrete masonry, and to synthesize the behavior of complex structural elements from the basic constituent properties. It appears that the complex behavior of concrete masonry assemblages such as shear walls and piers under both monotonic and cyclic loading in the nonlinear regime of material response can be rationally predicted from the basic component data.

APPENDIX I. - REFERENCES

1. Argyris, J.H., G. Faust, J. Szimmat, E. P. Warnke and K. J. William, "Recent Developments in the Finite Element Analysis of Prestressed Concrete Reactor Vessels," Nuclear Engineering and Design, Vol. 28, 1974.
2. Arya, S.K. and G. A. Hegemier, "A Nonlinear Material Model for Reinforced Concrete Masonry with Application to Shear Walls," Report No. UCSD/AMES/TR-77-5, University of California, San Diego, April 1978.
3. Arya, S.K., "A Method for Incorporating Interface Discontinuities in Finite Element Analysis with Application to Concrete Masonry Rheology," Weidlinger Associates, Report No. R-7522, prepared for University of California, San Diego, Aug. 1975.
4. Bathe, K. J., E. L. Wilson and R. H. Iding, "NONSAP- A Structural Analysis Program for Static and Dynamic Response of Nonlinear Systems," Report No. UC SESM 74-3, University of California, Berkeley, Feb. 1974.
5. Cervenka, V. and K.H. Gerstle, "Inelastic Analysis of Reinforced Concrete Panels," Publications, International Association for Bridges and Structural Engineering, Zurich, Switzerland, Vol. 31, 1971, and Vol. 32, 1972.
6. Ghaboussi, J., E. L. Wilson, and J. Isenberg "Finite Element for Rock Joints and Interfaces," Journal of Soil Mechanics and Foundations Division, ASCE, Vol. 99, No. SM10, October 1973.

7. Goodman, R. E., R. L. Taylor, and T. L. Brekke "A Model for the Mechanics of Jointed Rock," Journal of Soil Mechanics and Foundations Division, ASCE, Vol. 94, No. SM3, May 1968.
8. Hegemier, G. A., S.K. Arya, R.O. Nunn, M.E. Miller, A. Anvar, and G. Krishnamoorthy, "A Major Study of Concrete Masonry Under Seismic-type Loading," Report No. UCSD/AMES/TR-77-2, University of California, San Diego, Jan. 1978.
9. Lin, C.S. and A.C. Scordelis, "Nonlinear Analysis of RC Shells of General Form," Journal of the Structural Division, ASCE, Vol. 101, No. ST3, March 1975.
10. Rashid, Y.R., "Analysis of Prestressed Concrete Pressure Vessels," Nuclear Engineering and Design, Vol. 7, April 1968.
11. Schnobrich, W.C., "Behavior of Reinforced Concrete Structures Predicted by the Finite Element Method," Second National Symposium on Computerized Structural Analysis and Design, George Washington University, Washington, D. C., 29-31 March 1976.
12. Scordelis, A. C., "Finite Element Analysis of Reinforced Concrete Structures," Speciality Conference on the Finite Element Method in Civil Engineering, McGill University, Montreal, Canada, June 1972.
13. Zienkiewicz, O. C., et al., "Analysis of Nonlinear Problems in Rock Mechanics with Particular Reference to Jointed Rock Systems," Proceedings of the 2nd Congress of the International Society for Rock Mechanics, Belgrade, Yugoslavia, 1970.

APPENDIX II. - NOTATION

The following symbols are used in this paper:

- σ_1, σ_2 = principal stresses;
- ϵ_1, ϵ_2 = principal strains;
- σ, ϵ = octahedral shear stress, strain, respectively;
- x, y = global coordinate system;
- x', y' = principal stress coordinate system;
- r_x, r_y = reinforcement area ratios in x and y directions, respectively;
- $t, \Delta t$ = time, time interval, respectively;
- σ_t^*, σ_n^* = allowable shear and tensile strengths of an interface, respectively;
- c, μ = cohesion, coefficient of friction, respectively;
- c_0, c_1, \dots = coefficients of nonlinear cohesion law;
- μ_0, μ_1, \dots = coefficients of nonlinear coefficient of friction law;
- σ_t, σ_n = tangential and normal stresses at an interface, respectively;
- E = Young's modulus;
- G = shear modulus;
- λ = reduction factor for shear modulus of a cracked element;

- ν = Poisson's ratio;
 β = direction of major principal stress in masonry;
 f'_m = ultimate strength of masonry in compression;
 f_m = reduced strength of masonry in compression;
 f'_m = tensile strength of masonry;
 ϵ_{p}^{mt} = complete collapse strain of masonry in uniaxial compression;
 e' = octahedral shear strain at yield;
 f_y = yield strength of reinforcement;
 Δ = horizontal displacement;
 F = horizontal force corresponding to Δ ;
 δ = horizontal displacement of top lefthand corner of masonry shear wall;
 $\{\Delta u\}$ = incremental displacement vector;
 $\{d\sigma\}$ = incremental stress vector;
 $\{d\epsilon\}$ = incremental strain vector;
 $\{\sigma\}$ = total stress vector;
 $[D]$ = matrix of linear coefficients;
 $[T]$ = transformation matrix;
 $[K]$ = effective stiffness matrix;
 $\{R\}$ = effective load vector;
 $\{R\}$ = internal resisting force vector;

Superscripts

c, s = concrete masonry, steel, respectively.

THE FLEXURAL BEHAVIOUR OF BRICKWORK

By Lawrence, S.J.

ABSTRACT: Current masonry research in Australia centres around the improvement of methods for the design of non-loadbearing wall panels subject to wind loading without resort to the use of steel reinforcement. Many engineers believe that brickwork has greater potential tensile strength than codes and regulations permit. The current Australian Brickwork Code allows tensile design stresses of 0.07 MPa across the bed joints and 0.14 MPa parallel to them. A number of investigations in recent years have been aimed at measuring the flexural properties of brickwork in order to derive basic data for the design of wall panels and to provide an understanding of the way in which brickwork resists flexure.

Data are presented on the strength of brickwork when subjected to bending moments about axes parallel to and normal to the bed joints, and a relationship between these orthogonal strengths is derived. Similarly, data are presented and a relationship investigated for flexural stiffnesses in these two orthogonal directions.

Stretcher-bonded brickwork resists bending about an axis normal to the bed joints by a complex mechanism which involves a highly non-uniform distribution of stress between bricks and mortar. Investigations into this stress distribution are described and it is shown how changes in the pattern, caused by partial cracking of joints within the brickwork panel, produce changes in the flexural stiffness with increased bending moment.

The effect of stochastic variation in brickwork properties on the measured strengths of beam specimens is discussed and illustrated.

THE FLEXURAL BEHAVIOUR OF BRICKWORK

By Stephen J. Lawrence¹

INTRODUCTION

The most troublesome area for masonry designers in Australia today is the wind load resistance of infill panels in framed buildings or of upper storeys in loadbearing construction. The basic design parameter for these cases is the brickwork strength in flexure and this is determined by the tensile strength of bond between brick and mortar. Although there is a long history of investigations into bond strength and the influences of many factors have been identified, data on strengths in flexure are lacking and there are no suitable standardised test procedures for measuring this property. In addition, there is not yet sufficient understanding of the way in which test results from small specimens might relate to full-size structural panels.

In the absence of suitable data the Australian Brickwork Code (5)², in common with other masonry codes throughout the world, specifies very low permissible tensile stresses. The result is extreme conservatism in most cases. Allowable tensile stresses in Australia are 0.07 MPa across the bed joints and 0.14 MPa in the direction parallel to them.

The Experimental Building Station in Sydney is conducting a long-term project on the lateral load resistance of masonry walls and early efforts have been directed towards standardising test procedures for measuring flexural strength and stiffness and expanding the available collection of data on these properties. Not only are the magnitudes of strength and stiffness important but also the way in which these properties vary with orientation. The directions normal to and parallel to the bed joints are of prime importance. The degree of anisotropy determines the controlling factors for initial cracking and ultimate failure and should be taken into account in any realistic theoretical analysis of wall panels.

Early results showed an unusual form of load-deflection relationship for brickwork bent about an axis normal to the bed joints. Further investigation has revealed that this non-linear behaviour can be attributed to partial cracking; the effects on a full-size wall panel are being investigated.

Effort is also being devoted to investigating the form of stochastic variation in brickwork flexural properties and the effects of this variation on the performance of structural elements.

¹Engineer, Experimental Building Station, Sydney, Australia.

²Numerals in parentheses refer to corresponding items in the Appendix I - References.

TEST SPECIMENS

The requirements for a method of test are that it give a measure of both strength and stiffness and that it provide well controlled conditions which represent as closely as possible the conditions in a wall panel subjected to out-of-plane loading. In addition the specimen must not be too heavy or difficult to handle because there is large variability in brickwork properties and therefore a reasonable number of replicates must be tested. The most suitable specimen to satisfy these requirements is a section of brickwork tested as a simple beam with stiffness calculated from measurements of central deflection.

Apart from specimen size, self-weight is the only factor which distinguishes the behaviour of brickwork in a wall panel from that in a simple specimen tested in the horizontal plane. Simply testing the beam specimen in a vertical orientation, with loads applied horizontally, would not adequately reproduce the effects of self-weight as each beam would then only represent the top few courses in a wall. Since every bed joint in a wall is subjected to a different precompression due to self-weight, beams would have to be tested under various degrees of precompression to provide the necessary data to allow for this factor. This amount of testing is not feasible on the scale required so tests are being conducted without any compensation for the lack of self-weight on the bed joints. It is believed that once the mechanism of flexure is understood, the effect of self-weight can be allowed for theoretically.

Experience of simple beam tests on stretcher-bonded brickwork panels has shown that when the axis of bending is normal to the bed joints, with 'average' bond strength the failure will be on a straight line through bricks and perpend joints. Only in cases of very weak bond (or poorly controlled testing conditions) will 'stepped' failures involving only mortar joints arise. Similarly, experience of full-scale wall tests has shown that where the preferred crack orientation is vertical, the crack will run through bricks as well as perpend joints, rather than following a toothed line through bed and perpend joints. In other words the simple beam test correctly reproduces the failure mode occurring in a wall panel and so satisfies all the requirements for a test method.

For the determination of flexural properties where the axis of bending is normal to the bed joints, stretcher-bonded panels with at least three or four courses are necessary so that construction techniques can represent those used in full-size walls. Three-course panels are unsatisfactory because the properties vary markedly along the span of the beam. With these specimens, on any potential failure line there are two bricks and one perpend, and half a brick away on each side there are potential failure lines with two perpend and one brick. A panel four courses high does not have this problem and has therefore been chosen for this work.

Three different configurations of four-course panel have been examined and a full discussion of the results was presented previously (3). The smallest panel was three bricks long and was tested under a single

line load applied at mid-span. The problems with this arrangement are that high shear is combined with maximum bending moment at the centre of the span and that the load is applied directly over a potential failure line. An alternative which overcomes the second problem is a panel three and one half bricks long, with a central line load applied mid-way between two potential failure lines. However, there is still a triangular bending moment distribution with high shear and bending moment superimposed. The third alternative considered was a panel four bricks long with two line loads applied at approximately the third-points. In this configuration the loads span three potential failure lines, subjecting them to very nearly identical conditions of bending moment and zero shear force. Failure almost invariably occurs on one of these three lines. From early experiments with the three alternative configurations it was found that the failure stress obtained using a two-point load differed significantly from that obtained using a single load. The four-course by four-brick-long panel with a two-point loading has been standardised for determination of flexural properties about an axis normal to the bed joint and since it estimates the properties of a horizontal strip taken from a wall panel it is referred to throughout this paper as a horizontal beam.

The type of specimen for the determination of bending resistance about an axis parallel to the bed joints is specified in the Australian Brickwork Code (5) as a nine-brick-high stack-bonded pier, but the loading conditions are not well defined. For laboratory investigations a pair of line loads at approximately the quarter-points have been used. This loading configuration subjects four joints to very nearly identical conditions of bending moment and zero shear force and therefore the probability of failure of each of these four joints should be determined only by their relative strengths. The nine-high stack-bonded pier tested under a two-point loading is referred to throughout this paper as a bond pier.

Sufficient tests have now been carried out with these simple beam specimens to allow the relationships between horizontal and vertical strengths and between horizontal and vertical stiffnesses to be investigated.

FAILURE STRESSES

Brickwork is well known to be anisotropic in its properties and most codes imply a ratio of two between horizontal and vertical tensile strengths. Hendry (1) reported ratios of orthogonal strengths up to seven, and early testing at EBS (3) gave values between three and four. It is important to know the range of strength ratio which occurs in practice so that analytical methods can take the anisotropy into account. In addition, if a relationship between vertical and horizontal flexural strengths can be established, a simple one-way bending test such as the nine-high bond pier will provide all the necessary data on the flexural strength of brickwork in a particular situation. A simple test such as this can be easily carried out on site without the need for any sophisticated testing apparatus.

An early attempt (2) at finding a relationship between the strengths in orthogonal directions considered data from Australia and the United Kingdom and included results from tests with various configurations of specimen and load application. Despite the wide variety of sources, the relationship was very strong and took the form

$$f_H = 2.17 \sqrt{f_V} \text{ (MPa) } \dots\dots\dots (1)$$

With the availability of a greater body of data obtained under uniform conditions, a better estimate of the strength relationship can be made. It must be emphasised that this relationship only applies to the flexural strengths of small specimens tested in the manner described in the previous section, and that the way in which these strength results are applied to a wall panel will involve other considerations. Twenty-one data points were considered, each the mean of a sample of specimens. Sample sizes ranged from six to twelve with the majority being about nine. The data values are given in Appendix III Table A1. A regression analysis of these data gave a relationship of the same form as equation 1 with an exponent of f_V close to 0.5. For the sake of convenience the square-root relationship was used and a least-squares analysis, weighted according to the number in each sample, gave the following expression

$$f_H = 1.75 \sqrt{f_V} \text{ (MPa) } \dots\dots\dots (2)$$

The correlation coefficient was 0.89 and the data are shown with the regression line in Figure 1. The square-root relationship is a very simple one and it is recommended that it be used whenever an estimate of horizontal flexural strength or orthogonal strength ratio is required from a knowledge of the vertical flexural strength.

FLEXURAL MODULUS OF ELASTICITY

Very few data have ever been published on the flexural stiffnesses of brickwork about axes normal to and parallel to the bed joints. Sahlin (4) presents some results which show a range of modulus of elasticity from 10 000 MPa to 30 000 MPa and he also refers to results showing a higher modulus of elasticity horizontally than vertically. These data only refer to specific cases and do not provide any general guidance.

Deflections of brickwork horizontal beams are only about 0.3 mm before failure and those for bond piers are less than 0.1 mm; consequently the measurement of these deflections with sufficient accuracy requires sensitive instruments and careful control. Suitable measuring techniques have been developed at EBS and deflections are measured on every beam tested. Two LVDT-type displacement transducers are mounted on a light frame which rests over the beam supports so that the vertical deflection of each side of the beam relative to the supports is measured at centre span. This arrangement provides automatic compensation for any support movement or twisting

effect and the electrical average of the two transducer outputs is used to plot a load-deflection graph directly. From the slope of the load-deflection graph at any point an equivalent flexural modulus of elasticity can be calculated using simple beam theory.

Load-deflection graphs for bond piers are linear to failure, indicating elastic brittle behaviour. On the other hand the load-deflection graphs for horizontal beams usually exhibit a marked change of slope at about thirty to fifty per cent of the ultimate load. Figure 2 shows a typical load-deflection graph for a horizontal beam. The portions of the graph before and after the change of slope are approximately linear and a modulus of elasticity has been calculated for each portion. Evidence is presented in the next section to support the hypothesis that this change in slope corresponds to the cracking of a perpendicular joint.

The relationship between horizontal and vertical moduli of elasticity must be known so that anisotropy can be considered in prediction of the elastic behaviour. If the stiffnesses are nearly the same a standard isotropic plate analysis would be sufficient but a significant anisotropy in stiffness would modify the distribution of bending stresses to such an extent that it would have to be considered in analysis. Consideration of available stiffness data has shown a relationship between horizontal and vertical moduli of elasticity as follows

$$E_H = 2280 + 0.62 E_V \quad (\text{MPa}) \quad \dots\dots\dots (3)$$

Nineteen data points were included, each the mean of at least six specimens, and the correlation coefficient was 0.96. The data values are given in Appendix III Table A2. The alternative exponential relationship shown in equation 4 also gave a correlation coefficient of 0.96 and passes through the origin.

$$E_H = 9.73 E_V^{0.74} \quad (\text{MPa}) \quad \dots\dots\dots (4)$$

This is proposed as the most useful form of relationship and is shown in Figure 3 with the data points. Note that in all but a few cases of low elasticity the vertical stiffness is greater than the horizontal stiffness.

The relationship between moduli of elasticity before and after cracking in the horizontal beam has also been investigated. In this case the values were correlated for the 150 individual specimens and the line of best fit was found to pass very close to the origin. In order to simplify the relationship as much as possible a line was constrained to pass through the origin, resulting in the relationship given in equation 5 with a correlation coefficient of 0.84.

$$E_{H2} = 0.615 E_{H1} \quad (\text{MPa}) \quad \dots\dots\dots (5)$$

Figure 4 shows the 150 data points plotted with this relationship. The significance of this relationship is that the well-defined change of slope

in the load-deflection graph must represent a definite change in the physical behaviour of the panel. The cause of this change of slope, rather than being random, is likely to be the same in every panel. Future analyses of the mechanism of bending are expected to confirm that this change is the result of cracking in perpend joints; some evidence for this is presented in the next section.

THE DISTRIBUTION OF STRAINS IN STRETCHER-BONDED BRICKWORK

The first stage in investigating the mechanism of bending in stretcher-bonded brickwork has been the measurement of the distribution of strains in a brick forming part of a horizontal beam. Brickwork consists of relatively large, stiff, brittle bricks set in a relatively thin, soft mortar matrix. It could therefore be expected that the bricks would have high bending stresses near the centre of their length and that these stresses would diminish towards the ends as shear on the bed joints caused transference to the brick on each side. Figure 5 shows how this load transfer would take place.

In order to verify the proposed distribution of stresses, resistance strain gauges were placed in nine positions on a brick as shown in Figure 6. The brick was located near the centre of a horizontal beam which was loaded in the standard manner and subjected to load cycles as follows:

1. Loading to 7.2 kN which was estimated to be just below the failure load. The strain gauges were on the top surface of the panel.
2. Loading to 6.7 kN with the gauges on the bottom surface of the panel.
3. Repeat of 2.
4. Loading to failure at 8.1 kN with the gauges on the top surface of the panel.

The three gauges at each transverse cross-section of the brick gave quite uniform readings and were averaged. The two average end readings were similar but, as expected, they were significantly lower than the average reading at the centre of the brick. Figure 7 shows the ratio between centre reading and average end reading plotted against load for each of the four load cycles. On the first loading the ratio remained uniform at just below 1.5 as the load was increased. The same is true of the second load cycle until a load of 5 kN was reached, at which stage the end strains dropped and the centre strain increased markedly. This change is construed to have arisen from cracking in the perpend joints at the ends of the brick. After this cracking the ratio of centre to end strain rose above five, and on reloading (load cycle 3) the ratio remained higher than initially at about 2.8, showing that a permanent change in physical behaviour had taken place. In the fourth load cycle, after the panel was inverted again, the ratio reverted to about 1.5, as the cracks were on the

compression face of the panel. No change in ratio was observed in this load cycle, presumably because once cracks formed they completed failure through the full thickness of the panel and sudden collapse followed.

The measurements described above have demonstrated how the strain varies within a single brick and have shown how minor cracking can modify this strain distribution. It is proposed to take measurements of strain across mortar joints and to build up a model of the behaviour of bricks and mortar in a horizontal beam. Using the distribution of stress between bricks and perpend joints on a potential failure line it is proposed to perform a Monte Carlo analysis of the failure of horizontal beams. Such an analysis could be used to investigate the causes of failure, the effect of various statistical distributions of brick and mortar strength, and the effect of various fracture theories (elastic brittle, plastic, partially plastic etc.) on the statistical distribution of horizontal beam strengths. A greater understanding will thereby be gained of the behaviour of stretcher-bonded brickwork in horizontal bending.

STOCHASTIC EFFECTS IN BRICKWORK BEAMS

In these investigations of brickwork flexural properties the quantities of interest apply to individual joints or failure lines. Whenever a bond pier or horizontal beam is tested there is a sample of joints or failure lines and only one of these causes failure of the beam. Statistically, the problem is an extreme value one as the cause of failure is the joint or failure line with the lowest ratio of strength to applied bending stress. Corrections should be applied to obtain parameters for joint strength from the measured mean and variance of beam strength. Further corrections are required to determine the strengths of wall panels since another sampling process is involved. In the case of wall panels it is likely that averaging will take place and reduce the variability below the level of variability in individual joints.

For the case of bond piers the necessary statistical corrections have been known for some years and were discussed at length by Tucker (6). Bond piers are obviously a "weakest-link" problem with links in series and Tucker has considered the effects of various forms of loading on the measured strengths in such cases.

For stretcher-bonded panels the problem is more complex and the author is undertaking a Monte Carlo analysis as mentioned in the last section. This analysis will provide the necessary factors to correct beam results to the mean and variance of individual failure line strengths. Future work will show how these failure line strengths can be used to predict wall panel behaviour.

When considering the statistical distributions of individual properties such as brick transverse strength and perpend strength it may not be safe to assume the normal distribution. Some evidence has been found

that for brick compressive strength and bond strength in tension the variance increases in proportion to the mean squared. Large numbers of specimens were considered in that analysis and when further data are available the same analysis will be performed for brick transverse strength. If such a relationship exists between sample mean and variance the indications are that the parent distribution is logarithmic normal. The effect this may have on the distribution of panel strengths is unknown but can be determined by the Monte Carlo analysis referred to previously.

SUMMARY

The flexural strength and modulus of elasticity of brickwork must be known in two orthogonal directions : normal to and parallel to the bed joints. Investigations have shown that the best specimens for measuring these properties are a nine-brick-high stack-bonded pier and a four-course by four-brick-long stretcher-bonded panel, each loaded as a simple beam with two line loads.

Data from a large number of small beam specimens have been presented and it was shown that the relationship:

$$f_H = 1.75 \sqrt{f_V} \text{ (MPa) } \dots\dots\dots (2)$$

allows the horizontal flexural strength to be determined from the vertical flexural strength with sufficient accuracy for design purposes.

Data on flexural moduli of elasticity in the two orthogonal directions have been presented and the relationship:

$$E_H = 9.73 E_V^{0.74} \text{ (MPa) } \dots\dots\dots (4)$$

has been proposed for estimating E_H from E_V .

It has been shown that the load-deflection relationship for stretcher-bonded panels is bi-linear, with a distinct change of stiffness probably corresponding to cracking of perpend joints within the panel. The change in stiffness is such that the modulus of elasticity after cracking can be estimated from the modulus of elasticity before cracking by the relationship:

$$E_{H2} = 0.615 E_{H1} \dots\dots\dots (5)$$

It has been shown that an individual brick in a stretcher-bonded panel carries greater stress at the centre of its length than towards the ends, and that this stress is transferred to adjacent bricks by shear on the bed joints. Future tests will investigate the shear behaviour of a bed joint with a view to building up a model of the mechanism of action of a stretcher-bonded panel in simple bending.

Stochastic effects in brickwork beams have been discussed and the weakest-link theory is proposed for considering vertical bending. A Monte-Carlo simulation is to be carried out for horizontal bending to investigate the effects of different fracture theories on the statistical distribution of strength. It is suggested that the statistical distribution of basic properties such as brick strength may be logarithmic normal and that the effects this may have on beam strength should be investigated.

ACKNOWLEDGMENT

The work described in this paper forms part of the research program of the Experimental Building Station and is published with the permission of the Chief.

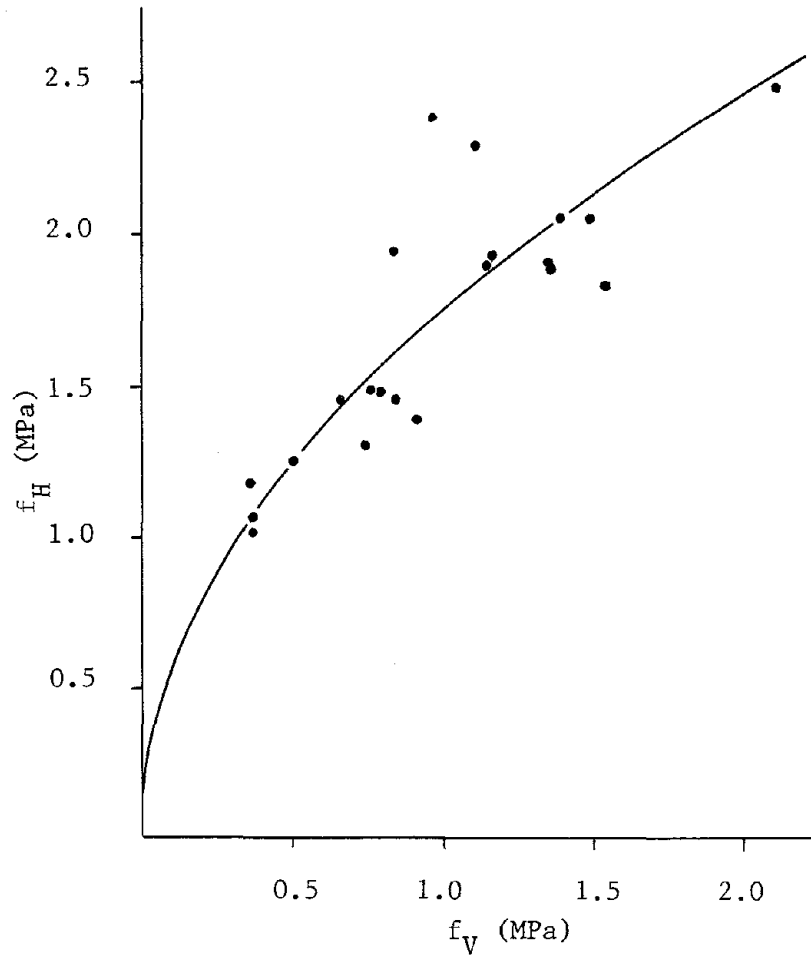


Figure 1. Relationship Between f_H and f_V

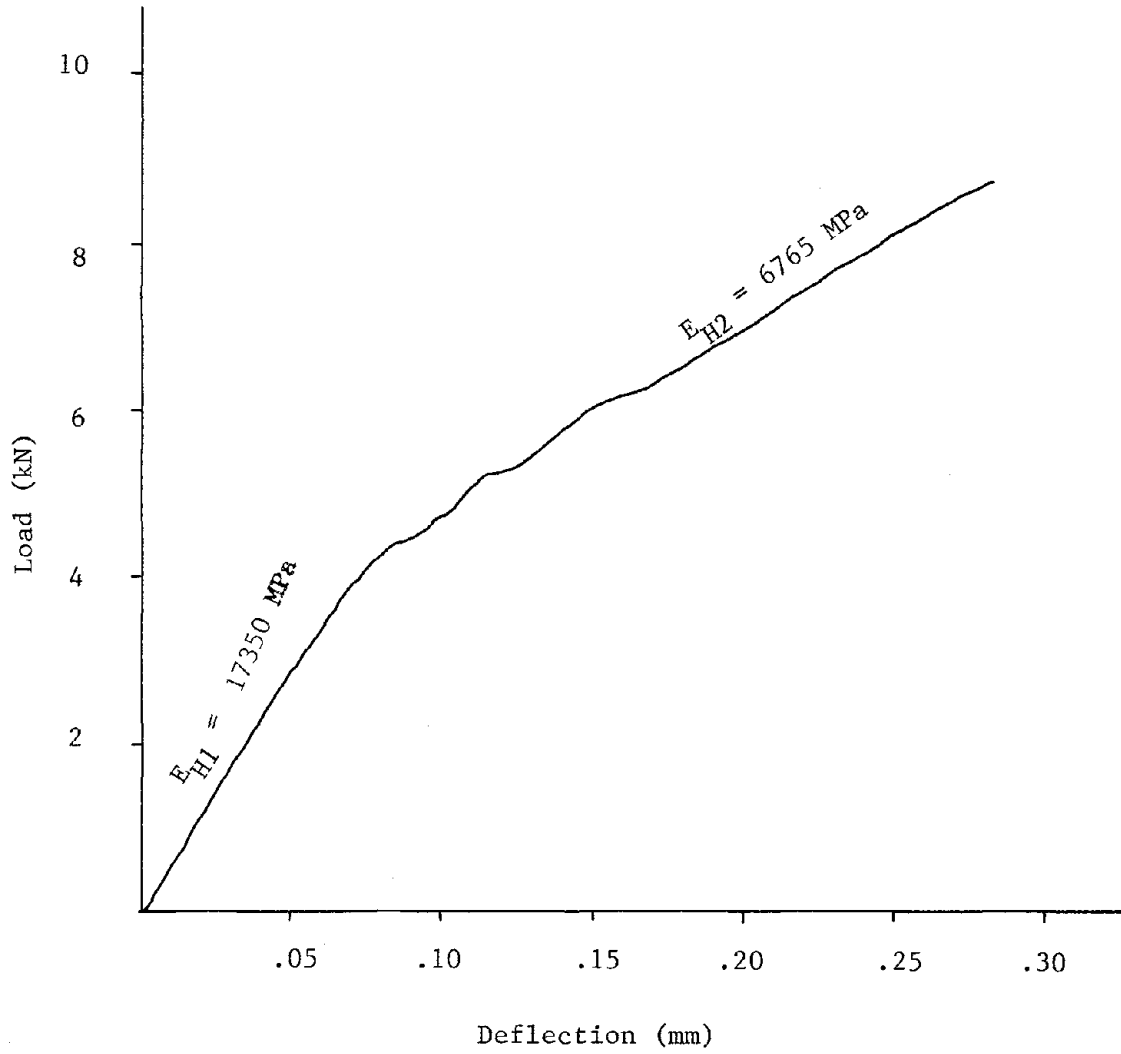


Figure 2. Typical Load/deflection Graph for Horizontal Beam

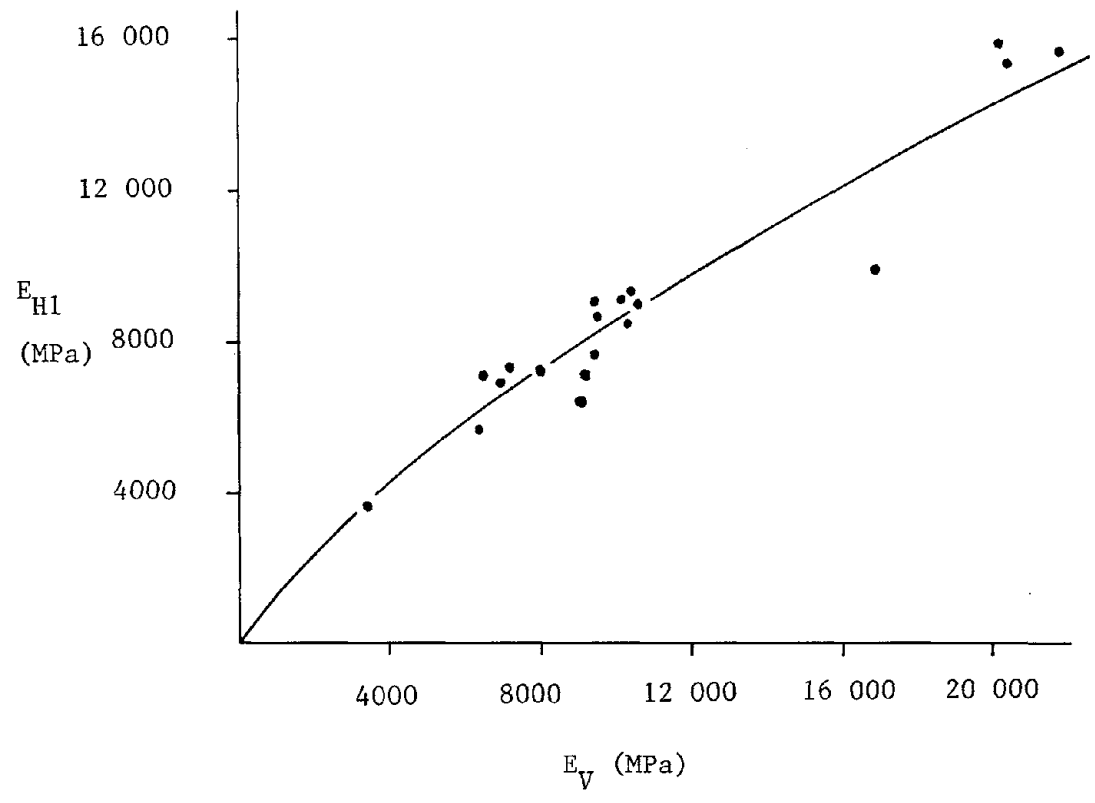


Figure 3. Relationship Between E_H and E_V

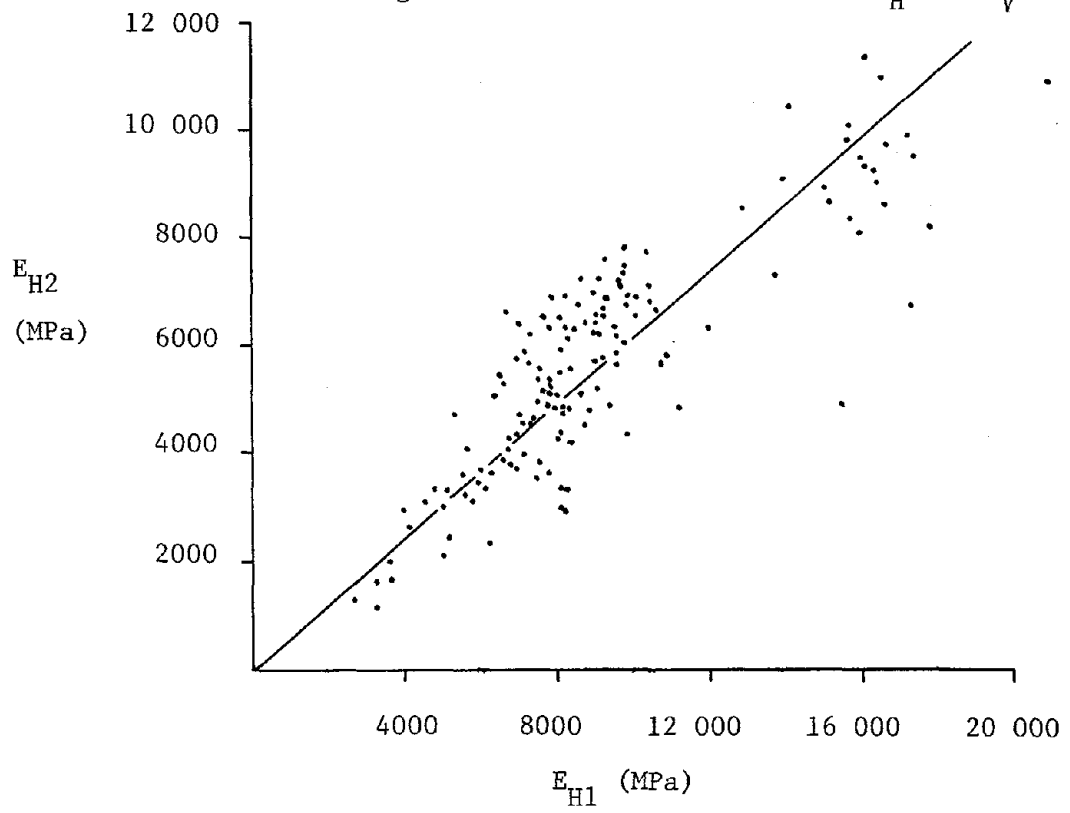


Figure 4. Relationship Between E_{H2} and E_{H1}

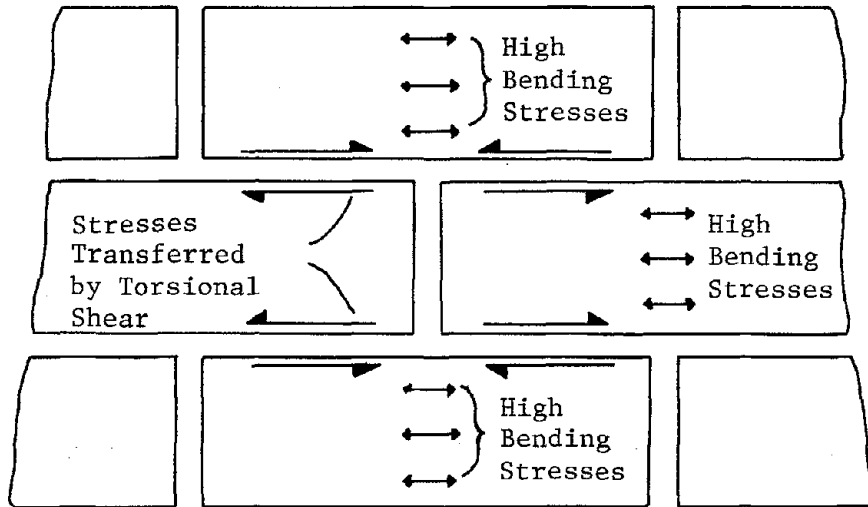


Figure 5.

Method of stress transfer by shear on bed joints

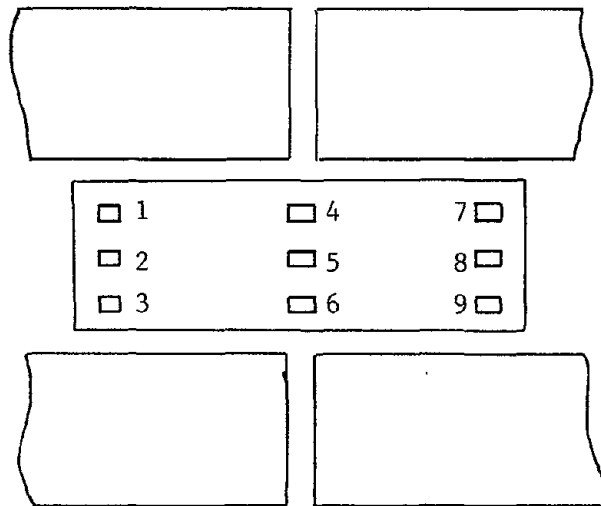


Figure 6.

Measuring points for distribution of strains in bricks

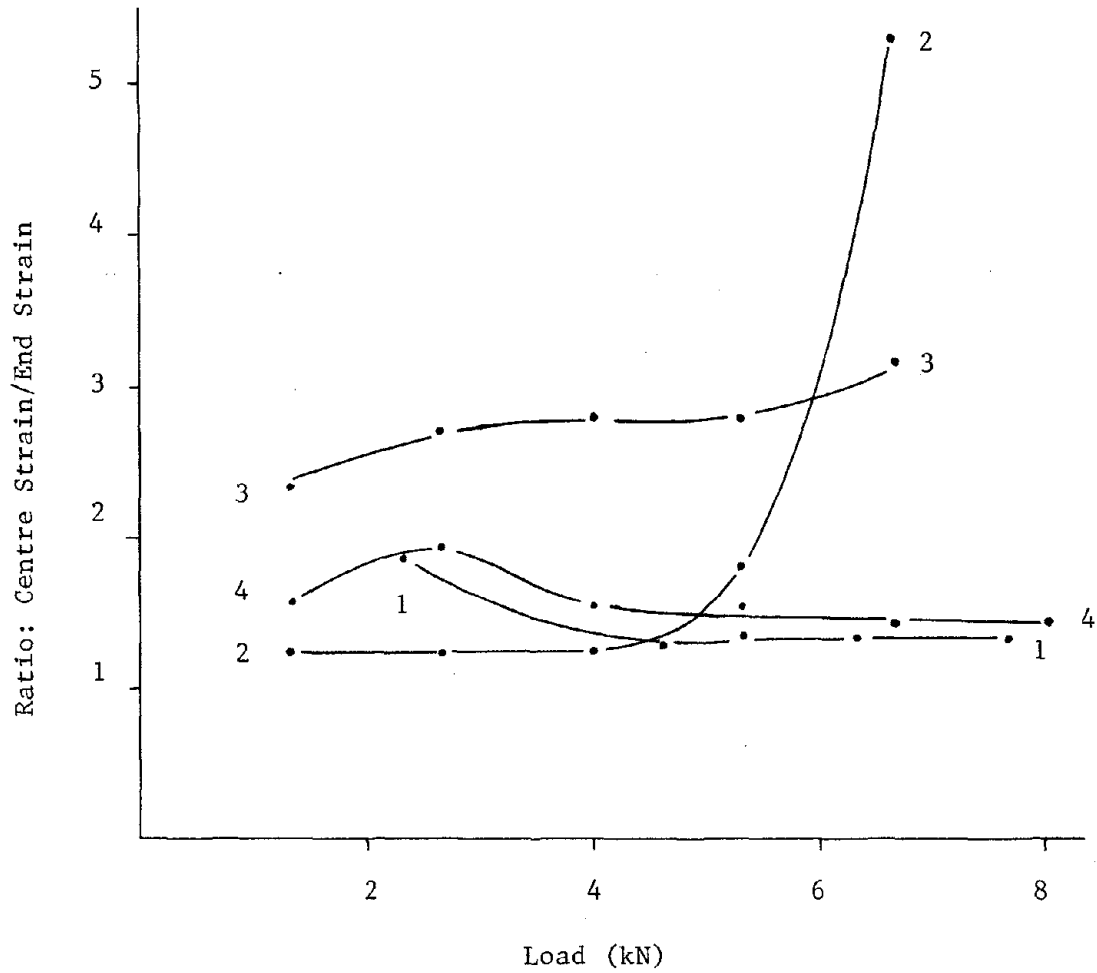


Figure 7. Ratio of Centre/End Strain in Brick Forming Part of a Stretcher-bonded Beam

APPENDIX 1 - REFERENCES

1. HENDRY, A.W. 'The Lateral Strength of Unreinforced Brickwork'. The Structural Engineer, V51, N2, Feb. 1973, pp. 43-50.
2. LAWRENCE, S.J. 'Flexural Strength of Brickwork Normal to and Parallel to the Bed Joints'. Journal of the Australian Ceramic Society, V11, N1, May 1975, pp. 5-6.
3. LAWRENCE, S.J. & MORGAN, J.W. 'Investigations of the Properties of Small Brickwork Panels in Lateral Bending'. Technical Record 418, Experimental Building Station, Sydney, 1975.
4. SAHLIN, S. 'Structural Masonry'. Prentice-Hall, New Jersey, 1971, Section H.4.
5. 'Brickwork in Buildings'. AS 1640-1975, Standards Association of Australia, Sydney, 1974.
6. TUCKER, J. 'Statistical Theory of the Effect of Dimensions of Loading upon the Modulus of Rupture of Beams'. Proceedings of the ASTM, V41, 1941, pp. 1073-1094.

APPENDIX II - NOTATION

- E_{H1} , initial modulus of elasticity of brickwork in the horizontal direction, i.e. when bent about an axis normal to the bed joints.
- E_{H2} , modulus of elasticity of brickwork in the horizontal direction after cracking.
- E_V , modulus of elasticity of brickwork in the vertical direction, i.e. when bent about an axis parallel to the bed joints.
- f_H , failure stress for brickwork in horizontal bending, i.e. when bent about an axis normal to the bed joints.
- f_V , failure stress for brickwork in vertical bending, i.e. when bent about an axis parallel to the bed joints.

APPENDIX III - DATA

Table A1. HORIZONTAL AND VERTICAL FAILURE STRESSES (MPa)

f_H	Number in Sample	f_V	Number in Sample
2.49	12	2.11	12
1.90	9	1.14	9
1.88	9	1.36	9
2.06	12	1.48	12
2.07	12	1.38	12
1.83	9	1.53	9
1.92	9	1.35	9
1.94	9	1.17	8
2.38	9	0.97	9
1.95	9	0.83	9
1.02	6	0.37	12
1.18	6	0.36	12
1.25	6	0.51	12
1.46	6	0.66	12
1.07	6	0.37	12
1.31	8	0.74	9
1.39	8	0.91	8
1.48	8	0.79	9
1.49	8	0.76	8
2.30	6	1.11	6
1.46	6	0.84	6

Table A2. HORIZONTAL AND VERTICAL MODULI OF ELASTICITY (MPa)

E_{H1}	Number in Sample	E_V	Number in Sample
7636	12	9385	12
7343	9	7161	9
6949	11	6947	9
8642	12	9524	12
9115	12	9452	12
9335	9	10440	9
9112	9	10227	9
8456	9	10341	8
15737	9	21767	9
15893	9	20170	9
6410	18	9070	12
7170	18	6410	12
9850	18	16890	12
15400	18	20440	12
9020	18	10560	12
5687	8	6036	9
3650	8	3361	8
7251	6	8004	6
7118	6	9160	6

DEPENDENCE OF MASONRY PROPERTIES
ON THE INTERACTION BETWEEN MASONRY
UNITS AND MORTAR

By Sneck, T.¹

Technical Research Centre of Finland, Espoo,
Finland

ABSTRACT: The application of the performance concept at the level of materials is described as an analysis and matching of the extrinsic factors affecting a material in use with the properties of the material. Principles on the use of the concept in masonry construction are outlined. Results of a Delphi-study are given and a Finnish masonry standard is reviewed. The interaction between masonry units and mortars is the central point, and the removal of water from the mortar by the suction of the masonry unit is the most important matter. Examples are given on the importance of the interaction in investigations of mortar strength, effects of sand, moisture penetration, winter masonry and the use of masonry cement.

¹Research Professor of Building Materials Technology,
Technical Research Center of Finland, SF-02150, Espoo 15, Finland.

DEPENDENCE OF MASONRY PROPERTIES
ON THE INTERACTION BETWEEN MASONRY
UNITS AND MORTAR

By Tenho Sneck¹

INTRODUCTION

The conventional approach to masonry specification is to use masonry units meeting specification requirements in combination with a mortar of a specified composition. If a performance oriented approach towards mortars and masonry is chosen, one has to start by defining the requirements and then to proceed by selecting or developing a solution which gives the wanted service in the conditions of use. This means that the construction has to perform under the action of the actual extrinsic factors, e. g. , stresses and loadings in a broad sense. In order to achieve this, the properties of the mortar have to be matched to the properties of the masonry units, and the evaluation has to be based upon the interaction between the mortar and the units.

THE PERFORMANCE CONCEPT

The performance concept starts from a consideration of human requirements and makes it possible to describe a solution freely, without binding it to any specific components, materials, etc. The definition by Eberhard and Wright [2] states:

"The performance concept is an organized procedure or framework within which it is possible to state the desired attributes of a material, component or system in order to fulfil the requirements of the intended user without regard to the specific means to be employed in achieving the results. "

It has not always been clear how to apply the performance thinking on the level of materials.

¹Research Professor of Building Materials Technology,
Technical Research Center of Finland, SF-02150, Espoo 15, Finland.

For this reason, the performance of materials, performance criteria and performance tests have been defined by the RILEM technical committee 31-PCM, Performance criteria for building materials, in following terms:

"For a defined requirement, the performance of a material is its response to the action of extrinsic factors. The nature of the response is due to the intrinsic properties of the material."

"The performance criterion is the definition of the limiting value or value range which satisfies the requirement for a given lifetime."

"A performance test aims to the prediction of the performance of a material as a part of a building element. A test has to be chosen where the response of the material to the action of the appropriate extrinsic factor or factors is illustrated and information concerning the intrinsic properties of the material needed to satisfy this action is collected."

In this way we try to design and operate a system which would not from the beginning restrict innovation, in fact, many hope that the performance concept would become an "invitation to innovation."

The system is operated at different levels of building, as buildings, building elements, compounds, material combinations, materials, etc. The properties or attributes describing the solution are chosen by starting with an analysis of the different human and technical extrinsic factors as the extrinsic factors fix the requirements to be fulfilled and the intrinsic factors fix the solution at a particular level. It is important to keep in mind that the solution at a lower level has to be consistent to the properties (and requirements) put up on a higher level. Different systems for the listing of the extrinsic factors exist. Below an example is given.

Extrinsic factors:

- Human factors, as physiological and sociological.
- Environmental (technical) factors, as the expected behaviour under the influence of loads and forces, fire, gases, water, solids; biological, thermal, optical and acoustic factors; electricity, energy, time, etc.

The performance concept may be principally seen as a design aid. In order to get a satisfactory final solution, it has to be applied at different stages of the building process. Design, manufacture, storage,

transport, erection, operation, maintenance, repair, replacement and demolition can be considered in this connection.

In its "pure" state, the performance concept operates in complete dependence on human requirements. Very often national and community needs and goals are likely to be deciding and a restrictive subsystem is then operating, and the performance concept forms a part of a systems approach [7].

MASONRY CONSTRUCTION

In masonry construction the aim is to build of masonry units and mortars a construction that has to withstand the effects of many factors from the inside and the outside of the building. Requirements upon its appearance are set up but many of the technical requirements are of great importance. The construction must resist different types of loads and forces, it must withstand effects from the climate and many actions caused by the use of the building. It must be loadbearing, it has to possess a certain strength, it must resist the penetration of rain, be weather and frost resistant, fire-proof, acoustically insulating, etc.

The most difficult matter within the concept is the predictive evaluation of the performance. Any kind of tests can be made to a building, a building element, a product, etc. According to the results of a Delphi-study [8] performed within the RILEM committee on "Performances of mortars and renderings", the most important level for the evaluation is "product combination", e.g., the interaction between mortars and masonry units. In the Delphi-study it was stated that the performance evaluation of masonry mortars may be based upon research performed at different levels of building. The answers were numbered from 7 to 1 with 7 = the most important and 1 = the least important level. The results are given in Table 1.

1.0	Building
2.0	Part of building
4.0	Building element (wall)
6.8	Product combination (masonry unit/mortar interaction)
5.8	Product (masonry unit, mortar)
4.5	Material (cement, lime, sand, admixtures)
3.7	Internal structure (chemical composition, pore properties, cohesion)

Table 1. Results of the Delphi-study

The results of the Delphi-study were accepted as the basis for the work of the RILEM-committee working with Mr. V. Saretok from Sweden as chairman. Several recommendations for testing methods will appear during 1978.

After a work for several years a Finnish standard for masonry structures [6] was introduced in 1972. The task of the masonry mortar is to bind the masonry units together in order to form a firm and durable structure meeting different technical, aesthetic and economic requirements.

According to research and a very long practical experience, the masonry requirements can in general be reached when mortars and masonry units meeting specification requirements are used. For conventional use, certain lime, lime-cement and cement mortars are listed in the "conventional" part of the standard. These mortars can be used together with specified masonry units, and the standard lists the allowed stresses for such combinations.

The performance oriented part of the standard is built around the philosophy stated above that the properties of the mortar have to be matched to the properties of the masonry units, and the evaluation has to be based upon the interaction between the mortar and the masonry unit.

The standard is mainly a norm on loads and stresses but it gives outlines for the application of the performance approach. This is most outstanding in the part describing masonry mortars. This is very much due to the work made within the Scandinavian Mortar Committee [1].

The standard makes it possible to develop and accept new masonry unit/mortar combinations where the allowable stresses of the standard could be used or even higher stresses could be applied. In every case it is necessary to make tests in order to present them for authorization to the permanent committee of masonry constructions.

The aim of the standard is to give practical directives for the selection, preparation and use of mortars in central mixing facilities and at building sites. The performance-oriented part of the standard was believed to promote development and innovations. This assumption has been proved to be correct but there would be great possibilities to go much further if a very R & D intensive approach would be chosen by the industries concerned.

PRINCIPLES OF INTERACTION

The suction of masonry units is the most important extrinsic factor affecting the fresh mortar, and, consequently, the properties of the hardened mortar and the properties of the combination. Water removal affects the mortar bed as a whole and the properties of the interface between the masonry unit and the mortar. Shrinkage and swelling of the mortar and the masonry unit due to moisture change and thermal movements also affect the quality of the joint.

When a masonry unit and the fresh mortar get into contact with each other, the suction varies dependent upon many factors connected both with the unit and the mortar. In some cases no water may be removed from the mortar, the other extreme being that almost all water is absorbed by the masonry unit. Strength and porosity of the mortar, bond, watertightness, etc. are among the properties which are dependent upon the suction. For instance, the strength of the mortar is not dependent upon its initial water content but on the water present after suction. This means that the suction is the deciding factor as far as the binder-water-ratio in the mortar is considered. The general rule is the same as for the water-cement-ratio in concrete: too much water results in a weak and porous mortar, if too much water is removed, the cement does not harden. The optimal conditions are, of course, to be found somewhere between these extremes.

The suction varies dependent upon the water absorption of the unit, the rate of absorption and the capillary suction force. The water absorption of the masonry unit gives a figure on how much water the unit is capable of removing from the mortar, the rate tells, generally, how rapidly the water is removed. The capillary suction force may become important in cases where the masonry unit consists of a material with very fine pores. This is the case with many sand-lime units. The fine pores exert a strong suction for a long time. This is quite different from the properties of clay bricks.

The amount of water absorbed from a mortar bed by a masonry unit may be quite different than from a free water surface. The initial rate of absorption (IRA) determined in this way cannot always be accepted as a reliable property describing the real suction.

The suction is reduced by the water absorbed by the masonry unit. A water gradient may be formed in the mortar. Soluble substances are transported with the water into the unit.

The suction exerted by the bottom masonry unit on the lower part of the mortar bed may result in the stiffening of the mortar. In that case the upper masonry unit will get into contact with a different kind of mortar than the bottom unit, and the properties of the interfaces may become quite different.

If the mortar hardens partly before the water is removed, the effects are different from the situation where the water is rapidly absorbed by the masonry unit. As the mortar already has a structure, it is not any more a plastic body, the transfer of water results in volume changes. Later, the fine pore structure of a hardened cement mortar may revert the water flow, and water may return from the masonry unit to the mortar if the pore structure of the masonry unit is coarser.

From thermodynamic points of view a good adhesion is impossible if the adhesive does not wet its substrate. This means that the adhesive has to get into a very good and even contact with its substrate. In the case of a substrate like a porous masonry unit the process of wetting becomes rather complicated. From one side, the properties of the mortar are altered by the suction. From the other side, the properties of the mortar change with the time of working.

Own preliminary tests on the instant adhesion of different masonry units to fresh mortars have shown that there are indications for rupture by adhesion in some cases and by cohesion in others. It also seems to be evident that the time of applying the mortar after its preparation is of vital importance. Indications by short-time tests on adhesion would be of interest for product development.

Interesting studies on the mortar layer in close contact with the masonry unit have been made and the formation of a layer of ettringite at the surface of bricks has been proved [3]. The ettringite forms some kind of bridge between the brick and the hydrated tricalciumsilicate. The authors seem to believe that the size of the ettringite crystals as seen in contrast to the pores in the brick have an influence on the bond. The crystals cannot enter in pores smaller than themselves.

In the manufacture of prefabricated masonry panels it is quite possible to use methods which are very different from ordinary methods. The possibilities to adopt special mortars are interesting. Also, the consistency of the fresh mortar can often be of such a nature that the mortar could never be used at an ordinary building site.

EXAMPLES ON THE EFFECTS OF INTERACTION

It is quite obvious that the most important matter is the development of a proper interaction between the mortar and the masonry unit. The scope of the rest of this paper is to give some examples.

Strength of mortar. -- Three lime-cement mortars were tested in combination with two types of sand-lime bricks. The tensile strength of the mortar hardened between the masonry units was tested with the splitting method. The strength of the three mortars was clearly higher between one type of bricks. The ratios were 1.7, 2.0 and 2.0. A strength difference of this order must influence the strength of masonry.

Effect of sand. -- Standards for masonry construction often give recommendations concerning the corn size distribution of the masonry sand. Often a test with standard prisms or other specimens is accepted as a quality test of the mortar.

A lime cement mortar was prepared by three sands:

- C = high content of coarse fraction
- S = standard sand
- F = high content of fine fraction

The bending and compressive strengths of standard mortar prisms were determined. Small columns were loaded to rupture. The columns were made by cutting bricks into two halves. Five such halves were built into a small panel. The bond of the mortars to the bricks was also measured. Clay bricks with an initial rate of absorption of 3 to 4 kg/m²min were used. The results are quite striking (Table 2).

Test	Sand type of lime-cement mortar		
	Coarse	Standard	Fine
Prism strength			
Bending	Second	Best	Clearly inferior
Compressive	Best	Second	Clearly inferior
Bond	About equal bond strengths		Clearly best
Small columns	Clearly inferior	Slightly inferior to "fine"	Best

Table 2. Effect of sand on strength of standard prisms, bond and compressive strength of small columns at rupture.

As the suction in the preparation of the standard prisms is rather low, the water content of the mortar remains high as the amount of water in a mortar made with fine sand is necessarily high from the beginning. A low prism strength is the result. The interaction with the masonry units results in the best bond and in the test with small columns in about the same strength as with the standard sand.

In the conventional way, the fine sand mortar would have been rejected after the prism tests.

Moisture penetration. --For long times there has been evidence on the importance of bond for the resistance of masonry to moisture penetration. As one example, the work by Ritchie and Davison may be quoted [5]. They conclude that leakage more usually occurs through channels at the brick-mortar interface. The extent of bond is critical and depends largely on the condition of the upper surface of the mortar bed when a brick is laid in it.

West et al. [11] have recently determined the effect of bricks with varying suction rates on the permeability of mortars cast between the bricks. The small mortar slabs were compared by measuring the capillary rise of water. The results tend to show that clay bricks with a very low or high suction rate gave mortars with a high porosity. There seems to be an optimum suction rate for unmodified mortars. With admixtures the results were changed.

Winter masonry. --Winter masonry forms a special example on the effects of the water content of the mortar during hardening. The possible damage due to the low temperature depends upon the amount of water in the mortar at freezing. In the investigations within the Scandinavian Mortar Committee [9] on winter masonry construction, tests of mortars, bond and the strength of small and large columns have been performed. The results show that damage in winter masonry can be avoided if at the time of freezing

- the water content of the mortar has been lowered enough by the suction of bricks, or
- the mortar has prehardened enough before freezing, or
- the mortar freezes immediately, e. g., as long as it is structureless.

In the first alternative a percentage of 6 % is given as a limit. The last alternative is not generally recommended as it might increase the compressibility of the masonry at the time of thawing.

It is very interesting that large columns loaded after freezing generally showed greater strength than did unfrozen columns of the same age. In some cases, their compression at rupture was higher.

In the Finnish standard [6] the three alternatives mentioned above are given. They are shortly summarized in [10] where also was stated that problems have arisen in connection with testing and approval of masonry unit/mortar combinations for winter masonry. Also certain matters concerning the design of the construction and the working operations must be clarified. The main obstacles are found with sand-lime bricks with a high water absorption capacity but with a slow rate of absorption, and with very frost resistant, hard burnt clay bricks with a very low water absorption.

A Scandinavian project group is active in this field with the objective of studying the problems. Some experimental work is done but the main activities are concentrated on writing instructions for the practice.

Masonry cement mortars. --Over a decade ago, there arose a new way of thinking which preferred a mortar where lime was "substituted" by an air entraining agent. It was thought that the single effect of the lime was to make the cement more workable. Thus, cement mortars with an air entraining agent were introduced instead of lime-cement mortars. It was believed that there was a possibility to have new mortars which would be equal to the different lime-cement mortars. This could be achieved by having different amounts of sand in the mix.

This was confirmed by testing mortar prisms with standard methods. One could obtain mortars with the same strength of both types. However, in all tests performed with masonry, the results did not follow this pattern.

Finnish masonry cements are mixtures of finely ground portland cement, fine limestone and admixtures, mainly with the air entraining effect. A system was developed where the old classes of standardized lime-cement mortars could be obtained by changing the ratio of masonry cement and sand. The results of tests with masonry panels did, however, show that the compressive strength and the modulus of elasticity were just about independent of the composition of masonry mortars from M 100/600 to M 100/800. (M 100/600 = 100 kg masonry cement and 600 kg sand).

The explanation was found in the interaction between the masonry unit and the mortar [4]. In bond test with bricks with an IRA varying from 1.5 to 1.9 kg/m²min, the bond strength was increasing with

leaner mortars. The bond strength of M 100/800 was about twice that of M 100/500. The strength of prisms made of the mortars very clearly increased with increasing amount of masonry cement. It may be possible that the opposite effects on the mortar strength and the bond are the explanation to the findings.

As a result, masonry constructions can be erected with own special rules concerning strength requirements, proportioning and mixing. Very strict requirements on the composition of masonry cement mortars are not necessary as the strength of the masonry does not depend on small variations in the proportions. Masonry cement is today the most used binder for masonry in Finland.

CONCLUSIONS

Examples are given on the possibility to develop masonry construction by studying the interaction between masonry units and mortars. This principle could make significant results possible if it would be applied more consequently than is happening today.

APPENDIX I - REFERENCES

1. Dührkop, H., Saretok, V., Sneck, T. and Svendsen, S.D., Mortar-Masonry-Rendering (in Finnish). Rakentajain Kustannus Oy, Helsinki 1966. (The same book has also been published in Danish, Norwegian and Swedish)
2. Eberhard, J.P., The Performance concept: A study of its application to housing. Volume One, National Bureau of Standards, pp. 3, 34, Washington, 1969
3. Farran, J., Grandet, J. and Maso, J.-C., Variations des concentrations de portlandite et d'ettringite dans les pates de ciment Portland au contact des terres cuites poreuses, C.R.Acad.Sc.Paris, t. 271, Série D, pp. 4...7
4. Leiritie, M., The use of masonry cement (in Finnish), Tiili (1973):3, pp. 19...21
5. Ritchie, T. and Davison, J.I., Factors affecting bond strength and resistance to moisture penetration of brick masonry, ASTM, Special Technical Publication No. 320, pp. 16...30, 1962

6. Masonry structures of clay bricks and sand-lime bricks (in Finnish), SFS-Standard 2803, RIL 85, Suomen Rakennusinsinöörien Liitto, Helsinki 1972
7. Sneck, T., An attempt to deal systematically with building materials, Industrialization Forum 5 (1974):3, pp. 3...8
8. Sneck, T., RILEM-MR/VTT Delphi study on masonry and rendering mortars, State Institute for Technical Research, Laboratory of Building Technology, Report 12, Otaniemi, 1972
9. Sneck, T., Koski, L., Oinonen, H., Svendsen, S.D., Waldum, A., Dührkop, H. and Helander, E., Winter Masonry, Division of Building Technology and Community Development, Technical Research Centre of Finland, Publication 1, Helsinki 1972
10. Sneck, T., Winter masonry construction, First Canadian Masonry Symposium, Publication, Calgary 1976, pp. 238... 246
11. West, H.W.H., Ford, R.W. and Peake, F., The effect of suction rate of bricks on the permeability of mortar, The British Ceramic Research Association, Technical Note No. 254, Stoke-on-Trent, 1976

STRAIN GRADIENT EFFECTS IN MASONRY

By Carl J. Turkstra and Gareth R. Thomas
Dept. of Civil Engineering, McGill University

ABSTRACT

For both concrete block and clay brick masonry walls under vertical loading, it has been noted that apparent failure stress seems to increase with load eccentricity. This "strain gradient effect" may have important practical implications.

In this paper, the distribution of stresses under eccentric load is considered in detail. Variations in patterns of local stresses in concrete block webs and throughout solid brick units are examined by means of finite element analysis. Combinations of these stresses with an elementary linear failure surface suggests a rationale for the existence of strain gradient effects. It is concluded that relatively large load eccentricity may not reduce wall axial load capacity and hence may be ignored in design.

STRAIN GRADIENT EFFECTS IN MASONRY

By Carl J. Turkstra¹ and Gareth R. Thomas²

INTRODUCTION

A number of experimental investigations indicate an apparent anomaly in the behaviour of eccentrically loaded masonry walls. Specifically, maximum compressive stress seems to increase with strain gradient. The effect was apparently first identified explicitly by Yokel, Mathey, and Dikker (7) in 1970 for concrete block walls. Similar effects for brick walls have since been identified (1,6). No rational explanation for the observed behaviour seems to have been given.

The purpose of this paper is to present the results of an investigation into possible reasons for the existence of the phenomenon. No attempt is made to predict the numerical magnitude of effects in particular walls which would require detailed experimental studies.

The present investigation involves an extension of the failure criteria proposed by Hilsdorf (3) to nonuniform stress situations. As such, the discussion is on a phenomenological level and seeks to explain the general nature of wall behaviour. Such understanding can provide confidence for the use of observed effects in design and can suggest likely response in situations not studied experimentally.

EXISTENCE OF THE EFFECT

Identification of strain-gradient effects came about through the following reasoning process. Firstly, experimentally measured stress-strain properties of masonry prisms in compression are nearly linear or at least fairly brittle without large ductile strains before failure. Plane sections seem to remain nearly plane as walls deform under loads applied at moderate eccentricities to the centroidal plane of the wall.

This pair of observations suggests that the capacity P under a load applied at an eccentricity e on a short wall should be related to the capacity P_o under pure axial force by

$$\frac{P}{P_o} + \frac{PeAt}{2P_o I} = 1 \quad (1)$$

where t , A and I are the thickness, net area and net moment of inertia of the wall respectively. Eq [1] can be expected to apply up to the eccentricity at which one edge of the wall is in tension. Assuming, as is reasonable, that tensile capacity is zero, the limiting or kern eccentricity e_k is equal to $2I/tA$. For a solid rectangle section $e_k = t/6$.

¹Assoc. Prof., Dept. of Civil Engrg., McGill Univ., Montreal, Que., Canada

²Asst. Prof., Dept. of Civil Engrg., McGill Univ., Montreal, Que., Canada

If behaviour is linear, failure at the kern eccentricity occurs with an axial force $P_k = P_o/2$ and moment $M_k = P_o I/tA$. The governing interaction equation then can be written

$$\frac{P}{P_o} + \frac{M}{2M_k} = 1 \quad [2]$$

To compare predictions based on Eqs. [1] or [2] to experimental behaviour, the strength data for pin ended masonry wallettes given by Fattal and Cattaneo (2) may be used. Data for brick wallettes are given in Table 1 and for concrete block wallettes in Table 2. These sets of results are plotted in Figs. 1 and 2. Both indicate that elementary theory underestimates capacity for eccentric load.

To consider increased capacity in the presence of a bending moment, Eq. [2] can be rewritten

$$\frac{P}{P_o} + \frac{\alpha M}{2M_k} \quad [3]$$

where α is a strain gradient effect factor. Calculated values of α for the concrete prism test results are also shown in Tables 1 and 2. In this case, α is given by

$$\alpha = \frac{e_k}{c} \left[\frac{P_o}{P} - 1 \right] \quad [4]$$

One conclusion suggested by these results is that small eccentricities can be ignored in design.

Finally, shown in Fig. 3 are results for brick wall tests taken from Ref. (5) for walls which may be expected to show very small slenderness effects (6). In this case, three alternate stress strain assumptions were used with conventional equilibrium analysis to develop the theoretical interaction diagrams shown. These results suggest that observed strain gradient effects are not due primarily to nonlinearity of stress-strain relationships.

It can be concluded that the elementary linear theory systematically underestimates the capacity of eccentrically loaded short walls. Eccentricities as large as one half of the kern eccentricity may not significantly reduce load capacity. It must be noted, however, that even small eccentricities can cause significant out-of-plane displacements, moment magnification (6,7) and instability.

BASIC FAILURE MECHANISMS

To understand the nature of masonry wall behaviour, stresses at points throughout the wall must be examined. Shown in Fig. 4 are conventional infinitesimal cubes taken from a brick masonry unit and mortar joint under a load P per unit length at an eccentricity e .

As mentioned by Hilsdorf (3), the typical stress element taken from a brick is subjected to compression in the direction of loading and tension in the two transverse directions. A typical mortar stress element, however, is under triaxial compressive stress. This combination of stresses is caused by the difference between the mechanical properties of bricks and mortar.

Shown in Fig. 5 is a simple hypothetical two dimensional linear failure surface for either brick or concrete. Points along the line represent failure combinations of the stress in the load direction σ_z , along the length σ_x , or through the thickness σ_y . C^* represents the failure stress under pure uniaxial compression while $T^* = \gamma C^*$ is the failure stress under uniaxial tension.

At any point in the wall and assuming linear properties, stress increases proportionally with load along a straight path as shown in Fig. 5. Failure will first occur at the point whose stress path first intersects the failure surface. It is essential to note that tensile transverse stresses reduce capacity while compressive lateral stresses increase capacity in the load direction σ_z . Thus, a mortar with little strength in an unconfined cube test can support much higher stresses in a wall joint.

Analytically, the stress history at any point can be written

$$\sigma_x = a_x P \quad [5-a]$$

$$\sigma_y = a_y P \quad [5-b]$$

$$\sigma_z = a_z P \quad [5-c]$$

where a_x , a_y and a_z are constants. Under axial load, a_z is simply the reciprocal of net area. In general, the constants a_x , a_y and a_z must be established by stress analysis.

For demonstration purposes, the hypothetical failure surface for transverse tension can be written

$$\sigma_x^* + \sigma_y^* + \gamma \sigma_z^* = \gamma C^* \quad [6]$$

where asterisks are used to denote failure combinations of stress. The actual shape of the failure surface and values of the parameters γ and C^* must be found from experiment. Results obtained by Koo (4) indicate that for clay brick, the failure surface is not linear but concave to the origin.

With these assumptions, failure load can be obtained as the least value of P satisfying

$$P[a_x + a_y + \gamma a_z] = \gamma C^* \quad [7]$$

for all sets $[a_x, a_y, a_z]$ for any point in the units in a wall. Consideration of failure in mortar joints does not seem to be warranted unless vertical tension occurs.

The physical manifestation of failure also depends on the combination of stresses involved. In particular, failure in the z direction involves crushing, while failure in the x or y direction implies tensile splitting and spalling respectively.

It has been observed in studies of concrete strength, that tensile strength depends on the extent of the stress field. Thus, specimens in pure tension have significantly lower strength than tensile regions in bending tests. This phenomenon can be attributed to the statistical nature of brittle tensile failure which leads to decreasing strength with increasing volume under high stress.

CONCRETE BLOCK BEHAVIOUR

An analytical study reported by Fattal and Cattaneo (2) provides the basis for an understanding of stress behaviour of concrete block masonry. In that study, a finite element analysis of the stress distribution in block webs was made, assuming face shell bedding of the block. With such bedding, force is applied through the two face shells approximately in proportion to the eccentricity of the applied load. Load is gradually transmitted from the face shell through the web in a shear lag type of phenomenon.

The finite element analysis involved forty-eight rectangular plane stress elements in the web and six bending elements for each face shell in one half of a block. Changes in web and shell thickness were ignored. These assumptions limit the reliability of numerical values but do not prevent useful insight into behaviour.

For each of the 48 web elements for a particular case of loading P and eccentricity e , principal normal stresses were calculated. These results provide the parameters a_x , a_z in Eqs. 5 with $a_y = 0$ for plane stress. Assuming that concrete tensile capacity is one-tenth of compressive strength ($\gamma = 0.10$) leads to the results of Table 3.

The complete results given in Ref. (2) indicate two critical stress regions in the webs. In region 1 of Fig. 6, near the top of the web in the center of a block, there are high transverse tensile stresses and low compressive stress. A second region, slightly lower near the face shell, experiences high tensile stresses and high compressive stresses. In evaluating the relative importance of these two regions it should be noted that thickening of the web near the face shell was ignored and, as a result, stresses near the face shell tend to be overestimated.

The pattern of stresses is consistent with the failure mode of experimental block prisms. Under axial load block wallettes tend to fail by vertical web splitting near the center of the block and near the face shells.

The qualitative conclusions to be drawn from the analysis is that the governing stresses do not increase proportionally with small load eccentricity but remain relatively constant. As eccentricity increases the direction and location of controlling stresses shifts towards a combined tension-compression situation near the face shell. After this location becomes critical, increases with eccentricity become more pronounced.

BRICK MASONRY BEHAVIOUR

To investigate the stresses in brick masonry walls, detailed analysis of stress variations in all three directions is required. As shown subsequently, results are sensitive to the boundary conditions imposed on the wall element under consideration.

In the present study, attention was focussed on the behaviour of a single brick and its mortar joints. An extensive finite element analysis of this basic combination was made for a variety of conditions. From symmetry and other considerations, attention can be restricted to only a part of the basic unit in a particular case.

In all cases, Poisson's ratio for both brick and mortar was taken as 0.18 while the ratio of moduli of brick to mortar was taken as 4.3. The ratio of pure tensile to pure compressive strength γ was assumed to be 0.08. Joint thickness was 0.47 in. with brick dimensions 9.2 x 4.2 x 2.7 in. These properties correspond to Hilsdorf's specimen no.2..(2).

Analysis was performed in two stages. Stresses caused by pure axial force were first computed followed by a separate calculation of stresses caused by a pure bending moment. Final results for any case are a combination of these two cases.

Prism Analysis

Figure 7 shows a prism subjected to a vertical load P and a moment M . A one eighth segment of a brick is identified at the prism mid-height which is far from the end effects. By imposition of the appropriate kinematic boundary conditions on planes I through IV shown in Fig. 8, it is possible to avoid the need to analyse the entire prism. Symmetry about the vertical plane I is implied by these restraints as well as multifold symmetry about horizontal planes II and III. Symmetry about plane IV is required for axial loading whereas antisymmetry is required for the case of applied moment. Normal stresses on the outside faces are zero.

It is not possible to apply prescribed vertical loads on plane II where the vertical stress distribution is not known. However, it may be assumed on the basis of experimental evidence that points on the plane move in a planar fashion. Thus under vertical load P , plane II will translate downwards relative to plane III. Under moment M there will be a rotation of plane II relative to Plane III. The ability to prescribe displacements in the finite element method is therefore an important feature in the present analysis.

The one eighth segment of the brick was idealized by thirty six hexahedral finite elements while twelve elements were used to represent half the mortar thickness. These elements have twenty nodes distributed as shown in Fig. 9. In the elements, quadratic distribution of displacements is assumed which implies a linear stress variation. Thus a general nonlinear variation of stress through the brick is approximated by a linear function within each finite element.

The mesh of elements used must be relatively fine to limit errors in the analysis. Although the results of a finite element analysis converge

to the exact values with an increasing number of elements, increased precision involves increased computer costs, and additional time in data preparation and interpretation of results. In the present situation, the problem of errors is particularly severe because transverse stresses are a small fraction of the vertical applied loads and are therefore quite sensitive to inaccuracies that may arise. However, on the basis of checks performed after the analysis, it is believed that the fine mesh used did indeed yield very accurate results.

Interesting aspects of behaviour are revealed by an examination of deflection patterns. Shown in Fig. 10 are horizontal displacements along a vertical line in the free end face of the brick and mortar. This plot shows clearly the interaction between brick and mortar with the mortar pulling the brick into tension and vice-versa. Fig. 11 shows a plan view of the displacements of various nodal points in the prism again under vertical load. It is apparent from this plot that vertical plane sections remain plane and vertical everywhere except close to the outside faces of the prism. Furthermore these planes translate without rotation.

Response to an applied moment is also rather surprising in that vertical plane sections remain vertical. However, such planes rotate about a vertical line in the plane of the wall. It is possible that this general behaviour could form the basis for a simplified analysis.

Detailed examination of the pattern and magnitude of lateral stresses indicated that the critical points in brick behaviour were points A, B, C, D, E, and F on the central vertical plane in a brick as shown in Fig. 10. Table 4 summarizes results for the ratio of lengthwise lateral stress σ_x and spalling stress σ_y to the peak vertical stress σ_z . In pure compression σ_z is simply the vertical load divided by the area while in pure bending, σ_z is the vertical stress at the outside edges given by the conventional formula.

Results for point B show that lateral tensile stresses σ_x are almost the same fraction of axial and peak bending vertical stresses. However, the region of high lateral stresses is very limited under applied moment but widespread under axial force. This could be expected to lead to higher average effective capacity.

An aspect of prism loading which can be expected to significantly affect prism behaviour is the effect of end lateral constraint since testing arrangements for relatively short specimens tend to inhibit displacements in the lengthwise direction. Displacements through the thickness are also constrained but to a significantly less extent.

To examine this effect, the analysis was repeated with an additional constraint of zero deflection in the lengthwise or x direction. The results shown in Table 5 indicate that for both axial load and moment, complete confinement leads to compressive rather than tensile lateral stresses in the lengthwise direction.

However, spalling tensile stresses remain and are almost independent of applied moment. Thus, with significant confinement, failure could be initiated by spalling stresses under a load independent of eccentricity. This would yield a significant apparent strain gradient effect.

Wall Analysis

When a basic brick and masonry element is part of a wall rather than a single brick prism, the principle effect is a change in boundary conditions. In the central region away from top, bottom, and edge conditions, a brick does not have a free end. Rather, the end is subjected to forces from a vertical mortar joint. The appropriate constraint on a vertical end plane is a rigid body translation.

For simplicity stack bond has been considered in this analysis. The finite elements of the prism analysis were used with the addition of twelve finite elements to represent one half of the thickness of a vertical mortar joint. The complete set of kinematic constraints is shown in Fig. 12.

To achieve the desired boundary conditions on the vertical plane V, analysis was performed in two steps. Firstly, points on plane V were prevented from movement in the x direction giving rise to a horizontal thrust normal to the plane that should not be present. The value of the thrust was computed as the integral of the σ_x stresses over the plane.

For the case of axial load, transverse stresses were modified by a constant value to eliminate this thrust. The correction step corresponds to a translation of plane V to a location such that the average horizontal stress in the wall is zero as would be the case away from edge effects in a uniformly loaded wall.

A similar procedure was used for the case of an applied moment. In this case the initial transverse stresses must be modified by a rotation of plane V to remove the net moment resulting from the initial solution with no motion of plane V.

Shown in Table 6 are lateral stresses on the centroidal vertical plane of a brick as before. Transverse lateral stresses are somewhat larger than those under prism conditions. Once again, transverse tensile stresses are localized under applied moment but are widespread throughout the brick under axial load.

Of particular interest is the fact that peak tensile stress under applied moment are approximately two-thirds those under axial force for the same peak vertical stress σ_z . The effects of this difference on load capacity can be estimated using the failure surface of Fig. 5.

The stresses at point B are $\sigma_z = P/A + Pet/2I$, $\sigma_x = 0.059 P/A + 0.04 Pet/2I$, and $\sigma_y = 0$ where P is load per unit length. For the brick

geometry assumed, these stresses can be written $\sigma_z = 0.238P + 0.340 Pe$ and $\sigma_x = 0.0140 P + 0.0136 Pe$.

Substitution into the failure surface of Eq. 7, assuming $\gamma = 0.08$ from Hilsdorf's data, leads to a capacity reduction factor $P/P_0 = 1/(1+1.24 e)$. Elementary theory from Eq. [1] yields $P/P_0 = 1/(1+1.43 e)$ which decreases with the eccentricity e more rapidly than the preceding expression.

Coupled with this strain gradient effect are two others. Firstly, as in concrete block walls, axial loads cause generalized lateral tensile stresses while bending moments cause only localized tensile stresses. Secondly, the tensile stresses in the direction of the wall thickness or the spalling stresses are nearly independent of applied bending moments.

SUMMARY AND CONCLUSIONS

In this study, an attempt has been made to establish a rationale for the strain gradient effect in masonry walls. In essence the approach is an extension of Hilsdorf's failure analysis to nonuniform stress fields. Estimation of the stress fields is based on finite element analysis.

Although numerical results are dependent on particular masonry unit and mortar characteristics, a number of general conclusions are suggested by the analysis. These are:

- (1) Experimental studies indicate that short wall capacity is not reduced by load eccentricity as elementary theory would predict.
- (2) This apparent increase in failure stress with eccentricity may arise because failure is associated with lateral tensile stresses whose magnitude and pattern depend on the combination of axial force and moment.
- (3) For concrete block walls with face-shell bedding, large transverse tensile stresses occur in the block webs. These stresses increase very slowly with load eccentricity and hence may be the source of a strain gradient effect.
- (4) For brick masonry walls, lateral tensile stresses in the lengthwise direction increase with load and to a lesser extent with load eccentricity. However, such stresses are highly localized under eccentric load conditions but widespread under pure axial force. Moreover, such transverse stresses are highly dependent on external constraint on deflections and under some test conditions might vanish or change sign. In such cases, spalling stresses can be significant. Since bending moments do not lead to significant spalling stresses, failure based on spalling or lengthwise splitting would not be sensitive to load eccentricity.

In practice, design of short masonry walls could be based on a modified interaction equation of the form

$$\frac{P}{P_o} + \frac{\alpha M}{M_k} = 1 \quad [8]$$

for eccentricities up to the kern eccentricity. In Eq. [8], P_o and M_k are the pure axial load capacity and theoretical kern moment capacity respectively. For eccentricities up to perhaps one half of the kern eccentricity the strain gradient effect factor α can be taken as zero for short walls. However, small eccentricities can cause significant out-of-plane bending for longer walls.

The results in this study have been based on limited finite element studies. While such studies can give valuable insight into behaviour, more accurate and detailed studies for particular experimental arrangements would seem to be of considerable value.

ACKNOWLEDGEMENTS

This study was supported by a research grant from the National Research Council of Canada.

REFERENCES

- (1) Burns, D., "Unreinforced Brick Masonry Walls Under Vertical Load", Technical Report No. SM72-1, Dept. of Civil Engineering, McGill University, Montreal, Quebec, Canada, 1972.
- (2) Fattal, S.G., and Cattaneo, L.E., "Structural Performance of Masonry Walls under Compression and Flexure", Building Science Series 73, National Bureau of Standards, Washington, D.C. June, 1976.
- (3) Hilsdorf, H.K., "An Investigation into the Failure Mechanism of Brick Masonry. Loaded in Axial Compression", Designing, Engineering and Constructing With Masonry Products, Ed. by F.B. Johnson, Gulf Publishing, Houston, Texas, 1969.
- (4) Khoo, C.L., "A Failure Criterion for Brickwork in Axial Compression", Thesis submitted in partial fulfillment of requirements for the degree of Doctor of Philosophy, Edinburgh University, Edinburgh, Scotland, 1972.
- (5) Structural Clay Products Institute, "Recommended Practice for Engineered Brick Masonry", McLean Virginia, 1969.
- (6) Turkstra, C.J. and Ojinaga, J., "The Moment-Magnifier Method Applied to Brick Walls", Proc. Fourth Int'l Brick Masonry Conf., Bruges, Belgium, April 1976.

(7) Yokel, F.Y., Mathey, R.G., and Dikkers, R.D., "Compressive Strength of Slender Concrete Masonry Walls", Building Science Series 33, National Bureau of Standards, Washington, D.C., Dec., 1970.

TABLE 1 - Brick Walette Data

Eccentricity		Axial Force P (kips) (3)	Force Ratio P/P_o		Failure Moment (in kips)		Gradient Factor α (8)
e(in) (1)	e/c_k (2)		Theory (4)	Exp (5)	Theory (6)	Exp (7)	
0	0	497.0	1.0	1.100	0	0	-
		408.5		.904			
		450.0		.996			
		451.8		1.0			
0.297	.500	465.0	0.66	1.029	89.45	138.1	-.056
		462.0		1.023		137.2	-.045
		495.0		1.096		147.0	-.175
		474.0		1.049		140.8	-.093
0.593	1.00	353.0	0.50	0.781	134.0	209.3	0.280
		356.5		0.789		211.4	.267
		331.5		0.734		196.6	.362
		347.0		0.768		205.8	.302

NOTE: Thickness $t = 3.56$ in, Net area $A = 112.5$ in², Net moment of inertia = 118.8 in⁴. Kern eccentricity = 0.593 in. Kern moment = 134.0 in k. Axial capacity $P_o = 451.8$ kips.

TABLE 2 - Block Wallette Data

Eccentricity		Axial Force P (in kips) (3)	Force Ratio P/P _o		Failure Moment (in kips)		Gradient Factor α (8)		
e(in) (1)	e/e _k (2)		Theory (4)	Exp (5)	Theory (6)	Exp (7)			
0	0	127.7	1.00	1.03	0	0	-		
		122.5		.99					
		122.5		.99					
		124.2		1.00					
.467	.311	120.0	.76	.97	44.1	56.0	.10		
		87.8		.71				41.0	1.32
		160.0		1.29				74.7	-.73
		122.6		.99				57.3	.03
.933	.620	115.1	.62	.93	71.5	107.3	.12		
		108.9		.88				101.6	.22
		117.1		.94				109.2	.10
		113.7		.91				106.1	.16
1.400	.931	82.5	.52	.66	90.0	115.5	.55		
		84.4		.68				118.2	.51
		82.3		.66				115.2	.55
		83.1		.67				116.3	.53

NOTE: Thickness $t = 5.6$ in, Net area $A = 88.4$ in², Net moment of inertia $I = 372.4$ in⁴, Kern eccentricity = 1.50 in, Kern moment = 93.4 in. kips, Axial capacity $P_o = 124.2$ kips.

TABLE 3 - Block Analysis

Eccentricity e/e_k (1)	Stress Ratios				Load Capacity P/P_o			
	Region 1		Region 2		Elementary Theory (6)	Region 1 (7)	Region 2 (8)	Experiment (9)
	a_x (2)	a_z (3)	a_x (4)	a_z (5)				
0	5.24	.45	4.44	12.93	1.00	1.00	1.00	1.00
0.311	5.35	.42	4.97	15.74	0.76	0.98	0.88	0.99
0.622	5.45	.38	5.50	16.54	0.62	0.96	0.80	0.92
0.933	5.58	.35	6.03	21.35	0.52	0.94	0.70	0.67

TABLE 4 - Lateral Stress in Brick Prism

Location (1)	Ratio of Lateral Stress to Vertical Stress (%)			
	Axial Load		Moment	
	σ_x/σ_z (2)	σ_y/σ_z (3)	σ_x/σ_z (4)	σ_y/σ_z (5)
A	-1.5	0	-1.6	0
B	-4.1	0	-3.9	0
C	-2.9	-2.2	0	0
D	-2.7	-3.3	0	0
E	-1.5	0	+1.6	0
F	-4.1	0	+3.9	0

NOTE: Ratio (σ_x/σ_z) for applied moment are based on the extreme fibre value of σ_z .

TABLE 5 - Effects of Confinement on Lateral Stresses

Location (1)	Lateral Stress σ_x/σ_z (%)	
	Axial Load (2)	Moment (3)
A	17.4	16.2
B	14.0	14.0
C	16.0	-
D	15.6	-
E	17.4	16.2
F	14.0	14.0

TABLE 6 - Lateral Stresses in Brick Wall

Location (1)	Ratio of Lateral Stresses to Vertical Stress (%)			
	Axial Load		Bending Moment	
	σ_x/σ_z (2)	σ_y/σ_z (3)	σ_x/σ_z (4)	σ_y/σ_z (5)
A	-3.6	0	-2.1	0
B	-5.9	0	-4.0	0
C	-5.0	-2.2	0	0
D	-4.7	-3.2	0	0
E	-3.6	0	+2.1	0
F	-5.9	0	+4.0	0

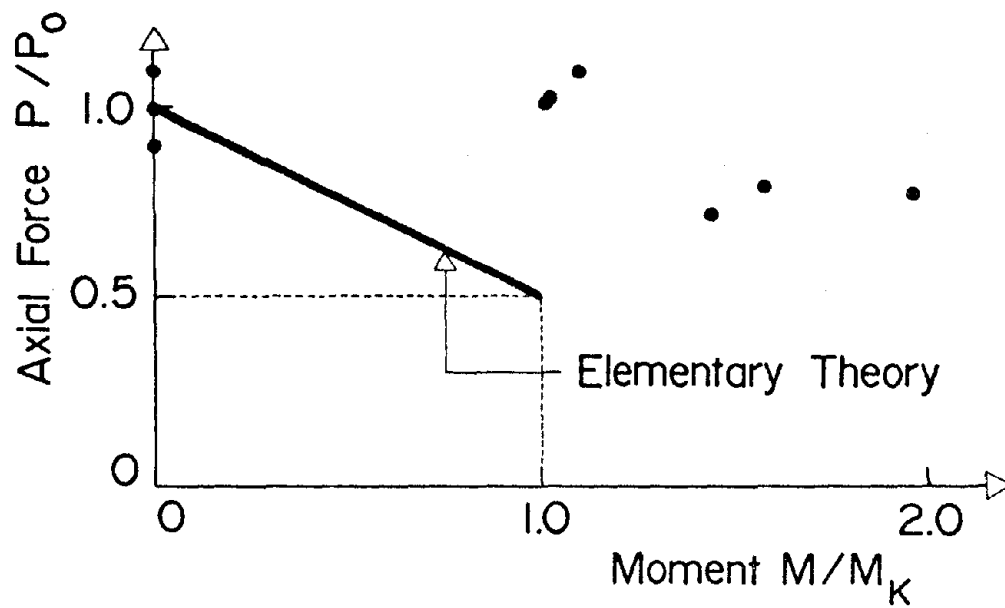


FIG. 1 BRICK WALLETTE DATA

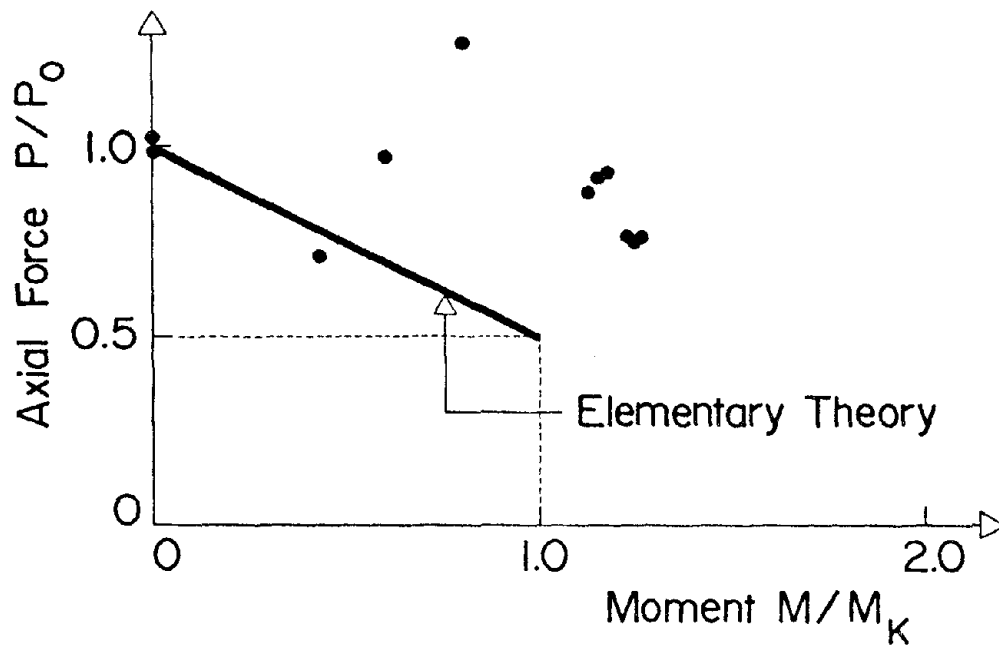
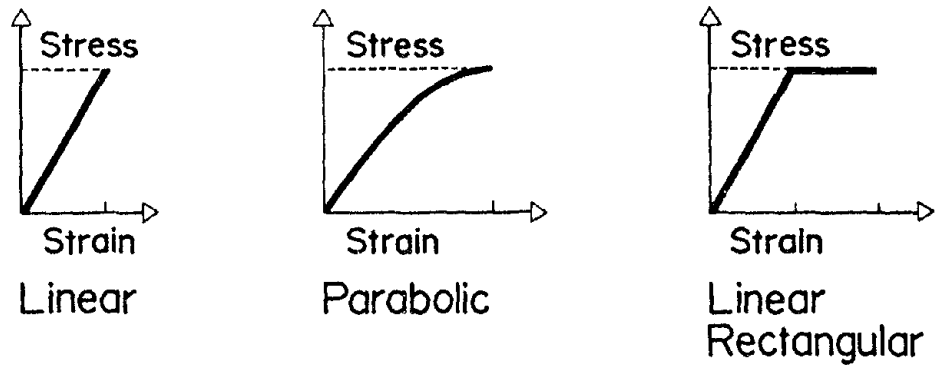
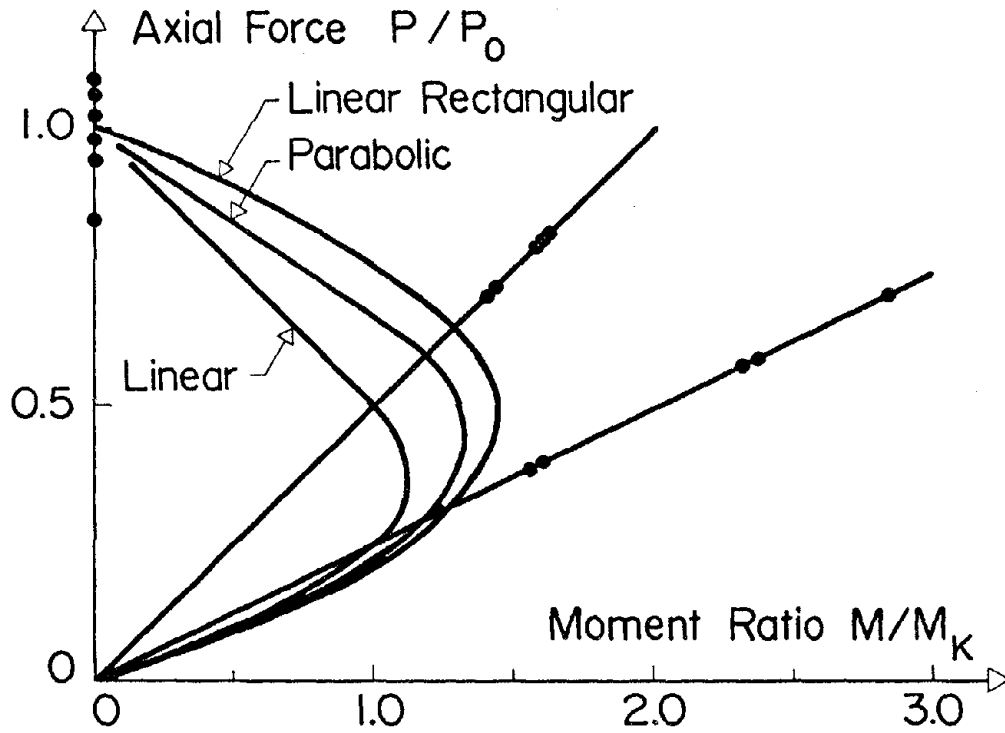


FIG. 2 BLOCK WALLETTE DATA



(a) Stress Strain Diagrams



(b) Experimental Results

FIG. 3 BRICK WALL DATA

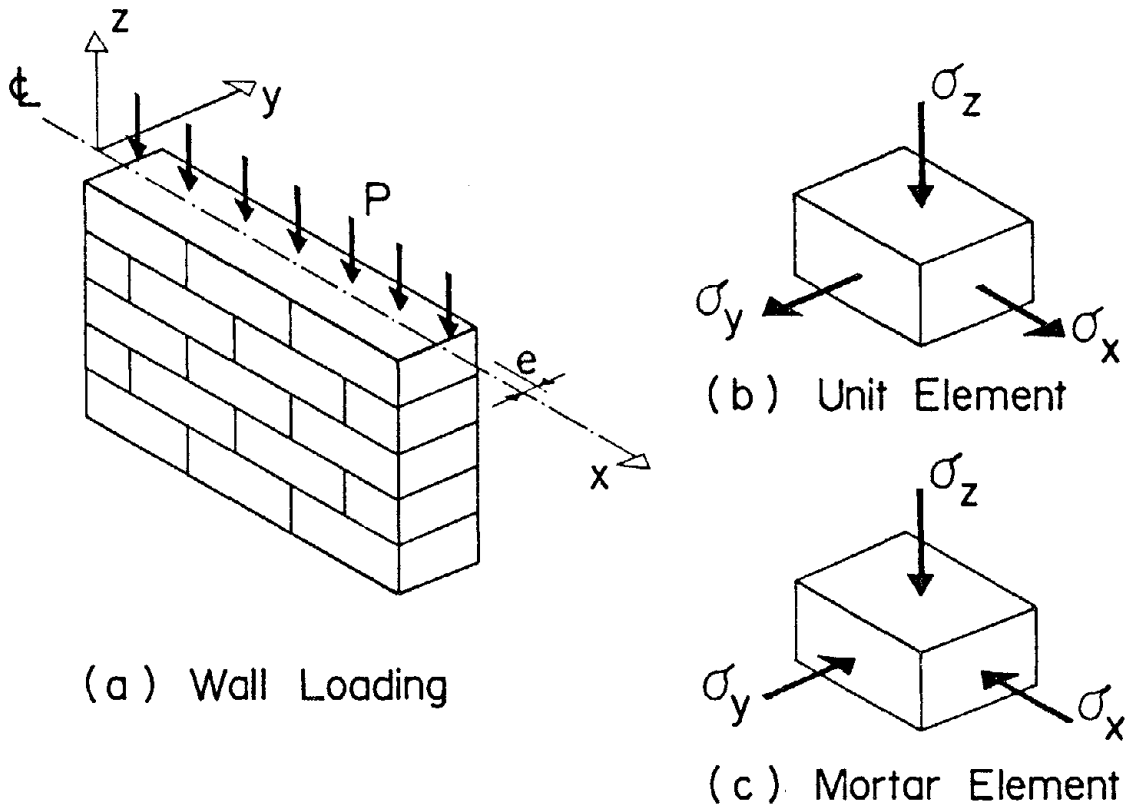


FIG. 4 GENERAL WALL SITUATION

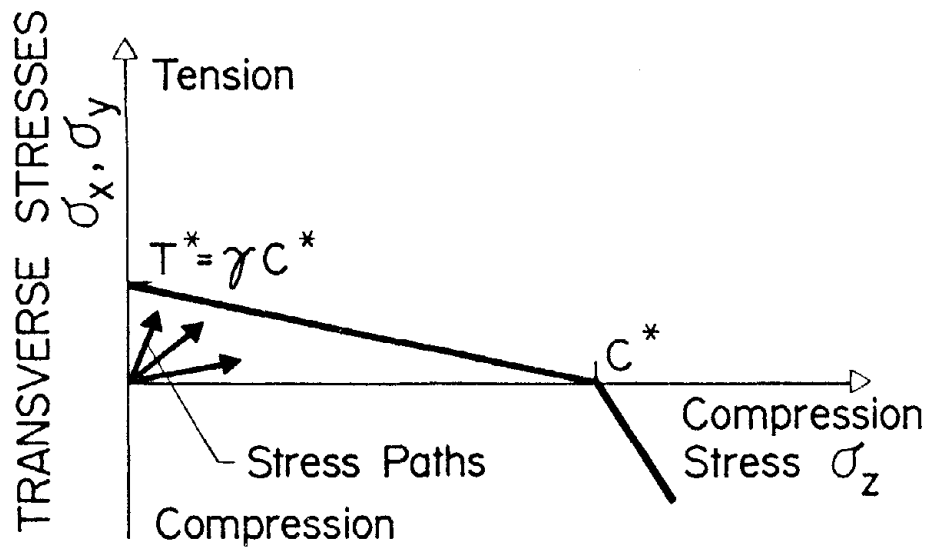


FIG. 5 FAILURE SURFACES

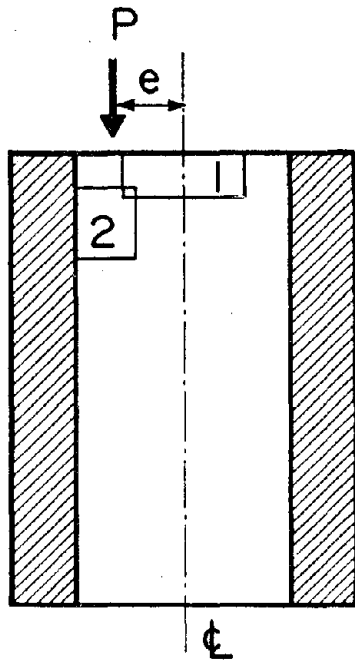


FIG. 6 CRITICAL BLOCK STRESS REGIONS

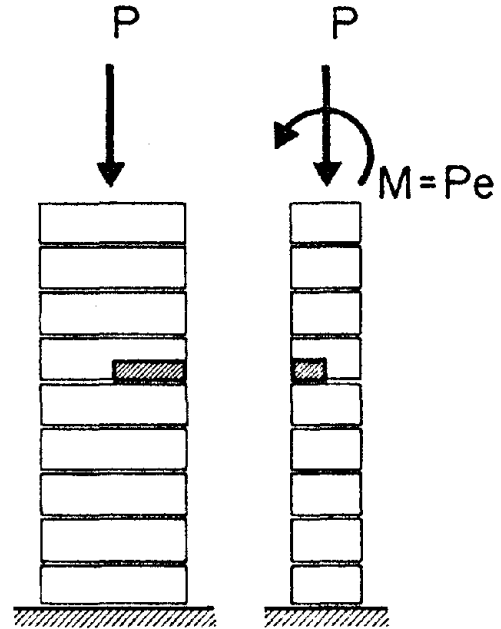


FIG. 7 BRICK PRISM

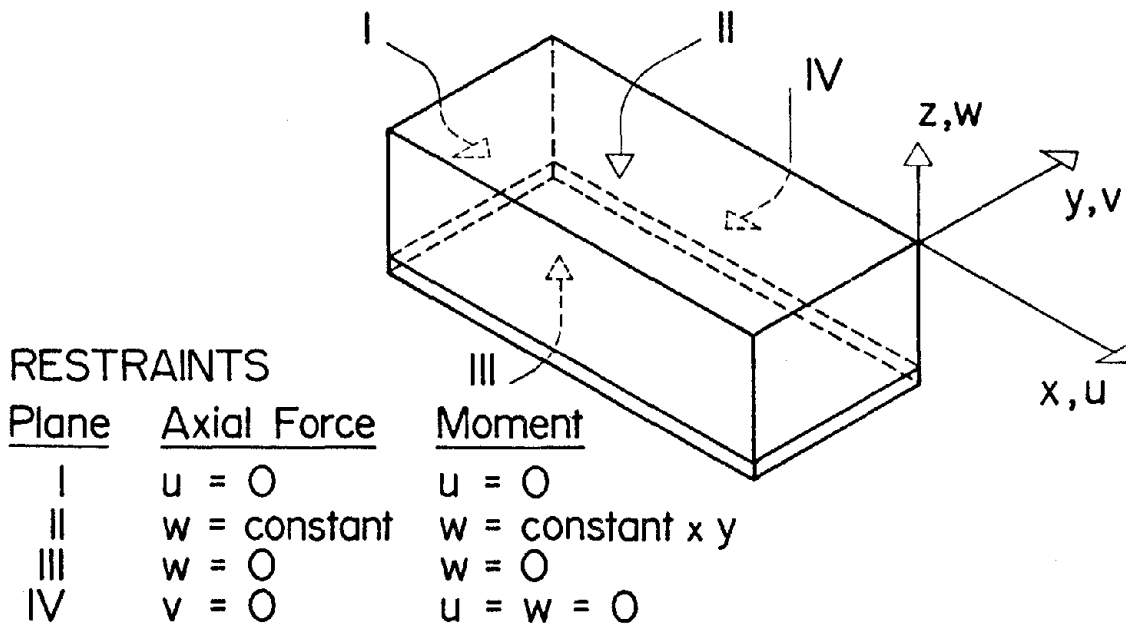
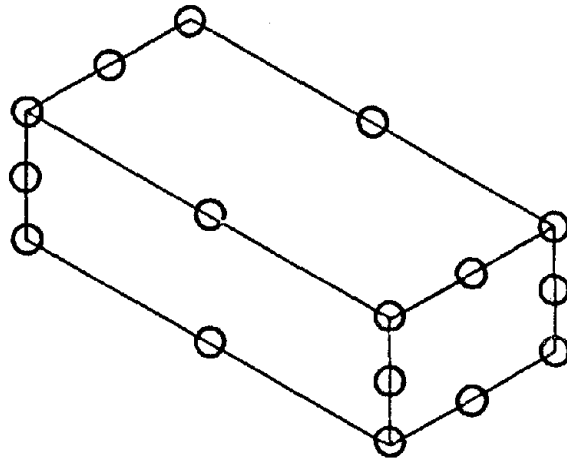
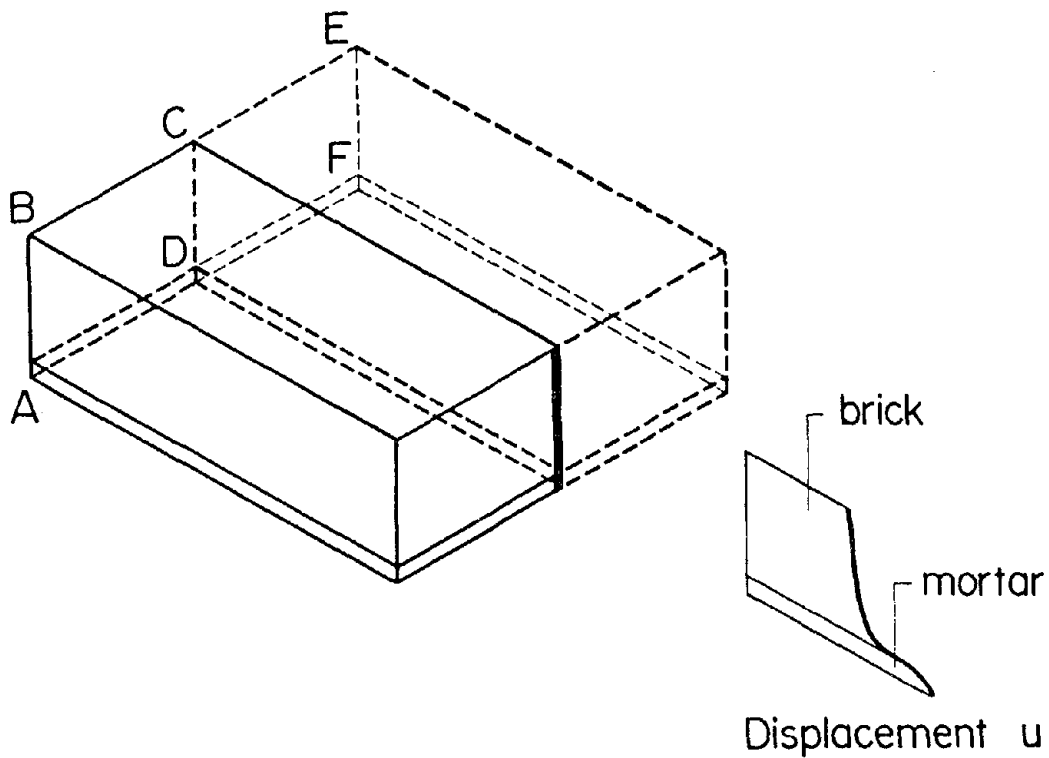


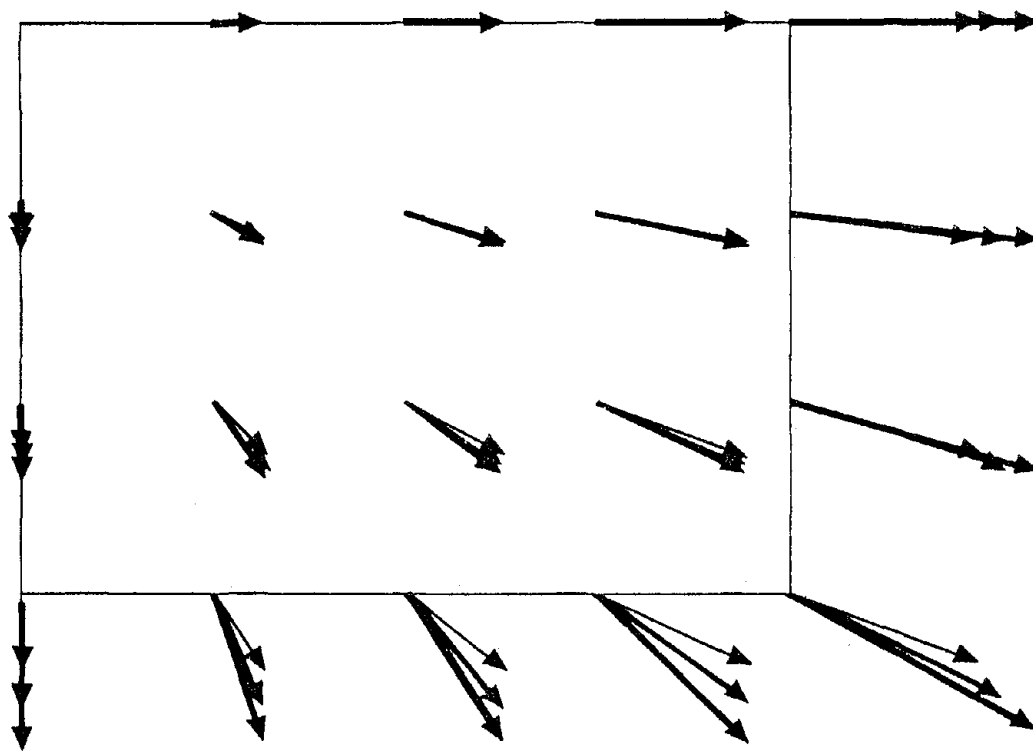
FIG. 8 KINEMATIC RESTRAINTS ON BRICK PRISM



**FIG. 9 THREE DIMENSIONAL HEXAHEDRAL
FINITE ELEMENT**

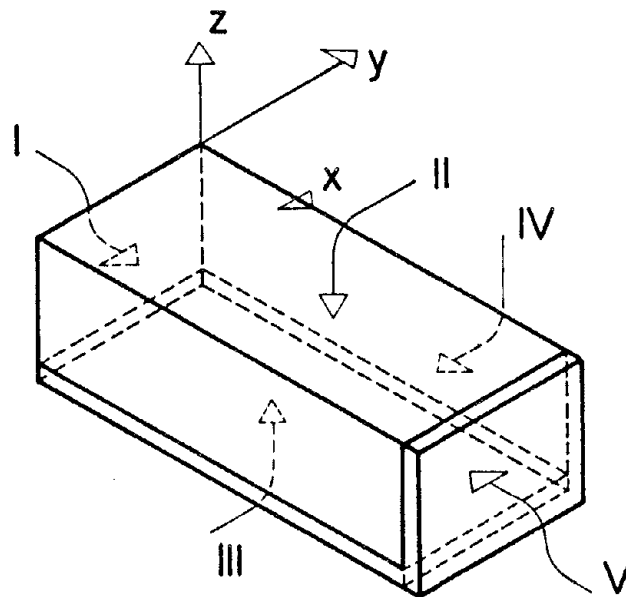


**FIG. 10 HORIZONTAL DISPLACEMENT ON
END SECTION**



→ ϕ mortar
→ mortar/brick interface
→ ϕ brick

FIG. II DISPLACEMENTS DUE TO VERTICAL LOAD



RESTRAINTS

<u>Plane</u>	<u>Axial Force</u>	<u>Moment</u>
I	$u = 0$	$u = 0$
II	$w = \text{constant}$	$w = \text{constant } x \ y$
III	$w = 0$	$w = 0$
IV	$v = 0$	$u = w = 0$
V	$u = \text{constant}$	$u = \text{constant } x \ y$

**FIG. 12 KINEMATIC RESTRAINTS
FOR BRICK WALL**

THE EFFECT OF STRENGTH AND GEOMETRY ON THE ELASTIC
AND CREEP PROPERTIES OF MASONRY MEMBERS

By Lenczner, D.

ABSTRACT: A survey is presented of the main factors which influence creep in masonry piers and walls. The effect of type of brick and mortar, stress level, presence of damp proof course, temperature and humidity, age, and degree of saturation of bricks at laying are considered. An expression is put forward giving creep strain in composite walls as a function of the elastic and creep parameters of component leaves. This is followed by a study of the effect of strength and geometry on the elastic and creep properties of masonry members. An approximate method is given for estimating the maximum creep strain in brickwork piers and walls. The only information required for this purpose is the strength of the brick units and small brickwork cubes.

THE EFFECT OF STRENGTH AND GEOMETRY
ON THE ELASTIC AND CREEP PROPERTIES
OF MASONRY MEMBERS

By David Lenczner¹

INTRODUCTION

For well over a decade the author has been engaged on a research programme to investigate the elastic and creep properties of masonry. Most of the tests were carried out on brickwork and some on blockwork members. The specimens used were hollow piers 12 courses high and storey high single leaf and cavity walls. Recently tests were also carried out on storey high piers.

With few exceptions the creep tests were carried out at a constant temperature of 20°C and 45-50 percent relative humidity. With one exception the bricks were laid air dry. In most cases the load was applied 28 days after laying. A range of stress levels was used in the tests but the upper limit was confined to just over one half of the strength of the masonry.

A considerable amount of data has already been obtained on the elastic and creep properties of masonry and most of it has already been published (1 to 7)².

This paper surveys the work carried out to date. The first part of the paper summarizes the more important findings resulting from this work. This is followed by an analysis in which the elastic and creep properties of masonry members are related to the strength of the members. A set of empirical equations is put forward which may be used to predict the instantaneous and long term movements in brickwork masonry members under sustained loads.

CREEP IN MASONRY PIERS

The elastic and creep properties of masonry depend on a number of factors. The more important ones are the strength and coefficient of absorption of the unit, the degree of saturation of the unit at laying, the type and strength of mortar, stress level, temperature, humidity and age at loading. A summary of results from the tests carried out on brickwork and blockwork piers with different types of brick, block and mortar are given in Table 1 in Appendix III.

¹Senior Lecturer in Bld. Tech., Univ. of Wales Inst. of Science and Tech., Cardiff.

²Numbers in parentheses refer to corresponding items in the Appendix I - References.

Depending on the stress level and the strength of bricks and mortar, brickwork piers creep for a period ranging from a few weeks to 12 months or more. Most of the creep will usually take place within the first nine months. The amount of creep varies inversely with the strength of the piers and their components. It has been found that the maximum load-strain (the strain caused only by the load) is roughly proportional to the instantaneous strain. For that reason it is convenient to relate the creep, or the maximum load-strain (instantaneous strain + creep), to the instantaneous strain. The ratio of maximum load-strain to the instantaneous strain, hereafter called the 'strain ratio' is a useful parameter in the study of creep in brickwork.

Creep in brickwork piers decreases with an increase in relative humidity. In an uncontrolled environment the temperature and moisture expansion may exceed numerically the creep strain. It follows that in such a situation the resultant strain in the piers under load may be less than the initial strain.

The presence of a layer of a bituminous damp proof course can increase the creep strain in brickwork piers two to threefold. Even above the layer of dpc the creep strain is considerably greater than when no dpc is present. The difference can be attributed to a smaller lateral restraint above the dpc and becomes more noticeable at stress levels approaching the yield stress of the dpc.

In absolute terms blockwork piers were found to creep considerably more than brickwork piers. To a large extent this was due to a lower strength of the blocks tested. It was also found that a considerable amount of creep occurred in the blocks themselves.

CREEP IN SINGLE LEAF AND CAVITY WALLS

Creep tests were carried out on single leaf and cavity storey high walls. Details of these tests are given in Table 1 in Appendix III. The main findings of these tests are given below:

A comparative study of movements in single leaf walls subjected to a constant load showed that between 20-40 percent of the maximum load-strain occurs in the bricks and the rest in the mortar bed joints. Bearing in mind that bricks account for approximately 85 percent of the height of a wall it is clear that, when compared on the basis of equal gauge length, the strain in the bricks is relatively small and that by far the highest proportion of the strain occurs in the mortar.

A series of tests were carried out to compare the creep behaviour of a composite brick/block cavity wall with similar walls composed of bricks and blocks respectively. A theory (8) was developed based on a modified Kelvin model which, from known elastic and creep parameters of the components, gave the creep strain in the composite. The required parameters can be obtained from independent

tests on the components or from published data.

The strain in a composite wall at time t after loading is given by³

$$\epsilon_c = \epsilon_{i,c} \left[2.5 - 1.2 \exp \frac{-E_c t}{\lambda_c} \right] \quad (1)$$

The theory also showed that

$$\epsilon_{i,c} = \frac{2\epsilon_1\epsilon_2}{\epsilon_1 + \epsilon_2} \quad (2)$$

$$E_c = \frac{E_1 + E_2}{2} \quad (3)$$

and

$$\lambda_c = \frac{\lambda_1 + \lambda_2}{2} \quad (4)$$

Comparison of experimental and theoretical values showed reasonably good agreement (8).

It appears on present evidence that the degree of saturation of bricks at laying has an effect on subsequent creep in walls and probably in piers too. Further tests are necessary to confirm this. The effect of age at loading, provided it is more than 14 days after laying, does not seem to have a marked influence on creep in walls. Small eccentricity of loading does not seem to affect the magnitude of creep in walls either.

EFFECT OF STRENGTH AND GEOMETRY ON THE ELASTIC PROPERTIES OF MASONRY MEMBERS

A comprehensive study was made of the factors which may influence the elastic properties of masonry members. The factors studied were types of unit and mortar as well as geometry of the member. The parameter chosen to represent the elastic behaviour of masonry was the elastic modulus. Attempts were made to relate the elastic modulus with masonry and mortar strength but without much success. There was, however, a much better relationship between the elastic modulus of masonry members and the compressive strength of the masonry unit.

Figure 1 shows the graph of the elastic modulus of masonry piers and walls made up with different bricks, blocks and mortar plotted against the strength of the masonry units. Where more than one stress level was used for a particular unit and mortar the mean value of the modulus was plotted and the scatter indicated by a band. The figure shows that in spite of the scatter which is inevitable in an inherently variable material like masonry, there is a well defined relationship between the elastic modulus of the

³For notation see Appendix II

masonry members, brick or block, wall or pier, and the strength of the unit. The geometry of the member does not appear to have any consistent effect on the modulus. The relationship may be represented approximately by a set of straight lines shown in the figure. These should give the lower limit of the modulus and thus should give the maximum probable elastic or instantaneous strain.

For units of compressive strength of 20 N/mm^2 or less the elastic modulus may be taken as $5,000 \text{ N/mm}^2$. For units with compressive strength between 20 and 70 N/mm^2 the modulus is given by

$$E = 300S - 2000 \quad (5)$$

For units with compressive of 70 N/mm^2 and above

$$E = 12,750 + 100S \quad (6)$$

THE EFFECT OF STRENGTH AND GEOMETRY ON THE CREEP IN BRICKWORK MASONRY MEMBERS

It has already been shown that the strain ratio is a useful concept which enables us to relate the maximum load-strain with the instantaneous strain. Using the information given in Table 1 in Appendix III graphs were plotted of the strain ratio against brickwork cube strength at 88 days for brickwork piers and single leaf walls. Due to insufficient tests blockwork members were excluded. These graphs are shown in Figure 2. As before, where more than one stress level was used for a given type of member the mean value of the strain ratio was plotted and the scatter indicated by a band.

Although the number of results is still relatively small, especially for brickwork walls, a certain trend begins to emerge. It appears that for brickwork piers, regardless of type of mortar, the relationship between the strain ratio and brickwork strength can be roughly represented by a straight line:

$$R = 3 - \frac{6W}{100} \quad (7)$$

For single leaf brickwork walls the variation between the strain ratio and brickwork strength follows a similar pattern, namely:

$$R = 4.7 - \frac{6.6W}{100} \quad (8)$$

A single result obtained so far for a brickwork cavity wall suggests that the values of strain ratio for cavity walls lies somewhere between those of piers and single leaf walls.

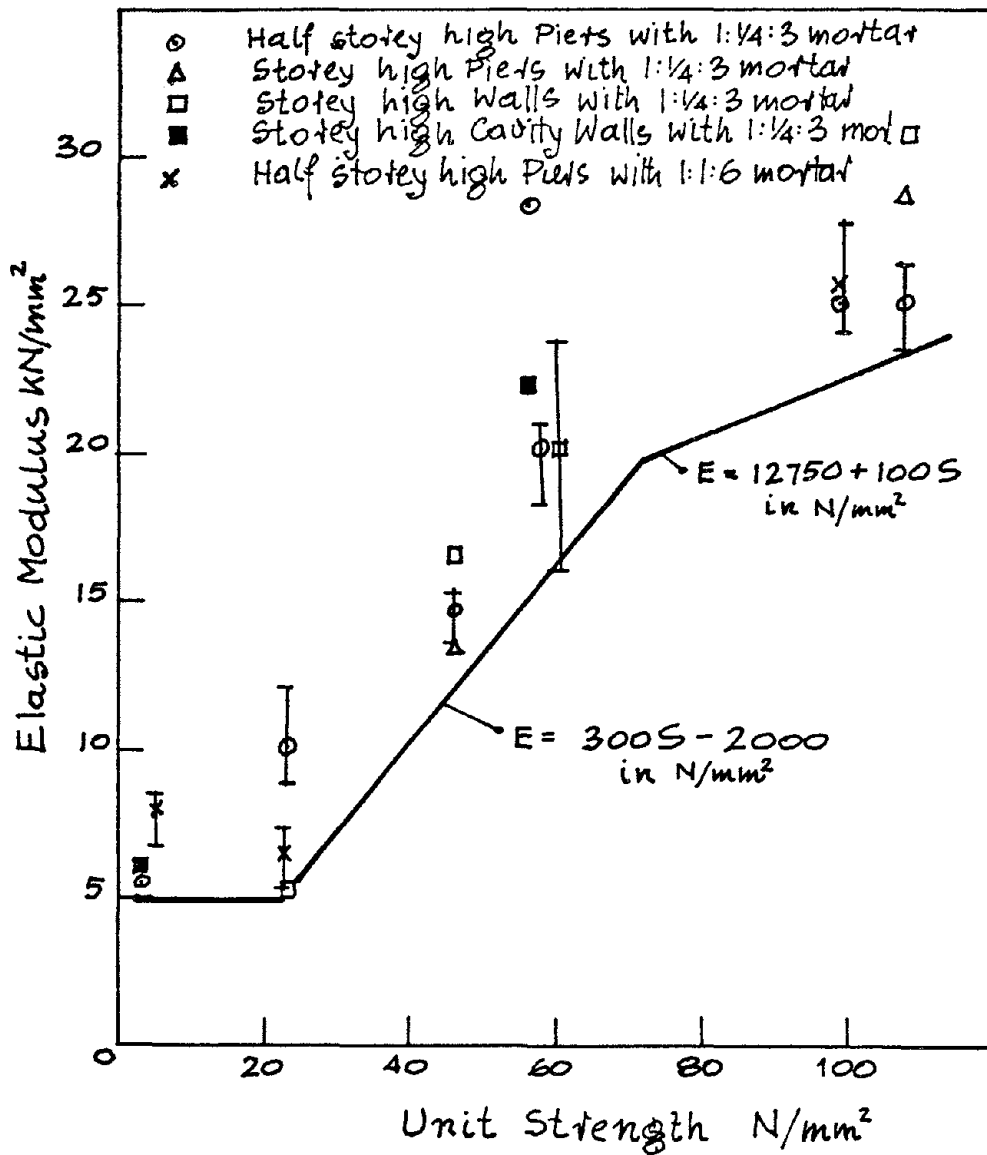
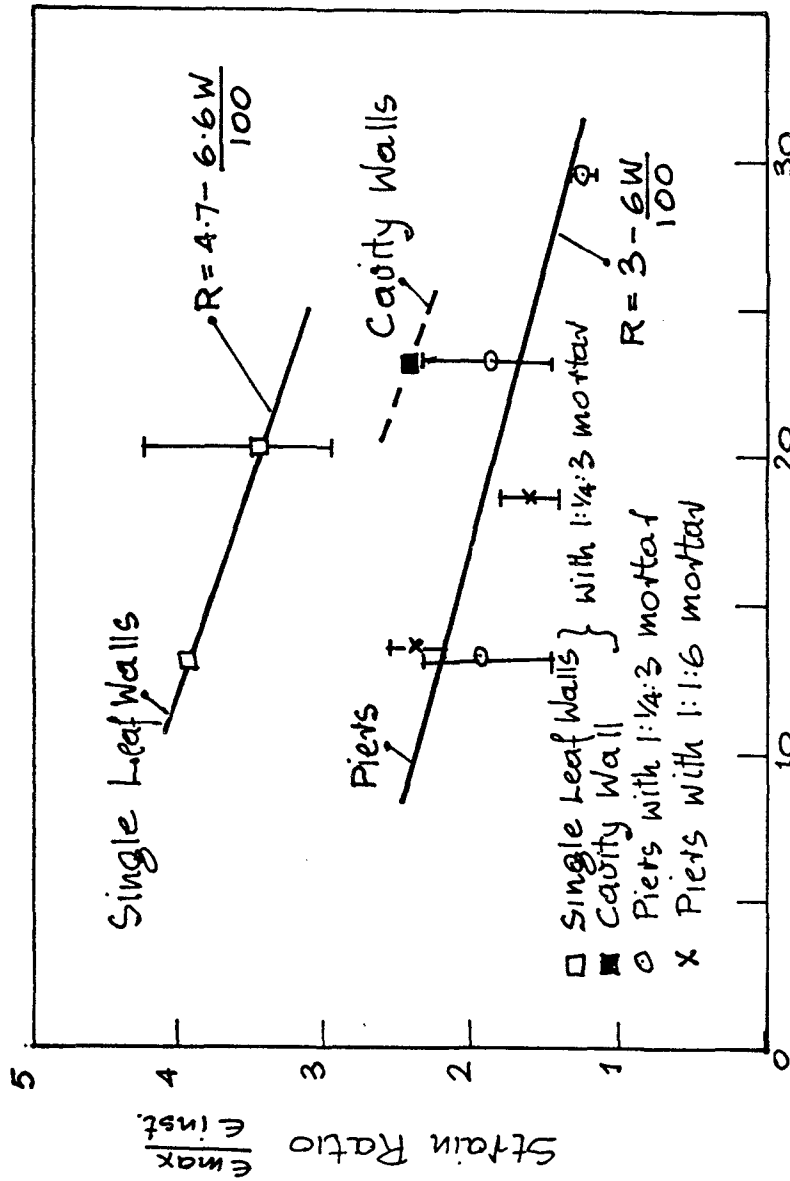


FIGURE 1. Variation of Elastic Modulus of Masonry Members with Strength of Masonry Unit.



Brickwork Cube Strength N/mm^2
 FIGURE 2. Variation of Strain Ratio for Walls
 and Piers with Brickwork Cube Strength

METHOD OF PREDICTING CREEP IN BRICKWORK

Using equations 5-8 it is possible to predict the maximum likely creep strain in brickwork piers and single leaf walls. The only information required is the compressive strength of the brick and brickwork cubes made with it. The recommended procedure is outlined below:

(a) Use equations (5) or (6) to determine the elastic modulus of pier or wall for a known brick strength. For a brick strength of 20 N/mm² or less take $E = 5,000 \text{ N/mm}^2$.

(b) For the known or design stress level determine the instantaneous strain of the pier or wall from

$$\epsilon_i = \frac{\sigma}{E} \quad (9)$$

(c) Determine the strain ratio for the known brickwork cube strength using equation (7) for piers and equation (8) for single leaf walls.

(d) Determine the maximum load strain from maximum load strain = strain ratio x instantaneous strain.

(e) Determine the maximum creep strain from maximum creep strain = maximum load strain - instantaneous strain.

SUMMARY AND CONCLUSIONS

The first part of the paper presented a brief review of the creep behaviour of masonry piers and walls. The creep behaviour of a brick/block cavity wall was also considered and an expression is given, based on a modified Kelvin model, for predicting the load-strain in the composite in terms of the elastic and creep properties of the components.

The second part of the paper considered the effect of strength and geometry on the elastic and creep properties of masonry members. An approximate method is given for estimating the maximum load and creep strains in brickwork piers and walls. The only required information is the strength of the bricks and brickwork cubes. It is hoped that with more experimental data it will become possible to improve the method to give a more accurate prediction of creep in masonry members.

ACKNOWLEDGEMENT

The work described in this paper is sponsored by the Science Research Council and The Structural Clay Products Ltd. of Great Britain.

The author wishes to express his thanks to both sponsors for

providing the funds for carrying out the research work and to Professor J.D. Geddes for providing the laboratory facilities.

APPENDIX I

REFERENCES

1. LENCZNER, D. 1970. "Creep in Brickwork". Proc. 2nd Inter. Conf. on Brick Masonry, SIBMAC, Stoke-on-Trent.
2. LENCZNER, D. 1973. "Creep in Brickwork with and without Damp-Proof Course". Proc. 4th Inter. Symp. on Loadbearing Brickwork, London, 1971. The Brit. Ceram. Socy.
3. LENCZNER, D. 1974. "Creep in Concrete Blockwork Piers". The Struct. Eng., Mar. Vol. 52 No. 3.
4. LENCZNER, D., WYATT, K. and SALAHUDDIN, J. 1975. "The effect of stress on Creep in Brickwork Piers". Proc. Brit. Ceram. Socy. Loadbearing Brickwork (5). 24 Sept.
5. LENCZNER, D. 1976. "Creep and Moisture Movement in Brickwork and Blockwork". Proc. of the Inter. Conf. on Performance of Building Structures. Vol. 1. Glasgow.
6. LENCZNER, D. and SALAHUDDIN, J. 1976. "Creep and Moisture Movements in a Brickwork Wall". Proc. 4th. Inter. Brick-Masonry Congress. Bruges. Section 2.
7. LENCZNER, D. and SALAHUDDIN, J. 1976. "Creep and Moisture Movements in Masonry Piers and Walls". First Can. Masonry Symp. Univ. of Calgary, Canada.
8. LENCZNER, D. 1977. "Creep in Brickwork and Blockwork Cavity Walls and Piers. The 5th Inter. Symp. on Loadbearing Brickwork. London, Dec. 1977. Brit. Ceram. Socy. (To be published).

APPENDIX II

NOTATION

- t = time after loading (secs.)
- E, E_1, E_2 = elastic moduli of member or components (N/mm^2)
- λ_1, λ_2 = coefficients of traction ($Nsec/mm^2$)
- E_c = elastic modulus of composite wall (N/mm^2)
- λ_c = coefficient of traction for composite wall ($Nsec/mm^2$)
- $\epsilon_i, \epsilon_1, \epsilon_2$ = instantaneous strains in member or components

$\epsilon_{i,c}$ = instantaneous strain in composite wall

ϵ_c = load-strain at time t in composite wall

E = elastic modulus of masonry member (N/mm^2)

S = compressive strength of brick or unit (N/mm^2)

W = brickwork cube strength at 28 days (N/mm^2)

R = strain ratio = $\frac{\text{maximum load strain}}{\text{instantaneous strain}}$

σ = stress level (N/mm^2)

APPENDIX III

TABLE 1

No.	Type of Specimen	Compressive strength of unit N/mm ²	Mortar type and strength N/mm ²	Masonry cube or pier* strength ² N/mm ²	Stress Level N/mm ²	Instant Strain x 10 ⁻⁵	Maximum Load-Strain x 10 ⁻⁵	Elastic Modulus kN/mm ²	Strain Ratio
1	Butterley Pier	99	1:1:3 16.1	29.5	1.70	6.1	7.8	27.9	1.28
2	"	"	"	"	2.80	11.6	13.9	24.1	1.20
3	"	"	"	"	4.34	17.7	21.6	24.6	1.22
4	"	"	"	"	6.00	24.6	31.9	24.4	1.29
AV. 1-4		99	16.1	29.5				25.3	1.25
5	Butterley Pier	99	1:1:6 7.8	18.7	2.30	8.5	11.9	27.3	1.40
6	"	"	"	"	2.91	12.1	17.5	24.1	1.45
7	"	"	"	"	3.86	14.9	24.6	25.9	1.65
8	"	"	"	"	4.65	18.4	33.1	25.2	1.80

TABLE 1 (continued)

Av. 5-8		99	7.8	18.7						25.7	1.58
9	National Star Pier	58	1:4:3 17.8	23.3	1.25	6.5	9.6	19.2	1.47		
10	"	"	"	"	2.39	11.4	23.0	21.0	2.02		
11	"	"	"	"	3.76	17.8	30.2	21.1	1.69		
12	"	"	"	"	4.95	24.1	36.9	20.5	1.61		
13	"	"	"	"	2.93	15.9	38.3	18.4	2.41		
14	"	"	"	"	4.95	23.9	46.9	20.7	1.96		
Av. 9-14		58	17.8	23.3				20.2	1.86		
15	Fletton Pier	23	1:4:3 19.3	13.2	1.1	12.0	17.1	9.2	1.43		
16	"	"	"	"	1.7	14.0	27.6	12.1	1.97		
17	"	"	"	"	2.3	26.0	60.3	8.9	2.32		

TABLE 1 (Continued)

Av. 15-17		23	1:1:3 19.3	13.2				10.1	1.91
18	Fletton Pier	23	1:1:6 5.1	13.6	1.03	15.7	37.2	6.6	2.37
19	"	"	"	"	1.45	27.3	69.1	5.3	2.53
20	"	"	"	"	1.98	27.4	60.0	7.3	2.19
Av. 18-20		"	5.1	13.6				6.4	2.36
21	Concrete Block Pier	5.6	1:1:6 8.5	4.2*	0.78	9.6	73.4	7.7	7.64
22	"	"	"	"	1.20	14.0	85.6	8.6	6.11
23	"	"	"	"	1.62	19.9	96.0	8.1	4.84
24	"	"	"	"	1.89	27.7	118.0	6.8	4.27
Av. 21-24									
25	Aglite Block Pier	3.3	1:1:3 23.3	-	1.06	18.15	62.8	5.4	3.46

TABLE 1 (Continued)

26	Rustic Brown Pier	56	1:1:3 23.3	30.4	1.13	3.50	7.8	28.3	2.23
27	Poynton Pier	46	1:1:3 17.5	20.9	1.96	14.3		13.7	
28	"	"	"	"	1.92	12.4		15.5	
Av. 27-28		46	17.5	20.9				14.6	
29	Poynton Storey High Pier	46	1:1:3 17.6	20.9	1.95	14.6		13.4	
30	Swillington Pier	108	1:1:3 17.6	36.2	1.92	7.2		26.7	
31	"	108	"		1.91	8.1		23.6	
Av. 30-31		108	17.6	36.2				25.1	
32	Swillington Storey High Pier	108	1:1:3 17.6	36.2	1.95	6.8		28.7	
33	Fletton Wall	23	1:1:3 19.3	13.2	1.20	23.4	92.2	5.1	3.94
34	Staffordshire Wall	60	1:1:3 17.2	20.2	3.73	15.7	66.5	23.8	4.24

TABLE 1 (continued)

35	Staffordshire Wall	60	1:4:3 17.2	20.2	3.45	21.3	62.7	16.2	2.94
36	"	"	"	"	4.51	22.4	71.1	20.1	3.17
Av. 34-36		60	17.2	20.2				20.0	3.45
37	Poynton Wall	46	1:4:3 17.6	20.9	2.00	12.1		16.5	
38	Swillington Wall	108	1:4:3 17.6	36.2	1.92	6.4		30.6	
39	Rustic Brown Cavity Wall	56	1:4:3 23.3	30.4	0.91	3.7	8.9	22.1	2.41
40	Ag-lite Block Cavity Wall	3.6	23.3	-	0.94	18.3	39.1	5.6	2.14

REINFORCED BRICKWORK LINTEL SHEAR STUDY UTILIZING SMALL SCALE BRICKS

by

G. T. Suter* and H. Keller*

ABSTRACT

The basic objective of the work dealt with in the paper is to help define brickwork lintel ultimate shear strength values for a future North American masonry code based on limit states design. Past work by the authors and others has led to a satisfactory definition of ultimate shear capacities for ordinary reinforced brickwork lintels. However, what still remains to be investigated and what represents the primary objective of this paper, is the effect of a varying grout cavity width on the shear capacity of grouted beams. Such an investigation could be carried out by utilizing full scale or small scale bricks, where small scale masonry units have the advantage of faster construction, reduced weight, easier handling and hence overall time savings. While small scale brickwork studies have been successfully employed, particularly in Britain, all such studies were limited to unreinforced brick masonry and hence when the authors decided to utilize small scale units for their investigation of the effect of a varying grout cavity width on shear capacity, basic work in reinforced brickwork was required to prove the validity of small scale versus full scale results. To provide this evidence, the authors carried out a research program over a three year period involving a total of thirty-seven beams. Approximately one half of the beams consisted of small scale members while the remainder were full scale lintels for comparison purposes. Besides the scale effect, other key variables investigated were the shear arm ratio and the width of the grout cavity.

The two most significant results of the investigation indicate firstly, that small scale beams can indeed be utilized to predict the shear strength of full scale lintels and secondly, that the shear capacity of grouted beams can be conservatively calculated from the separate shear capacities of the grout and brick sections according to their relative widths.

*Associate Professor and Research Engineer, respectively,
Department of Civil Engineering, Carleton University, Ottawa, Canada.

REINFORCED BRICKWORK LINTEL SHEAR STUDY UTILIZING SMALL SCALE BRICKS

G. T. Suter* and H. Keller*

INTRODUCTION

The basic objective of the work dealt with in the paper is to help define brickwork lintel ultimate shear strength values for a future North American masonry code based on limit states design. Past work by the authors and others (6,8) has led to a satisfactory definition of ultimate shear capacities for ordinary reinforced brickwork (RB) lintels. For the typical elevation and cross section of RB lintels shown in Fig.1, this work has indicated that the ultimate shear strength of RB lintels is dependent mainly on the ratio of shear span to effective depth or shear arm ratio, a/d , as seen in Fig.2, and to a lesser degree on the percentage of reinforcement, ρ ; it has been argued that the masonry compressive strength, f_m' , has little, if any, effect on shear capacity (8).

An investigation of shear capacity of grouted reinforced brickwork (GRB) lintels was initiated at Carleton University because the present Canadian masonry code (1) specifies an allowable shear stress of $0.7\sqrt{f_m'} \leq 0.35$ MPa for both RB and GRB types of members regardless of the fact that reinforced concrete (RC) members exhibit a shear resistance which is typically two to three times that of RB members. Since GRB members represent a composite construction of RB and RC, their composite shear behaviour warrants a separate investigation. For the typical GRB elevation and cross section shown in Fig.1, limited research has indicated two basic points (7):

- The ultimate shear stress of GRB lintels increases markedly with decreasing a/d values similar to the cases of RC and RB lintels.
- The shear capacity of GRB beams falls between that of RC and RB beams and since composite action exists between brickwork wythes and grouted concrete core, the GRB shear capacity can be safely derived from the separate shear capacities of the grout and brick sections according to their relative widths b_g and b_b .

Since GRB lintel shear research has been limited so far to a single width of grout cavity, what still remains to be investigated and what represents the primary objective of this paper, is a study of the effect of a varying grout cavity width on the shear capacity of grouted beams. Such an investigation could be carried out by utilizing full scale or small scale bricks, where small scale masonry units have the advantage of faster construction, reduced weight, easier handling and hence overall time savings. While small scale brickwork studies have been successfully employed, particularly in Britain, all such studies were limited to unreinforced brick masonry and hence when the authors decided to utilize 1/3 scale units for their investigation of the effect of a varying grout cavity width on shear capacity, basic work in reinforced brickwork was required to prove the validity of small

*Associate Professor and Research Engineer, respectively,
Department of Civil Engineering, Carleton University, Ottawa, Canada.

scale versus full scale results. To provide this evidence, the authors carried out a research program over a three year period involving a total of 37 beams. Approximately one half of the beams consisted of 1/3 scale members while the remainder were full scale lintels for comparison purposes.

The investigation is divided into two test programs as presented in the following two sections. The objective of the first program was to determine any possible scale effect when dealing with small scale rather than full scale RB and GRB lintels. Once validity of the small scale work had been established, the objective of the second test program was to ascertain the possible effect of a varying grout cavity width on GRB beam shear capacity.

STUDY OF SCALE EFFECT

General

For research purposes, small scale members have the advantage of ease of construction, material savings, reduced load requirements and ease of handling. For the reinforced lintel shear study dealt with in this paper, 1/3 scale brick units were available from the British Ceramic Research Association. These coreless bricks were manufactured by means of a standard extrusion process and had a compressive strength of about 38 MPa. In order to establish the validity of shear test results obtained through the use of 1/3 scale brick units, five RB and three GRB beams were built and tested in 1/3 scale to compare with the respective full scale beam results reported on earlier (2, 7, 8).

Test Program

Since the full scale RB and GRB beams have been dealt with previously (2, 7, 8), the following sections will concentrate on the 1/3 scale RB and GRB members and make only minimal reference to the full scale results as required for comparison purposes. In order to ensure that only the possible scale effect would have a bearing on full scale versus 1/3 scale shear capacities, the following parameters were kept constant:

1. All beams were built in running bond 5 bricks high as indicated in the typical elevation and cross sections of Fig. 1.
2. All beam cross sections contained a high percentage of reinforcement of about 1.5 percent. This also ensured that beams would generally fail in shear rather than in flexure.
3. Anchorage plates welded to the reinforcement were

provided at the ends of all beams to prevent premature bond failures which might obscure true shear capacities.

4. Type S mortar was used throughout in agreement with Canadian code requirements (1). The approximate mix proportions by volume were $1:\frac{1}{2}:4$ for cement:lime:sand, respectively.
5. Pairs of beams, one beam being full scale and the other being 1/3 scale, refer to the same a/d ratio. Since the a/d ratio is known to have a significant effect on shear capacity, paired beams exclude this effect.
6. All beams were tested under the two-point loading arrangement depicted in Fig. 1. The distance between point loads was kept constant at about 600 mm for full scale beams and at about 150 mm for 1/3 scale beams.

Concerning 1/3 scale RB lintels, a total of five beams were built with a/d values ranging between 1 and 5. The single wythe 34×132 mm cross section contained three 4.85 mm diameter deformed bars in the lowest bedjoint. The effective depth was 105 mm as compared to 273 mm for corresponding full scale members. The average strength of the steel was 372 MPa. The average masonry compressive strength, $f_m' = 19.1$ MPa, was determined by means of two-stack prisms as shown in Fig. 3. Incidentally, the same type of prism was used for the f_m' determination of all other beams because such a specimen more closely represents the compression region in a beam than the standard five or six-stack prism.

Concerning GRB lintels for investigation of scale effect, a total of six beams were built all with an a/d ratio of 3. The six beams consisted of three pairs, each pair representing a different ratio of b_g to b as depicted in Fig.1. According to the terminology indicated, the three pairs of beams therefore consisted of $1-\frac{1}{2}-1$, $1-1-1$ and $1-2-1$ GRB beams. While the results for both the full scale and 1/3 scale beams will be utilized in the following section, only the 1/3 scale lintels will be described more fully here since previous work has dealt with the full scale study (2,7). For the third scale GRB beams a grout mix by volume of one part normal Portland cement to four parts sand was used. At the time of beam testing, approximately 28 days, an average grout strength of 10.0 MPa was obtained for 75×150 mm waxed paper cylinders. For the three prisms, whose sizes correspond to the respective grout cavity widths of the $1-\frac{1}{2}-1$, $1-1-1$ and $1-2-1$ GRB lintels, an average grout strength of 19.7 MPa was obtained. Since the prisms were produced by pouring grout into a space formed by bricks and lined with permeable paper, the prism results reflect more closely the true grout strength in the beams. Steel reinforcing with an average yield stress of 374 MPa was furnished by 9.5 mm deformed bars. The effective depth was about 108 mm as compared to about 270 mm for corresponding full scale members.

Test Results and Discussion

Most significantly, all pairs of beams, whether RB or GRB, displayed similar cracking behaviour and similar shear failure modes. This then represents the first important basis for utilizing third scale reinforced lintels to predict full scale behaviour.

For the RB scale effect study, results are presented in Table 1 and Fig.2. Two key observations can be made from this evidence:

1. The shear strength of 1/3 scale RB lintels increases significantly with decreasing a/d values particularly in the range of low a/d values. This finding is in agreement with full scale behaviour.
2. Ultimate shear stresses obtained for 1/3 scale lintels agree well with the results from full scale beams shown in Fig.2. As has been discussed elsewhere (8), it must be recognized here that shear capacities even for identical beams vary considerably and that a plot of shear stress, v_u , versus a/d displays significant scatter regions particularly for a/d values less than 3. If in Fig.2 an average curve were drawn for the 1/3 scale results, such a curve would correspond very closely to the average curve given for the full scale results. It can therefore be concluded that no significant scale effect is evident for RB lintels.

The basis of discussion of a possible scale effect on the shear capacity of GRB beams will be made by means of the results presented in Table 2. The results show that for each pair of beams, i.e. full scale $1\frac{1}{2}$ -1 versus 1/3 scale $1\frac{1}{2}$ -1, etc., the difference in ultimate shear strength is less than 10 percent. This finding is particularly interesting since it indicates that GRB lintels behave similarly to RB lintels and that both types of beams are not significantly influenced by the scale effect. This situation is quite different from the case of RC beams where shear capacity increases with decreasing beam depth (4). Kani argued that while the crack spacing Δx is virtually independent of RC beam depth, the crack length s is greatly dependent on beam depth. The so-called crack factor $\Delta x/s$, which Kani showed to be a function of relative beam strength, would hence increase with decreasing beam depth. This reasoning does not apply to RB lintels where cracks usually develop at the brick-mortar interface. Here the crack spacing is dependent on the length of brick used in the beam. Hence $\Delta x/s$ does not behave as in RC beams as long as the brick length changes in the same ratio as the beam depth. This was the case in the scale effect study of the present paper. In GRB lintels, cracks were observed to develop in the mortar joints first and subsequently propagate through the grout core. This indicates that although the grout core is essentially a RC beam, its crack formation is governed by the composite brick facing, hence a GRB lintel acts more closely like a RB lintel and is virtually independent of the scale effect.

In summary then it can be stated that for both the RB and GRB lintels no significant scale effect is evident between full scale and 1/3 scale members.

STUDY OF GROUT CAVITY WIDTH EFFECT

General

In the previous section the validity of small scale work has been established. Based on this evidence, the effect of a varying grout cavity width on the shear capacity of GRB beams will now be investigated using 1/3 scale GRB lintels.

Test Program

In order to determine clearly the influence of a varying grout cavity width on beam shear resistance, five pairs of equal a/d value GRB lintels incorporating narrow (1- $\frac{1}{2}$ -1) and wide (1-2-1) grout cavities were designed as shown in Fig.4. Two widely differing widths were selected because these would reveal any possible influence of a varying grout cavity width on v_u . The use of paired beams eliminated the substantial influence of a/d on the v_u of GRB lintels and a range of a/d ratios between 1 and 7 was chosen according to the known shear resistance of full scale GRB beams (7). The constant parameters of this test program were parameters 1 to 5 listed in the previous section as well as those listed below:

1. A fine-to-coarse grout was used in accordance with Canadian code requirements (1). The approximate mix proportions by volume were 1:4 for cement:sand; a slump of about 250 mm was maintained throughout. Average grout strengths of 10.0 MPa were obtained for 75 × 150 mm waxed paper cylinders as well as 20.4 MPa and 17.9 MPa for 19×19×38 mm and 70×70×140 mm prisms, respectively. Note that prism sizes corresponded to the respective grout cavity width of the 1- $\frac{1}{2}$ -1 and 1-2-1 GRB lintels.
2. An average masonry compressive strength, $f_m' = 15.7$ MPa, was determined by means of the two-stack prisms shown in Fig.3.
3. The average yield strength of the 9.5 mm bars was 374 MPa.
4. One day after construction of the brickwork wythes, beams were grouted and then covered with polyethylene for curing. Six days later the polyethylene cover was removed and the beams were allowed to cure under normal laboratory conditions until testing at 28 days.

5. All beams were tested under the two-point loading arrangement shown in Fig.1. The distance between point loads was kept constant at about 150 mm.

Since shear failures seldom take place simultaneously in both shear spans, bandaging of the first shear failure by means of external steel plates and tie rods generally permitted a second shear failure to be obtained in the other shear span. While the results of both failures for each beam are shown in Fig.5, for the sake of simplicity only the average results per beam are listed in Table 3.

Test Results and Discussion

At equal a/d ratios, pairs of 1/3 scale GRB lintels with narrow and wide grout cavities exhibited almost identical cracking patterns and similar shear failure modes (2). All other parameters being equal, this indicates that GRB lintels with different b_g/b ratios essentially act in a similar manner.

Results of 1/3 scale GRB lintel tests are presented in Table 3 together with one set of full scale results at $a/d = 3$. Fig.5 depicts the individual shear stress results with their corresponding average lines plotted versus a/d ratios for 1/3 scale GRB lintels. The diagram shows that 1-2-1 GRB lintels exhibit increased shear strengths over their 1- $\frac{1}{2}$ -1 counterparts for the whole a/d range investigated.

In order to assess GRB strengths with respect to the basic RB and RC shear strengths, the average GRB failure lines from Fig.5 are depicted again in Fig.6 together with RB and RC capacities (7); also shown are the two full scale GRB results at $a/d = 3$. It can be seen from Fig.6 that the GRB capacities lie between the RB and RC curves and that, as expected, the 1-2-1 curve is closer to the RC capacity line. Note that the two full scale GRB results fall close to the 1/3 scale curves, again indicating the absence of a scale effect, and also that the positioning of the two GRB lines agrees with the full scale 1-1-1 evidence presented previously (7).

The question still remains if the 1- $\frac{1}{2}$ -1 and 1-2-1 GRB shear capacities can be considered as the combined shear strength of RB and RC beams. Based on the relative widths of the grout and brick sections and also on the RB and RC curves shown in Fig.6, so-called 'derived' GRB shear strengths were calculated and listed in Table 4. Note that for convenience all shear capacities are expressed as a function of RC strength. When the tabular results are plotted as shown in Fig.7, a comparison of the derived versus the experimental GRB results shows relatively good agreement for all a/d values. This holds for 1- $\frac{1}{2}$ -1 as well as 1-2-1 GRB beams. Since the derived curves are slightly below the experimental curves, the approach of determining GRB capacity as a combined strength of RB and RC sections is conservative. It can also be noted again from Fig.7 that as the width of the grouted section diminishes, the GRB capacity line approaches the RB line and alternatively, as the grout width increases the GRB line moves toward the RC line. It is unlikely that the GRB line would match

the RC line even for very wide grout cavities unless grouts of lower water/cement ratios similar to normal concrete beams were used.

CONCLUSIONS

Based on tests reported in the first part of this paper, 1/3 scale RB and GRB beams can be utilized reliably to predict corresponding full scale beam behaviour and capacities. This conclusion holds for the full range of a/d values of practical interest.

Results of the second study indicate that GRB beam shear capacities fall between RC and RB shear strengths and that wider grout cavities lead to increased capacities closer to those for RC beams. The GRB results further indicate that composite action exists between brick wythes and grout core and that GRB shear capacities can be conservatively calculated from the separate RB and RC sections according to their relative widths.

ACKNOWLEDGEMENTS

The investigation was carried out in the Structures Laboratory of the Department of Civil Engineering at Carleton University. The authors wish to express their appreciation to B. Davies, D.A. Aylen and H. Kempthorne for their contributions to the experimental programs.

The authors acknowledge with thanks the financial support provided by the National Research Council of Canada and the Masonry Research Foundation of Canada.

Thanks are also due to Domtar Construction Materials Ltd. and the British Ceramic Research Association for providing full scale and 1/3 scale bricks, respectively.

APPENDIX I - REFERENCES

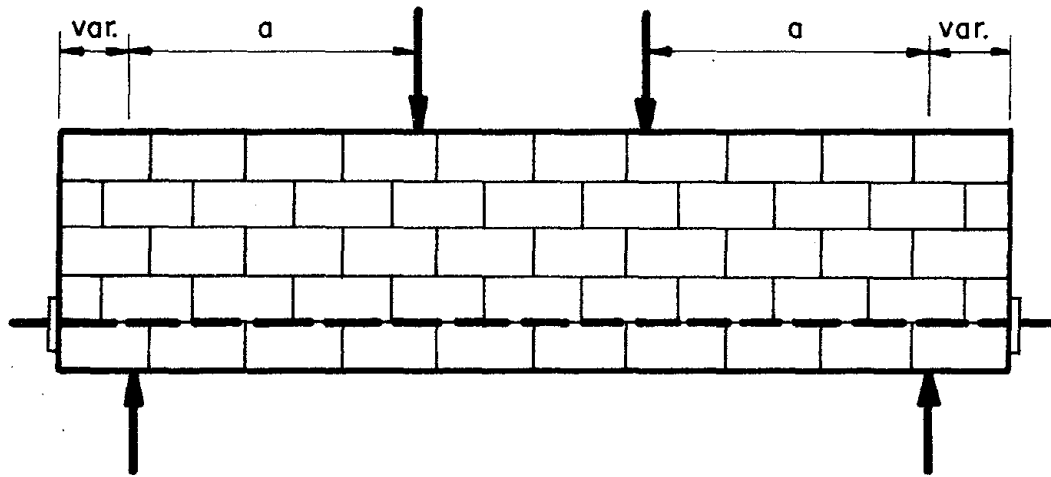
1. Canadian Standards Association, "CSA Standard S304 - 1977 Masonry Design and Construction for Buildings".
2. Davies, B.J., "Shear Strength of one third scale Grouted Reinforced Masonry Beams", M.Eng. Thesis, Carleton University, December 1976.
3. Kani, G.N.J., "Basic Facts Concerning Shear Failure", ACI Journal, Vol. 63, No. 6, June 1966.
4. Kani, G.N.J., "How Safe are Our Large Reinforced Concrete Beams", ACI Journal Vol. 64, No. 12, March 1967.
5. Keller, H., "Shear Strength of Grouted Reinforced Masonry Beams", M.Eng. Thesis, Carleton University, September 1975.
6. Suter, G.T. and Hendry, A.W., "Shear Strength of Reinforced Brickwork Beams", The Structural Engineer, Vol. 53, No. 6, June 1975, pp 249-253.
7. Suter, G.T. and Keller, H., "Shear Strength of Grouted Reinforced

Brickwork Beams", Congress Proc., Fourth International Brick Masonry Congress, Bruges, April 1976.

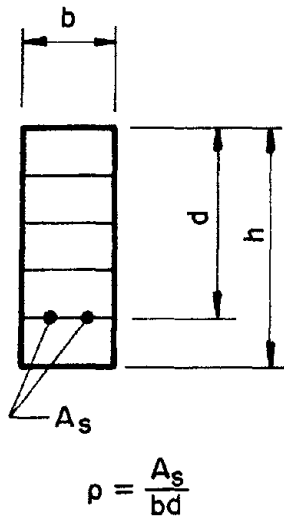
8. Suter, G.T. and Keller, H., "Shear Strength of Reinforced Masonry Beams and Canadian Code Implications", Proc. of the First Canadian Masonry Symposium", Calgary, June 1976.

APPENDIX II - NOTATION

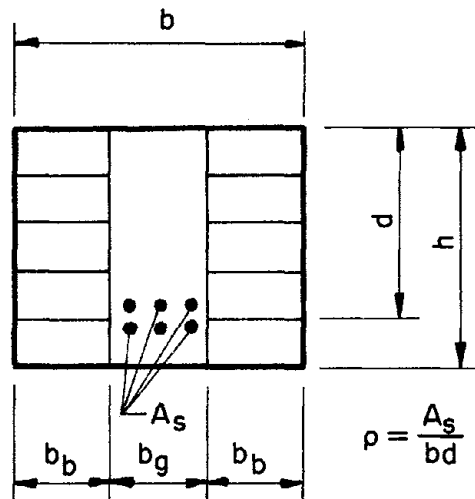
A	= cross-sectional area of reinforcing bars;
a^s	= shear span as shown in Fig.1;
a/d	= ratio of shear span to effective depth;
b	= width of beam section;
b_b	= width of one brick wythe;
b_g	= width of grout cavity;
d	= effective depth as shown in Fig.1;
f_m'	= brickwork compressive strength;
s	= length of crack;
v_u	= ultimate shear stress;
Δx	= spacing of cracks;
$\Delta x/s$	= crack factor;
ρ	= percentage of tensile reinforcement = $\frac{A_s}{bd}$



BEAM ELEVATION



RB CROSS SECTION



GRB CROSS SECTION

TERMINOLOGY:
 WHEN $b_g = \frac{1}{2}b_b$, REFER TO 1- $\frac{1}{2}$ -1 BEAM
 WHEN $b_g = b_b$, REFER TO 1-1-1 BEAM
 WHEN $b_g = 2b_b$, REFER TO 1-2-1 BEAM

FIG. 1 TYPICAL BEAM ELEVATION AND CROSS SECTIONS

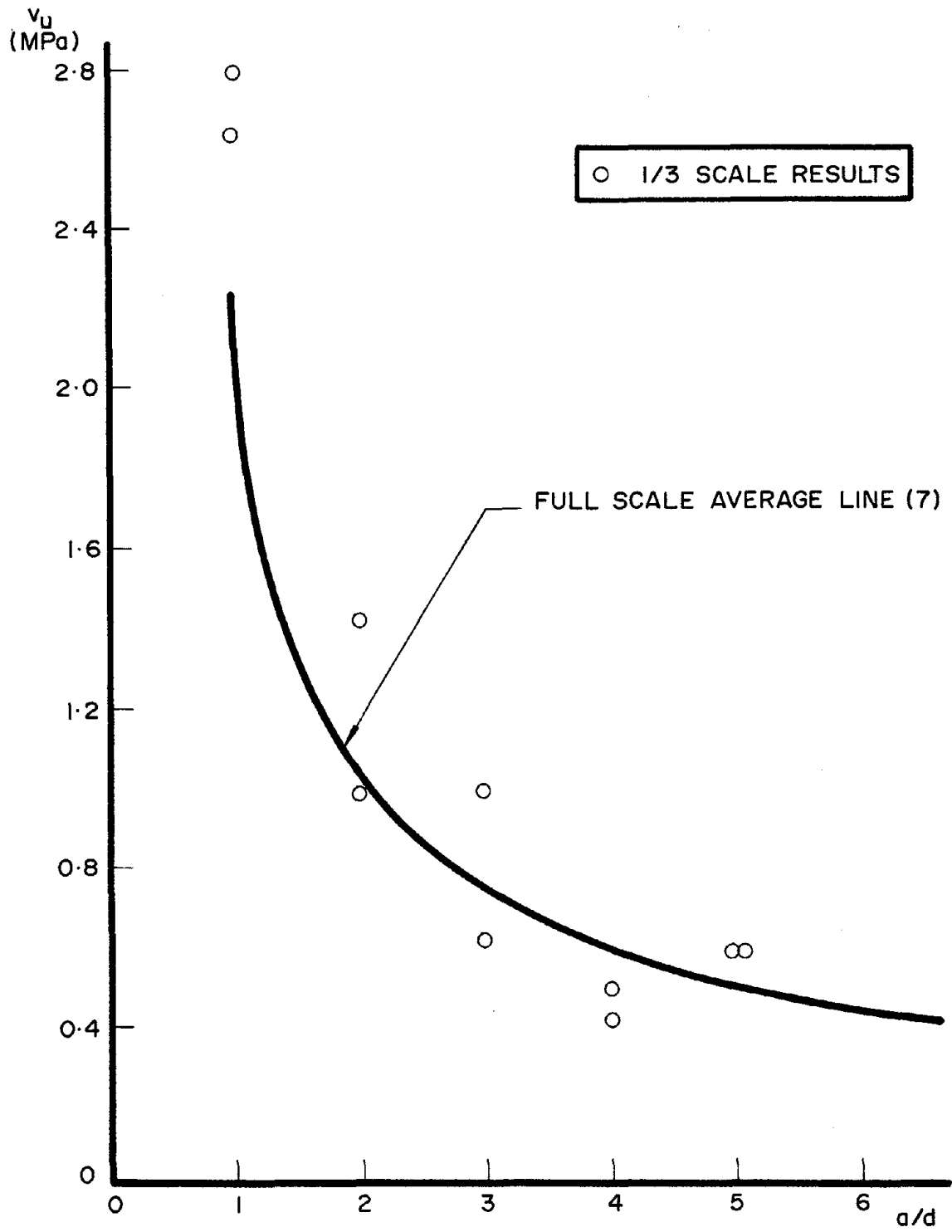


FIG. 2 1/3 SCALE VERSUS FULL SCALE RB RESULTS

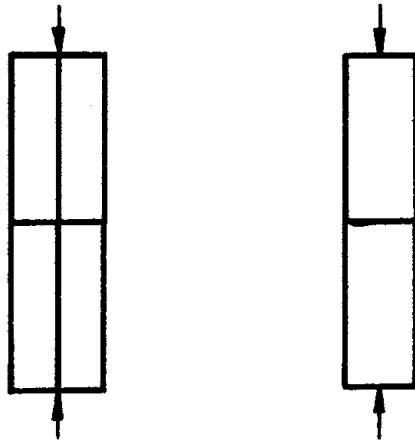


FIG. 3 TWO-STACK PRISM COMPRESSION SPECIMEN

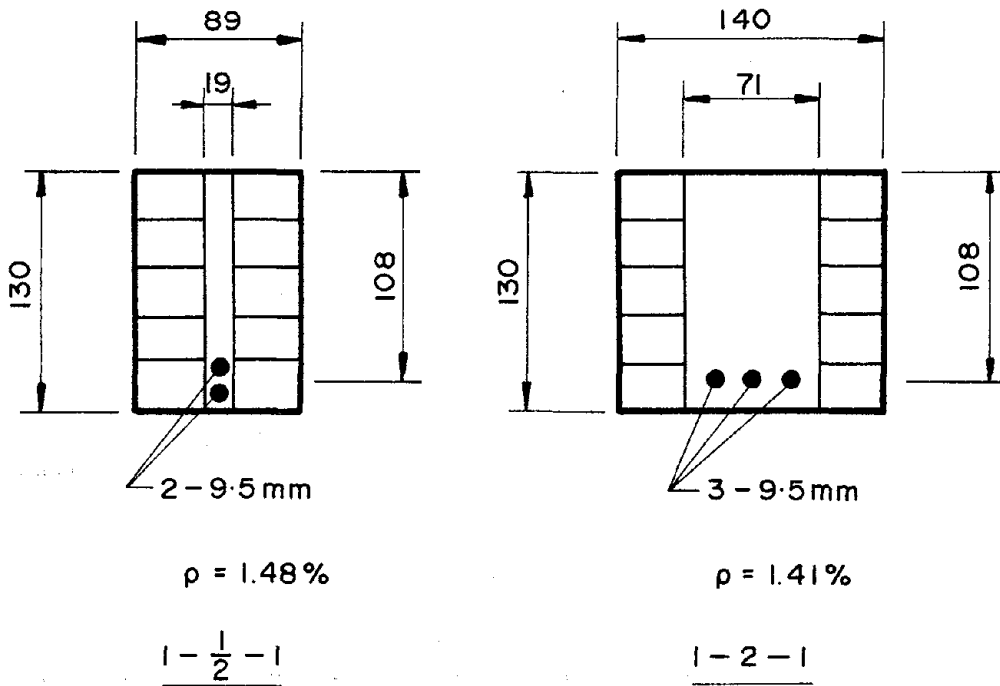


FIG. 4 1/3 SCALE GRB LINTEL CROSS SECTIONS

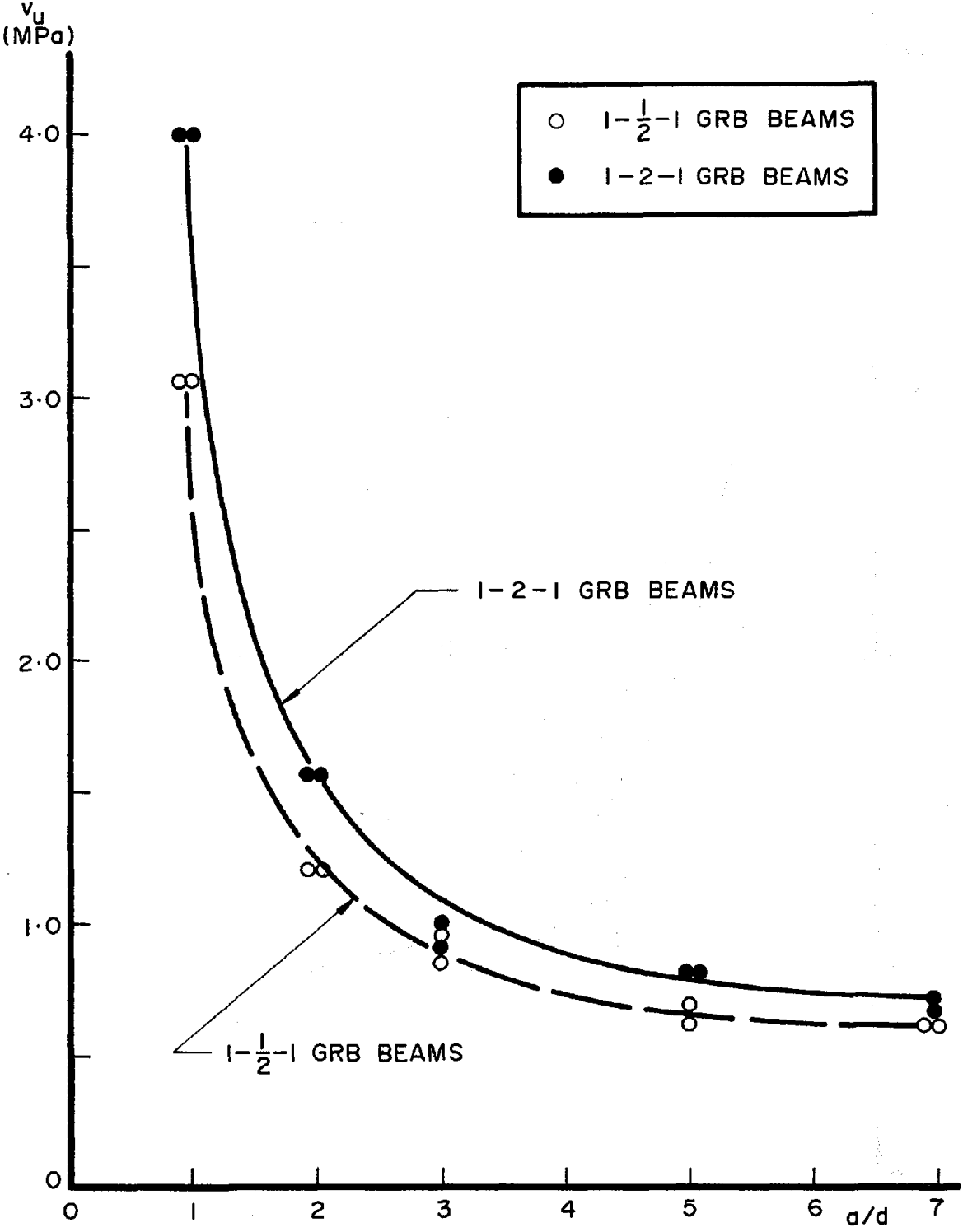


FIG. 5 INFLUENCE OF GROUT CAVITY WIDTH ON SHEAR STRENGTH

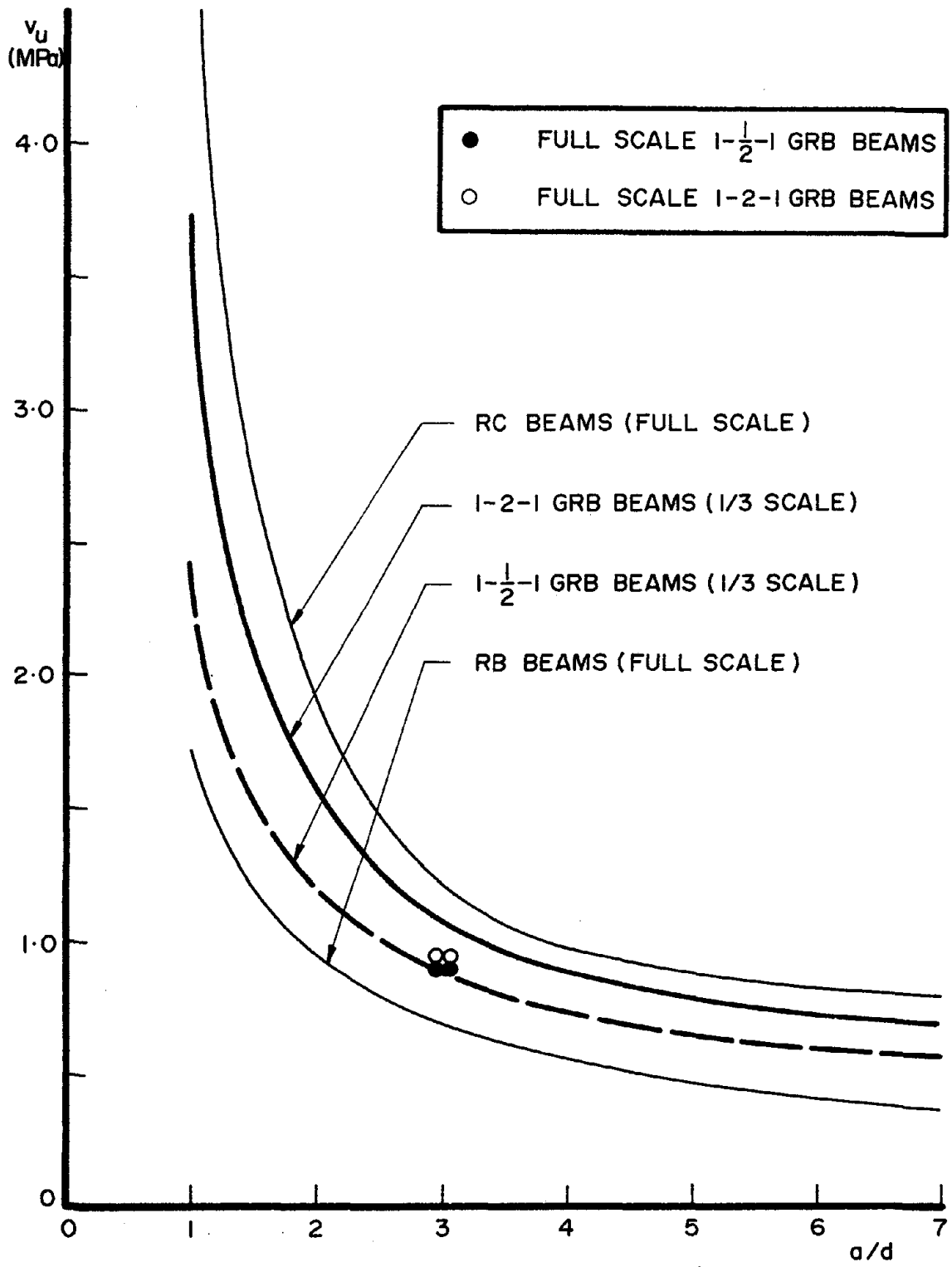


FIG. 6 INFLUENCE OF a/d ON v_u FOR RC, RB AND GRB BEAMS

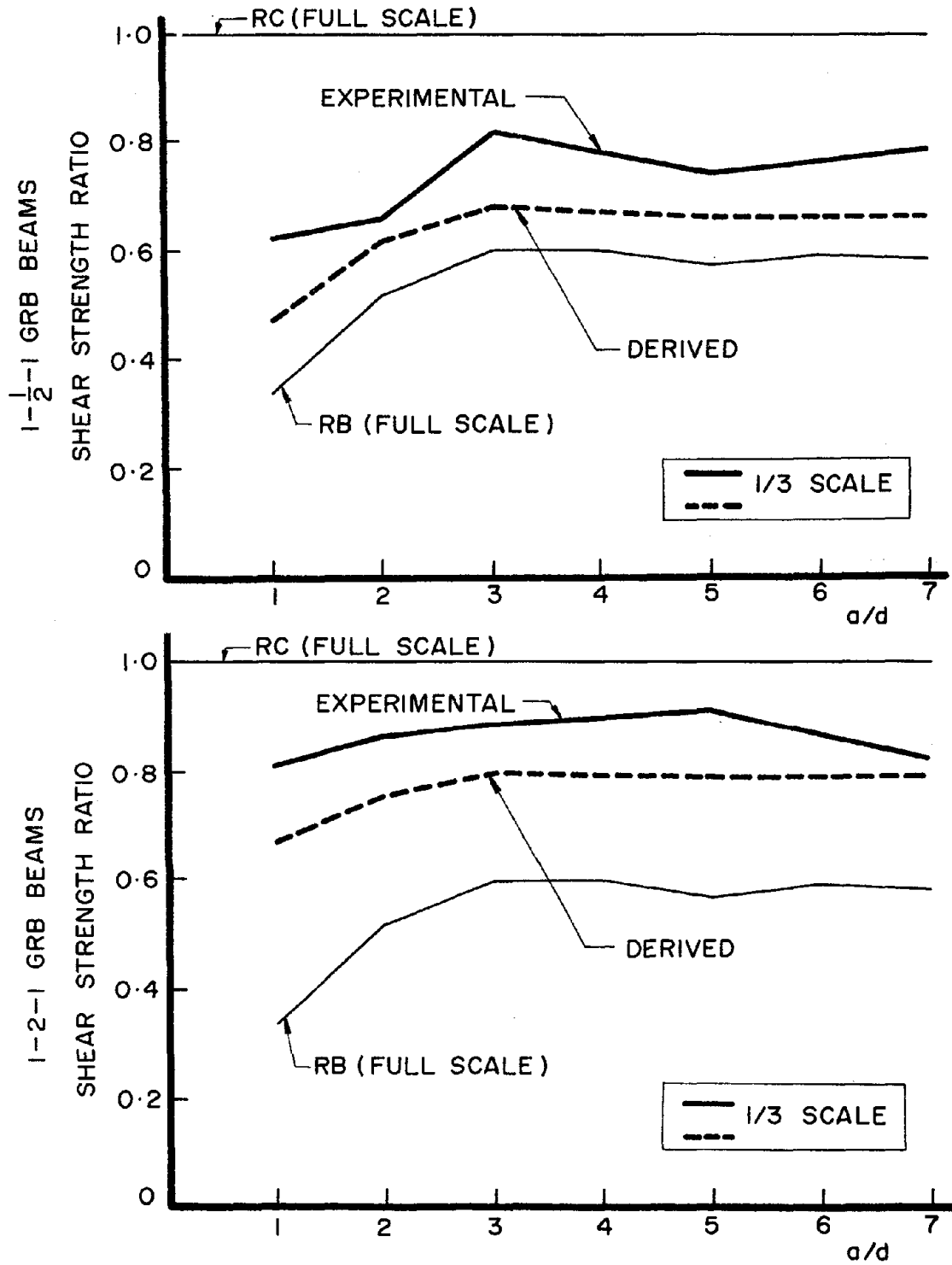
FIG. 7 SHEAR STRENGTH RATIO VS. a/d FOR GRB LINTEL SERIES

TABLE 1 - FULL SCALE VS. 1/3 SCALE RB SHEAR STRESS RESULTS

a/d	FULL SCALE (5) v_u (MPa)	1/3 SCALE v_u (MPa)
1	1.91	2.72
1.5	1.35	-
2	0.95	1.21
3	0.92	0.80
4	0.59	0.45
5	0.46	0.59
6	0.43	-
7	0.35	-

TABLE 2 - FULL SCALE VS. 1/3 SCALE GRB SHEAR STRESS RESULTS (MPa)

a/d	FULL SCALE (2)			1/3 SCALE (2)		
	1- $\frac{1}{2}$ -1	1-1-1 (5)	1-2-1	1- $\frac{1}{2}$ -1	1-1-1	1-2-1
3	0.94	0.89	0.91	0.89	0.84	0.95

TABLE 3 - STUDY OF GROUT CAVITY WIDTH EFFECT*(2)

a/d	1/3 SCALE SHEAR STRESS**	
	1- $\frac{1}{2}$ -1 v_u (MPa)	1-2-1 v_u (MPa)
1	3.06	3.99
2	1.21	1.57
3	0.89 (0.94)**	0.95 (0.91)**
5	0.66	0.81
7	0.62	0.68

*note that the shear stresses presented represent the average result of two separate shear failures obtained for each beam.

**except as noted in the table: the two beam test results in parentheses represent full scale results.

TABLE 4 - SHEAR STRENGTH RATIOS BASED ON RC STRENGTHS

a/d	RC (3)	RB (5)	EXPERIMENTAL GRB BEAM SHEAR STRENGTH RATIOS		DERIVED SHEAR STRENGTH RATIOS	
			$1-\frac{1}{2}-1$	1-2-1	$1-\frac{1}{2}-1$ $\frac{2RB + 0.5 RC}{2.5}$	1-2-1 $\frac{2RB + 2 RC}{4}$
1	1	0.34	0.62	0.81	0.47	0.67
2	1	0.52	0.66	0.86	0.62	0.76
3	1	0.60	0.82	0.89	0.68	0.80
4	1	0.60	-	-	-	-
5	1	0.57	0.74	0.91	0.66	0.79
6	1	0.59	-	-	-	-
7	1	0.58	0.78	0.82	0.66	0.79

COMPRESSION TESTS OF CLAY-UNIT STACKBOND PRISMS

John Baur¹, J. L. Noland², and James Chinn³

ABSTRACT: The primary object of the research was to study the influence upon ultimate compressive strength of prisms, of basic masonry parameters, e.g., unit flatwise compressive strength, initial rate of absorption of the unit, mortar cube uniaxial compressive strength, mortar cement/water ratio, mortar lime/water ratio, mortar retentivity, and mortar flow. Several mortar mixes were used as well as several strengths of 8 in. x 2 in. (nominal) extruded wire-cut clay masonry units. All prisms were 4 units high.

A secondary motive was to verify that simple, but rigorously followed, construction and test procedures would yield consistent test results.

The results indicated the influence of mortar strength upon prism strength and the influence of unit strength upon prism strength. A series of multiple regression analyses ultimately revealed that unit flatwise compressive strength and mortar cement/water ratio (or mortar cube strength) together were the most significant parameters affecting prism strength. Consistency of results indicated that the experimental procedures used were satisfactory.

¹Howard Dutzi & Associates, Inc., Colorado Springs, CO; formerly graduate student, University of Colorado.

²Principal, Atkinson-Noland & Associates, Inc., Boulder, CO.

³Professor, Department of Civil, Environmental, & Architectural Engineering, University of Colorado, Boulder, CO.

COMPRESSION TESTS OF CLAY-UNIT STACKBOND PRISMS

John Baur¹, J. L. Noland², and James Chinn³

INTRODUCTION

The compressive test of a small masonry subassemblage has been widely used as a basis to establish the ultimate compressive strength, f_m' , for use as a basis of design allowables, and as a component of quality control (1,2,5,7,8,10,11,13). In the United States, Canada and Australia, the subassemblage generally used consists of two or more units laid up in single-wythe stackbond (1,8,11,13).

Recognizing the possible limitations of results due to single-wythe, stackbond construction, the prism test may be used to assess the influence of mortar and unit properties upon ultimate compressive strength. However, specimen preparation and test procedures should be such that extaneous effects are minimized.

OBJECTIVES

The objectives of the research (3) reported in this paper were two-fold. The primary interest was, through statistical analyses, to study the influence of the individual constituents upon the ultimate compressive strength of masonry prisms. A secondary goal was to demonstrate that, with reasonable care in preparation and testing of prisms, consistent data could be obtained thus verifying the applicability of prism tests as a method of quality control and as a means of establishing ultimate compressive strength.

THE TEST SPECIMEN

The test specimen used throughout the project was a four-unit stackbond prism laid up with 3/8 in. mortar joints. The selection of the number of units was based upon the concept that due to friction restraint at the test machine-prism interface, at least three joints would be required to permit failures somewhat representative of full-scale masonry behavior. This was based upon a review of the nature of

¹Howard Dutzi & Associates, Inc., Colorado Springs, CO;
formerly graduate student, University of Colorado.

²Principal, Atkinson-Noland & Associates, Inc., Boulder, CO.

³Professor, Department of Civil, Environmental, & Architectural
Engineering, University of Colorado, Boulder, CO.

clay masonry failure (5,6,7,11) and of a limited number of preliminary tests. It was of interest to note that the four-unit prism has been adopted in Australia (10).

The joint thickness used was simply to be consistent construction practice in the U.S.

SCOPE

The tests conducted were in two major categories. The first series consisted of compressive tests of 41 prisms constructed with nominal 4 in. x 8 in. clay paver units, i.e., completely solid. The second series used 44 prisms constructed with a nominal 4 in. x 8 in. cored unit whose void area was such that it qualified as a "solid" unit, i.e., void area less than 25% of gross. The paver series was intended to provide baseline data against which results using a common cored unit could be compared.

COMPONENT MATERIALS

Units. The units used were manufactured using local clays and the stiff-mud wire-cut process. Typical actual dimensions of the units are shown in Fig. 1 and their physical properties are presented in Table I. Flatwise compressive strength and initial rate of absorption (IRA) properties were determined in accordance with ASTM C67 "Standard Methods of Sampling and Testing Brick" (2).

The units were selected to represent a wide range of IRA values and flatwise compressive strengths (f'_b).

Mortar. Selection of mortar mixes to be used in the research was made to include mixes commonly used in the masonry industry and representative of a wide range of cement content relative to sand and lime. One mortar mix was chosen from each of four categories of mixes as defined by ASTM C270 (1). The mixes chosen and their ASTM classifications are:

M - 1:½:3

S - 1:½:4½

N - 1:1:6

O - 1:2:9

Cement used in all mortar batches was fresh Martin-Marietta, Type I. The lime was Flintkote "Miracle Lime", type S, a hydrated lime packaged in fifty pound sacks.

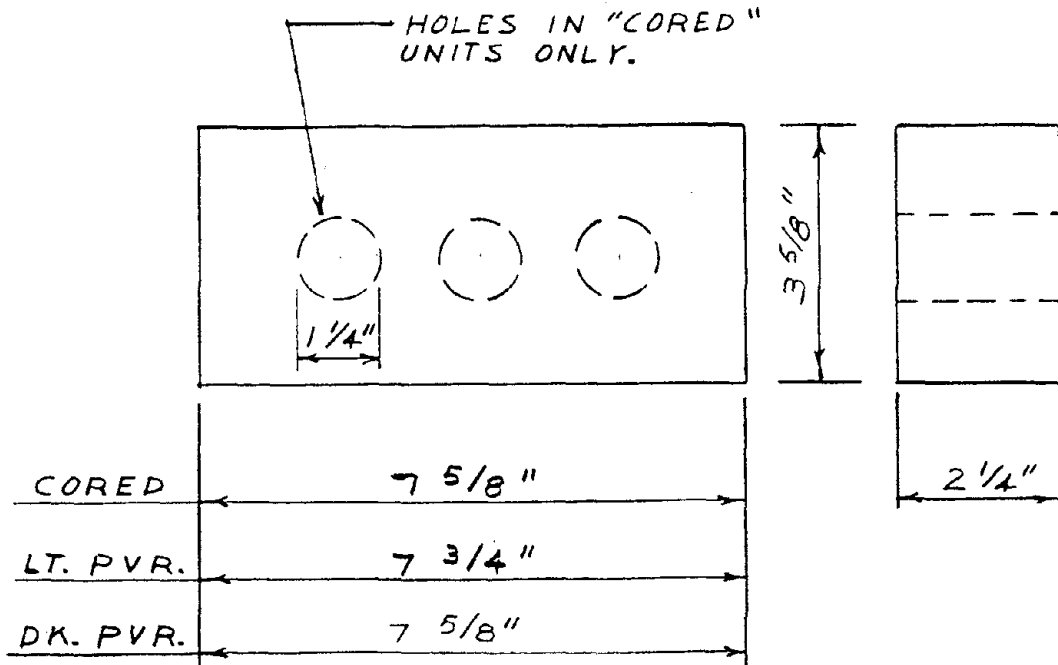


Figure 1. Clay Unit Dimensions

TABLE I
CLAY UNIT PROPERTIES

Clay Unit Designation	Initial Rate of Absorption (g/30 in ² /min)	Flatwise Compression Strength (psi) ¹		
		Mean	Standard Deviation	
Solid	Light Paver (LP)	20	11100	1832
	Dark Paver (DP)	10	13670	1463
	Desert Tan (DT)	7.8	14834	1466
	Dark Buff (DB)	16.2	10805	1287
Cored	Chestnut Brown (CB)	13.9	10518	665
	Dapple Gray (DG)	17.8	7970	864
	White Grain (WG)	60.4	3257	113
	CB Red (CBR)	17.9	14260	800
	CB White (CBW)	16.5	13387	43
	CB Brown (CBB)	20.5	9853	88
	CB Orange (CBO)	30.6	6989	1362

¹Based on gross area

A commercially available blended sand was used which satisfied the requirements of ASTM C144-70. The average fineness modulus was 2.25. The results of two independent sieve analyses are plotted in Fig. 2 along with the ASTM C144 limits.

The physical parameters of the materials used in the research were measured periodically throughout the program both to ensure consistent quality of the materials and to provide data which could be used in determining the effect these parameters would have on the ultimate compressive strength of the masonry specimen.

Water retentivity of the mortar mixes used in the program was measured in accordance with Section 26 of ASTM C91 "Methods of Testing Masonry Cement Mortars" (1). Fig. 3 shows a plot of the retentivity test results when related to percent lime of the particular mix. The plot shows a high correlation between the two variables and is quantified by a high coefficient of determination, r^2 .

Mortar strength was measured through the use of seven day uniaxial compressive tests on 2-inch mortar cubes. The results of these tests were compared with those presented in "Effect of Constituent Proportions of Uniaxial Compressive Strength of 2-Inch Cube Specimens of Masonry Mortars" a thesis by Donald Frey (4).

All mortar was prepared by weighing the individual ingredients in order to obtain consistent properties (4).

PREPARATION OF SPECIMENS

The compression test specimens consisted of four units laid up in stackbond and capped on each end. The specimens were constructed under laboratory conditions by an experienced mason whose workmanship was considered to be excellent. All mortar used in the compression specimens was mixed in a Hobart Mixer, Model N-50, in accordance with procedures set forth in Section 6 of ASTM C305, "Mechanical Mixing of Hydraulic Cement Pastes and Mortar of Plastic Consistency" (1). Bed joints were furrowed lightly or not at all. All joints were 3/8 inches thick and tooled by the mason to a concave finish.

After the top unit had been laid, the specimen was allowed to air cure for approximately four hours so that an initial set of the mortar could take place. The specimen was then carefully placed in a fog room at 100% humidity for seven days of wet curing. At the end of that period the specimen was removed from the fog room and air cured in the laboratory which was generally at 70 degrees Fahrenheit and 20-50% humidity. Air curing proceeded until the test date which was either 14 or 28 days from the construction date.

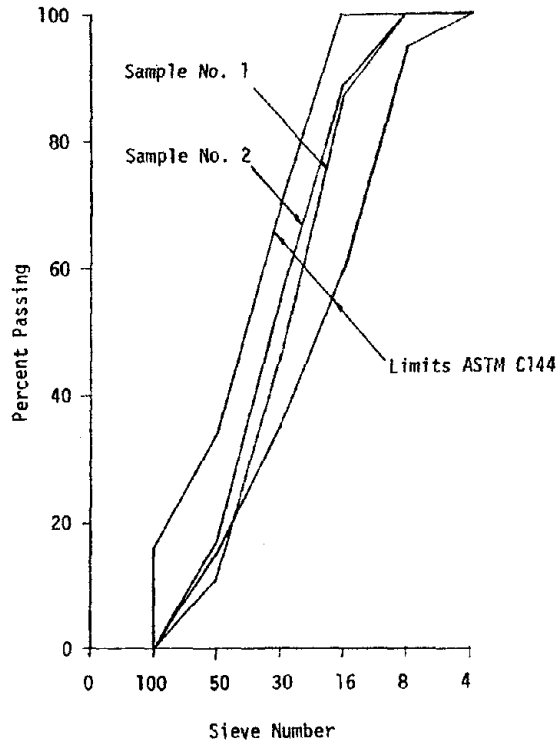


Figure 2 Comparison of Sample Sand with ASTM Specifications

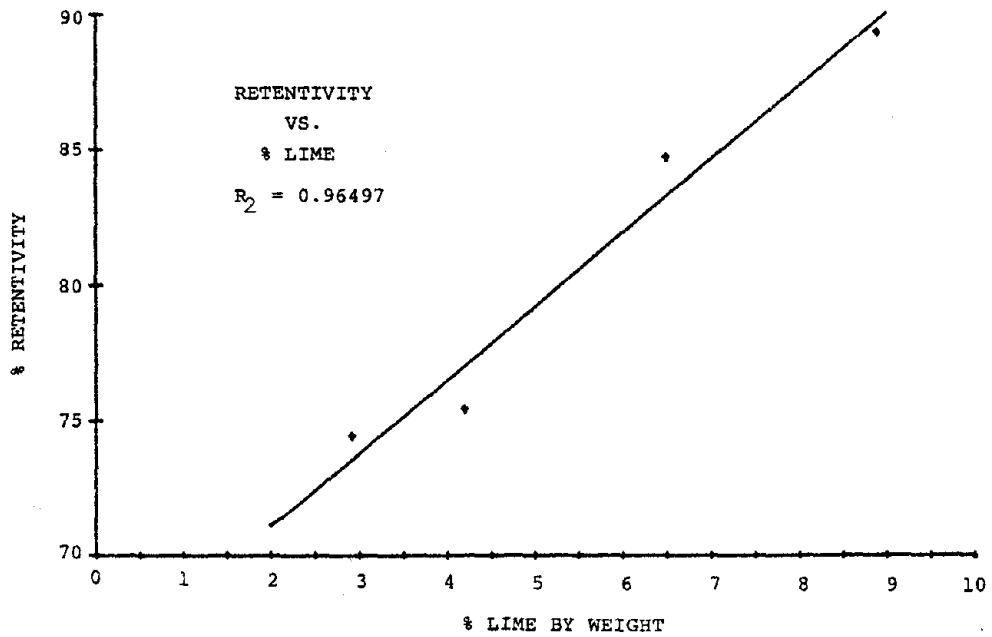


Figure 3. The Relationship of Water Retentivity to Percent Lime of Mortar

An area of specimen preparation which received particular emphasis was the development of a procedure for applying test caps to the specimen ends which would be uniform in thickness and parallel to each other. The emphasis given to this aspect of specimen preparation was dictated by the conviction that non-parallel specimen ends result in premature and eccentric failure of the specimen, thereby introducing an uncontrolled variable into the testing procedure.

To meet the requirement for parallel ends, a capping device was fabricated using 7075-T6 Aluminum Alloy. The device consisted of a one-inch base plate with upright corner guide plates extending at right angles from the base plate. Measurement of the angle of the cap to perpendicularity of the longitudinal axis of the specimen, showed that angle to be less than 0.5 degrees, a limit imposed by Section 3, ASTM C617, "Standard Method of Capping of Cylindrical Concrete Specimens" (1). Test results on specimens with caps parallel to within those limits appeared to be consistent to within an expected range of statistical variation.

The capping material used was a sulfur-clay compound marketed commercially under the name "Cylcap", and meets the requirements set forth in Section 4 of ASTM C617 (1).

TEST SERIES

The test series was designed to permit the influence of mortar characteristics and unit characteristics to be evaluated. The basic approach essentially was to vary one parameter while holding others constant. The data in Tables II and III present the specific values of parameters varied for the paver-unit prism series and the cored-unit prism series.

The basic sample size was three. In one case, however, an additional sample was tested because, at the time, the mortar cube strength seemed low. In two other cases, one prism each was damaged prior to the test. Since the results of the remaining two were so close, replacement specimens were not built.

TESTING PROCEDURE

Compression Testing. All compression testing was performed in accordance with ASTM Specification E447, "Compression Strength of Masonry Prisms" (1). Testing was done in a 300,000 pound capacity Baldwin-Southwart Universal Testing Machine. Load was applied to the tops of the specimens through a spherical bearing block, thus minimizing eccentricity in loading. A cast iron bearing block was used

TABLE II
PAVER UNIT PRISM TEST SERIES

Subset Number	Number of Specimens	Mortar Types Used in Test	Clay Unit Type	Initial Flow
I	15	1:¼:3, 1:½:4½ 1:1:6, 1:2:9	DP	130
II	18	1:¼:3, 1:1:6	DP	110, 120, 140
III	8	1:¼:3, 1:1:6 1:2:9	LP	130

TABLE III
CORED UNIT PRISM TEST SERIES

Clay Unit Type	Number of Specimens	Mortar Types Used in Test	Initial Flow
DT	9	1:¼:3, 1:1:6, 1:2:9	130
DB	9	1:¼:3, 1:1:6, 1:2:9	130
CB	9	1:¼:3, 1:1:6, 1:2:9	130
DG	9	1:¼:3, 1:1:6, 1:2:9	130
WG	8	1:¼:3, 1:1:6, 1:2:9	130

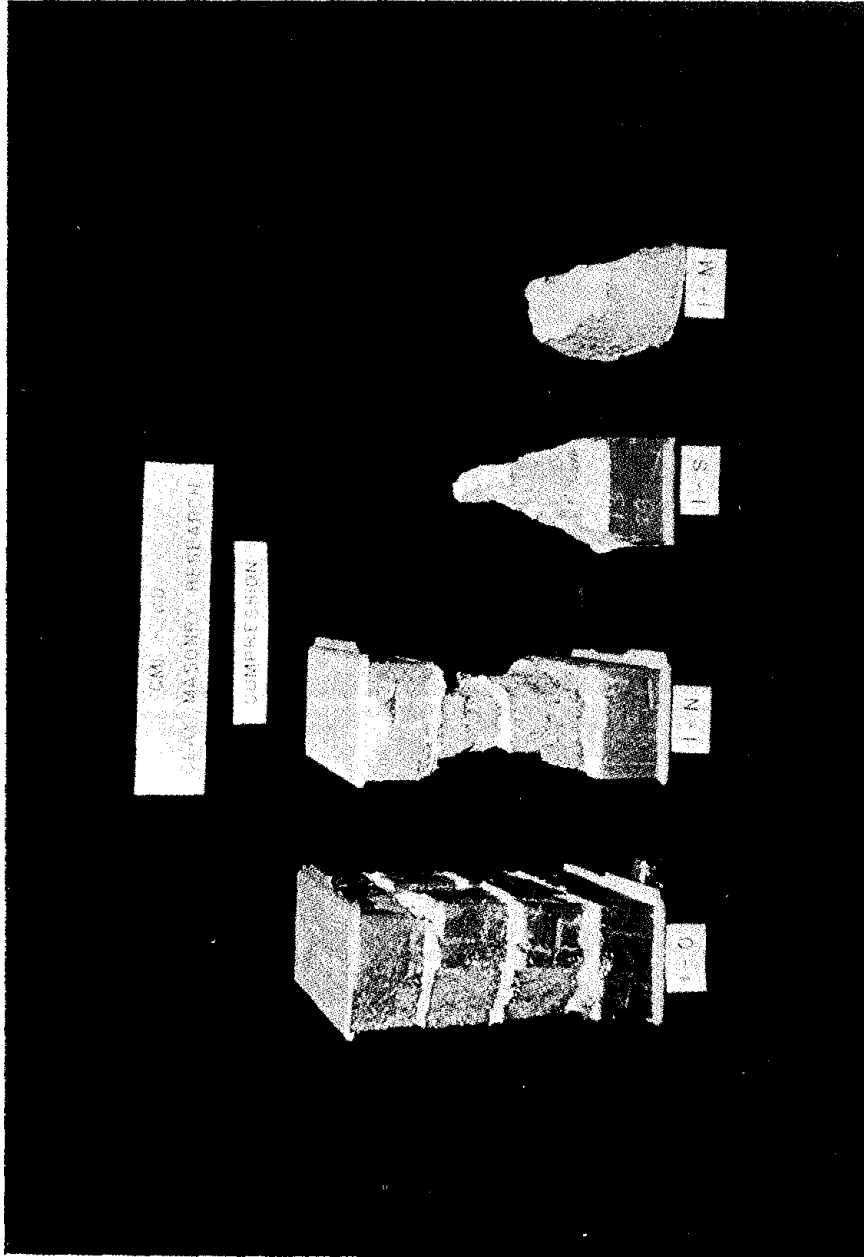


Figure 4. Compression Failures

TABLE IV
 COMPRESSION TEST RESULTS - PAVER UNIT PRISMS

Clay Unit Type	Clay Unit Comp. Str. f'_b (psi)	Mix	Mortar Properties				Prism Str. f'_m (psi)
			Comp. Str. - f'_c (psi)	Flow	C/W ¹	L/W ²	
DP	13670	1:1/4:3	5951	130	1.71	0.18	12627
DP	13670	1:1/4:3	5951	130	1.71	0.18	12590
DP	13670	1:1/4:3	5951	130	1.71	0.18	12701
DP	13670	1:1/2:4 1/2	2762	130	1.14	0.24	8762
DP	13670	1:1/2:4 1/2	2762	130	1.14	0.24	8614
DP	13670	1:1/2:4 1/2	2672	130	1.14	0.24	8752
DP	13670	1:1:6	1188	130	0.81	0.35	6829
DP	13670	1:1:6	1188	130	0.81	0.35	6617
DP	13670	1:1:6	1188	130	0.81	0.35	6783
DP	13670	1:1:6	1244	130	0.81	0.35	7317
DP	13670	1:1:6	1244	130	0.81	0.35	7887
DP	13670	1:1:6	1244	130	0.81	0.35	6838
DP	13670	1:2:9	369	130	0.50	0.43	4565
DP	13670	1:2:9	369	130	0.50	0.43	5053
DP	13670	1:2:9	381	130	0.50	0.43	5062

TABLE IV (continued)
 COMPRESSION TEST RESULTS - PAVERS

Clay Unit Type	Clay Unit Com.Str. f' _b (psi)	Mix	Mortar Properties				Prism Str. f' _m (psi)
			Comp.Str.-f' _c (psi)	Flow	C/W ¹	L/W ²	
DP	13670	1:1/4:3	6582	110	1.82	0.19	13363
DP	13670	1:1/4:3	6582	110	1.82	0.19	11154
DP	13670	1:1/4:3	6582	110	1.82	0.19	12369
DP	13670	1:1/4:3	5259	120	1.67	0.18	13474
DP	13670	1:1/4:3	5259	120	1.67	0.18	12332
DP	13670	1:1/4:3	5259	120	1.67	0.18	14688
DP	13670	1:1/4:3	5203	140	1.55	0.16	12995
DP	13670	1:1/4:3	5203	140	1.55	0.16	12332
DP	13670	1:1/4:3	4922	140	1.55	0.16	12590
DP	13670	1:1:6	1447	110	0.85	0.36	7492
DP	13670	1:1:6	1447	110	0.85	0.36	7823
DP	13670	1:1:6	1447	110	0.85	0.36	8117
DP	13670	1:1:6	1353	120	0.83	0.35	7473
DP	13670	1:1:6	1353	120	0.83	0.35	7556
DP	13670	1:1:6	1353	120	0.83	0.35	7278

TABLE IV (continued)
 COMPRESSION TEST RESULTS - PAVERS

Clay Unit Type	Clay Unit Comp. Str. f'_b (psi)	Mix	Mortar Properties				Prism Str. f'_m (psi)
			Comp. Str. - f'_c (psi)	Flow	C/W ¹	L/W ²	
DP	13670	1:1:6	1134	140	0.79	0.33	6258
DP	13670	1:1:6	1134	140	0.79	0.33	7307
DP	13670	1:1:6	1134	140	0.79	0.33	7418
LP	11100	1:1/4:3	5694	130	1.67	0.18	8202
LP	11100	1:1/4:3	5863	130	1.67	0.18	8484
LP	11100	1:1:6	1188	130	0.80	0.34	5741
LP	11100	1:1:6	1209	130	0.80	0.34	5662
LP	11100	1:1:6	1209	130	0.80	0.34	5856
LP	11100	1:2:9	381	130	0.49	0.42	4709
LP	11100	1:2:9	381	130	0.49	0.42	4718
LP	11100	1:2:9	381	130	0.49	0.42	5089

¹ Cement/Water ratio of mortar as mixed and based on weight measurements.

² Lime/Water ratio of mortar as mixed and based on weight measurements.

TABLE V
COMPRESSION TEST RESULTS - CORED UNIT PRISMS

Clay Unit Type	Clay Unit Comp. Str. f'_b (psi)	Mix	Mortar Properties ¹			Prism Str.- f'_m (psi) Net Area	
			Comp.Str.- f'_c (psi)	C/W ²	L/W ²		
CB	10518	1:1/4:3	5710	1.67	0.18	7972	9991
CB	10518	1:1/4:3	5710	1.67	0.18	9226	11563
CB	10518	1:1/4:3	5710	1.67	0.18	6943	8701
DB	10805	1:1/4:3	5710	1.67	0.18	8766	10829
DB	10805	1:1/4:3	5710	1.67	0.18	8325	10284
DB	10805	1:1/4:3	5710	1.67	0.18	8846	10927
WG	3257	1:1/4:3	5710	1.67	0.18	2422	3004
WG	3257	1:1/4:3	5710	1.67	0.18	2790	3388
WG	3257	1:1/4:3	5710	1.67	0.18	2620	3181
DT	14834	1:1/4:3	5710	1.67	0.18	10460	12995
DT	14834	1:1/4:3	5710	1.67	0.18	9700	12050
DT	14834	1:1/4:3	5710	1.67	0.18	10240	12725
DG	7970	1:1/4:3	5710	1.67	0.18	5743	7168
DG	7970	1:1/4:3	5710	1.67	0.18	5504	6869
DG	7970	1:1/4:3	5710	1.67	0.18	5329	6651
CB	10518	1:1:6	1203	0.80	0.34	4866	6098
CB	10518	1:1:6	1206	0.80	0.34	5090	6379
CB	10518	1:1:6	1206	0.80	0.34	5109	6403
DB	10805	1:1:6	1197	0.80	0.34	5926	7321

TABLE V (continued)
 COMPRESSION TEST RESULTS - CORED

Clay Unit Type	Clay Unit Comp. Str. f' _b (psi)	Mix	Mortar Properties ¹			Prism Str.-f' _m (psi)	
			Comp.Str.-f' _c (psi)	C/W ²	L/W ²	Gross Area	Net Area
DB	10805	1:1:6	1188	0.80	0.34	5344	6602
DB	10805	1:1:6	1188	0.80	0.34	6041	7463
WG	3257	1:1:6	1194	0.81	0.34	2449	3038
WG	3257	1:1:6	1269	0.81	0.34	2243	2782
WG	3257	1:1:6	1269	0.81	0.34	2153	2671
DT	14834	1:1:6	1206	0.79	0.34	5499	6931
DT	14834	1:1:6	1203	0.79	0.34	6207	7823
DT	14834	1:1:6	1200	0.79	0.33	6848	8630
DG	7970	1:1:6	1188	0.78	0.33	4522	5620
DG	7970	1:1:6	1178	0.78	0.33	4459	5542
DG	7970	1:1:6	1170	0.78	0.33	4396	5463
CB	10518	1:2:9	416	0.49	0.42	3106	3893
CB	10518	1:2:9	416	0.49	0.42	3181	3987
CB	10518	1:2:9	416	0.49	0.42	3331	4175
DB	10805	1:2:9	416	0.49	0.42	4837	5632
DB	10805	1:2L9	416	0.49	0.42	4304	5011
DB	10805	1:2:9	416	0.49	0.42	4997	5818
WG	3257	1:2:9	416	0.49	0.42	2117	2626

TABLE V (continued)
 COMPRESSION TEST RESULTS - CORED

Clay Unit Type	Clay Unit Comp. Str. f'_b (psi)	Mix	Mortar Properties ¹			Prism Str.- f'_m (psi)	
			Comp. Str.- f'_c (psi)	C/W ²	L/W ²	Gross Area	Net Area
WG	3257	1:2:9	416	0.49	0.42	2225	2702
DT	14834	1:2:9	416	0.49	0.42	4447	5610
DT	14834	1:2:9	416	0.49	0.42	4687	5913
DT	14834	1:2:9	416	0.49	0.42	4447	5610
DG	7970	1:2:9	416	0.49	0.42	3350	4181
DG	7970	1:2:9	416	0.49	0.42	3534	4411
DG	7970	1:2:9	416	0.49	0.42	3599	4491

¹ Flow = 130% in all tests.

² See Footnotes to Table IV.

beneath the specimens. Load was applied at a moderately rapid rate until half the predicted strength was reached, after which the rate was regulated to induce failure after one minute but before two minutes from the half-way point. A professional testing company was employed to test the prisms whose strength exceeded the 300,000 pound capacity of the machine.

Failure of specimens made with high lime, low strength mortars tended to be slower and less explosive than did failure of those made with high strength, low lime mortars. Illustrations of four failed compression specimens are shown in Fig. 4. The prism on the far left, made with 1:2:9 mortar, was almost wholly intact, while the specimen made from 1:½:3 mortar failed so violently that only fragments of the size shown on the far right remained.

TEST RESULTS

Test Results. The results of Test Series I and II are presented in Tables IV and V respectively. The ultimate compressive stress for Series II is reported in terms of net area (area in contact with mortar) as well as in the usual manner of using gross area.

ANALYSES OF RESULTS

Statistical analyses were performed of the data collected using Subprogram Regression (9) and the CDC 6400 computer at the University of Colorado.

Ultimate prism failure stress (f'_{mt}) was the dependent variable, while other parameters, e.g., unit compressive strength (f'_b), initial rate of absorption (IRA), mortar cube strength (f'_c), cement/water ratio (C/W), lime/water ratio (L/W), and mortar flow¹ were considered for independent variables.

Bivariate Regression Analyses. Prior to performing multiple regression analyses, bivariate regression analyses were performed on various combinations of the candidate independent variables to detect any close relationships thereby avoiding redundancy in the subsequent multiple regression analyses. A close relationship between percent lime and retentivity (depicted in Fig. 3) was observed; retentivity was therefore not used in the multiple regression analyses. A similar relationship was observed to exist between mortar cube strength and cement/water ratio indicating that one or the other could be used in multiple regression analyses, but both would cause redundancy. A close relationship was also observed between unit compressive strength and initial rate of absorption.

¹C/w, L/W and flow are as-mixed values.

Bivariate analyses were performed to establish the relationship between ultimate cored-unit prism compressive stress and unit compressive strength for each of the three different mortar mixes used for the cored-unit prisms, i.e., 1:½:3, 1:1:6, and 1:2:9. Test data for cored unit prisms from reference 12 were analyzed as well to include results for 1:½:4½ mortar. Since the SCPI¹ prisms tested (12) were of a different slenderness ratio $(h/t)^2$ than those tested for this research, the results were converted to values compatible with the h/t of this study by using correction factors specified by SCPI (11). A second-order least-squares fit for the data corresponding to each mortar mix is presented in Fig. 5. The plots indicate that, for the data considered, prism strength increased as the unit strength increased for a given mortar, and that prism strengths were higher for low-lime mortar than for high-lime mortar. It may be noted also that the influence of unit strength is greater for low-lime mortar than for high-lime mortar.

Fig. 6 is a plot of prism compressive strength against two-inch mortar cube strength. Quadratic least-squares lines are shown for each of six types of cored clay units; five for the cored clay units used in this study and one for the unit of reference 12. The graph illustrates, for the data considered, the increase in prism strength with the increase in mortar cube strength. It may be noted that the influence of mortar strength upon prism compressive strength is less pronounced for the prisms of lower strength units.

The strength of the bivariate relationships between prism compressive strength and unit strength, and mortar cube strength observed was not too great, being in the range $r^2 = 0.5$ to 0.7 .

Multiple Regression Analyses. Several multiple regression analyses were performed (3) using Subprogram Regression (9)³ in which the candidate individual independent parameters (f'_b , C/W , L/W) were input. Analyses were performed based upon a linear form,

¹ SCPI (Structural Clay Products Institute) is now BIA (Brick Institute of America).

² h = height of prism.
 t = least lateral dimension.

³ The program uses a stepwise multiple regression procedure which successively selects the most influential of the independent variables as predictors of the dependent variable.

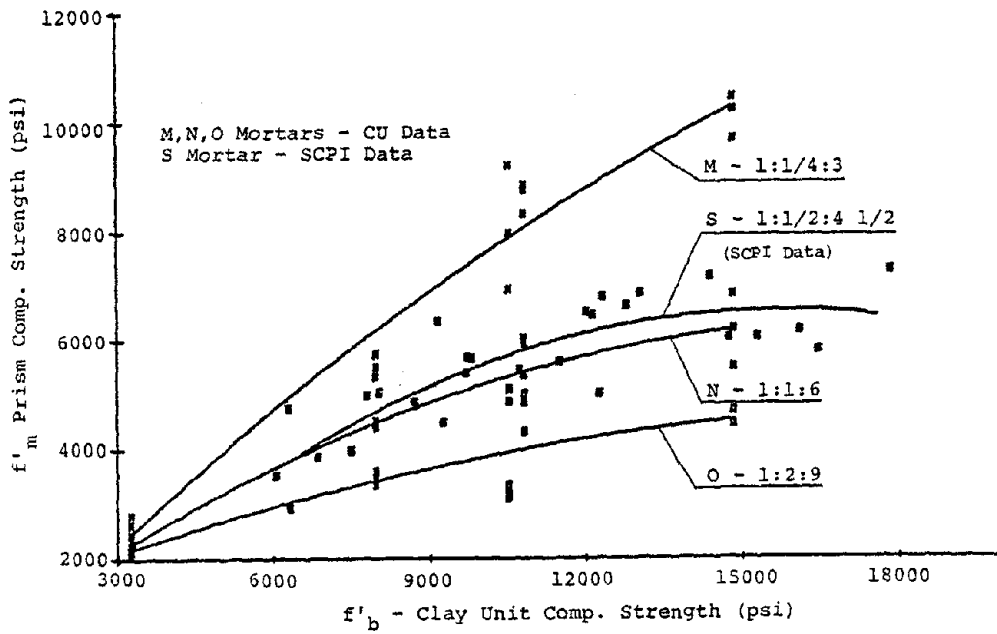


Figure 5. Relationship of Prism Strength to Clay Unit Strength

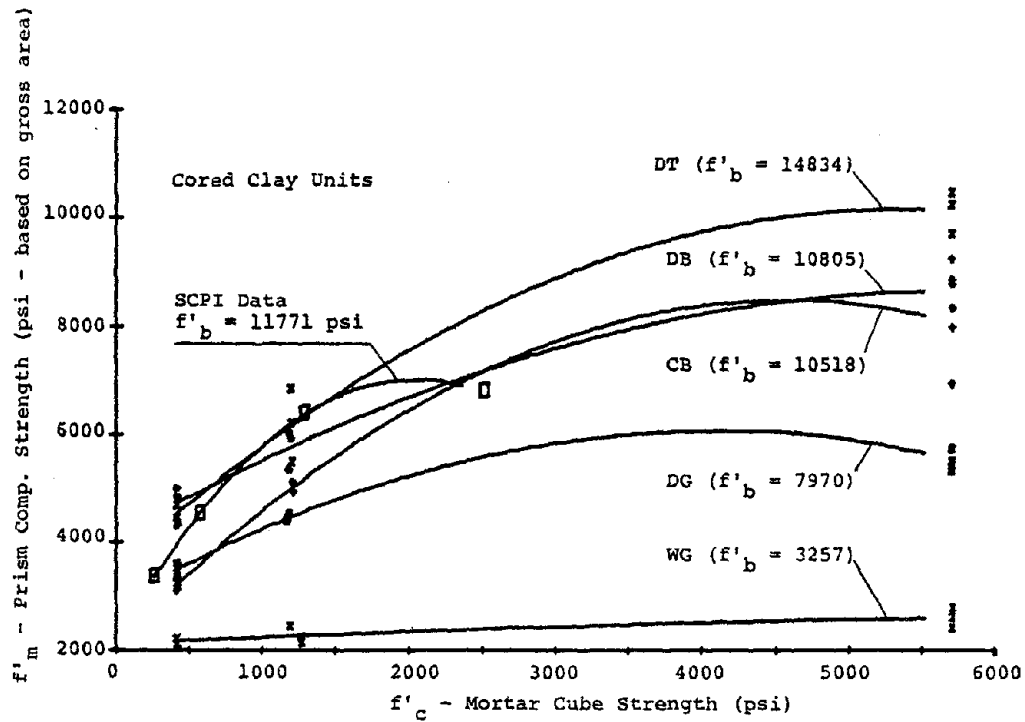


Figure 6. Relationship of Prism Strength to Mortar Cube Strength

$$y' = A + B_1x_1 + B_2x_2 + \dots + B_kx_k \quad (1)$$

in which y' is the estimated value of y

A is the y intercept, and

B_k are the regression coefficients

and based upon an exponential form¹,

$$y' = Ax_1^{B_1} x_2^{B_2} \dots x_k^{B_k} \quad (2)$$

The exponential form of predictor expression resulted in higher coefficients of determination (r^2). Table VI is a partial presentation of the combinations of independent variables used and the corresponding coefficients of determination.

It may be observed that including IRA along with variables f'_b and C/W or L/W produces little or no improvement in prediction accuracy as measured by r^2 . This could have been expected due to the strong bivariate relationship previously observed between f'_b and IRA. Similarly, the inclusion of L/W to the combination of f'_b and C/W produced little improvement.

Since mortar cube strength is a commonly measured value, f'_c was substituted for C/W to determine the strength of the resulting expression. As may be noted from combinations 12, 13, and 14, the accuracy of prediction is slightly less than the corresponding expressions 7, 8, and 9 using C/W and further, inclusion of L/W and IRA improves accuracy only slightly.

The exponential forms of predictor equation for the prisms tested in this study for independent variables f'_b and C/W are,

$$\text{for paver-unit prisms: } f'_{mt} = -450 + 0.85(f'_b)^{0.973} (C/W)^{0.693} \quad (3)$$

$$\text{for cored-unit prisms: } f'_{mt} = -489 + 8.0(f'_b)^{0.724} (C/W)^{0.499} \quad (4)$$

¹It was necessary to linearize the exponential form by taking logarithms of each side, i.e.,

$$\ln(y') = \ln(A) + B_1 \ln(x_1) + \dots + B_k \ln(x_k)$$

in order to determine experimental exponential expressions using Subprogram Regression (9).

TABLE VI
 MULTIPLE REGRESSION - EXPONENTIAL FORM

Combination Number	Independent Variables Included	Coefficient of Determination-r ²	
		Power-Unit Prisms	Cored-Unit Prisms
7	f' b, C/W	0.926	0.930
8	f' b, L/W	0.922	0.919
9	f' b, C/W, IRA	0.926	0.946
10	f' b, L/W, IRA	0.922	0.936
11	f' b, C/W, L/W	0.939	0.930
12	f' b, f' c	0.918	0.930
13	f' b, f' c, L/W	0.935	0.929
14	f' b, f' c, IRA	0.918	0.946

When f'_c replaced C/W the expressions become

$$\text{for paver-unit prisms: } f'_{mt} = - 620 + 0.09(f'_b)^{0.964} (f'_c)^{0.315} \quad (5)$$

$$\text{for cored-unit prisms: } f'_{mt} = - 488 + 1.36(f'_b)^{0.725} (f'_c)^{0.234} \quad (6)$$

and in each of (3), (4), (5), and (6),

f'_{mt} = predicted ultimate prism compressive stress, psi

f'_b = unit flatwise ultimate compressive stress, psi

f'_c = mortar ultimate uniaxial compressive stress, psi

The exponents in the foregoing equations are obviously unique to the data obtained in the study conducted. Out of curiosity, the exponents of f'_c were fixed at 0.5, that of f'_b at 1.0, and the predictor equations reformulated with the following results:

$$\text{for paver unit prisms: } f'_{mt} = 2438 + 0.01 f'_b \sqrt{f'_c} \quad (7)$$

with $r^2 = 0.913$ and a 90% confidence interval of ± 1745 psi.

$$\text{for cored-unit prisms: } f'_{mt} = 2494 + 0.007 f'_b \sqrt{f'_c} \quad (8)$$

with $r^2 = 0.905$ and a 90% confidence interval of ± 1742 psi.

Experimental values of f'_{mt} are plotted against the predicted values of f'_{mt} and the 90% confidence band for each case in Figs. 7 and 8. It may be noted that Equations (7) and (8) are nearly the same.

CONCLUSIONS

The results of the research indicate that of the parameters evaluated, flatwise unit compressive strength and mortar cube strength together are the more important factors influencing prism strength and can be the basis of expressions which predict ultimate prism compressive strength. Inclusion of additional parameters, e.g., lime/water ratio of the mortar, and initial rate of absorption improved the accuracy of prediction only slightly as did substituting the cement/water ratio of mortar for mortar cube strength.

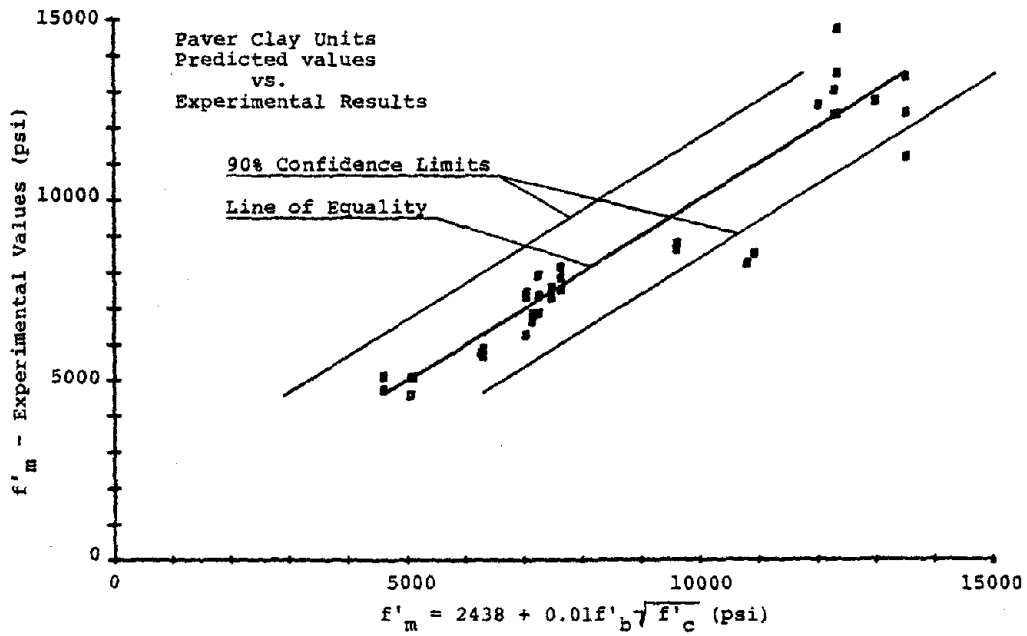


Figure 7. Predicted f'_m vs. Experimental Results - Pavers

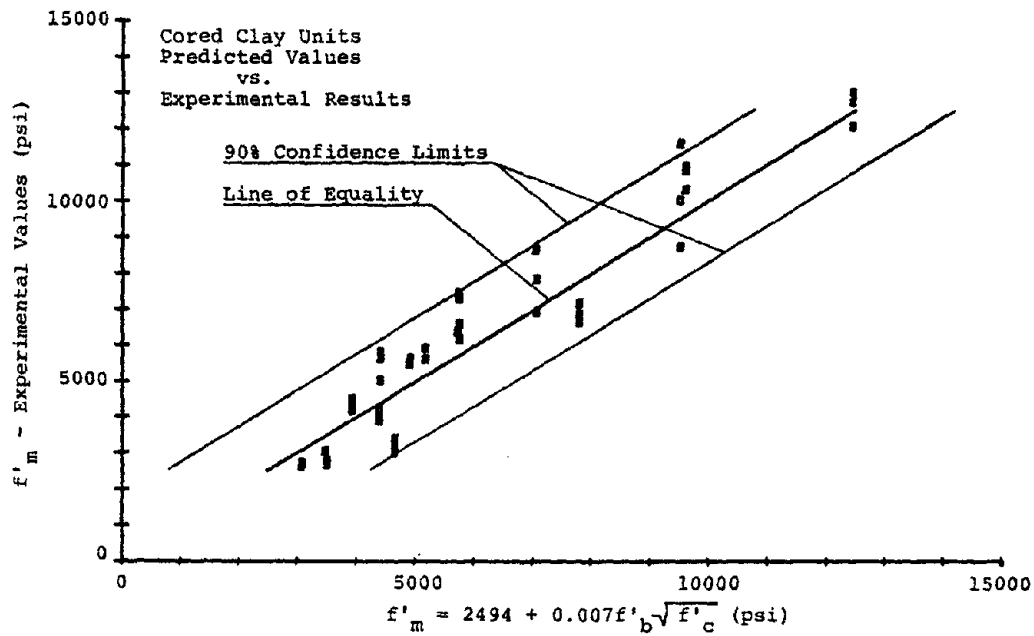


Figure 8. Predicted f'_m vs. Experimental Results - Cored

While the coefficients of determination of the predictor equations derived are quite high, it must be noted that the expressions apply to the data collected and cannot be considered generally applicable. In a statistical sense, the test sample was small; additional data could well reduce the coefficients of determination and cause a change in the expressions. Further, slenderness of the prisms was held constant.

The results indicate to the authors that stackbond prisms constructed and tested with rigorously followed but simple procedures can yield constant data.

ACKNOWLEDGEMENTS

The research was supported by a grant from the Colorado Masonry Institute and the Northern Colorado Masonry Guild. The project was monitored by Robert J. Helfrich, Technical Director, Colorado Masonry Institute. Professor C. C. Feng, University of Colorado, provided administrative control.

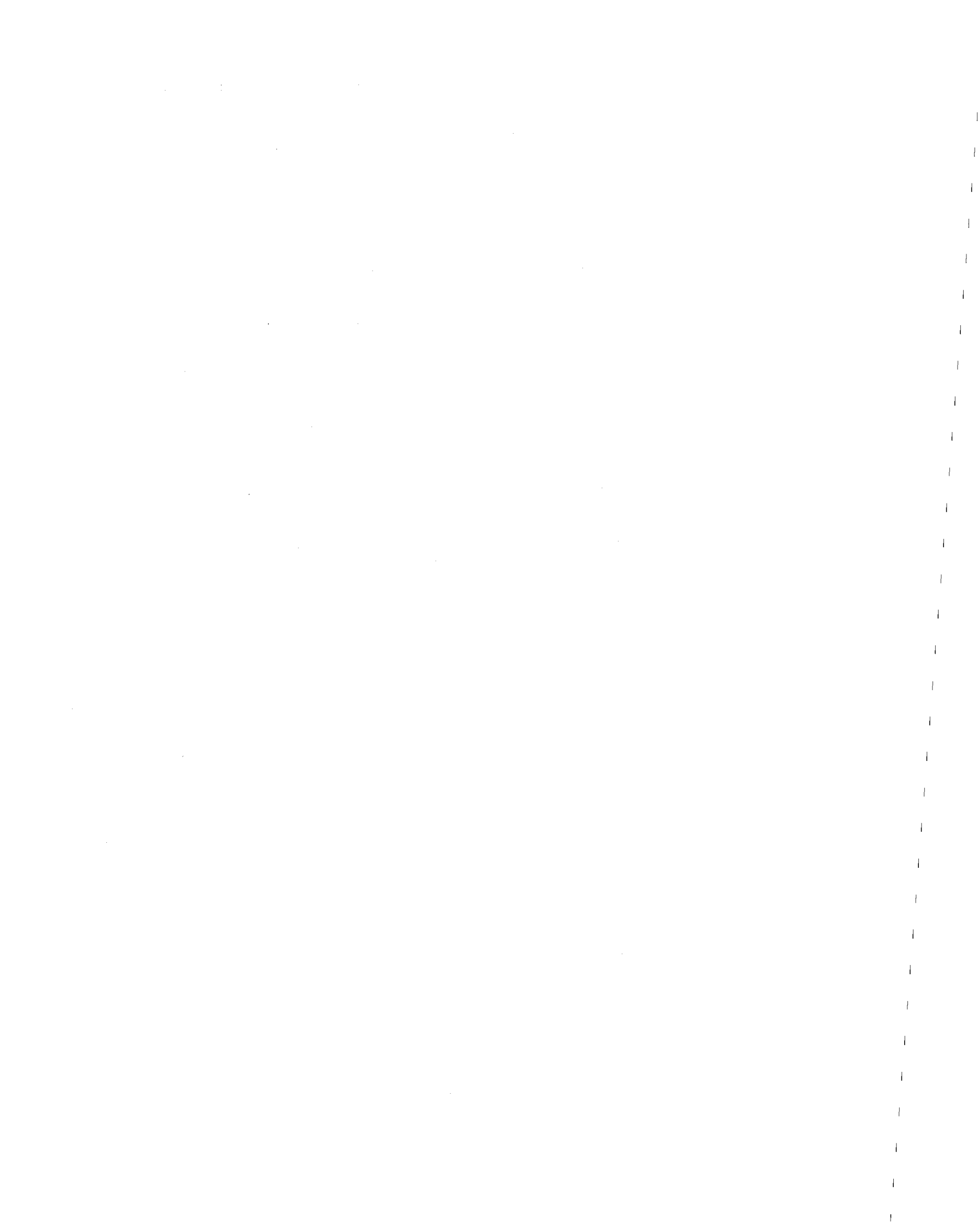
Materials were supplied by Colorado Brick Company, Lakewood Brick and Tile, and Rio Grand Supply, all in the Denver, Colorado area.

APPENDIX I - REFERENCES

1. American National Standards Institute, "Building Code Requirements for Reinforced Masonry", ANSI A41.2, 1960 (R1970).
2. Annual Book of ASTM Standards, American Society for Testing and Materials, Philadelphia, PA, 1973.
3. Baur, John C., Tension Bond and Compressive Strength of Small-Scale Masonry Specimens, M.S. Thesis, University of Colorado, Boulder, 1977.
4. Frey, D., Effects of Constituent Proportions on Uniaxial Compressive Strength of 2-Inch Cube Specimens of Masonry Mortars, M.S. Thesis, University of Colorado, Boulder, 1975.
5. Foster, P.K. and Bridgeman, D.O., "Prism Tests for the Design and Control of Brick Masonry", Technical Report No. 22, New Zealand Pottery and Ceramics Assoc. 1973, also Proceedings of the Inst. of Civil Engrs., London, March, 1973.
6. Hilsdorf, H.K., "Investigation into the Failure Mechanism of Brick Masonry Loaded in Axial Compression", Designing, Engineering and Constructing with Masonry Products, Gulf Publishing Co., Houston, 1969.
7. Mayes, R., Clough, R., A Literature Survey--Compressive, Tensile, Bond and Shear Strength of Masonry, Report No. EERC 75-15, College of Engineering, Univ. of California, Berkeley, 1975.
8. National Building Code of Canada, Assoc. Committee on the National Bldg. Code, National Res. Council of Canada, Ottawa, 1975.
9. Nie, N., Hull, C., Jenkins, J., Steinbrenner, K. and Bent, D., Statistical Package for the Social Sciences, McGraw-Hill, 2nd Ed., 1975.
10. Standard Association of Australia Brickwork Code, Standard Assoc. of Australia, Standards House, Sidney, N.S.W., 1974.
11. Structural Clay Products Institute, Recommended Practice for Engineered Brick Masonry, McLean, VA, 1969.
12. Structural Clay Products Institute, "Small Scale Specimen Testing - National Testing Program", Research Report No. 1, SCPRI, McLean, VA, 1964.
13. Uniform Building Code, ICBO, Whittier, California, 1976.

APPENDIX II - NOTATION

- f'_b - flatwise compressive strength of a masonry unit per ASTM C67.
- f'_c - uniaxial compressive strength of two-inch mortar cube.
- f'_{mt} - ultimate prism compressive stress, measured or predicted.
- C/W - mortar cement to water ratio by weight.
- L/W - mortar lime to water ratio by weight.
- IRA - initial rate of absorption, grams/30 in /min, of masonry unit.
- r^2 - coefficient of determination



A DESIGN GUIDE FOR REINFORCED AND PRESTRESSED BRICKWORK

By B. A. Haseltine¹

ABSTRACT: Reinforced brickwork has been used in a rather small way in the U.K. for many years, but the design guidance that was available was very poor. The existing Code of Practice covers only the design of reinforced walls, but nothing else; it is written in permissible stress terms. All U.K. codes are being revised at present into limit state terms, and the code on unreinforced masonry is nearly ready for publication. Being aware that it would be many years before the part on reinforced masonry would be produced, a group of engineers under the auspices of the British Ceramic Research Association have prepared a design guide for the use of prestressed and reinforced clay brickwork, in limit state terms.

This paper describes the design guide with particular reference to the Design Principles, Reinforced Brickwork Walls and Columns axially loaded, Reinforced Brickwork to resist lateral loads, the Design of Walls and Columns subjected to vertical and lateral loads, Reinforced Brickwork beams, Prestressed Brickwork, the detailing, materials, properties, and workmanship aspects of the material, the research carried out to support the guide is briefly described.

¹Jenkins and Potter, United Kingdom, Chairman of the Drafting Committee for the Design Guide

A DESIGN GUIDE FOR REINFORCED AND PRESTRESSED BRICKWORK

By B A Haseltine¹

BSc(Eng) ACGI DIC FICE MConSE

1.0. INTRODUCTION

Since 1948, in the United Kingdom and elsewhere in the world where UK codes are recognised, there has been a Code of Practice called Structural Recommendations for Loadbearing Brickwork (CP111)⁽¹⁾. The latest version was issued as long ago as 1970, although there was an amendment in 1971. The Code contains recommendations for the design of both unreinforced and reinforced walls, but no guidance on any other type of reinforced element of structure. It is, of course, in permissible stress terms as would be expected from the period of issue.

There has been a very considerable use of unreinforced load-bearing masonry in the UK since the early 1960s including many tall buildings which have been described already in the literature^(2,3,4). Unreinforced brickwork is still considered the most economical structure for flats, houses, halls of residence and other buildings having a regular plan form and an even spacing of walls. However, the use of reinforced brickwork has been limited because:

- a) The code, CP111, deals only with walls.
- b) The basis of design in CP111 is the modular ratio approach, where the E-value of the brickwork has to be assumed.
- c) Plain brickwork walls usually carry sufficient vertical load without the need for reinforcement.
- d) No allowance for seismic loads is required in the UK.
- e) No-one has publicised, until recently, the use of reinforced brickwork.

Codes in the UK are being revised to use the limit state philosophy. The concrete one⁽⁵⁾ has been published for some time (1972), and the loadbearing masonry code would also have been published but for unforeseen delays. However, the draft only deals with unreinforced masonry (brickwork and concrete blockwork) and work will not start for some time on the part dealing with reinforced and, probably, prestressed masonry.

¹ Partner, Jenkins and Potter, Consulting Engineers, London.

Because of the lack of guidance, and hence encouragement, in the use of reinforced brickwork, the Structural Ceramics Advisory Group (SCAG) of the British Ceramic Research Association, a group of engineers, architects, contractors and brickmakers, commenced work on their own Design Guide in 1972, and after 22 meetings it was published in 1977⁽⁶⁾.

2.0. DESIGN PRINCIPLES

The purpose of design is defined as the achievement of acceptable probabilities that the part of the structure being designed will not become unfit for the use for which it is required, i e that it will not reach a limit state.

Two limit states are recognised:

a) the ultimate limit state. In this an assessment using the design loads should ensure that an ultimate limit state is not reached as a result of rupture of one or more critical sections, by overturning, buckling or twisting, caused by elastic or plastic instability. The layout on plan is required to ensure a robust and stable design, with some allowance for accidental loads.

b) the serviceability limit state. In this it is required that deflection and cracking should not adversely affect the appearance or efficiency of the structure.

2.1. Loading. - The loads to be applied should ideally have been determined statistically, but it is recognised that it is rarely possible to do this at the moment and so code loadings are required to be used, multiplied by a partial safety factor γ_f to give the design load. For the combination dead plus imposed load, γ_f is taken as 0.9 or 1.4 on the dead load and 1.6 on the imposed. For the combination dead plus wind load γ_f is the same on dead load, but 1.4 on wind load. When dead, imposed and wind loads are considered, γ_f is taken as 1.2 on all three.

2.2. Materials . - The design strength of the material is the characteristic strength divided by another partial safety factor γ_m , which varies for brickwork in compression (γ_{mm}), brickwork in shear (γ_{mv}), steel (γ_{ms}) and for certain other uses.

For the ultimate limit state, γ_{mv} is taken as 2.5 and γ_{ms} as 1.15. γ_{mm} varies depending on the degree of manufacturing and construction control. For the worst of both γ_{mm} is 3.5 and for the best 2.5. When construction control is special, but manufacturing is normal, γ_{mm} is 2.8 and for the reverse it is 3.1. Lower factors apply to design for the serviceability limit states.

The characteristic strength of steel is given in the concrete code, and the same figures are recommended for reinforced and

prestressed brickwork. The limit state version of the unreinforced code for masonry will give characteristic compressive strengths of brickwork, and the same figures have been adopted in the design guide for use in direct compression, Table 1, but an enhancement factor of 1.5 is allowed for bending compression. The figures in Table 1 apply only when the bricks are loaded in the usual way; they have to be corrected for slenderness effects.

Table 1 - Characteristic compressive strength of brickwork (f_k) normal to bed joints (N/mm^2)

Mortar Grade and mix	Compressive strength of brick (N/mm^2)					
	15	20	35	50	70	100
(i) 1: $\frac{1}{4}$:3	6.0	7.4	11.4	15.0	19.2	24.0
(ii) 1: $\frac{1}{2}$:4 $\frac{1}{2}$	5.3	6.4	9.4	12.2	15.1	18.2

An appendix allows prism tests to be used to determine the characteristic compressive strength, but, unlike American practice, there is little confidence in the UK that there is a proper correlation between prism strength and brickwork strength.

Two types of shear are considered - racking shear in walls and shear in flexural members. Racking shear in walls is dependent in part on the degree of pre-compression and is taken as $0.35 + 0.6$ times the design load (taken as $0.9 \times$ dead load), in N/mm^2 . This is the same figure as is used in unreinforced brickwork. With certain limitations the characteristic shear strength of members in flexure is taken as $0.35 N/mm^2$, but this figure seems to be rather low when applied to retaining walls, for example, and this is an area for more research work.

2.3. Analysis

For the purposes of analysis, stress strain curves are given for brickwork (Figure 1) reinforcement (Figure 2), prestressing steel (Figure 3) and prestressing strand (Figure 4).

For the verification of structural safety it is required that the design strength of a member should equal or exceed the effects of the design loads.

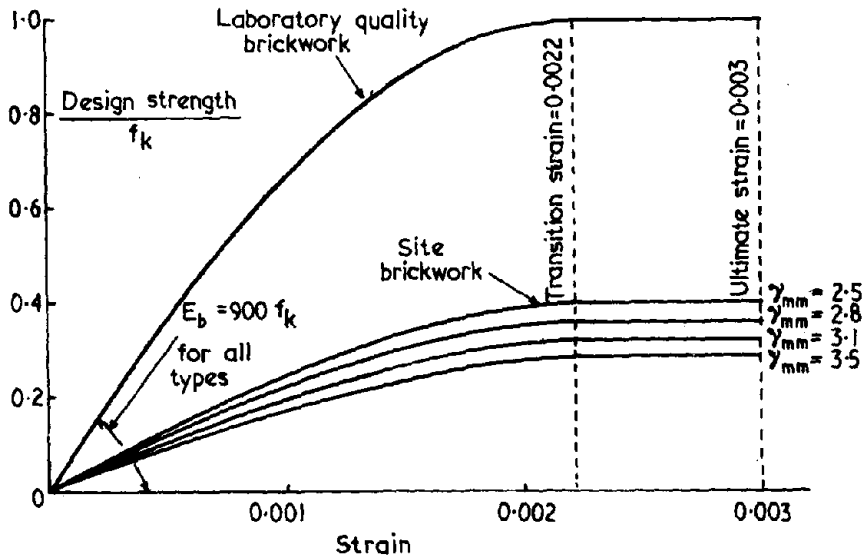


FIGURE 1 - Idealized design short-term stress-strain relationships for brickwork.

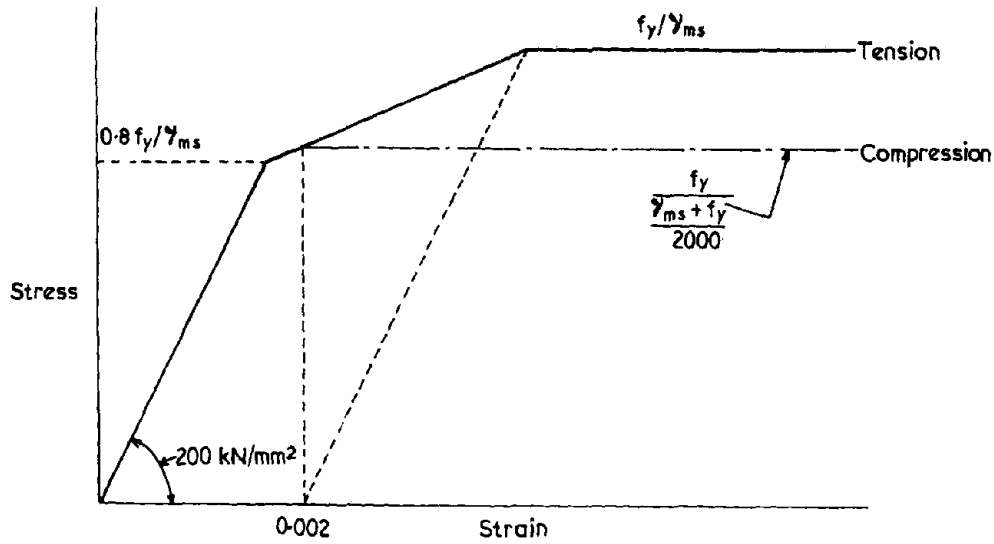


FIGURE 2 - Short-term design stress-strain curve for reinforcement.

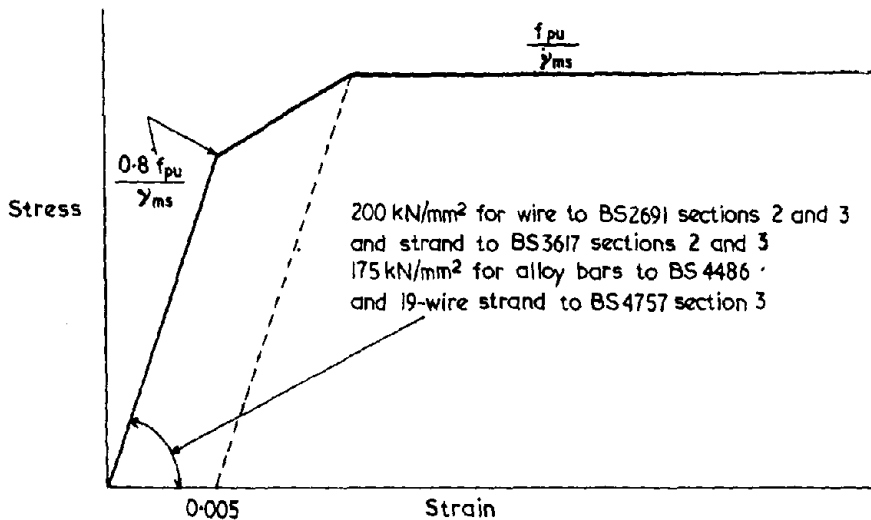


FIGURE 3 - Short-term design stress-strain curve for normal and low relaxation products.

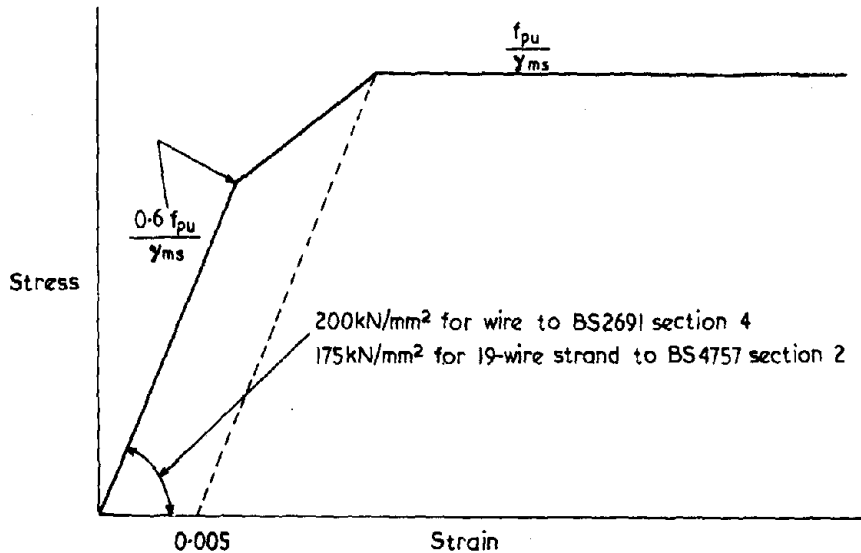


FIGURE 4— Design stress-strain curve for 'as-drawn wire' and 'as-spun' strand.

3.0.

RESEARCH FOR THE GUIDE

Ideally, a great deal of research would have been carried out to verify all the design principles and formulae given for the various practical cases. It was recognised that much research has been done in other countries, but it was not found practicable to make a great deal of use of this, as it is often not directly applicable to UK practice and materials. A research programme has been prepared to remedy this deficiency, but two areas were investigated before publication.

3.1. Stress/Strain relationships. - Figure 1 was prepared from the results of research into the stress/strain behaviour of four brick/mortar combinations by the British Ceramic Research Association, reported at the Fourth International Masonry Conference in Bruges (7). The curve in Figure 1 is extremely idealised, as is the case with a similar curve in the concrete code, but it represents the shape of a conservative compressive stress block. Work has started to obtain a similar curve for calcium silicate brickwork.

3.2. Prisms Loaded in Different Ways. - Almost all the available information on the strength of brickwork in compression assumes that the bricks are laid with frogs up and filled and that they are loaded on their bed faces. For reinforced loadbearing walls or retaining walls this is valid, but for beams it is unhelpful, since bricks will usually be loaded in another aspect and most have lower strengths when tested on end or on edge as compared to their bed face strength.

A series of prism tests was, therefore, carried out by the British Ceramic Research Association with several different types of bricks laid in bonds that loaded them on other than the bed face as well as in the normal direction. Figure 5 shows the bonds and Table 2 the types of brick used in the research.

Figure 5 - Bonds of prisms tested for effect of loading on edge or on end.

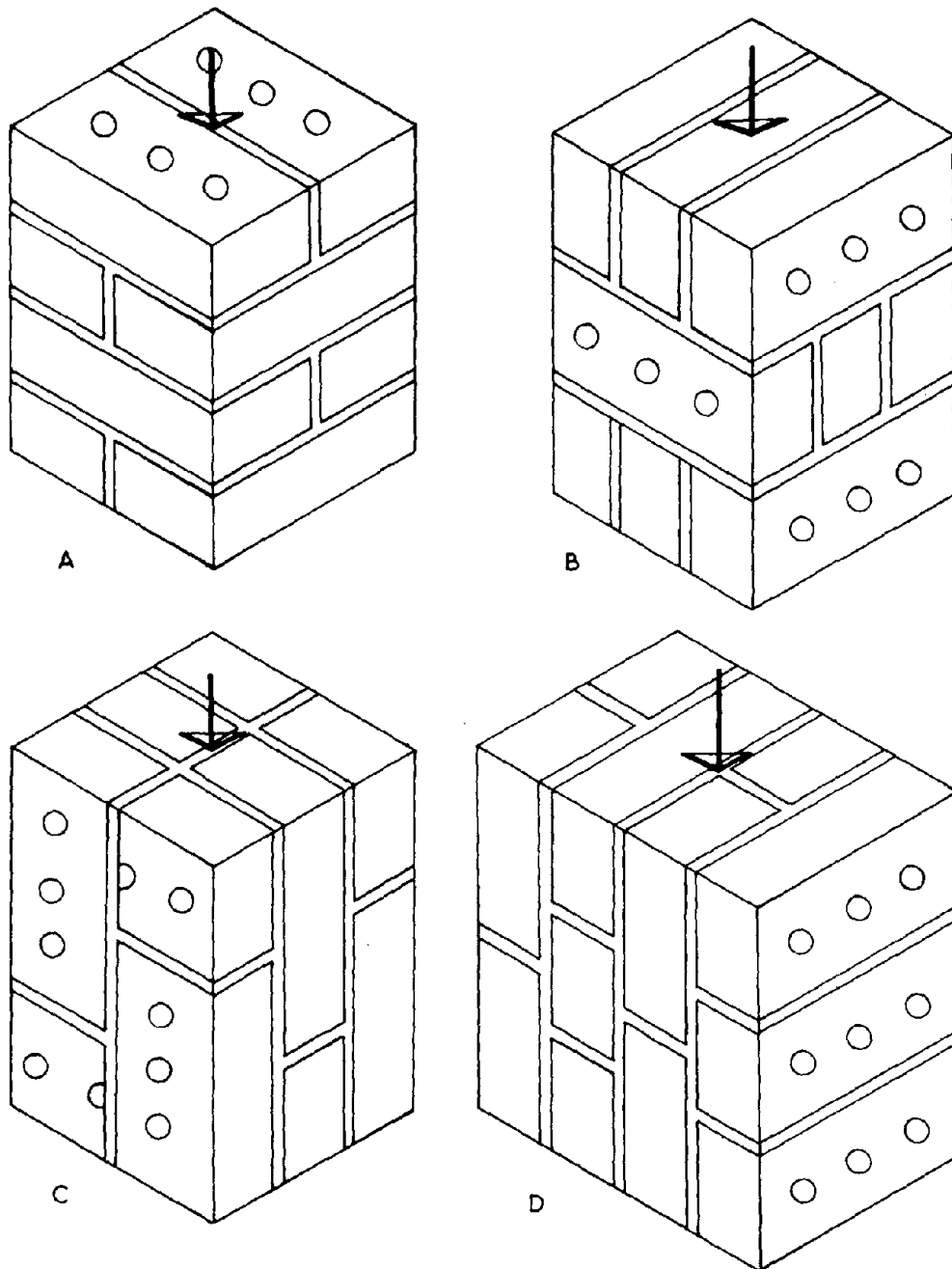


Table 2 - Details of Bricks

Brick	Description	Mean Crushing Strength N/mm ²		
		On Bed Face	Between Headers	Between Stretchers
1	3 hole wirecut	52.6	9.07	19.0
2	16 hole wirecut	63.1	8.74	23.3
3	23 hole wirecut	73.2	8.58	15.7
4	Staffordshire Blue Engineering	71.8	45.3	53.8
5	Semi-Dry Pressed Deep Single Frog	27.9	14.4	15.6
6	Stiff Plastic Pressed Double Shallow Frog	53.9	37.5	48.6

The results of the tests were most interesting. It was found that solid and deep frogged brick prisms had virtually the same strength when the bricks themselves were being loaded along their length or width as comparable prisms loaded in the conventional way. It was, therefore, concluded that no distinction need be made in the guide about the direction of loading of solid or frogged bricks. However, it was found that perforated bricks carried much less load when the direction of loading was other than on the bed face. It has been recommended in the guide that users test the particular perforated brick that they intend to use, but as a lower bound, perforated brickwork loaded on end or across the bricks should be assumed to be only 0.4 times the strength in the direction perpendicular to the usual bed face.

3.3. Retaining Walls. - A group of brick manufacturers has sponsored some tests on reinforced retaining walls, and the results were made available to the drafting committee. They are now published by Structural Clay Products Ltd (8, 9).

4.0.

DETAILED CLAUSES

The guide is sub-divided into a number of sections which cover the main uses of reinforced and prestressed brickwork. Some of the more important aspects are described below.

4.1. The Design of Reinforced Brickwork Walls and Columns with Vertical Axial Loading. - This section really replaces that in the present CP111, where walls are to be reinforced to help in their loadbearing capacity. A formula for the design strength is given, together with rules for calculating the effective height of a wall and its slenderness effects. This is the section that will probably be least used, since there are so many high strength bricks available in the UK that unreinforced walls can carry all the loads usually required.

4.2. The Design of Reinforced Brickwork to Resist Lateral Loads.
This covers three principal groups of elements:

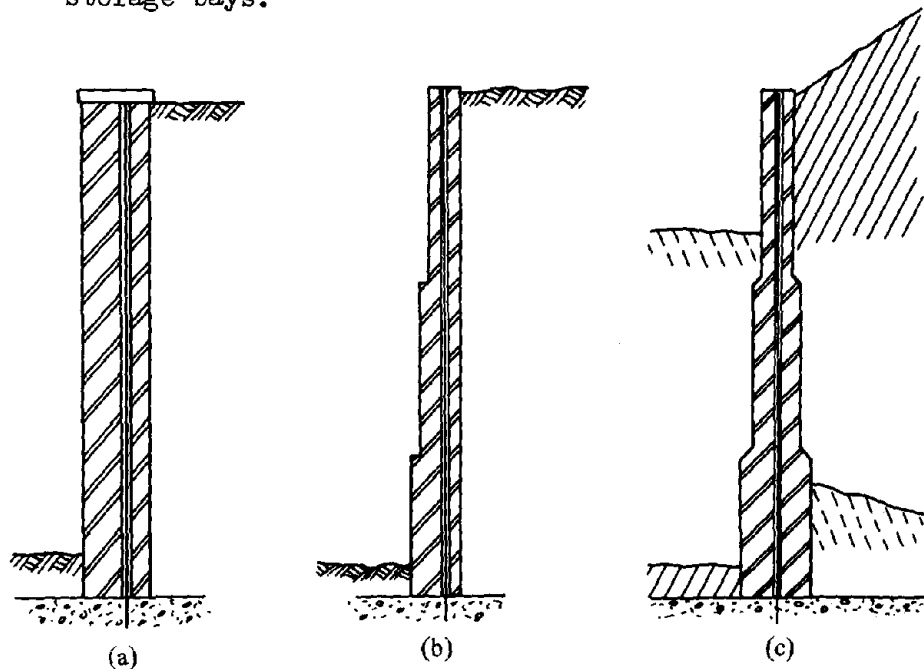
a) External panel or boundary walls (and to a lesser extent partitions) with no primary structural function but which, because of their size, shape or fixings cannot be shown to resist lateral forces when unreinforced.

b) Retaining walls whose prime function is to resist lateral pressures perpendicular to their faces from earth, liquids or stored materials such as grain.

c) Piers or buttresses which are loaded along their major plan dimension instead of perpendicular to it.

It is an important section, as one of the most popular uses of reinforced brickwork in the UK is for retaining walls. Considerable help is given to designers in the way in which reinforcement can be added to brickwork, e g Figure 6, but the actual design of the reinforced section is left to the part dealing with beams (4.4.). Another recent publication has amplified the design guide in respect of retaining walls (10).

Figure 6 - Cantilever retaining walls, grouted cavity or Quetta bond wall: (a, b) thickened on unloaded face; (c) thickened on both faces as dividing wall between storage bays.



4.3. The Design of Walls and Columns Subjected to simultaneous vertical Loads and Moments, or Horizontal Loads. - This covers, in the main, the design of eccentrically loaded walls or those carrying vertical loads, and in addition, substantial horizontal loads, e g a wall in a basement carrying the vertical loads from above, but resisting earth pressure as well. However, if the net eccentricity is less than 1/20th of the wall thickness, bending can be ignored. The simple relationship

$$\frac{\text{Moment due to design loads}}{\text{Design moment of resistance}} + \frac{\text{vertical design load}}{\text{design vertical load resistance}} \leq 1$$

is used for these combined actions.

4.4. The Design of Reinforced Brickwork Beams. - Tension arising from bending is the principal reason for incorporating reinforcement in brickwork, and so the design approach given for beams is also applicable to all bending cases. A large number of ways of incorporating reinforcement are given, for instance those in Figure 7.

The formulae for the resistance moment of a section are given; the compression case has been derived from the stress/strain curves in Figure 1.

Design moment of resistance =

$$\text{either } \frac{0.3 \cdot b \cdot d_{ef}^2 \cdot 1.5 f_k}{\delta_{mm}}$$

$$\text{or } \frac{A_s f_y \cdot z}{\delta_{ms}}$$

where z is the lever arm which equals

$$d_{ef} \left[1 - \frac{0.53 A_s}{b \cdot d_{ef}} \frac{f_y}{\delta_{ms}} \frac{\delta_{mm}}{1.5 f_k} \right] \text{ but not } > 0.95 d_{ef}$$

and b width of beam

d_{ef} effective depth

f_k characteristic compressive strength

A_s cross sectional area of reinforcement

f_y characteristic tensile strength of reinforcement

Information is given for shear resistance and bond effects

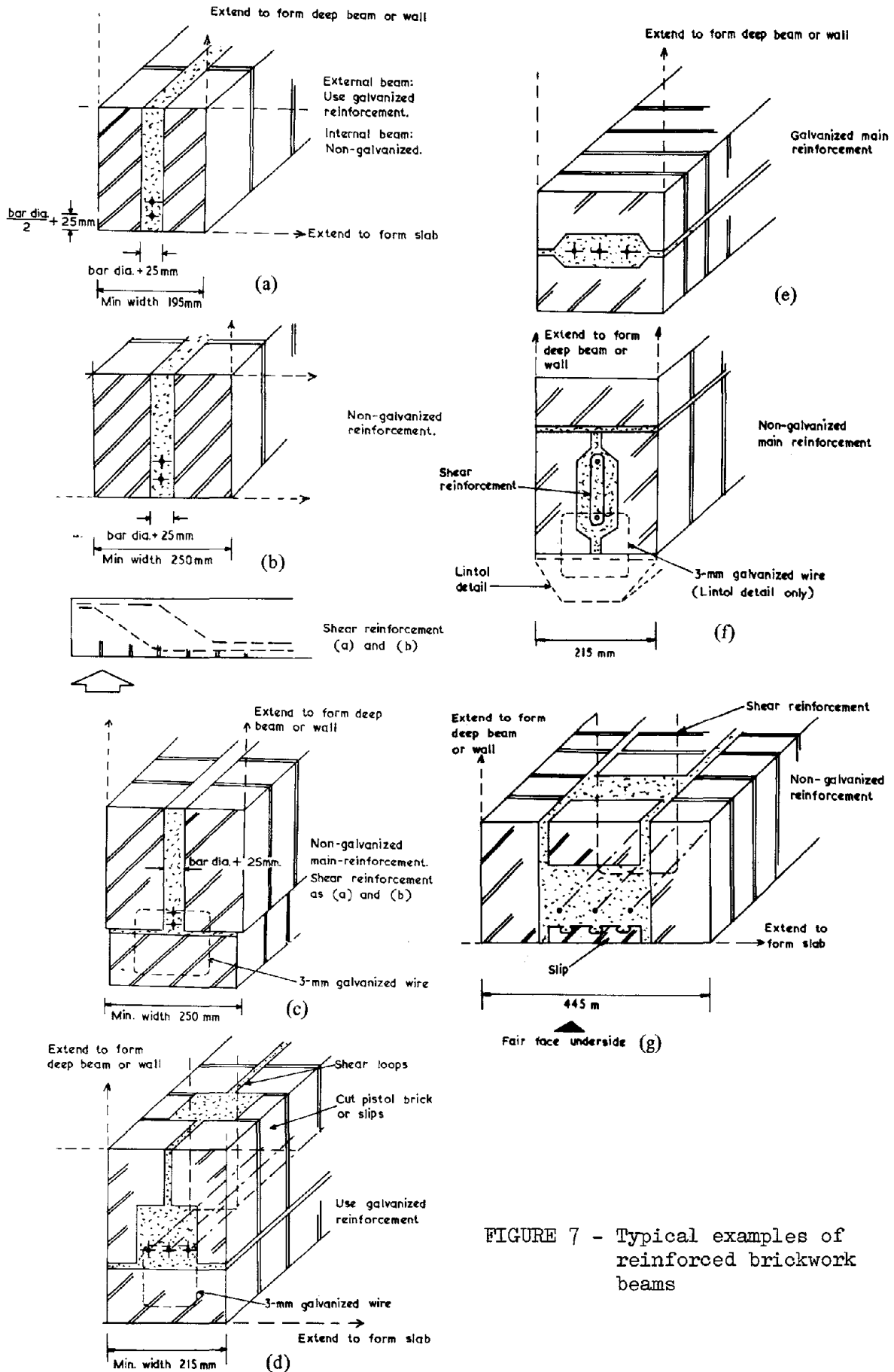


FIGURE 7 - Typical examples of reinforced brickwork beams

4.5. The Design of Prestressed Brickwork. - It is assumed that brickwork will be post-tensioned. In most respects the design guidance given follows exactly that in the appropriate part of the concrete code. The main differences are in respect of shrinkage and creep effects, when considering losses.

4.6. Detailing Reinforced and Prestressed Brickwork. - The minimum areas of reinforcement, maximum and minimum bar sizes and spacings are reproduced here in Table 3. Anchorage bond, curtailment, secondary steel, nominal shear reinforcement and column links are dealt with in the guide.

One of the most important areas of detailing is the matter of cover. This produced a lot of discussion in drafting, and in the end a simple performance requirement has been given - "Reinforcement in brickwork should have sufficient cover of mortar grout or concrete to ensure that it is able to act structurally and to give protection against corrosion". This is further supplemented for external walls etc. "All reinforcement within 100 mm of the face of the brickwork should be galvanised to BS729, be stainless steel, or have a similar degree of protection".

4.7. Materials and Properties. - This section, and the following one on Work on Site, lean heavily on the "Model Specification for Clay Brickwork" (11) published also by British Ceramic Research Association. Grouts have been specified, as these do not receive attention in the Model Specification.

4.8. Work on Site. - The main additions to the Model Specification are a table of minimum grout strengths, items on 'low-lift' grouted cavity walls, 'high-lift' grouted cavity walls, Quetta and similar bonds, reinforcement and prestressing tendons.

5.0.

CONCLUSIONS

The design of reinforced and prestressed brickwork has received attention in only a few countries and as far as is known, apart from the subject of this paper, there is no limit state guidance for designers using this material.

It is recognised that much research needs to be done to verify the design rules given in the guide, but they are founded on well known principles, derived for the design of reinforced and prestressed concrete. The guide is recognised as being an interim document, and users have been invited to comment on its use in practice. In the meantime a research programme has been planned to further verify the design principles.

Table 3 - Reinforcement Requirements

Maximum bar diameter	6 mm in bed joints 25 mm elsewhere
Maximum bar spacing in walls (other than pocket)	500 mm
Minimum spacing between bars	10 mm in bed joints 25 mm elsewhere
Minimum area of reinforcement (% of gross cross-sectional area, unless otherwise stated)*	
<i>LOCATION</i>	<i>Secondary reinforcement</i>
Beams	0.2% As necessary to suit shear force or nominal shear reinforcement in accordance with Section 8.1.3.
Columns	0.2% Only required where tensile strength of surrounding brickwork is not adequate to restrain main reinforcement. In accordance with Section 8.1.4.
Walls	0.05%
(a) Grouted cavity designed to span one way	0.2% total, not more than $\frac{1}{3}$ of which is in either direction
(b) Grouted cavity designed to span two ways	
(c) Quetta bond	0.2% Not normally required (Horizontal reinforcement in bed joints may be used to give some measure of two-way spanning, or to control cracking).
(d) Pocket-type walls	0.2% Not necessarily required, but desirable especially with widely spaced pockets or where the wall needs to be tied back to the concrete (see Figure 13 B, C and D); also helpful to control cracking

*The minimum areas of reinforcement given above do not apply to small bars, or proprietary strip reinforcement, in bed joints.

ACKNOWLEDGEMENTS

The design guide on which this paper is based is published by the British Ceramic Research Association, whose Director, Mr. A Dinsdale, has kindly given permission for the extracts to be used.

REFERENCES

1. 'Structural Recommendations for load-bearing walls' CP111:1970. British Standards Institution
2. Haseltine, B A: 'Some load-bearing brick buildings in England'. Designing Engineering and Construction with Masonry Products. Edited by Franklin B Johnson, Gulf Publishing Co.
3. Jenkins, R A S; Haseltine, B A: 'Recent Experiences with Calculated Load-bearing Brickwork' Proceedings of the British Ceramic Society, 11, 1968.
4. Haseltine, B A and Au, Y T: 'Design and Construction of a Nineteen-Storey Load-bearing Brick Building'. Proceedings 2nd International Brick Masonry Conference. Edited by H W H West and K H Speed, Stoke-on-Trent, British Ceramic Research Association, 1970.
5. 'The Structural Use of Concrete'. CP110 1972. British Standards Institution.
6. 'Design guide for reinforced and prestressed clay brickwork' SP91. British Ceramic Research Association.
7. Powell, B and Hodgkinson, H R: 'The determination of stress/strain relationship of brickwork': Proceedings 4th International Brick Masonry Conference, Bruges. Groupment National de l'Industrie de la Terre Cuite, 1976.
8. Maurenbrecher, A H P; Bird, A B, Sutherland, R J M and Foster, D: 'Reinforced Brickwork: vertical cantilevers. 1'. SCP10. Structural Clay Products Ltd.
9. Maurenbrecher, A H P; Bird, A B, Sutherland, R J M and Foster, D: 'Reinforced Brickwork: vertical cantilevers. 2', SCP11.
10. Haseltine, B A and Tutt, J N: 'Brickwork retaining walls'. The Brick Development Association
11. 'Model Specification for Load-bearing Clay Brickwork'. SP56: 1975. British Ceramic Research Association.

MASONRY IN BUILDING CODES

By Walter L. Dickey, S.E.*

ABSTRACT: Early master mason activity, developed by successive approximation and by intuition, produced magnificent structures. Modern code documentation of masonry design and of reinforced masonry provisions followed in turn much later. Seismic consideration and design methods followed, with requirements to improve performance. Resulting fallacy, and validity, of arbitrary requirements is clarified.

Need for reorganization of code provisions and for development based on authentic data summarized.

*Consulting Structural Engineer, Los Angeles, California

MASONRY IN BUILDING CODES

by

Walter L. Dickey*

INTRODUCTION

This North American Masonry Conference is a great step for mankind! It presents what is probably the largest surge of authentic testing, research and development in masonry information. Perhaps we are seeing a sleeping giant stirring for an awakening.

Following the introductory session is a session on Codes, i.e., the control of design. This is because we in The Masonry Society, and in the National Science Foundation, recognize the importance of and deplore the state of modern design codification of man's oldest permanent construction.

It deserves better! It has served man for centuries, even millennia, with its excellent qualities of strength, durability, permanence, fire resistance, thermal resistance, weather resistance, beauty, flexibility of design and function. It has provided man and his family with protection from the elements, and from enemy carnivores and homo sapiens. It has provided him with shelter for home, for livelihood and work, for his soul and worship, grand palaces to rule in, and to be ruled from. It has ranged from hovels to majestic monuments.

We should not now ask - "What can our masonry do for us?", but, "What can we do for our masonry?"

There are several things we should do. We should give it understanding (it needs it) and T.L.C. (Tender Loving Care) so that we may provide for better design understanding, with better code statement of design and construction requirements. One item we might hopefully remember is the note sent a minister by his wife at the start of his sermon. It was simply KISS. One member saw the note, was touched, and commented on its tenderness. The minister explained that he also appreciated it, it meant Keep It Simple Stupid.

This is especially appropriate in masonry because possible scatter of test results and quality do not warrant complex refinements of method or equations for a high degree of complexity and precision in practice. Let us hope for KISS as we progress and develop.

*Consulting Structural Engineer, Los Angeles, California

OBJECTIVE

The objective of this discussion is to present:

1. Historical background pertinent to the development of Codes.
2. A brief look at the recent modern Code development, since 1933.
3. Amplify and clarify items of apparent confusion or contradiction, and fallacy or fact.
4. Emphasize need for considering new provisions for post-failure performance as it affects assumed input for seismic, blast, tornado, or vibratory response.
5. Emphasize dire need for more true, basic and authentic information, in addition to intuitive design.
6. Emphasize simplification of design for the major portion of masonry construction, which does not require sophisticated complex numerical manipulation to prove satisfactory application, i.e., KISS.

HISTORICAL

The long history of masonry resulted in many intuitive design principles and satisfactory use of masonry, what might be called traditional use.

A list would be endless.-I saw some examples in a recent trip, e.g.

Segovia with its 8-story height of columns supporting two miles of aqueduct across the valley, started in 100 BC and still functioning (in spite of two large earthquakes that have occurred.)

Cordoba, beautiful areas of columns, arches and ornamentation from the 1200's.

The gorgeous Alhambra and Generalife. Arched, ornamented and filigreed, built in the 800 year reign of the Moors.

The Gothic, Romanesque, and Renaissance cathedrals of Europe, unbelievably grand, majestic and tall, arched, domed, groined, with fantastic artistic flying buttresses and pilasters - built in the 1200's through 1600's, lighted through delicately carved masonry patterns supporting beautiful stained glass.

Those were developed by what we now might call intuitive design, or cut-and-try, or "successive approximations" or "iteration". We do not know how the master masons actually prepared the trestle boards, except that the design was without formal Codes. One Master is reputed to have used a model design method. Strings were suspended from an inverted foundation plan and weights were added at locations of intersecting loads. The shape of the weighted strings were along the line of force (tension) which shapes could be inverted and would be correct for the compressive forces in the lines of asymmetrical arches.

By whatever methods, the results were eminently satisfactory. Traditional rules were developed early, -in antiquity, in what we might call B.C., "Before Codes". For example the h/t ratio of the Segovia aqueduct columns is about what we use now. The h/t of the Rothenberg city walls between pilasters, built in the 1200's, is about what we might use under our present codes.

There was also our early American continuation and then application of basic engineering use. This was, in modern times, improved and codified by many, such as by the now Brick Institute of America and the National Concrete Masonry Association.

Then after the catastrophic failure of masonry buildings in the Long Beach earthquake of 1933 reinforced masonry began its continuous growth in the Uniform Building Code.

RECENT DEVELOPMENT (1933 - 1978)

There have been recent developments in unreinforced design, especially as shown in the BIA and NCMA publications on design and codes and in the adoption by ICBO, BOCA, Southern Code, etc. However the newer subject of reinforced masonry will be discussed in this brief presentation in the light of UBC. It was introduced into the UBC, the large Los Angeles City, and the California State provisions in 1933 and 1934, primarily crystallized by the 1933 Long Beach Earthquake.

It then experienced a continuous growth and refinement in those codes, especially in the UBC, which is reviewed, refined, up-dated and reprinted every 3 years.

However, since it was influenced by the specter of earthquakes the design requirements of reinforced masonry were not separated in principle from the sometimes hysterical reactions to quakes, and the consequent post-failure performance prescriptive protective provisions.

This has injected some arbitrary, or empirical, limits and requirements not completely based on scientific research and analysis, both for design and for construction requirements.

In addition there was another non-integrating factor. There was no strong entity for research and development like PCA and ACI in concrete, and the similar organizations in steel and in timber. The masonry industry is a fragmented one.

One example would be the organization (?) of the Brick Manufacturers group. They were separate from the Block industry, separate from the Contractors, separate from the Bricklayers. The East was split from the West. The West, e.g., California, was split into a North and a South. The largest manufacturer in the South split off on his own. The other industry portions were similarly splintered. To say the masonry industry was fragmented would be true, but an understatement!

Now we have great hopes for the integrating influence of The Masonry Society, hoping it will bring together the Brick and Block manufacturers, the East and West, the contractors, the craftsmen, the architects, engineers, building officials, all who use masonry.

CONFUSION AND CONTRADICTIONS, FALLACY AND FACT

Due to the above type of development, part intuition, part engineering, part practice, partial information, part tradition, mixed by committees, the resulting Code is a hybrid (some have used worse description).

Some specific examples are mentioned to clarify the above general statements and to emphasize the need for code improvement.

One example is a partial content of the UBC Masonry Chapter. There is Reinforced masonry; Partially Reinforced masonry; Unreinforced masonry; Engineered Unreinforced masonry; and Traditional Unreinforced; -a little voluminous and slightly confusing.

There are a few of the other miscellaneous examples which will be pointed out in a theme of reducto ad absurdum. This is not to be scornful, but in the hope of encouraging improvement in the codes that have actually provided us with so many excellent masonry buildings.

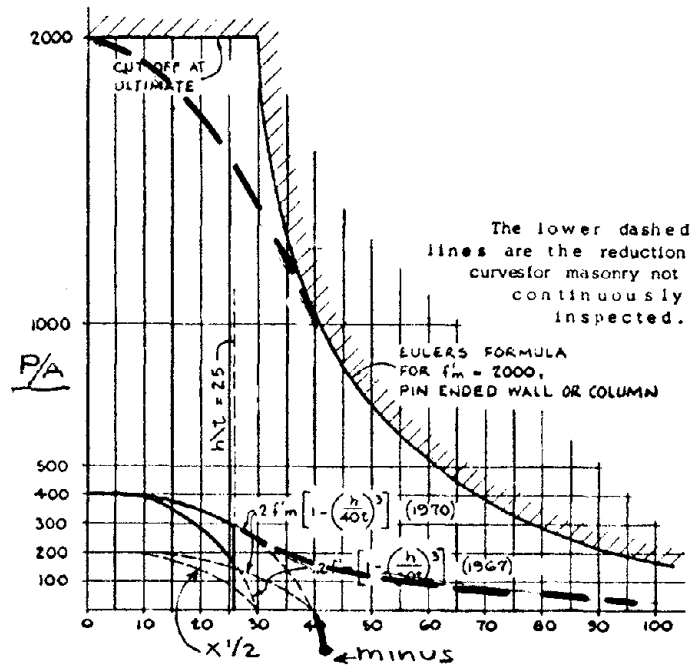
1. The reduction factor for walls and columns is $\left[1 - \left(\frac{h}{40t} \right)^3 \right]$

There is implication this is a buckling factor, but this is questionable. It does serve to reduce the design value of bearing walls, but at $h/t = 25$, the arbitrary maximum height permitted, it reduces the strength to about 75% of short column. This is really a negligible reduction when we consider that 1500^{psi} masonry is used at 300 psi, i.e., a ratio of 1:5, and there is a wide scatter of field quality and strength.

2. The limit of h/t of 25.00 is obviously not valid. If a wall at h/t of 25 has 3/4 of its full value, a wall at h/t of 26 would be almost

as strong, instead of 0 capacity.

3. The shape of the reduction curve is not correct, it goes to 0 at an h/t of 40, and to minus values at values greater than 40 - i.e., the capacity would increase! A small few cities have recognized this and have extended the curve beyond the h/t of 25 by a curve of the general shape of $1/5$ of an appropriate Eulers curve. Others should be similarly enlightened!



Buckled shape of column is shown by dashed line	(a)	(b)	(c)	(d)	(e)	(f)
Theoretical K value	0.5	0.7	1.0	1.0	2.0	2.0
Recommended design value when ideal conditions are approximated	0.65	0.80	1.2	1.0	2.10	2.0
End condition code						
			Rotation fixed and translation fixed	Rotation free and translation fixed	Rotation fixed and translation free	Rotation free and translation free

4. The curve makes no direct recognition of end conditions - which can introduce factors of from 2 to 1/2, a range of 4:1 or 400%.

5. The curve is inaccurate in not considering solid vs hollow wall construction. It is obvious that a hollow shape has a much better radius of gyration and hence better unit stress capacity for similar amounts of material.

6. The Code requires that piers whose width is less than 3 times its thickness shall be designed as columns.

An example was an 8" wall with windows leaving piers 20" wide. According to code they must be designed as columns, with 4 or more bars, and heavy ties, all at half stress because they are less than 12" thick. The plan section would be as shown in drawing - an obviously impractical construction. The computed capacity might be:

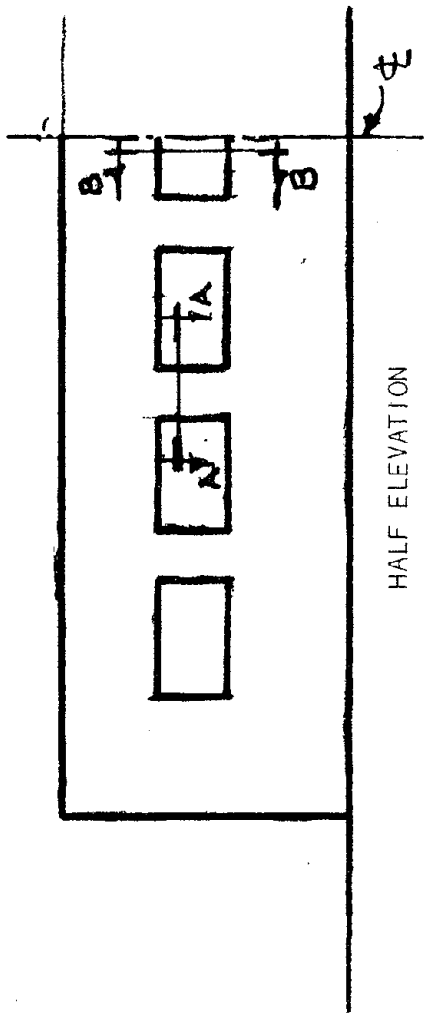
$$1/2 \quad [.18 \times 1500 \times 146'' + .65 \times 20,000 \times 4 \times .2] = 24,944$$

Or - the piers may be 6" thick with a/d of 20:6 or greater than 3:1 with the pier section shown in the drawing - and 2 bars.

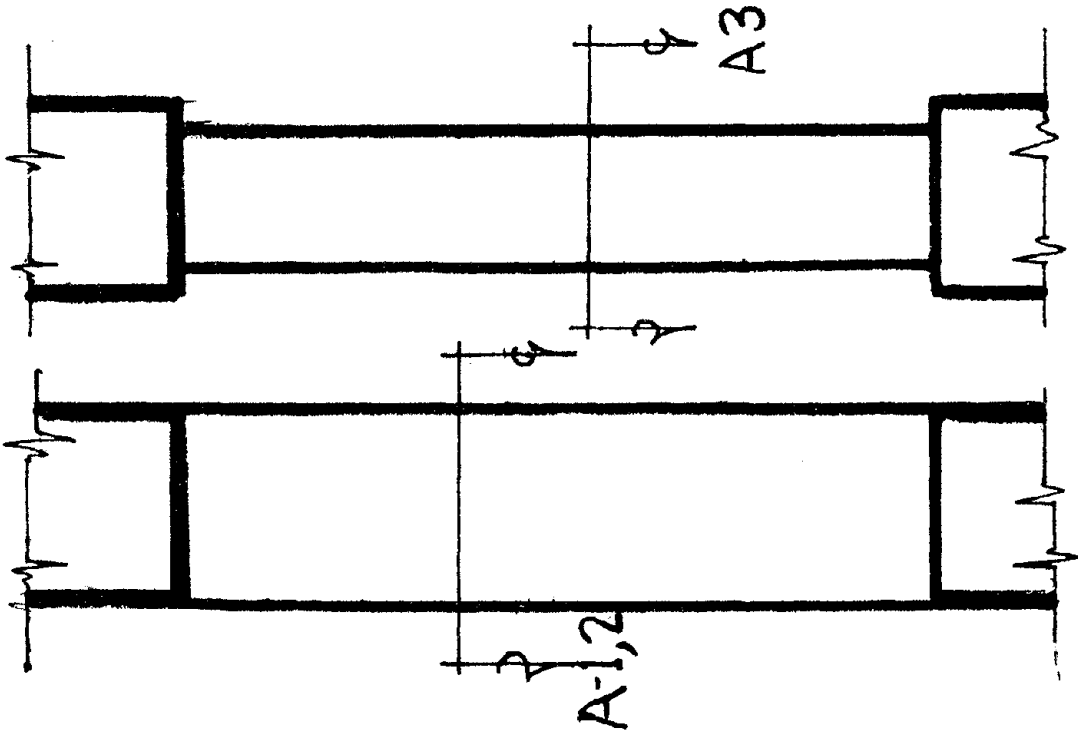
The computed capacity would be $.2 \times 1500 \times .07'' = 32,175\#$

Intrinsically the code would arbitrarily require the 6" pier instead of the 8" pier and would indicate that the alternate 8" column it required would not be as strong as the 6" pier.

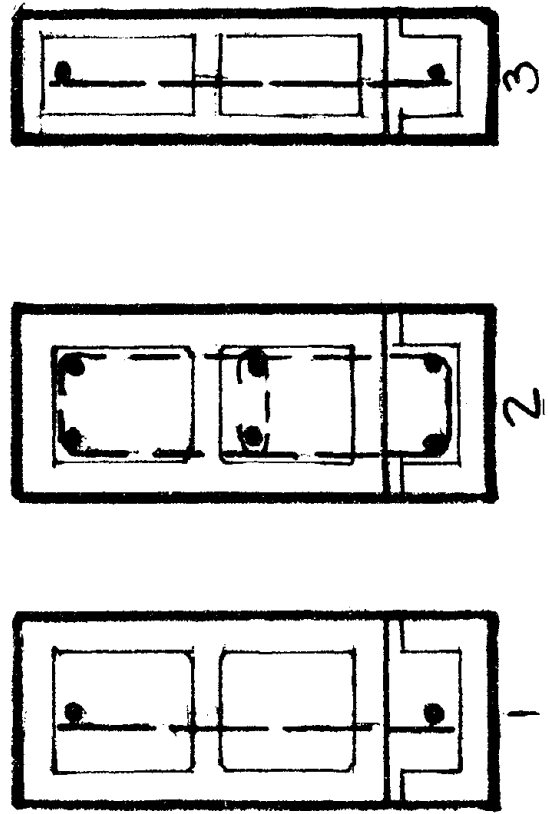
Fallacies in pairs!



HALF ELEVATION



ALTERNATE SECTION B-B



ALTERNATE SECTION A-A

7. The Code requirements for arbitrary column tie spacing was not due to a test program developed for masonry. It was merely a use of concrete column tie spacing which had been developed for use in concrete columns at rather high stress and monolith with beams and slabs. The size and spacing was adopted without regard for masonry joinery and function, e.g., 3/8 or 1/2" bars in 1/4 or 3/8 joints, and for columns that are generally not part of a frame or slab integration, but all are required to have that non-cost-effective installation.

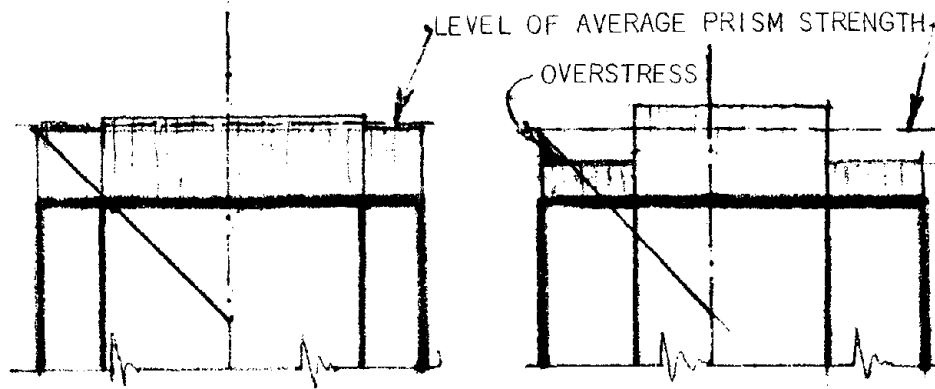
8. The Code requires an arbitrary area of steel, a percentage not less than .0007 x the gross area. This is regardless of whether the masonry is solid, or hollow with 1/2 the masonry net area. Also regardless of whether it is of concrete masonry which shrinks or is of clay brick which expands in time. Also regardless of weight, heavy weight or light weight. This is not a design factor, it is merely to improve post seismic failure performance.

9. The Code requires spacing not more than 4' in Reinforced nor 8' in Partially Reinforced. This arbitrary limit is simply a number. It disregards the type of masonry or the thickness of the wall, i.e., 4' for a 16" or 12" thick wall or for a 4" thick wall. Again this is an arbitrary seismic performance requirement - not a rational design factor. It is because of a "feel" for need for "basketing".

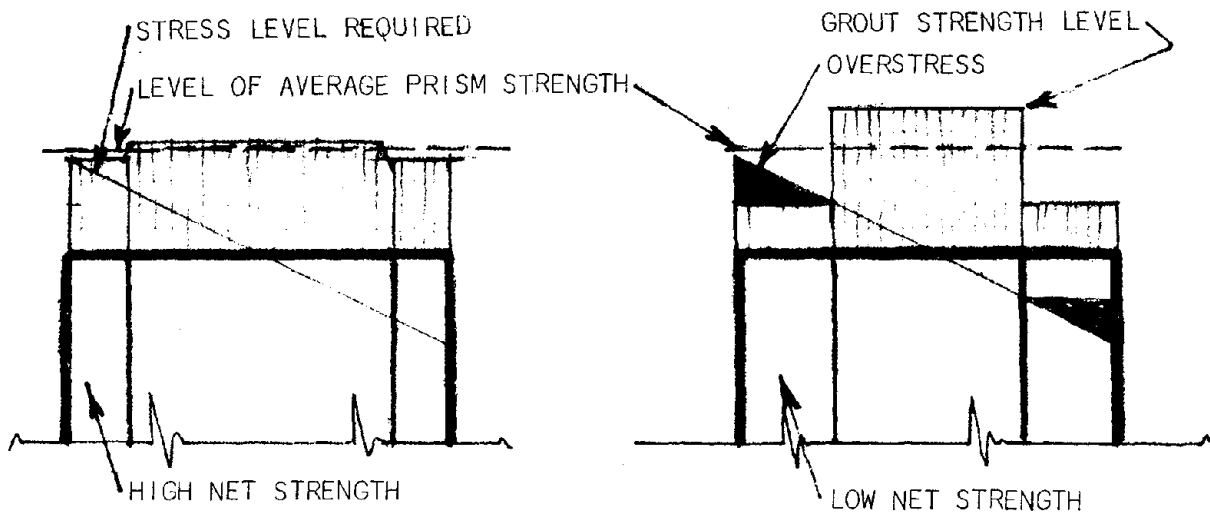
10. The Code limits the height of grout lift in a pour to 4' in hollow construction irrationally without regard for absorption of units, width of grout space or consistency of grout. There have been many pours greater and one Code approved height was 6' but the UBC requires maximum of 4.00 feet, though 8' is consistently used satisfactorily in residential construction.

11. Bearing walls "shall not be less than 6", yet thousands of bearing walls have been built 4", and investigation indicated that 5" would be the most economically effective thickness for masonry use in buildings as built today, but this system, of course, could not be used. That 6" limit was thought by some to provide constraints on pouring or reinforcement placement, but these controls are in other parts of the Code.

12. The Standards require strength to be determined on gross area of hollow units. But what we need for design, is control of the strength in the outer fibers. Gross strength test readings can be provided either by units of a weak material containing small coring (hard to grout) or by units of a strong material, and larger cores (with better grouting).



REINFORCED



UN-REINFORCED

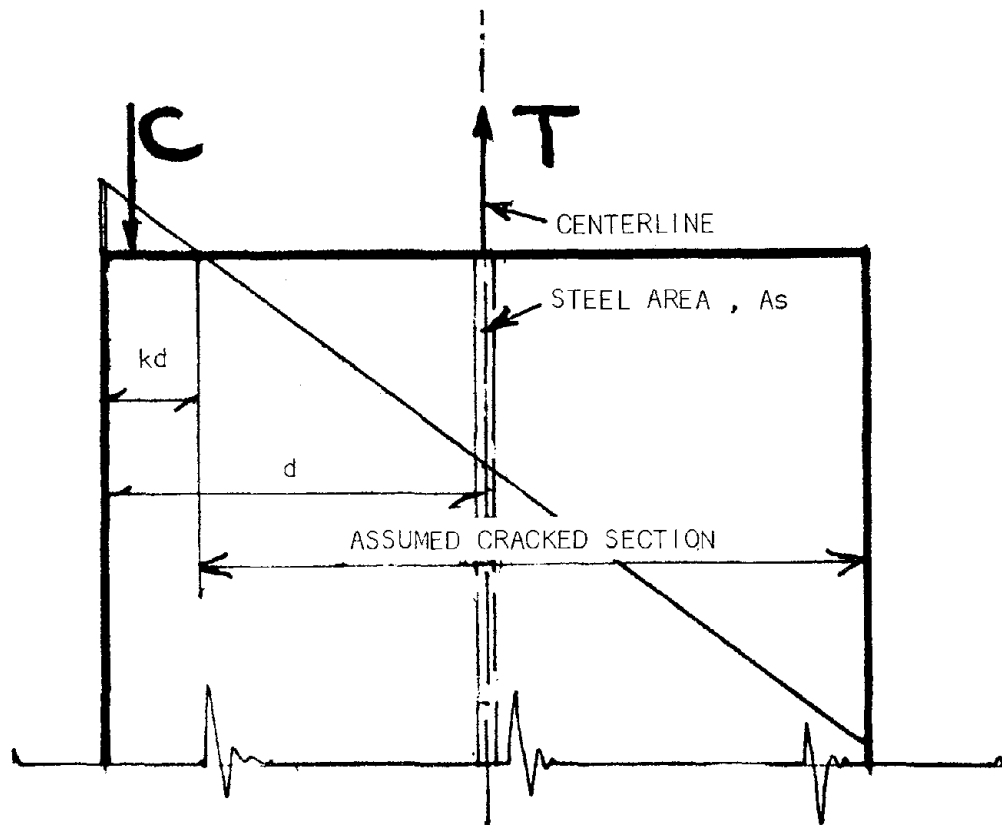
NET vs GROSS AREA STRENGTH. This shows the effect of high strength and low strength material providing the same hollow unit gross area strength. The dashed line shows the average prism strength that could be provided by grout with the two different strengths of unit (same gross area strength.) The sloping line shows the stress level required by bending. In the cases of high strength unit material the level is satisfactory, but not for the low strength unit - although gross area strength of unit and prism strength tests would indicate satisfactory wall assemblage,

The incorrect indication would be for reinforced as well as unreinforced.

13. The growing importance of shear resistance for lateral resistance of structures is hampered by the Code not permitting use of increased shear value or capacity caused by added axial compressive force.

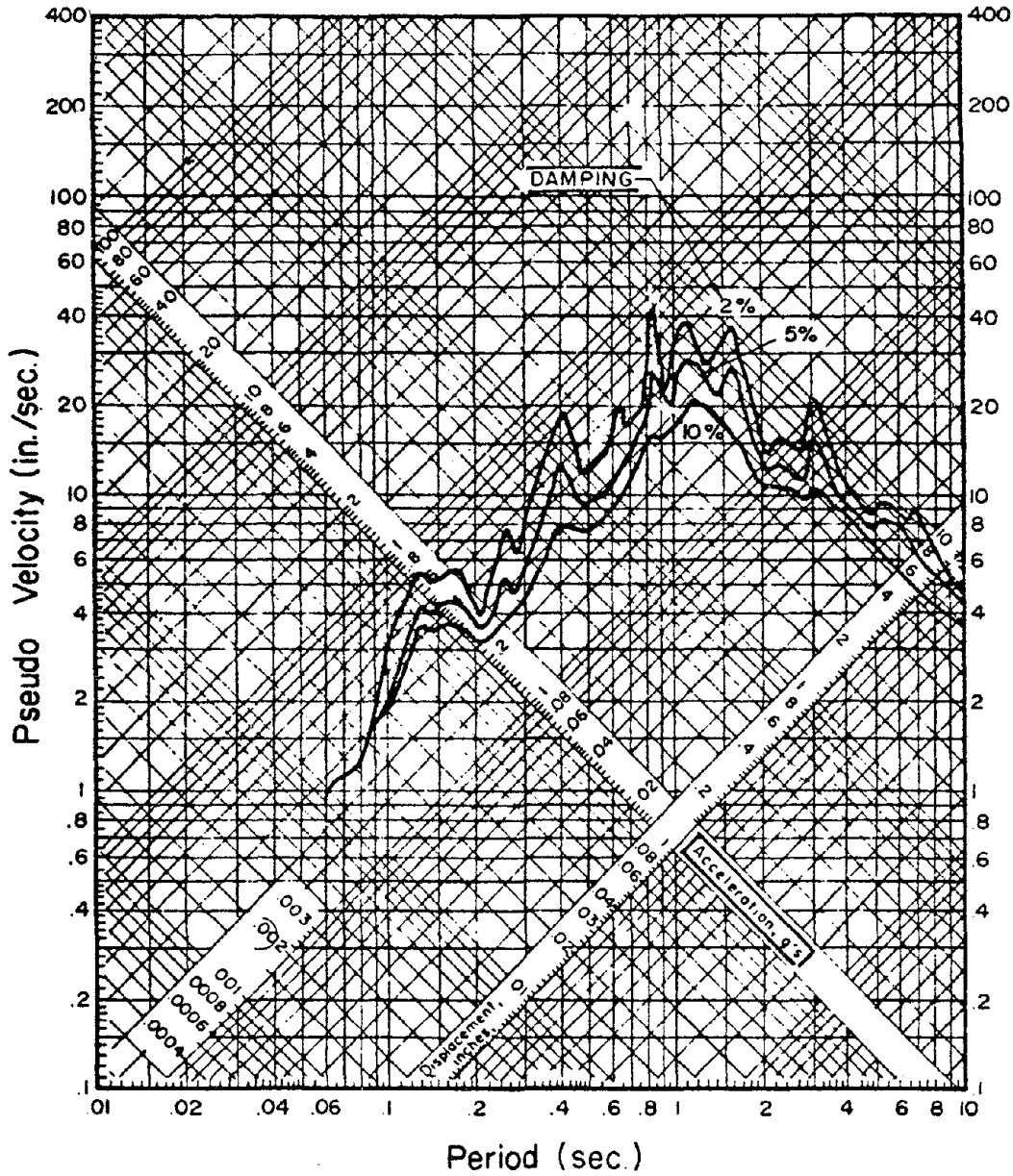
14. Calculations following Code provision indicate the strengthened reinforced masonry shows less computed capacity than the unreinforced!

15. It is obvious that reinforced masonry does not act as we design it. The assumption in a normal wall design is that it cracks on the tension side - most of the way through the wall, for the tension steel to work - but we know the wall does not function in that manner!



16. The Code does not provide for grouping of those increasingly important items that provide for increased performance and proper utilization of the high damping characteristics, ductility and energy absorption, so necessary in our increasing sophistication of seismic resistance, as in spectral response. If it did we might find that instead of a worst material for survival in an earthquake, unit masonry might be the best!

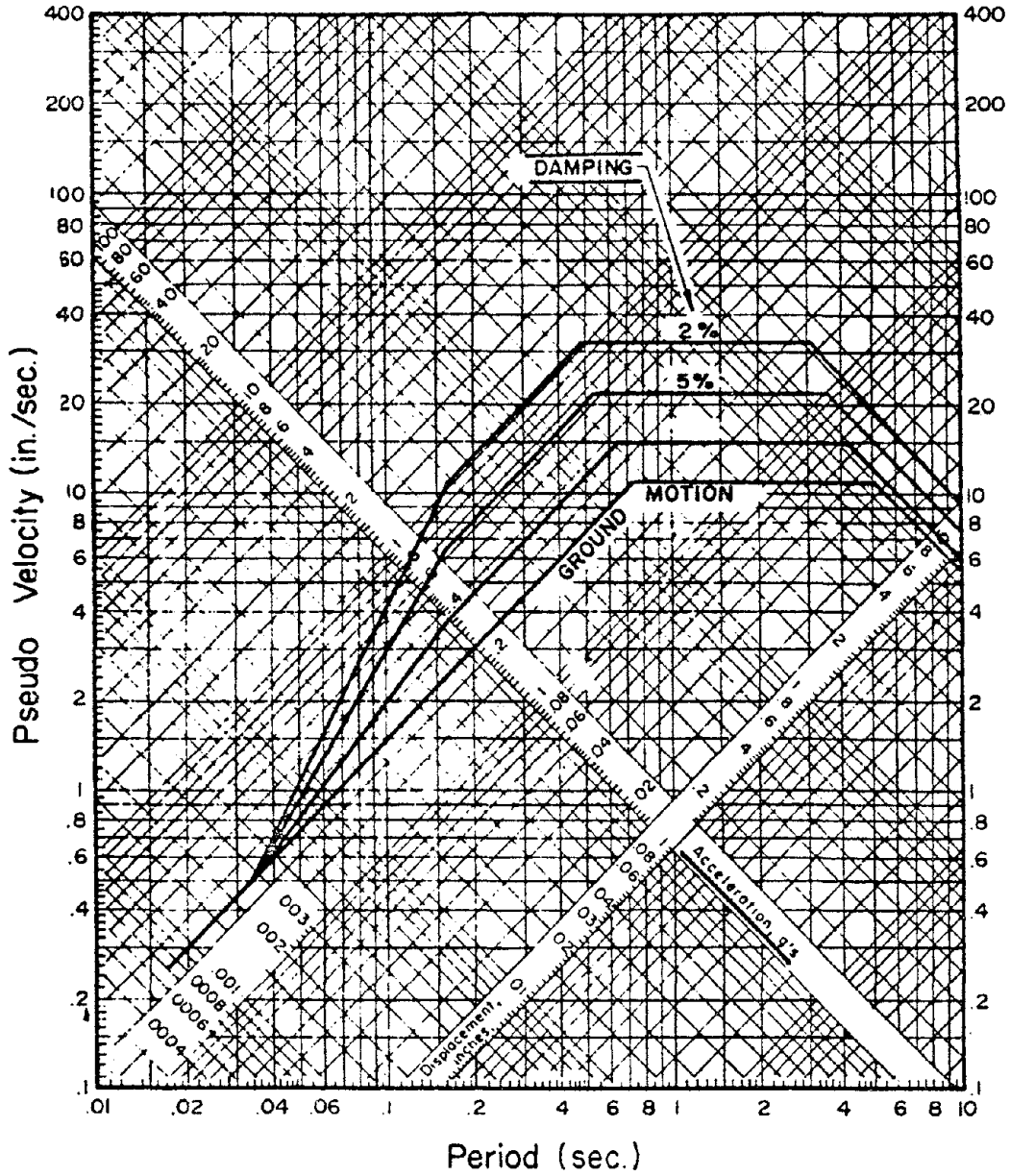
The following charts from the ATC-2 and other design stipulations show importance of relation of damping, period, and acceleration response.



RESPONSE SPECTRA

DAMAGE THRESHOLD LEVEL
(Unsmoothed)

Appendix A, ATC-2.



RESPONSE SPECTRA

DAMAGE THRESHOLD LEVEL
(Newmark-Hall Procedure)

17. The present Code does not provide well for retrofit, which is generally a specific problem requiring specific design and unusual conditions. Problems of retrofit have emphasized the need for basic performance.

SUMMARY

The Masonry codes have developed by empirical methods, with less theoretical research than other construction methods. Unfortunately many were developed by committees, rather than by a Thomas Jefferson. But are on the brink of an era of tremendous development.

This Conference, with its 90 papers on new research and development is one symptom.

The "stirring of the pot" by ATC-3 is another symptom.

The formation of The Masonry Society is a symptom. One of the first projects of this organization, and probably the greatest recognized common need is for the development of improved design, and consequent code improvement.

This must be done however with full recognition that all the parameters should not be combined in a way that will be cumbersome and awkward, to encourage error. The avoiding of error is more important than development of precision. Great precision is not warranted in the application of masonry design.

While the reinforced masonry methods were developing in the West, prodded by the specter of quakes and resultant catastrophic failures, the traditional conventional or rule of thumb design was being refined. It had resulted in so many more, and satisfactory structures. Both methods were being massaged to improve their usage, making them more adaptable to our changing needs and economy.

There were certain eddies in that current of progress, it was not smooth, especially as the western and eastern influences merged, there were conflicts such as;

Long time service records vs "new and better ways"

Cost vs safety, especially under new loadings

Reinforced vs unreinforced

State of the art of engineering vs state of the art of information and the dearth of knowledge of masonry material integration.

The confusion was worse than it might have been because there was no well defined unifying influence. The masonry industry is fragmented!

But - there has been growing changes - at an exponential rate, a small explosion here and there, then many, all contributing to some big explosions.

This might be demonstrated by a package of fire crackers in a Chinese New Year celebration, let's hope we have a New Year, a New Era.

A STRUCTURAL ENGINEER'S RATIONALIZATION OF THE MASONRY BUILDING CODE

By Don T. Pyle and Donald C. Weber

ABSTRACT: The major building codes such as UBC present a number of apparent inconsistencies in the determination of allowable stresses and material properties and in design procedures. This, coupled with the current state of the art in masonry design, testing and construction, present serious obstacles to the structural engineer.

This paper discusses some of the problems and inconsistencies that must be resolved by the structural engineer designing with reinforced masonry. Some of the design guidelines and philosophy of a major structural engineering firm are presented.

A STRUCTURAL ENGINEER'S RATIONALIZATION
OF THE MASONRY BUILDING CODE

By Don T. Pyle¹ and Donald C. Weber²

INTRODUCTION

Twenty years may seem a long time in our lives; yet it is an instant in the long history of man's involvement with masonry. Interestingly, though, when we started the practice of consulting structural engineering approximately 20 years ago, masonry was not really considered a structural material by our colleagues. In most cases it was something the architect used to cover the structure we designed. In the occasional situations where the masonry walls were used structurally to support loads, an imperical or rule of thumb procedure was mostly used as the "design" approach.

Much has happened in these last 20 years and we have now come to the point where many creative and interesting engineered uses of masonry are occurring in building construction on a more or less routine basis...uses which utilize the structural advantages of masonry materials.

This does not mean the problems involved in design and construction using masonry are all solved. With the hold over of rule of thumb design procedures, the evolutionary nature of changes in building codes, the special interest groups, and lack of uniformity and direction in the masonry industry, the consulting structural engineer faces many difficult and time consuming decisions and procedures. Nevertheless, in order to better serve our clients, it is our opinion the many advantages of masonry construction warrant the extra time, difficulty, and risk involved.

Our firm specializes in structural engineering and has been one of the leading designers of masonry structures in the Denver and Colorado areas. In order to avoid potential problems and to standardize our design procedures, we have, over the years, established some office guidelines. These have attempted to reflect our actual design experience on past projects, to better define and simplify the many choices that are allowed and must be made, and to reconcile some of the inconsistencies that are currently in most building codes.

It is the purpose of this paper to discuss some of these office guidelines and the design philosophy involved, and to point out some of the unresolved difficulties inherent in current engineering design of masonry structures.

¹Don T. Pyle, Principal, KKBNA, Inc. Consulting Engineers

²Donald C. Weber, Principal, KKBNA, Inc. Consulting Engineers

THE PROBLEM OF DETERMINING MASONRY STRENGTH

The designer wishing to use engineered masonry construction is at the outset faced with a problem of selecting a consistent set of material properties for use in his design. The current (1976) edition of the Uniform Building Code selects as the significant parameter for this purpose f'_m , the ultimate 28-day compressive strength of masonry prisms, and establishes two alternate procedures for determining this value.

In the first procedure the ultimate strength of the masonry is determined from tests of prisms made from the materials to be used, and made under the same conditions that will be encountered in the actual construction. In lieu of this procedure, an alternate method is allowed which assumes a prism strength as a function of the type of the masonry unit to be used.

As would be expected, the procedure of assuming f'_m values based only on the type of masonry unit used approximates a lower bound of prism strengths obtained in actual practice and while safe, may severely penalize a project where structural performance is a governing criteria. It is at this point the problems begin to arise.

If the designer wants to utilize the full potential strength available to him, he must have tests conducted on the proposed materials, prior to accomplishing the structural design. However this is frequently impractical. It is sometimes difficult to get authorization for the tests, delays may result, or the owner or architect may not select the masonry unit until late in the design phase.

If the prior testing is not possible or justified, the designer must assume a value of f'_m based on his prior experience with the material. In any case, he must specify that prisms be made in advance of and during the course of construction to verify that the strength assumed in the design is achieved in the actual construction.

While it is recognized the assumed prism strengths given in UBC are conservative, establishment of an appropriate value (without specific testing) is largely a matter of experience and luck. There is a surprising lack of reliable information available to the designer regarding prism strengths that can be expected from a given combination of materials installed with reasonable care by competent workmen. To further compound the problem, there have been only a relatively few applications of masonry construction in our area of practice where prism tests were required, hence we find that the techniques for making and testing masonry prisms are not well developed. In some cases where prism tests have been required, the results have exhibited a wide range of scatter, making confident interpretation of the results impossible.

To circumvent these problems our office has taken the approach of attempting to evaluate the cost impact of the use of the lower range of prism strengths. In some instances, non-structural considerations such as thermal conductivity, fire resistance, and sound control dictate the thickness of the masonry and actual stresses are acceptable even if low prism strengths are assumed.

In masonry construction with high stresses and other cases where h/t ratios approach the code maximums, stress levels are often the governing design criteria and prism strength has a major impact on the cost of construction. In such cases we normally specify prism strengths 20 to 30 percent greater than the code minimums and require testing to verify the assumed values.

THE PHILOSOPHICAL PROBLEM OF WORKING STRESS (ELASTIC) DESIGN

The design procedures for reinforced masonry have been adapted from the procedures used for reinforced concrete design at the time when reinforced masonry came into use. In recent years, research has shown that elastic or working stress design procedures do not adequately represent the structural behavior of reinforced concrete and the method has been abandoned in favor of the more realistic ultimate strength design approach.

From a philosophical standpoint we have no reason to expect that reinforced masonry acts any more like an elastic material than does reinforced concrete. Yet with the absence of research necessary to apply ultimate strength design procedures to reinforced masonry, we are forced into using a method which, while yielding safe designs, gives us no way of knowing what factor of safety we are designing into our structures. If reinforced masonry is to be competitive as a structural material, these design procedures must be re-evaluated in the light of current technology.

THE PROBLEM OF DETERMINING ALLOWABLE STRESSES

For masonry construction where "special inspection" is provided, the Uniform Building Code allows increases in the allowable masonry stresses of 100 percent over work where only normal inspection is provided. To qualify under this provision, the work must have continuous inspection at all times during the installation of the masonry by an inspector who is approved by, and who reports to, the building official.

In our area of practice, we have encountered a great reluctance on the part of owners to bear the cost of this additional inspection, even when we can show that it would result in a net savings in the cost of the project. Consequently we find the masonry construction we are involved with almost never qualifies for the "special inspection" stresses in a strict sense.

The obvious intent of the "special inspection" provision is to recognize the importance of field quality control in achieving the required strength in the finished product. While there is no question that field quality control is an essential ingredient of good masonry construction, the following questions arise: 1) Are the code provisions with respect to "special inspection" realistic (e.g. does full time inspection of the work really bring about an improvement in workmanship resulting in a 100 percent increase in masonry strength)? 2) Do the

code provisions adequately account for problems related to poor workmanship which occur when full time inspection is not provided? 3) Are there instances where we as designers are justified in using higher stresses even though special inspection, in the strict sense, is not provided?

First, it must be noted some systems of masonry construction are more vulnerable to workmanship related problems than others. For example, low lift grouted construction where the work is covered up immediately as it progresses and where there are a great number of splices in the vertical reinforcement, is inherently more susceptible to quality control problems than high lift construction where the cells to be grouted are accessible for inspection until the grout is placed.

In view of the above, there appears to be logical justification for using higher allowable stresses with some masonry systems even when only normal inspection will be provided. But since current codes make no differentiation between the quality control problems associated with various systems, the designer would be accepting a greater professional liability exposure if he chose to do so. If problems with masonry elements were to occur, it would be very difficult to defend a design that was not in compliance with the code even if it could be shown that the problems were not directly related to the stress level.

From the standpoint of logic, it seems reasonable to assume masonry laid in stacked bond is weaker than when adjacent units are interlocked as in running bond. UBC recognizes this weakness by reducing the length of wall considered effective under a concentrated load or the width of tee beam flange effective in bending when stacked bond is employed, but if we are designing a reinforced masonry beam, we are told to use the same allowable vertical shear stress in the masonry regardless of whether we are using stacked or running bond. There is an obvious inconsistency here.

The use of reduced allowable stresses in the masonry as a method of assuring adequate strength when full time inspection is not provided is not necessarily an effective way of achieving the desired result and may even be counterproductive in some instances. The factor of safety of a reinforced masonry component is not predictable on the basis of masonry stress alone. If the designer is faced with physical limitations on thickness, the net affect of reducing the allowable masonry stress is to increase the amount of reinforcing required which may compound the quality control problem by making construction more difficult and result in a weaker and less ductile finished product. The old axiom that "more is better" is not necessarily true when applied to the amount of reinforcing in a masonry wall.

Tension stress perpendicular to mortar joints is another confusing subject. In actual practice the developable tensile stress is highly variable and is subject to many factors. The UBC currently has an allowance of 4 to 72 psi. Yet why can you not lift a prism test sample by the top unit without the real possibility of breaking the sample (this represents an average tensile stress of approximately 1 psi)?

Also, based on usual code required wind pressures, calculations show most existing, unreinforced masonry walls are overstressed. Yet few walls actually fail in service due to wind pressure. Obviously, there are many other factors and redundancies that increase the strength of walls in actual buildings. However, we feel a general allowance of 4 to 72 psi in tension for all situations is not wise and should be applied only with considerable engineering judgment.

PROBLEMS RELATED TO ACCEPTANCE CRITERIA

Another common problem is the difficulty of monitoring quality control during the construction process. We refer here primarily to problems of measuring the acceptability of the finished product.

The concrete test cylinder is a well accepted, routine procedure for the evaluation of completed concrete structures. This is not to say such tests are a fully reliable and suitable testing procedure... they are not. However, structural masonry has a long way to go even to reach this rather imprecise level. For example:

1. There is no standard ASTM field test for mortar. Several tests are used for this but none seem to solve the problem; they are either unsuitable, or have poor repeatability with inexperienced testing personnel. Thus it is our opinion such tests are not a suitable and reliable field test for mortar acceptability.
2. The prism test is probably the best test available for acceptance of a completed masonry assemblage. We have used it with reasonable success on a number of projects. However, it is not an ideal test; it is limited by the capacity of available testing machines; it measures only one property, compressive strength; it is susceptible to considerable variations due to workmanship, handling and testing procedures; and, it can never represent a random, statistical sample of the finished product since it is built specifically for each test.
3. The lack of standardized, well developed and routine procedures in testing, and especially the lack of experience with masonry evident in many of the commercial testing labs, is a serious deterrent to good quality control. We have spent many hours trying to justify acceptance of walls that have produced below specification tests, or attempting to placate a justifiably upset client when the masonry tests are erratic or meaningless.

PROBLEMS RELATED TO WORKMANSHIP

The long history of unreinforced and "rule of thumb" masonry has produced too many tradesmen and masonry contractors who do not have a real understanding of reinforced, "engineered" masonry as a truly structural material. The main concern in the trade has been how many

square feet of wall can be laid and the appearance of the exposed surface of the work.

Yet the structural engineer is frequently concerned most of all with the interior construction of the wall. The mason without adequate supervision, will frequently neglect items of major importance to the structural engineer. For example, things we find regularly are insufficient lap of joint and bar reinforcing, improper construction of corners, columns and bearing seats, inadequate tie between wythes, unfilled joints, substitution of concrete block for brick when it doesn't show, and omitted bond beams and reinforcing steel. But once the wall is closed up, no one can tell what's inside. This has been a major deterrent for the structural engineer to take full advantage of the unique structural properties of masonry.

SUMMARY

The design of masonry can be a difficult, time consuming and challenging task for the structural engineer who attempts to take full advantage of the unique capabilities of structural masonry. Yet the rewards can be as satisfying as the challenge is difficult. It is our hope the Masonry Society will be able to bring unity to the industry and provide the mechanism required to solve the many problems facing the masonry designer.



A SIMPLE TECHNIQUE FOR DETERMINING STRENGTH OF BRICK

By Parviz F. Rad

ABSTRACT: Compressive strength and flexural strength are the major strength characteristics determined for bricks. However, due to differences in geometry, a single brick usually yields a strength value quite different from that of prisms or walls of brick. This paper advocates the use of a small impact device to determine the strength and chipping characteristics of bricks. This technique has been successfully used in rock mechanics and has promising potentials of successful use in brick identification. The single most important advantage of this technique is its simplicity of specimen preparation and data collection. The test device consists of a steel tube 3 inches by 26 inches. A handful of brick pieces of varying sizes are placed on the bottom of the tube and impacted with a standard weight. Strength and durability of bricks can be inferred from the results of comparisons between the original size distribution and distribution after impacts. The correction factors needed for normalizing the data from various size distributions can be obtained for each brick by conducting a series of pilot experiments on representative size distributions. The advantages of this system are low capital cost, ease of operations, and ease of specimen preparation even from broken, old, and small pieces of bricks.

A SIMPLE TECHNIQUE FOR DETERMINING STRENGTH OF BRICK

By Parviz F. Rad¹

INTRODUCTION

Compressive Strength and Flexural strength are the major strength characteristics determined for bricks. However, due to the differences in geometry between a single brick and a structural wall, a single brick normally yields a higher strength value. A further complicating factor is the fact that a structural wall is a composite structure made of bricks and mortar. The properties of the wall are then dependent on properties of individual components as well as the quality of the bond between them. Various modifications have been recommended for the flexural test and compression test of bricks and brick prisms in order to account for the size effect and composite effect. However, the relation between strength of brick and that of a wall has not been fully explained yet.

This paper advocates the use of a small impact device to determine the strength and chipping characteristics of bricks. This technique has been used successfully in rock mechanics and has promising potentials of successful use in brick identification.

PROCEDURES, TECHNIQUES

The single most important advantage of this technique is its simplicity of specimen preparation and data collection. Figure 1 shows a schematic of the impact device. It consists of a steel tube with an inside diameter of 3.02 inches and a height of 24.75 inches. A 5.28 lb. steel weight is dropped through this cylinder from a height of 22 inches onto brick samples. A comparison between the original size distribution and that after several impacts will yield the Impact Strength Index and provides means of estimating strength and chipping properties.

¹Associate Professor of Civil Engineering, Clemson University, Clemson, South Carolina

The original technique used for rocks involves using ten irregular shaped rocks averaging 7.5 cu cm each. The specimens are sorted by screening to select the minus 1-inch, plus 3/4-inch material. Since the specimens will be irregularly shaped, the desired volume could be obtained more accurately by weighing the material and dividing the weight by the value of density. The total weight (in grams) of the ten specimens is 75 cu cm multiplied by the specific gravity of the material. The specimens are then divided into groups of five sets of two specimens to each set.

Each set of two specimens is placed in the bottom of the cylinder and impacted with the standard weight.

The number of drops for each set of two specimens vary from 3 to 40. The same number of drops are used for each set of two specimens until the five sets are broken. The broken material for each sample is combined on a 0.5-mm screen (35 mesh) and hand shaken for 40 seconds. The minus 0.5 mm material is then weighed in grams and divided by the specific gravity to determine the solid volume of the material.

An impact strength index is then determined by dividing the number of drops used for each group of specimens by the volume of the minus 0.5 mm material from the five sets of specimens:

$$ISI = \frac{nP}{W} = \frac{n}{V} \quad (1)$$

where ISI = the Impact Strength Index
 n = the number of drops used on each group of two specimens,
 ρ = the specific gravity
 w = the weight of the minus 0.5 mm material from five groups of specimens,
 and V = the solid volume of the minus 0.5 mm material from five groups of specimens.

After the Impact Strength Index is determined for one assay, larger or smaller number of drops are tried to determine the minimum value of Impact Strength Index. This minimum will be used in all calculations and comparisons because it represents the most efficient use of energy required to produce the minus 0.5 mm material.

As an attempt to further simplify this technique, a series of impact tests were conducted in Clemson University in which the original size distribution of the brick was at the discretion of the experimenters. This size distribution was arbitrarily chosen but carefully measured and maintained throughout the tests.

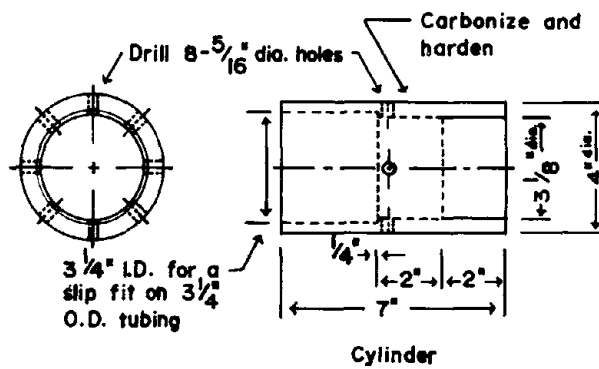
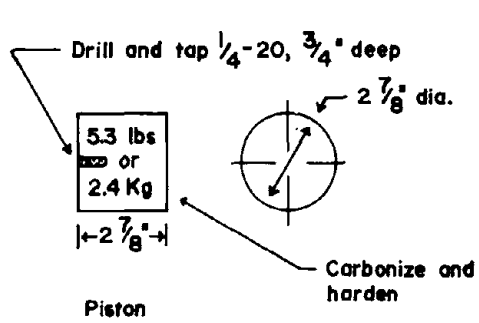
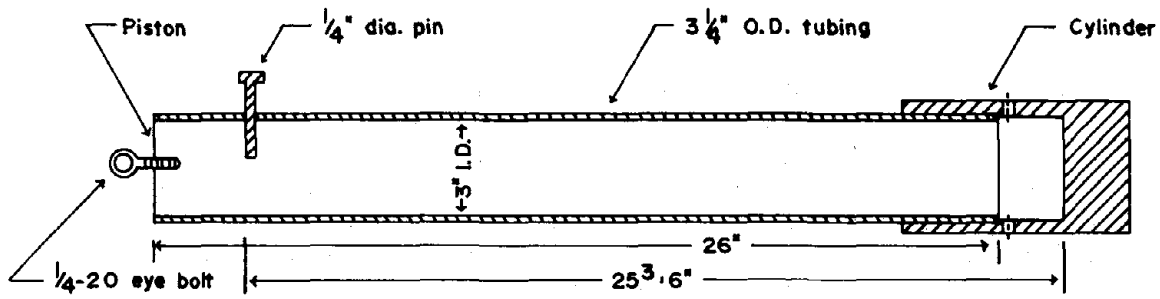
RESULTS AND DISCUSSION

Figure 2 shows the variation of Impact Strength index for Richtex Brick for various impacts. The ISI shows a marked decrease for the first 8 drops and gradually increases for further impacts. The minimum ISI is estimated to be .75. Figure 3 shows the variation of ISI for Southern brick. Although a significant amount of scatter is evident, the minimum ISI can be conveniently estimated to be .72. Ease of estimating the minimum is another advantage of this technique. Although care should be taken to get a well behaved set of data, lack of uniformity will not affect the value of ISI significantly.

The value of impact strength can be obtained for any sieve if a complete size distribution of the specimens is available. However, virtually all sieves result in the same trend as that of the ISI obtained by the standard technique from the specified sieve. This observation led to a further refinement and simplification of the impact technique. In a second series of experiments bricks were broken to approximately .2 inch and smaller and then a series of impact tests were conducted on these specimens. It is important to note that the specimens contained chips of various sizes before impact. Figures 4 and 5 show the size distribution of Southern Brick and Richtex brick before and after impacts. Values of ISI similar to those obtained for figures 2-3 can be obtained from any one of these sieves.

SUMMARY AND CONCLUSIONS

Strength and durability properties of bricks can be inferred from the results of the proposed simple impact test. The major advantages of this technique are freedom in choosing the original size distribution of specimens, low capital cost, and ease of operations. The correction factors needed for normalizing the data from various size distributions can be obtained for each brick by conducting a series of experiments on representative size distributions.



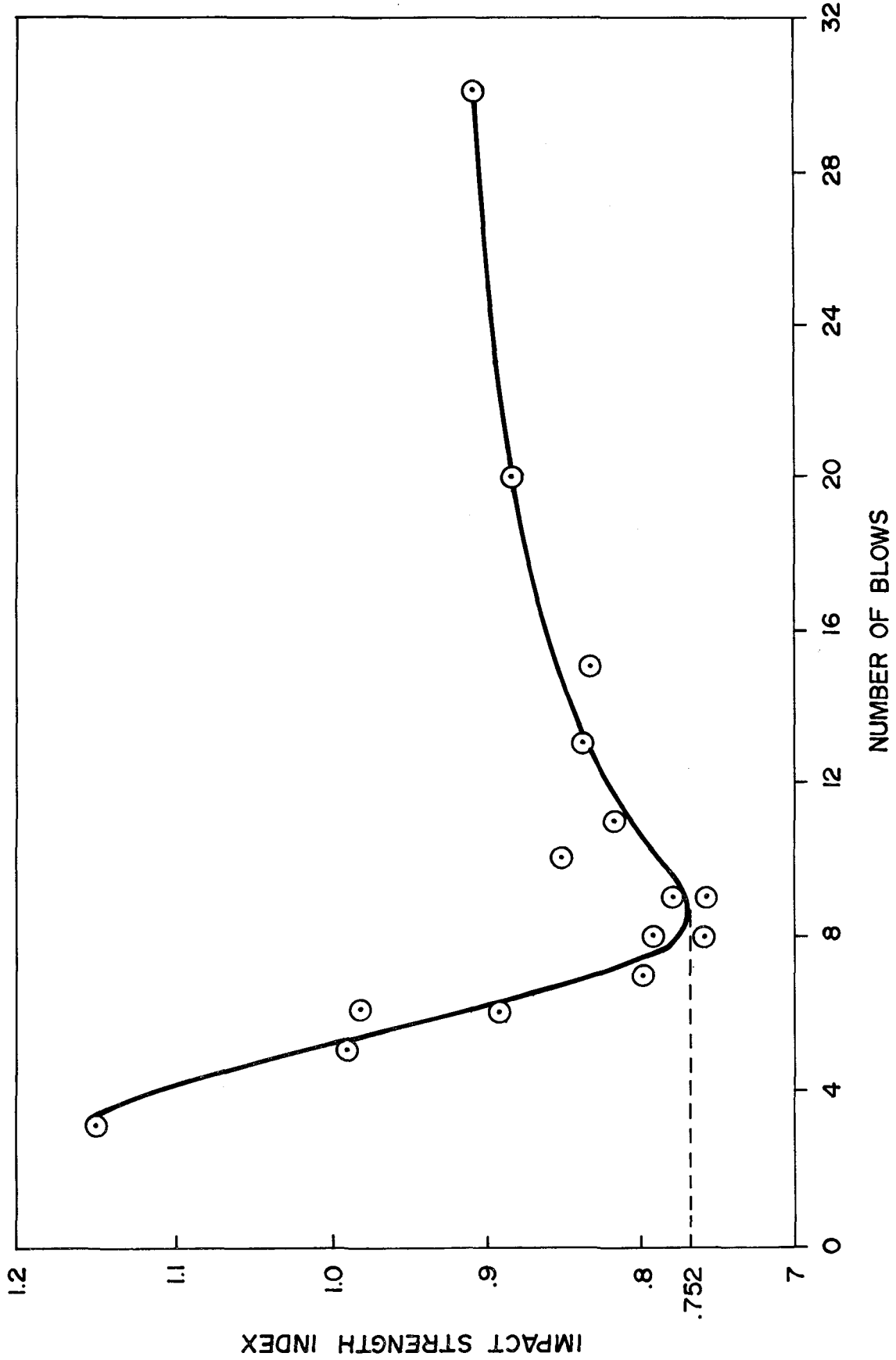


Figure 2 Impact Strength Index Of Richtex Brick For Various Blows

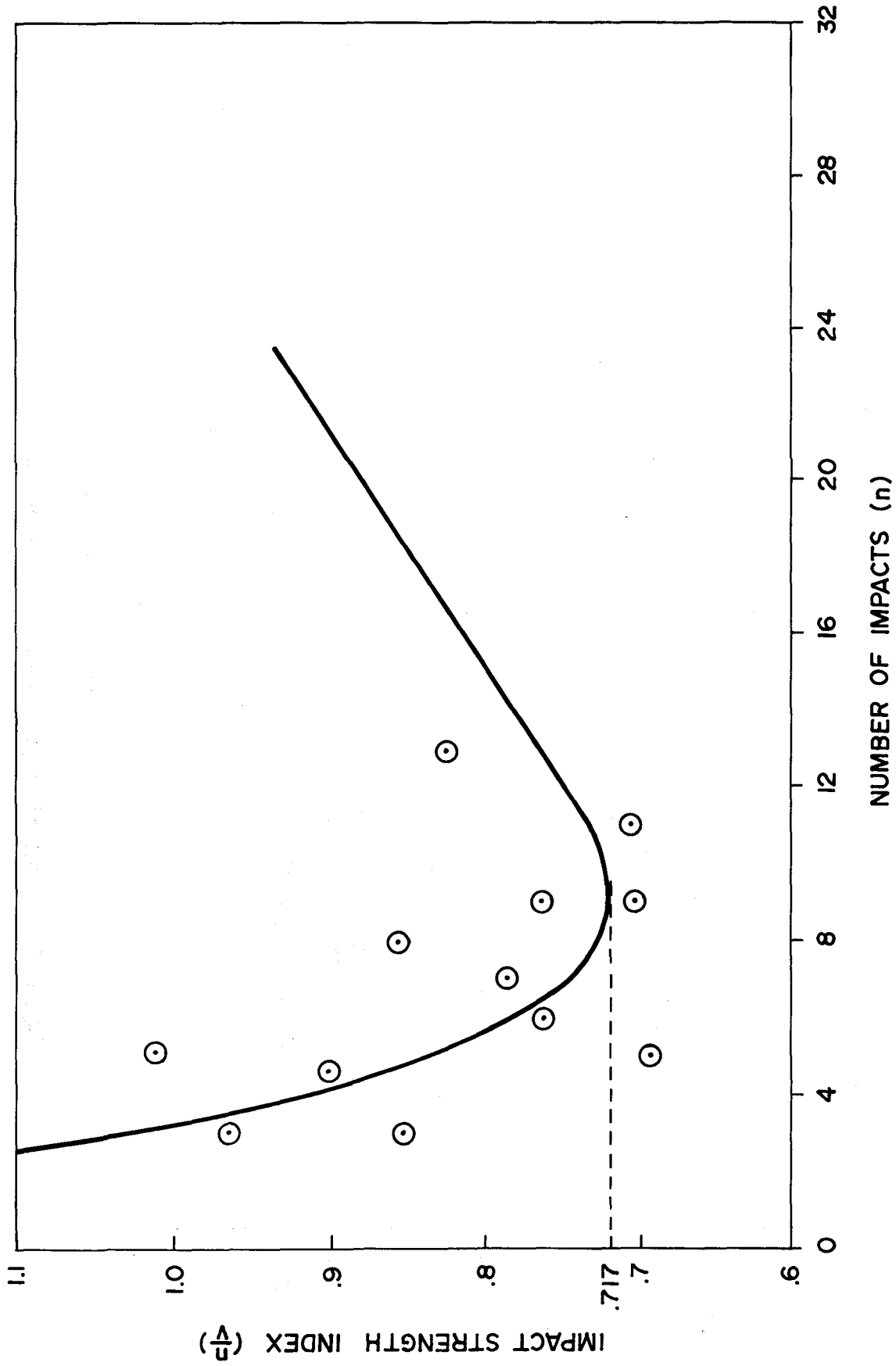


Figure 3 Impact Strength Index Of Brick Southern For Various Blows

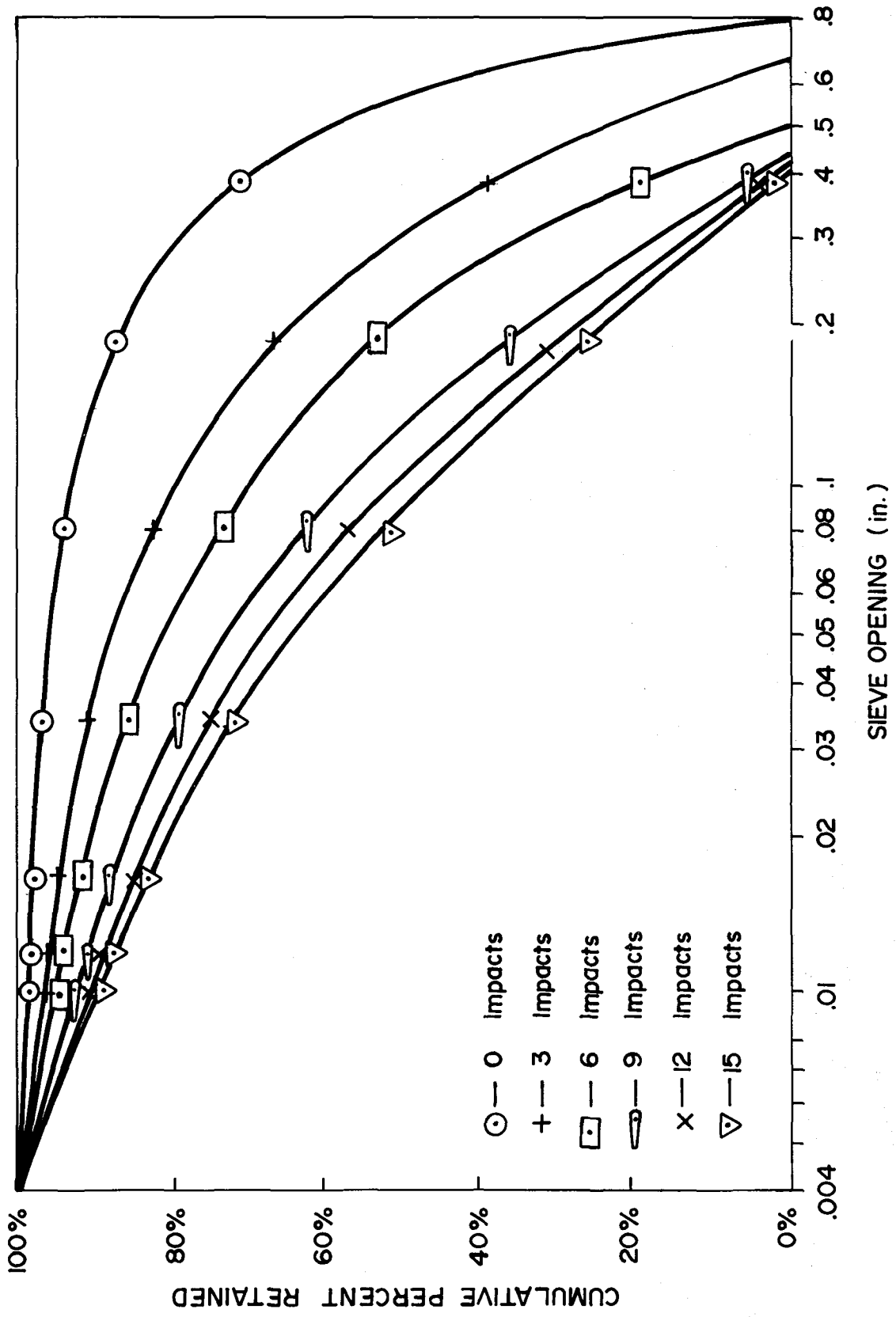


Figure 4 Sieve Analysis of Impacted Particles Richtex Brick

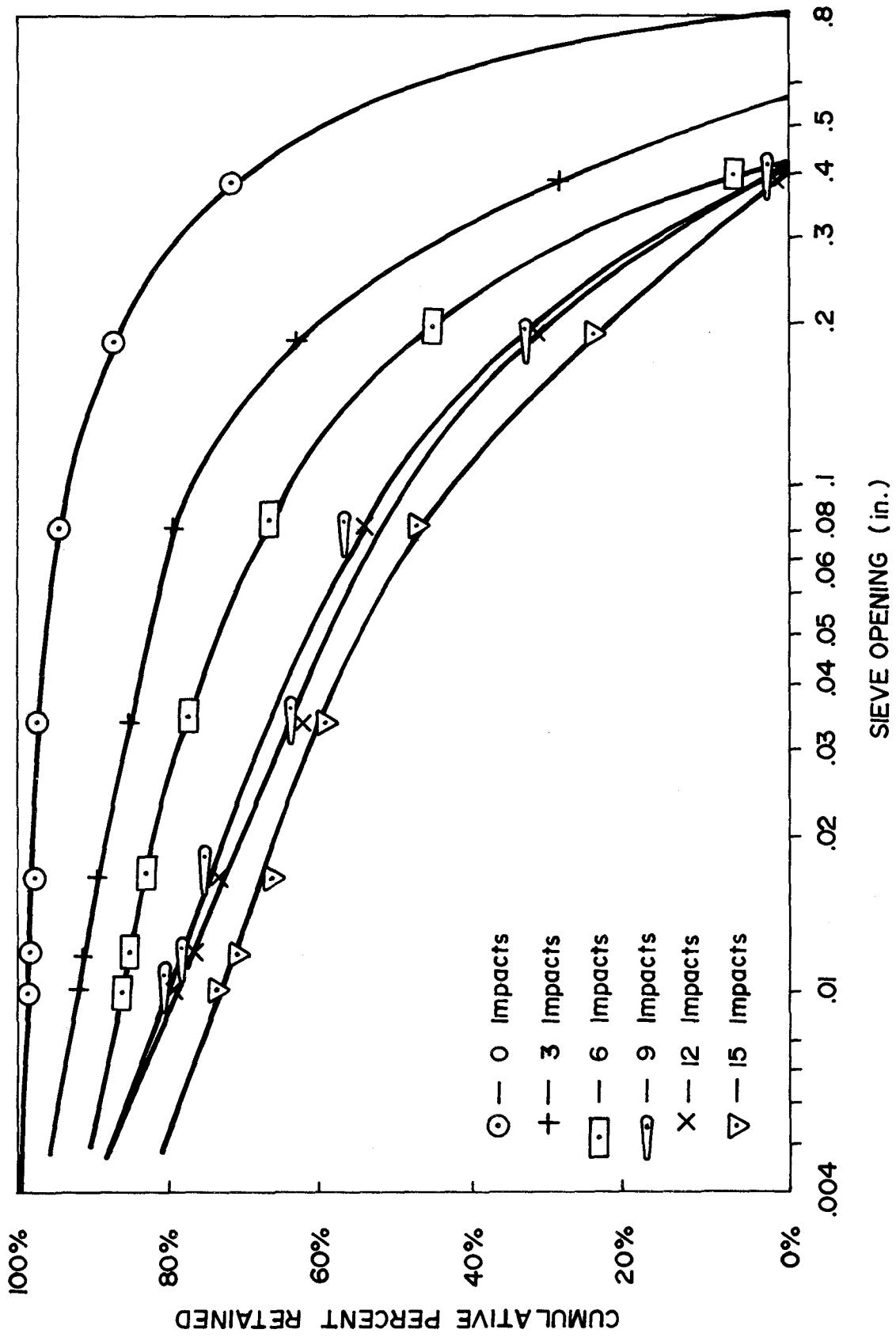


Figure 5 Sieve Analysis Of Impacted Particles Southern Brick

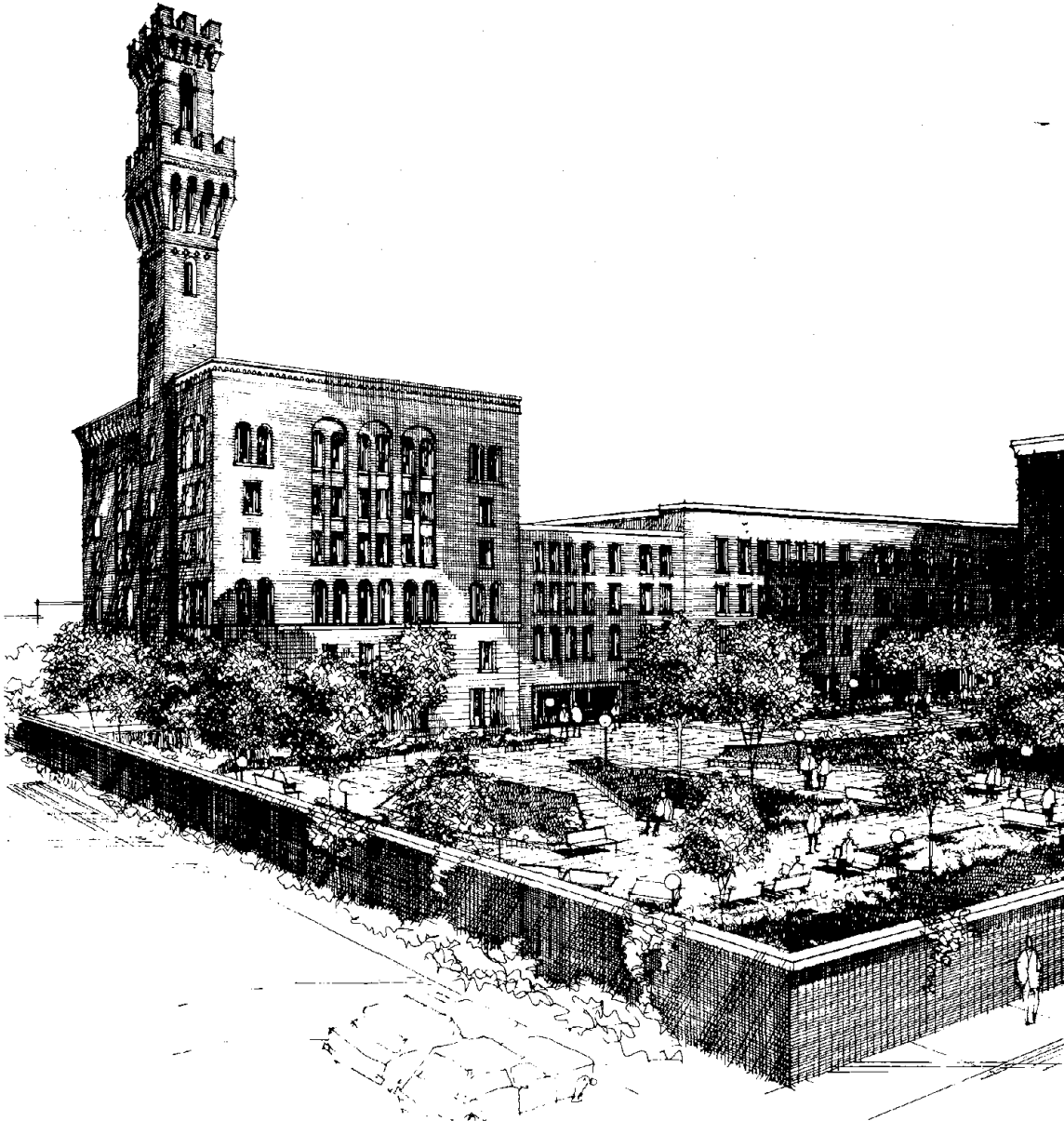
RESTORATION OF THE PINE STREET INN TOWER

By John M. Looney, P.E.
Chief Engineer
CBT/Childs Bertman Tseckares & Casendino Inc.
Boston, Massachusetts

ABSTRACT: Boston's old Fire Headquarters had been abandoned for many years and had deteriorated to the point that the city had condemned it. This historic landmark was selected to be the new home for the Pine Street Inn. This paper will describe how our office evaluated the existing condition of the hazardous 156 foot high fire tower and rebuilt it to a safe condition.

RESTORATION OF THE PINE STREET INN TOWER

By John M. Looney, P.E.¹



¹Chief Engineer, CBT/Childs Bertman Tseckares & Casendino Inc, Boston, Massachusetts

INTRODUCTION

Four years ago our office, CBT/Childs Bertman Tseckares & Casendino Inc. was hired by the Pine Street Inn to find a new home. The Inn is a private, non-profit organization that provides food, shelter and limited medical care to its indigent, predominately alcoholic 'guests.' The new facility would need to house approximately 300 men and 50 women. After a considerable search we chose the old City of Boston Fire Headquarters and its three adjacent buildings. It was thought that the 156 foot high tower of the old Fire Headquarters would serve as an effective beacon for the Inn's 'guests.' One year earlier the City of Boston had condemned the tower building because of severe deterioration. This paper will describe how our office developed repair methods to save this landmark.

HISTORICAL BACKGROUND

In 1892 the City of Boston built their new Fire Headquarters on Bristol Street in Boston's South End. City architect, Edmond Wheelwright, modeled the building after the town halls of Florence and Siena, Italy. The Fire Department used the tower for ladder practice, fire lookout and fire alarm purposes. The Department's 'old guard' admits that even today the tower building brings back memories of their 'fearless youth,' when leaping six stories into a net below was as easy as rolling out of bed.

The building and tower were built of yellow New Jersey fire brick, with Amherst stone trimmings and balconies. The tower is a 14 foot square shaft rising up 125 feet to a low roof. At this point a series of interlocking arches and corbels dramatically increase the size of the tower to 18 feet square. Above the low roof the walls step back and rise another 30 feet to the high roof. At the high roof another series of arches, corbels and piers form a crown to top off the tower. (See photo No. 1)²

The building was thoroughly fireproof as befits a fire station. The exterior walls were two feet thick. All partitions were brick and the steel beams covered with terracotta. The building was completely sprinkled inside and outside and heavy steel shutters could be closed over the

²Photographs of the tower appear in Appendix I.

windows in case of fire. All these precautions were taken to insure that a fire would not put the city's vital fire alarm system out of commission. The cost of the building exclusive of the fire alarm apparatus was \$81,000.

After the Fire Department moved out in 1951, the building served as a warehouse and factory and fell into disrepair. In the early 1970's the building was abandoned.

The Pine Street Inn received funding to renovate the buildings from the Massachusetts Department of Community Affairs through the Boston Housing Authority. One of the stipulations for the money was that the historic Fire Headquarters building was to be restored to its original appearance and structural integrity. Several local citizen groups had also applied pressure to prevent the Pine Street Inn from even moving into the area and the restoration of the tower was one item that had helped to mollify them. Originally we had wanted to save the tower but now we were committed to it whether it seemed possible, never mind economical, or not.

EXISTING CONDITION OF THE TOWER

Because of the ravages of vandals and New England weather, the tower had deteriorated to a point where large sections of the top parapet threatened to crumble and fall to the ground, cracks ran up the corners and the brick corbels below the low roof seemed to defy the laws of gravity in remaining in place. In short the tower appeared in such a poor state that we wondered whether it would not have been better to tear it down.

The parapet around the top of the tower is two feet thick and about three feet high. On top of the parapet sit eight, four foot piers. Vandals had removed all of the copper flashing around the inside of the parapet and the water had deteriorated the brickwork. As the bricks became loose vandals had picked them out and thrown them off the tower. In some sections of the parapet two wythes had been removed. The resulting porous surface acted like a sponge and allowed the water to completely penetrate the wall. The outside four inch veneer had bulged more than three inches in some locations. (See photo No. 2). One of the piers had been stripped to where it resembled an upside down pyramid and at the base of several others the mortar had desintegrated to the point where bricks could also be picked out by hand. (See photo No. 4).

Water had penetrated the piers that support the high roof and they had bulged and twisted. Several of the piers had split open and one had a one-inch gap running up its narrow face. At the low roof the copper flashing had also been removed allowing water to penetrate down into the large corbeled arches below. Some of the cap stones weighing several hundred pounds had been pushed off their piers. A few of them had fallen to the roof of the building below and had broken large holes in it.

Below the low roof are the distinctive and dramatic corbels and arches that appear to be hanging off the tower in danger of tipping over. The mortar at the top of these corbels had completely disintegrated and only the weight of the bricks above the arches appeared to be holding this part of the tower together. (See photo No. 6). The tower's southeast corner corbel was completely shattered and many large cracks ran vertically down the edge of the tower below that corbel. We surmised that lightning had struck the tower at this point because of a bare copper lightning rod attached to the tower near this area. (See photo No. 6). Large cracks ran practically the full height of the tower at each corner.

The cast iron stairs, that wind their way up inside the tower had deteriorated so badly that several treads broke off when weight was put on them. The stairs stop just below the low roof and ladders provide access to the remainder of the tower. Most of the supports for these ladders had rusted completely through and some of the rungs had corroded to less than half their original diameter.

DEVELOPING METHODS OF REPAIR

Because the Pine Street Inn would lease the buildings from the Boston Housing Authority and the Boston Housing Authority is a public agency, the contract documents had to conform to Massachusetts Public Bidding Laws. This meant that the bidding had to be open to any qualified contractor, the contract had to be awarded to the lowest responsible bidder and, most important for us, the extent of the work had to be clearly defined to preclude any increase in its scope after it had started.

Several masonry contractors were asked to examine the tower and suggest methods of repair. All balked at the complexity of the task and their replies were always the same; "Its a beautiful piece of work but I wouldn't touch it unless it were on a cost plus basis." In a cost plus contract

the contractor is reimbursed for all labor, materials and equipment he uses and he receives a percentage of the total cost for his profit. Since 'cost plus' was out of the question the problem became how to evaluate accurately such an intricate structure in such an advanced state of decay built 85 years ago by craftsmen whose work no one seemed able to understand or duplicate now. (See photo No. 1).

It was decided that the repair methods should be developed one step at a time. The first step was to accurately determine the tower's present condition. Every inch of the tower inside and out was examined. Binoculars were used to study those areas that were too far away to see clearly. A camera, with a telephoto lens, was used to photograph the exterior of the tower. The interior was also photographed. Problems were recorded on sketches of the tower. The second step involved using a combination of both the photos and the sketches to evaluate the existing condition of the tower. After careful study, the following items were determined; that the freezing and thawing of the water that had penetrated the bricks had caused the bulk of the damage, and areas where the flashing had been removed appeared to have suffered the most, that large sections of brick had lost their mortar and were in immediate danger of falling from the tower and finally that because of the thickness of the walls (over three feet at their base) the stresses in them were thankfully low. (See photo No. 4).

Tracings were made of various horizontal sections of the tower from actual field measurements for the next step. These tracings were superimposed over each other in order to determine the relationship between the walls, corbels and piers. This process revealed that the walls at the corbels at the low roof were over four feet thick which meant that the structure supporting them was perhaps sounder than it seemed from the outside.

Study of the field notes, photos and the scale drawings indicated one important fact. The large cracks in the exterior did not appear on the inside, indicating that the damage might extend only as far as the exterior veneer. The forces of nature were peeling off the exterior skin of the tower as one peels off the skin of an onion. If this was the cause of the damage, the repair of the tower would consist mainly of replacing the damaged bricks and sealing the walls to prevent water from entering them again.

CONTRACT DOCUMENTS

The repair of the tower could be bid as a separate entity or it could be part of a total masonry sub-bid. The advantage of the first was that contractors who specialize in this type of work could bid it. However, the possibility of finding three qualified contractors appeared slight. Also, the bidders would have to apply a factor to cover unforeseen problems. Because of these concerns the second method was chosen. The total estimated masonry sub-bid was over \$200,000 and the complex tower repair would only constitute one third of that. A masonry sub-bid of that size as well as the fact that two thirds of the work would be straightforward would increase the possibility of getting enough contractors to bid the work.

The scope of the repair work had to be clearly indicated in the contract documents and many approaches were studied. One method of applying pictures to the originals was considered. The problem with this method was that not every part of the tower could be clearly photographed. The method finally adopted was to draw a plan of each of the five levels of the tower and indicate the scope of work on each plan. In addition a comprehensive document for the mason to follow in repairing the brickwork was needed. As much information as possible was condensed onto a single sheet in the form of a series of tower repair notes (see Appendix II).

A drawing showing the entire height of the tower on every side, interior and exterior was made. All repair work was shown on these drawings by circling the areas to be repaired and keying the required repairs to a repair schedule (see Appendix III).

REPAIR OF THE TOWER

The contract documents were completed in April of 1976. Before bidding could start the various city and state agencies had to review them. When a bid date had not been set by September, the then owner of the building, the Boston Redevelopment Authority, was informed that the tower was structurally unstable and repair work had to be done before winter. If water penetrated the bricks and froze, large sections of brick could fall off the tower and injure passersby. With the Boston Redevelopment Authority's blessing, a brief specification and a couple of drawings were developed to remove the hazardous top of the tower.

Bids were solicited from several contractors that specialized in chimney building and repair and work proceeded immediately. The piers on top of the the parapet wall were so loose that a crane was able to lift them up in one piece and lower them to the ground. The stone copings and the yellow bricks were stacked up inside the building and used later to rebuild the top of the tower. At this point the Boston Redevelopment Authority began receiving protest calls as the men dismantled the parapet. Everyone was assured that the tower would be restored to its original appearance at a later date.

In the Spring of 1977 Coronis Construction Co. of Winchester, Massachusetts came in as the low bidder for the project. After the scaffolding had been set up around the tower, the contractor began replacing the broken bricks on the corners. The exterior veneer was removed and the back up brick examined for cracks. When no cracks were found the corners were rebuilt using salvaged bricks from the site. (See photo No. 8).

The top was then started. The first step in rebuilding it was to repair all the loose bricks in the small corbels and arches. The exterior wythes of the arches were not tied back to the rest of the tower and the bricks were being held in place by gravity alone. Several ways to tie these arches back were discussed with the masons working on the tower, and the way finally decided upon indicated their exceptional skill and ingenuity. The chief problem facing them was that if any bricks were removed the whole arch would cave in and cause the arches on either side to collapse as well. Thus the arches had to remain intact. Screw jacks were placed horizontally between the scaffolding and wood blocking placed across the face of the arches. A slight amount of horizontal pressure was then applied to the arches while a long thin bar was used to chip out all the loose, crumbly mortar behind the bricks. As the mortar was cleaned out the pressure from the jacks was increased. Eventually, the entire arch was pushed back to its original position and a header course was placed along the top to tie the veneer to the rest of the wall (see photo No. 9). Next the two foot thick parapet was built up from the roof level. Photographs of the original parapet helped the masons rebuild the top to its original shape.

A stone coping covered the original parapet and small pieces of stone ran across the front of the piers at the same level. These stones gave the appearance of a band around the tower. Two of the larger stones were broken and

several of the smaller ones were missing. (See photo No. 2). Instead of trying to match the missing stones, a cast-in-place coping was used and the outside edges were formed to match the original shape of the stones. This concrete coping not only provided a waterproof cap for the parapet but also provided additional reinforcing for the top of the tower (see photo No. 3). The masons rebuilt the piers to their original size and shape on top of this new concrete coping. (See photo No. 5).

Each corner of the tower was rebuilt by one mason, and it was interesting to note that each mason became very possessive of 'his' corner. They took great pride in their work and proved themselves to be true craftsmen in carrying on a centuries old tradition.

The most difficult part of the tower to repair were the large corbels just below the low roof. The southeast corner corbel had been shattered by lightning. (See photo No. 6). The extent of the damage was not known and the drawings called for the entire corbel to be removed and rebuilt. The magnitude of this task was tremendous. The whole corner of the tower would have to be shored and braced. The masons felt that the tower would collapse if this section of wall were removed and they suggested peeling the outside veneer off and examining the interior wythes first. The masons removed the outside veneer and examined the back up bricks carefully. Fortunately, only the outside veneer was damaged; the force of the lightning had been dissipated in the exterior bricks. Therefore only the veneer had to be replaced and no extensive repair was needed. (See photo No. 7). The bricks above the large corbels were so loose that they started to move when the corbels were being worked on. (See photo No. 6). The masons had to rebuild the corners above the corbels before the corbels themselves could be repaired. This particular job was akin to building a brick wall from the top down. Stainless steel tie rods were installed just above the corbels in order to relieve some of the strain these ten ton pieces of brick work put on the tower.

Before winter arrived all of the loose and broken brick work had been repaired and at this writing the repointing, cleaning and the replacement of the stairs were all that remained to be done to complete the restoration of the tower.

CONCLUSION

The restoration of yesterday's intricate brick work would seem to present an insurmountable challenge to the modern engineer. Many of the old skills are lost and the construction industry is no longer based on a labor intensive economy. Budget limitations, deadlines, dealing with neighborhood groups, the various authorities and labor problems are enough to undermine the simplest of building programs. This paper has shown how one office dealt with these sorts of problems and managed to save a historic landmark. While the methodology outlined in this paper may not be the final answer for dealing with a complex restoration problem, it at least demonstrates some of the basic techniques and analysis which are necessary. The writer only hopes that this paper will give some encouragement to those who are faced with similar tasks in the future.

APPENDIX I

41-11

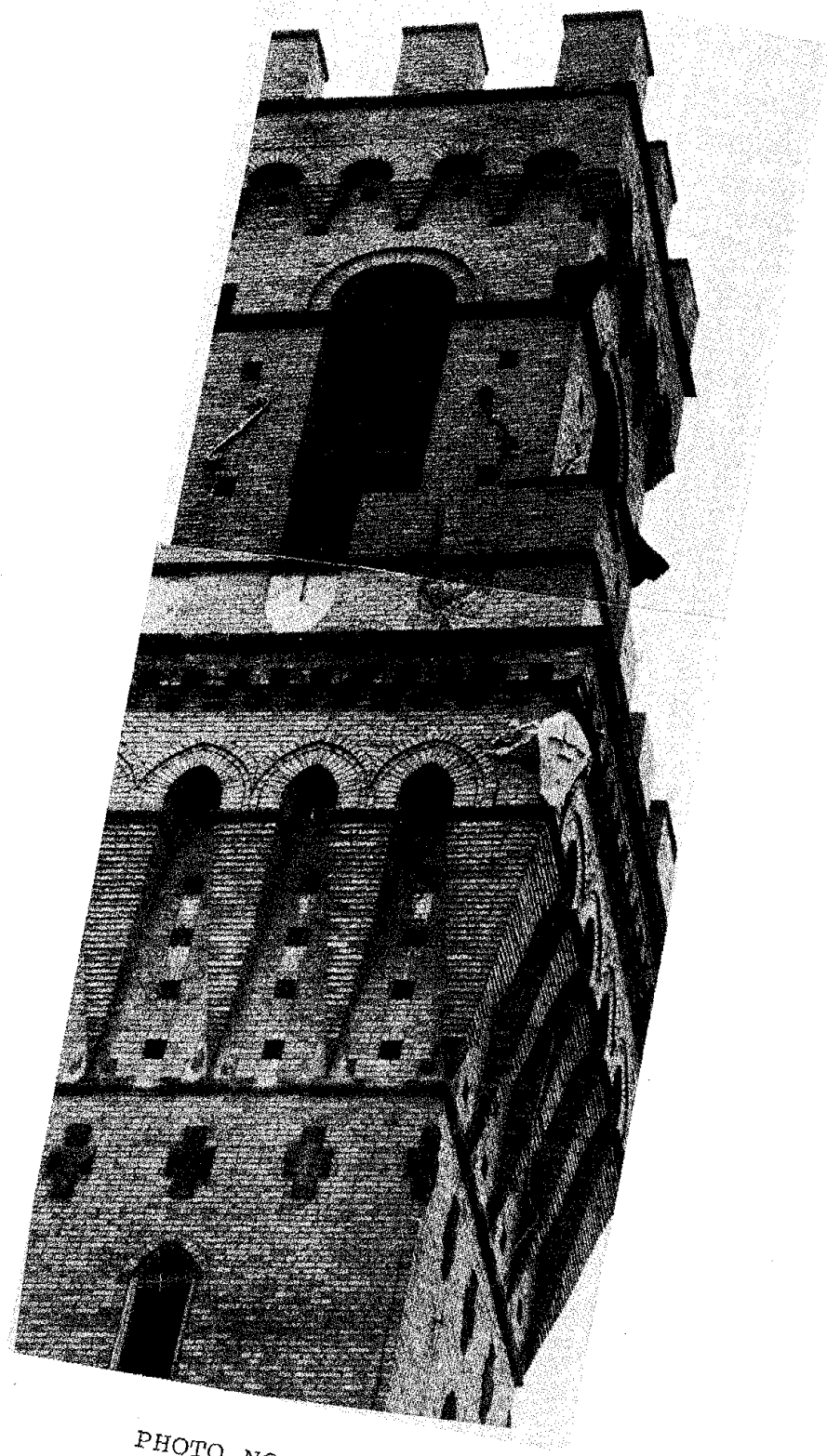


PHOTO NO 1

41-12



PHOTO NO 2



PHOTO NO 3

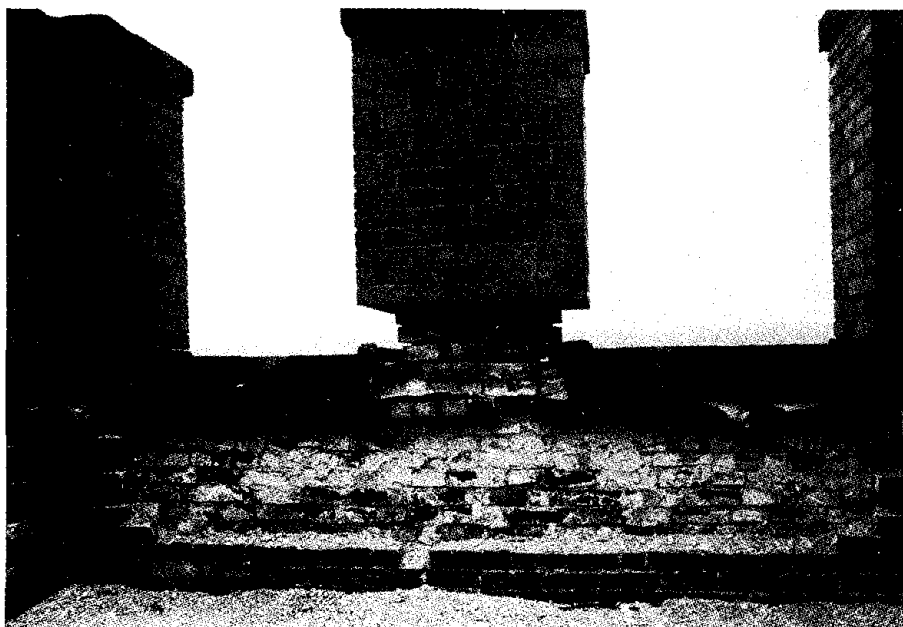


PHOTO NO 4

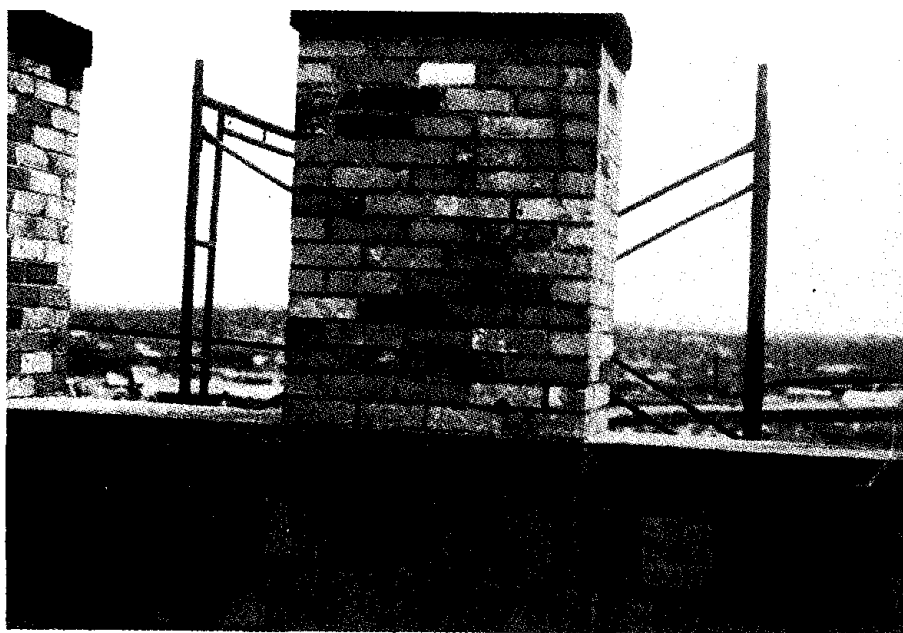


PHOTO NO 5

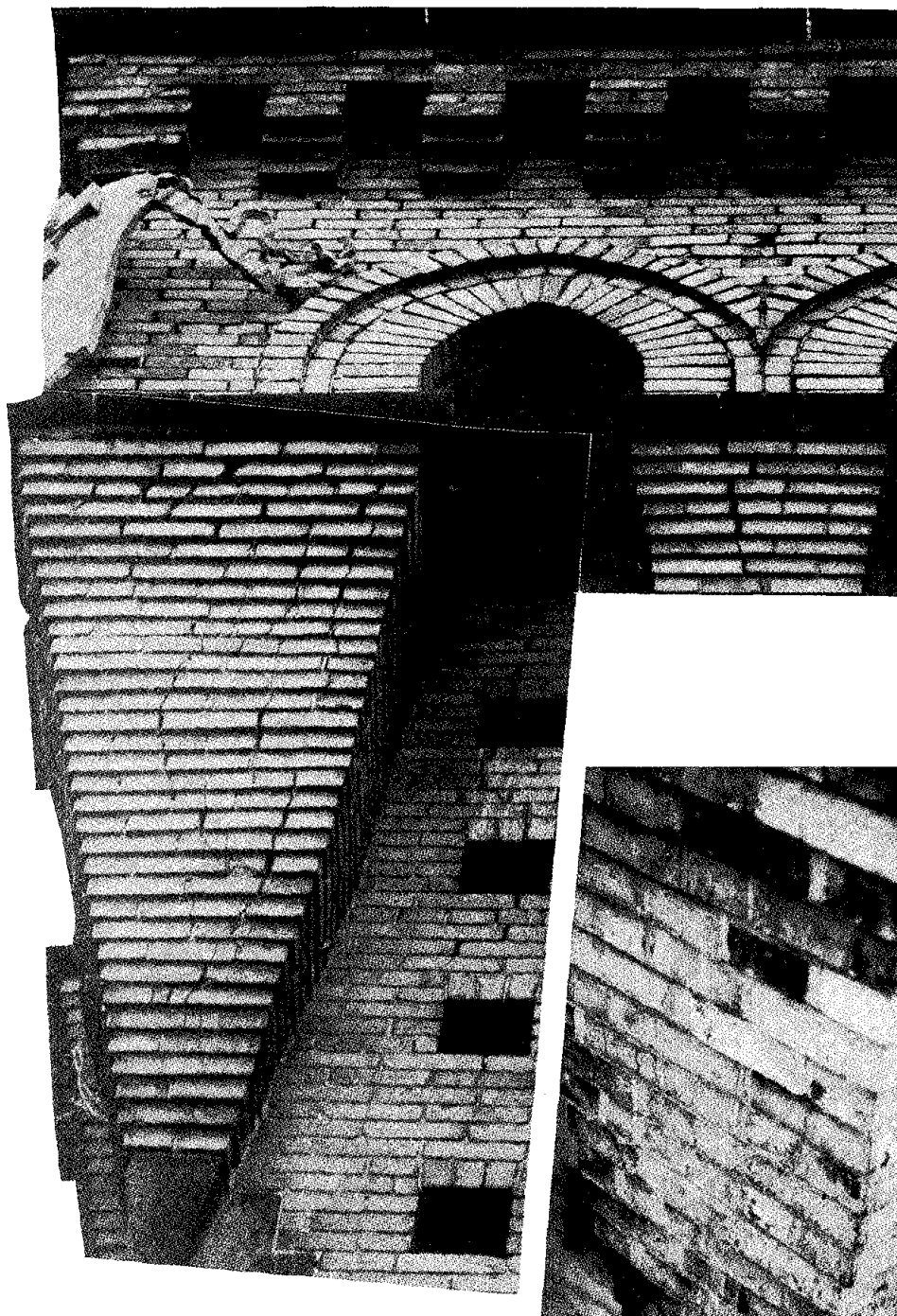


PHOTO NO 6



PHOTO NO 7

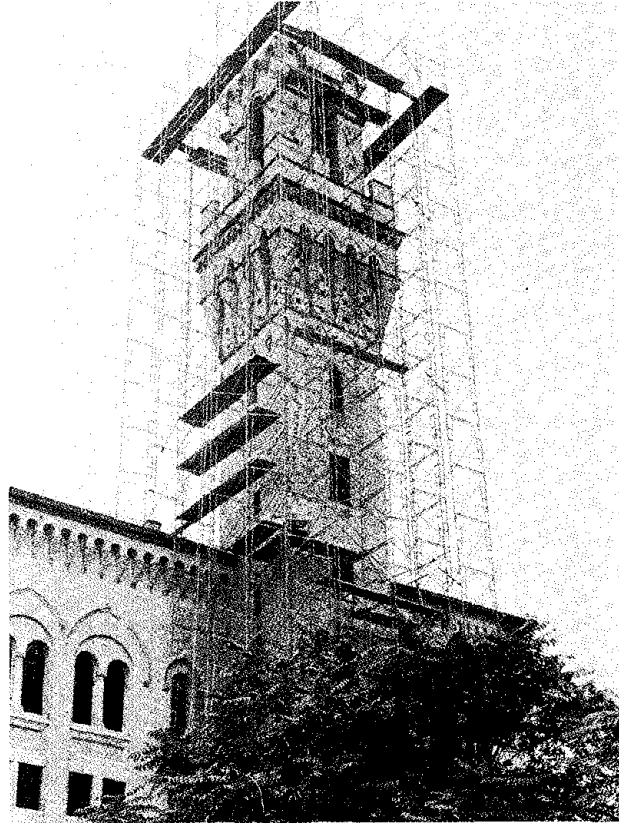


PHOTO NO 8

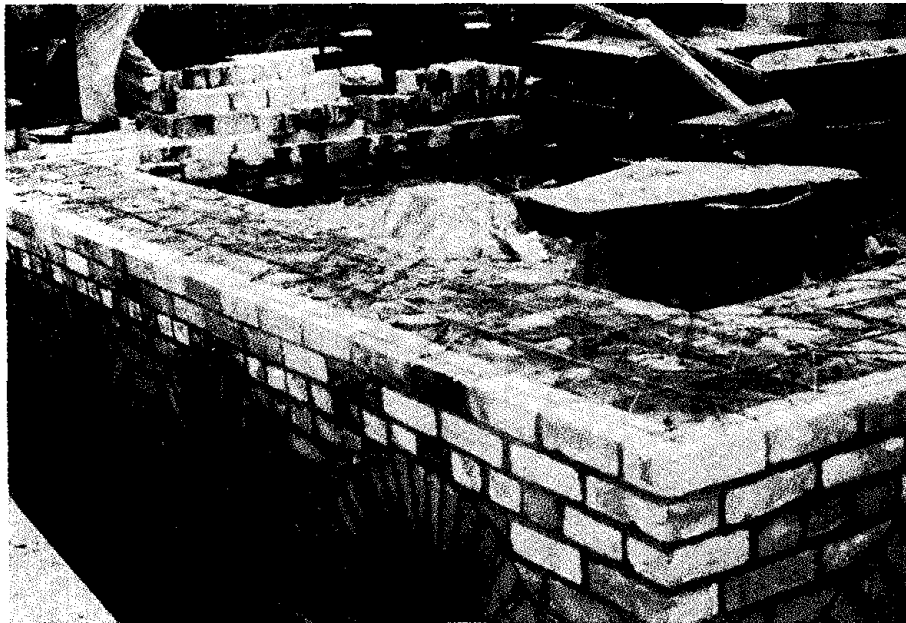


PHOTO NO 9

Appendix II

Tower Repair Notes:

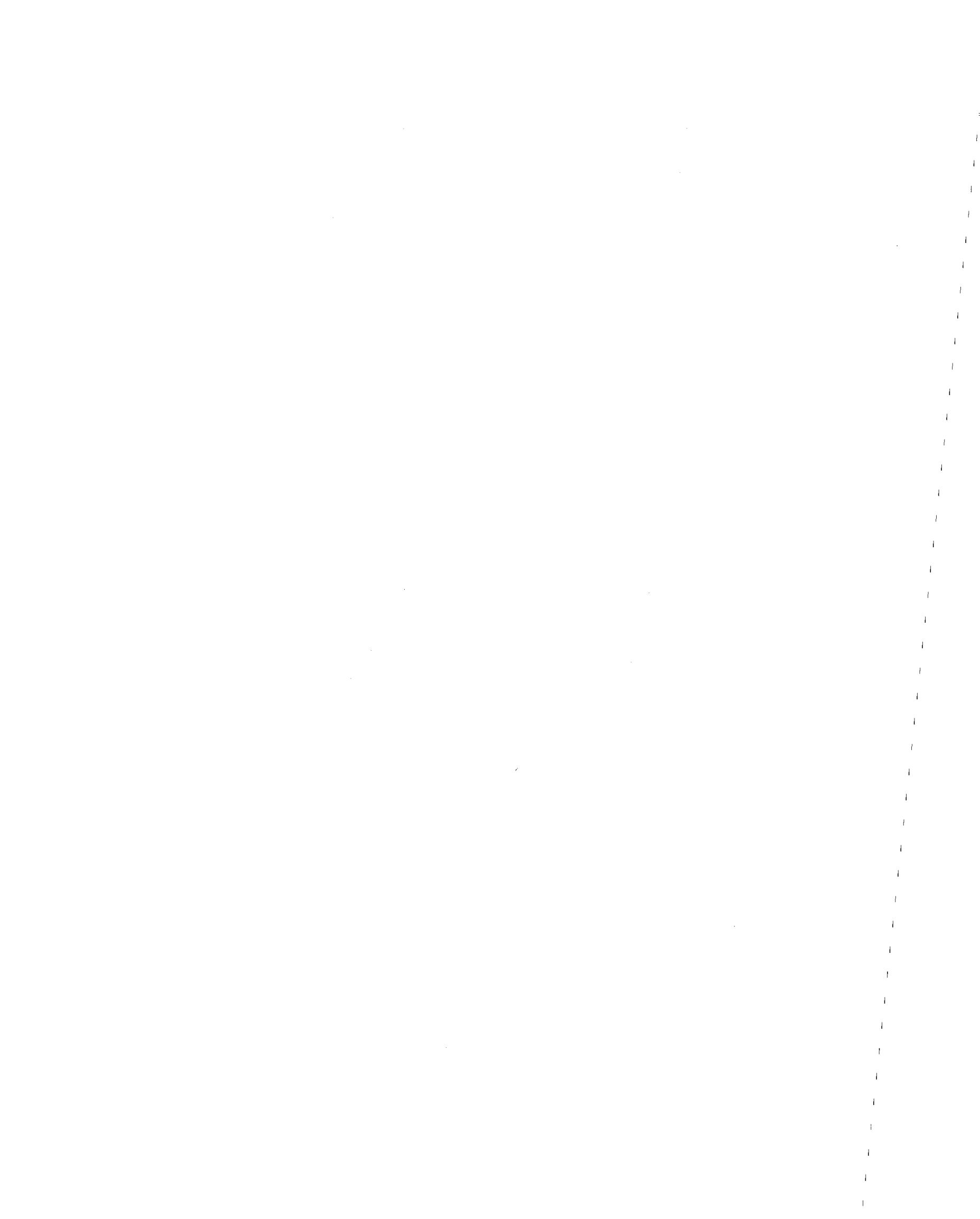
1. The intent is to provide repair work to match in character and appearance the original work, and to provide complete repair and renovation of all defective existing brick and stone work, including replacement of missing or damaged bricks and stones, repair of existing brick arches, and the complete re-pointing of all masonry joints to replace missing, crumbling, or decaying mortar. The present brick is a "yellow New Jersey fire brick." Some brick is available from the walls that will be demolished on the site. The cap stones and trimming stones are "Amherst stone." The natural color is light buff. Light buff concrete of matching color may be used to replace broken and missing stones.
2. Each bidder shall visit the site and examine the tower to ensure his knowledge of conditions affecting the work.
3. All information given relating to existing materials and conditions to be encountered is furnished for the information and convenience of the bidders and neither the owner nor the architect warrants or guarantees that such materials, or conditions will be the same as those encountered during construction.
4. Re-pointing: remove all defective brick work. Cut out all crumbling and decaying existing mortar from defective joints at least 1/3 deep. Where severe, replace entire bricks in fresh mortar. Clean surfaces to receive new mortar by wire brushed scrubbing with water, and/or other means subject to approval of architect.
5. Blend the repair work into the existing work by tooth-ing.
6. Anchor all repair work to the existing construction by use of metal masonry ties.
7. The re-pointing and the repair schedule apply to both the exterior and interior faces of the tower.
8. The repair schedule is intended as a guide to indicate the scope of work, but shall not be constructed to limit the scope.
9. Store existing structure where required during construction.

10. See sheet s-7 for tower level plans.
11. Stones from the top are stored on the site.

Appendix III

Repair Schedule:

- A) Replace missing, loose and/or broken face brick and any loose or broken back-up brick. Re-build to match existing.
- B) Remove any loose and/or broken face brick and any loose and/or broken back-up brick and re-build to match existing.
- C) Remove unsound section of wall or pier and re-build to match existing.
- D) Remove any loose and/or broken bricks and re-build arch to match existing.
- E) Remove any loose and/or broken bricks and re-build corbeling to match existing.
- F) Re-build to original height and re-place coping.
- G) Brick up solid existing opening or chase.
- H) New opening or enlarge existing opening. Provide new lintel angles as specified in the general notes sheet s-1.



THE CENTER FOR EDUCATIONAL DEVELOPMENT -
A MEDIUM SCALE SEISMIC UPGRADING

Harold A. Davis¹

ABSTRACT: During the 1960's, many substantial buildings in San Francisco were vacated or abandoned by industrial and commercial occupants, creating a surplus of unused floor space. Most of these buildings were old, poorly ventilated, without adequate parking facilities, and dangerously inadequate in seismic capacity, thereby becoming presumed liabilities to their owners rather than assets.

Far West Laboratory for Educational Research and Development obtained a federal grant to relocate in San Francisco and purchased a 43-year-old warehouse building at 15th and Folsom Streets in the city. Proposed use of the space included a school (part of the San Francisco School District), offices, and retail facilities for selected light industry.

The seismic upgrading requirements of Title 21 were met with gunite backing on the brick walls and new concrete wall elements. By adding major grade beams attached to the existing structure, it was possible to continue to use the existing pile foundations.

Disruption to the existing structure was kept to a minimum by drilling hundreds of holes of varying size and location in the existing concrete and brick fabric of the building. These holes were then filled with epoxy bonding agents and reinforcing bars. The exterior appearance of the building was maintained virtually unchanged by placing all new elements on the inside. The flexibility of the interior space was maximized by locating all shear elements on the exterior perimeter of the building.

¹Structural Engineer, Rutherford & Chekene, San Francisco, CA.

THE CENTER FOR EDUCATIONAL DEVELOPMENT
A MEDIUM SCALE SEISMIC UPGRADING

By Harold A. Davis¹

INTRODUCTION

Many engineers are now familiar with the problems and technical details of rehabilitation work and seismic upgrading, both for public agencies and private owners. The reconstruction and upgrading of unreinforced masonry structures is a problem which is now becoming more and more a necessity of solution, especially in California and other major urban centers. The economics of new construction vs. rehabilitation make rehabilitation a more frequent choice than in the past. Some of the design investigations will be described as well as details of the reinforcing elements added to upgrade the structure. The project I wish to review, the Center for Educational Development, includes some unique features deserving our examination for ideas on design investigation, analysis and implementation.



FIGURE 1

¹Structural Engineer, Rutherford & Chekene, San Francisco, CA

The Center for Educational Development is located in the Mission District of San Francisco, at Fifteenth and Folsom Streets. The site borders a residential, small commercial retail area and light-to-medium industry. Main traffic thoroughfares such as freeways, bridges and transit facilities like BART (under construction when our involvement with this building started) are nearby. When planning began, the San Francisco Chamber of Commerce actively campaigned to save older existing structures by urging real estate investors to consider rehabilitation as an alternative to the demolition of older, neglected buildings, or to relocation outside the city itself. The Cannery and Ghirardelli Square projects had recently been completed and stood as guideposts for future efforts along the same lines. (See Figure 1)

The problem, as it faced us in 1969, was this: the building is six stories, containing some 300,000 square feet of floor space, measuring approximately 190 feet by 255 feet. Constructed in 1926-27, it was the second structure to occupy the same site, built and used as a warehouse for merchandising and retail concerns such as Woolworth's. In 1969 it stood empty and neglected, a visual deterrent to change. Exterior walls were varying thicknesses of unreinforced brick masonry, supported on the flat-slab concrete frame.

At this point, Far West Laboratory, an energetic team of educational research and development professionals from Berkeley, were looking for space to house 75,000 square feet of offices and an experimental school in the same building. Thanks to funding from the Office of Education of HEW, this building was purchased with part of a \$4.75 million federal grant. The grant was to pay for all construction work on the condition that there be no major disruption to the exterior of the building, and that unused space retain a certain flexibility and ease of future occupancy. Also, the structure had to be approved for public school occupancy. The architect and consultants were selected and discussions began on the basic philosophy or design approach to this problem.

The first questions are familiar to many of you who have experience in rehabilitation work: Does it meet the code? How much do we have to do? What's the minimum? How much will it cost? Why are your fees so high? These are certainly important and basic considerations, but the answers to such questions alone do not provide a sufficient basis for proceeding on a project of this scale. The design professions (and I include structural engineers in this category) need to be made more aware of issues related to planning, esthetics, community impact, and flexibility for future uses. What I propose to discuss is how our solutions for these questions were developed, integrated with other design requirements, and implemented to produce the final result.

We began with a set of drawings for the existing construction which provided enough information to allow preparation of comprehensive calculations of the existing capacity for vertical loads. The building was originally designed for an unreduced live load of 200 psf on all floors, (heavy warehouse occupancy) a fact which we were able to make great use of. We performed testing on concrete cores, made detailed measurements, cut chases in brick walls, and water leveled the floors. Our first surprise came from the results of the water leveling -- as much as nine inches of differential settlement, and no major, fundamental cracking to show for it. (See Figure 2)

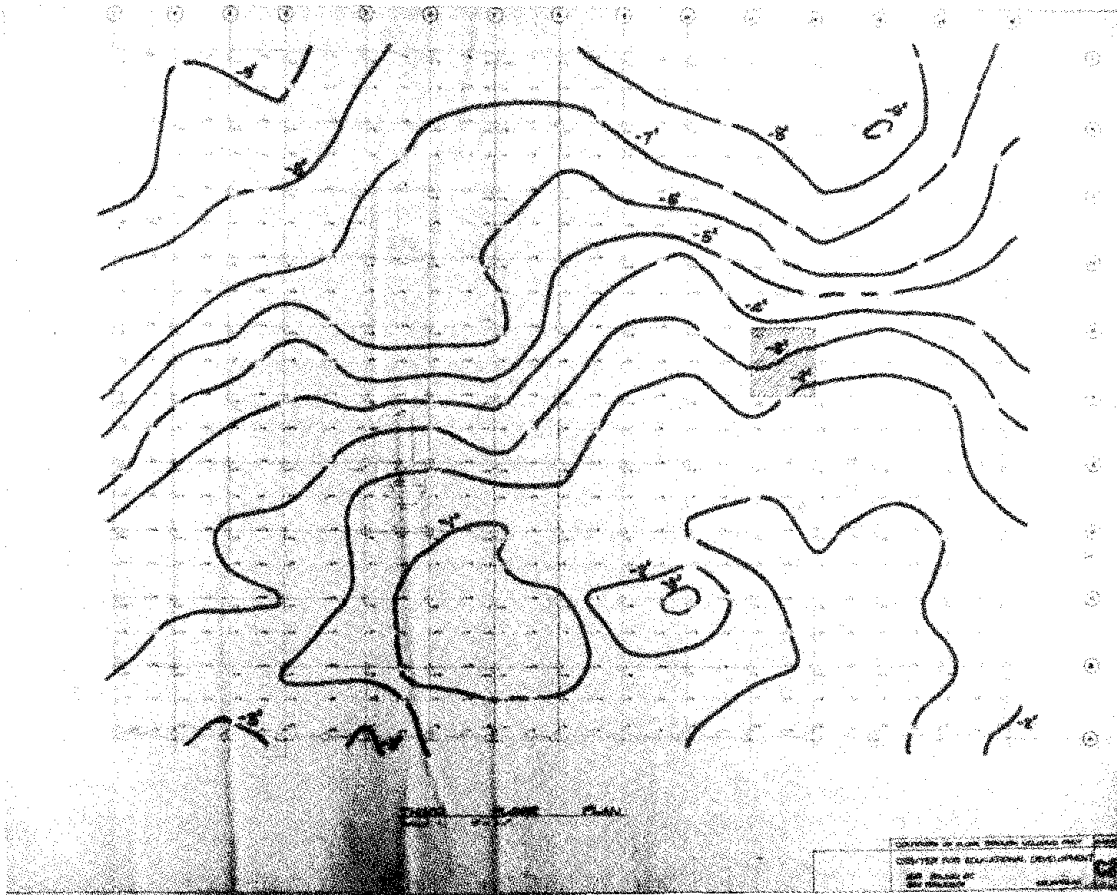


FIGURE 2

The structure is founded on wood piles, of unknown depth and tip size. We verified the number, butt sizes, and conditions by visual observation in several exploration pits. An initial soils investigation was performed by Shannon & Wilson, to see if correlation could be established between the settlement picture and the use of piling, and to determine if the building was doomed to permanent or short-term foundation failure.

Results showed that there could indeed be a logical explanation for the differential, but without information on driving, depth or size, we could reach no definite conclusions, especially if new dead loads were to be required. As the preliminary development of structural schemes and requirements proceeded, it became apparent that dead load would be increased, and therefore two pile load tests were required. (See Figure 3)

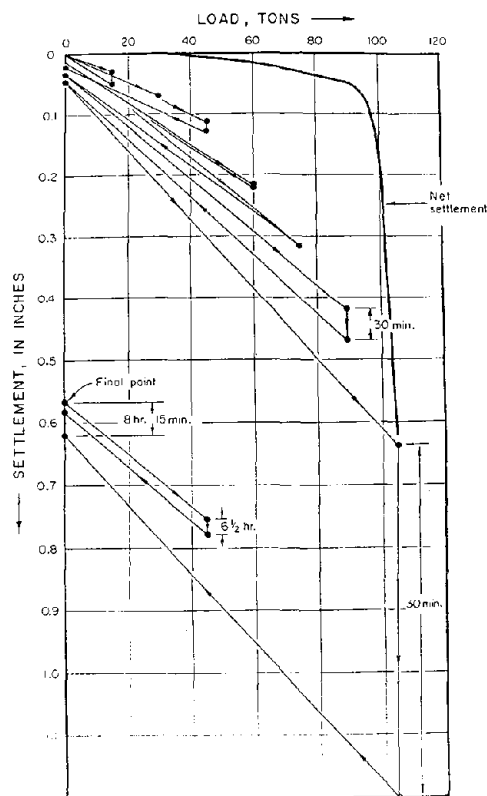


FIGURE 3

These tests indicated that substantial increase in dead load and real live load were possible. We concluded then that the settlement was gradual, due to differing conditions for pile bearing (and possibly driving and that the rate of settlement had decreased considerably because of the age of the fill which some of the structure is founded on. We cored the ground floor slab and learned that the ground had settled away from the slab in areas of the building which were 'high', but was right up against the slab-on-grade where the building was most depressed.

At this point, we were convinced that certain engineering factors should be considered major parameters to any proposed architectural solutions:

A. Dead load could be added, but a limit was set which would require some trade-off in weight with the existing loads.

B. Shear-wall type solutions were desirable for lateral forces.

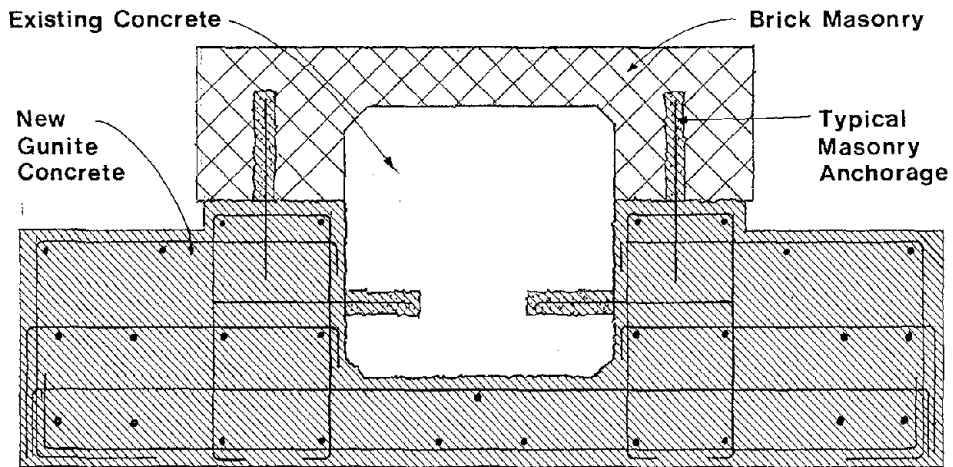
- C. Floor slabs were adequate to support the 50 psf and 100 psf loads, based on the slab load test.
- d. Application of new dead and real-live loads were required to be distributed evenly over the building to avoid costly foundation revisions.
- E. New seismic resistance elements should be located on the perimeter.

About six months after starting the project, we began to firm up our ideas on the system of lateral bracing to be used. It was clear to everyone involved that the solutions to the engineering problems would have a major impact on architectural planning and design. We operate on the conviction that in a rehabilitation project like this, the structural engineer occupies the position of leadership, and if he is sensitive to the overall needs of the project his work is in the nature of a creative contribution rather than just solutions to limited technical problems. In response to the original appearance of the building and the fact that projected occupancies were offices and schools, we proposed that the lateral scheme use the form of the building as an outline, and that the entire exterior wall become a new concrete shear wall. From the sixth floor down, pier and spandrel elements become larger and larger; window and door openings diminish. At first, no judgement was made whether the concrete elements would be poured-in-place or gunite, but as the design progressed, gunite clearly seemed the more appropriate material.

The design detail sections are worth examining -- not to count reinforcing bars, but to demonstrate the relationship between our design and the original construction. Figures 4 through 7 show a Pier Sections and Spandrel Sections, both on the first floor and on the sixth floor.

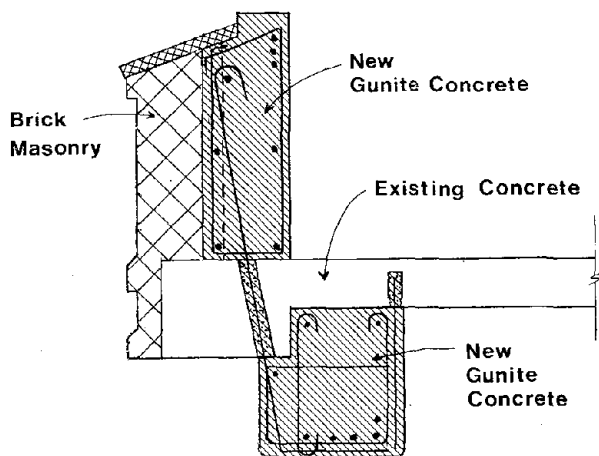
Foundation work was limited to the construction of a major perimeter grade beam to receive the nearly vertical wall elements and distribute the load to the existing pile caps. The ground floor slab had failed in many bays due to the ground settlement, so a new flat slab was designed, with the old slab cut away from the columns to remove any possible load transfer and to provide space for a drop panel.

The decision to use gunite rather than cast-in-place concrete was based partly on considerations of economy in formwork, but also was influenced by the necessity of achieving positive bond on a variety of surfaces. Some of these surfaces would require temporary ports, chases and intricate placing schemes to receive concrete properly and develop bond.



PIER SECTION- FIRST FLOOR

FIGURE 4



FIRST FLOOR SPANDREL SECTION

FIGURE 5

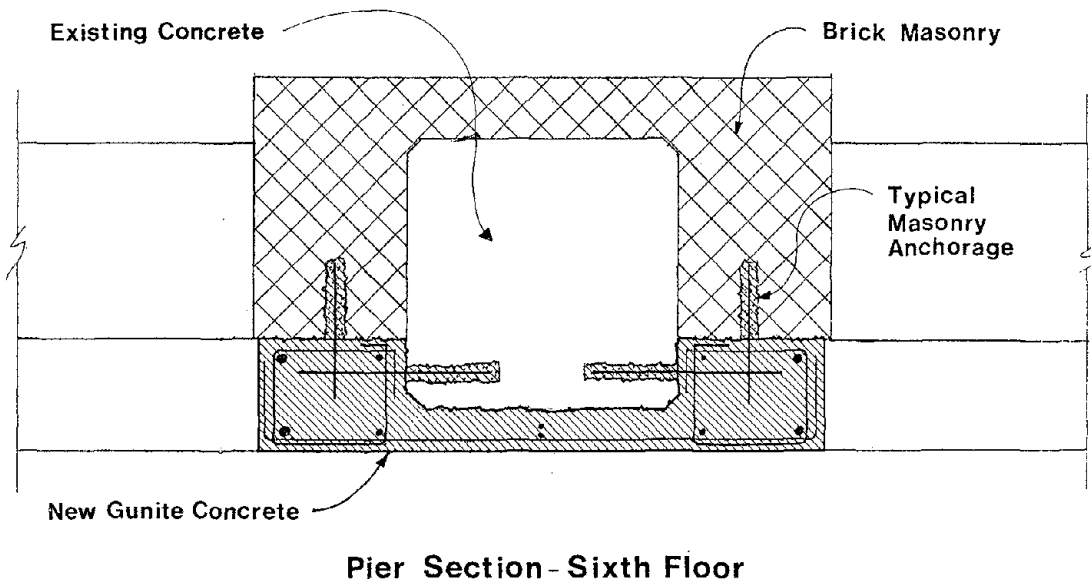


FIGURE 6

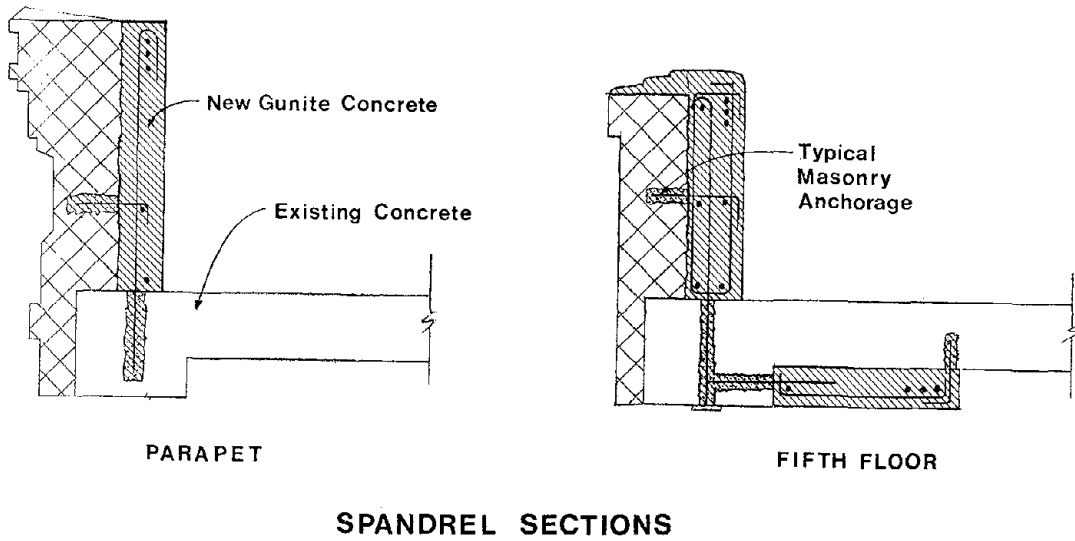


FIGURE 7



Figure 8 shows the construction work itself. Foundation work was the first phase following demolition. While foundation construction proceeded, holes and chases were drilled in slabs, columns, and brick walls throughout the building. (See Figure 9)

FIGURE 8



FIGURE 9

Existing wythes of masonry were anchored to the new concrete elements by rebar anchors set in 8"Ø holes drilled by core barrel. Holes were filled prior to guniting by an pneumatically applied dry pack material. (See Figure 10)

The installation of reinforcing was a major, time-consuming portion of the work. Because of the number and distribution of the bars, and clearances necessary for gunite work, very close coordination between the men drilling the holes and the reinforcing installation was necessary. Our construction observation required one man to be assigned on a continuing basis to assist the owner's project representative and review conflicts as they developed. (See Figure 11, 12)

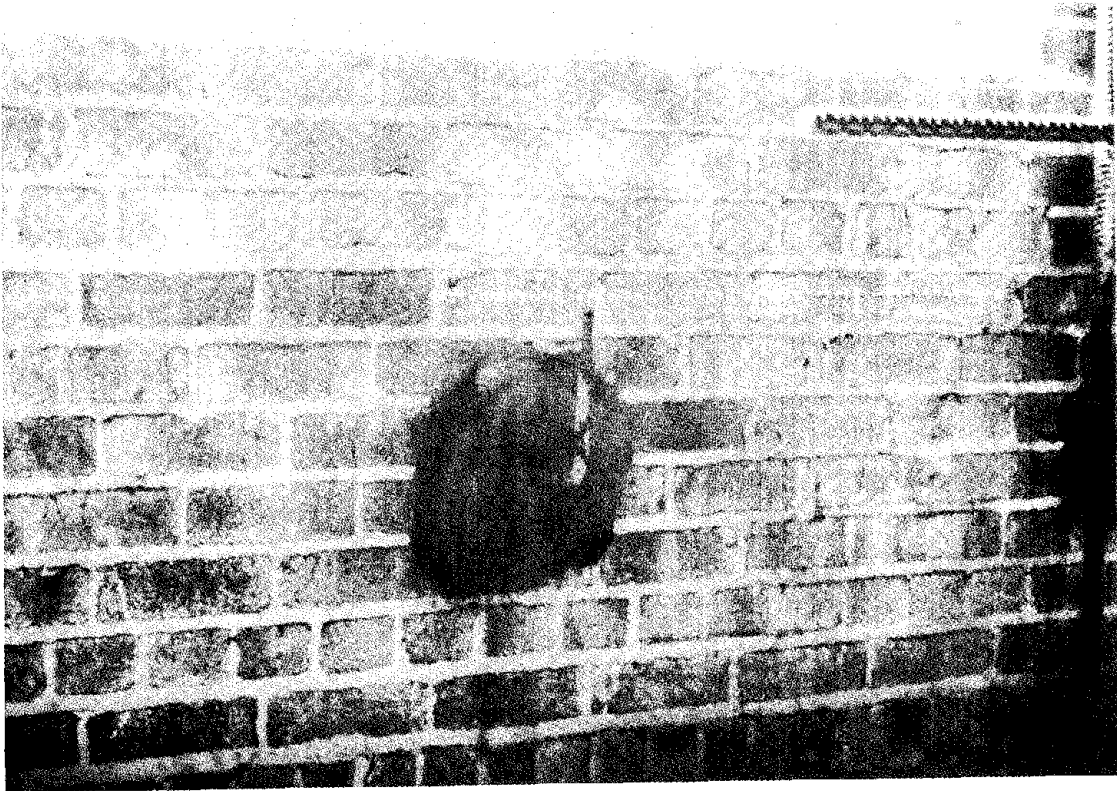


FIGURE 10

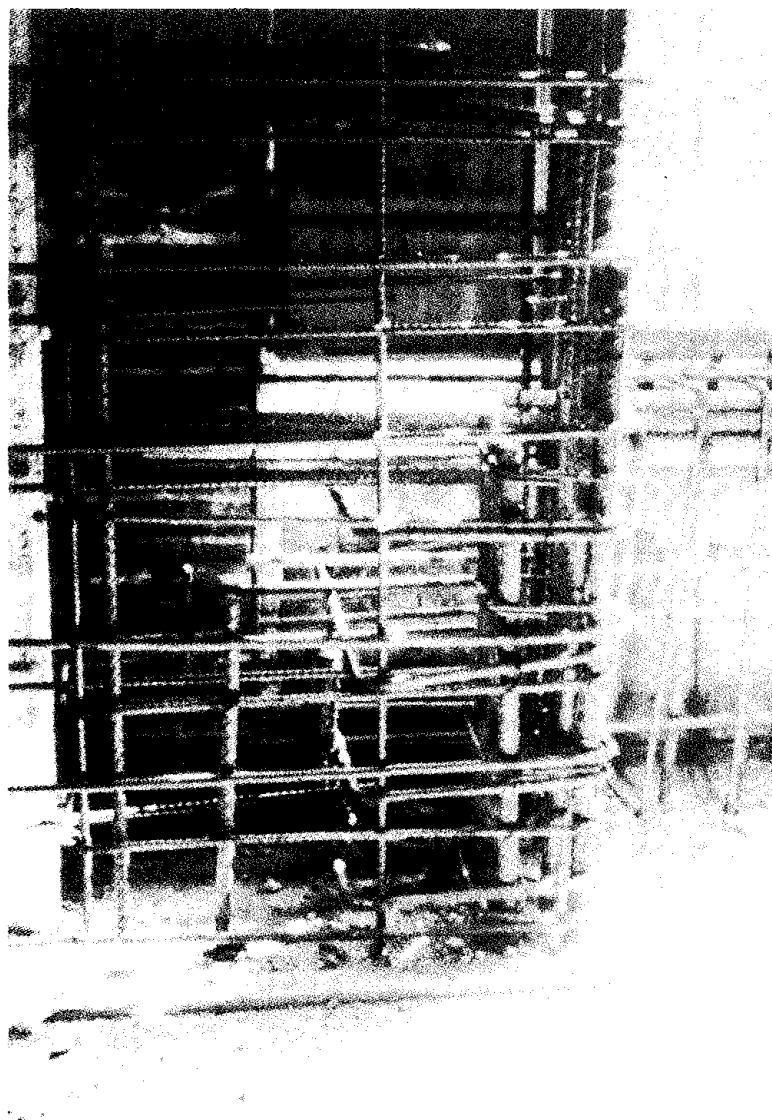


FIGURE 11

42-12

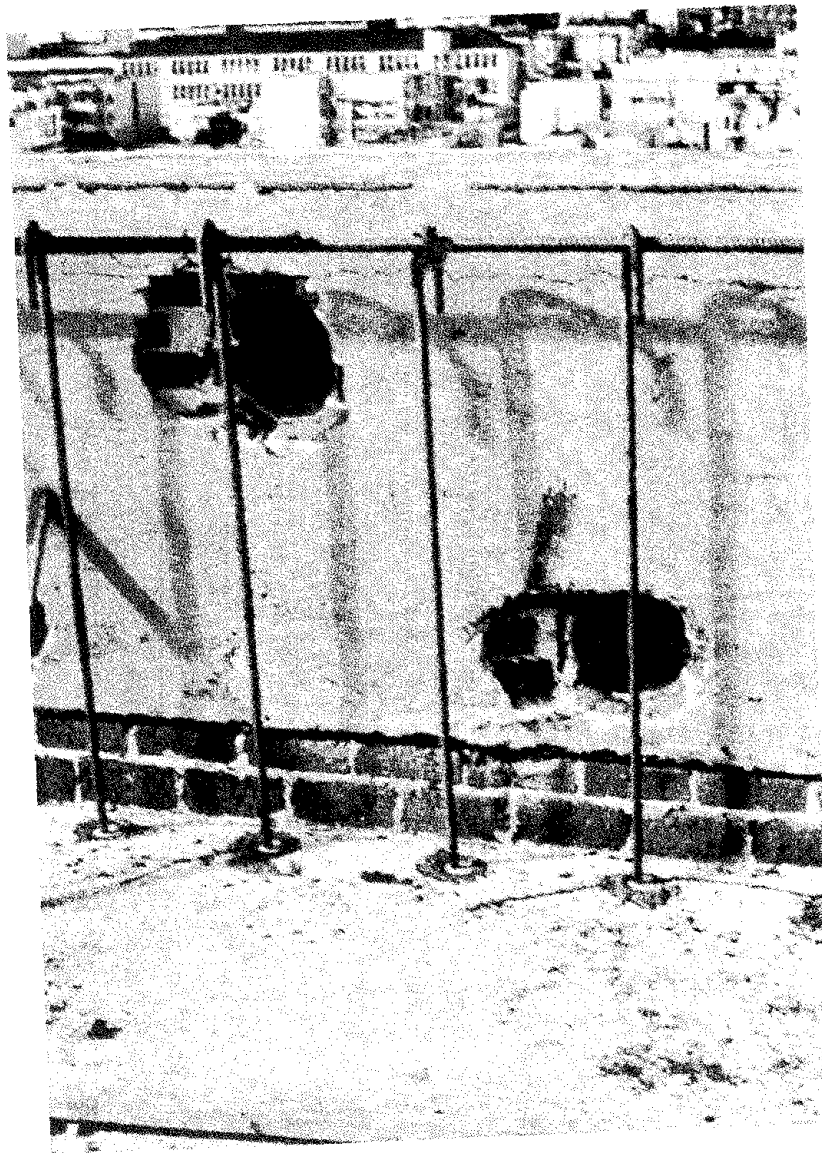


FIGURE 12

As soon as possible after the completion of reinforcing, screed wires were set, back forms installed and gunite applied. Masonry and concrete surfaces were thoroughly sand blasted. Although difficulties in mixing and application did occur at first, they were soon overcome. Only the workmanship of the nozzle men remained problematic. The key to gunite, of course, is the proper compaction of the material in place, and the elimination of rebound material from the section. OSA requirements determined the minimum core testing, but on several occasions, additional cores were taken because of low breaks or cores which indicated the inclusion of rebound.

The finish coat, applied by plasterers, was between 1/4" to 1/2" in thickness. This dimension was originally intended to be an integral application with a wood float finish, but nozzle men simply were not able to control the tolerances to that degree, so plasterers were called in to apply the finish. Figure 13 shows the general shape and appearance of spandrel and pier section (at the 1st floor) after the forms are stripped.

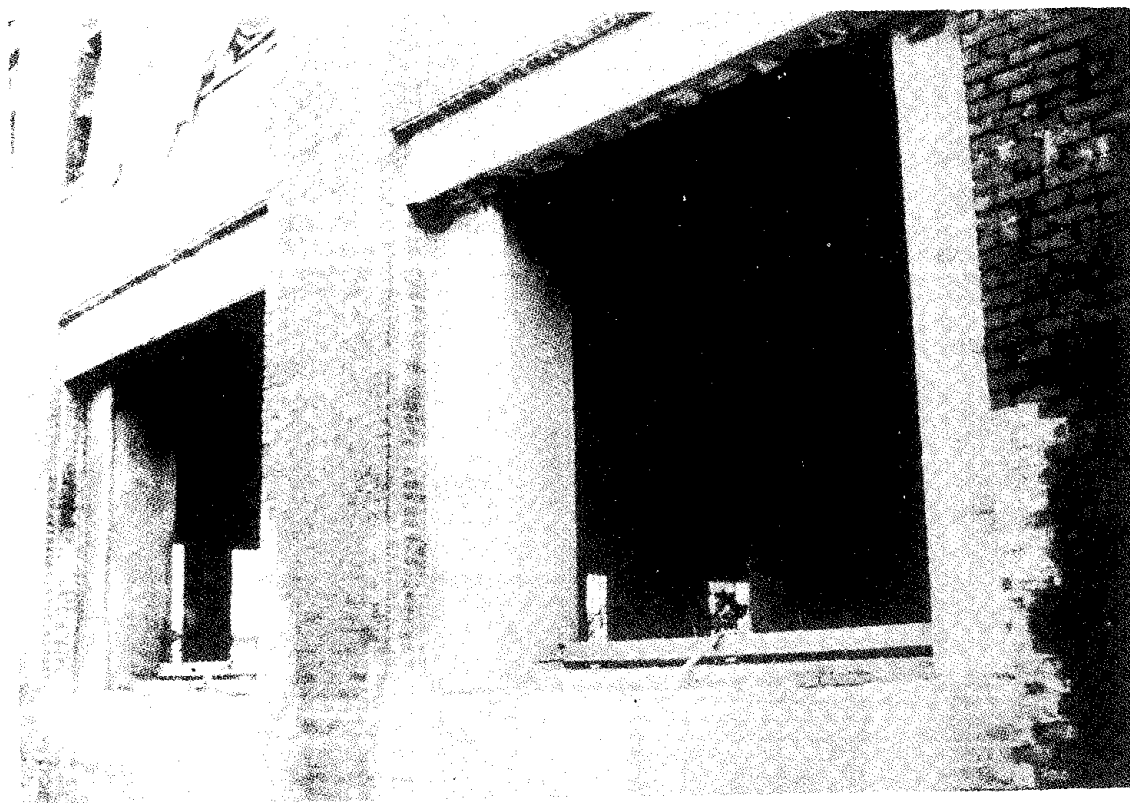


FIGURE 13

The finished building originally housed offices, mechanical service areas, and a television studio on two floors (5th and 6th), and combined joint-use space on the first floor for community groups and the Laboratory. There is also a pre-school children's center on the first floor.

Our solution to the seismic upgrading has produced a scheme which did not significantly alter the exterior appearance, provided total interior flexibility for space planning, and met the criteria for OSA-approved school occupancy without further structural modifications. School occupancy of the second, third and fourth floors has not yet occurred, but numerous proposals have been discussed. A major facility of higher learning is currently planning to develop two or more floors into new classroom and office space. A Mexican museum has recently been established in the building, exhibiting Mexican and Mexican-American paintings, traditional crafts, and other works of art.

Figures 14 and 15 show some aspects of the completed work, and demonstrate how the structural work was integrated into the architectural solution.

Total cost of the construction was \$3,500,000 or roughly \$11.50 per square foot, bid in 1971. The Architect was Esherick Homsey Dodge and Davis, San Francisco. The contractor was DeNarde Construction Company of San Francisco.

SUMMARY

A large concrete frame and brick wall industrial building was rehabilitated and remodeled for an educational facility and office. Integration of requirements for seismic design and foundation loads resulted in a solution permitting maximum space planning flexibility, as well as minimum change in the exterior appearance. Construction aspects involved close coordination of a multitude of holes, chases and removals for reinforcing steel in gunite. Completed construction cost was approximately \$11.50 per square foot in 1973.

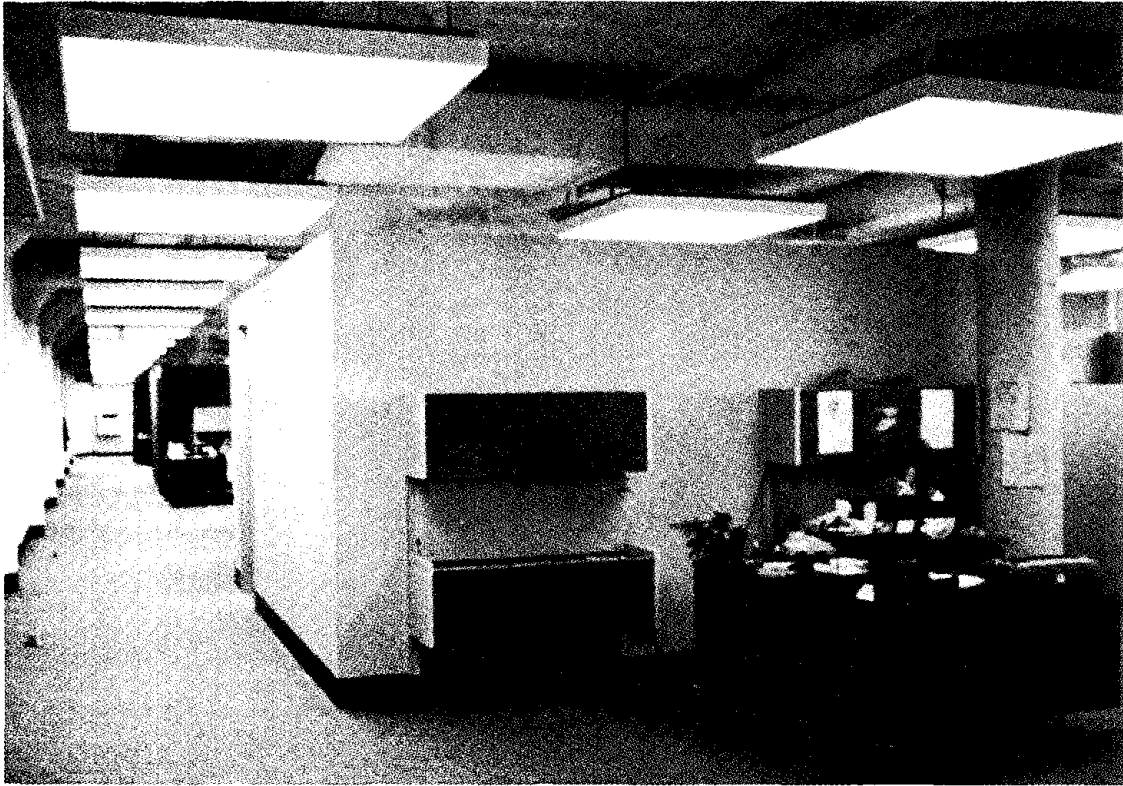


FIGURE 14

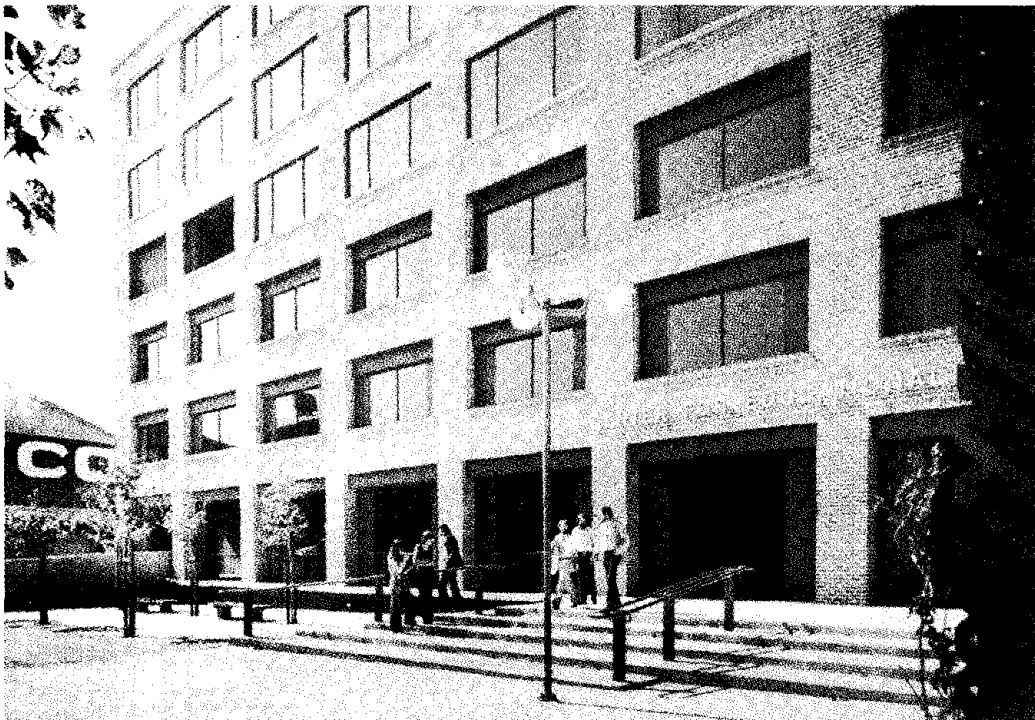


FIGURE 15



LOW COST FACILITY FOR TESTING THE ULTIMATE EARTHQUAKE RESISTANCE OF
MASONRY STRUCTURES

By Keightley, W. O., Department of Civil Engineering and Engineering
Mechanics, Montana State University, Bozeman, Montana

ABSTRACT: A shock table, 6m x 7m, which can impart horizontal half-sine acceleration pulses to the foundations of 20-test structures has been constructed around the frame of a used railway wagon. The shocks, of 0.1 second duration and up to 2g amplitude, are generated by impacts from two other heavily loaded wagons which roll down short inclines and collide through heavy springs with the platform wagon. Tests of half-scale models of one-room low grade masonry houses reveal the weakness of walls transverse to the shocks, demonstrate the effectiveness of vertical steel bars in the building corners and of encircling reinforced concrete bands at lintel level, and raise questions about the anchorage of corner reinforcing bars in the foundation. A proposal is made for construction of a similar facility with capability of shaking to the point of collapse structures weighing from 100 to 200 tons.

LOW COST FACILITY FOR TESTING THE ULTIMATE EARTHQUAKE
RESISTANCE OF MASONRY STRUCTURES

by

W. O. Keightley¹

INTRODUCTION

The design of a reinforced masonry structure which is to be built in a region subject to earthquakes is based on a large body of simplifying assumptions as to the behavior of materials, joints, and large assemblages of materials, as well as assumptions as to the nature, intensity, and duration of the ground shaking. When the ground shaking is strong enough to cause serious damage to the structure, most of the assumptions about the structure will be incorrect. Proof of the value of the presently used methods of designing comes from observing the performance of structures during strong shaking, but to date not much performance data has accumulated for modern types of construction.

Greater assurance of the reliability of today's methods and materials can be had by large scale destructive testing, which means subjecting the foundations of structures to simulated earthquake motions strong enough to cause damage to the point of collapse. Testing of this kind is expensive because large structures must be built and then destroyed. In addition, facilities for simulating three-dimensional ground motion at high force levels do not exist, and those which are capable of one-, or two-dimensional motion are expensive to construct and expensive or unavailable for rent for the period of time necessary to build a reinforced masonry structure in the usual fashion and carefully test it. Nevertheless, as masonry structures increase in height and numbers, and depart more from designs and methods tested by experience, some tests to destruction of large assemblages under simulated earthquake loading should be made. As one testing machine manufacturer puts it, "One test is worth a thousand expert opinions."

This paper describes a low cost testing facility which has been recently constructed in India, capable of destroying 20-ton structures. Suggestions are given for constructing a similar facility to test much larger structures. Although the facility cannot simulate earthquake motion, but is capable of imparting only uniaxial acceleration pulses, it is believed that it can reveal much useful information about the performance of masonry structures up to the point of collapse.

DESCRIPTION OF THE FACILITY

The principles of the low cost test facility can be grasped from Figure 1. Three railway wagon (car) underframes, with wheels, were

¹Professor, Department of Civil Engineering and Engineering Mechanics, Montana State University, Bozeman, Montana.

mounted on a 36-m long railway track, the central portion of which was depressed to create a short ramp at each end. Integral with the center frame there was constructed a stiff steel platform, 6m x 7m, as shown in Figure 2. Houses to be tested were built on top of this platform. The other two frames were fitted with sides and bottoms, and then loaded with boulders and sand to become movable 32-ton dead loads.

To conduct a test, one dead load wagon and the platform wagon were positioned on the track as shown in Figure 1. The other dead load wagon was pulled partway up the incline, and then released to roll down and collide with the platform wagon through heavy coil springs which had been mounted on its ends. The platform wagon would thus receive an acceleration pulse and be driven forward into collision with the stationary dead load wagon. This second collision resulted in another acceleration pulse being given to the platform wagon, but in the opposite direction. Once the wagons had been brought to rest after this pair of collisions, the process was repeated, except that the roles of the two dead load wagons were interchanged.

The amplitude of the acceleration pulses was controlled by the height from which the dead load wagons were released. Theoretical expressions for the amplitude and the duration of an acceleration pulse are shown in Figure 1. These expressions are based on the assumption that all the mass associated with each wagon, including wheels and payload, can be treated as a single rigid unit, although actually the test structures are far from being rigid, and there was looseness in the connection between the axles and the frame. Measured values of amplitude and duration, however, were reasonably close to the computed values at higher acceleration levels.

The track for this facility was made of new rails (90 lbs/yard) spiked to wood ties on broken stone ballast. The underframes and the wheels came from 50-year old rolling stock condemned by the Indian Railways, but with rehabilitation of bearings and wheels on two wagons. Rated loaded gross weight of each wagon in railway service had been about 35 tons. Figure 3 shows the track and the frame used for the platform wagon, and Figure 4 shows the entire facility near completion, including the surrounding building. Total cost of the facility, including the building, was approximately \$12,500. Of this amount, \$3,300 was spent for the 3 wagons, and \$1,900 for 7 tons of structural steel and plate.

Hand operated winches were used to draw the dead load wagons up the inclines; release was effected by driving out a steel connecting pin with a sharp blow from a sledge hammer. In Figure 7 can be seen the coil springs on the ends of the platform wagon, which are necessary to moderate the impacts. These were salvaged from the buffers of the wagons. The springs on each end could resist 70 tons before becoming solid, meaning that a maximum acceleration of 2g could be imparted to a rigid 35-ton platform wagon.

PERFORMANCE OF THE FACILITY

Data from only one set of tests is available to evaluate the performance of the facility, and this appears in Table 1. Four half-scale one room brick structures, representing typical peasant houses in India, were constructed symmetrically on the platform. Made with half-scale bricks, their outside dimensions were 1.75m in the direction of the shocks, by 2.17m, by 1.60m high above the plinth, capped with a 7.6cm concrete roof slab, with walls 11.5cm thick. Three walls contained a window, and one shear wall contained a door. Weight of each structure was 3.7 metric tons. Two of the houses were laid in mud mortar, and two in 1:6 cement mortar, one of each kind unreinforced, and the other reinforced with an encircling reinforced concrete band at lintel level and with a vertical steel bar set in cement mortar in each corner and surrounding each opening. Vertical steel reinforcing bars in the walls were anchored by welding them to plates anchored in the roof slabs, and by embedment four courses deep into the brick-cement mortar foundations which were built around light steel angles welded to the platform.

Records of accelerations of the platform during two shocks, shown in Figure 5, exhibit roughly the half-sine shaped pulses which are expected. The oscillations which follow the pulses in the upper traces, shock no. 3, were caused by free vibrations of the structures on the platform. These oscillations do not appear in the lower traces, shock no. 17, because by this time all of the structures except one had been destroyed and were now piles of rubble resting in their former locations on the platform to preserve balance. The peak acceleration in the second pulse in each pair of pulses is about 80% of the peak in the primary pulse, indicating that some energy has been lost in the primary collision and in rolling between collisions.

In Table 1 significant discrepancies are noted among peak accelerations pertaining to the same release point of the dead load wagons and between the two edges of the platform, the latter indicating twist about a vertical axis. Some factors affecting these discrepancies are: (1) The wheels of the dead load wagons had been coarsely machined, leaving ridges on the rims which cut grooves in the rails, thus slowing the rolling. It is believed that this cutting process definitely affected the first few runs and possibly affected later runs if the wheels had been displaced laterally and thereby cut new grooves. (2) Tests of the recording instruments showed that the two channels of instrumentation were unequally affected by line voltage variations, one by a change in gain of 12% as the line voltage varied over a not unusual range. These conditions create some doubt as to the actual variations that might be expected under ideal conditions, but undoubtedly variations will exist due to changes in properties of the test structures as damage progresses, due to slight variations in the point of release of the dead load wagons, and due to wobbling of the wagons as they roll down the inclines.

PERFORMANCE OF THE STRUCTURES

Damage to the structures when they were near the point of collapse is pictured in Figures 6 through 10. The unreinforced mud mortar structure failed, not in the shear walls, but by collapse of the walls transverse to the impacts. Vertical cracks at the building corners and a horizontal crack in the transverse walls one course below the roof slab appeared after shock No. 5, and these determined the course of failure. During subsequent impacts, the tops of the transverse walls displaced further and further, and they finally fell in shock No. 8, with the shear walls also in bad condition. In an earthquake, with excitation in both directions, the roof would have fallen sooner because the damaged transverse walls would not have been able to sustain the shear caused by transverse ground motions. For more realistic testing it is recommended that future test structures be aligned so that the impacts occur along a diagonal, thus loading walls both transversely and parallel to their surfaces.

The unreinforced cement mortar structure was the next to fail, starting with a crack appearing at the junction of the foundation and the walls entirely around the structure after shock No. 6, and also cracks in the shear wall below the window. One method of protecting a structure against earthquakes is to build it on a sliding foundation so that it more or less stands still when the ground shakes. This base crack to some degree served this purpose, but due to rough surfaces, the coefficient of friction along the crack probably varied greatly, so that under subsequent impacts the base shear was concentrated at a few points, leading to local failures. The walls broke into large chunks which shifted unequally on the foundation, and in shock No. 10 the west transverse wall fell, with shear walls in a collapsing condition. The importance of a uniform and low coefficient of friction in a sliding base structure was made apparent.

The reinforced mud mortar structure, being more flexible, experienced less base shear than the cement structure, but this shear was concentrated at the cemented corners and the door jambs, where there was also tension from the reinforcing bars. Cracks started first in the mud portions of the shear walls after shock No. 6, but probably caused no weakening of the structure. At the next shock, cracking at the upper level of the foundation began at the corners, extending down through four courses of brick to the bottom of the anchorage of the vertical bars. The foundation masonry had been broken open during construction to insert the corner bars and was then recemented. Possibly these cold joints were responsible for the early failure at this point. During subsequent shocks, the lower ends of the corners displaced outward in diagonal directions, while the reinforced corner columns remained rigid and uncracked up the lintel band where they were broken. There was little damage above the lintel band. It was difficult when viewing the structure as it was near collapse to determine from which direction the shocks had come.

After shock No. 14, only the reinforced cement mortar structure remained standing, with small well distributed cracks. It was rigid, but had not cracked along the base as the plain cement structure did because the vertical reinforcing bars prevented the corners from lifting. As the shock intensity increased, cracks appeared in the shear wall below the window sill, and extended diagonally into the corner of the foundation, down to the bottom of the steel anchorage. The masonry piers alongside the door and masonry above the lintel band remained in good condition. Failure progressed by the breaking and diagonal displacement of all four corners, and failure of the shear wall containing the window.

A PROPOSED LARGE CAPACITY FACILITY

Before a large capacity testing facility is built, some thought should be given not only to the cost of the facility and its maintenance, but also to the cost of the testing and the extent to which the facility might be used. Large test structures are expensive to build, instrument, and test. Probably no one is prepared at the present time to commit himself to financing tests of 1000-ton structures, except in the case of existing structures which are scheduled for demolition. Mechanical oscillators can be attached to the floors of such structures and they can be resonated to the point of light to moderate damage. However, it is not often that condemned structures of the proper type can be found and permission be obtained for the testing. In the author's opinion, a reasonable facility for testing masonry structures today would be a platform 12m x 12m, with a capacity in the range 100 to 200 tons.

It can be argued that since large scale testing is expensive, the testing facilities should be sophisticated so as to provide as much knowledge as possible for each dollar spent. This is good reasoning, but the initial outlay for the testing facility, and the staffing and maintenance costs represent a major hurdle.

Proposed for consideration here is simply an enlarged version of the 20-ton facility which has been described. Shortcomings of the facility can easily be pointed out: (1) It is not possible to generate a realistic earthquake motion to create significant resonance in a structure. Only widely separated pairs of pulses are possible, and these are influenced to some degree by the properties of the structure under test. (2) Vertical accelerations and independent transverse horizontal accelerations cannot be generated. (3) Soil-structure interaction and the effect of travelling waves through the foundation cannot be studied. (4) There is much uncertainty in predicting how a structure would behave during a prescribed earthquake from observation of the behavior of only a part of it or of a scaled down model of it during these simple tests. This latter shortcoming is true of all testing today.

The advantages of such a facility are: (1) low initial cost, (2) low maintenance and staffing requirements, and (3) low level operating

technology. The chief benefits of the testing would probably be: (1) the discovery of unexpected structural weaknesses and modes of failure, (2) the opportunity to experiment with new constructional features intended to improve earthquake resistance, (3) the opportunity to compare the strengths of structures employing new materials, techniques, and designs with strengths of present construction, (4) the gaining of a better idea of the extent of damage that might be caused by earthquakes of a certain intensity, and (5) the gaining of general knowledge that would advance the state of the art of earthquake resistant design.

The test platform would be built around several wagons placed side by side on several sets of rails embedded in a concrete slab. The wagons would be shimmed to a common height, and the original spring mountings retained. The rolling dead load would consist of several wagons rigidly connected side by side. As an alternative to excitation by impacts from wagons rolling down inclines, it might be possible to simply bring the platform wagon up to a prescribed speed by means of a power winch and then permit it to impact massive abutments. Many wagons in use today are about 12m long and are rated at 50 to 60 tons live load. It is believed that five such wagons side by side could carry 150-ton structures and impart base accelerations up to 2g. It is recommended that used wagons and rails be purchased to reduce costs, and that the facility be located in an area which has a long construction season and in which the level of masonry construction activity is high.

SUMMARY

A simple shock facility made from used railway equipment, capable of destroying 20-ton masonry structures with acceleration pulses of up to 2g, has been described. Results were presented from one set of tests in which four half-scale one room low grade masonry houses were shaken to destruction. It was pointed out that this type of facility has many shortcomings, but its simple technology and low cost are attractive features. Useful observations resulted from the tests described in spite of their simplicity. It was proposed that a similar but larger facility of capacity 100 to 200 tons be constructed for testing large scale models or full scale portions of masonry buildings. It is believed that use of such a facility will bring more realism into the methods of earthquake resistant design.

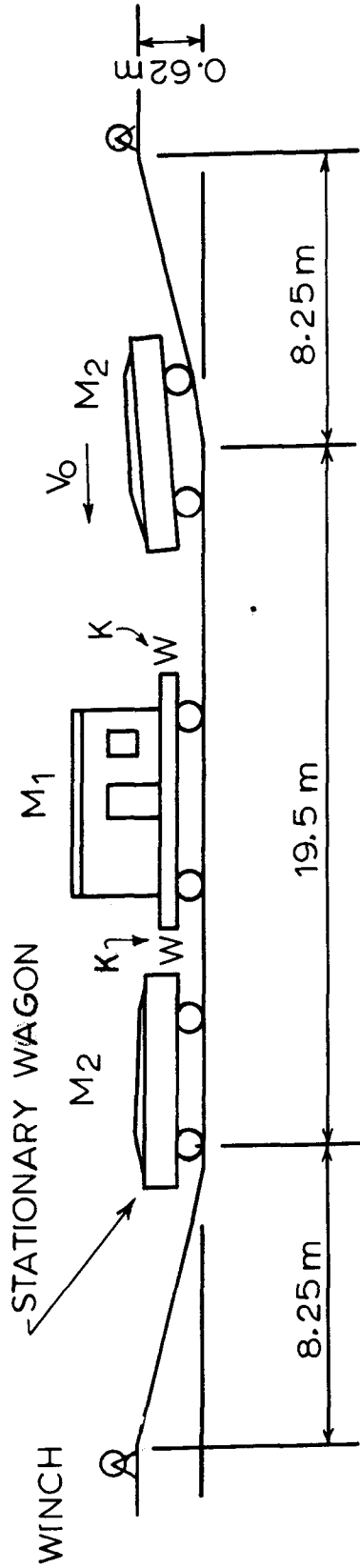
ACKNOWLEDGMENT

The 20-ton capacity facility was constructed at the School of Earthquake Engineering, University of Roorkee, Roorkee, U.P., India, where the author worked as an Indo-American Fellow in 1976-1977, in a program sponsored by the Indo-U.S. Subcommittee on Education and Culture. Funds for construction were provided by the University of Roorkee, the Fellowship program, and the U.S. National Science Foundation, which also paid for round trip travel to India for the author's family. The staff of the Earthquake Engineering School assisted in all phases of the work. M. Qamaruddin, a research scholar in the Earthquake Engineering School, supervised the design and construction of the test structures as a portion of his thesis work.

Table 1. Acceleration of the Shock Table

Shock	Direc- tion From	Dead Load Wagon Position	Maximum Horizontal Acceleration			
			initial impact		rebound	
			s. side	n. side	s. side	n. side
1	E	14.5	negligible			
2	E	15.5	0.22 g	0.20	0.14	0.10
3	E	15.5	0.40	0.34	0.30	0.29
4	W	15.5	0.51	--	0.47	0.36
5	W	15.5	0.57	0.47	0.46	0.37
Transverse walls of PM cracked						
6	E	17	1.05	0.78	0.96	--
Base crack all around PC, shear wall cracks in PM, RM						
7	E	17	0.83	0.84	0.71	0.84
Transverse walls of PC bending, foundation cracks in RM						
8	W	17	Power failure			
PM demolished, small cracks in RC						
9	W	17	1.24	1.18	1.16	1.01
All walls of PC have wide cracks						
10	W	17	--	0.22 vert	--	--
PC demolished, large foundation cracks in RM						
11	W	17	--	0.19 vert	--	--
12	W	17	--	0.32 vert	0.97	--
13	W	17	1.26	0.36 vert	1.06	0.55 vert
14	E	18	1.30	1.27	1.30	1.46
RM demolished						
15	E	19	1.85	0.49 vert	1.40	0.31 vert
16	E	19	1.84	0.30 vert	1.52	0.30 vert
17	E	19	1.78	0.21 vert	1.45	0.18 vert
18	E	18	1.60	1.56	1.36	1.47
19	E	19	1.95	1.83	1.68	1.63
RC demolished.						

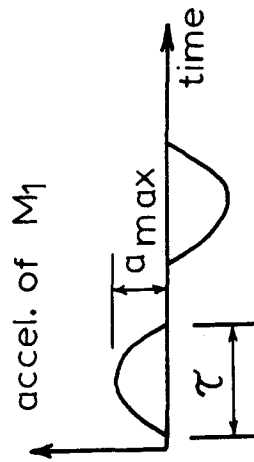
Mortars: PM: plain mud, PC: plain cement, RM: reinf. mud, RC: reinf. cement



Treating M_1 AND M_2 as rigid

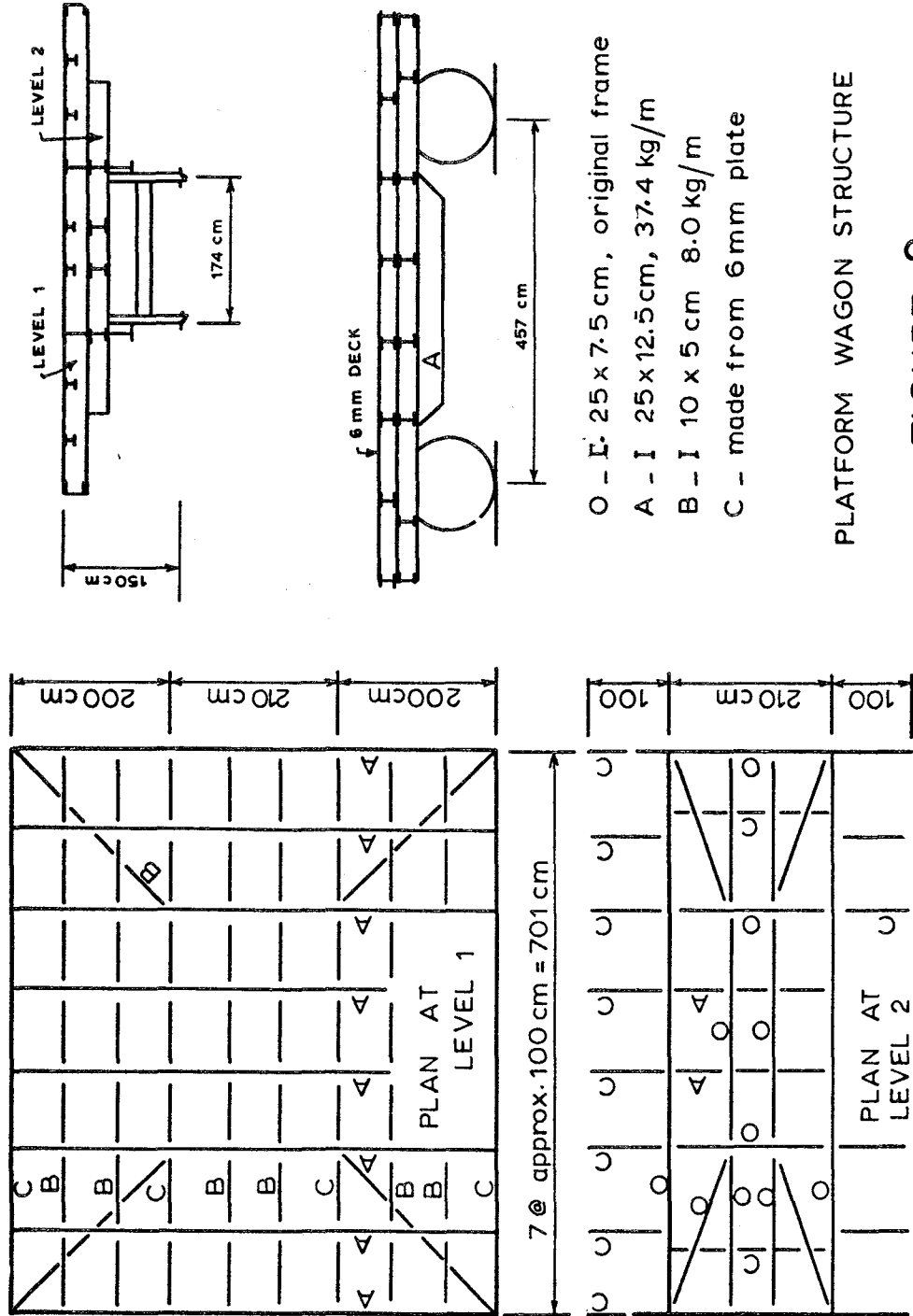
$$\tau = \frac{\pi M_1 \sqrt{\alpha}}{\sqrt{KM_1(1+\alpha)}}, \quad \alpha = \frac{M_2}{M_1}$$

$$a_{max} = \frac{\tau V_0 K}{\pi M_1}$$



Railway Wagon Shock Test Facility

FIGURE_1



- O - I: 25 x 7.5 cm, original frame
- A - I 25 x 12.5 cm, 37.4 kg/m
- B - I 10 x 5 cm 8.0 kg/m
- C - made from 6 mm plate

PLATFORM WAGON STRUCTURE

FIGURE_2

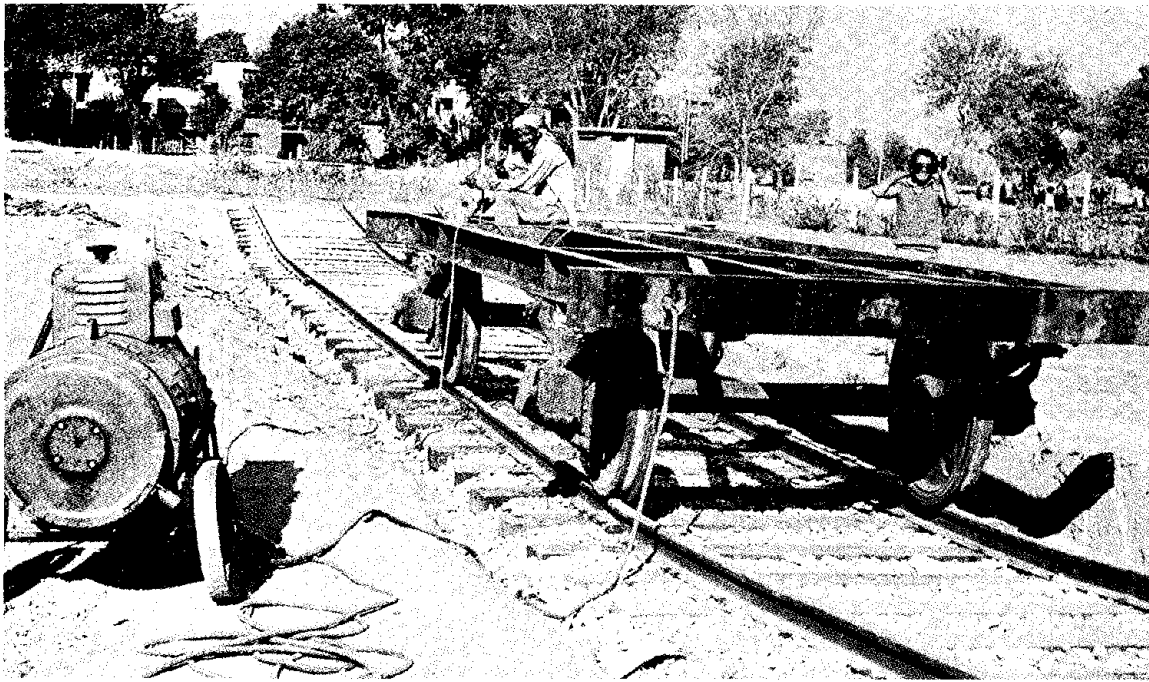


FIG. 3.-Original Wagon Frame

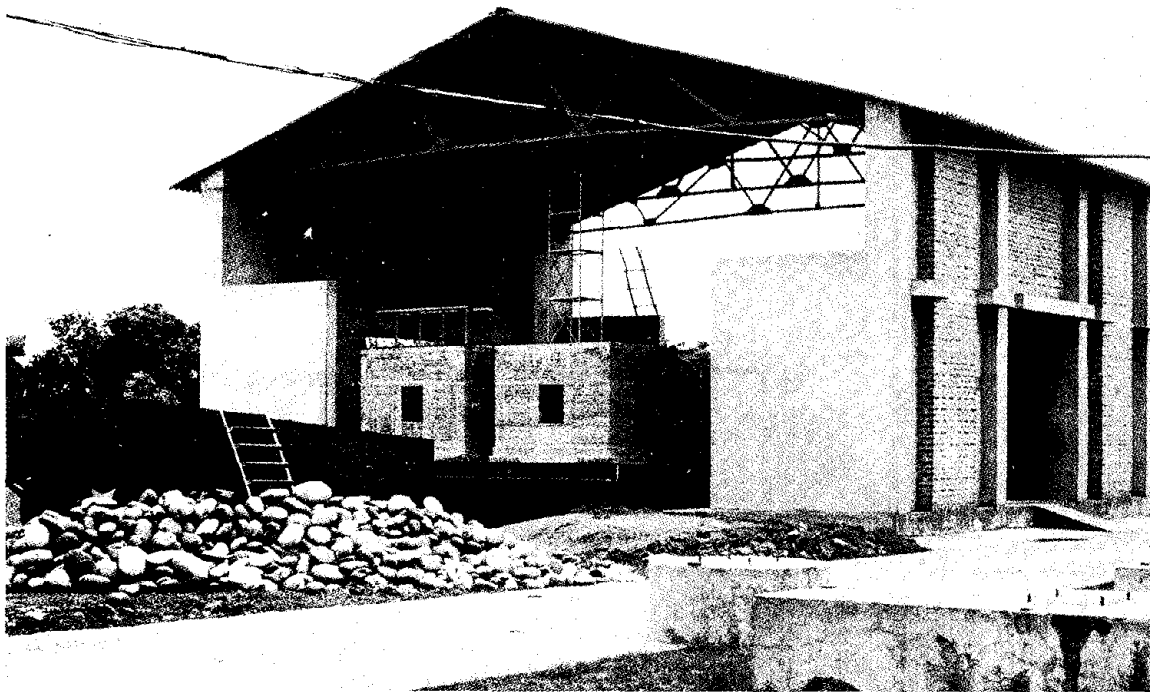
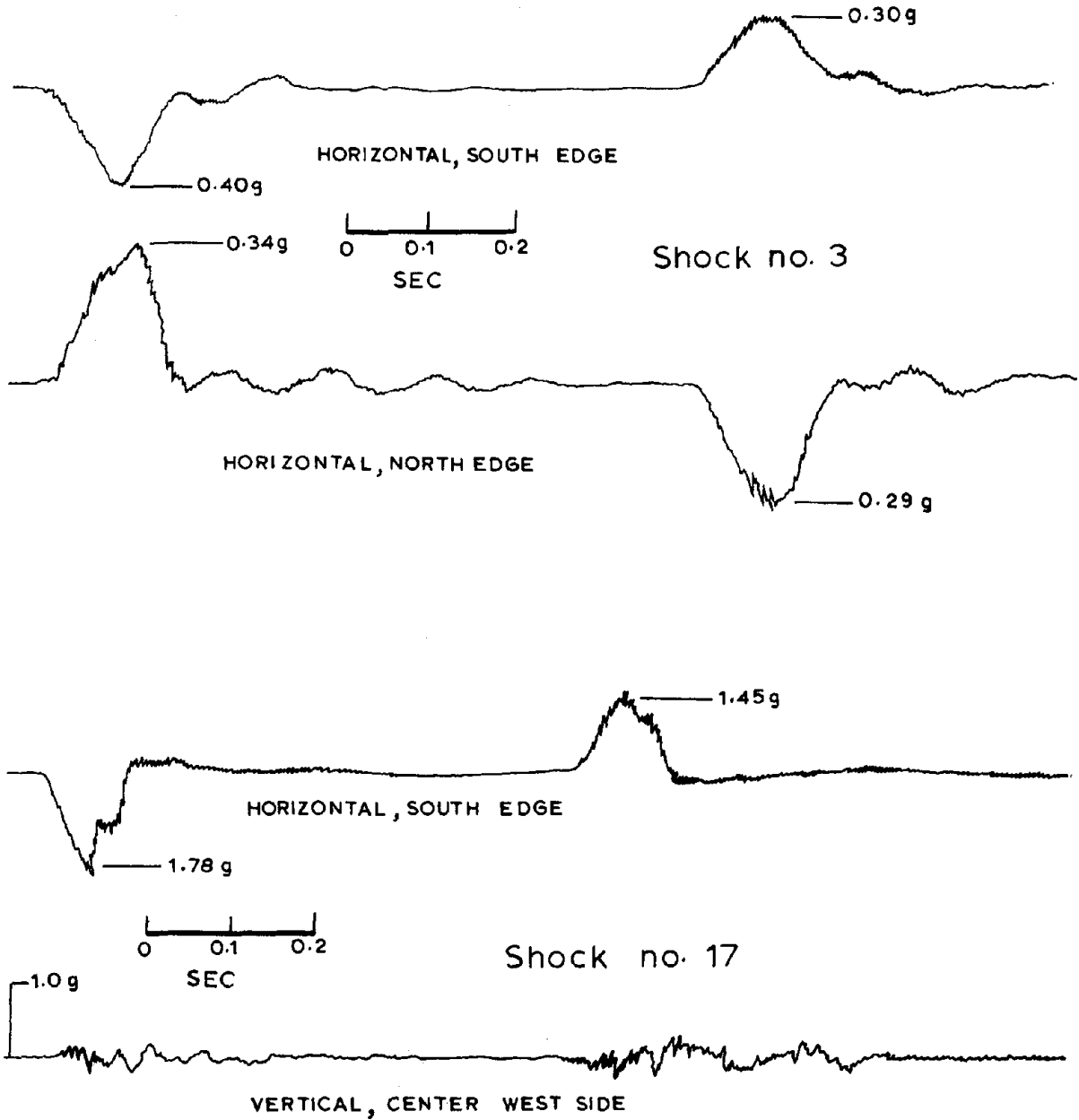


FIG. 4.-Facility Near Completion



ACCELERATIONS OF PLATFORM
(Traced)

FIGURE_5

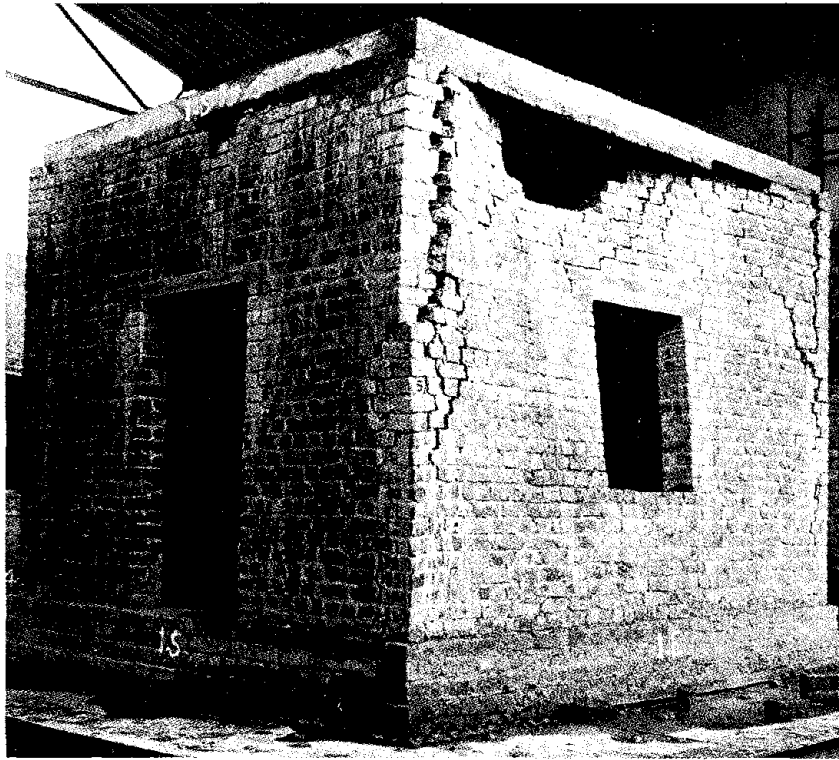


FIG. 6.-Unreinforced Mud Mortar, Transverse Wall

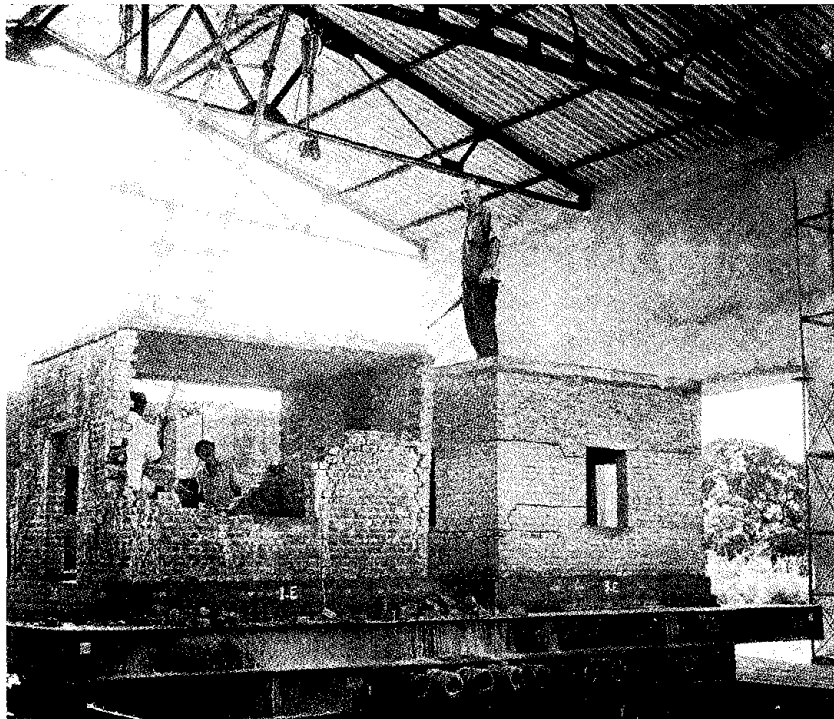


FIG. 7.-Removing Slab From Unreinforced Mud Structure

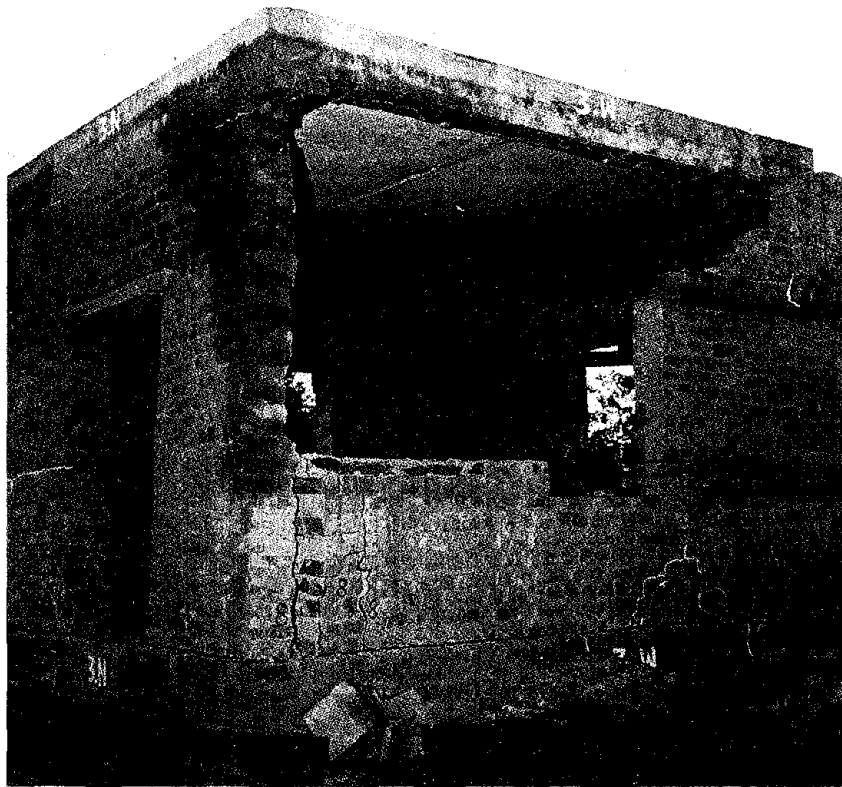


FIG. 8.-Unreinforced Cement Mortar, Transverse Wall

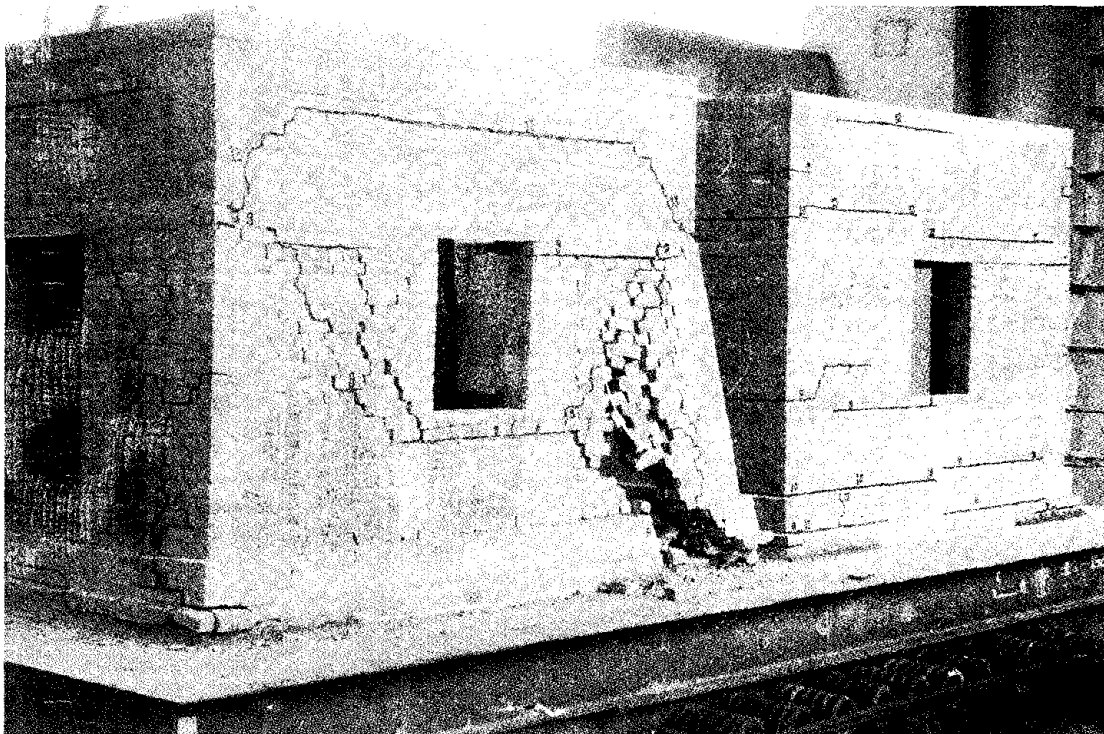


FIG. 9.-Reinforced Mud Failure, Reinforced Cement Standing

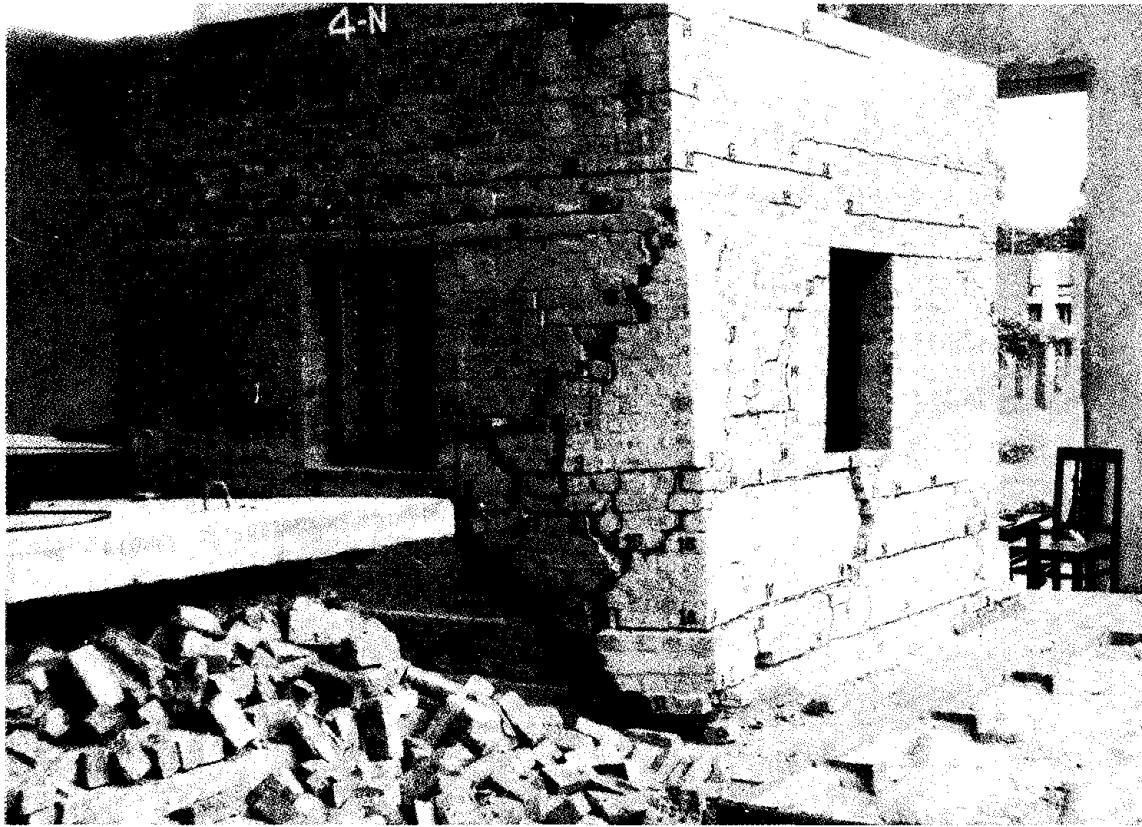
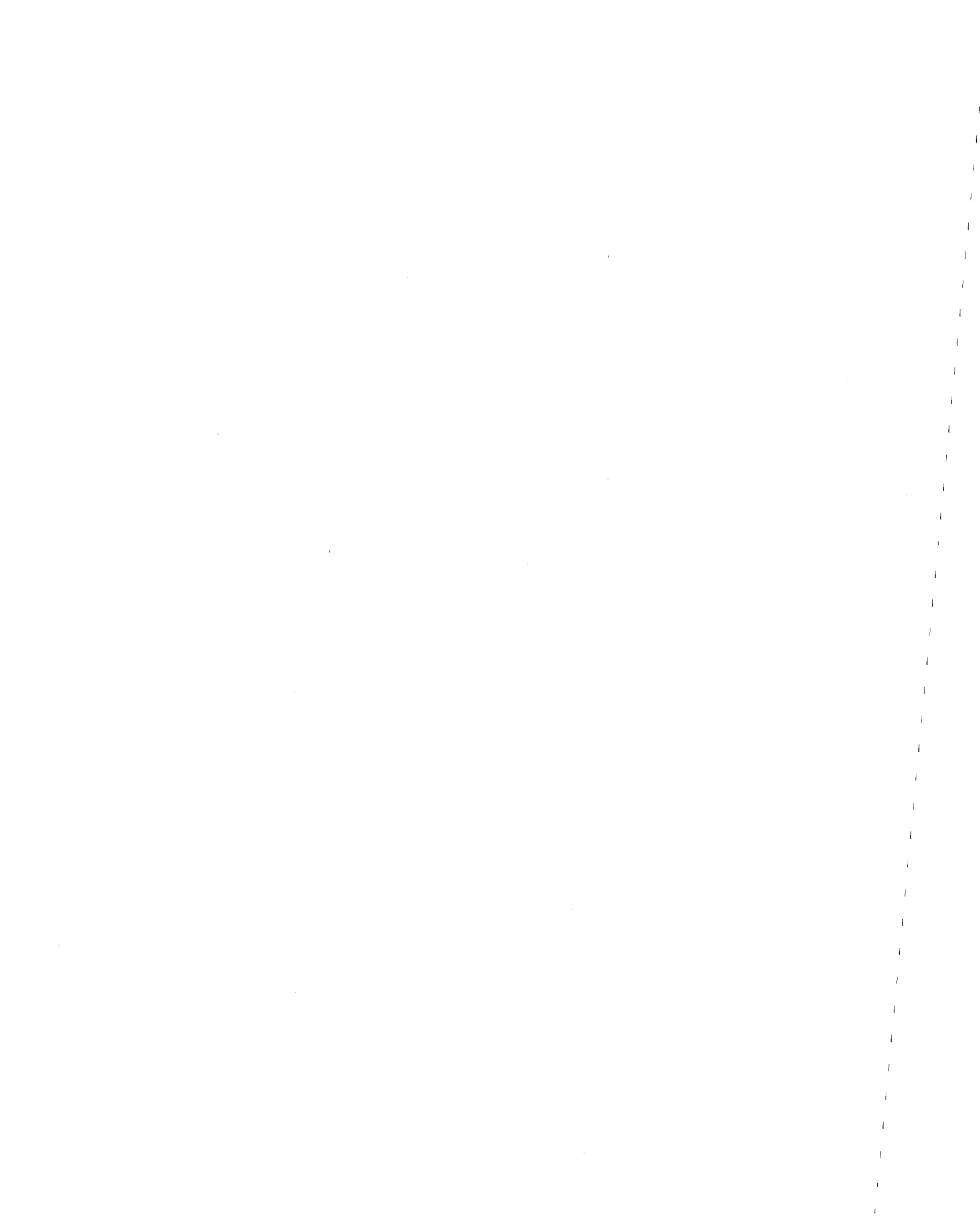


FIG. 10.-Failure of Reinforced Cement Mortar Structure



AN INVESTIGATION OF THE DYNAMIC RESPONSE OF THE PARK LANE TOWERS TO EARTH-
QUAKE LOADINGS.

By Medearis, K.

ABSTRACT: The Park Lane Towers complex is located in Denver, Colorado, and currently consists of four high-rise towers. Each of the towers is about 206' high, having twenty main levels above ground plus a two-level penthouse. These high-rise structures are somewhat unique because of their predominantly reinforced masonry construction. In order to learn more about the dynamic response of such structures to earthquake loadings, the Colorado Masonry Institute engaged Kenneth Medearis Associates to perform an applied research study of the Park Lane Towers. Modern, computer-oriented analysis techniques, wherein mathematical models of the structures were subjected to earthquake ground motion time-histories, were utilized for the study. Three different earthquake time-histories were used, two having motions corresponding to a Richter magnitude of about 5.6, and the other, magnitude 7. The former are appropriate for the Denver area, with the latter being relatable to more seismically severe locations, such as Southern California. The magnitude 7 earthquake was utilized to determine how the Towers would respond to ground motions much larger than anticipated in the design. This paper describes the Park Lane Towers dynamic response studies.

AN INVESTIGATION OF THE DYNAMIC RESPONSE
OF THE PARK LANE TOWERS TO EARTHQUAKE LOADINGS

By Kenneth Medearis¹

INTRODUCTION

The 20 story Park Lane Towers in Denver, Colorado, are among the tallest load-bearing masonry buildings in the world. There are four towers in all, each about 206' high. As such, these significant structures were designed to satisfy a number of pertinent criteria, including the withstanding of static lateral forces associated with earthquake and wind in accordance with the provisions of the Uniform Building Code (UBC).

The Colorado Masonry Institute, recognizing the growing acceptance of the dynamic analysis of structures subjected to seismic ground motions, engaged Kenneth Medearis Associates (KMA) for an applied research study of the Park Lane Towers. The scope of the original research included dynamic analyses of the Towers for earthquake ground motions that might be experienced in the Denver area, micro-vibration measurements of the structure dynamic characteristics, and interpretation of results. In addition, three permanent seismic motion monitoring instruments were installed in the Towers for the purpose of response recording and further study. Subsequent research considered the response of the Towers to a strong motion, Richter magnitude 7 earthquake. The associated responses, as anticipated, exceeded design levels, necessitating a form of non-linear analysis.

DISCUSSION

The response of the Towers is similar to that of a cantilever beam undergoing flexural vibrations. The Towers are essentially identical, thus only one was analyzed. The tower was ultimately modeled as a frame structure, shear and bending deformations being considered for all elements (Figure 1). The precast floor panels were assumed to act only as diaphragms, i.e., rigid in their own plane and flexible normal to that plane.

A comparison of the stiffness and stress distributions for the beam and column frame representation and finite element plane stress models was made to verify the adequacy of the former. A typical beam and column model of an E-W exterior wall, two stories high, was subjected to a static lateral load at the upper level, as indicated in Figure 2. The resultant axial forces, shears, and moments were calculated at mid-height of the second level. These internal forces (Figure 3) were then applied as loadings to a plane stress finite element model of the portion of the structure below, as depicted in Figure 4. The applied axial force was distributed uniformly over the piers, the moments linearly, and the shears

¹Principal, Kenneth Medearis Associates, Research, Engineering, Computer Consultants, Ft. Collins, Colorado.

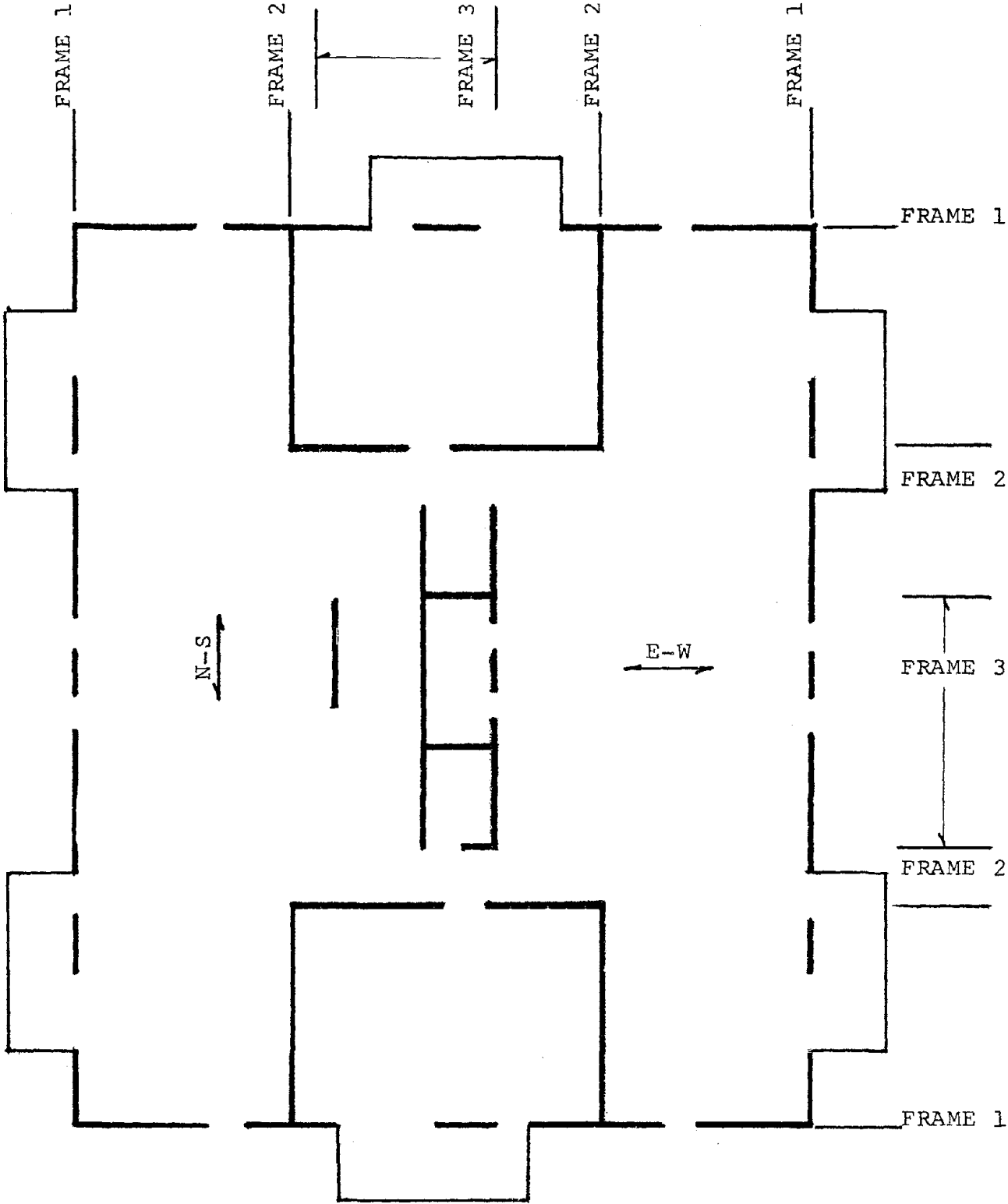


FIGURE 1. FRAMING PLAN

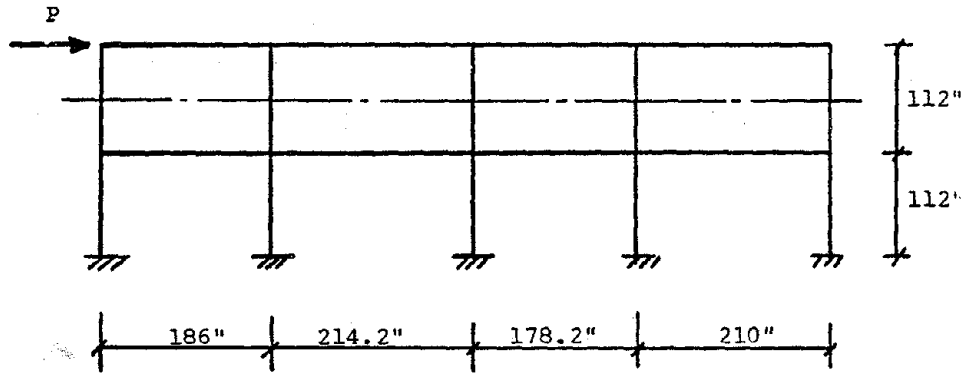


FIGURE 2. BEAM AND COLUMN SUB-STRUCTURE

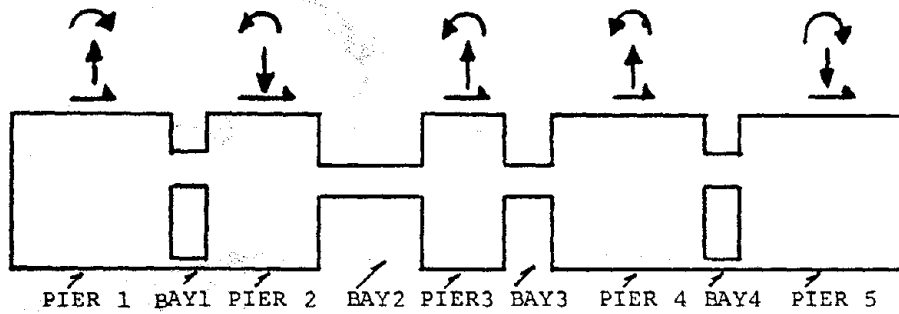


FIGURE 3. FINITE ELEMENT SUB-STRUCTURE

quadratically. The resulting displaced configuration of the finite element model is depicted in Figure 5. The lateral stiffness was considered to be the ratio of the shear force to the displacement, the obtained results being as follows:

	<u>Displacement</u>	<u>Stiffness</u>
Beam and Column Model	.191"	52,300 kips/inch
Finite Element Model	.190"	52,300 Kips/inch

The beam and column model is clearly adequate.

The most critical area for stresses was found to be in the short beams above and below openings. Those stresses, for the two models, were thus compared, the agreement being found to be excellent. The beam and column model was thus deemed sufficiently accurate for analysis purposes.

ANALYTICAL RESULTS

Computer runs were made for earthquake motions occurring in the direction of both major structure axes directions using story masses derived using either dead load or dead load plus 1/2 live load. The UBC seismic design method recommends using only dead load in obtaining lateral forces. However, it is more realistic to recognize that, during most of the lifetime of a structure, a certain amount of live load will be present, and that a substantial portion of this load may be assumed fixed to the structure. The most probable loading is a combination of dead load plus some fraction of the design live load. It is believed that responses determined using dead load and dead load plus 1/2 live load bracket the most probable results. It is generally true that an increase in loading corresponds to more critical static stress states in a structure. However, this is not necessarily the case for dynamic stresses. A change in mass usually alters the nature of dynamic response, and may increase or decrease its amplitude. This is in contrast with the UBC method of static seismic analysis wherein lateral forces are proportional to the assumed weights. Accurate assessment of the weight of a structure is thus more important in dynamic analysis because one cannot rely on certain assumptions being conservative or non-conservative.

Initial response calculations were made using uncracked sections, dead load only, and ground motions corresponding to a 5.6 Richter magnitude earthquake. The results indicated high stress levels, thus the cracked member section concept was utilized for subsequent calculations. This reduced stiffness was accompanied by a corresponding reduction in some frequency and response levels. The first five natural frequencies for the cracked section models, in cycles/second, are as follows:

	f_1	f_2	f_3	f_4	f_5
N-S, DL + $\frac{1}{2}$ LL	.902	3.589	7.800	13.049	19.417
N-S, DL	.908	3.651	8.195	13.781	20.069
E-W, DL	.799	3.231	6.923	11.157	15.900
E-W, DL + $\frac{1}{2}$ LL	.738	2.979	6.403	10.314	14.695

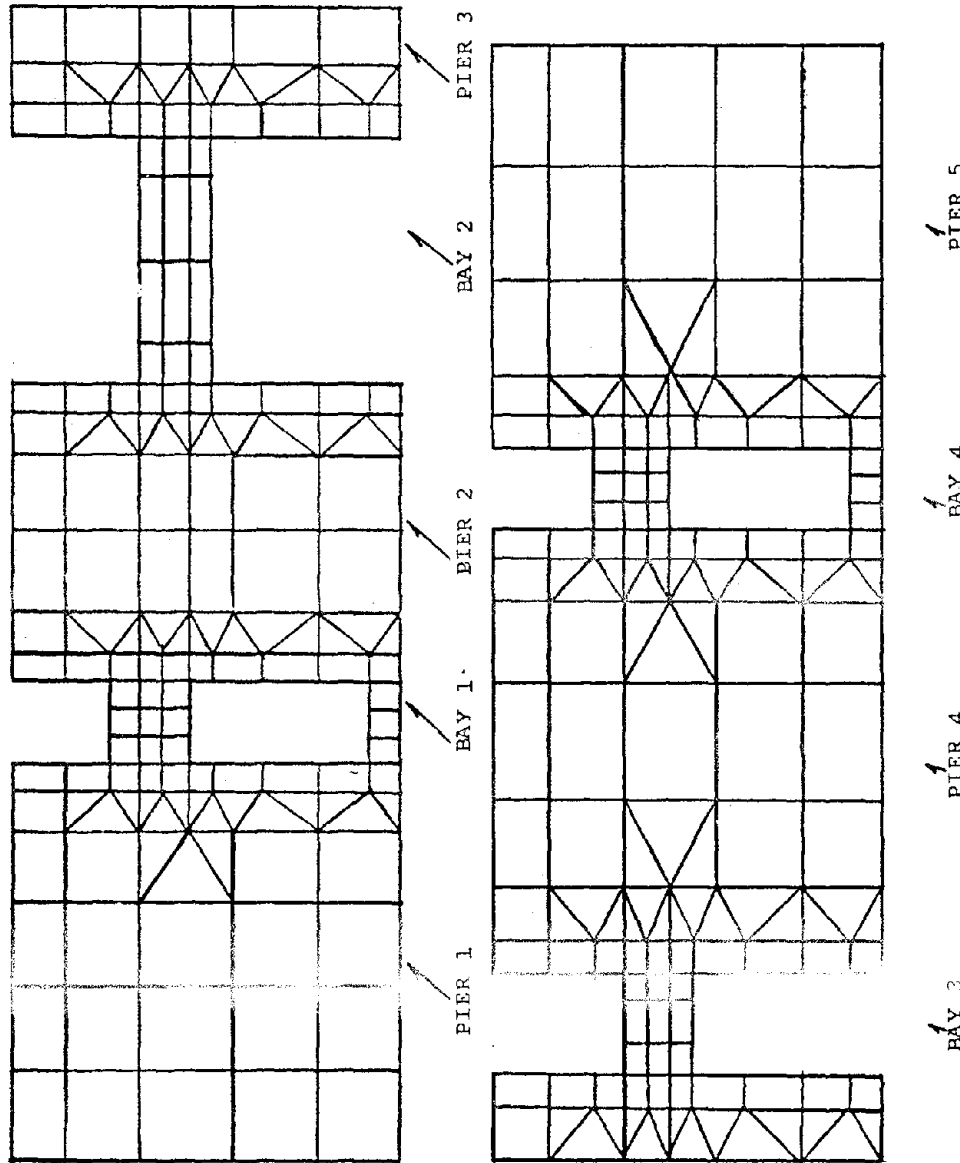
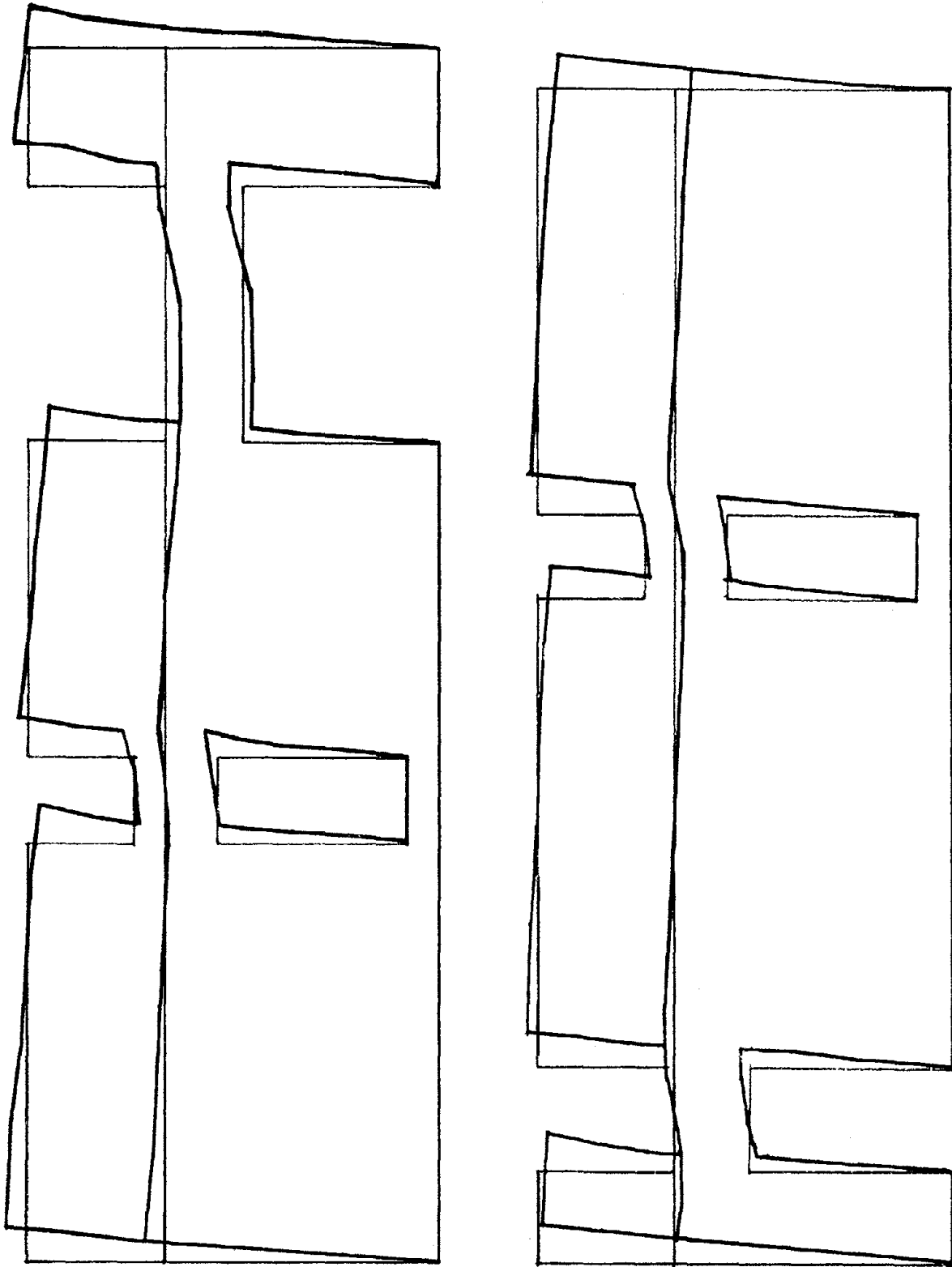


FIGURE 4. PLANE STRESS FINITE ELEMENT MODEL -
 321 NODE POINTS - 337 ELEMENTS

FIGURE 5. FINITE ELEMENT MODEL - DISPLACED CONFIGURATION



The first four normal modes of vibration for the E-W direction, dead load only, are given in Figure 6.

Envelopes of maximum story displacement and moment for earthquake E-1 (magnitude = 5.6) acting in the E-W direction are plotted in Figures 7 and 8. These envelopes represent the maximum values that occur at a given level over the entire ground-motion time history and do not necessarily occur at the same time. It may be noted the UBC response levels are significantly lower in all cases. Also, the dead load and dead load + 1/2 live load dynamic response curves are similar in magnitude and character.

EXPERIMENTAL EFFORT

An experimental effort was also carried out in conjunction with the dynamic earthquake analysis of the Park Lane Towers. This effort consisted of taking measurements of the tower micro-vibrations at various levels in the directions of its principal axes. To elaborate, all structures are constantly moving, or vibrating, even on calm days. Such movements were monitored on the Park Lane Towers using a sensitive vibration instrument, typical motion records being given in Figure 9.

The micro-vibration records were subsequently digitized and computer-analyzed to obtain the natural frequencies of the structure. The first five frequencies, in cycles/second, were found to be

	f_1	f_2	f_3	f_4	f_5
N-S	1.3	4.2	8.0	13.7	20.7
E-W	1.2	3.7	6.9	13.7	20.2

These values are in reasonable agreement with those computed theoretically using cracked sections models. However, results for the uncracked sections model are clearly more appropriate for comparison with the micro-vibration (micro-motion) results. The first five natural frequencies for the former are:

	f_1	f_2	f_3	f_4	f_5
N-S, DL + $\frac{1}{2}$ LL	1.13	4.20	8.70	14.07	20.58
N-S, DL	1.14	4.29	8.20	14.88	21.88
E-W, DL	1.05	4.01	8.29	12.95	17.95
E-W, DL + $\frac{1}{2}$ LL	.97	3.73	7.70	12.02	16.67

The agreement between the experimental and uncracked theoretical frequencies is quite good, the latter generally being slightly less. This is probably due to the effects of nonstructural elements, such as partitions, which contribute additional stiffness to the structure. Much of this stiffness would probably be lost through local failure during high amplitude response, however.

The results of the experimental investigation were deemed to be quite significant because they provided verification of the adequacy of the

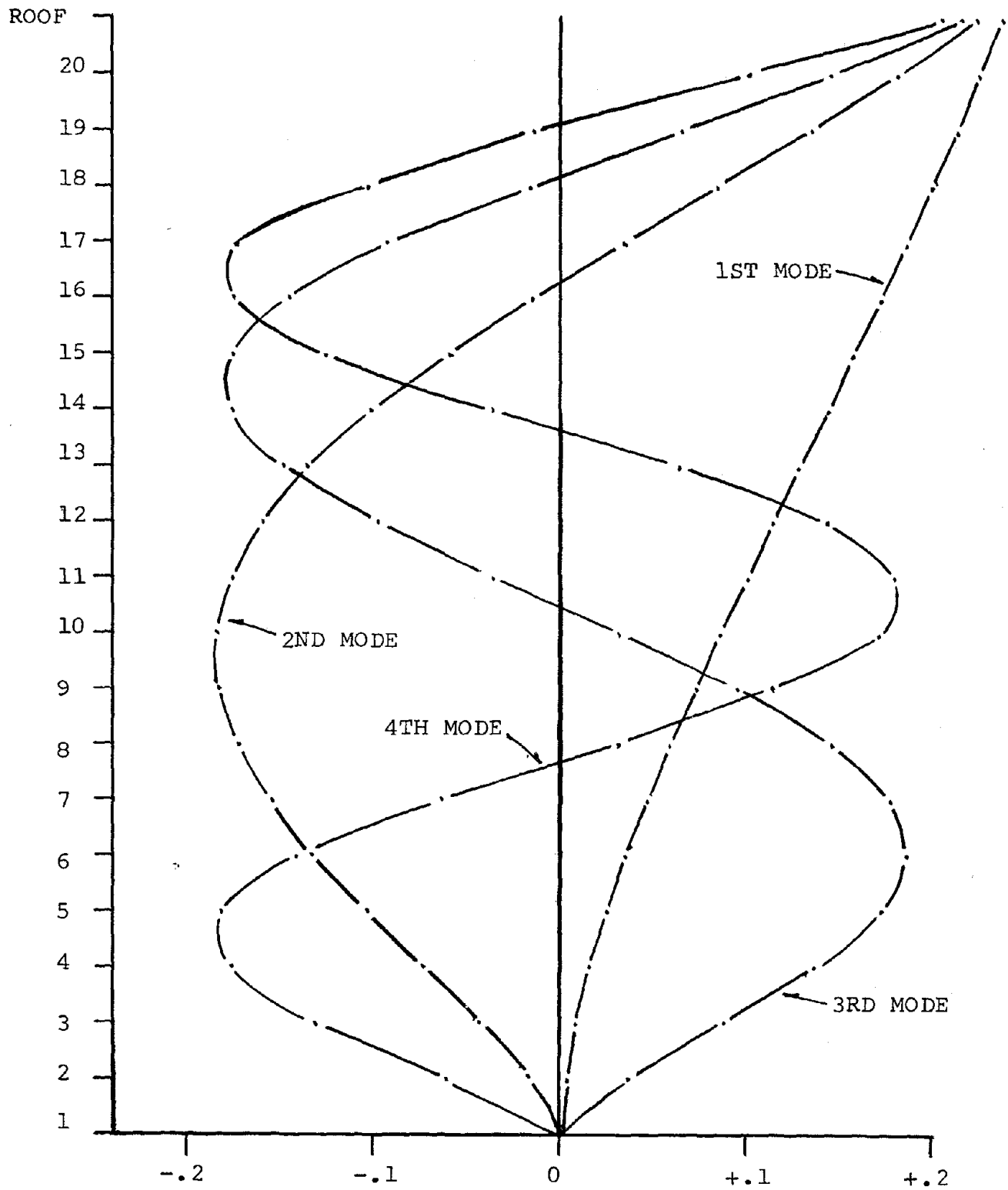


FIGURE 6. TYPICAL NORMAL MODE SHAPES - E-W DIRECTION

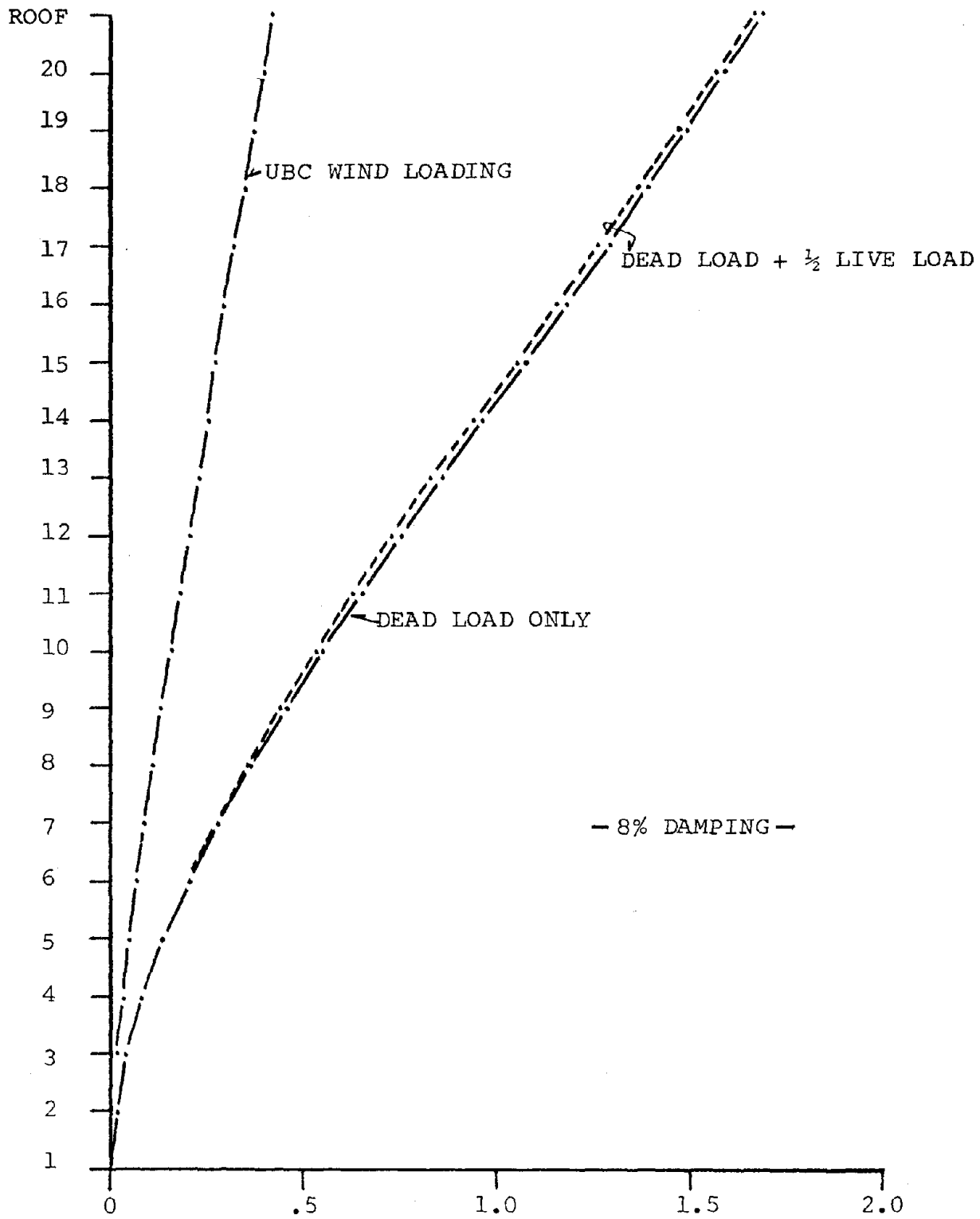


FIGURE 7. MAXIMUM STORY DISPLACEMENTS, INCHES -
E-W DIRECTION, EARTHQUAKE E-1

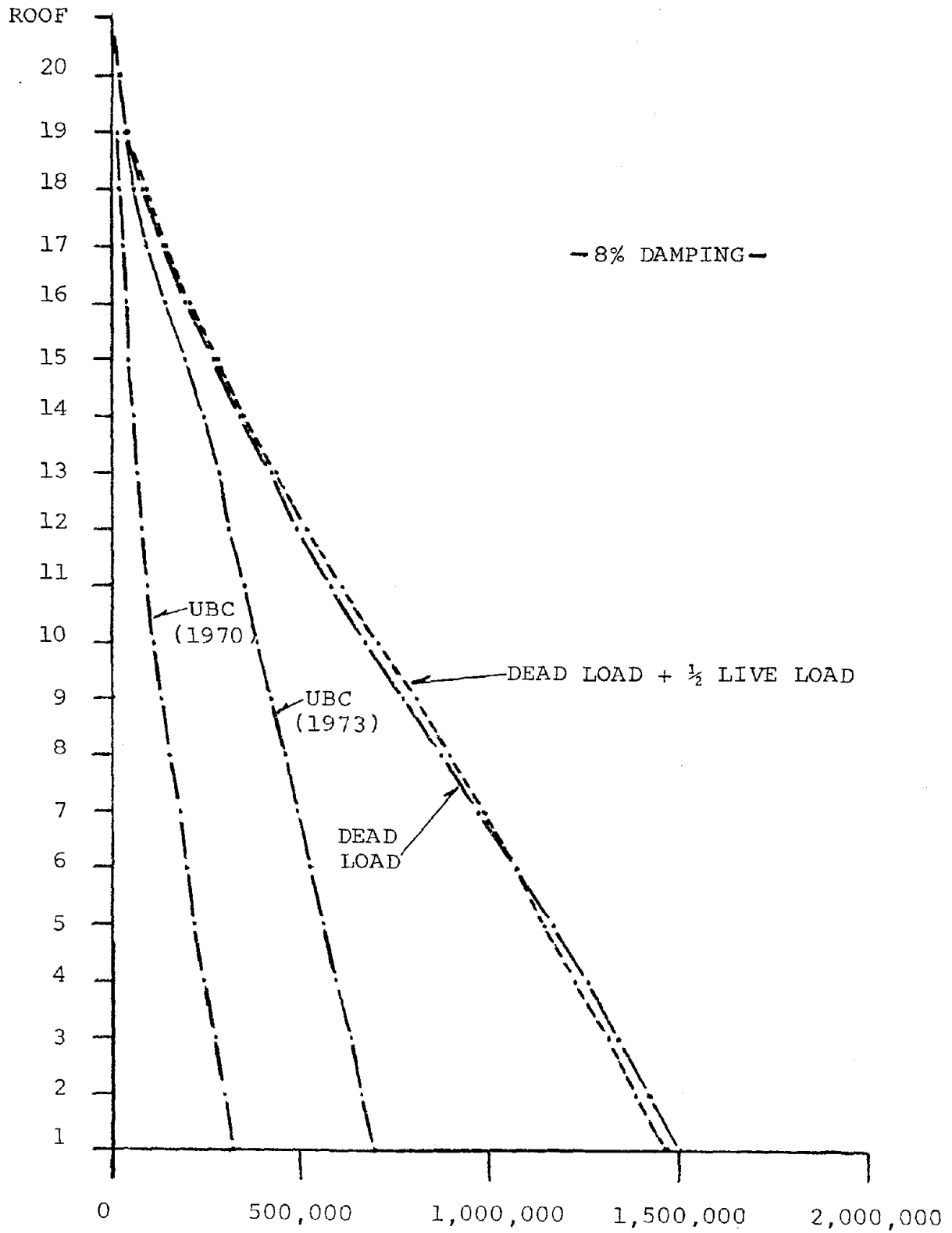


FIGURE 8. MAXIMUM STORY MOMENTS, INCH-KIPS - E-W DIRECTION,
EARTHQUAKE E-1

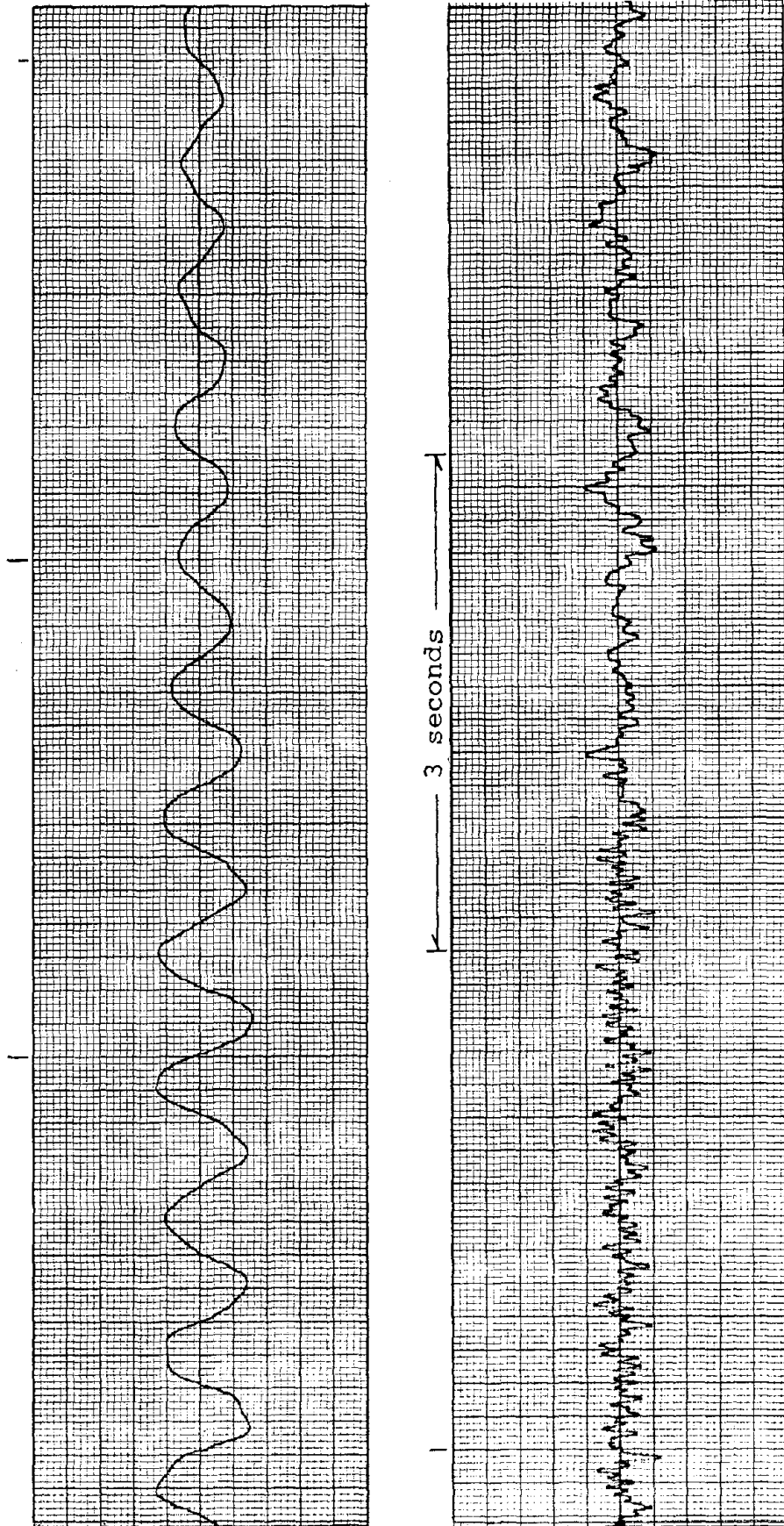


FIGURE 9. TYPICAL MICRO-VIBRATION MEASUREMENT TRACES -
PARK LANE TOWERS

analytical model and assumed elastic properties.

STRONG MOTION RESPONSE

The response of the Park Lane Towers to a strong-motion earthquake was evaluated as a corollary effort of interest. The higher level ground motions utilized correspond to an earthquake, herein referred to as BE-1, having a Richter magnitude of about 7. This seismic level is considered to be quite excessive for the Denver area, being more appropriate for areas of major seismic risk, such as California. The associated response levels, of course, exceed those anticipated in the design of the structures, thus the analysis results should not be construed as reflecting the adequacy of the buildings with regard to sustaining the normally anticipated seismic loadings.

The analytical model was initially based on linear load-deformation relationships, although there was little doubt that stresses would be in the yielding, non-linear range. This indeed proved to be the case. However, the obtained results provided valuable insight, especially in regard to the possible upper bounds of the response. Configuration of frames and elements was identical with that previously utilized (Figure 1). The somewhat hypothetical, elastic, responses of the E-W model, with dead load only, to the original (E-1) and higher (BE-1) ground motions are compared in Figure 10.

Overstresses associated with the E-1 earthquake, lesser ground motions, were mainly limited to the spandrel and header beams. The response of the model to the BE-1 ground motions was indicative of more extensive yielding in both beam and column sections. Damping values as high as 16% may be obtained where considerable cracking has occurred, and that value was deemed reasonable for this investigation.

Considerable yielding of structural members was apparent even at the higher damping level. Information concerning the non-linear, cyclic-loading characteristics of reinforced masonry is currently not available, thus an iterative analytical procedure was utilized to obtain approximate, but realistic, response results. In this analysis, member areas and inertias were changed in accordance with the overstress condition indicated by the results of each iteration, and the response recalculated. Convergence of results was usually obtained in less than 10 iterations. In the final configuration, plastic hinges had formed in all exterior wall spandrel beams and a number of columns. The yielded exterior wall columns are graphically depicted by the cross-hatched areas in Figure 11. No beam or column exceeded its estimated ultimate load-carrying capacity, thus, despite the formation of plastic hinges throughout the structure, general collapse was not indicated.

The change in lateral stiffness also had a significant effect on the vibrational characteristics of the structure. The values of the first five natural frequencies, in cycles/second, of the original and reduced stiffness E-W models (DL only) clearly illustrate this effect. They are

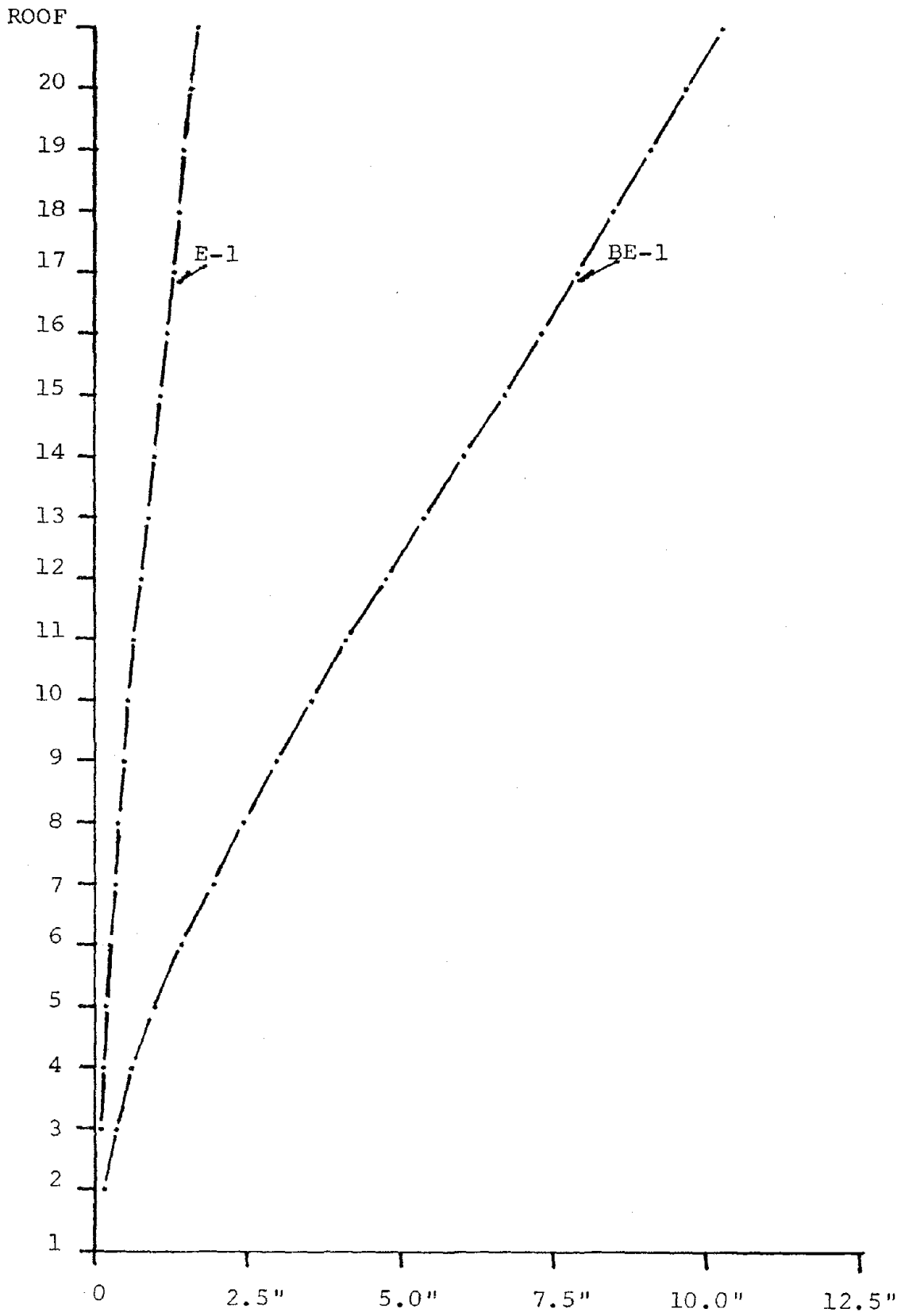


FIGURE 10. MAXIMUM STORY DISPLACEMENTS, INCHES - 8% DAMPING,
E-W DIRECTION, DEAD LOAD ONLY

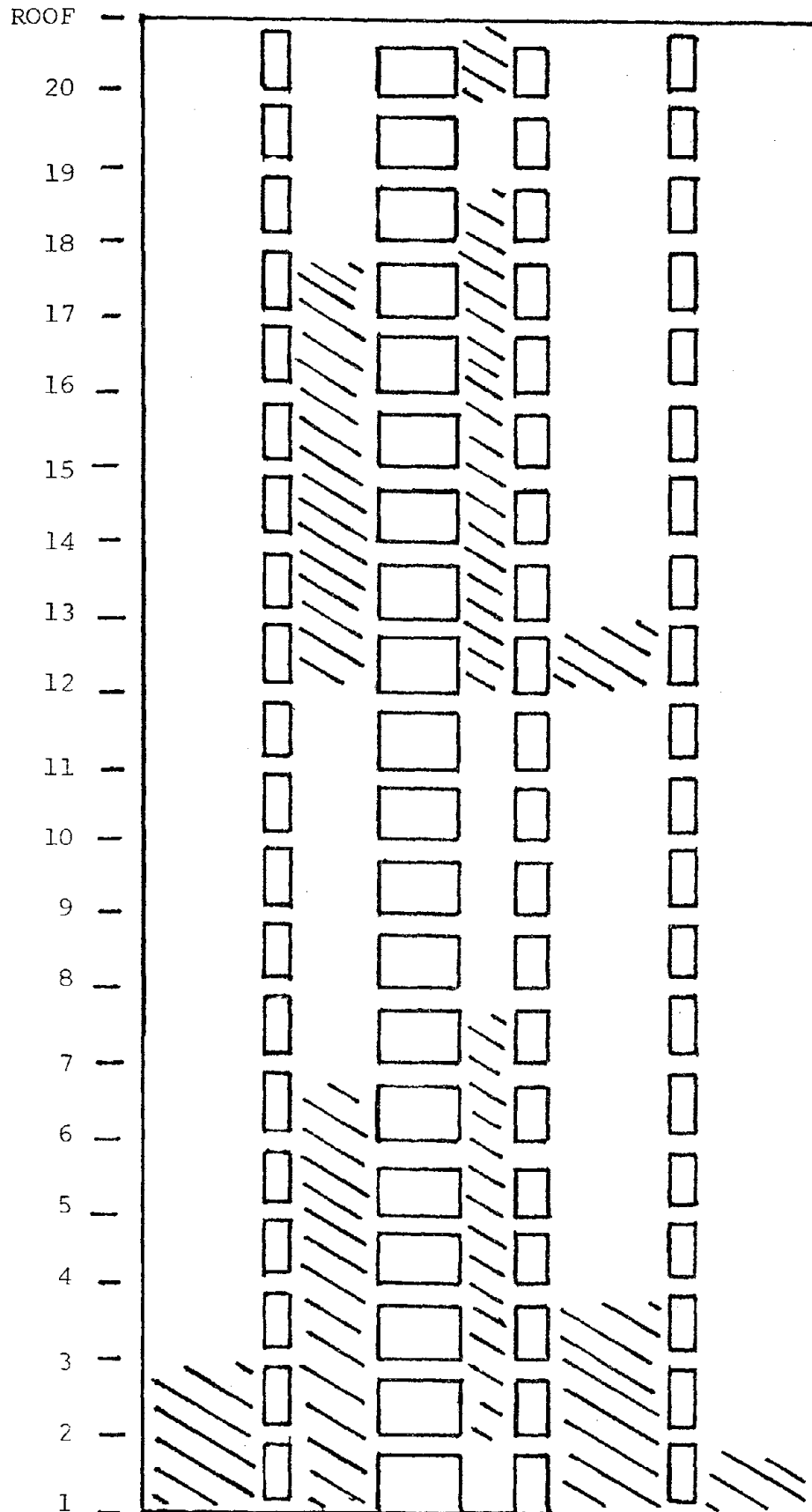


FIGURE 11'. EXTERIOR YIELD ZONES - EARTHQUAKE BE-1, E-W DIRECTION,
DEAD LOAD + $\frac{1}{2}$ LIVE LOAD, 16% DAMPING

given below:

	f_1	f_2	f_3	f_4	f_5
Initial Stiffness	.799	3.231	6.923	11.157	15.900
Reduced Stiffness	.399	1.657	3.650	5.995	8.621

SUMMARY COMMENTS

One of the Park Lane Towers has been dynamically analyzed for earthquake loadings that might reasonably be expected to occur in the Denver area. The predominantly reinforced masonry wall construction of these high-rise structures make them somewhat unique. Modern computer-oriented analysis techniques were utilized throughout the investigation. These were supplemented with experimental verification measurements taken using sensitive vibration monitoring instruments. The experimental results were found to be in good agreement with those obtained analytically.

As anticipated, some structural members were found to be overstressed under dynamic earthquake loading; others were not. The former result is somewhat typical for structures designed to Uniform Building Code (UBC) static seismic requirements. Of importance is the fact that overstresses occurred primarily in header and spandrel beams and could probably have been initially avoided at a relatively minor increase in construction cost. It may be noted that some of the overstress conditions would never have surfaced using a UBC static seismic analysis.

A limited study was made of the response of the Park Lane Towers to a strong motion earthquake having a Richter magnitude of about 7, i.e., a motion far more than that for which they are designed. An approximate, non-linear analysis was utilized for that study, but the obtained results are believed to be realistic. The associated response levels, of course, far exceeded those anticipated in the design of the buildings, and extensive yielding of the various structural elements was apparent. The overall results, however, indicate the Park Lane Towers would survive a severe earthquake, although there would probably be some localized material failures. Damage to non-structural components was also deemed probable because of the larger deflections accompanying the strong-motion response. It should be noted that net tensions occurred in certain columns, primarily at the corners. Although the redistribution of such tensions to other structural members merits additional study, it seems clear the specifying of additional wall reinforcing at corners would, in general, be desirable.

The results of this investigation indicate that it is quite feasible to utilize reinforced masonry for high-rise construction in earthquake-prone areas. However, it should be required that such structures, as well as those constructed of other materials, be rigorously analyzed for appropriate earthquake loading using modern dynamic analysis techniques.

Details of the overall research effort are given in:

Medearis, K., "An Investigation of the Dynamic Response of the Park Lane Towers to Earthquake Loadings," a report to, and available from, Colorado Masonry Institute, 3003 E. 3rd Ave. at Milwaukee, Denver, CO 80206.

THE EFFECT OF FLOOR AND WIND LOADS APPLIED SEPARATELY OR SIMULTANEOUSLY
TO TWO-STORY HIGH WALLS

by H. R. Hodgkinson¹

ABSTRACT

The British Ceramic Research Association has, for the past seven years, been carrying out an extensive investigation of the performance of brick walls when subjected to lateral loads arising from wind forces. Most of this work has been on plain storey height walls within framed structures, both with and without window openings.

This paper is concerned with the performance of two-storey high walls as used in domestic accommodation. It describes the structural testing of a number of two-storey high single leaf walls, together with their associated floor and roof timber. This structural testing has involved the simultaneous application of lateral loads to the walls (simulating wind loads) and loads to the floors. The walls have been built of several different types of bricks and of various configurations, both plain and with returns - both bonded and tied. The testing has shown up the shortcomings of some of the metal tying devices widely used in traditional British building practice; as a result of this, improved tying devices have been developed which are also described in the paper.

1. Principal Scientific Officer, British Ceramic Research Association.

THE EFFECT OF FLOOR AND WIND LOADS APPLIED SEPARATELY OR SIMULTANEOUSLY
TO TWO-STORY HIGH WALLS

by H. R. Hodgkinson¹

INTRODUCTION

The British Ceramic Research Association has, for the last seven years, been engaged in a very extensive programme of research to determine the resistance of masonry walls to lateral loading arising from wind forces.⁴ This work has been primarily concerned with infill panel walls in reinforced concrete framed buildings. The largest group of walls in the programme has been plain single leaf walls without openings and built of various combinations of bricks or blocks and mortar and with different degrees of peripheral restraint. A smaller number of two-leaf cavity walls and walls with door and window openings have also been tested.

The infill panel wall is the most vulnerable to damage by wind loading. Structural walls which carry a compressive load are not in general susceptible to wind damage because, as has been demonstrated by earlier work², they behave as 3-pinned arches and the magnitude of the compressive load is sufficient to generate adequate lateral resistance; the strength of the bricks and mortar is largely irrelevant. Walls in single-storey domestic housing, although carrying a compressive load arising from the roof weight, are vulnerable because in the worst wind loading condition there is a suction on the roof which effectively removes the precompression on the wall. Similarly in two-storey domestic housing, which is the most common in the United Kingdom, the upper storey behaves like the single storey building. The lower storey loading is somewhat more complicated because the wall carries the compressive load of the upper storey wall, possibly the roof load and the first-floor dead and imposed load which may be applied eccentrically, when, depending on whether the wind load on the wall is positive or negative, the floor load may act on the wall to augment or partially offset the wind loading.

This paper describes a number of tests on various configurations of two-storey high walls built in combination with roof and floor timbers, and to which lateral, floor and roof loads were applied.

BASIS OF EXPERIMENTATION

A total of eight walls have been built and tested so far, using three different bricks and one mortar, 1:1:6 Portland cement:lime:sand. All but the first of the walls, which was exploratory in nature and has previously been reported³, were built within a very rigid steel space frame, which provided support for the outboard ends of the floor joists, and also provided the reaction against the applied lateral loads. The photograph Figure 1 shows Wall No. 8 in place in the test frame.

1. Principal Scientific Officer, British Ceramic Research Association.

The details of the three bricks are given in Table 1. Bricks 1 and 3 were British Standard-sized bricks, but Brick 2 was a special brick of 140 mm width with the single frog divided into two to provide a hand hold.

Bricks 1 and 2, which were both frogged and of a high water absorption, were laid frog uppermost and had their suction rates corrected to about 1 kg/m²/min before laying.

Three of the walls were plain and approximately 2 m long; the other five had two returns and were approximately 5 m long. All the walls were two-storeys high (2 x 2.6 m) and were complete with floor joists and top restraint. The configuration of the walls is summarised in Table 2. The floor joists were of 225 x 50 mm softwood and were supported in the test wall by joist hangers; in the early tests these hangers were of conventional pattern, but in the later tests were of a modified construction as described later. A floor of 18 mm chipboard was attached to the floor joists. The restraint at the top of the wall was provided by 225 x 50 mm softwood joists, in some cases lying parallel to the wall and in the other cases running at right angles to the wall.

METHOD OF TEST

Lateral loads were applied to the walls using a number of light-weight inflatable airbags connected through a manifold to a compressor. The reaction from these airbags was taken on wooden clad metal frames of the same area as the test walls, and positioned about 20 mm away from the walls. The floor load was similarly applied by airbags resting on the floor and reacting against reaction frames which were tied down to the floor of the laboratory. All the walls were firstly subjected to a floor overload, and then a constant floor load was maintained while an increasing lateral pressure was applied to the wall.

INSTRUMENTATION

The pressures applied to the walls and floors were measured by water manometer. The lateral deflections of the walls were measured by a multiplicity of linear transducers mounted horizontally to bear on the middle of the unloaded side of the wall at the bottom and top and usually every three courses in between; other transducers were mounted along the length of the wall at selected heights. Where applicable, other transducers were mounted to detect any uplift and rotation of the returns. The deflections of the floor joists were monitored by similar transducers mounted underneath the floor. All the linear transducers were coupled to a data logger with punched tape output, from which computer plots of the wall deflections could be derived. In the case of a few of the walls, strain gauges were affixed to measure the compressive and tensile strains arising from the eccentric loading.

RESULTS AND DISCUSSION(a) Plain Walls Without Returns

Walls 1, 3 and 5 were respectively 1.83, 2.0 and 2.0 metres long and without returns. In each case the lateral load was applied to the inner face of the wall. Initially a uniformly distributed floor load of 5 kN/m^2 was applied with no resulting damage to the wall; at this load the deflections of the floor at the middle of a 3.2 m span were 7.4, 8.3 and 6.0 mm respectively. Then a constant floor load of 2.1 kN/m^2 (the design load) was sustained while the lateral load was applied to the wall in increments of 0.5 kN/m^2 . In all three walls the upper storey failed first; at this juncture the air supply to the upper storey airbags was disconnected and the loading to the lower storey continued. The results for all three walls are given in Table 3 and a typical computer plot of the deflection immediately prior to failure (for Wall No. 5) given in Figure 2.

Concurrently with the test walls, wallettes were built for the determination of the ultimate flexural strengths of the brickwork. These wallettes were tested under 4-point loading in such a direction that the direction of tensile stress was at right angles to the bed joint. These values for tensile strength are compared in Table 4 to the ultimate tensile strengths of the upper storeys of the three walls (calculated from the applied pressure), assuming simply supported end conditions. From the table it will be seen that there was no advantage accruing from the use of the wider bricks other than that arising from the greater section modulus. The design lateral load chosen for the walls was 1.0 kN/m^2 , based on B.S. Code of Practice 3:Ch.V:Pt.2.⁴ Clearly in this situation the upper storey walls with only 2 sided restraint could be structurally inadequate, and the remainder of the test walls were built with additional peripheral restraint provided by returns.

(b) Walls with Returns

Wall 2 was 4.5 m long and had two bonded returns at the ends, each 0.9 m long and 102 mm thick. Walls 4, 6 and 8 were each 5.27 m long and had one return 0.55 m long bonded to one end and another return 0.88 m long tied in, approximately 0.8 m from the other end. The leading dimensions and the arrangement of the floor and ceiling timbers are shown in Figure 3. The purpose of the tied returns was to simulate an internal stiffening wall; they were tied to the main wall by Tee-ties (Figure 4) 450 mm long and 3 mm thick, placed every 4 courses. Wall 7 had two 1 m returns which were each tied to the main wall, one 0.16 m from one end and the other 0.71 m from the other end. The floor joists were cut back to a trimmer to represent the staircase well and there were three small windows, two in the lower storey and one in the upper storey.

Walls 2, 4, 6 and 8 represented part of a gable wall including the corner, in which case the maximum lateral load would arise from an external negative pressure and the most onerous loading condition would be this lateral load together with the maximum (dead and live) floor load.

As with the plain walls, an initial floor overload of 5 kN/m^2 was applied, followed by a constant design floor load of 2.1 kN/m^2 with a lateral load applied to the inner face.

The results of all the walls with returns are given in Table 5. For Wall 2, only the strength of the lower storey is reported, because deficiencies in the timber restraint to the top of the wall rendered the value for the top storey meaningless. A typical computer plot for a wall (No. 8) just prior to failure is shown in Figure 5a (top storey) and Figure 5b (lower storey). Walls 4, 6 and 8 are directly comparable because their configurations are identical, apart from the bricks. Their typical mode of failure (Figure 6a) was a more or less horizontal crack near to the top of the upper storey, and a four-sided restraint (back of envelope) crack pattern in the lower storey. As with the plain walls, the results show that the use of the wider brick produces a strength advantage only proportionate to the increase in section modulus. The performance of Wall 4 was superior to Wall 6, but this superiority was less than the disparity between the ultimate flexural strengths of brickwork built of the two bricks, but this is explained by the fact that the strength of the wall is only partly dependent on the strength of the brickwork.

In no case was there relative movement between the tied return and the wall, and the short length of wall beyond the tied return did not crack, thus indicating that the tied return afforded a similar degree of peripheral restraint as the bonded return. In every case the failing pressure of the lower storey was higher than the upper storey, indicating that the eccentricity of the floor load was not adversely affecting the strength of the lower wall, as might have been expected.

Wall No. 7 differed from the other walls with returns in two respects. It was of a much more complex shape (Figure 7), being punctured by three windows and having restraint provided for only part of its length at first floor level, due to the presence of a stair well. In the preceding tests, the most arduous combination of possible loading was a floor load combined with lateral pressure on the inside of the wall (simulating external suction). Wall 7 however represented a section of a gable wall which would not be subject to external suction effects. Reference to British Standard Code of Practice No. 3: Chap. 5:Part 2⁴ showed that wind pressure produced a more onerous loading than suction and so the wall was tested with external load simulating wind pressure together with the minimum floor load of 0.55 kN/m^2 . In addition, a load equivalent to a roof load of 0.88 kN/m^2 was applied by kentledge to the top of the wall.

The wall failed (Figure 6b) as one panel at a load of 4.5 kN/m^2 , and the deflection plots indicated that failure started in the upper storey and spread to the lower. From this it can be assumed that because the eccentric loading occurred close to the buttressing wall positions its effect on the failure of the panel as a whole was small. The design wind pressure for this wall was 0.87 kN/m^2 , so that the partial safety factor was 5.2. The flexural strengths of the brickwork, as determined by tests on wallettes, were 2.26 N/mm^2 and 0.68 N/mm^2 in the two orthogonal directions. Using these values, a partial safety factor for materials of 5.1 was obtained by calculation using the method evolved by Haseltine⁵

for laterally loaded walls. The corresponding minimum required partial safety factor is 2.5. Of the three walls 4, 6 and 8, the upper storey of wall 6 was the weakest element, having a failure load of 3.2 kN/m^2 . In relation to the design wind load of 0.87 kN/m^2 this gave a partial safety factor for materials of 3.6.

(c) The Performance of Tying Devices and Joist Hangers

In the course of this programme of work some of the shortcomings of some of the metal tying devices widely used in traditional British building practice were shown up.

Little research has been done on typical joist hangers or straps when used in conjunction with brick masonry. Manufacturers of such devices have largely confined their testing to production line strength tests in a steel rig, and design has been founded on calculations of strength of the device based solely on the dimensions of the steel, and in isolation from its performance in combination with the masonry. The B.C.R.A. has produced a document ⁶ giving guidance on the design of tying details, based on good current practice, but there is a necessity for an investigation of such criteria as load limits and eccentricities for straps and hangers in actual use in masonry.

It is common practice in the U.K. to provide restraint at the top of a cavity wall by proprietary straps which are typically $30 \text{ mm} \times 5 \text{ mm}$. These are attached to ceiling ties of trussed rafters by woodscrews, pass through the inner leaf and turn down into the cavity to lie alongside the interior face of the inner leaf. They thus provide reasonable restraint to a wall subject to exterior suction, but little restraint to a wall under exterior pressure. In this series of experiments the ceiling ties have been positively fixed to the masonry to provide some degree of restraint against lateral loads in both directions.

For walls 2 and 3 the $30 \text{ mm} \times 5 \text{ mm}$ straps were attached to the masonry by woodscrews inserted into superior quality plastic plugs in the top course of bricks. When the lateral load was applied to the wall the plastic plugs pulled out of the brickwork; for all subsequent test walls (except No. 7) the $30 \text{ mm} \times 5 \text{ mm}$ straps were modified as illustrated in Figure 8 by the addition of a 6 mm mild steel plate welded on, the latter being attached to the brickwork by three woodscrews and two masonry bolts. In the initial stages of Test 4 the woodscrews attaching the straps to the ceiling joists proved insufficient and the straps were increased in length to 1000 mm to permit additional screws. In this modified form, the straps were more than adequate in that they were intact when the brickwork failed, and each was capable of sustaining a lateral load in excess of 5.5 kN without relative movement between the masonry and strap, and between timber and strap.

In situations where the support of floor joists by building into the walls is not appropriate or suitable, it is common British practice to use metal joist hangers. These are in the form of a stirrup in which the joist sits, and with a tongue which is laid in the bed joint of the masonry.

The connection between the wooden joist and the hanger is by a pair of nails or screws passing through holes in either side of the hanger. Tests on the earlier walls in the series showed that under load the woodscrews pulled sideways in the grain of the wood and the connection was grossly inadequate. An improved experimental joist hanger was developed and was used in Walls 4 - 8. The design, which is illustrated in Figure 9, incorporates two bolts which clamp the timber securely. The joists are drilled in situ, using the holes in the hanger as a drilling jig, so that the bolts also act as dowels and the inevitable random length of joist which would occur in site practice has no adverse effect on the rigidity of the connection. The tongue of the hanger is split and splayed to augment anchorage in the mortar joint. The design also incorporates a stand-off, to permit 12 mm of thermal insulation material between the hanger and the masonry, but this is an optional feature which may be omitted. Examination of the computer plot of horizontal deflection showed that there was virtually no lateral movement of the wall at the first floor level, indicating the total effectiveness of the joist hanger.

An attempt was made by two methods to determine the magnitude of the eccentricity of loading of the lower storey wall due to the application of the floor load through joist hangers. On a number of walls vibrating wire strain gauges were affixed to determine the magnitude of the compressive and tensile stresses in the lower storey. The strain gauges used to determine the stresses in the brickwork were 100 mm long; they were affixed to two adjacent bricks and straddled one mortar joint. The gauge encompassed 10 mm (nominal) of mortar and 90 mm of brick whereas the ratio of mortar to brick in the generality of the brickwork was 10 mm of mortar to 65 mm of brick. Since the values of Modulus of Elasticity for the mortar and the brick were not identical, the stress-strain relationship for the specimen of brickwork spanned by the strain gauge was not representative of that of the wall. Consequently it was necessary to calibrate the strain gauges by affixing them to prisms built of the same masonry and measuring the strain under a known applied compressive stress. The stiffening effect of the returns on walls 4, 6 and 8 was such as to make the strain gauge readings unreliable, and only the results obtained on the plain walls were considered. These indicated that the point of application of the load lay within the middle third of the joist hanger. Supplementary tests were carried out using an adaptation of the method evolved by Watstein and Johnson⁷ using a joist hanger mounted in a small specimen of brickwork. This was set on a load-detecting fixture in such a manner that the overturning moment produced by the load applied from the wooden joist could be measured. Two methods of attaching the joist to the hanger were used (a) the customary two woodscrews and (b) the bolted and gripped connection of the B.C.R.A. modified hanger. Calculations of moments from these experiments indicated that the load was applied between 5 mm and 17 mm outside the wall. There was thus a range of results by both methods and a discrepancy between the two, so that the need for further investigation is indicated.

CONCLUSIONS

1. Two-storey high plain walls without returns built of standard 102.5 mm wide bricks and restrained only by floor and roof timbers, such as might be obtained by floor to ceiling fenestration, are only adequate to withstand wind loads arising from the lower speed ranges. The use of wider bricks gives enhanced resistance proportional to the greater section modulus.
2. The additional restraint provided by short return walls renders such two-storey high walls adequate to withstand most wind loads arising in the U.K. and U.S.A., i.e. of the order of a maximum basic wind speed of 50 m/sec, based on a 50 year mean recurrence interval.
3. The strength of such walls can be predicted satisfactorily by the modified yield line theory evolved by Haseltine for the design of laterally-loaded walls.
4. The types of masonry to timber fixing commonly used in the U.K. are, in certain circumstances, structurally inadequate and there is scope for development work in this field.
5. The degree of eccentricity of loading imposed on a wall by the application of a floor load through metal joist hangers is in the approximate range 20-40 mm outside the face of the wall. The experimental determination of this eccentricity has not yet been satisfactorily solved and further work is indicated.

ACKNOWLEDGEMENTS

The author thanks Mr. A. Dinsdale, O.B.E., Director, British Ceramic Research Association, for permission to publish this paper.

He wishes to thank Mr. H.W.H. West, Mr. B.A. Haseltine and Mr. B. Powell for helpful discussions, and the members of the wall testing team who carried out the experimental work.

REFERENCES

1. West, H.W.H., Hodgkinson, H.R., Haseltine, B.A. and Tutt, J.N.
The resistance of brickwork to lateral loading.
J. Inst. Struct. Engs. 55, 10 411. Oct 77.
2. West, H.W.H., Hodgkinson, H.R. and Webb, W.F.
The resistance of walls to lateral loading.
Proc. Brit. Ceram. Soc. No. 21, 1973.
3. West, H.W.H., Hodgkinson, H.R. and Haseltine, B.A.
The effect of floor and wind loads applied separately or
simultaneously to a two-storey height wall.
Proc. Fourth International Brick Masonry Conference,
Bruges 1976.
4. British Standard Code of Practice No. 3 : Chapter V : Part 2,
Wind Loads, 1972.
5. Haseltine, B.A. and West, H.W.H.
A simplified guide to the design of laterally loaded walls.
British Ceramic Research Association, Special Publication 90,
1977.
6. Design Guide for strapping and tying of load-bearing brickwork in
low-rise construction.
British Ceramic Research Association, Special Publication 93,
1977.
7. Watstein, D. and Johnson, P.V.
Experimental determination of eccentricity of floor loads
applied to a bearing wall.
National Bureau of Standards, Building Science Series 14, 1968.

TABLE 1

Details of Bricks

	Brick 1	Brick 2	Brick 3
Description	Semi-dry pressed single frog 16% frog	Semi-dry pressed twin single frog 21% frog	Wirecut 23 holes 19% perforation
Dimensions mm	215 x 102.5 x 65	215 x 140 x 65	215 x 102.5 x 65
Mean crushing strength N/mm ²	30.5	28.8	55.8
Water absorption %	24.6	23.8	7.6
Suction rate (dry) kg/m ² /min	2.50	2.73	0.86
Approx. suction rate (corrected) kg/m ² /min	1	1	-

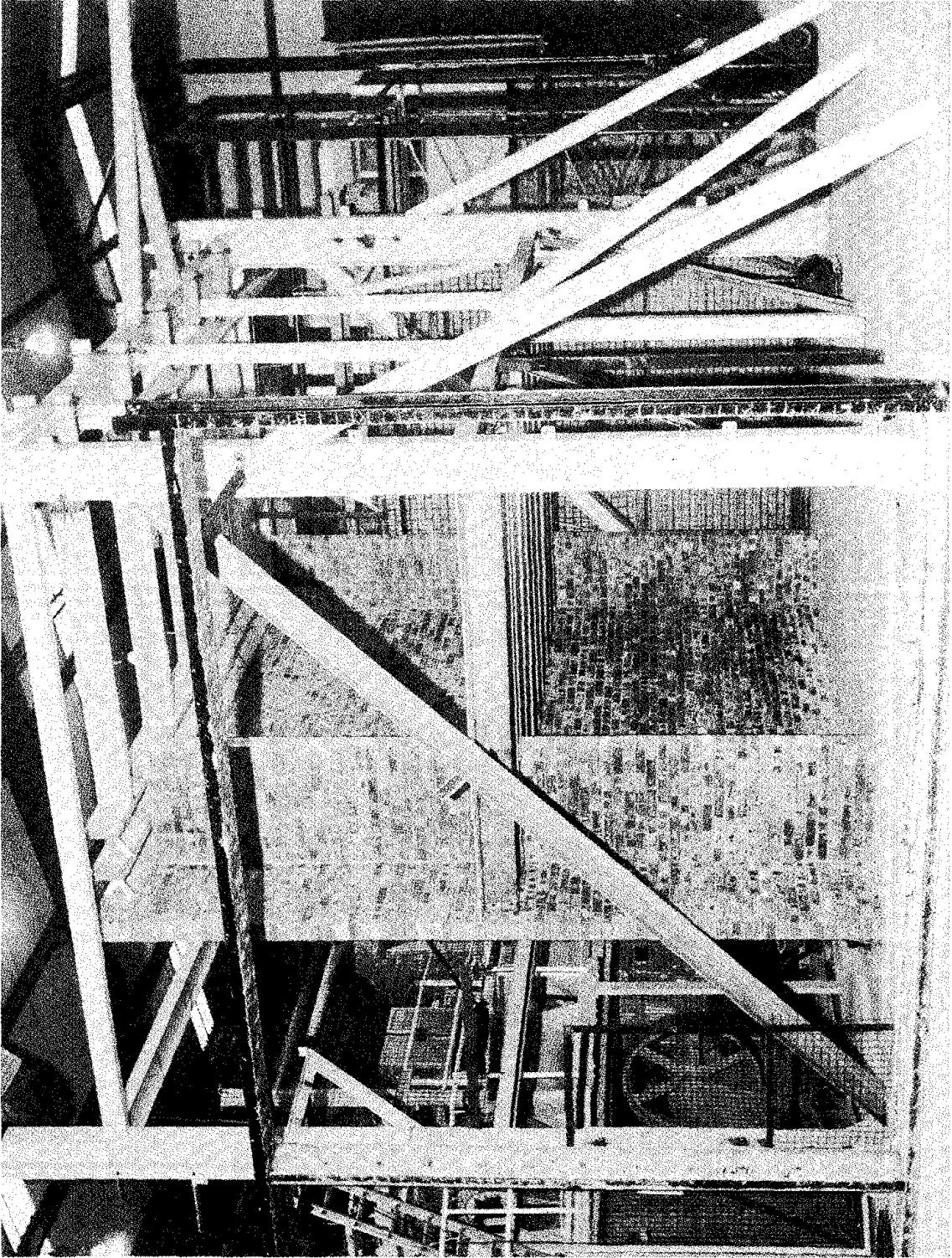


FIGURE 1

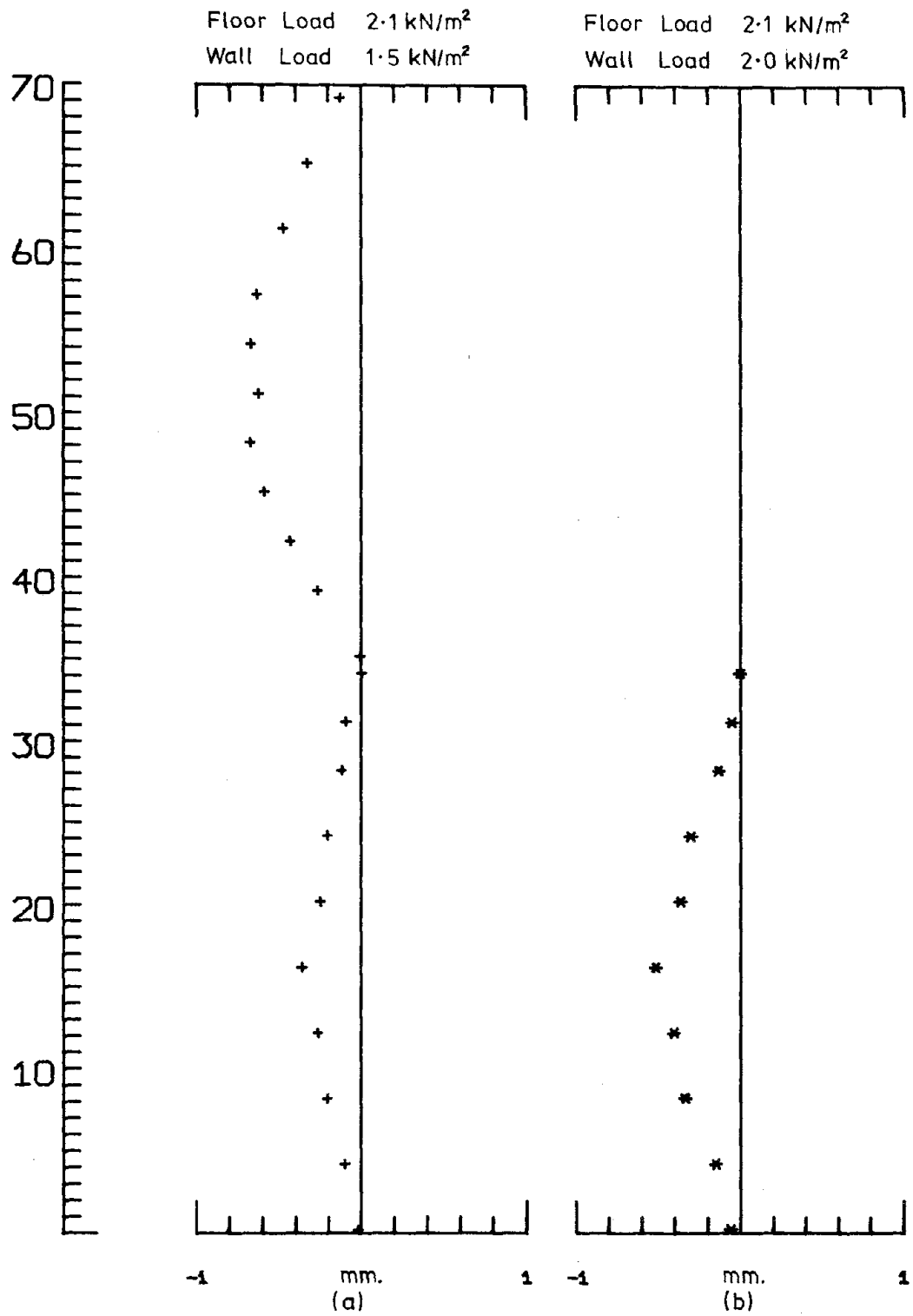
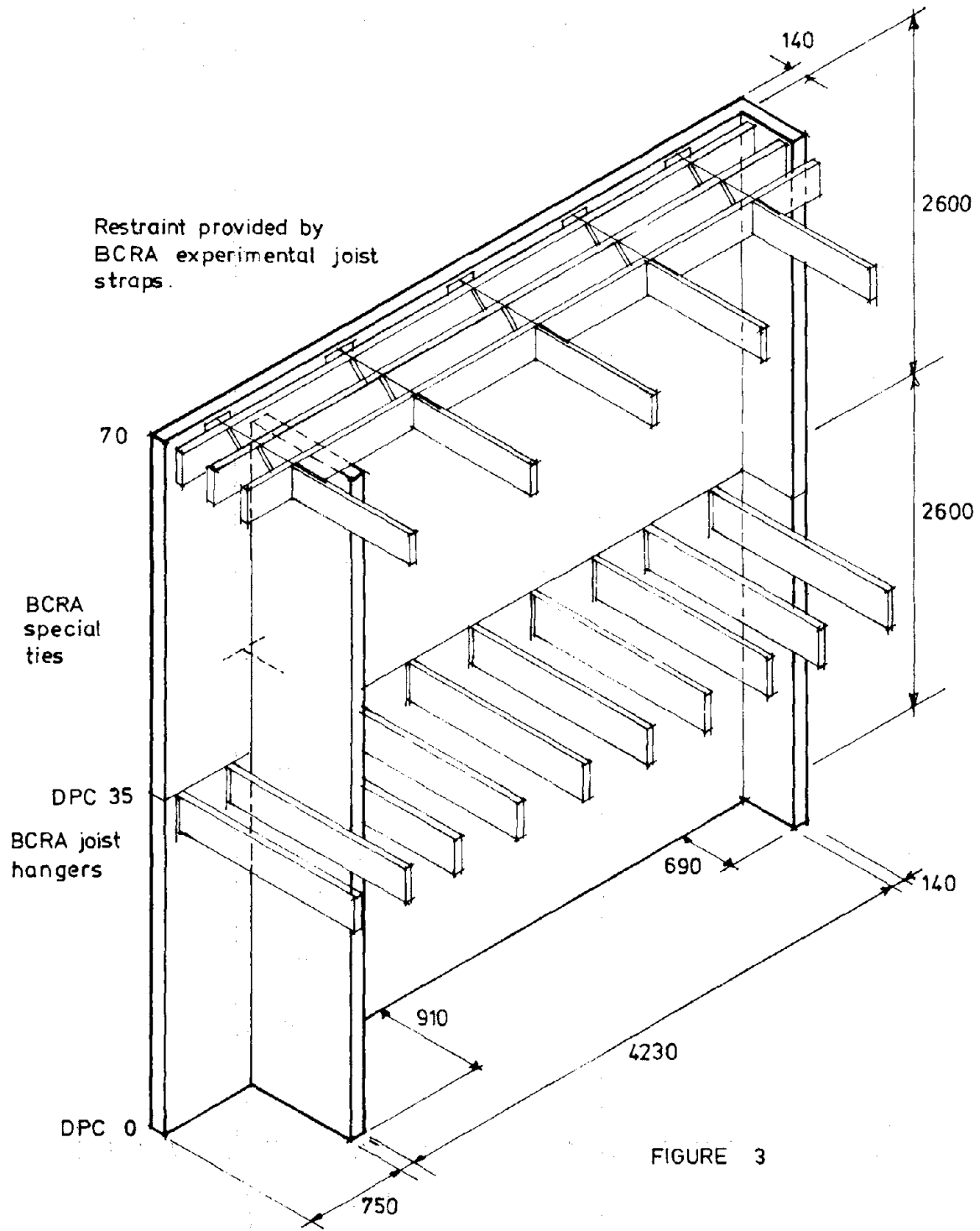


FIGURE 2



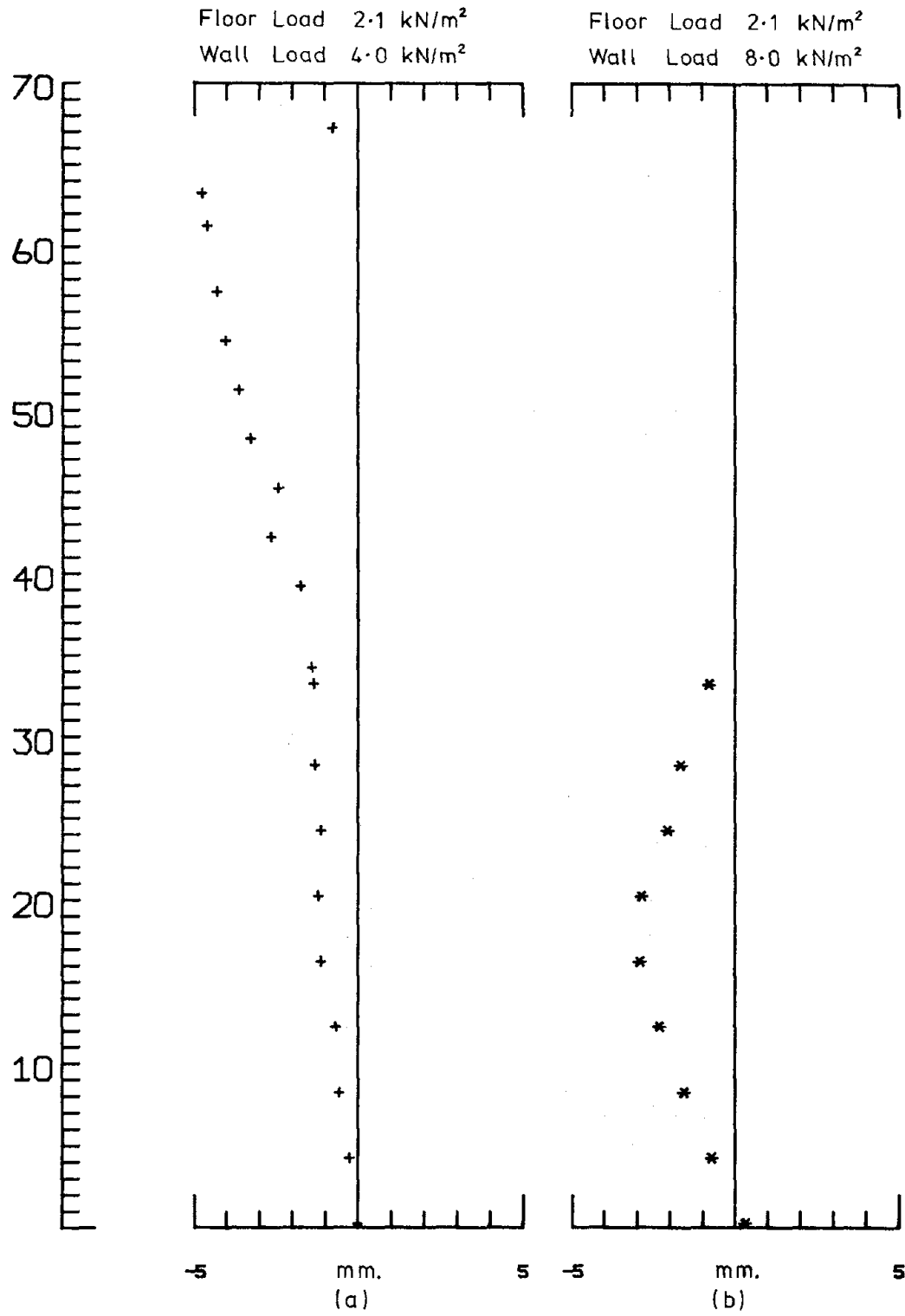
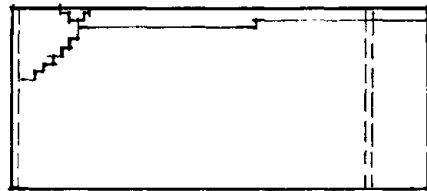
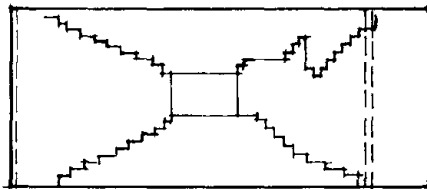


FIGURE 5



Upper Storey



Lower Storey

FIGURE 6a

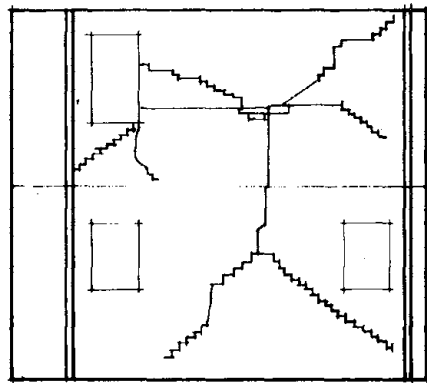


FIGURE 6b

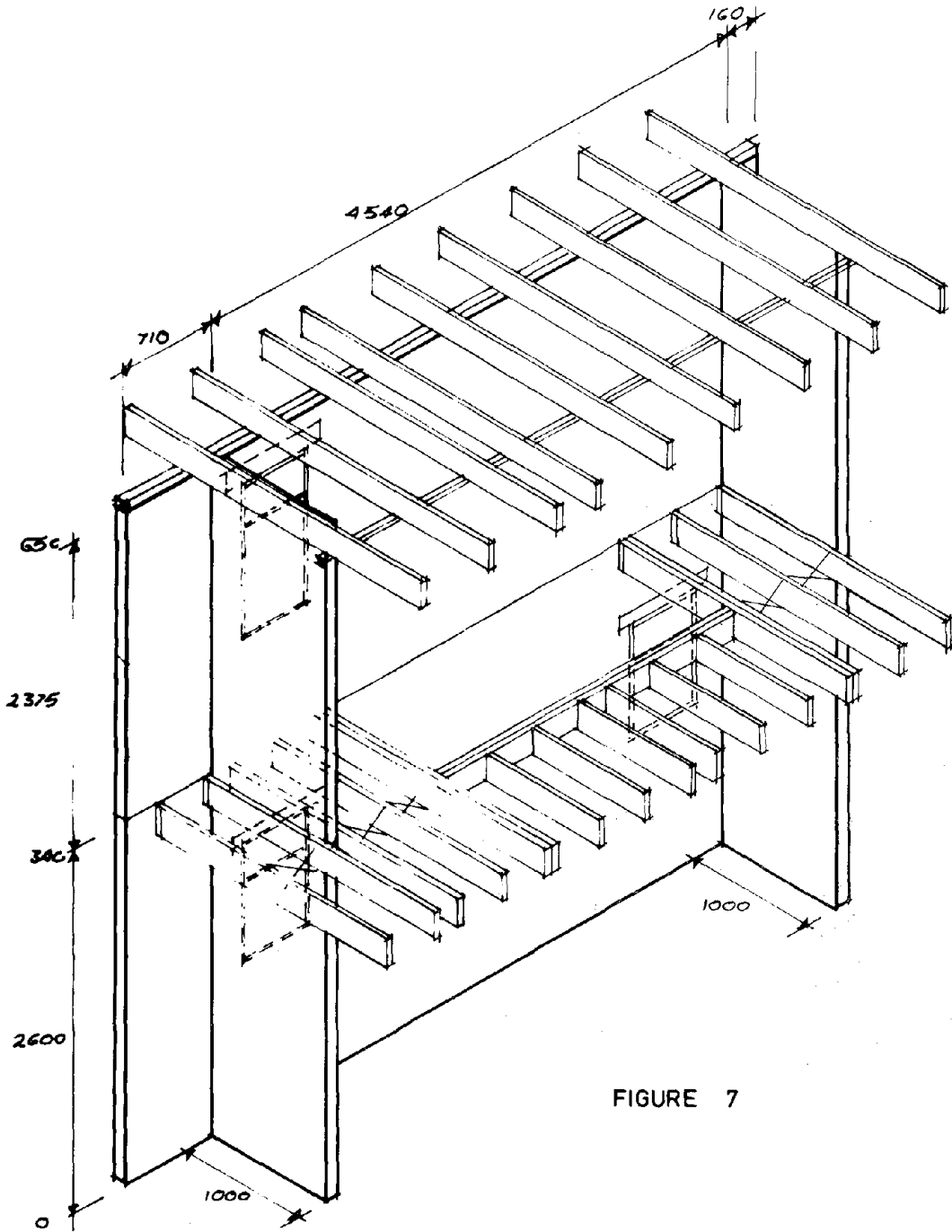
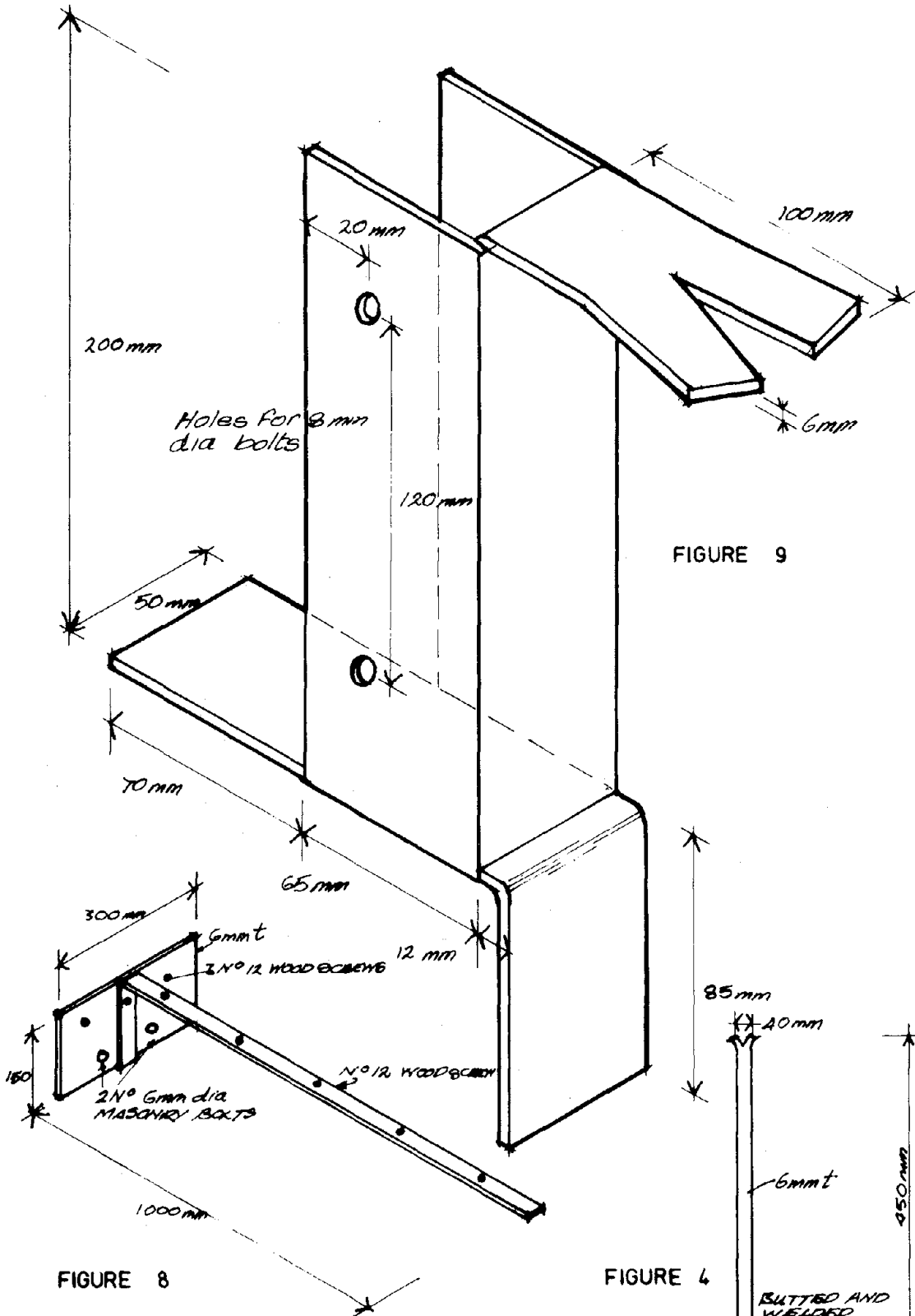


FIGURE 7



SEISMIC RESEARCH ON MULTISTORY MASONRY BUILDINGS
UNIVERSITY OF CALIFORNIA, BERKELEY, 1972 TO 1977

By Mayes, R.L., Clough, R.W., Hidalgo, P.A., and McNiven, H.D.

ABSTRACT: This paper describes the scope and provides a summary of the results of the seismic research program on multistory masonry buildings that has been ongoing at the Earthquake Engineering Research Center, University of California, Berkeley, since September, 1972. The program to date has consisted of two major phases. The first phase consisted of seventeen in-plane shear tests on a double-piered concrete block test specimen. The second phase, which is still in progress, consists of eighty in-plane shear tests on a single pier test specimen. The tests include hollow concrete block, hollow clay brick, and grouted core clay brick specimen.

The paper includes a section on the design implications of the results obtained to date in both the Berkeley test program and a similar test program being performed in New Zealand.

SEISMIC RESEARCH ON MULTISTORY MASONRY BUILDINGS
UNIVERSITY OF CALIFORNIA, BERKELEY, 1972 TO 1977

Ronald L. Mayes¹, Ray W. Clough²,
Pedro A. Hidalgo³ and Hugh D. McNiven⁴

INTRODUCTION

The masonry research program was initiated at the Earthquake Engineering Research Center, University of California, Berkeley, in September, 1972, and has continued for the past five years. The program currently has two major parts: The first is an experimental study of multistory masonry buildings, and the second is an experimental study of masonry housing construction and is described in references [3,4].

The program on multistory buildings has been in progress for five years and consists of three major parts. The first, which has been completed, is a series of seventeen in-plane shear tests on a double-piered test specimen [8]. The second, which is in progress, consists of a series of eighty in-plane shear tests on a single pier test specimen [9]. The third, which is planned to begin in October, 1978, consists of a series of tests on spandrel girders. In addition to this experimental work, recent Uniform Building Codes (UBC) have been evaluated to determine their adequacy in protecting masonry structures against severe damage or collapse in an earthquake [7].

After an extensive review of literature [5,6] dealing with earthquake resistance of masonry, it was concluded that exterior wall panels penetrated by numerous window openings (Fig. 1) were the components of multistory masonry buildings most frequently damaged in earthquakes, and it was decided to make an experimental study of the seismic behavior of such components. A testing fixture was designed to subject typical full-scale window piers to combined static vertical (gravity) and cyclic lateral (seismic) loads (Fig. 2), and the stiffness and strength of a series of seventeen double pier wall panels were measured (Fig. 3). Results of these tests indicated significant variations of the pier behavior with the various test parameters--type of grouting, types of reinforcing, rate of loading, etc. The results were not conclusive and demonstrated the need for more extensive tests to establish definitive parametric relationships.

The cost of the double pier tests, both in money and time, precluded carrying out the extensive parametric variations which are needed by this

¹Assistant Research Engineer, Earthquake Engineering Research Center (EERC), Univ. of California, Berkeley, Calif., and Principal, Computech, Berkeley, Calif.

²Prof. of Civil Engrg. and Asst. Director, EERC, Univ. of California, Berkeley, Calif.

³Visit. Assoc. Research Engineer, EERC, Univ. of California, Berkeley, Calif.

⁴Prof. of Engrg. Science, Univ. of California, Berkeley, Calif.

test procedure, and consequently, a single pier test system was devised which greatly simplified the investigation (Fig. 4). Preliminary studies showed that single pier results could be obtained which were comparable to the double pier tests; hence a large number of single pier tests were planned for 1976 to 1978.

Details of both the double and single pier test programs are discussed in the following sections.

TEST OBJECTIVES

In determining the shear strength of masonry piers and panels, the first step is to evaluate the mode of failure. Because most failures in past earthquakes have been characterized by diagonal cracks, many research programs have concentrated on this type of failure mechanism. Test techniques used by Blume [1], Greenley and Cattaneo [2], and others induce the diagonal tension or shear mode of failure. Scrivener [13], Meli [10], Williams [14], Priestley and Bridgeman [11] recognized that there were two possible modes of failure for cantilever piers. In addition to the shear or diagonal tension mode of failure, they recognized that for certain piers, a flexural failure could occur. This mechanism is characterized by yielding of the tension steel of the wall, followed by a secondary failure at the compressive toe, with associated buckling of the reinforcement once confinement is lost. Meli [10] described the flexural failure as similar to that of an underreinforced concrete beam; i.e., with extensive flexural cracking and strength limited by yielding of the reinforcement with failure finally due to crushing of the compressive corner or to rupture of the extreme bars.

Because the double pier tests were the first fixed ended piers to be tested cyclically, the objective of the tests was to determine the effect of various parameters and compare the results with those obtained by others on cantilever piers. Both the shear and flexural modes of failure were included in the investigation.

The thirty-one tests reported herein for the single pier tests are part of a total program of eighty tests. One of the main objectives of these tests was to thoroughly investigate the effects of different parameters on the shear mode of failure. It was evident from the double pier test program that the flexural mode of failure in a fixed ended pier had desirable inelastic characteristics, however, these were not as desirable as those obtained by Priestley in cantilever piers. Furthermore, it was recognized that for fixed ended piers, with height to width ratios commonly found in multistory buildings, the amount of horizontal reinforcement required to force a flexural mode of failure was substantially greater than required by current codes. Therefore, it was decided to investigate the effects of lesser amounts of horizontal reinforcement on the shear mode of failure to determine if desirable inelastic behavior could be obtained. Single pier test parameters other than the amount of reinforcement included types of masonry construction and the effect of partial grouting.

TEST SPECIMEN

a) Double Pier Specimen. The overall dimensions of the seventeen double piers test specimen are the same and are shown in Fig. 3. The test

specimen was designed to satisfy as closely as possible the boundary conditions of piers in a real structure. The piers, which had a height (5 ft 4 in.) to width (2 ft 8 in.) ratio of two, were the elements of interest. The top and bottom spandrels were heavily reinforced (using #7 rebars as shown in Fig. 3) in an attempt to prevent their failure, although this objective was not achieved in all cases.

The panels were constructed from standard two core reinforceable hollow concrete blocks, nominally 6 in. wide by 8 in. high by 16 in. long. The core of each block has an area of approximately 51.4 sq. in. with a ratio of net (concrete) to gross (block) area of 58 percent.

Both the piers and the top and bottom spandrels were fully grouted in fifteen specimen, but only the cores containing the vertical rebars were grouted in the piers of Tests 11 and 12 (partially grouted).

The series of seventeen tests was planned to determine the effect of the bearing stress, the rate of loading, the quantity and distribution of reinforcement, and the effect of partial grouting on the strength and deformation properties of the piers, as shown in Table 1. In general, the specimen were constructed in identical pairs, one being tested dynamically; the other under pseudo-static conditions. Test specimen 1 and 2 were considered to be the basic panel, while all other pairs of panels had variations of one or two major properties that varied from those of Tests 1 and 2. Specimen 17 was unique; it did not have an identical mate.

Tests 1, 2, 5, 6 and 9 to 12 had 2-#6 vertical rebars in each jamb of the pier, providing a ratio of 0.0092 of the area of reinforcement to the gross cross-sectional area. Tests 3 and 4 had 2-#4 vertical rebars in each jamb, giving a reinforcement ratio of 0.0042. Tests 7 and 8 had 2-#6 vertical rebars in each jamb and 3-#5 horizontal bars at the quarter points in each pier, giving a reinforcement ratio of 0.014. Tests 13 to 16 had a substantial amount of reinforcement (0.0168), arranged to ensure a flexural failure. In addition to the horizontal and vertical bar reinforcement, Tests 15 and 16 had steel plates inserted in the mortar joints at each of the three courses at the top and bottom of each pier [8]. The piers of Test 17 were completely unreinforced.

The standard two core reinforceable hollow concrete blocks, when tested as single units, had an average gross compressive strength of 1714 psi (2944 psi net strength). The average gross tensile strength of the unit was 267 psi. The mortar was specified as standard ASTM Type M (i.e., 1 Cement: 1/4 Lime: 2-1/4 to 3 Sand), with a minimum strength of 2500 psi. The grout was also specified according to ASTM specifications. Because each of the nine sets of panels was built at different times, the grout and mortar strength for each set varied according to normal workmanship.

b) Single Pier Specimen. The overall dimensions of the thirty-one single pier test specimen were the same: 4 ft 8 in. high and 4 ft wide (1.17 height to width ratio). The top and bottom flanges that transfer the loads from the loading beam and to the base were 8 in. high and 5 ft 4 in. long. These flanges were fully grouted and contained shear keys to transfer the load to the specimen. Three different types of masonry construction were used; namely, hollow concrete block (HCBL), hollow clay brick (HCBR), and double wythe grouted core clay brick (CBRC).

The HCBL specimen were constructed from standard two core reinforceable hollow concrete blocks, nominally 8 in. wide by 8 in. high by 16 in.

long. The net to gross cross-sectional area was 58 percent. The average gross compressive strength was 1800 psi (3000 psi net). The average gross tensile strength of the units was 293 psi. The HCBR specimen were constructed from standard two core reinforceable, hollow clay brick units, nominally 8 in. wide by 4 in. high by 12 in. long. The net to gross cross-sectional area was 61 percent. The average gross compressive strength was 3430 psi (5717 psi net). The average tensile strength of the units was 248 psi. The CBRC specimen were constructed from two wythes of clay brick units nominally 4 in. high by 4 in. wide by 12 in. long. The grouted core between the two wythes was nominally 2 in. thick giving the test specimen a nominal thickness of 10 in. The average compressive strength of these clay brick units was 5440 psi. The average tensile strength was 253 psi.

The mortar used for all construction was the standard ASTM Type M, and the grout was 1C:3S:2G, where G refers to 10 mm maximum size local gravel.

The variables of the test specimen are listed in Table 2. When vertical rebars are used, they are placed one at each jamb of the pier. The horizontal rebars, when included, are evenly distributed over the height of the pier. The F and P in the grouting column refer to full and partial grouting. Partial grouting means that piers are grouted at rebar locations only.

TEST EQUIPMENT AND PROCEDURE

The test equipment shown in Figs. 2 and 4 permits lateral loads to be applied in the plane of the piers, using two displacement controlled actuators with a combined maximum capacity of 150 Kip. A vertical load may be applied to the piers through the springs and rollers shown above the spandrel beam in Fig. 2 and above the lateral loading beam in Fig. 4. The Thomson Dual Roundway Bearings connecting the springs to the loading beam allow the piers to move freely with minimal friction force.

In the single pier test setup, the two hinged external steel columns restrain the rotation of the top of the pier, forcing it towards a condition of rotation fixity at the top and bottom. An additional compressive load was imposed on the pier by the unequal forces developed in the two hinged columns during the cyclic loading.

The loading sequence for each test consisted of groups of three sinusoidal displacement cycles applied at a specified actuator amplitude and frequency. In the case of the double pier tests, the actuator displacement amplitude followed the sequence at 0.02 in., 0.04 in....0.08 in., 0.12 in. ...0.20 in., 0.25 in....0.50 in., 0.60 in....1.50 in. This sequence was changed during the single pier tests to 0.02 in., 0.04 in., 0.08 in., 0.10 in., 0.12 in., 0.14 in., 0.16 in., 0.20 in., 0.25 in....0.60 in., 0.70 in....1.20 in.

TEST RESULTS

The results presented in Tables 1 and 2 for the double pier and single pier tests, respectively, include tabulations of the maximum shear forces; for the double pier, the applied bearing stress, and for the single pier, the compressive load corresponding to the maximum shear force. It should be noted that in the double pier tests, the actual compressive load of the

piers varied as a function of the overturning moment resulting from the applied shear force. For the single piers, the compressive load generally increased as the input displacement increased. Also included are comparisons of the envelopes of the hysteresis loops (average force versus deflection results) for most tests (Figs. 6 to 16). The hysteresis envelopes are a plot of the absolute average of the maximum positive and negative forces and corresponding displacements for each of the three cycles of loading at a given input displacement. The ultimate shear forces given in Tables 1 and 2 are the average and peak values. The peak ultimate value is the maximum shear force obtained in any one cycle of loading. The average ultimate value is the maximum value obtained from the hysteresis loops. This is always less than the peak value, and except for a few cases, it is generally within 90 percent of the peak value.

In evaluating the inelastic characteristics of the pier behavior, the hysteresis envelopes provide a good visual picture; however, they must be considered in conjunction with other parameters to fully evaluate the inelastic behavior. The other parameters include the energy dissipated per cycle, the ultimate strength, indicators of ductility, and comparisons of crack patterns at equal displacements. The usefulness of hysteresis envelopes is that they provide visual comparisons of ductility and ultimate strength; however, they give no indication of the energy dissipated per cycle.

The hysteresis envelopes (average maximum force-deflection curves) are used as a frame of reference for the discussion of the test results. The question to be considered is what constitutes desirable inelastic behavior. It is difficult to answer this question in quantitative terms; but Figs. 5a, b, and c are useful for a qualitative discussion of three different aspects of the behavior encountered in the test program. Figure 5a shows a set of four force-deflection relationships, each with the same ultimate strength (F_1). Obviously, the inelastic force-deflection relationship becomes more desirable in passing from curves A through D. Figure 5b shows a set of four force-deflection relationships with different ultimate strengths. The relative desirability of these curves is more difficult to evaluate, as it is a function of the imposed interstory deflection. If the interstory deflection never exceeds d_1 , then piers with the force-deflection relationships given by B, C and A are preferable to those of D. If the interstory deflection increases to d_2 , then B, C and D are preferable to A; and finally, if the interstory deflection increases to d_3 , then the order of increasing preference is A, B, C and D. Hence the relative desirability of the force-deflection relationships in Fig. 5b depends on the intensity of the expected earthquake. For a moderate earthquake where the interstory deflection may not exceed d_1 , the order of increasing preference would be D, C, A and B. If, however, a large earthquake is considered, and the interstory deflection could be of the order of d_3 , the order of increasing preference would be A, B, C and D (It should be noted that the interstory deflection resulting from a particular earthquake is a function of the dynamic characteristics of the building.).

For the two force-deflection relationships given by Fig. 5c, obviously B is preferable to A, as it is able to resist a greater lateral force and has the same characteristics when the interstory deflection exceeds d_1 . With the foregoing discussion in mind, the effect of the various test parameters on the hysteresis envelopes of the piers will be discussed.

DISCUSSION OF THE TEST RESULTS

The discussion of the test results is presented in two sections; one on the effect of horizontal reinforcement, and the other on the effect of partial grouting. Under each section the results of the three materials of construction are presented separately.

a) Effect of Horizontal Reinforcement. Although not discussed in detail in this paper, increasing amounts of horizontal reinforcement with all materials of construction generally improved the crack pattern, even though the hysteretic behavior was not always improved.

Hollow Concrete Block Series--For the double pier tests, Fig. 6 shows a comparison of Tests HCBL-21-1, 2, 7 and 8. Clearly the shape of the hysteresis envelopes is improved with the addition of the 3-#5 horizontal rebars. The horizontal reinforcement forced a flexural type of behavior, although the final mode of failure was shear. Fig. 7 shows a comparison of Tests HCBL-21-3, 4 and 13 to 16. The addition of a large amount of horizontal reinforcement in Tests 13 and 14 did improve the shape of the hysteresis envelopes, although this was not as significant as that noted for Tests 7 and 8. With the addition of the plates in the mortar joints in Tests 15 and 16, the full flexural capacity of the piers and the resultant desirable type of flexural behavior was obtained.

For the single pier tests, a similar trend was noted. However, in this case, relating the quantity of horizontal reinforcement to the flexural capacity is difficult because the flexural capacity increases at each stage of loading due to the increase in compressive load resulting from the test fixture arrangement. The discussion of the single pier tests is therefore presented in qualitative terms. It should be noted that the mode of failure for all single pier tests was shear. For the fully grouted piers with vertical rebar, the effectiveness of horizontal reinforcement is dependent on the quantity, as seen in Figs. 8 and 9. If the quantity of horizontal reinforcement is expressed by $A_{hs}f_y$ as a percentage of the average ultimate shear strength of the horizontal unreinforced wall (45 Kip for HCBL-11-3, then with a quantity less than 65 percent (HCBL-11-9), the effect of horizontal reinforcement was not significant. The shape of the hysteresis envelope did not change, although there was an 18 percent increase in the average ultimate strength for HCBL-11-4. If the percentage of horizontal reinforcement was greater than 130 percent (HCBL-11-6 and 11), the inelastic characteristics of the wall were substantially improved. The combined shear action of the masonry and horizontal reinforcement in this case was capable of forcing a flexural type of behavior, although the mode of failure was still shear. The result of this was a significant increase in the peak ultimate strength. In terms of the UBC ratios of steel area (based on the gross area of the pier) horizontal reinforcement up to a ratio of 0.0017 did not significantly improve the inelastic behavior. The behavior was substantially improved when the ratio increased to 0.0033; this is 4.5 times the minimum required by the Code.

Hollow Clay Brick Series--For fully grouted piers with vertical rebar, the effect of increasing amounts of horizontal reinforcement after 1-#5 was

added was not significant, as seen in Figs. 10 and 11. The shape of the hysteresis envelopes for all test specimen with one or more horizontal rebars was improved over the two cases with none--HCBR-11-3 and 8 (Figs. 10 and 11). Unlike the hollow concrete block walls, it appears that the hollow clay brick material is not able to act in combination with horizontal reinforcement to force a flexural type of behavior and thus obtain improvement in inelastic behavior. In terms of the UBC ratios of steel area, horizontal reinforcement equal to 0.0008 improves the inelastic behavior of the pier when compared with horizontally unreinforced walls; however, increasing the ratio above this value does not result in any improvement in the inelastic performance.

Grouted Core Clay Brick Series--For the piers with #5 vertical rebar (Fig. 12), the shape of the hysteresis envelope was improved when the 5-#5 horizontal rebars were added, although the average ultimate strength was approximately the same for all tests. For the piers with #8 vertical rebar (Fig. 12), the shape of the hysteresis envelope gradually improved as additional horizontal reinforcement was added. Also, the average ultimate strength gradually increased, although the increase was small in comparison to the amount of steel added. This type of behavior indicates a trend towards the flexural type of behavior even though the actual mode of failure was shear.

b) Effect of Partial Grouting.

Hollow Concrete Block Series--For the double pier Tests HCBL-21-1, 2, 11 and 12, the inelastic behavior of the partially grouted walls is comparable to the fully grouted walls if net shear stresses are used (Fig. 13).

For the single pier tests, partially grouted walls with no horizontal reinforcement had less desirable inelastic behavior when compared with the fully grouted walls (Fig. 14). As expected, the partially grouted walls were significantly more flexible and carried significantly less total load. They also had less desirable hysteresis envelopes. The average ultimate shear stress based on the net area of the partially grouted walls was also less than for the corresponding fully grouted walls. Partially grouted walls with horizontal reinforcement also had less desirable inelastic behavior when compared to fully grouted walls (Fig 15), although this difference was not as great as that for walls with no horizontal reinforcement. The partially grouted walls were more flexible and carried less total load. The shape of the hysteresis envelopes was less desirable, although not significantly. With regard to average ultimate shear stress based on net area, the partially grouted walls had approximately the same value as fully grouted walls.

Hollow Clay Brick Series--Partially grouted walls, regardless of the amount of horizontal reinforcement up to a ratio of 0.0016, had significantly less desirable inelastic characteristics when compared with the fully grouted walls (Fig. 16). The partially grouted walls carried 40 percent or less total load than the fully grouted piers; and the shape of the hysteresis loops was substantially less desirable than for the corresponding fully grouted walls. The ultimate average shear stress based on net area was 55 percent or less than obtained with the fully grouted pier.

SUMMARY OF TEST RESULTS

1. For fully grouted hollow concrete block piers with vertical reinforcement in the jambs, the inelastic behavior was improved only when the ratio of the horizontal steel area to the gross cross-sectional area of the pier exceeded 0.0032. With a ratio of 0.0016 or less, the inelastic behavior was not significantly different from the pier with no horizontal reinforcement.
2. For fully grouted hollow clay brick piers with vertical reinforcement in the jambs, a ratio of horizontal steel area of 0.0008 improved the inelastic behavior when compared with a horizontally unreinforced pier. Additional increases in horizontal reinforcement up to 0.0041 produced no further improvement in the inelastic behavior.
3. For grouted core clay brick walls, improved inelastic behavior was obtained as the amount of horizontal reinforcement was increased; however, the improvement was not as significant as that noted for hollow concrete block walls, and it also was dependent on the amount of vertical reinforcement.
4. Partial grouting in hollow concrete block walls decreased the effective inelastic behavior of piers with no horizontal reinforcement when compared with the fully grouted piers in the single pier tests. However, this conclusion is not applicable to the double pier test results. For piers with horizontal reinforcement, the inelastic behavior of the partially grouted walls was not significantly different from the fully grouted walls.
5. Partial grouting in hollow clay brick walls, regardless of the amount of horizontal reinforcement (up to a ratio of 0.0016), significantly decreased the inelastic behavior of piers when compared with fully grouted piers.
6. Fully grouted hollow clay brick and grouted core clay brick walls are able to resist approximately twice as much shear load as fully grouted hollow concrete block walls.

DESIGN IMPLICATIONS OF THESE AND OTHER TEST RESULTS

The only extensive code related study the authors have performed to date has been an evaluation of the design force and stress levels of recent Uniform Building Codes for multistory masonry buildings [7]. The study concluded that the trend towards increasing conservatism, which is evidenced in recent UBC code changes concerning masonry structures, is justified. Moreover, the study suggests that the codes should be more conservative for masonry buildings of moderate height. This study was envisaged to be the first part of a continuing effort to utilize relevant research data in evaluating masonry codes. It made no attempt to develop a design methodology or recommend specific code changes. It is hoped these can be done when the eighty single pier tests are complete. However, based on the results presented herein, code writers should consider the following:

- 1) Fully grouted hollow clay brick and grouted core clay brick piers have significantly greater strength than corresponding fully grouted hollow concrete block walls.
- 2) Partially grouted hollow clay brick walls have significantly less desirable inelastic characteristics than fully grouted walls.

The most specific design orientated recommendations available to the authors are those presented by Priestley. Priestley, et al, [11,12] have performed several extensive series of tests on cantilever piers and have

shown that very desirable inelastic behavior can be obtained with the flexural mode of failure. For cantilever piers, Priestley has shown that it is necessary to provide sufficient shear strength with horizontal reinforcement to exceed the flexural strength using a capacity design approach. Priestley has recommended that the total area of shear steel crossing a potential 45° shear crack in a pier be calculated as follows:

$$V_D = \frac{\phi_o}{\phi_f} V_B \quad (1)$$

where V_B is the shear force required to induce yielding of all the vertical steel in the pier, ϕ_f is the flexural undercapacity factor, and is recommended as 0.7 for masonry design, ϕ_o is the flexural overcapacity factor and represents the ratio of maximum feasible flexural strength to ideal flexural strength based on nominal material strengths and is recommended as 1.25 for 40 ksi steel and 1.4 for 60 ksi steel. V_D is the shear force used to calculate the required area of horizontal steel, A_{hs} , as follows:

$$A_{hs} = \frac{V_D}{\phi_s f_y} \quad (2)$$

where ϕ_s is the shear capacity reduction factor and is recommended as 0.85 and f_y is the yield stress of the horizontal steel.

The major problem associated with this design methodology is one of sliding shear along the base of the pier or wall when the flexural mode of failure is forced to occur. This was evident in Priestley's tests and led to a limitation of the design shear force in his recommended design methodology. A few simple calculations will show that the required amount of horizontal reinforcement far exceeds the amounts of horizontal reinforcement required by the current Uniform Building Code.

Consistent with the desirable characteristics obtained for the flexural mode of failure, Priestley has recommended that in the conceptual design of a building, all walls be designed to act as cantilever walls so that desirable inelastic structural behavior is attained. It is clear that this may be a difficult architectural constraint, and, consequently, the inelastic behavior of walls other than cantilever must be investigated.

Priestley also comments that the perforated shear wall of Fig. 1 will have a tendency to form a soft first story in a large earthquake unless it is designed elastically for realistic forces. This infers that a building will have to be designed for a larger force than is used in most current codes. This inference was validated by the authors study [7] in which a low ductility factor was assumed for the structural elements.

The test results on the fixed ended test specimen presented herein indicate that the desirable inelastic behavior is decreased with the addition of vertical load and that large amounts of horizontal reinforcement are not always effective in developing the flexural capacity of a pier.

An example of the effect of vertical load is seen in the double pier Tests HCBL-21-7 and 8 (Fig. 6) in which a desirable elastoplastic type of behavior was not obtained. In this case the bearing stress was 250 psi.

The ineffectiveness of increasing amounts of horizontal reinforcement is indicated in single pier Test HCBL-11-11, which should have a greater ultimate strength than HCBL-11-6. Both tests have similar ultimate loads and inelastic behavior. A similar result was obtained for hollow clay brick walls in Tests HCBR-11-7 and 12.

The authors are not yet sure if this discrepancy with Priestley's results is attributable to the reasonably high compressive load induced in the single pier tests or to the difference between cantilever and fixed ended pier tests. However, it is clear that these differences should be resolved before applying Priestley's design methodology.

ACKNOWLEDGMENTS

The research reported in this paper has been jointly funded by the National Science Foundation, the Masonry Institute of America and the Western States Clay Products Association. The sponsorship of these institutions is gratefully acknowledged. There are many colleagues and students who have participated in this program over the past five years. These include Prof. N. Mostaghel, Prof. M. Khojasteh-Bakht, Dr. Y. Omote, students S. W. Chen, A. Anwar, J. Kubota, A. Agarwal and A. Shaban. Many helpful suggestions have been made by prominent members of the masonry industry, including Messrs. W. D. Dickey, J. Amrhein, D. Wakefield, J. Tawresey, L. Thompson, D. Prebble, S. Beavers, and other members of technical committees of various masonry organizations. D. A. Sullivan Co. has fabricated the pier specimen. Thanks also are due to the laboratory staff headed by D. Steere and I. Van Asten.

APPENDIX I - REFERENCES

1. Blume, J.A. and Prolux, J., "Shear in Grouted Brick Masonry Wall Elements," Report to Western States Clay Products from J.A. Blume and Associates, August 1968.
2. Greenley, D.G. and Cattaneo, L.E., "The Effect of Edge Load on the Racking Strength of Clay Masonry," Proceedings, Second International Brick Masonry Conference, Stoke-on-Trent, April 1970.
3. Gulkan, P., Mayes, R.L., Clough, R.W. and Hendrickson, R., "An Investigation on the Seismic Behavior of Single-Story Masonry Houses," to be published in the Proceedings of the Sixth European Conference on Earthquake Engineering, Dubrovnik, Yugoslavia, September 1978.
4. Gulkan, P., Mayes, R.L., Clough, R.W. and Hendrickson, R., "An Experimental Investigation on the Seismic Behavior of Single-Story Masonry Houses," North American Masonry Conference, Boulder, Colorado, August 1978.
5. Mayes, R.L. and Clough, R.W., "A Literature Survey--Compressive, Tensile, Bond and Shear Strength of Masonry," EERC Report No. 75-15, University of California, Berkeley, June 1975.
6. Mayes, R.L. and Clough, R.W., "State-of-the-Art in Seismic Strength of Masonry--An Evaluation and Review," EERC Report No. 75-21, University of California, Berkeley, October 1975.

7. Mayes, R.L., Omote, Y., Chen, S.W. and Clough, R.W., "Expected Performance of Uniform Building Code Designed Masonry Structures," EERC Report No. 76-7, University of California, Berkeley, May 1976.
8. Mayes, R.L., Omote, Y. and Clough, R.W., "Cyclic Shear Tests of Masonry Piers, Volume I--Test Results," EERC Report No. 76-8, University of California, Berkeley, May 1976.
9. Mayes, R.L., Clough, R.W., Chen, S.W., McNiven, H.D. and Hidalgo, P., "Cyclic Loading Behavior of Masonry Piers," to be published in the Proceedings of the Sixth European Conference on Earthquake Engineering, Dubrovnik, Yugoslavia, September 1978.
10. Meli, R., "Behaviour of Masonry Walls under Lateral Loads," Proceedings of the Fifth World Conference on Earthquake Engineering, Rome, 1972.
11. Priestley, M.J.N. and Bridgeman, D.O., "Seismic Resistance of Brick Masonry Walls," Bulletin of the New Zealand National Society for Earthquake Engineering, Vol. 7, No. 4, December 1974.
12. Priestley, M.J.N., "Seismic Resistance of Reinforced Concrete Masonry Shear Walls with High Steel Percentages," Bulletin of the New Zealand National Society for Earthquake Engineering, Vol. 10, No. 1, March 1977.
13. Scrivener, J.C., "Concrete Masonry Wall Panel Tests with Predominant Flexural Effect," New Zealand Concrete Construction, July 1966.
14. Williams, D.W., "Seismic Behaviour of Reinforced Masonry Shear Walls," Ph.D. Thesis, University of Canterbury, Christchurch, New Zealand, 1971.

APPENDIX II - NOTATION

A_{hs} = area of horizontal steel reinforcement

V_D = design shear force

V_B = shear force required to induce yielding of all vertical steel

f_y = yield stress of steel

ϕ_f = flexural capacity reduction factor

ϕ_o = flexural overcapacity factor

ϕ_s = shear capacity reduction factor

TABLE 1. DOUBLE PIER TEST RESULTS

Specimen Designation	Test Frequency (cps)	Grouting Full (F) or Partial (P)	Prism Strength (psi)	Bearing Stress (psi)	Vertical Rebar			Horizontal Rebar			Ratio of Total Area of Rebar to Gross Area of Wall $P_h + P_v$	Average Ultimate Shear Force (kips)	Peak Ultimate Shear Force (kips)
					No. of Bars	Yield Strength (ksi)	$P_v = \frac{A_{vs}}{A_g}$	No. of Bars	Yield Strength (ksi)	$P_h = \frac{A_{hs}}{A_g}$			
HCBL-21-1	0.02	F	2280	250	4-#6	79.0	0.0092	---	---	---	0.0092	24.0	26.0
- 2	3	F	2280	250	4-#6	79.0	0.0092	---	---	---	0.0092	31.0	33.2
- 3	0.02	F	2115	125	4-#4	54.1	0.0042	---	---	---	0.0042	26.0	27.3
- 4	3	F	2115	125	4-#4	54.1	0.0042	---	---	---	0.0042	22.8	26.0
- 5	0.02	F	2430	0	4-#6	78.1	0.0092	---	---	---	0.0092	18.5	20.5
- 6	3	F	2430	0	4-#6	78.1	0.0092	---	---	---	0.0092	21.7	25.5
- 7	0.02	F	2630	250	4-#6	78.1	0.0092	3-#5	67.8	0.0048	0.0140	39.0	40.7
- 8	3	F	2630	250	4-#6	78.1	0.0092	3-#5	67.8	0.0048	0.0140	44.0	48.4
- 9	0.02	F	2362	500	4-#6	78.5	0.0092	---	---	---	0.0092	28.7	29.5
-10	3	F	2362	500	4-#6	78.5	0.0092	---	---	---	0.0092	32.7	34.1
-11	0.02	P	2253	250	4-#6	74.8	0.0092	---	---	---	0.0092	18.9	20.0
-12	3	P	2253	250	4-#6	74.8	0.0092	---	---	---	0.0092	20.6	21.8
-13	0.02	F	1880	125	4-#4	50.8	0.0042	3-#7 2-#5	62.9	0.0126	0.0168	26.0	29.1
-14	3	F	1880	125	4-#4	51.7	0.0042	3-#7 2-#5	62.9	0.0126	0.0168	24.0	28.8
-15	0.02	F	2105	125	4-#4	51.8	0.0042	3-#7 2-#5	64.0	0.0126	0.0168	33.6	35.2
-16	3	F	2105	125	4-#4	51.3	0.0042	3-#7 2-#5	64.0	0.0126	0.0168	32.4	36.2
-17	3	F	1908	250	---	---	---	---	---	---	---	20.7	23.7

TABLE 2. SINGLE PIER TEST RESULTS

Specimen Designation	Test Frequency (cps)	Grouting Full (F) or Partial (P)	Prism Strength (psi)	Vertical Rebar			Horizontal Rebar				Ratio of Total Area of Rebar to Gross Area of Wall $P_h + P_v$	Average Ultimate Shear Force (kips)	Peak Ultimate Shear Force (kips)	Compressive Load at Ultimate (kips)
				No. of Bars	Yield Strength (ksi)	$P_v = \frac{A_{vs}}{A_g}$	No. of Bars	Yield Strength (ksi)	$P_h = \frac{A_{hs}}{A_g}$	$A_{hs} \cdot f_y$ (kips)				
HCBL-11-1	1.5	F	1330	No	--	--	No	--	--	--	--	45.0	46.6	44.0
-2	1.5	P	1330	No	--	--	No	--	--	--	--	26.2	26.3	42.2
-3	1.5	F	1833	2-#5	70.8	0.0016	No	--	--	--	0.0016	45.0	49.1	25.1
-4	1.5	F	1833	2-#5	70.8	0.0016	1-#5	47.9	0.0008	14.7	0.0024	53.1	54.9	39.1
-5	1.5	P	1330	2-#5	70.8	0.0016	1-#5	47.9	0.0008	14.7	0.0024	42.5	46.7	30.2
-6	1.5	F	1833	2-#5	70.8	0.0016	4-#5	47.9	0.0032	58.8	0.0048	80.0	82.7	52.7
-7	1.5	F	1905	2-#8	69.2	0.0041	No	--	--	--	0.0041	52.5	65.8	33.3
-8	1.5	P	1330	2-#8	69.2	0.0041	No	--	--	--	0.0041	33.8	37.9	29.2
-9	1.5	F	1905	2-#8	69.2	0.0041	2-#5	47.9	0.0016	29.4	0.0057	53.8	56.9	41.9
-10	1.5	P	1330	2-#8	69.2	0.0041	2-#5	47.9	0.0016	29.4	0.0057	43.1	50.6	31.2
-11	1.5	P	1330	2-#8	69.2	0.0041	4-#6	73.9	0.0046	130.6	0.0086	84.4	87.7	50.8
HCBR-11-1	0.02	F	2535	No	--	--	No	--	--	--	--	86.2	98.5	116.1
-2	0.02	P	2535	No	--	--	No	--	--	--	--		23.7	76.5
-3	0.02	F	2535	2-#5	75.0	0.0016	No	--	--	--	0.0016	96.2	98.9	52.3
-4	0.02	F	2722	2-#5	71.3	0.0016	1-#5	70.0	0.0008	21.5	0.0024	120.0	124.8	114.3
-5	0.02	P	3053	2-#5	71.3	0.0016	1-#5	70.0	0.0008	21.5	0.0024	45.0	52.4	53.7
-6	0.02	F	2722	2-#5	71.3	0.0016	5-#5	64.2	0.004	98.5	0.0056	105.0	105.3	61.9
-7	0.02	F	2535	2-#5	75.0	0.0016	5-#5	72.6	0.004	111.4	0.0056	90.0	96.2	85.3
-8	0.02	F	2866	2-#8	69.2	0.0041	No	--	--	--	0.0041	85.0	85.6	43.4
-9	0.02	P	3053	2-#8	69.2	0.0041	No	--	--	--	0.0041	36.2	49.1	37.3
-10	0.02	F	2722	2-#8	72.9	0.0041	2-#5	68.7	0.0016	42.2	0.0057	100.0	104.8	54.2
-11	0.02	P	2722	2-#8	72.9	0.0041	2-#5	68.7	0.0016	42.2	0.0057	32.6	37.1	26.7
-12	0.02	F	2535	2-#8	76.0	0.0041	5-#6	73.9	0.0058	163.2	0.0099	92.6	98.7	85.0
-13	0.02	F	2722	2-#8	72.9	0.0041	5-#6	74.7	0.0058	165.0	0.0099	111.2	116.1	110.0
CBRC-11-1	0.02	P	2507	No	--	--	No	--	--	--	--	110.0	118.6	141.9
-2	0.02	F	2507	2-#5	71.7	0.0013	No	--	--	--	0.0013	111.2	117.1	92.7
-3	0.02	F	2507	2-#5	71.7	0.0013	1-#5	68.3	0.0006	21.0	0.0019	105.0	114.5	89.5
-4	0.02	F	2507	2-#5	71.7	0.0013	5-#5	66.3	0.0032	104.8	0.0045	113.8	128.6	132.5
-5	0.02	F	2507	2-#8	72.9	0.0033	No	--	--	--	0.0033	98.8	104.3	76.4
-6	0.02	F	2507	2-#8	72.9	0.0033	2-#5	73.9	0.0013	45.3	0.0046	117.6	130.4	100.3
-7	0.02	F	2507	2-#8	72.9	0.0033	5-#6	74.7	0.0046	165.0	0.0079	125.0	127.3	80.9

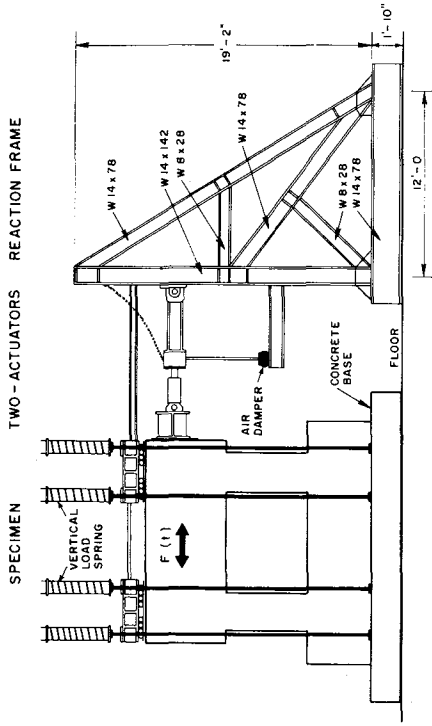


FIGURE 2 DOUBLE PIER TEST SET-UP

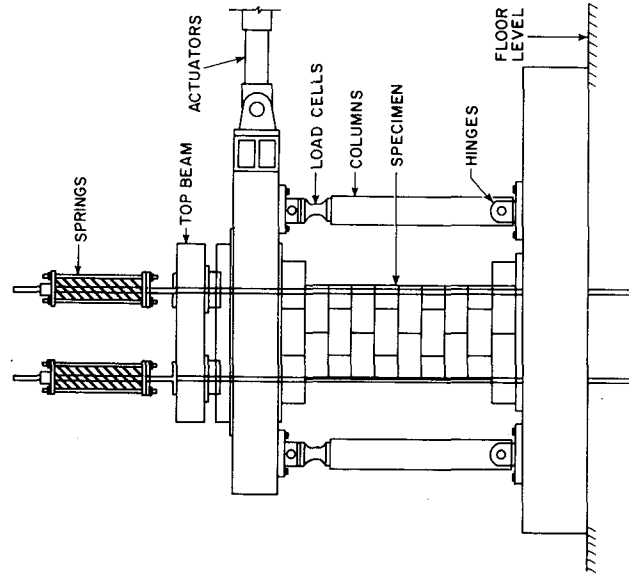


FIGURE 4 SINGLE PIER TEST SET-UP

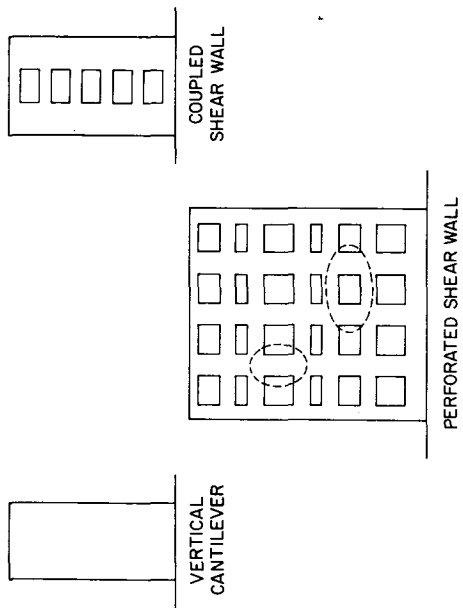


FIGURE 1 TYPICAL SHEAR WALLS

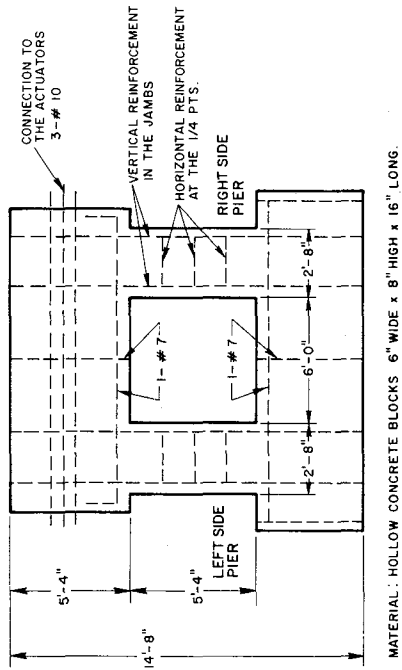
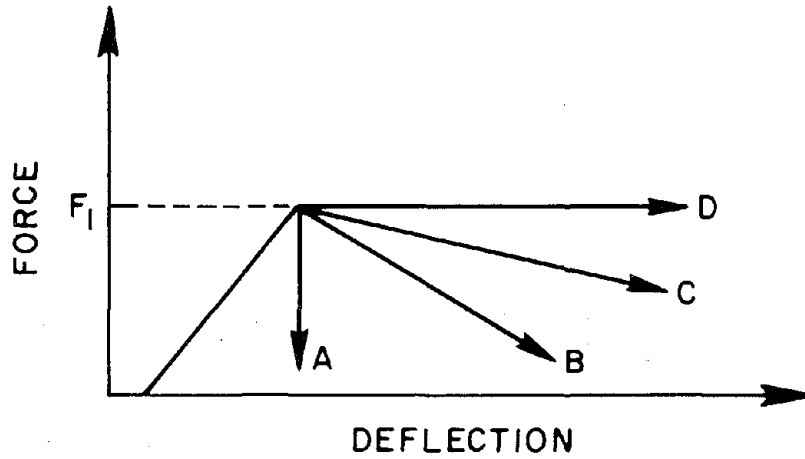
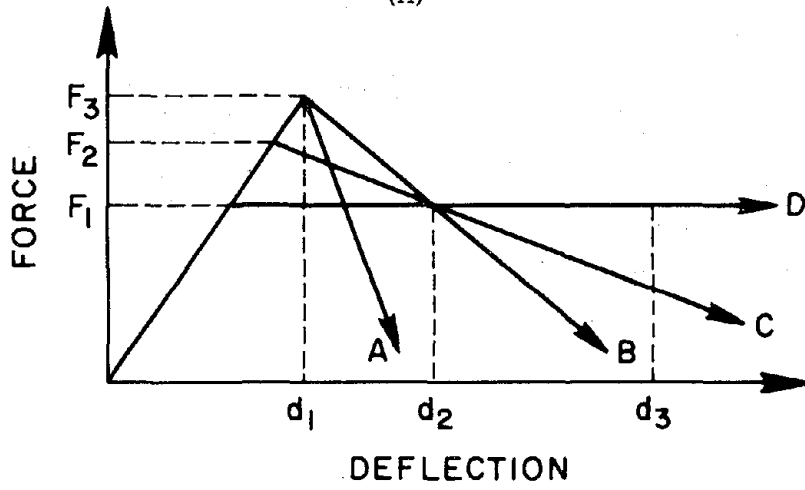


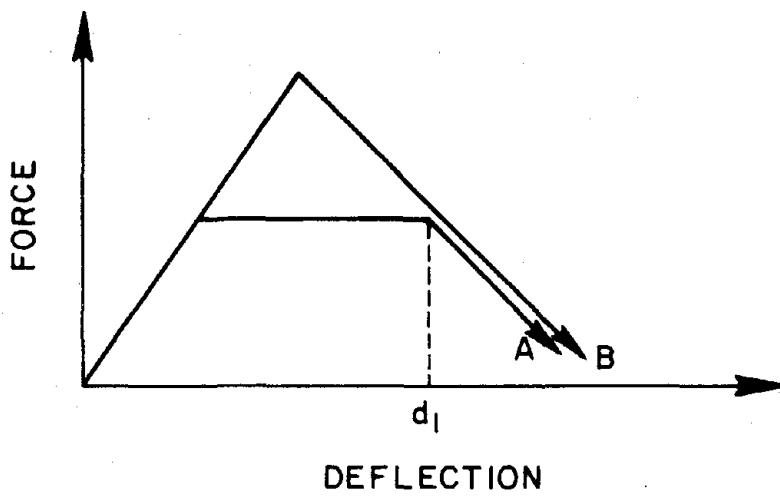
FIGURE 3 TYPICAL DOUBLE PIER TEST SPECIMEN



(A)



(B)



(C)

FIGURE 5 IDEALIZED HYSTERESIS ENVELOPES

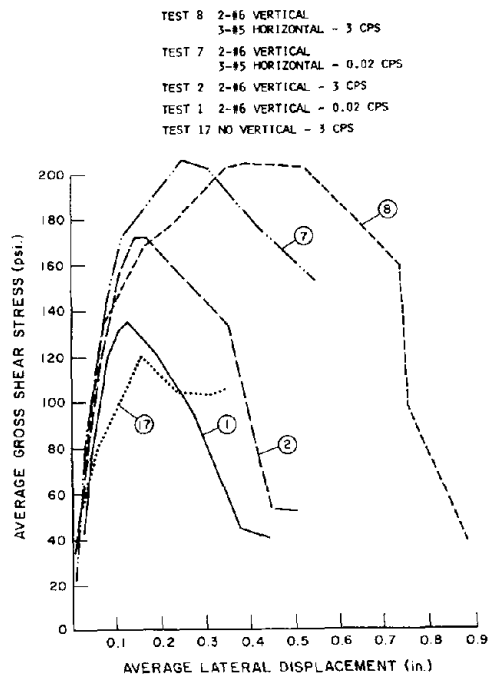


FIG. 6 HYSTERESIS ENVELOPE
DOUBLE PIER 2:1 HCBL
EFFECT OF HORIZ. REINF.

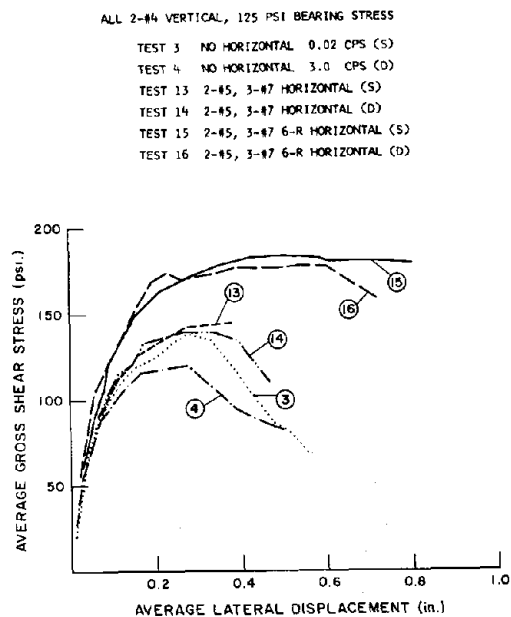


FIG. 7 HYSTERESIS ENVELOPE
DOUBLE PIER 2:1 HCBL
EFFECT OF HORIZ. REINF.

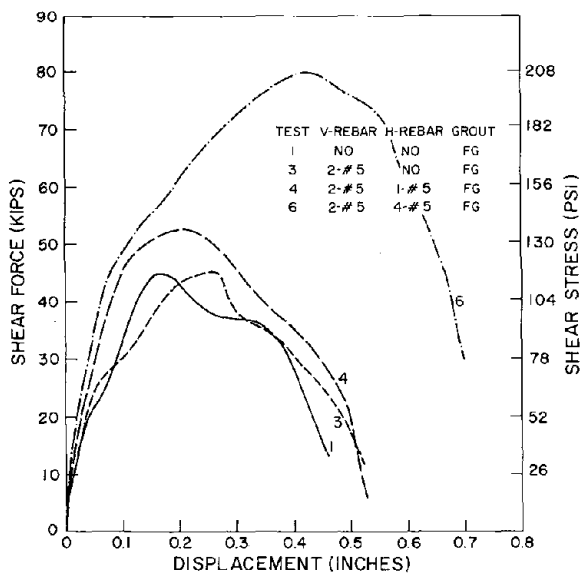


FIG. 8 HYSTERESIS ENVELOPE
SINGLE PIER 1:1 HCBL
EFFECT OF HORIZ. REINF.

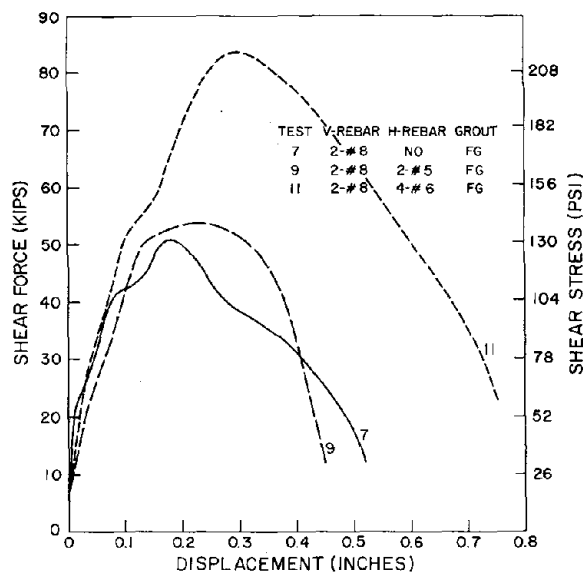


FIG. 9 HYSTERESIS ENVELOPE
SINGLE PIER 1:1 HCBL
EFFECT OF HORIZ. REINF.

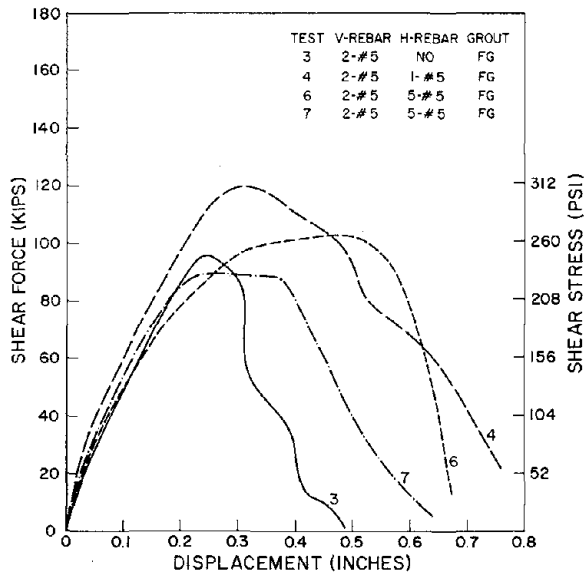


FIG. 10 HYSTERESIS ENVELOPE
SINGLE PIER 1:1 HCBR
EFFECT OF HORIZ. REINF.

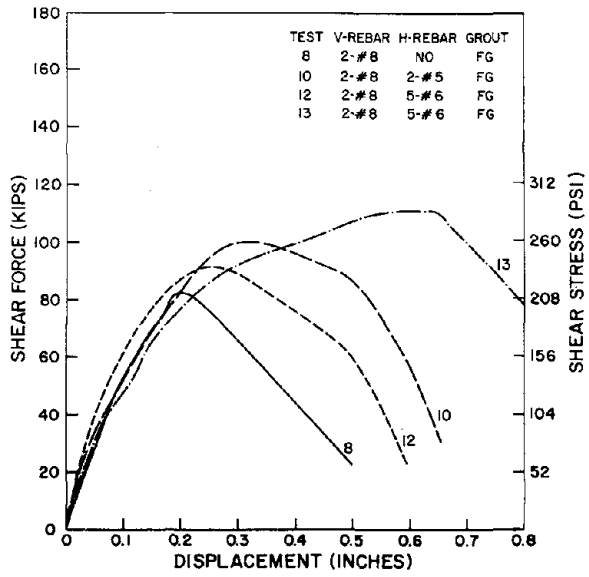


FIG. 11 HYSTERESIS ENVELOPE
SINGLE PIER 1:1 HCBR
EFFECT OF HORIZ. REINF.

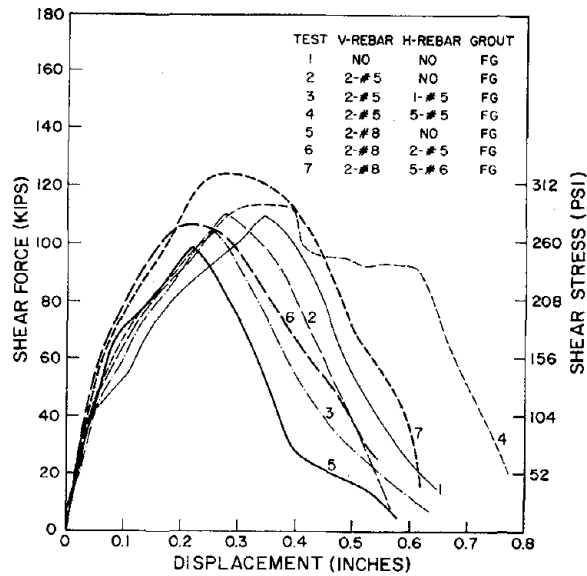


FIG. 12 HYSTERESIS ENVELOPE
SINGLE PIER 1:1 CBRC
EFFECT OF HORIZ. REINF.

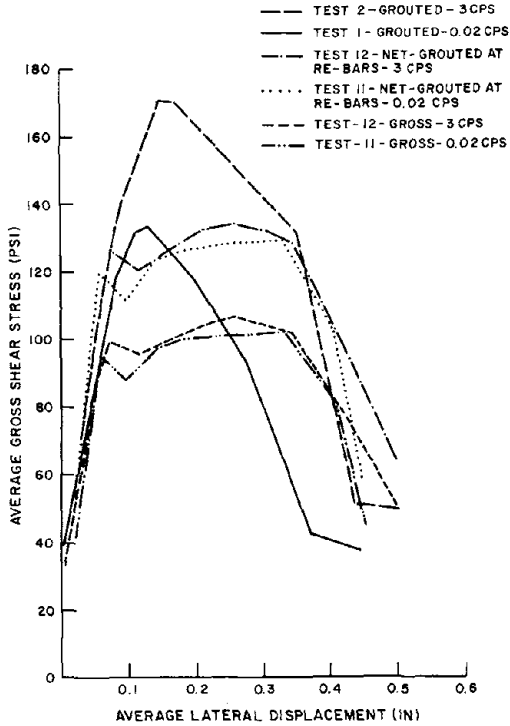


FIG.13 HYSTERESIS ENVELOPE
DOUBLE PIER 2:1 HCBL
EFFECT OF PARTIAL GROUTING

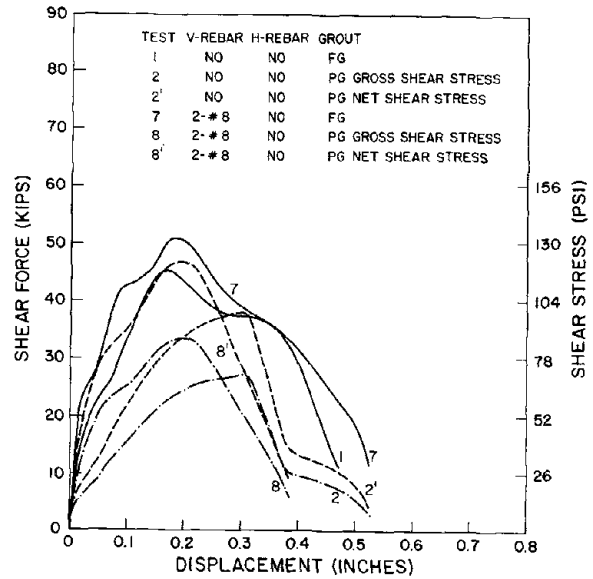


FIG.14 HYSTERESIS ENVELOPE
SINGLE PIER 1:1 HCBL
EFFECT OF PARTIAL GROUTING

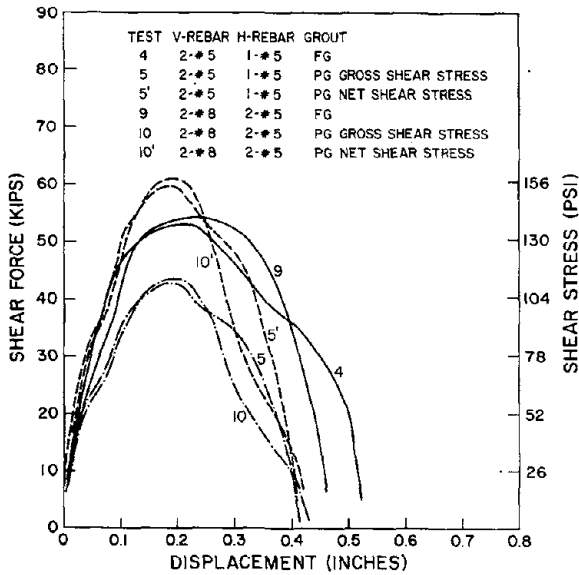


FIG.15 HYSTERESIS ENVELOPE
SINGLE PIER 1:1 HCBL
EFFECT OF PARTIAL GROUTING

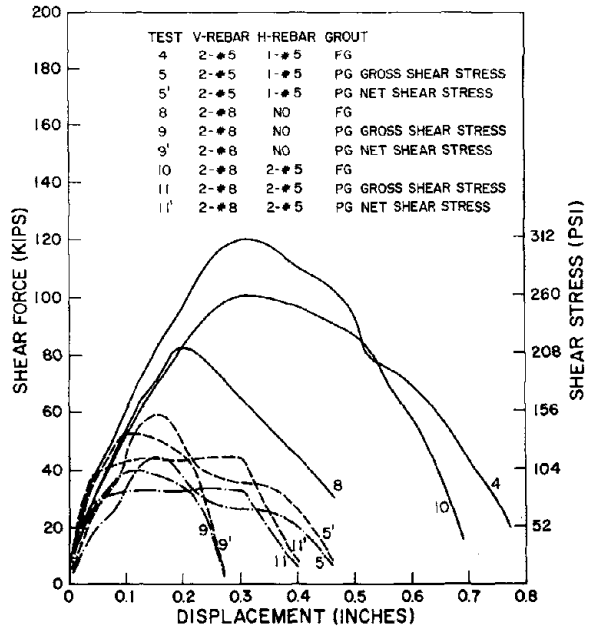
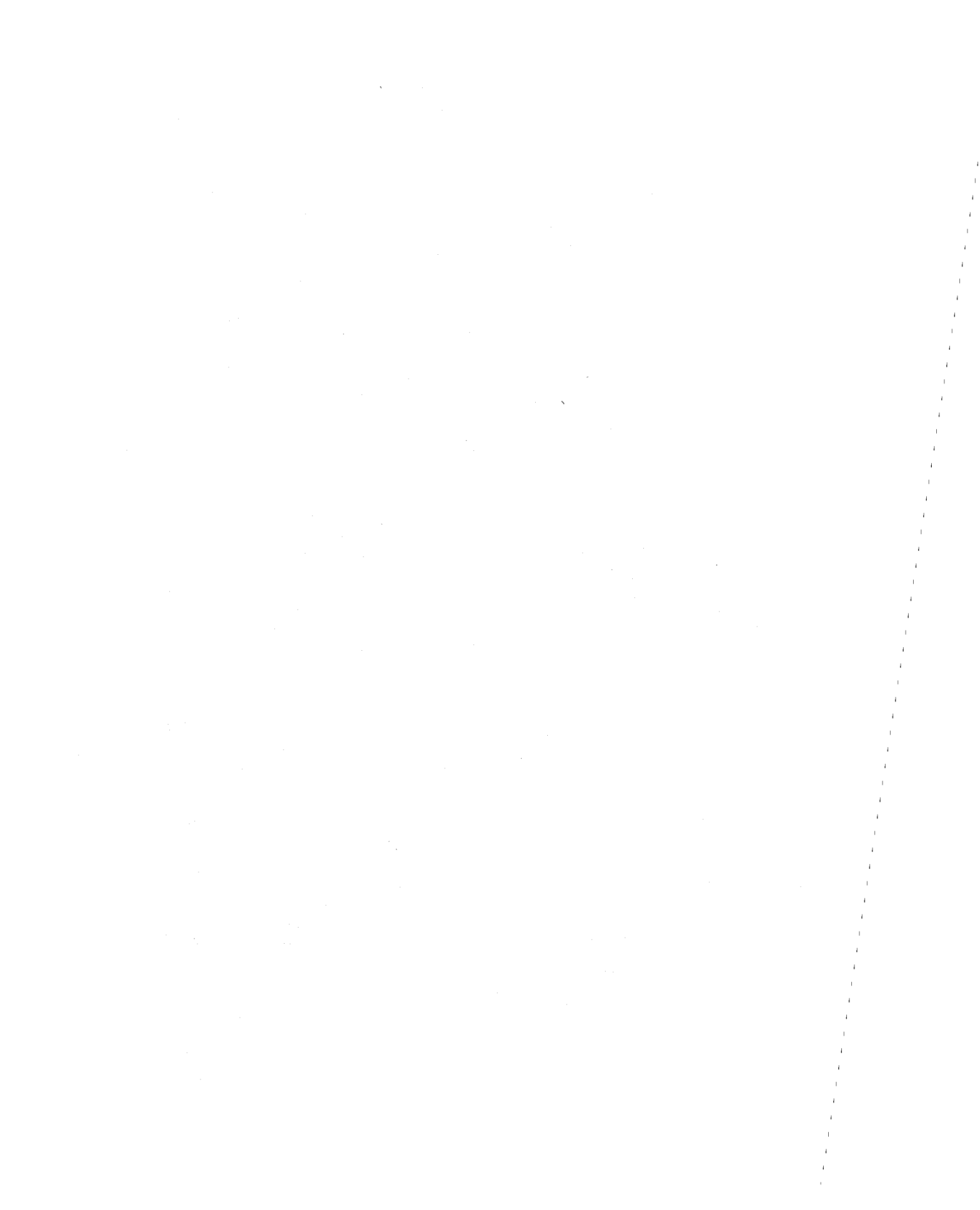


FIG.16 HYSTERESIS ENVELOPE
SINGLE PIER 1:1 HCBL
EFFECT OF PARTIAL GROUTING



AN EXPERIMENTAL INVESTIGATION ON THE SEISMIC BEHAVIOR
OF SINGLE-STORY MASONRY HOUSES

by

P. Gulkan,¹ R.L. Mayes,² R.W. Clough,³ and R. Hendrickson⁴

ABSTRACT

Observations on the seismic behavior of a simple masonry house subjected to simulated earthquake motions on the University of California, Berkeley, shaking table are presented. The house was constructed such that similar masonry components were placed both parallel and transverse to the table motion. Measurements indicated that the orientation of the timber trusses comprising the roof assembly, base fixity of the in-plane walls, and cracks which developed in the walls affected the overall response in a complex manner. In general, a nominal amount of reinforcement appeared to have a beneficial effect on preventing the formation of cracks which could lead to failure. Additional pseudo-static tests were conducted on typical timber roof-masonry wall connection details to assess their adequacy for resisting seismic forces.

¹Visiting Assoc. Research Engineer, Earthquake Engineering Research Center (EERC), Univ. of California, Berkeley, California.

²Assist. Research Engineer, EERC, Univ. of California, Berkeley, California, and Principal, Computech, Berkeley, California.

³Prof. of Civil Engineering and Assist. Director, EERC, Univ. of California, Berkeley, California.

⁴Former Assist. Specialist, EERC, Univ. of California, Berkeley, California.

AN EXPERIMENTAL INVESTIGATION ON THE SEISMIC BEHAVIOR
OF SINGLE-STORY MASONRY HOUSES

by

P. Gulkan,¹ R.L. Mayes,² R.W. Clough,³ and R. Hendrickson⁴

INTRODUCTION

To evaluate U. S. Department of Housing and Urban Development (HUD) criteria for single-story masonry dwellings, an experimental investigation of the design and construction requirements for these dwellings in Uniform Building Code Seismic Zone 2 regions of the United States was embarked upon at the Earthquake Engineering Research Center (EERC), of the University of California, Berkeley. Because of limited information on the shear strength of masonry structural elements and the response of masonry structures to earthquakes, the investigation was directed towards testing masonry houses constructed with full-scale components using the EERC shaking table. Cyclic pseudo-static displacement type tests were also performed on typical masonry-timber roof connections to assess their adequacy for resisting the forces developed during seismic excitations.

This paper is a progress report for the first year of the experimental research, and presents an overview of the significant results determined on the basis of the experiments carried out during that period.

DESCRIPTION OF THE TEST STRUCTURE

The basic purpose of the project is to evaluate experimentally the seismic resistance of masonry dwellings of typical construction in less active seismic regions of the United States. To date, no experimental study has been reported for masonry structures subjected to simulated earthquakes, although the inadequate seismic resistance of poorly designed or constructed masonry buildings has traditionally been given heavy emphasis in post-earthquake survey reports (1, 3, 6). During the planning phase of the study the primary objective was to obtain a structure which would be simple in concept and yet would contain the most significant components,

¹Visiting Assoc. Research Engineer, Earthquake Engineering Research Center (EERC), Univ. of California, Berkeley, California.

²Assist. Research Engineer, EERC, Univ. of California, Berkeley, California, and Principal, Computech, Berkeley, California.

³Prof. of Civil Engineering and Assist. Director, EERC, Univ. of California, Berkeley, California.

⁴Former Assist. Specialist, EERC, Univ. of California, Berkeley, California.

such as wall panels, corners, and wall-footing and roof-wall connections. Limitations on size imposed by the earthquake simulator facility (7) coupled with these requirements resulted in the design and fabrication of the structure depicted in Fig. 1. While maintaining geometrical symmetry, similar wall segments and corner units built in duplicate were placed at 90 degrees to one another so that both in-plane and out-of-plane wall behavior could be observed simultaneously. Both partially reinforced and unreinforced components were used. Another point of interest was the orientation of the timber truss units which supported the roof. In Fig. 1 the photograph shows the trusses in the direction of the table motion. Later experiments were conducted with the roof structure rotated 90 degrees.

The masonry unit used was a standard hollow concrete block unit 4 in. high, 6 in. wide and 16 in. long with a nominal compressive strength of 1,000 psi based on the gross area. Type S mortar of the Uniform Building Code with volume proportions of 1C:1/2L:4-1/2S was used. The average compressive strength of the mortar was 2,650 psi. The grout used for the top course of all walls and for the vertical cells containing reinforcement was the standard 1C:3S mixture. It had an average strength of 6,300 psi. Reinforcement consisted of one medium grade #4 vertical bar placed in each end cell of wall panels W1 and W2, and three #4 bars placed in the reinforced corner units C1 and C3 (Fig. 1). These bars were measured to have an average yield strength of 54,000 psi and an average ultimate strength of 80,000 psi. Also, the top two horizontal mortar joints of each wall and corner unit contained a 9-gage wire mesh.

The roof trusses were toe nailed at a spacing of 2 ft to a single 2 in. by 6 in. top plate with three 16-penny nails at each end. Additionally, every other truss was attached to the top plate with a proprietary metal strap. Roof-to-wall connection was achieved through three 10-1/2 in. long, 5/8 in. diameter anchor bolts on each wall and corner unit embedded 8 in. into the masonry.

The masonry segments were built upon footings 7-1/2 in. high and 16 in. wide. Through a specially designed attachment system (Fig. 1), the horizontal translation and rotation of each individual footing could be controlled. During the early tests, only translations were prevented. During later stages the footings of the in-plane walls W1 and W3 were bolted to prevent the observed uplift of the footings. Transverse walls W2 and W4 were left free to rotate at the footing level at all times with the assumption that this would more closely approximate actual conditions.

In addition to the roof assembly which weighed 2,600 lb., concrete slabs totaling 12,000 lb. were attached to the top of the plywood sheathing. This provided a total roof load per unit length of wall periphery of approximately the same as that of a typical 40 ft by 50 ft prototype unit.

DESCRIPTION OF THE TESTS

Although the roof structure shown in Fig. 1 is stiffer than what a full-size house might be expected to have, no attempt was made to modify the base motions applied to the test specimen for "scaling" purposes. The test

specimen was subjected to a series of base motions of increasing intensity. The base motions used were the N-S component of the 1940 El Centro, the S69E component of the 1952 Kern County (Taft), and the N76W component of the 1971 San Fernando earthquake recorded at Pacoima Dam. In Fig. 2 the range of the response spectrum ordinates for elastic systems with 2 percent damping is indicated for all three types of base motions normalized to a maximum peak acceleration of 1 g. Also superimposed on the same figures for comparison are the corresponding response spectra of the original ground motions normalized to the same peak.

The house was tested under a wide spectrum of conditions. In addition to the variations in the type and intensity of base motions, cracks which formed during the tests were repaired by plastering the affected masonry walls with a fiber glass based surface bonding mortar on both surfaces. The roof truss orientation was changed, and the base fixity of the footings of the in-plane walls was also changed.

The response of the masonry structure was monitored through a wide array of transducers. By means of displacement measuring devices, deflections of the wall panels, as well as the relative motions between the timber and the masonry components, were recorded. Also, accelerometers were used to obtain a more complete understanding of the response. Table 1 provides a summary of the conditions that prevailed at the beginning of each test run, along with a summary of important developments.

The reference number used to designate a given test run consists of a letter followed by a decimal number. The letter T, E, or P represents the Taft, El Centro, or Pacoima signals. The number indicates the peak table acceleration of that test run, expressed as a fraction of g. It should be noted that unreinforced wall W3 was cracked along the mortar joint of the eighth course from the bottom while it was being moved onto the shaking table. This was epoxy-repaired before the tests commenced. The first crack that developed was in this joint during test T-0.214. The out-of-plane walls W2 and W4 did not crack during the first thirteen tests when the roof trusses were orientated in the direction of table motion and these walls acted as bearing walls. The maximum base motions during this series of tests were T-0.267 and E-0.282. After the roof trusses were rotated 90 degrees, the unreinforced out-of-plane wall W4 cracked during test E-0.311. This was then repaired with the fiber glass reinforced plaster, and did not crack again until test P-0.492.

The in-plane and out-of-plane partially reinforced walls remained uncracked during all phases of testing. The maximum base motions used during the first phase of tests had peak accelerations of the order of the actual recorded Taft and El Centro earthquakes. During the second phase when the roof structure was rotated 90 degrees, the peak table accelerations exceeded the corresponding peaks of the Taft and El Centro earthquakes, but remained well below the peak of the original Pacoima record.

OBSERVED RESPONSE

Masonry structures are complicated systems because of the inherent nonlinear characteristics of the constituent materials, effects of cracking, and boundary conditions as well as loading circumstances (2, 4). The difficulty involved in interpreting the measured response of the structure tested on the shaking table is further exacerbated because of the differences introduced by reorienting the roof trusses, repairing damaged sections, and implementing deliberate variations in the fixity conditions of the footings. Moreover, the structure was subjected to three different types of base motions during which the peak accelerations varied by as much as an order of magnitude. One must frequently gloss over these differences in order to bring out the more important characteristics of the response parameters. In order to illustrate the bulk of the observations that follow, two test runs have been selected. These are Tests 10 and 19, in which the Taft earthquake was used. The peak table acceleration recorded in Tests 10 and 19 were 0.267 g and 0.248 g, respectively. The orientation of the roof structure was different for the two tests. In Test 10, walls W2 and W4 were load-bearing, while in Test 19, walls W1 and W3 were load-bearing. Due to limitations of space, the discussion of the response will be made only with respect to the following quantities:

- (1) Input table motion
- (2) Out-of-plane displacements of the reinforced wall segment W2, and the unreinforced wall segment W4
- (3) In-plane displacements of the reinforced and unreinforced walls W1 and W3
- (4) Displacements of the reinforced and unreinforced corner units C3 and C4
- (5) Relative slip of the timber top plate with respect to W1 and W3
- (6) Acceleration on two sides of the roof

The respective time history plots for these quantities are given in Figs. 3 and 4 for the two selected test runs. In the following discussion, corresponding frames in these two figures should be considered simultaneously.

The table motion during similar runs was remarkably repeatable. This is visually verified by comparing the table acceleration traces in Figs. 3 and 4, and accounts for the narrow band of variation for the velocity response spectra ordinates presented in Fig. 2(a). The fidelity of the simulated motion to the original ground motion can, of course, best be evaluated in terms of the response spectra for both. Here, an absolute reproduction of the original spectrum is not as essential as obtaining a ground acceleration history which may justifiably be called an expectable earthquake due to its temporal and spectral characteristics.

The displacement histories of Test 10 for the reinforced and unreinforced out-of-plane load-bearing walls W2 and W4, respectively, indicate insignificant differences in response. The transverse displacements of

these walls were measured at the top, as well as the central one-third points. These displacement histories are superimposed on the same frame for each case to allow an estimation of the displacement profiles to be made at any given instant of time. Inspection of Figs. 3(b) and (c) reveals that both transverse walls vibrated at the frequency of the structure as a whole in the first "cantilever" mode, and both had remarkably similar peak displacements--0.42 in. at the top, 0.25 in. at two-thirds the wall height, and 0.12 in. at one-third the wall height. All of these maximum displacements were reached simultaneously. This picture is totally altered for Test 19 in Figs. 4(b) and (c) when the walls were not load-bearing. In addition to displacement magnitudes decreasing significantly (note that the scales for displacements are not the same in Figs. 3 and 4), there appears to be a slight increase in the frequency indicating the existence of local modes. Also, peak displacements are no longer attained simultaneously along the height, especially for W4 for which the peak amplitude at the top and two-thirds height are both 0.065 in. From about 12 seconds into the response, the displacement at the top is less in magnitude than that at the next location below it, indicating a "kink" due to local cracking along the height.

A striking difference in the response mechanism is illustrated by the in-plane displacements of W1 (reinforced) and W3 (unreinforced) together with readings of the slip of the top plate interconnecting the roof assembly relative to these two units. With the trusses parallel to table motion, Test 10, Fig. 3(d), the in-plane displacements measured at the top are of the same order of magnitude as the transverse wall displacements. Also, W3 developed a cracking plane along the entire length of the wall at the mortar joint of the eighth course from the bottom, and the motion recorded as deflection at the top was probably slippage along this plane. What was recorded as the in-plane displacement of W1 was due in part to the uplift of the footing under it. Both walls were bolted to the table after Test No. 13. Still, because of the great difference in the stiffness of W1 and W3, relative slip readings of the top plate showed great differences as indicated in Fig. 3(g). After the rotation of the roof, when W1 and W3 became load-bearing walls, the magnitudes of these displacements as well as the relative slip readings were reduced to only a fraction of their previous values. It should be noted also that during this test the walls were not restrained from uplift. This is readily observed from a comparison of Figs. 3(d) and (g) with Figs. 4(d) and (g). The same trend is noted for the corner units C3 (reinforced) and C4 (unreinforced) with the latter going through slightly greater amplitudes of displacement than its counterpart in both cases. Displacement readings at two different heights are shown in Figs. 3(e) and (f) and 4(e) and (f). Accelerations recorded on either side of the roof and superposed on the same diagram for comparison show an amplification ratio of 2 with respect to the table acceleration in the case when the trusses were parallel to motion (Fig. 3(h)) as compared to the state when their orientation was rotated through 90 degrees (Fig. 4(h)). The former figure also indicates a substantial amount of twist in the roof response due to the different stiffnesses of W1 and W3.

TESTS OF TIMBER ROOF-MASONRY WALL CONNECTIONS

An integral part of the research directed toward the assessment of the behavior of masonry assemblages under dynamic loading conditions has been the identification and evaluation of the mechanisms through which inertia forces generated at the roof level are transmitted to the masonry components and ultimately to the foundation (5). To this end, the five types of typical connection details shown in Fig. 5 were tested in duplicate concurrently with the shaking table tests. In addition to a simulation of the in- and out-of-plane connections of the shaking table specimen, typical connections for industrial buildings were also included in the test series as shown in Figs. 5(d) and (e). Figure 6 shows the overall force-deformation response of a connection of the type given in Fig. 5(a). Analysis and interpretation of the data obtained from this phase of the research is expected to give an indication of the strength requirements for typical connections in seismic design.

FUTURE TESTS

Following the examination and evaluation of the results from the first test specimen, specimens with increasing complexity are to be tested in the program. Figure 7 shows the features of the second model which is due to be tested during March, 1978. Future tests will include different reinforcing and opening details as well as clay brick units for the building material.

SUMMARY

The research program reported in this paper has the objective of providing experimental information to determine the seismic resistance of typical one-story masonry dwellings constructed in moderately seismic regions of the United States. Evaluation of selected quantities describing the behavior of the first test specimen which was simple in plan, but which contained significant components of a masonry structure, indicates the following:

- (1) The response of the test specimen to the base motions was complex and was affected by the orientation of the roof structure, the base fixity of the in-plane walls and the cracks that developed in the unreinforced walls.
- (2) The overall behavior is strongly dependent on the orientation and vibratory characteristics of the roof assembly. The in-plane response of walls is governed entirely by the inertia effects transmitted from the roof. The out-of-plane response depends on the constraint provided by the roof.
- (3) With the roof trusses oriented in the direction of the table motion, the test specimen was subjected to twelve consecutive base accelerations patterned after the Taft and El Centro earthquakes. During this series, the maximum peak table accelerations

were of the same order of magnitude as the original ground motions. After the roof structure was rotated through 90 degrees, the structure was subjected to sixteen additional motions. In general, the peak table accelerations recorded during these tests were considerably larger than the corresponding original motions with the exception of the Pacoima signal.

- (4) The first observed damage in the unreinforced walls occurred in the in-plane wall W3 when the test specimen was subjected to the Taft base motion with a peak acceleration of 0.214 g. It is not clear if the crack was initiated by the repair necessitated during the moving of the test specimen onto the shaking table. The out-of-plane unreinforced wall W4 was essentially undamaged during all tests while it was a load-bearing wall. When it was nonload-bearing, it remained undamaged when the test specimen was subjected to a sequence of Taft motions, but was cracked during Test E-0.311 when the peak acceleration of the El Centro motion was approximately equal to the peak of the original accelerogram.
- (5) The nominal amount of reinforcement used in the reinforced walls and corner specimens was sufficient to prevent any damage from occurring throughout all the tests.
- (6) The surface bonding material used to repair the cracked, unreinforced walls appeared to be quite effective. Following the repair of both in-plane and out-of-plane walls, the test specimen had to be subjected to base motions of substantially increased intensity before cracking occurred again.

ACKNOWLEDGMENTS

The research project reported in this paper is an ongoing three-year effort sponsored by the U.S. Department of Housing and Urban Development under Contract No. H-2387. The concrete block units were donated by the California Concrete Masonry Technical Committee through arrangements made by the Masonry Institute of America, and are gratefully acknowledged. D.A. Sullivan Co. fabricated the test structure. Planning of the tests was carried out with the suggestions of an Applied Technology Council Advisory Panel, consisting of Messrs. R.D. Benson, J. Gervasio, J. Kesler, O.C. Mann, L. Pritchard, and R.L. Sharpe. The government technical representative on the project was Mr. W. J. Werner. Messrs. L. Chang and A. Gerich also provided coordination with the Department of Housing and Urban Development. Student assistants T. Nearn and P. Buscovich did the laboratory work, D. Steere implemented the data acquisition setup with care, and the personnel of the Structural Research Laboratory headed by I. Van Asten contributed to nearly every phase of the investigation.

REFERENCES

1. Davis, R.E.. "Effect of Southern California Earthquake upon Buildings of Unit Masonry Construction," report to Committee C-12 on Mortars for Unit Masonry of the American Society of Testing Materials, Department of Civil Engineering, University of California, Berkeley, May 31, 1933.
2. Hegemier, G.A., et al, "Earthquake Response and Damage Prediction of Reinforced Concrete Masonry Multistory Buildings, Parts I and II," Proceedings of the Sixth World Conference on Earthquake Engineering, New Delhi, India, 1977.
3. Mayes, R.L., and Clough, R.W., "State-of-the-Art in Seismic Shear Resistance of Masonry--An Evaluation and Review," Earthquake Engineering Research Center Report No. 75-21, University of California, Berkeley, October, 1975.
4. Mayes, R.L., Omote, Y., and Clough, R.W., "Cyclic Shear Tests of Masonry Piers, Volume I--Test Results," Earthquake Engineering Research Center Report No. 76-8, University of California, Berkeley, May, 1976.
5. Mayes, R.L., Clough, R.W., and Omote, Y., "Seismic Research on Masonry, University of California, Berkeley, 1972-1977," Earthquake Resistant Masonry Construction: National Workshop Proceedings, edited by R.E. Crist and L.E. Cattaneo, National Bureau of Standards Building Science Series No. 106, September, 1977.
6. Meehan, J.F., et al, "Managua, Nicaragua Earthquake of December 23, 1972," Earthquake Engineering Research Institute, Oakland, California, 1973.
7. Rea, D., and Penzien, J., "Dynamic Response of a 20 ft by 20 ft Shaking Table," Proceedings of the Fifth World Conference on Earthquake Engineering, Rome, Italy, 1973.

TABLE 1: LIST OF DYNAMIC TESTS AND TESTING CONDITIONS

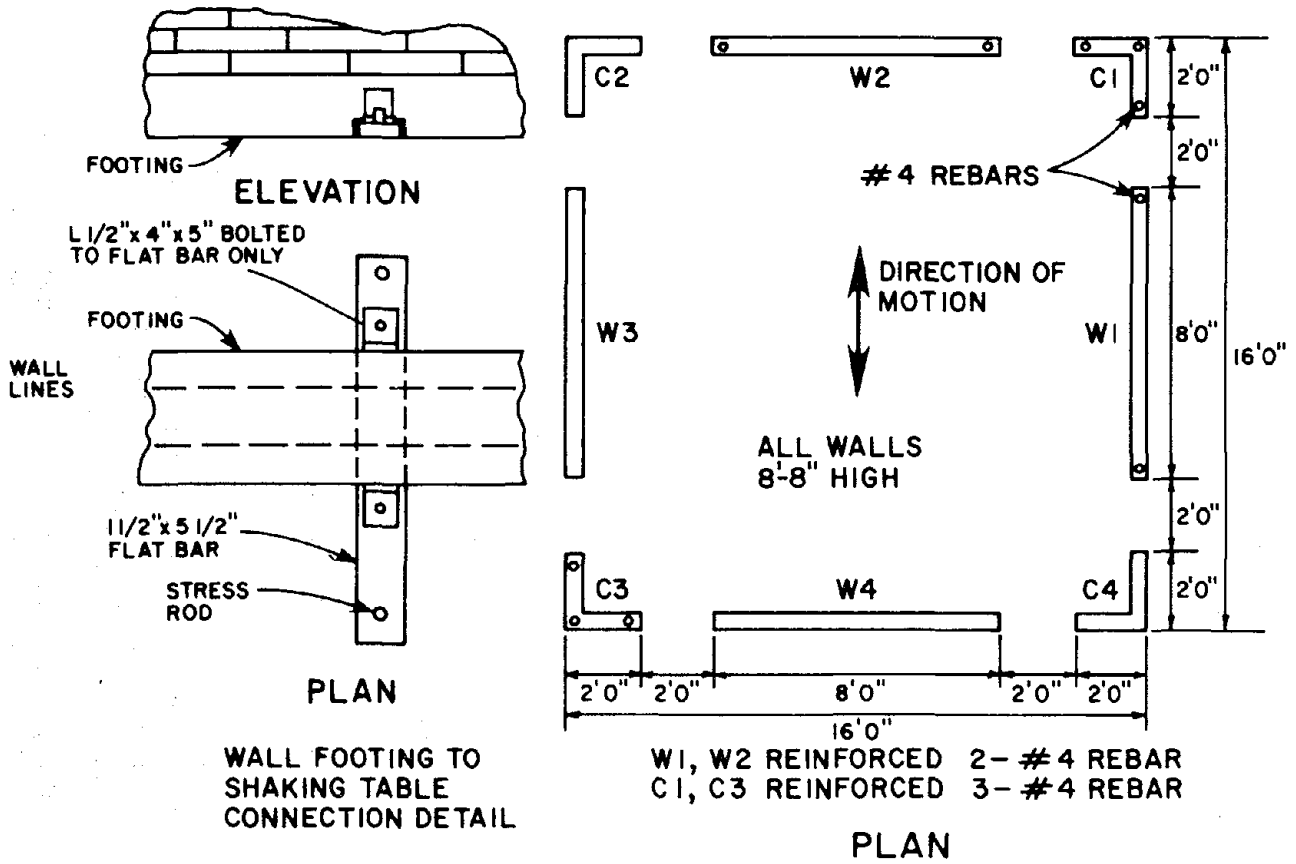
<u>Test Sequence</u>	<u>Reference Number</u>	<u>Base Motion/ Span Setting</u>	<u>Remarks</u>
1	T-0.002 ⁽¹⁾	Taft/000	No weights attached to the roof; trusses oriented in the direction of table motion
2	T-0.026	Taft/040	
3	T-0.050	Taft/080	
4	T-0.066	Taft/100	Concrete weights totaling 12,000 lbs. attached to the roof assembly
5	T-0.081	Taft/150	
6	T-0.122	Taft/200	
7	T-0.147	Taft/250	
8	T-0.190	Taft/300	
9	T-0.214	Taft/350	W3 cracked along the mortar joint of the 8th course from bottom; slippage along this plane
10	T-0.267	Taft/400	Crushing at ends of crack in W3
11	T-0.285 ⁽²⁾	Taft/300	Crack in W3 restrained by stressed metal tubing; new crack plane along 2nd course from bottom

(1) This value represents the "noise" in the recorded signal, hence peak values given may be off by this much.

(2) Command system malfunctioned, resulting in a significantly altered base motion on the table.

Table 1 (continued): List of Dynamic Tests and Testing Conditions

12	E-0.140	E1 Centro/200	
13	E-0.282	E1 Centro/400	W3 cracked along 5th and 6th courses from bottom; footing underneath W1 bolted onto table
14	T-0.051	Taft/080	Roof rotated 90 degrees; W3 and C4 repaired; footing under W3 bolted
15	T-0.062	Taft/100	
16	T-0.092	Taft/150	C2 repaired
17	T-0.119	Taft/200	
18	T-0.193	Taft/300	
19	T-0.248	Taft/400	
20	E-0.209	E1 Centro/300	
21	E-0.311	E1 Centro/450	W4 cracked along joint of 1st course from bottom and 6th course from top
22	E-0.214	E1 Centro/300	W4 repaired
23	E-0.323	E1 Centro/450	
24	E-0.455	E1 Centro/600	C2 cracked at 7th course from top
25	P-0.247	Pacoima/200	
26	P-0.386	Pacoima/300	
27	P-0.492	Pacoima/400	W3 failed by cracking at 1st joint from bottom; W4 cracked at 6th course from top
28	P-0.627	Pacoima/500	C4 crushed at corner junction
29	E-0.592	E1 Centro/750	Imminent collapse of structure; reappearance or growth of all previous cracks; loosening of roof



WALL FOOTING TO SHAKING TABLE CONNECTION DETAIL

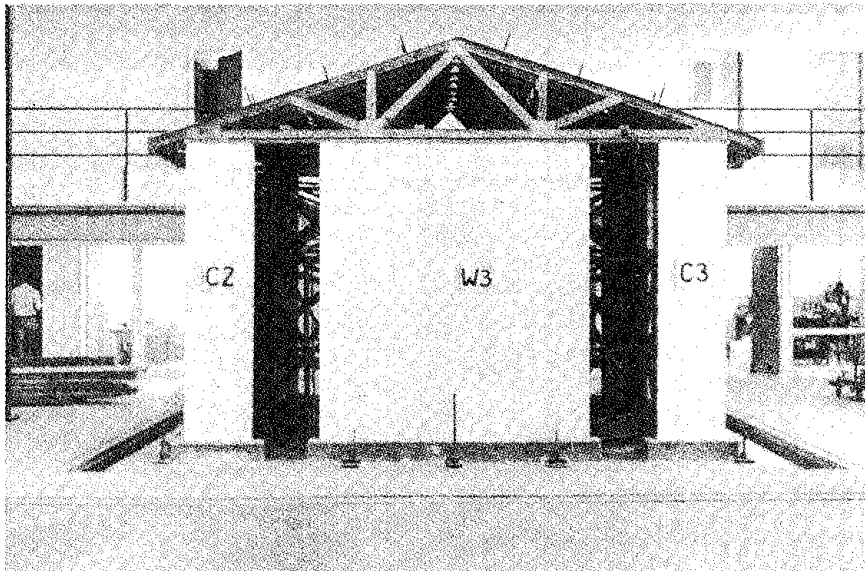


Figure 1. Test Structure

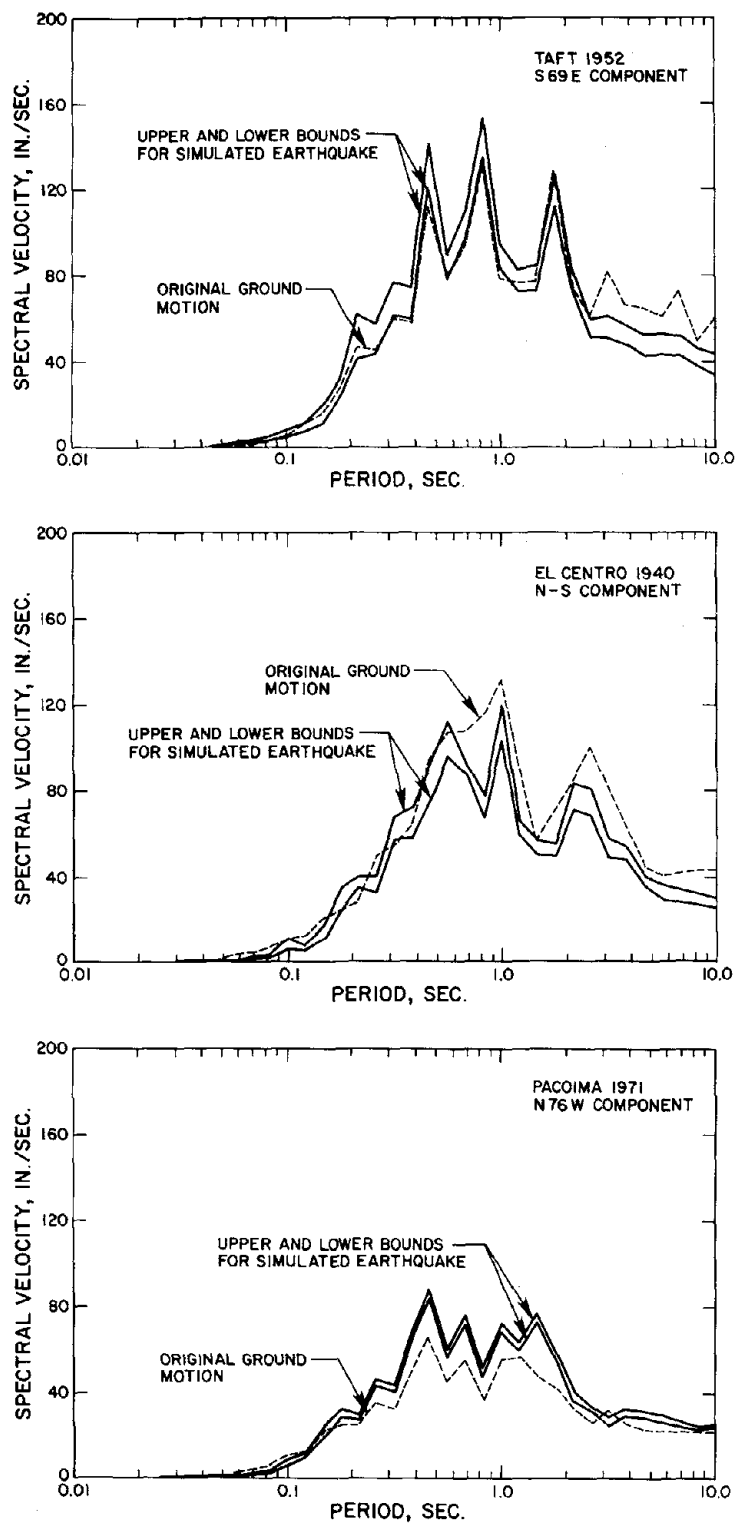


Figure 2. Normalized Response Spectra for Simulated and Original Earthquakes

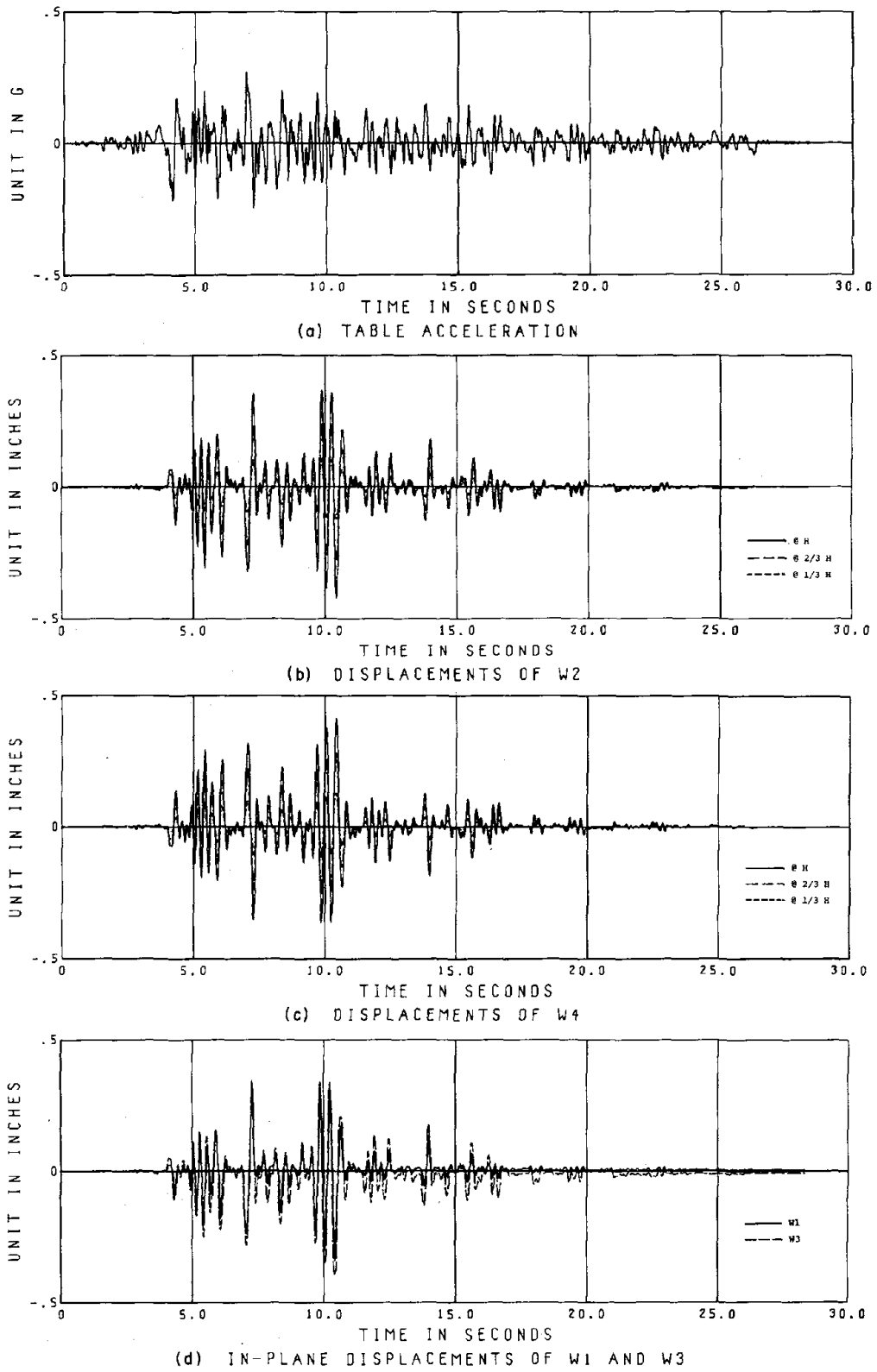


Figure 3. Measured Response: Trusses Parallel to Table Motion

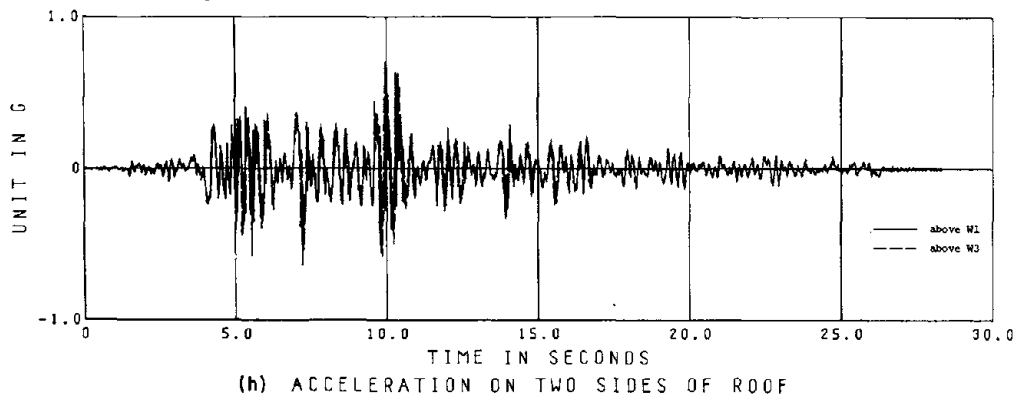
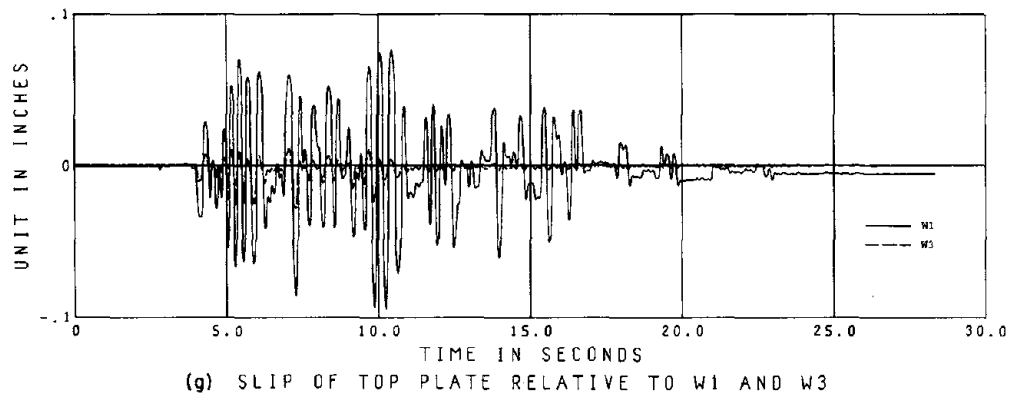
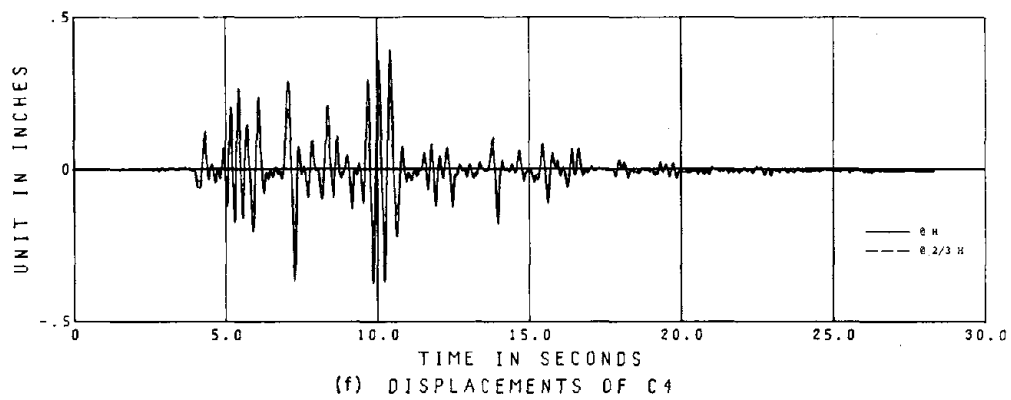
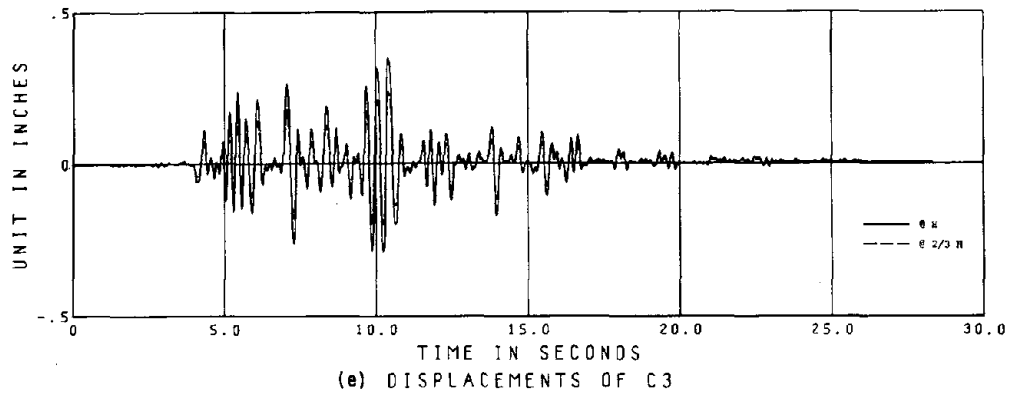
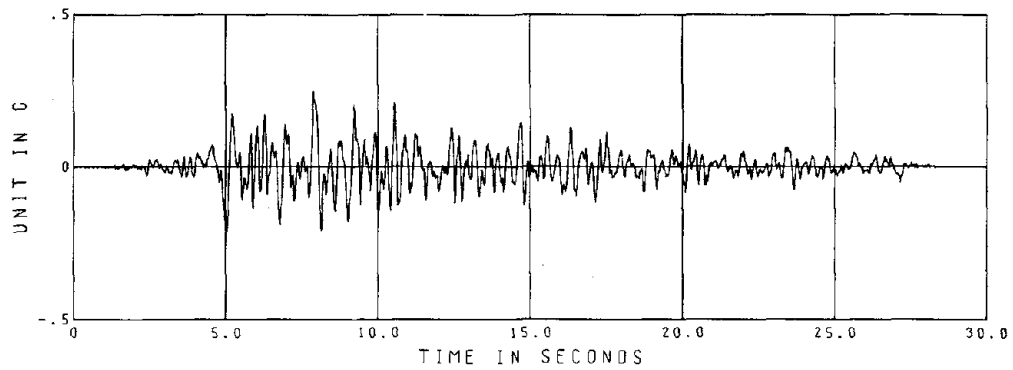
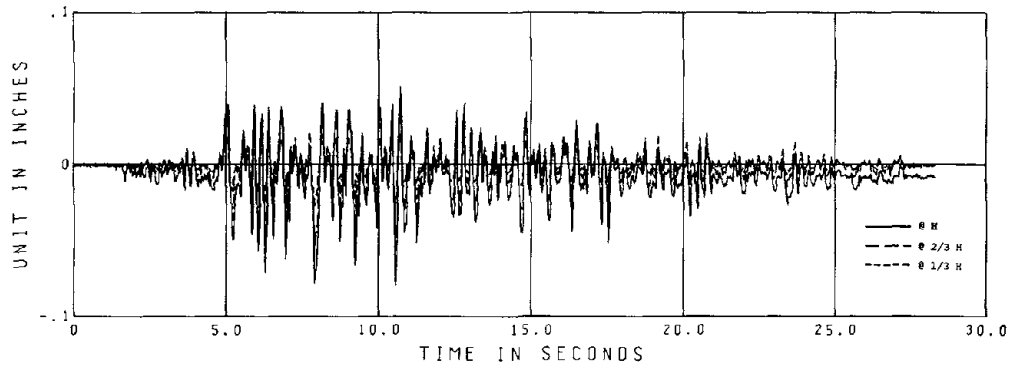


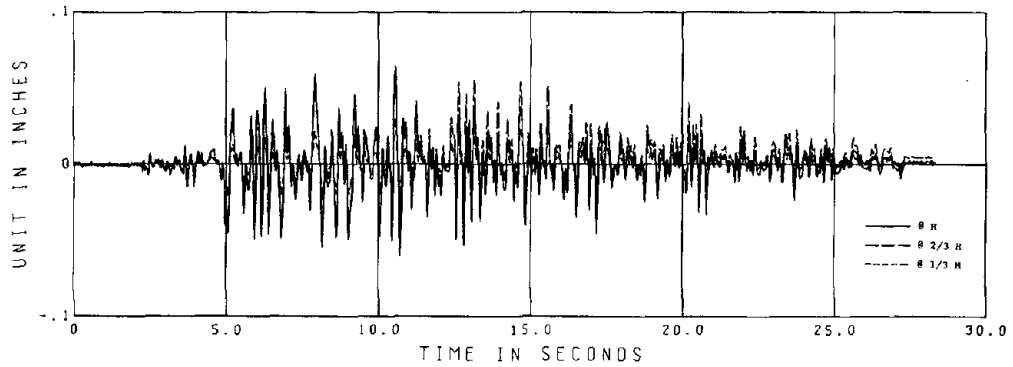
Figure 3 (Cont.). Measured Response: Trusses Parallel to Table Motion



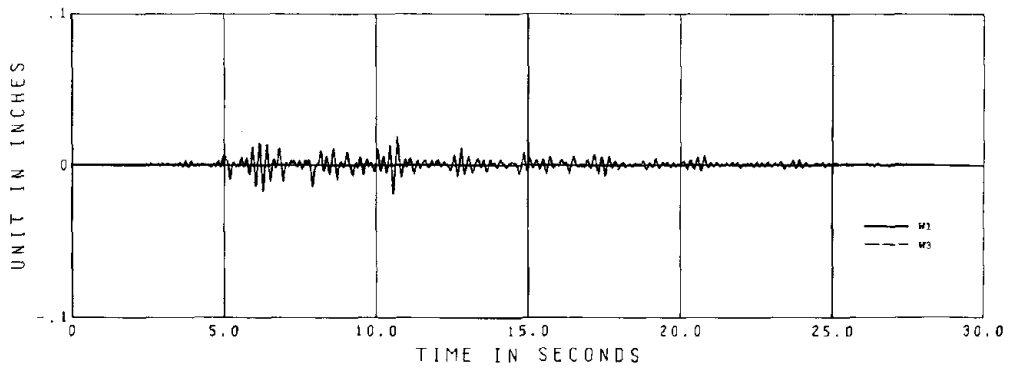
(a) TABLE ACCELERATION



(b) DISPLACEMENTS OF W2

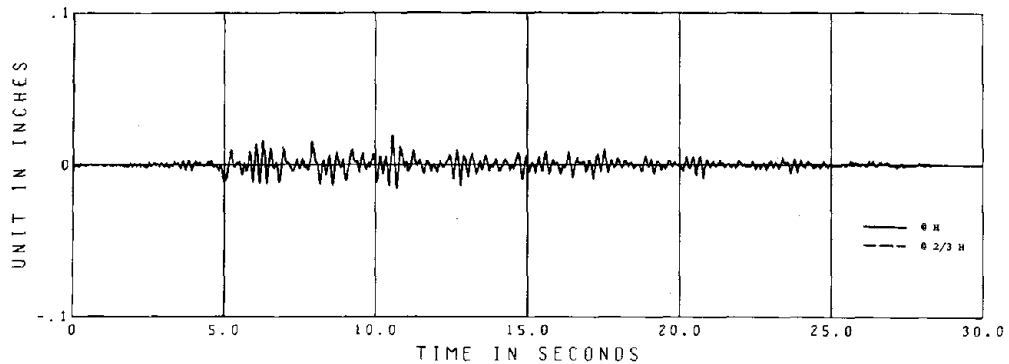


(c) DISPLACEMENTS OF W4

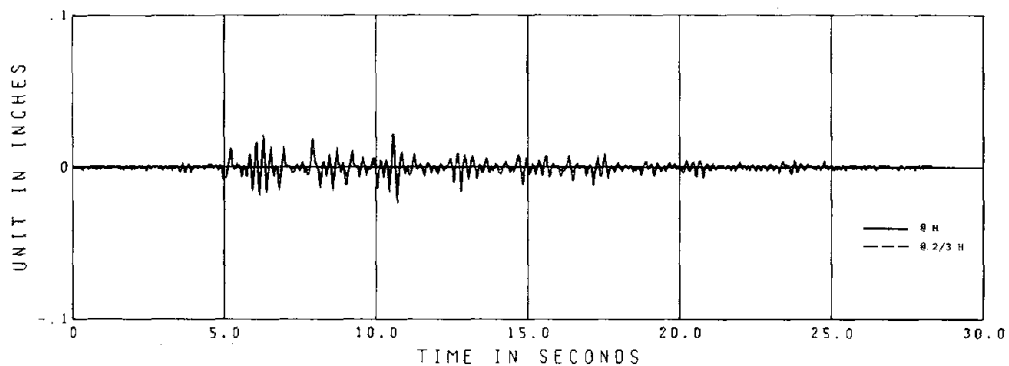


(d) IN-PLANE DISPLACEMENTS OF W1 AND W3

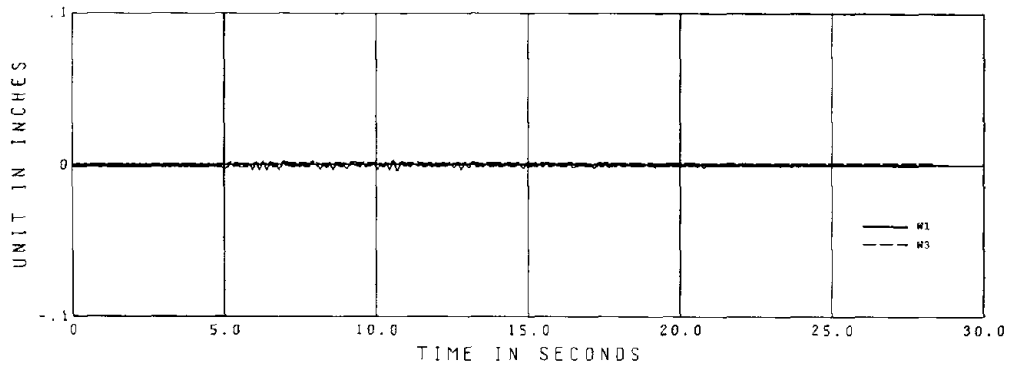
Figure 4. Measured Response: Trusses Transverse to Table Motion



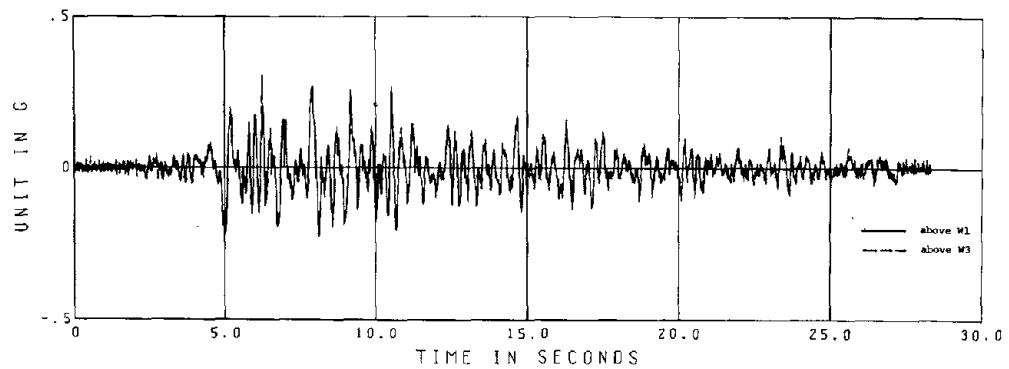
(e) DISPLACEMENTS OF C3



(f) DISPLACEMENTS OF C4



(g) SLIP OF TOP PLATE RELATIVE TO W1 AND W3



(h) ACCELERATION ON TWO SIDES OF ROOF

Figure 4 (Cont.). Measured Response: Trusses Transverse to Table Motion

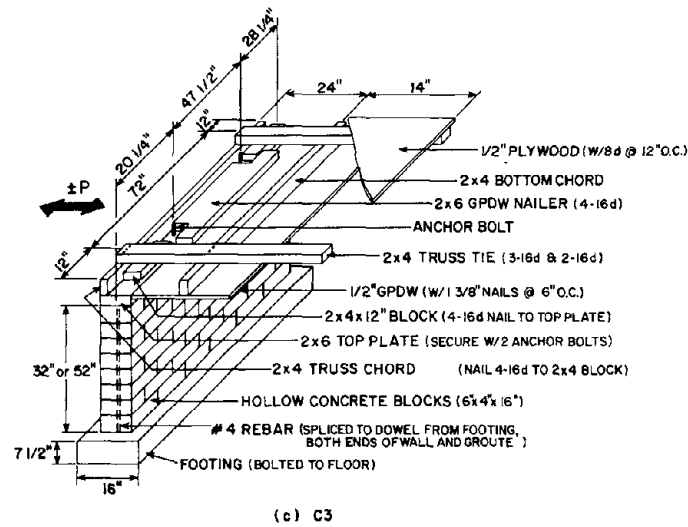
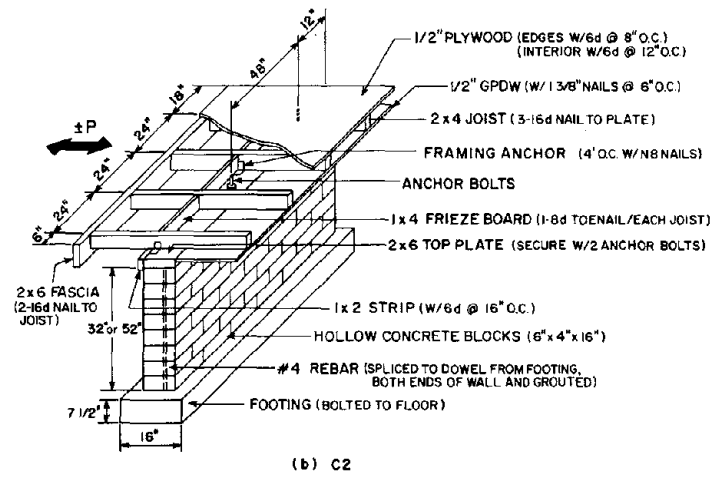
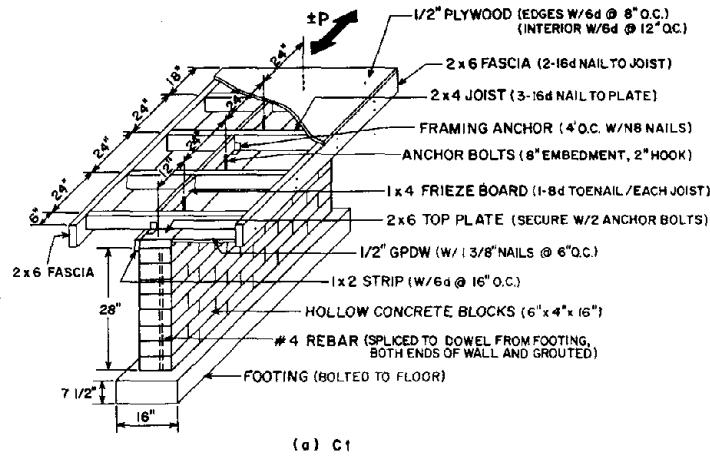
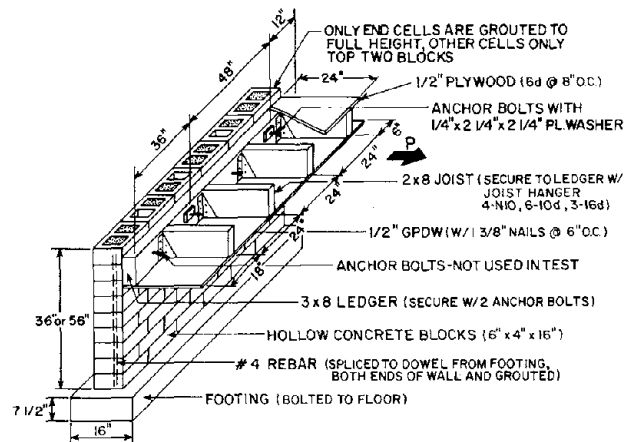
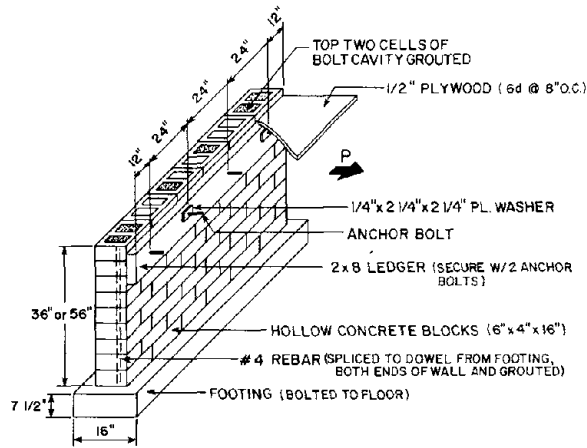


Figure 5. Connection Test Specimens



(d) C4



(e) C5

Figure 5 (Cont.). Connection Test Specimens

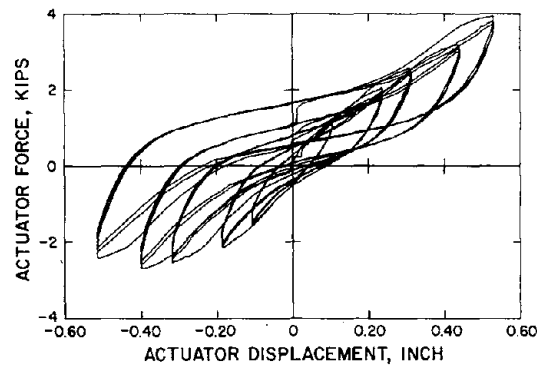


Figure 6. Measured Response of a Connection of Type C1

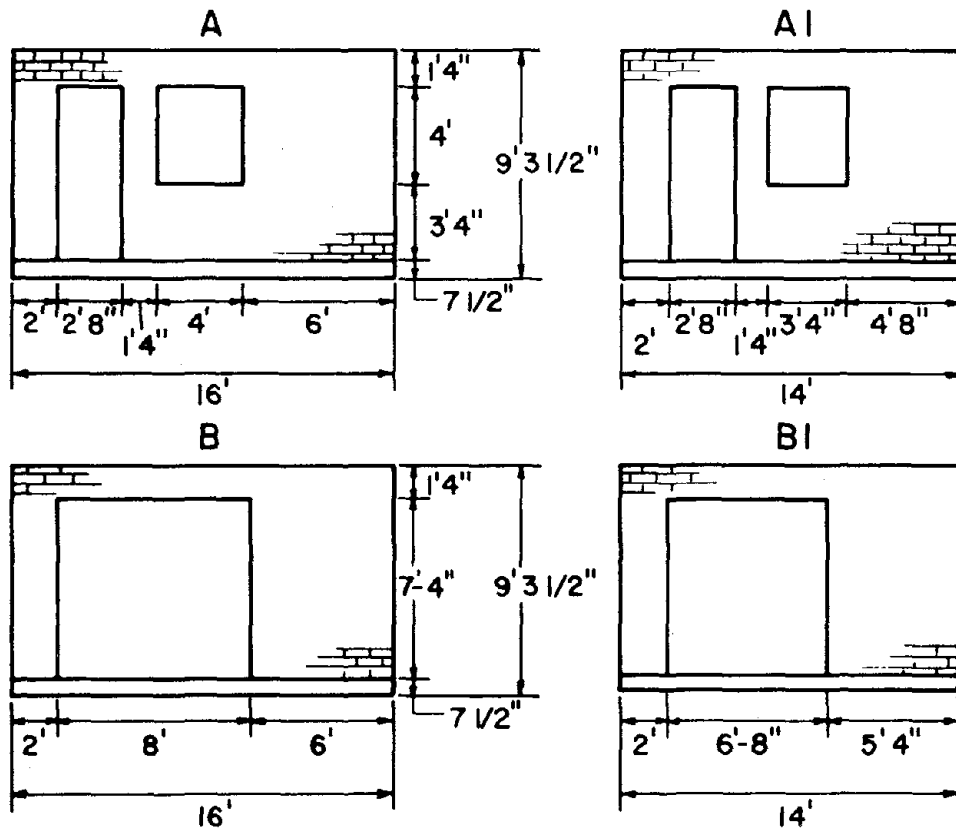
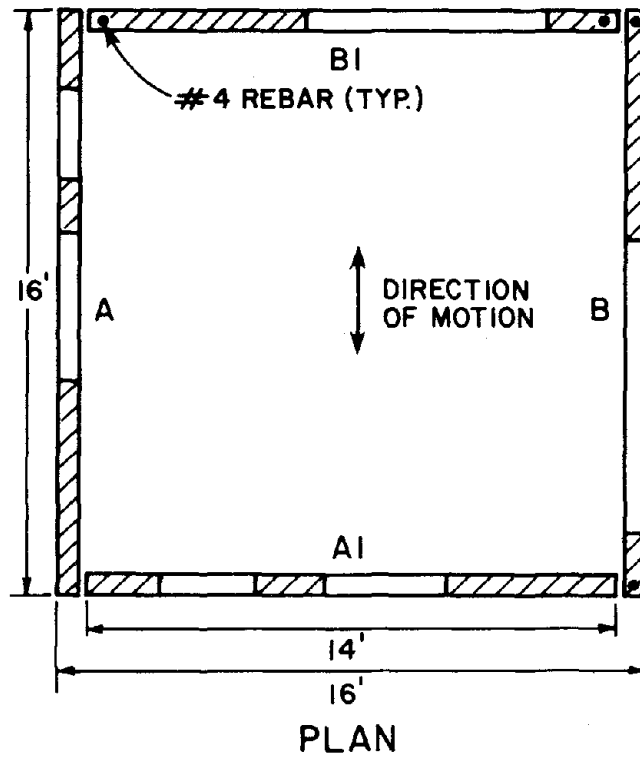


Figure 7. Details of the Second Masonry House

STABILITY UNDER SEISMIC LOADING OF BUILDINGS WITH
FULLY CRACKED WALL-FLOOR JOINTS¹

by

W. Nachbar² and R. Furgerson³

ABSTRACT

Structural collapse by loss of kinematic integrity is studied. In particular, the failure of a floor slab and shear-wall model structure by loss of support is considered. It is assumed that all floor slab to shear-wall connection reinforcement has failed, and that motions of the floor slab relative to the shear-walls and due to acceleration applied to the foundation are restrained by friction only. Coulomb friction with a constant coefficient of friction is used in the analysis. Our previous work has shown that a Coulomb friction law with a constant coefficient of friction is a good approximation to the experimentally observed frictional behavior of cracked joints in concrete masonry blocks, provided that the blocks have slid against one another a distance that is found to be short compared to shear-wall widths seen in standard construction practice. The collapse time is defined as the instant when the floor slab first ceases to be in contact with its supporting walls. Since vertical displacements are not considered in the present model, this definition of collapse implies loss of structural integrity. The seismic foundation acceleration input is simulated by a sinusoidal oscillation contained within an envelope that has a shape representative of a type of earthquake. A number of envelope shapes are considered. The results of computations show that the relationship between collapse time and maximum foundation acceleration, earthquake duration and predominant frequency is surprisingly well-defined. Although derived from a much simplified model, these results defining safe and unsafe parametric regimes can be of use to engineers and building designers.

¹Research was sponsored by the National Science Foundation under Grant NSF ENV 74-14818.

²Professor, Department of Applied Mechanics and Engineering Sciences, University of California, San Diego, La Jolla, California, 92093.

³Research Assistant, Department of Applied Mechanics and Engineering Sciences, University of California, San Diego, La Jolla, California, 92093.

STABILITY UNDER SEISMIC LOADING OF BUILDINGS WITH
FULLY CRACKED WALL-FLOOR JOINTS¹

by

W. Nachbar² and R. Furgerson³

INTRODUCTION

Damage assessment photographs of structures subject to earthquake ground motion frequently show that the seismic forces break connections holding major substructures together allowing them to move as individual rigid bodies. Stairwells, elevator shafts, precast floor slabs, roof channels and reinforced concrete roadway bridge spans are seen to be examples of such substructures. Reference (2) contains many excellent photographs of such substructures more or less intact after being overthrown from their foundations or sliding off their supporting uprights.

The following analysis describes a failure of this class through the solution of rigid body equations of motion for a simplified shear-wall floor slab system subject to a realistic friction law between the floor slab and shear-wall and a simulated seismic acceleration applied to the shear-wall foundation. The solution predicts the elapsed time after onset of acceleration of the kinematic failure of the system by loss of support. Further, the results show a surprisingly well-defined relation between the time that the system can resist the applied acceleration and the predominant frequency and maximum amplitude of the applied acceleration.

¹Research was sponsored by the National Science Foundation under Grant NSF ENV 74-14818.

²Professor, Department of Applied Mechanics and Engineering Sciences, University of California, San Diego, La Jolla, California, 92093.

³Research Assistant, Department of Applied Mechanics and Engineering Sciences, University of California, San Diego, La Jolla, California, 92093.

DESCRIPTION OF THE MODEL

Consider the assembly of a rigid floor slab supported by two rigid walls built into a rigid foundation, Fig. 1. An analysis of sliding concrete block experiments suggests that Coulomb friction with a coefficient of 0.6 is an appropriate friction condition to prescribe⁴. The slab is constrained to move with the walls by Coulomb friction only. A prescribed acceleration, $a(\tau)$, acts on the foundation.

MATHEMATICAL MODEL AND NUMERICAL SOLUTION TECHNIQUE

Including Coulomb friction with its stick-slip character introduces significant complications in the integration of the equations of motion. Heretofore, the rather dubious substitution of an "equivalent" viscous or velocity dependent friction law to render the equations of motion more tractable analytically has been made. By contrast, this work relies wholly on numerical methods to integrate the unsimplified equations.

The floor slab begins slipping on the walls when the magnitude of the base acceleration in g's exceeds the friction coefficient, if the slab is sliding over the walls, it will stop sliding if the magnitude of the base acceleration in g's is less than the friction coefficient and the velocities of the slab and walls are equal. The describing equations follow:

Let

$y_s(\tau)$ = nondimensional displacement of the floor slab
from its $\tau = 0$ location

$y_b(\tau)$ = nondimensional displacement of wall
from its $\tau = 0$ location

$y_s(\tau) = \dot{y}_s(\tau) = y_b(\tau) = \dot{y}_b(\tau) = 0$ at $\tau = 0$

then

$$\left. \begin{array}{l} \ddot{y}_b(\tau) = a(\tau) \\ \ddot{y}_s(\tau) = a(\tau) \end{array} \right\} \begin{array}{l} \text{if floor slab is not} \\ \text{sliding on the walls} \end{array}$$

floor slab will slide if

$$|a(\tau)| > a_s$$

$$\left. \begin{aligned} \ddot{y}_b(\tau) &= a(\tau) \\ \ddot{y}_s(\tau) &= -a_s \operatorname{sign}(\dot{y}_s - \dot{y}_b) \end{aligned} \right\} \begin{array}{l} \text{if floor slab is sliding} \\ \text{on the walls} \end{array}$$

floor slab will stop sliding if

$$|a(\tau)| < a_s \quad \text{and} \quad \dot{y}_b(\tau) = \dot{y}_s(\tau)$$

A brief description of the solution technique follows; reference (5) contains complete details of the code.

The integration of the initial value problem proceeds by marching, with a polynomial approximation of the slab and wall velocities updated at each time step. Tests for changes in motion regime, slipping or sticking, are then performed on the solution.

If the slab and walls were sticking at the previous time step, the magnitude of the acceleration is computed. If the magnitude of acceleration is less than a_s , the motion regime is unchanged and the solution is again advanced a time step. If the magnitude of acceleration is larger than a_s , then slipping begins at some time between the current solution time and the last solution time. A Newton iteration calculates the time at which slipping begins,

$$\text{previous time} < \tau < \text{present time such that } |a(\tau)| = a_s.$$

The integration from the previous time is repeated with a step size to advance the solution to the time of slipping, the motion regime is changed, and the slipping equations are then advanced to the intended time with the displacement and velocities of the slab and walls at the time of slipping as the initial conditions. Marching then proceeds with the original time step.

If the slab was sliding on the wall at the last time step, the solution is advanced integrating the equations of motion for the slipping regime and the solution there is tested. If $|a(\tau)| > a_s$, marching proceeds to the next time step. If $|a(\tau)| < a_s$, then the difference of the polynomials approximating the wall and slab velocities is formed. If the difference of velocities changes sign in the interval, the velocities are presumed to be equal somewhere in the interval. The time when the velocity difference is zero is calculated, and the integration of the slipping equations is advanced from the previous time to the time of sticking, time of zero velocity difference. The equations for sticking floor slab and walls are integrated from the time of sticking to the intended time. Afterward, marching proceeds using the

original step size.

Detail drawings of building plans¹ and photographs of construction underway³ show that a reasonable floor slab bearing length is one half the wall thickness, $\delta = 1$. The difference in displacements, $\delta(\tau)$, is tested at each time step. Should the magnitude of the difference exceed 1, the assembly is considered to have collapsed, and the time at the present integration step is taken as the collapse time.

While it is true that distance from the focus of an earthquake, depth of focus, whether the soil is firm or whether it is soft and layered, and other geological concerns control what the local earthquake ground accelerations will be⁵, it is expeditious to regard earthquake ground motion accelerograms as showing quickly varying random oscillations within a much smoother envelope which rises to a peak then slowly decays.

The function $(e^{-\alpha t^* \tau} - e^{-\beta t^* \tau})$ is a smooth, 2 parameter envelope function which is qualitatively similar to those of recorded accelerograms. Specifying τ_{rise} and τ_{dur} allows the parameters α and β to be evaluated. This was done for 3 pairs of τ_{rise} and τ_{dur} to yield 3 envelope functions with characteristics representative of a fast rising, a moderately rising, and a slowly rising envelope function as seen in published earthquake ground motion accelerograms. Table 1 shows the correspondence between the chosen nondimensional characteristic times and real time for an "8 inch" wall. Choosing the acceleration function, $a(\tau)$, as

$$a(\tau) = A \frac{2(t^*)^2}{d} \frac{g}{S_{\text{max}}} (e^{-\alpha t^* \tau} - e^{-\beta t^* \tau}) \sin \omega \tau$$

where

$$S_{\text{max}} \equiv \max_{\tau > 0} \left\{ (e^{-\alpha t^* \tau} - e^{-\beta t^* \tau}) \sin \omega \tau \right\}$$

gives the oscillatory motion within an envelope of realistic proportion. Fig. 2 shows the superposition of the North-South component of the accelerogram of the El Centro earthquake of 1940 and the fast rising envelope scaled to a similar height versus nondimensional time.

RESULTS AND DISCUSSION

For each of the three envelope shapes, the collapse time is computed for amplitude A in the range of $0.7 \geq A \geq 1.15$ and for frequency f in the range $0.5 \leq 1.125$. Because of the finite duration

of earthquakes, the smaller collapse times represent greater hazard than the larger collapse times. The product of a scaling parameter, which is a reference nondimensional time, and the reciprocal of the nondimensional collapse time is called γ_c ; γ_c is plotted on the vertical scale of the cartesian coordinate system in reciprocal time - envelope amplitude - frequency space, in brief the γ -A-f space. The larger values of γ_c are the more significant. Computations were made with different scaling parameters to find a scaling parameter which makes the surfaces of γ_c in γ -A-f space relatively independent of the envelope shape. Scaling parameters of τ_{rise} , τ_{max} , τ_{dur} , and 1 were tried. The greatest similarity is shown in the surfaces $\gamma_c(A, f) \equiv \tau_{\text{rise}}/\tau_c$ and $\gamma_c \equiv \tau_{\text{max}}/\tau_c$; these surfaces are shown in Figs. 3 to 8. The cross-hatching in these figures represents lines parallel to the amplitude and frequency axes following the surface $\gamma_c(A, f)$. One notes that, for a given frequency, the collapse factor increases rapidly with amplitude after a critical amplitude is reached. Fig. 9 gives an indication of this steepness in the area of critical amplitude. On the other hand, the collapse factor γ_c decreases with increasing frequency at a fixed amplitude.

In addition, the complete displacement histories for certain A and f in the critical area were examined to demonstrate that the interval of integration (Sect. 2) was chosen adequately long to reach collapse in all possible cases. Fig. 10 shows such a displacement record with the peak relative displacement $\delta(\tau)$ per cycle decreasing for $\tau > \tau_{\text{max}}$. Such records also justify the use of the Coulomb friction model, as experiments (Ref. 4) show that for concrete blocks sliding along cracked grouted and mortared surfaces, the friction ratio μ approaches the asymptotic Coulomb friction value after sliding about 0.4 inches. The present calculations show sliding of many times that distance before the collapse time is reached.

τ_{\max}	value of τ at maximum of the acceleration envelope
τ_{rise}	value of τ at which the prescribed acceleration envelope first attains half maximum value
μ	friction ratio: frictional force/normal force

	Nondimensional Time	Real Time (seconds)
fast rising envelope		
τ_{rise}	= 3.38	0.33
τ_{\max}	= 27.78	2.75
τ_{dur}	= 732.11	72.48
moderately rising envelope		
τ_{rise}	= 8.92	0.88
τ_{\max}	= 37.89	3.75
τ_{dur}	= 113.80	11.27
slow rising envelope		
τ_{rise}	= 12.81	1.27
τ_{\max}	= 63.13	6.25
τ_{dur}	= 266.23	26.36

Table 1. The correspondence between the chosen nondimensional characteristic times and real time for an "8 inch" wall, $t^* = .099$.

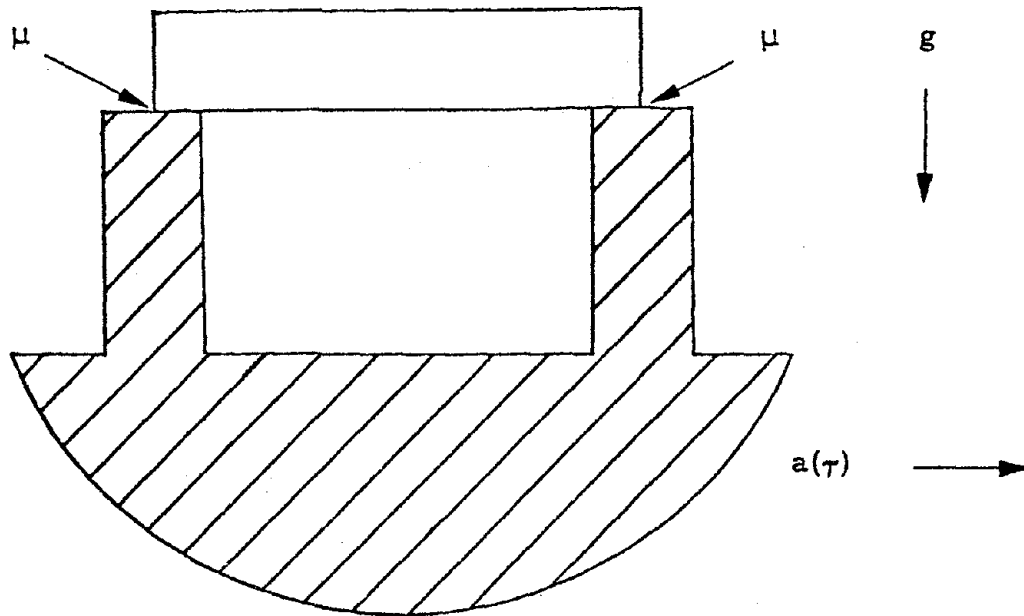


Fig. 1. Configuration of the idealized wall-floor slab assemblage.

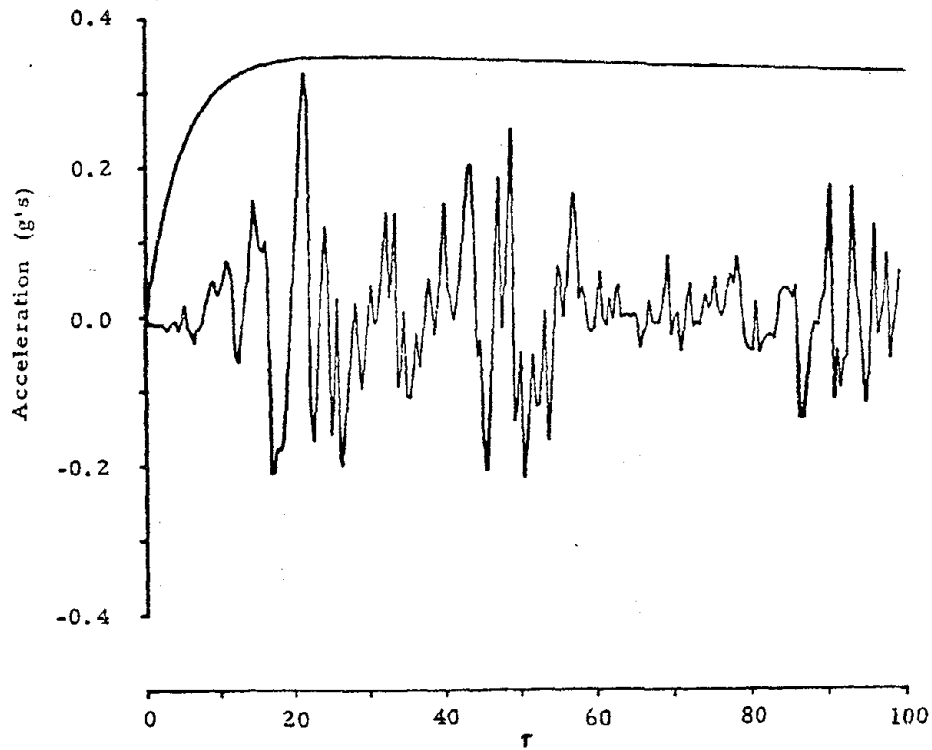


Fig. 2. Comparison of the fast rising acceleration envelope with an earthquake accelerogram (El Centro, 1940) versus nondimensional time τ .

APPENDIX I - REFERENCES

1. Amrhein, J. E. Reinforced Masonry Engineering Handbook. Masonry Institute of America, Los Angeles, Ca. 1972.
2. Jennings, P. C., ed. Engineering Features of the San Fernando Earthquake February 9, 1971. Earthquake Engineering Research Laboratory, EERL 71-02, California Institute of Technology, Pasadena, Ca. 1971.
3. Johnson, F. B., ed. Designing, Engineering, and Constructing with Masonry Products. Proceedings of the International Conference of Masonry Structural Systems, University of Texas at Austin, Austin, Tx. 1969.
4. Nachbar, W., R. Furgerson. "Statistical Analysis of Post-Fractured Concrete Masonry Joints," Report No. AMES-NSF TR-76-8, University of California, San Diego, 1976.
5. _____ . "Collapse Under Seismic Acceleration of an Idealized Wall-Floor Slab System with Frictional Constraints," Report No. AMES-NSF TR-77-2, University of California, San Diego, 1977.
6. Newmark, N. M., E. Rosenblueth. Fundamentals of Earthquake Engineering. Prentice-Hall, Inc., Englewood Cliffs, N. J., 1971.

APPENDIX II - NOTATION

$a(\tau)$	prescribed nondimensional acceleration, $a \equiv \frac{d^2}{d\tau^2} y(\tau)$
a_{\max}	$\max_{\tau > 0} a(\tau) $
a_s	nondimensional acceleration at which the floor slab begins sliding: $a_s \equiv 2(t^*)^2 \mu g/d$
d	width of the wall (feet)
f	frequency of base oscillation (Hz)
g	acceleration of gravity (32.2 ft/sec^2)
t	time (seconds)
t^*	a characteristic time defined by $(d/(2g))^{1/2}$
$u(\tau)$	relative horizontal displacement between the wall and the floor slab
$y(\tau)$	prescribed nondimensional displacement of base
y_{\max}	$\max_{\tau > 0} y(\tau) $
A	maximum expressed in "g's" of the prescribed nondimensional acceleration, $a(\tau)$
α, β	parameters controlling the shape of the acceleration envelope
$\delta(\tau)$	nondimensional relative displacement, $u/(d/2)$
ω	nondimensional frequency, $2\pi ft^*$
γ_c	collapse factor proportional to $(\tau_c)^{-1}$
τ	nondimensional time, t/t^*
τ_c	value of τ at collapse
τ_{dur}	value of τ at which the prescribed acceleration envelope decreases to half maximum amplitude

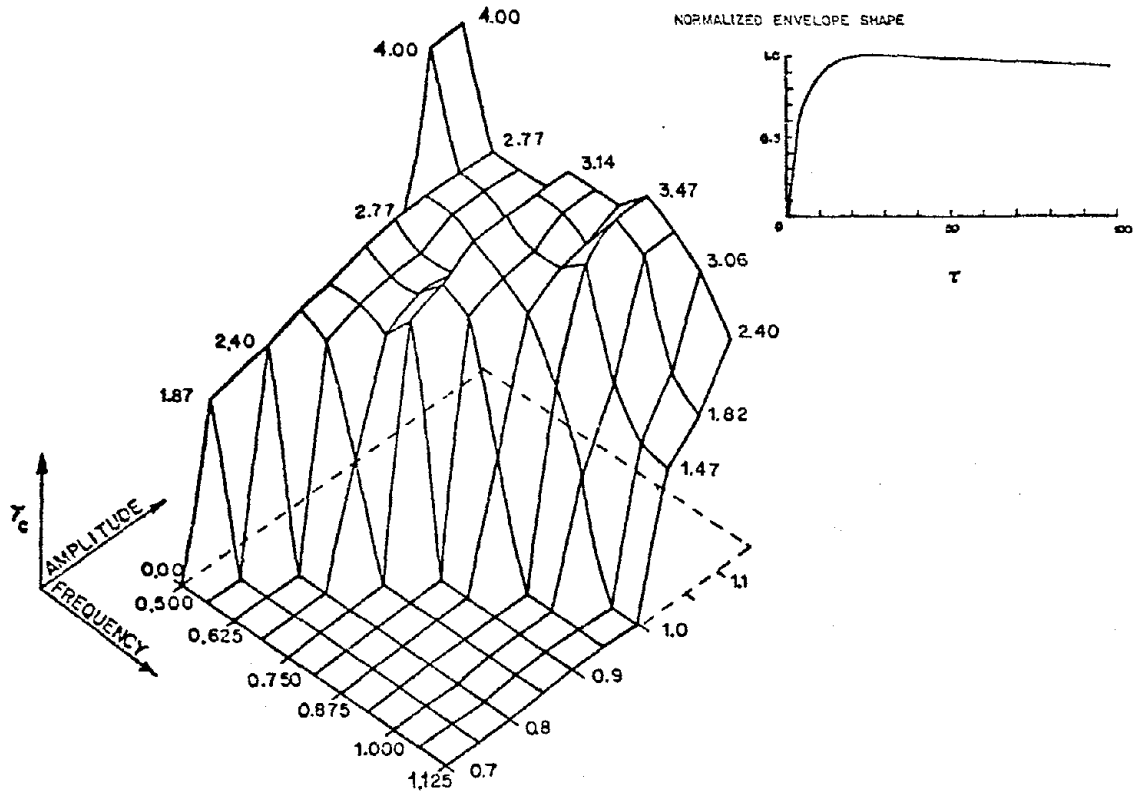


Fig. 3. Surface γ_c (A, f) for the scaling parameter τ_{max} , $\gamma_c \equiv \tau_{max}/\tau_c$, computed with the base acceleration contained in a fast rising envelope.

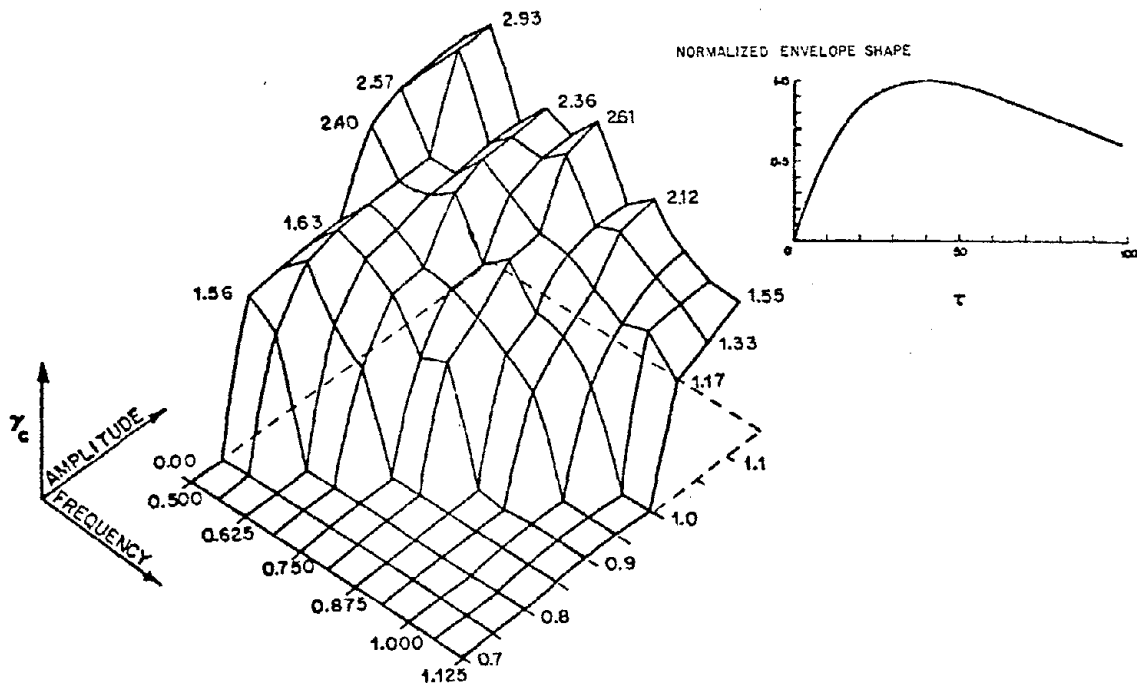


Fig. 4. Surface γ_c (A, f) for the scaling parameter τ_{max} , $\gamma_c \equiv \tau_{max}/\tau_c$, computed with the base acceleration contained in a moderately rising envelope.

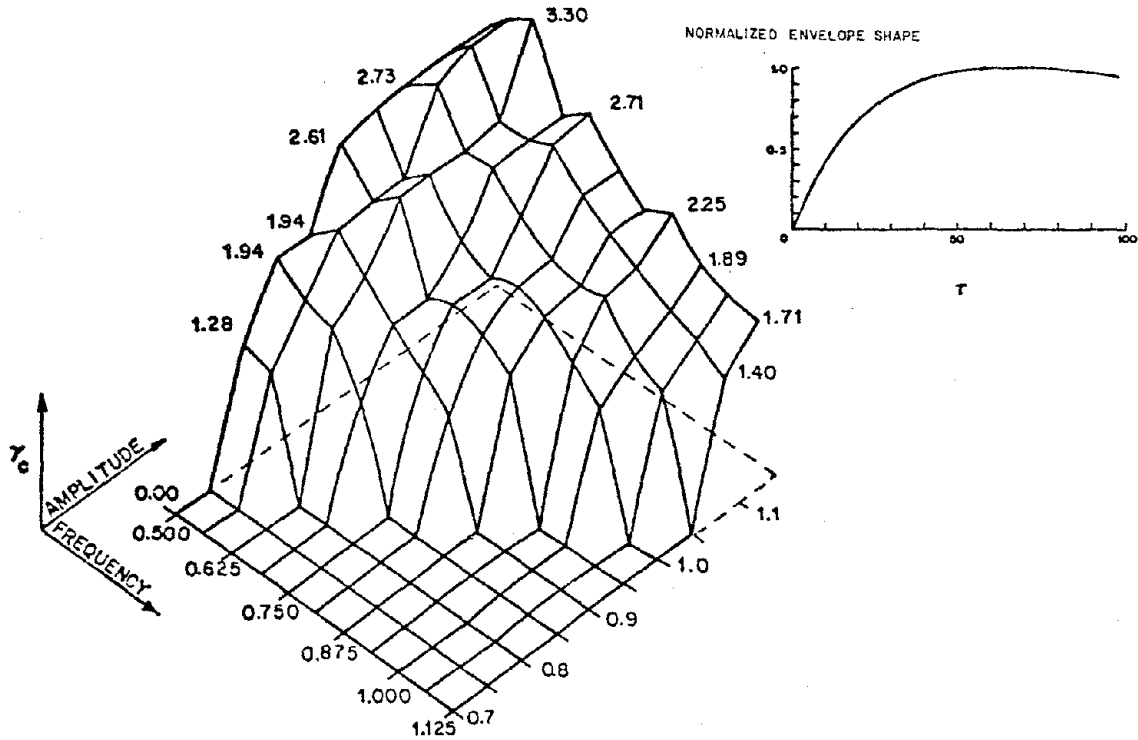


Fig. 5. Surface $\gamma_c (A, f)$ for the scaling parameter τ_{max} , $\gamma_c \equiv \tau_{max}/\tau_c$, computed with the base acceleration contained in a slowly rising envelope.

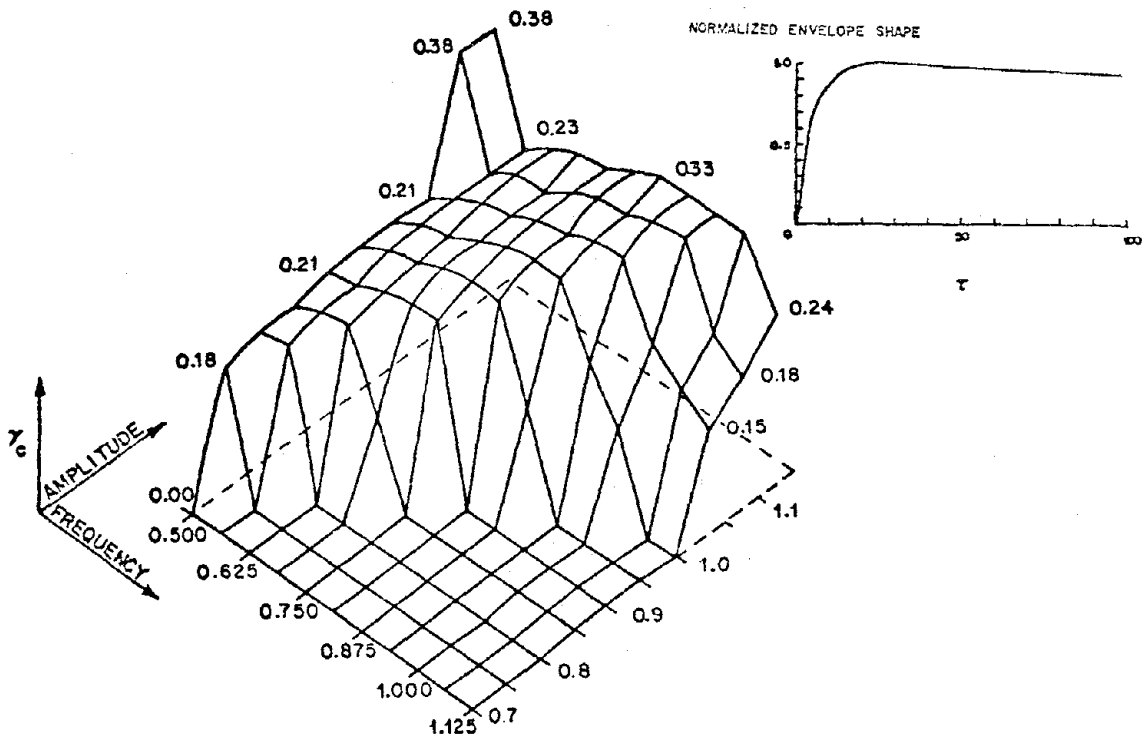


Fig. 6. Surface $\gamma_c (A, f)$ for the scaling parameter τ_{rise} , $\gamma_c \equiv \tau_{rise}/\tau_c$, computed with the base acceleration contained in a fast rising envelope.

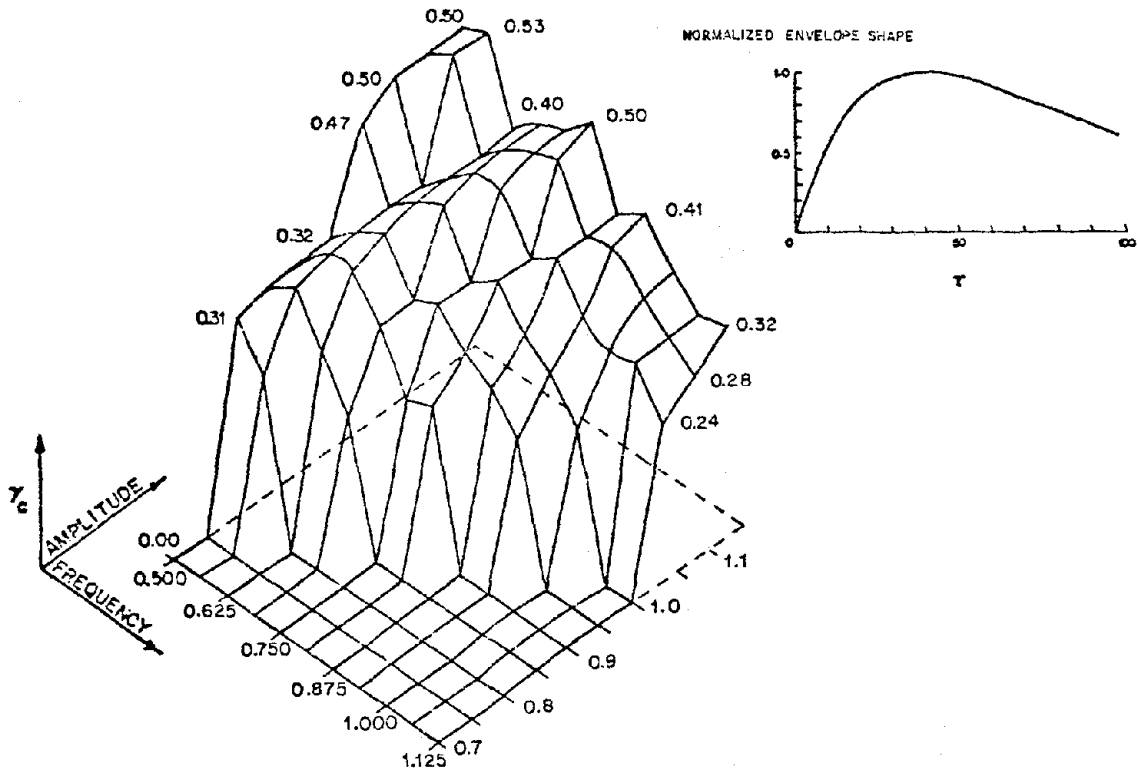


Fig. 7. Surface $\gamma_c (A, f)$ for the scaling parameter τ_{rise} , $\gamma_c \equiv \tau_{rise}/\tau_c$, computed with the base acceleration contained in a moderately rising envelope.

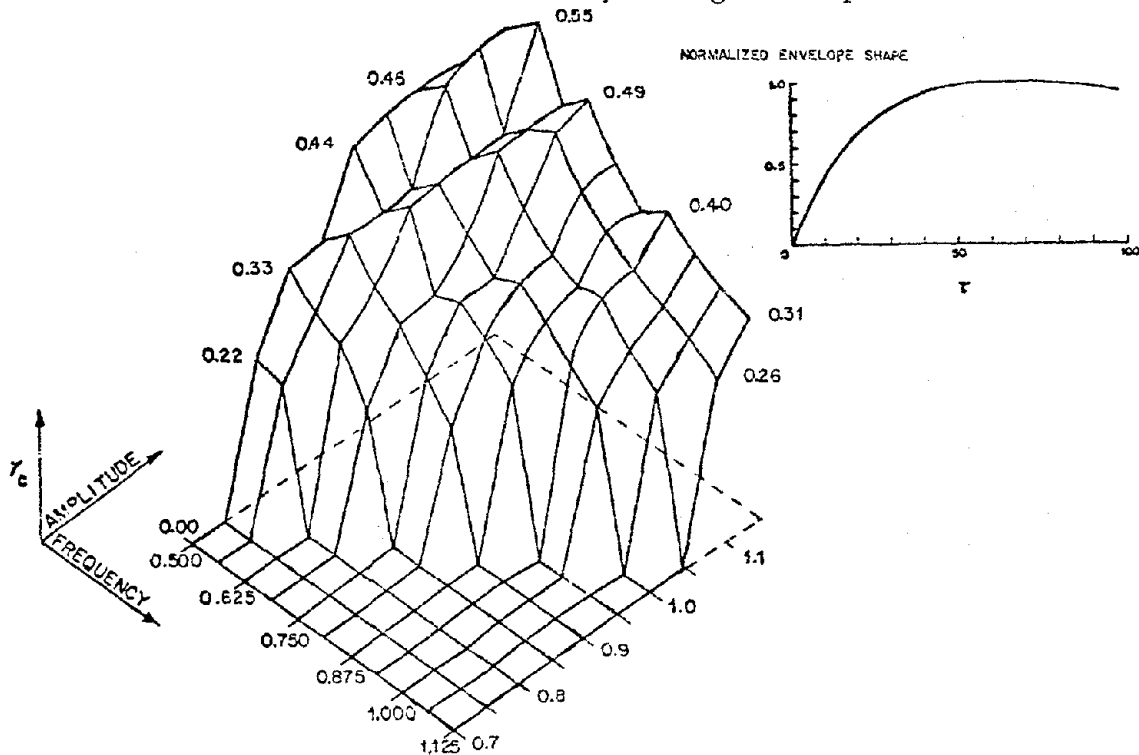


Fig. 8. Surface $\gamma_c (A, f)$ for the scaling parameter τ_{rise} , $\gamma_c \equiv \tau_{rise}/\tau_c$, computed with the base acceleration contained in a slowly rising envelope.

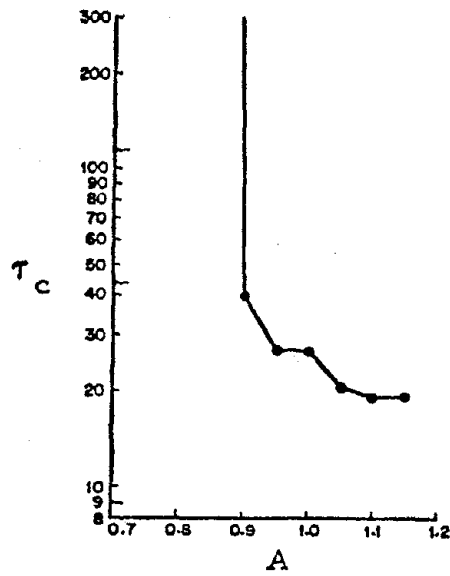


Fig. 9. Nondimensional collapse time τ versus amplitude A given fixed frequency $f = 0.75$ Hz. and moderately rising acceleration envelope.

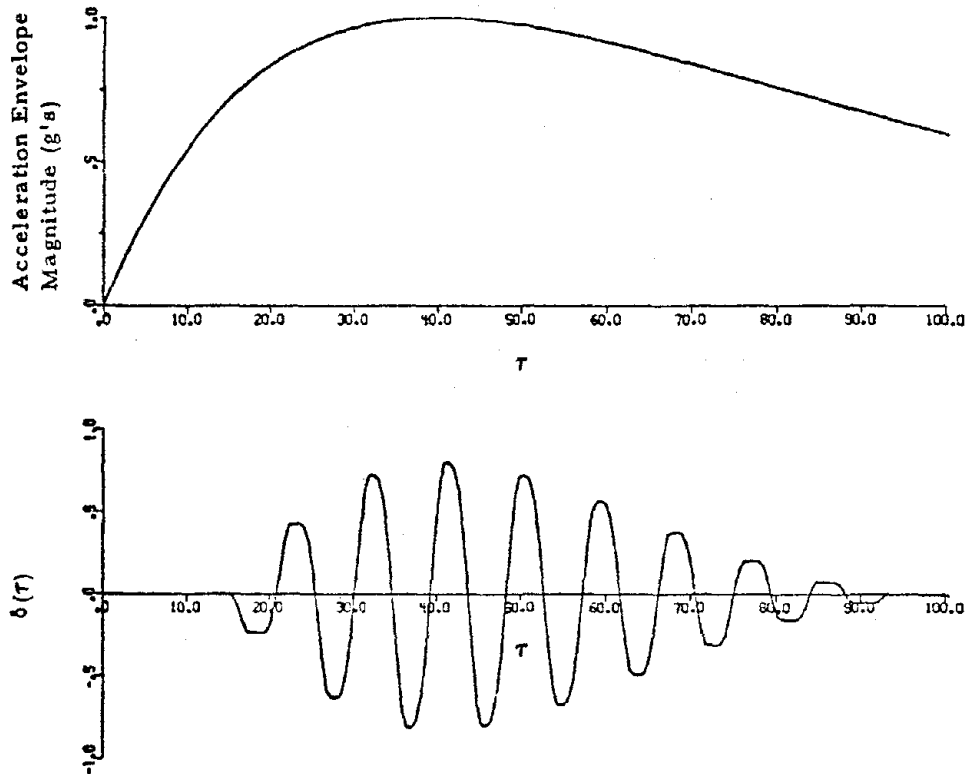


Fig. 10. Nondimensional relative displacement $\delta(\tau)$ versus nondimensional time τ with acceleration envelope versus nondimensional time τ for $A = 1.0$, $f = 1.125$ Hz and moderately rising acceleration envelope.

HIGH RISE BUILDING VIBRATION PROPERTIES:
AN UNEXPECTED BEHAVIOR MECHANISM

Irving J. Oppenheim¹

A twenty storey reinforced masonry apartment building was the subject of experimental and analytical studies. The building, basically rectangular in plan, has seven pierced shear walls in the short plan direction. All walls are constructed of two wythes of concrete block, enclosing a grouted core containing the longitudinal reinforcement.

Acceleration records at roof level were obtained under ambient and man-induced vibrations. A Fast Fourier Transform of the ambient records provided frequency information in the E-W, N-S, and torsional directions. The man-induced vibrations provided direct observation of structural frequencies, and a measurement of damping. The building was then the subject of an elastic modal analysis performed by the analysis program ETABS; the building was analyzed under two behavior assumptions. In one analysis the wall sections were considered coupled, while in the other they were uncoupled; as built, the walls were designed as uncoupled. Quite surprisingly, the building behavior as measured was in exact correspondence with the coupled wall mechanism.

On closer examination, the reason for this coupled wall behavior was apparent. The detail of supporting the lintels had them embedded in the wall for a distance of 8 inches. The bearing stress in the wall, acting over that embedment length, supplied a fixity moment to the lintel ends, transforming them from simply supported lintels into fixed ended coupling girdles of limited capacity. Theoretical calculations of fixity moments were prepared, along with behavior under design loads and recommendations for designers.

¹Associate Professor of Architecture and Civil Engineering,
Carnegie-Mellon University, Pittsburgh, PA, 15213.

HIGH RISE BUILDING VIBRATION PROPERTIES:
AN UNEXPECTED BEHAVIOR MECHANISM

By Irving J. Oppenheim¹

INTRODUCTION

A twenty storey masonry apartment building was studied. The ambient vibrations at roof level were measured, and those records processed to obtain frequency and damping estimates. A complete elastic analysis was performed, using the analysis program ETABS, to attempt the reproduction of measured frequency values. Surprisingly, the analytical results implied coupled shear wall behavior, even though the design was executed as uncoupled. A reason for this unsuspected behavior was found on examining the lintel detail. Theoretical limits for lintel fixity were developed, and a lateral load analysis performed to estimate the significance of such effects.

The masonry apartment building is an interesting structural type. It represents the convergence of numerous factors (functional, structural, material, and construction) which produce a highly efficient architectural/structural solution. This paper begins with a short examination of shear wall structural types, and their interaction with the building design itself.

STRUCTURAL TYPES FOR SHEAR WALL BUILDINGS

If buildings are grouped into office or apartment categories, there are numerous functional factors which shape the engineers choice of a structural system. A brief review of those factors follows, in an attempt to spotlight the structural efficiency of reinforced masonry walls for apartment construction.

Office buildings may often be characterized by the following three features:

1. Elevator, stair, and service requirements extensive enough to require a "core" area no less than 20% of the plan area.
2. The use of forced air climate control.
3. A desire to provide flexible wall-free areas.

A particular structural type evolves from these factors, and is shown in Figure 1a. The floor depth required for the mechanical system permits large girder spans. The engineer can then concentrate his shear wall group around the core, and span to the exterior wall. (It should be noted

¹Associate Professor of Architecture and Civil Engineering,
Carnegie-Mellon University, Pittsburgh, PA 15213

that in the absence of a mechanical system depth requirement, the engineer might find it difficult to justify girder depth decisions.) This system transfers the lateral load to a small number of central walls, and lateral load quickly governs such a design. The analyst often turns to coupled wall design, employing deep coupling girders between wall sections. With a typical storey height of 12 feet, there is ample structural depth for floor and coupling girders.

Apartment buildings could be characterized by negating the three factors which applied to office construction; a totally different structural type evolves. There is little benefit in providing clear span, so walls are closely spaced. Without a mechanical system depth requirement, a minimum floor depth is desirable; in practice this often is an 8 inch slab spanning about 20 feet between parallel walls. The system which evolves, for a double loaded corridor, is typified by Figure 1b or 1c. In either case, the significant structural feature is the large number of wall sections available to resist lateral load. Such a design is not likely to require resolution by coupled wall behavior; designs are typically uncoupled walls with a storey height near 9 feet.

BUILDING DESCRIPTION, PENN CIRCLE TOWERS

The structure which was tested, a twenty storey apartment building, is located in Pittsburgh. Tasso Katselas, architect, and Gensert-Peller Associates, engineers, were the professionals who designed the building (together with its twin, and other buildings in the complex) in 1969. The building, pictured in Figure 2, is regular in its upper 17 storeys. In the bottom three storeys, the walls flare out to reduce stresses induced by lateral load. A typical section is shown in Figure 3. The structural plan for the middle and upper floors (Figure 4) shows seven walls in the E-W direction, and five walls running N-S. All walls are 14 inches thick, consisting of two five-inch concrete masonry units enclosing a four inch grouted core.* The masonry cross-section is not uniform, as blocks with different densities (between 25% and 100% solid) were specified as required. While wind loading governed wall design in the E-W direction, a zone I seismic loading was critical for the N-S direction. The floor system is 8 inch deep Celldex (a prestressed concrete plank system) with poured troughs to ensure diaphragm action. Almost all spandrels and lintels were from a group of precast concrete rectangular sections.

The close wall spacing resulted in numerous walls being available to resist lateral loads. The individual wall sections, acting as uncoupled shear walls create a satisfactory load carrying system, with the mild expedient of the aforementioned bottom storey flaring. As a system of uncoupled walls, no continuity was required with the lintels. Lintels were designed as simply supported beams, and framed into the wall as shown in Figure 5. It will shortly be shown that the lintels instead

* Exterior wythes employ brick rather than concrete block.

act as coupling girders, even though not designed as such. One point must be emphasized; the lintels in this particular building are in no danger of being overloaded as a result of that coupling action. The engineer provided compression steel (to control long term deflection) and shear stirrups, which mitigate any serious problem which could have arisen.

TEST RESULTS, AMBIENT AND MAN-INDUCED VIBRATIONS

Ambient and man-induced vibrations [1,2,3,4] were measured at roof level on several different occasions. All readings were taken with a Kinometrics VM-1 single channel vibration monitor. Motion records were produced on paper strips, from which hand-digitization was performed. Typical records are shown in Figure 6, at locations indicated in Figure 4. Man-induced vibrations were used to determine the lowest frequencies of vibration in the E-W and N-S directions; those same records yielded damping estimates of 1.1% of critical damping, obtained from the logarithmic decrement. The lowest torsional frequency, and the second frequency in the E-W direction, were obtained from a plot of the Fourier Transform (Figure 7) of the ambient vibration records. The measured frequencies are presented in Table I.

TABLE I MEASURED FREQUENCIES OF VIBRATION

<u>Mode Description</u>	<u>Frequency, Hz</u>
E-W 1	1.16
E-W 2	4.40
N-S 1	1.48
Torsional 1	1.72

ANALYTICAL RESULTS, ETABS PROGRAM

Analytical predictions of vibration frequencies were obtained using the computer program ETABS. [5] The inertial mass, mass center, and polar moment of inertia were calculated at each storey. Every flexural element was modelled individually; flexural and shear deformations were considered along with "rigid depths" to model shear walls as columns. There were a total of 26 wall sections in plan with 200 different wall cross sections used in modelling the building.

Two analyses were performed, corresponding to uncoupled and coupled wall construction. The coupled wall analysis treated lintels as having rigid supports. The floor slab was not considered to couple wall segments; the floor is constructed of planks running at right angles to the wall. Had the floor slab been cast-in-place, it would have been appropriate to consider it too as a coupling mechanism.

It has been the experience of researchers that analytical results often prove reliable in the short plan dimension, but not in the long plan or torsional directions. That was the experience in this case, where results in the E-W direction were the most reasonable. The analysis required the assumption of an effective elastic modulus for the walls; a value of 2500 KSI was chosen. The results are shown in Table II.

TABLE III MEASURED AND ANALYTICAL E-W FREQUENCIES, Hz

Mode Description	Measured	Analytical (Uncoupled)	Analytical (Coupled)
E-W 1	1.16	0.68	1.18
E-W 2	4.40	3.37	4.49

A first examination of the results indicates that coupled wall action more accurately models the measured behavior than does uncoupled action. This is, of course, partly due to the fortuitous (though unplanned) choice of an elastic modulus which yields a fundamental frequency within 2% of the measured frequency. A more meaningful measure for comparison would be the ratio of the second frequency to the first; this quantity is a characteristic of the structural behavior mechanism, and is independent of elastic modulus. It is listed in Table III.

TABLE III CHARACTERISTIC FREQUENCY RATIO, E-W₂/E-W₁

Measured	Analytical (Uncoupled)	Analytical (Coupled)
3.79	4.96	3.80

Examination of Table III clearly indicates that behavior mechanism is not of the uncoupled walls. Instead, the building behavior is apparently predicted by coupled wall action, where the lintels themselves act as coupling girders. The next section will clearly show how this behavior is brought about.

THEORETICAL BASIS OF LINTEL FIXITY

Examination of Figure 5, the lintel support detail, provides a mechanism for coupled wall behavior. Although the lintel was designed as simply supported, it has been embedded in the wall to a depth of 8 inches. For low values of moment, that embedding will suffice to fix the lintel against rotation, and to create coupling action. How strong is that end fixity? Does it remain in effect at high load levels?

Figure 8a shows the lintel end condition, with bearing stress, f_b , present in the wall. A first (lower) bound for the lintel end fixity limit may be found from the rigid limit state.

$$M_o' = 0.5 f_b b w^2$$

In the typical fifth storey wall, the bearing stress, f_b , is taken as 300 psi. That corresponds to a moment of 134 K-in.

An upper bound to the lintel end fixity limit may be found from the ultimate strength limit state, shown in Figure 8b.

$$M_u' = 0.335 f_c' b w^2$$

In this example the moment would be 1200 K-in. A theoretical M- θ relationship for the lintel/wall connection could then be imagined in Figure 9. Of course, the ultimate moment capacity of 1200 K-in. is not likely to be achieved; local failure of the concrete and mortar in the wall would certainly precede it. Moreover, the end fixity is not "rigid" above moments of say, 100 K-in. A hypothetical M- θ relationship has been indicated, and experimental studies are needed in the future.

Had the lintels been designed as singly reinforced, their negative moment capacity would have been minimal, certainly less than the end fixity capacity. In that case, lateral forces could induce excessive cracking in the upper part of the lintel near its support. Even with light reinforcement, the danger associated with excessive cracking remains, because of the presence of high shear in that region. Again, this particular design is quite adequate; this note of caution is addressed to designers who might be reluctant to provide top steel and shear reinforcement in the apparent "absence" of loads requiring that capacity of the member.

EXAMPLE ANALYSIS UNDER WIND AND EARTHQUAKE LOADS

The coupled wall analytical model was subjected to a lateral wind pressure of 30 psf, and a Newmark-Hall design spectrum for a ground acceleration of 4% g, with 2% of critical damping. Lintel end moments were in the range of 100 to 150 K-in. for the lateral wind loading. The elastic modal response produced end moments generally five times as high as produced by the wind loading.

The end moments produced under wind load are significant. They approach the strength of the reinforced cross sections, and are associated with rotations which would represent serious cracking in the absence of top steel. The end moments are not significantly larger than M_o' , and are much smaller than M_u' . Lintel end fixity is certain to occur at those levels of end moment. For analysts familiar with coupled shear wall design, a representative α_H factor between 2.0 and 3.0 would characterize the behavior of the coupled walls.

The results of the earthquake spectral analysis are not too meaningful, as they predict stresses far beyond the elastic range. It should, however, be recognized that an earthquake loading is likely to place extreme demands on the deformation of those embedded lintels.

SUMMARY

Man induced and ambient vibration tests provided measures of structural frequencies for the masonry building studied. Comparison with analytical results from elastic analysis indicated that coupled wall behavior was present. Examination of the lintel detail showed that embedment of the lintels in the wall was sufficient to fix the ends of the lintels, and turn them into coupling girders.

This behavior was observed at low stress levels. The lintel end fixity was shown (theoretically) to be high enough to surpass the moment capacity of lightly reinforced lintel sections. Actual behavior of the lintel/wall combination remains to be studied experimentally; tests are being planned for next year at Carnegie-Mellon University. Analysis under lateral loads did indicate the likelihood that design wind loads or earthquake effects would induce high moments in the lintels. Those moments could approach or exceed the lintel capacity, and are within the limits of end fixity provided by the wall detail.

This behavior is no cause for concern if top steel and stirrups are provided, as they were in this design. Engineers should be aware of potential cracking in those lintels if such reinforcement is not provided.

ACKNOWLEDGEMENTS

This work was possible only through the contributions of numerous people. Tasso Katselas and Richard Gensert, the designers, were available to provide the information on the building itself. The management and staff of the building were helpful to us when doing the numerous vibration measurements. Many students contributed to the study, with the computer analysis performed by Enrico J. Betti.

APPENDIX I - REFERENCES

1. Crawford, R., and H.S. Ward, "Determination of the Natural Periods of Buildings", Bull. Seism. Soc. Amer., Vol. 54, No. 6, December 1964.
2. Hudson, D.E., W.O. Keightley and N.N. Neilsen, "A New Method for the Measurement of the Natural Periods of Buildings", Bull. Seism. Soc. Amer., Vol. 54, No. 1, February 1964.
3. Medearis, K., "An Investigation of the Dynamic Response of the Park Lane Towers to Earthquake Loading", Colorado Masonry Institute, 1974.
4. Stephen, R.M., J.P. Hollings, J.G. Bouwkamp and D. Jurukovski, "Dynamic Properties of an Eleven Story Masonry Building", EERC 75-20, Berkeley, CA, 1975.
5. Wilson, E.L., J.P. Hollings, and H.H. Dovey, "Three Dimensional Analysis of Building Systems (Extended Version)", EERC 75-13, Berkeley, CA, 1975.

APPENDIX II - NOTATION

- b - width of lintel
- f_b - bearing stress in wall
- f_c' - crushing stress of block
- M_o' - lintel end fixity limit from the rigid limit state
- M_u' - lintel end fixity limit from the ultimate strength limit state
- w - length of embedment

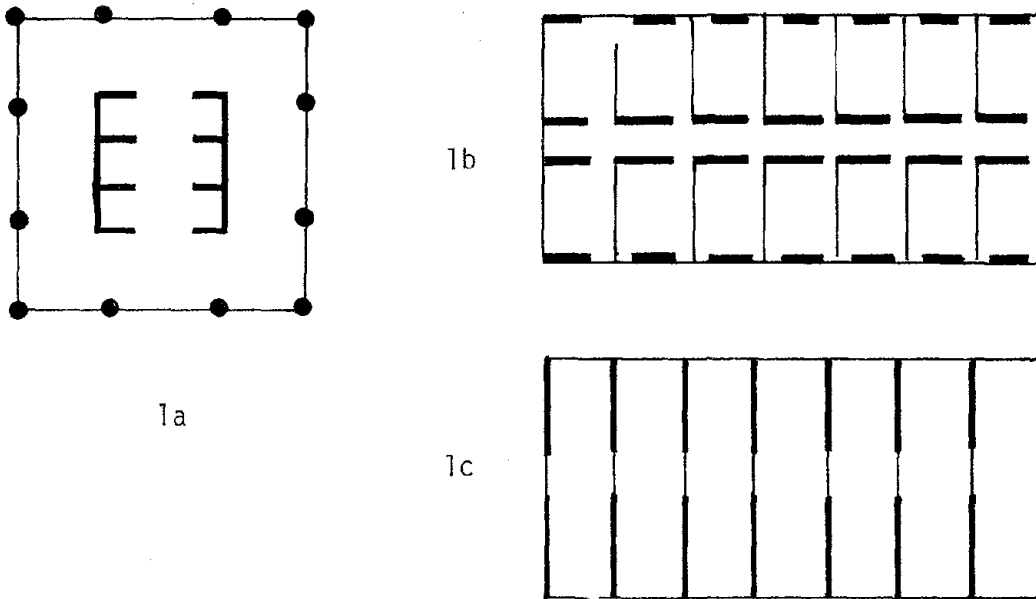


Figure 1. Types of Shear Wall Buildings



Figure 2 Photograph of Structure

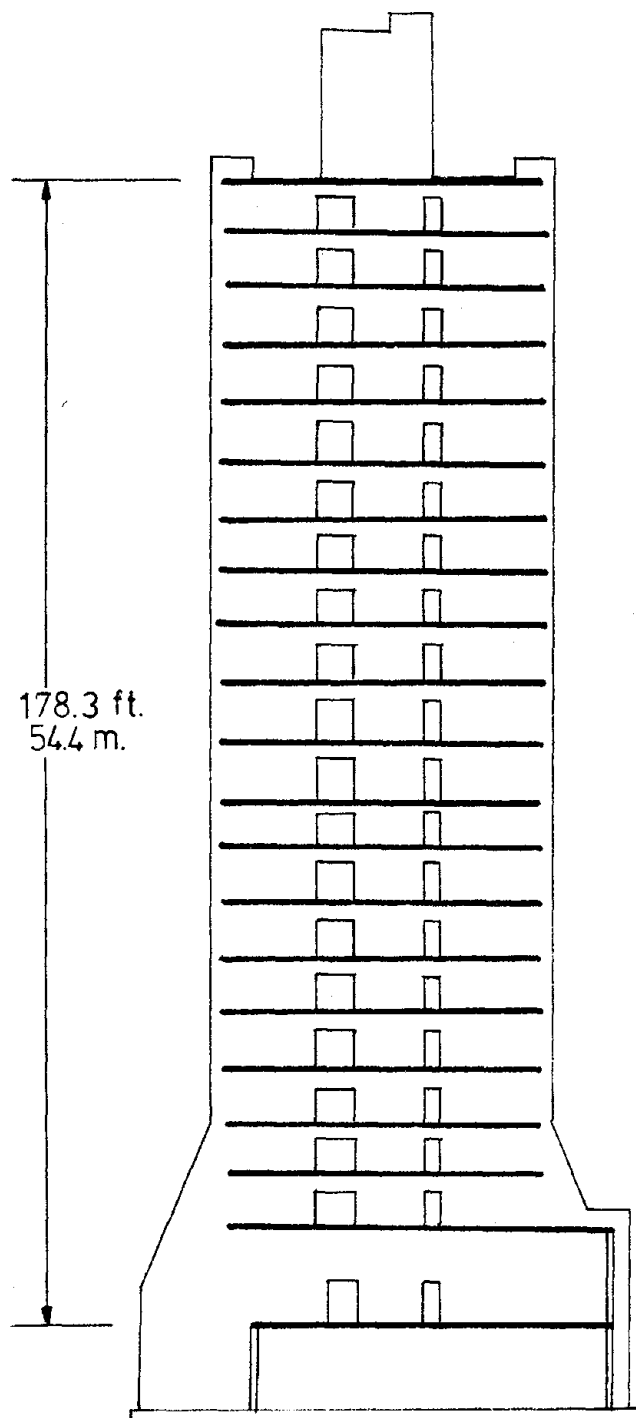


Figure 3 Section through Structure

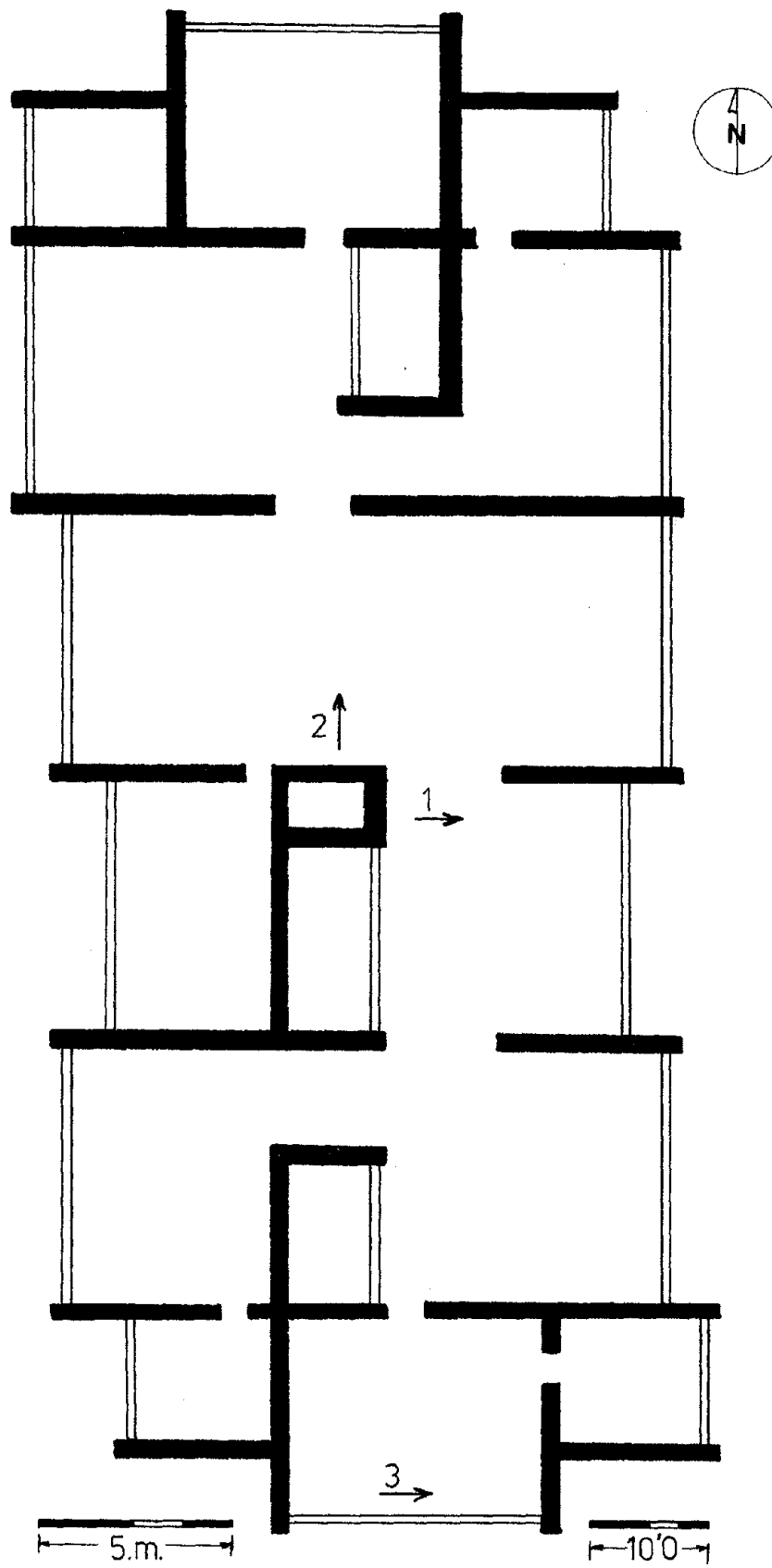


Figure 4 Plan of Typical Floor

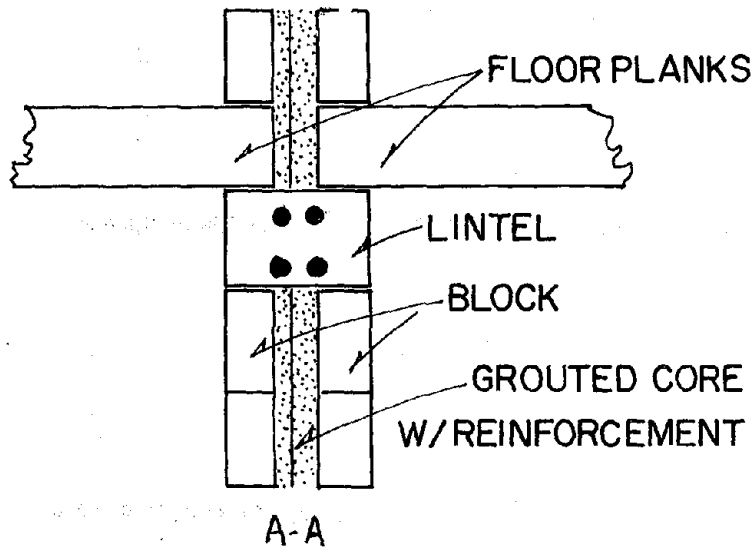
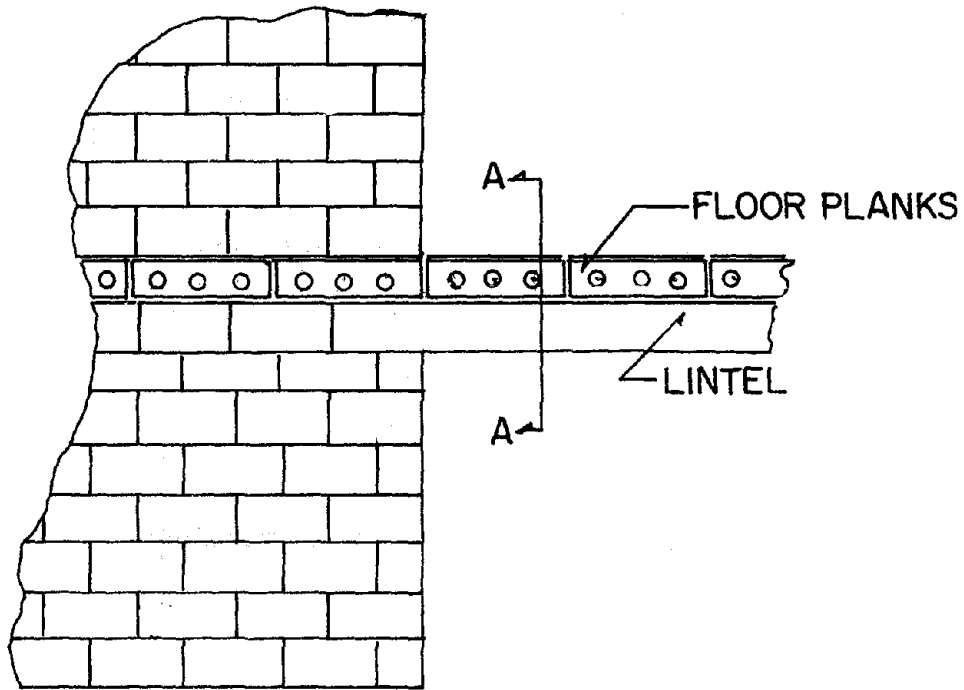


Figure 5 Lintel Detailing

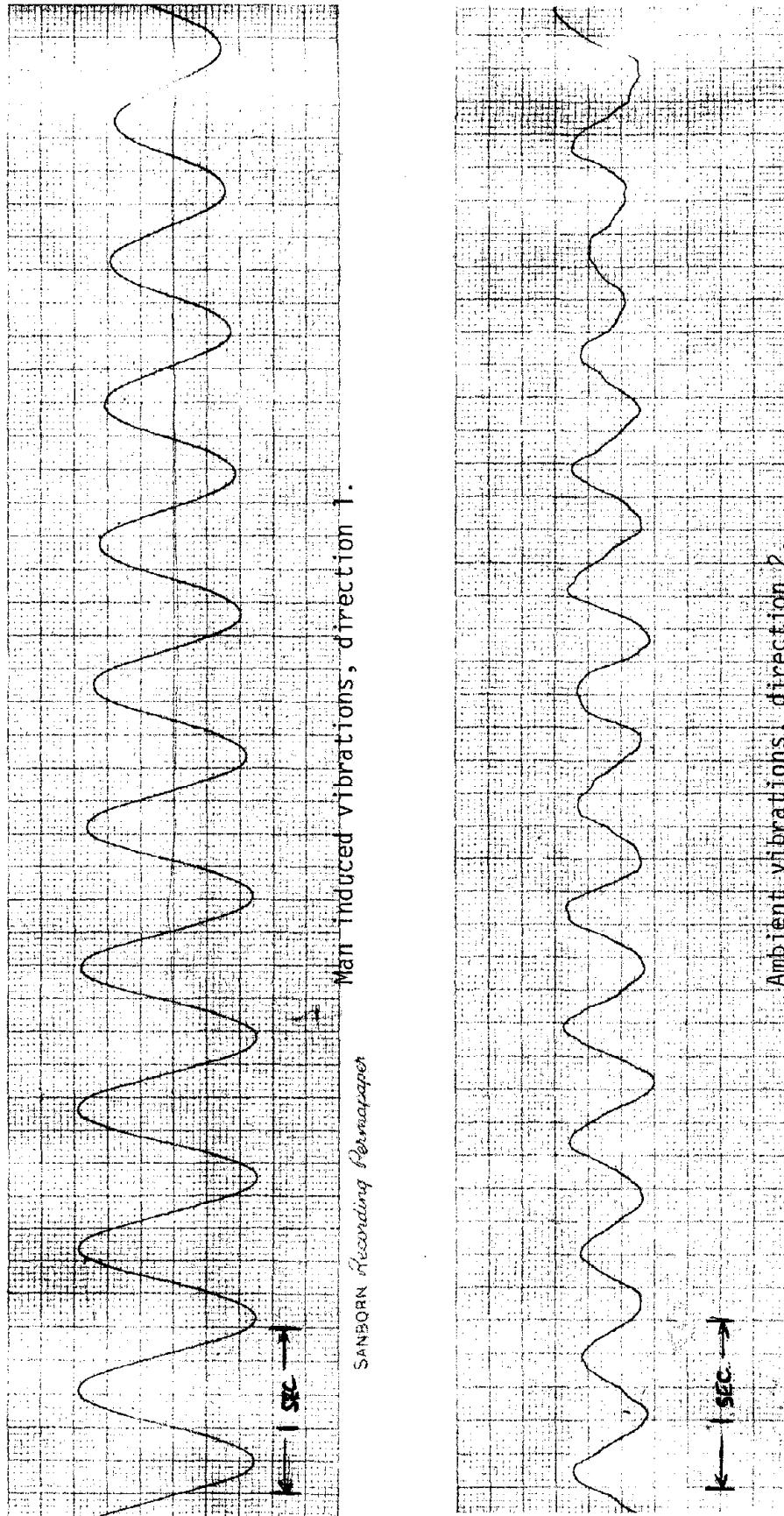


Figure 6 Typical Vibration Records

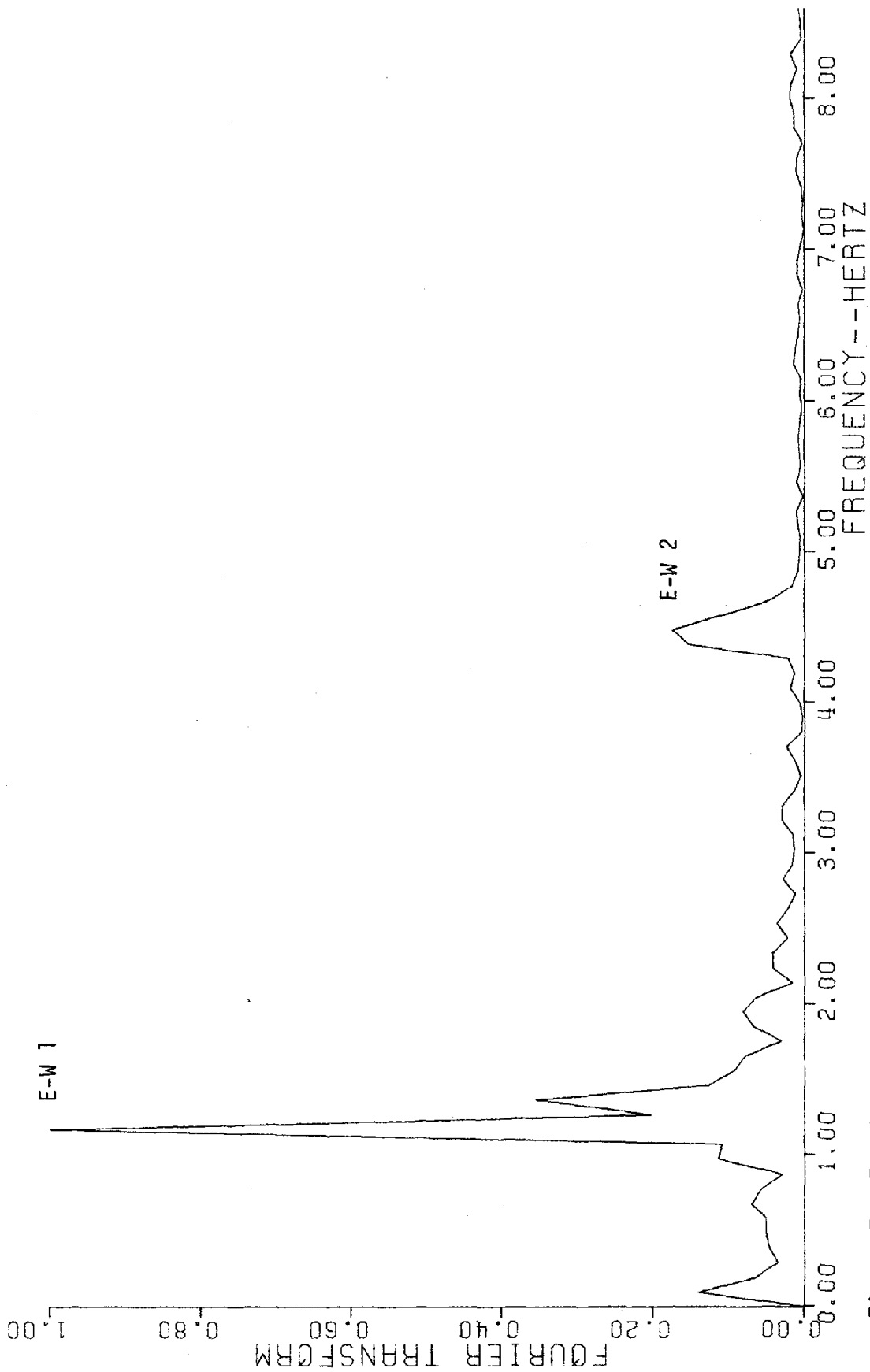


Figure 7 Fourier Transform Plot

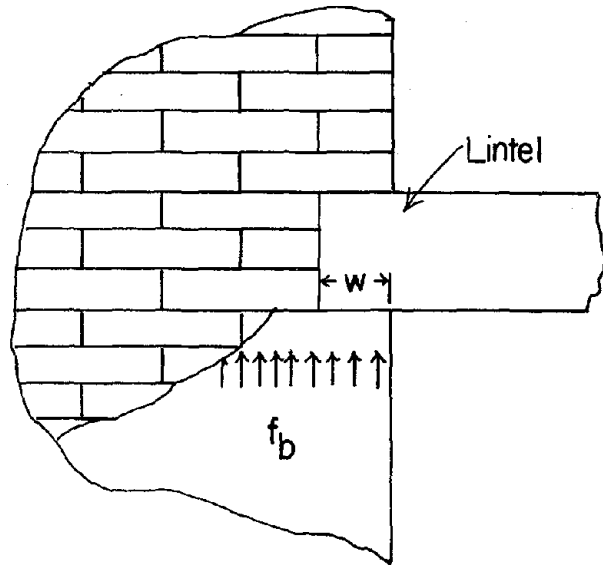


Figure 8a Lintel, f_b

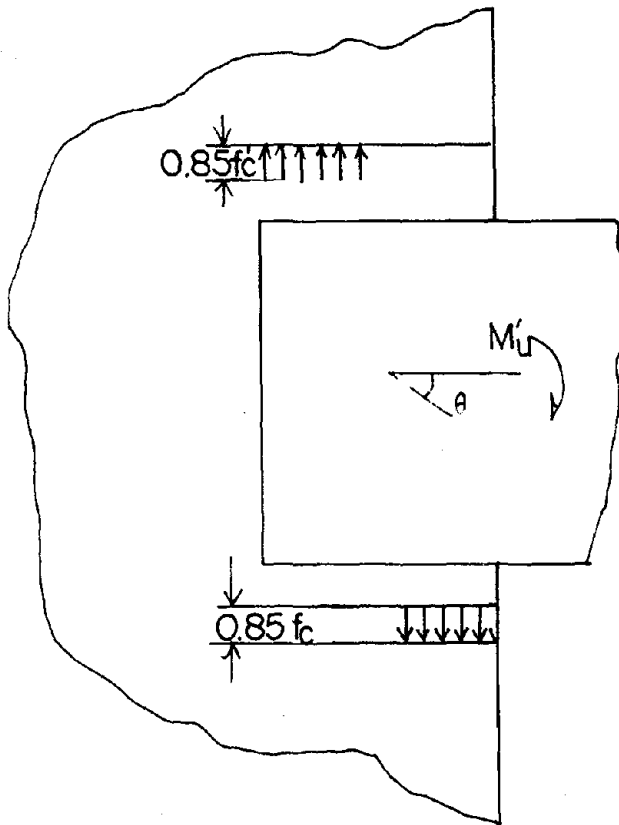


Figure 8b, Lintel at M'_u

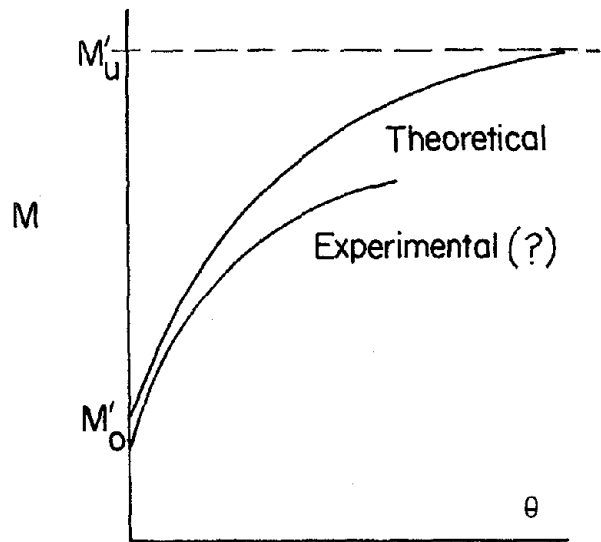
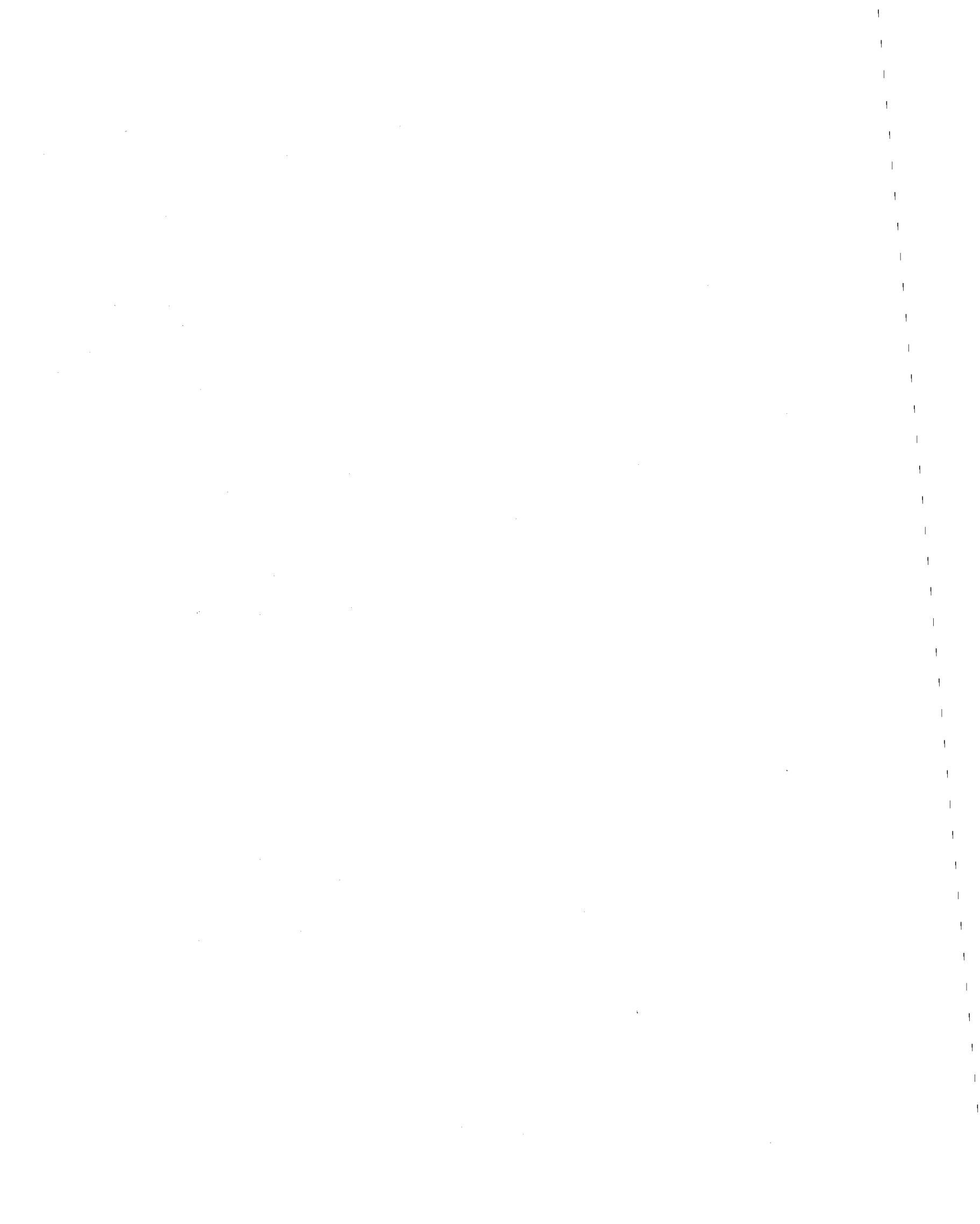


Figure 9 M- θ Relationship



INTERACTION BETWEEN UNREINFORCED MASONRY STRUCTURES AND THEIR ROOF
DIAPHRAGMS DURING EARTHQUAKES

By Adham, S.A., and Ewing, R.D.

ABSTRACT: Numerous wood roof diaphragms are found in existing masonry buildings in highly seismic zones. The effect of varying the stiffness of these diaphragms on the response of masonry buildings was studied. A lumped-mass analytical model representing the masonry-wall/diaphragm interaction was developed. This model was then subjected to earthquake acceleration time-history input that corresponds to the intensity level of the Los Angeles area. Plywood, diagonal, and straight-sheathed diaphragms were examined. Results of this study indicate that the response of a wood diaphragm is highly nonlinear, and that low amplitude tests are not adequate for predicting the response of these diaphragms in highly seismic zones. It was concluded that softer wood diaphragms will attenuate the input earthquake accelerations and result in shear forces transmitted to the masonry walls that are lower than those obtained from stiffer diaphragms as expected; however, the corresponding midspan deflections will be larger.

INTERACTION BETWEEN UNREINFORCED MASONRY STRUCTURES AND THEIR
ROOF DIAPHRAGMS DURING EARTHQUAKESBy Samy A. Adham¹ and Robert D. Ewing²

INTRODUCTION

Wood diaphragm roofs supported on unreinforced masonry walls are found in numerous existing masonry buildings in highly seismic zones. Reports of damage from past earthquakes indicate that such diaphragms have suffered little or no damage during these earthquakes.

Studies by Blume et al. (1, 2) and Rea et al. (3) on full-scale school buildings indicated that (a) wood roof diaphragms had periods ranging between 0.17 and 0.75 sec; (b) to reduce the response of these buildings to earthquake motions, roof diaphragms should be stiffened. However, these results were obtained from low-amplitude vibration tests and therefore are limited to low magnitude earthquake shaking.

Static tests of full-scale lumber and plywood-sheathed diaphragms were conducted by several investigators (4 through 17). The results of these tests indicate that the behavior of these diaphragms is highly nonlinear. Therefore, these diaphragms would exhibit longer periods when subjected to high intensity earthquake shaking.

This paper presents some results obtained using computer analyses to study a simple lumped mass model of a one-story building with a wood diaphragm roof supported on masonry walls. These calculations demonstrate (1) some basic phenomena and the potential effect that the energy-absorption capacity of wood diaphragms will have on the response of existing masonry buildings, (2) the effect that stiffening these diaphragms will have on the response of masonry buildings to earthquake loading, and (3) the usefulness of computer analyses as a tool for studying these effects. The results were obtained from a preliminary study that is part of a proposed program for evaluating seismic hazards in existing unreinforced masonry buildings.

ANALYTICAL MODEL

System Description.— The one-story building considered in the following calculations consists of a wood-diaphragm roof supported at four sides by 13-in. solid masonry walls as illustrated in Fig. 1. The uniform load of the roof is assumed to be 30 lb/sq ft and the wall uniform load as 130 lb/sq ft.

¹Senior Staff Engineer, Agbabian Associates, El Segundo, California

²Associate, Agbabian Associates, El Segundo, California

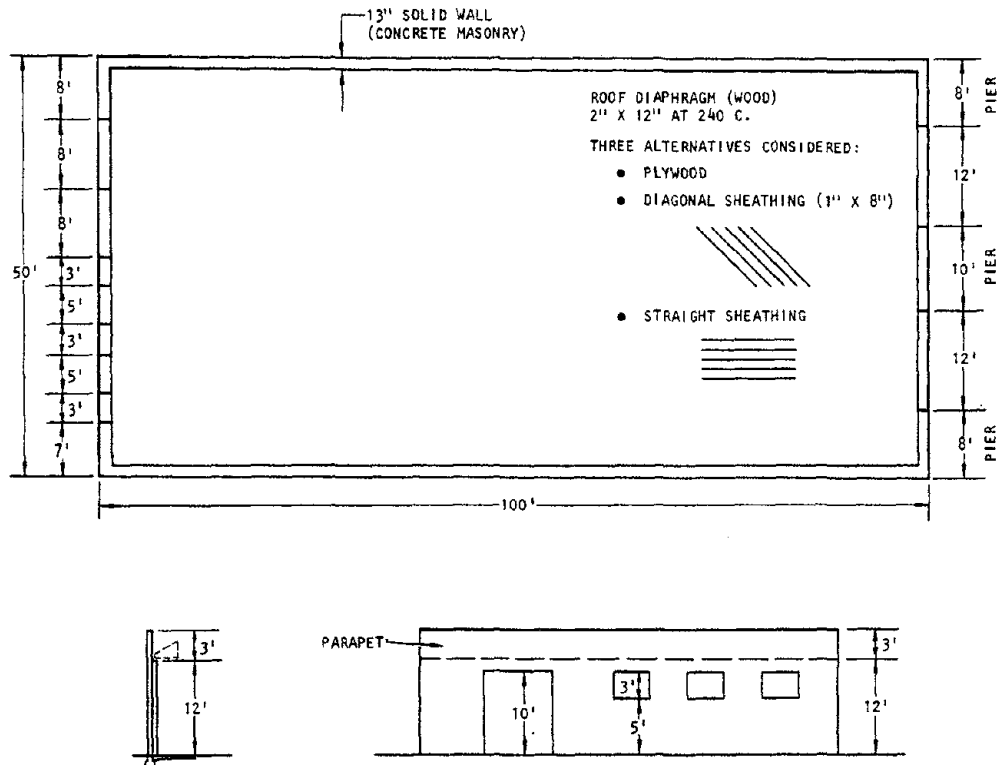
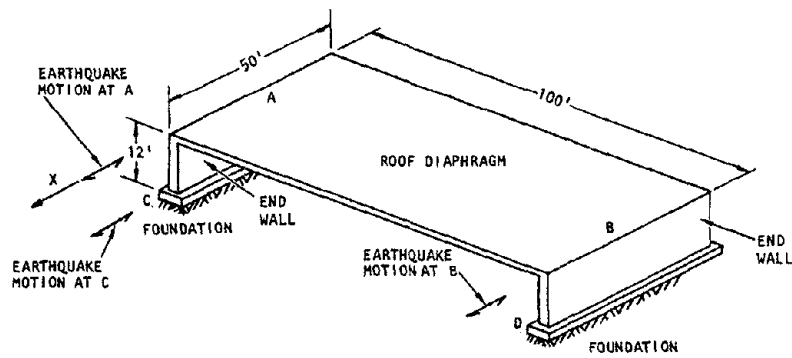
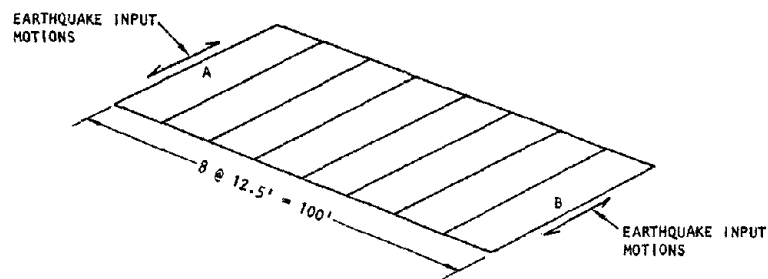


FIG. 1. ONE-STORY UNREINFORCED MASONRY BUILDING WITH A WOOD DIAPHRAGM ROOF



(a) SYSTEM CONFIGURATION



(b) EIGHT-SEGMENT DIAPHRAGM MODEL

FIG. 2. DIAPHRAGM/WALL CONFIGURATION AND MODEL CONSIDERED IN EXAMPLE ANALYSIS

The roof diaphragm is modeled as a deep shear beam (Fig. 2a). This beam is divided into a series of segments, as shown in Fig. 2b and 2c. The 100-ft-long masonry wall was assumed to crack when subjected to shaking normal to its plane. Therefore, only its weight will be included in the model.

For the present phase of the analysis, the two end walls are assumed rigid. A study of wall overturning under seismic loading (18) indicated that for the height-to-width ratios in this structure the earthquake input motions will be transmitted from the foundation level (Fig. 2a, Levels C and D) to the top of the end shear walls (Levels A and B) with little modification. A four-segment model was used for preliminary calculations. However, the final results were based on the more refined eight-segment model shown in Fig. 3.

Material Properties.— From full-scale tests on plywood diaphragms (19) it appears that for cyclic monotonic loading, the deflection may be expressed by

$$\Delta = CWL \quad (1)$$

where

Δ = Midpoint diaphragm deflection in inches (total deflection is attributed to in-plane shear deformation)

C = Flexibility coefficient

W = Total load in kips in diaphragm assumed uniformly distributed over diaphragm length

L = Diaphragm span in feet

Use of the single constant C to describe flexibility appears to be applicable for diaphragm span/depth ratios of 2 to 4.

The plot on Fig. 4 indicates that the diaphragm will cycle at approximately constant deflection for repetitions of reloading (19).

The simple idealized load/deflection relation, shown in Fig. 5, describes a monotonically increasing loading curve in compression and an unloading curve in tension. The hysteretic curve indicates a permanent set of $0.5 \Delta_{\max}$. This idealization was included in the present analysis.

As illustrated in Fig. 5, the data on plywood were presented by the relation

$$\Delta = 5 \times 10^{-4} WL \quad (2)$$

for

W = 5 kips

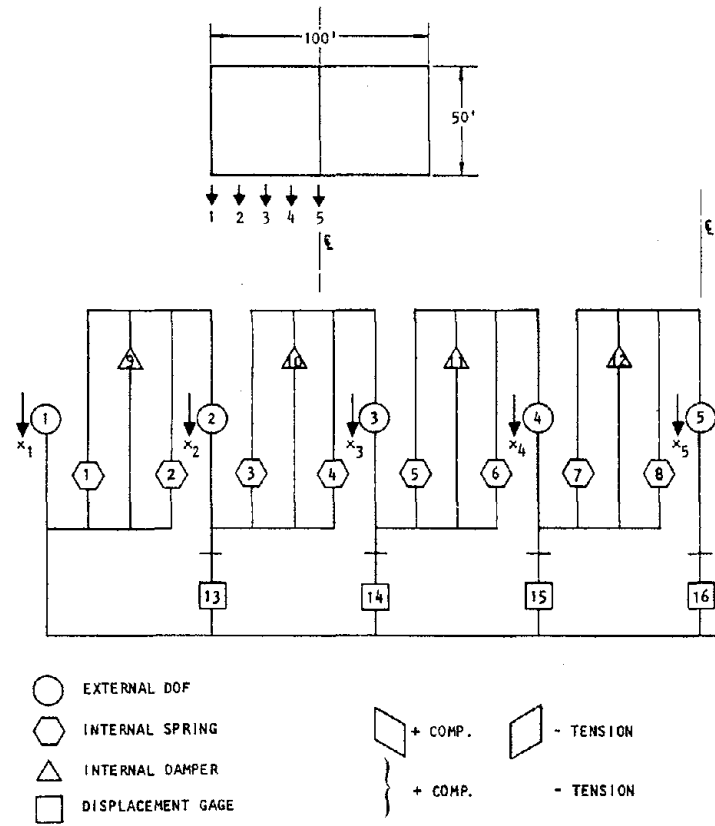


FIG. 3. LUMPED PARAMETER MODEL (8 SEGMENTS - HALF MODEL)

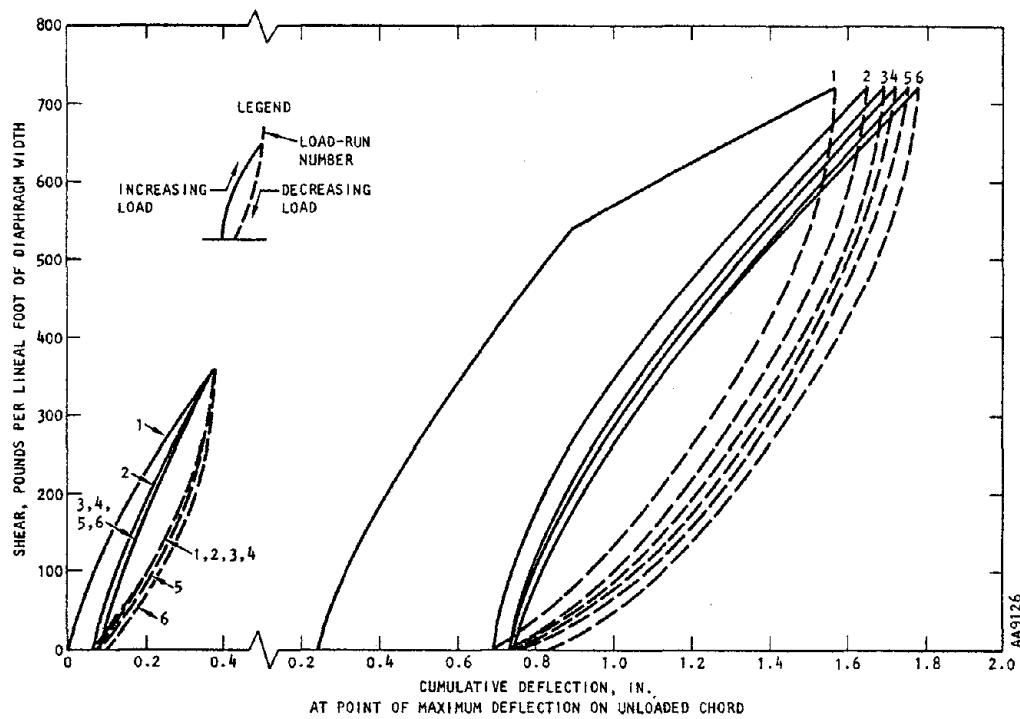
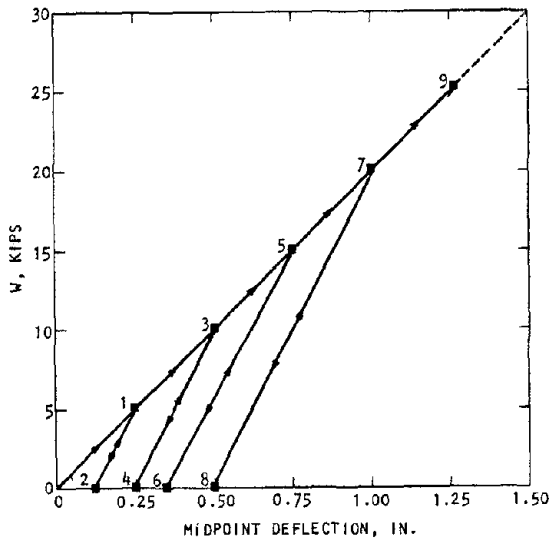
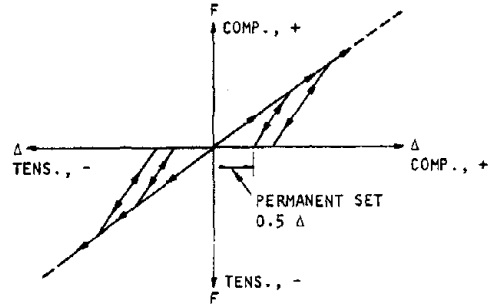


FIG. 4. REPETITIVE LOADING AT 360 AND 720 PLF (19)



$\Delta = 5 \times 10^{-4} WL$ FOR DEFLECTION OF EACH CYCLE
 PERMANENT SET ON LOAD REVERSAL = 1/2
 PLOTTED FOR PLYWOOD: 100' SPAN, 50' DEPTH

(a) SIMPLE LOAD DEFLECTION MODEL FOR PLYWOOD DIAPHRAGMS



(b) LOADING-UNLOADING CYCLE

FIG. 5. IDEALIZED LOAD DEFLECTION RELATIONS USED IN DIAPHRAGM MODELS OF THIS STUDY

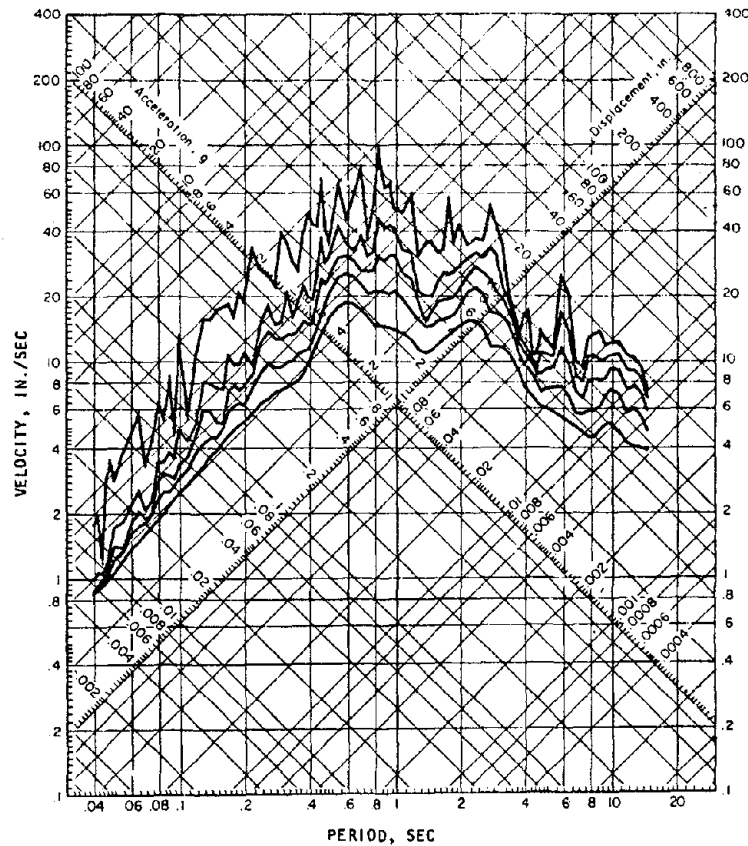


FIG. 6. RESPONSE SPECTRUM OF IMPERIAL VALLEY EARTHQUAKE, 18 MAY 1940: EL CENTRO SITE, IMPERIAL VALLEY IRRIGATION DISTRICT, COMP SOOE

and

$$L = 100 \text{ ft}$$

$$\Delta = 0.25 \text{ in.}$$

The stiffness of the plywood diaphragm is expressed as

$$K = \frac{1}{CL} \quad (3)$$

or

$$K = \frac{1}{5 \times 10^{-4} L}$$

or

$$K = 20 \text{ kips/in.}$$

For the four-segment model, the stiffness per segment is

$$k = \frac{K}{4} = 5 \text{ kips/in.}$$

For the eight-segment model

$$k = \frac{K}{8} = 2.5 \text{ kips/in.}$$

A summary of material properties used for the diaphragms analyzed in this study is given in Table 1.

TABLE 1. STIFFNESS OF ROOF DIAPHRAGM USED IN THE PRESENT ANALYSIS

Roof Diaphragm	Load/Deflection Relation	Stiffness/Segment, k, kips/inch		
		Diaphragm Stiffness, kips/inch	Preliminary Model, 4 Segments	Final Model, 8 Segments
Plywood	$\Delta = 5 \times 10^{-4} WL$	20	5	2.5
Diagonal	$\Delta = 2.5 \times 10^{-3} WL$	4	1	0.5
Straight	$\Delta = 10 \times 10^{-3} WL$	1	0.25	0.125

In addition to the hysteretic damping provided by the hysteretic cycles of Fig. 5, a 10% critical damping was used in the analyses of some cases to account for viscous damping provided by the roofing materials (viscous damping shown in Table 2).

Input Motions.— The intensity of ground shaking used in this study represents the level of shaking expected in a highly seismic area such as Los Angeles. Effective peak acceleration for such an area is 0.40 g (20

The N-S component of the 1940 El Centro record was scaled to the 0.40 g level and used as input to diaphragm models. The response spectra for this record are shown in Fig. 6. The critical orientation of these motions for the diaphragm analyses is shown in Fig. 2.

DISCUSSION OF RESULTS

A number of parametric cases were run as summarized in Table 2. The length of the record used for cases 1 through 6, in addition to case 8, was 15 sec. The length of record used for cases 7 and 9 was 30 sec.

Both elastic and hysteretic material properties were assumed in the analysis. Viscous and hysteretic damping were included in 8 cases, as illustrated in Table 2. The results of the calculations are provided at the middle of the diaphragm (DOF 5 in Fig. 3). The relative peak displacements shown in Table 2 and Figs. 7 through 13 correspond to the maximum difference between input displacements and the absolute displacements of the middle point of the diaphragm at the same instant of time.

The first set of results corresponds to cases 1 through 3 and were obtained using a preliminary four-segment model. The diagonal-sheathed model (case 2) has a longer response period than the plywood model (case 1); and as a result, the peak acceleration at the middle of the case 2 diaphragm is lower than that of the case 1 diaphragm (0.06 g vs. 0.20 g). However, these response periods are in the approximately constant displacement portion of the response spectra (Fig. 6); and the relative peak displacement of case 2 is only slightly higher than that of case 1 (7.4 in. vs. 6.2 in.), as illustrated in Fig. 7.

The straight-sheathing diaphragm (case 3) has the longest period among the three diaphragms studied (9.30 sec). Maximum acceleration of 0.02 g and relative peak displacement of 12 in. were calculated at the middle point.

The second set of results corresponds to cases 4 through 7. Four diaphragms of varying material properties and damping were analyzed. Fig. 8 and Table 2 illustrate how the response of the diaphragm is affected by increasing the number of segments in the diaphragm model. The results of case 5, compared to those of case 1, indicate that the second and third natural modes provide a considerable contribution to the response. The 6.2 in. peak displacement of case 1 was increased to

TABLE 2. SUMMARY OF DIAPHRAGM ANALYSIS RESULTS

Case No.	Diaphragm	Number of Segments	Earthquake Input*	Material Property	Type of Damping	Calculated Period T in seconds	Acceleration at Center in gravities	Relative Peak Displacement at Center in inches†	
1	Plywood	4	El Centro 1940 N-S Component	Elastic	Viscous	1.80	0.20	6.2	
2	Diagonal Sheathing					3.00	0.06	7.4	
3	Straight Sheathing					9.30	0.02	12.0	
4	Plywood	8		El Centro 1940 N-S Component	Elastic	No Damping	2.80	0.20	11.0
5	Plywood				Elastic	Viscous	2.80	0.14	10.4
6	Plywood				Hysteretic	Hysteretic	3.00	0.20	8.0
7	Plywood				Hysteretic	Hysteretic and Viscous	3.00	0.12	10.7‡
8	Straight Sheathing				Hysteretic	Hysteretic	10.60	0.02	11.0
9	Straight Sheathing				Hysteretic	Hysteretic and Viscous	11.50	0.006	9.0‡

* Earthquake input motions scaled to 0.40 g peak ground acceleration. NOTES:

† Relative peak displacements were calculated by subtracting the absolute input displacement from the absolute peak midpoint displacement.

‡ 30-sec record used for cases 7 and 9.

15-sec record used for cases 1 through 6 and case 8.

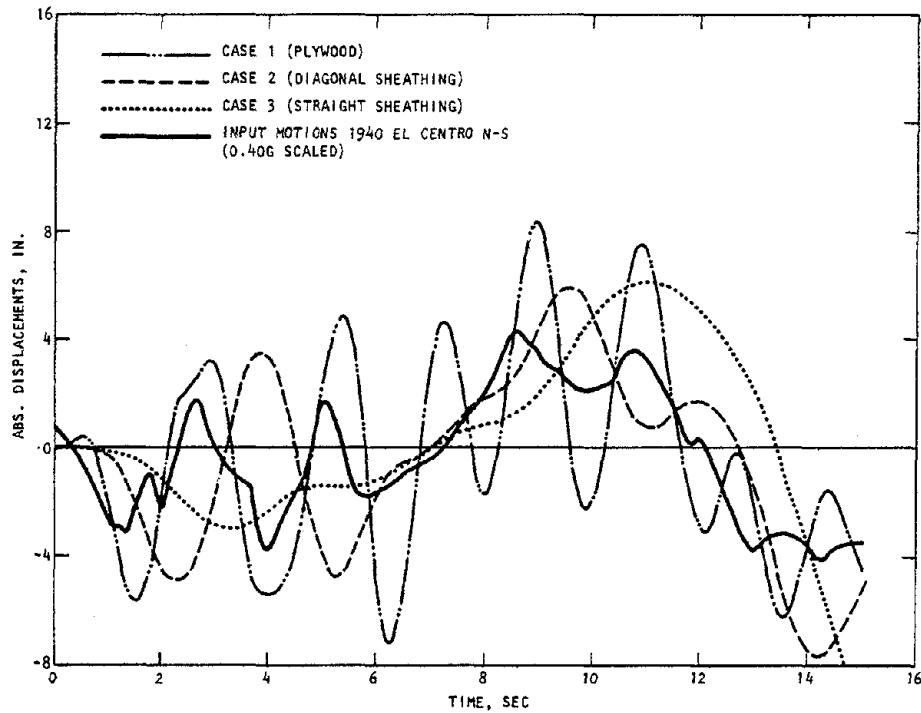


FIG. 7. COMPARISON OF ABSOLUTE DISPLACEMENT AT MIDPOINT OF DIAPHRAGM MODELS, CASES 1, 2, 3
(IN FIG. 7 TO 13 THE RELATIVE PEAK DISPLACEMENTS WERE CALCULATED BY SUBTRACTING THE ABSOLUTE INPUT DISPLACEMENT FROM THE ABSOLUTE PEAK MIDPOINT DISPLACEMENT)

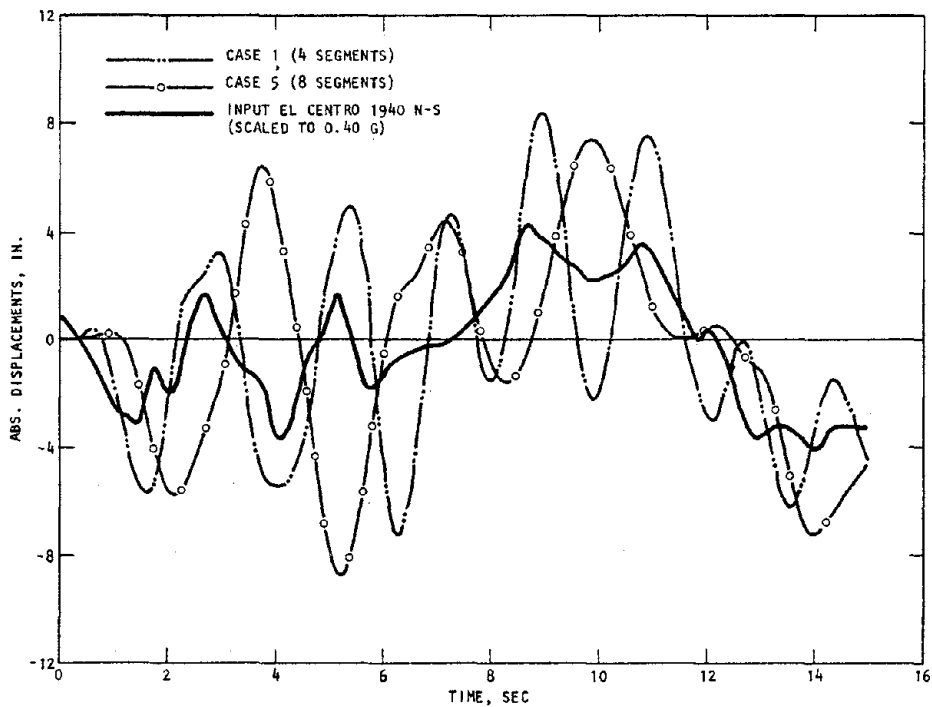


FIG. 8. COMPARISON OF ABSOLUTE DISPLACEMENTS AT MIDPOINT OF PLYWOOD DIAPHRAGM MODELS, CASES 1 AND 5

10.4 in. in case 5 by including the contribution of the second mode (Fig. 8). This resulted in shifting the response to a lower acceleration region. The contribution of the higher modes, particularly the second mode, to the acceleration is minimal; and the final result was a reduction in peak acceleration from 0.20 g for case 1 to 0.14 g for case 5 (Fig. 9). Therefore, the four-segment model behaves like a stiffer structure with a higher acceleration (0.2 g), shorter period (1.8 sec), and smaller displacement (6.2 in.); whereas the eight-segment model performs like a more flexible structure with a lower acceleration (0.14 g), longer period (2.8 sec), and larger displacement (10.4 in.). It is observed that the El Centro input, with its strong long-period content, when applied to the eight-segment model, provides considerable interaction with the periods of the plywood diaphragm (Fig. 10).

When the diaphragm material is represented by hysteretic characteristics, as shown in case 6, the structural response corresponds to contributions from a band of diaphragm frequencies, bounded by values related to the slopes of the loading and unloading curves (Fig. 11). The period of the diaphragm is lengthened from 2.8 sec (case 4) to 3.0 sec (case 6) for the plywood diaphragm. Because of the combination of higher damping and more frequency contribution to the response, the relative peak accelerations are about the same for cases 4 and 6, as illustrated in Fig. 12 (0.2 g). However, the peak displacement for case 6 is 8 in., which is smaller than that of case 4, due to the damping effect.

The difference between cases 6 and 7 is that the latter has viscous damping in addition to the hysteretic characteristics. In addition, case 7 was run to 30 sec, whereas case 6 was run for only 15 sec. The peak acceleration for case 6 is 0.20 g as compared to 0.12 g for case 7. Therefore, viscous damping appears to have a considerable effect on attenuating peak accelerations in these diaphragms. The relative peak displacement for case 7 is 10.7 in., compared to 8 in. for case 6 (Table 2). However, case 6 may show higher displacements if run for an additional 15 sec.

For the straight-sheathed diaphragm, the natural periods are 10.6 and 11.5 sec for cases 8 and 9, respectively. The effect of the additional viscous damping in case 9 results in a reduction of the response of the diaphragm from 11.0 in. for case 11 to 9.0 in. for case 9. The peak acceleration of the midpoint is 0.02 g and 0.007 g for cases 8 and 9, respectively. These values indicate no significant changes in the peak acceleration calculated for the four-segment model of case 3. The results illustrate the considerable attenuation of peak acceleration that is provided by these relatively soft diaphragms. The shear force transmitted to the ends of these diaphragms is reduced from 7.5 kips for the plywood diaphragm (case 7) to 0.54 kips for the straight-sheathing diaphragm (case 9).

A comparison of the response of the plywood and straight-sheathed diaphragms indicate that the periods of the latter are much longer, whereas the peak accelerations are much lower. The peak displacements vary between 8 and 11 in. for both diaphragms (Figs. 12 and 13).

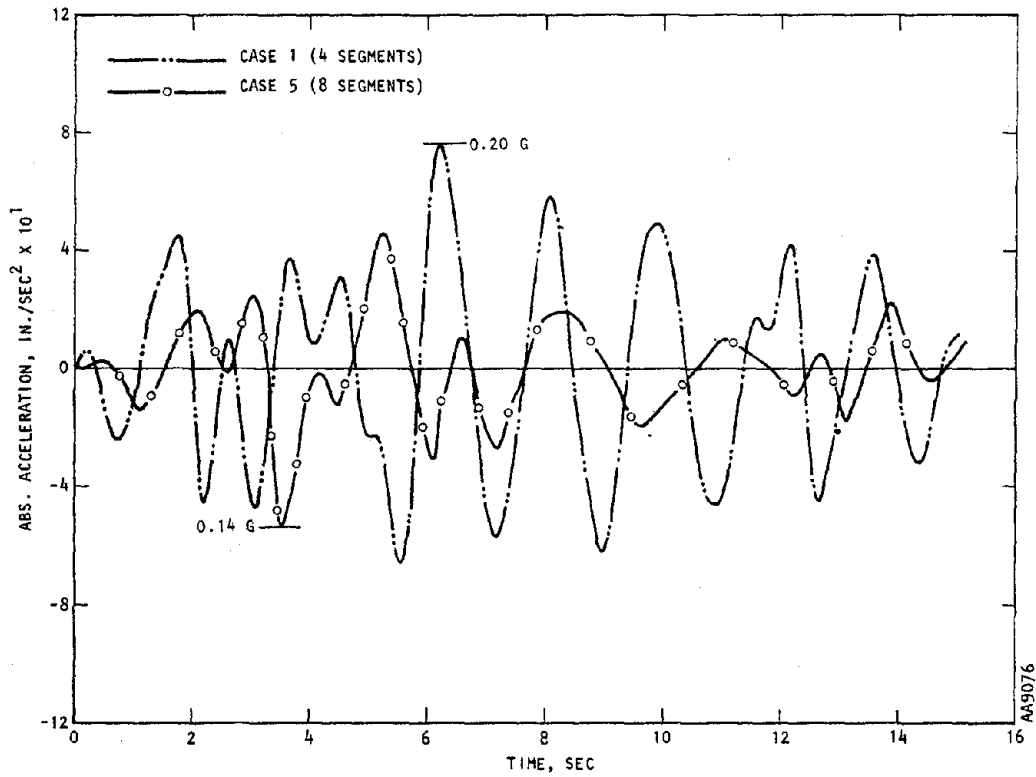


FIG. 9. COMPARISON OF ACCELERATION TIME-HISTORY RESPONSES AT MIDPOINT OF PLYWOOD DIAPHRAGM MODELS, CASES 1 AND 5

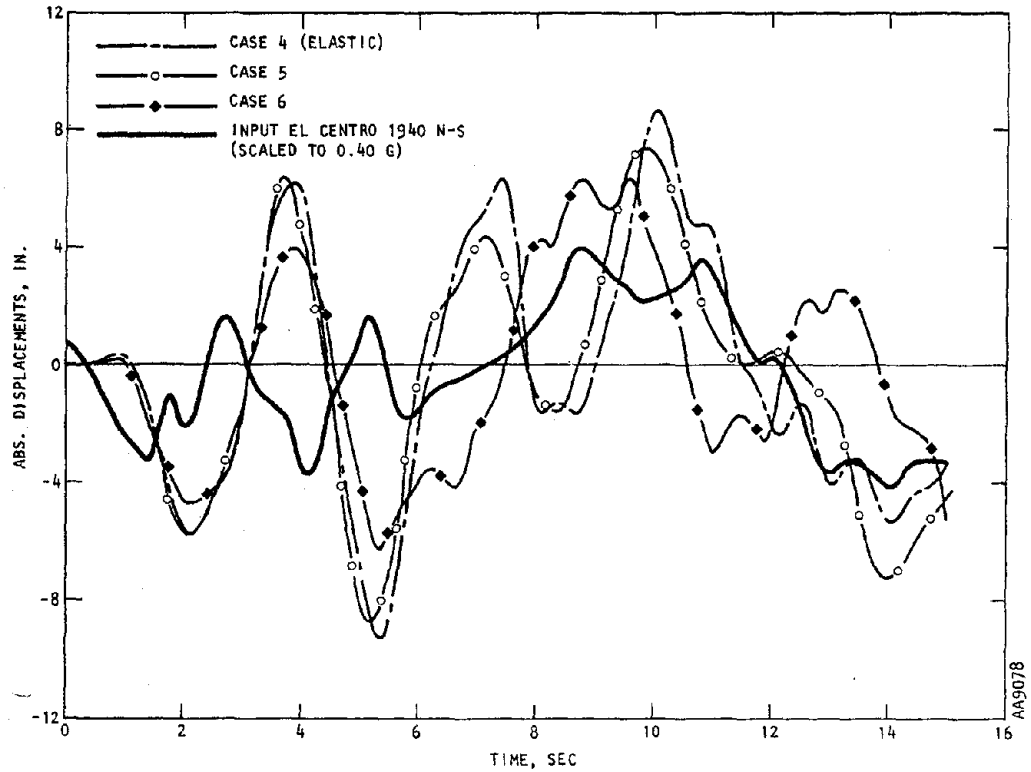


FIG. 10. COMPARISON OF ABSOLUTE DISPLACEMENTS AT MIDPOINT OF PLYWOOD DIAPHRAGM MODELS, CASES 4, 5, 6

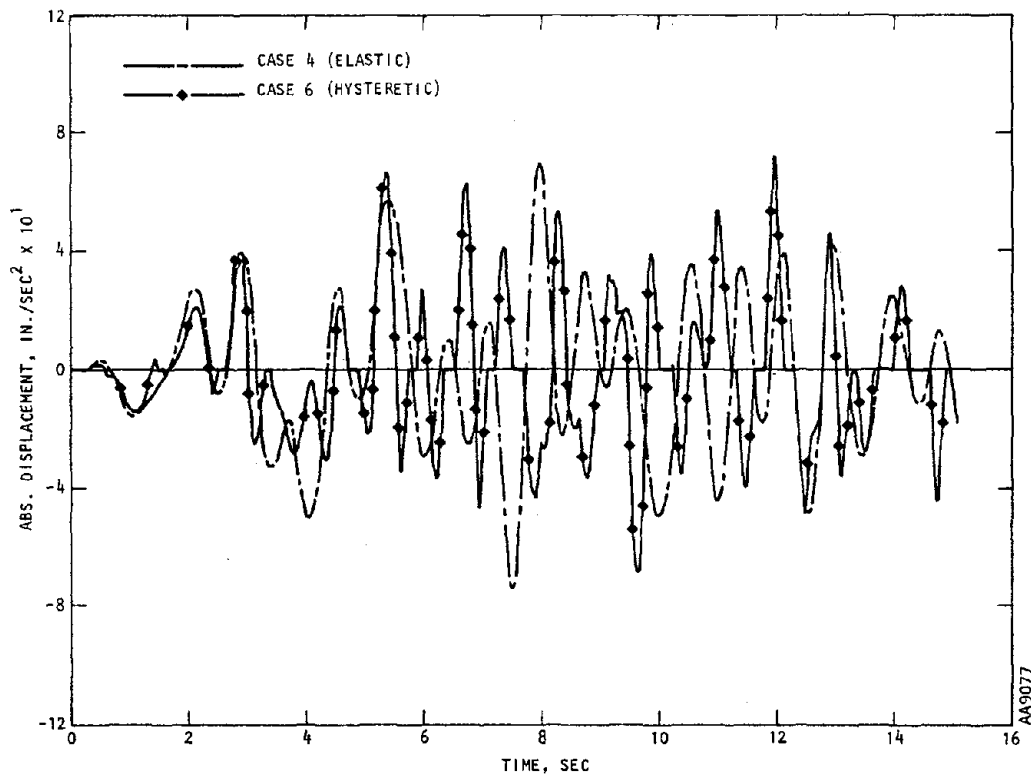


FIG. 11. COMPARISON OF ACCELERATION TIME-HISTORY RESPONSES AT MIDPOINT OF PLYWOOD DIAPHRAGM MODELS, CASES 4 AND 6.

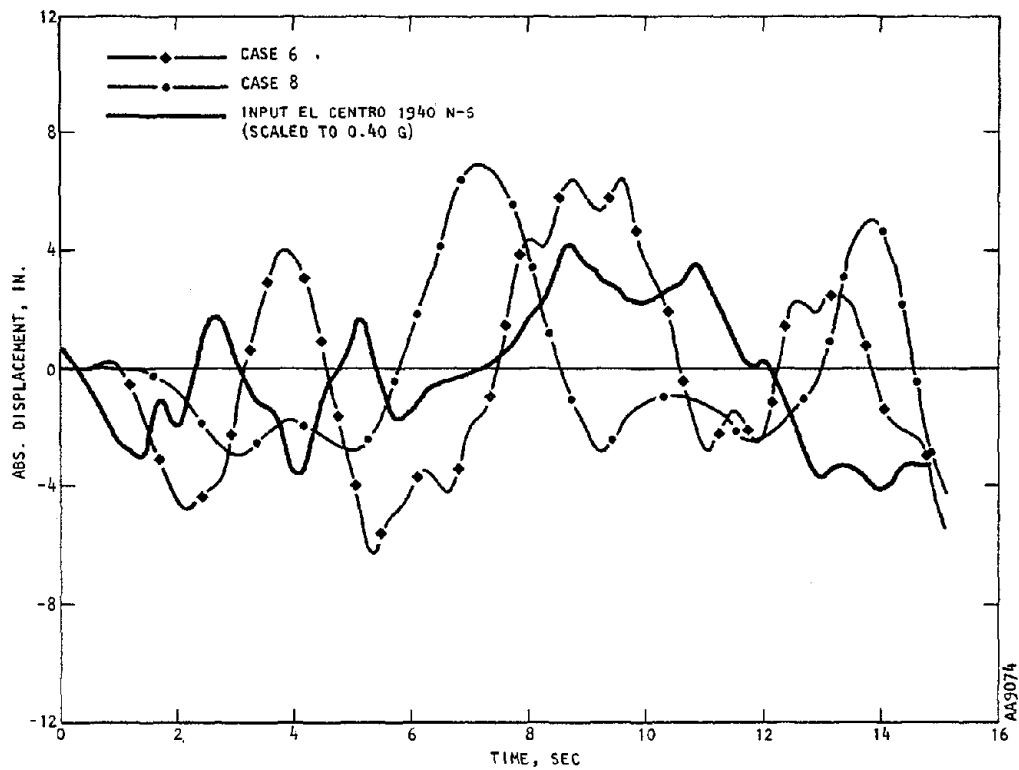


FIG. 12. COMPARISON OF ABSOLUTE DISPLACEMENTS AT MIDPOINT OF PLYWOOD AND STRAIGHT-SHEATHED DIAPHRAGM MODELS, CASES 6 AND 8

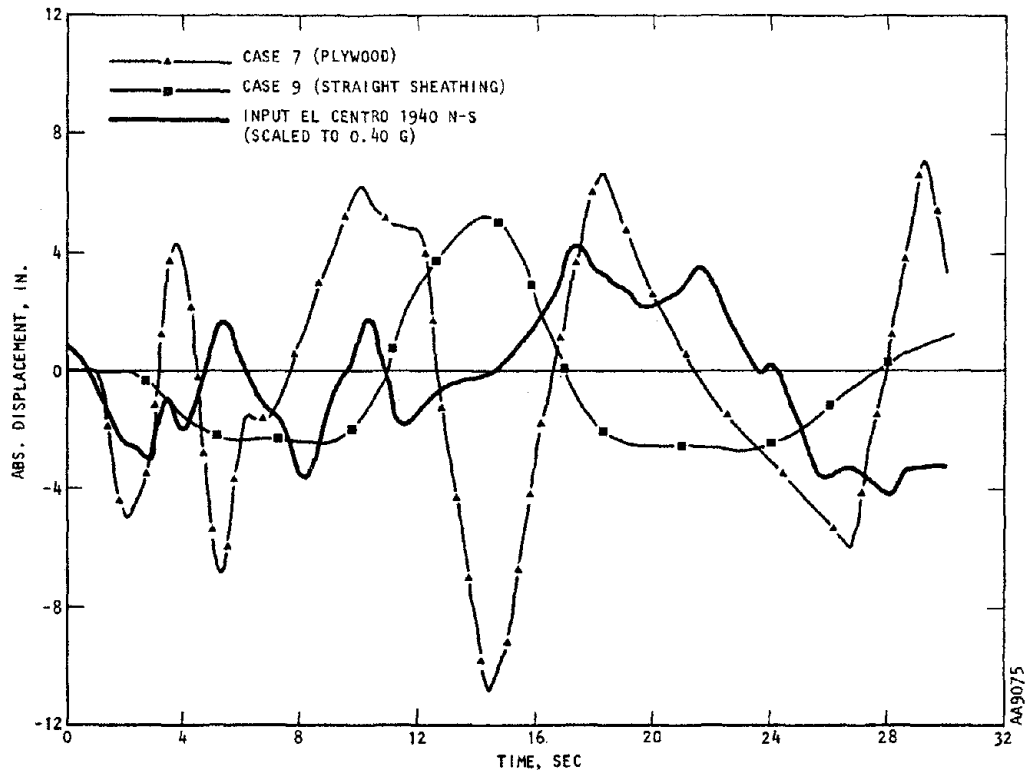


FIG. 13. COMPARISON OF ABSOLUTE DISPLACEMENTS AT MIDPOINT OF PLYWOOD AND STRAIGHT-SHEATHED DIAPHRAGM MODELS, CASES 7 AND 9

The previous results indicate that the eight-segment model provided a better representation of the response of the diaphragms. Addition of the second-mode contribution resulted in a more intense response with longer periods and larger displacements.

The results also indicate that the El Centro record has a wide and strong long-period content. Therefore, this input was critical for studying the response of the above diaphragms. However, the El Centro record has strong long-period peaks and valleys. Therefore, its use must be substantiated by other records with strong long-period content. The results also indicate that the viscous damping effect of roofing materials reduced both the acceleration and the displacement of the diaphragm.

It is of interest to note that the results of this study indicated diaphragm periods ranging from 1.8 sec for case 1 to 11.5 sec for the softest diaphragm of case 9. These results are in contrast to those obtained by Blume et al. (1, 2) and Rea et al. (3), where relatively shorter periods ranging between 0.17 and 0.75 sec were obtained from low amplitude testing of full-scale school buildings. This discrepancy is probably a result of the highly nonlinear character of these diaphragms, which results in lengthening the periods of these diaphragms when they are subjected to the input level of the 0.40 g scaled El Centro used in this study.

CONCLUSIONS

Conclusions of this study can be summarized as follows: (1) Wood diaphragms studied in this phase had periods that range between 1.80 and 11.5 sec and are strongly influenced by the long-period content of the earthquake ground motions; (2) response of wood diaphragms is highly nonlinear when subjected to the level of shaking expected in highly seismic zones; (3) low amplitude tests are not adequate for predicting the response of these diaphragms in highly seismic zones; (4) softer wood diaphragms will attenuate the input earthquake accelerations and result in shear forces transmitted to the masonry walls that are lower than those obtained from stiffer diaphragms, as expected; however, the corresponding midspan deflections will be larger.

ACKNOWLEDGMENTS

This research effort has been supported by the National Science Foundation under Contract No. C-AEN77-19829. The support is gratefully acknowledged. The analyses reported were performed in close collaboration with the firms of Kariotis, Kesler and Allys, and S.B. Barnes and Associates.

REFERENCES

1. Blume, J.A.; Sharpe, R.L.; and Elseser, E. *A Structural-Dynamic Investigation of Fifteen School Buildings Subjected to Simulated Earthquake Motion*. Sacramento, CA: State of Calif. Dept. of Public Works, 1961.
2. Blume, J.A. *The Earthquake Resistance of California School Buildings - Additional Analyses and Design Implications*. Sacramento, CA: State of Calif. Dept. of Public Works, 1962.
3. Rea, D.; Bouwkamp, J.G.; and Clough, R.W. *Dynamic Properties of McKinley School Buildings*, EERC 68-4. Berkeley, CA: Univ. of Calif. Nov 1968. (PB 187 902)
4. Forest Products Lab. (FPL). *Diaphragm Action of Full-Scale Diagonally Sheathed Wood Roof or Floor Panels*. Madison, WI: FPL, Apr 1955.
5. Atherton, G.H. and Johnson, J.W. *Diagonally Sheathed Wood Diaphragms*. Corvallis, OR: Oregon Forest Research Lab., Oct 1951.
6. Stillinger, J.R.; Johnson, J.W.; and Overholser, J.L. *Lateral Tests on Full-Scale Lumber-Sheathed Diaphragms*. Corvallis, OR: Oregon Forest Products Lab., Oct 1952.
7. Stillinger, J.R. *Lateral Tests on Full-Scale Lumber-Sheathed Roof Diaphragms*. Corvallis, OR: Oregon Forest Research Lab., Oct 1953.
8. Johnson, J.W. *Lateral Tests on Full-Scale Lumber-Sheathed Roof Diaphragms of Various Length-Width Ratios*. Corvallis, OR: Oregon Forest Research Lab., Oct 1954.
9. Johnson, J.W. *Lateral Tests on 12-by-60 ft and 20-by-80 ft Lumber-Sheathed Roof Diaphragms*. Corvallis, OR: Oregon Forest Research Lab., Oct 1955.
10. Burrows, C.H. and Johnson, J.W. *Lateral Test on Full-Scale Roof Diaphragm with Diamond-Pattern Sheathing*. Corvallis, OR: Oregon Forest Research Lab., Oct 1956.
11. Stillinger, J.R. "Lateral Tests on Full-Scale Lumber and Plywood-Sheathed Roof Diaphragms," in *Symp. on Methods of Testing Building Construction*, ASTM-STP-166. New York: Amer. Soc. of Mech. Eng., 1955.
12. Oregon Forest Labs. (OFL). *Lateral Tests on Full-Scale Lumber and Plywood-Sheathed Roof Diaphragms*. Corvallis, OR: OFL, Mar 1956.
13. Countryman, D. *Lateral Tests on Plywood Sheathed Diaphragms*. Tacoma, WA: Douglas Fir Plywood Assoc. Lab., Mar 1952.
14. Oregon Forest Research Lab. (OFRL). *Lateral Tests on Full-Scale Plywood-Sheathed Roof Diaphragms*. Corvallis, OR: OFRL, Oct 1953.
15. Countryman, D. and Colbenson, P. *1954 Horizontal Plywood Diaphragm Tests*. Tacoma, WA: Douglas Fir Plywood Assoc. Lab., Oct 1954.
16. Douglas Fir Plywood Assoc. (DFPA). *1954 Horizontal Plywood Diaphragm Tests*. Tacoma, WA: DFPA, Jan 1955.
17. Johnson, J.W. *Lateral Test on a 12-by-60 ft Plywood Sheathed Roof Diaphragm*. Corvallis, OR: Oregon Forest Research Lab., Jan 1955.
18. Adham, S.A. and Ewing, R.D. *Methodology for Mitigation of Seismic Hazards in Existing Unreinforced Masonry Buildings, Phase 1*. R-7815-4610. El Segundo, CA: Agbajian Assoc., Mar 1978.
19. Tissel, J.R. *Horizontal Plywood Diaphragm Tests*. Tacoma, WA: Douglas Fir Plywood Assoc., 1966.
20. Applied Technology Council (ATC). *Recommended Comprehensive Seismic Design Provisions for Buildings, Final Review Draft*, ATC-3-05. Palo Alto, CA: ATC. Jan 1977.

ABSTRACT
COAL ASH UTILIZATION IN MASONRY CONSTRUCTION

BY John H. Faber¹

The great progress in design and construction of concrete structures over the past 40 years has, with some exceptions, not seen great change in the selection of proportions of concrete materials for improving properties. Ash, a reclaimable material, offers seven basic benefits when employed in mixes:

1. improving plasticity without increasing water,
2. correcting deficiency in extreme fines in some sands,
3. increasing formation of cementitious compounds,
4. counteracting or reducing cement-aggregate reactions or damage due to sulfate attack,
5. improving impermeability,
6. improving cement/water ratio, and
7. adding strength to the end product.

Ash is being produced in more areas with attendant economies. The process of producing ash may permit recovery of scarce metals and valuable oxides. The recycling of waste materials is still in its infancy and has a tremendous future.

¹ Executive Vice President, National Ash Association, Washington, D.C.

COAL ASH UTILIZATION IN MASONRY CONSTRUCTION

By John H. Faber¹

INTRODUCTION

In the past 40 years, tremendous strides have been made in the design of concrete structures and in construction methods and equipment for mixing, transporting, and placing concrete. However, with the exception of lightweight aggregate, chemical admixtures, and high-strength reinforcing steel relatively few changes have been made in the selection of proportioning of concrete materials for improving properties of structural concrete.

Structural engineers and architects have shown a general lack of interest in the use of pozzolans - fly ash - in concrete mix designs. Fly ash is unequivocally considered a good admixture for concrete and structural fly ash concrete has given a good account of itself.

One can only assume these same engineers have found it much easier to order concrete from ready-mix dealers by designing the compressive strength without considering the benefits they could obtain from the use of a pozzolan.

Perhaps, the best way to introduce my assigned topic is to define the word pozzolan. What is a pozzolan? The modern term pozzolan is derived from the ancient term "pozzuolana" which referred to a volcanic ash found near Pozzuoli, Italy. The Romans produced a pozzolanic cement by grinding this material with lime and used it in the construction of aqueducts and other structures. Thus, in so doing, they also fathered the recycling movement.

By definition, ASTM characterizes a pozzolan as follows:

"A pozzolan is a siliceous or silicious and aluminous material which in itself possesses little or no cementitious value but will, in finely divided form and in the presence of moisture, chemically react with calcium hydroxide at ordinary temperatures for form compounds possessing cementitious properties."

¹ Executive Vice President, National Ash Association, Washington, D. C.

Silica is the principal constituent of all pozzolans along with substantial amounts of alumina, and some iron oxides. And, chemically, fly ash is about 80 percent silica, alumina, and iron with small amounts of other elements. Physically, fly ash particles resemble glass ball bearings or spheres and are about the same fineness as face powder.

Being a residue of the burning process that transforms coal into electric power, ash has unique properties that require less energy in turning out acceptable construction materials and improving the quality of others in specific applications.

Ash is firmly entrenched as the sixth most abundant mineral resource with 1976 production amounting to 61.9 million tons. According to figures from the U. S. Department of Interior's Minerals Yearbook, ash ranks behind stone, sand/gravel, coal (all types), iron ore, and portland cement. (See Figure 1)²

Last year's totals, being recorded as this paper is written, are expected to climb to about 65 million tons and by 1985 substantially greater tonnages are on the horizon. A recent survey by the National Coal Association indicates the electric utility industry will have 259 new coal-fired stations on stream by that date (See Figure 2)³. Production totals will be in excess of 100 million tons with this new capability. At present a majority of the available ash is produced east of the Mississippi River, but many of the new stations will be located in the West near the new sources of coal being developed. (See Figure 3)⁴

When fully operational the new stations will have a dramatic impact on ash availability. It will mean many areas of the country, particularly the Southwest, will have commercial amounts of these versatile construction materials available to them for the first time at locations that will minimize transportation costs. I'm happy to report to you that satisfied ash users and producers in that part of the country are getting themselves ready to take advantage of these coal by-products. An Ash Management Conference is to be held at Texas A & M University on September 25-27 and an Ash Short Course is being planned in Phoenix, Arizona early in 1979.

The advent of these new sources will also bring with them a need for adjusting marketing techniques. Why? Well, basically, it is because the sub-bituminous coal ashes are quite different in chemical and physical composition than the bituminous ash available from Eastern producers.

In 1976, there were 42.8 million tons of fly ash produced in the United States. Even though the utilization factor reached an all-time high of 13.3 percent or about 5.7 million tons we had a surplus of 37.1 million tons. Realistically, however, that does not mean all that tonnage was or is available although there is a decided trend toward dry collection systems rather than sluice ponds and the separation of fly ash and bottom ash. (See Figure 4)⁵

Of the 5.7 million tons of fly ash utilized about 16 percent or 912,000 tons were used in the partial replacement of cement in concrete or concrete products.

If you don't get anything else out of my remarks here today, I would hope to impress you with the fact it is imperative that the producer, marketer, and the ultimate user know and understand the recommended fly ash before attempting to prescribe its application. Ash is not a miracle material nor a panacea for all your masonry problems.

Not all ashes are the same. Each is plant specific. Variances in equipment, burning techniques, station loading, and coal sources all have an impact on the nature of the ash. Additionally, the installation of equipment and the use of additives to meet emission standards can also alter the characteristics of the ash. Likewise, the introduction of pulverized solid waste into boiler furnaces as a fuel supplement could further change the make-up of the coal by-products.

The characteristics of fly ash that make it valuable for use in concrete are its (1) high fineness, (2) low carbon content, (3) a high percentage of fused silica, and (4) spherical shape which contributes toward great plasticity.

Let's take a look at how fly ash works in concrete. When Portland cement hydrates it gives off lime as a by-product. The silica found in the fly ash combines with the lime that is liberated to form cementitious compounds which adds appreciably to the development of strength, durability, and other performance qualities important in concrete. In other words, the fly ash or pozzolan combine with the lime to make a form of cement.

Another point to remember is that for every 100 pounds of cement that is put into concrete up to 15-20 pounds of free lime is liberated after hydration. As you all know, lime is soluble and therefore subject to leaching out of the concrete. The inclusion of the fly ash in the mix ties up the free lime and makes additional insoluble cementitious compounds.

This chemical reaction does not require any complicated curing procedure because pozzolans operate at ordinary temperatures to form these strength giving compounds. Naturally, this action continues only as long as the cement hydrates and liberates lime.

Fly Ash Benefits

Generally speaking there are seven basic reasons or benefits why fly ash is most commonly employed in concrete mixes. They include:

- (1) improving plasticity of mix without increasing water;
- (2) correcting deficiency in the extreme fines in some sands to put more fat in the concrete;
- (3) increasing formation of cementitious compounds as mentioned before;
- (4) counteracting or reducing cement-aggregate reactions or damage due to sulfate attack;
- (5) improving impermeability of concrete;
- (6) improving water/cement ratio;
- (7) adding strength to end product.

Additionally, there are a couple of important economic factors that must be considered. First, because it is much lower in cost than Portland cement, fly ash has to be rated an economic replacement. Secondly, some contractors feel fly ash concrete requires less hand work after pulling forms and this represents significant labor savings. And cost savings today is the bottom line any way you look at it.

The use of a good quality fly ash is a must in the production of high strength concrete. A fly ash with an ignition loss of 3 percent or less is preferable. The strength gain achieved from the use of 10 to 15 percent fly ash (by weight of cement) simply cannot be attained through additional cement.

Tests have been actually conducted where cement was replaced by fly ash on a volume-per-volume basis of up to 30 percent.

For many years fly ash was used chiefly in mass concrete where its slower strength-gaining curve, its fineness, and reduction in heat of hydration peaks combined to achieve the desired performance qualities. Fly ash is still used in virtually all mass concrete for dams or spillways.

Now fly ash concrete is used on all types and sorts of structures from the simplest foundation wall to the 1,100 foot high, 100-story John Hancock Center in Chicago. No longer is it uncommon to hear of using fly ash concrete for industrial floors, high-rise building construction, residential construction, precast products, tunnels, and other common applications.

There are no established physical and chemical criteria for determining the value of a given fly ash as a concrete admixture. Therefore, it is advisable to test a fly ash with the materials with which it will be used.

Reputable fly ash suppliers for concrete will provide information on its physical and chemical characteristics, and samples for analysis and testing. And many operate their own labs or will contract required work-ups. Such data is valuable and/or essential in forming an initial evaluation of its applicability to a specific job.

Thus, no attempt will be made to get into the critical area of mix designs in this presentation.

If fly ash is being employed to increase strength, it most likely will be used as an admixture. That is, it will be in addition to the regular amount of cement and not as a partial substitute for it. This will hold true in a majority of applications.

In jobs for which the specifications are aimed at a given strength at three months or more, some fly ashes may be of value as a partial cement replacement. However, it is well to remember that replacement of as little as 10 percent of the cement with a like amount of fly ash will reduce all strengths up to 28 days. On the other hand, used as an admixture, it will usually cause an increase in strength at all ages although its total effect will be more noticeable after three months.

Let's get back to the benefits for a moment. Plasticity, is or should be, an important factor in pouring a wall. For example, the more plastic the mix the less honeycombing will take place. As you know, this will minimize the segregation of the coarse aggregate from the matrix and reduce the probability of shrinking and cracking. Also, the ball bearing effect of the fly ash acts more or less as a dry water and reduces the amount of vibration that is necessary.

Impermeability or water tightness is one of the most important qualities of concrete. The very fineness of fly ash aids in producing a dense, impermeable concrete by filling out deficiencies in the fine aggregate. Laboratory results have proven fly ash concrete is water tight concrete.

Concrete used in underground applications, such as foundation walls, must be able to resist the destructive effects of mild acids, the aggressive action of sulphate soils, the passage of water, and not leach lime salts onto finishes. Research and actual practice has shown that fly ash concrete answers the need in all cases.

Fly ash has proved to be of great value in combating deterioration of concrete subject to sulphate attack. For example, it has been used in concrete exposed to sea water and sulfate or acid bearing soil waters. It has been especially effective in cases where a low cement content concrete has been specified. It is generally used at a rate of one part fly ash to from 2 to 5 parts Portland cement - either by weight or absolute volume. Virtually all fly ashes tested greatly improved the resistance of concrete to sulfate attack regardless of the type of cement used.

Pozzolans will also substantially improve the pumpability of a concrete mix by taking advantage of the spherical shape of the fly ash particles. This has been proven and documented, particularly in high-rise construction and where it is necessary to move the mix over or under obstacles on the job site.

The pozzolans used primarily in the eastern and mid-western section of the country is fly ash - the resultant by-product of the burning process in fossil fuel power stations. The lower the carbon content and the higher the fineness, the more active the fly ash is for use as a pozzolan. The beneficiation of fly ash to produce specification material while desirable, is also more costly.

Carbon, as you no doubt have heard, is one of the most controversial constituents in fly ash to be used in concrete work. It has been repeatedly established that carbon affects the amount of air-entrainment. Thus, a low carbon content is extremely desirable in the fly ash to ease the control of air content. No one appears to know definitely if a high carbon content, per se, has a detrimental effect on concrete but the universal practice appears to be to limit the carbon content to a small percentage - below 6% is recommended.

New Breed of Ash

Two new breeds of fly ash that are now or soon will be entering the market place which are worth mentioning are: First, lignite ash is available in the midwest - principally in the Dakotas, Minnesota, Canada - and have been successfully used in Portland cement concrete. And, secondly, the advent of sub-bituminous coals (so-called western coal) in coal burning power stations will produce an ash with different characteristics. The lignite ashes have been incorporated into the ASTM C-618.77 specifications now for the first time.

Generally speaking, there are four major differences between the lignite ash and bituminous ash which require some new guidelines in mix designs. First, the index of refraction of the lignite fly ash is higher; secondly, the average particle size of the lignite ash is considerably coarser; thirdly, the presence of free lime is greater; and finally, the color is brown as compared to the grey or cement-like hue of eastern ashes.

One important factor worth emphasizing again is the tendency for the lignite ash to set after being moistened because of the reaction of the hydrated lime with the silica in the ash. If you do this in the bed of a truck or a mixer truck you had better be looking for a place to dump the load within a half-hour or stop and buy yourself a jackhammer.

Energy Saver

Another way of introducing fly ash into your mix designs is through the utilization of Type 1-P cement. In 1-P cement the ash was added during the production process. It is noteworthy to mention that 1-P requires only about 80 percent of the fuel consumption that it takes to produce a ton of standard Type 1 cement. As the nation becomes more energy conscious this must become an increasingly important factor to the cement industry. And, it might also be one way of alleviating or extending available supplies of cement in some areas of the country.

The cement industry, one of the nation's premier energy consumers, is thus becoming a major beneficiary of ash utilization. About 20-28 percent of the sales cost of cement corresponds to the cost of energy used. The production of blended cement is a good example since fly ash or granulated boiler ash can replace clinker. The replacement of 20 tons of clinker with fly ash in 100 tons of cement corresponds to 4 tons of coal saved plus 1,025 KWH of electricity. Additionally, the industry can increase its capacity by about 20 percent by using a like amount of fly ash with Portland cement in the final grinding phase of the process.

As mentioned earlier, most of the current ash production is centered east of the Mississippi River where the bulk of the fossil fuel is mined. However, this will shift further west by the mid-80's when the impact of the new steam generating plants begins to show.

How do you account for this? Well, overly simplified, it is more efficient and less expensive to transport coal by wire than by any other mode. And that is why the bulk of the western coal will go to western markets.

The economic benefits and costs of using power plant ash will vary geographically just as the cost of transporting all other essential masonry ingredients - sand, gravel, limestone, cement, and admixtures is reflected from region to region. What may be an economic bonanza for one area or one company may turn out to be a horror story for someone else. One has to assume the profit motive will continue to be the dominant motive in our free enterprise system.

However, it is rather difficult to always place a dollar sign on the technological advantages of a material to produce the best end result. The U. S. Corps of Engineers found it expedient to ship thousands of tons of fly ash from the midwest to the vast hydro dams in the west and even today ash is being transported from West Virginia to Georgia and Massachusetts by railroad tank car.

I guess what I am trying to say is that when designing a concrete mix employing fly ash, first clearly define the performance features that are specified or desired and then go after the best materials to do the job.

Regardless of what your needs are, we, in the ash industry, feel that concrete utilizing fly ash can be provided more economically.

Product acceptance has been and continues to be the major deterrent holding back the development and utilization of fly ash in another construction application - lightweight aggregate - here in the United States. One English firm, Lytag Limited, has just opened their fourth facility in the United Kingdom and presently convert over 1 million tons of fly ash per year into useful building products. Lytag has already utilized over 10 million tons of fly ash in aggregate production and justifiably, I think, claim to be the world leaders in the recycling of power plant ash.

And I'm happy to report they are shopping around here in this country for a plant site that is close to an ash source and has the required market potential as well. These are the critical factors leading to a management decision committing the required \$4 million for plant facilities.

Lightweight aggregate has a wide variety of uses in the building and construction industry where lightweight, fire resistance, thermal and sound insulation qualities make it ideal for use in structural concrete, building blocks, refractory concrete products, or overlays (cladding). It has also proved highly effective for accident prevention in escape ramps for trucks on steep grades and is widely used on the continent as a growing and drainage medium in horticulture.

The process is a relative operation whereby the ash is fed into pelletizers, the "green" pellets are moved by conveyor belt into a sinter strand which cures and hardens the aggregate at temperatures of 1,300° C. It is then passed through grading screens into storage hoppers and/or on-site stockpiles.

Another large facility in England is making a light weight aggregate from coal mine refuse and fly ash.

Another exciting prospect is the recovery of scarce or precious metals and other valuable oxides from fly ash. The time frame for the commercial application of laboratory techniques is being shortened by inflationary trends and the continued uncertainty of foreign imports. The imposing roster of metals that are available in ash include copper, vanadium, manganese, aluminum, iron, zinc, chromium, nickel, titanium, magnesium, strontium, barium, lithium, calcium, and lead.

The recycling of waste materials is still in its infancy and has a tremendous future. We in the ash industry are full-fledged participants and we invite you to join us.

Figure 1

PRODUCTION OF MINERALS AND SOLID MINERAL FUELS IN THE UNITED STATES

	Millions (Short Tons)					
	1972	1973	1974	1975	1976	Est. 1977
1. Stone	920.4	1,060.1	1,043.5	903.0	901.7	915.6
2. Sand/Gravel	914.3	983.6	904.6	789.4	885.2	898.2
3. Coal (All Types)	602.4	598.5	610.0	654.6	741.5	747.0
4. Iron Ore	77.8	90.6	84.9	78.9	76.7	53.7
5. Portland Cement	77.9	82.7	75.9	65.2	69.2	74.0
6. Coal Ash	46.3	49.3	59.5	60.0	61.9	63.9
7. Clays	59.4	64.3	60.7	49.0	52.4	56.3
8. Phosphate Rock	40.8	42.1	45.6	48.8	49.2	49.2
9. Salt	45.0	43.9	46.5	41.0	44.2	43.0
10. Slag (Air Cooled)	25.0	28.8	29.8	25.3	22.9	NA
11. Lime	20.2	21.0	21.6	19.1	20.2	19.7
12. Gypsum	12.3	13.5	11.9	9.8	12.0	13.9

Minerals Yearbook

Metals, Minerals, & Fuels, U. S. Department of Interior

Note: 1 Ton = 907 Kg

Figure 2

NEW COAL-FIRED PLANTS BY REGION**New Coal-fired Units
Planned for 1977-86**

Region (and States)	Units	Megawatts
New England (CN, ME, MA, NH, RI, VT)	1	600
Middle Atlantic (NY, PA, NJ)	7	5,500
East North Central (IL, IN, MI, OH, WI)	50	22,124
West North Central (IA, KS, MN, MO, NE, ND, SD)	40	18,727
South Atlantic (DE, DC, FL, GA, MD, NC, SC, VA, WV)	31	18,444
East South Central (AL, KY, MS, TN)	30	14,940
West South Central (AR, LA, OK, TX)	59	32,398
Mountain (AZ, CO, MN, NV, NM, UT, WY)	36	13,952
Pacific (CA, OR, WA)	5	2,630
Total U.S.	259	129,315

SOURCE: National Coal Association

Figure 3

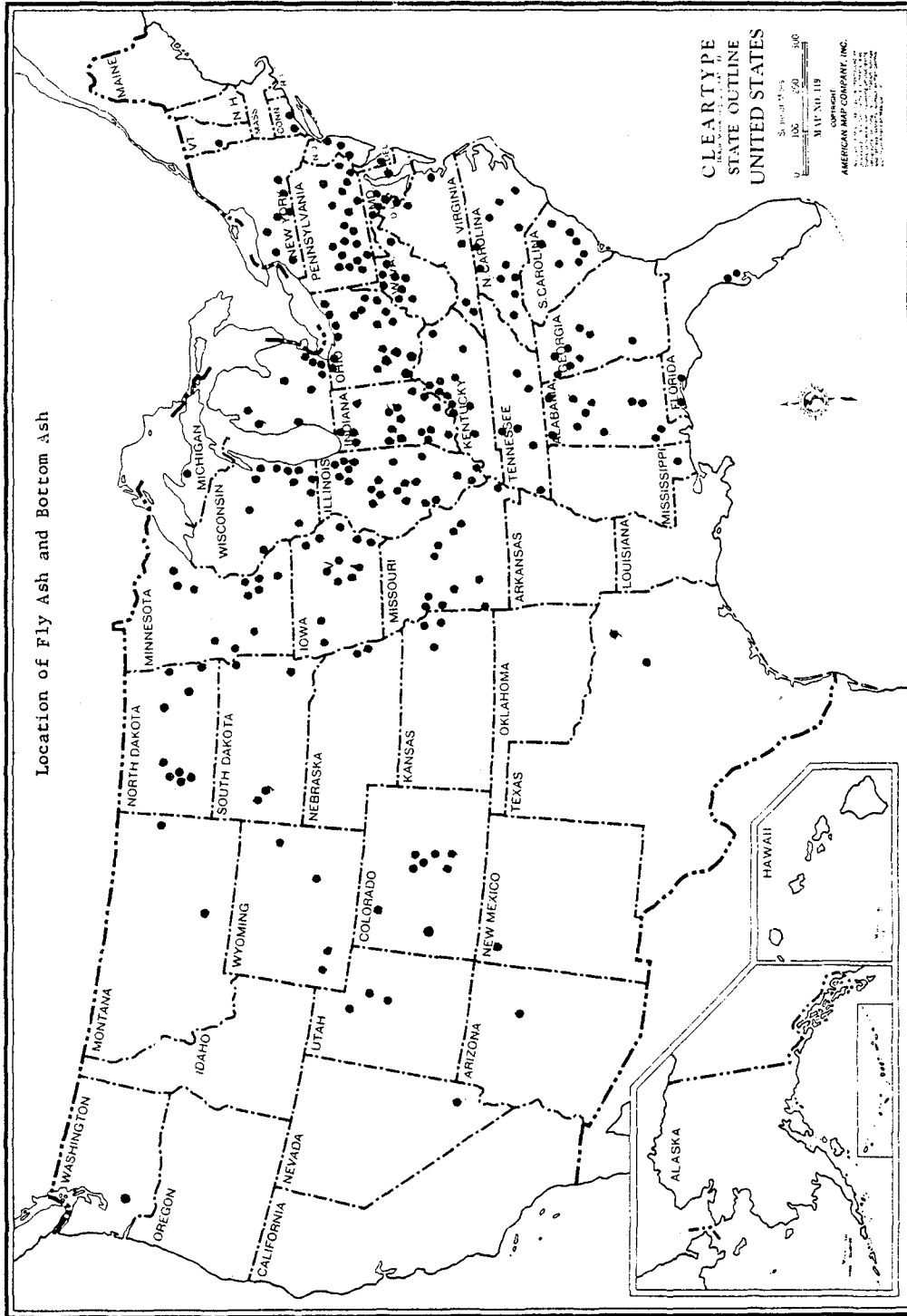


Figure 4

Ash Collection & Utilization 1976

(Million Tons)

	Fly Ash Tons x 10 ⁶	Bottom Ash Tons x 10 ⁶	Boiler Slag (if separated from Bottom Ash) Tons x 10 ⁶
1. Total Ash Collected	42.8	14.3	4.8
2. Ash Utilized	5.7	4.5	2.2
3. Utilization Percentage			
A. COMMERCIAL UTILIZATION			
a. Used in Type 1-P cement- ASTM 595-71 or mixed with raw material before forming cement clinker	9	2	2
b. Partial replacement of cement in concrete or concrete products	16	—	—
c. Lightweight aggregate	2	2	—
d. Stabilization and roads	4	15	10
e. Fill for roads, reclamation & ecology dikes, etc.	26	—	—
f. Filler in asphalt mix	4	—	—
g. Ice control	—	10	5
h. Blast grit and roofing granules	—	—	55
i. Miscellaneous	9	20	14
B. ASH REMOVED FROM PLANT SITES AT NO COST TO UTILITY	5	23	8
C. ASH UTILIZED FROM DISPOSAL SITES AFTER DISPOSAL COSTS	25	28	6
	100	100	100

COMPARATIVE RESULTS

Ash Collected	1966*	1973	1974	1975	1976
Fly Ash	17.1	34.6	40.4	42.3	42.8
Bottom Ash	8.1	10.7	14.3	13.1	14.3
Boiler Slag		4.0	4.8	4.6	4.8
TOTAL ASH COLLECTED - TONS x 10 ⁶	25.2	49.3	59.5	60.0	61.9
Ash Utilized					
Fly Ash	1.4	3.9	3.4	4.5	5.7
Bottom Ash	1.7	2.3	2.9	3.5	4.5
Boiler Slag		1.8	2.4	1.8	2.2
TOTAL ASH UTILIZED - TONS x 10 ⁶	3.1	8.0	8.7	9.8	12.4
Percent of Ash Utilized					
% Fly Ash	7.9	11.4	8.4	10.6	13.3
% Bottom Ash	21.0	21.9	20.3	26.7	31.5
% Boiler Slag		44.3	50.0	40.0	45.8
Percent of Total Ash Utilized	12.1	16.3	14.6	16.4	20.0

*First year that data was taken

**1967-1972 data omitted from tabulation because of space limitation.

Compiled by the National Ash Association and Edison Electric Institute.

Figure 4a

COMPARATIVE ASH COLLECTION AND UTILIZATION IN THE U. S. - 1966 TO 1976

Year	Ash Collected in Millions of Tons				Ash Utilized in Millions of Tons				Ash Utilization in Percent			
	Fly Ash	Bottom Ash	Boiler Slag	Total Ash	Fly Ash	Bottom Ash	Boiler Slag	Total Ash	Fly Ash	Bottom Ash	Boiler Slag	Total
1966 ^a	17.1	8.1	-	25.2	1.4	1.7	-	3.1	7.9	21.0	-	12.1
1967	18.4	9.1	-	27.5	1.4	2.3	-	3.7	8.2	25.0	-	13.5
1968	19.8	7.3	2.6	29.6	1.9	1.8	1.5	5.2	9.6	25.0	57.8	17.6
1969	21.1	7.6	2.9	31.7	1.9	2.0	1.0	4.9	9.1	25.6	33.0	15.3
1970	26.5	9.9	2.8	39.2	2.2	1.8	1.1	5.1	8.1	18.6	39.1	13.0
1971	27.8	10.1	5.0	42.8	3.3	1.6	3.7	8.6	11.7	16.0	75.2	20.1
1972	31.8	10.7	3.8	46.3	3.6	2.6	1.3	7.5	11.4	24.3	35.3	16.3
1973	34.6	10.7	4.0	49.3	3.9	2.3	1.8	8.0	11.4	21.9	44.3	16.3
1974 ^b	40.4	14.3	4.8	59.5	3.4	2.9	2.4	8.7	8.4	20.3	50.0	14.6
1975	42.3	13.1	4.6	60.0	4.5	3.5	1.8	9.8	10.6	26.7	40.0	16.4
1976	42.8	14.3	4.8	61.9	5.7	4.5	2.2	12.4	13.3	31.5	45.8	20.0

^aFirst year that data was taken

^bIn 1974 a more comprehensive data collection program was developed, thus resulting in a substantial increase over previous year

Note: 1 ton = 907 kg

CONSTRUCTION AND QUALITY CONTROL
OF HIGH LIFT GROUTED REINFORCED MASONRY

Robert W. Harrington¹

ABSTRACT: The following items are discussed:

1. History of both reinforced and reinforced grouted masonry.
2. Materials. The physical characteristics of brick (clay, concrete, sand-lime) should be given to point out that the same high quality materials used in unreinforced masonry are also the materials of reinforced as well as reinforced grouted masonry. This would also hold true for mortar, grout, reinforcing steel and web wire reinforcement.
3. Procedures in plain masonry, reinforced and reinforced grouted masonry (low and high lift).
4. Reinforced vs. Reinforced Grouted Masonry. In reinforced masonry web wire reinforcing and pencil rods can be used in mortar joints. In reinforced grouted masonry all of the structural reinforcing steel must be embedded in grout if evaluated for steel requirements.
5. High Lift Grouted - Low Lift Grouted. The procedural differences between the two systems should be discussed. Advantages and disadvantages of each should be weighed. The intermingling of procedures causes problems. High lift requires cleanouts, grout control dams, mechanical pumping procedures, consolidation and reconsolidation. Low lift requires none of these.
6. Testing and Quality Control. When is testing necessary? What items of quality control should be watched? Substitution of materials? Who should substitute? Written authorization? The role of the Inspector.
7. Efflorescence and Cleaning. Is sandblasting a recommended cleaning procedure? What chemicals are available? What are the do's and don'ts and the pitfalls of cleaning? How do you avoid efflorescence? What do you do about efflorescence if it exists?
8. Painting and Waterproofing. Should masonry be painted? What materials can be used? What materials should be avoided? What factors should be evaluated in waterproofing? What kinds of waterproofing should be used? What waterproofing should be avoided and what conditions?
9. Inspection. Spot inspections vs. part time inspection vs. full time inspection. Is inspection a necessity or is it an unwarranted expense?

¹Harrington & Company, San Francisco, CA.

CONSTRUCTION AND QUALITY CONTROL
of
HIGH LIFT GROUTED REINFORCED MASONRY

By Robert W. Harrington¹

INTRODUCTION

HISTORY

It is not necessary to mention more than a few thoughts and ideas on the History of Masonry. Plain masonry has been with us since the days of the cave men. From the time man first accumulated a few stones to make a fire pit; Masonry was born and the great monuments of man need only to be mentioned to be recognized. The Roman Aquaducts and the Egyptian Pyramids were basically constructed of Masonry. None of these, however, were constructed of either Reinforced or Reinforced Grouted Masonry.

The ancient castles, the great churches and cathedrals were constructed of Masonry, but again these were not reinforced. Reinforced Masonry was first used about 1825 in England for construction of the Thames Tunnel, which was 26 years before concrete (known then as "New Cement") was first used.

The "New Cement" now Portland Cement, was so named because the mortar and concrete resembled the natural stone from Portland, England.

In 1923, India used a million square feet of Reinforced Masonry per year for three consecutive years.

In 1950, Japan reported in Engineering News Record that Masonry, when reinforced, offered high tensile strengths to resist earthquakes.

In San Francisco, the 1906 earthquake damage was about equal in Masonry and concrete construction.

In the 1925 Santa Barbara Earthquake, Reinforced Masonry and reinforced concrete performed well. Unreinforced Masonry and unreinforced concrete failed miserably.

¹Harrington & Co., Construction Consultants, S.F.
Fellow of Construction Specification Institute
Professional Engineer, Registered State of California

During the 1933 Earthquake in Long Beach, unreinforced masonry and unreinforced concrete failed so badly, it was outlawed for all State of California schools and public buildings by a State Safety Act; Title 21.

In Los Angeles in 1935, the idea of using a cement-sand grout to bond the brick wythes together instead of using bonding headers was first proved to be practical by the Clay Products Institute of California under the direction of Norman W. Kelch, Registered Architect and Director and M. C. Poulsen, Registered Civil Engineer. Since then thousands of tests on shear resistance and tensile strengths have been conducted to prove their sound engineering principles.

In 1955 in San Francisco, a committee (Manley W. Sahlberg, State Division of Architecture; Oscar F. Person, Masonry Contractor and Robert W. Harrington, Masonry Institute) directed Testing Project No. 922 for the Masonry Joint Industry Board of San Francisco. This first testing program on High Lift Grouting techniques was developed, tested and refined and then documented in the printed report. Most of today's knowledge on High Lift Reinforced Grouted Masonry is based directly on Testing Project No. 922.

MATERIALS

The materials of Reinforced Grouted Masonry should be the same high quality materials as used in unreinforced masonry.

BRICK: The brick should be of good sound quality with a compressive strength of 5000 psi plus. The absorption should be not more than 8% on the cold water test and a C/B ratio of 0.75. The material in the brick, whether it be clay, shale, concrete, sand-lime or whatever, the physical characteristics should be of the same quality. These requirements are not excessive but if a lesser unit is manufactured it should be used as a veneer or of some other use but not as the basic material for Reinforced Grouted Masonry.

MORTAR: The American Society for Testing and Materials (ASTM) lists at least two Specifications for Mortar. The first is ASTM: C270-73. This Specification lists all five types of mortar to be used in all types of masonry. This Specification is much too broad in scope. The proper Specification is ASTM: C476-71. This Specification has only two types of mortar. The "PM" mortar that is 1 part Portland Cement : 1 Part Masonry Cement : $4\frac{1}{2}$ parts sand. The preferred Specification is the "PL" mortar, that is 1 part Portland Cement : $\frac{1}{2}$ part lime and $4\frac{1}{2}$ parts sand. No place in any of the ASTM Specifications are there any substitutions, such as fireclay, allowed. The Uniform Building Code does not even recognize fireclay or any admixtures as an equal or

substitute. These specific mixes are a most important part of the overall strength that is to be developed into the wythes of the Reinforced Grouted Masonry.

STEEL & WIRE REINFORCEMENT: The steel to be used in Reinforced Grouted Masonry should be of good quality and should be acceptable under the Intermediate Grade ASTM A615-Grade 40. Excessive rust and mill scale should be avoided.

GROUT: The grout used in Reinforced Grouted Masonry and the proper placement of that grout, is the single most important feature of the Reinforced Grouted Masonry System. The grout is the single ingredient that replaces the header, the wall tie and performs the miracle of combining as many as six completely separate and heterogeneous materials into a completely homogeneous mass.

The ASTM Specification for grout is ASTM C476-71. This is the same Specification number as we use for mortar. It is convenient, easy to use, and it defines both the Fine Grout used in grout spaces of 3" or less and the Coarse Grout usually used in High Lift Reinforced Grouted Masonry.

Building Codes will also allow the use of a Class A mortar to which additional water has been added to be used as a grout. This grout should only be used in emergencies or extremely small projects.

PROCEDURES

Masonry is a broad term to describe a type of construction that covers many and various combinations of building units that are bonded together with a cement adhesive. It is a well known fact that mixing together of non-compatible materials and techniques can cause many problems.

Masonry is not complicated, nor is it difficult, providing one will take the time to study, recognize and understand. There are many of the procedures that are the same but in the fine points there are many differences. Let me explain some of the likenesses and some of the differences.

Plain masonry has always been known for its ability to withstand high compressive loads. It is not uncommon to have brick units in the 8,000 to 12,000 psi strengths, and mortar with a composition of 1 cement : $\frac{1}{2}$ lime : and $4\frac{1}{2}$ sand will make a test sample of 2500 to 3000 psi.

Combining the brick and mortar will give a composite wall section with a compressive strength of 5000 psi to 6500 psi.

The tensile strengths of this combination is very low, probably in the range of 1% - 3% of the compressive strengths.

Recognizing this fact immediately points to the advantages of reinforcing steel in Masonry.

In addition to the Masonry units and the mix of the mortar, the size of the mortar joints will also effect the overall strengths of the Masonry walls. For example, using a 8,000 psi brick and a $1:\frac{1}{2}:4\frac{1}{2}$ mortar and a $\frac{1}{2}$ " mortar joint, we should expect a 3000 psi composite wall. If the mortar joint is increased to 1" the overall strength would be 1500 psi and conversely, if the mortar joint is decreased to $\frac{1}{8}$ " the expected strengths should be 6000 psi.

Recognizing that the size of the mortar joint can make considerable difference in the overall strength, consider the advantages of adding steel to the masonry to combine the high compression strengths of masonry with the high tensile strengths of steel.

When the design calls for Reinforced Masonry, the steel can be added to the mortar joint. But mortar joint reinforcing cannot be greater than $\frac{1}{2}$ the thickness of the mortar joint. This limits the size of the steel to a $\frac{1}{4}$ " bar in a $\frac{1}{2}$ " joint or a $\frac{3}{16}$ " wire in a $\frac{3}{8}$ " joint, etc.

When the design calls for Reinforced Grouted Masonry, we have the opportunity to use the stronger and smaller mortar joints plus larger rebars, usually #4 ($\frac{1}{2}$ ") or #6 ($\frac{3}{4}$ ") and the steel must be placed in the collar joint and embedded in grout. In walls from 8" to 12" in width, the steel should be placed in a single curtain at the center of the wall. Unless (of course) the design is a retaining wall where the lateral load would be in one controlled direction.

LOW LIFT REINFORCED GROUTED MASONRY

The system of constructing Reinforced Grouted Masonry by the Low Lift procedure has a number of limitations. Many of these procedures have been discussed time and time again in the field, not because the rules are illogical but many times because of a lack of understanding.

The Low Lift rules and reasons are as follows:

RULE # 1 - The outside wythe of masonry shall not be carried ahead of the inside wythe more than 16".

Reason 1a - A four inch or single wythe of masonry and mortar, built ahead, will dry out quickly, especially when exposed on both sides.

Reason 1b - A dried out wythe of masonry doesn't have the high overall strength of a properly cured wythe.

Reason 1c - A single wythe of masonry can be easily

bumped, breaking the bond between the mortar and the masonry unit. Wind and other construction vibrations will also be detrimental.

RULE # 2 - The back up and the pouring of the grout shall be one course at a time and the heights of the grout pour shall not be more than four inches. The grout pour shall also be at half heights of the units, i.e., from the center of the course below to the center of the last course laid.

Reason 2a - The purpose of the procedure of laying up masonry units and grouting is to form a homogeneous mass from several separate components. This can be best done in a series of short layers that are still of the consistency that they may bond together.

Reason 2b - Grouting one course at a time in layers from the center of the course below, to the center of the last course laid will not allow the following: a straight bonding joint across the wall; the very fluid grout to push the most recent laid masonry unit out of line; the grout pressure to break the bond between the mortar and masonry units of the last course laid and the masonry units in the last course laid to be pulled in from alignment as the excess water from the grout is absorbed.

Reason 2c - Grouting one course at a time in layers from the center of the course, below to the center of the last course laid, will allow: the mason to have complete control in forming a homogeneous mass; for the absorption of the excess water from the mortar and grout without fear of pushing or pulling masonry units out of alignment; for proper consolidation and reconsolidation of the grout; the mason to be sure that no air pockets or foreign materials are in the grout core and the mason to properly position the reinforcing steel in accordance with the design.

RULE # 3 - No wall ties or bonding headers shall be used in Low Lift Reinforced Grouted Masonry.

Reason 3a - When the procedures of RULE # 2 are followed, none will be needed.

RULE # 4 - No wall joint(collar) or grout spaces shall be greater than 3 inches without floaters.

Reason 4a - This will allow for a shiner to be floated in the grout space and still allow for the mandatory 1/4" of grout coverage between masonry units or between the steel and masonry units.

Reason 4b - This will also help to absorb the excess water from the fluid grout mix and will help stabilize the setting and curing characteristics.

RULE # 5 - At the end of a day or when work is to be stopped for more than one hour, the horizontal construction (cold) joint shall be formed by bringing the two wythes to the same elevation and the grout core shall be stopped approximately $1\frac{1}{2}$ " below the top.

Reason 5a - Horizontal construction cold joints should be recognized for what they are and handled accordingly.

Reason 5b - The grout lift $1\frac{1}{2}$ " below will give a mechanical key. It will also provide a continuity in the laying of the masonry units, pouring of the grout, consolidation and reconsolidation in the wall above.

HIGH LIFT REINFORCED GROUTED MASONRY

The system of constructing Reinforced Grouted Masonry by the High Lift procedure has a number of individual construction requirements. Many of the rules in this system are resisted daily in the field because of a lack of understanding.

The High Lift rules and reasons are as follows:

RULE # 1 - The outside wythe or tier of masonry shall be constructed not more than 16" ahead of the backup.

Reason 1a - A single wythe or tier of masonry and mortar built ahead will dry out quickly, especially when both sides are exposed.

Reason 1b - A dried out wythe of masonry doesn't have the high overall strength of a properly cured wythe.

Reason 1c - A single wythe of masonry can be easily bumped, breaking the bond between the mortar and the masonry unit. Wind and other construction vibrations will also have detrimental effects.

Reason 1d - Stirrup wall ties shall be place 16" on center vertically. 16" is a good reasonable wythe height limit.

RULE # 2 - The outside wythe or tier of masonry units shall be constructed not more than 12" when using stacked bond.

Reason 2a - This has all of the logic of RULE # 1, except that stirrup wall ties shall be placed 12" on center vertically when using stacked bond.

RULE # 3 - Wall ties shall be not less than #9 bright basic wire in the form of a rectangle with no kinks, water drips, or deformations and shall not be bent up or down in placement.

Reason 3a - The wall ties (a #9 wire in a rectangle)

shall be strong enough to retain the hydrostatic pressure of the grout.

Reason 3b - No drips or kinks or deformations in the wall ties are allowed. Thus the tie will not give under the hydrostatic pressure. Bright basic wire is acceptable since the ties will be solidly embedded in the grout.

Reason 3c - Since both wythes of the wall is brought to the same height, each 12" or 16" as provided in RULES # 1 and 2, bending wall ties is not necessary.

RULE # 4 - Cleanouts shall be provided for each grout pour.

Reason 4a - At the bottom of each grout pour there must be a way to clean out the mortar droppings and any other foreign substance that might be dropped in the grout space. Even with an expert mason, there is always the possibility of mortar droppings.

Reason 4b - The cleanouts are cleaned daily to remove mortar droppings, sawdust, dirt, dust and other foreign materials.

RULE # 5 - All High Lift Grouted Reinforced Masonry shall have full head and bed joints. These are defined as completely full, except there may be a protrusion or a recess equal to the size of the mortar joint on the side adjacent to the grout core.

Reason 5a - When the grout is poured in High Lift, the outside wythes must be strong and capable of withstanding the pressure of the grout.

Reason 5b - All mortar protrusions that project into the grout core more than the thickness of the mortar joint must be cut off so it will not interfere with the pouring of the grout.

Reason 5c - Protrusions that are more than a joints thickness will be dried out, not cured mortar and will have a low strength. These should be removed and not become a part of the wall.

Reason 5d - Indentations or recesses in the mortar joints that do not exceed the size of mortar joints will be easily filled with grout to form a solid wall.

RULE # 6 - Grout control dams shall be designed into High Lift Grouted Reinforced Masonry to provide horizontal grout control.

Reason 6a - Grout with a 9" to 11" slump will flow laterally 40 feet or more. Grout must be contained in a controlled area of placement.

Reason 6b - All grout pours must be completed to full height of the wall within one day. Control dams will allow grout to be placed in only the intended areas.

RULE # 7 - The grout should be pumped or placed at a center point between grout control dams.

Reason 7a - This will allow for control of height of the lift.

Reason 7b - This will keep all of the reinforcing steel from becoming covered with grout before imbedment.

RULE # 8 - Grout lifts shall not exceed four feet.

Reason 8a - Fluid grout will have a high hydrostatic pressure on the wythes or tiers of masonry units.

Reason 8b - Blow outs are very costly and will cause unnecessary delays.

Reason 8c - Proper consolidation is extremely difficult at a depth of more than four feet.

RULE # 9 - A grout pour may consist of two or more lifts and shall be completed in one day.

Reason 9a - The purpose of High Lift is to provide a completely homogeneous and continuous grout core without a single cold joint. It must be completed in one day.

Reason 9b - A one grout lift wall has a maximum height of four feet; a two grout lift wall an approximate eight feet and a three grout lift wall an approximate twelve feet, etc.

Reason 9c - Mechanical pumping and transit mix grout is encouraged to provide needed speed of placement.

RULE # 10 - Consolidation and reconsolidation of the grout lift must be performed in accordance with the Designer's requirements.

Reason 10a - Consolidation is necessary so that no air bubbles have been trapped or the grout has not bridged or hung up when pouring.

Reason 10b - Reconsolidation is necessary to allow the grout to slump properly into place after the excess water has been absorbed from the grout, reducing its volume.

RULE # 11 - Reinforcing steel must be properly located and held firmly in place.

Reason 11a - When grout is placed and then consolidated and reconsolidated, steel must be firmly held or it can be moved from its proper position.

RULE # 12 - Grout shall be poured full wall height without stopping for more than one hour.

Reason 12a - No cold joints are allowed in the High Lift Grouted method.

Reason 12b - If an emergency situation occurs and grouting is delayed, the Architect or Engineer on the project shall determine the corrective procedures.

RULE # 13 - No grout slurry is needed or allowed.

Reason 13a - With a proper designed mix, slurry is not necessary.

Reason 13b - With proper control dams, slurry is not necessary.

Reason 13c - If the pouring of the grout has not been properly performed, the use of slurry will not overcome this deficiency.

Reason 13d - Slurry improperly used, can be a detriment.

TESTING AND QUALITY CONTROL

The only mention of Quality Control and Inspection in the High Lift Grouted Reinforced Masonry Testing Project No. 922 is on Page 3, where it states that, "Quality control and inspection are deemed necessary." I know that when the report was written, it was believed that the facts of the High Lift Grouting technique were so thoroughly documented that more explicit details of inspection need not be outlined.

Today, I am of a completely different opinion. Inspection, Testing and Quality Control are very important in the success of High Lift Grouted Reinforced Masonry. The lack of Quality Control and uniform purpose of direction is one of the main reasons that today we still find Reinforced Masonry Low Lift Reinforced Grouted Masonry and High Lift Reinforced Grouted Masonry all being designed with the same relative low working stress. The use of 1500 psi as the F'_m for a well designed reinforced masonry wall is a waste of good construction materials.

Today, we are confronted with adverse heat transmission

coefficients and acoustical limitations and yet we have not conquered the simple advantages of the High Lift Reinforced Grouted Masonry system in establishing a means of using higher design stresses.

The simple prism test to establish the F'_m for reinforced masonry is one of the most overlooked and ^munused advantages in the Building Code.

Designers could easily use 2600 psi design working stress. The Industry has spent most of its time in advancing alternate suggestions of procedures and short cuts in achievements.

As a matter of policy, the testing program for High Lift Reinforced Grouted Masonry, asked that new ideas and suggestions be offered. The Committee suggested that qualified substitutions of techniques and combinations of material be given every opportunity for success. The ideas that have come forth in the past 19 years, since the basic testing was done, are many.

It has been suggested that lime be added to the grout, which would allow the substitution of a high absorption brick, instead of an acceptable unit.

Instead of trying to downgrade the workmanship in a potentially good system, to meet the low values usually assigned, the Industry should take advantage of the proven facts in High Lift Reinforced Grouted Masonry and upgrade its outlook.

It has been suggested that we could substitute masonry or plastic cement for the Portland Cement and lime. It has also been suggested that fireclay be allowed instead of lime in the mortar, and that a 5" slump, 5 sack concrete be used instead of a 10" slump, 8 sack grout as an economy move. None of these suggestions are acceptable or are they in any way equal, but nevertheless they have been suggested.

One item of the original testing that has been changed, is the recommended use of slurry at the bottom of the grout pour. The idea of using slurry was born from the pouring of concrete when slurry helps seal a cold joint. In High Lift Reinforced Grouted Masonry, the rich fluid grout has more than enough plasticity to meet the cement requirement at the foundation and no other cold joints are allowed.

When cleaning out the grout space, how much water should one use? It is not how much water, but how effective it has been used. A clean grout space is, simply that. The original testing used water, however, compressed air or other cleaning techniques are acceptable.

Racetrack Grouting is a term used when grout is placed all

around the top of the building's walls. It is usually a team effort. The first team pumping grout, the second team doing the consolidation and the first team back around again for the second lift. I dislike this type of grouting because the first team covers all of the rebar with grout that usually in hot weather, dries on the steel, completely covering it with what turns out to be a very poor and low strength material. Another disadvantage is the possibility of the grout in the second lift hanging up on the steel creating a blockage and a potential void.

What is the role of the Inspector? This is the most difficult job of any in the construction field. The Inspector should see everything and yet he should know nothing if he is asked an opinion or a question. He should be everywhere at one time without appearing to be in the way or looking over anyone's shoulders. He should write clear, complete and brief reports, covering everything that has happened all day every day, without getting carried away. (This should also be in plain, forthright and unimpeachable English.)

He should be in direct contact with both the Architect and or Engineer and the Contractor without seeming to favor either over the other. He must also have a complete file of requests and authorization for every substitution or change.

The Quality Control of High Lift Reinforced Grouted Masonry is not difficult. Quality Control means simply: FOLLOW THE RULES, doing the best possible job to stay within the parameters of the research and tested program. Everyday we hear of people that have performed an outstanding feat of unbelievable proportions. I only hope that none of these are in High Lift Reinforced Grouted Masonry, as we have had enough dreams, and are now ready to face facts and hard work.

The High Lift Reinforced Grouted Masonry system is not a cure all, nor is it a perfect or undaunted. It is, however, a system that has stood up well over the past 19 years and although, at times, it may have seemed that everyone was trying to prove it wrong, it is still the best, most economical system and results in the highest strength masonry in existence today.

HOW THE HIGH LIFT GROUTING SYSTEM WAS DEVELOPED

By Oscar F. Person, Person-Western, Inc.

ABSTRACT: This paper presents information about the inception and development of the high lift grouting system for masonry construction. It also presents information supported by Testing Project No. 922, "The Method of Reinforced Concrete in Masonry Construction Using High-Lift Grout System."

This report is based upon the experience of a masonry contractor who has been in business for more than 40 years. Cases illustrating the use of the high lift system, and recommendations for its successful application in modern masonry, are included.

HOW THE HIGH LIFT GROUT SYSTEM WAS DEVELOPED

By Oscar F. Person¹

INTRODUCTION

The High Lift Grouting system for masonry construction was developed in California to meet the needs of the industry in earthquake zone areas. The system developed by Oscar F. Person, Manley W. Sahlberg and Robert W. Harrington was first published as Testing Project No. 922, "New Method of Reinforced Concrete and Masonry Construction using High Lift Grouting System."

This paper covers the development of this system and points up its advantages in modern masonry construction.

THE PROBLEM

A common statement made by architects and engineers alike was: "We love masonry. It's flexible for design, provides a variety of attractive materials which make beautiful homes and buildings." But, we can not trust masonry contractors or the masons. Poor workmanship was an especially important problem in earthquake areas. Inspection of this workmanship often showed that reinforcing steel was not properly installed and adequately covered with grout. It also showed that the grout mix was short on cement, that masonry units were not properly embedded in mortar and that water penetration into the finished buildings was prevalent.

THE SYSTEM'S DEVELOPMENT

During the period of 1955-60, I worked very closely with the Division of Architecture, State of California and with Robert W. Harrington to promote 40 million dollars worth of residence halls for State colleges and other projects in masonry.

It was at this time, I realized more than ever what problems the design profession was having with masonry buildings. It became apparent that inspection was one of the major areas of concern. I started asking questions: The general contractor always have full time inspection when concrete is poured? Why not have full time

1 Owner of Person-Western, Inc., Masonry contractor, Burlingame, California.

inspection of masonry by properly trained inspectors? Why shouldn't the properly trained inspectors have certification from the mixing plants when the grout was delivered. I concluded all these inspection procedures should be accomplished and made this recommendation to the State Architect.

During this period our firm, Person & Wik (later changed to Person-Western) was working on many school jobs where grout was poured in 18 and 24-inch lifts. After observing one job after another, I came to the conclusion that in order to gain the trust and confidence of the engineers and architects, we in the masonry industry, had to gain better control of the installation of our walls and turn out a better finished product.

In 1957 Wik and I tried the high lift grouting system on a number of small jobs to prove its practability and gain the confidence of building inspectors. One such building was a small apartment building in Burlingame. This building was laid out in jumbo brick with a grout core of about 3 inches. We proceeded to lay the walls up to the full height of 8 feet - 6 inches, and in some areas, up to 10 feet. We ordered ready mixed grout and poured the walls up to the full height. The walls were excellent, never created a problem of any kind or a call back!

This success prompted me to start working on the high lift grouting system in earnest.

DEVELOPMENT OF CLEAN-OUTS

I decided that providing clean-outs was one important element of this system. This was accomplished by leaving out every other brick in the first course of a brick wall, and every other face shell in a block wall. This idea provided a good method of cleaning and flushing out the walls. Once this was accomplished it was a simple matter to put the steel in place and call for inspection of the walls. Of course, the horizontal bars were put in place as the walls were layed up.

The first major job to use this clean-out system was the Palmacia Village in Hayward (now Southland Shopping Center). A major structure in the center was Sears-Roebuck. It was designed by Reynolds & Chamberlain; Pregnoff-Mathew were the structural engineers.

Having known Pregnoff for many years, I had gained his confidence. I therefore, asked him if he would permit us to pour the full height of the 30 foot walls in that building. Pregnoff wrote, saying "Oscar, you can have the clearance on this provided that you take full charge yourself." He advised the architects he would accept my procedure on

the job. Thus, this Sears-Roebuck building became one of the first on which high lift grouting was used to any large extent.

We didn't have a grout pump in those days, but we had a big Loraine Crane with the 2-yard bucket and an elephant trunk to carry the grout down into the walls which had a 4-inch grout core.

When we were ready to pour this job, we notified most of the building inspectors in the East Bay area and Manley Sahlberg from the State Division of Architecture to witness the grouting.

In the meantime, in preparation for the pour, I developed what I called a "stirrup-tie" designed to hold the two wythes of brick in the wall together. These metal ties had been placed in the wall, as it was constructed, about 16 or 18 inches apart both ways.

When we were ready to pour, twenty or more building inspectors and several engineers were on hand to see how it worked. I stood next to the wall. Two men yelled, "Mr. Person, run. The walls are not going to hold." I did not move, but ordered the pour of 8 sack cement grout. The pour caused the wall to vibrate. At that time, I was convinced that you couldn't get any better vibration than was being accomplished by dropping the grout from a height of 20 to 30 feet. There was no segregation because the grout was a proper mixture.

I felt that this grout pour procedure was a big success! Manley Sahlberg spoke out immediately to say, "Oscar, you have developed something that even surprises me. You've got a good system here, and there's no question about it. I am convinced that a liquid grout, properly handled and properly certified by the materials yard, is excellent for this system. Now we have to prove it to the engineering and architectural professions."

DEVELOPMENT OF TEST PROJECT NO. 922

I volunteered \$10,000 to be put up by Person & Wik to start a test project on high lift grouting procedures. I asked Manley Sahlberg if he would work with me and I suggested that we ask the Brick & Tile Association and its manager, Robert W. Harrington, to participate. Later I also asked the San Francisco Masonry Promotion Trust Fund to contribute.

This was the beginning of the testing project which is quite well known as Testing Project No. 922.

From the outset Mr. Sahlberg insisted that we keep complete records

of the testing so that we would be able to certify what had been accomplished.

Our first step was to make an agreement with Abbott-Hanks Laboratories to become the inspectors on the job to certify the results of the test. Then we proceeded with extensive testing which proved the value of the system. Procedures and results of this testing were reported in a printed "Progress Report of Testing Project No. 922...." published in September 1959.

Since Manley Sahlberg was thoroughly sold on the idea, he reported the results directly to Anson Boyd, California's Chief State Architect at that time. Both Boyd and Peterson, Chief Structural Engineer of the State got very interested in the system. They gave their approval. Peterson said, "Mr. Boyd and I have had many disappointments in masonry in Southern California. The poorest project under Oscar Person's system is better than the best system we are provided today. Therefore, I am endorsing it." That was the breakthrough for "high lift grouting" in California. Today, we are very proud of the success of the system.

FOUR FOOT LIFTS

I wrote the first high lift specifications for the state of California which were approved by Manley Sahlberg and recommended to the state. At that time, we asked for only 4 foot lifts because we learned that masonry contractors were not putting proper ties in the masonry walls. We also noted that many were trying to get by with poor workmanship.

When I saw the way the ties were being installed, I said, "We don't dare recommend any higher lifts than 4 feet because we will have one blowout after another. We agreed that masonry contractors needed to be educated about the manner of properly installing ties in a brick wall where you have grout cores anywhere from 2 to 4 to 6 to 8 inches wide.

Today, after more experience has been gained, I recommend very strongly that 4 feet lifts only be used under special conditions where high lift grouting is not feasible. Based on experience, I recommend that grout be poured as high as up to 20 to 30 feet. There's no doubt that if the proper grout mixture is used, the higher the drop the better the consolidation.

I am suggesting that the 8-foot lift limit called for in the state of California's school house section and many building departments, is outdated.

THE WEIGHT OF THE MASS

Early in the development of the system, Mr. Sahlberg said, "Oscar, we engineers have not realized the value of the "weight of the mass." When pouring the proper grout mixture in the wall, the weight of the mass and the high drop gives you unbelievable vibration. However, you do have to vibrate the top three feet where there's no weight of the mass factor because you do not have a sufficient drop. Be sure to either puddle or vibrate it properly in order to get a solid and sound wall, especially where you are connecting to the roof.

WATER PENETRATION

Masonry materials are the finest ever developed by man! However, we have failed, in the past, to install them properly to meet the challenge of modern design. If the high lift grouting method is properly used, you should have no problem of moisture penetration. The proof is in the pudding. Our firm has been in business for over 40 years and I can say that we have had very little problem with moisture. There must be something wrong with the installation if people cannot waterproof the buildings.

EXAMPLES OF SUCCESSFUL HIGH LIFT GROUTING

I could point to a large number of high lift jobs to substantiate the success of this system, but since space is limited here, I present these few examples among our major California contracts:

1. The Royal Coach Motor Hotel, San Mateo. We poured the brick towers on this structure with a 9-inch grout core at 18 foot high lifts with no problems whatsoever. The concrete block walls were poured up to 20-feet high. In six hours, we poured 125 yards of grout using two pumps and four trucks.
2. The Sears-Roebuck building in San Rafael. The 20-foot walls in this building were poured at full heights. Compliments on this job were received from both the architect and engineer.
3. Sheraton Hotel, Burlingame. The first story of this hotel was poured 18 feet, the rest were poured story high, but every floor was poured in one lift.
4. The Coast Guard Station on Treasure Island (San Francisco). The specifications on this job stated that, under no

circumstances, could we pour over 8-feet. I asked for a special meeting with the engineers and with the Navy Department to explain the high lift system. They said they were with me 100%. The job was completed and we received many compliments; never had a call back on the building.

5. San Carlos High School. Manley Sahlberg's office sent four engineers to watch when we were making our high lift pours with instructions not to interfere. We poured 29 feet high lifts with complete success. Three test cores were taken. One was of part of the wall and foundation, one in the center and one at the top. The best core was the one taken from the foundation and the bottom of the wall, because of the weight of the mass!

PROPER MIXTURE IS IMPORTANT

Using brick or concrete block in the high lift grouting system is like building a form. This form is made of absorbent materials. Excess water will be absorbed by the concrete block or brick units. If the walls are wet on the outside after your grout pour, you have the proper consistency of water. If the wall is completely dry, especially using the lightweight aggregate, the grout is too dry! I believe that one of the worst problems in using the high lift grouting system, is grout that is poured dry or does not have the proper cement ratio. I feel very strongly, that an extra sack of cement is better than any admixture you want to use. Cement adds strength, admixtures do not!

I recommend a 7½ or 8 sack of cement grout; 7½ sacks in concrete block construction, and 8 sacks for brick walls, especially when working with small, very tight cores. Cutting down on the cement content of grout is the worst problem we have in the high lift grouting system today!

CONCLUSION

In summary, these are the most important considerations for successful high lift grouting:

1. Be sure to provide cleanouts wherever the vertical steel is located.
2. Lay up the walls with the least amount of mortar droppings inside.
3. Locate dams or barriers in the wall approximately 18 to 20 feet apart to limit the grout flow. This procedure will also strengthen the wall and help it resist wind.

4. In brick work, the proper stirrup-tie should be 2 inches shorter than the width of the walls and properly imbedded in mortar.
5. Horizontal reinforcing steel should be properly installed during the course of laying up the masonry units.
6. The grout space should be reasonably clean. Clean this space with either air or water. In hot climates, however, water should be used to slow down the curing of the masonry.
7. If the proper mortar mix is used, one day is ample time to allow before pouring grout. However, job conditions should be considered.
8. Inspection should be called and an approval given by the engineer or inspector before cleanout holes are plugged.
9. I recommend that only full height pours be used, and that the four-foot lift be used only in special circumstances.
10. Slump should be the maximum without separation--approximately 10½ to 11 inches.
11. The cement ratio recommended for the grout is 8 sacks for brick; 7½ sacks for concrete block walls...with no admixtures.
12. In high lift grouting, consolidation is needed at the top three feet of the wall.

THE USE OF CONCRETE UNIT MASONRY IN NUCLEAR POWER PLANTS

By Grant, J.M., and Wu, A.Y.

ABSTRACT: Concrete Unit Masonry (CUM) has found increasing acceptance and utilization in the design and construction of nuclear power plants. Its use overcomes the inflexibilities of poured-in-place concrete within a fast track construction schedule that involves simultaneously both engineering design and field construction. CUM allows the delayed installation of walls and partitions to accommodate temporary construction access openings, and postpones the determination of wall penetrations for cables, ducts, and pipes otherwise needed for the early installation of poured-in-place concrete.

Stringent criteria unique to nuclear power plant construction for seismic integrity, radiation shielding, and for barriers against fire, flooding, gaseous incursion and pressurization, as well as against some forms of missiles are satisfactorily accommodated by CUM systems derived from available materials and components. Certain masonry systems that find use in normal construction applications are not generally suitable for the demands of nuclear work. Opportunities to increase construction productivity of CUM may be found in the field administration and coordination of the many factions and contracts required in nuclear power plant work.

THE USE OF CONCRETE UNIT MASONRY IN NUCLEAR POWER PLANTS

By James M. Grant,¹ and Allan Y. Wu²

INTRODUCTION

This paper addresses the use of concrete unit masonry (CUM) in the design and construction of nuclear power plants, the special conditions encountered, unique requirements and constraints, and the virtues and limitations of this material in a high-technology industry. A survey of CUM built into nuclear plants over the past 20 years shows increasing utilization despite increasingly stringent design criteria and quality control.

Although the current political climate generates some questions regarding additional use of nuclear energy, industry sources have projected that the nuclear share of electric generation will increase from the present rate of 13% to 28%, over the next ten years. Today's nuclear power plants are also much larger in size than those of ten and twenty years ago. Table 1 shows the significant increase in the use of concrete unit masonry construction as plant size has been extrapolated upwards.

While concrete is generally used for structural load-bearing walls and foundations, there has been increasing acceptance of reinforced concrete unit masonry construction for nonload-bearing partitions serving as fire walls, radiation shielding barriers, and similar heavy construction separations.

The nuclear systems of some plants (such as the boiling water reactor) call for larger amounts of radiation shielding, and hence greater amounts of concrete unit masonry than appear in other types of nuclear plants. On the other hand, seismic criteria and consequential high design stresses tend to negate some applications of concrete unit masonry in earthquake-prone regions such as the western seaboard.

The cost of masonry construction weighed against overall project costs is not a significant item when considering that a single-unit 1,300-megawatt capacity power plant represents a capital cost of about \$1.4 billion in today's dollars. However, masonry considered in itself is a substantial cost item since a two-unit nuclear power plant can contain masonry work on the order of \$7 million.

¹Chief Architect, San Francisco Power Division, Bechtel Power Corp., San Francisco, Calif.

²Staff Architect, San Francisco Power Division, Bechtel Power Corp., San Francisco, Calif.

SPECIAL REQUIREMENTS FOR POWER PLANT CONSTRUCTION

Nuclear power plant construction is characterized by a high degree of conservatism in engineering design and quality control of construction. Stringent design criteria are imposed on all aspects of the plant related to the nuclear safety systems. Seismic assumptions and functional considerations of radiation shielding, fire barriers, flooding, etc, must be addressed in building material selection.

Nuclear power plants by their nature require large amounts of radiation shielding to ensure biological protection for operating staff. In the earlier, relatively small and simple plants, such protection was afforded by poured-in-place concrete. As plants increased in size and complexity, construction and design schedules indicated a need for building systems that allowed more flexibility than had been previously available by the system of massive wall structures of poured concrete. Complete and accurate determination of block-outs for piping, ducts, and electrical cables is usually not possible when load-bearing walls are first designed. Furthermore, access requirements for installing large items of equipment dictate the need for temporary openings or deferred construction.

Examination of these current requirements suggests the need for a structural system that can support massive radiation shielding walls while also allowing for flexibility of access and penetration. The system which has developed combines a structural steel frame of columns, girders, and beams with concrete floor slab platforms supporting concrete unit masonry walls.

Photo Figure A shows a typical wall with penetrations.

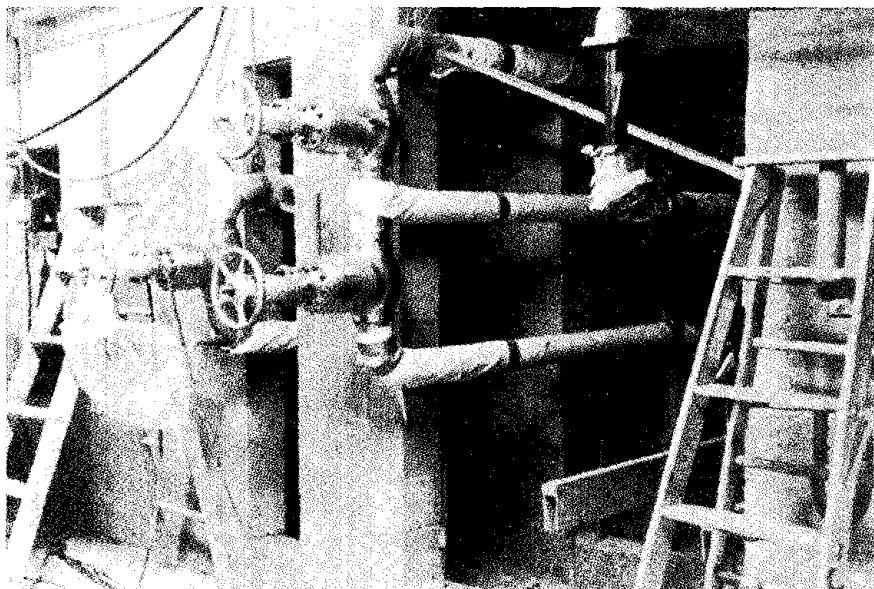


Figure A

STRUCTURAL CONSIDERATIONS

Concrete unit masonry has certain structural limitations in meeting high seismic factors as well as large loads imposed by piping systems, mechanical equipment, and other such sources common in nuclear power plants. Structural applications of masonry under seismic criteria are handicapped by the lower allowable stresses imposed by model codes such as UBC, compared to the ultimate strength design method allowed for reinforced concrete. Compressive stresses due to flexure often govern the structural design. Areas of buildings or entire structures that contain vital components or equipment essential to the controlled safe shutdown of the nuclear system are classified as "Seismic Category I." The seismic design of these buildings must be based on dynamic analysis.

Geographic regions that are seismically active normally are classified for high ground acceleration values. An example of a low risk assessment is a "G" value of 0.2 while another is influenced by fault zones in an active area, and is required to meet a "G" value of 0.5. These two "G" values refer to a free field ground acceleration value for a Safe Shutdown Earthquake (SSE).

The Safe Shutdown Earthquake has been defined as that earthquake which is based upon an evaluation of the maximum earthquake potential considering the regional and local geology, as well as seismology and specific characteristics of local subsurface material. The SSE is that earthquake which produces the maximum vibratory ground motion for which safety-related systems and components classified as Seismic Category I are designed to remain functional.

An additional analysis must be made for an Operating Basis Earthquake (OBE), which is usually one-half of the SSE value. The OBE has been defined as that earthquake which, considering regional and local geology, together with seismology and specific characteristics of local subsurface material, could reasonably be expected to affect the plant site during the 40-year operating life of the plant. Structures and systems of the plant necessary for continued safe operation are designed to remain functional, with a suitable margin, under vibratory ground motion produced by an OBE.

The "G" values for the particular items being considered (such as a wall or pump) are dependant on the dynamic characteristics of the item, the structure at the support point, and the supports of the item. All other structures not required for vital safety-related functions are classified as Non-Seismic Category I and their seismic design may be accomplished by methods of static analysis using model code requirements except when failure of such structures adversely affects a Seismic Category I item, in which case the design must be checked for Seismic Category I criteria for the SSE.

Design of masonry partitions and walls that include varying configurations, heights, thicknesses, openings and penetrations, etc, require a case-by-case evaluation. Generally, where walls span between two floor levels, they are designed as simple beams supported at the floor and ceiling. Low walls that are connected neither to the overhead ceiling nor to adjoining structures are usually required to be designed as vertical cantilevers. Thick walls of proportionately limited height are usually sufficiently stable so as not to require highly-stressed moment connections at their base. Although the design of the wall connections at the floor and ceiling involve relatively low shear values, consideration must be given to ensuring structural integrity and to prevent adverse impact upon the primary structural system.

To avoid the transmittal of loads from overhead structures, separation of the tops of non-bearing walls and partitions from the overhead structural system is sometimes required. Figure B shows a common condition at the top of a non-bearing masonry wall. In addition to the structural separation provision, the restraint connection must also reconcile criteria for radiation shielding, fire, and air pressure.

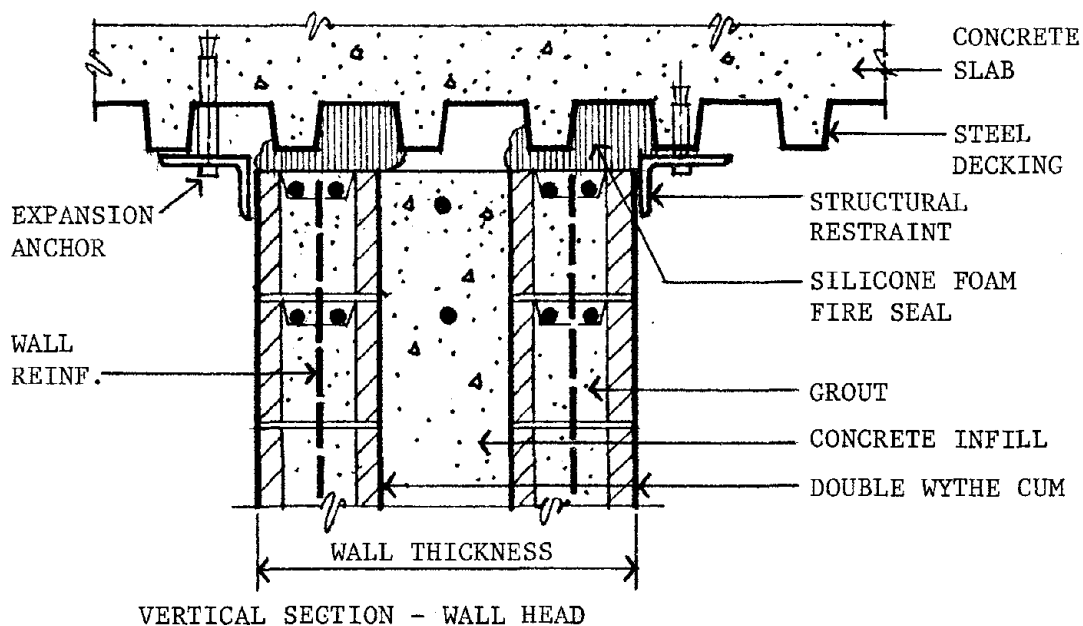


Figure B

The floor connection must reconcile construction access needs with structural reinforcing steel placement. Floor surfaces at temporary wall openings must be free from hazards and interferences to personnel and small vehicles. The large amounts of vertical reinforcing steel frequently required, ranging up to No. 7 bars as close as eight inches on centers, create formidable barriers and obstacles to safe access.

Furthermore, fast-track design-build schedules need to accommodate a considerable number of changes in wall locations or dimensions that impact floor anchors and other connections. Various solutions have been developed to meet these needs, as discussed below.

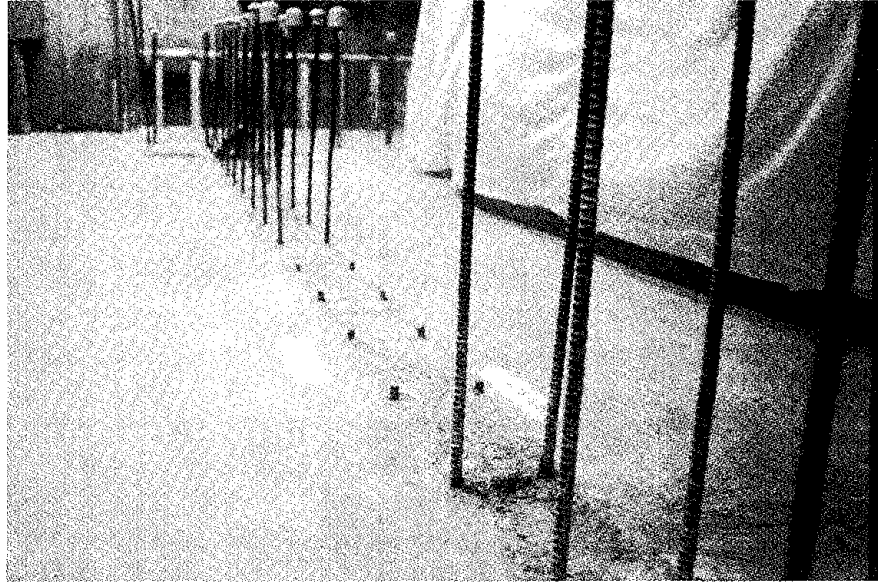


Figure C

Common cast-in-the-slab floor dowels have not been an entirely satisfactory method. Cold bending of bars larger than No. 4 can cause unacceptable damage to the steel. To overcome the hazards of the vertical cast-in-place floor dowels, cast-in threaded inserts have been proposed. The threaded dowels are installed just prior to construction of the masonry and minimize the hazards and obstacles of cast dowels. However, the same limitations of wall location adjustments remain. Drilling and setting of dowels with epoxy grout into the floor overcome some of the deficiencies of the above two methods but raise concern for costs and the possibility of severing cast-in-floor conduits, or floor slab reinforcing.

Drilled expansion anchor inserts to receive threaded dowels are frequently used to allow unimpeded access and flexibility to cope with partition location adjustments. Such anchors incur the same problems as grouted dowels regarding existing conduit and reinforcing steel.

Casting steel plate embedments into the floor slab and stud welding the dowels to the embed have been proposed for high bending moment conditions beyond the capacity of conventional anchorage. However, this anchorage method does not accommodate late changes of wall location.

The approach being used on some projects is to select one of the methods noted above according to the specific conditions that determine its appropriateness.

RADIATION SHIELDING BARRIERS

Availability, cost, and density of the shielding system and its components are significant factors that must be thoroughly investigated in order to optimize design.

Radiation barriers have design requirements that can usually be satisfied by masonry construction, i.e., high mass uniformity of units, modular dimensions, capability of forming various wall thicknesses and configurations, and resistance to long-term, high-radiation exposure. The effectiveness of the shielding barrier against alpha, beta, or gamma radiation is a function of the density or mass of the constituent materials in combination. However, barriers to protect against neutron radiation (in the vicinity of the reactor) are not as effective in masonry, although they may be used, depending upon the energy level of the neutron radiation.

Most shielding barrier walls consist of two wythes of eight-inch thick unit masonry solidly grouted, sandwiching a concrete core infill. In some cases, shielding barriers two to three feet thick have been constructed wholly of unit masonry with grouted cells. The economy of this method tends to diminish as the thickness exceeds two feet; it then becomes advantageous to specify a concrete core type design.

The density of the masonry units is determined by the aggregates used and the degree of compaction attained in manufacture. Where local sources offer high-density sand and gravel, it is possible to specify masonry units with densities up to 140 pcf. The current recommended range for masonry unit density is 130 to 135 pcf in conformance to ASTM C-90. The total shielding effectiveness of a wall becomes a combination of the densities of masonry units, mortar, grout, and (in double walls) concrete infill. The mortar is not a large enough percentage of the total wall to make a special density mix worthwhile.

Concrete used as core infill between masonry wythes can be obtained with densities of 142 to 145 pcf without the use of special aggregates. Grout tends to be limited by the density of the sands available, but the addition of pea gravel can increase grout density.

Special heavyweight aggregates such as barite, magnetite, and ilmenite, can be added to any or all components, but generally do not prove to be economical except in unusual situations where space limitations govern or radiation levels are high. High-density shielding using heavy-weight concrete, steel, or even lead may be used in small quantities for remedial situations.

Design requirements frequently call for removable wall panels in shielding barriers to facilitate equipment maintenance and removal. Such panels must maintain the integrity of the shielding barrier and comply with structural design criteria. Removable access panels are also required to be reasonably portable either in whole or in parts. These removable panels have in some cases been built from solid masonry units laid with dry joints offset to prevent radiation shine or streaming. Structural restraint has been provided by the use of heavy cellular steel deck sections positioned and fastened to prevent lateral movement due to earthquake. In other cases, precast log-type concrete elements have been used.

OTHER BARRIERS

In addition to the requirements for seismic resistance and radiation shielding, certain walls in nuclear power plants must be capable of serving as barriers against fire, water flooding, air, gas and vapor pressures, noise, the impact of missiles generated by natural phenomena, and forced entry.

The risk of a possible release of radioactivity due to fire has resulted in high standards for fire protection in nuclear plants. CUM can readily comply with the fire ratings required by building code and insurance underwriters, but a demanding aspect of fire resistance is maintaining the rating at wall penetrations. For this purpose materials have been developed and tested that will meet the requirements of ASTM E119; also withstand impact of a hose stream; maintain air pressure seal; offer equivalent radiation shielding capabilities; and allow movement of the penetration assembly due to thermal expansion. Figure D shows a detail with the capability to meet such criteria.

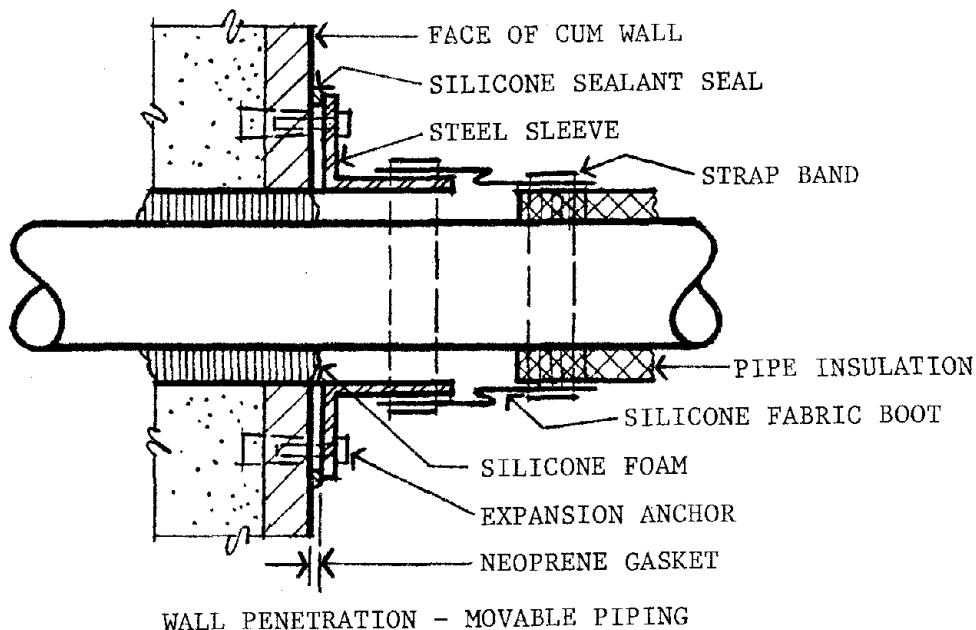


Figure D

Large inventories of water are normal to the process systems in a nuclear power plant; therefore, floods from these systems and from natural sources are hazards that are addressed in the design of safety-related systems. One frequently-used design approach requires the construction of watertight compartments with watertight doors to contain or protect essential systems. Masonry construction offers adequate structural properties to resist most design water pressures.

Where hazardous gases are involved, such as chlorine or carbon dioxide, regulatory requirements demand low-leakage construction; in these cases masonry surfaces must be filled and coated to eliminate porosity.

Industrial processes in nuclear power plants inevitably generate high noise levels that in many instances have to be contained to meet OSHA requirements limiting the noise exposure of employees. Concrete unit masonry can often meet this need. A solidly grouted masonry wall eight inches thick can provide a sound transmission class (STC) rating between 56 and 58. Where reduction of reflected noise is of primary importance, masonry units of sound-absorbing design have been specified.

Concrete unit masonry is generally considered to be effective as a barrier against missiles such as those from tornadoes or machinery failure, but its effectiveness still has to be measured with precision. Data is lacking regarding the development of secondary missiles from the impact point.

Another use of solid masonry construction is in industrial security applications. Current criteria for hardened security occupancy call for barriers capable of stopping high-powered rifle fire in accordance with U.L. Standard 752, Class IV. Eight-inch solid grouted masonry meets this requirement.

MASONRY AND SPECIAL COATINGS

Nuclear power plants set extremely high housekeeping standards to achieve the degree of cleanliness demanded by radiation control. Where decontamination is a requirement, room surfaces are generally coated with impervious sealers or coatings to minimize deposits of contaminants and to allow for their easy removal. The CUM's ability to receive these special coatings is an important consideration; some masonry has a coarser texture than is ideal for coating. Care is required to specify acceptable surface textures.

AVAILABLE MATERIALS AND SYSTEMS

CONVENTIONAL MASONRY CONSTRUCTION

The masonry system finding high acceptance in nuclear power plant construction uses "A" or "H" concrete block units, in the common 8 x 8 x 16 size, with vertical and horizontal reinforcing, and with all cells filled solid with grout. Cement mortar is the normal bonding agent. This system is suitable for both single and double wythe wall configurations. Epoxy adhesive in lieu of mortar has been investigated but apparently not used to date. Availability of units with faces ground for epoxy adhesive bonding, as well as contractors familiar with its use, seem to have affected its selection, even though the epoxy system seems to offer a faster and stronger wall installation than cement mortar bonding.

COMPONENT MASONRY SYSTEM

The component masonry system provides advantages not available in conventional masonry systems where structural requirements impose reinforcing steel spaced eight inches on centers, or closer. Although the component masonry system can be used for wall thicknesses of 8" and thicker, it is best suited for thicknesses over 14 inches. By the addition of a third wythe, the system can accommodate wall thicknesses up to 48 inches. Use of ultimate strength values for the concrete wall design offers wider wall application compared to the limited strength designs based on lower stresses allowed for conventional masonry construction. Furthermore, the larger proportion of concrete fill results in greater average wall density and consequently improved radiation shielding characteristics.

A cost analysis of the component system has shown it to be more economical than the basic double-wythe conventional grout and concrete systems in the range of thicknesses from 16 inches up to about two feet. Beyond this thickness, its advantages tend to be offset by the need for an additional wythe and the dual systems of reinforcing; however, both masonry systems are more economical than conventional poured-in-place concrete by a factor of one-half or smaller. Furthermore, the component masonry units can be considered non-structural framework rather than an essential part of the structural wall, and hence are relieved of the costly imposition of stringent quality control.

SURFACE BONDING SYSTEMS

The surface bonding system (with a glass fiber-reinforced Portland cement surface coating), that has been competing with conventional cement mortar systems in some building types, has not found similar acceptance in nuclear plant work.

The concerns that need resolution before it can be utilized in nuclear applications are as follows:

- 1) Instability of the units to grout placement and to accommodate random openings.
- 2) The need to dampen the wall surfaces both prior to and after the application of the bonding coating.
- 3) Hazards of overspray.
- 4) Lack of test data to ascertain compatibility of the surface bonding substrate with the high performance nuclear coatings.

MORTARLESS SYSTEMS AND TIELESS UNITS

Proprietary mortarless systems that depend on interlocking keys rather than bonding have generally not found acceptance in nuclear plant work. This appears to be due to the fact that the units cannot accommodate reinforcing steel, and other types of cellular configurations have closed ends that restrict placement of extensive vertical reinforcing.

Another proprietary masonry unit incorporates integral notches and lugs that separate and position reinforcing bars without ties, thus eliminating the expense of iron workers. Our evaluation of this system is not complete.

CONSTRUCTION CONSIDERATIONS

Construction productivity with respect to masonry installations involves many factors that are not easily controlled on nuclear projects. Structural requirements and construction practicalities have a strong bearing upon the type of masonry system selected. The masonry system must address the limitations of being installed between existing floor slabs with large amounts of reinforcing steel.

Evolutionary design changes that are reflected in adjustments to the building fabric, including masonry work, have an adverse impact when they are considered over the six to seven years needed to construct a plant. Union work rules can greatly impact productivity in many trades, and cause slippage in contingent construction, as well as delays in delivery of components or equipment requiring deferred construction of masonry walls in order to afford temporary access openings.

One recommendation to improve productivity calls for use of six-inch nominal thickness in place of the more common eight-inch nominal thickness. However, inquiries of masonry contractors indicated preferences to the contrary. The limited-size cells of six-inch wide units is a constraint for effective grout placement that tends to offset the initial material cost advantages. Masons also tend to prefer the customary handling and stability of the common eight-inch unit.

Use of mechanical scaffolding can be cost-effective where long and high masonry walls are required. These conditions are not the norm in the compartmentalized arrangements typical of nuclear plants.

Additional opportunities for construction productivity improvements may be found in the field administration and management of the work. Interfacing the requirements of related but separate contracts requires careful coordination and scheduling integration which can be negated by a delay in contingent construction. To maintain acceptable productivity and economy in constructing masonry partitions and walls, adequate amounts of work must be released to the masonry contractor on a continuous basis. Masonry work is frequently subject to intermittent construction and deferred wall installations in order to accommodate temporary construction access and design changes due to the higher priority of primary mechanical/electrical system installation. Delayed construction imposes access limitations that require innovative material handling devices and procedures. Figures E and F show two examples of field developed devices, a hoisting cage, and a hand truck with forks, that allow for efficient delivery of block units through limited access openings.

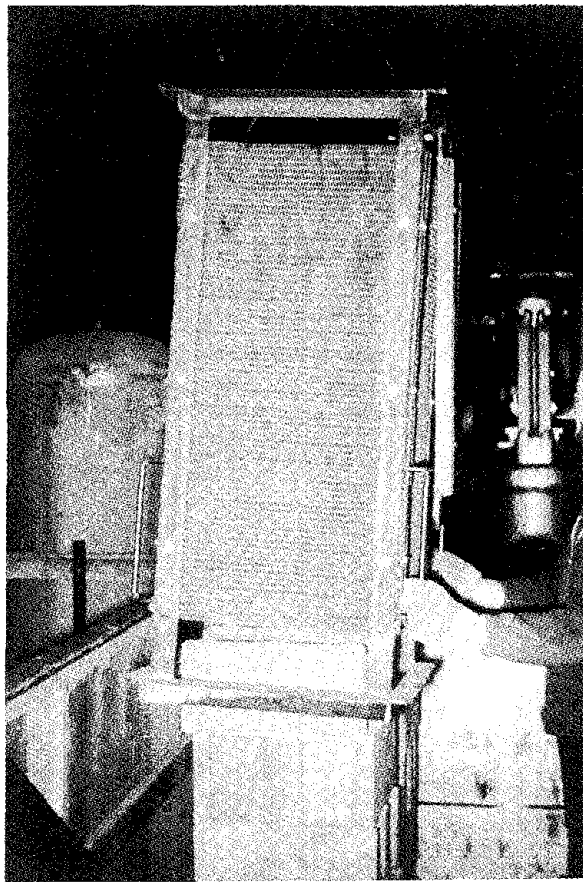


Figure E

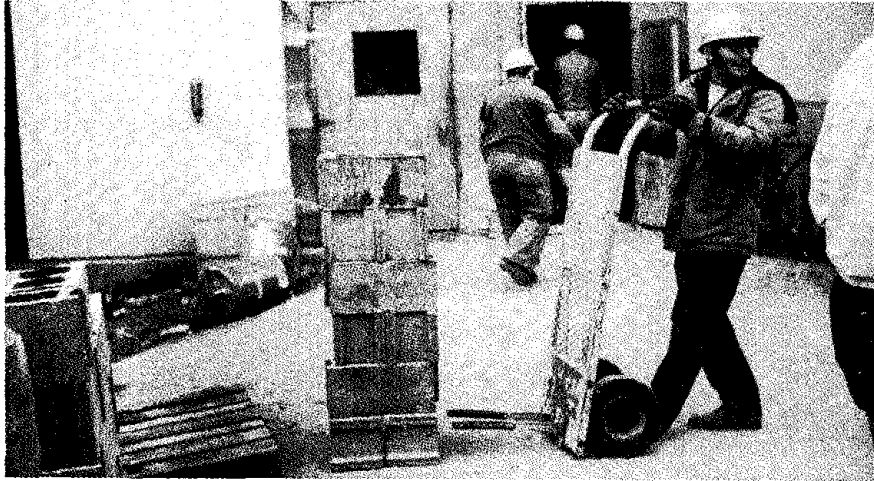


Figure F

SUMMARY AND CONCLUSIONS

The record shows that concrete unit masonry can satisfy many of the requirements for walls and partitions in nuclear power plants. Concrete unit masonry has the qualities of ruggedness to withstand the abuse of long periods of construction activity while meeting the requirements of the various barrier walls that have been described. Concrete unit masonry walls have also demonstrated a flexibility in their construction that facilitates temporary access openings and the provision of wall penetrations for piping, ducts, cable trays, and similar services.

While being able to provide radiation shielding mass comparable to poured-in-place concrete, concrete unit masonry offers the economy of being self-forming, and is more competitive than poured concrete in most applications. Though concrete unit masonry does not attain the same structural capability as poured reinforced concrete, it can be designed to meet the stringent structural requirements for seismic criteria demanded of partition walls found in nuclear power plants.

We see the need for special care in selecting appropriate masonry systems, preventing the intrusion of dowels into traffic lanes, and selecting densities for radiation barriers that are consistent with economy and availability. Our experience indicates that masonry densities above 135 pounds per cubic foot should only be specified after carefully checking material sources to assure adequate deliveries and cost control. Special consideration is needed in field administration and coordination to ensure that the masonry contractor is afforded continuity of work to maintain an economical operation.

The use of concrete unit masonry in nuclear power plants has grown due to its satisfactory performance as well as to the increasing size of the plants. We would expect to see a continuation of this trend along with continued development and refinement of masonry systems, their components, and our approach to their design and utilization.

TABLE 1
AMOUNTS OF MASONRY USED ON NUCLEAR PLANTS

PLANT & TYPE	SIZE MWe	COMMERCIAL OPERATION	MASONRY AMOUNT (S.F.)*
BWR-1	59	8/63	7,500
BWR-2	180	8/60	8,500
BWR-3	550	7/71	20,000
PWR-1	705	12/71	27,000
BWR-4	670	12/72	193,000
BWR-5	550	1/75	123,000
PWR-2	836	12/74	74,000
BWR-6(2)	1,065 each	7/74 12/74	150,000
PWR-3	1,030	5/76	300,000
BWR-7(2)	1,050 each	2/81 5/82	400,000
BWR-8(2)	1,050 each	4/83 4/85	540,000
BWR-9(2)	1,067 each	5/84 5/86	735,000
PWR-4	1,180	1986	225,000

*Square Feet, is measured by the surface area of each wythe at double wythe concrete core combination wall systems, and the wall area of single wythe walls.

TABLE 2

CONCRETE UNIT MASONRY PROPERTIES, CRITERIA & CHARACTERISTICS

PROPERTIES	CRITERIA	CHARACTERISTICS
Fire Resistance	ASTM E119 ASTM E84	Non-combustible, capable of fire resistance ratings of 3 and 4 hour.
Structural - Seismic	Spectral Analysis Category I Structures. UBC Chapter 23 for Non-Category I Structures. UBS Chapter 24 for Masonry Design.	Spectral Analysis: Ranges from 0.20 to 1.50 G. UBS Seismic: Generally 0.10 G. Ultimate strength design for reinforced concrete. Working stress design used for masonry design. Reinforced unit masonry not presently used for support of critical equipment and piping restraints.
Structural - Pressure Boundary	UBC Chapter 24 and Industry Standards	Standard of 1.5 psi differential used, not critical for reinforced masonry design.
Structural - Flooding	UBC Chapter 24	Not critical for reinforced masonry design.
Structural - Severe Winds, Tornado and Missiles	ANSI A58.1, NRC Standard Review Plan, Section 3.5.1.4	Exterior walls only - limited to reinforced concrete (component masonry unit system) ultimate strength design.
Structural - Locally Imposed Loading	UBC Chapter 24 and Industry Standards	High concentrated load imposed from piping restraints, etc; non-bearing masonry partitions not used for supporting loads of this type.
Radiation Shielding	ANSI N101.6, 10CFR20 (Section 10). ASTM C637	Adequate mass for most applications; compatible with penetration details, removable shielding panels; suitable for alpha, beta, and gamma radiation shielding, and 40-year plant life.

TABLE 3

CONCRETE UNIT MASONRY

DESIGN REQUIREMENTS & CAPABILITY

DESIGN REQUIREMENT	CAPABILITY
Deferred and Intermittent Construction	Small unit sizes and method of construction give flexibility.
Varying Wall Thicknesses and Configurations	Modular system with core fill between wythes is adaptable.
Wall Penetrations and Block-Outs	Small components and modular construction well suited for a wide range of block-outs, pipe sleeves, and penetrations.
Resistant to Abrasion and Construction Abuse	Tough surface properties, and capability to replace damaged face shells.
Water Resistance	Inorganic, rotproof, verminproof, and when treated, relatively waterproof.
Suitable for Coatings	Compatible surface textures readily available. (Requires filler to allow finishing with smooth paints and thin film coatings.)
Chemical Resistance	Relatively inert against most chemicals and corrosives; special treatment required for concentrated acids and caustics.
Noise Resistance	High mass and attenuation for good noise barriers. Sound absorbing units available.
Gas & Vapor Permeability	Makes adequate low pressure barrier when appropriately treated.
Cost Economics	Lower cost than comparable systems.

USES OF CHEMICALLY RESISTANT MASONRY IN LINING AIR AND WATER POLLUTION CONTROL EQUIPMENT

By Harry Clyburn* and Walter Lee Sheppard, Jr. # P.E.

ABSTRACT: This paper provides a short description of this discipline not taught in engineering schools. Masonry linings are discussed in relation to the processes involved in the removal of contaminants from waste products prior to their disposition. Processes range from the incineration of wastes, scrubbing of waste gases, venting of waste gases to the atmosphere, collection of liquid wastes (including scrubbing liquids), separation and neutralization of waste liquids, and their disposition.

The methods of employment of masonry linings in the equipment used in the subject processes are detailed, to demonstrate how such linings can be employed in mild steel or concrete structures to replace equipment which, without such a lining, would have to be manufactured out of or clad with an expensive alloy.

The design differences between all alloy metal construction and masonry lined steel or concrete are indicated, together with criteria for the selection and specification of suitable masonry units and bonding mortars under varying conditions.

*Pennwalt Corp., Philadelphia, PA.

#C.C.R.M. Inc., Havertown, PA.

USES OF CHEMICALLY RESISTANT MASONRY IN LINING AIR AND WATER POLLUTION CONTROL EQUIPMENT

By Harry Clyburn * and Walter Lee Sheppard, Jr.[#], P.E.

INTRODUCTION

There are basically three types of masonry construction: common brick and stone (used for residential and industrial structures), refractory masonry (used in furnaces, incinerators and the like) and chemically resistant masonry (used both as structural material and as protective lining material where the structure will be exposed to corrosive chemicals, in vapor or liquid state). These three types of masonry are handled differently and require different craft techniques.

Brick masons and stone masons who build houses etc., are concerned with a combination of structural integrity and appearance. Since this is the common type of structure their techniques will not be discussed here. Next best known is refractory masonry used to line furnaces, etc. where instead of using wide, full joints the mason tries to achieve the absolute minimum of joint thickness by making a soup of his mortar, dipping the brick into it, and then laying it. Obviously structures erected in this manner are full of air voids since no joint can be absolutely tight, and with low structural strength is often supported by metal anchors or hangars. Chemically resistant masonry is very different from these other two types, requiring full structural integrity, total absence of air voids in the structure, and with a few exceptions, a prohibition on anchors, hangars, or other similar penetrations of the brick work. The reasons behind these differences are made clear by a quick look at the limitations and the purposes of, and the uses for, this type of structure (1).

There are three limitations that should be kept in mind.

1. Though excellent in compression, they are weak in tension, torsion and shear, since they contain no reinforcing, but rely entirely on the bond of a mortar to the surfaces of the brick.
2. They have a measurable absorption, and so are not gas-tight, nor can they restrain a liquid head.
3. They are brittle and inflexible. Unlike steel which can be bent and straightened, such movement will destroy a brick structure.

* Pennwalt Corp., Philadelphia, PA # C.C.R.M. Inc., Havertown, PA

With these limitations, then what reason could one possibly have to use a masonry lining in a process vessel or in equipment designed for pollution removal or waste control? The answer lies in the protection that masonry can provide to a structure. The proper design and selection of a masonry lining can allow the designer to employ carbon steel vessel with, say, a rubber lining, protected with "acid-resistant" brick which can be furnished on fairly short delivery and at a lower expense, to fill requirements which might otherwise be satisfied only with a much more expensive alloy construction and available only on a long lead time. In addition, when an alloy or special metal vessel fails due to chemical or other cause, repairs are costly and total replacement may be required at even a higher cost than the initial expenditure. When a masonry lined vessel is damaged or starts to leak, it is almost always possible to remove part of the lining from the damaged area, repair the vessel, replace the lining and return the vessel to service, all at nominal cost, - a considerably lower expense than that of replacing an alloy vessel.

Chemically resistant masonry, when used to provide protection to the substrate, is normally employed in conjunction with a membrane, since as noted above masonry is neither liquid-tight nor gas-tight, and the corrosive medium will penetrate it and eventually reach the substrate unless such membrane is provided.

Examples of the uses of chemically resistant masonry as protection might be: "acid" brick flooring laid over an asphalt membrane, on top of a concrete floor in a chemical plant, protecting the concrete substrate from acid spillage and then asphalt from mechanical damage from fork-lift traffic; a brick lining in a pickling tank in a steel mill in which the brick provides thermal insulation for a rubber lining on the steel walls and bottom of the tank, reducing the contact temperature of the contained sulfuric acid from 212 °F to 160 °F, which is an acceptable thermal limit for the rubber lining.

The third type of protection may be somewhat harder for the uninitiated to visualize, but the following is an example: Pickling (chemical cleaning) of stainless steel is done in a mixture of nitric and hydrofluoric acid. Pickling tanks to handle this operation are today usually made of steel with PVC sheet linings, protected by carbon brick joined with a carbon filled hot applied sulfur mortar. However in the 30's, when stainless steel was developed PVC sheet had not been created. Since material selection was limited, the first tanks built to handle this process were built of carbon steel, lined with Goodrich Triflex rubber and faced with 9" of carbon

brick laid in carbon filled sulfur mortar. B. F. Goodrich was well aware that the nitric acid would ruin the rubber, but there was nothing else that was believed to be any better so the tank was lined in this manner with the hope that the customer would get a year's life out of it before it would have to be re-lined. The tank performed successfully through the war years and served without maintenance for a total of seventeen years before it became obsolete - not from the failure of the lining, but because the mill changed to larger shapes that could not be fitted into the old tank. It was decided to remove the lining to find out why it had not failed. When the brick was stripped away it was found that the first layer of rubber (Triflex is a 3 layer laminate), was completely charred - turned to carbon - by the nitric acid. But the brick lining had prevented this charred corrosion product from being removed so that it remained and acted as a barrier to further attack. The other two layers under it were still alive and springy.

WASTE PROCESSES

Wastes can be classified as solid, liquid and gaseous. Solid wastes that are of concern to us are those which can not be used in landfill because they can break down and cause pollution. Wastes of this type are often incinerated, and converted to gas and ash. The gas is treated in the same manner as gaseous wastes - that is scrubbed (or cleaned) and vented to the atmosphere, the scrubbing liquid being treated in the same manner as liquid wastes. The ashes, usually a very small part of the total, may become fertilizer or landfill, or they may be further processed to recover some valuable ingredient in the ash.

Liquid wastes may be either incinerated, with the resultant products treated in the same manner as those created by the incineration of solids; or the liquid may be treated, the contaminants neutralized or removed, and the water in the liquid returned to plant use.

Gaseous wastes are either scrubbed directly or pre-cooled and then scrubbed, the scrubbed gas, vented to the atmosphere and the scrubbing liquid treated to remove the contaminant, then the cleaned liquid re-circulated (2).

EQUIPMENT USED IN WASTE HANDLING

The following tabulation covers most of the types of equipment used in handling wastes:

1. Furnaces to burn wastes: solid, liquid, or gaseous.
2. Ducts to carry exit gases from furnace to conditioner (or cooler, or scrubber).
3. Conditioner or cooler. (This step appears only when exit gases are very hot. It does not appear in lower temperature systems).
4. Ducts carrying gases from conditioner to scrubber (or precipitator).
5. Scrubber. (Precipitator rarely (though sometimes) requires lining).
6. Ducts carrying scrubbed gas to stack.
7. Chimney.
8. Liquid scrubbing system (piping, pumps and storage equipment).
9. Equalizer tanks used to hold and balance non-incinerated liquid wastes.
10. Treatment vessel or neutralizer for scrubbing liquid, or for non-incinerated liquid wastes.
11. Piping or trenches carrying non-incinerated liquid wastes from areas of release to equalizer and from equalizer to neutralizer for treatment.
12. Manholes along pipe line carrying liquid wastes.
13. Floors under equipment where liquid wastes are spilled.

APPLICATIONS FOR CHEMICALLY RESISTANT MASONRY

Furnaces, per se, do not normally employ chemically resistant masonry in their linings. However, at least one manufacturer of such equipment designs his burner as a two compartment structure, the actual burner in the first compartment, which is lined only with refractory brick (3), and the second, where temperatures are lower, lined with a refractory brick facing, over a fireclay "acid" brick (4) laid in a silicate (5) mortar on top of a membrane lined carbon steel shell.

and bell and spigot clay pipe (13) transmitting such wastes to equalizers or collecting tanks are usually joined with furan mortars, sometimes backed with sulfur mortars, sometimes backed with epoxies. The equalizer and neutralizer tanks are most often concrete (14) with asphalt membranes, and brick linings laid in furan mortars. Manholes (15) placed along the sewer line should receive similar linings.

MATERIAL SELECTION IN FURTHER DETAIL

We frequently find that engineers, especially those who have not had past experience in the use of chemically resistant masonry, tend to think of special alloys in selecting materials of construction for some of these pieces of equipment. Generally it can be said that thin gauge stainless steel is roughly comparable to or a little less expensive than rubber lined carbon steel inner lined with "acid" brick. However in the case of the more complex and more expensive alloys or metals, consideration should certainly be given to substituting the carbon steel-rubber-brick system.

A paper has been offered to an NACE meeting (16) that provides comparisons of the costs from actual installations which paper certainly deserves the designers' attention. There is an additional use for such masonry linings in alloy vessels, where the inner temperature is too high for the economical use of the alloy, but where a masonry lining may provide sufficient insulation to drop the skin temperature into the economic range.

The selection of supporting structures for the equipment considered in this paper is usually either steel for items 1 to 6, concrete outer shell with either brick, steel or FRP self-supporting liners for 7, and concrete for items 9 through 13, except item 11, and except that at some plants, where the liquid volumes are small lined steel or wood stave holding tanks are employed for item 9. Item 8 may employ alloy or plastic piping; alloy, plastic, or lined carbon steel pumps, and storage tanks for re-cycled scrubbing liquid of lined steel, wood stave, FRP or lined concrete. Item 11, if using trenches, will employ concrete, or if pipe, vitrified clay, plastic or lined steel. Lined concrete pipe is not usually recommended though some successful installations of this type are noted.

The membranes (17) selected to protect the supporting structures are: for concrete usually glass fabric reinforced hot applied, unfilled, oxidized ("blown") asphalt, with a ball-and-ring softening point 110^oF to 130^oF; for steel usually sheet or fluid applied rubber, or plasticized p.v.c. sheet. FRP acts as its own membrane. Wood

The ducts leading from the furnace to the conditioner are usually unlined, as is usually the duct to the scrubber if no conditioner is interposed between furnace and scrubber. There are, however, exceptions. If highly corrosive waste products are present in the exit gases, which corrosives condense at high temperatures (example: SO_3 , and SO_2 in an oxidizing atmosphere), then it is sometimes advisable to line the duct, preference being to 2" of foamed borosilicate glass block (6) faced with refractory brick, or sometimes with a layer of potassium silicate mortar (7).

In the past conditioners have followed refractory design employing "hung" refractory brick. Such designs have required considerable maintenance, and preference here should be for foamed borosilicate glass block (6) faced with "acid" brick joined (8) with high temperature furan mortar (9), except at the gas entry (and other dry zones) where the mortar would be a potassium silicate (7).

The duct from conditioner to scrubber, is often lined with borosilicate foamed glass (6) faced with "acid" brick (8). The brick mortar would be a potassium silicate (7) if the duct is dry, but if liquid water is entrained in the gas, then the high temperature furan (9) should be employed.

The scrubber design has a great deal to do with the lining selection, and there are few generalizations that can be made. There are four basic types: open body, packed tower, tower with trays, and venturi. Perhaps a hybrid may be encountered containing parts of each. The references cite papers with more details of scrubber linings (2).

The duct from scrubber to stack can best be lined using only the foamed borosilicate glass block (6). The supporting structures here are usually all carbon steel.

Chimney design and lining depends on exit gas temperature (10). If always above the dew point of the highest dew point contaminant (total removal of all contaminants is considered outside economic reality), held above that temperature with a re-heater, then a steel liner may be used. However if below this temperature a chemically resistant lining must be applied to a steel liner, or an FRP liner used instead of steel. But if there is the possibility of fluctuating temperatures from high to low and back, due to down time or failure of water pumps or possible by-pass of gases, then only an "acid-resistant" brick lining with the appropriate mortar (probably a potassium silicate) will be trouble free.

Floors subject to chemical spills, or spills of acid laden scrubbing liquid are most often protected with "acid" brick laid in furan mortar on an asphalt membrane (11). The same protection is carried into trenches and sumps (12) receiving such liquid wastes,

may be unlined if the liquids contain acids that cause wood to swell (sulfuric acid is an example), or lined with a loose neoprene or p.v.c. liner if the liquid contains acids that cause wood shrinkage or degradation, (such as nitric, hydrochloric, or hydrofluoric).

Selection of the appropriate masonry unit to employ in the lining is dependent on chemical content of the gases and that of the scrubbing liquids, on the dew points of residuals after scrubbing, on the maximum and minimum temperatures in the specific area to be lined, on the thermal drop needed through the system, on the acceptable amount of heat loss, and on the thickness and weight of lining that is acceptable.

First consideration should probably be given to the foamed borosilicate glass block (6) mentioned earlier since it provides the optimum in insulation combined with minimum in weight, and thickness, in installation costs, and in installation time. However, it should not be used, surface exposed, to live steam impingement, or to liquids bearing more than 50 ppm of hydrofluoric acid or acid fluorides, or to alkalis such as sodium carbonate (soda ash), potassium carbonate, sodium or potassium hydroxide, lime, etc., or to temperatures in excess of 960° F.

Next consider shale, fireclay, and carbon brick (8) alone or in combination with the foamed glass block, and/or further combined with insulating or refractory brick (18).

Mortar selection also depends on thermal conditions and liquid exposures. In hot and normally dry areas, but where there can be condensation contaminated with acid during idle periods, a refractory type silicate mortar is usually the selection (191), and in wet-dry areas that are often quite hot and are never subject to steam impingement, potassium or sodium silicates or pure silica mortars should be considered. Resin mortars should be used in all areas that are continually wet, if there is either steam impingement, or the possibility of excursions into the alkali pH ranges. Mortar selection procedure is therefore too technical and too varied to be covered in this paper in more than a general way, and the designer should consult the manufacturer for a firm recommendation geared to his specific design and exposures.

DIFFERENCES IN DESIGN: ALLOY AND MASONRY LINED EQUIPMENT

In designing steel or concrete vessels to receive masonry linings, the following factors should be born in mind:

(1) The masonry (and membrane) lining must have adequate thickness to provide the thermal, mechanical and chemical protection for which it is intended. Therefore, adequate space must be provided to accomplish this. Internal dimensions of the equipment must be determined after the thickness is computed and not guessed at (22).

(2) The masonry lining must be supported by the vessel structure. Therefore, the vessel design must include provision to carry not only the weight of the lining, but to restrain and support any stresses that may be created by cycling operations (23).

(3) Human applicators must be able to construct the lining, and if need be repair it, from inside the vessel, therefore the design must take this into account.

(4) It is easy to design and fabricate rectangular cross-section horizontal ducting. But "acid brick" cannot be laid flat unless they have support. Therefore, covers and duct tops must be arched to permit the brick lining their under-sides to be supported by thrust against the walls. (There is an exception to this. The borosilicate foamed glass block can be used as a lining for the under-side of flat surfaces).

(5) Outlets and penetrations through the wall of cylindrical (or conical or spherical) vessels must be desinged so that the lining of the connecting outlet (etc.) mates with the brick lining in the interior of the vessel. For this reason the steel (or concrete) shell must be designed with side outlets at least one course of brick (4" approximately) above the floor, preferably more, to allow space for a "bulls eye" course in the wall around the outlet.

(6) Intersections of two cylinders, though handled without too much difficulty in metal fabrication, are not easy to line with brick, especially if the two cylinders are roughly the same diameter. Designs of this type should be avoided, or if that is not possible, discuss with an engineer experienced in masonry lining work prior to finalizing the drawings.

(7) "Acid" brick linings have coefficients of thermal expansion in the range of 4×10^{-6} , while steel expands 80% more. Concrete structures also have higher coefficients - in the vicinity of 5.8×10^{-6} .

The design must take this into account in order to assure continuous support of the substrate for the lining. Failure to do this will allow the masonry to go into tension - an unacceptable condition - and the lining will pull apart. The design must also take into account all stresses due to thermal changes so that excessive compressive forces do not build up and cause failure. Cylinders, cones and spheres are generally the best for masonry linings since "arch" configurations are always the strongest in masonry. Rectangular designs give least trouble when the walls and bottoms are "bowed" outward from the center (wider at center than at ends). Such design builds an arch into the wall and bottom, providing greater strength and stability (25).

(8) Western hemisphere clay brick all grow over a period of time, though neither uniformly nor at uniform speed. This growth has been measured up to a maximum in the vicinity of 0.16% of any dimension and may be attained within a year or so, or perhaps over a ten year period. Growth is accelerated by hot, wet cycling conditions and is least noticeable in steady state dry conditions. In designs where the brick are held in compression (such as the lining of cylindrical vessels) the growth is restrained and unnoticeable unless a brick must be replaced, at which time it is noticed that the replacement brick will not fit unless it is trimmed. However, on flat surface such as floors, trench linings, and flat rectangular walled tanks the growth is sufficient to cause "heaving". The ends of the masonry structure are restrained, so the growth forces within the structure relieve themselves by pushing away from the flat surface - upwards from a floor, outwards from a wall. The designer may prevent this in vessel design by "bowing" the walls and bottom (see #7). In floor design expansion joints to take up the growth (in addition to allowing for thermal elongation) must be provided.

(9) As in all structures, but to a greater extent than in alloy design, expansion must be provided for. There are many kinds and designs of expansion joints and the designer should compute carefully the maximum movement that can be anticipated and provide for it with a joint size double that of anticipated expansion. Expansion joints are the weakest parts of masonry structures and care must be taken to prevent them from becoming sources of trouble in operation (26).

(10) The designer must keep in mind that all brick linings must be primarily self-supporting. A relationship between height and length of a wall, and its thickness determines the stability of the wall. In contoured vessels (cylinders, bowed wall rectangles, etc.) the arch effect forces the wall against its support, and thickness is only important as it is required to protect membrane and substrate. However in a straight wall, failure to make the wall thick enough to provide a base of support will ensure its collapse (27).

References

1. "Handbook of Chemically Resistant Masonry" by Walter Lee Sheppard, Jr. (CCRM - 1977), (hereafter HCRM) pp. 1-4.
2. "Uses of Chemically Resistant Masonry in Air Pollution Control" by Walter Lee Sheppard, Jr., paper No. 5 presented to Air Pollution Control Equipment Corrosion Equipment Corrosion Seminar, Atlanta, GA. Jan. 17-19, 1978. "Material and Corrosion Problems in Gas Scrubbing Systems" D. W. McDowell, Jr. and W. L. Sheppard, Jr., paper presented to National Association of Corrosion Engineers, San Francisco, CA, March 14-18, 1977.
3. HCRM pp. 11-13.
4. HCRM pp. 7-8.
5. HCRM pp. 17-19.
6. HCRM pp. 10-11.
7. HCRM pp. 17-18.
8. HCRM pp. 6-8.
9. HCRM pp. 22, 193.
10. HCRM pp. 125-129.
11. HCRM pp. 31-39.
12. HCRM pp. 39-44.
13. HCRM pp. 90-94. Water & Sewage Works - Dec., 1975, Vol. 122 No. 12 pp. 64-67.
14. HCRM pp. 61-72.
15. HCRM pp. 100-106.
16. "Engineered Brick Lined Process Vessels", R. R. Pierce, published in Materials Protection and Performance, Dec., 1972, Vol. 11 No. 12, pp. 32-37.

17. "Membranes Behind Brick", W. L. Sheppard, Jr., Chemical Engineering May 14, 1972, Vol. 79 No. 11, pp. 122-126; June 12, 1972 Vol. 79 No. 13, pp. 110-116. HCRM p. 162.
18. HCRM pp. 11-14.
19. HCRM p. 19.
20. HCRM pp. 16-19.
21. HCRM pp. 20-23.
22. The mathematics necessary to compute thermal drops are discussed in HCRM pp. 112-124.
23. Requirements for concrete vessels to be brick lined, see HCRM pp. 61-63; for steel see pp. 72-76.
24. HCRM p. 82.
25. HCRM pp. 47, 64-68.
26. Expansion joints and their designs are discussed in detail in HCRM. See especially pp. 24, 25, 30, 31, 34, 37-39, 65, 69, 82, 85.
27. HCRM pp. 39, 40, 46, 47, 49, 57, 71, 72. See also paper No. 6, by AA Boova "Chemical Resistant Masonry, Flake and Fabric Reinforced Linings for Pollution Control Equipment", conference on Corrosion Problems in Air Pollution Control Equipment, Atlanta, GA January 17-19, 1978 pages 2-3.

SURFACE BONDING CEMENT: A NEW TECHNOLOGY FOR MASONRY

Richard D. Klausmeier

ABSTRACT: A new technology has been added to the masonry industry-- surface bonding cement. Surface bonding cement is a fiberglass reinforced concrete that is used to bond hollow unit masonry together without the use of mortar. The 1/8 in. thick glass-reinforced skin on each side of the wall bonds the units together and seals the masonry in one step.

The first course of concrete units is placed in a mortar bed. Subsequent courses are stacked dry. The dry walls are dampened and the surface bonding trowled on. The surface bonding cement gains much of its strength within 24 hours.

Tests have been conducted to establish the moisture penetration resistance, fire resistance, as well as the various structural characteristics. The National Concrete Masonry Association has issued recommended design allowables and a short form specification has been developed.

¹President, the Q-Bond Corporation of America, Denver, Colorado.

SURFACE BONDING CEMENT: A NEW TECHNOLOGY FOR MASONRY

By Richard D. Klausmeier¹

INTRODUCTION

The masonry trade has an old and proud tradition dating back to the early placement of stone to make structures. The stone mason selected his materials, cut and fit each stone so that the whole edifice took on the character that the designer wanted. There was great pride in building a structure that had lasting beauty as well as lasting durability.

When masonry building units progressed to the production stage, the mason maintained his position of skill and level of workmanship. The cutting of stone decreased and the use of mortar increased. This trend has continued to the present time. Evidence of masonry work is available throughout the world.

Masonry construction is generally thought of as the cutting and placing of stone, decorative stonework, bricklaying, and hollow unit masonry construction. Hollow unit masonry, commonly referred to as concrete blocks also includes the modern lightweight aggregate blocks. This paper concentrates on concrete block construction.

Since the late 1960's a new masonry technique has gained wide acceptance in the building industry. That new technique is surface bonding and the new material used is glass fiber reinforced surface bonding cement, referred to as surface bonding mortar in the proposed ASTM standards.

Under standard concrete block construction, the concrete blocks are laid in a mortar bed. The assumption might be that the mortar glues the blocks together and that the mortar also weather seals joints. Neither of these assumptions can withstand close scrutiny. The mortar is a relatively poor adhesive and has little strength in tension. The mortar also serves as a matrix of capillary channels to pass water, thus not serving to seal the wall. Concrete blocks soak up moisture and must be protected lest they function as a sponge. The use of concrete blocks in construction is widespread and widely accepted as good construction.

¹President, The Q-BOND Corporation of America, Denver, Colo.

Surface bonding cement is used to bond concrete blocks together without the use of mortar. The glass fiber reinforced skin bonds the blocks together and seals them all in one step.

Generally speaking, surface bonding cements are commercially available as a pre-mixed dry blended material delivered in 50-80 lb. bags. To make the material useable only requires the addition of water and mixing. Surface bonding cement will usually contain cement, silica sand, lime, chopped strand and a water proofing agent

The construction procedure for surface bonded walls is similar to that of conventionally built block except that NO MORTAR is used.

CONSTRUCTING WITH SURFACE BONDING CEMENT

FIRST COURSE

The block wall should be built on a firm foundation not likely to shift. Level the first course of blocks in a mortar bed without mortaring between the blocks. (Fig. 1) Leave necessary openings for doors. Level the first course carefully so that upper walls will be level. Make sure control joints and all vertical reinforcing has been installed.



Figure 1

Except for the first course eliminate mortar and horizontal joint wire mesh reinforcement. Be sure your building conforms with the local masonry building codes.

All blocks are not made to perfect dimensions; therefore, when blocks are laid end to end without mortar the length of the wall needs to be checked. Lay out the first course dry to check overall dimensions. Some blocks may need excessive roughness knocked off.

STACKING THE WALLS

Start by stacking the blocks three courses high at the corners. Using a mason's line from corner to corner, stack the blocks to the line in a running bond pattern. (Fig. 2)

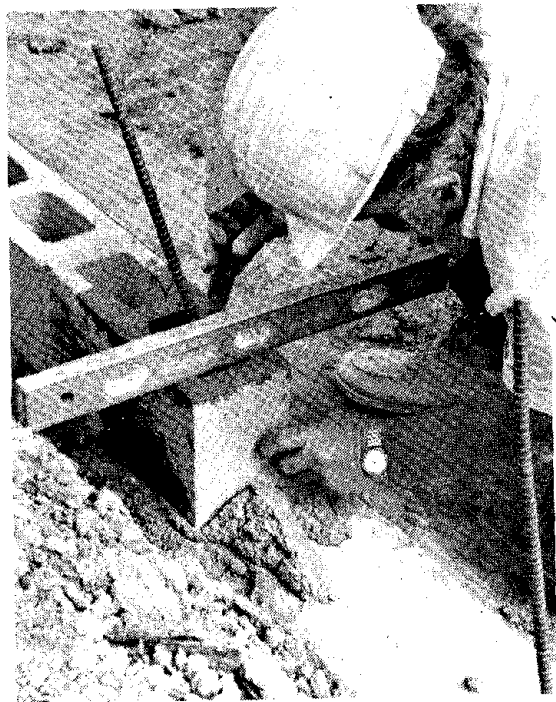


Figure 2

Check corners and the face of the walls with a level. Stack the block tightly together. Insert wooden frames to maintain correct openings for windows and doors.

Because blocks are not all perfect, shimming may occasionally be necessary. To shim, use metal wall ties, mortar, or surface bonding cement. A perfectly smooth wall is not necessary; surface bonding cement will hide the block lines and many irregularities. Just make sure the blocks are bearing securely against one another. Cover the top of the wall to prevent rain or snow from getting in the wall.

MIXING SURFACE BONDING CEMENT

Using a container such as a wheelbarrow (or mortar mixer) put in $1\frac{1}{2}$ gals. of water. Pour in a 50 lb. bag of surface bonding cement, mix with hoe or other mixing tool. Slightly more water may be needed to get a creamy, workable (but not runny) mixture. A small amount of water may be added up to 30 minutes after mixing if mixture begins to thicken. A 50 lb. mix should be used in about one hour by one person. Mix that becomes unworkable should be discarded and not added to another batch.

APPLYING SURFACE BONDING CEMENT

The block walls should be wetted well (but not soaked) before applying surface bonding cement. Wetting prevents the dry block from absorbing water from the bonding mixture. In very dry climates more care will be needed to offset quick evaporation. Surface bonding cement should be applied when the surrounding temperature will be above 40° for 24 hours after application.

Surface bonding cement is easily worked with an ordinary plasterer's trowel. (Fig.3) Apply surface bonding cement to a minimum of $\frac{1}{8}$ inch thick, using upward strokes and sweeping in a diagonal direction, covering the blocks and joints. Surface bonding cement must be applied to BOTH SIDES of the wall.

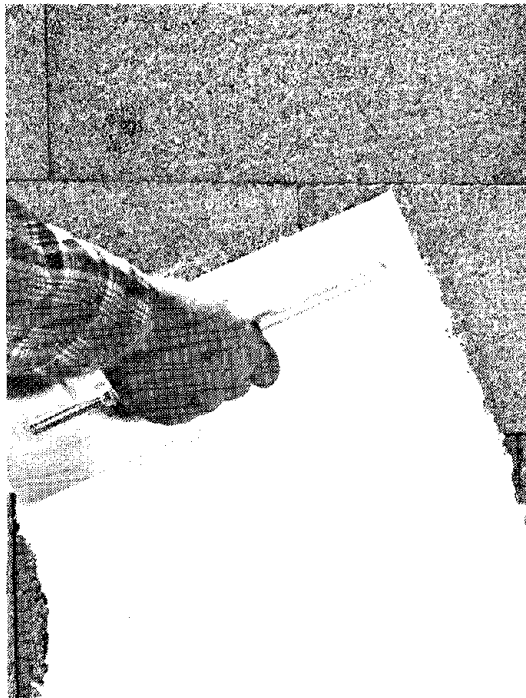


Figure 3

For high production, a spray pump can be used to apply the surface bonding cement to the wall. Excessive troweling should be avoided. Stop at natural breaks such as doors, windows or corners.

CURING

Surface bonding cement takes its set in one hour and will gain much of its ultimate strength in 24 hours. To insure maximum performance from your surface bonded wall, the surface must be dampened twice each day with a fine spray during the first 48 hours after application. (Fig. 4) This is particularly necessary under dry climatic conditions. In cold weather, keep the surface bonding cement from freezing during the first 48 hours.

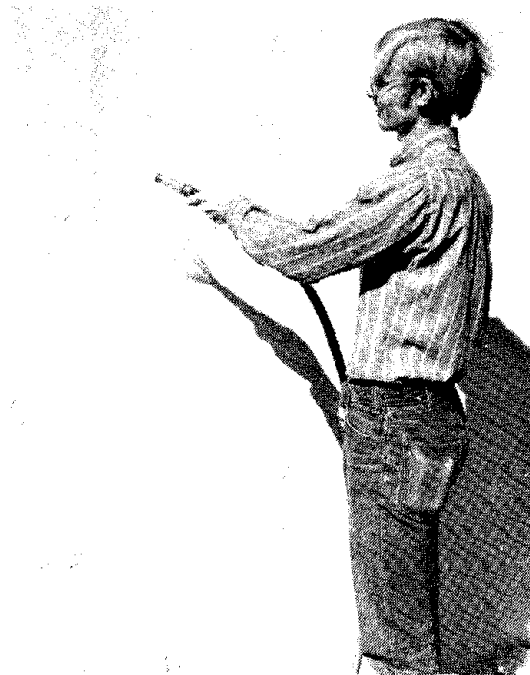


Figure 4

In the event you desire to add a subsequent texture coat to your surface bonded wall, it should be done within 24 hours after the original coating. Using a bonding adhesive additive in the texture coat allows application at any time.

TEST RESULTS

Test results of surface bonded wall systems show that in comparison with conventional mortared walls they have more strength in flexural and racking, resist moisture penetration better, and retain a good fire rating. (See Table 1) (1,2)

TABLE 1
COMPARISON OF SURFACE BONDED WALLS AND CONVENTIONAL
MORTARED LIGHTWEIGHT BLOCK WALLS

Test	Wall Thickness	Wall System	Surface Bonding Thickness	Results	Percent of Conventional
Compression (ASTM E-72)	8 Inch	Type S Mortar		504 psi	100
		Surface Bonded	.10	308 psi	57
Flexural (ASTM E-72)	8 Inch	Type S Mortar		29 lb/ft ²	100
		Surface Bonded	.10	47 lb/ft ²	164
Beam Third Point Loading (ASTM E-72)	8 Inch	Surface Bonded	.09	340 psi	
Racking (ASTM E-72)	8 Inch	Type N Mortar		2970 lb/ft	100
		Surface Bonded	.10	4170 lb/ft	140

FIRE RESISTANCE* (ASTM E-119-73)

	Thickness	Block wt.	Duration of Test	Rate
Surface Bonded	.11	94.3 lbs/ft ³	2 hr 6 min	2 hr

WATER RESISTANCE (F.S. TTP-0035)

	Wind Velocity	Thickness	Duration of Test	Water Penetration	Rating
Surface Bonded	98mph	.10	8 hrs	0	Excellent

* Also passed double loading of 100 psi and hose stream test

As a result of tests, The National Concrete Masonry Association (NCMA) has established design data for Surface Bonded Walls. (See Table 2) (3)

TABLE 2

RECOMMENDED DESIGN ALLOWABLE STRESSES FOR
NONREINFORCED SURFACE BONDED WALLS
OF HOLLOW CONCRETE MASONRY UNITS

General: "American Standard Building Code Requirements For Masonry,"
ANSI Standard A41.1, except as noted below.

ALLOWABLE STRESSES:

Compressive: 45 psi based on gross area with unground masonry
bearing surfaces

85 psi based on gross area with ground masonry
bearing surfaces

Shear: 10 psi based on gross area

Flexural: Horizontal Span:
30 psi based on gross area when units are drystacked
in interlocking (running bond) pattern

18 psi based on gross area when units are drystacked
in non-interlocking (stack bond) pattern

Vertical Span:
18 psi based on gross area

A proposed ASTM Standard is in the final stages of acceptance.

In a research project under a National Science Foundation Grant, James R. Cagley is investigating the feasibility of surface coatings or treatments to accomplish seismic hardening of existing unreinforced masonry walls. (4) The author came to the following conclusions:

The use of surface bonding cement to accomplish seismic hardening of unreinforced masonry walls is a potentially economic solution to a problem that at present only has expensive solutions.

This solution does not address all of the problems inherent in hardening of existing building such as anchoring of diaphragms or lack

of chord elements, but it does offer substantial additional safety for the buildings' inhabitants and those people outside the building who might get hit by falling masonry. The confining effect of the coating and ductility it furnishes are equally as important as the added sheer capacity.

If the use of this material tests out as anticipated, it will result in an immediately available solution for economical hardening of existing unreinforced masonry walls. This solution together with rational engineering judgment could be used to upgrade thousands of buildings in a short period of time.

SHORT FORM SPECIFICATION

The first course of concrete masonry units shall be laid in a full bed of mortar or surface bonding cement, but without mortar between the blocks. Starting with the second course, all blocks will be stacked in a running bond pattern. Surface bonding cement shall be applied to both sides of the block, covering the block and joints to a minimum thickness of 1/8 inch according to instructions on the manufacturer's bag.

DIMENSIONS FOR BLOCK WALLS TABLE 3

DIMENSIONS OF WALLS AND WALL OPENINGS CONSTRUCTED WITH SURFACE-BONDED CONCRETE BLOCKS¹

Number of Blocks	Length of wall	Number of Courses	Height of wall
1	1' 3 5/8"	1	7 5/8"
2	2' 7 1/4"	2	1' 3 1/4"
3	3' 10 7/8"	3	1' 10 7/8"
4	5' 2 1/2"	4	2' 6 1/2"
5	6' 6 1/8"	5	3' 2 1/8"
6	7' 9 3/4"	6	3' 9 3/4"
7	9' 1 3/8"	7	4' 5 3/8"
8	10' 5"	8	5' 1"
9	11' 8 5/8"	9	5' 8 5/8"
10	13' 0 1/4"	10	6' 4 1/4"
11	14' 3 7/8"	11	6' 11 7/8"
12	15' 7 1/2"	12	7' 7 1/2"
13	16' 11 1/8"	13	8' 3 1/8"
14	18' 2 3/4"	14	8' 10 3/4"
15	19' 6 3/8"	15	9' 6 3/8"

¹ Standard 16 inch blocks, 15 5/8" long by 7 5/8" high.

USES OF SURFACE BONDING

The uses for surface bonding cement are literally limited only by the imagination of the user or designer. Fish ponds, dams, outdoor sculpture and molding are some of the unusual applications. More practical projects have included every kind of building from storage shed to huge warehouses hundreds of thousands of square feet and including both low cost and custom homes, shopping centers, racquetball courts, churches and even McDonald Restaurants. Extensive building is presently underway and the growth of the surface bonding concept appears to be on a steady incline.

Designers, owners and contractors like the savings and appearance of surface bonded walls. This most dramatic development in masonry provides another technique that allows the mason to build with skill while combining innovation with tradition. Economy, speed of construction, strength and beauty are all characteristics of the surface bonding system. Add to this the increased productivity and it is clear why masons repeatedly comment about surface bonding being the wave of the future. New technology combined with the pride and skill of the mason will make his trade even more important in the future.

REFERENCES

1. National Concrete Masonry Association, "Structural Properties and Moisture Resistance of Concrete Masonry Walls Constructed with Q-BOND", Report of Research for The Klausmeier Corporation, May 1974.
2. The Ohio State University, "Standard ASTM Fire Endurance and Hose Stream Test on A Load Bearing Wall Assembly", Building Research Laboratory Report No. 5660 for The Klausmeier Corp., June 1974.
3. NCMA-TEK 88, "Surface Bonding (Design details and special properties)", National Concrete Masonry Association, 1978.
4. Cagley, J.R., "Seismic Hardening of Unreinforced Masonry Walls Through A Surface Treatment", March 1978, p. 22.

A SIMPLIFIED FLEXURAL BOND TEST FOR CLAY BRICK MASONRY

By Huizer, A. and Ward, M. A.

ABSTRACT: The accepted flexural test for clay brick masonry involves the use of specimens that are heavy, unwieldy and fragile. As a result the specimens are both inconvenient and impractical to transport and test. A new test is proposed which replaces the end thirds of the flexural beam with light alloy end pieces. The specimen to be manufactured in the laboratory or on site is therefore reduced to a two, three or four high brick prism. The end pieces are designed to minimize torsional stress due to uneven bearing surfaces, etc. This, coupled with the fact that the specimens are less likely to be damaged due to their reduction in size and weight, results in a significant reduction in within-batch variability.

A SIMPLIFIED FLEXURAL BOND TEST FOR CLAY BRICK MASONRY

By Arie Huizer,¹ and Michael A. Ward²

INTRODUCTION

In many applications, such as cavity walls and non-structural veneers, the structural performance of clay brick masonry is dependent upon adequate in plane flexural strength. Where wind related forces are the design loads the flexural strength of the unreinforced masonry panel is the principal design parameter.

The American Society for Testing Materials (ASTM) and the Australian Standards Association (AS) have developed test methods to establish the flexural bond strength of clay brick masonry, designated respectively as ASTM E518 (1)³ and AS 1640 (2). Unfortunately both test methods specify test specimens that are difficult to manufacture and which are easily damaged in transport or handling during the test itself. In addition the method of test in each standard is unsatisfactory since it gives results with unacceptably high coefficients of variation, nominally greater than 30%.

In the proposed test method the flexural test is performed on a two- or three-brick high prism segment. The specimens are easy to manufacture and handled without damage. The simple loading rig utilized minimizes the alignment problem during the set-up procedure which results in a significant improvement in the test coefficient of variation.

PROPOSED TEST METHOD

The proposed test is a flexural test which employs demountable extension sections fixed to both ends of the two- or three-brick prism segment. Load is applied on each of the end bricks of the segment which gives a uniform bending moment over the central section of the segment,

¹Instructor II of Civ. Engrg., Univ. of Calgary, Calgary, Alberta.

²Prof. and Head of Civ. Engrg., Univ. of Calgary, Calgary, Alberta.

³Numerals in parentheses refer to corresponding items in the Appendix I.--References.

i.e. either one or two mortar joints. The supports for the extension sections are designed to ensure that a uniform bending moment occurs over the prism segment without any torsional effect from the support reactions. The complete test set-up is shown in figures 1 and 2.

TEST PROGRAM

In order to evaluate the new test method, a comparative test program was conducted using the procedure specified in AS 1640, figure 3, and the proposed method. The Australian test is essentially a field test and was chosen for comparison purposes since the new test was originally conceived for field testing. In the Australian method the load is applied to the beam specimen using a brick stack (see figure 3).

The new test procedure used both two- and three-brick segments. The loading rates were established for the new test so that the increase in extreme fibre stress with time was nominally the same for both the new and the old procedures, nominally 13.8 kPa/min.

The brick chosen for this study was a locally produced wirecut 4 in. modular standard brick. The brick meets all requirements of CSA Specification A82.1(4). The nominal dimensions of this brick are 3 5/8 in. x 2 1/4 in. x 7 5/8 in. and it has ten perforations.

Two mortar types were used, type N and S as specified in CSA A179(5) and ASTM C780 (6).

All test prisms were cured in laboratory air for 28 days. The mortar cubes were moist cured as specified in CSA A179.

The stress at failure is the modulus of rupture of the specimen calculated from

$$\sigma_f = \frac{My}{I}$$

RESULTS

The mortar compressive strength results are given in table 1.

Mortar Type	No. of Specimens	Strength MPa
N	12	8.20
S	12	13.8

Table 1. Mortar Compressive Strength
(according to CSA A179)

The modulus of rupture and coefficient of variation for each of the mortar/brick/test method combinations are given in table 2. Table 3 gives the pooled coefficients of variation for all test methods used in this study and a method developed by Lawrence (3).

Test Method	Mortar Type (CSA A179)	No. of Specimens	Average Modulus of Rupture MPa	Coefficient of Variation - per cent
9 Brick Prism	N	12	0.99	50.3
	N	12	0.51	53.3
2 Brick Prism Segment	N	12	1.34	14.1
	S	12	1.88	15.8
3 Brick Prism Segment	N	12	0.65	14.7
	S	12	1.81	11.7

Table 2. Summary of Flexural Test Results, all Methods

The latter is of interest to this study since Lawrence's specimen and test procedure is essentially the same as ASTM Test Specification E 518-76.

Test Procedure	Coefficient of Variation (per cent)
2-brick prism segment	15.0
3-brick prism segment	13.2
9-brick prism (AS 1640)	51.8
Lawrence* 9-brick prism (essentially ASTM E518)	27.6

* 10-hole wire cut bricks only

Table 3. Pooled Coefficients of Variation - all
Test Methods

DISCUSSION

For a test method to be useful for pre-construction evaluation of materials or for control purposes on site it should be relatively easy to perform (inexpensive) and give meaningful results. In flexure tests on masonry assemblages it is obvious that neither of these criteria is met using either the Australian or ASTM test methods. The nine- and ten-brick prisms are heavy and unwieldy and hence are easily damaged during handling. Both procedures also give unacceptably high coefficients of variation, probably due in part to unavoidable damage to the specimens themselves and problems arising from the loading set-up.

The new procedure is however more acceptable. The two- or three-brick segments are easy to manufacture and handle and the extension segments are easily fixed to the specimen. In place, the design of the extensions ensures a relatively uniform stress distribution in the specimen. The coefficients of variation obtained with the new test method are only nominally one half of the best result obtained with any of the other methods.

CONCLUSION

The proposed test procedure to determine the flexural strength of plain masonry has been shown to be a superior test to current laboratory and field test methods, in particular AS 1640 and ASTM E518. Its principal advantages are (1) that the use of the two- or three-brick segment in place of the nine- and ten-brick beam almost ensures that the test specimen will not be damaged during handling; and (2) that the test variance is reduced due to (1) and the uniform stress distribution ensured by the end piece design.

FUTURE WORK

Since the four high prism is the accepted standard for the compressive strength test for masonry, work should be undertaken to determine whether a four-brick prism could be as effectively used for flexure testing using the prism end pieces. There would be clear advantages if the same prism configuration could be used for compression and flexure testing.

ACKNOWLEDGEMENTS

This research was made possible by a grant from IRAP through the Alberta Masonry Institute.

APPENDIX I

REFERENCES

- (1) ASTM E518-76, Standard Test Methods for "Flexural Bond Strength of Masonry".
- (2) AS 1640 - 1974, "Brickwork in Buildings," Standards Association of Australia, Sydney, 1974. (SAA Brickwork Code).
- (3) LAWRENCE, S. J., "The Relationship between the Strengths of Brickwork Bond Piers and Shear Couplets," Technical Record TR52/75/938, Experimental Building Station, Sydney, 1977.
- (4) CSA Specification A82-1, 1965, "Burned Clay Brick."
- (5) CSA-A179M-1976, "Mortar and Grout for Unit Masonry".
- (6) ASTM C780-74, Standard Test Methods for "Preconstruction and Construction Evaluation of Mortars for Plain and Reinforced Unit Masonry".

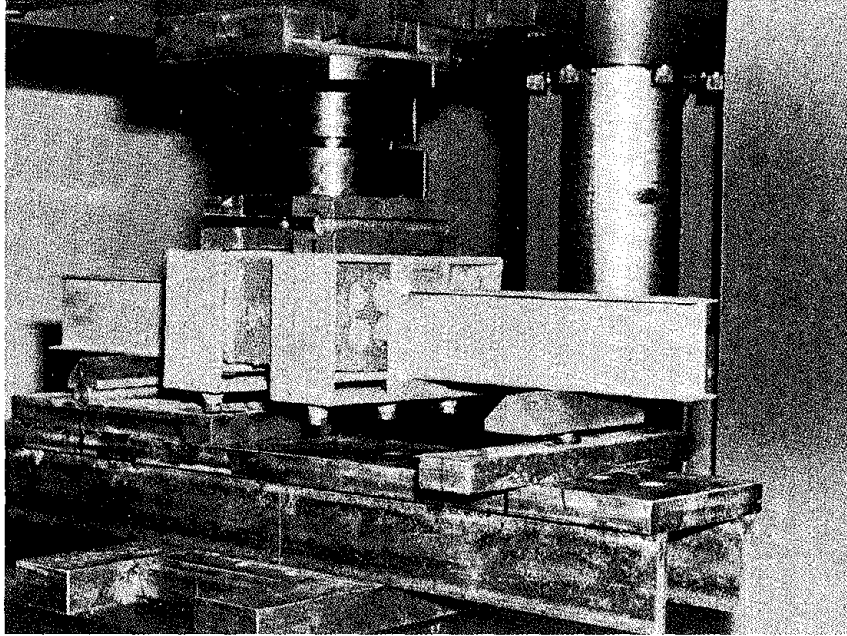


Figure 1. Proposed Test Method

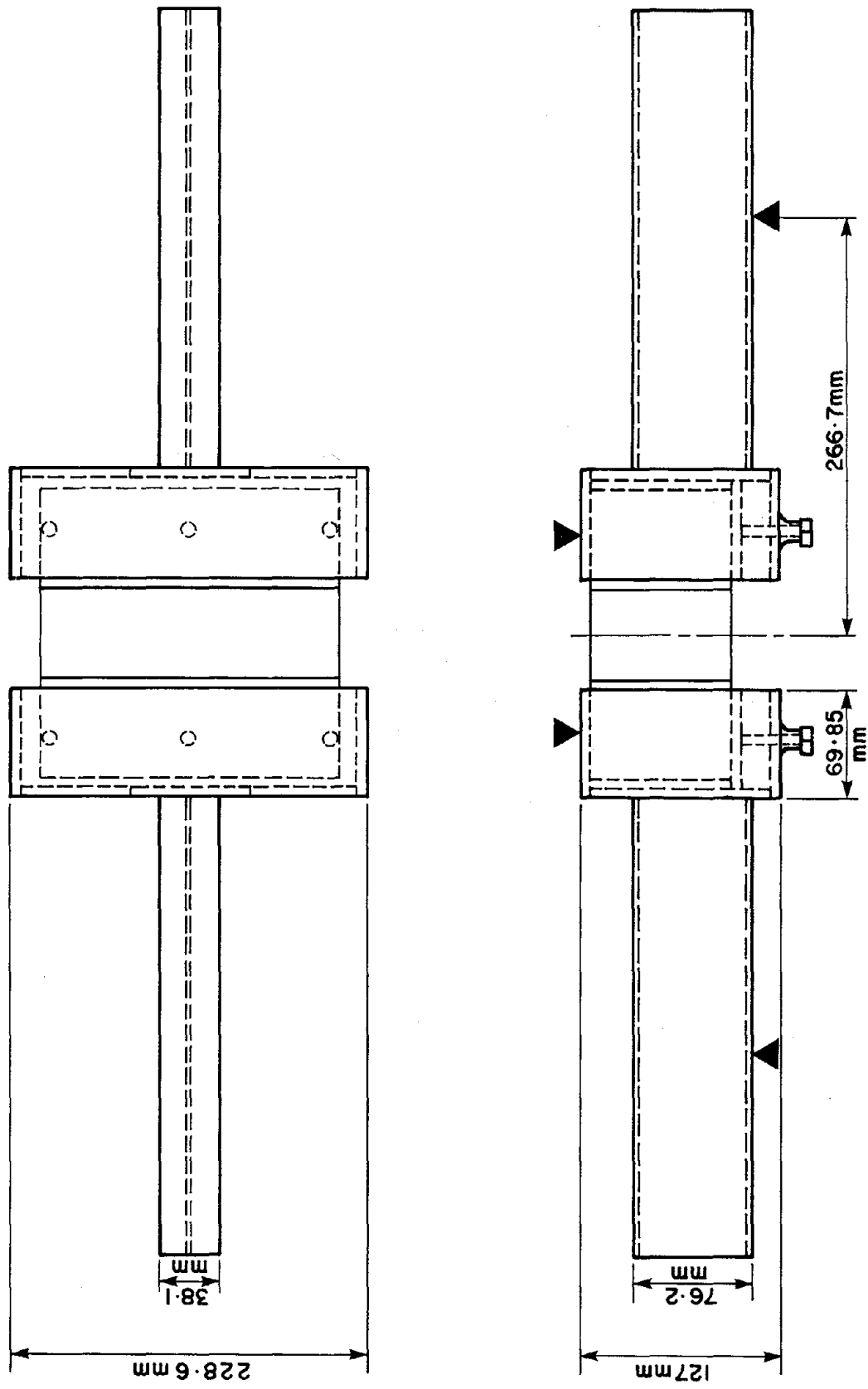


Fig. 2 TESTING ARRANGEMENT

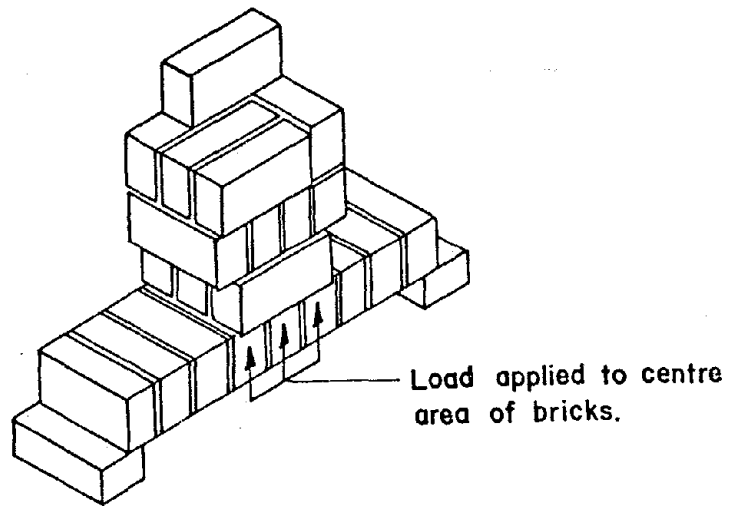


Figure 3. Australian Flexure Bond Arrangement

QUALITY CONTROL OF LOAD BEARING CONCRETE BLOCK WALLS

By Elnicky, E. J.

ABSTRACT: On October 6, 1977, a significant step in bringing people back into the "Central City" of Fort Wayne was accomplished with the groundbreaking for the Edsall House apartments, a 202 unit senior citizens housing complex. The project, estimated to take about 15 months to complete is divided into three five-story masonry buildings valued at 4.5 million dollars. The entire Edsall House development is adjacent to a Senior Citizens Center which is valued at 2.5 million dollars.

The architect specified fluted masonry load-bearing block wall construction for the project. To establish the 28-day ultimate compressive strength ($f'm$) of the block, prism tests were conducted in accordance with Section 3.2 of "Specification for the Design and Construction of Load-Bearing Concrete Masonry," (NC MA-1970).

In conjunction with the above tests, 36 additional prisms were tested to ensure that the design $f'm$ value was met. From the test data, a statistical analysis was performed to determine the basic characteristics of the prisms.

The significance of the project is the quality control of the masonry work as determined by prism tests. It is the first time in the Fort Wayne area that prism tests have been performed. The results and conclusions drawn from these tests are of value to block suppliers, architects, engineers and building contractors.

QUALITY CONTROL OF LOAD BEARING CONCRETE CLOCK WALLS

By Edward J. Elnicky¹

INTRODUCTION

In order to ensure that a building is safe and long-lasting, a program of quality control is essential. In Fort Wayne, Indiana, the Edsall House (a 202-unit, three 5-story buildings, senior citizen housing complex) is being built of concrete masonry block wall construction. To determine and verify the ultimate compressive strength (f'_m) of the load-bearing concrete block walls, a series of prism tests has been performed. Therefore, the purpose of this paper is threefold: (1) to examine the procedures used to determine f'_m , (2) to review the specifications and procedures used for the testing of prisms during the course of construction, (3) to analyze by means of a statistical analysis the 36 prisms used for quality control.

DETERMINATION OF f'_m INITIAL f'_m

The determination of f'_m was a process of learning, testing and evaluating prism test results to see if load bearing concrete block wall construction could be used for the Edsall House apartment complex. The reason for this statement is that prism tests have not been performed in the Fort Wayne area for at least twenty years. One of the major problems involved with prism tests is the need for a large capacity compression testing machine. This problem was solved by using the testing facilities at the Indiana University-Purdue University regional campus. The machine used was a Tinius Olsen Standard Super "L" universal testing machine with a range capacity of 400,000 pounds.

The architect specified fluted concrete block wall construction, but did not specify the number of flutes nor color to be used. This was to be decided upon by making two block wall mockups, one 8-flute and the other 4-flute. A set of five prisms (two block high H/d ratio equal to 2.0, 4-flute two cell) was then tested at seven and 28 days to determine f'_m . When the average seven day f'_m value proved adequate (3580 psi net area), another set of five prisms (two block high, H/d ratio equal to 2.0, 4-flute block, correct color) was made and tested. Prior to this, a set of five prisms (two block high, H/d ratio equal to 2.0, 8" x 8" x 16", 2-core regular limestone foundation block) was constructed and tested. The average seven and

¹Assistant Professor, Civil Engineering Technology, Purdue University at Fort Wayne, Indiana.

28-day f'_m value for the foundation block were 2080 psi and 2110 psi respectively. This is an increase in strength of 1.4%. The 4-flute prisms were then tested, and the average seven and 28-day f'_m values were 3790 psi and 3940 psi respectively. Because only a 1.4% and 4.0% increase in f'_m was obtained from the 28-day breaks, it was decided by the architect that seven-day break values would be used for quality control.

DESIGN f'_m

The Uniform Building Code which is used in Fort Wayne, Indiana, specifies that the ultimate compressive strength (f'_m) may be assumed to be 1350 psi for hollow concrete units and 1500 psi for the same units grouted solid (1). Prisms were made and tested to establish the f'_m values for both the foundation and 4-flute block. From these tests, the average seven day f'_m values were found to be 2080 psi (foundation block) and 3790 psi (4-fluted block). The foundation blocks used in the construction of the load bearing walls were grouted solid but prism tests were made using hollow blocks. After evaluating the initial test results, an f'_m value of 1500 psi was selected as the design f'_m value for the Edsall House apartment complex. This provided an extra amount of safety which the structural engineer felt necessary because of the lack of experience in making and testing prisms in the Fort Wayne area. Quality control prisms would be used to verify this f'_m value for both the foundation and 4-flute block walls.

PRISM SPECIFICATIONS

PRISM SAMPLING

Job specifications for the Edsall House require "At least one field test during construction per each five thousand square feet (5000 square feet) of wall but not less than three such tests for each of the lower three floors of the building; the upper floors require one test per floor (3)." The latter portion of this specification was used to determine when prism tests would be performed. Periodic inspections were also done by the architect during wall construction. An area of concern was the possibility of the mortar freezing due to low temperatures during the latter part of October. To prevent freezing, walls and prisms were covered. Adverse weather conditions forced the job to shut down early in December with sporadic work being done during the winter months. Construction is scheduled to resume in early March or as soon as weather conditions permit. Prisms will continue to be tested to verify the remainder of the work.

PRISM CONSTRUCTION

"The test prisms should be a representative sample of the actual composition of the wall (4)." To establish this, block, grout and workmanship shall be the same as that used in the actual wall structure.

The mason supervisor built all the prisms using block and mortar that was currently being used in the construction of the load bearing walls. The initial prisms were constructed with the job superintendent, block representative, and other representatives on hand. Prisms were constructed adjacent to the job trailer on level sheets of 3/4" x 4' x 8' plywood.

PRISM HANDLING AND CURING

Prisms were cured on the job site for 48 hours then banded with 3/4-inch plywood placed on the top and the bottom of the prism. They were then transported to the laboratory for five more days of curing, then taken to the Indiana University-Purdue University regional campus at Fort Wayne for testing.

PRISM CAPPING AND TESTING

The purpose of capping is to provide a smooth bearing surface for the load to be transmitted evenly throughout the prism. Prisms were first thoroughly examined for possible damage in transport before removing bands and plywood. The bearing surfaces were then rubbed with a carborundum stone to provide a surface free from any rough spots. Prisms were not capped with either sulfur mortar or high-strength gypsum plaster because of the difficulty in handling the prisms. Instead corrugated fiber board was placed on both bearing surfaces to transmit the load throughout the prism. Testing was done by using a Tinius Olsen Standard Super "L" universal testing machine with a capacity of 400,000 pounds. Prisms had a height to thickness (H/d) ratio of 2.0; therefore, a correction factor of 1.00 was applied to the ultimate compressive strength of the specimens (2).

BLOCK AND MORTAR TESTS

Individual block tests were performed by an independent testing firm, and the block exceeded the requirements of A.S.T.M. C-90, Grade NI and NIT. Cube mortar tests were performed on the Type S mortar used and exceeded the specified compressive strength of 1800 psi in 28 days.

STATISTICAL ANALYSIS

MEAN AND STANDARD DEVIATION

Statistical quality control implies the use of numbers and mathematical relationships to determine if a material, quantity or process meets job specifications. Using a sample size of 15 from the data given in Appendix III, a mean f'_m value of 2200 psi was calculated with a standard deviation of 284 psi for the foundation block. Figure 1 shows the relationship between the mean f'_m (sample size 3) and each foundation block set. While Figure 2 illustrates this same relationship for the 4-flute block. A sample size of 21 was used to compute a mean f'_m value of 3920 psi with a standard deviation of 414 psi for the 4-flute block.

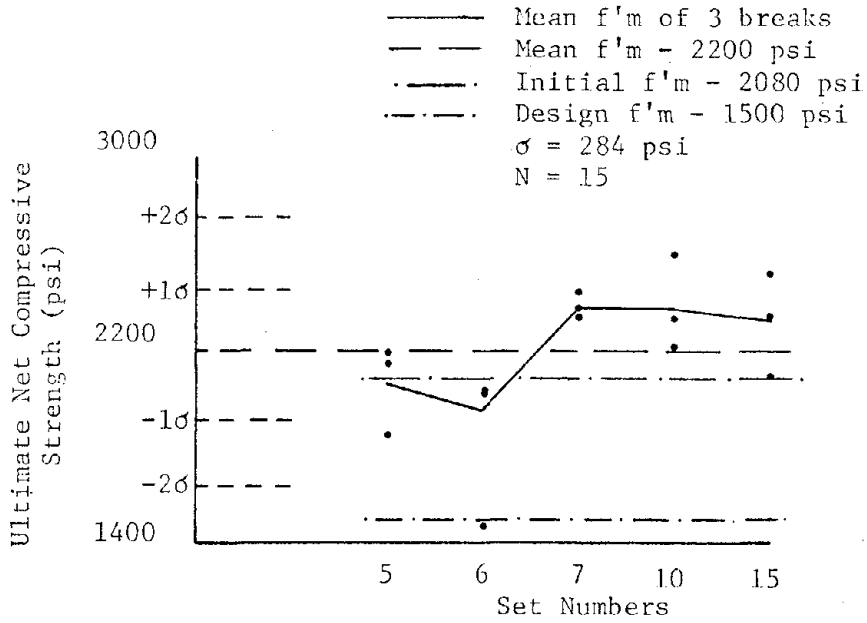


FIG. 1 - SET NUMBERS (FOUNDATION BLOCK) VERSUS ULTIMATE COMPRESSIVE STRENGTH (PSI)

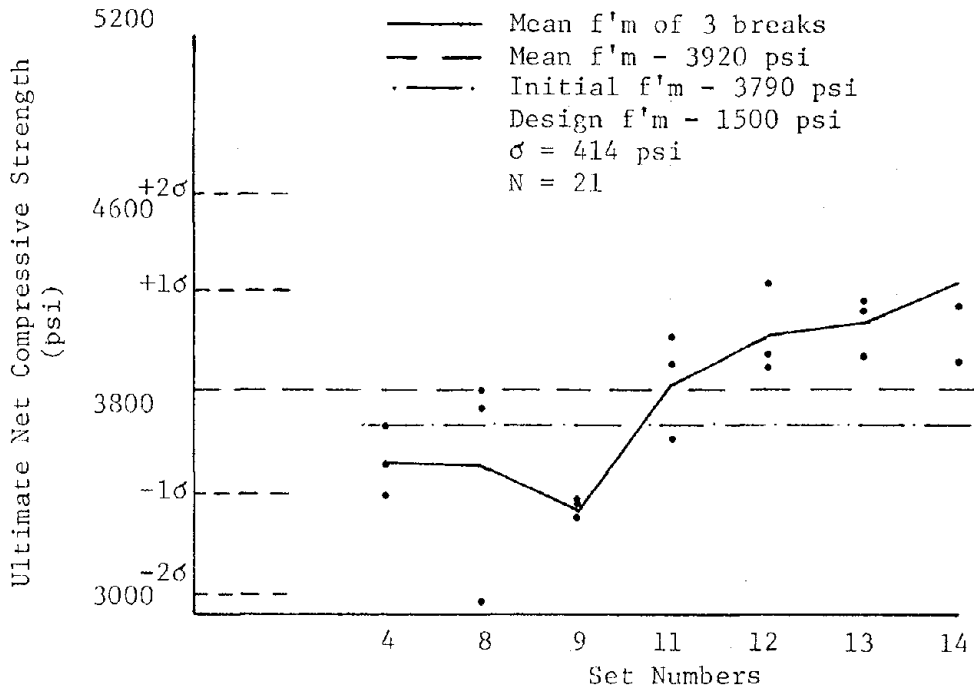


FIG. 2 - SET NUMBERS (4-FLUTE BLOCK) VERSUS ULTIMATE NET COMPRESSIVE STRENGTH (PSI)

From Figures 1 and 2, it is noted that there are two low prism breaks. One in Set 6 (foundation block) and the other in Set 8 (4-flute block). Upon examining the prisms in Set 6, a damaged corner was discovered. This could account for the low test break. There is no apparent reason for the low test break in Set 8.

The relationship between the mean f'_m value for each building is given in Figures 3 and 4. Figure 3 shows this relationship for the foundation block while Figure 4 illustrates this same relationship for the 4-flute block. In both Figure 3 and 4, the mean f'_m value is greater than the initial and the design f'_m values. This indicates that the block being placed in the building is meeting specifications.

RANGE

The range is another measure of the dispersion or degree of scatter among test results. Table 1 lists the range for both the foundation and 4-flute block for all three buildings and the overall range for the prism breaks.

TABLE 1 - f'_m RANGE

Building	Foundation Block psi	4-Flute Block psi
A	700	890
B	390	890
C	410	810
ABC	1120	1810

SUMMARY

Quality control is vital on any construction project and is necessary for the safety and proper performance of any structure. The Edsall House Project was one where prism tests were used to establish and control the ultimate compressive strength (f'_m) of the concrete masonry load bearing block walls. By having a method of control (prism tests) the architect, contractor and owner had assurance of the performance of the load bearing walls.

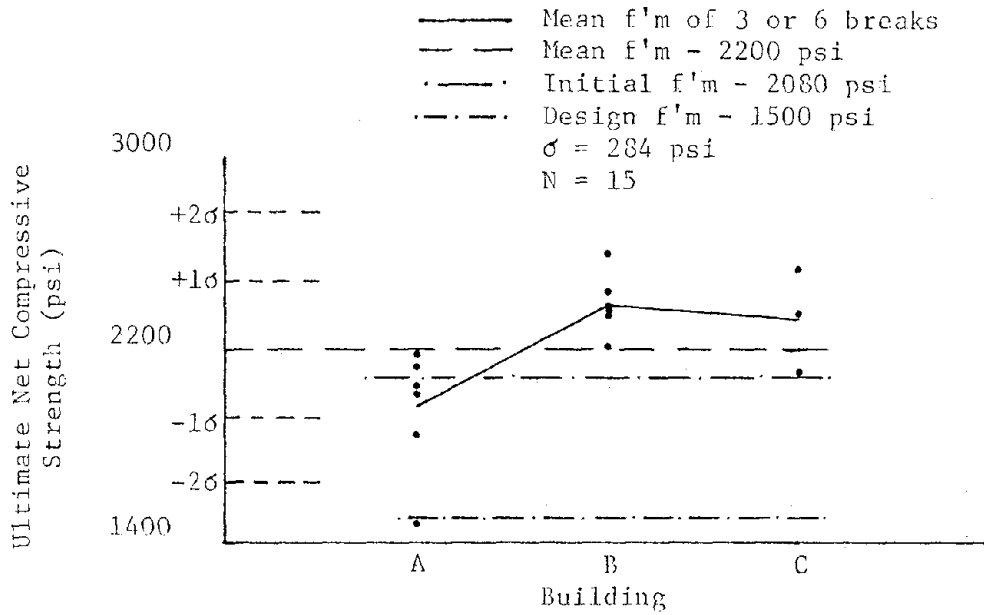


FIG. 3 - BUILDING (FOUNDATION BLOCK)
VERSUS ULTIMATE NET COMPRESSIVE
STRENGTH (PSI)

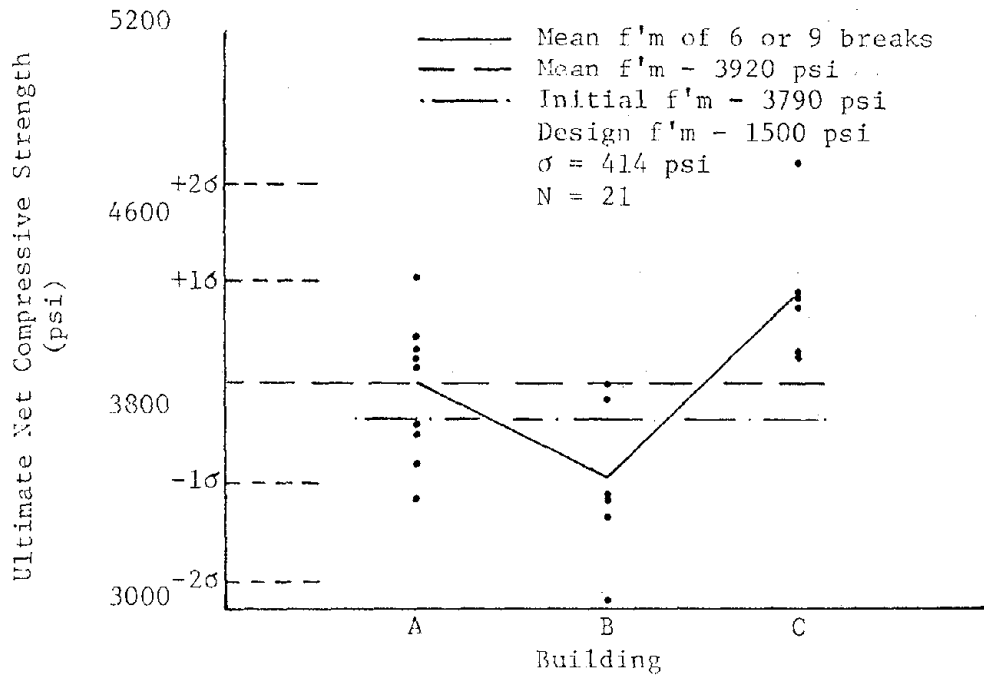


FIG. 4 - BUILDING (4-FLUTE BLOCK)
VERSUS ULTIMATE NET
COMPRESSIVE STRENGTH (PSI)

The result of these prism tests, being a feasible method of quality control in the Fort Wayne area, has led to the planning of another load bearing masonry block wall apartment complex in Fort Wayne, Indiana.

ACKNOWLEDGMENTS

The writer wishes to express his thanks to the following firms for their help in the procurement of data and other necessary information: D. M. Snyder & Associates; Grinsfelder - McArdle, Associates, Inc.; Masolite Concrete Products, Inc.; and Materials Inspection & Testing, Inc.

APPENDIX I - REFERENCES

1. "Concrete Masonry Units", Section 2404, Uniform Building Code, 1976, p. 158.
2. "Concrete Masonry Units", op. cit., p. 157.
3. "Masonry", Division 4, Section C, Specifications for the Edsall House, 1977, p. 6.
4. "Prism Testing for Engineering Concrete Masonry", Information Series number 22, National Concrete Masonry Association, 1970, p. 3.

APPENDIX II - NOTATION

The following symbols are used in this paper:

f'_m = ultimate net compressive strength;
 N = number of tests;
 σ = standard deviation.

APPENDIX III - PRISM TEST DATA

Set	Date Made	Bldg.	Age	Type	Total Load lbs	Net f'_m psi*
1	9/30	Orig. Set	7	4- Flute	193,000	3290
			7		227,500	3880
			28		240,000	4140
			28		247,000	4260
			28		233,500	4030
2	10/14	Orig. Set	7	Found.	133,000	2110
			7		129,000	2050
			28		119,500	1900
			28		143,000	2270
			28		136,500	2170

APPENDIX III (Cont'd) - PRISM TEST DATA

Set	Date Made	Bldg.	Age	Type	Total Load lbs	Net f'm psi*
3	10/21	Set Used	7	4- Flute	218,000	3770
			7		332,500	3810
			28		236,000	4020
			28		223,000	3800
			28		235,000	4000
4	10/28	A 1st Floor	7	4- Flute	222,000	3780
			7		212,500	3620
			7		205,000	3490
5	10/28	A 1st Floor	7	Found.	137,500	2180
			7		116,000	1840
					134,000	2130
6	11/7	A 1st Floor	7	Found.	127,000	2020
			7		128,000	2030
			7		93,000	1480
7	11/7	B 1st Floor	7	Found.	150,000	2380
			7		153,000	2430
			7		148,000	2350
8	11/7	B 1st Floor	7	4- Flute	227,000	3930
					176,000	3040
					223,000	3860
9	11/7	B 1st Floor	7	4- Flute	200,000	3460
			7		196,000	3390
			7		200,500	3470
10	11/18	B 1st Floor	7	Found.	164,000	2600
			7		139,500	2210
			7		147,000	2330
11	11/22	A 2nd Floor	7	4- Flute	243,000	4140
			7		218,000	3720
			7		237,000	4040
12	11/22	A 2nd Floor	7	4- Flute	240,000	4090
			7		236,000	4020
			7		257,000	4380
13	11/28	C 1st Floor	7	4- Flute	250,000	4260
			7		252,000	4300
			7		239,000	4070

APPENDIX III (Cont'd) - PRISM TEST DATA

Set	Date Made	Bldg.	Age	Type	Total Load lbs	Net f'm psi*
14	11/28	C	7	4- Flute	237,000	4040
		1st	7		252,000	4290
		Floor	7		282,000	4850
15	11/28	C	7	Found.	158,000	2510
		1st	7		148,000	2350
		Floor	7		132,500	2100

*Net area foundation block = 63.0 in²

*Net area 4-flute block = 58.7 in²

Test Methods for Masonry Mortars

by E.L. Jessop and B.W. Langan
Department of Civil Engineering
University of Calgary
Calgary, Alberta
Canada

ABSTRACT: Test methods for determining the properties of fresh mortar have been reviewed. Particular attention has been paid to those methods used for determining the workability of mortar, i.e, the flow table, Mo-meter, dropping ball, cone penetrometer, slump and Russian cone. Comparative test data relating these tests are presented together with data assessing the ability of the individual methods to detect small variations in workability over the range of low to site workabilities. Other test methods considered include those used to determine water retentivity and consistency retentivity, together with procedures for determining the constitutive proportions of the mortar and air content.

TEST METHODS FOR MASONRY MORTARS

by

E. L. JESSOP¹ and B. W. LANGAN²1. SUMMARY

In this paper we present our thoughts on the specification of mortar, discuss the various test methods included in the mortar standards of a number of countries in the world for determining the characteristics of fresh mortar, and recommend which of these test methods are the most suitable for use in both pre-construction evaluation and on-site quality assurance programs.

2. INTRODUCTION

In North America ASTM C270 (1) and CSA A179 (2) are the standards by which mortar is specified, and they are very similar. Davison (3) has reviewed the development of ASTM C270, observing that,

- a) the original objective of the drafting committee was to write a performance-type specification.
- b) the objective was not achieved because consumer members of the committee were unable to relate the laboratory test methods in the draft specification with known field programmes and producer-members could not appreciate consumer concern that certain tests be included.
- c) the format of the current specification is a compromise presenting alternative "prescription-type" (proportion) and "performance-type" (property) specifications.

We are of the opinion that a mortar specification should directly relate to the method by which the mortar is prepared on-site.

On-site mortar is prepared by volume or weight proportions. Hence, an appropriate mortar specification is one which states requirements for the composition of the mortar; in other words, a prescription-type (proportion) specification. A performance-type (property) specification is more appropriate for masonry than mortar alone.

-
1. Research Director, Alberta Masonry Institute and Associate Professor (part-time), Department of Civil Engineering University of Calgary, Calgary, Alberta, Canada.
 2. Instructor II, Department of Civil Engineering, University of Calgary, Calgary, Alberta, Canada.

Prior to specifying mortar by its proportions, the mix should first be evaluated in the laboratory to determine its suitability for use with the chosen masonry units via tests on prism or panel assemblages.

On-site, for quality-assurance purposes, the sooner a test yields data the better; hence, emphasis should be placed on fresh mortar testing rather than on hardened mortar testing. The important characteristics of fresh mortar are listed in Table 1.

3. TEST METHODS FOR FRESH MORTAR PROPERTIES

3.1 Workability

The workability of fresh mortar is of fundamental importance to the mason. Perhaps the best definition of this characteristic, certainly as far as the mason is concerned, is..."the property that enables a mortar to spread, when trowelled, into all cracks and crevices of the unit". (4)

Researchers, in attempting to be more scientific in their search for a suitable definition of this characteristic, have variously recognized that workability is a complex rheological property embodying such properties as plasticity, consistency, cohesion, adhesion and viscosity. Some of the test methods included in Table 1 under the heading "Workability" measure one or more of these properties.

Flow Table:

The most common test method in use throughout the world for assessing the workability of mortar is the Flow Table which measures the percentage increase in the diameter of a mortar sample, originally moulded in the shape of a truncated cone, after it has been subjected to a prescribed amount of work.

The method was originally developed as a test for mortars of laboratory workability with flow values between 100 and 130 percent, the prescribed energy input being 25 drops of the table in 15 seconds. In Australia, where this test method is used on mortars of site workability, it was observed that many of the mortars used overflowed the table under this amount of energy input (5). Therefore, the requirement that mortar be subjected to only 12 drops of the table in 7 seconds has been proposed.

It is of passing interest to note that the Flow Table of European Standards (6) is a larger apparatus than that used in North America (7, 8) and Australia (9).

The Flow Table is strictly a laboratory test method. The massive base shown in Figure 1 is essential to the obtaining of reproducible results.

Mo-Meter:

This method of test (10) originated in Sweden as a means of assessing the consistency of mortar, and is included in the mortar standards of a number of European countries.

The Mo value is the number of drops, 25 mm onto a heavy base, required to empty a specific container originally filled with a sample of the mortar.

The Mo-Meter is intended to be used on-site as well as in the laboratory; the apparatus is also shown in Figure 1.

Correlation Data:

Figure 2, taken from reference (11), shows the lack of correlation between the data obtained by each method on a number of different mortars.

Cone Penetrometers:

Two different pieces of apparatus are reviewed here. In North America (12) and Western Europe (13), the form of apparatus is as shown in Figure 1, and we refer to this simply as the cone penetrometer. Eastern European countries (14) use an apparatus that, for want of a better name, is referred to as the Russian cone, illustrated also in Figure 1.

The method measures the depth of penetration by a cone of specified dimensions and mass under its own weight.

The cone penetrometer is basically a Vicat apparatus developed originally for use as a test for cement consistency, modified to allow greater depth of penetration in mortars.

The Russian cone is much larger than the cone of the cone penetrometer. In the laboratory, the Russian Cone apparatus is similar to that of the cone penetrometer. The Russian cone may be used on-site detached from its base, hand-held and inserted directly into the mortar in the mixers, thus eliminating the necessity for sampling and remoulding mortar.

Correlation Data:

The Cone Penetrometer and Russian Cone are similar test methods. Figure 3 shows the relationship between the limited data obtained by each method on samples of mortar of varying workability. Each point is an average of at least 3 readings.

Dropping Ball:

Originally developed at the Building Research Station in Great Britain, this simple test method (15, 16) is an adaptation of one used to measure the consistency of plaster. The penetration into a smoothed mortar surface of a Perspex ball dropped from a prescribed height is measured.

Slump Cone:

The proposed revision to the Australian standard (9) includes a slump test for evaluating the workability of mortar which is based on the similar test method used for concrete but employing a slump cone one-half the size. This apparatus is also shown in Figure 1.

Comparative Test Data:

Figures 4 through 8 show comparative test data obtained by utilizing the various test methods on the same mortar(s).

Methods of test which impart energy to the mortar, such as the Flow Table and the Mo-Meter, which we describe as dynamic tests, are best suited to mortars of stiffer consistency or lower workability while the remaining methods, which we describe as static tests, are best suited to mortars of higher workability.

A means of evaluating the various test methods is to compare their variability and sensitivity in use on mortar of known mix proportions but varying consistency due to different water contents. This has been done and the results of sensitivity are presented in Table 2 and shown in Figure 9, while the results of variability are summarized in Table 3.

Over the range of low to site workabilities (in terms of the flow table values from 90 to 140 percent), the cone penetrometer and the Russian cone appear to be the most sensitive static tests while the flow table is the most sensitive dynamic test. Sensitivity is here defined as the largest change in readings over the range considered.

For mortars in the range above that of normal site workability, both the dynamic tests are rendered impractical as specified, i.e., the mortar overflows the table and it is impossible to fill the container of the Mo-Meter. A reduction in the number of drops, as mentioned earlier, allows the flow table to be used for mortars in this range. The static tests most sensitive in this range of workabilities are the slump and cone penetrometer.

Table 3 summarizes the variability, of the test methods under discussion, on mortar of site workability. Included in this table are the specified and achieved accuracies for each method of test. Ten repetitive tests were conducted to establish the standard deviation and coefficient of variation. In comparing the statistics,

one must bear in mind the accuracy of each test procedure and thus the effect on the statistics presented, i.e., a test method with a coarser scale may give a lower coefficient of variation than a test with a finer scale; in other words, a coarser scale may mask inherent test variations.

Notwithstanding the above, the Russian Cone appears to be the most useful test for monitoring site workability, not only because of the low coefficient of variation but of its ease of use. The flow table still appears to be an excellent laboratory test.

3.2 Retentivity

Two types of retentivity tests appear in mortar standards, one for assessing the ability of a mortar to retain its water under the action of a short duration absorptive force; the other, for assessing the ability of a mortar to retain its initial consistency or workability over an extended period of time.

Water Retentivity:

Basically two types of apparatus are specified in mortar standards. In one, the absorptive force is generated by use of a vacuum, while in the other, blotting or filter paper is used; in both, it is the intent that the absorptive force simulate that of a masonry unit.

Figure 10 shows the ASTM apparatus (17). In this method the value of water retentivity is calculated as the ratio of "Flow after suction" to "Flow after initial mixing", expressed as a percentage. In other words, the water retentivity of a mortar is expressed as the workability of the mortar before and after vacuum suction has been applied.

In contrast to the ASTM approach, the British standard (15) requires that water retentivity be calculated as the ratio of the mass of the water retained in the mortar after suction to the original water content.

It should be noted that any method of determining water retentivity, be it by vacuum suction or blotting paper, which requires the comparison of workabilities before and after suction rather than water contents, is not particularly suitable for establishing a minimum value of water retentivity in all mortars, i.e., 70 percent in ASTM standards, since high air content mortars subject to suction will lose workability by virtue of both loss of water and air, not just water alone.

Consistency Retentivity:

This property of fresh mortar may be assessed by repeating over a period of time any one of the workability tests described earlier in this paper, the value for consistency retentivity being expressed as the ratio of the workability at time t_1 to the workability at time t_0 .

4. TEST METHODS FOR FRESH MORTAR PROPORTIONS

The ability to determine quickly and accurately the proportions of the constitutive materials in a sample of fresh mortar is highly desirable.

4.1 Wet-Sieve Analysis:

This method of test (2, 12) requires that the water content of a mortar be determined on one sample, the aggregate content of a known mass of mortar on a second sample and the mass of the "dust" fraction of aggregate which approximates the fineness of the cementitious material on a sample of the aggregate. Given this information, the ratio of aggregate to cementitious material of the mortar can easily and accurately be calculated. The value obtained is, of course, by mass proportions not by volume.

The equipment necessary to conduct this test is shown in Figure 11.

4.2 Chemical Analysis:

The British standard (15) gives a chemical procedure for determining the proportion of portland cement to lime in a cement-lime mortar based on the known chemical composition of the two materials.

The method has not so far been adapted for determining the proportions of portland cement to masonry cement in mortars containing both these cements. However, it would appear possible to do so provided samples of the masonry cement are suitable for prior testing. This test is definitely a laboratory procedure.

We have no data at this time for the accuracy and coefficient of variability associated with this test.

4.3 Air Content:

The air content of fresh mortar mixed for a specified length of time may be thought of as being characteristic of the mix rather than as a constitutive material, in the sense that the air is introduced into the mix as an ingredient of the cementitious materials and is modified by the mixing action.

Masonry cement mortars have characteristically high air contents while lime mortars have characteristically low air contents.

There are three test methods recognized in the various standards for determining the air content of a mortar.

Gravimetric Method: (9, 15, 23)

This method requires detailed knowledge of the components of the mortar, i.e., mix proportions, the density of each of the constitutive materials and of the mortar; thus, although several standards reference this method, we consider it to be inappropriate for masonry mortar testing, especially so for site-prepared mortar.

Volumetric Method: (12)

This method requires no information about the mortar mix nor about the properties of the constitutive materials, permitting the determination of air content by water or alcohol replacement under agitation.

The apparatus is shown in Figure 12. The main disadvantage to this test is the degree of physical effort required during the agitation process.

A small "Chase air indicator" shown also in Figure 12. uses alcohol only to replace the air and yields values of air content with very little effort but having a high coefficient of variability.

Pressure Method: (12, 14, 24)

This method also requires no information about the mortar mix proportions or the properties of the constitutive materials and is a very simple method. A sample of mortar is put under pressure whence the air bubbles leave the body of the mortar and the mortar consolidates. The air content is read directly. A pressure meter is shown in Figure 12.

A proven accurate method from concrete technology, the pressure method is the test to be used for mortar.

Comparative Test Data

Figure 13 shows data from the same mortars obtained by the Chase air indicator and the pressure method. While there is obvious relationship, the correlation is not good and the scatter can be attributed mostly to variability in the Chase values.

5. RECOMMENDATIONS

On the basis of our experience with the application of the various test methods for fresh mortar discussed in this paper, we recommend that:

- a) in pre-construction testing, for gauging the site workability of the mortar, the Flow Table method should be used; the same method should be used to determine the consistency retentivity of the mortar intended for use on-site;
- b) on-site, to monitor workability if necessary, the Russian cone should be used;
- c) on-site, for quality assurance purposes, the mix proportions should regularly be checked using the wet-sieve analysis technique, and air content monitored by the pressure method.

Note that for tests b) and c) characteristic values should be established during pre-construction testing and that the objective of a quality-assurance program should be to control the mix proportions of the mortar.

6. ACKNOWLEDGEMENT

We acknowledge the financial support provided by a National Research Council of Canada IRAP grant.

REFERENCES

1. American Society for Testing and Materials, "Mortar for Unit Masonry", ASTM Standard C270-13, Part 16, 1977, pp. 146-150.
2. Canadian Standards Association, "Mortar and Grout for Unit Masonry", CSA Standard A179M, 1976.
3. Davison, J. I., "Development of the ASTM Specification for Mortar for Unit Masonry (C270)", Masonry: Past and Present, ASTM STP509, 1975, pp. 10-24.
4. Davison, J. I., "Mortar Technology", Proceedings, First Canadian Masonry Symposium, Calgary, Alberta, Canada, June 1976, pp. 12-21.
5. Anon, "Mortar Tests with the ASTM Flow Table" Experimental Building Station, TR 52/75/423, Department of Housing Construction, Australia, 1975.
6. Institute Belge de Normalisation, "Consistance Etalement a la Table Secousses", NBN 813-01, Belgium, 1969.
7. Canadian Standards Association, "Masonry Cement", CSA Standard A8, 1970.
8. American Society for Testing and Materials, "Flow Table for Use in Tests of Hydraulic Cement", ASTM Standard C230-68, Part 13, 1977, pp. 213-217.
9. Standards Association of Australia "Mortar for Masonry Construction", Proposed Revision to AS123-1963, July 1974.
10. Institute Belge de Normalisation, "Consistance - Mesure au Mobilmetre", NBN 813-02, Belgium, 1969.
11. RILEM/CIB Commission W3, "Report of the Work on Jointing Mortars of RILEM/CIB Commission W3 on Mortar and Renderings", Building Research Station, United Kingdom, 1965.
12. American Society for Testing and Materials, "Preconstruction and Construction Evaluation of Mortars for Plain and Reinforced Unit Masonry", ASTM Standard C780-74, Part 16, 1977, pp. 436-451.
13. Institute Belge de Normalisation, "Consistance - Penetration d'un Cone", NBN 813-09, Belgium, 1969.
14. Polski Komitet Normalizacyjny, "Mortars - Mechanical and Physical Tests", PN - 71/B - 04500, Poland, 1973.

15. British Standards Institution, "Methods of Testing Mortars and Specification for Mortar Testing Sand", BS 4551, 1970.
16. Institute Belge de Normalisation, "Consistance - Enfoncement d'une Bille", NBN 813-08, Belgium, 1969.
17. American Society for Testing and Materials, "Masonry Cement", ASTM Standard C91-75, Part 13, 1977, pp. 55-61.
18. American Society for Testing and Materials, "Bleeding of Cement Pastes and Mortars", ASTM Standard C243-65, Part 13, 1977, pp. 221-224.
19. Institute Belge de Normalisation, "Ressuage - Methode Au Tetrachlorure de Carbone", NBN B14-204, Belgium, 1972, 6 pp.
20. Institute Belge de Normalisation, "Ressuage - Methode a la Pipette", NBN B14-205, Belgium, 1972, 4 pp.
21. Institute Belge de Normalisation, "Mesure de la Stabilite d'Occlusion de l'Air", NBN B14-202, Belgium, 1973, 2 pp.
22. Institute Belge de Normalisation, "Mesure de la Prise et de la Stabilite", NBN 813-11, Belgium, 1970, 6 pp.
23. Institute Belge de Normalisation, "Mass Volumique du Mortier Frais Compacte", NBN B14-203, Belgium, 1972, 3 pp.
24. Institute Belge de Normalisation, "Teneur en Air du Mortier Frais Methode a Pression Variable", NBN 813-15, Belgium, 1971, 6 pp.
25. American Society for Testing and Materials, "Time of Setting of Concrete Mixtures by Penetration Resistance", ASTM Standard C403-77, Part 14, 1977, pp. 255-257.
26. Institute Belge de Normalisation, "Retention d'eau", NBN 813-07, Belgium, 1969, 3 pp.
27. Building Research Station, "Tests of the Working Properties of Mortars", Building Research Station Note No. C687, United Kingdom, 1959.
28. Huizer A., Ward M. A., Morstead H., "Field and Laboratory Study Using Current and Proposed Procedures for Testing Masonry Mortar" ASTM STP 589, 1975, pp. 107-122.
29. Jessop, E. L., "Variability in Masonry Mortar Quality and its Control", Phase One Completion Report on Masonry Research, Alberta Masonry Institute, March 1977.

TEST METHODS FOR DETERMINING THE PROPERTIES OF FRESH MORTAR

TABLE I

COUNTRY	PROPERTY	WORKABILITY	CONSTITUTIVE PROPORTIONS	AIR CONTENT	WATER RETENTIVITY	CONSISTENCY RETENTIVITY
AUSTRALIA		Flow Table (9) (ASTM) Slump Cone (9)		Gravimetric (9)	Vacuum (ASTM) (9)	
		Flow Table (6) (European) Cone Penetrometer (12) Dropping Ball (15) Mo-Meter (10)		Gravimetric (22) Pressure (23)	Filter Paper (25)	
BELGIUM			Ratio of Agg. to Cementitious Material (2)		Vacuum (7)	
CANADA		Flow Table (7) (ASTM)				
GREAT BRITAIN		Flow Table (14) (ASTM) Dropping Ball (14)	Chemical Analysis of Lime or Cement-Based Mortar (14)	Gravimetric (14) Pressure (14)	Filter Paper (14)	Dropping Ball (14)
POLAND		Russian Cone (13)		Pressure (13)	Vacuum (13)	
UNITED STATES		Flow Table (8) (ASTM) Cone Penetrometer (11)	Ratio of Agg. to Cementitious Material (11)	Pressure (11) Volumetric (11)	Vacuum (16) (ASTM)	Cone Penetrometer (11)

TABLE 2 - RESULTS OF WORKABILITY TESTS

TEST	Total Water Content (liters)		Type N Mortar	11.761**	14.261
	9.092*	10.511			
Flow Table (%) (12 Drops)	68	89	104	123	
Flow Table (%) (25 Drops)	92	122	141	150+ (beyond limit)	
Mo-Meter (Drops)	66	34	28	0 (beyond limit)	
Dropping Ball (mm)	7.6	11.5	14.0	17.5	
Cone Penetrometer (mm)	39	59	63	77	
Russian Cone (mm)	50	80	103	125	
Slump (mm)	8	16	55	94	

* Low Workability

** Site Workability

TABLE 3 - ACCURACY AND VARIABILITY OF WORKABILITY TESTS

TEST	ACCURACY		MEAN VALUE	STD DEVIATION	COEFFICIENT OF VARIATION (%)
	SPECIFIED	TEST METHOD			
Flow (25 days)	± 1 mm	± 1 mm	141.3	± 6.3	4.5
Mo-Meter			27.7	± 4.5	16.1
Dropping Ball	± 0.1 mm	± 0.025 mm	13.99	± 1.06	7.6
Cone Penetrometer	± 1 mm	± 1 mm	62.9	± 3.8	6.1
Russian Cone	± 5 mm	± 2.5 mm	103.0	± 2.5	2.4
Slump		1.0 mm	69.5	± 10.9	15.7

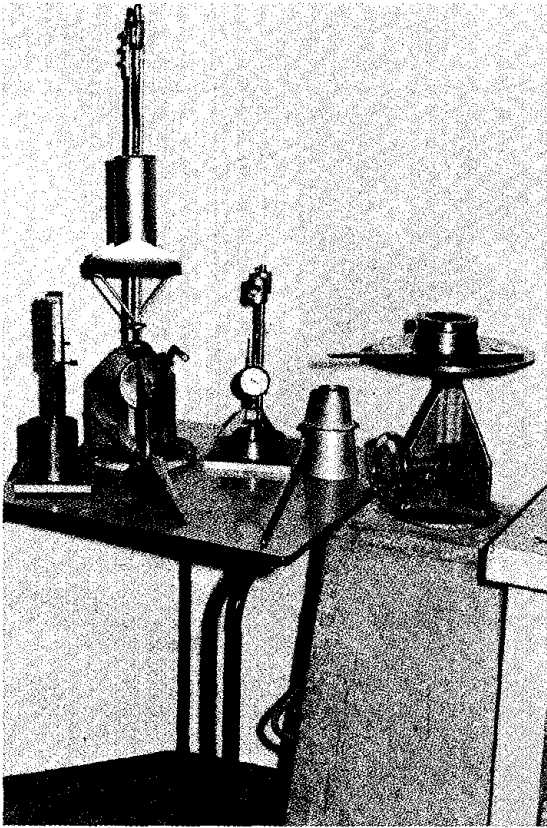


Figure 1
Test Methods for Determining the
Workability of Mortar

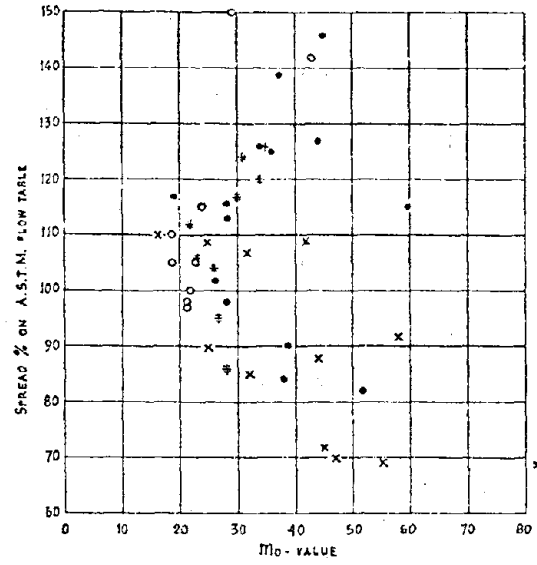


Figure 2
Comparison of ASTM Flow Table
and Mo-Meter

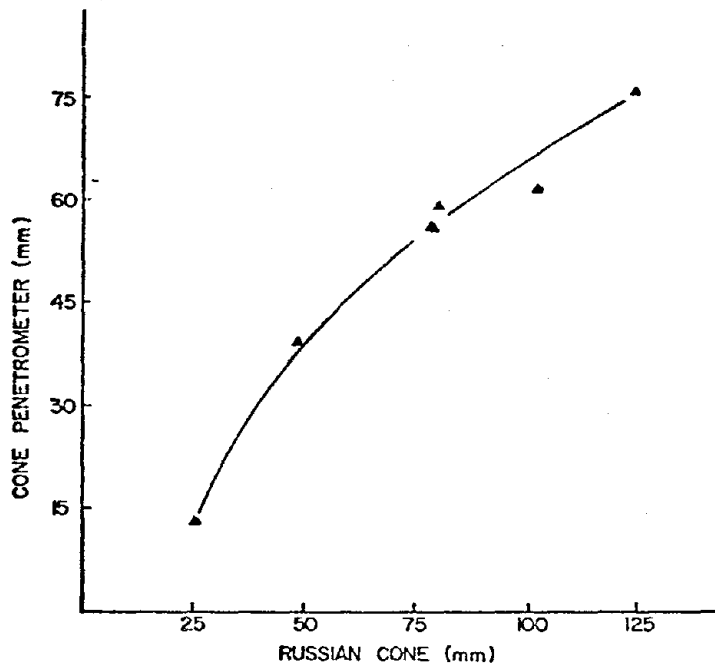


Figure 3
Comparison of Cone Penetrometer and Russian
Cone

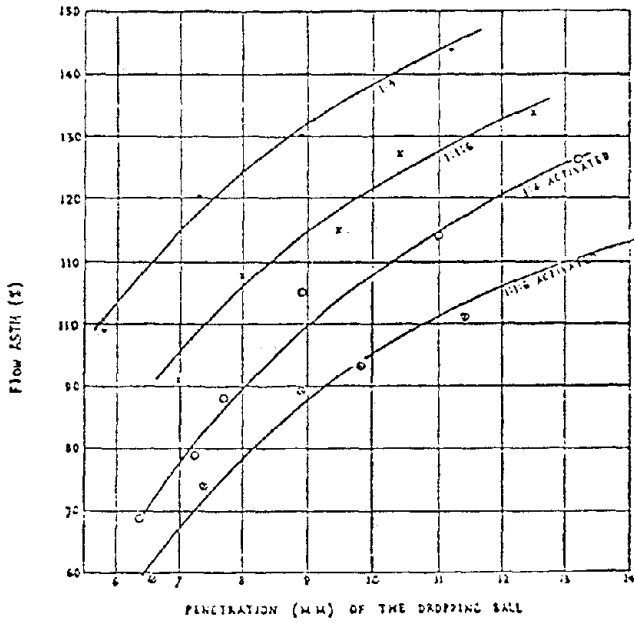


Figure 4

Comparison of ASTM Flow Table and Dropping Ball

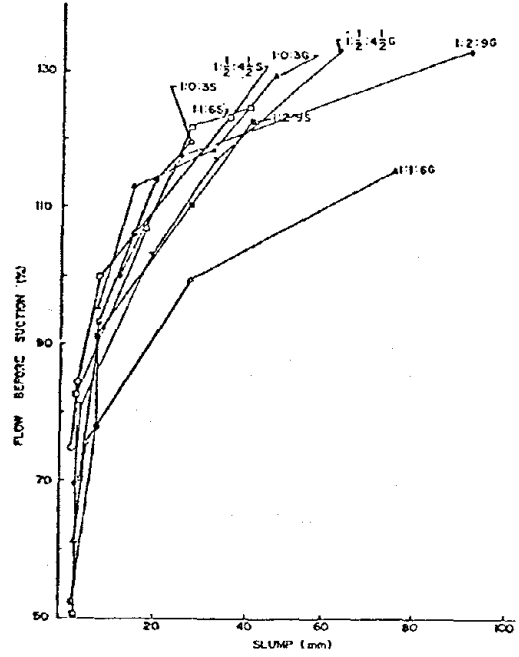


Figure 5

Comparison of ASTM Flow Table and Slump

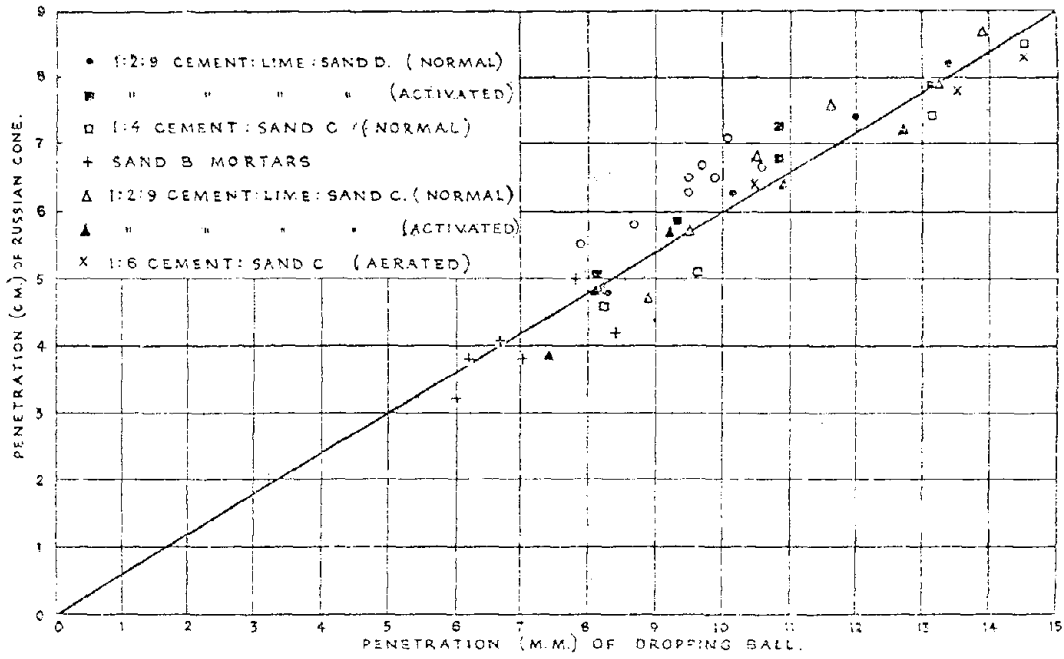


Figure 6

Comparison of Russian Cone and Dropping Ball

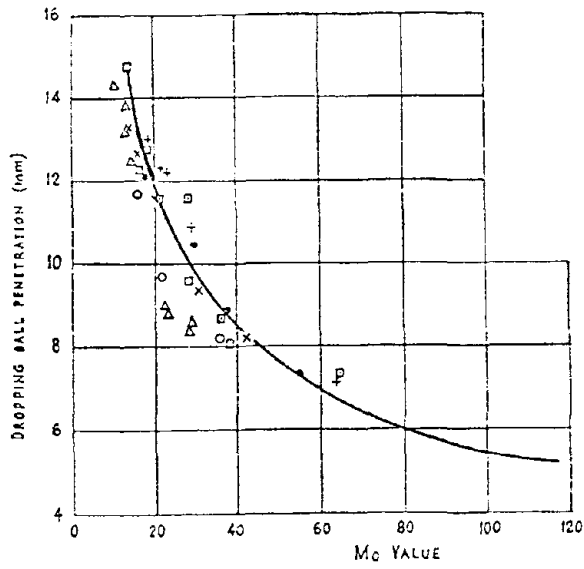


Figure 7

Comparison of Dropping Ball and Mo-Meter

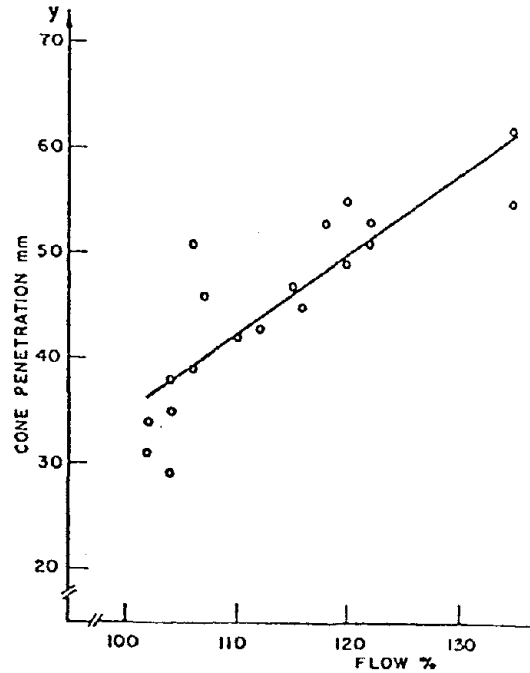


Figure 8

Comparison of Cone Penetrometer and ASTM Flow Table

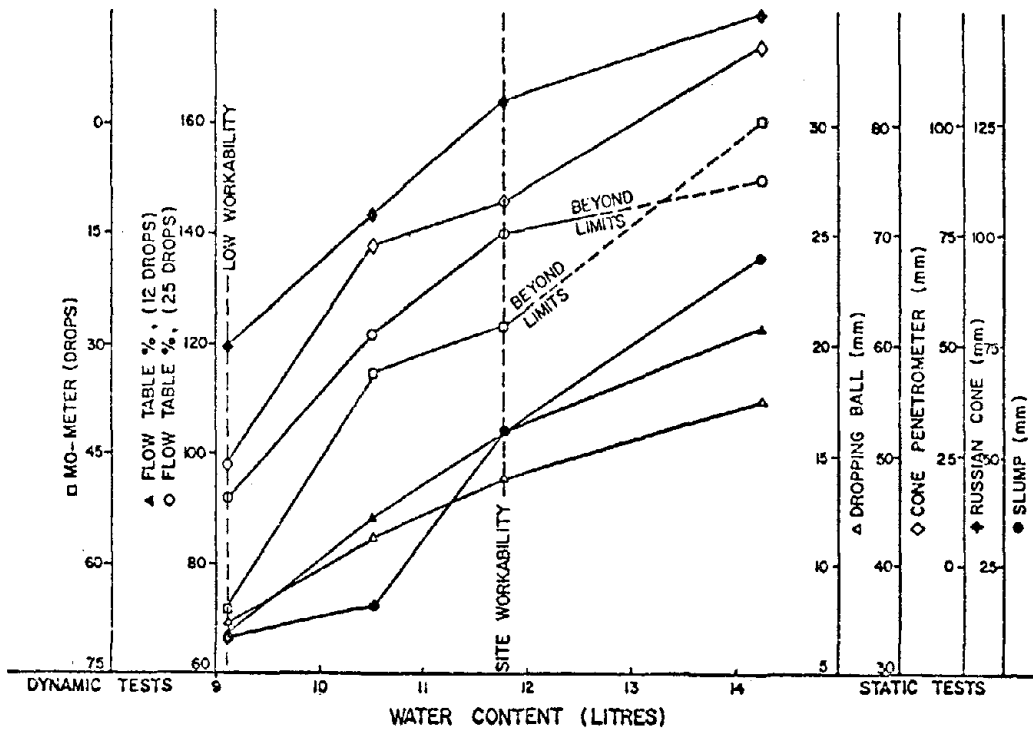


Figure 9

Sensitivity of Workability Tests

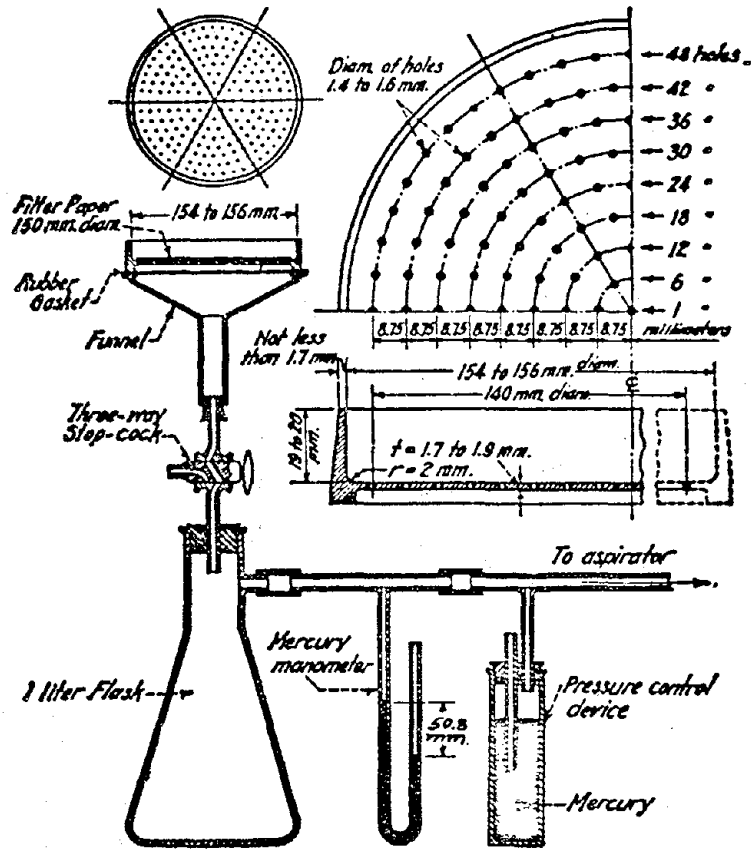


Figure 10
Apparatus for Determining Water Retention

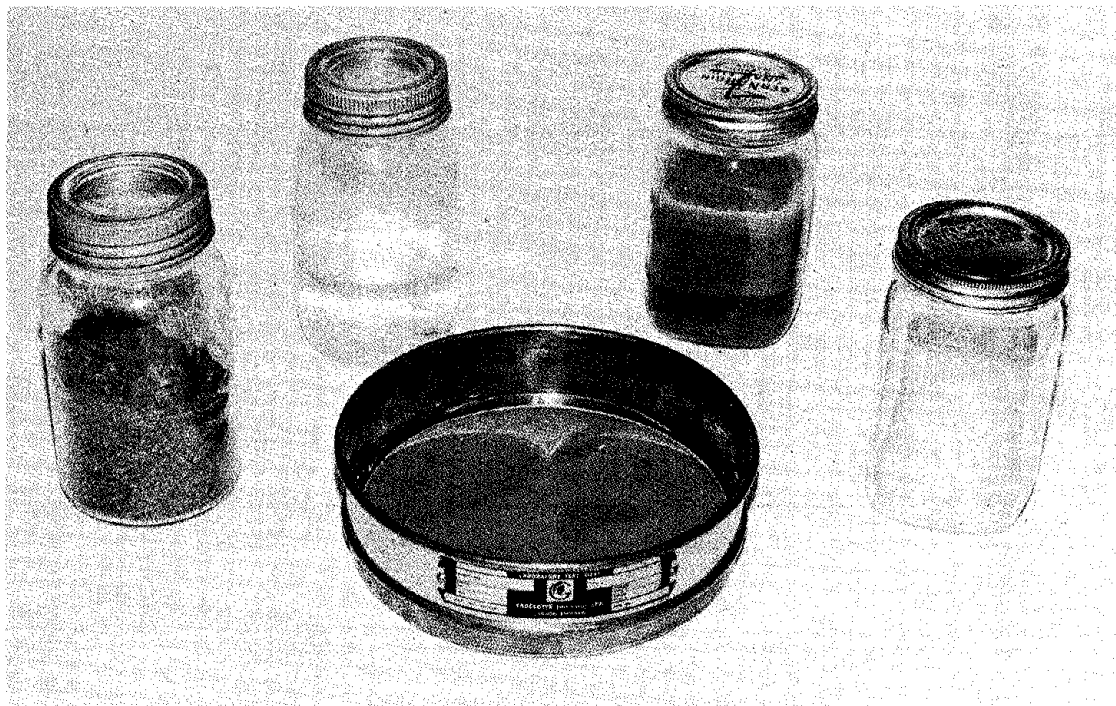


Figure 11
Apparatus for Wet Sieve Analysis

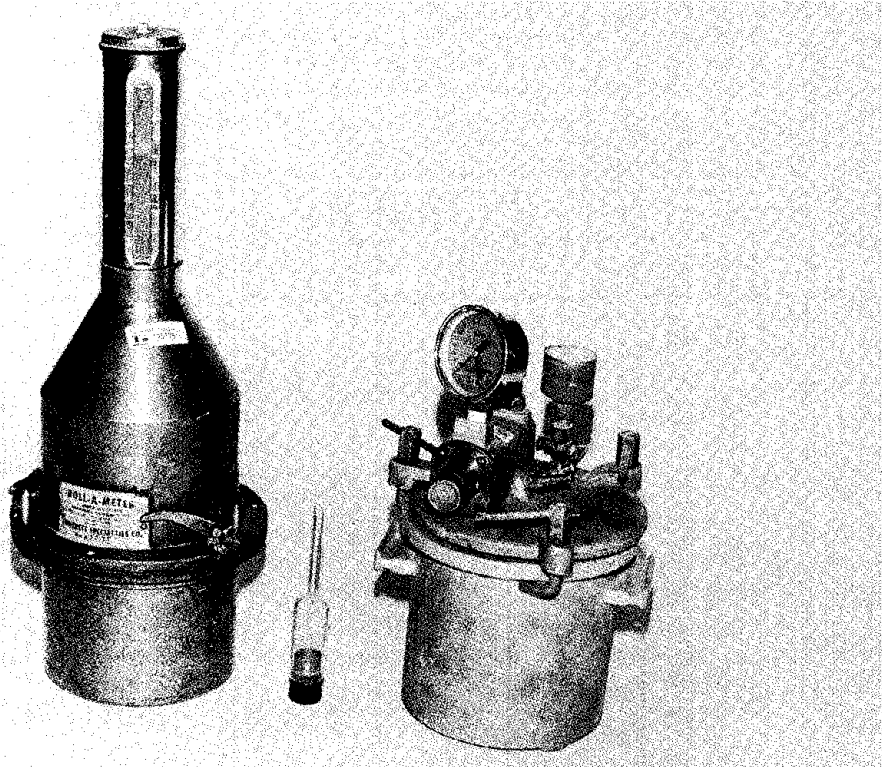


Figure 12
Apparatus for Determining Air Content

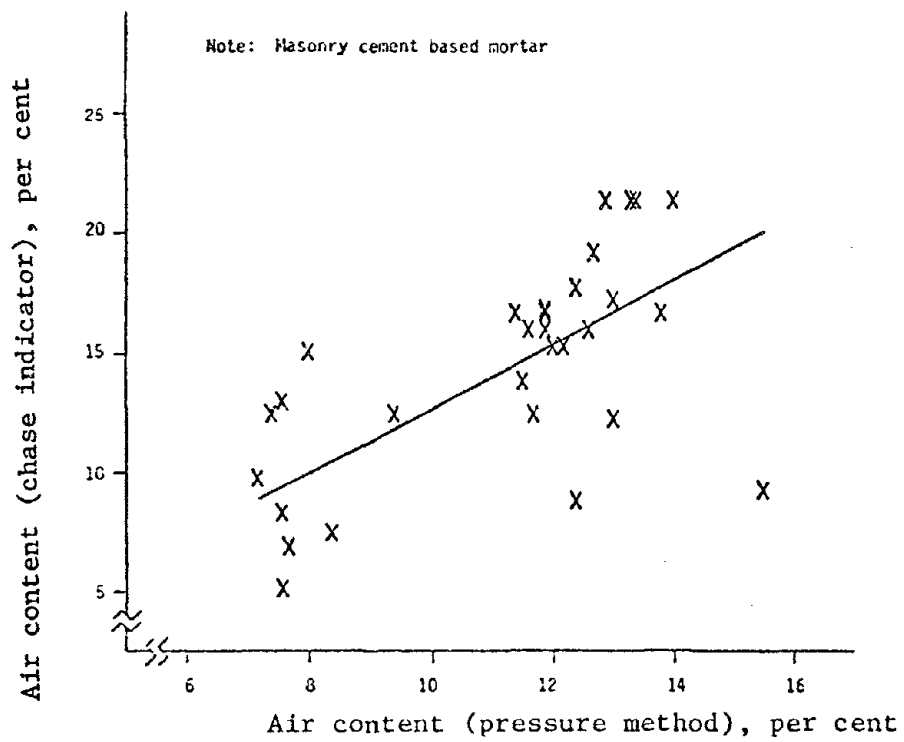


Figure 13
Comparison of Air Contents by Chase and Pressure Methods

NON-DESTRUCTIVE TESTING TECHNIQUES TO EVALUATE
EXISTING MASONRY CONSTRUCTION

by Luke M. Snell¹

ABSTRACT: One of the first requirements for a structural evaluation of an existing masonry structure is to determine the location and properties of the materials of construction. This evaluation can include the location and/or the quality of the grout or concrete within the masonry units, and the location and size of the steel reinforcements. It is desirable to select evaluation techniques that minimize damage to the structure; therefore, several non-destructive testing techniques have been applied to the evaluation of masonry construction.

The following non-destructive techniques that apply to the evaluation of masonry construction are briefly discussed:

1. Hammer Test
2. Probe Holes
3. Low Frequency Ultrasonics
4. Gamma Radiography
5. Pachometer

¹

Senior Materials Engineer, Law Engineering
Testing Company, Nashville, Tennessee

NON-DESTRUCTIVE TESTING TECHNIQUES TO
EVALUATE EXISTING MASONRY CONSTRUCTION

By Luke M. Snell,¹

INTRODUCTION

One of the requirements for an evaluation of an existing structure is to determine the integrity and properties of the in-place materials. Since many details of the original construction are hidden from view, the visual examination usually gives incomplete answers. A methodology of evaluating the in-place materials must, therefore, be selected. The evaluation technique must identify the general condition of the entire structure plus determine the locations and types of abnormalities. It must be cost effective, timely, and cause a minimal amount of structural and aesthetic damage.

In the last 50 years, several non-destructive testing (NDT) techniques have been developed to evaluate reinforced concrete structures. Some of these techniques have been applied directly to the evaluation of masonry construction. Other techniques were modified because of the several heterogeneous components (various types of masonry units, mortars, mortar reinforcements, cell reinforcements and grouts) that are included in masonry construction. The purpose of this paper is to briefly discuss some of the NDT techniques that have been used for field evaluations.

¹ Senior Materials Engineer, Law Engineering
Testing Company, Nashville, Tennessee

HAMMER TEST

The hammer test is probably the easiest and quickest of the NDT methods. This procedure will allow the investigator to determine the integrity of the individual masonry units and the bond between the mortar and the masonry units. The investigator can also determine if the cells are filled with grout. The technique requires an investigator to lightly tap the masonry unit with a hammer and listen to the resultant sound. Typically, the filled and well-bonded masonry construction will have a dull thud. Masonry construction with abnormalities or ungrouted cells will have a distinctive ring. This procedure obviously requires an experienced person with a good sense of hearing and a delicate touch.

This procedure is rather unsophisticated and many people do not consider it an "engineered test" because of its simplicity. However, this procedure does allow the experienced investigator to quickly survey a structure and identify areas where additional testing may be warranted.

PROBE HOLES

The probe hole procedure is performed by penetrating the areas of investigation with a small masonry bit and probing the hole with a stiff wire. After probing the hole, the investigator can determine the location and uniformity of the inner cell grout. The investigator can also measure the wall thickness of the masonry units.

The probe holes provide a positive examination of the individual masonry units since they are penetrated and examined. The equipment (bits, power drill and stiff wire) is relatively inexpensive and easy to use.

The probe hole method does damage the surface of the masonry units and repairs may be required for aesthetics as well as to insure that the units remain weather tight. To minimize damage and the need for repairs, the use of probe holes should be limited.

LOW FREQUENCY ULTRASONICS

Low frequency ultrasonics involves the use of a soniscope and two transducers (transmitter and receiver). The transmitter would be placed on one side of the wall and the receiver would be placed on the other side of the same wall, opposite the

transmitter. A low frequency ultrasonic sound wave would be sent from the transmitter to the receiver. The investigator would then examine the wave patterns on the soniscope to determine the time for the low frequency ultrasonic signals to be transmitted through the masonry unit and the relative strength of the received signals. If the received signals are approximately as strong as the transmitted signals, the investigator can assume that the masonry units are continuous (without voids or cracks). If the received signals are weaker than the transmitted signals, the investigator can assume that the masonry units are not continuous (containing voids or cracks).

The soniscope can also be used to estimate the strength of masonry construction. This procedure requires a correlation of the average pulse velocity through masonry units and mortars as determined with the soniscope and the compressive strength of cores or prisms that were removed from the wall and tested. This correlation would be required for each job. A general correlation developed from field data of pulse velocity (average of 10 readings) and site conditions are shown below:

<u>AVERAGE PULSE VELOCITY</u> <u>(FEET PER SECOND)</u>	<u>CONDITIONS REPRESENTED</u>
Below 4000	Cracks and/or voids, questionable construction (strength less than 500 psi)
4000 to 6000	Low strength masonry construction (strength of 500 to 1500 psi)
Above 6000	Moderate to high strength masonry construction (strength over 1500 psi)

The low frequency ultrasonic signals across construction with more than one wythe are usually quite weak and require careful visual observations by an experienced investigator. Reductions in signal strength are attributed to energy losses occurring as the signals travel through the various media. Attempts to use equipment with gated clocks have proven unreliable since a strong output signal would be required to stop the gated clock. This strong output signal is not normal; therefore, the use of this particular equipment has been unsuccessful.

The soniscope and transducers are quite expensive and usually only available from researchers and consultants that specialize in construction materials evaluation. The operator should be an engineer that is experienced in this procedure since it requires detailed field interpretation of the wave patterns on the soniscope. For these reasons, the cost of this testing procedure may be prohibitive for routine investigations.

The low frequency ultrasonic test procedures can be a rapid and sophisticated testing procedure for evaluation of the continuity and strength of the masonry walls. The writer recommends that if this procedure is to be used, that a firm or an individual experienced in the use of low frequency ultrasonics review the scope and purpose of the evaluation program prior to the start of the investigation.

GAMMA RADIOGRAPHY

Gamma radiography requires the use of a gamma radiation source, X-ray film and dark room equipment. The procedure requires that the gamma radiation source be set up on one side of the area to be examined with the X-ray film on the opposite side. After the source exposes the film (usually requiring several minutes), the film is processed. The engineer or radiographic technician can interpret the X-ray film and determine the location of steel reinforcements and void areas within the masonry. The steel reinforcements will be evidenced by a light line on the film. Void areas within the masonry would be evidenced by dark, irregular patches.

The use of gamma radiation requires extensive safety procedures. The equipment and personnel must be licensed with the state regulatory agencies. The areas where X-rays are to be taken must be isolated by roping off the area for the duration of the exposure. The safety requirements, trained personnel, and expensive equipment can cause the cost of this technique to be prohibitive for routine projects. Gamma radiography techniques have been cost effective for only specialized investigations, such as distressed precast masonry units. This procedure has usually been used to provide a permanent record of the details of construction for possible litigation.

PACHOMETER

The pachometer is a magnetic detector and its operation is based on the presence of steel which causes a variation in the magnetic field. This variation can be correlated to the depth or the size of the reinforcement. The equipment is used by scanning the surface

of the masonry units with the probe. When a maximum reading is obtained, the probe is stopped and the dial is read. The location of the steel reinforcement is assumed under the probe. The dial reading can be used to estimate either the size or depth of the steel in lightly reinforced construction. In heavily reinforced masonry or construction with both joint and cell reinforcement, information about the steel depth or size is difficult to determine. Each reinforcement will cause a variation in the magnetic field, thus, the details of the reinforcement at a particular location cannot be separated. When these details are needed, probe holes will usually be included in the investigation.

CONCLUSIONS

The applications of NDT methods to masonry construction is relatively new. The present methods discussed above have been successfully applied to evaluating masonry construction. Many refinements to the present testing methods and new testing techniques, are necessary for advancements. The writer is confident that several of the new developments, such as low energy penetration, microwave absorption and acoustic emission tests will find unique applications for the field evaluation of masonry construction.

AN APPLICATION OF THIN WALL MASONRY

By Pyle, Don T.

ABSTRACT: Single wythe masonry walls, coupled with concrete floor and roof framing systems, are especially suited to construction of multi-unit residential projects and small office buildings. In spite of the current popularity of single wythe construction, it presents considerable design difficulties to the architect and structural engineer. A construction system and a special masonry to concrete connection, using standard construction materials and procedures, are proposed to solve some of the design problems and to reduce construction cost.

AN APPLICATION OF THIN WALL MASONRY

By Don T. Pyle¹

INTRODUCTION AND DISCUSSION

Recent advances in material technology and structural engineering design practice have resulted in increasing use of "Thin Wall" (single wythe) masonry construction. The ever increasing cost of new construction has made this type of masonry work especially attractive in some situations, where savings in both material and labor can be achieved over more traditional multi-wythe wall systems.

Single wythe masonry construction is especially well suited to multi-unit residential projects such as apartments and dormitories, and to small multi-story office buildings. For a number of reasons this type of masonry construction is frequently coupled with a concrete flat slab or plate for the floor and roof framing.

Yet, in spite of the appeal and economy of this building system, it presents considerable difficulties to the architect and structural engineer. If the floor and roof are to be supported on the masonry walls, an important problem is the question of how to detail and design the typical exterior bearing wall section. The traditional approach has been to "build in" the floor or roof system in order to transfer vertical and horizontal forces between the wall and floor. With single wythe construction, this type of detailing is difficult or impossible to accomplish. The floor or roof must pass through the wall (resulting in exposure of the floor or roof system on the opposite side, and considerable change in the architectural design) or the floor or roof system must terminate at the near face of the wall (resulting in eccentricity of load application and difficult or potentially expensive connections between the floor/roof and wall).

On the other hand, if the floor and roof are not supported on the masonry walls, another set of problems must be faced: how to control long term deflections at the perimeter of the floor/roof slabs, and how to conveniently and economically transfer forces between the masonry shear walls and the floor/roof framing systems.

One common solution to the deflection problem is the use of concrete spandrel beams formed and placed as part of the floor/roof sys-

¹Principal, KKBNA Consulting Engineers, Denver, CO

tem. However this involves more material, form work and labor, and significantly increases the cost of a normal flat plate framing system.

Supporting the flat plate on masonry bearing walls rather than on columns also solves the deflection problem. However this may severely restrict the floor plan. Also, many general contractors are less comfortable with this system since they often find it more difficult to control construction scheduling and sequencing.

Continuous steel ledge angles are frequently bolted to the edge of concrete slabs to support the masonry cladding. This can add considerable cost, and result in the structural system supporting the masonry walls even though the masonry walls are entirely capable of supporting themselves.

To overcome some of these design and cost disadvantages, the author has used a variation of these conventional approaches with considerable success on several recent projects. The construction system proposed is described as follows:

1. The floor and roof framing consist of conventional flat plates or slabs supported on interior and exterior columns. However the columns are designed for vertical load only since the masonry walls will be used to provide lateral stability.
2. After construction of the floor slabs has progressed to one or more floors above the ground level, laying of the exterior single wythe masonry walls can begin, independent of the concrete construction schedule.
3. The key to the proposed system is the means used to connect the floor slabs to the masonry walls. Using standard inexpensive hardware and the theory of shear friction, the connection is economical, easy to make, and theoretically strong enough to transfer considerable force between the wall and slab system.
4. The masonry walls are designed to resist the lateral forces normal to their surface, lateral shear forces to provide overall building stability for seismic and wind loading, and vertical live and dead loads from the edge of the floor slab to control edge deflections caused by application of live load and long term creep deflection.

Some of the advantages to be gained from this system are: the use of simplified, conventional construction procedures and systems, work most contractors are familiar with; the ability of the contractor to schedule concrete work for the structure and masonry work independently of each other; use of the masonry to support its own weight, to control floor/roof edge deflections, and to provide all of the building's lateral stability; maximum flexibility of floor plan layout with minimum restrictions due to column and wall locations, and wall openings; and elimination of the usual expense of spandrel beams and/or ledge angles.

THE CONNECTION

Specific details of the proposed shear friction connection are shown in Figure A. The connection is designed to carry direct tension, plus horizontal and vertical shear in the plane of the masonry wall. For the shear design, the standard shear friction design procedures for reinforced concrete have been utilized. Based on this theory, a 5/8" steel bolt is good for an allowable load of approximately 2 kips, more than adequate for the usual type of building project proposed.

SUMMARY AND CONCLUSIONS

A simplified method for providing structural connections between single wythe masonry walls and concrete floor/roof systems has been presented. It is the author's opinion this connection solves several of the problems the architect and structural engineer must face in the design of one class of typical masonry buildings, and eliminates some of the costly elements that are often used. The author feels the proposed connection has sufficient merit to warrant a research and development program to further develop its potential and capability.

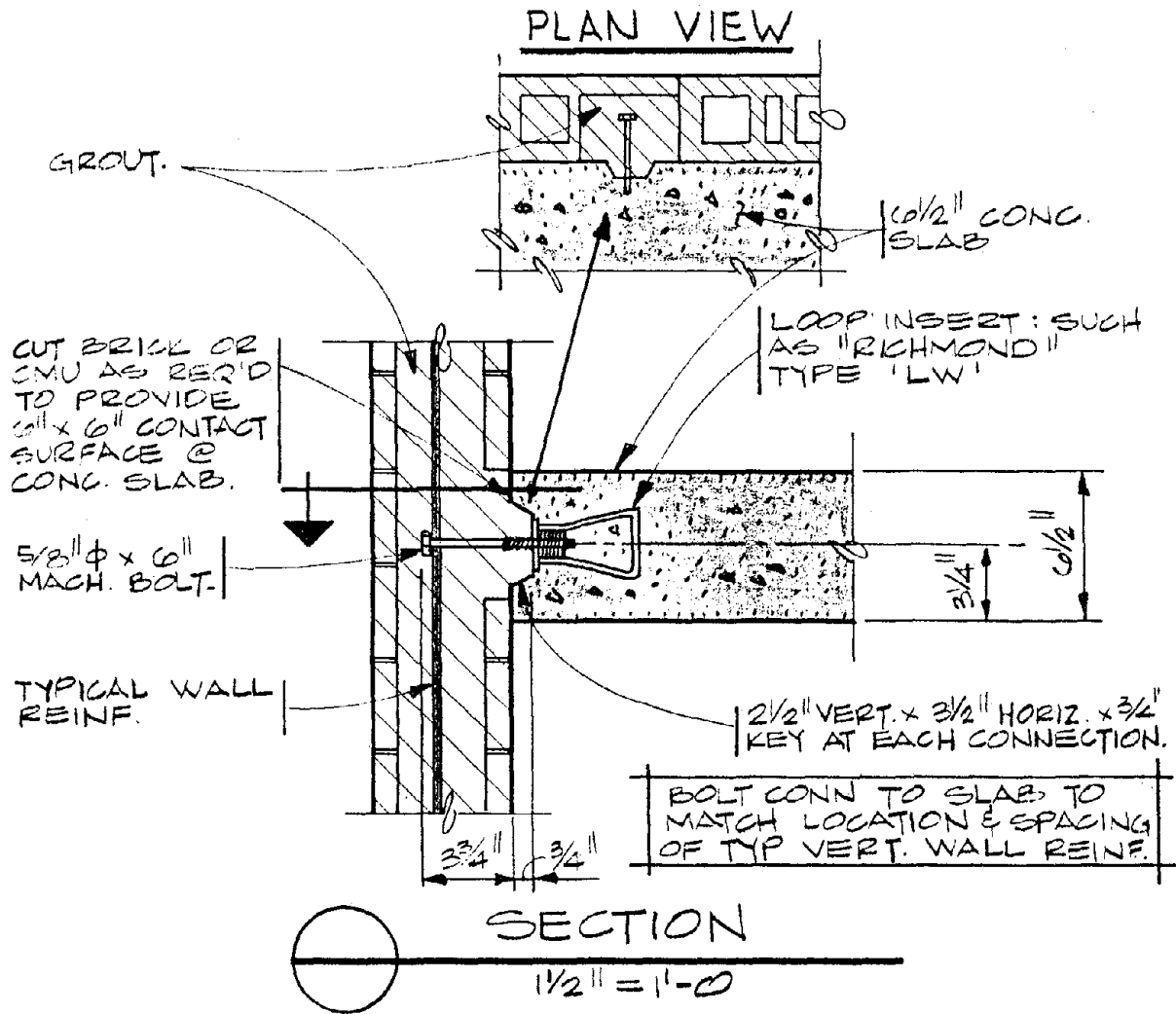


FIGURE A

CASE STUDY - COMPUTERIZED DESIGN FOR LOAD BEARING MASONRY

By Vannoy, D.,¹ Harvey, H. E.,² and Colville, J.³

ABSTRACT: A seven story load bearing masonry building (Locust House) is analyzed using a computer program for the rational analysis of masonry structures which was developed by the Masonry Institute of Maryland. The Locust House is scheduled for beginning of construction in the spring of 1978 and completion 15 months later. Located in Westminster, Maryland the building has 73,500 square feet of space and is a government assisted housing for the elderly.

This paper illustrates how data is prepared for input into the computer program for a typical building using the Locust House as a case study. The results from the program give the required compressive strength for each wall on every floor for all loading combinations used in design. From the case study, this paper illustrates and discusses how changes in floor plan and wall dimensions are changed to develop an effective and economical final design for Locust House using the computer program.

Architects and engineers will find the accurate and comprehensive information provided in the printout an extremely useful and time saving tool for design review. In addition, the printout provides a firm with a permanent record of the analysis.

¹ Assistant Professor, University of Maryland, College Park, Md., 20742

² Structural Engineer, Gaudreau, Inc., Architects-Planners-Engineer, Baltimore, Md.

³ Associate Professor, University of Maryland, College Park, Md., 20742

CASE STUDY
COMPUTERIZED DESIGN FOR LOAD BEARING MASONRY

By Donald W. Vannoy,¹ Harold E. Harvey,²
and James Colville³

INTRODUCTION

A seven story load bearing masonry building (Locust House) is analyzed using a computer program for the rational analysis of masonry structures which was developed by the Masonry Institute of Maryland (1)⁴. The Locust House is scheduled for beginning of construction in the spring of 1978 and completion 15 months later. Located in Westminster, Maryland the building has 73,500 square feet of space and is a government assisted housing for the elderly.

This paper illustrates how data is prepared for input into the computer program for a typical building using the Locust House as a case study. The results from the program give the required compressive strength for each wall on every floor for all loading combinations used in design. From the case study, this paper illustrates and discusses how changes in floor plan and wall dimensions are changed to develop an effective and economical final design for Locust House using the computer program.

Architects and engineers will find the accurate and comprehensive information provided in the printout an extremely useful and time saving tool for design review. In addition, the printout provides a firm with a permanent record of the analysis.

DESCRIPTION OF PROJECT

This is a privately owned project developed under the Rental Housing Program of the Maryland Community Development Administration. Under this program the owner may obtain long term (up to 42 years) low interest financing that combines the construction loan and permanent loan for 90% of the total development cost. The agency obtains its

¹ Assistant Professor, University of Maryland, College Park, Md., 20742

² Structural Engineer, Gaudreau, Inc., Architects-Planners-Engineer, Baltimore, Md.

³ Associate Professor, University of Maryland, College Park, Md., 20742

⁴ Numerals in parentheses refer to corresponding items in the Appendix I.

mortgage capital from the sale of tax exempt bonds. The projects are not low income developments but seek an economic mix of tenants. The object is to utilize the savings which accrue from the low interest bonds to produce quality housing at rents marketable to families with incomes of \$9000 to \$19000. In addition, under certain circumstances, higher income tenants will be admitted, and a portion of the units are eligible for rent subsidies from the Federal Section 8 HUD (Department of Housing and Urban Development) Program. These subsidies can assist families with incomes as low as \$2000.

Westminster, a small city of 7,000 is located 30 miles northwest of Baltimore. It is the county seat of Carroll County, historically a thriving agricultural county. During the last 15 - 20 years the County has gradually become, on a large scale, a collection of bedroom communities for the Baltimore Metropolitan area. Also, the County has been somewhat successful in its efforts to attract light industrial development. Simultaneous with these two trends has been the construction of shopping centers and their incidental commercial development on the perimeter of the City. The result of these 3 factors is a typical town center struggling to maintain some of its previous position as the center of business and commerce. Locust House is located on a mid-town site near the commercial areas in need of revitalization. The 1.14 acre site is covered 21% with building and 20% with parking. The remaining 59% is devoted to careful landscaping and extensive planting. The project was required to meet strict architectural and landscaping requirements of the City Planning Commission. Locust House is thus expected to make a significant contribution to the revitalization process.

Locust House is a rectangular, slightly H shaped, double loaded corridor, 65 foot high building containing 98 rentable one bedroom units of 531 square feet. As a means of assuring adequate quality housing, the Community Development Agency requires compliance with the HUD Minimum Property Standards. The HUD standards require seismic design in accordance with the Uniform Building Code and provisions to prevent progressive collapse. The local building Code is the 1975 BOCA Code. In Appendix B of BOCA, the American National Standards Institute's "Building Code Requirements for Minimum Design Load Requirements for Buildings and Other Structures" ANSI - A58.1 - 1972 is listed as an accepted Engineering Practice. Section 6 of this standard is the result of recent research and is a comprehensive wind code. Therefore, it was adopted as the criteria for wind loads, applying a 50 year storm. The design data and material properties are summarized in Table 1.

Westminster is an old, very traditional town with virtually all significant buildings finished in brick. To be in harmony with its surroundings, brick facing thus became a requirement from the outset. Slag aggregate concrete masonry units are an economical readily available building material in the region, and it was felt that bearing and shear walls of this material would provide the most lightweight, economical and convenient system of vertical elements that could be designed

TABLE 1DESIGN DATA AND MATERIAL PROPERTIES

DESIGN DATA

TOTAL FLOOR AREA	73,500 Ft.
NO. OF STORIES	7
NO. OF UNITS	98 Rentable units
TOTAL BUILDING HEIGHT	65 Ft.

STRUCTURAL DESIGN REQUIREMENTS (design based on allowable loads and stresses)

*Stresses:

- fc-3300 p.s.i. for slabs on grade
- fc-3000 p.s.i. for all other poured concrete
- fs-24000 p.s.i. for all reinforcing steel
- fy-36000 p.s.i. (yield point) for all structural steel

*Soil Bearing Capacity: 4000 P.S.F. for total load
2500 P.S.F. for dead load

*Live Loads:

- Roof - 20 P.S.F.
- Stairs - 100 P.S.F.
- Social Area, Laundry Room and Elevator Machine Room - 100 P.S.F.
- Corridors - 80 P.S.F.
- All Other Floors - 40 P.S.F.
- Snow Load - varies as per 1975 BOCA Code
- Seismic Loads and Design - as per 1976 Uniform Building Code
- Wind Loads - as per BOCA Code appendix B and A.N.S.I. A58.1-1972.

to meet seismic and progressive collapse requirements. Furthermore, the use of engineered masonry design concepts results in thin economical elements that satisfy vertical load requirements. Dry floor and roof systems were selected because of their economy, speed of construction, and freedom from weather related delays. Lightweight precast prestressed concrete quad tees were chosen for the floors. The roof system is open web steel joists and steel deck. Masonry elevator and stairwell walls were chosen because of their fire resistance and ease of supporting guide rails and stair framing. Because concrete masonry bearing walls were a natural adjunct to the brick masonry facing, masonry shaftways and stairwells, and the bearing walls worked well with the chosen floor and roof systems, and because of the factors described above. Hollow concrete masonry bearing and shear walls were used.

COMPUTER PROGRAM FOR THE RATIONAL ANALYSIS OF MASONRY STRUCTURES

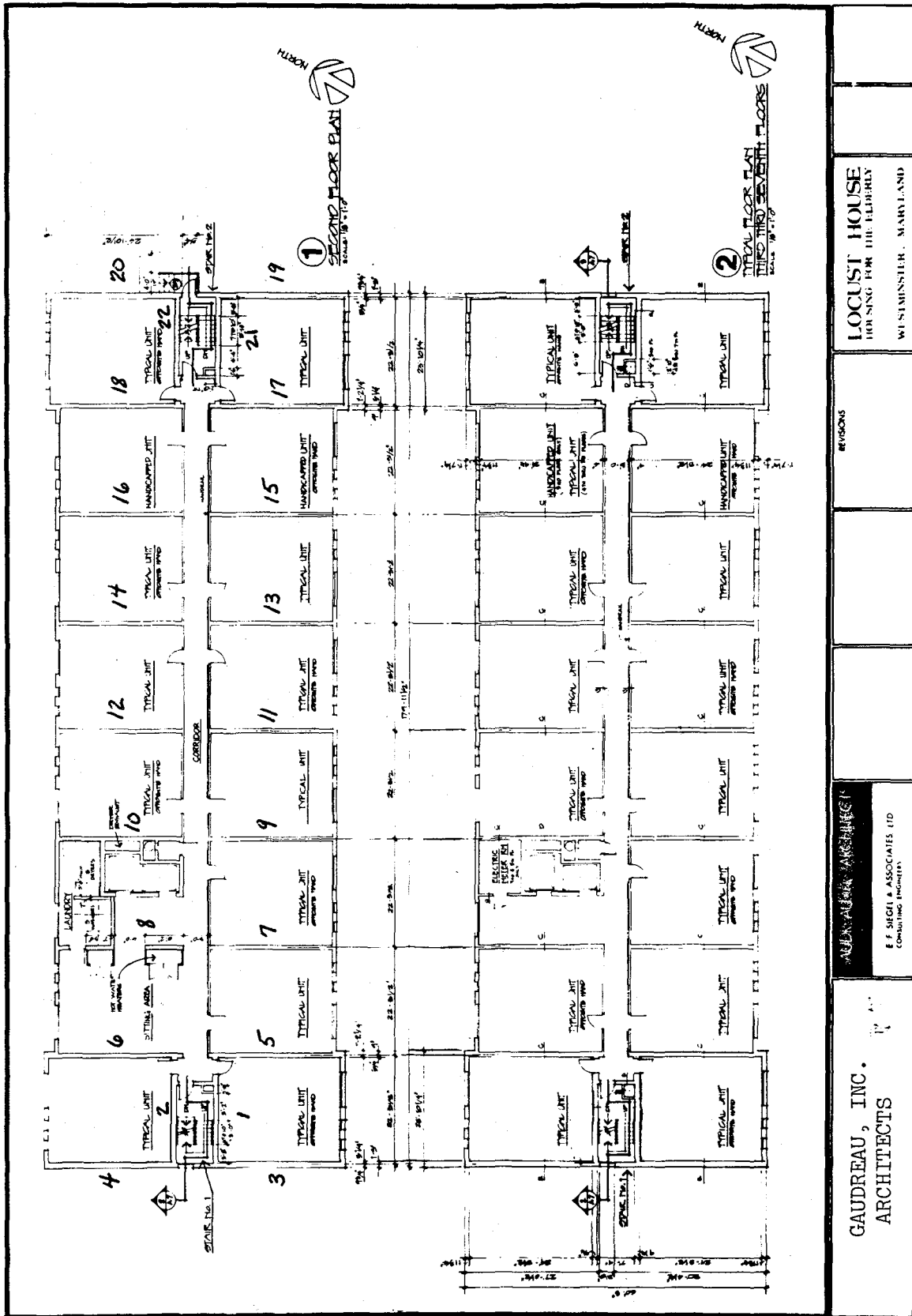
A computer program for the rational analysis of non-reinforced engineered masonry construction from the Masonry Institute of Maryland, Inc. was used in this project. This program follows the Building Code Requirements for Engineered Brick Masonry, August 1969, published by the Brick Institute of America, and the Specification for the Design and Construction of Load-Bearing Concrete Masonry, February 1975, published by the National Concrete Masonry Association.

From the floor layout in Figures 1 and 2, the walls are number from 1 to 22 as shown. The data input forms are completed for the project according to the instructions provided by the Masonry Institute of Maryland and are shown in Figures 3 to 8.

The computer output includes echo printing of all input data for checking purposes and to provide a record of the problem, but the printing will not be shown here due to space imitation. The results of the stress analysis are then printed for every wall on every floor. A copy of the results for walls 11 to 20 on floors 1 to 7 is shown in Figure 9 as an example of the printout from the program.

The wall number and floor number are identified in the first two columns. For each wall the required compressive strength f'_m which is assumed equal to the compressive stress $f_m/0.20$ is printed for each of seven different load combination as follows:

- Case 1 - Total load and parallel wind
- Case 2 - Dead load and parallel wind
- Case 3 - Dead load and reduced live load
- Case 4 - Total load and perpendicular wind or earthquake
- Case 5 - Dead load and perpendicular wind or earthquake
- Case 6 - Total load and parallel earthquake
- Case 7 - Dead load and parallel earthquake



FIGURES 1 AND 2. TYPICAL FLOOR PLANS

INPUT DATA FORMS
FOR
RATIONAL ANALYSIS OF MASONRY STRUCTURES
(REV. 6/76)
See
Addendum #1

1. Job Identification

Job Name: Locust House
 Engineer/Architect: Gaudreau INC.

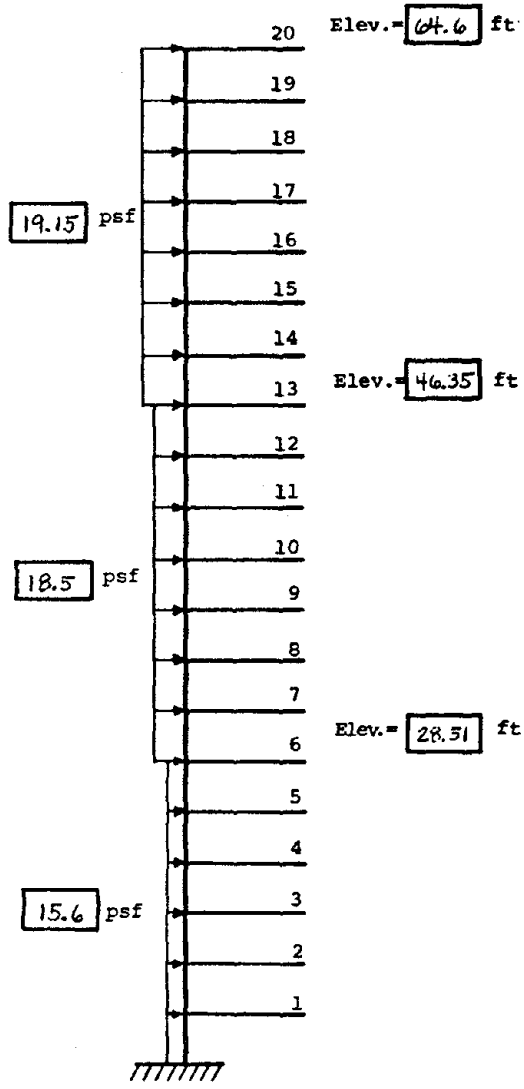
2. General Information

Number of Floors = Importance Factor =
 Earthquake Zone = Soil Factor =
 Live Load Reduction Factor
 (Check One) Uniform Building Code Baltimore City Code

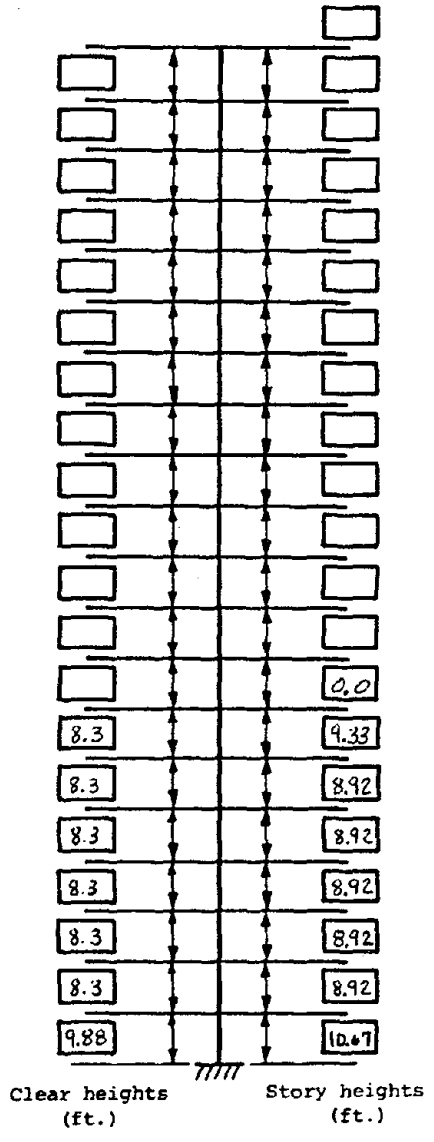
3. Gravity Loads

Roof Live Load = psf.
 Roof Dead Load = psf.
 Floor Live Load = psf.
 Floor Dead Load = psf.
 Miscellaneous Weight = kips.

FIGURE 3. INPUT DATA FORM - GENERAL INFORMATION AND GRAVITY LOADS



4. Wind Load Data



5. Story Heights

FIGURE 4. INPUT DATA FORM - WIND LOAD DATA AND STORY HEIGHTS

6. Table 1 - Wall Locations

Wall No	x-Coordinate ft	y-Coordinate ft	Wall No	x-Coordinate ft	y-Coordinate ft
1	9.69	26.36	26		
2	9.69	34.69	27		
3	0.68	15.73	28		
4	0.68	57.15	29		
5	23.23	14.43	30		
6	23.23	46.66	31		
7	45.52	15.27	32		
8	45.52	45.81	33		
9	67.81	15.27	34		
10	67.81	45.81	35		
11	90.10	15.27	36		
12	90.10	45.81	37		
13	112.39	15.27	38		
14	112.39	45.81	39		
15	134.68	15.27	40		
16	134.68	45.81	41		
17	156.97	15.27	42		
18	156.97	45.81	43		
19	179.26	15.73	44		
20	179.26	57.15	45		
21	170.02	26.36	46		
22	170.02	34.69	47		
23			48		
24			49		
25			50		

FIGURE 5. INPUT DATA FORM - WALL LOCATIONS

7. Building Plan Dimensions

The overall plan dimensions of the building may be different at each floor level. Thus the plan dimensions, measured from the reference axis, for each floor level are needed.

Table 2 - Building Plan Dimensions

Floors	x_1 ft	x_2 ft	y_1 ft	y_2 ft
1	0.0	179.71	0.0	61.08
↓	↓	↓	↓	↓
7	0.0	179.71	0.0	61.08

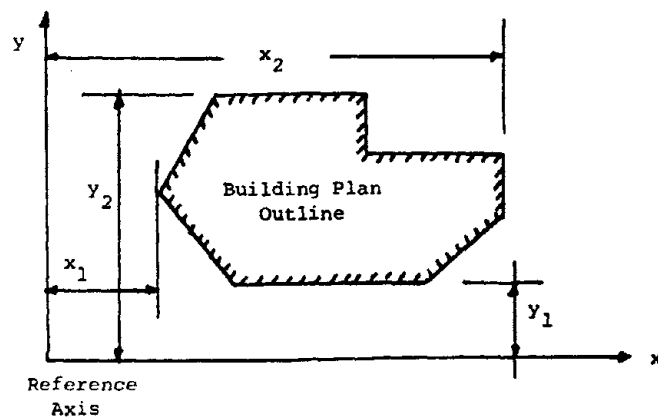


FIGURE 6. INPUT DATA FORM -- BUILDING PLAN DIMENSION

8. Table 3 - Wall Loading Data

Wall No	SL (ft)	SS (ft)	EL (ins)	ES (ins)	DF	TRIB (ft ²)	TOTA (ft ²)
1	6.40	0.0	4.5	0.0	0.0	93.0	138.0
2	6.40	0.0	4.5	0.0	0.0	93.0	138.0
3	10.81	0.0	2.65	0.0	1.0	323.0	323.0
4	10.81	0.0	2.65	0.0	1.0	284.0	284.0
5	10.81	10.81	2.65	2.65	1.0	590.0	590.0
6	10.81	10.81	2.65	2.65	1.0	590.0	590.0
7	10.81	10.81	2.65	2.65	1.0	548.0	548.0
8	10.81	10.81	2.65	2.65	1.0	548.0	548.0
9	10.81	10.81	2.65	2.65	1.0	548.0	548.0
10	10.81	0.0	2.65	0.0	1.0	274.0	274.0
11	10.81	10.81	2.65	2.65	1.0	548.0	548.0
12	10.81	10.81	2.65	2.65	1.0	548.0	548.0
13	10.81	10.81	2.65	2.65	1.0	548.0	548.0
14	10.81	10.81	2.65	2.65	1.0	548.0	548.0
15	10.81	10.81	2.65	2.65	1.0	548.0	548.0
16	10.81	10.81	2.65	2.65	1.0	548.0	548.0
17	10.81	0.0	2.65	2.65	1.0	590.0	590.0
18	10.81	0.0	2.65	2.65	1.0	590.0	590.0
19	10.81	0.0	2.65	0.0	1.0	323.0	323.0
20	10.81	0.0	2.65	0.0	1.0	284.0	284.0
21	6.40	0.0	4.5	0.0	0.0	93.0	138.0
22	6.40	0.0	4.5	0.0	0.0	93.0	138.0
23							
24							
25							

FIGURE 7. INPUT DATA FORM - WALL LOADING DATA

9. Table 4 - Wall Data

Wall No	Floors	I _x ft ⁴	I _y ft ⁴	C ₁ ft	C ₂ ft	Area ft ²	t ft	Unit wt lbs/CF	Type	Cavity Factor
1	1→2	0.0	523.46	9.32	9.32	18.08	1.00	128.0	6	0.0
1	3→7	9.99	135.14	9.32	9.32	4.66	1.00	220.0	4	
2	1→2	0.0	523.46	9.32	9.32	18.08	1.00	128.0	6	
2	3-7	9.99	135.14	9.32	9.32	4.66	1.00	220.0	4	
3	1-7	465.0	5.34	14.96	14.96	6.23	.67	183.0	3	
4	1-7	315.46	4.7	13.15	13.15	5.477	.67	183.0	3	
5	1-7	352.07	4.87	13.64	13.64	5.681	.67	183.0	4	
6	1	218.0	0.0	6.5	6.5	13.0	1.0	128.0	6	
6	2-7	352.0	4.87	13.64	13.64	5.681	.67	183.0	4	
7	1-7	282.15	4.52	12.67	12.67	5.277	.67	183.0	4	
8	1	218.0	0.0	6.5	6.5	13.0	1.0	128.0	6	
8	2-7	282.15	4.52	12.67	12.67	5.277	.67	183.0	4	
9	1-7	282.15	4.52	12.67	12.67	5.277	.67	183.0	4	
10	1-7	282.15	4.52	12.67	12.67	5.277	.67	183.0	4	
11	1-7	282.15	4.52	12.67	12.67	5.277	.67	183.0	4	
12	1-7	282.15	4.52	12.67	12.67	5.277	.67	183.0	4	
13	1-7	↓	↓	↓	↓	↓	↓	↓	↓	
14	1-7	↓	↓	↓	↓	↓	↓	↓	↓	
15	1-7	↓	↓	↓	↓	↓	↓	↓	↓	
16	1-7	↓	↓	↓	↓	↓	↓	↓	↓	
17	1-7	352.07	4.87	13.64	13.64	5.681	.67	183.0	4	
18	1-7	352.07	4.87	13.64	13.64	5.681	.67	183.0	4	
19	1-7	465.0	5.34	14.96	14.96	6.233	.67	183.0	3	
20	1-7	315.46	4.7	13.15	13.15	5.477	.67	183.0	3	
21	1-2	0.0	523.46	9.32	9.32	18.08	1.0	128.0	6	
21	3-7	9.99	135.14	9.32	9.32	4.66	1.0	220.0	4	
22	1-2	0.0	523.46	9.32	9.32	18.08	1.0	128.0	6	
22	3-7	9.99	135.14	9.32	9.32	4.66	1.0	220.0	4	0.0

FIGURE 8. INPUT DATA FORM - WALL DATA

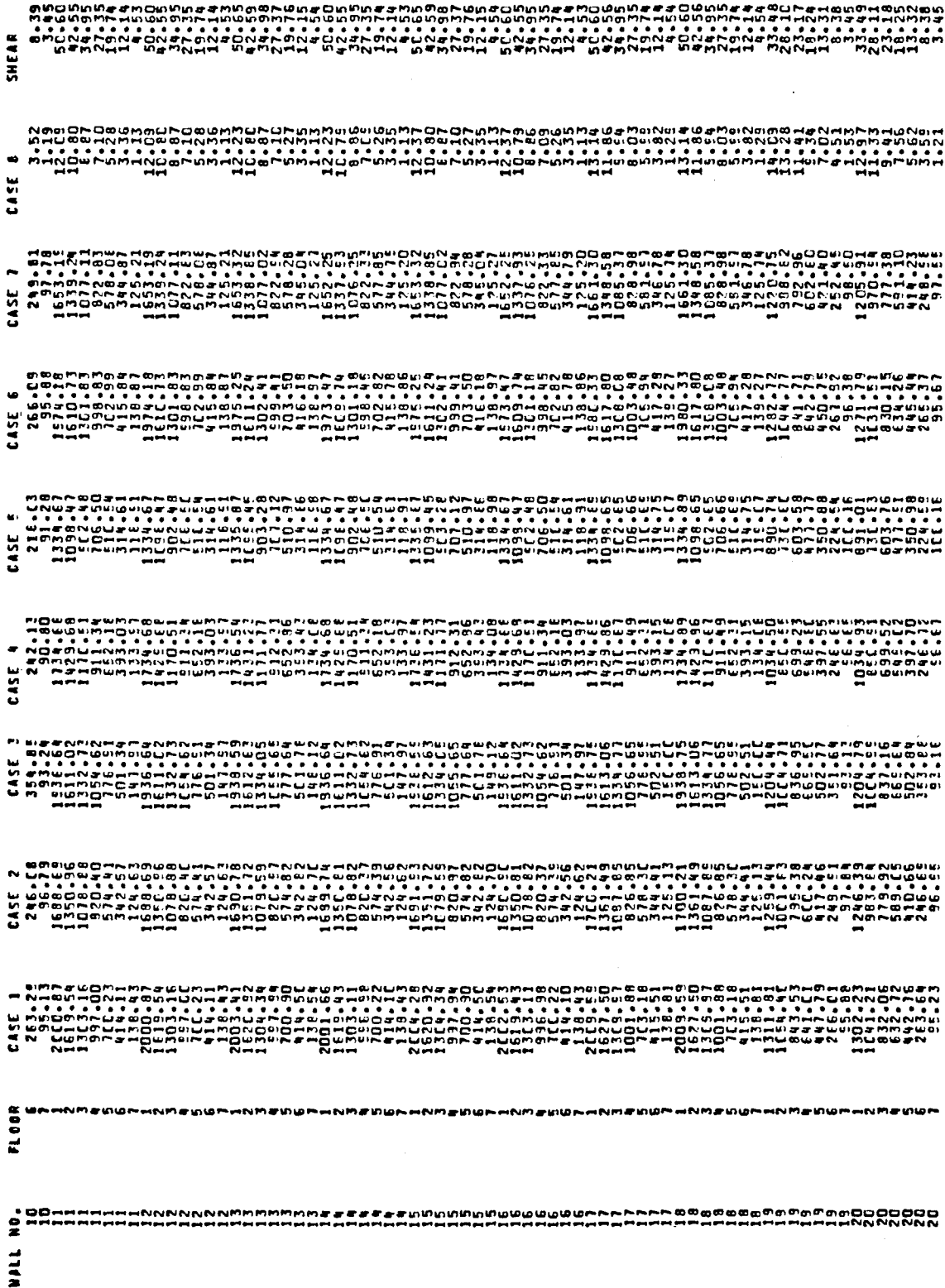


FIGURE 9. COMPUTER OUTPUT - STRESS IN WALLS FOR SEVEN LOADING CASES

Four cases 4 and 5, only the largest perpendicular (bending) load is considered. Thus, for all load bearing interior walls, the perpendicular load is the seismic load. For an exterior load bearing wall the perpendicular load may be either due to wind or earthquake, whichever is greater. For non-load bearing walls the compressive stress is not computed. Rather, the transverse load in pounds per square foot is printed. This load should be checked by the user to determine whether or not the wall needs reinforcement.

In addition, the nominal horizontal shear stress in the wall is printed as Case 8. This is the shear due to either wind or earthquake, whichever is greater. Also, the allowable shear stress increase which is equal to one-fifth the dead load stress is printed under the heading SHEAR.

Several other checks are made by the program. For example, if the wall is in tension, a message stating (tension in wall) is printed in order to permit the designer to determine the reinforcing steel required for walls in tension. The following information is also printed along with the above message:

- Case 1 Live load at top of wall (lbs./ft.)
- Case 2 Dead load at top of wall (lbs./ft.)
- Case 3 Reduced live load at top of wall (lbs./ft.)
- Case 4 Live load at bottom of wall (lbs./ft.)
- Case 5 Dead load at bottom of wall (lbs./ft.)
- Case 6 Reduced live load at bottom of wall (lbs./ft.)

In addition for brick masonry walls the eccentricity (in feet) of the gravity load with respect to the wall centerline is printed under the case 7 heading. Also the magnitude of the moment in the plane of the wall is given under the case 8 heading. For concrete block walls the equivalent eccentricity (in feet) is given under the case 7 heading. In order to identify the loading corresponding to the above data, the required compressive strength is set equal to zero. Thus, for example, if the message (tension in wall) is printed three times, then following these statements in the next line of output three values of required compressive strength would be equal to 0.0. Using the loading data given and knowing the critical load combination, it should be possible to design the needed reinforcing steel.

Also, if overturning is a problem, the program will print the wall number, floor number, bending moment at both extreme fibers (in lbs./sf.), the wall dead load stress (in lbs./sf.), the wall total load stress (lbs./sf.), and a statement indicating whether the overturning is caused by wind or seismic load. From this data, it should be possible to design the required wall reinforcement and examine the severity of the overturning. Finally for brick masonry, if the slenderness ratio of the wall exceeds the allowable ratio, the message (slenderness ratio exceeds allowable) is printed.

The advantage of using the computer program is in the flexibility that is now available to the designer. The designer can make modifications to the original conception layout, e.g. wall height, wall length, thickness, spacing, etc., and quickly obtain stresses for every wall, floor by floor, for the building. The time saved in manual calculations is fantastic. Minor architectural changes in the final phase of design can be checked quickly. Otherwise, these changes may not be made due to the required manhours involved in the laborious calculations that would be required by hand.

Some of the design highlights are discussed in the next section, which show the use of the results of the seven different load combinations. This will illustrate how a designer uses the results to finalize the design.

DESIGN HIGHLIGHTS

The transverse walls between units and the exterior end north-south walls were made bearing walls because:

- (1) The exterior longitudinal walls contained numerous openings. (see Figure 10)
- (2) This would allow venting of explosions for progressive collapse design.
- (3) Lateral forces across the narrow dimension of the building could be easily resisted; i.e., the untopped gird floor and the steel roof deck would satisfy diaphragm requirements and bearing walls would also function as shear walls without being severely over worked.
- (4) Masonry walls would decrease sound transmission between units.

Stairwells are placed longitudinally at each end of the building and their longitudinal side walls function as the shear walls in the east-west direction. Shear walls and uninterrupted bearing walls with no openings were hollow 8" walls. The east-west shear walls required reinforcing and mortar fill in the cells at each end; below the 3rd Floor high shear stresses required 75% solid c.m.u. (concrete masonry units). Normal strength block was used in all bearing and shear walls except typical interior bearing walls above the 7th floor and below the 3rd Floor. Higher strength masonry was required in the top floor walls to satisfy bending stresses when the wall is functioning under progressive collapse as a beam supporting roof, 6th and 7th Floor loads after an assumed explosion causing collapse of 6th Floor walls below. The computer program printout indicated that typical 1st and 2nd floor bearing walls were overstressed as normal masonry under all loading conditions except Case IV. The most severe stresses occurred on the 1st Floor under Case VI, Dead Load and Parallel Earthquake, and required 1800

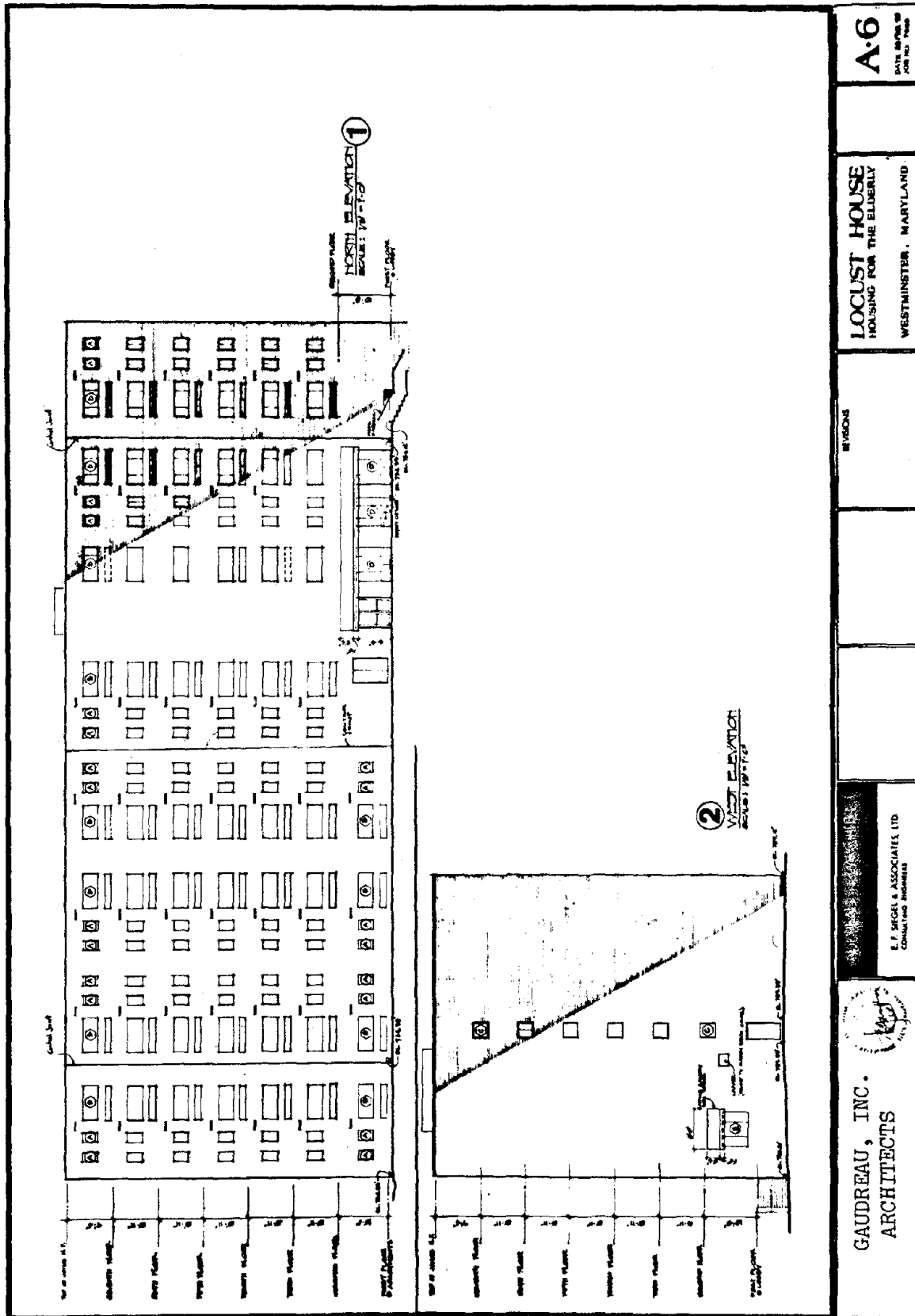


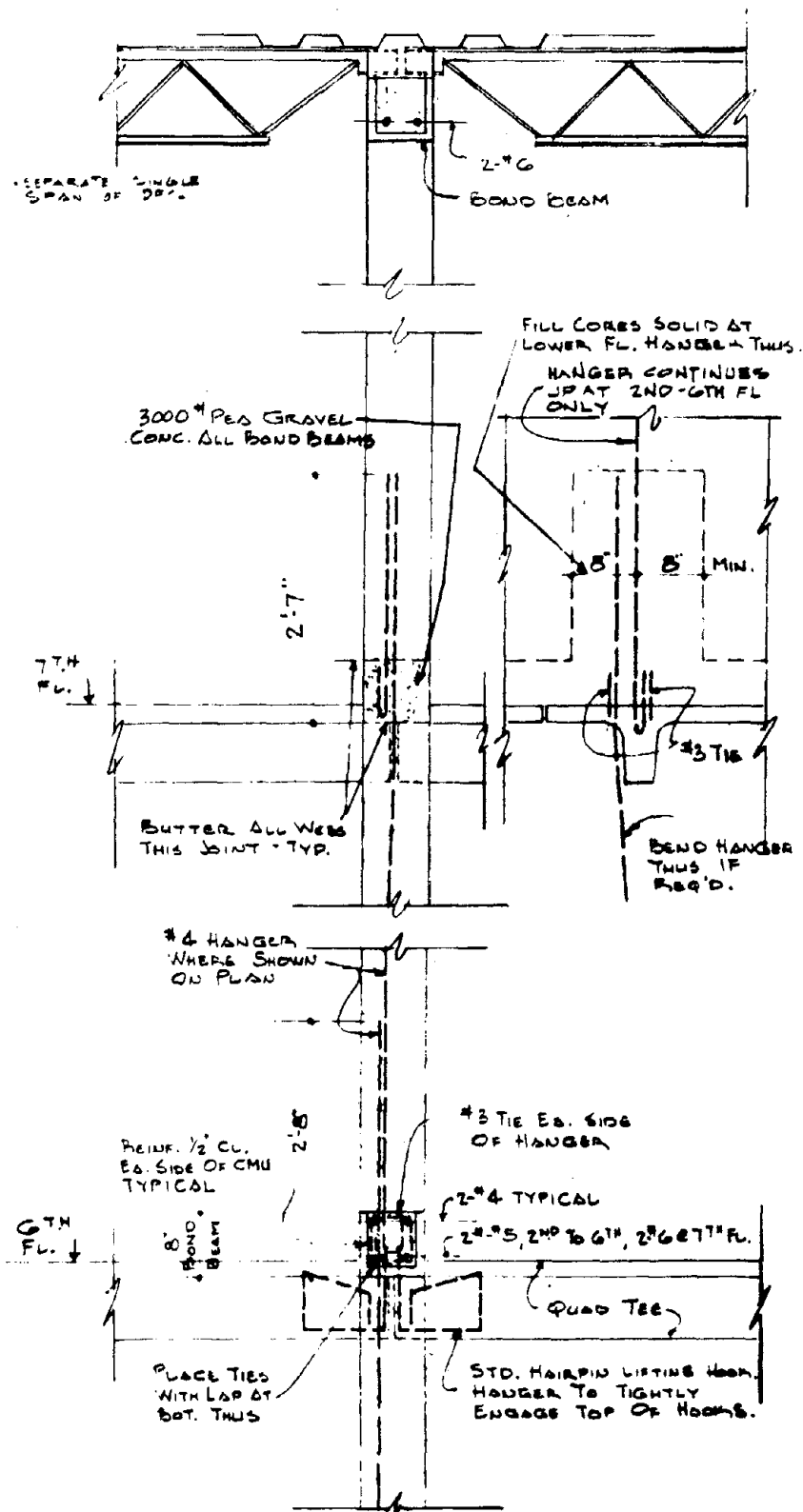
FIGURE 10. NORTH AND WEST ELEVATION

pounds per square inch masonry. Therefore, this was the higher strength selected for all these conditions. Table 3-1 of the N.C.M.A. Specification indicates that 3500 PSI c.m.u. with Type M or S mortar would furnish masonry of that strength, and they were thus specified for the high strength walls. Web areas were neglected throughout because of the difficulty and uncertainty of achieving buttering of the c.m.u. webs, given the present state of the construction art.

The longitudinal exterior walls were made steel stud and brick veneer construction due to its speed of construction, ease of installing insulation, windows and mechanical electrical work, ease of meeting wind design requirements, its small seismic load and low cost. Floor and Roof Systems were designed and detailed as diaphragms to satisfy wind and seismic loads. Although Maryland is subject to only small earthquake risks, the Zone 1 seismic loads were more critical than wind. The quad tee floor units have inserts cast into the slightly beveled longitudinal edges of the flanges at 5 foot spacing. After the units are placed, a short bar is placed in the joint and welded to both inserts to transfer diaphragm shear between units. The bond beam (see Fig. 11) in each bearing wall at each floor level and at the roof serves several functions:

- (1) It provides the tensile reinforcement for the positive bending of the wall beam above and the negative bending of the wall-beam below in case of possible blow out of the end of a bearing wall and cantilever action is then needed.
- (2) Also, it completes the connection between the quad tee and the progressive collapse hanger located at each corner of the tee unit.
- (3) It connects end to end the quad tees and is the chord or flange portion (at the East and West end walls under single panel mode or at each wall under multiple panel truss mode) of the diaphragm to resist east-west lateral loads.
- (4) At the roof and each floor it is an efficient means of providing for transfer of north-south lateral forces into the wall from the respective diaphragms.

The economical application of any type precast floor or roof system depends to a very large extent upon the simplicity and repetitiveness of the layout of the units, the requirement for very few non-standard units, the careful treatment of openings architectural-ly, mechanically and structurally and the clarity of the contract drawings and specifications indicating these conditions. From the architectural layout of LocustHouse it was obvious from the outset that with care much of these could be achieved; thus there was no hesitation to proceed with the tentative choice of a quad tee floor system. (see Figures 12 & 13). Standard units will be used throughout except for

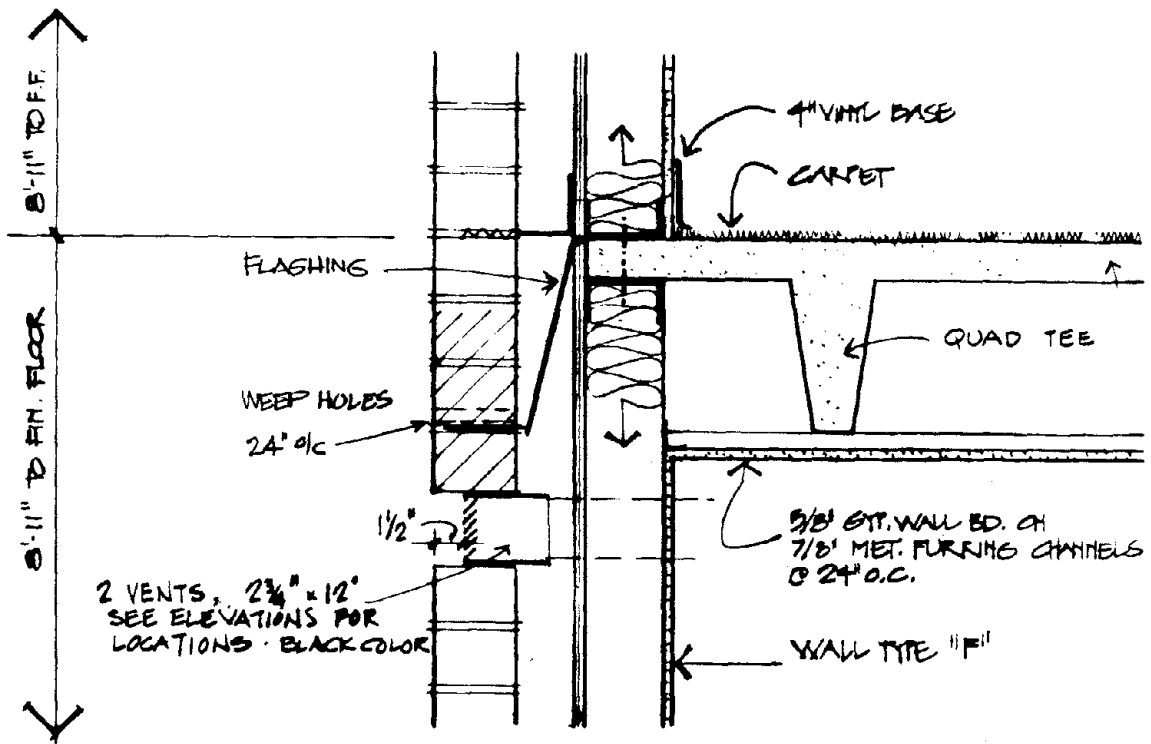


TYPICAL BEARING WALL - SECTION S-8

(EXCEPT WEST WALL OF ELEVATOR)

3/4"=1'0"

FIGURE 11. BOND BEAM SECTION



WALL SECTION @ TYP. FLOOR (2-7)

FIGURE 12. WALL SECTION @ TYP. FLOOR (2-7)

the end bays and the elevator area. This was accomplished by careful coordination of Architectural and Structural Drawings, i.e. the adjustment of the air space dimension of Wall Type F, Fig. 14 so that the outside face of studs coincided with that of the quad tees. The plumbing fixture locations were checked for pipe interference with quad tee webs and any necessary adjustments were made and dimensioned. (See Figure 15). Architectural, Mechanical and Structural Drawings were coordinated to proportion and place the openings for the two make-up air risers clear of quad tee webs.

All the earlier efforts to achieve an efficient and successful project utilizing engineered masonry will likely be wasted unless a comprehensive quality control program is set up before construction begins. For Locust House the masonry section of the Specifications was titled Engineered Masonry and this program was included therein as follows:

1.4 Special Coordination:

1.4.1 The contractor shall hold a preconstruction meeting at least 15 days before start of engineered masonry construction, and before laying up of sample wall. The Architect, with the Structural Engineer and the Testing Agency, will direct the meeting. Attendance shall be mandatory for:

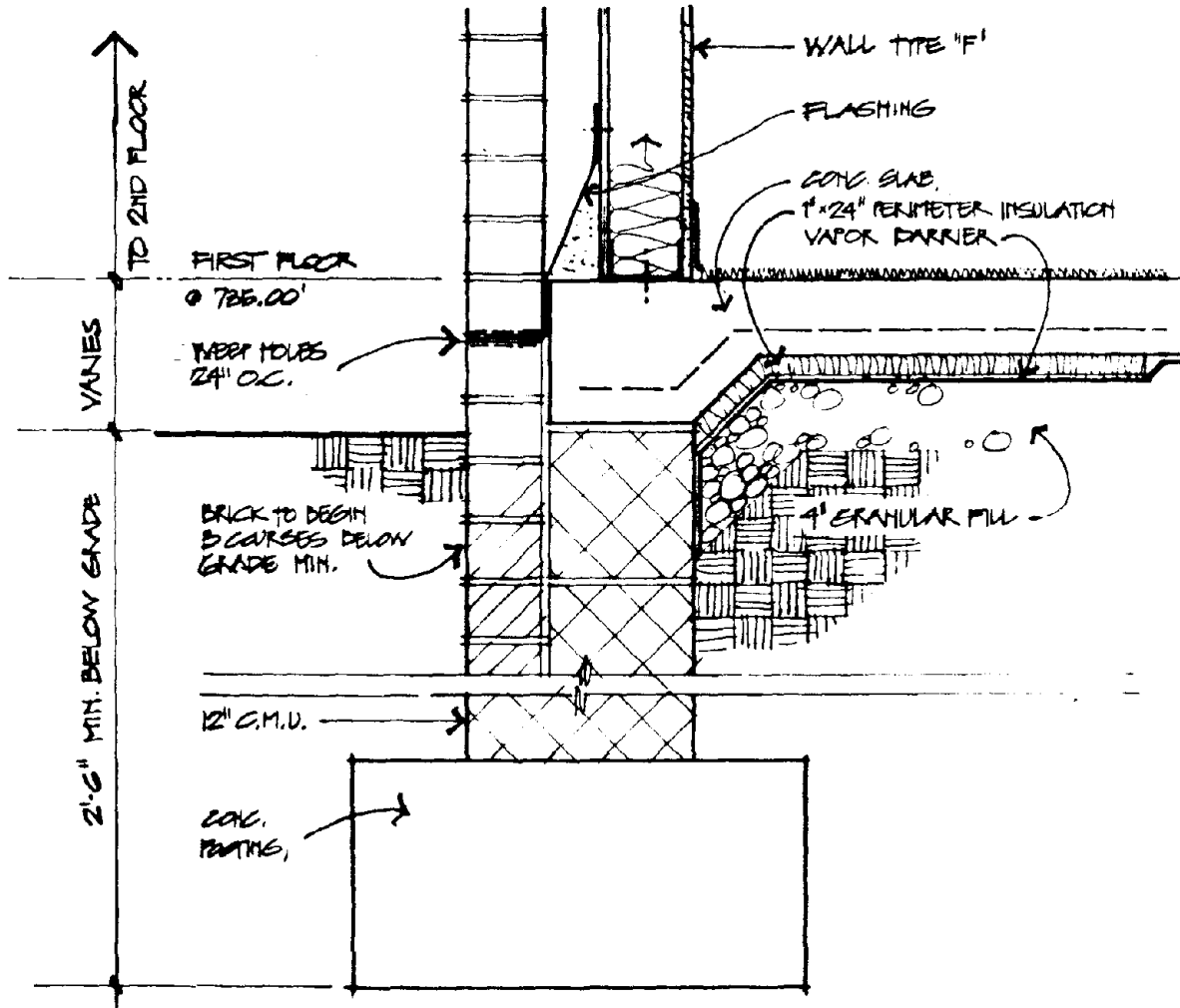
- (1) Contractor's project manager and superintendent.
- (2) Masonry subcontractor's superintendent, foreman, at least 2 mason mechanics, and the mechanic who will oversee the mortar production.
- (3) Representatives of the masonry unit and lime or masonry cement suppliers.

1.4.2. The Architect will discuss structural concept, mortar requirements, methods and sequence of engineered masonry construction, special masonry details, standards of workmanship, and quality control requirements.

1.6 Quality Control

.1 Test masonry prisms of each type of c.m.u. and each type of mortar according to the National Concrete Masonry Association's TEK Bulletin 22. The Testing Agency shall test sets of 3 prisms:

- (1) 1 set at least 21 days before start of engineered masonry construction.



WALL SECTION @ 1ST FLOOR

FIGURE 13. WALL SECTION @ 1ST FLOOR

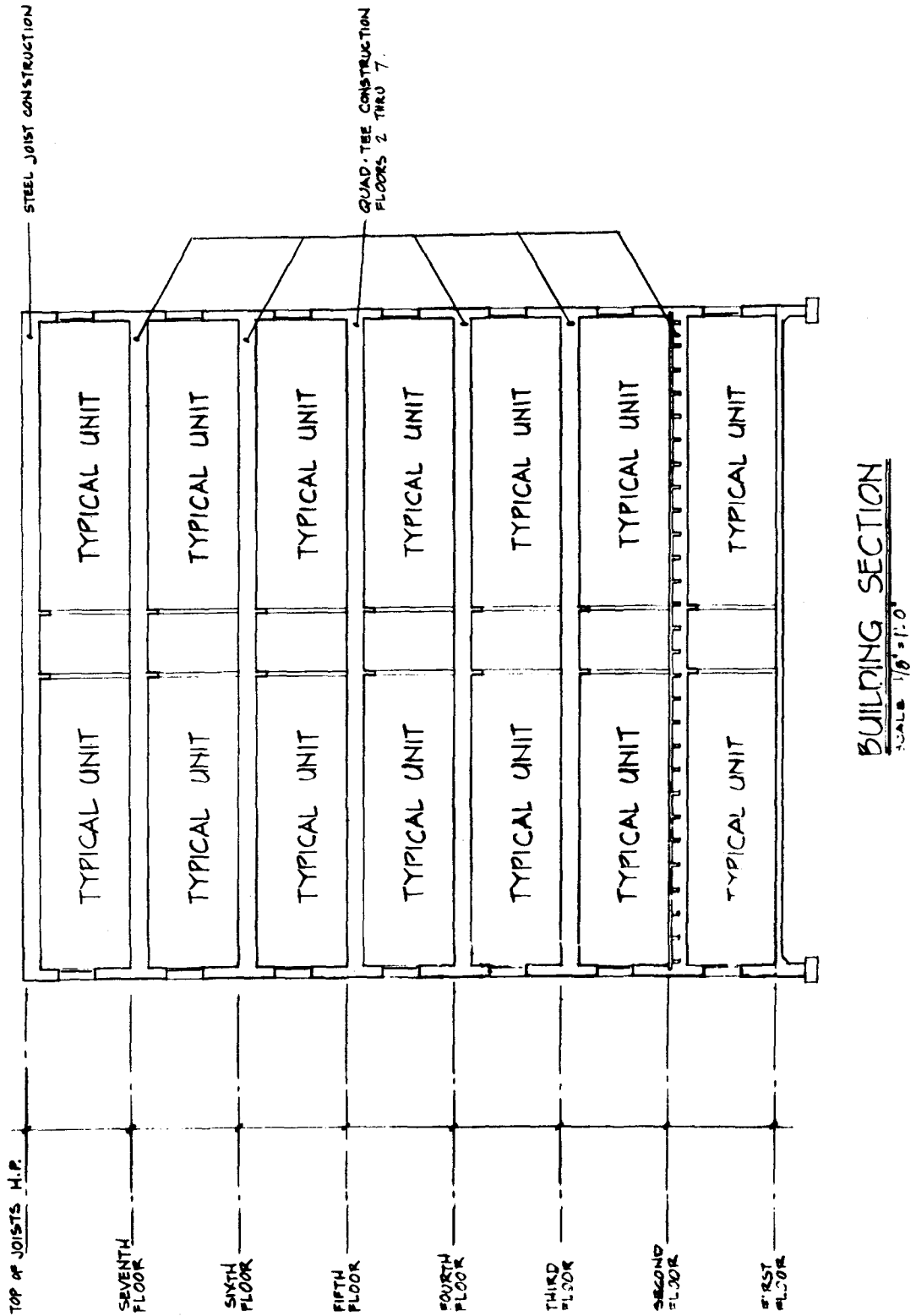
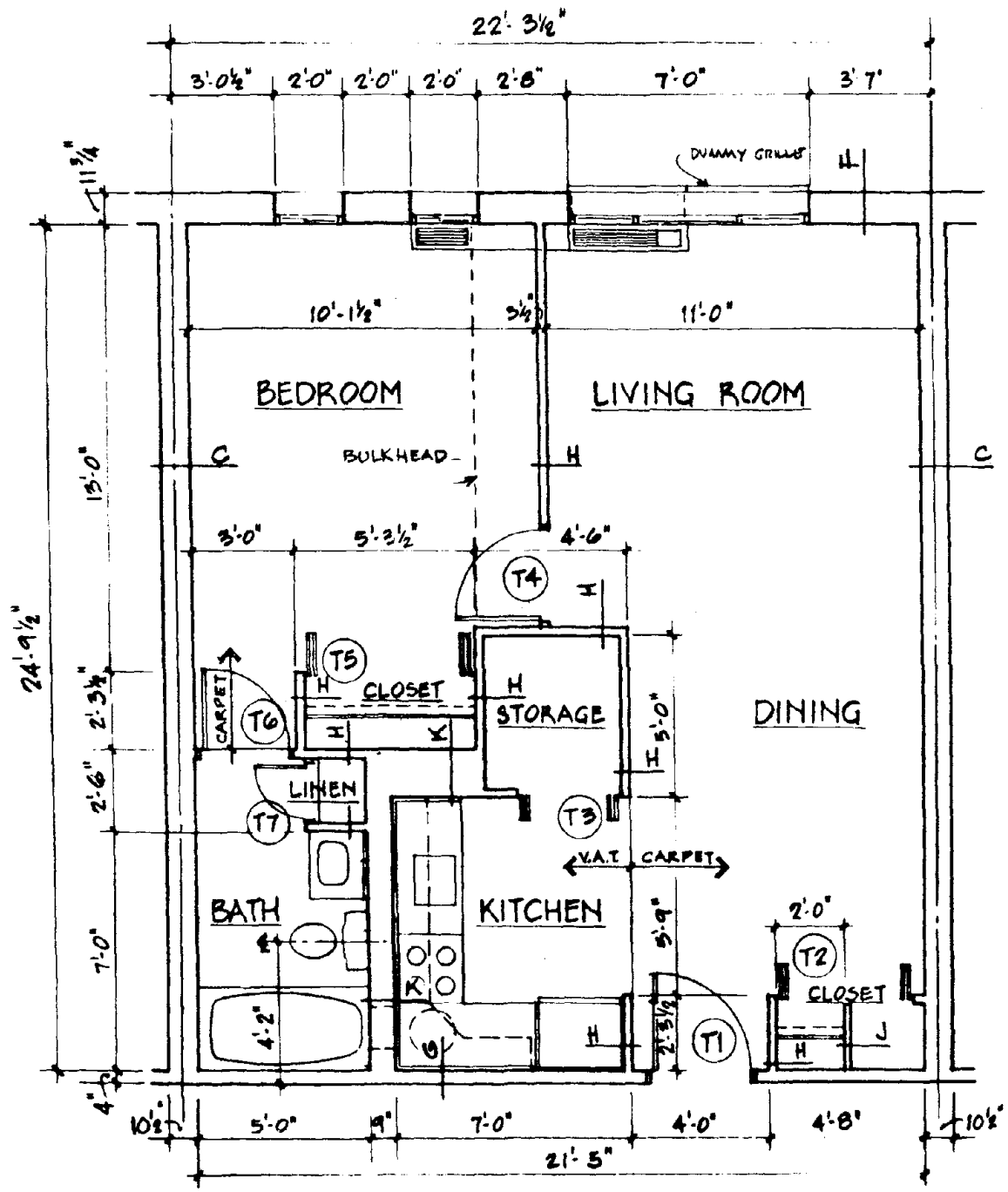


FIGURE 14. BUILDING SECTION



TYPICAL UNIT PLAN

SCALE: 1/4" = 1'-0"

FIGURE 15. TYPICAL UNIT PLAN

(2) 1 set at start of engineered masonry construction;

(3) 1 set in the course of each story height of engineered masonry work.

.2 Test mortar prisms according to ASTM C109. The Testing Agency shall test sets of 3 prisms:

(1) 1 set at least 21 days before start of engineered masonry construction.

(2) 1 set at start of engineered masonry construction.

(3) 1 other set at time determined by Architect.

.3 The Testing Agency, or other qualified party approved by the Architect, shall conduct continuous on-site inspection of the construction of the engineered unit masonry work.

The primary purpose of the former is to explain the reasons for quality control and the somewhat stringent provisions of the plans and specifications and thus to obtain motivation for careful workmanship from all members of the team.

SUMMARY

This paper illustrates the use of the computer program for rational analysis of non-reinforced engineered masonry construction from the Masonry Institute of Maryland, Inc. The advantage of using the computer program is in the flexibility that is now available to the designer. The designer or owner can make modification to the original conception layout and quickly obtain stresses for every wall, floor by floor, for the building. Thus, savings can be realized from laborious hand calculations. Minor architectural changes in the final phase of design can be checked quickly. Locust House which was designed by Gaudreau, Inc. was used in this paper as a typical building design example.

ACKNOWLEDGMENTS

The authors acknowledge with thanks the support provided by the Masonry Institute of Maryland and Gaudreau, Inc., Architects-Planners-Engineer.

APPENDIX I

1. Colville, James, "Report on Computer Program for the Rational Analysis of Masonry Structures", Masonry Institute of Maryland, Baltimore, Maryland, January, 1976.

-ABSTRACT-

TWO STORY MASONRY BUILDING
SUPPORTED ON A 24 FOOT DEPOSIT OF ORGANIC FILL

BY: DONALD R. HEIL, AIA*

Constructed and owned by the Metropolitan Sanitary District of Greater Chicago, the "Nu-Earth Service Center" at Forest View, Illinois has some unique design features:

- 1) It is the first and only masonry building in the world supported by a 24 foot deposit of sewage sludge.
- 2) Foundation walls are specially reinforced to bridge cavities in the supporting fill material.
- 3) The masonry walls are specially designed to tolerate differential settlement without cracking.
- 4) The building was designed and constructed by Plant personnel as a slack-time project.

The building structure consists of a reinforced concrete spread footing, 12 inch thick reinforced masonry shear wall panels interspersed with 4 foot wide, translucent, floor-to-ceiling wall panels. The masonry shear walls are tied together by a steel decking system that is designed for diaphragm action. Two and a half years after its erection, there is no sign of a crack in the masonry.

The service building is divided into a two story office section for operations control and a heavy equipment repair shop. Adjacent to the building is a 50-ton capacity truck scale.

* Associate Professor of Architecture
Washington State University
Pullman, Washington

TWO STORY MASONRY BUILDING
SUPPORTED ON A 24 FOOT DEPOSIT OF ORGANIC FILL

DONALD R. HEIL, AIA *

The Metropolitan Sanitary District of Greater Chicago (MSD) has been hauling huge quantities of sewage sludge (since 1931) from its air drying beds at the West-Southwest Sewage Treatment Works (Stickney, Illinois) to the Harlem Avenue Solids Management Area (HASMA) near Forest View, Ill.

The Harlem Avenue Dump (as it was formerly known) is sited on an irregular parcel of land, about sixty acres (24 hectares), bordered by steep earthen dikes which entrap the sludge deposits and support the encircling rail haulage system.

The MSD by 1973 had accumulated a 35-foot high plateau of sludge and remaining dump space was virtually nil. Attempts were made to find a new site, but for sludge, nothing was available.

The problem was finally resolved in 1974 when it was accidentally discovered that the dump was quietly functioning as a biological compost heap. It simply converts waste into "Nu-Earth", a rich black soil that looks and smells like black dirt, is high in nitrogen, phosphorous and humus and has a solids content of about 65%. With a little help from the news media, and free delivery service for orders of one truckload or more, Nu-Earth became an overnight success. Deliveries to the public in equivalent dry tons of solids were:

47,000 tons in 1974
102,000 tons in 1975
81,000 tons in 1976
127,000 tons in 1977

As may be surmised from production quantities, a massive excavation and truck delivery system was placed in operation, and it soon became apparent that a building was needed for an operations center where delivery orders would be received and dispatched, where excavation activities could be coordinated, and where heavy equipment could be repaired.

The normal procedure for procuring such a building involves initiating an engineering feasibility study, preliminary design and a Federal Grant application. After filing an environmental impact statement, there will be meetings, more meetings, discussions, etc. With a bit of luck, construction might have gotten underway in about five years or so.

Unfortunately, the building was needed immediately, not six or seven years later. With some advise and a lot of guts, it was just possible the building could be started immediately, utilizing plant supplies, equipment and maintenance personnel to do the job.

* Associate Professor of Architecture
Washington State University
Pullman, Washington

TWO STORY MASONRY BUILDING (2)

Selecting a building material was easy. The Sanitary District routinely uses brick to raise manhole covers, repair sewers, and reline steam boilers. In between repair jobs, District bricklayers have slack time which could be used for erecting a building. Red shale face brick was selected for the exterior due to its beauty, quality and cheap price (\$87.00/1000 bricks). No wonder almost all "little old school houses" were made of red brick. For back-up wall material, we selected 8" x 8" x 16" (20 cm x 20 cm x 41 cm) hollow concrete masonry units. This was even cheaper, per unit area of wall than the red brick (\$0.44/concrete block).

Selection of a building site was dictated by the following operating considerations:

- 1) Must be near the entrance to Solids Management Area, at a location where the truck haulage roads converge, where incoming empties can be weighed, and where outbound trucks can be weighed and dispatched.
- 2) Must be on a high vantage point where all operations activities (truck and railroad) can be readily observed from a control room.

There was only one logical location for the building, but it presented a slight problem. "The site was underlain by 24-feet (7.3 meters) of sewage sludge." Thanks to years of consolidation, the slushiness was gone and the stuff now had the consistency of soft clay. An unconfined compression test on a boring sample yielded a value of 0.68 tons per square foot (65k N/m²).

The obvious solution was to drive piling through the sludge, past a layer of loose sand, and into the dense gravel some 35-feet below the site. The only difficulty with this solution is that District maintenance crews are not equipped for pile driving, and the work is far too expensive to be performed with a purchase requisition (ceiling limit of \$2,500.00)

The Nu-Earth Program was developed on ingenuity, and wasn't to be deterred by a minor foundation problem. The sludge had already proven capable of carrying heavy trucks when topped with stone and broken concrete to distribute wheel load, so why not use it for supporting a building?

Heedful of the \$2,500 limit on material requisitions, the size of the building was held to a modest two story height, a width of 34 feet (10.4 m) and a length of 71 feet (21.6 m). At the west end of the main floor is a washroom, showers, locker room and lunch area for equipment operators. Directly above, on the second floor, is a 32 foot (9.8 m) by 12 foot (3.7 m) operations control room. The windows from this vantage point provide a commanding view of pit operations and a bird's eye observation of the trucks as they drive to the scale for weighing. An equipment repair shop occupies the rest of the building. In floor area, the shop is 32 feet (9.8 m) wide by 56'4" (17.2 m) long and has a ceiling height of 16'8" (5.1 m).

TWO STORY MASONRY BUILDING (3)

The most taxing part of the project was waiting for a hoisting (operating) engineer with a little slack time to dig the foundation. Two months were lost before an operator was available, and (as chance would have it) we were given an operator who wasn't strong on backhoe experience. He made a disasterous start by knocking down an overhead telephone line, ran over the survey stakes and dug up an underground power cable someone forgot to warn him of. After an auspicious start, there were a few problems with line and grade, but the over-dig was corrected by back-filling with crushed stone, and the alignment difficulties were corrected by hand trimming and wheel-barrel work. At the end of August, 1975, excavation work was completed and thereafter, the job proceeded smoothly.

Poor bearing capacity for the foundation was compensated by providing extra wide continuous footing under each of the walls. Cavities and super-soft spots were bridged by the foundation walls which were specially reinforced to act as deep beams.

The real design challenge of the structure was to provide for long term shrinkage of the underlying soil. The adjacent pit excavation was draining the water table and soil shrinkage was a virtual certainty. Not having a practical way to stop soil shrinkage, we turned to a design that allows the building to rock and roll without cracking.

Bone, like masonry, is hard and fairly rigid, yet nature makes animal skeletons flexible by segmenting the bone (picture the backbone of a snake), and connecting it with a flexible material (cartilage). In a like manner, the masonry walls of the Nu-Earth Service Center were segmented, the four foot (1.2 m) spaces between segments being linked by sandwich type, translucent, fiberglass wall panels (manufactured by Kallwall Corp. of Manchester, N.H.). The building has a total of seven such wall panels, which by strange coincidence, come to a total price of \$2,485.00 (\$15. under the limit for a material requisition). Two 14' x 14' (4.3 m x 4.3 m) roll type steel doors provide additional flexibility for the walls.

To insure movement will not take place in the masonry segments, every second horizontal joint of concrete block is tied to the face brick and reinforced with "three wire heavy duty block-truss". For vertical reinforcement, #4 bars are grouted inside the block cores at intervals of about four feet (1.2 m). The rest of the block cores are filled with vermiculite masonry insulation

At the top of each masonry wall segment is a well anchored steel plate to which galvanized steel roof decking is welded for diaphragm action. With this system, horizontal wind forces are transferred to the roof deck, then to the side walls where the force is carried to the foundation by shear action.

TWO STORY MASONRY BUILDING (4)

Over the shop, the 18 gage ribbed roof deck is supported by 16-inch (40.6 cm) rolled steel beams spaced seven feet (2.1 m) on centers. Over the control room, the decking is supported by 6" x 4" (15.2 cm x 10.2 cm) tubular steel beams that span the 12 foot (3.7 m) width of the room. In their painted condition, the steel tubes look like wood beams, greatly enhancing the appearance of the room. In general, the steel decking system is stiff enough to be an effective structural diaphragm, yet flexible enough to accommodate differential settlement.

Some of the more conventional features of the New Earth Service Center are a:

- 1) Precast concrete floor system for the operations control room, part of which cantilevers into the shop area, providing an entry balcony reached by a steel stairway.
- 2) Combination acrylic plastic dome skylight and roof scuttle over the control room entry balcony.
- 3) Two inches (5.1 cm) rigid fiberglass board for insulation of roof system.
- 4) Roofing over the insulation board consists of one ply of 43# asphalt base felt, two plies of asbestos cap sheet, and a spray-on surface membrane of fiberglass reinforced asphalt. Pipe vents and other openings are flashed with a neoprene seal.
- 5) 440 volt plug receptacles for welding machines usage in shop area, in addition to 110 volt outlets.
- 6) Ceiling mounted electric radiant heaters for the shop area and a heat pump for the control room and locker-wash room area.
- 7) Metal clad Pella casement windows.
- 8) Provision for a future 10-ton (9.1 metric tons) bridge crane to be hung from roof beams.
- 9) Cast iron roof drains, catch basins and extra heavy drain pipe.
- 10) "Cavitette" aeration system for treatment of waste water from building.
- 11) 50 ton (45.4 metric ton) truck scale mounted in reinforced concrete floating foundation. Weight is determined by an electronic load cell with remote readout and printer located in the control room.
- 12) Electronic alarm system that utilizes microwave motion detectors (installed following two break-ins).

TWO STORY MASONRY BUILDING (5)

Construction was conducted by the "fast track method" in which actual building work proceeds simultaneously with design. To our surprise, it really worked (and with very few foul-ups.) Design and coordination of construction was handled by engineer-administrator types who (like the tradesmen) did the job as a fill-in (in between operating problems, citizen complaints, maintenance troubles, conferences, budget request, discipline cases, etc.). Somehow or other both design and the construction commenced together and both finished at the same time.

One side benefit of the fast track method is that it necessitated bringing the trade formen and leadmen into the basic planning process. They were consulted on alternatives and relative difficulties of each. In some cases, where the District lacked suitable construction equipment (for example, concrete forms) the foreman advised on the type of equipment to rent. If there were two alternatives of equal merit, we always took the tradesman's suggestion. By being a part of the planning process, the tradesmen not only contributed valuable suggestions, but took greater pride in the work - - it was something personal to them and they were eager to prove their suggestion were good ones.

Construction of the service center proceeded swiftly from August of 1975, until December when winter weather slowed up progress. In January of 1976 the roof decking was welded in place, thus ending all hazard of wind damage to the masonry walls. Thereafter, construction moved in short, scattered spurs as tradesmen became available.

CONCLUSIONS:

- 1) As of this writing (some 2½ years after the masonry walls were first erected) there are no signs of cracks in the masonry, thus proving that "flexible masonry design" is not only possible but practical.
- 2) There have been no difficulties caused by poor bearing capacity of the underlying soil (sludge). Even the truck scale remains level and in good adjustment, proving that difficult soil condition need not necessitate a highly expensive foundation. The only hint of unusual soil condition is a slight water bed effect when a train runs past the building.
- 3) The building is not likely to win an architectural award (too many sacrifices in fenestration due to cost restrictions and special structural considerations), however, it is a very pleasant building to work in, and the men who built it are very proud of their accomplishment.
- 4) It took but fourteen months from the first sheet on the drawing board till the building was occupied. This didn't set a record, but it is considerably faster than the projected five to seven years for a Federal Grant Project. Further, we believe the savings in foundation costs, labor expense and material price escalation more than offset the benefit of a Federal Grant.

TWO STORY MASONRY BUILDING

(6)

ACKNOWLEDGMENTS

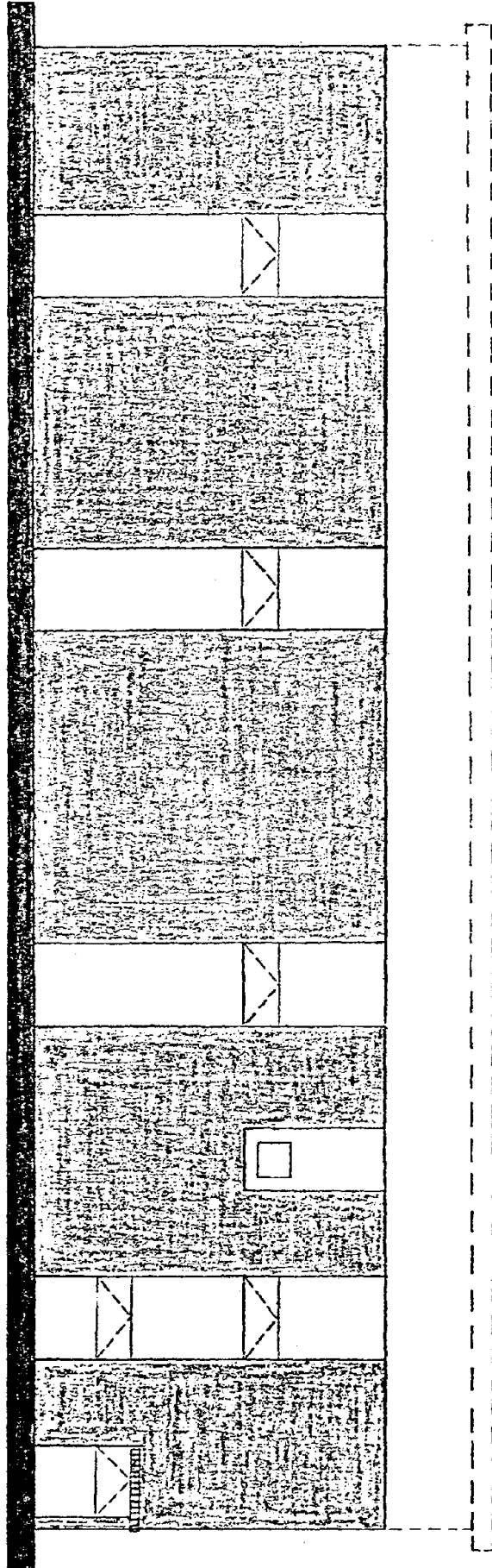
Planning & supervision of the Nu-Earth Service Center was performed entirely by the WSW Plant staff. Surprisingly, the engineers who coordinated the project prefer to be anonymous. "Such unorthodox handling could damage our bureaucratic image."

The Plant tradesmen have no such reservations, they are unabashedly proud of their contributions. My congratulations to the Master Mechanic - Bob Bartuska, his assistants - Bill Robertson, Pete Yore, Tim O'Connell, and the foremen and leadmen - Jim Airdo (Cement Finishers), Bob Arlow (Bricklayers) Henry Burrowes (Pipefitters) Norm Cullerton (Electricians) Emil DelBoccio (Sheetmetal workers) George Enda (Painters) Ruphin Kukulski (Carpenters) Joe Mixan and Bob Kilb (Plumbers) George Schaefer and Jack Mezera (IRONWORKERS) and George Wirtz (Hoisting Engineers).

POST-SCRIPT

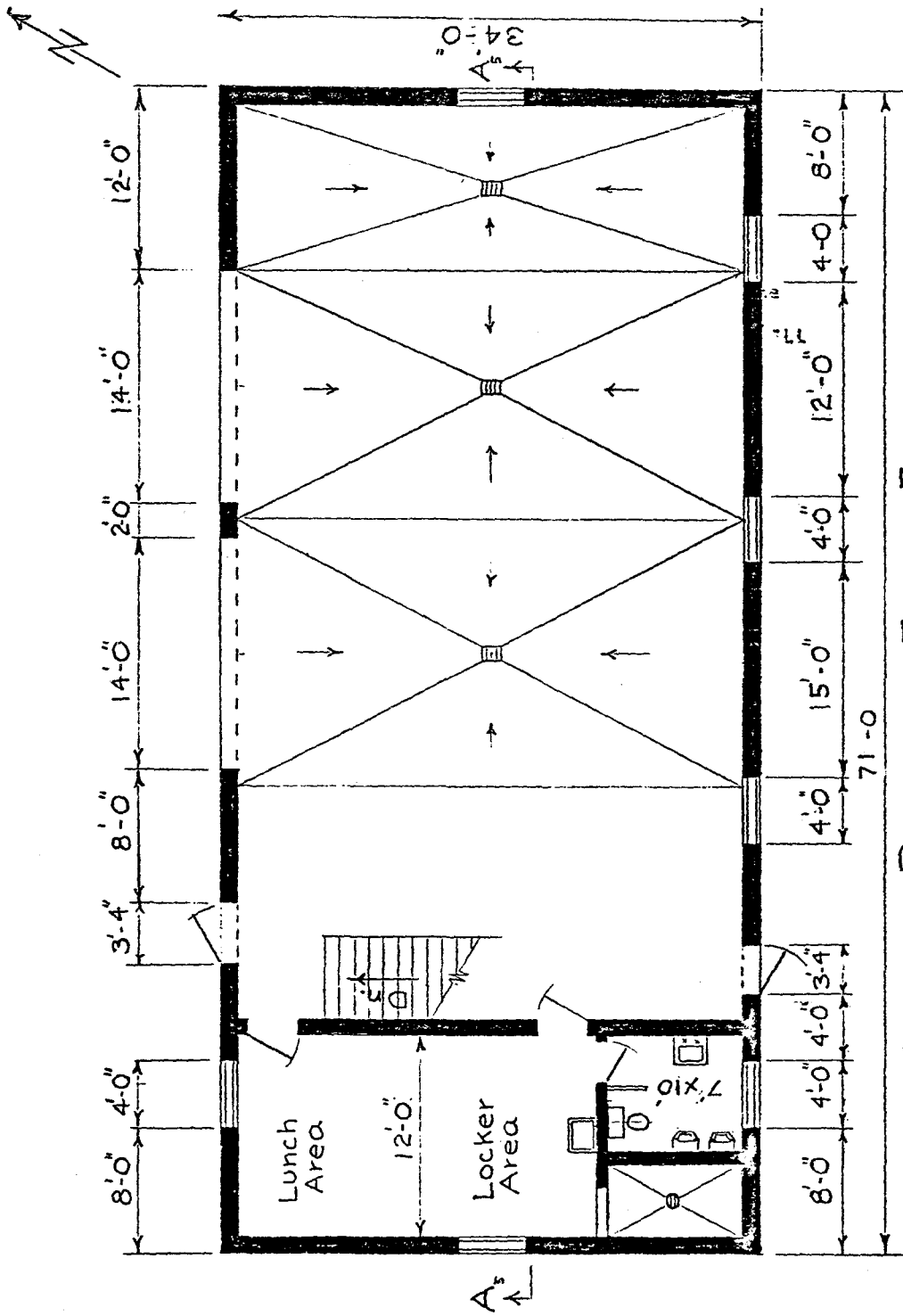
The use of Nu-Earth for home gardens is now under attack by environmentalists. The question at issue is whether crop uptake of heavy metals from the sludge is sufficient to pose a health hazard. On a short term basis, there is no evidence of ill effect from crops grown with Nu-Earth. The long term effects however have yet to be determined.

In May of this year, Nu-Earth was sent to eighteen different agricultural research centers throughout the United States. Under EPA sponsorship, these centers will study uptake of heavy metals. (Locally, Colorado State University at Fort Collins is one of the eighteen agricultural research centers so selected.) Pending resolution of the heavy metals question, the MSD has voluntarily restricted Nu-Earth distributions to non-food-chain usage. The healthy octogenarian retirees from the MSD who have used Imhoff sludge in their gardens for forty years or more suggest it will eventually be proven safe.

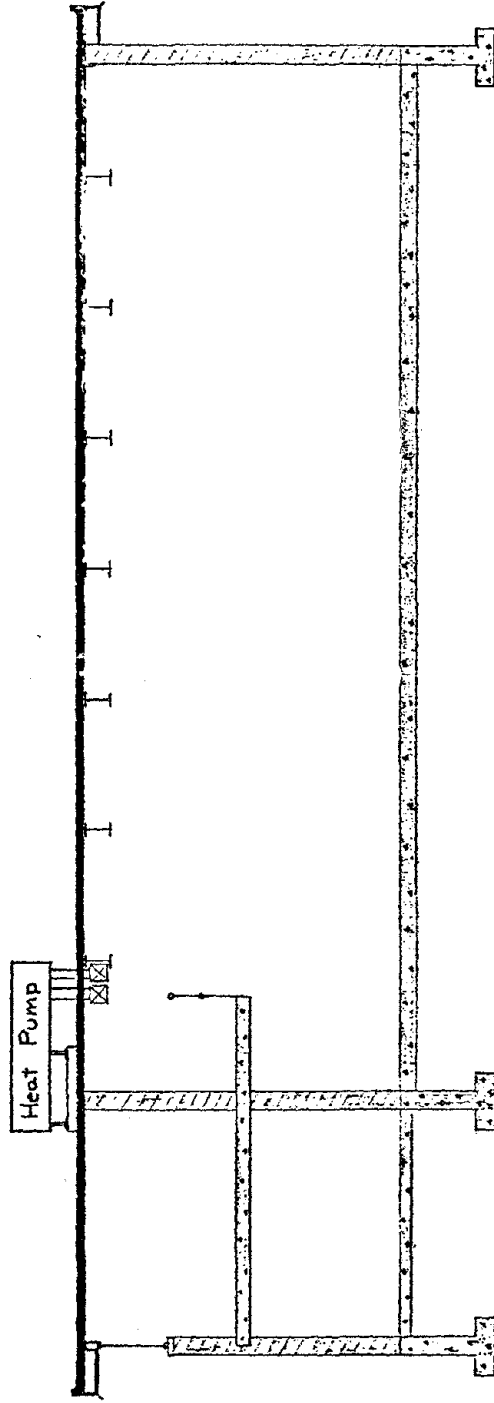


SOUTH ELEVATION OF SERVICE CENTER FOR NU-EARTH

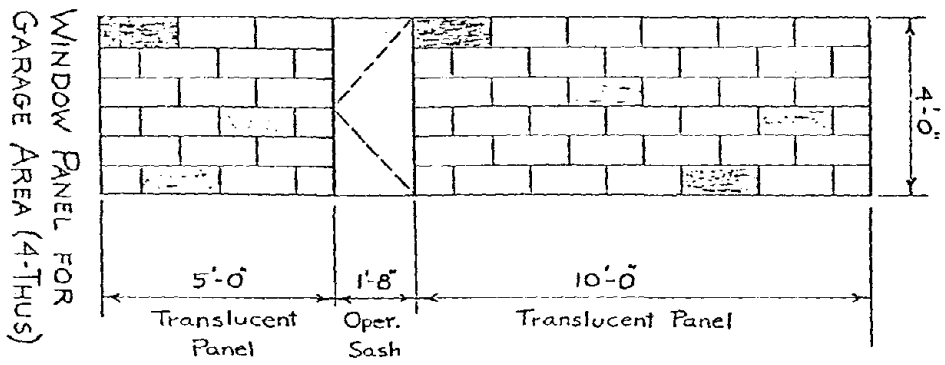
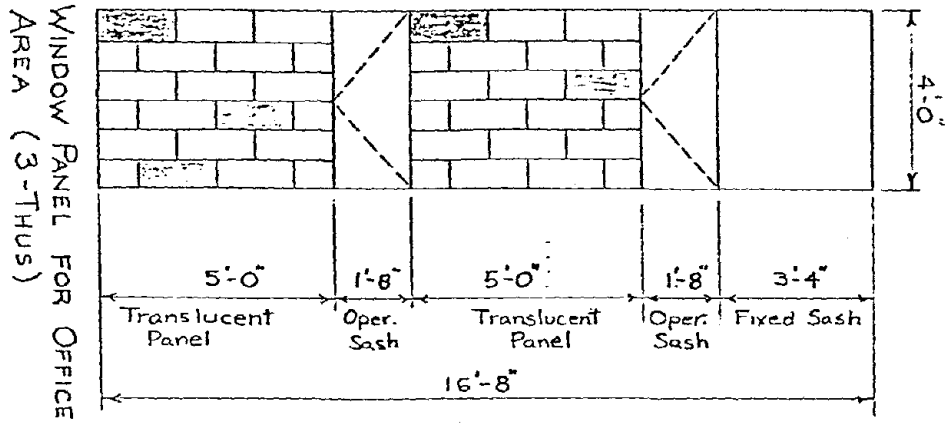
Sheet A-1
Scale 1/8" = 1'-0"

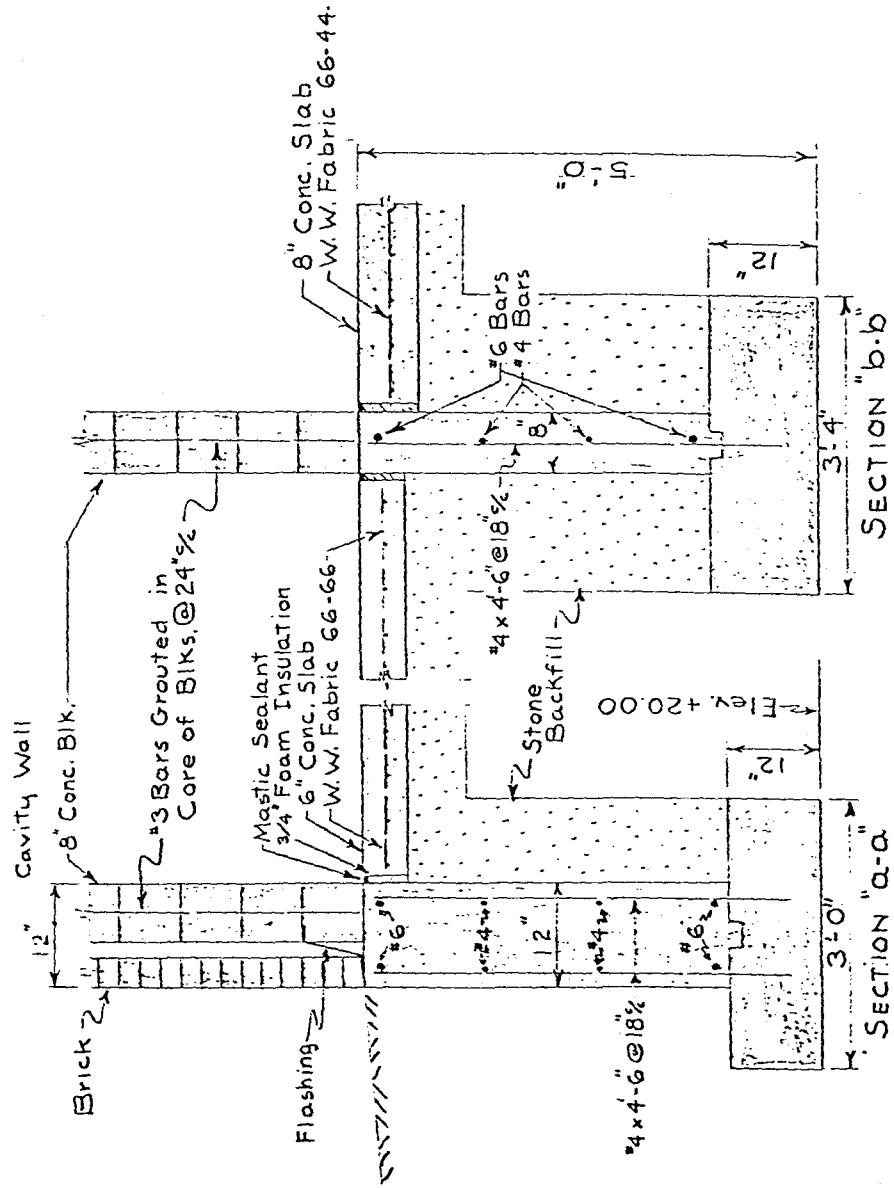


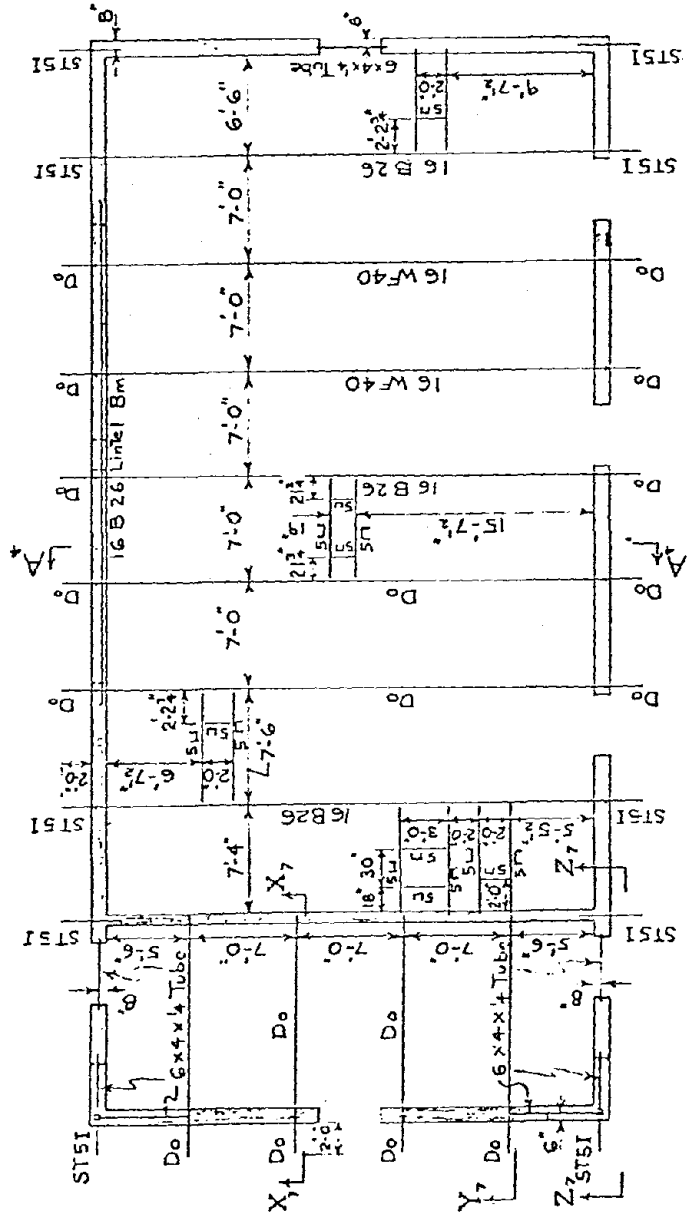
PLAN OF FIRST FLOOR
SERVICE. CTR. FOR NU-EARTH DISTRIBUTIONS



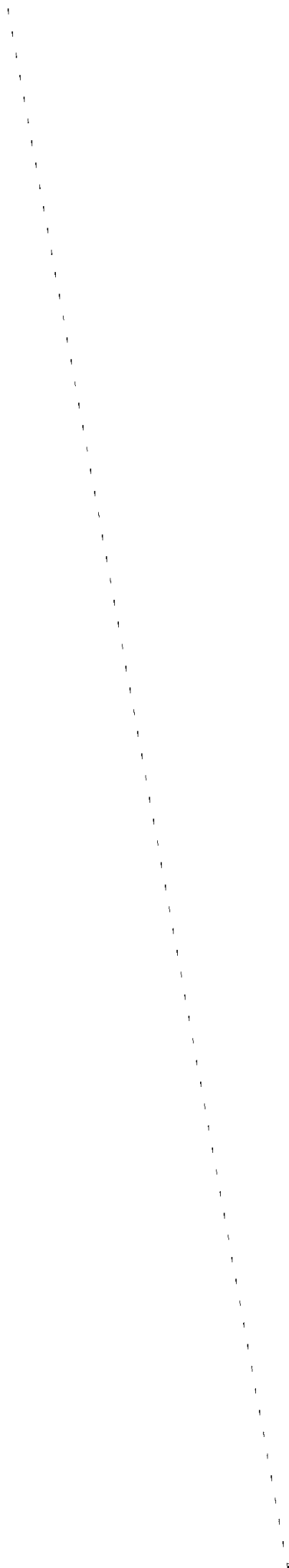
SECTION A-A,
SERVICE CENTER FOR NU-EARTH DISTRIBUTIONS







ROOF FRAMING PLAN FOR NU-EARTH SERVICE CENTER



AUTOMATED DESIGN OF MULTISTORY MASONRY SHEAR WALL STRUCTURES

By Hill Jr., Louis A. and Chasey Jr., Richard H., Arizona State University

ABSTRACT: This paper discusses a computer program which provides automated, practical design of multistory masonry shear wall structures. Automated techniques provide an economic means for data-controlled design, without the need to learn a Problem Oriented Language. Structured programming techniques are used to simplify revision and/or replacement of subroutines necessitated by code changes as well as improvements and refinements in design and analysis methods. Overall program configuration used top-down programming to insure that data structure and program modules consistently maintained integrity and flexibility. Program modules, however, were consistently prior tested using bottom-up programming to insure that they performed their assigned tasks accurately under all possible conditions.

User input is minimized by utilizing the typically repetitious nature of both horizontal and vertical structure geometry. User options provide data controlled flexibility of design criteria, unit material and labor costs, seismic and wind zones, material strengths, allowable stresses, etc.

Working stresses are used in the design of all structural elements and connections. Iterative selections are then checked against applicable code requirements and revised as necessary. The Uniform Building Code (1976) is used but care is taken to allow for ready incorporation of future code revisions, including the method of analysis based on artificial seismic time histories.

Output conforms to standard design office procedures and includes user data-specified selectivity. In general, input data is checked for reasonableness and echoed to guard against gross errors. Masonry thicknesses and reinforcing steel details (i.e., design results) are output in a well organized format for providing structural drawings. Analyses include load combinations, and stress checks for all elements. This output is in a form to facilitate checking by the responsible engineer and any regulatory agencies which must approve the plans. A bill of materials and a cost estimate are also provided.

AUTOMATED DESIGN OF MULTISTORY MASONRY SHEAR WALL STRUCTURES

By Louis A. Hill Jr.,¹ and
Richard H. Chasey Jr.²

INTRODUCTION

Practical automated design of multistory masonry shear wall structures is provided by the computer program discussed in this paper. The program utilizes standard techniques of reinforced masonry shear wall design and analysis, in conjunction with procedures and values specified by the Uniform Building Code. Automated techniques provide a means of data-controlled design, eliminating the need to learn a Problem Oriented Language. Required input is minimal. A selection of data-controlled design criteria allows the engineer-user flexibility in modifying the design according to his needs. Output includes input data, analysis computations, design results and a cost estimate.

As research introduces improvements and refinements in design and analysis techniques, and as code requirements are revised, portions of this program will have to be changed. Revision and/or replacement of these portions will be facilitated by use of structured programming techniques. At present, buildings with stepped floors or having more than one independent tower cannot be designed. This program is also limited to buildings with vertical walls which are parallel and/or perpendicular. Walls, however, can be continuous, discontinuous, contiguous, or isolated.

INPUT

Formulation of program input received careful consideration. Input data provides the sole means of communication to the program, and must include information about the geometry of the structure, loads, and analytical controls for the design process.

An overview of the structuring of data input is provided by Fig. 1, User Sheet. Input cards shown on the User Sheet are detailed in Figs. 2 and 3, which show Typical Cards. Except for the first

¹Professor and Chairman, Civil Engineering, Arizona State University, Tempe, Arizona.

²Graduate Student, Civil Engineering, Arizona State University, Tempe, Arizona.

Figure 1. User Sheet

NUMBER OF CARDS

ORGANIZATION OF INPUT CARDS

LEGEND

must use 3 {

(0) ID Cards

GEOMETRY

1 card {

(I) Geometric Control Card

Coordinates of Ends of Walls (alternately called joints or nodes)

NN/3 Cards {

(II) Coordinate Cards [NN is Number of Nodes]

Geometry for Level #1

NW sets:
1 set for
each wall {

(III) Wall Control Card [NW is Number of Walls]

{ NOP Cards
per wall

(IV) Pier Cards [NOP is Number of Piers per
Wall]

Geometry for Upper Levels

1 set
for
each
level
that
differs
from
level
below {

{ NWA sets:
1 set for
each wall
added

{ NOP Cards
per wall

(V) Wall-Change Control Card

(III) Wall Control Cards

(IV) Pier Cards [Note: Value of NOP changes
with each wall]

{ NWC sets:
1 set for
each wall
added

{ NOP Cards
per wall

(III) Wall Control Cards [Note: Leave all spaces
blank except where
changes occur]

(IV) Pier Cards

{ NWD/10 Cards

(VI) Wall Delete Cards [NWD is Number of Walls
Deleted]

Parapet Data (Skip if none exist, i.e., if IP = 0 on Geometric
Control Card)

IP/10 cards {

(VII) Parapet Cards

[IP is Number of Parapet
Walls]

LOADING

1 card {

(VIII) Load Control Card

varies {

(IX) Load Card(s) [Note: Unless loads differ on every
floor, a zero or blank is
required in the first odd-
numbered column after the last
differing load--this may
necessitate a card with only a
zero in column 1 to complete
sequence]

ANALYTICAL CONTROLS

1 card {

(X) Analytic Control Card

COST DATA

1 card {

(XI) Unit Costs Card

if used; 1 per level {

(XII) Multipliers

three cards of legend, which provide the user with the means to title and identify his program, all data cards have an identical format. This system is used both (1) to facilitate preparation of coding for a building and (2) to expedite typing of input data. Excluding the legend cards, twelve types of data cards are shown on the User Sheet, relatively in order of use. Observe that the data cards break down logically into four main types: (1) legend, (2) geometry, (3) loading, and (4) analytical controls and cost data.

GEOMETRY. Because both horizontal and vertical geometry of shear wall structures is typically repetitious, care has been taken to develop a method which minimizes input for such occurrences. Simultaneously, freedom is allowed for using the program to design structures with non-repetitive portions.

The (I)Geometric Control Card establishes the number of stories in the building, whether the building has parapet walls and how many, the number of joints, and the number of walls on the first level. Coordinates of the "ends of all walls" are entered on (II)Coordinate Cards.

Once this basic data has been read, specific information for the first level is required, starting with a (III)Wall Control Card. This card establishes the location of the wall, its function in the structure, the number of piers, and its height. With the basic wall information complete, information is required on (IV)Pier Cards--for each pier of that particular wall. Thus, geometry of the first level is defined by a set of cards, always with a (III)Wall Control Card followed by a sufficient number of (IV)Pier Cards to define the geometry of openings for that specific wall.

After the geometry has been established for the first level, geometry is entered for the upper levels. Only new information defining changes from the floor immediately below need be supplied. If everything on any subsequent level is identical with the level immediately below, then absolutely no entries are required. If any wall changes at a particular floor level from that of the wall directly below it, a (V)Wall-Change Control Card is necessary. This is the first card in a set which contains:

- (a) (IV)Wall Control Cards for any walls added beyond that of the level below, followed by their respective (IV)Pier Cards AND/OR
- (b) (III)Wall Control Cards followed by their respective (IV) Pier Cards for all walls which are changed (only entries for changes are required, all other spaces should be left blank) AND/OR
- (c) (VI)Wall Delete Cards.

Using this system, for any higher level floor the entries could be: Nothing at all or a (V)Wall-Change Control Card with any combination of add, change, or delete sets following it. The configuration of the

Figure 2. Typical Cards

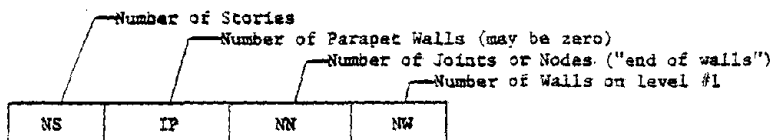
(0) ID Card

Use any or all 80 spaces for TITLE and IDENTIFICATION

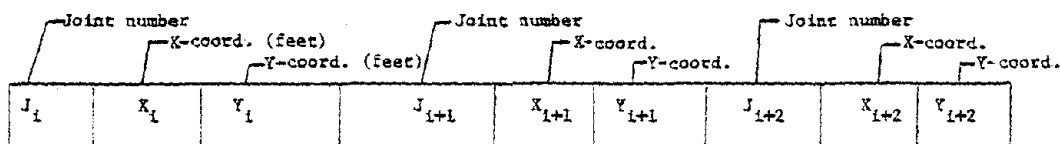
FORMAT FOR ALL DATA CARDS:

1. Maximum of 10 values in any card
2. Use a decimal point with every number
3. Start numbers on card as follows: Column of data: 1 2 3 4 5 6 7 8 9 10
Column on card: 1 9 17 25 33 41 49 57 65 73

(I) Geometric Control Card

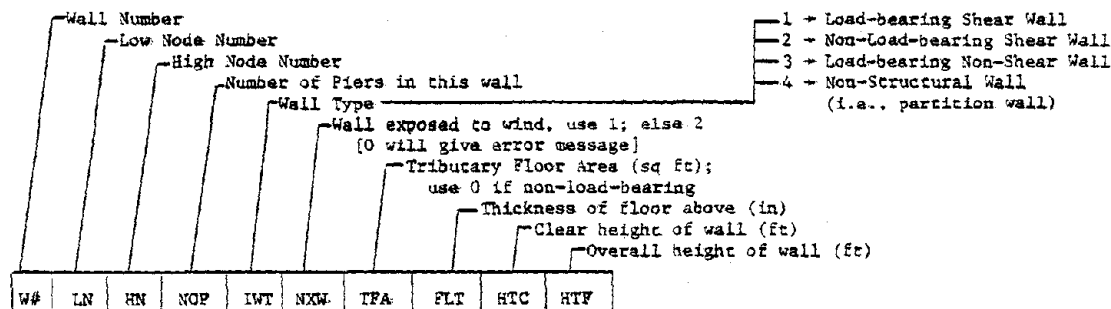


(II) Coordinate Card



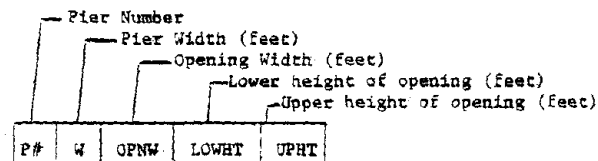
Comment: Use maximum of 3 nodes per card; do not skip spaces; will use NN (see Geometric Control Card) ÷ 3 cards in all.

(III) Wall Control Card

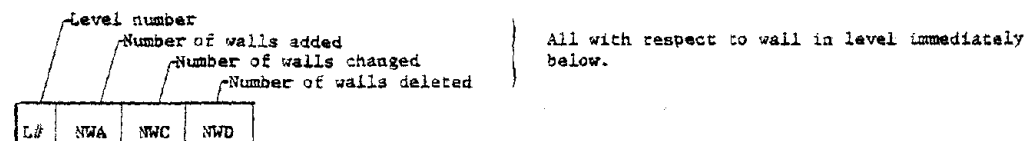


Comment: Use either HTC or HTF, but not both. (Needed only on first card of level.)

(IV) Pier Card



(V) Wall-Change Control Card



(VI) Wall-Delete Card

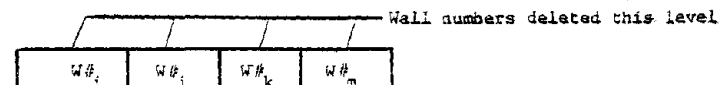
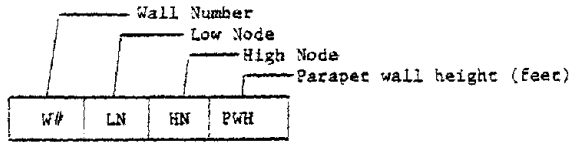
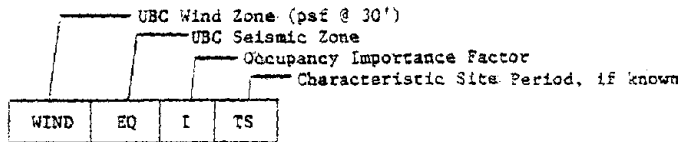


Figure 3. Typical Cards

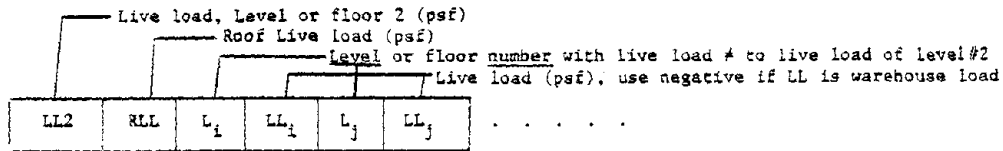
(VII) Parapet Card



(VIII) Load Control Card

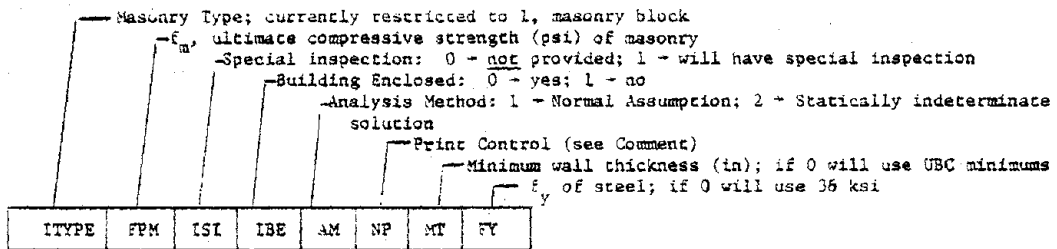


(IX) Load Card



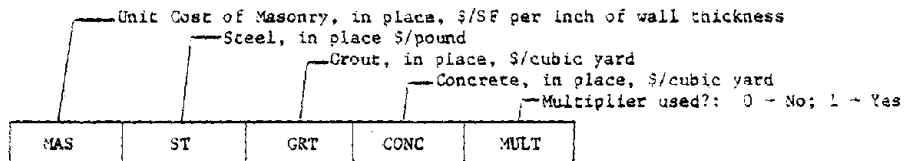
Comment: Unless loads differ on every floor, a zero or blank is required in the first odd numbered column after the last differing load--this may necessitate a card with only a zero in column 1 to complete sequence.

(X) Analytical Card



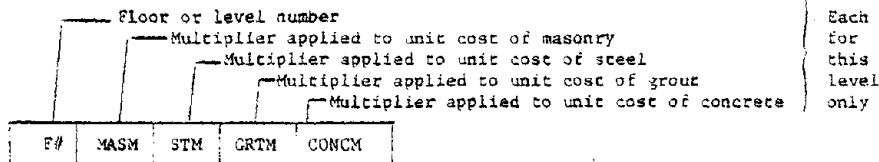
Comment: NP>1 Input Values and Design Results including Cost Estimate
 NP>2 Analysis used for Final design
 NP>3 Analysis for each iteration

(XI) Unit Costs Card



Comment: Multipliers, as input on "multiplier cards" if used, provide a means to adjust unit, in place, costs for different floor levels.

(XII) Multiplier Card



Comment: A multiplier of 1.00 can also be signified by a zero or blank.

structure at any level is always compared with the level immediately below.

The geometry is completed by (VII)Parapet Cards--only if parapets have been declared to exist in the previously read (I)Geometric Control Card.

LOADING. Once geometry of the structure is complete the (VIII)-Load Control Card establishes both wind and seismic zones, and specifies the occupancy importance factor as well as the characteristic site period if it is known. Input of loads is completed by reading a sufficient number of (IX)Load Cards to specify: (1) live load at the second level, (2) roof load and (3) live loads on all other levels which differ from that of the second level. When floor is used as a warehouse, the negative of live load is input to signal that part of the load is to be used for lateral seismic force.

All dead loads are computed from the structure itself. Floor loads and tributary areas to walls remain unchanged throughout the design process. Dead loads of the walls, however, change with changing thicknesses during the iterative design process.

CONTROLS. The type of masonry used, the ultimate compressive strength of the masonry, whether or not special inspection is provided, and whether or not the building is enclosed are all contained on the (X)Analytical Control Card. This card also contains a control for the type of analysis to be used on the walls and establishes the amount of output which is to be provided by the program. The analytical method most commonly used in longhand computations is provided by entering a 1, but does not yield story drifts. A more precise, statically indeterminate method is normally recommended, provided by entering a 2.

The (X)Analytical Control Card also contains two pieces of optional information, which are set automatically if not supplied. Unless otherwise specified, the minimum wall thickness is six inches and the yield strength of steel is 36ksi.

The next card, (XI)Unit Cost Card, specifies estimated unit costs to be used for the building. In the case of high rise structures, when multiplier values indicating cost variations with height above grade are available, they can be supplied on (XII)Multiplier Cost Cards.

EXAMPLE. Illustrations of examples of multistory shear wall buildings using information from the User Sheet of Fig. 1 and Typical Cards from Figs. 2 and 3 will be available for review at the conference. Due to space limitations, however, these are not included in the paper.

ANALYSIS AND DESIGN

ASSUMPTIONS. The floor systems are assumed to be perfectly rigid and to function as diaphragms which transfer the story shear forces to the shear walls in accordance with the relative rigidities of the walls. Shear walls in a plane perpendicular to the direction of the applied shear force are assumed to offer negligible resistance; only walls parallel to the applied shear force are included in lateral resistance computations, except for polar moment of inertia.

Rigidities are computed assuming: (1) wall material is linearly elastic, homogeneous and isotropic, (2) bottom pier edges do not rotate and (3) no elastic shortening occurs in the wall segments directly above openings.

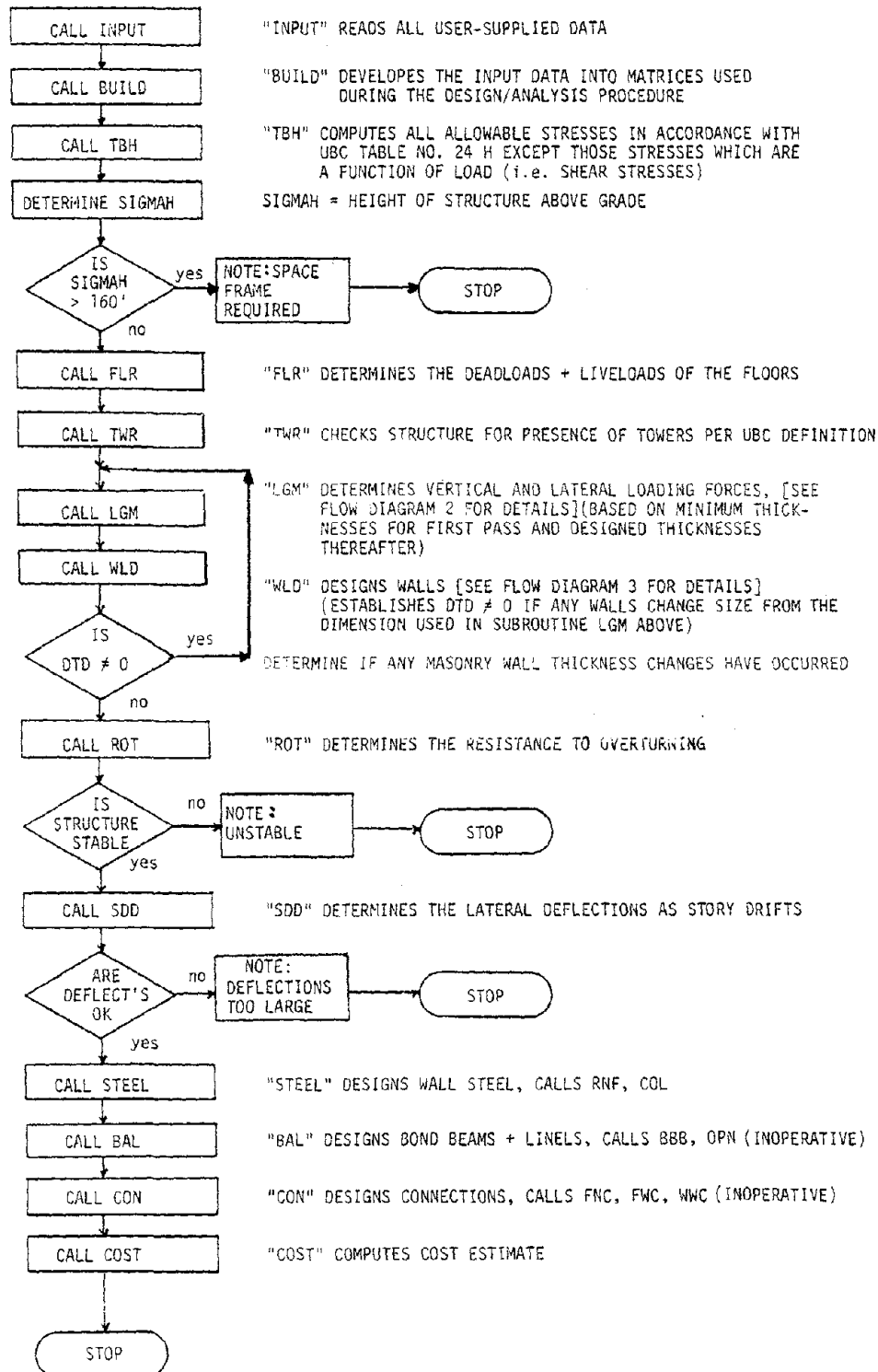
BASIC PROCEDURE. The basic procedure for the analysis and design of structural elements is illustrated in Flow Diagram 1. After the user supplied input has been read, the allowable stresses are computed in accordance with code specifications and stored. Allowable stresses which are functions of load (i.e., shear stresses) are computed elsewhere. The total height of the structure is then checked against the code specified maximum; computation is terminated if the building is too tall. Floor dead loads and live loads are computed and distributed to load-bearing walls according to the tributary floor areas. The structure is checked for the presence of towers, in accordance with the UBC definition, in order to determine governing seismic forces.

Once the preliminaries are complete, the program enters an iterative procedure which generates forces due to loads and establishes thicknesses of masonry walls. The Load Generation Module (discussed in more detail below) utilizes masonry dimensions established during the last iteration of wall design. Alternately, on the first pass code or user specified minimum wall thicknesses are used. Wall forces are computed for seismic, wind and gravity loads. With wall forces determined, walls are analyzed by WLD (discussed in more detail below) and masonry dimensions revised as necessary. If any dimensional changes occur, the procedure is repeated. If no dimensional changes occur, convergence has been reached and the program proceeds.

With walls designed, the structure is checked for lateral stability about each axis. In accordance with the UBC, if the factor of safety is less than 1.5, the program terminates. The structure is also checked for lateral stiffness by checking story drifts against code specified maximums, terminating if deflections are too large.

If the structure satisfies all these criteria, the program designs the wall steel and computes the cost of the structure. Although currently inoperative, Flow Diagram 1 shows where bond beams, lintels and connections will be designed.

FLOW DIAGRAM 1: MULTISTORY REINFORCED MASONRY SHEAR WALL BUILDING DESIGN (MRM)



DETERMINING LOADS. Loads are generated in the Load Generating Module, LGM, illustrated in Flow Diagram 2. Gravity loads and structure masses are computed in module DLC for every iteration because both are functions of masonry dimensions. The dead load, and in some cases part of the live load, are used to determine seismic forces. Wind shearing and overturning forces are computed in module WFS on the first pass only. Seismic shearing and overturning forces are computed in module SMV for each iteration. Base shear and overturning moments are computed and distributed in accordance with code specified procedures. If towers are present, additional lateral forces are computed and the governing force determined in module TFS.

ANALYSIS AND DESIGN OF WALLS. All walls in a structure need not be designed as load-bearing shear walls. The engineer-user may, therefore, specify walls to resist no gravity load, walls to resist no horizontal shear forces, or non-structural partition walls. Such specifications must, of course, be consistent with construction methods actually used, particularly with respect to joints and connections.

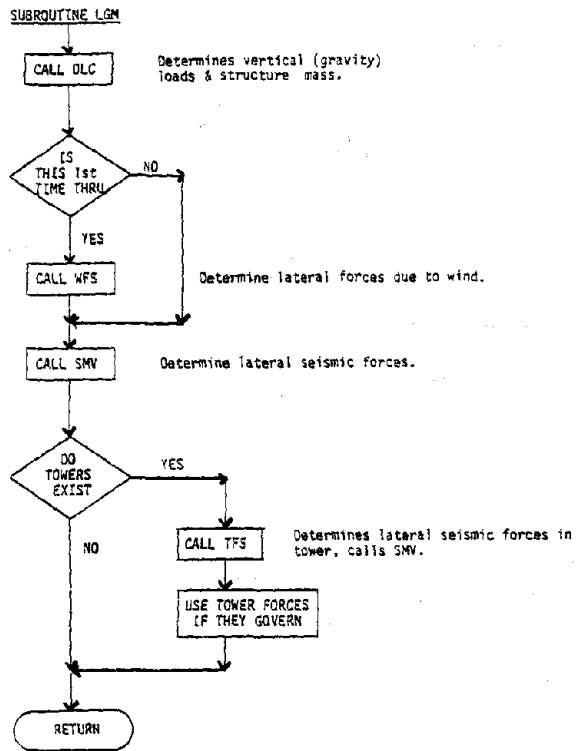
The analysis and design of the structural masonry walls is accomplished in the Wall Design Module WLD illustrated in Flow Diagram 3. This module does one level at a time, sequentially. For each level, the relative rigidities and other wall properties are determined in module MBLD1, illustrated in Flow Diagram 4. When no change has occurred in wall thicknesses, their properties also are unchanged (from the previous iteration) and therefore are not recomputed. Each wall is analyzed, and if necessary, wall thicknesses are changed in module SBW, illustrated in Flow Diagram 5.

MASONRY WALL PROPERTIES. MBLD1 uses two methods to compute wall/pier rigidities. Method 1 uses WST1 and is the simpler of the two. It computes wall rigidity by dividing the wall between openings into piers. Method 2, used by WST2, divides the entire wall into piers and uses a statically indeterminate method for computation of rigidities.

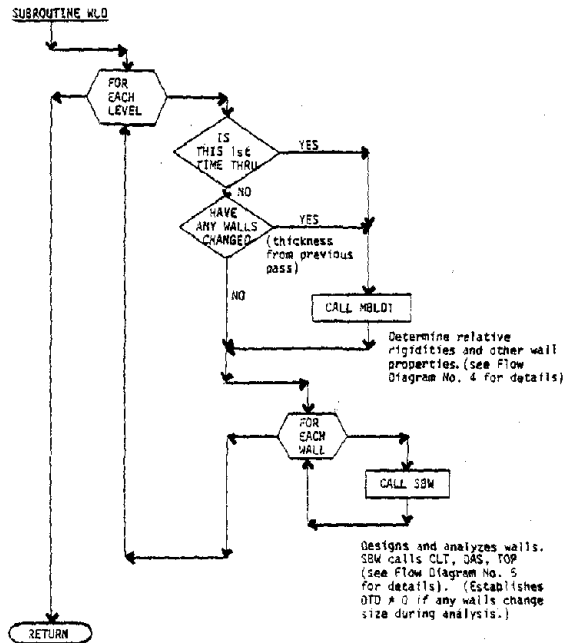
AI computes the static properties of each wall: the cross sectional area, centroid and moment of inertia for each wall plus the polar moment of inertia (in units of rigidity-ft²) and the center of rigidity for the entire level. Eccentricities and torsional forces are calculated within MBLD1.

WALL ANALYSIS. Within SBW (Flow Diagram 5), CLT checks wall thickness against minimum code requirements and DAS determines the actual stresses in the piers of the walls--for each loading condition. Structure walls are analyzed for five different load conditions: (1) dead load plus live load plus lateral load due to wind, (2) dead load plus lateral load due to wind, (3) dead load plus live load plus seismic lateral load, (4) dead load plus seismic lateral load and (5) 1/2 dead load plus seismic lateral load.

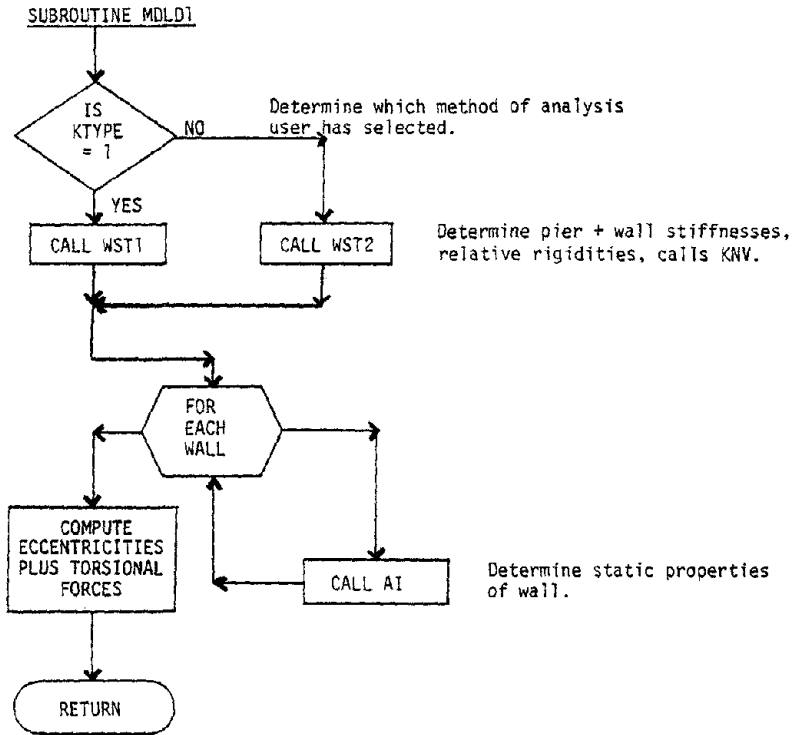
FLOW DIAGRAM 2: LOAD GENERATING MODULE (LGM)



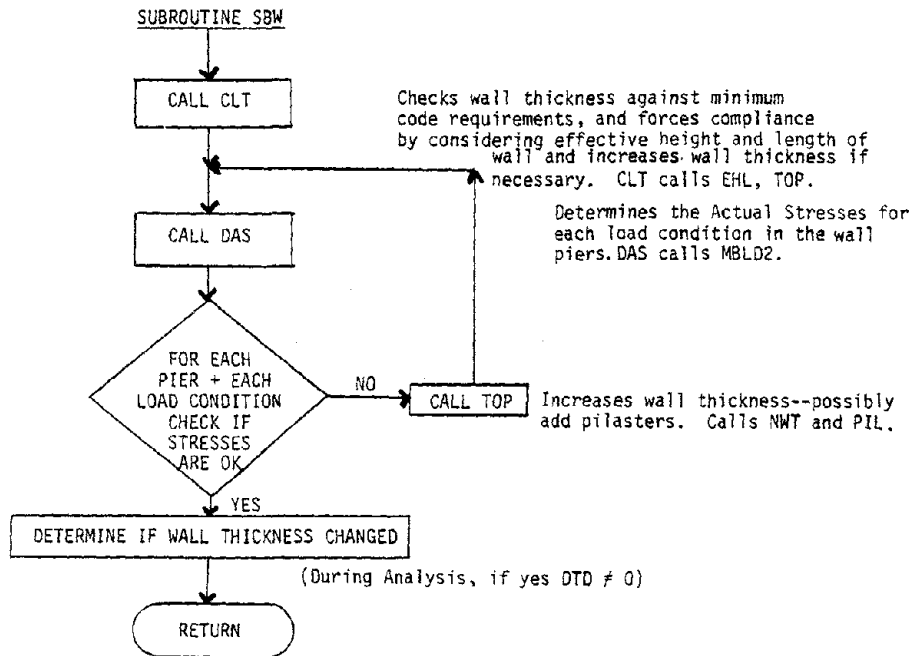
FLOW DIAGRAM 3: WALL DESIGN MODULE (WLD)



FLOW DIAGRAM 4: MASONRY WALL PROPERTIES (MBLD1)



FLOW DIAGRAM 5: WALL ANALYSIS (SBW)



Wall analysis results in unit stresses for each pier of the wall, as caused by each of the five loading conditions. The following are computed: (1) axial unit stress, (2) bending unit stress, (3) overturning unit stress, (4) shearing unit stress, (5) maximum tensile unit stress, (6) maximum compressive unit stress.

Once the unit stresses have been determined, they are checked against allowable masonry stresses and other code requirements. If actual stresses exceed allowable stresses, or if other code requirements are not met, wall thickness is increased (in some cases pilasters may be added). The process is repeated for each wall within each level, and for each level until all walls in the structure have been analyzed.

FLAG. A flag, DTD, is set if any walls have changed thickness. This flag controls computations of new loads when convergence has not been reached.

OUTPUT

This program was developed for use in the design office and thus the style of printed output conforms closely to standard procedure. The format facilitates preparation of drawings, checking of designs by the responsible engineer, and provides data to assist regulatory agencies in approving the plans. An outline of program print out is shown rather than actual output because of space limitations. It is planned to have several different building designs available for review at the conference.

OUTLINE OF PROGRAM PRINT OUT:

- I. Introduction
 - A. Program Title
 - B. Brief Program Description
 - C. User Supplied Title and Identification
- II. Input Echo
 - A. Structure Data
 - B. Design Criteria
 - C. Floor/Roof Data
 - D. Node Coordinates
 - E. Wall-Pier Data
- III. Analysis Computations
 - A. Base Shearing Forces
 - B. Distribution of Forces
 - C. Level, Wall and Pier Properties
 - D. Stresses in Piers of Walls

IV. Wall Design Results

- A. Masonry Thickness
- B. Vertical Steel
- C. Horizontal Steel

V. Lateral Criteria

- A. Resistance to Overturning
- B. Story Drift

VI. Cost Estimate

Although input is checked for reasonableness, it is echoed to provide additional safeguard against error. In addition, such input is useful when studying the design results.

Analysis print out includes the loads generated by gravity, wind and seismic forces. Values are shown for each iteration or for only the analysis used in the final design. All necessary identifying data is shown with computed properties of the masonry walls (rigidities, relative rigidities, moments of inertia, etc.), computed properties of each level (polar moments of inertia, center of rigidity, torsional eccentricities, etc.), intermediate calculations and stresses for all elements.

Design results include masonry thickness and horizontal and vertical steel for walls. These results are organized to provide ease in preparation of structural drawings.

Output also indicates resistance to overturning, story drifts, and a cost breakdown. A print control system is utilized to provide flexibility in the amount and detail of output. This flexibility was also an invaluable aid in the process of testing and debugging the program.

PROGRAMMING TECHNIQUES

STRUCTURED PROGRAMMING. As used in this paper, a structured program is composed of a series of modules, each module performing some specific function. By definition, a module has only one entrance and only one exit (except for possible error exits). Flow through the program is module by module, sequentially, along a straight-line path until each function has been performed and the program is complete.

Modules are primarily subroutines, although mini-modules are often used within subroutines to accomplish particular loops, and maxi-modules combine subroutines into larger constructs. Programs

written employing structured programming techniques tend to optimize human effort, sometimes at the expense of machine efficiency. They are easy to follow, easy to change and easy to correct.

Segmenting the program into modules aids the programming in a number of ways. Segmenting allows formulation of a program which is larger and more complex than could otherwise be completely grasped, in detail, at any given moment. Segmenting also allowed incorporation of the work of others into the project, increasing programmer efficiency. Thus, members of a group can function simultaneously and independently toward completion of a single project. Well defined modules increase efficiency by being available as tools each time a specific task is to be performed.

TOP-DOWN FORMULATION. The Top-Down concept provided a holistic approach to conceptualizing, writing, and debugging this program for the design of multistory masonry buildings. Flexibility was provided to effectively and efficiently add to, revise, or replace portions of the program because tasks are well defined, have clearly delineated boundaries, and the order and sequence of computation is always clear. Top-Down programming also helps insure that program data structure is complete so that all modules receive necessary data and can return results of computations to appropriate storage locations.

The main program was tested using a top-down procedure. Before subroutines had been thoroughly tested by a bottom-up procedure, "dummy" subroutines were used to echo call lists and insure proper transfer of data. A number of these "dummy" subroutines also supplied a set of internally fixed or generated data to be used by subroutines in later portions of the program.

BOTTOM-UP FORMULATION. In contrast to Top-Down, the Bottom-Up formulation focuses on the details; the primary objective is to insure that individual elements work perfectly.

Bottom-Up testing was used to independently validate portions of the program. Such testing started at the "bottom" and proceeded to the "top", i.e., testing began with those subroutines which call no others, using a "dummy" program designed specifically to test it thoroughly.

A typical testing sequence can be illustrated by referring to Flow Diagram 5 on Wall Analysis. Subroutines, MBLD2, NWT, and EHL were validated independently. At the next level, TOP was validated using previously validated NWT and a "dummy" PIL. At the third level, CTL (using EHL and TOP, which used NWT and "dummy" PIL) and DAS (using MBLD2) were tested independently with their own "dummy" test programs. These were then combined and tested together by a "dummy" program calling SBW.

The procedure was sometimes modified because of difficulties in providing sufficient data for a thorough test; in such cases a combination of lower-level top-down testing was combined with bottom-up testing.

VALIDATION. Judicious use of Top-Down and Bottom-Up formulation and testing, used in conjunction with structured programming, has greatly aided in insuring a program which is error free. These techniques provided a systematic way of program debugging and led to substantial savings in time.

Because this program designs a building, and because the occupants of such buildings depend upon structural integrity for their safety, it is encouraging to have the assurance provided by this combination of techniques.

SUMMARY AND CONCLUSIONS

Use of structured programming in conjunction with Top-Down and Bottom-Up formulation and testing has led to the development of an efficient and effective program for designing multistory reinforced masonry buildings. Having started with the holistic view, additions and refinements can be made rather easily.

BUILDING GEOMETRY. The program needs to be expanded to handle: (1) buildings having walls that are not parallel and perpendicular to each other, (2) buildings having independent towers, and possibly (3) buildings having floors which are stepped with respect to one another. All of these changes can be made with only minor modifications to the existing program plus the replacement of specific subroutines.

DETAILS. Initial work has been done on the design of details. Completion of this work will result in a complete design of bond beams, lintels, and connections.

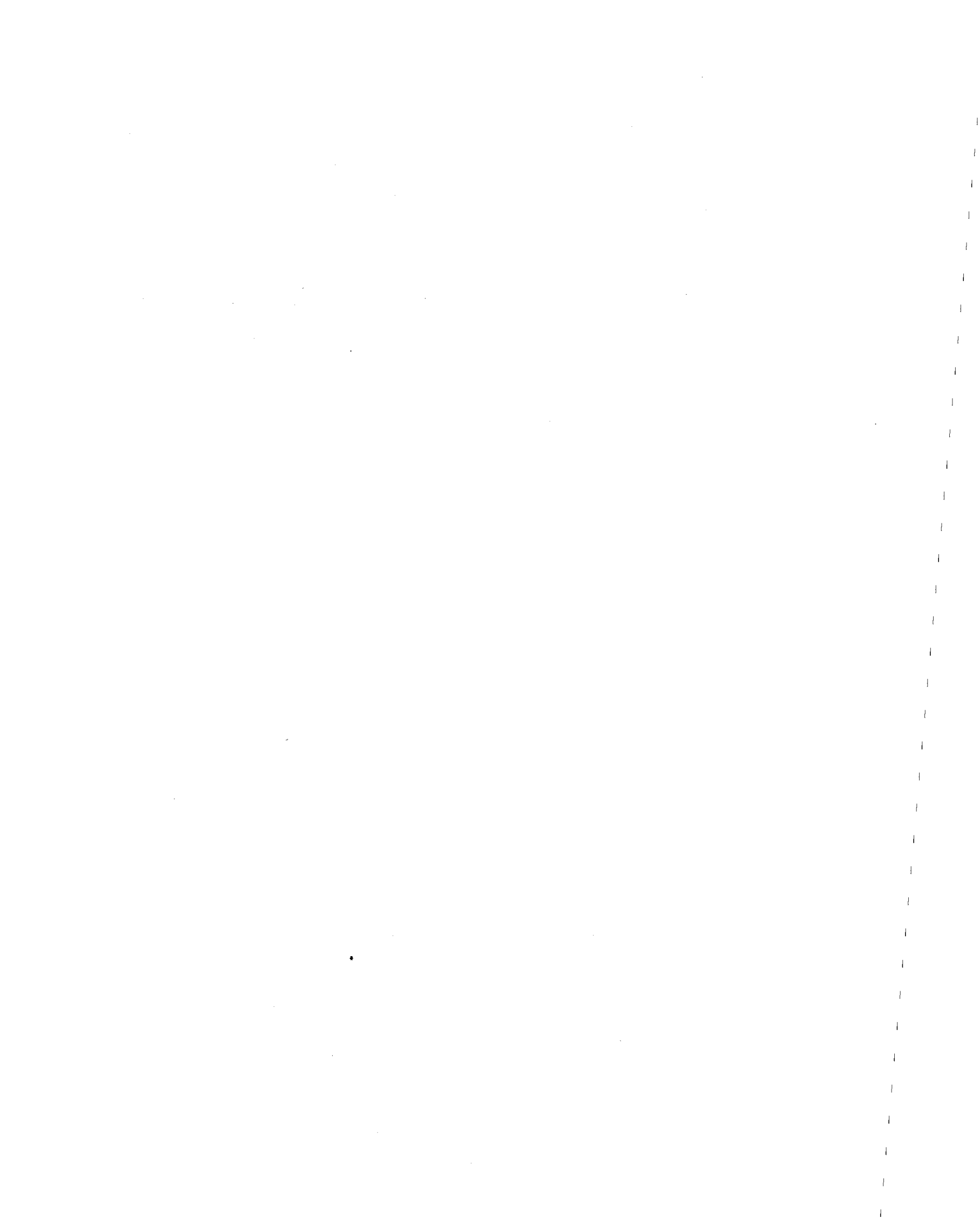
Of large scope, it is desirable to automate the design of floor systems of a general nature so that tributary loads to walls will be computed within the program itself.

Another undertaking of similar magnitude is the refinement of the dynamic analysis of the structure to include the latest theoretical refinements.

PARAMETRIC STUDIES. With very minimal alterations, the program provides the capability for doing parametric studies related to cost of the structure in different parts of the country, and with respect to changing costs associated with the height above the ground floor level. Eventually, such studies could be useful in comparing different structural systems for buildings.

Another easily implemented interesting parametric study is to design a series of building shapes, for a succession of heights-- each starting with the lowest wind and seismic zones and going to the highest. This process would provide a cost comparison relating differences inherent in varying lateral forces. Such information could prove valuable by giving definitive guidelines in the choice of structural configurations, dependent upon geographical location and cost factors.

As it stands, the program provides a means to compare costs between structures which have special inspection and those which do not. Such comparisons would relate overall cost of structures, including the differential costs of supervising labor.



MASONRY BUILDINGS: CONSTRUCTION ON SUBSIDENCE SITES

By Hall,¹ Harold Clifford

ABSTRACT: This paper deals with a basis for structural design of shallow foundations for support of rigid masonry structures on subsidence sites. It is assumed that the structure is to be located on a surface which will settle in the future, within certain limitations. Examples of subsidence sites include mined sites, thick clay soils, and filled sites. Both superstructure and substructure design considerations are treated; deflection (deformation) of the building is a primary consideration. The paper represents design practice in the author's consulting office for this type of problem; it is based on the author's experiences and on British and European practice.

¹ President, H. C. Hall, Consulting Civil Engineer, Inc., Hart, Michigan

MASONRY BUILDINGS: CONSTRUCTION ON SUBSIDENCE SITES

By Harold Clifford Hall¹

INTRODUCTION

Special procedures are required for design of masonry structures where uncontrolled deep-seated movements in the underlying soil or bedrock are expected. This paper deals with the unique goal and associated problems of successful construction of masonry buildings on subsidence sites.

The writer has, in recent years, been involved with site evaluation and design of buildings proposed for subsidence sites in the Wyoming Valley (Wilkes-Barre and Scranton area), Pennsylvania, where deep mining of multiple seams of coal has been carried out over the past 100 years. This work, performed for an agency of the U. S. Government, included the preparation of a Manual (4) for the guidance of government engineers in site evaluation, subsidence prediction, and plan review. The corresponding practices of engineers in England and Europe were summarized by Chen et. al. (1) of Michael Baker, Jr., Inc., Consulting Engineers of Beaver, Pennsylvania.

This paper represents the practice of this engineering office for this type of problem.

PURPOSE OF THIS PAPER

The provisions made in this paper may severely limit the architect's design options. On the other hand, proper engineering design should significantly enhance the chances that the structural unit will survive large subsidence-related strains, possibly without damage, and that human life and safety may be reasonably protected. Thus, the purpose of this paper is to outline a basis for responsible design of a rigid masonry structure on a subsidence site.

SUBSIDENCE SITE DEFINED

Notorious subsidence zones include heavily-mined coal fields, as well as areas where water tables have lowered. We assume that, for such a site, future subsidence will not be "minor" or "ordinary",

¹Consulting Engineer, Hart, Michigan

Numerals in parentheses refer to corresponding items in the Appendix I.--References

in the usual sense. Areas of significant subsidence may be well known to the reader. The causes of subsidence, as recognized in this paper, are summarized as follows:

1. Mined and cavernous sites; karst areas. Changes occurring in underground cavities; it is assumed that these changes, despite the mechanism of movement, will cause subsidence at the ground surface.
2. Clay sites. Major time-dependent consolidation caused by vertical stress in underlying soil. This settlement may be associated with any or all of the following factors:
 - a) the weight of the structure,
 - b) the weight of new fill,
 - c) lowering of the water table.
3. Dessiccation shrinkage of clay. Often caused by uptake of water by roots of trees.(2)
4. Filled sites. Consolidation due to internal ravelling (5), disintegration, or decomposition of fill materials; e.g., an uncontrolled fill of random materials such as building rubble. Also, consolidation of cohesive fill soil due to dissipation of excess pore pressure, especially if inadequately compacted.

Our definition of "subsidence" sites excludes "unstable" sites where shear failures are to be expected, (e.g., sliding or very weak bearing materials which cannot support footings), as well as earthquake zones. This paper applies only to sites where the bearing soil is sufficiently strong to provide adequate foundation support, but where large strains are expected under the proposed structure associated with changes occurring in or below these bearing materials.

MASONRY CONSTRUCTION

A masonry building may seem inappropriate for a subsidence site because of masonry's low tolerance to differential movement.(1,3) However, rigid masonry superstructures on subsidence sites are not uncommon throughout the world. In England, high-rise (13 or more story) buildings of rigid masonry have been built on subsidence sites; these buildings, small in plan area, are founded on stiff reinforced concrete rafts.(1)

SITE STUDIES AND INVESTIGATIONS

This paper does not deal with the methodology for investigation and evaluation of subsidence sites, nor with techniques for prediction of the amount, mode, or timing of any future movement. The potential for future movements, and the time-frame within which such movements can occur, can differ markedly from site to site for many reasons. The designer ought to avail himself of local experience and information regarding the potential for, and the rate, type and amount of future movements, including data, judgment and past history in the area. He should investigate the possibility of rapid or sudden subsidence, and whether a pothole could develop in the ground surface. On the other hand, if gradual rates of change in surface contours are predicted, these time-rates should be investigated. Future changes in surface contours should be predicted, and whether ground-stretching or surface-compression strains are to be expected.

THE ELEMENT OF RISK

Actual design should be undertaken by design professionals, equipped by training and experience to properly evaluate the site, to assess the significance and rate of future subsurface movement, to gauge the likelihood of success and the degree of risk, and to carry out a competent, appropriate design. A thorough site investigation is minimally necessary. Beyond question, some subsidence sites are not feasibly buildable; even those sites which may be buildable will incorporate an inevitable element of risk. Costly repairs and corrective measures may be required; the future cost of these measures should be anticipated by the owner. Because the circumstances are unique possibly involving liability to the designer, the details and significance of these risks ought to be realistically defined by the designer to the owner, at the outset.

DESIGN PRACTICE

Within the limitations defined in this paper, the following text describes our current general design approach to this type of problem. It should be emphasized that design decisions must depend upon actual building requirements and site conditions.

A. Site Preparation and Building Configuration

After grading, the site should be level; grade changes should ideally be "cut" rather than "fill", if possible, so as to minimize or reduce new vertical stresses in underlying materials. Also, a sufficient thickness of strong materials must underlie the foundation so as to satisfy the stability requirements of soil mechanics.

The plan of each building unit should ideally be simple and regular, e.g., a square or rectangular plan; complex plan geometrics should be avoided. The planned width or length of the building unit should probably not exceed about 80 feet, although larger structural units are possible depending on the nature and degree of the subsidence problem. The purpose of limiting the plan dimension of each structural unit is to minimize the relative size (and, thus, the cost) of the foundation, and to minimize risk; longer building units are riskier than shorter units. Large buildings can be constructed, comprised of contiguous structural units; no dimensional limit exists since individual units would be structurally independent of one another, although adjacent. However, special structural and geometric criteria will apply to the inter-face or "hinge" area. Damage in this area may be unavoidable. An appropriate gap will be required. Consideration could be given to a relatively small "link" unit, located between the larger buildings; a link unit would ideally be constructed so as to be more readily repaired at relatively less cost; possibly wood or light steel framing would be appropriate. Although separation between adjacent structural units is important, the appearance of a single monolithic building can be preserved. Shielding over the joint area should be large enough to account for reasonable increases and decreases in width.

Inherently heavy or sensitive structures, including warehouses and buildings which house sensitive machinery, as well as other special-problem structures, may be inappropriate as rigid buildings on subsidence sites. Although heavy buildings are possible, live and dead loads should ideally be as light as feasible, consistent with rigidity, so as to minimize the cost of foundation construction. Also, any building for which minor or temporary tilting-type deformation is intolerable should probably not be considered.

The building should preferably not incorporate a basement; as feasible, below-grade construction should be minimized. The main floor of the building should ideally be constructed at one level which should be at, or near, exterior grade. Steps in the main floor level are undesirable. The main floor level should probably be the surface of the concrete foundation raft, or directly supported thereon.

Where horizontal strains are expected, the zone around the periphery of the foundation should be backfilled with compressible material and should be properly drained so that the compressible fill material does not become water-logged and frozen. Examples of porous, free-draining, compressible fill materials include: chipped wood mulch; weak light-weight expanded ash particles; rock-wool or other suitable insulation. This zone of compressible material should be at least twelve inches in thickness and should surround the entire periphery of the foundation; it should allow lateral movement of the foundation without the development of significantly large passive resistance. Entrance slabs must span structurally over this compressible zone. Roof water and other drainage must be directed away. The surface of the compressible zone should be either paved with

asphaltic concrete, covered with decorative mulch, or similarly treated. It may be planted as feasible. The surface surrounding building units should slope so that positive drainage occurs away from the building area. Other design provisions to account for anticipated horizontal strains are provided below.

A building of about two-story height is desirable; that is, the dimension from main floor to roof should ideally be no more than about 20 feet. Despite the height of the building, consideration must be given to predicted changes in joint width, and to design stresses in the masonry as the subsidence occurs. For tower-like buildings, no internal masonry jointing is needed or desirable because towers are small in plan relative to their height; however, masonry stresses must be considered for various design conditions, including out-of-plumbness.

The suspended framing, floor and roof systems, should be of light construction. Joists, beams, and slabs must be well anchored into all contiguous masonry walls; this anchorage requirement applies to the bearing walls, and to walls which parallel the floor or roof framing.

Settlement checkpoints should be located on the exterior of the foundation, at corners, and at intermediate points along the walls, placed so as to permit a surveyor to readily measure vertical movement. Checkpoints should be established so as to monitor movement across joints in walls, and between building units. The first hint of movement may be revealed at the inter-face between structural units. Periodic monitoring of movements should be carried out throughout the life of the structure. A continuous record of all evidence of movements at and near the structure should be maintained. As the history of movement is developed, extrapolation of the data can be useful in refining predictions of future movement. If no significant vertical, horizontal, or rotational movements are detected, the time interval between sets of measurements can be greater (say, three months) so as to minimize the cost of monitoring. However, if progressive movement is detected or suspected, the time interval should be decreased to once or twice per month until it can be established whether a problem exists and, if so, whether the rate of movement is significant or ominous. Measurement of strains within the building may be readily recorded; as stated, changes in joint widths within and between buildings should be monitored. This type of monitoring can be done at relatively small cost utilizing simple equipment. If evidence is detected which might indicate stresses in the foundation, the services of a structural engineer should be obtained who would examine the data and determine whether over-stress may be developing. If over-stress exists or is predicted, a plan for corrective measures should be carried out before damage becomes significant. Corrective measures might include jacking of the foundation back to a level condition.

Pressure grouting under the foundation may be required in the future; because of this possibility, grout pipes should be incorporated into the foundation during construction at appropriate locations.

Underground pipes which serve the building unit, such as water, gas and sewer, should be articulated at the location where they enter the building. The purpose of this articulation is to account for relative movement between building and surrounding soil at the location where the pipes enter the building. Particular attention must be given to the gas service line, since rupture of such a gas line could have disastrous consequences.

Where pipes in the superstructure extend across joints within structural units, and between adjacent units, the pipes must be appropriately designed to accommodate movement. Greater movement may, of course, be expected at such joints in the plane of the roof than in the floors below. Also, the amount of anticipated movement between structural units is much greater than within the unit itself.

Under-floor utilities, such as sewers, water and gas pipes, should be placed in chases under the main floor so as to be accessible to the surface for maintenance and repair. They should not be encased in the foundation concrete.

B. Masonry Wall Construction

The structural unit should be constructed as a three-dimensional rigid monolith utilizing masonry walls and partitions. Masonry walls should provide structural support to floor and roof; posts or columns are less desirable. It may be necessary that the structural unit be segmented using crack-control joints which extend as a continuous vertical plane through the entire building. Although the usual maximum spacing of these through-building joints would be in the order of 25 to 40 feet, the actual spacing would depend on the building's geometry. The superstructure of a two-story 40' x 80' structural unit, for example, could be segregated by two of these joints into three more-or-less equal zones of about 40' x 26'8". On the other hand, the superstructure of a tower-like building would probably not be jointed. The through-building joints would be continuous through floor and roof construction so that relative movement could occur. The joint width should allow compression movement of at least 3/4 inch. The greatest movement is to be expected at or near the roof level. These joints should not be placed at or near locations of doorways and windows, since if movement occurs, the dimensions of door and window openings should ideally not be changed. Smaller window and door openings are preferable to larger openings.

All masonry wall construction whether bearing or non-bearing should be well reinforced horizontally. Vertical reinforcement may be needed, as well; for vertically reinforced walls, hollow-unit masonry is suggested; the block cores would be filled with concrete, and the reinforcing steel would be continuous from top to bottom of the wall. Walls should be bonded together at intersections and at corners. Vertically reinforced walls should be adequately anchored down to the

foundation using dowels. The purpose of horizontal and vertical reinforcement, and anchorage, is to produce a strong, stiff, three-dimensional monolith capable of resisting strains.

Where joints in walls or floors are provided, the architectural treatment should account for the maximum expected amount of movement; aesthetic problems can be minimized or eliminated by proper design of joint covers. Roof leaks can be minimized if particular attention is given to joints in the roof structure so as to account for the sum of temperature movement and foundation-related movement.

According to British practice, a relatively weak lime mortar is preferred; it is believed that "softer" mortar will produce a more flexible wall. However, in our view, this concept would be inappropriate where vertically reinforced masonry is to be used; also, the use of "weak" mortar seems more appropriate for brick than block masonry because the units are smaller.

C. Foundation Design and Construction

The "Building Code Requirements for Reinforced Concrete" (ACI 318) of the American Concrete Institute should govern the structural design of the foundation for the ordinary foundation considerations, for the subsidence problem, and for the releveling process.

The subsidence, it is assumed, would tend to cause deformation in the foundation of greater magnitude than the superstructure could tolerate. For this reason, we assume that the raft foundation must incorporate flexural and shear strength to resist deformation in the building.

The design of the reinforced concrete foundation raft should account for dead loads, plus reduced live loads, on roofs and floor. Any reduction in live load should be in accordance with the judgment of the structural engineer; the purpose of reducing live loads is to realistically account for only the maximum probable loading to be delivered to the foundation.

The foundation within each structural unit should be of heavy, continuous, monolithic reinforced concrete. It should have two-way strength and adequate stiffness as herein recommended. It should be designed for cantilevering (negative moment), and for simple span (positive moment), in accordance with the designer's judgment, guided by the design assumptions described herein. See Figures 1 and 2. The designer should recognize that the location of maximum negative and positive moment is not fully predictable. The design, and the reinforcing steel placement, should be governed accordingly.

The raft foundation should be designed for deflection as well as stress. The following deflection allowances should be based on the spans shown in Figures 1 and 2. The amount of deflection which can

occur due to positive moment should not exceed 0.001 times the assumed simple span. The maximum amount of deflection due to negative moment, or cantilevering, should not exceed that which is consistent with a radius of curvature of 5,000 feet. This aspect, deflection, will probably control the size (cross-sectional area) of beams or slabs; the concrete stresses (flexure and shear) in the raft possibly may not govern. The member, in any event, should have relatively large shear area and large moment of inertia. It should be designed with sufficient concrete area so that web reinforcement (ties or stirrups) are not required as shear reinforcement; low shear stresses are desirable under assumed design conditions. Deep narrow beams should be avoided; ideally, the width of the beam should not be less than half the depth.

The reinforced concrete foundation should not be placed directly on bedrock. A zone of compacted sand, of at least two foot thickness, containing no more than about 15 percent finer than the 200 mesh sieve, should be placed as a cushion between the foundation and the underlying materials. The judgment of the project soil engineer is required relative to the details of this sand cushion.

If horizontal strains are expected, the concrete raft should be designed for frictional or drag forces which would develop along the interface with the underlying soil. The entire base (soffit) of the reinforced concrete foundation unit should be a level plane. The concrete foundation should ideally be a two-way flat slab of uniform thickness. However, if a beam system is to be used, close beam spacings are preferred, e.g., about 3 to 4 foot centers, maximum. If a two-way ribbed ("egg-crate") type foundation is selected, the coffering should be open air voids so as to minimize resistance to horizontal strain; they should not be filled with soil. The amount of horizontal drag force can be estimated by calculating the vertical unit stress being transmitted by the foundation to the underlying soil and by application of a suggested coefficient of friction of 0.7. The actual friction coefficient used should be selected according to the best judgment of the project soil engineer. This procedure would allow the designer to estimate the point or area where the maximum tension force is likely to occur along the length of the raft. The maximum force may then be calculated and the required reinforcing steel area determined accordingly.

All reinforcing steel should have a minimum yield strength of 60,000 psi.

Top and bottom horizontal reinforcing bars will be required in the foundation raft because positive and negative moments can occur at unpredictable locations. If beams are used, top and bottom reinforcing bars should be placed as a cage using tie bars. The tie bars should be of at least 3/8 inch diameter, spaced at no greater spacing than the vertical distance between the top and bottom reinforcing bars in the beam. The purpose of these ties is to assure accurate placement of the main reinforcing bars.

The raft concrete should be of high quality and should have a minimum 28 day strength of 4,000 psi. Where carbon-rich soils exist, a sulfate-resisting concrete may be appropriate. Foundation concrete should be placed in a single pour, if possible. Construction joints within a given foundation unit should be eliminated or, if they are necessary, should be minimized. Construction joints should be vertical, and provided with proper keyways for transfer of shear stresses, and with proper dowels (deformed reinforcing bars) through the joints so as to account for contraction stresses in the concrete.

The design of the building, including the foundation raft, should assume that the entire structure may tilt out of level. Ideally, the design should provide for restoration to a level condition without extraordinary expense; if releveling is required, high-capacity hydraulic jacks would probably be utilized. It is suggested that jacking points or locations, such as alcoves, be provided in the foundation where these jacks may be readily placed. An experienced structural engineer should observe the jacking operation, supported by surveying services as required. Careful coordinated jacking, along with careful measurement and monitoring of building movement, should prevent accidental damage to the raft and building. The structure would be gradually restored to a level, plumb condition. It is obvious that few jacking points would be preferred, rather than many points, in order to avoid complex indeterminacy and to minimize the likelihood of accidental over-stress and damage.

Pressure grouting under the foundation base would be coordinated with the releveling procedure so as to restore uniform support between the base of the foundation and the top of the underlying soil.

The design of the foundation should account for the possibility of "plan-skew" type distortions. As before, a fully continuous two-way slab is preferable for resisting these distortions, rather than a "pierced" slab or set of grade beams. Such a slab will more satisfactorily resist the forces which tend to distort the building into a skewed configuration. In any event, despite the pattern of forces exerted on the raft, it should be sufficiently strong to prevent damage. For this reason, if a beam-type of foundation is selected, a strong slab should be incorporated as an integral part of the beam system.

CONCLUSIONS

This paper provides a basis for design and construction of a masonry building on a site where future subsidence is expected, but where a conventional solution to the subsidence problem is not possible or feasible. Unstable sites such as potential landslide areas are excluded. Some considerations which should receive careful treatment in order to increase the likelihood of a successful project, are as follows:

- 1) A thorough and comprehensive site and subsurface investigation;
- 2) Proper preparation of the site;
- 3) Choice of appropriate building-unit size, geometry, and configuration;
- 4) Design of a suitable raft foundation;
- 5) Appropriate design of a rigid, reinforced masonry super-structure.

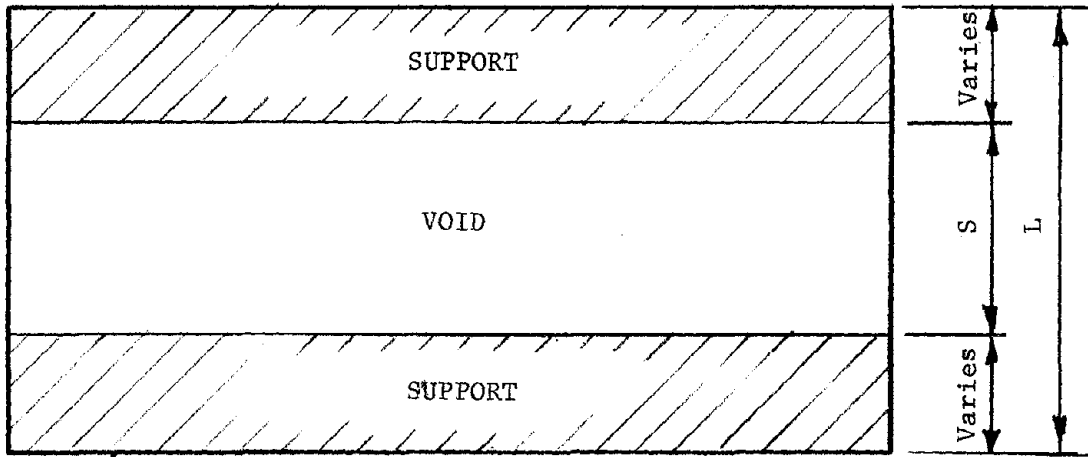
Despite all efforts to mitigate the problem by site evaluation, and to reduce risk by the construction of an appropriately designed building, some risk will probably be unavoidable. The owner may be required to bear the cost of future repairs and restoration.

It is recommended that engineers, architects, and builders who have dealt with this or similar problems, publish their data and experiences so that the profession as a whole may benefit.

- - - - -
APPENDIX I.-REFERENCES
- - - - -

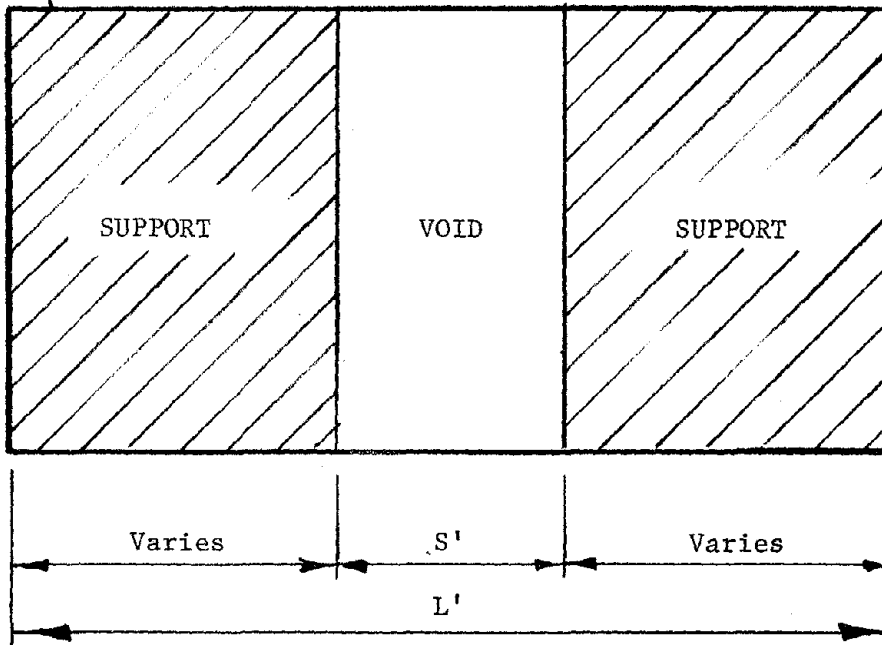
1. Michael Baker, Jr., Inc., "Architectural Measures to Minimize Subsidence Damage," Report ARC-73-111-2551, Appalachian Regional Commission, Washington, D.C., 1974.
2. Wallace, George B., and Otto, William C., "Differential Settlement at Selfridge Air Force Base," Proceedings, Design of Foundations for Control of Settlement, Evanston, Illinois, Soil Mechanics and Foundations Division, American Society of Civil Engineers, 1964, p.249.
3. Feld, Jacob, "Tolerance of Structures to Settlement," Proceedings, Design of Foundations for Control of Settlement, Evanston, Illinois, Soil Mechanics and Foundations Division, American Society of Civil Engineers, 1964, p.555.
4. Soil Testing Services, Inc., "Mine Subsidence Evaluation Manual," U. S. Department of Housing and Urban Development, Regional Office, Philadelphia, Pennsylvania, 1974.
5. Sowers, George F., "Foundation Problems in Sanitary Landfills," Journal of the Sanitary Engineering Division, ASCE, Vol. 94, No. SAI, Proc. Paper 5811, February, 1968, p.103.

APPENDIX II - FIGURES



PLAN
No Scale

Heavy, two-way, Reinforced
Concrete Raft Foundation



Note: Bars shall be based on maximum conditions, and shall be continuous full length of raft.

Splice: 30 diameters minimum

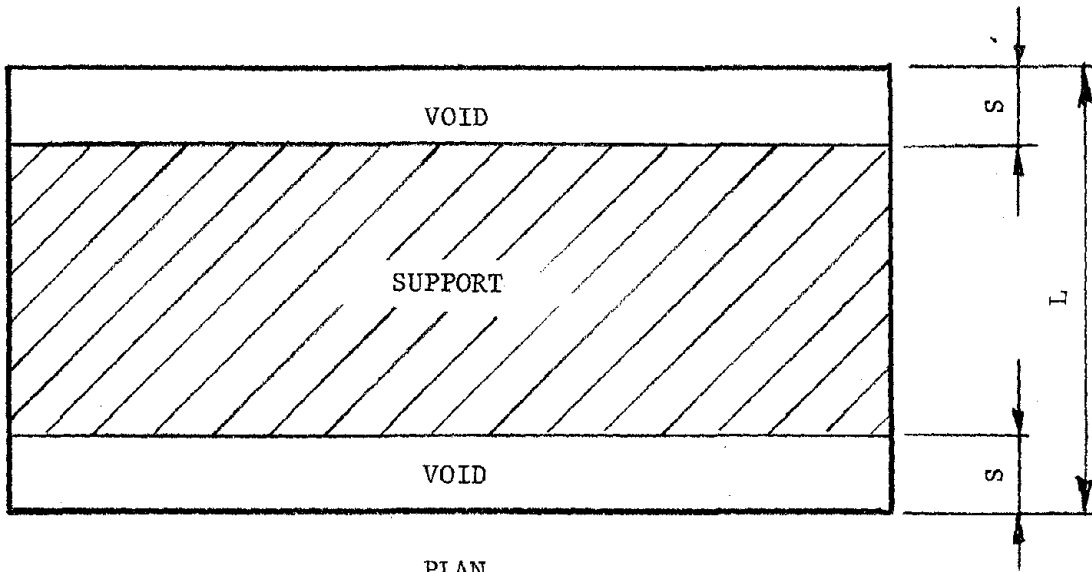
PLAN
No Scale

S & S' are Simple Spans

$$S = \frac{2L}{3}$$

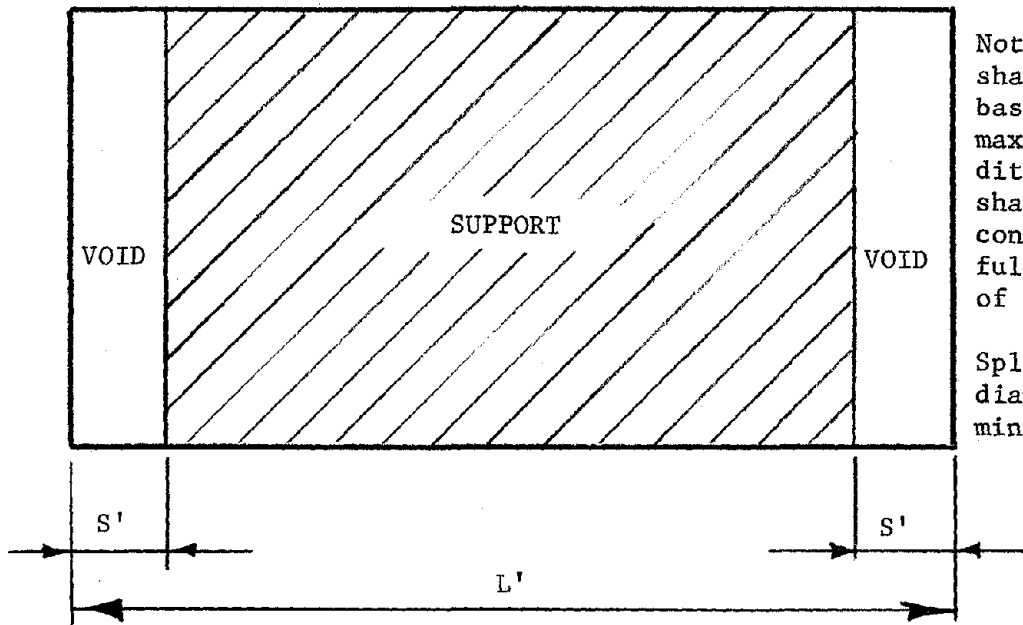
DESIGN FOR POSITIVE MOMENT (BOTTOM BARS) but $S \leq 20$ ft.

FIGURE 1



PLAN
No Scale

Heavy, two-way, Reinforced
Concrete Raft Foundation



PLAN
No Scale

DESIGN FOR NEGATIVE MOMENT
(TOP BARS)

FIGURE 2

Note: Bars shall be based on maximum conditions, and shall be continuous full length of raft.

Splice: 30 diameters minimum

S & S' are cantilever spans

$$S = \frac{L}{8} \text{ for } L > 64 \text{ ft.}$$

S = 8 ft. for $L \leq 64$ ft., except that

$$S = 0.4L \text{ for } L \leq 20 \text{ ft.}$$

A CONTRIBUTION TOWARDS THE DESIGN OF
HEAVILY LOADED MASONRY WALLS ON REINFORCED CONCRETE BEAMS

B. Stafford Smith¹ and Luigi Pradolin²

ABSTRACT: The paper describes a series of vertical loading tests to collapse of masonry walls on steel and reinforced concrete beams. The purpose of the tests was to determine whether a design method developed to account for the composite arching action of masonry walls on steel beams would be appropriate, or would have to be changed, when used for the design of walls on reinforced concrete beams. The principle of the existing design method is that the behaviour of a wall-beam structure is governed by the relative stiffness of the wall and beam.

The tests were made to compare the detailed behaviour of masonry walls on steel beams with those of similar walls on reinforced concrete beams of similar initial stiffness.

Six tests were conducted on wall-beams 6 ft span by 4 ft high. These were in three pairs, each pair including a wall on a steel beam and a similar wall on a similar stiffness reinforced concrete beam. Beams of low, medium and high relative stiffness were included.

The tests showed that the behavior of the two types of wall-beam structure differ to the extent that modifications to the design method should be made. Recommendations for the changes in the design method are proposed.

¹Professor of Civil Engineering, McGill University, Montreal.

²Graduate student, McGill University, Montreal.

AN EXPERIMENTAL COMPARISON BETWEEN MASONRY WALLS ON
REINFORCED CONCRETE BEAMS AND ON STEEL BEAMS

By Bryan Stafford Smith¹ and Luigi Pradolin²

INTRODUCTION

If a masonry wall is supported on a beam over an opening and is subjected to a heavy top loading, the beam tends to bend away from the wall in the middle of the span. Consequently the distribution of vertical stress between the wall and the beam is concentrated near the ends of the beam. This has the detrimental effect of increasing the maximum stresses in the ends of the wall to magnitudes substantially above the average value. However, a simultaneous and beneficial effect is to reduce the bending moments and deflections in the beam to substantially lower values than for the same load distributed uniformly across the span.

A useful analogy for the composite behaviour of a wall on a beam is a tied arch structure in which the wall acts as the arch and the beam serves as a tie to prevent the arch from spreading (Fig. 1). The distribution of vertical stress between the wall and beam has been shown in a number of theoretical and experimental studies (1,2) to be approximately equivalent to triangular distributions, as shown in Fig. 2.

The resistance of the beam to separation from the wall depends upon its flexural rigidity relative to the in-plane vertical stiffness of the wall. The stiffer the beam, the longer the effective lengths of contact α (Fig. 1). Conversely, if the stiffness of the beam is less, the lengths of contact are also less, thereby raising the stresses in the masonry and reducing the bending moments in the beam. When designing the beam from considerations of bending strength, this reduction of moment might allow the use of an even lighter, more flexible, beam which would further reduce the lengths of contact and bending moments, whilst again increasing the wall stresses. This sequence could be repeated until either the bending strength of the beam is reduced to a value lower than the diminishing bending moments, producing beam failure, or until the maximum compressive stress in the wall increased up to the masonry strength, to cause a crushing failure. In the majority of full-scale tests which have been made, the latter mode of failure has occurred, thereby justifying the

¹Professor of Civil Engineering, McGill University, Montreal

²Graduate Student, McGill University, Montreal

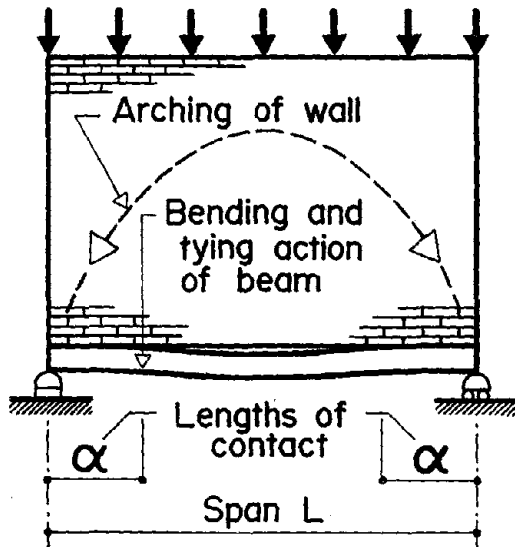


FIG. 1 COMPOSITE ARCHING ACTION OF WALL - BEAM STRUCTURE

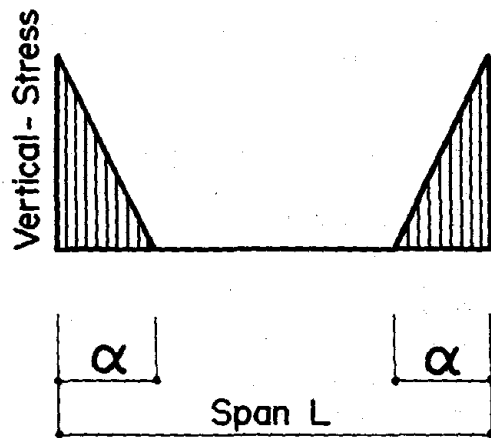


FIG. 2 APPROX. DISTRIB. OF VERTICAL STRESSES ON BEAM

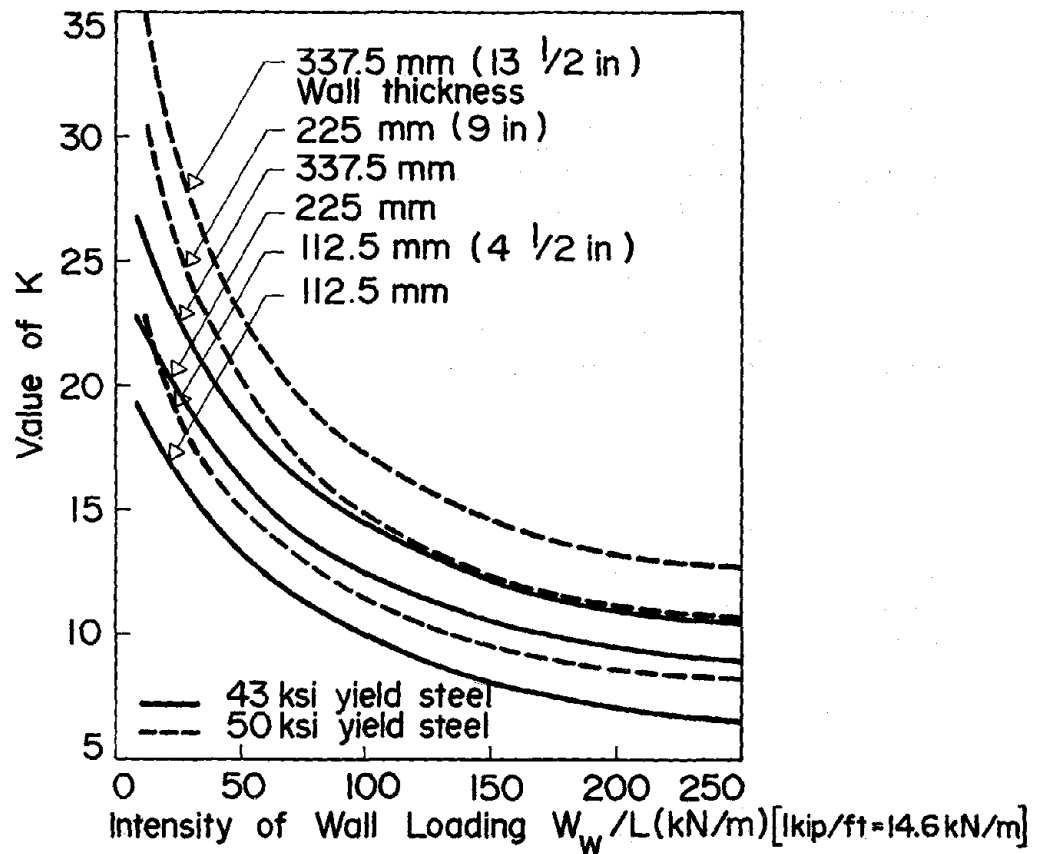


FIG. 3 VALUE OF K AS A FUNCTION OF W_w/L

authors' concern about the wall-beam designer's traditional pre-occupation with the beam bending mode of failure.

The above considerations of beam bending moments and wall compressive stresses, whilst of primary importance in the design problem, are not the only ones. Other factors must also be considered; for example, the horizontal component of the arching action, which produces high shearing stresses along the bedding planes in the corners of the masonry wall. If the height to length ratio of the wall is low these stresses might produce a spreading failure of the arch. Also a shear failure of the beam is possible, especially if it is of reinforced concrete. However, excessive deflections of the beam in practically proportioned wall-beam structures appear from experimental evidence to be very unlikely.

A design method has recently been developed (2) which attempts to take all the above factors into account. The method was written specifically for masonry walls on steel beams. The experimental work described in this paper was intended to compare the behaviour of masonry walls on reinforced concrete beams with similar walls on steel beams. If it could be shown that their modes of behaviour up to and including failure are essentially similar, it should then be possible, by making minor modifications, to adapt the wall-steel beam design method for wall-concrete beam structures.

This paper gives first a brief explanation of the existing design method and then describes a series of six large-scale wall on beam tests which compare the behaviour of steel and concrete beam structures. The results are then used to make tentative recommendations concerning the adaptation of the design method.

A DESIGN METHOD FOR WALL-BEAM STRUCTURES

The method (2) is based on the assumption that α , the length of contact between the wall and beam, can be estimated by

$$\alpha = \frac{BL}{K} \quad 1$$

in which L is the span, B is a constant determined experimentally and K is a parameter based on the relative stiffness of the wall and beam, thus

$$K = \sqrt[4]{\frac{E_w t L^3}{EI}} \quad 2$$

in which E_w and t are the elastic modulus and thickness of the wall, respectively, and EI is the flexural rigidity of the beam; B has been shown experimentally to be approximately equal to unity (2). It is assumed also that the vertical stress over the length of contact has a triangular

distribution, as in Fig. 2.

For calculating wall stresses, B is taken conservatively as 0.75 and, for calculating beam moments, as 1.5. On the basis of these assumptions expressions were written for the loads necessary to cause either a wall failure or a beam failure. The method was developed to give design clauses which may be summarized as follows:

1. Select a beam with a second moment of area I within the range

$$I = \frac{W_w^4}{9.5L^3 p_b^4} \pm 20\% \quad 3$$

and whose section modulus S also satisfies the equation

$$S \leq \frac{W_w^2}{3p_{st}p_b t} + \frac{W_s L}{8p_{st}} \quad 4$$

in which W_w and W_s represent the total wall and slab loads and p_{st} and p_b represent the permissible steel and masonry stresses, respectively.

2. If a section cannot be found to satisfy equations 3 and 4, then a section is to be selected using

$$S \leq 1.2 \left[\frac{W_w L}{4Kp_{st}} + \frac{W_s L}{8p_{st}} \right] \quad 5$$

for which a value of K appropriate to the intensity of the wall loading is obtained from Fig. 3. The I of this section should be not less than the value given by Eq. 3.

Finally a check should be made to ensure that the depth of the section is not less than L/25.

The purpose of these three formulae is that Eq. 3 produces a beam which is stiff enough to distribute the wall load so that the allowable wall stresses are not exceeded. Eq. 4 provides a check to ensure that the selected beam is strong enough to carry the bending imposed on it. If none of the available beams with I between the limits of Eq. 3 is strong enough, it is then necessary to choose a stronger beam using Eq. 5. Step 2 neglects consideration of the wall stresses on the presumption that a stronger beam will also be stiffer than required. The requirement for a minimum depth of L/25 is to restrict the possibility of excessive deflections.

The design method was developed in its present form for use with steel beams. However, the principles of the method should be applicable also to the design of masonry walls on reinforced concrete beams if it can be shown that reinforced concrete beam structures behave substantially the same as steel beam structures.

The concern of the experimental project has been to establish comparability of behaviour between the two types of structure.

PREVIOUS EXPERIMENTAL WORK

The limited scope of the tests reported here, restricts them to making only a small contribution to the total need for experimental knowledge of wall-beam structures. It is relevant therefore, to refer to some earlier experimental work in this field.

A number of full-scale tests have been made at the British Building Research Establishment by Burhouse (3) and Weeks (4). The tests were on masonry walls of different heights on encased steel and reinforced concrete beams. They demonstrated the reduction in beam bending moments and the concentrations of wall stresses due to the composite arching action. They also showed the vulnerability of low walls to fail by sliding along the bedding planes, which destroys the arching action.

In 1977, (5), a series of three full-scale tests on masonry walls supported on encased steel beams, was reported. The purpose of the tests was to study some of the assumptions made for a design method (2) and to verify the conservatism of the method. The tests, in which the walls were similar but the beams were of widely different stiffnesses, demonstrated very clearly the dependence of the wall strength on the beam stiffness.

THE TEST RIG AND WALL-BEAM SPECIMENS

The test rig shown in Fig. 4 consists of a steel reaction girder, comprising 2 I sections side by side, which supports and allows load to be applied to the specimens. The wall-beam specimens sit on the reaction beam with a rotating support at one end and a rotating - sliding support at the other. Eight 30 ton Simplex hollow rams, four attached to each side of the reaction beam, apply load to the top of the wall by a system of prestressing cables, cross arms and a 5 in. x 3 in. hollow steel section member which bears full length along the top of the wall and distributes the load evenly. The rams are driven in parallel by a single hand pump and their load is measured by a pressure gauge at the pump.

Six specimens were tested, three with steel beams and three with singly-reinforced concrete beams. These were grouped in three pairs; each pair incorporating a steel beam and a reinforced concrete beam of similar flexural stiffness. The three pairs differed in the flexural stiffness of the beams; they included beams of low, medium and high stiffness.

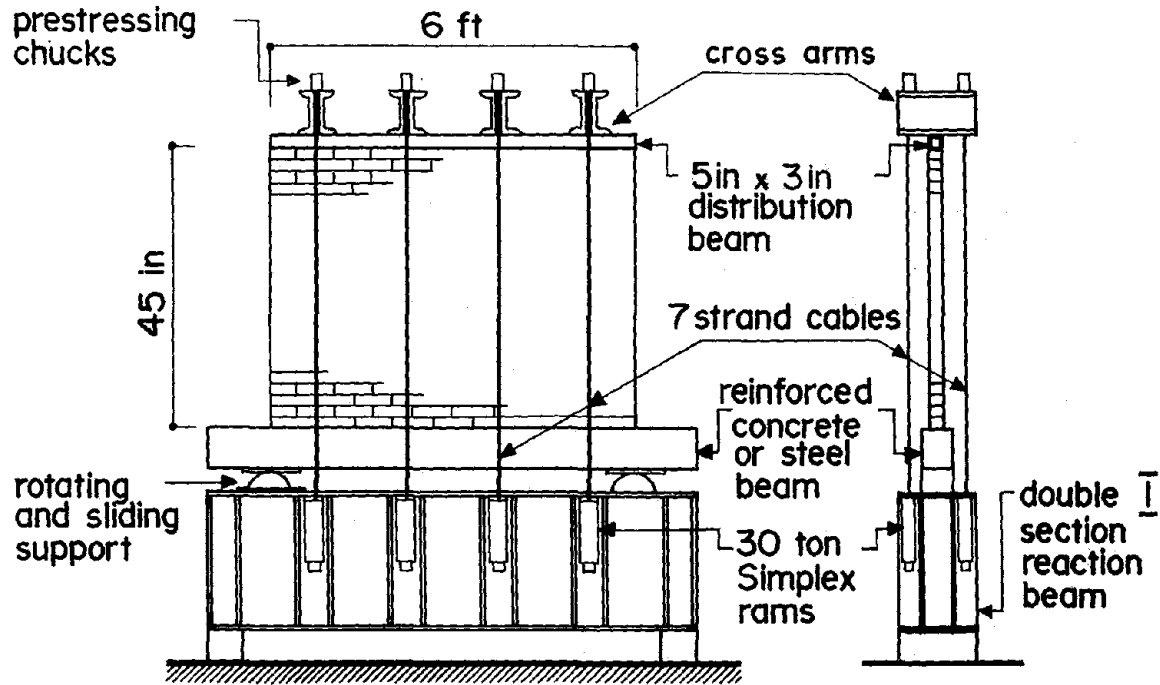


FIG. 4a ELEVATION OF TEST RIG

FIG. 4b END VIEW

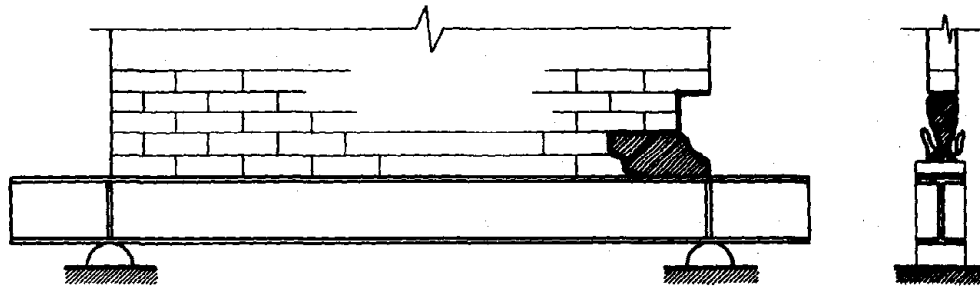


FIG. 5a WALL FAILURE ON INTERMEDIATE STEEL BEAM

FIG. 5b END VIEW

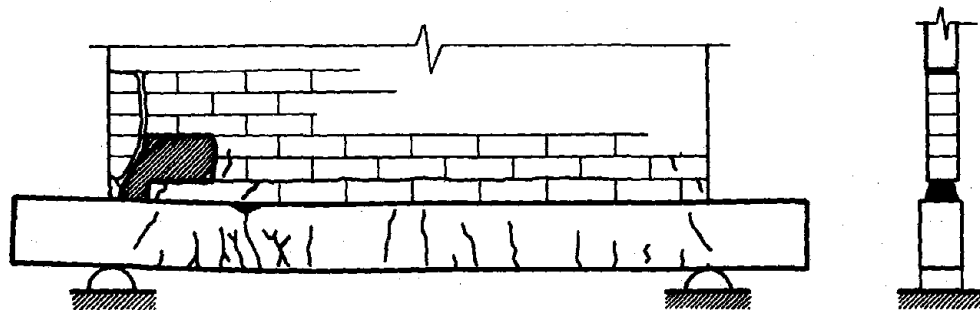


FIG. 5c WALL FAILURE ON INTERMEDIATE RC BEAM

FIG. 5d END VIEW

The walls were constructed to be as identical as possible using 17 courses of 4000 psi solid concrete brick of nominal dimensions 7 7/8 in. x 3 5/8 in. x 2 1/4 in., with 1/2 in. thick Type N mortar jointing. Concrete bricks were used because all the available clay bricks with specified strengths would have produced wall-beam specimens too strong for the test rig, which was limited by the strength of the 3/8 in. dia. loading cables. The length of the walls and the beam span was 6 ft., and the height was approximately 45 in. This gave a height to length ratio of 0.625 which was deliberately larger than a minimum of 0.6, considered necessary to develop a satisfactorily high arch.

The instrumentation on the wall consisted of Demec gauge points for measuring vertical strains at points just above the wall-beam interface and up the edge of the wall. These were applied to both faces at one end of the wall.

The bending and axial strains in the steel beam were recorded by electrical resistance gauges fastened to the inner faces of the flanges and at the mid-height of the web, on both sides of the beam. The concrete beams were instrumented with electrical resistance gauges on each of the two main reinforcing bars at mid-span. Demec points were also placed on both faces of the beam at mid-span to record longitudinal strains at levels 1/4 in. below the top of the beam, at mid-depth and at the level of the main reinforcement. Deflections of the beams were recorded by dial gauges at mid-span and at the quarter points.

The properties of the masonry were found from tests on half-brick samples, 2 in. cubes of the mortar and simple 4 - brick stacks of the brickwork. 8 in. x 4 in. dia. cylinders of the beam concrete were tested axially for compressive strength. The reinforced concrete beams were tested for flexural stiffness before the wall was constructed.

TESTING PROCEDURE

Each wall was tested after a 14-day curing period. Uniform increments of load were applied by hand-pumping the rams. The loading increments were approximately equal to one-fifteenth of the estimated ultimate load in each case. As the loading approached ultimate these increments were halved.

After each load increment, readings were taken of the hydraulic pressure, electrical strain-gauges, Demec points and dial gauges. As the test progressed, observations were also made of cracking in the wall and the concrete beams. Close attention was also paid to ensure symmetrical functioning of the loading rig about the central plane of the wall.

In the final stages of each test it was necessary for the safety of the experimenters to abandon the dial gauge and Demec readings.

However, electrical strain and ram pressure readings were continued up to collapse.

OBSERVATIONS, RESULTS AND DISCUSSION

All six specimens followed a very similar pattern of behaviour. The first indications of distress were occasional loud cracking sounds from the wall, in some cases at load levels as low as one-third ultimate; however, these were not accompanied by any visual evidence of cracking. Next, in specimens with concrete beams, bending cracks began to appear in the beams. In the later stages of loading, these were remarkable in extending almost to the top of the beam, presumably a result of the axial tying stresses. It was also possible in the later stages of loading to observe horizontal cracks along the wall to beam interface, or in the lowest bedding planes of the masonry, in the mid-span region. Such cracking served to demonstrate the tendency of the beam to separate from the wall.

The first visual indications of real distress in the wall appeared usually at about two-thirds of the ultimate load, when small flakes of mortar began to slough off the end faces of the lowest bedding joints. As the ultimate load was approached, cracks began to appear in the masonry in the faces and ends of the lower corners of the wall. The facial cracks were inclined along the direction of the "arch" whilst the end cracks were vertical. The ultimate modes of failure for the intermediate beam specimens are illustrated in Figs. 5. Failure finally occurred in five of the six specimens when one corner of the wall collapsed. The immediate consequence was to shift that end of the arch towards mid-span onto the nearest sound masonry. In the reinforced concrete beam specimens, this inward shift of the arch thrust and the resulting increased moment on the beam precipitated bending failure of the beam. These failures demonstrated yielding of the reinforcement and crushing of the concrete at the top of the beam, both directly below the newly located end of the arch. In the low stiffness steel beam, the wall failure was followed immediately by a shear failure in the web of the beam. Each of the steel beams had been given vertical web stiffeners directly above the supports, but this did not anticipate the shift in the concentrated arch load as the wall collapsed. In the specimen with the stiffest steel beam the lengthwise distribution beam on top of the wall, which was initially a 5 in. deep I section, twisted and collapsed before the specimen failed. The member was replaced by 5 in. x 3 in. hollow steel section which performed well in all subsequent tests.

Before considering the results of the tests it should be remarked that one anticipated difference between the behaviour of the reinforced concrete and steel beam specimens was the progressive cracking of the former as the load increased, and the consequent reduction in the bending stiffness. This contrasts with the constant stiffness of the steel beam. Another expected difference was the segmentation of the concrete beam and a discontinuity of its profile compared with the continuous elastic curve of the steel beam. Neglecting other effects, the reduction in beam

stiffness would have been expected to decrease the length of contact, increase the wall stresses and reduce the beam bending moment. The possible effects of segmentation and whether they would worsen or relieve the effects of beam softening could not be predicted.

Preliminary answers to these questions are provided by the interface stress distribution diagrams. Examples of these, for the specimens with low beam stiffness are shown in Fig. 6. At low loading, both the steel and reinforced concrete beam specimens have stress distributions which extend along the span beyond the regions of measurement. As the loading is increased, the stress distributions tend to concentrate towards the ends of the span and settle on a more definite length of contact. There are, however, no distinct differences between the lengths of contact for the two types of beam.

An important difference is shown to occur between the wall stress distributions of the low stiffness pair of beams (Fig. 6). The stresses at the ends of the wall in the steel beam specimen are peaked whereas, in the reinforced concrete beam specimen they are flattened. If this had been observed from only a single test on a reinforced concrete beam specimen it might have been attributed to the inelastic behaviour of the masonry at higher stresses. However, for that explanation to be correct, the steel beam test would have shown a similar result.

It appears therefore that the flattening, with a platform of uniform stress distribution near the end, could be due to the segmentation of the concrete beam. The difference in stress distribution was also observed, but to a lesser extent, in the intermediate beam specimens, except that at loads approaching ultimate the stress distribution in the wall on the steel beam also began to flatten. This presumably, was due to the non-linear behaviour of the masonry at high stress. In the stiff beam tests, neither specimen showed flattening of the stress distribution until very high loading was reached. Again this was probably due to the non-linear behaviour of the masonry.

It is evident from these preliminary results that the anticipated increase of the wall stresses, due to the softening of the reinforced concrete beam with increasing load, does not materialize in practice. On the contrary, available evidence indicates that, possibly due to segmentation, the arching stresses in a masonry wall on a reinforced concrete beam are more evenly distributed near the ends of the span, than in the case of a similarly stiff steel beam specimen, especially when the beams are of low stiffness. At lower loads this probably gives a more assured performance of the masonry, however, at higher loads the stresses in the wall on the steel beam tended to flatten also, suggesting that closer to the ultimate load, the performance of masonry walls on reinforced concrete beams and those on steel beams are not very different.

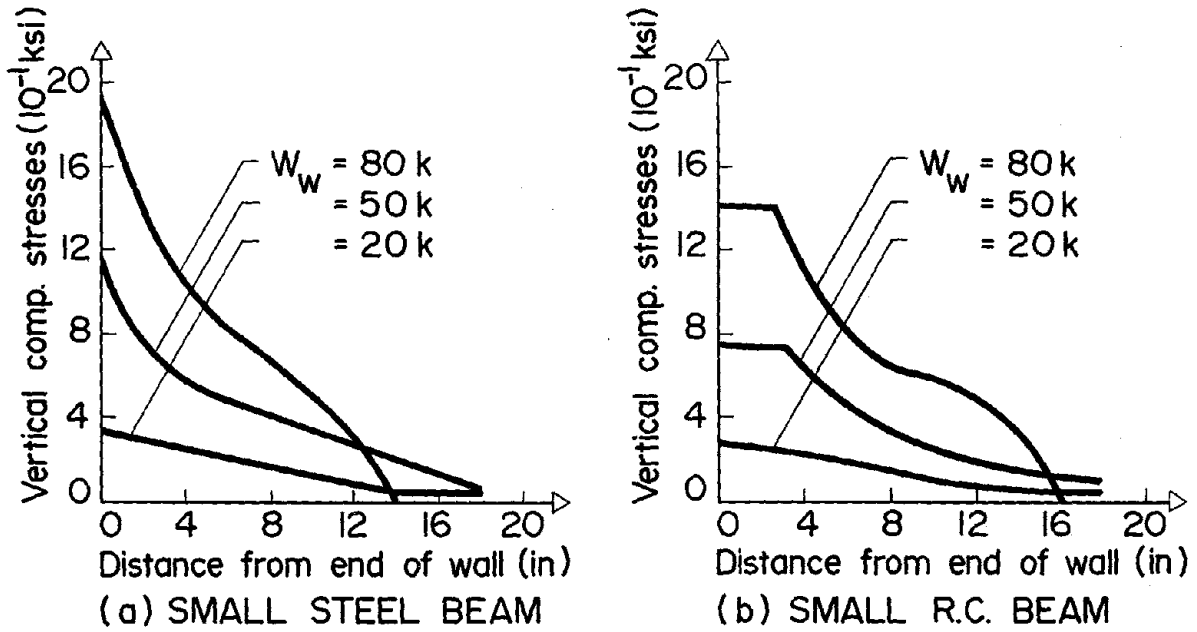


FIG. 6 DISTRIBUTION OF VERTICAL COMPRESSIVE STRESS BETWEEN WALL AND BEAM

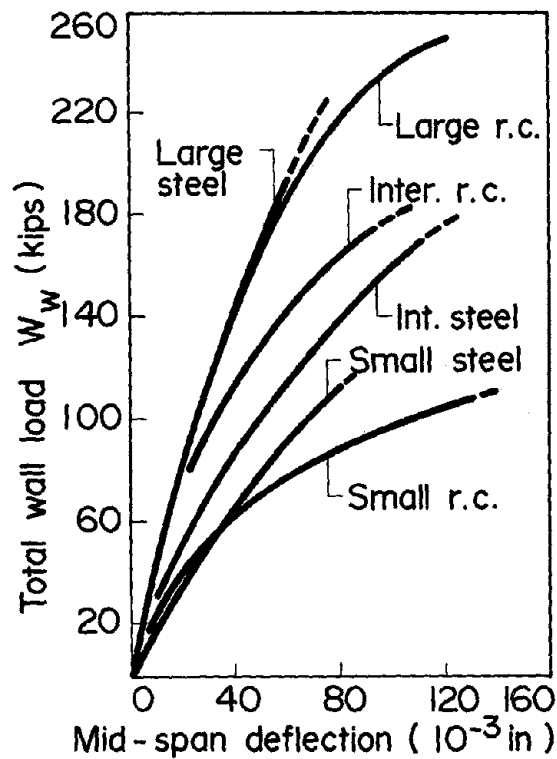


FIG. 7 WALL LOAD VS BEAM DEFLECTION

Table 1 compares the ultimate loads of the two types of structure. It appears from the results that, for similar initial beam stiffnesses, masonry wall-steel beam specimens are slightly stronger than masonry wall-reinforced concrete beam specimens. However, a factor which might have played a part in this small difference was that end cleats were included on the steel beams to prevent the wall from spreading outwards. These might inadvertently have restrained the masonry against vertical crushing at its most vulnerable point, thereby increasing the ultimate load. Load-deflection curves for the specimens are shown in Fig. 7. These do not merit extensive consideration except to note that in each of the three pairs of specimens the reinforced concrete beam deflected distinctly non-linearly relative to the steel beam specimen. This non-linearity was more evident in the low stiffness beam specimens. Although at loading close to ultimate the reinforced concrete beams deflected more than the corresponding steel beams, the deflections in the working load range were similar for both types. Therefore, as for masonry wall-steel beam structures, deflections are not a matter of great concern in the design of walls on reinforced concrete beams.

Finally, the strain distributions, derived moments and tie forces across the mid-span sections of the large beams are shown in Fig. 8. The bending moment in these large beam specimens was only one-quarter of the distributed load moment. In the intermediate and small beam specimens the fraction was even less; the recorded value in the small steel beam specimen was as low as one-twelfth of the uniformly distributed load moment.

The values of tie force in the beam have been shown theoretically, and confirmed experimentally, to be practically independent of the beam size.

CONCLUSIONS

The described tests and discussion lead to the following preliminary conclusions.

1. The modes of wall failure and ultimate strengths of masonry wall-reinforced concrete beam specimens are similar to those for masonry wall-steel beam specimens.
2. The lengths of contact of masonry walls on reinforced concrete beams and on steel beams of the same initial stiffness, are similar.
3. The stress distributions in walls on steel beams tends to peak at the ends whereas those in walls on reinforced concrete beams tend to flatten with lower maximum stresses. This effect is very distinct with low stiffness beams but less so for very stiff beams. At loads close to ultimate the stress distribution at the ends of walls on steel beams tends to flatten also.
4. In reinforced concrete beams which support walls, the tying effect gives a tensile bias to the concrete stress distribution, increasing the depth of cracking. The stirrups must be adequate, therefore, to carry the whole of the shear force at all points in the beam.

5. As a general conclusion it can be stated that the composite behaviour of masonry walls on reinforced concrete beams compares closely enough with that of walls on steel beams to allow the adaptation of the steel beam design method.

REFERENCES

1. Stafford Smith, B. and Riddington, J.R., "The Composite Behaviour of Elastic Wall-Beam Systems", Proc. Instn. Civ. Engrs., Part 2, 1977, 63, June.
2. Riddington, J.R., and Stafford Smith, B., "Composite Method of Design for Heavily Loaded Wall-Beam Structures", Proc. Instn. Civ. Engrs., Part 1, 1978, 64, February.
3. Burhouse, P., "Composite Action Between Brick Panel Walls and their Supporting Beams", Proc. ICE, Vol. 43, pp. 175 - 194, June 1969.
4. Weeks, G.A., Private Communications Concerning tests on Full-Scale Wall on Beam Structures at the Building Research Establishment.
5. Stafford Smith, B., Khan, M.A.H. and Wickens, H.G., "Tests on Wall-Beam Structures", Proc. 6th International Symposium on Load-Bearing Brickwork, London, December 1977.

ACKNOWLEDGEMENT

The authors wish to record their appreciation of the Canadian National Research Council and the Ministère de l'Éducation du Québec for providing the financial support for this project.

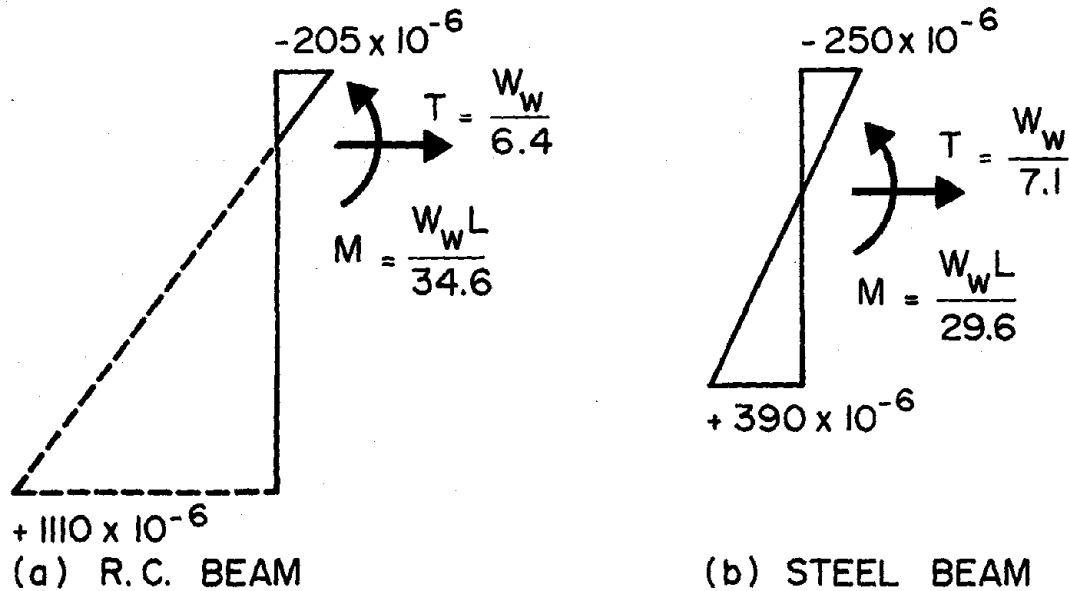


FIG. 8 STRAINS ACROSS MID-SPAN SECTION OF LARGEST SIZE BEAMS FOR $W_w = 230$ k

WALL - BEAM SPECIMEN	BEAM TYPE OR SIZE	STIFFNESS EI OF BEAM (kip. ft. ²)	ULTIMATE LOAD (kips)
SMALL STEEL BEAM	W6 x 15.5	6062	125
SMALL R.C. BEAM	4 ³ / ₄ in x 8 ¹ / ₈ in	6506	112
INTERMEDIATE STEEL BEAM	W8 x 28	19696	210
INTER. R.C. BEAM	5 in x 12 in	25302	182
LARGE STEEL BEAM	W10 x 54	61625	273 +
LARGE R.C. BEAM	8 in x 14 ³ / ₄ in	54346	257

N.B. EI VALUES FOR THE R.C. BEAMS ARE BASED ON INITIAL UNCRACKED SECTIONS

TABLE I. BEAM PROPERTIES AND WALL-BEAM ULTIMATE STRENGTHS

SOME FUNDAMENTAL FACTORS IN THE STRUCTURAL DESIGN OF MASONRY BUILDINGS.

by Professor A.W. Hendry.

ABSTRACT: This paper reviews a number of basic factors underlying the structural design of masonry buildings. Considerations affecting the plan arrangement of walls are first considered. Closely allied to this is the requirement to ensure general robustness of a building and, in particular, the avoidance of collapse resulting from accidental damage. The choice between plain and reinforced masonry is discussed and reference is made to the possibility of extending the scope of masonry construction by the use of reinforced or prestressed elements. Codes of practice for masonry buildings are now being framed in terms of the limit states approach and this has required the selection of appropriate partial safety factors. Recent theoretical work by Macchi and by Beech is referred to and reference is made to the new British Code of Practice, due to be published in 1978. Finally, the analysis of masonry structures is considered in relation to vertical and lateral loads. Currently, rather crude methods are used in design calculations but, as a result of recent research work, more rational procedures are becoming available.

SOME FUNDAMENTAL FACTORS IN THE STRUCTURAL DESIGN OF
MASONRY BUILDINGS

By Arnold W. Hendry¹

INTRODUCTION

During the past two decades the structural design of masonry buildings has moved considerably from dependence on empirical rules and practices to a basis more consistent with structural engineering principles as applied to materials such as steel and concrete. The purpose of this paper is to review progress in certain fundamental aspects of structural design in this medium. These will include measures to ensure general stability and resistance to accidental damage, analysis for vertical and lateral loading and the selection of safety factors.

Wall Layout

The first consideration in the design of masonry buildings is to determine the plan arrangement of the walls in accordance with the function for the building. From the structural point of view the wall arrangement is important, firstly as a means of providing lateral strength and rigidity and, secondly, in order to ensure that the building is generally "robust" in the sense that any local damage to the structure does not result in catastrophic collapse.

Possible wall arrangements are almost unlimited¹ and in any particular case tend to evolve from the site plan and the required sizes and disposition of rooms. The arrangement is not particularly critical from the structural view-point provided that a reasonable balance is allowed between walls oriented along the principal axes of the building so as to permit the development of adequate strength and rigidity against lateral forces applied in these directions. The design should always be such that side-sway is for all practical purposes eliminated. The forthcoming British code of practice² for masonry structures seeks to achieve general stability by requiring that buildings should be designed to resist, at any level, a horizontal load equal to $1\frac{1}{2}\%$ of the permanent dead load above that level. This in itself is not altogether sufficient to ensure a satisfactory structure as it could be met by concentrating lateral resistance, say by a stair well or service shaft whilst leaving a large part of the building vulnerable to collapse as a result of local damage. (see Fig. 1).

1. Prof. of Civ. Engrg., Univ. of Edinburgh,

Very unsymmetrical wall arrangements are to be avoided as they will give rise to torsional effects which are difficult to calculate and which may produce undesirable stress conditions.

The Ronan Point accident in England some years ago (3) gave rise to specific requirements being incorporated in the Building Regulations of that country (4) aimed at preventing catastrophic collapse resulting from accidental damage to a structure, for example from a gas explosion or vehicle impact. It has been shown (5,6) that it is possible to make a reasonable assessment of the liability to and extent of such damage in a masonry building and an extensive test programme (7) has shown that it is in fact quite difficult for the commoner incidents such as domestic gas explosions to result in serious damage to an unreinforced brickwork building whose plan form has been designed with that degree of technical common sense which any qualified structural engineer should possess. Nevertheless, the new British masonry code will contain "cookery book" style prescriptions for the insertion of arbitrary horizontal and/or vertical ties in buildings, presumably for the benefit of those who are lacking the time or competence to check out their designs on a rational basis. It is fortunate that these proposals do not appear to destroy the economic advantage of masonry construction. The accidental damage regulations in the U.K. do not at present extend to structures of less than five stories and in such cases gas explosions do frequently result in severe damage but in the nature of things are unlikely to result in severe loss of life.

Plain and Reinforced Brickwork

The essential difference between plain and reinforced masonry is that the former is incapable of resisting significant tensile stresses whereas the latter acts in a manner similar to reinforced concrete, tensile stresses being taken by suitably placed steel.

Most brickwork buildings are constructed in plain masonry without reinforcement but in seismic areas it is essential to use reinforced brickwork in order to provide resistance to dynamic forces of considerable magnitude. In Europe and Australia, therefore, brickwork structures are normally unreinforced whereas in the United States and New Zealand, reinforced brickwork is generally required.

Apart from construction in seismic areas, however, there is a field of application for reinforced brickwork elements in building construction in situations where the nature of plain masonry imposes undue limitations on the design. One such case is the possible use of large span reinforced brickwork wall beams in the lower floors of multi-storey (8,9) buildings where it is not possible to continue the wall layout of the upper storeys to the foundation level. A practical example of this method of construction has been described (10) and the extension of the concept to cantilever beams has been explored (11).

The limitation of plain masonry arising from lack of tensile strength can also be overcome by prestressing (12,13) although this technique has not so far been widely applied.

The potentialities of reinforced and prestressed masonry should therefore be kept in mind at the preliminary design stage of brick or block structures which are conceived primarily in terms of plain masonry.

Design guides for reinforced masonry covering North American (14,15) and British practice (16) are available although in Britain this has not yet reached the stage of a code of practice.

Limit State Design of Masonry

The basic aim of structural design is to ensure that a structure should fulfil its intended function throughout its lifetime without excessive deflection, cracking or collapse. Conventionally this has been achieved by dividing the ultimate strength of a wall, allowing for slenderness and eccentricity of loading, by an arbitrary safety factor, sufficiently large to avoid not only collapse but also cracking at working loads. In recent years there has been a general move in the direction of handling the structural safety and serviceability problems through consideration of "limit states" and partial safety factors. The new British code is based on this approach and other similar codes are in process of preparation.

Considering the ultimate limit state of a particular structure, we have the condition that for failures to occur:

$$\text{where } R^* - S^* \leq 0$$

$$R^* = \frac{R_k}{\gamma_m}$$

$$S^* = f(\gamma_f \cdot Q_k)$$

The various symbols have the meanings defined in the International Standards Organisation document ISO 2394 (17) and summarised in Appendix 1. The safety requirement is satisfied by ensuring that the probability of failure is very small, that is

$$P[R^* - S^* \leq 0] = p$$

where P is the probability of occurrence of the expression within the brackets and p is the required value of this probability. In practice this will be in the range of 10^{-5} to 10^{-6} .

If the necessary statistical data are available it is possible to calculate the safety factors necessary to achieve a required probability of failure. This has been done by Macchi (18) in terms of a global safety factor. Macchi produced sets of curves showing the relationship between the safety factor and the coefficient of variation of the strength of the material, of the loads and of the eccentricity and slenderness reduction factors. These curves, shown in Fig. 2 show that, other things being equal, the safety factor required to ensure a given probability of failure rises quite rapidly with the coefficient of variation of the strength of the material.

These curves are based on the assumption of normal distribution and Beech (19) has suggested that lognormal or truncated normal distributions have greater validity. The latter result in a much less steep rise in the factor of safety with increase in coefficient of variation of material strength, as may be seen in Fig. 3.

Limit state codes, as presently used, use two or more partial safety factors. Thus assuming homogeneity of units, the condition at the ultimate limit state is given by

$$\frac{R_k}{\gamma_m} = \gamma_f \cdot Q_k$$

or

$$\frac{R_k}{\gamma_m \gamma_f} = Q_k$$

It would appear from this that the product $\gamma_m \cdot \gamma_f$ is equivalent to a global safety factor but, as Beech has pointed out, the probability of failure associated with the product of two partial safety factors is generally different from the product of the partial probabilities. For this and other reasons this author has argued (20) in favour of working in terms of mean values of actions and resistances and global safety factors. However, the partial safety factor and characteristic strength approach has already been adopted in some codes and it might now be difficult to reverse this practice.

The partial safety factors, γ_m , adopted in the draft British code are summarised in Appendix 2. Rather similar values are proposed in the model code being prepared by Commission 23A of CIB (21).

Analysis of Brickwork Structures

Limit state design calls for the comparison of the effects of load actions with the strength of the material. This in turn calls for the use of suitable methods of structural analysis to estimate the effects of loads on the structure in terms of forces, bending moments and deformations and for the use of appropriate methods of calculating the resistance of masonry elements and of establishing deformation limits.

Unreinforced masonry is a brittle material and although its stress-strain relationship is non-linear, it is customary to use elastic analysis to determine the forces at particular sections of a structure. Calculation of resistance of a wall to eccentric vertical load is now sometimes based on the assumption of a rectangular internal stress block,

neglecting tensile strength. In the past, methods of analysis have been relatively crude but the construction of taller buildings in brick masonry and the general need for increased economy in the use of materials has led to the development of more refined methods. Similarly, the resistance of brickwork was, in the past, on an entirely empirical basis but is now increasingly supported by analytical studies.

Considering first of all lateral loading, large scale and model experimentation (22, 23) have demonstrated that it is possible to analyse the distribution of lateral loads amongst the shear walls of a cross-wall structure by an equivalent frame analysis. The usual procedure of allocating the wind moments between the walls in proportion to their stiffness without considering flexural effects in the floor slabs leads to an over-estimation of moments and deflections. On the other hand, the well known shear continuum method appears to over-estimate the stiffness of the structure. Finite element analysis gives good results but, in the case of the structures investigated experimentally, no greater accuracy than a suitable frame analysis.

More recently, attention has been directed to the problem of load and moment distribution due to vertical floor loading taking into account wall/floor slab interaction. Experimental results suggest that this can also be achieved by a frame analysis with two important provisos: firstly, that the moment transmission capabilities of the joints are not exceeded and secondly that, where necessary, cracking of the brickwork resulting from the development of tensile stress is allowed for (24 - 27).

Methods of analysis of this type are in process of development and comparison with experimental results is promising. The outcome of research in this area will go a long way towards lifting the structural design of masonry buildings out of the realms of pure empiricism and guess-work which has undoubtedly inhibited the adoption of this material by structural engineers.

Conclusion

This paper attempts to summarise certain fundamental trends in the structural design of masonry structures which, when more fully developed, will place the design of these structures on the same technical and scientific level as those built in steel and concrete. The subjects referred to are too extensive to discuss in detail within the space available but may be followed through the references quoted.

It may be concluded that progress during the past decade has been impressive and, from the response to the present conference, may be expected to continue at least at the same pace in future.

REFERENCES

1. Stockbridge, J.G. "Case studies and critical evaluation of high-rise load bearing brickwork in Britain". Designing, Engineering and Construction with Masonry Products. ed. F.B. Johnson, Gulf Publishing Co., Houston, Texas, 1969, pp 427-433.
2. - "The Structural Use of Masonry", Inst. Struct. Eng., London, 1974 (Proc. of a Symposium on the draft code: the actual code will be published in 1978 by the British Standards Institution).
3. - "Report of the Inquiry into the Collapse of Flats at Ronan Point, Canning Town", H.M.S.O., London, 1968.
4. - The Building (Fifth Amendment) Regulations, 1970, H.M.S.O., London.
5. Morton, J., Davies S.R., and Hendry, A.W. "The Stability of Load-bearing Brickwork Structures Following Accidental Damage to a Major Bearing Wall or Pier". Proc. Second Int. Brick Masonry Conf., (SIBMAC), B. Ceram. Res. Assoc., Stoke-on-Trent, England, 1971, pp 276-281.
6. Sinha, B.P., and Hendry, A.W. "The Stability of a Five Storey Brickwork Cross-wall Structure Following the Removal of a Section of a Main Load-bearing Wall". The Structural Engineer, Vol. 49, No.10, 1971, pp. 467-474.
7. Astbury, N.F.
West, H.W.H.,
Hodgkinson, H.R.,
Cabbage, P.A., and
Clare, R. "Gas Explosions in Load Bearing Brickwork Structures". B. Ceram. Res. Assoc., Special Publication No.68, 1970.
8. Flowman J.M.,
Sutherland, R.J.M. and
Couzens, M.L. "The Testing of Reinforced Brickwork and Concrete Slabs forming Box Beams". Struct. Engr. Vol. 45, No.11, 1967, p 379.
9. Gero, J.S. "Prestressed masonry reinforced concrete space structure" Designing, Engineering and Constructing with Masonry Products, ed. F.B. Johnson, Gulf Publishing Company, Houston, Texas, 1969, pp.210-215.

10. Buckton, G. "Modern Development Utilizing the Interaction of Deep Brick Panels and Reinforced Concrete Beams to Support Multi-storey Construction". Proc. SIBMAC, B. Ceram. R.A., Stoke-on-Trent, England, 1971, pp 331-336.
11. Haseltine, B.A. and Fisher, K. "The Testing of Model and Full size Composite Brick and Concrete Cantilever Wall Beams". Proc. B. Ceram. Soc. No.21, 1973, pp 243-260.
12. Mehta, K.C. and Fincher, D. "Structural Behaviour of Pretensioned Prestressed Masonry Beams", Proc. SIBMAC, B. Ceram, R.A., Stoke-on-Trent, England, 1971, pp 215-219.
13. Curtin, W.G., Adams, S. and Sloan, M. "The Use of Post Tensioned Brickwork in SCD System". Proc. B. Ceram. Soc., No.24 1975, pp 233-245.
14. - "Recommended Practice for Engineered Brick Masonry". Brick Institute of America, McLean, U.S.A., 1969.
15. Amrhein, J.E. "Reinforced Masonry Engineering Handbook". Masonry Institute of America, Los Angeles, U.S.A., 1972.
16. - "Design Guide for Reinforced and Prestressed Clay Brickwork". B. Ceram. R.A., Stoke-on-Trent, England, Special Publication, No.91, 1977.
17. - "General principles for the verification of the safety of structures". International Standard ISO 2394, International Organisation for Standardisation, Switzerland, 1973.
18. Macchi, G. "Safety Consideration for a Limit State Design of Brick Masonry". Proc. SIBMAC, B. Ceram. R.A., Stoke-on-Trent, England, 1971, pp 229-232.
19. Beech, D.G. "Some Problems in the Statistical Calculation of Safety Factors". Proc. Fourth Int. Brick Masonry Conf., Brugge, Belgium, 1976, Paper 4.b.8.

20. Beech, D.G. "The Concept of Characteristic Strength"
Proc. B. Ceram. Soc. (In press).
21. Lewicki B., and Motteu, H. "Structures by Load-bearing walls (W 23A)"
Construction Research International, Proc. 7th CIB Triennial Congress, Edinburgh 1977, Vol.1, pp 77-90.
22. Sinha, B.P., Maurenbrecher, A.H.P., and Hendry, A.W. "Model and Full-scale Tests on a Five-Storey Cross Wall Structure Under Lateral Loading". Proc. SIBMAC, B.Ceram. R.A. Stoke-on-Trent, England, 1971, pp 201-208.
23. Hendry, A.W. "Wind load analysis of multi-storey brickwork structures", B.D.A. Research Note Vol. 1 No.3, 1971.
24. Hendry, A.W. "The compressive strength of certain multi-storey brick masonry walls". Proc. 7th CIB Congress, Edinburgh, 1977, Vol.B, pp 213-224.
25. Sinha, B.P. and Hendry, A.W. "An Investigation into the Behaviour of a Brick Cross-Wall Structure". Proc. B. Ceram Soc. (In press).
26. Colville, J. and Hendry, A.W. "Tests of a Load Bearing Masonry Structure". Proc. B. Ceram. Soc. (In press).
27. Germanino, G. and Macchi, G. "Experimental Research of a Frame Idealisation for a Bearing-Wall Multi-Storey Structure". Proc. B. Ceram Soc. (In press).

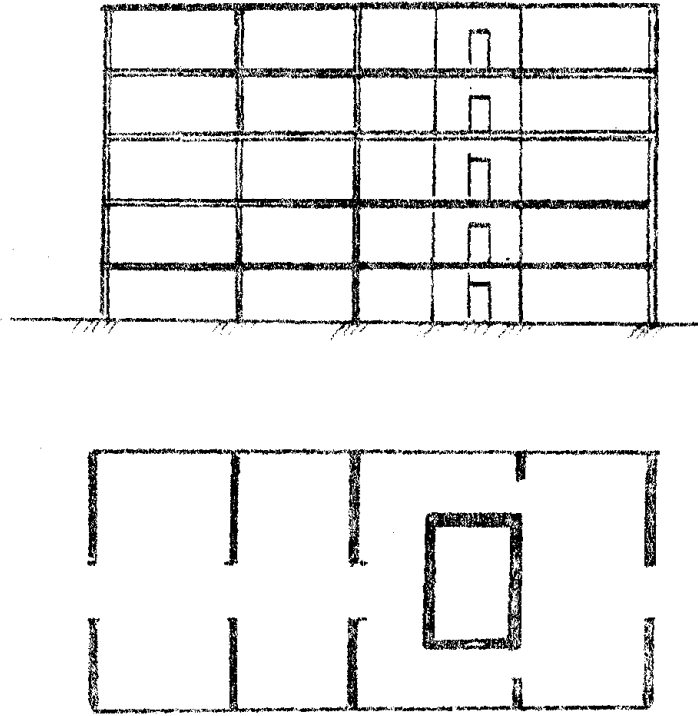


FIG. 1

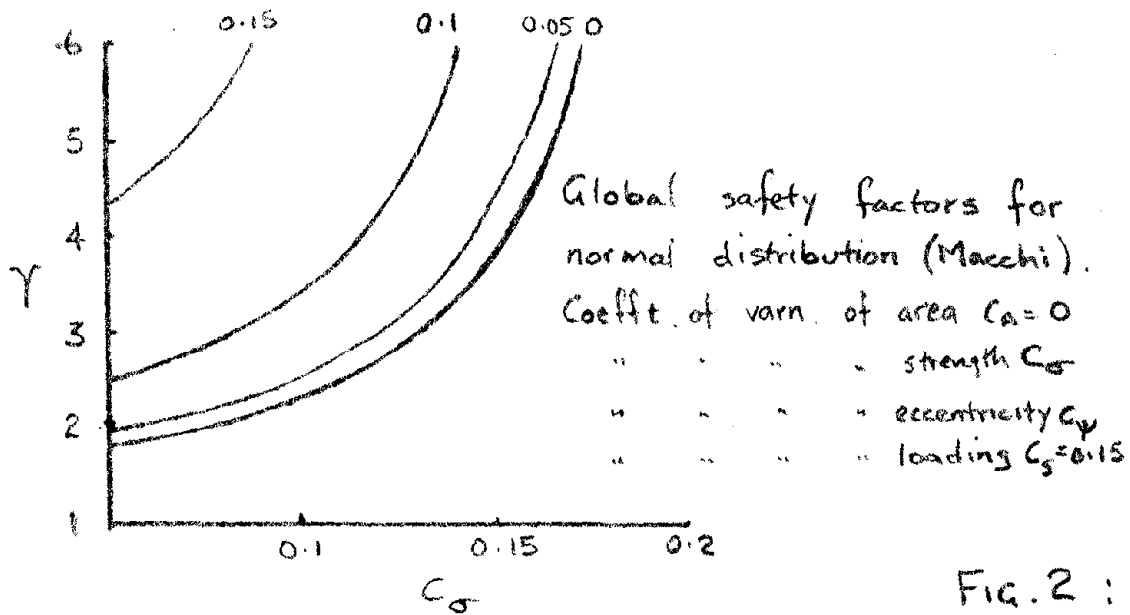


FIG. 2 :

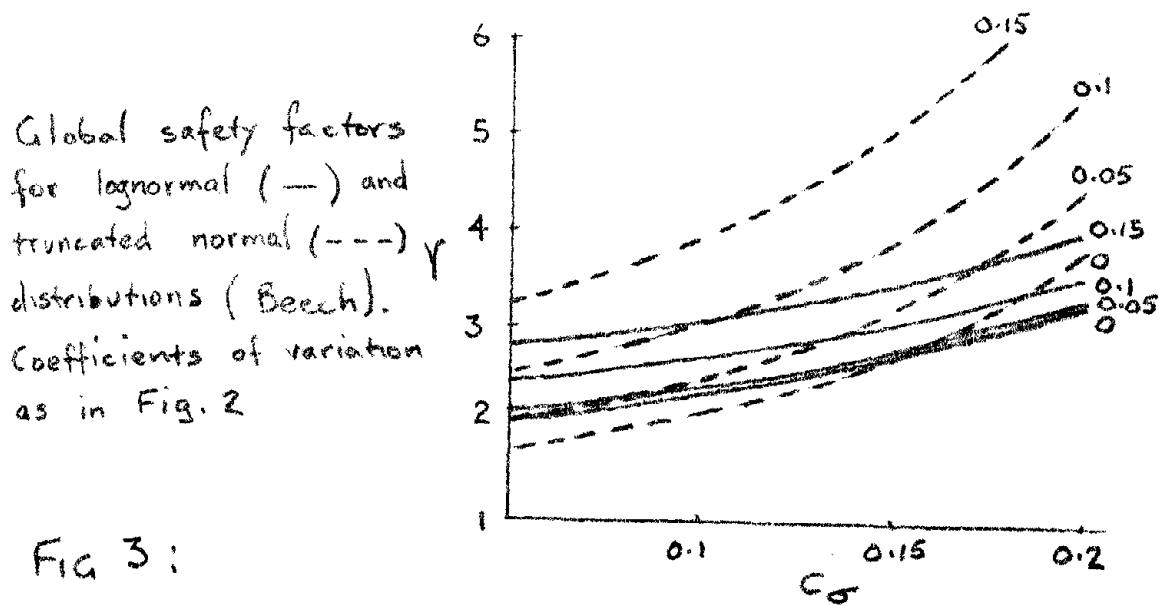


FIG 3 :

APPENDIX 1Definitions and Symbols used in ISO 2394Characteristic Values1. Characteristic strength of materials

$$R_k = R_m - ks$$

where

R_m is the arithmetic mean of the different test results
 s is the standard deviation
 k is a coefficient depending on the probability accepted a priori of obtaining test results less than R_k .

2. Characteristic actions

$$Q_k = Q_m (1 + k \cdot \xi)$$

where

Q_m is the value of the most unfavourable loading, with a 50% probability of its being exceeded, up to abnormally high values, once in the expected life of the structure;
 ξ is the relative mean quadratic deviation of the distribution of the maximum loading;
 k is a coefficient depending on the probability, accepted a priori, of maximum loadings being greater than Q_k .

The value of the average loading Q_m is derived from the statistical analysis of a number of structures of the same type as that under consideration and with similar durability.

A modified definition of Q_k applies when the reduction of a load may endanger the stability of a structure.

3. Partial safety factors for strength of materials

The design strengths, R^* , are defined by:

$$R^* = \frac{R_k}{\gamma_m}$$

The reduction coefficient, γ_m , is in principle a function of two coefficients γ_{m1} and γ_{m2}

γ_{m1} is intended to cover the possible reductions in the strength of the materials in the structure as a whole as compared with the characteristic value deduced from the control test specimen;

γ_{m2} is intended to cover possible weakness of the structure arising from any cause other than the reduction in the strength of the materials allowed for γ_{m1} including manufacturing tolerances.

In general, for calculation purposes, a single coefficient will be used; thus

$$\gamma_m = \text{function} (\gamma_{m1}, \gamma_{m2})$$

4. Partial safety factors for loads and loading effects

The design loading effects, S^* , are determined from the characteristic actions, Q_k , by taking account of a coefficient γ_s , in the following relation:

$$S^* = \text{effects of } (\gamma_s \cdot Q_k)$$

(increase of the characteristic actions and assessment of their effects using non-linear theory).

For particular cases where there is proportionality between the actions and the resulting loading effects, the following relation may be used:

$$S^* = \gamma_s (\text{effects of } Q_k)$$

To allow the values of γ_s to be derived, the following treatment may be accepted. The coefficient γ_s is assumed to be a function of partial coefficients γ_{s1} , γ_{s2} and γ_{s3} .

where

γ_{s1} takes account of the possibility of unfavourable deviation of the loads from the characteristic external loads, thus allowing for abnormal or unforeseen actions;

γ_{s2} takes account of the reduced probability that various loadings acting together will all be simultaneously at their characteristic value;

γ_{s3} is intended to allow for possible adverse modification of the loading effects due to incorrect design assumptions (introduction of simplified support conditions, hinges, neglect to thermal and other effects which are difficult to assess), constructional discrepancies such as dimensions of cross-section, deviation of columns from vertical, and accidental eccentricities.

In general, for calculation purposes, a single coefficient will be used; thus

$$\gamma_s = \text{function} (\gamma_{s1} \gamma_{s2} \gamma_{s3})$$

APPENDIX 2Values of Material Partial Safety FactorsProposed in New British Limit State Code

	Category of Construction Control	
	Special	Normal
Category of manufacturing : Special	2.5	3.1
Control of structural units: Normal	2.8	3.5

Definitions of Categories of Control:

(a) Manufacturing control

Normal category. This category should be assumed when the supplier is able to meet the requirements for compressive strength in the appropriate British Standard but does not meet the requirements for the special category below.

Special category. This may be assumed where the manufacturer (a) agrees to supply consignments of structural units to a specified strength limit, referred to as the "acceptance limit" for compressive strength, such that the average compressive strength of a sample of structural units taken from any consignment and tested in accordance with the appropriate British Standard specification has a probability of not more than $2\frac{1}{2}\%$ of being below the acceptance limit.

Construction control

Normal category. This category should be assumed whenever the requirements of special category construction control are not satisfied.

Special category. This category of construction control may be assumed where:

(a) the designer, either by frequent visits to the site of the presence of a permanent representative on site, ensures that the work is built in accordance with CP 121: Part 1: 1973, and with such specifications as he may prescribe.

and

(b) preliminary compressive strength tests carried out on the mortar to be used, indicate compliance with specified strength requirements; regular testing of the mortar used on site, shows that compliance with the specified strength requirements is being maintained.



BUCKLING OF PLAIN MASONRY WALLS WITH INITIAL DOUBLE CURVATURE

By Hatzinikolas, M., Longworth, J., and Warwaruk, J.

ABSTRACT: Masonry walls loaded in double curvature tend to fail in the first buckling mode. The buckling loads for masonry walls with initial double curvature imperfections or moments are evaluated using the energy approach and fifth order polynomials for interpolating functions. Results for a number of full scale walls tested under double curvature moments are compared with the analytical results.

BUCKLING OF PLAIN MASONRY WALLS
WITH INITIAL DOUBLE CURVATURE

By M. Hatzinikolas¹, J. Longworth², J. Warwaruk³

INTRODUCTION

Recently a number of researchers have studied the application of the moment magnifier method to the design of load bearing masonry walls. The method has been shown to give satisfactory results for walls bent in single curvature and for eccentricities within the kern. Most significant is the work of Dikkers, R.D. and Yokel, F.Y. (1) and that of Faltal, S.G. and Cattaneo, L.E. (2). For walls subjected to double curvature bending it is assumed that the moment magnifier method will give satisfactory results because of the increased buckling load. In this paper a method of evaluating the critical load for masonry walls with initial double curvature bending is presented and test results for a number of full scale specimens are reported.

BUCKLING OF MASONRY WALLS

Solutions to the buckling problem of walls or columns without tensile strength were proposed by Chapman, J.C. and Slafford, J. (3) and by Yokel, F.Y. (4). The solution of the differential equations presented in Reference (4) for walls in single curvature bending gives the following expression for the critical load:

$$P_{cr} = 0.285 \frac{9}{4} \pi^2 \frac{(0.5t - e)^3 EI_o}{L^2} \quad [1]$$

where E = the modulus of elasticity of the masonry
 t = thickness of the wall
 e = eccentricity of the applied load
 L = the length of the wall.
 I_o = uncracked moment of inertia.

This solution can be approximated with an accuracy of 3.8% by

$$P_{cr} = 8\pi^2 \left(0.5 - \frac{e}{t}\right)^3 \frac{EI_o}{L^2} \quad [2]$$

¹ Graduate Student, The University of Alberta, Edmonton, Canada
T6G 2G7

² Professor of Civil Engineering, University of Alberta, Edmonton,
Canada T6G 2G7

³ Professor of Civil Engineering, University of Alberta, Edmonton,
Canada T6G 2G7

The first buckling mode is a lower energy configuration than the second mode, and as a result of this, regardless of the loading condition and initial imperfection, the member tends to assume this configuration. When this happens, the cracks created by the end moments on one side of the wall will close and, in effect, this side will be uncracked. The member may then be analyzed as a "stepped-column" as shown in Figure 1.

Initially the location of the point of inflection is given by

$$\alpha = \frac{e_1}{e_1 + e_2}$$

where e_1 = the smaller of the two end eccentricities
 e_2 = the larger of the two end eccentricities

The moment of inertia of the cracked section may be approximated on the basis of Equation 2 as:

$$I_1 = 8\left(0.5 - \frac{e_2}{t}\right)^3 I_0$$

and the section can be now analyzed as the column shown in Figure 2.

EVALUATION OF BUCKLING LOAD OF EQUIVALENT SECTION BY THE ENERGY METHOD

The total potential energy at buckling for any member subjected to combined bending and axial load is given by

$$\Pi_B = 1/2 \int_0^L EI_0 (y'')^2 dx - 1/2 P_{cr} \int_0^L (y')^2 dx \quad [3]$$

where y = the buckled shape.

For an elastic structure the total potential Π_B is composed of the strain energy and the potential of the applied load. The equilibrium condition is expressed mathematically as:

$$\delta \Pi_B = 0 \quad [4]$$

To solve the buckling load for the stepped column an appropriate buckled shape is selected and the condition of Equation 4 is imposed on the total potential relation.

To obtain the best possible shape for the buckling configuration, a finite element approach is used with a fifth order interpolating function.

Equation 3 is rewritten to account for the different section properties in the two segments as follows:

$$\begin{aligned} \Pi_B = & 1/2 \int_0^{\alpha L} EI_0 (y''')^2 + 1/2 \int_{\alpha L}^L EI (y''')^2 dx - \\ & 1/2 P_{cr} \int_0^L (y')^2 dx \end{aligned} \quad [5]$$

Letting $y = \langle \phi \rangle \{ \theta \}$

Then

$$\begin{aligned} y' &= \langle \phi' \rangle \{ \theta \} \\ y'' &= \langle \phi'' \rangle \{ \theta \} \\ (y')^2 &= \langle \phi' \rangle \{ \theta \} \langle \phi' \rangle \{ \theta \} = \{ \theta \} [\phi'] \{ \theta \} \\ (y'')^2 &= \langle \phi'' \rangle \{ \theta \} \langle \phi'' \rangle \{ \theta \} = \{ \theta \} [\phi''] \{ \theta \} \end{aligned}$$

where y = deflection
 y' = slope
 y'' = curvature
 $\langle \phi \rangle = \langle \phi_1 \phi_2 \phi_3 \phi_4 \phi_5 \phi_6 \rangle$, the interpolating functions,

and

$$\{ \theta \} = \begin{bmatrix} y_1 \\ y_1' \\ y_1'' \\ y_2 \\ y_2' \\ y_2'' \end{bmatrix}$$

Since end deflections y_1 and y_2 are zero, the interpolating functions ϕ_1 and ϕ_4 must be zero.

Changing the limits of integration and substituting for y'' and y' in Equation 5, the following relation is obtained for the total potential

$$\begin{aligned} \Pi_B = & 1/2 \frac{EI_0}{L} \int_0^{\alpha} \{ \theta \} [\phi''] \{ \theta \} dn \\ & + 1/2 \frac{EI_1}{L} \int_{\alpha}^1 \{ \theta \} [\phi''] \{ \theta \} dn - 1/2 P_{cr} L \int_0^1 \{ \theta \} [\phi'] \{ \theta \} dn \end{aligned}$$

Applying Equation 4 to the above, the equilibrium condition may be expressed as

$$\begin{aligned} \delta \Pi_B = & \frac{EI}{L} \int_0^{\alpha} [\phi''] \{ \theta \} dn + \frac{EI_1}{L} \int_{\alpha}^1 [\phi''] \{ \theta \} dn - \\ & P_{cr} L \int_0^1 [\phi'] \{ \theta \} dn = 0 \end{aligned}$$

$$\text{or, } \int_0^\alpha [\phi'''] \{\theta\} dn + \beta \int_\alpha^1 [\phi'''] \{\theta\} dn = \frac{P_{cr} L^2}{EI_0} \int_0^1 [\phi'] \{\theta\} dn$$

$$\text{where } \beta = \frac{I_1}{I_0}$$

The above relation can be reduced to

$$[K] \{\theta\} = \lambda [K_g] \{\theta\} \quad [6]$$

where $[K]$ = bending stiffness matrix
 $[K_g]$ = geometric stiffness matrix

This equation is solved as an Eigen value problem to find λ .

For $L^2/EI_0 = 1$ the above relation can be solved to obtain the coefficients which will give the buckling load $P_{cr} = \lambda EI_0/L^2$ for values of α and β . Table 1 is a tabulation of λ values as found using this method. The interpolating functions and the boundary conditions used are given in the Appendix. Table 1 can be used to evaluate P_{cr} for any stepped column of constant modulus of elasticity by entering with α and β finding λ and multiplying λ by EI_0/L^2 .

The advantages of using this method are:

- (a) High order polynomials will approximate very closely a sine curve and other shapes that a stepped column can assume as a result of initial bending and variations in the geometric properties. It is found that a fifth order polynomial is quite adequate in this case.
- (b) Using a determinant search method and approaching the solution from the left will assure the selection of the best shape to minimize the energy stored in the system.

EXPERIMENTAL PROGRAM AND RESULTS

Ten plain walls were built using 8x8x16 two core C-90 blocks and type S mortar. The end eccentricities and the slenderness ratios of the walls tested are listed in Table 2.

The walls were tested in a 1.6 million pound capacity testing machine at ages varying from 28 to 65 days. Deflections were monitored throughout each test and the deflected shapes at selected loads were plotted. The tendency of the walls to fail in their first buckling modes is shown in Figure 4 and 5. Figure 6 shows the calculated and experimental buckling loads. The theoretical analysis was based on $I_0 = 1200 \text{ in.}^4$ and $E = 1.35 \times 10^6 \text{ psi}$. Table 2 gives a summary of test results. As expected, the experimental results were lower than the theoretical buckling loads because material failures occurred before the buckling loads were reached. This type of failure is more probable than buckling failure for small eccentricities and slenderness ratios less than 30. However the mode of failure was in close agreement with the

assumed first mode. Movement of the point of inflection with increasing load was observed, which further strengthens the assumption that the first buckling mode is the more critical, regardless of the end conditions. Figure 5 shows a comparison of test results with theoretical values.

CONCLUSIONS

Masonry walls subjected to double curvature bending tend to buckle in their first buckling mode. The critical loads for such walls can be obtained using energy methods and fifth order polynomials for interpolation functions. The results, using one element and fifth order interpolating functions, are good estimates of the buckling loads. For a wall with a constant moment of inertia, the error is 0.048%. The coefficients for evaluating the critical loads for walls subjected to double curvature bending can be used in the moment magnifier method in designing such walls.

ACKNOWLEDGEMENTS

This study was performed in the Department of Civil Engineering at the University of Alberta. Financial assistance from the Canadian Masonry Institute, the Alberta Masonry Institute and the National Research Council of Canada is acknowledged.

REFERENCES

1. Dijkers, R.D. and Yokel, F.Y., "Strength of Brick Wall Subject to Axial Compression and Bending", Proceedings of Second International Brick Masonry Conference held in Stoke-on-Trent, England, April 1970.
2. Fattal, S.G. and Cattaneo, L.E., "Structural Performance of Masonry Wall Under Compression and Flexure", U.S. Department of Commerce, National Bureau of Standards, Ernest Ambler, Acting Director, Issued June 1976.
3. Chapman, J.C. and Slafford, J., "The Elastic Buckling of Brittle Columns", Par No. 6147, Proceedings of the Institution of Civil Engineers, London, Volume 6, pp. 107-125, January 1957.
4. Yokel, F.Y., "Stability and Load Capacity of Member with No Tensile Strength", Journal of the Structural Division, Proceedings of the American Society of Civil Engineers, July 1971.

APPENDIX

EVALUATION OF INTERPOLATING FUNCTION

All mathematical operations involving interpolating functions and the solution of the buckling problem were carried out using a computer.

Since deflections are zero at both ends ϕ_1 and ϕ_4 are zero. The remaining four functions are shown schematically in Figure 3. The boundary conditions to be satisfied by these functions ($\phi_2, \phi_3, \phi_5, \phi_6$) are as follows:

η	y	y'	y''	functions
0	0	1	0	ϕ_2
1	0	0	0	
0	0	0	1	ϕ_3
1	0	0	0	
0	0	0	0	ϕ_5
1	0	1	0	
0	0	0	0	ϕ_6
1	0	0	1	

The functions which satisfy these conditions are:

$$\begin{aligned}\phi_2 &= -3\eta^5 + 8\eta^4 - 6\eta^3 + \eta \\ \phi_3 &= -1/2 (\eta^5 - 3\eta^4 + 3\eta^3 - \eta^2) \\ \phi_5 &= -3\eta^5 + 7\eta^4 - 4\eta^3 \\ \phi_6 &= 1/2 (\eta^5 - 2\eta^4 + \eta^3)\end{aligned}$$

Differentiating these functions once yields

$$[\phi'] = \begin{bmatrix} \phi_2' & \phi_2' & \phi_2' & \phi_3' & \phi_2' & \phi_5' & \phi_2' & \phi_6' \\ & & \phi_3' & \phi_3' & \phi_3' & \phi_5' & \phi_3' & \phi_6' \\ \text{symmetric} & & & \phi_5' & \phi_5' & \phi_5' & \phi_6' & \\ & & & & & \phi_6' & \phi_6' & \end{bmatrix}$$

Substitution of the functions and integration of the above matrix from 0 to 1 results in

$$\int_0^1 [\Phi'] \, dn = \begin{bmatrix} 0.22857 & 0.016666 & -0.014285 & 0.004762 \\ & 0.0015873 & -0.004762 & 0.000793 \\ \text{symmetric} & & 0.228571 & -0.016667 \\ & & & 0.001587 \end{bmatrix} = [K_g]$$

where $[K_g]$ is the geometric stiffness matrix.

The interpolating functions are then differentiated twice and the matrix $[\Phi'']$ is obtained as:

$$[\Phi''] = \begin{bmatrix} \phi_2'' & \phi_2'' & \phi_2'' & \phi_3'' & \phi_2'' & \phi_5'' & \phi_2'' & \phi_6'' \\ & & \phi_3'' & \phi_3'' & \phi_3'' & \phi_5'' & \phi_3'' & \phi_6'' \\ \text{symmetric} & & & & \phi_5'' & \phi_5'' & \phi_5'' & \phi_6'' \\ & & & & & & \phi_6'' & \phi_6'' \end{bmatrix}$$

After substitution of the corresponding functions, integrating this matrix and evaluating $[\Phi'']_0^\alpha + C[\Phi'']_\alpha^1$, the bending stiffness matrix, $[K]$, is obtained.

For the case of a column with constant EI_1 ($\alpha = 0$) this matrix is

$$[K] = \begin{bmatrix} 5.4857 & 0.3143 & +3.0857 & -0.11428 \\ & 0.0857 & 0.1143 & 0.01428 \\ \text{symmetric} & & 5.4857 & -0.31428 \\ & & & 0.00857 \end{bmatrix}$$

Solving the relation

$$[K] \{\theta\} = P_{cr} \frac{L^2}{EI_0} [K_g] \{\theta\}$$

for $\frac{L^2}{EI_0} = 1$

and the geometric and bending stiffness matrices, $[K_g]$ and $[K]$ as evaluated above, using the power sweep method, $P_{cr} = 9.8734354$ which compares very closely with the exact value of π^2 . Table 1 is obtained by evaluating $[K]$ and solving relations for various values of α and β from 0.0 to 1.

Table 2 - Loading Conditions and Test Results

Wall No.	h/t	e_1 (inches)	e_2 (inches)	Load at failure (kips)
E1	17.97	+3.54	-3.54	85.0
E2	15.87	+3.54	-3.54	115.0
E3	13.77	+3.54	-3.54	135.2
E4	13.77	+2.54	-2.54	156.6
E5	13.77	+1.27	-1.27	220.4
G5	17.97	+2.54	-3.00	150.6
G6	17.97	+2.54	-3.54	144.4
G7	17.97	+1.27	-1.27	196.6
G8	17.97	+3.00	-3.54	117.0
G9	17.97	+3.00	-3.00	148.2
M1	24.20	0.00	0.00	139.2

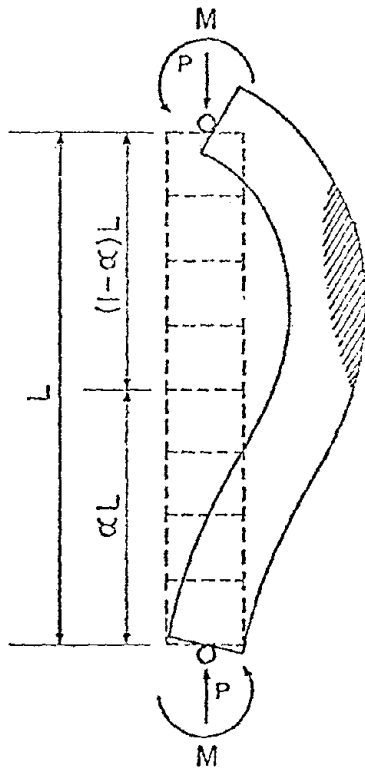


FIGURE 1: CRACKED SECTION AT BUCKLING UNDER THE ACTION OF AXIAL LOAD AND DOUBLE CURVATURE BENDING

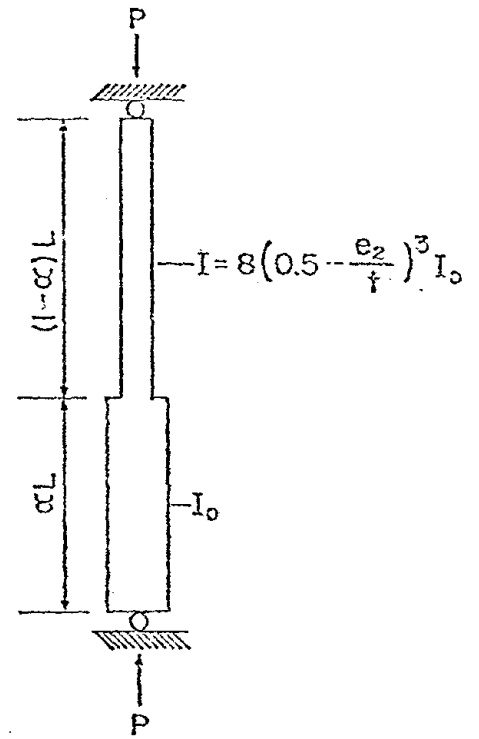


FIGURE 2: EQUIVALENT SECTION

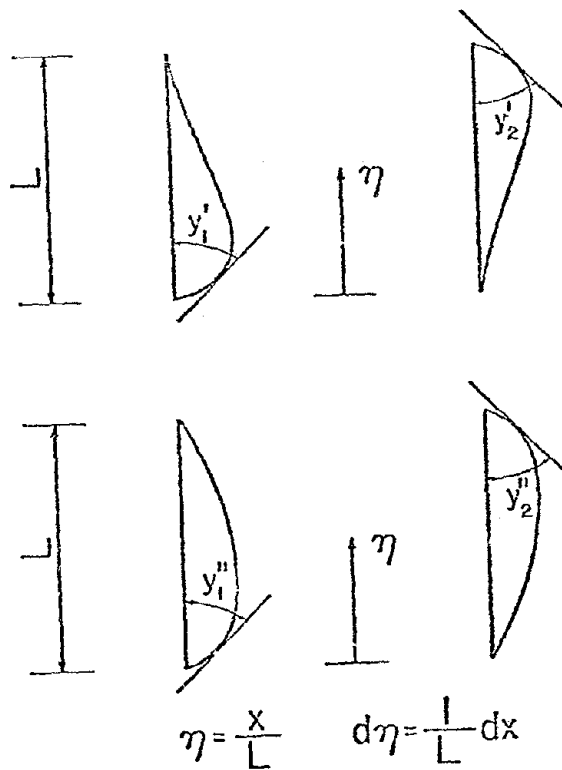
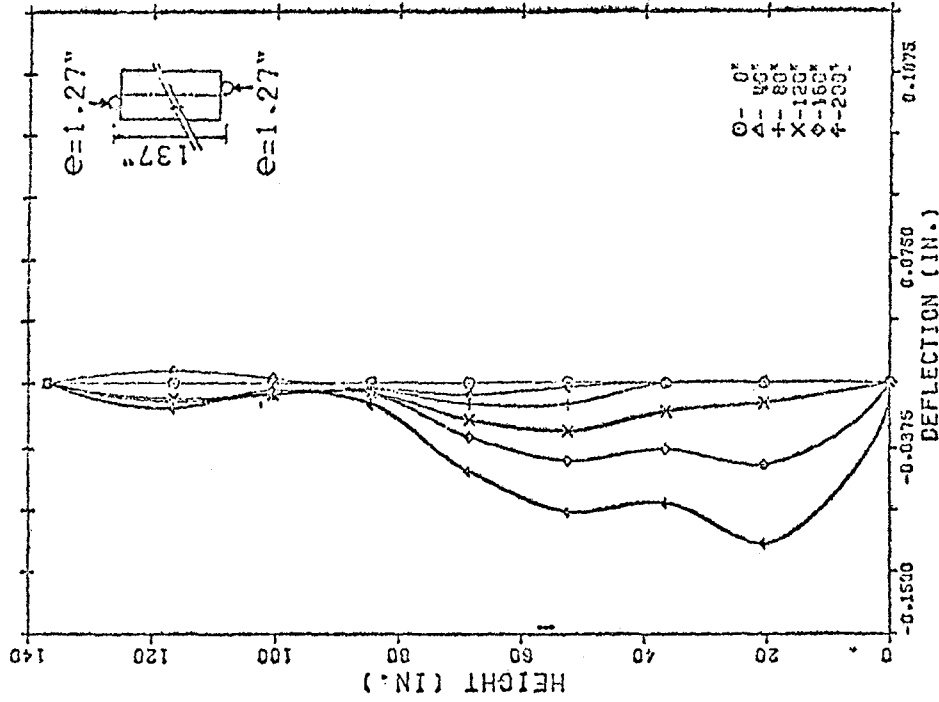
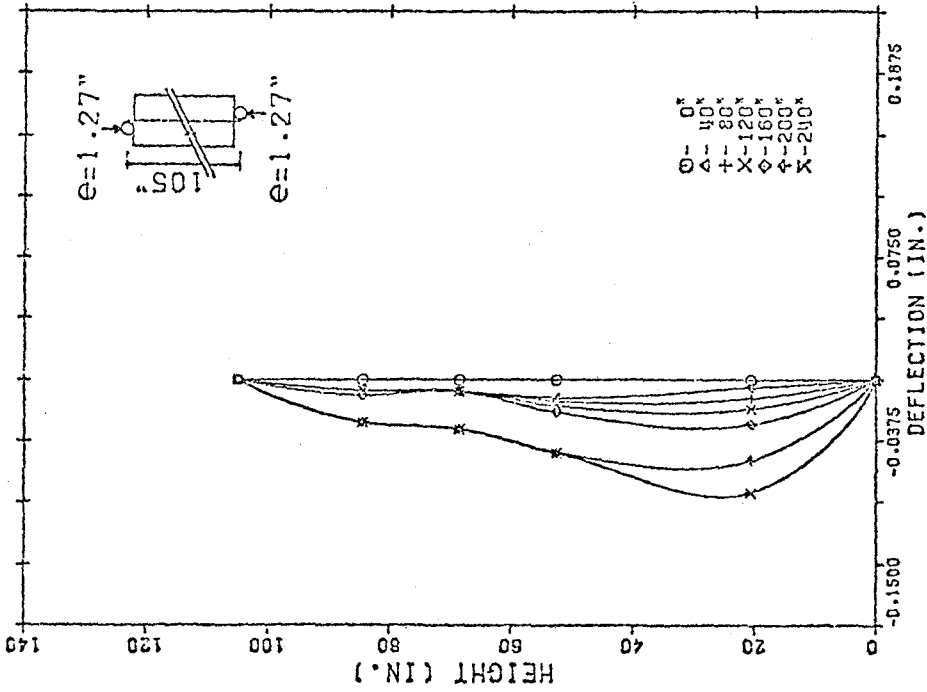


FIGURE 3: INTERPOLATING FUNCTIONS

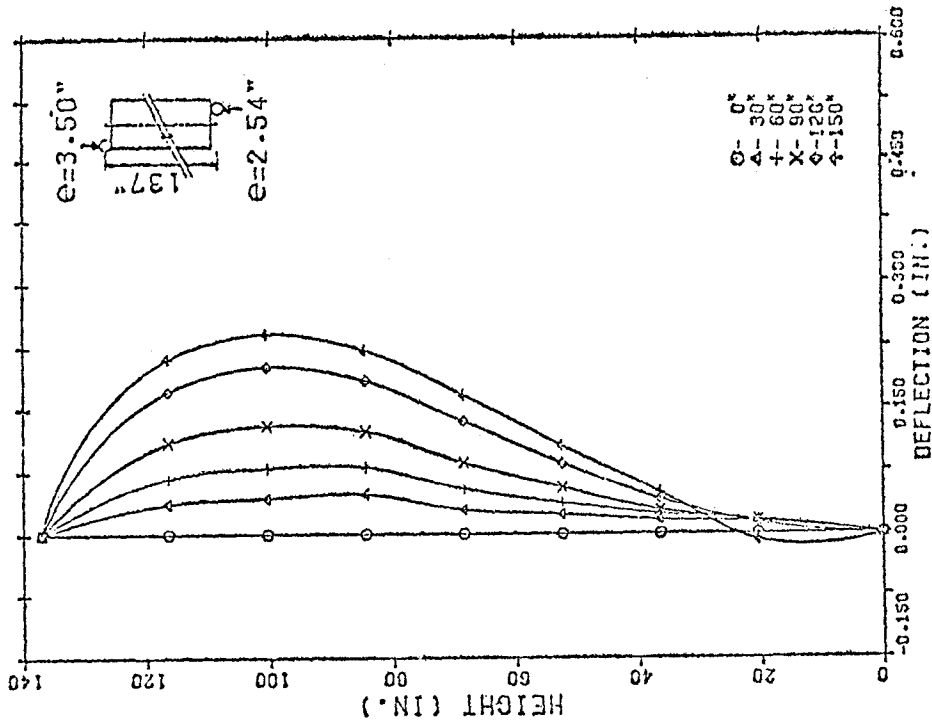


WALL G7 AT 40 KIP INC.

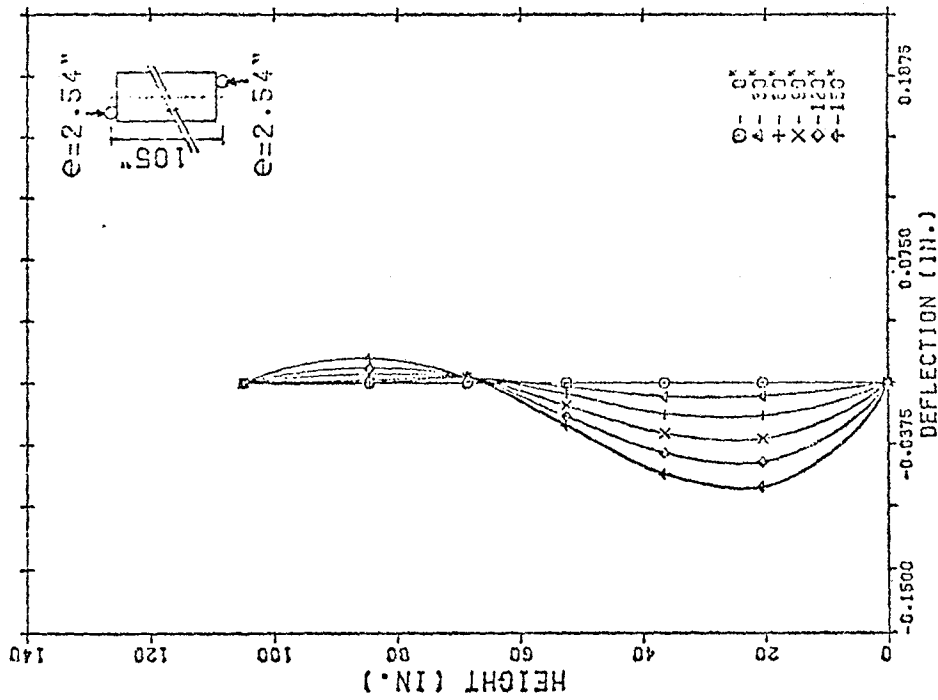


WALL E5 AT 40 KIP INC.

FIGURE 4: LOAD DEFLECTION CURVES FOR WALLS LOADED IN DOUBLE CURVATURE WITH THE LOAD APPLIED AT THE "KERN" POINT.



WALL E4 AT 30 KIP INC.



WALL G6 AT 30 KIP INC.

FIGURE 5: LOAD DEFLECTION CURVES FOR WALLS LOADED IN DOUBLE CURVATURE WITH ECCENTRICITY LARGER THAN THE "KERN".

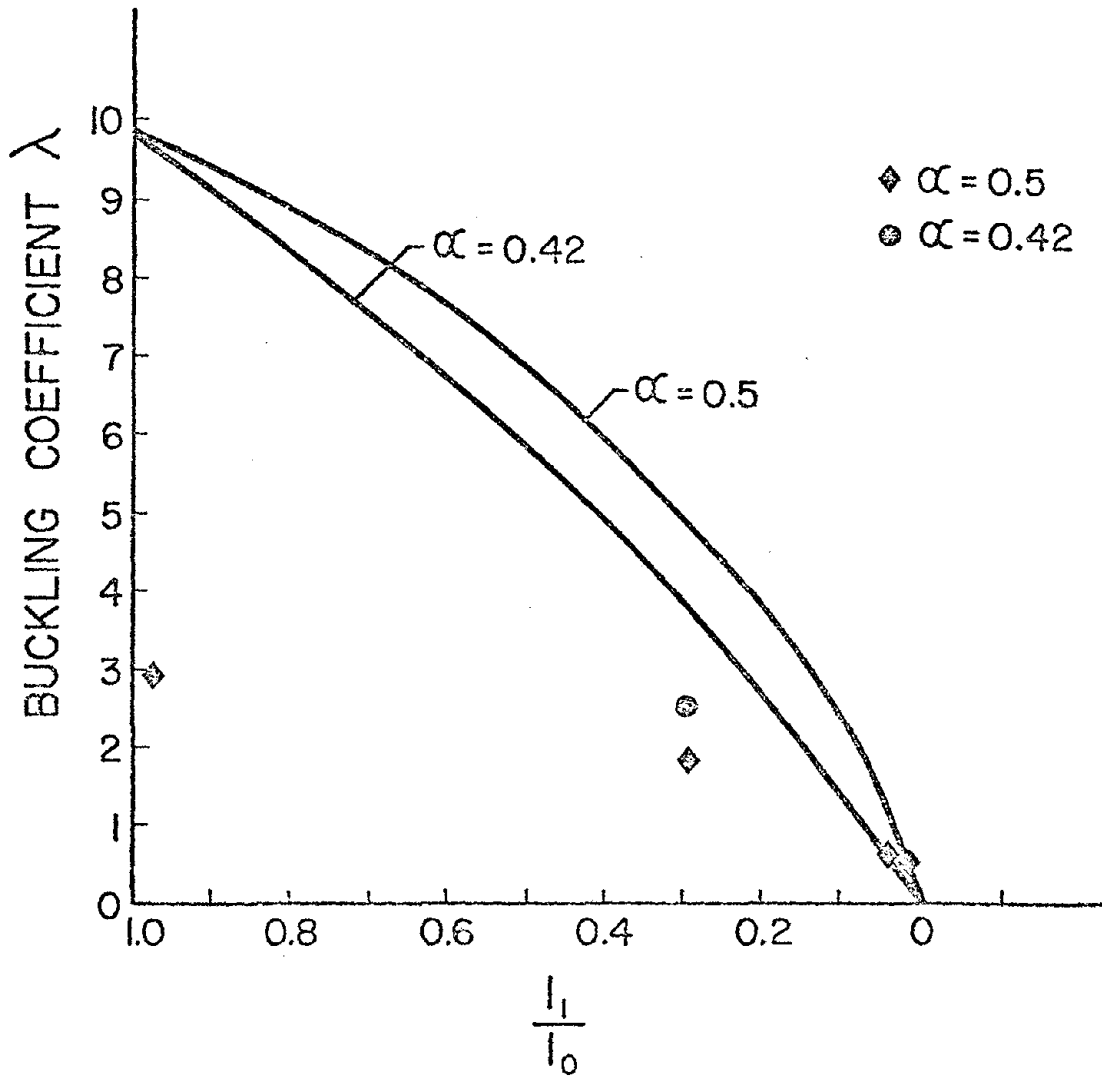


FIGURE 6. RELATION BETWEEN CALCULATED AND EXPERIMENTAL RESULTS

AN AUTOMATED DESK METHOD FOR ANALYZING LOAD BEARING
MASONRY STRUCTURES

By Van Pelt, Jack M., P.E.¹

ABSTRACT: The analysis of load-bearing masonry structures involves complex and time-consuming engineering calculations. The purpose of this paper is to discuss the impact of a preliminary automated method of analysis using an inexpensive programmable printing desk calculator to obtain the same results in final form for publication. The overall approach is discussed and individual programs which have been developed are assessed. The current capability of the analysis tool is reviewed and comments are solicited from experienced masonry structural engineers for incorporation into the finalized method.

¹Consulting Engineer, Littleton, Colorado. Consultant to Colorado Masonry Institute, Denver, Colorado.

AN AUTOMATED DESK METHOD FOR ANALYZING LOAD BEARING MASONRY STRUCTURES

By Jack M. Van Pelt, P.E.¹

INTRODUCTION

The analysis of load-bearing masonry structures involves complex and time-consuming engineering calculations. Large computers can certainly handle these calculations, but for many an engineer the direct interface with his own analysis tool is more desirable for both economic and practical reasons. For many also, that analysis device is a desk calculator with little or no programming capability and requires laborious calculations with many double checks for accuracy.

The rapid advances in microelectronics and in programmable printing calculators in the last several years is allowing economic replacement of the unprogrammable variety with corresponding advances in convenience and engineering efficiency.

This paper discusses the ongoing development of an analysis approach using an advanced programmable desk calculator. Also discussed is the rationale for the initial selection of the analysis tool, its current capability, and what the currently developed programs allow the user to accomplish. Programs remaining to be developed under the 8-Task approach are also discussed and an estimate of when all programs will be completed is given.

THE ANALYSIS TOOL

In early 1976 the author was asked by the Colorado Masonry Institute (CMI) to compare various computer and programmable calculator systems and to recommend one that was economical, versatile, would have the capability to produce reinforced masonry design tables and would also be compatible with the development of an automated load-bearing analysis for masonry structures.

After a period of investigation and comparison of a range of system capabilities from pocket programmables under \$500 to microcomputers in the \$10,000 range, a preliminary recommendation was made. The recommendation was to lease a Texas Instruments SR-60 Programmable Prompting Calculator (base price under \$2,000) with an option to buy

¹Consulting Engineer, Littleton, Colorado. Consultant to Colorado Masonry Institute since January 1976. Results reported in this paper cover the period from January 1977 - February 1978 with progress continuing.

it. After further demonstrations and tests of the calculator to work problems of specific interest, CMI obtained one of the first five units delivered to Colorado (Fig. 1).

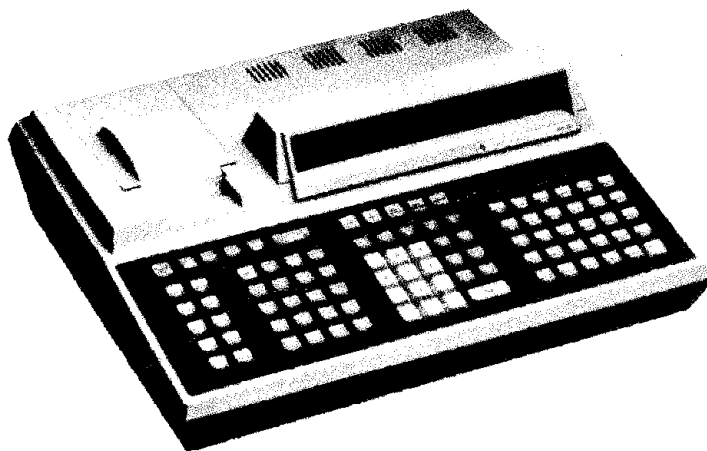


Fig. 1 - SR-60 Programmable Calculator

Since that time, as experience was gained with the calculator, the storage memories were expanded from the basic 480 steps (key strokes) and 40 data memories to the current 3840 steps and 310 data memories. An option is also available for additional memory expansion but has not been necessary. Options were also planned for auxiliary equipment to plug into the basic calculator (e.g., typewriter or plotter), but the output of the thermal printer was found adequate to produce final results for programs written thus far.

The usefulness of the SR-60 for masonry structural design tasks is enhanced by the fact that it is basically a scientific calculator. It has 95 keys (many with double functions) of which 45 keys are scientific functions. This greatly reduces programming time and space over calculators or computers without this feature. As a calculator it carries 12 calculating digits and has a limited precision capability as well as specified roundoff of displayed or printed results. The basic calculator is a convenient desk size (17 x 14.7 x 5.5 inches), consumes 40 watts (at 120 volts) of power and has a portable weight of 16 lbs.

Various program libraries are also available from Texas Instruments for evaluation of special mathematical and statistical functions and for working financial problems plus electrical, civil, mechanical, and various other basic engineering problems. All programs are stored on 2½-inch by 10-inch magnetic cards.

Whether pre-recorded or user-generated programs are being used, the prompting feature of the calculator is most useful. Since alphabetical as well as numerical input is available for programming,

alphabetical messages can be displayed requesting the user for a specific input (e.g., enter prism strength) when it is needed by the program. It is the prompting feature which allows a user to interface with the calculator in a very direct way.

In addition to its capability for listing programs and data memory contents, the printer can also be used in a trace mode for editing of programs under development. Writing of programs is greatly simplified since no special program language must be learned and input is alphabetical or algebraic. Some of the programming features include 15 user-defined keys, 77 labels, indirect memory addressing, 4 subroutine levels, and 10 flags.

During the period the calculator has been in use 17 programs have been written varying in complexity from relatively simple programs of less than 480 steps to programs exceeding 3300 steps. Some typical examples of varying complexity are listed as follows:

1. A program to generate tables of reinforced concrete and clay masonry wall section properties of moment of inertia and section modulus (under 480 steps).
2. A program to generate tables of reinforced masonry wall resisting moments (about 1200 steps).
3. A program for generating tables of combined vertical and lateral load-carrying capacities of reinforced masonry walls (under 1920 steps).
4. A program to determine the center of rigidity of any floor (over 3000 steps).

The analysis tool was found to be quite versatile and economical and programming experience is not required to write simple programs within a short time of first use. Further examples of application are discussed in the later section describing the load-bearing analysis programs. Other possible future technical applications of the SR-60 include cost estimating and thermal analysis of masonry structures. The calculator can also be used to generate payroll data for a small business and has many other applications.

OVERALL ANALYSIS APPROACH

The goal of this analysis is to progress through the design of a masonry structure with load-bearing walls and design the walls for the wind conditions, seismic conditions, and local code considerations for the particular part of the country under consideration. It is designed for use with buildings of one or more rectangular-shaped planform and elevation units (Fig. 2) up to 25 stories high.

The general approach used is similar to the approach described by Amrhein (2) in the chapters on building design. The overall approach in this paper is valid for load-bearing masonry structures with shear-resisting walls and would be applicable to hand analysis or to any other scientific calculator or computer system. Programs

generated for other systems would, of course, differ from those generated for the SR-60, depending upon the specific requirements of the system used.

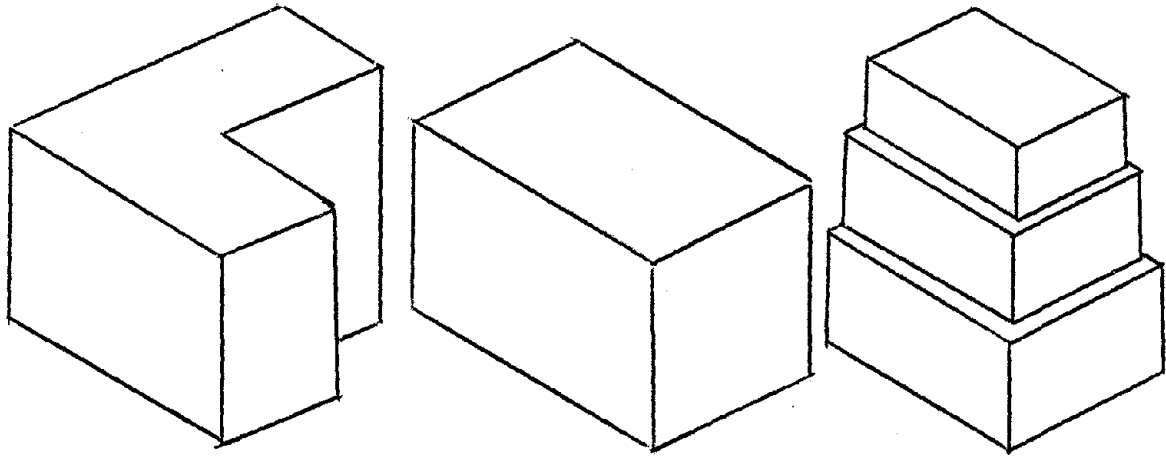


Fig. 2 - Examples of Building Types Considered

The approach used in this analysis is to take the procedure and break it down to 8 specific tasks. These tasks then become one or more calculator programs to be used as tools by the structural engineer for the complete analysis of the building (Fig. 3).

- Task 1 - Select Design Criteria and Determine Gravity Loading
- Task 2 - Determine Mass and C.G. Locations of Walls, Floors, etc.
- Task 3 - Determine Wall Rigidities and Centers of Rigidity
- Task 4 - Determine Lateral Force Design
- Task 5 - Obtain Design Lateral Force and Moment Distribution on the Building
- Task 6 - Determine Shear and Overturning Moments on All Shear Walls
- Task 7 - Find Wall Unit Shears and Flexural Stresses
- Task 8 - Design Load-Bearing Walls

Fig. 3 Overall Load Bearing Analysis Approach

The advantage of this task approach is that as the engineer goes through the various phases he can stop at any point and quickly determine the effect of varying design constraints or loading assumptions before proceeding through the whole analysis. This should save substantial time in the long run. Brief descriptions of the tasks follow:

Task 1 - Select Design Criteria and Determine Gravity Loading - The first part of this task would be to gather structural floor plans, floor area layouts, and building elevation drawings for use throughout all of the tasks. General design criteria and code references used would be listed as well as pertinent weight, strength, and dimension data on the structural wall system planned. In addition, lateral force criteria on the wind zone and seismic zone would be called out at this time. Further descriptions of the nomenclature and standard building and wall coordinate systems used are given under later discussions of the programs.

The second part of the task is to determine all of the live and dead loads (gravity loading) on the roof and individual floors of the structure.

Task 2 - Determine Mass and C.G. Locations of Walls, Floors, etc. - In this task all dead loads would be detailed as well as weights and locations of structural walls, floors, and concentrated loads to determine weight and C.G. (center of gravity) locations for each floor as a unit acting under wind or seismic forces and for the building as a whole.

Task 3 - Determine Wall Rigidities and Centers of Rigidity - In Task 3 the relative rigidities of all walls on a given floor are determined considering the wall types, locations, number of flanges, prism strengths, and basic dimensions. This information is required to determine the center of rigidity for floors of buildings with rigid diaphragms that can transmit torsional moments to the floor and influence shearing stresses on the individual walls. In addition, the center of rigidity for each floor is compared to C.G. location to evaluate torsional eccentricity for later use.

Task 4 - Determine Lateral Force Design - In this task the base seismic and wind shears are calculated for the principle axes of the building and design base shears are selected. Other factors including building periods and lateral force coefficients are also evaluated.

Task 5 - Obtain Design Lateral Force and Moment Distribution on the Building - In Task 5 the governing lateral forces (wind or seismic) are distributed to individual floors and story shears and overturning moments are calculated. Total overturning moments on the building are also obtained and compared to corresponding weight restoring moments as a measure of building stability.

Task 6 - Determine Shear and Overturning Moments on All Shear Walls - From the results of Task 5 and previous tasks, shear forces are distributed and overturning moments determined for all shear walls.

Task 7 - Find Wall Unit Shears and Flexural Stresses - The purpose of this task is to determine the unit shear stresses and flexural stresses (due to overturning moment) for all walls with and without reinforcement.

Task 8 - Design Load-Bearing Walls - In the final task individual load-bearing walls are evaluated with all vertical and lateral loads present and necessary reinforcement is determined. At this point (or earlier in some cases) assumptions concerning prism strength or wall thickness may be reassessed if necessary. Depending upon the complexity of the structure and the experience of the structural engineer, as many individual walls as necessary are evaluated.

DESCRIPTION OF PROGRAMS AND CONVENTIONS

As with any systematic approach involving automated analysis techniques, a system of standard nomenclature and conventions must be adopted. For this analysis the familiar right-handed coordinate system convention is used and examples of its application are shown as the discussion progresses.

An example of a building layout is shown in Fig. 4. The longest dimension of the building is selected as the x-direction and the face of the building is placed near the x or y-axis as indicated. Location of overall areas are numbered as shown on the layout and also on the reference grid describing the convention (Fig. 4). The rule used is to start at the area (or areas) with the smallest y-value location (YD1) and number the area with the smallest x-value location (XD1) No. 1, the next highest x-value location No. 2, etc. and then proceed to the next higher y-value location and continue.

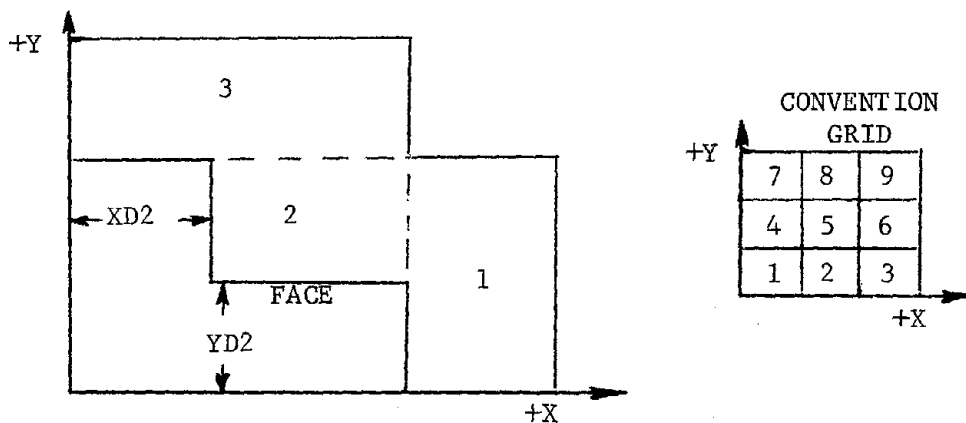


Fig. 4 - Building Layout Convention

The location of the origin is selected to contain all parts of the building within the first quadrant to eliminate negative inputs to programs for the location of any item in the structure. In the example shown (Fig. 4) the y-location of area No. 1 and the x-location of area No. 3 are both zero. If some of the upper floors had smaller dimensions those x and y locations would have positive values. This general procedure for locating areas is also used for locating and

numbering wall types and individual walls as will be seen later.

The vertical dimension of the coordinate system is the height (H). The origin corresponds to ground level and floors are numbered from 1 (at ground level) consecutively to the top floor.

The normal procedure would be first to gather all data on the building (numbering areas and walls), design criteria, wind profiles, etc. during Task 1 to initially provide all program inputs required. For purposes of clarity in this discussion, however, these items will be shown only at the time they are first needed.

Common Features of Programs - In an effort to reduce the amount of writing, hand calculation, and tabulations of data, maximum use has been made of the thermal printer output for a display of all titles, inputs and wind calculations to fit on a standard 8½ x 11 inch page. Printing is produced on 2½ inch wide thermal paper. In all programs the input data is first requested and titles are printed while input is made. After the first page of titles is complete and calculations are made, the data is then printed for the first page. This procedure continues for the remaining pages produced. A full scale reproduction (for 8½ x 11 scale) of part of a program output is shown (Fig. 5).

SUBJECT--4 STORY APT.
JOB NO-- 001

PAGE NO--4
DATE--2-23-78
BY-- JVP

LOADING (PSF)

ROOF

DEAD LOADS

(1) ROOFING+INSUL.	16.0
(2) SLAB=	
8 IN. L.W. CONC	73.0
(3) WALL TYPE	0.0

Fig. 5 - Output of Thermal Printer

Dashed lines are printed at the top and bottom of each page for ease of mounting on a standard page for ready reproduction. Extra space is also available on the page for any special notes. In the example shown (Fig. 5) the user is first asked for roofing and insulation weight (psf), then for the type of slab, its weight, etc. In most cases the request for the data remains in the calculator display until the input is entered.

In addition to the printed program output, a partial or complete listing of the program in the calculator or a listing of data memory contents may be printed out at any time.

Another common feature of all programs is the SR-60 User Instructions. These are produced on a standard 8½ x 11 inch form and vary from 2 to 4 pages for most programs. The example (Fig. 6) shows what information is in the display at a particular step in the program and gives the user instructions on the input required. These instructions would only be referred to periodically since the prompting message in the display is normally sufficient.


TITLE		GRAVITY LOADING PROGRAM		PAGE	2	OF	3	SR-60		
No. 15 & 16		CARDS	REGS	STEPS	AUX	User Instructions				
STEP	DISPLAY	INSTRUCTION		PRESS	GOTO					
6	T.O.T. NO. OF FLOORS =	KEY IN TOTAL NO. OF FLOORS		ENTER						
7	NUMBER OF TOP FLOOR =	KEY IN NUMBER OF TOP FLOOR		ENTER						
8	ARE FLOORS SLABS?	YES, IF SLABS/NO, IF FRAMING		YES/NO						
9	ALL FLOOR LD.S. SAME?	YES, IF ALL FLOOR LOADING IDENTICAL		YES/NO						

Fig. 6 - User Instructions

General program descriptions including equations used and special instructions would also be included with each program. Program descriptions, instructions, copies of listings, and magnetic program cards (in holders) fit easily into a three-ring notebook binder.

Generally used units are feet and inches, inches, pounds, kips, psf, and psi. Convenience features to reduce input are present in most programs (e.g., if individual floor heights are the same the number of inputs is reduced).

Gravity Loading Program - The purpose of this program is to identify and summarize the roof and floor gravity loads that the structural wall system must sustain. The program can handle both rigid slabs (Fig. 5) and wooden framing for floors and roofs (Fig. 7). Roof data is first requested and then floor data. Common floor data is indicated and input/output is reduced if this is the case. Total dead loads, live loads, and dead plus live loads are summarized for each floor. Program running time is under 2 min. per floor.

Mass Program - The purpose of the mass program is to determine mass and center of gravity data for each floor and for the total structure. The input and output of dead loads is organized to allow direct use of the data in determining torsional moments in the shear wall rigidity calculations. For this purpose the weight acting on the walls

FLOOR NO. =	2.
DEAD LOADS	
(1) FLOORING	5.0
(2) FLOOR JOISTS	3.0
(3) CEILING	5.0

	13.0
(4) PARTITIONS	10.0
(5) OTHER =	N/A

	0.0
TOTAL DEAD LOAD	23.0
TOTAL LIVE LOAD	40.0

TOTAL DEAD+LIVE LD.	63.0

Fig. 7 - Gravity Loading Program Output Sample

of a given floor consists of those walls plus the weight of the floor (or roof) above and any fixed concentrated loads attached to it. In this way (for rigid diaphragms only) when the diaphragm is acted on by earthquake forces the proper mass affecting the shear walls on the floor is accounted for.

Inputs to the program include the location, dimensions, and weight per sq. ft. of each floor (or roof) area and each wall plus the location and weight of each concentrated load. Floors common to the floor above are not re-input by the user. For a common wall in a given direction (up to 10) weight and dimension data is given once for a particular wall type and only the changing location is requested (e.g., 3.09 indicates that wall type No. 3 has 9 walls). It is possible to have up to 49 wall types in each direction and wall types and individual walls are numbered in the same manner as areas (Fig. 4).

Output of the program includes the input data plus the calculated floor (or roof) areas for each level and their total weight plus the weight and C.G. location for each floor and the total building. Samples of output are shown (Fig. 8) with outputs in feet and inches. The equations used are simple area and moment calculations and running time is under 2 min. per roof/floor area or per wall on floors without commonality.

Rigidity Program - The purpose of this program is to determine wall rigidity data and center of rigidity for each floor of a building. Center of gravity data from the Mass Program is used to determine torsional eccentricity for earthquake calculations with rigid diaphragms.

The program is rigorous in the sense that wall moments of inertia (along the wall) are calculated and differing clay masonry and concrete masonry prism strengths and moduli limits are considered. Up

FLOOR NO=	1.	SHEAR WALLS	
-----		-THIS FLOOR	
FLOOR ABOVE		N-X TYPES=	1.00
DISTRIB. LOAD		N-X WALLS=	1.00
AREAS COMMON		N-Y TYPES=	2.00
MT/SQ. FT (PSF)=	60.00	N-Y WALLS=	2.00
		H-WALLS=	8.00
TOT AREA		WALL NO=	1.00
-----		MT/SQ. FT (PSF)=	20.00
A (SQ. FT)=	2529.99	LM=	24.00
W (KIPS)=	151.80	X-WALL	
XG=	37.07	YM=	30.00
YG=	23.06	YV=	10.00

Fig. 8 - Mass Program Output Sample

to two flanges per wall formed by intersecting walls are also considered. The rigidity is herein defined as the inverse of the deflection (from shear and bending) of a cantilever wall under a 100,000 lb. horizontal force directed along the wall at the top (see also Ref. 2) as follows:

$$R_C = \frac{1 \times 10^{-6}}{\left(\frac{.0333 (HW)^3}{(E_M) (I_{CC})} \right) + \left(\frac{.12 (HW)}{(E_V) (A)} \right)} \quad (1)$$

where:

- R_C = Rigidity of a cantilever wall (per in)
- A = Total cross sectional area of wall/flanges (sq. in.)
- I_{CC} = Moment of inertia along wall system about centroidal axis (in⁴)
- E_M = Modulus of elasticity (psi)
- E_V = Modulus of rigidity (psi)
- HW = Wall height (in.)

Wall numbering for this program is identical to the numbering used for the Mass Program when flanges are not present. With flanges the number of wall types would change somewhat. Calculations for centers of rigidity are of the same type as for C.G. locations and the former is compared with the latter to obtain torsional eccentricity. A minimum torsional eccentricity of 5 per cent floor length (1) is assumed when calculated eccentricities are lower.

Program running time is approximately 2 to 2½ minutes per wall type for each non-common floor. Time varies with the number of flanges present. An example of output is shown in Fig. 9 based on data from Hanson (3).

WALL NO=	51.04	FLOOR Z	
Y-WALL		-----	
N-TYPE=	4.		
LN=	12.06	FLOOR NO=	2.
RIGIDITY (<IN)=	32.741	FLOOR LENGTH (DMM)=	113.04
XN=	0.00	XG=	56.08
YN=	0.00	YG=	32.06
XN=	113.04	XR=	56.08
YN=	113.04	YR=	36.08
WALL NO=	52.04	EX (= .05DMM)=	5.08
Y-WALL		EY (= .05DMM)=	5.08
N-TYPE=	4.		
LN=	1.00		
RIGIDITY (<IN)=	0.028		
XN=	0.00		
YN=	0.00		
XN=	113.04		
YN=	113.04		

Fig. 9 - Rigidity Program Output Sample

Base Shear Program - The purpose of the program is to determine the total base shear along each principle axis of a structure for both seismic and wind lateral forces and to define the governing base shears.

This program is the first step in the lateral force design of a building. It uses results from the Mass Program and provides information for the Building Shear and Overturning Moment Distribution programs. For seismic calculations, the user has the option of selecting the equations and constraints from the 1976 UBC (4) or programming in a code of his choice. The 1976 Denver Building Code (1) is used for an example and the main differences are shown as follows:

Total Seismic Base Shear Equation

$$V = ZIKCSW \quad (1976 \text{ UBC}) \quad (2)$$

where:

V = Total seismic base shear (kips)

Z = Zone coefficient

I = Occupancy coefficient (1.0 for 1976 Denver Code)

K = Framing coefficient (normally 1.33)

S = Structure/site interaction coefficient (1.0 for 1976 Denver Code)

W = Total building load (kips)

C = Lateral force coefficient

and

$$C = \frac{1}{15 \sqrt{T}} \leq .12 \quad (1976 \text{ UBC option}) \quad (3)$$

or

$$* C = \frac{.05}{3 \sqrt{T}} \leq .10 \quad (1976 \text{ Denver Code option}) \quad (4)$$

(Fixed at .10 for buildings under 3 floors)

where T is the building period in seconds

Wind base shear is calculated using a wind pressure profile as shown in Fig. 10. To simplify calculations in later programs the profile (for the particular locale) is adjusted conservatively by selecting wind pressure heights at the nearest lower floor level.

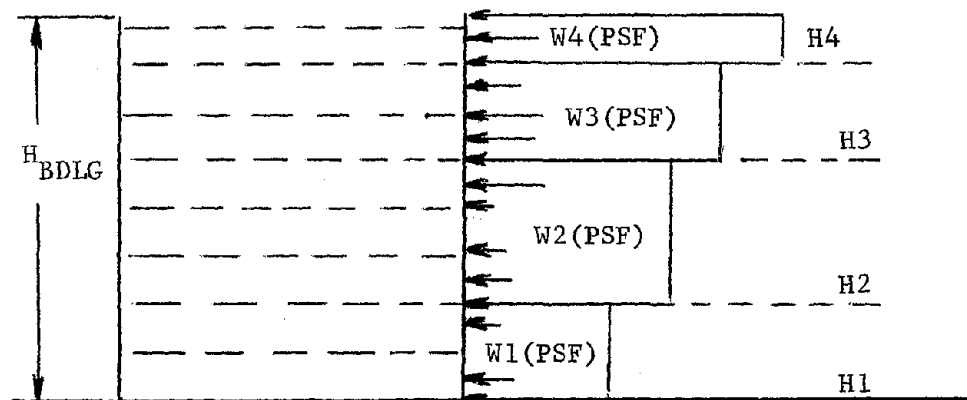


Fig. 10 - Wind Pressure Profile Sketch

For calculation purposes an average horizontal building dimension normal to the wind direction is used to calculate wind forces and allows quick determination of the governing base shear. If differences between seismic and wind base shears are marginal, both shears can be determined accurately in the story shear calculations of the following programs. Fig. 11 shows samples of output of the seismic calculations, wind pressure profile, and design base shear. Running time is under 6 minutes and seismic or wind calculations may be omitted if not desired.

Building Shear and Overturning Moment Distribution Programs - These two programs together accomplish Task 5 by assisting the structural engineer in determining the shear and OTM (overturning moments) for each floor of a building due to seismic and/or wind forces along the principal axes. In a final summary, the governing design shears and overturning moments for the building are given and the building restoring moments are compared.

The first program is used for general inputs which are needed for both programs (e.g., the number of floors and floor heights) and also for seismic inputs and calculations. The equations used for determining story shear and overturning moment are basically the same as in Ref. 2. The same options exist for building code constraints as in the Base Shear Program and appear in the calculation of the whiplash force (F_T) at the roof of the building, as follows:

$$F_T \text{ (1976 UBC)} = 0 \text{ for } T \leq 0.7 \text{ sec.} \quad (5)$$

$$\text{or } = .07 TV \leq 0.25V$$

and $*F_T$ (1976 Denver Code) = 0 for $(H_{Bldg}/D_{Max}) \leq 3.0$ (6)
 or = $.004V (H_{Bldg}/D_{Max})^2 \leq .15V$

where: T = Bldg period (sec)
 V = Seismic base shear (kips)
 H_{Bldg} = Height of bldg. (ft)
 D_{Max} = Horizontal dimension of bldg. along the principal axis (ft)

After general inputs are made the user has the option of omitting seismic inputs and calculations if not required. Samples of output using the 7-Story Apartment Building of Ref. 2 are shown in Fig. 12. Running time for the first program (with seismic calculations) is approximately 2 minutes per floor. Basic inputs and total seismic building shear and overturning moments can be temporarily stored on magnetic cards if execution of the second program must be delayed.

<p>SEISMIC BASE SHEAR V=ZIKCSW -----</p> <p>ZONE= 3.</p> <p>Z-ZONE COEFF= 1.00 I-OCCUP COEFF= 1.00 K-FRAMING COEFF= 1.33 S-SITE COEFF= 1.00</p> <p>X-DIRECTION</p> <p>D(MAX)= 143.08</p> <p>T-PERIOD(SEC)= 0.271</p> <p>*C-LAT FORCE COEFF 0.077</p> <p>V-SEISMIC(KIPS)= 904.14</p> <p>Y-DIRECTION</p> <p>D(MAX)= 87.04</p> <p>T-PERIOD(SEC)= 0.348</p> <p>*C-LAT FORCE COEFF 0.071</p> <p>V-SEISMIC(KIPS)= 832.16</p>	<p>MIND BASE SHEAR V=LKZDELTA H*W(PSF) -----</p> <p>MIND PRESS PROFILE REF U(PSF)= 30.00</p> <p>H1= 0.00 W1(PSF)= 15.00 H2= 27.00 W2(PSF)= 20.00 H3= 45.00 W3(PSF)= 25.00 H4= 100.00 W4(PSF)= 30.00 H5= 500.00</p> <p>X-DIRECTION</p> <p>LY(MAX)= 87.04</p> <p>V-WIND(KIPS)= 110.48</p> <p>DESIGN BASE SHEAR -----</p> <p>X-DIRECTION</p> <p>V-SEISMIC(KIPS)= 904.14</p> <p>Y-DIRECTION</p> <p>V-SEISMIC(KIPS)= 832.16</p>
---	--

Fig. 11 - Base Shear Program Output Sample

The second program is used for the wind inputs and calculations and for summarizing the governing building design base shears, overturning moments, and restoring moments. If seismic forces are known to govern, the wind inputs and calculations may be omitted. Equations for calculating wind story shear and overturning moment are similar to Ref. 2 and the program also accounts for buildings with multiple floor widths and variable floor heights. Samples of output for the 7-Story Apartment Building (2) are shown in Fig. 13. Running time is approximately 10 minutes plus 1½ minutes per floor.

BLDG SHEAR/MDM DISTR (DIMENSIONS-FT.IN)		ZF-STORY SEIS SHEAR Y-DIRECTION	
		FLOOR NO.	ZF (KIPS)
N-FLOORS=	7.	7.	193.31
H-BLDG=	65.00	6.	376.94
H-PARAPET=	2.00	5.	529.96
		4.	652.37
		3.	744.19
		2.	805.40
		1.	836.00

FLOOR LEVELS		ZFH-STORY SEIS OTM Y-DIRECTION	
FLOOR NO.	HEIGHT	FLOOR NO.	OTM (FT-KIPS)
1.	0.00	7.	1739.80
2.	9.00	6.	5132.23
3.	18.00	5.	9901.85
4.	27.00	4.	15773.23
5.	36.00	3.	22470.91
6.	45.00	2.	29719.47
7.	54.00	1.	37243.47
ROOF	63.00		

Fig. 12 - Bldg. Shear/OTM Distrib. Program (Part 1) Output Sample

ZF-STORY WIND SHEAR Y-DIRECTION		BLDG DESIGN BASE SHEAR/OTM	
FLOOR NO.	ZF (KIPS)		
7.	23.25	X-DIRECTION	
6.	55.67	V-SEISMIC (KIPS) =	906.00
5.	84.76	OTM-SEIS (FT-KIPS) =	40361.95
4.	110.62	Y-DIRECTION	
3.	133.25	V-SEISMIC (KIPS) =	836.00
2.	152.65	OTM-SEIS (FT-KIPS) =	37243.47
1.	172.04	X-DIRECTION	

ZFH-STORY WIND OTM Y-DIRECTION		BLDG DESIGN BASE SHEAR/OTM	
FLOOR NO.	OTM (FT-KIPS)		
7.	210.11	X-DIRECTION	
6.	711.15	NO =	71.05
5.	1474.02	D (MAX) =	143.08
4.	2469.63	D (MAX) DIST. =	0.00
3.	3688.88	RST. MDM (FT-KIPS) =	628465.20
2.	5042.69	OTM/RST. MDM =	0.06
1.	6591.06		

Fig. 13 - Bldg. Shear/OTM Distrib. Program (Part 2) Output Sample

Programs to be Developed - The six programs previously discussed cover the requirements for Tasks 1 through 5 and bring the user to the point of having design lateral forces and overturning moments for all floor levels. Also known at this time are the dead and live loading requirements, the dead loads for all floors and the total building plus rigidity characteristics of all walls.

In Task 6 a program (or programs) will be developed to allow distribution of shear and overturning moments to each structural wall on a floor. In the case of rigid diaphragms the forces will be distri-

buted according to the relative rigidities of the shear walls and torsional moment effects will be considered. For non-rigid diaphragms lateral forces will be distributed by the tributary load areas of the diaphragms. Overturning moments will be calculated for both cases.

In Task 7 a program will be developed to take the shear force along the top of each wall and with the known wall dimensional and moment of inertia data, determine the unit shear stress and flexural stress due to overturning moment. Unit shear stress will also be compared with maximum allowable shear stress with and without shear reinforcement. A portion of the latter task may be accomplished by table look-up, depending upon program complexity.

In the final task (Task 8) a program (or programs) will be developed to allow investigation of each load-bearing wall, considering all vertical and lateral loads (including direct wind loads) to check the structural adequacy of the masonry units used, and to determine the amount of shear reinforcement and vertical steel required for the final design. Table look-up will probably be used to determine steel spacing, and masonry unit sizes or strengths can be adjusted to meet requirements, if necessary.

Programs to be developed will be similar in input and output format to those already developed. Running times for the various programs will allow the structural engineer to greatly reduce the time devoted to the design calculations for load-bearing masonry walls, through improved accuracy and direct interfacing with all segments of the analysis tool (e.g., the 7-Story Apartment Building (2) takes less than 4 hours to run the first six programs and the total analysis is estimated to take less than two weeks). Completion of all programs for the analysis is expected in late 1978 and comments on completed and planned programs and methods used are solicited.

SUMMARY AND CONCLUSIONS

A programmable prompting calculator such as the SR-60 by Texas Instruments is an economic replacement for standard desk calculators for masonry structural and other calculations and provides a good compromise for many applications, compared to rental or purchase of a larger computer. The prompting feature allows the user to interface with the calculator in a very direct way.

It is unnecessary for engineers to learn a programming language to use this tool and programs written for load-bearing analysis of masonry structures can easily be modified to reflect local code restrictions in various sections of the country.

The overall approach is applicable to hand analysis or to other scientific calculator or computer systems (programs would vary, depending upon the system) and permits use with buildings with floor plans or elevations made up of one or more rectangles. Up to 25 stories for the building, and a maximum of 98 wall types (10 walls per type) on each floor can be processed.

The 8-Task approach presented has the time-saving advantage of allowing the engineer to stop at any phase in the analysis and quickly see the effect of varying design constraints or loading assumptions before proceeding through the complete analysis.

Programs for 5 of the 8 Tasks have been completed and allow the user to input data in convenient units (e.g., feet and inches) and outputs are in a form to fit on a standard 8½ x 11 in. page for final publication.

The present series of programs brings the user to the point of defining lateral forces and overturning moments for all floor levels. Also known are the dead and live loading requirements, the dead loads for all floors and the total building, plus rigidity characteristics of all walls. Completion of remaining programs is expected in late 1978.

Comments are solicited from experienced masonry structural engineers on the methods used in the analysis and on programs completed and planned, to allow consideration and incorporation into the finalized method.

ACKNOWLEDGMENTS

The writer wishes to thank Mr. Robert J. Helfrich, P.E., Technical Director of the Colorado Masonry Institute, Denver, Colorado, for his guidance and support in the formulation of the overall automated analysis method. In addition, the discussions with Mr. James E. Amrhein, P.E., Author of "Reinforced Masonry Engineering Handbook" (2), Messrs. George C. Hanson, P.E. and Joseph W. Sallada, P.E. of Sallada-Hanson and Associates, Denver, Colorado, were very valuable.

APPENDIX I - REFERENCES

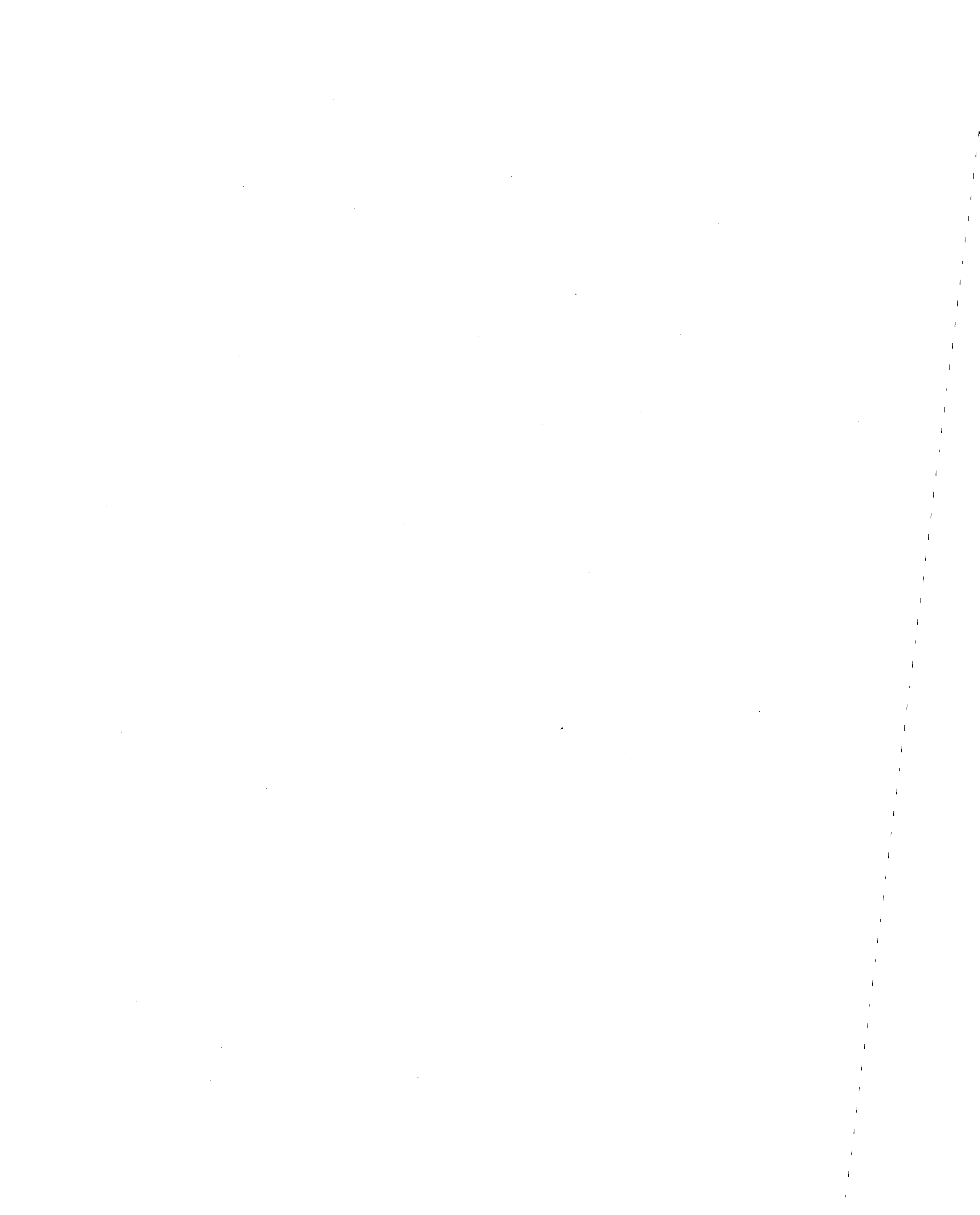
1. "Building Code of the City and County of Denver", Ordinance No. 69D of the Series of 1976.
2. Amrhein, James E., "Reinforced Masonry Engineering Handbook", Second Edition, Masonry Institute of America, Los Angeles, CA, in cooperation with Western States Clay Products Assoc., San Francisco, CA., 1973.
3. Hanson, George C., P.E., "Van Schaack Office Building, Colorado Springs, CO. - Structural Design Calculations", Sallada-Hanson and Associates, Inc., Feb. 1975.
4. "Uniform Building Code, 1976 Edition", International Conference of Building Officials.

APPENDIX II - NOTATION

- A = Floor/roof area, total cross sectional area of wall/flanges
 BLDG Σ = Building summary
 C,*C = Lateral force coefficient
 C.G. = Center of gravity
 CMI = Colorado Masonry Institute, Denver, CO.
 D(MAX) = Reference building dimension for seismic calculations
 D(MAX)DIST. = Distance to building from coordinate axis
 E_M = Wall modulus of elasticity
 E_V = Wall modulus of rigidity
 EX = X component of C.G. to center of rigidity distance
 EY = Y component of C.G. to center of rigidity distance
 FLOOR Σ = Floor summary
 $F_T,*F_T$ = Seismic whiplash force at top of building
 FT.IN. = Program notation for feet and inches (e.g., 16.09 = 16 ft. 9 in.)
 H = Vertical axis of right-handed coordinate system (positive height)
 HI = Height to ith wind pressure on the building
 H-BLDG = Height of building
 H-PARAPET = Height of parapet above roof level
 HW = Height of wall
 H-WALLS = Height of walls on the floor
 I_{CC} = Moment of inertia of shear wall about centroidal axis
 I = Occupancy coefficient in seismic eqn.
 K = Framing coefficient in seismic eqn.
 (KIPS) = 1000 lbs.
 LX MAX = Maximum average width of building for Y-direction wind
 LY MAX = Maximum average width of building for Y-direction wind
 Lx Σ DELTA HxW(PSF) = Wind base shear formula notation
 N-FLOORS = No. of floors in building from ground-up
 N-TYPE = No. of walls of this type
 N-XTYPES = No. of X-direction wall types on the floor
 N-XWALLS = No. of X-direction walls on the floor
 N-YTYPES = No. of Y-direction wall types on the floor
 N-YWALLS = No. of Y-direction walls on the floor
 OTM = Overturning moment (e.g., for wall, floor or building)
 OTM/RST.MOM = Ratio of building OTM to building restoring moment
 (PSF) = Pounds per sq. ft. (e.g., floor wt, wall wt, wind pressure)
 (PSI) = Pounds per sq. in.
 R_C ,RIGIDITY(/IN) = Rigidity of cantilever wall along wall
 REF W(PSF) = Wind pressure at reference altitude
 RST.MOM = Building restoring moment

S = Site/structure interaction coefficient (seismic)
 SR-60 = Texas Instruments SR-60 Programmable Prompting
 Calculator
 STEPS = No. of calculator key strokes in an SR-60 program
 T = Building period for seismic calculations
 UBC = Uniform Building Code
 V = Base shear
 V-SEISMIC = Seismic base shear
 V-WIND = Wind base shear
 W,W-BLDG = Weight or load on building
 WallNo. = Wall type No. and individual No. of walls of type
 (e.g., 51.09)
 WI = Wind pressure above ith height (HI)
 X = Horizontal axis of coordinate system along build-
 ing length
 XD = Distance to floor/roof area in X-direction
 XG = Distance to C.G. in X-direction
 XR = Distance to center of rigidity in X-direction
 XW = Distance to wall in X-direction
 X-WALL = A wall running in X-direction
 Y = Horizontal axis of coordinate system along build-
 ing width
 YD = Distance to floor/roof area in Y-direction
 YG = Distance to C.G. in Y-direction
 YR = Distance to center of rigidity in Y-direction
 YW = Distance to wall in Y-direction
 Y-WALL = A wall running in Y-direction
 Z = Zone coefficient in seismic eqn. for Zone No.
 ΣF = Story seismic or wind shear
 ΣFH = Story seismic or wind OTM

 * = Designates second building code option used
 (1976 Denver Code)



DIMENSIONAL CHANGE AND ITS CONTROL IN CLAY MASONRY CONSTRUCTION

by Wyatt, K.J.*

ABSTRACT: The paper deals firstly with the nature of the dimensional changes that commonly occur in burnt-clay masonry construction, including the familiar cyclical movements caused by changes in temperature and moisture content. Particular attention, however, is devoted to long-term dimensional change resulting from two causes: firstly, the irreversible long-term moisture expansion that has been studied so extensively in Australia, and, secondly, the creep or time-dependent shortening that occurs in masonry under the action of sustained compressive stress. It is shown that long-term moisture expansion is by far the most important factor contributing to dimensional change in masonry. Some recommendations are made on typical spacing of control joints.

*Senior Lecturer, Faculty of Architecture, University of New South Wales, Sydney, Australia.

DIMENSIONAL CHANGE AND ITS CONTROL
IN CLAY MASONRY CONSTRUCTION

K. J. WYATT*

INTRODUCTION

Despite the fact that clay masonry has a history of use extending over millenia, and despite the fact that it is well known that clay masonry expands and contracts in response to changes in its environment, we are still today producing buildings which suffer damage because the designer has failed to make adequate provision for the movements that will occur.

The aim of this paper is to examine the nature of dimensional change in clay masonry, and to suggest some simple rules that will give reasonable assurance that damage will not occur.

BRICKWORK MOVEMENTS

Thermal Expansion.

The amount of movement that results from a change in body temperature depends upon the coefficient of linear thermal expansion and on the magnitude of temperature change.

In the United States, Ross⁽¹⁾ measured the thermal expansion of 139 brick samples drawn from across the country. The mean coefficient of thermal expansion was found to be $3.4 \times 10^{-4}\%$ /degree F ($6.1 \times 10^{-4}\%$ /degree C) with a standard deviation of $0.56 \times 10^{-4}\%$ /degree F ($1.0 \times 10^{-4}\%$ /degree C). In England, the BRE⁽²⁾ quotes design values for expansion that infer a coefficient of $6 \times 10^{-4}\%$ /°C, whilst in Australia the SAA Brickwork Code⁽³⁾ specifies $8 \times 10^{-4}\%$ /°C. Thus a value of $8 \times 10^{-4}\%$ /°C for design purposes should be adequate in that, on Ross' figures, it would be exceeded in less than 10% of instances.

It is more difficult to nominate appropriate values for the range in temperature to be used in computing movements for thermal expansion. In Australia, the SAA Loading Code⁽⁴⁾ nominates a seasonal range of mean dry bulb temperature of between 11° and 17°C (depending on locality) and an extreme air temperature range of between 42° and 53°C. It is probable that the mean range of temperature in the external skin of a brick wall will be nearer to the seasonal range rather than the extreme range because of the heat capacity of the masonry.

Again, the season during which the wall is constructed will tend to determine whether the wall undergoes expansion or contraction. Grimm⁽⁵⁾ points out that horizontal thermal contraction of the brick typically does

*Senior Lecturer, Faculty of Architecture, University of New South Wales, Sydney, Australia.

DIMENSIONAL CHANGE AND ITS CONTROL IN CLAY MASONRY CONSTRUCTION

By Wyatt, K.J.

not induce contraction of the wall but rather induces fine cracks between bricks and mortar. Consequently, he proposes that a design temperature range of +65°F (35°C) be adopted in USA even though the extreme air temperature range is about 120°F (66°C). In a similar way, the BRE⁽²⁾ proposes a design range of 28°C as does the SAA Brickwork Code.

Consequently, if it is possible to make a realistic estimate of the maximum temperature range likely to be experienced in a particular wall, a thermal coefficient of $8 \times 10^{-4}\%/^{\circ}\text{C}$ should be assumed; if no such estimate is possible, it would be wise to assume a range of at least 25°C, giving a design thermal expansion of 0.02% minimum.

Reversible Moisture Expansion.

Reversible movements caused by moisture expansion are usually smaller than thermal movements, and are frequently neglected by designers. The BRE⁽²⁾ suggests that the dimensional change between oven-dry and saturated is likely to be between 0.002 and 0.01%. West⁽⁶⁾ has reported tests on briquettes in which, as the moisture content increased from zero to 16%, the dimensions increased by 0.015%. In the British work reported by Bonnell and Butterworth⁽⁷⁾, over one hundred brick types were tested, and the vast majority had reversible strains less than 0.01%; in only two instances did the strain exceed 0.025%.

Thus, for the range of moisture content likely to be encountered on site, an allowance for reversible moisture strains of 0.01% should be adequate.

Long-term Permanent Moisture Expansion.

All burnt clay products undergo an irreversible expansion, caused by reaction with atmospheric moisture; it commences as soon as the product is removed from the kiln and continues for many years. In the case of bricks, it has been shown that this expansion, if unrestrained, may amount to as much as 0.3%.

Very many factors affect the magnitude of the eventual unrestrained expansion of bricks. The type of clay or shale from which the bricks were made and the kiln temperature at which they were fired exert a dominant effect.

Wyatt and Marshall⁽⁸⁾ tested samples of extruded manganese bricks drawn from different parts of a kiln during a commercial firing. The accelerated test procedure of McDowall and Birtwistle⁽⁹⁾ was used, and the results indicated that the average long-term expansion of bricks drawn from the cooler part of the kiln was four times greater than that of bricks from the hot part, even though the actual temperature difference of the kiln did not exceed 60°C. Thus, even when specimens are drawn from the same firing, using the same clay body, large variations in potential expansion may occur. The variations become even larger if one examines the bricks produced in a number of plants, even though these plants may all lie in

DIMENSIONAL CHANGE AND ITS CONTROL IN CLAY MASONRY CONSTRUCTION

by Wyatt, K.J.

the one geographic region. Table 1 shows the predicted mean expansions of sixteen brick types tested by the author; all bricks were commercially produced in Sydney, Australia, using local clays and shales. It can be seen that the potential expansions range from 0.002% to 0.120% (for pressed bricks) or 0.132% (for extruded bricks).

Table 1: Predicted Unrestrained Expansion of Sydney Bricks.

Description	Method of Forming	5 Year Expansion (%)
Manganese Wire-cut Face	Extruded	0.002
Red Textured Face	Extruded	0.025
Red Textured Face	Extruded	0.035
Buff Textured Face	Extruded	0.030
Cream Textured Face	Extruded	0.107
Cream Wire-cut Face	Extruded	0.125
Cream Striated Face	Extruded	0.132
Grey Common	Pressed	0.002
Grey Common	Pressed	0.015
Grey Common	Pressed	0.038
Red Face	Pressed	0.012
Red Face	Pressed	0.027
Red Face	Pressed	0.047
Red Face	Pressed	0.120
Red-mottled Face	Pressed	0.095
Yellow Face	Pressed	0.045

In consequence of this extreme variability, there is little point in recommending an "average", or even a "design", value for permanent moisture expansion of bricks. McDowall and Birtwistle's method of test for potential expansion is a simple procedure involving a 4-hour steam treatment of 24-hour-old specimens. This method should be used in all instances. For the very rare occasions when it is impossible to conduct an accelerated test of the bricks, it would be wise to pessimistically set an arbitrary value of 0.20% for light coloured bricks and 0.12% for dark bricks. Such values will of course impose severe limitations on the spacing of control joints - limitations that could well have been lifted if the predictive test had been conducted.

DIMENSIONAL CHANGE AND ITS CONTROL IN CLAY MASONRY CONSTRUCTION

by Wyatt, K.J.

Values such as those just quoted are typically obtained in laboratory-controlled tests at constant temperature and humidity on kiln-fresh bricks. Quite different values may be obtained when these same bricks are used in walls on site. It has been noted by Smith⁽¹⁰⁾, for example, that bricks stored out-of-doors had about 20% less expansion than bricks stored at constant temperature and humidity; for brickwork the differential was even greater, in that outdoor walls had expansions of only 60% of those of individual bricks stored indoors. On the other hand, Wyatt⁽¹¹⁾ has shown that the expansions of unrestrained bricks and brickwork are identical when both are stored indoors under the same atmospheric conditions (Fig.1).

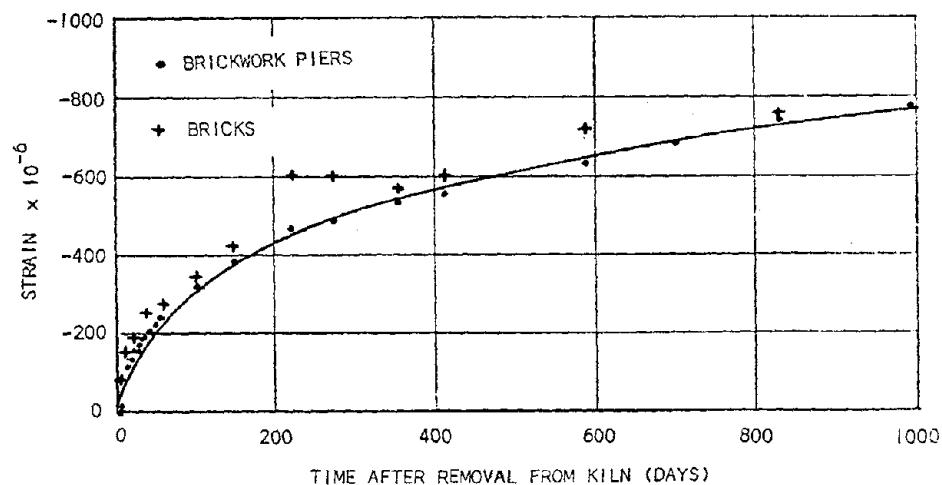


Fig.1

Other investigators have noted a correlation between expansion and building aspect. However it must be said that, for almost every research paper asserting a particular relationship between indoor brick expansion and outdoor brickwork expansion, one can find another paper asserting a different relationship. The effect of restraint and the consequent creep is almost certainly the reason for the contradictory evidence that is available.

Creep.

Limited research into creep of clay masonry has been conducted by Lenczner and his co-workers at Cardiff, and a summary of this work is available⁽¹²⁾. Among the more important conclusions reached by Lenczner in this summary are:

1. At normal working stresses, creep in brickwork piers will effectively cease within one year of the application of the load. The creep strain during this period rarely exceeds the instantaneous strain that occurs during loading.

DIMENSIONAL CHANGE AND ITS CONTROL IN CLAY MASONRY CONSTRUCTION

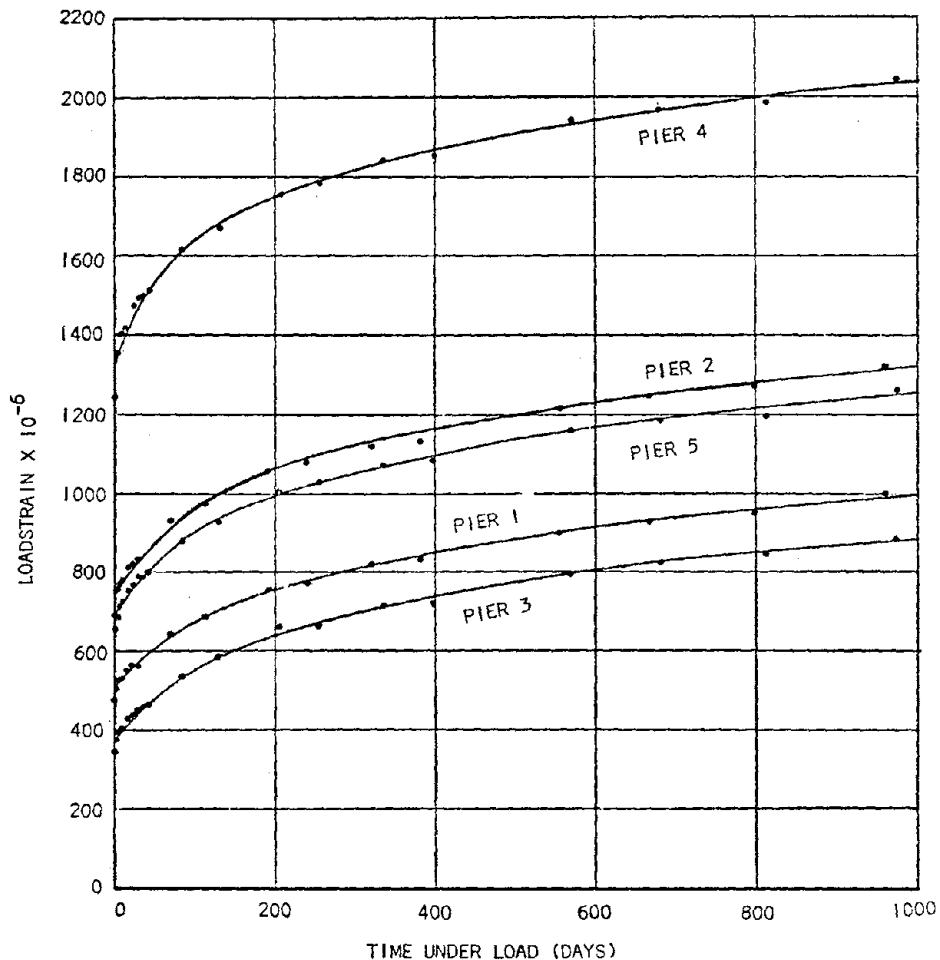
by Wyatt, K.J.

2. Creep in brickwork walls using 1:¼:3 mortar was up to 4½ times greater than in piers at comparable stress levels.
3. Measurements on brickwork using 1:¼:3 mortar show that about two-thirds of the creep in a wall occurs in the mortar joints, even though these amount to only about 10% of the height of the wall. Therefore, creep in the mortar is of much greater significance than creep in the bricks.

It has been shown by Wyatt and Morgan⁽¹³⁾ that the relationship between creep-strain and time can be well-represented by a logarithmic expression of the form:

$$e = A + B \ln (t + C)$$

where A, B and C are empirical constants. A relationship of this type assumes that creep progresses indefinitely at a continuously-decreasing rate; results obtained by the author⁽¹¹⁾ from experiments extending over three years have confirmed this behaviour (Fig.2). Wyatt *et al*⁽¹⁴⁾ have shown that, for low stress levels, the rate of creep is proportional to stress (or, more precisely, is proportional to the stress/strength ratio), whilst at higher stresses the creep varies with the cube of this ratio.



DIMENSIONAL CHANGE AND ITS CONTROL IN CLAY MASONRY CONSTRUCTION

by Wyatt, K.J.

Thus, although a small amount of research work that has been done in recent years, we are still unable to define quantitatively the creep behaviour of brickwork. For the present, we can do no better than make a series of assumptions that do not disagree with the bulk of the existing evidence. These are:

1. Within the working stress range, creep-strain varies with the ratio of applied stress to brickwork strength. Because Young's Modulus is usually regarded as being a function of brickwork strength, it follows that elastic strain also varies with the ratio of stress to strength. Hence it is reasonable to anticipate a relationship between creep strain and short-term elastic strain.
2. Creep strain increases with the logarithm of time under stress.
3. For brickwork laid up in a cement-rich mortar, the creep strain is likely to equal the elastic strain after about two years under constant stress. About half of this strain is likely to occur quite quickly, within the first three months or so. Even if the stress is maintained for as long as ten years, the creep strain is unlikely to be more than one-and-a-half times the elastic strain.
4. For lime-rich mortar, creep strains are likely to be larger than for cement-rich mortars; very little information is available but there are some indications⁽¹²⁾ that the creep strain may reach one-and-a-half times the elastic strain after only two or three years under stress.

The SAA Brickwork Code suggests that the short-term modulus of elasticity be taken as 750 times the brickwork compressive strength; similar values are found in other Codes. For brickwork sustaining a compressive stress equal to, say, 10% of the brickwork strength, the elastic strain will be $0.1/750 = 0.013\%$; the long-term creep strains in cement-mortar brickwork are therefore unlikely to exceed 0.02%, or 0.03% in lime-mortar brickwork. It should be noted that if the brickwork is stressed at an early age (one month or less after laying) the elastic strains are likely to be considerably larger than implied by the Code value for Young's Modulus; the creep strains will also be larger.

Total Movements.

Typically, the movements caused by the mechanisms examined above are as follows:

Unrestrained Thermal Expansion	0.02%
Unrestrained Reversible Moisture Expansion	0.01%
Unrestrained Long-term Moisture Expansion	0.12 to 0.20%
Creep Contraction under Working Stress	0.03%

DIMENSIONAL CHANGE AND ITS CONTROL IN CLAY MASONRY CONSTRUCTION

by Wyatt, K.J.

The range of values for long-term moisture expansion is appropriate to Australia; recent research in other countries indicates that these values would not be excessively high for very many parts of the world. The main point to be made when considering these figures is the over-riding importance of long-term expansion when compared with reversible movements; a 50% error in estimating reversible movements would alter the total movement be less than 10%. There is little benefit in making a precise calculation of predicted movement unless the designer is prepared to conduct tests to predict the long-term moisture expansion.

CONTROL JOINTS

From a consideration of the amounts of movement described in the preceding sections, it is possible to nominate suitable control joint spacing for various conditions, as follows:

1. Horizontal Movement.

Control joints should be positioned so as to permit:

Thermal movement	- 0.02%
Reversible moisture expansion	- 0.01%
Long-term moisture expansion	- 0.06% for dark brickwork
(in absence of test data)	- 0.10% for light brickwork
Total	- 0.09 to 0.13%

(The values shown for long-term moisture expansion are 0.5 times the values for individual bricks, to allow for the effects of partial restraint on the brickwork).

The SAA Code limits the amount of movement at a joint to 15 mm; for the typical movements listed above, this would require joints of about 25 mm width spaced at between 11 and 16 m. For parapet walls, because of the virtual absence of partial restraint, spacings of joints should be half those for other walls. Because external corners are highly vulnerable to damage, the first joint should be positioned at half the normal spacing from any corner.

2. Vertical Movement in Concrete-framed Buildings.

Control joints should be positioned so as to permit the following movements:

Thermal movement	- 0.02%
Reversible moisture expansion	- 0.01%
Long-term moisture expansion	- 0.12 to 0.20%
Shrinkage and creep of concrete frame	- 0.12%
Total	- 0.27 to 0.35%

DIMENSIONAL CHANGE AND ITS CONTROL IN CLAY MASONRY CONSTRUCTION

by Wyatt, K.J.

Movement of this order corresponds to differentials between the masonry and the frame of about 7 to 10 mm per storey height. Many structures have been built without making allowance for movements of this magnitude, and a number of them have suffered extensive damage ranging from local crushing of brickwork near supporting nibs at floor level to dislodgement of entire brickwork panels. It is fortunate that three factors often combine to reduce the differential movement to a value that can be absorbed by the structure without undue distress. They are:

- (1) The initial shortening of the concrete frame occurs very rapidly; with good fortune much of it will have occurred before the masonry is constructed.
- (2) It is not uncommon for the bricks for a high-rise building to be ordered in advance and stockpiled; much of the long-term expansion will have taken place during this stockpiling.
- (3) Because the frame exercises a severe restraint to the masonry, high stress may well be generated; they will be accompanied by a very high rate of creep in the young mortar. Creep often will act beneficially to relieve high stress before severe damage results.

Unless the construction process can be carefully scheduled as to use these three factors to control differential movements, horizontal control joints equivalent to one bed joint per storey height should be provided.

3. Vertical Movement in Load-bearing Masonry Buildings.

Control joints should be positioned so as to permit the following movements:

Thermal movement	- 0.02%
Reversible moisture expansion	- 0.01%
Long-term moisture expansion	- 0.12 to 0.20%
Elastic shortening of loaded leaf	- 0.02%
Creep shortening of loaded leaf	- 0.03%

If, as is preferable, only the inner leaf of a cavity wall is load-bearing, joints are required to provide for the differential movement that may occur between the two leaves. When the same brick-type is used for both leaves, it is necessary to allow only for thermal expansion of the outer leaf and elastic and creep shortening of the inner leaf; a total differential strain of about 0.07%, which can usually be accommodated without difficulty. If the brickwork of the inner leaf has a smaller long-term moisture expansion than that of the outer leaf, the differential between the two expansions must be included in the computation. For example, sometimes in Sydney pale-coloured face

DIMENSIONAL CHANGE AND ITS CONTROL IN CLAY MASONRY CONSTRUCTION

by Wyatt, K.J.

bricks with expansions of about 0.15% are used on the outer leaf, whilst the inner leaf uses commons of negligible expansion potential; the differential strain then becomes about 0.22%, requiring joints of 6 mm width at each storey. It is not recommended for the inner leaf to have a larger expansion potential than the outer leaf, since this would cause the control joint to become wider with the passage of time, causing sealing problems.

Where, in special circumstances, both leaves of construction are required to be load-bearing, both leaves should undergo the same strains, and should therefore use the same materials.

CONCLUSIONS

Of the various factors that cause dimensional change in clay masonry construction, long-term permanent moisture expansion is by far the most important in that it produces strains that may be as much as ten times larger than the strains produced by other causes. Consequently, for design purposes it is very important that an accurate estimate be made of the potential long-term expansion. The method proposed by McDowall and Birtwistle⁽⁸⁾ is recommended for this purpose.

The expansions resulting from this and other causes may be greatly modified by the effects of restraint, and as yet there is no fully satisfactory method whereby restraint may be taken into account in computing the width and spacing of control joints. Further work on the interaction between expansion and creep in restrained brickwork is required.

Because of these uncertainties, the recommendations for control joint spacings made in this paper make generous provision for dimensional strain. As more evidence becomes available, these recommendations should be able to be progressively refined.

REFERENCES

1. Ross, C.W. "Thermal Expansion of Clay Building Bricks", J. Res. of Nat. Bur. of Stds., Research Paper RP1414, U.S. Government Printing Office, 1941.
2. Building Research Establishment, "Cracking in Buildings", BRE Digest No. 75, U.K., 1966.
3. AS 1640-1974, Standards Association of Australia Brickwork Code.
4. AS 1170-1971, Standards Association of Australia Loading Code.

DIMENSIONAL CHANGE AND ITS CONTROL IN CLAY MASONRY CONSTRUCTION

by Wyatt, K.J.

5. Grimm, C.T., "Design for Differential Movement in Brick Walls", J. Struc. Div., Proceed. ASCE, V 101, No. St.11, Nov. 1975.
6. West, H.W.H., "Moisture Movement of Bricks and Brickwork", Trans. Br. Ceram. Soc., 66, 137, 1967.
7. Bonnell D., and Butterworth, B. "Clay Building Bricks of the United Kingdom", HMSO, London, 1950.
8. Wyatt, K.J. and Marshall, R.J. "Testing for Quality Control in Brick Production", J. Aust. Ceram. Soc., V 8, N 3, November 1972.
9. McDowall, I.C. and Birtwistle, R. "Predicting the Long-term Moisture Expansion of Fired Clay Products", SIBMAC Proceedings, Br. Ceram. Res. Assoc., Stoke-on-Trent, England, 1971.
10. Smith, R.G. "Expansion of Unrestrained Flatton Brickwork", Trans. Br. Ceram. Soc., 73, 6, pp 191-198, September 1974.
11. Wyatt, K.J. "Restrained Moisture Expansion of Clay Masonry", J. Aust. Ceram. Soc., V 12, N 2, Sydney, 1976.
12. Lenczner, D. and Salahuddin, J. "Creep and Masonry Movements in Masonry Piers and Walls", SIBMAC Brick Masonry Conference, Calgary, 1976.
13. Wyatt, K.J. and Morgan, J.W. "The Role of Creep in Brickwork", Arch. Sc. Rev., V 17, N 2, Sydney, 1974.
14. Wyatt, K.J., Lenczner, D., and Salahuddin, J. "The Analysis of Creep Data for Brickwork", Brit. Ceram. Soc. Confce. on Load-Bearing Masonry, London, 1974.



RATIONAL ANALYSIS OF MASONRY STRUCTURES

By James Colville¹ and Donald Vannoy²

ABSTRACT: A procedure for the rational analysis of load bearing masonry structures is developed. This procedure follows the Building Code Requirements for Engineered Brick Masonry, August, 1969, published by the Brick Institute of America, and the Specification for the Design and Construction of Load-Bearing Concrete Masonry, February 1975, published by the National Concrete Masonry Association.

Equations for determining the distribution of lateral load to resisting shear walls, which consider that some of the walls do not extend the full height of the building and that wall properties may change from floor to floor, are presented. Following this a strength analysis is performed which indicates the required compressive strength of each wall at each floor level for seven critical combinations of vertical and lateral loads. The strength analysis considers both the effects of slenderness and eccentricity of gravity loading.

The procedure described in the paper has been incorporated into a computer program which is available to the profession through the Masonry Institute of Maryland.

¹Associate Professor of Civil Engineering, U. of MD, College Park, MD 20742

²Assistant Professor of Civil Engineering, U. of MD, College Park, MD 20742

RATIONAL ANALYSIS OF MASONRY STRUCTURES

by

James Colville¹ and Donald Vannoy²

INTRODUCTION

A computer program for the rational analysis of non-reinforced engineered masonry construction is described herein. This program follows the Building Code Requirements for Engineered Brick Masonry, August 1969, published by the Brick Institute of America, and the Specification for the Design and Construction of Load-Bearing Concrete Masonry, February 1975, published by The National Concrete Masonry Association. Thus most of the basic assumptions are based on generally accepted engineering analysis procedures. However, in order to present the main limitations and applications of the program, a brief review of the basic assumptions and restrictions is given. Use of the program is available through the Masonry Institute of Maryland.

LOADS

The two basic types of loads considered in the analysis are gravity loads and lateral loads. The gravity loads consist of dead and live loads and it is assumed that the floor loads are the same at each level of the structure and that all areas, at each floor level, receive the same loading. The roof live and dead loads may be different than the corresponding floor loads.

A reduction in the floor live load is considered using either one of the following procedures as specified by the designer:

- (a) if the loaded floor area exceeds 150 sq. feet and the magnitude of the live load is not more than 100 psf, the reduction is taken as 0.08 percent per square foot of loaded area but may not exceed 60% or the value of R from the following equation

$$R = 100(D+L)/4.33L \quad (1)$$

in which D = dead load in psf. and L = live load in psf.

- (b) the reduction depends on the number of floors supported as given below:

1 floor supported - R = 15%;	5 floors supported - R = 35%
2 floors supported - R = 20%;	6 floors supported - R = 40%
3 floors supported - R = 25%;	7 floors supported - R = 45%
4 floors supported - R = 30%;	8 or more floors supported - R = 50%

¹Associate Professor of Civil Engineering, U. of MD, College Park, MD 20742

²Assistant Professor of Civil Engineering, U. of MD, College Park, MD 20742

Also, the effect of a checkerboard live load distribution is considered for each wall in the structure. The lateral loads are due to either wind or earthquake forces. The wind load depends on the exposed area of the building and the magnitude of the wind pressure. It is assumed that a maximum of three different wind pressure magnitudes may be considered in the analysis and that changes in wind pressure magnitudes do not occur between floors. The wind load is considered to be a uniformly distributed loading, and the resultant wind load at each floor level is obtained from tributary area principles and the wind pressure magnitude.

The lateral loads due to earthquake forces are based on the requirements of the Uniform Building Code, (UBC), published by the International Conference Building Officials, 1976 Edition or the BOCA Basic Building Code, 1975 Edition, as specified by the designer. In either procedure the dynamic forces resulting from an earthquake are replaced by equivalent static forces. The total lateral force, V , called the base shear is

$$V = ZIKCSW \quad (\text{UBC}) \quad ; \quad V = ZKCW \quad (\text{BOCA}) \quad (2)$$

in which C is a coefficient whose magnitude depends on the period of the structure, K is a framing coefficient related to the ductility of the structure, Z represents the earthquake zone, I is an occupancy importance coefficient, S is a numerical coefficient for site-structure interaction, and W is the total dead weight of the structure. For the analysis considered here

$$C = 1/(15\sqrt{T}) \leq .12 \quad \text{for UBC, or } C = 0.05/\sqrt[3]{T} \leq 1.0 \quad \text{for BOCA,}$$

where $T = 0.05 H/\sqrt{D}$, in which H is the height of the building in feet and D is the dimension of the building in feet in a direction parallel to the applied force. For load bearing masonry K is taken as 1.33. The lateral load due to an earthquake is considered to be a triangular distribution load and a portion of the base shear V is considered as a concentrated load, F_t , applied at the top of the building. Thus

$$F_t = 0.07 TV \leq .25V \quad (\text{UBC}) \quad ; \quad F_t = .004V(H/D_s)^2 \leq .15V \quad (\text{BOCA}) \quad (3)$$

in which $F_t = 0$ if $T \leq 0.7$ secs, or $(H/D_s) \leq 3.0$. The remaining force, $(V-F_t)$ is distributed to each floor in accordance with the equation

$$F_x = (V-F_t) \frac{w_x h_x}{\sum_{i=1}^n w_i h_i} \quad (4)$$

In Eq. (4), F_x is the lateral force at level x , w_x = the weight of the floor at level x , h_x = the height of level x above the base. The denominator of Eq. (4) represents the sum of the weights of the floors, w_i , times the height to that floor, h_i , summed over n = number of stories, including the roof.

The wind and seismic forces are of course assumed to act in the direction of either principal axis of the building. The procedure presented above is, therefore, applied to both principal directions.

WALLS

The program is valid only for structures where the vertical and lateral loads are resisted by wall elements, rather than beam and column members. For support of vertical loads, the walls may be considered to be either load bearing or non-load bearing.

All walls are considered to participate in resisting horizontal forces. Thus for lateral loads, all walls are considered to be shear walls, although it is assumed that there are no coupled walls.

Each wall unit may be solid brick, hollow or solid concrete block, and any combination of these masonry units may be used throughout the structure. Also, an exterior wall may consist of a loaded wythe of masonry tied to an unloaded wythe such that a portion of the transverse wind load is carried by the unloaded wythe. Wall section properties may change from floor to floor, and, the program can consider structures in which some walls do not extend the full height of the building.

LATERAL LOAD DISTRIBUTION

Lateral loads are assumed to act in the direction of either principal axis of the structure. Wind forces will cause bending in those exterior walls perpendicular (or transverse) to the direction of the wind, while seismic forces will cause bending in all walls, interior and exterior, load bearing and non-load bearing, perpendicular to the direction of the seismic force.

The lateral loads will be distributed from the transverse walls to the shear walls which are parallel to the load direction by the floor and roof diaphragms of the structure. The shear walls are assumed to act as vertical cantilevers in transmitting the lateral loads to the foundation.

The distribution of lateral load to the shear walls is a function of the rigidity of the horizontal diaphragms and shear walls, and the torsional effects of the lateral loads.

In the analysis procedure developed herein, it is assumed that the floor and roof diaphragms are infinitely rigid. Rigid diaphragms transmit lateral loads to the shear walls in proportion to the relative stiffnesses of the shear walls. Also, rigid diaphragms are capable of transmitting torsional moments to the shear walls in proportion to their relative rigidities and distances from the center of rigidity. However, two other factors, considered herein, which complicate the determination of the lateral force in each wall unit are:

- 1) Some of the walls do not extend the full height of the building;
- 2) The properties of each wall may change from floor to floor

A procedure for determining the lateral load in each wall unit is developed below. In this procedure the lateral load in each wall unit at each floor level is determined working from the upper story to the ground

floor. The procedure may be simply presented by considering the structure shown in Fig. 1. Once the necessary equations are developed for this structure, they may be generalized to consider more complicated structures. First of all, although wall 3 does not extend the same height as walls 1 and 2, it is assumed, for simplicity of coding, that all walls extend to the top of the structure. Thus; $I_{33} = A_{33} = 0$. Considering the top story of the structure (Fig. 2) and letting R_{i3} , $i = 1, 2, 3$ be the unknown lateral load carried by each wall unit, i , at the third floor,

$$R_{13} + R_{23} + R_{33} = P_3 \quad (5)$$

Also the top deflection of each wall unit (considering both flexural and shear deflections) is

$$\delta_t = \frac{R_{i3} h_3^3}{3EI_{i3}} + \frac{3R_{i3} h_3^3}{A_{i3} E} + \theta_{i3} h_3 \quad (6)$$

in which θ_{i3} is the rotation of the wall unit i at the base of the 3rd floor. The rotation θ_{i3} is assumed to equal the rotation at level 2 caused by the loading shown in Fig. 3.

Thus

$$\theta_{i3} = \frac{R_{i3} h_3}{E} \left(\frac{h_2}{I_{i2}} + \frac{h_1}{I_{i1}} \right) + \frac{R_{i3}}{E} \left(\frac{h_2^2}{2I_{i2}} + \frac{h_2 h_1}{I_{i1}} + \frac{h_1^2}{2I_{i1}} \right) \quad (7)$$

For a high rise structure, the computation of the second term in Eq. (7) becomes increasingly tedious. Also in a typical high rise structure, the story heights h_1 , h_2 , h_3 etc. do not vary significantly. Thus an approximate value of θ_{i3} is obtained.

$$\theta_{i3} = \frac{R_{i3} h_3}{E} \left(\frac{h_2}{I_{i2}} + \frac{h_1}{I_{i1}} \right) + \frac{R_{i3} h_3^2}{2E} \left(\frac{1}{I_{i2}} + \frac{3}{I_{i1}} \right) \quad (8)$$

Substituting Eq. (8) into Eq. (6) and combining terms gives

$$E\delta_t = R_{i3} \left[\frac{Ch_3^3}{3I_{i3}} + \frac{3h_3}{A_{i3}} + \frac{Lh_3^2}{I_{i3}} \right] \quad (9)$$

in which

$$C = \left[1 + \frac{3}{2} \left(\frac{I_{i3}}{I_{i2}} + \frac{3I_{i3}}{I_{i1}} \right) \right] \quad (10)$$

$$L = h_1 + h_2 \quad (11)$$

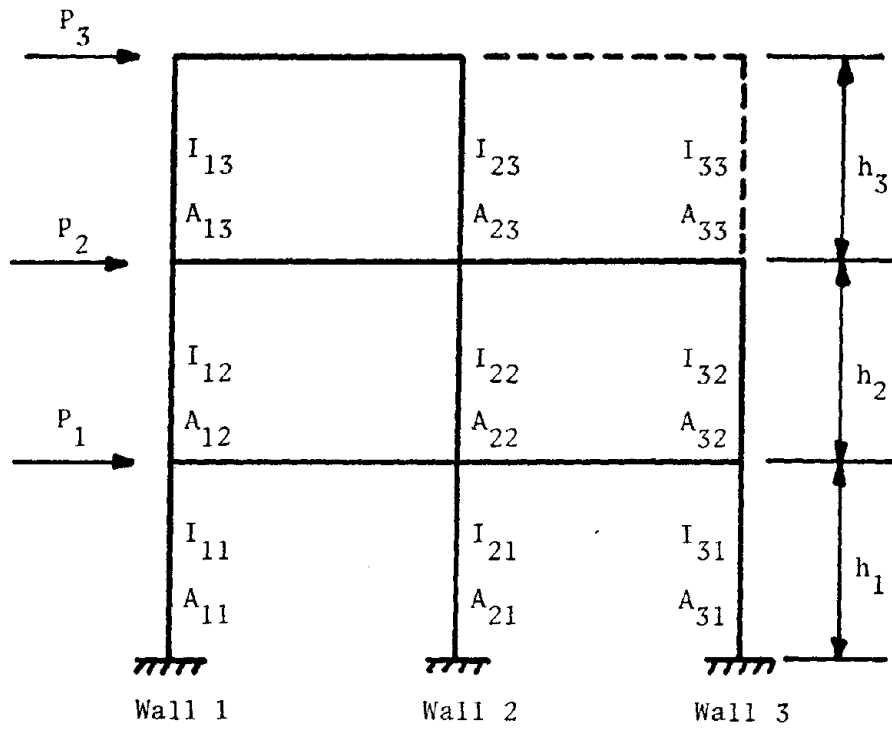


Figure 1 - Typical Structure

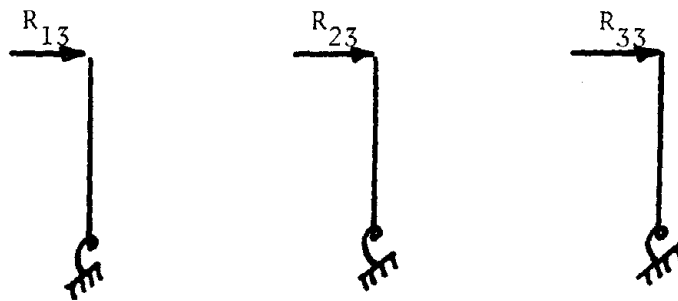


Figure 2 - Top Story Loading and Support

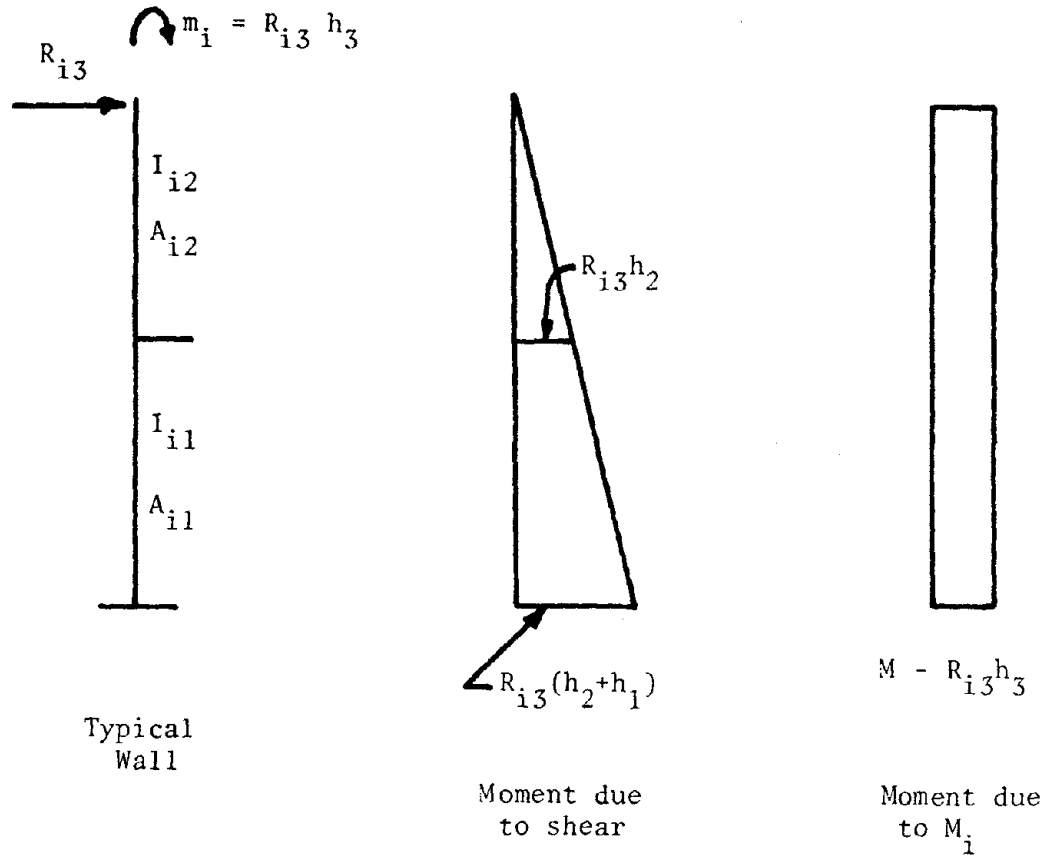


Figure 3 Loading on Structure for Computations of Rotations

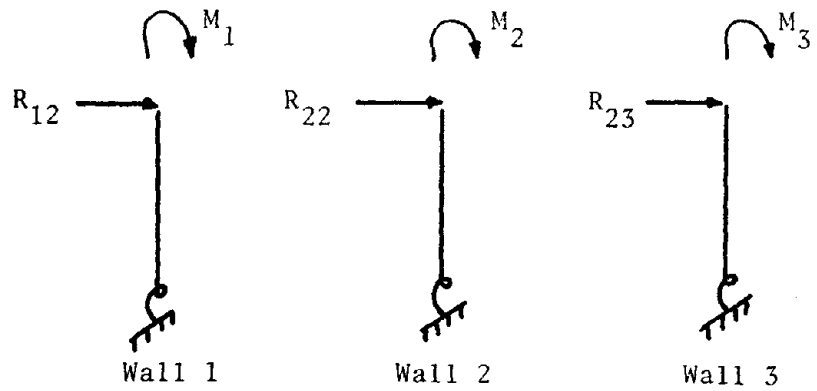


Figure 4 - Second Story Loading and Supports

and

$$\bar{I}_{i3} = \frac{L}{\left(\frac{h_2}{I_{i2}} + \frac{h_1}{I_{i1}}\right)} \quad (12)$$

Equation (9) can now be written as

$$E\delta = \frac{R_{i3}}{K_{i3}} \quad (13)$$

in which

$$K_{i3} = \frac{3I_{i3}A_{i3}\bar{I}_{i3}}{Ch_3^3 A_{i3}\bar{I}_{i3} + 9I_{i3}\bar{I}_{i3}h_3 + 3I_{i3}A_{i3}Lh_3^2} \quad (14)$$

Assuming that the top deflection of all walls is the same,

$$R_{23} = K_{23}R_{13}/K_{13}; \text{ and } R_{33} = K_{33}R_{13}/K_{13} \quad (15)$$

Substituting these relations into Eq. (5) and solving for R_{13} gives

$$R_{13} = \frac{K_{13}P_3}{K_{13} + K_{23} + K_{33}} \quad (16)$$

Generalizing Eq. (16) for any number of walls, NW, and any number of stories, n, gives

$$R_{in} = \frac{K_{in}P_n}{\sum_{j=1}^{NW} K_{jn}} \quad (17)$$

It should be noted that since $I_{33} = A_{33} = 0$, it follows that $K_{33} = 0$ giving $R_{33} = 0$. Or, in other words, no portion of the load P_3 is resisted by wall 3.

Considering the 2nd story of the structure, the loads are as shown in Fig. 4. The sum of the forces in the walls now equals the total lateral load above the level being considered. Thus

$$R_{12} + R_{22} + R_{32} = P_2 + P_3 \quad (18)$$

Also, the moments M_i , $i = 1, 2, 3$ at the top of the wall units equal the moments caused by the shears in the walls above. Thus, $M_1 = R_{13}h_3$; $M_2 = R_{23}h_3$; and $M_3 = R_{33}h_3 = 0$.

The deflection at level 2 is

$$\delta_{tE} = \frac{M_1 h_2^2}{2I_{i2}} + \frac{M_1 L h_2}{\bar{I}_{i2}} + \frac{R_{i2}}{K_{i2}} \quad (19)$$

In which $L = h_1$; $\bar{I}_{i2} = L/(h_1/I_{i1})$ and K_{i2} is as given by Eq. (14), replacing the subscript 3 by the subscript 2.

Equation (19) may be rewritten as

$$\delta_{tE} = \frac{M_1}{K'_{i2}} + \frac{R_{i2}}{K_{i2}} \quad (20)$$

in which

$$K'_{i2} = \frac{2I_{i2}\bar{I}_{i2}}{\bar{I}_{i2}h_2^2 + 2I_{i2}Lh_2} \quad (21)$$

Since the top deflections are equal,

$$\frac{M_1}{K'_{i2}} + \frac{R_{i2}}{K_{i2}} = \frac{M_2}{K'_{22}} + \frac{R_{22}}{K_{22}} = \frac{M_3}{K'_{32}} + \frac{R_{32}}{K_{32}} \quad (22)$$

Using these relations, substituting into Eq. (18) gives

$$R_{i2} = \frac{K_{i2}}{\sum_{i=1}^3 K_{i2}} \left[(P_2 + P_3) + \sum_{i=1}^3 \frac{K_{i2} M_i}{K'_{i2}} - \frac{M_1}{K'_{i2}} \sum_{i=1}^3 K_{i2} \right] \quad (23)$$

Generalizing this equation for any number of walls, NW, and any number of floors, n, the shear in any wall, i, at any floor level, j, may be given as follows

$$R_{ij} = \frac{K_{ij}}{NW \sum_{\ell=1}^{NW} K_{\ell j}} \left[\sum_{m=j}^n P_m + \sum_{\ell=1}^{NW} \left(\frac{K_{\ell j} M_\ell}{K'_{\ell j}} \right) - \frac{M_i}{K'_{ij}} \sum_{\ell=1}^{NW} K_{\ell j} \right] \quad (24)$$

For the first floor of the structure, since it is assumed that the base of each wall is fixed, the deflection at level 1 is

$$\delta_{tE} = \frac{M_1 h_1^2}{2I_{i1}} + \frac{R_{i1} h_1^3}{3I_{i1}} + \frac{3R_{i1} h_1}{A_{i1}} \quad (25)$$

Thus Eq. (24) can again be used to compute the lateral force in each wall unit, except that

$$K_{ij} = \frac{3I_{ij}A_{ij}}{A_{ij}h_1^3 + 9I_{ij}h_1} \quad (26)$$

and

$$K'_{ij} = 2I_{ij}/h_1^2 \quad (27)$$

Thus, Eqs. (17) and (24) may be used to determine the total shear in each wall unit. However, in most structures it will be necessary to consider the effects of torsion. The torsional moment at each floor level is equal to the total resultant lateral load at the floor multiplied by e_j = the distance between the line of action of the resultant load and the centroid of resistance of the shear walls.

The location of the centroid of resistance of the shear walls from any suitable reference line, is given as

$$\bar{x}_j = \frac{\sum_{i=1}^{NW} (R_{ij} X_{ij})}{\sum_{i=1}^{NW} R_{ij}} \quad (28)$$

where X_{ij} represents the distance of a particular wall from the reference line. The location of the resultant wind or seismic load at each floor level is computed by the program, and the eccentricity at each floor level may be computed. For seismic loads this distance is assumed to be at least 5% of the plan dimension of the structure.

Thus the force in each wall unit for lateral load parallel to the wall is

$$V_{ij_x} = R_{ij_x} + \frac{R_{ij_x} e_j c_{ij}}{\frac{R_{ij_x} x_i^2}{W_{xj}}} \quad (29)$$

For bending perpendicular to the walls the transverse bending load depends on whether or not the wall is exposed to direct wind load. Thus for interior walls, not exposed to wind, the transverse bending load, w , in pounds per square foot is

$$\omega = 0.2Z (\rho)t \quad (30)$$

in which t = wall thickness in feet, and ρ is the unit weight of the wall material in pounds per cubic foot. The value of the zone factor, Z , has been given above.

For exterior walls, the transverse bending load is either the value from Eq. (30) or the magnitude of the wind pressure at the level of the wall, whichever is greater.

The bending moment caused by transverse loading is assumed to be $w h_u^2/12$, in which h_u = clear height of wall between floors. However, for those walls in the top floor the bending moment is taken as $w h_u^2/10$.

FLOOR TO WALL CONNECTIONS

For an assumed hinged floor to wall connection, the wall bending moment is assumed equal to the eccentricity of the floor reaction, based on a triangular bearing plate stress distribution, times the floor reaction. Half of this moment is resisted by the wall above the floor and half is resisted by the wall below. The full moment is resisted by the top wall at the intersection of the wall and roof. It is also assumed that 1/4 of the first floor moment is resisted at the ground level of the wall.

For an assumed fixed floor to wall connection, the wall moments are computed assuming the connection is hinged for dead load and fixed for live load. Thus the dead load wall moment is computed as described above for a hinged connection. For the wall moment due to live load, a distribution factor is required. For exterior walls, a distribution factor of 0.5 is recommended. This results in a moment above and below the floor level equal to $w L^2/24$. For interior walls, the recommended distribution factor is 0.33 giving a moment equal to $w L^2/36$. These moments are somewhat conservative and are considered adequate for analysis.

It should be noted that, at the roof line, the roof to wall connection is always considered hinged.

STRENGTH ANALYSIS

The strength analysis performed by the program considers only the effects of gravity and lateral wind or seismic loads. Blast loads, temperature stresses and stresses caused by differential foundation movement are not considered. For stresses due to wind or earthquake in combination with dead and live loads, the allowable masonry stresses are increased 33 1/3 percent.

The required compressive strength of each wall at each floor level is computed for seven combinations of the vertical and horizontal loads as follows:

- Case 1. Total vertical load (dead load plus live load) with wind acting parallel to the wall.
- Case 2. Dead load with wind acting parallel to the wall.
- Case 3. Dead load and reduced live load.
- Case 4. Total load (dead load plus live load) and lateral load perpendicular to the wall.

Case 5. Dead load and lateral load perpendicular to the wall.

Case 6. Total load (dead load plus live load) and earthquake load acting parallel to the wall.

Case 7. Dead load and earthquake load parallel to the wall.

For cases 4 and 5, non-load bearing walls will probably be in tension and may require reinforcing. For non-load bearing brick walls, the lateral load on the wall (in-psf) is printed. The investigator must determine whether or not the non-load bearing wall is properly designed for the lateral load indicated. In determining the required compressive strengths, the effects of slenderness and virtual eccentricities are considered, as described below

(a) Brick Masonry

The required compressive strength f'_m is computed using the equation

$$f'_m = P / [0.2A C_e C_s (FS)] \quad (31)$$

in which C_e = eccentricity coefficient, C_s = slenderness coefficient, A = wall area, P = axial load on the wall, and $FS = 1.33$ for cases 1, 4, 6 and 1.0 for all other cases. It should be noted that P is the load at the base of the wall caused by the appropriate loading. The value of C_s is obtained from the following equation

$$C_s = 1.2 - (h/t) [5.75 + (1.5 + e_1/e_2)^2] / 300 \leq 1.0 \quad (32)$$

The ratio e_1/e_2 is always ≤ 1.0 and is positive when the member is bent in single curvature, and negative when the member is bent in double curvature. Values of e_1 and e_2 are computed for each combination of gravity loading, considering checkerboard effects and transverse bending where necessary.

The program also indicates those walls where the slenderness ratio, h/t , exceeds the allowable ratio as given by the following equation

$$h/t \leq 10(3 - e_1/e_2) \quad (33)$$

The eccentricity coefficient is

$$C_e = 1.0 \text{ if } e/t < 0.05$$

$$C_e = 1.3 / [1 + 6 (e/t)] + 0.5 (e/t - 0.05) (1 - e_1/e_2) \quad (34)$$

if $0.05 < e/t < .167$

$$C_e = 1.95 / (0.5 - e/t) + 0.5 (e/t - 0.05) (1 - e_1/e_2)$$

if $0.167 < e/t < 0.333$

In these equations e represents the virtual eccentricity and if the transverse load exceeds 10 psf, e_1/e_2 is taken as 1.0. For bending about both principal axes of a wall (cases 1, 2, 6 and 7) Eqs. (34) are modified as required by the Recommended Practice for Engineered Brick Masonry.

If e/t exceeds 0.333, the wall is in tension and an appropriate message is printed. Also, if overturning is a problem an error message is printed. The program also prints the increase in the allowable horizontal shearing stress due to the dead weight of the wall and the horizontal shear stress in each wall at each floor level from either wind or earthquake loading (whichever is greater) is computed and printed.

(b) Concrete Block Masonry

The required compressive strength f'_m is computed using the equation

$$f'_m = P/[0.2AR' (FS)] \quad (35)$$

in which R' is a reduction factor, which is defined below, and the other terms are the same as those used in Eq. (31). The equations developed below for R' follow the procedures outlined in The Application of Non-Reinforced Concrete Masonry Load-Bearing Walls in Multistory Structures, published in 1969, by the National Concrete Masonry Association. As outlined in this design manual, floor load eccentricities are not considered except for Case 3.

(1) Cases 1, 2, 6 and 7

For each of these loading conditions, the wall unit is subjected to both axial and bending loads. The bending moment, M , is in the plane of the wall. The interaction formula requires that

$$\frac{f_a}{F_a} + \frac{f_m}{F_m} \leq 1 \quad (36)$$

in which $f_a = P/A =$ axial stress, $f_m =$ bending stress, $F_a = 0.2 f'_m R =$ allowable axial stress, and $F_m = 0.3 f'_m =$ allowable bending stress. In the expression for the allowable axial stress, the factor R for walls equals $[1 - (h_u/40t)^3]$ where h_u is the clear story height, and $t =$ wall thickness. Substituting into Eq. (36) and solving for f'_m gives

$$f'_m = P/[0.2AR'] \quad (37)$$

in which

$$R' = \frac{R}{(1+2AeR)} \quad (38)$$

In Eq. (38), $e = M/P$ and thus the expression for R' to be used in Eq. (35) is available. For unsymmetrical walls, R' is evaluated using the smallest possible value of $S = I/c$. In addition, if $e = M/P$ exceeds S/A , the wall will be in tension, and the values of f'_m and f'_m are printed so that the designer will be able to determine how much reinforcement is required. Also for cases 1 and 6, FS in Eq. (35) equals 1.33.

(2) Cases 3, 4, 5

For these loading conditions, the factor R is considered in both terms of Eq. (36) giving

$$\frac{P}{0.2 f'_m AR} + \frac{Pe}{S(.3 f'_m)R} \leq 1.0 \quad (39)$$

Solving for f'_m gives

$$f'_m = \frac{P}{.2A} \left[\frac{S + .667eA}{RS} \right] \quad (40)$$

Thus

$$R' = \frac{RS}{S + .667eA} \quad (41)$$

in which for Case 3, $e =$ the unbalanced moment at the top of the wall from the floor gravity load divided by the total gravity load in the wall. For cases 4 and 5, e in Eq. (41) equals the transverse bending moment (defined previously) divided by the gravity load at mid-height of the wall.

If e , as defined, exceeds S/A , the wall is in tension, and, for hollow block units, an appropriate message is printed. However, for solid block units, if e exceeds $t/6$ but is less than $t/3$, values of f'_m are computed using the uncracked section modulus.

The uncracked thickness, $t_1 = (t+6e)/(12 e/t)$ and the corresponding eccentricity, $e' = e + (t-6e)/(24e/t)$

Thus

$$R' = \frac{\bar{R} t_1}{(1+4e'/t_1)t} \quad (42)$$

Where

$$\bar{R} = \left[1 - \left(\frac{h}{40t_1} \right)^3 \right] \quad (43)$$

Thus using the value of R' given from Eqs. (38), (41) or (43), whichever is applicable, the required compressive strength f'_m may

be computed from Eq. (35).

SUMMARY

A procedure for the rational analysis of load bearing masonry structures has been presented. This procedure has been incorporated into a computer program which is available to the profession through the Masonry Institute of Maryland.

ACKNOWLEDGMENTS

The work described herein was supported by the Masonry Institute of Maryland.



USE OF THE PRISM TEST TO DETERMINE COMPRESSIVE STRENGTH OF MASONRY

by Maurenbrecher, A.H.P.

ABSTRACT: This paper reviews the use of small masonry specimens (prisms) to determine the design compressive strength. The requirements of a number of masonry codes are compared, and the more important factors influencing prism tests are discussed.

USE OF THE PRISM TEST TO DETERMINE
COMPRESSIVE STRENGTH OF MASONRY

By A.H.P. Maurenbrecher¹

INTRODUCTION

Masonry prisms are small specimens used for predicting the full-scale properties of masonry such as compressive strength, shear strength, elastic modulus and shear modulus. This paper examines factors affecting prism compressive strength and presents a review of prism requirements contained in different masonry design codes.

Prisms are used to obtain the design compressive strength as an alternative to tabular values, which are based on unit strength and mortar type. They give more accurate values and, in most cases, higher allowable stresses than the tabular values because the latter are conservative to allow for the variation in units, mortar and construction. In addition to obtaining the design strength, prisms are used for quality control to ensure that the design strength is achieved on site.

Prisms range from two block high, stack-bonded specimens, normally used for concrete blockwork in North America, to small walls used for research purposes. Because of handling difficulties, test machine limitations and cost, prisms are usually made as small as possible while still giving adequate results for design use. This question of size has been a major subject of discussion in the development of prism testing. (2, 10-12, 24, 27)

PRISM STRENGTH

Prism behaviour should reflect the masonry to be used in a building. This implies similar workmanship, joint thickness, bond pattern, thickness, curing and failure mode. Depending on circumstances, some of these factors have a greater effect on strength than others.

Prism Dimensions.- The minimum size of a prism depends on the units, mortar, capping, and limitations caused by handling, size and capacity of the test machine and cost.

¹Research Officer, Division of Building Research, National Research Council of Canada, Ottawa, Canada K1A 0R6.

Number of Courses.- Where the mortar joints have a significant effect on masonry strength (mainly dependent on mortar and unit strength and the ratio of joint thickness to unit height) there should be enough courses to allow adequate representation of the interaction of the mortar and the units. Minimum numbers recommended are 3 to 5 courses (Table 1). Prisms made of standard bricks of low height usually have a larger number of courses than prisms containing higher units such as concrete blocks.

Height.- Prisms are normally tested between steel plates which are much stiffer than the masonry and restrict by friction the lateral expansion at the ends of the prism. This inhibits the normal vertical tensile splitting failure, thereby increasing the failure load. As prism height is increased, these end effects are confined to a small proportion of the prism height so that a further change in height has little effect on prism strength. Normally the strength becomes approximately constant at heights greater than three to five times the prism thickness but this may also depend on the capping material inserted between the prism and the steel plates. Lower height to thickness ratios may be adequate for hollow concrete block prisms, probably because the slenderness of the webs and flanges is more important than the overall prism slenderness.(27) On the other hand some grouted hollow blockwork may need higher ratios to reflect the interaction of the grout and the blockwork. (4, 24) Shorter prisms than desirable may be necessary because of handling difficulties or height limitations in the test machine but then a reduction factor must be applied to the test results. These reduction factors vary and should be based on results of tests that have compared the small prisms to large prisms or walls using the same type of unit, mortar and capping. Many codes contain correction factors based only on the results of brickwork pier tests (17) as pointed out by Foster and Bridgeman. (10)

Bond Pattern and Thickness.- Bond pattern where units are laid horizontally does not normally have an important effect on strength (14, 30, 32) but there are exceptions. Many hollow blocks with recessed ends cannot be laid with full mortar bedding since the cross webs do not line up. Therefore if a stack-bonded prism is used, only the face shells should be bedded in mortar, although some results indicate that the ultimate stress based on net-bedded area may be similar for full-bedded and face shell-bedded prisms. (26, 28)

The thickness of the prism should be the same as that of the wall. It has been shown that multiple wythe solid walls fail at lower stresses than single wythe walls. (16, 13, 33) Similarly with composite construction the prisms should be composite.

Capping.- The capping material between the prism and the steel plates can also affect strength. The capping ensures a more uniform distribution of the load applied to the ends of the prism. The more common cappings (Table 1) give similar results assuming the bearing surfaces are reasonably flat and the height to thickness ratio is such that end effects are small but materials such as rubber are not recommended as they induce premature splitting failure. Various capping procedures are commonly used. If the top and bottom of the prism are

single units they can be ground flat beforehand (no capping) or fibre-board (27, 28) can be used if the unit has a flat surface. Other methods include capping with mortar, dental plaster or sulphur (Table 1). These latter cappings can also be used together with fibreboard or plywood sheets. (31) The use of fibreboard merits further investigation since it has the advantage of being simple, cheap and quick. Hast (14) has shown it reduces the frictional restraint of the steel plates and produces a uniform stress distribution on flat surfaces in contrast to such materials as rubber which tend to flow outwards under pressure causing a triangular pressure distribution. Some attempts have been made to have a capping which has lateral expansion characteristics similar to that of the masonry thus allowing smaller prisms, but the capping would be restricted to a particular prism and masonry.

Workmanship.- Prisms should be constructed by a professional mason rather than, for example, by laboratory technicians, to try to ensure that the workmanship is as similar as possible to that expected on supervised sites. For example, many masons tend to furrow the mortar joints, which reduces the strength of masonry using solid masonry units.

Curing Conditions.- Test specimens are normally cured in air (Table 1). Codes usually specify humidities in the range 30 to 70%, greater than 90% or combinations of the two, such as initial curing under polythene (humidity > 90%) for 3 to 7 days. (6, 7, 9) As an example of the possible effect of curing on strength, James (16) found that the 28-day strength of single wythe brickwork walls and prisms cured uncovered and exposed to the sun was approximately 10% less than those cured under polythene in the shade.

High moisture content in units, especially concrete blocks, may reduce the strength of masonry. Strength reductions of up to 15% have been observed when air dry concrete blocks have been saturated. (27, 28) Because of this, prisms are usually tested air dry even though they may initially be cured at high humidity, but for masonry in very humid environments the humidity should be taken into account. (23)

Test Age.- The standard test age is 28 days (Table 1). Shorter times in many cases would be more convenient, especially if prisms are used for quality control, while longer periods are sometimes used to take into account the increase of strength with age. The Dutch code (23) allows tests up to 10 weeks when using cement-lime mortars. The strength increase with time can be significant, especially if fresh concrete blocks are used. (28)

Loading Rates.- Loading rates, usually specified in terms of load as opposed to strain, range from 14 - 28 MPa/min in the Australian code (31) to 2.4 MPa/min in the Dutch code. (23) This range of loading has not been shown to have a significant effect on ultimate strength.

The method of load control may cause differences in ultimate strength. For example, some standards (9) require that the load rate control should not be altered near failure even though the load rate is falling. This procedure approximates to a constant strain rate instead of load rate and will tend to give lower results.

The initial short term ultimate load test may give higher results than a long term test but the difference may be reduced due to the increase of strength with age. Russian literature (29) gives ratios of 0.6 to 0.8 of long term to short term strength but their code makes no allowance for this strength drop in design since in practice the stresses due to long term loads are considerably lower than the short term ultimate stress. On the other hand, the Dutch code (23) includes a reduction factor of 0.8 for masonry strength based on a short term test.

Number of Tests.- Most codes specify a minimum of 5 or 6 tests (Table 2). Note that these numbers are a minimum and should only be used for control tests or where a good estimate of the variation in strength is known beforehand. A minimum number of 10 replicates is recommended to obtain an estimate of the mean strength and especially so for its variation (e.g., standard deviation) although a statistically desirable figure is 30 or more. (3)

In practice, a figure of 30 or more would probably only be used for units and small prisms in research programs. For design, a minimum of 10 replicates is recommended, the actual number dependent on the variability of the materials and the size of the prism. If smaller numbers are used, higher mean prism strengths should be specified for a given design strength (see later section on Compressive Strength).

CODE REQUIREMENTS

Prism Test.- Table 1 shows the prism requirements contained in ten different codes. An increasing number of codes allow prism tests to determine masonry compressive strength as an alternative to using tabular values based on unit strength and mortar type, and in some cases tabular values are not even allowed. The Australian brickwork code (31) requires that design stresses be based on prism tests for buildings exceeding eight storeys. The CIB draft code (20) recommends them when design stresses exceed 1.8 MPa and in addition specifies storey-height wall tests when stresses exceed 3 MPa. These latter values are provisional and may be modified if prism strength is much larger than required.

Some codes such as the Russian (29) do not contain specific requirements for obtaining the design stresses experimentally although use of experimental data is allowed while the British draft code (6) recommends tests on storey-height walls as an alternative to tabular values (normally two replicates are tested). The Swiss code (13, 19) requires preliminary wall and unit tests to be done at a central laboratory to enable a particular masonry unit to be classified as standard, high or very high quality. After classification no further tests are required, but the manufacturer must guarantee the quality of his product. If the manufacturer has masonry tests carried out three times annually, a lower factor of safety is allowed -- four instead of five. Short and storey-height walls are tested both axially and eccentrically at the kern point (two replicates for each case).

The Dutch, Spanish and Mexican codes (23, 18, 15) use the prism test to obtain design stresses if there are no previous experimental values but prisms are not used for quality control. Instead, as with

the British (6) and Swiss (13, 19) codes, quality control is usually carried out on the units and the mortar.

U.S. codes (5, 21) and the present Canadian code (8) specify or recommend prisms for quality control if design stresses are based on prisms while the Australian code (31) requires them for all sites. The CIB draft code (20) recommends them when the design stress exceeds 3 MPa, although there is a possibility prisms may not be required if the masonry strength is much larger than necessary.

Compressive Strength.- Most codes, especially those written in terms of limit states philosophy, use a design prism strength which is lower than the mean strength to allow for variability in results. Table 2 lists the reduction factors. These reductions try to ensure that only a small percentage of the masonry strength falls below the design prism strength. For the Canadian and New Zealand codes (8, 25) this is 10%, for the Dutch, Spanish, Australian and CIB codes (23, 18, 31, 20) it is 5% while for the Mexican code (15) it is 2%. Many tests using units from different consignments are necessary to be confident that the design strength falls above the given percentages. If the number of tests is small, the CIB and New Zealand draft codes (20, 25) increase the reduction factor (in other words a higher prism strength must be achieved for a given design prism strength).

DISCUSSION

Design Compressive Strength.- The following discussion on design stresses outlines possible approaches for achieving more reliable results.

1. The use of design stresses based on tabular values in terms of unit strength and mortar type could be improved. In the Canadian code (8) there are only two tables covering brick and block units; they tend to be conservative since they cover a range of different units, wall thicknesses and construction techniques. Additional tables would need to be based on wall tests.
2. The present use of prism testing could be extended. Normally they are carried out for a given building or buildings (if the same unit is used) but to be more reliable ten or more prisms should be tested and in some cases fairly large prisms may be needed. This can be costly especially if the tests have to be repeated for every building. To reduce cost, small standardized prisms, such as two block high and four brick high, stack-bonded specimens, could be specified but to use the results with confidence, they need to be correlated to storey-height walls. This would need an initial extensive test program to cover the units, mortar and types of construction used.
3. Alternatively, to reduce duplication of testing and overall cost, the masonry industry could commission prism and wall tests for units and mortar used in structural masonry. The results could then be used for all future applications with control tests on the units and mortar to see that they conform with those used in the original tests.

Combinations of these three approaches could also be used.

Quality Control.- Prisms are envisaged primarily as a preliminary test to obtain design stresses and not for quality control on site as this can be achieved by testing the individual units, the mortar components and the mortar. In contrast to in-situ concrete construction, the major component of masonry, the unit, is prefabricated and therefore easily checked beforehand. Assuming the mortar proportions are properly controlled, the variation in strength for a given mortar type has little influence on masonry strength. Another drawback to prisms on site can be their size and weight; many are difficult to handle and thus are easily damaged during transport from site to the test laboratory. Workmanship is an important factor but prisms built on site do not necessarily incorporate faults in the walls. Workmanship faults, many of which can be checked visually, should be avoided by proper supervision.

SUMMARY

This paper has presented a short review of factors affecting prism strength and the approach taken by a number of masonry codes. It has shown the size and use of the prism varies and in many cases further improvement in procedure is needed so that prism results can be used with more confidence.

This paper is a contribution from the Division of Building Research, National Research Council of Canada and is published with the approval of the Director of the Division.

APPENDIX. — REFERENCES

1. American Society for Testing and Materials E447-74, "Compressive strength of masonry prisms," 1974.
2. Anderson, G.W., "Stack-bonded small Specimens as Design and Construction Criteria." SIBMAC Proceedings. H.W.H. West and K.H. Speed, eds. British Ceramic Research Association, Stoke-on-Trent, England, 1971, pp. 38-43.
3. Beech, D.G., "The Concept of Characteristic Strength." Presented at the British Ceramic Society Symposium on Load-bearing Masonry, London, 1977.
4. Boulton, B.F., Progress Report: "Concrete Masonry Prism Testing," New Zealand Concrete Research Association. Special Laboratory Report No. 2, Porirua, New Zealand, 1976.
5. Brick Institute of America. "Testing for Engineered Brick Masonry Quality Control," Technical Note 39b. McLean, Va., 1976.
6. British Standards Institution, "Draft Code of Practice for the Structural Use of Masonry, Part 1: Unreinforced Masonry," Document 76/12191, London, 1976.
7. California Concrete Masonry Technical Committee, "Recommended Testing Procedures for Concrete Masonry Units, Prisms, Grout and Mortar," Calif., 1975.
8. Canadian Standards Association, CSA Standard S304-1977, "Masonry Design and Construction for Buildings."
9. Canadian Standards Association. "Method of Test for Compressive Strength of Masonry Prisms," Draft Standard CSA A369.1, 1978.
10. Foster, P.K., and Bridgeman, D.O., "Prism Tests for the Design and Control of Brick Masonry," Technical Report No. 22, New Zealand Pottery and Ceramics Research Association, Lower Hutt, New Zealand, 1973.
11. Francis, A.J., Horman, C.B., and Jerrems, L.E., "The Effect of Joint Thickness and other Factors on the Compressive Strength of Brickwork." SIBMAC Proceedings. H.W.H. West and K.H. Speed, eds., British Ceramic Research Association, Stoke-on-Trent, England, 1971, pp. 31-37.
12. de Grave, A., and Motteu, H., "Testing and Calculation of Masonry: Recommendations Based on Research in Belgium," SIBMAC Proceedings, BCRA, Stoke-on-Trent, England, 1971, pp. 266-272.
13. Haller, P., "Masonry in Engineered Construction," Comments on the New SIA Standard No. 113. NRC Technical Translation 1270, Ottawa, Canada, 1967.

14. Hast, N., "Measuring Stresses and Deformations in Solid Materials (The Causes of Rupture in Brickwork and Some Other Problems)," Centraltryckeriet, Stockholm, 1943.
15. Instituto de Ingeniería. Norma 403. "Diseño y construcción de estructuras de mampostería" (Masonry Design and Construction). Universidad Nacional Autónoma de México. Mexico City, 1977.
16. James, J.A., "Investigation of the Effect of Workmanship and Curing Conditions on the Strength of Brickwork," Third International Brick Masonry Conference. Bundesverband der Deutschen Ziegelindustrie, Bonn, 1975, pp.192-201.
17. Krefeld, W.J., "The Effect of Shape of Specimen on the Apparent Compressive Strength of Brick Masonry," Proceedings ASTM, Vol. 38, No. 1, 1938, pp. 363-369.
18. Ministerio de la Vivienda. Norma MV 201-1972. "Muros Resistentes de Fábrica de Ladrillo," (Structural Brickwork Walls). Madrid.
19. Monk, C.B., and Gross, J.G., "European Clay Masonry Load-bearing Buildings," Structural Clay Products Institute (now BIA). McLean, Va., 1965.
20. Motteu, H., "Draft of International Recommendations for Masonry Structures." CIB Working Committee W23A, Bearing Walls. 1976 Meeting at Edinburgh. Proceedings edited by B.P. Sinha and published by Department of Civil Engineering and Building Science, Edinburgh University, 1976.
21. National Concrete Masonry Association. "Specification for the Design and Construction of Load-bearing Concrete Masonry, Arlington, Va., 1970.
22. National Concrete Masonry Association. "Prism Testing for Engineered Concrete Masonry," Technical Note 22, Arlington, Va., 1970.
23. Netherlands Standards Institute, NEN 3853-1976, "Regulations for the Calculation of Building Structures: Masonry Structures" (in Dutch).
24. New Zealand Concrete Research Association. "Concrete Masonry Prism Testing," Special Laboratory Report No. 1, Porirua, New Zealand, 1975.
25. New Zealand Standards Association. "Draft Code of Practice for Masonry Buildings. Part A Materials and Workmanship." DZ 4210/342. 1973.
26. Richart, F.R., Moorman, R.B.B., and Woodworth, P.M., "Strength and Stability of Concrete Masonry Walls," Bulletin No. 251, Urbana, Ill., 1932.

27. Roberts, J.J., "The Effect of Different Test Procedures upon the Indicated Strength of Concrete Blocks in Compression," Magazine of Concrete Research, Vol. 25, No. 83, 1973, pp. 87-98.
28. Self, M.W., "Structural Properties of Load-bearing Concrete Masonry," in Masonry: Past and Present, ASTM STP 589, 1975, pp. 233-254.
29. Sementsov, S.A., "Physical and Mechanical Properties of Masonry," Chap. 2 in Masonry Designer's Manual. S.A. Sementsov and V.A. Kameiko, eds. Translated by Israel Program for Scientific Translations, 1971.
30. Sinha, B.P., and Hendry, A.W., "The Effect of Brickwork Bond on the Load-bearing Capacity of Model-brick Walls," Proceedings, British Ceramic Soc. No. 11, Load-bearing Brickwork 2, 1968, pp. 55-67.
31. Standards Association of Australia, AS 1640-1974: SAA Brickwork Code, Sydney.
32. Structural Clay Products Research Foundation (now Brick Institute of America). "Compressive, Transverse and Racking Strength Tests of Four-inch Brick walls," Research Report No. 9, SCPRF, Geneva, Ill., 1965.
33. Structural Clay Products Research Foundation (now BIA). "Compressive and Transverse Strength Tests of Eight-inch Brick Walls," Research Report No. 10, SCPRF, Geneva, Ill., 1966.
34. Structural Clay Products Institute (now BIA). "Recommended Practice for Engineered Brick Masonry," McLean, Va., 1969.

TABLE 1. - Prism Test Requirements

	Spain(1)* MV201 (18)	Netherlands NEN3853 (23)	CIB Draft (20)	Australia(1) AS1640 (31)	New Zealand Draft (25)	Mexico 403 (15)	Canada		USA	
							S304(12) (8)	A369.1 Draft (9)	NCMA(18) (22)	ASTM E447(20) Method B (1)
h	--	≥ 700 mm	≥ 5 courses	4 courses	≥ 5 courses(8)	≥ 3 courses	≥ 380 mm	≥ 300 mm	≥ 400 mm	≥ 380 mm
h/t	≈ 2 (42)	--	3 - 5	≥ 2	--	2 - 5(10)	1.5 - 5(13)	1.4 - 10	1.5 - 3(19)	≥ 2
t	brick length	--(3)	as wall	brick thickness	as wall	--	as wall	as wall	as wall	as wall
b	brick length	--(3)	≥ 2 unit lengths	brick length	--	--	--	≥ unit length(14) ≥ 190 mm(15)	--	--
b/t	≈ 1	≈ 1	≥ 1	--	≥ 1	--	≥ 1	≥ 1	≥ 1	≥ 1
Curing no. of days	28	28(4)	28	28(5)	28(9)	28	28(9)	≤ 28	28(9)	28(9)
temp., °C	--	20	20	≥ 10(6)	--	--	24 ± 8	20 ± 10	24 ± 5	24 ± 8
humidity, %	≥ 90(2)	50 - 70	60	≥ 90(7)	--	--	30 - 70	≥ 90(16) and 30 - 70	50 - 70	30 - 70
Test procedure	mortar	--	--	mortar and 4 mm plywood	--	(11)	sulphur or dental plaster	fibreboard(17)	sulphur or dental plaster	sulphur or dental plaster
loading rate, MPa/min	--	2.4	3	14 - 28	10 - 20	(11)	P _u /2 + P _u 1 - 2	P _u /2 + P _u 1 - 2	P _u /2 + P _u 1 - 2	P _u /2 + P _u 1 - 2
duration, min	--	≥ 3	≥ 1	--	--	--	--	--	--	--

h = height; t = thickness; b = length; P_u = maximum load.

*see notes to Table 1.

Notes to Table 1:

- (1) Brick masonry.
- (2) Prism covered by a damp cloth.
- (3) $bt > 0.04 \text{ m}^2$.
- (4) Up to 10 weeks allowed if a cement-lime mortar is used.
- (5) Likely to be reduced to 7 days in the next code version.
- (6) Lower temperatures are allowed but curing period is then extended.
- (7) Prism covered by vapour-proof sheet.
- (8) A lower number is allowed if this does not affect the strength.
- (9) Seven day test allowed if its relationship to the 28-day test is established.
- (10) Four is standard; other ratios require a correction factor.
- (11) Same as concrete cylinder requirements.
- (12) Requires conformance with ASTM E447.
- (13) Brick masonry: 2 to 5 (5 is standard; others require correction factors).
Concrete block and structural clay tile: 1.5 to 3 (2 is standard; others require correction factors).
- (14) Hollow masonry units.
- (15) Solid and grouted masonry units.
- (16) 90 for first 7 days only.
- (17) Mortar, plaster or sulphur, is used in addition to fibreboard if the prisms do not have plane surfaces (most single concrete block and brick units have adequate surfaces).
- (18) Concrete masonry.
- (19) Two is standard; other ratios require correction factors.
- (20) BIA Tech Note 39A "Testing for Engineered Brick Masonry: Determination of Allowable Design Stresses" recommends prisms be built to ASTM E447, Method B.

TABLE 2. - Prism Strength Reduction Factors

Country	Reduction Factor ^{(1)*}		
Spain (18)	$1 - 1.64v$	$n \geq 6$	
Netherlands (23)	$1 - 1.64v$	$n \geq 6$	
CIB ⁽²⁾ (20)	$1 - 1.64v$	$v = R/qf_m$	$5 \leq n \leq 10$
		$v = s/f_m$	$n > 10$
Australia (31)	$1 - 0.38R/f_m \leq 4/3 f_{min}/f_m$		$n = 6$
New Zealand ⁽³⁾ (25)	$1 - q_1 R/f_m$	$f_m \geq q_2 R$	
Mexico ⁽⁴⁾ (15)	$1/(1 + 2.5v)$	$n \geq 9$	
Canada (8)	$1 - 1.5$	$n \geq 5$	
USA			
BIA (34)	$1 - 1.5(v - 0.1) \leq 1$	$n \geq 5$	
NCMA ⁽⁵⁾ (22)	$f_m \leq 1.25 f_{min}$	$n \geq 3$	

*Notes to Table 2:

(1) Unless otherwise stated:

$$v = s/f_m \quad \text{where} \quad \begin{array}{l} s = \text{standard deviation;} \\ f_m = \text{mean prism strength.} \end{array}$$

$$R = f_{max} - f_{min} \quad \text{where} \quad \begin{array}{l} f_{max} = \text{maximum prism strength;} \\ f_{min} = \text{minimum prism strength.} \end{array}$$

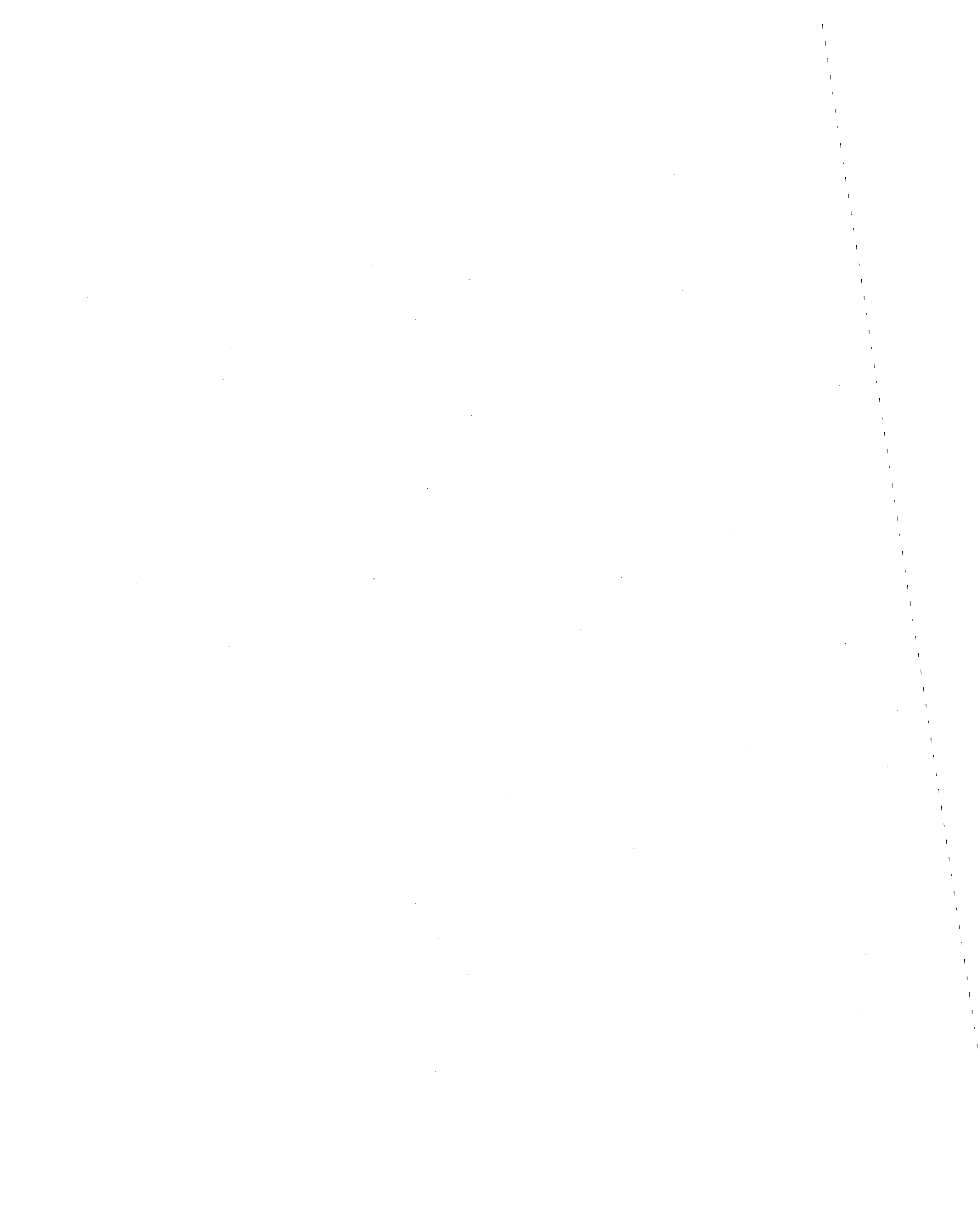
(2) q is a coefficient which depends on the number of tests

n	5	6	7	8	9	10
q	2.33	2.53	2.70	2.85	2.97	3.08

(3) q_1 and q_2 are coefficients based on the number of tests.

(4) Tests from a minimum of 3 different unit consignments.

(5) 5 tests recommended.



THE BENEFITS OF HIGH-STRENGTH MASONRYDean D. Froerer*ABSTRACT

This paper presents an analysis of the Uniform Building Code, 1976 Edition, Chapter 24, comparing the stresses allowed for conventional hollow unit masonry and high-strength masonry complying with ICBO Research Report Number 2730. The benefits derivable by the use of such high-strength masonry in building designs consist of space efficiency, economy, greater load capacity with less reinforcing steel/grout and smaller bearing areas.

Allowable axial load plots for reinforced, hollow unit masonry walls grouted solid and ungrouted are given as a function of wall height for several thicknesses. Allowable axial column stresses as a function of reinforcing steel for selected slenderness ratios are also presented in a graphical manner. Comparable data showing allowable vertical loads for unreinforced brick masonry walls and columns is displayed similarly.

Flexural coefficients for balanced, tension-reinforced masonry rectangular beams are plotted as a function of ultimate compressive masonry strength. This data assumes the allowable steel stress to be 20,000 psi. In addition, allowable flexural shear values are established for reinforced masonry beams when the unit shearing stress is less than that allowed on the masonry and also when shear reinforcement is required to resist all of the shear.

The allowable shear stress in walls varies and depends on the strength of the masonry and the height-length ratios. Long, low walls have higher allowables than short, high walls. Figures showing the interaction between line shear, height-length ratios for shear walls with shear reinforcement are given for several wall thicknesses. Bearing area requirements for reinforced masonry subjected to concentrated loads are presented graphically for two extremes of masonry strength.

Values given for four-inch thick walls are for units complying with ICBO Research Report Number 3118. It should also be noted that all of the preceding information is based on requiring special inspection.

*Senior Structural Engineer, KPFF Consulting Engineers, Seattle, Washington

THE BENEFITS OF HIGH-STRENGTH MASONRY

Dean D. Froerer*INTRODUCTION

An analysis of the Uniform Building Code, 1976 Edition, Chapter 24, is presented which compares the stresses allowed for conventional hollow unit masonry and high-strength masonry complying with ICBO Research Report Number 2730. The benefits derivable by the use of such high-strength masonry in building designs consist of space efficiency, economy, greater load capacity with less reinforcing steel/grout and smaller required bearing areas.

Data is presented for the following masonry elements and special inspection is required per Chapter 24 of the Uniform Building Code (1976 Edition).

1. Wall -- Axially loaded (reinforced).
 - a. Hollow masonry, grouted solid.
 - b. Hollow masonry, not continuously grouted.
2. Columns -- Axially loaded (reinforced).
3. Walls -- Eccentrically loaded (unreinforced).
4. Columns -- Eccentrically loaded (unreinforced).
5. Flexural Members -- Bending (reinforced).
6. Flexural Members -- Shear (reinforced).
 - a. With no shear reinforcement.
 - b. With shear reinforcement.
7. Walls -- Shear (reinforced).
 - a. Interaction with bending and direct shear reinforcement.
8. Bearing -- Concentrated loads.

REINFORCED MASONRY WALLS - Axially Loaded
 Uniform Building Code: Section 2418 (j)

"The axial stress in reinforced masonry bearing walls shall not exceed the value determined by the following formula:

$$f_m = 0.20 f'_m \left[1 - \left(\frac{h}{40t} \right)^3 \right]^4$$

The above allowable stress when multiplied by the actual thickness for grouted walls or by the net effective thickness for hollow walls yields the allowable compressive line load.

Figure 1a presents the data for grouted walls and Figure 1b the data for hollow units. Data corresponding to two masonry strengths is shown -- $f'_m = 1500$ psi or 1350 psi representing conventional strength masonry according to Section 2404 (c) 3 of the UBC; $f'_m = 2600$ psi representing high-strength masonry according to ICBO Research Report No. 2730. It should be noted that neither of these assumed strengths require prism tests.

*Senior Structural Engineer, KPFF Consulting Engineers, Seattle, Washington

It should also be noted that the data given for walls in Figures 1a and 1b are for axial loading only; however, wind loading up to 30 psf will have no impact on the allowables due to the dominance of the axial load.

For example, from Figure 1a it can be seen for wall heights less than 12.5 feet, 6-inch H-S units will carry more load than 8-inch CO units. This, of course, results in the saving of space and money.

Figure 1b shows that for wall heights less than 9 feet, 4 inch H-S units surpass 6-inch CO units in load capacity; and for wall heights less than 12.5 feet, 6-inch H-S units exceed 12-inch CO units. This results in dramatic savings of approximately 50 percent.

REINFORCED MASONRY COLUMNS - Axially Loaded
Uniform Building Code: Section 2418 (k)

"The axial load on columns shall not exceed:

$$P = A_g (0.18 f'_m + 0.65 p_g f'_s) \left[1 - \left(\frac{h}{40t} \right)^3 \right] "$$

The above expression, when divided by the gross column area, depends on the masonry strength, amount of reinforcing steel and the slenderness ratio. The allowable steel stress has been fixed at 20,000 psi for convenience.

Figure 2 presents the allowable axial column stress as a function of reinforcing steel for three values of slenderness ratio. Identical sets of data are given for two masonry strengths -- $f'_m = 1500$ psi, UBC Section 2404 (c) 3, and $f'_m = 2600$ psi, ICBO Report No. 2730.

From Figure 2 it can be concluded that in general the use of higher-strength masonry units result in greater load capacity with less material.

UNREINFORCED BRICK MASONRY WALLS AND COLUMNS- Eccentrically Loaded
Uniform Building Code: Section 2419 (c)

"Allowable vertical loads P on unreinforced walls and columns shall be computed as follows:

Where the maximum virtual eccentricity e does not exceed $t/3$,

$$P = C_e C_s f_m A_g "$$

C_e = Eccentricity coefficient.

C_s = Slenderness coefficient.

The above expression, when converted to axial stress and multiplied by actual thickness of the various masonry units, determines the allowable compressive line loads.

Figure 3 presents the data for an assumed eccentricity normal to the plane of the wall equal to one-sixth the thickness. The same two masonry strengths as were assumed for Figure 1a are considered; i.e., $f'_m = 1500$ psi and 2600 psi.

It can be seen from Figure 3 that more load can be carried using the higher-strength masonry unit or equal load can be handled using smaller higher-strength units; e.g., 4-inch H-S in place of 6-inch CO.

Figure 4 presents the data for an assumed eccentricity normal to the plane of the column equal to one-sixth the thickness. Masonry strengths corresponding to CO ($f'_m = 1500$ psi) and H-S ($f'_m = 26000$ psi) units are considered.

It is clear from Figure 4 that greater loads can be carried by columns constructed of H-S units.

Even though Section 2312 (j) 2 of the Uniform Building Code requires that all masonry elements within structures located in Seismic Zones 2, 3 and 4 be reinforced so as to qualify as reinforced masonry, this data is presented for possible application in zones of lesser seismic risk.

REINFORCED MASONRY FLEXURAL MEMBERS -- Bending Compression
Uniform Building Code: Section 2418 (e) Table No. 24-H

"All members shall be designed to resist at all sections the maximum bending moment and shears produced by dead load, live load, and other forces as determined by the principle of continuity and relative rigidity."

The allowable bending compressive working stress is given by:

$$f_m = 0.33 f'_m \text{ not to exceed } 900 \text{ psi}$$

The above masonry stress, combined with the allowable steel stress and modular ratio, enable the evaluation of the flexural coefficient K.

Figure 5 presents the data for balanced, tension-reinforced rectangular beams. The allowable steel stress has been assumed to be 20,000 psi.

From Figure 5 it can be seen that for masonry units having $f'_m = 2600$ psi (ICBO No. 2730) the bending capacity is approximately 73 percent greater than for masonry units with $f'_m = 1500$ psi (Section 2404 (c) of the UBC). Thus, the use of higher-strength masonry can result in significant material savings.

REINFORCED MASONRY FLEXURAL MEMBERS -- Shear
Uniform Building Code: Section 2418 (h) Table 24-H

"The shearing unit stress v in reinforced masonry flexural members shall be computed by:

$$v = \frac{V}{b_j d} \text{ " which is limited to the following values:}$$

$$v = 1.1\sqrt{f'_m} \text{ not to exceed } 50 \text{ psi}$$

with no shear reinforcement, and

$$v = 3.0\sqrt{f'_m} \text{ not to exceed } 150 \text{ psi}$$

with shear reinforcement.

The above formulae give the allowable shear on masonry flexural elements when the unit shearing stress is less than that allowed on the masonry (Figure 6a) and also when shear reinforcement is required to resist all of the shear (Figure 6b).

The data in Figures 6a and 6b yields the allowable shear for rectangular beams as a function of masonry strength.

The data in Figure 6a shows a 17 percent advantage of high-strength masonry over conventional-strength masonry, whereas there is a 29 percent advantage demonstrated in Figure 6b.

REINFORCED MASONRY SHEAR WALLS

Uniform Building Code: Section 2418 (e) Table 24-H

The allowable shear stress in walls varies and depends on the strength of the masonry and the height/length ratios. Long, low walls have higher allowables than short, high walls. Shear walls with shear reinforcement are governed by the following formulae:

$$V = 1.5\sqrt{f'm} \text{ not to exceed 75 psi}$$

for $\frac{M}{Vd}$ values ≥ 1 , and

$$v = 2.0\sqrt{f'm} \text{ not to exceed 120 psi}$$

for $\frac{M}{Vd} = 0$.

The above expressions for shear stress multiplied by wall thickness yield the allowable line shear.

Figure 7 shows the interaction between line shear, height/length ratio for two masonry strengths and several thicknesses.

It is to be noted from Figure 7 that the higher-strength masonry consistently provides greater line shear capacity than does the conventional-strength units.

BEARING ON REINFORCED MASONRY-Concentrated Loads

Uniform Building Code: Section 2417 (j) Table 24-H

The allowable stresses on masonry for bearing are higher than the allowable axial compression stress for walls and columns. The values vary according to bearing area as indicated:

$$f_{brg} = 0.25 f'm \text{ not to exceed 900 psi}$$

on full area, and

$$f_{brg} = 0.30 f'm \text{ not to exceed 1200 psi}$$

if bearing is on one-third or less of area.

The above bearing stresses, when divided into the concentrated load values, determine the required bearing area necessary for those particular loads.

Figure 8 shows that smaller bearing areas are required for the higher-strength masonry (ICBO No. 2730) than for the conventional-strength masonry (UBC Section 2404 (c) 3).

SUMMARY

The following identifies the benefits derivable by the use of high-strength masonry in building designs.

Space efficient

Economical

Greater load capacity

Less reinforcing steel

Less grout

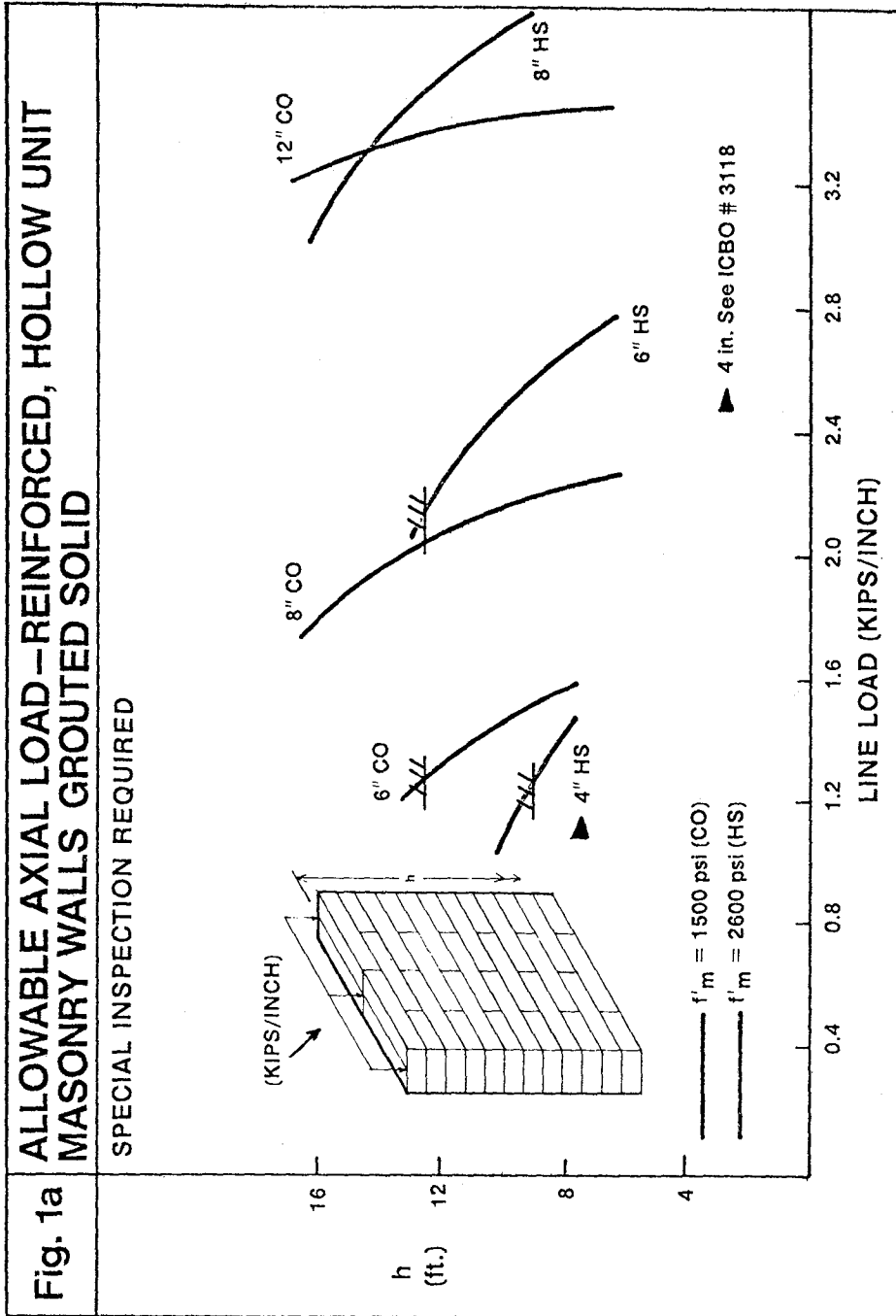
75% greater bending capacity

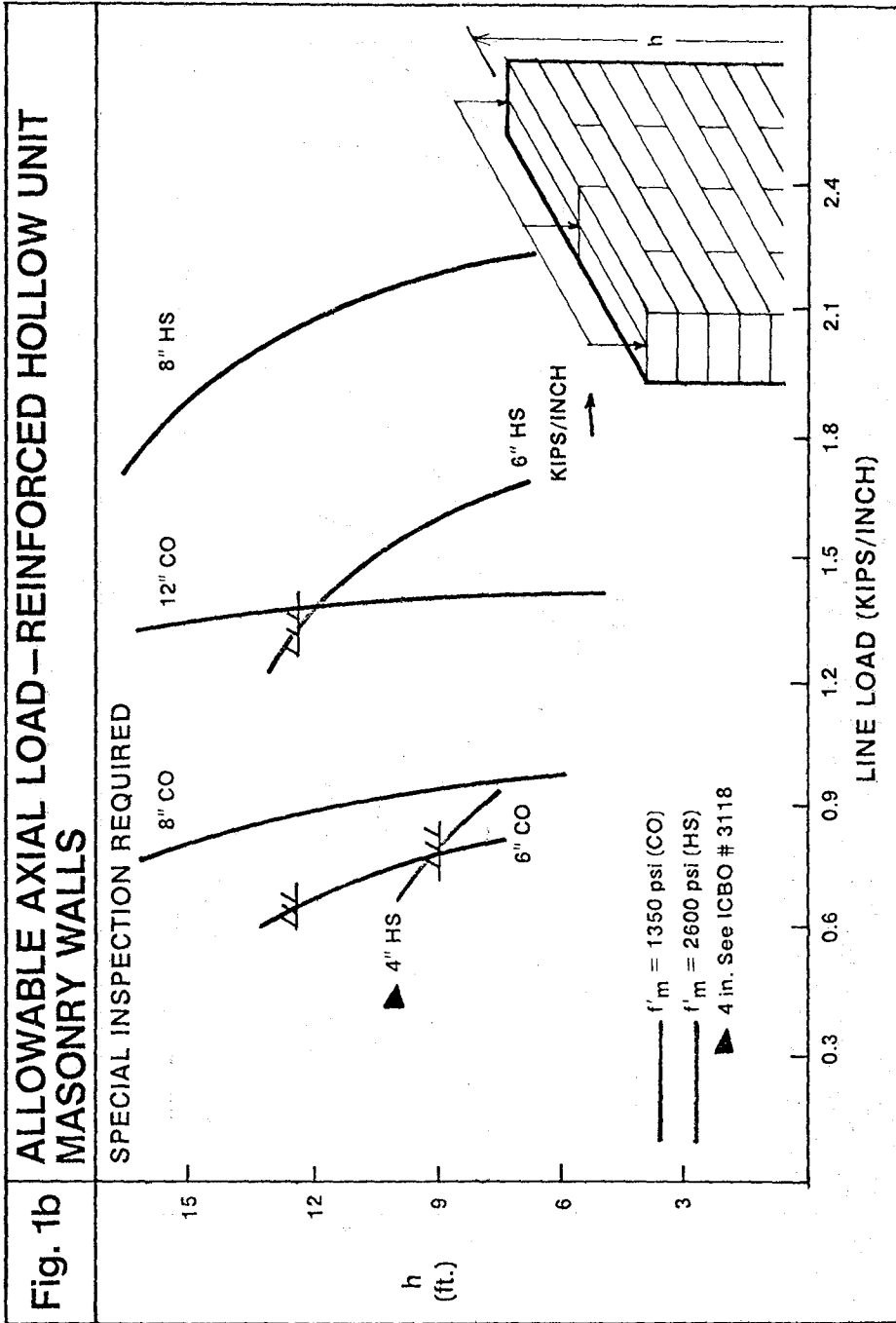
17% greater shear capacity with no shear reinforcement

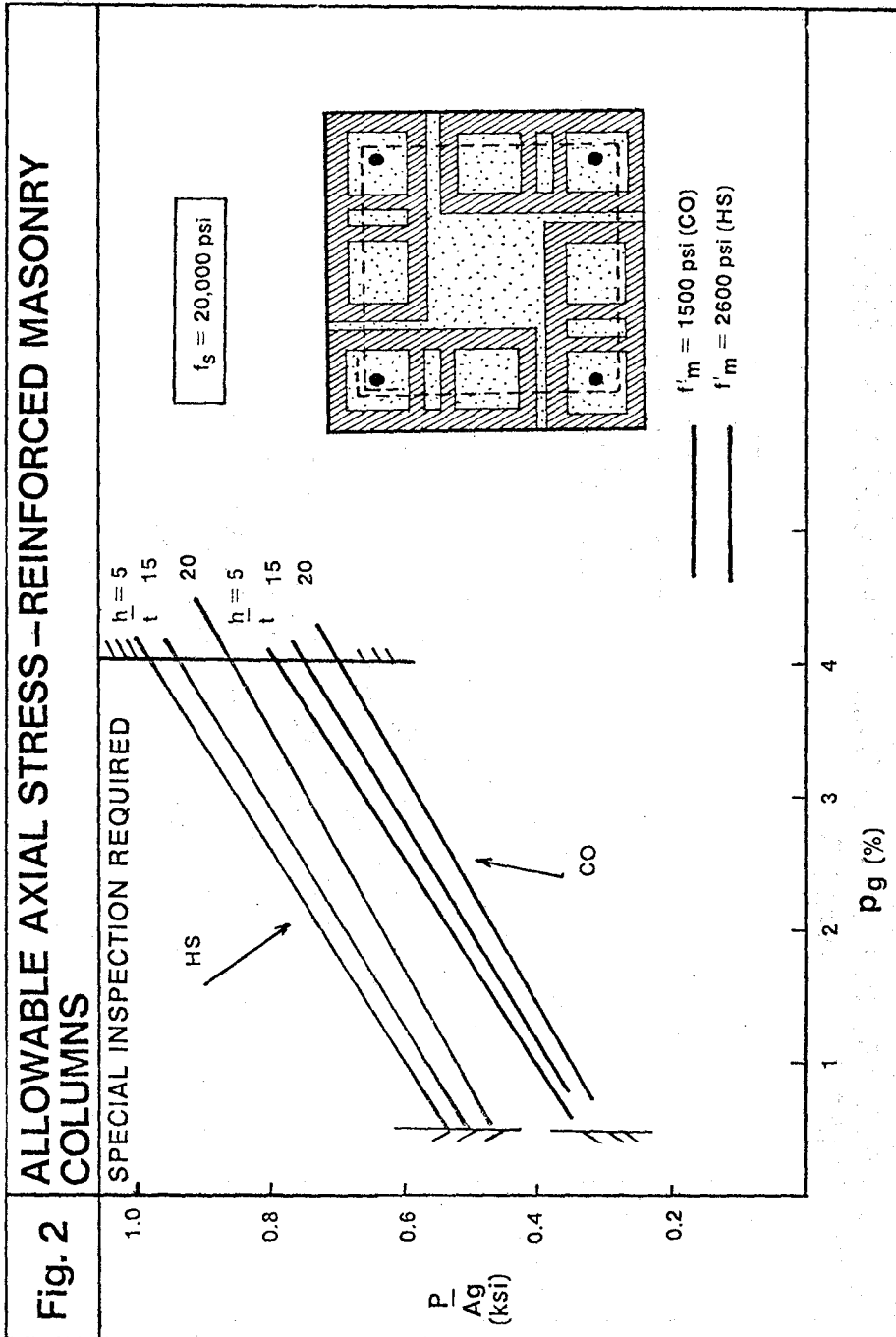
29% greater shear capacity with shear reinforcement

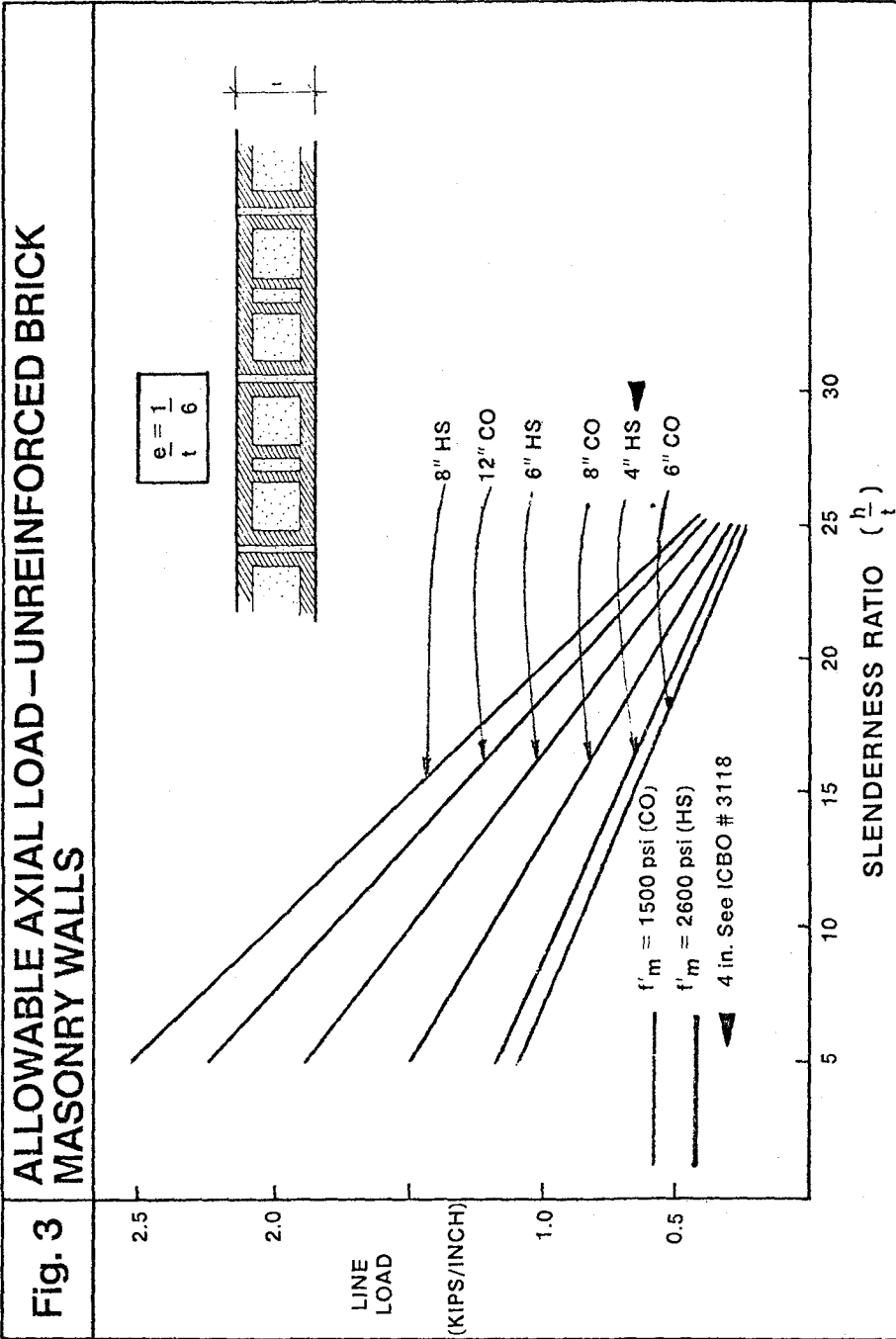
Smaller bearing areas

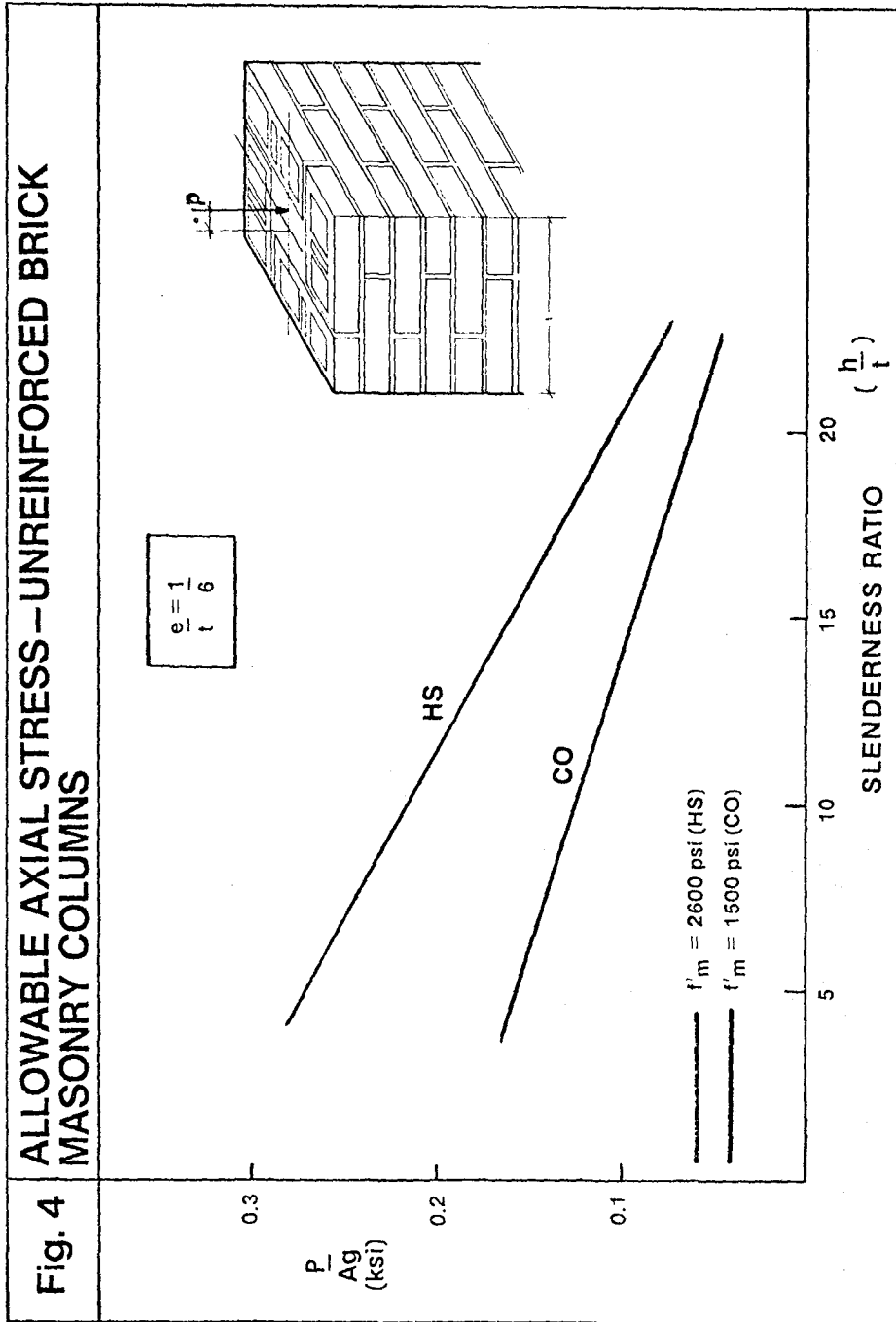
It should also be noted that the factor of safety with respect to masonry crushing is greater than five when designed according to Code and, as such, no additional reductions in allowable loads are included in this data.

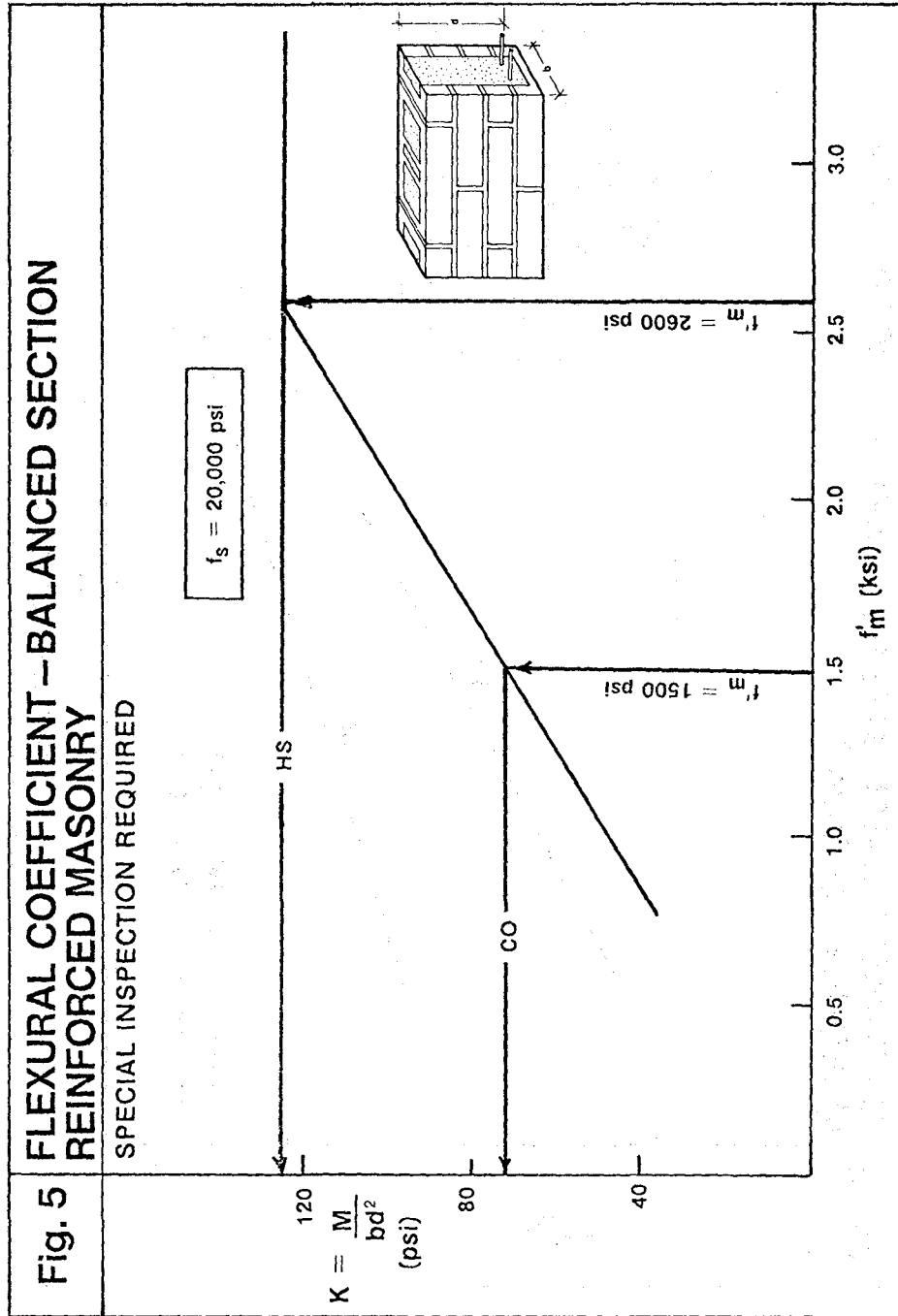


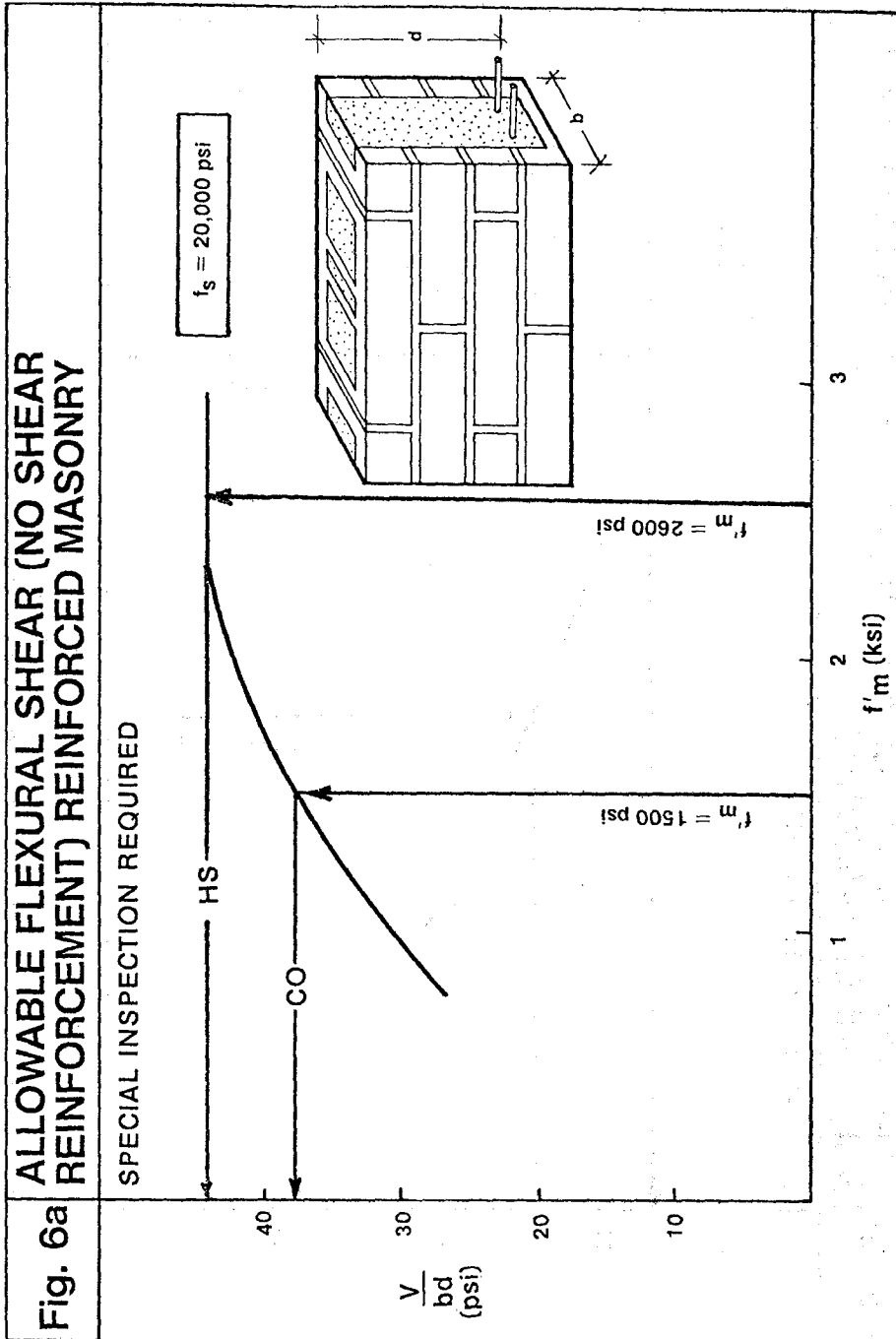


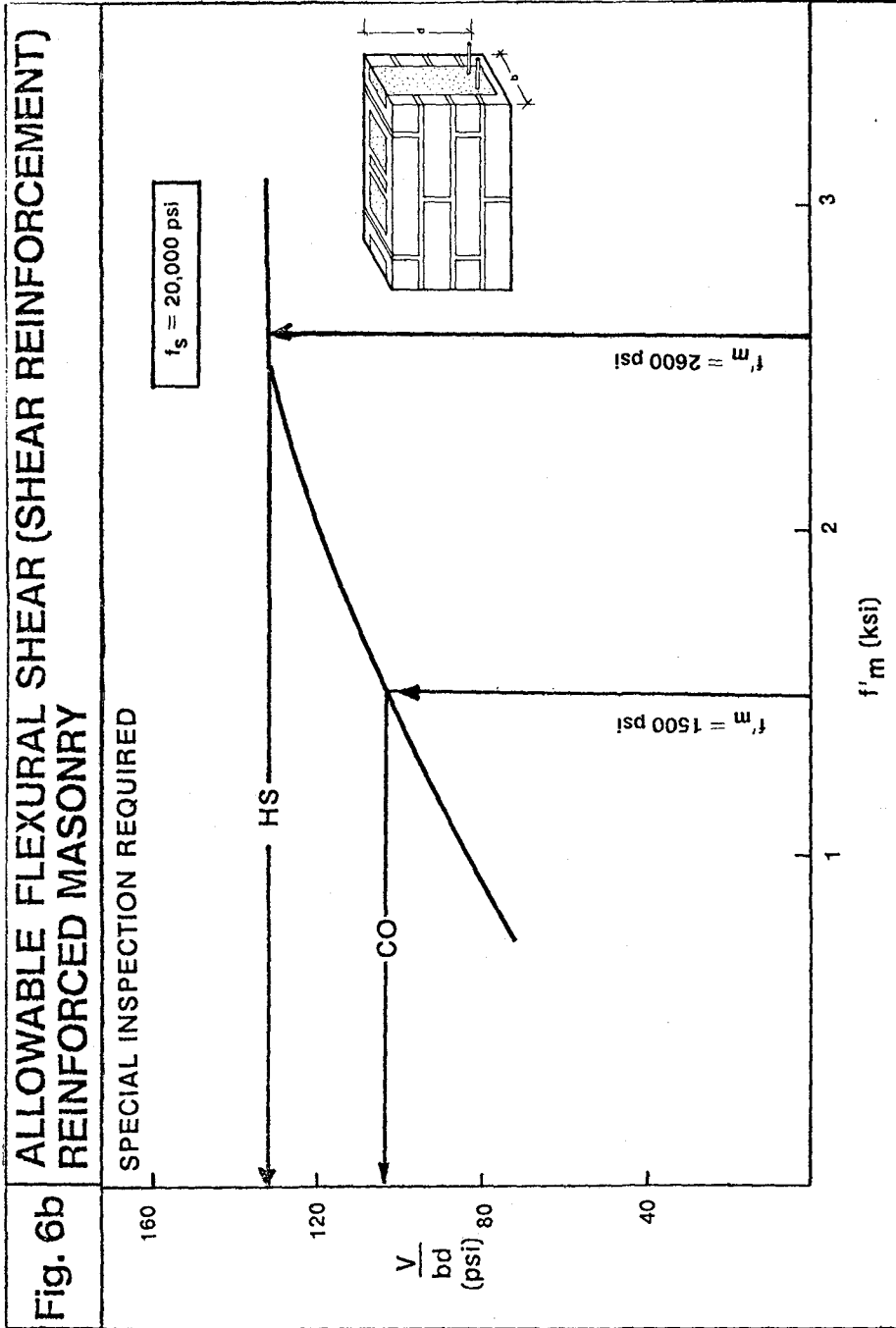


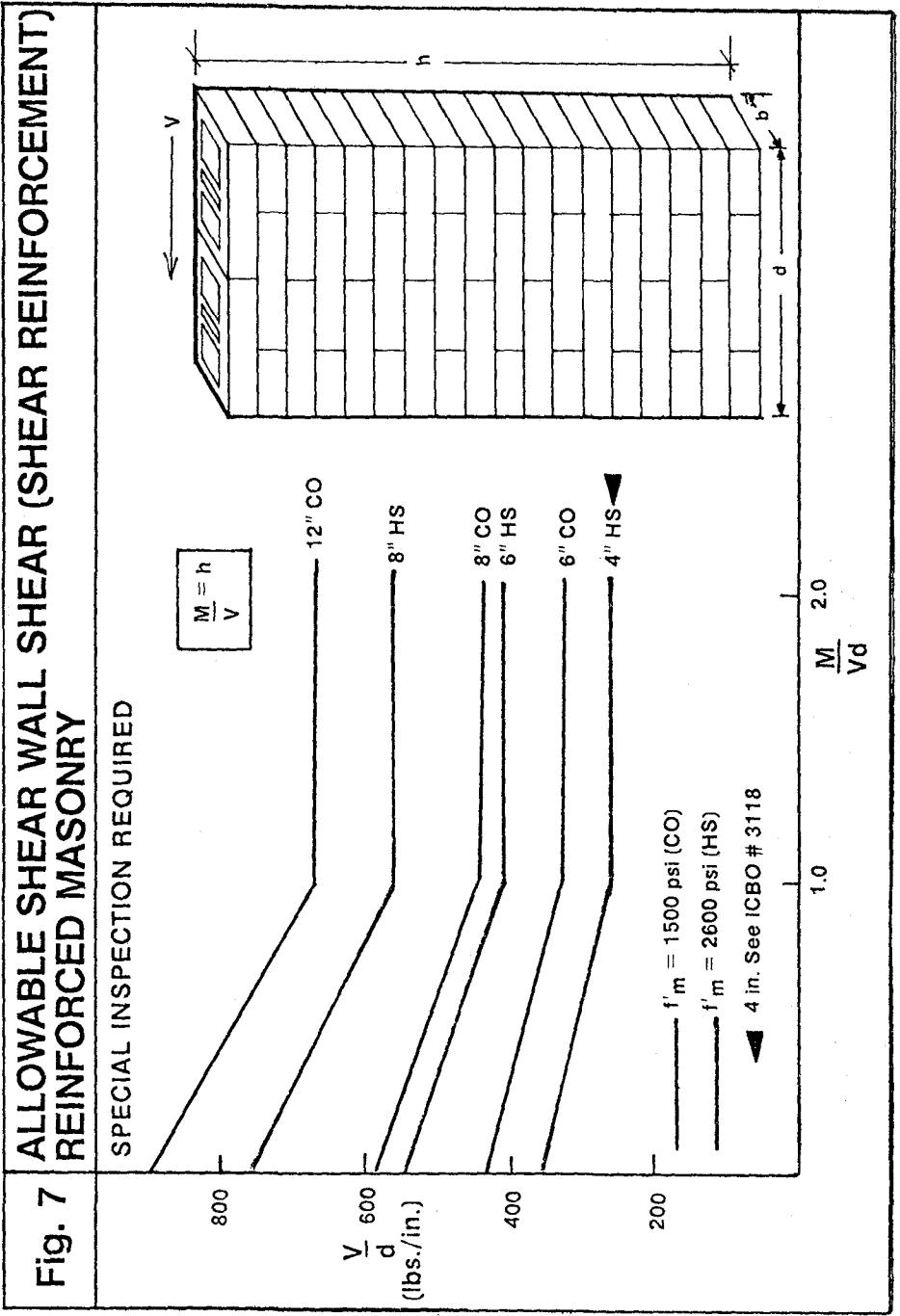


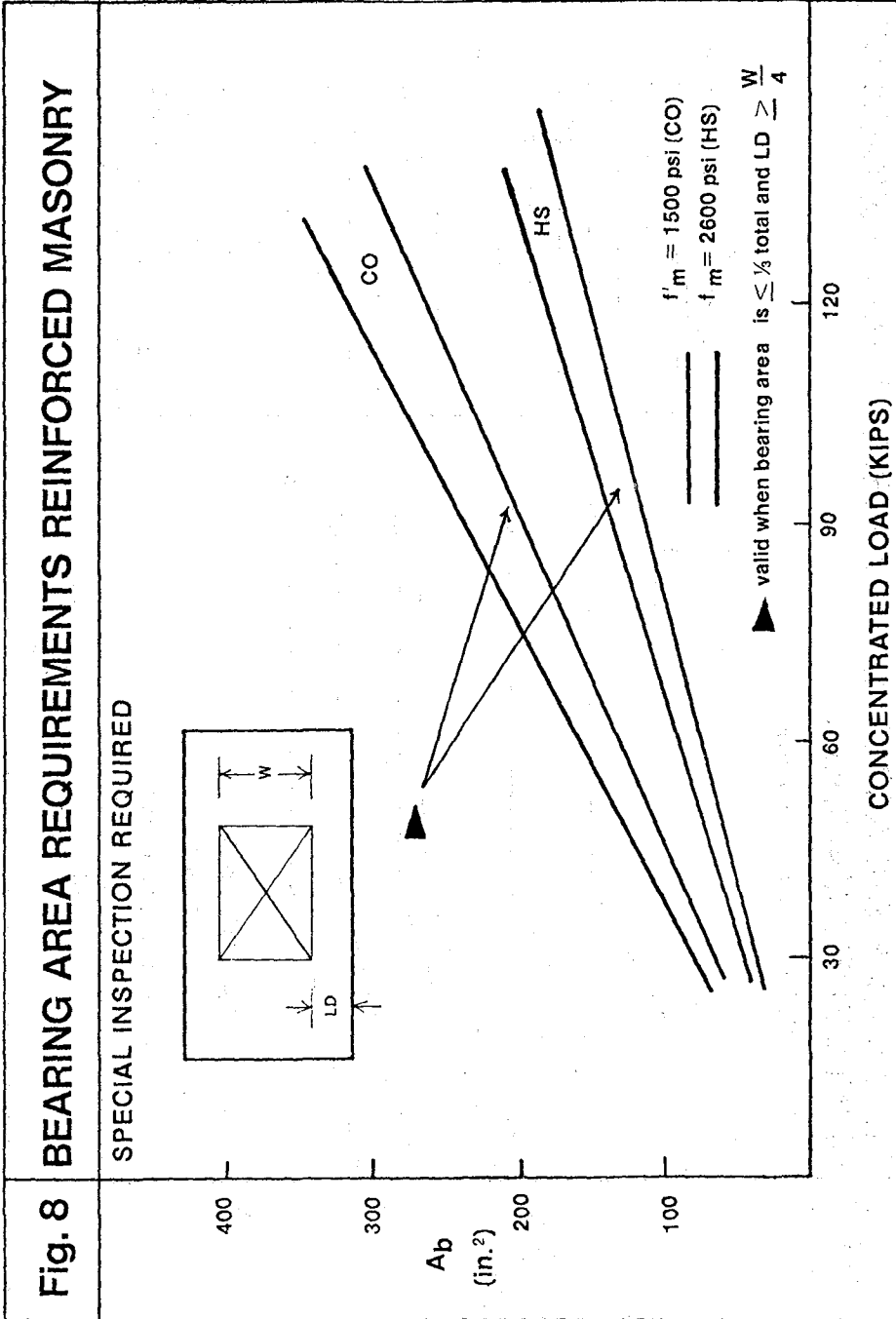












Nomenclature

A_b	total direct bearing area
A_g	gross cross-sectional area
b	width of rectangular section
C	stress reduction factor
CO	conventional strength masonry
d	depth from compression face of beam to centroid of longitudinal tensile reinforcement
e	eccentricity
f_{brg}	bearing unit stress
f_m	allowable compressive unit stress in masonry
f'_m	ultimate compressive masonry strength
f_s	allowable stress in reinforcement
h	clear unsupported distance
H-S	high-strength masonry
j	ratio of distance between centroid of compression and centroid of tension to depth d
LD	least dimension
M	external moment
P	maximum concentric column axial load
P_g	ratio of area of vertical reinforcement to gross area
t	least thickness
v	shearing unit stress
V	total shear
W	width direct bearing area



BASIC PRINCIPLES OF STRUCTURAL MECHANICS OF TALL MASONRY BUILDINGS

By P. T. Mikluchin

ABSTRACT: Uniqueness of structural performance of tall masonry buildings is outlined. Uniform analytical approach to three-dimensional structural analysis of tall masonry bearing wall buildings is presented. Investigation of distribution of stresses, strains and deformations due to static loads is carried out and used as a basic for the dynamic analysis subsequently outlined. Static and dynamic stability problems are discussed. Dynamic problems of stress and strain distribution in masonry structures subjected to wind and seismic forces are outlined. Necessity of dynamic approach to the consideration of wind-induced vibrations is mentioned. Simultaneous occurrence of axial and flexural-torsional vibrations and their interdependence are discussed. Problems of structural integrity and progressive collapse are considered. Possibility of limit states design approach is discussed.

BASIC PRINCIPLES OF STRUCTURAL
MECHANICS OF TALL MASONRY BUILDINGS

By Plato T. Mikluchin

1. INTRODUCTION

An attempt is made to present a conceptual framework, underlying the basic principles of structural mechanics of tall masonry buildings considered in their totality, together with the outline of the structural analysis of such buildings, subjected to the action of static and dynamic forces.

Generally, modern tall masonry bearing wall buildings are three-dimensional, multicellular constructions, consisting, principally, of sets of vertical thin-walled prismatic or curvilinear shells of various geometric configurations, interconnected with sets of horizontal slabs and behaving, in response to the action of external forces as continuous, integral structures.

From the standpoint of structural mechanics such buildings are vertical cantilevered three-dimensional structures, rigidly or flexibly fixed at the bottom and free to move at the top, and possessing well defined boundary conditions.

Complete structural continuity of all constituent elements in three-dimensional space, if desired, can be achieved in the construction of tall masonry buildings.

Structural framework in such buildings becomes a complete three-dimensional continuum.

Due to this circuit continuity there are no inert or passive structural parts in such buildings. Every point, within the structure participates in responding effectively to any force acting on a building.

Tall masonry bearing wall structures, properly constructed, and, if necessary, reinforced, show a superior structural performance in resisting the effects of various combinations of static and dynamic forces acting on such structures.

President, P.T. Mikluchin & Associates Limited, Consulting
Structural Engineers, Toronto, Ontario.

2. BASIC ASSUMPTIONS

A series of assumptions which can be readily justified, are introduced in this paper for the purpose of constructing a logical framework of theory of design of tall masonry buildings.

2.1 Assumptions Concerning the Geometry of Buildings.

Vertical bearing elements (walls) can have any geometric configuration in horizontal plane. Such walls could be in form of vertical curvilinear shells, polygonal prismatic shells, tubular multicellular structural elements, extending full height of the structure, or any other combinations of vertical walls with arbitrary arrangement in their layout.

Wall thickness can vary along the contour of the building but should remain constant along the full height of the structure.

Horizontal elements (floors) have the same thickness.

They are equally spaced along the vertical axis of the structure.

2.2 Assumptions Concerning the Structural Behaviour of Buildings

Vertical elements are flexible structural members, possessing definite axial and flexural-torsional characteristics.

All horizontal elements are assumed to be infinitely rigid in their own planes.

If the length and width of a structure, in plan, are of the same order of magnitude, this assumption can easily be justified. In case of long and narrow buildings, this assumption does not introduce any considerable errors, provided the degrees of stiffnesses of constituent bearing walls are sufficiently uniform along principal axes of the structure.

If these stiffnesses are not distributed uniformly, the deformations of the floors in their planes should be taken into account. Floor slabs are assumed to have zero rigidity in the direction perpendicular to their planes.

2.3 Assumptions Concerning the Mechanical Properties of Building Materials

Despite the fact that masonry materials in buildings consisting of masonry units and mortars sometimes combined with reinforcement and metal anchors, cannot be regarded, on a microscopic scale, as elastic, isotropic and homogeneous, the assumption of elasticity, isotropy and homogeneity, when applied to the whole masonry structure, on microscopic scale, does not lead to any

considerable discrepancies between the theoretical and experimental results.

This means that the hypotheses of Theory of Elasticity concerning the relationship between created within the structure by the action of external forces are considered to be valid.

If material of bearing walls in a building is not linearly elastic, such building can be analyzed with the help of the method outlined below, provided the nonlinearity is expressed in precise form and the results of analysis are accordingly modified.

3.1 Types of Tall Masonry Buildings

Tall load-bearing multistory masonry buildings with various wall layouts can be divided into the following types:-

Buildings with open multicellular wall layout.
Buildings with closed multicellular wall layout.
Buildings with mixed multicellular wall layout.

Each of these types of buildings could be subdivided into two sub-types:

buildings of multicellular cross-sectional profile with floor slabs acting as horizontal diaphragms, possessing infinite rigidity in their planes and zero rigidity perpendicular to their planes and

buildings of multicellular cross-sectional profile with floor slabs, possessing finite rigidity in their planes and zero rigidity perpendicular to their planes.

Majority of modern masonry bearing wall buildings belong to either first type or third type. Buildings with closed multicellular wall layout are used seldom and are limited to specialized structures.

4.1 Static Analysis of Tall Masonry Buildings

On the basis of the assumptions outlined above a comprehensive theory of analysis of tall masonry buildings can be developed and the general principles of practical design can be established. The aim of such analysis is to investigate the overall structural behaviour of tall buildings subjected to the action of external forces.

The results of the analysis will provide the designer with the information concerning the distribution, direction and magnitude of internal stresses and strains within the body of the structure and the changes in the exterior form of the structure itself.

On the basis of this analysis a designer can design structures possessing necessary strength, stiffness, stability and resistance to static and dynamic forces and effects.

4.2 Analysis of Internal Stresses and Strains Due to Action of External Forces

In order to determine the internal stresses and strains in any point of a structure, subjected to the action of a system of external forces, and evaluate the deformations of such a structure, the general theory of thin walled structures in form of vertical curvilinear of prismatic shells (1,2) in appropriately modified form can be used. All basic assumptions of general theory of thin walled structures are considered to be valid.

4.3 Basic Differential Equation of Equilibrium

The basic eighth order differential equation, which establishes the relationship between the external forces and internal stresses and strains in a shell can be presented in the following form:

$$\Omega \Omega \phi(z,s) + \frac{12}{h^3} \cdot \frac{\partial^4 \phi(z,s)}{\partial z^4} = P(z,s) \quad \dots (1)$$

where:

$$\Omega = \frac{\partial^2}{\partial s^2} \left(R \frac{\partial^2}{\partial s^2} \right) + \frac{\partial}{\partial s} \left(\frac{1}{R} \cdot \frac{\partial}{\partial s} \right)$$

- $\phi(z,s)$ - stress function,
 h - thickness of the shell,
 z and s - co-ordinates of a point on the middle surface of the shell (z is directed along vertical z -axis, " s " is directed along the contour of the shell).
 $P(z,s)$ - a given load function, expressed through the components P_z, P_s, P_n , of the vector of intensity of external forces acting on the shell,
 $R=R(s)$ - radius of the middle surface of the shell.

The stress function $\phi(z,s)$ which satisfies the differential equation (1) and given boundary conditions provides the solution of the problem. All stresses and displacements in any point of the structure can be expressed by means of stress function $\phi(z,s)$.

It can be shown that differential equation (1) is equivalent to a system of two symmetrical equations establishing direct relationship between normal force $N(z,s)$ and transversal bending moment $G(z,s)$ in the following form:

$$\frac{\partial^2 [\sigma(z,s)h]}{\partial z^2} + \Omega G(z,s) = P(z,s) \quad \dots (2)$$

$$\Omega \sigma(z,s) - \frac{12}{h^3} \cdot \frac{\partial^2 G(z,s)}{\partial z^2} = 0 \quad \dots (3)$$

In cases when floor slabs can be considered as absolutely rigid diaphragms in their own planes, and, consequently profiles of bearing walls as nondeformable, transversal bending moment $G(z,s)$ becomes zero.

Then from equation 3 we obtain:

$$\Omega \sigma(z,s) = \frac{\partial^2}{\partial s^2} \left(R \frac{\partial^2 \sigma(z,s)}{\partial s^2} \right) + \frac{\partial}{\partial s} \left(\frac{1}{R} \frac{\partial \sigma(z,s)}{\partial s} \right) = 0 \quad \dots (4)$$

and the solution of the problem can be obtained from this single equation.

Equation (4) is the basic differential equation which could be used for the solution of problems connected with analysis of stress and strain distribution in vertical prismatic thin-walled structures in form of various types of bearing walls, arranged in any desirable combinations, and floors acting as rigid diaphragms.

Although stress function $\phi(z,s)$ obtained from equation (1) gives a solution of the problem of stress and strain distribution in the structure in a very general form, quite often the system of equations (2,3) can provide more direct solution.

Equations (1) or (4) can be used for structural analysis of tall buildings with bearing wall systems of arbitrary open layout with rigid or flexible, in their own planes, horizontal floor slabs. The theory described above can easily be modified and applied to the design of tall buildings with semi-open or closed layouts of bearing walls.

For this purpose, geometric factors, characterising the flexural-torsional rigidity of the cross-section of bearing walls have to be modified. But the general approach to the solution of the problem of stress and strain distribution remains the same.

In case when bearing walls used in tall buildings, instead of being curvilinear in their layout, have configurations in form of prismatic polygonal vertical shells with finite number of vertical shells with finite number of vertical rectangular panels, system of equations (2,3) can be replaced with the equivalent system:

$$\begin{aligned} \sum a_{ik} \sigma_k''(z) + \sum b_{ik} G_k(z) + P_i(z) &= 0 \\ \sum b_{ik} \sigma_k(z) - \sum c_{ik} G_k''(z) &= 0 \end{aligned} \quad \dots (5)$$

Where $\sigma(z,s)$ and $G(z,s)$ are unknown functions, representing longitudinal normal stresses and transverse bending moments, acting along K-ridges of prismatic shells. Coefficients a_{ix} , b_{ix} , c_{ix} are constants expressed in terms of geometric characteristics of the shell under consideration.

4.4 Determination of Normal Stresses

Taking into consideration the fundamental equations of the Theory of Elasticity, solution of equation (4) can be presented in the following form:

$$\sigma(z,s) = F_1(z) + F_2(z)y(s) + F_3(z)x(s) + F_4(z)w(s) \quad \dots (6)$$

where: $F_1(z); F_2(z); F_3(z); F_4(z)$ = functions of integration
 = co-ordinates of the middle surface of bearing walls
 = sectorial co-ordinate

It can be shown that functions F_1, F_2, F_3, F_4 in the equation (6) have the following meaning:

$$\sigma(z,s) = \frac{P(z,s)}{A_s} + \frac{M_x(z)}{I_x} y(s) + \frac{M_y(z)}{I_y} x(s) + \frac{M_B(z)}{I_W} w(s), \quad \dots (7)$$

Where: $N(z,s)$ - total normal force parallel to z-axis
 A - cross-sectional area of bearing wall
 $M_x(z)$ - bending moment with respect to x-axis
 I_x - moment of inertia with respect to x-axis
 $M_y(z)$ - bending moment with respect to y-axis
 I_y - moment of inertia with respect to y-axis
 $M_B(z)$ - bimoment
 I_W - sectorial moment of inertia.

In order to determine $M_B(z)$ it is necessary to express the bimoment as a function of the angle of rotation, $\theta(z)$, related to the flexural centre:

$$M_B(z) = -E I_W \theta''(z) \quad \dots (8)$$

Value of $\theta''(z)$ may be obtained from the following equation:

$$E I_W \theta^{IV}(z) - G I_p \theta''(z) + m(z) = 0 \quad \dots (9)$$

Where: EI_W - sectorial rigidity
 GI_p - torsional rigidity
 $m(z)$ - external torsional moment per unit length in z-direction.

This equation, with corresponding boundary conditions, determines an angle of rotation, $\theta(z)$, as a function of the co-ordinate z . The general solution of equation 9 has the following form:

$$\theta(z) = C_1 + C_2 \frac{z}{\rho} + C_3 \sinh \frac{\kappa}{\rho} z + C_4 \cosh \frac{\kappa}{\rho} z + \bar{\theta}(z) \quad \dots (10)$$

where: C_1, C_2, C_3, C_4 - are constants of integration
 $\bar{\theta}(z)$ - particular solution of the differential equation

$$\kappa = \rho \sqrt{\frac{GI_p}{EI_W}} \quad - \text{ flexural-torsional coefficient.}$$

All derivatives of equation (10) may be readily obtained and evaluated. The angle of rotation, $\theta(z)$, is related to the flexural centre, whose co-ordinates, x_C and y_C are:

$$x = \frac{\int y(s) h w(s) ds}{\int y^2(s) h ds} \quad y = \frac{\int x(s) h w(s) ds}{\int y^2(s) h ds} \quad \dots (11)$$

4.5 Determination of Shear Stresses

In addition to $G(z,s)$ it is necessary to determine the magnitude of shear stresses $\tau(z,s)$. They can be found from the following equation:

$$\tau(z,s) = \frac{E}{h} [\xi'''(z)h ds + \xi'''(z)S_y(s) + \eta'''(z)S_x(s) + \theta'''(z)S_w(s)] \quad \dots (12)$$

where: $S_y(s) = \int x(s) h ds$
 $S_x(s) = \int y(s) h ds$
 $S_w(s) = \int w(s) h ds$

ξ, η, ζ, θ - are deformations of the shell along x, y, z , - directions at any point of the shell.

Equation (12) may be presented as the following form:

$$\tau(z,s) = F_1'(z) + F_2'(z)S_y(s) + F_3'(z)S_x(s) + F_4'(z)S_w(s) \quad \dots (13)$$

Where: $F_1(z), F_2(z), F_3(z), F_4(z)$ are certain functions.

These functions have the following meaning:

$$\tau(z,s) = \frac{M_K(z)}{I_P} h + \frac{V_X(z)}{I_y h} S_y(s) + \frac{V_Y(z)}{I_x h} S_x(s) + \frac{M_W(z)}{I_W h} S_w(s) \quad \dots (14)$$

where: $M_K(z)$ - torsional moment
 I_P - torsional moment of inertia
 $V_X(z)$ - shear force on xoz plane along x-axis
 $M_W(z)$ - warping torsional moment

The moments $M_K(z)$ and $M_W(z)$ may be expressed as functions of the angle of rotation θ :

$$M_K(z) = GI_P \theta' (z) \quad \dots (15)$$

$$M_W(z) = M'_B (z) = -EI_W \theta''' (z) \quad \dots (16)$$

Total torsional moment $M_T(z)$

$$M_T(z) = M_K(z) + M_W(z) \quad \dots (17)$$

Constants of integration C_1, C_2, C_3, C_4 can be determined considering the given boundary conditions. For tall masonry structures number of these conditions always equals four (two at each end of the structure).

4.6 Determination of Displacements

Having determined all normal and shear stresses it is necessary to evaluate the magnitudes of various displacements in any given point of the structure.

These displacements can be determined by adding vectorially the displacements resulting from external loading in two principal directions and torsional moments. The displacement resulting from torsional effects is obtained by multiplying the appropriate $\theta (z)$ value, by the distance from the flexural centre to the point under consideration.

5.1 Problem of Static Stability of Tall Masonry Buildings

In general case of tall multistory masonry bearing wall structures with thin-walled open or closed cross-sections, phenomenon of instability can take place, due to combined action of axial, torsional and flexural effects. [2]

Majority of modern masonry buildings, with normal dimensions in plan possess a high degree of stability. However, if such buildings are very high and slender, the analysis of stability should be undertaken.

In case of tall buildings, symmetrical in their layout with respect to principal axes, subjected to the action of exterior forces, such building before the loss of stability exhibit axial and flexural deformations only.

After the loss of stability, in addition to axial and flexural deformations, torsional deformations take place, accompanied by the general warping of the whole cross-section of the structure. A qualitatively new form of general deformation of the structure takes place. If the loss of stability is characterised by the flexural deformations only, this form of instability is flexural form of instability.

If the loss of stability is characterised by the appearance of flexural and torsional deformations this form of instability is flexural-torsional form of instability.

In general case of non-symmetrical arrangements of bearing walls this second form of instability should be investigated. Generally, structures similar to thin-walled multistory buildings possess seven degrees of freedom. Consequently seven types of deformations with corresponding systems of internal stress distributions can take place, in such structures. These deformations are:

- a) Axial deformations parallel to z-axis
- b) Shear deformations parallel to x-axis
- c) Shear deformations parallel to y-axis
- d) Torsional deformations about z-axis
- e) Flexural deformations about x-axis
- f) Flexural deformations about y-axis
- g) Warping deformations of all cross-sections.

In case of structures subjected to the action of vertical forces only, all potential energy accumulated in the structure, before the loss of stability, would be compression energy. After the loss of stability, this energy would be distributed among the above mentioned seven states of deformations within this structure. This distribution of potential energy depends mainly on the geometric shape and dimensions of the structure. Analysis of thin-walled tall structures shows that portion of energy which is going into creation of the state of warping, corresponding to the seventh degree of freedom, is very substantial and cannot be neglected in the analysis of the problem of stability.

Consequently, the classical theory of stability must be modified accordingly by taking into account the effect of warping. In this connection it must be pointed out that since the critical loading, acting on the structure always consists of certain combinations of gravity forces, the bifurcation loads could seldom be considered as realistic criteria determining the stability limits for tall slender bearing wall structures.

In other words the first type of instability, when sudden qualitatively new forms of deformations of this structure could take place, is improbable.

The second type of instability, when no qualitatively new form of deformations of the structure appear, but only quantitative changes in initially developed form of deformations continue to take place is the realistic type of instability for tall buildings.

5.2 Basic Differential Equations of Stability

The phenomenon of loss of stability of tall bearing wall buildings can be analyzed by means of a system of differential equations of stability.

Without going into the derivation of this system of equations it can be shown that using basic system of differential equations of equilibrium and analyzing the process of the transition from one form of equilibrium to the other form, which, becomes unstable, it is possible to derive a general system of differential equations of stability of multistory bearing wall structures, subjected to the simultaneous action of axial and flexural forces. [1]

In these equations unknown functions are displacements resulting from the change of flexural deformations, which take place during the stable form of equilibrium, into flexural-torsional deformations occurring after the loss of stability.

Such system of equations describes the general case of the loss of stability of tall masonry buildings.

5.3 Solutions of the System of Differential Equations of Stability

The exact solution of this system of equations can be obtained for a limited number of cases. If the loads are constant, solution can be found without difficulties. In general case, the approximate solution based on the application of one of the variational methods, can be obtained.

Equating the determinant of this system of equations to zero, we obtain an equation for determination of the magnitude of critical load. Roots of this equation give us three values of critical loads, corresponding to three flexural-torsional forms of loss of stability, the smallest of these three values is the critical load. The method described above is valid for the most general case of complex system of loads acting on a structure and non-symmetrical, irregular plan layout of bearing walls.

As it was mentioned earlier, the investigation of stability is necessary only for very tall and slender buildings. In the context of this paper, problem of stability is meant to refer to the investigation of stability of the total structure in three-dimensional space. This kind of stability could be defined as overall stability. In the portions of the structure where stresses and strains are the highest, local stability should also be investigated. This kind of stability could be defined as local stability. Main goal of stability analysis is the determination of the magnitude of the critical load and the probable deformed shape of the structure after the loss of stability.

6.1 Problem of Dynamic Stability of Buildings

Tall slender bearing wall structures exposed to wind or earthquake loads, experience simultaneous dynamic action of axial and flexural-torsional stresses and strains, For some types of structures with the certain degree of stiffness, frequency and magnitude of internal dynamic stresses and strains created by external forces, may cause a set of critical vibrations in three dimensional space, even in cases when the stresses are below the critical value. In such cases the amplitude of vibrations can reach very large values. This phenomenon is known as dynamic instability. Differential equation of stability condition for a structure can be derived and solved. [2]

If the analytical solution of this equation becomes unbounded then the analyzed structure is dynamically unstable.

Usually, presence of non-linear elastic response of the structure and soils, non-linear behaviour of wind and earthquake forces, and non-linear damping affect over-all dynamic behaviour of the structure and produce stabilizing effect.

7.1 Dynamic Analysis of Buildings

Dynamic behaviour of tall masonry structures is essentially determined by the following factors:

Stiffness distribution of the structure; mass distribution within the body of the structure; energy absorption capacity of the structure.

The knowledge of dynamic characteristics of a masonry structure is necessary for the evaluation of magnitudes of loads, resulting from the action of wind and earthquake forces. The fundamental natural frequency of vibrations of the structural system is of paramount importance for the solution of dynamic problems occurring in tall slender masonry structures.

If the external dynamic forces acting on the structure, possess certain frequency, it is necessary to check it against the natural frequencies of vibrations of the structure. If these frequencies coincide, the phenomenon of resonance takes place, accompanied by the rapid growth of stresses and deformations, which, if allowed to develop, would, ultimately lead to the destruction of the building. In order to prevent the occurrence of the resonance, it is necessary to explore the problem of dynamic processes governing the action of external forces and the behaviour of the structure.

Dynamic characteristics of external forces are given or determined on the basis of information contained in building codes or other appropriate sources.

7.2 Differential Equations of Vibration of Tall Buildings

Dynamic characteristics of the structure under consideration can be determined from the solution of the problem of natural vibrations of the structure in three-dimensional space. For the solution of this problem the well known Principle of D'Alembert allows us to study the dynamic problem as the static problem provided that to the system of external static forces, a system of inertial forces, expressed as functions of displacements of the structure, is added.

In expressing inertial forces through the mass and acceleration of force of gravity we can obtain the system of four differential equations, describing free natural vibrations of the tall masonry structures.

It could be shown from this system of equations that first equation describes axial vibrations of the structure along OZ axis and is independent of other equations. Second, third and fourth equations form a special interdependent system, describing flexural-torsional vibrations of the whole structure. In case of structure possessing two axis of symmetry all four equations become independent. In this case, first equation describes axial vibrations along OZ axis, second and third equations describe flexural vibrations in ZOY and ZOX planes, and fourth equation describes torsional vibrations about the vertical axis OZ located in the flexural center of the structure.

It means that independent flexural vibrations in ZOY and ZOX planes and torsional vibrations about OZ axis can take place only then, when the center of gravity of the structure coincides with the flexural centre. In all other cases flexural and torsional vibrations are always interdependent and should not be treated separately.

For dynamic analysis of the structure, three principal frequencies, K_{nx} , K_{ny} , K_{nw} are of fundamental importance. K_{nx} , K_{ny} - are frequencies of flexural vibrations in Zox , ZOY planes.

K_{nw} - is the frequency of torsional vibrations of the structure about z -axis, going through the flexural center.

7.3 Dynamic Effects of wind Forces

Tall slender bearing wall buildings should be designed using a dynamic approach, when considering the effects of wind gusts. This has to be done in all those cases, when the tall slender buildings under consideration are likely to be susceptible to wind-induced vibrations.

Buffetting vibrations are the most common vibrations of the structure, subjected to the turbulent wind action, which is created by fluctuating wind pressures, acting on the exterior surface of the building. The effect of these vibrations should be considered together with the effect of the static wind pressure. The resulting stresses could be much higher than stresses due to the mean wind pressure.

Load magnification effect created by gusts acting in resonance with the structure oscillating at the fundamental natural frequency, characteristic for this particular structure should be taken into account in design of buildings.

Structural behaviour of tall slender bearing wall structures subjected to the action of randomly fluctuating wind-forces can be studied by considering such structures as vertical cantilevers, whose dynamic characteristics are determined by definite natural frequencies and corresponding damping values of buildings under consideration.

Knowing the intensity of wind turbulence for the particular location of the building and geometric and structural characteristics of this building, such as height, length, width, fundamental natural frequency of vibrations of the structure and its damping capacity, it is possible to carry out a complete structural analysis of the building, subjected to wind forces. Since, in general, almost all tall slender buildings are subject to torsional deformations due to the action of random exterior forces, then the designer must be cognizant of the fact, that if torsional rigidity of the building is insufficient, then in certain cases, a phenomenon of torsional flutter of the building could take place. If flexural rigidity of horizontal floor slabs is insufficient then vibrations of floor slabs in their own plane can occur, creating a complex three-dimensional vibrations of the whole structure.

7.4 Dynamic Effects of Seismic Forces

Dynamic analysis of tall buildings requires a general evaluation of structural response of these buildings, subjected to the action of earthquake forces.

An average response spectrum approach could be used for this purpose.

The response of a structure can be obtained from the analysis of the deformed state of the structure and by summing the contributions of its natural modes.

The natural modes and corresponding periods of vibrations for any tall structure can be found from the system of four differential equations mentioned earlier.

The lateral forces $P_{i,j}$ acting on a tall building, for any mode i , of vibrations and at any floor level j , have to be determined.

All design lateral forces, story shears, and bending and torsional moments and lateral displacements can be obtained, considering the forces $P_{i,j}$ from each natural mode i , as individual loading cases.

Torsional moments M_j at any floor j , can be determined from

$$M_j = P_j \cdot e_d \quad \dots (18)$$

Where P_j - lateral force at j floor level, e_d - distance from the center of mass to the flexural center.

Total torsional moments at floor $j = k$ are

$$M_k = \sum_{j=n}^K M_j \quad \dots (19)$$

The lateral displacements D_j , j for any mode i , and floor level j , can be determined.

In general, in order to determine the displacement D_k at level $j=k$, it is sufficient to consider only the displacements in the fundamental mode.

In case of tall slender masonry bearing wall buildings, it is advisable to consider vertical displacements due to the action of the vertical component of the seismic motion.

Some of the codes require the consideration of so called coupled analysis, where torsional modes must be considered coupled with translational modes if the centers of mass and flexural center are separated more than $0, 10 D_n$, where D_n is a base dimension of structure normal to the direction of seismic force.

If the approach described in this paper, is used, this coupling procedure is not necessary, because the simultaneous effects of flexural and torsional phenomena have been already taken into account.

8.1 Problems of Structural Integrity

The planning and design of tall masonry buildings shall be governed by the general demands of the principle of structural integrity and adequate strength and stability requirements, in order to eliminate or minimize the probability of progressive collapse. Progressive collapse is a phenomenon, characterized by the propagation of the initial local failure, which could take place in any location in the building, to the other parts of the building, through the sequence of chain reaction failures and leading to eventual collapse of the building or a large portion of it.

In case of dynamic forces, acting on a building the concept of structural integrity is of great importance.

The possibility of occurrence of this phenomenon should be constantly kept in mind during the process of design of tall masonry buildings. Due to the increase in numbers of tall masonry buildings, proper construction practices, adequate reinforcement and anchorage of walls, slabs and joints are of paramount importance.

Strategically chosen plan layout of bearing walls containing the favourable arrangement of longitudinal and transversal walls should be a goal of a designer.

In addition to the proper layout of walls, the other measures could be of value. For instance, returns on external and internal walls contribute to strength and stability of the building. Potential effects of arching and beam action of bearing walls are important for beneficial three-dimensional behaviour of building. Changes in the direction of spans in certain areas of floors are also helpful. Other ingenious measures can be used for increasing the structural integrity of the buildings.

9.1 Masonry Buildings and Limit States Design

Limit states design can be used as an alternative method to existing procedures for static and dynamic design of tall bearing wall structures. Such structures should be safe from collapse and be serviceable during the normal life of the building.

Critical stages reached by the structure, during the process of loading, and characterized by particular types of collapse and unserviceability are called limit states. The class of limit states related to the problem of safety of the buildings are termed, ultimate limit states. They include the reaching of load bearing capacity, overturning, sliding, fracture.

The class of limit states, related to the problem of serviceability are termed serviceability limit states. They include among others, excessive deflections, cracking, vibrations.

The principal purpose of limit states design is to avoid the reaching of limit states, in order to prevent various types of failure.

10.1 Conclusion

Modern tall masonry buildings subjected to the action of static and dynamic forces should be designed as three-dimensional thin-walled structures, acting as one whole complex.

Reduction of a 3 dimensional structural system to a series of 2 dimensional elements does not and cannot reflect the actual performance and overall structural behaviour of an original space structure.

Such an artificial operation results in unnecessary expenditure of structural material in a substitute system and makes it difficult to assess the actual factor of safety of the original structural system.

It means that no continuous space structure can be reduced to a series of discrete plane elements, however, ingeniously chosen without wasting additional structural material and making the system less reliable.

Design of modern tall masonry buildings is a complex process, involving the solution of a series of problems, concerned with creation of a continuous three-dimensional multicellular structure, satisfying certain imposed physical space requirements, architectural and engineering demands and economic considerations.

Optimal arrangement of principal bearing walls is of great importance for obtaining well functioning and structurally sound masonry buildings.

The successful development of a well chosen topological system of bearing walls layout requires on the part of the designer, an intimate knowledge of architectural and engineering concepts, creative imagination, experience, intuition and refined aesthetic sensibilities.

REFERENCES

1. Timoshenko, S.P., Theory of Bending, Torsion and Buckling of thin-walled Members of open Cross-Section. Journal of the Franklin Institute, 1945.
2. Vlasov, V.A., Thin Walled Elastic Beams. National Science Foundation, Washington, D.C., 1961.
3. Coull A., and Smith, B.S., Analysis of Shear Walls (A Review of Previous Research), Tall Buildings, Pergamon Press Limited, London, 1967 pp. 139-155.
4. Tso, W.K. and Biswas, J.K., "Analysis of Core Wall Structure Subjected to Applied Torque," Building Science, Vol. 8, 1973, pp. 251-257.
5. Mikluchin, P.T., Design of tall masonry buildings with complex layout. The International Conference on Masonry Structural Systems, University of Texas, Austin, Texas, U.S.A. 1969.
6. Michael, D., "Torsional Coupling of Core Walls in Tall Buildings," Structural Engineer, Vol. 47. 1969, pp. 67-71.
7. Stamato, M.C., Three Dimensional Analysis of Tall Buildings, ASCE-IABSE International Conference on Planning and Design of Tall Buildings, Lehigh University, Bethlehem, Pa., 1972.
8. Richter, P.J., Reddy D.P., Agbabian, M.S., Three Dimensional Dynamic Analysis of Multistory Concrete Office Building. ACI Publication Sp 36-8. 1973.
9. Coull, A., and Irwin, A.W. Analysis of load distribution in multistory shear wall structures. The Structural Engineer, London. V.48, No. 8. 1970.
10. Mikluchin, P.T., with Tamberg K.G., Torsional Phenomena Analysis and Concrete Structure Design. A.C.I. Publication SP35-1, 1973.
11. Davenport, A.G., New approaches to the Design of Structures against wind action. Proc. Canadian Structural Engineering Conference, Toronto, 1968.
12. Wind Effect on Buildings and Structures, International Wind Conference, Tokyo, Japan. September 1971.
13. Response of Buildings to Lateral Forces, by the American Concrete Institute Committee 442, Journal of the American Concrete Institute, Vol. 68, No. 2, Feb. 1971, pp. 81-106.

14. National Building Code of Canada, 1975, NRCC No. 13982.
15. Blume, J.A., Structural Dynamics of Cantilever-Type Buildings, Proceedings, Fourth World Conference on Earthquake Engineering, Santiago, Chile, 1969.
16. Newmark, N.M. and Rosenblueth, E., Fundamentals of Earthquake Engineering, Prentice Hall, Inc., Englewood Cliffs, N.J., 1971.
17. Fintel, M., Ductile Shear Walls in Earthquake-Resistant Multistory Buildings. Journal of ACI. Vol. 71, June, 1974.
18. Mikluchin, P.T., Morphotectonics of Masonry Structures, The Proceedings at the International Conference on Masonry Structural Systems, University of Texas, Austin, Texas, U.S.A. 1969.
19. Haller, P., The Technological Properties of Brick Masonry in Masonry in High Buildings, Technical Translation 792, National Research Council, Canada, 1959.
20. Hendry, A.W., Wind Load Analysis of Multi-storey Brickwork Structures, Research Note Vol. 1, #3, January, 1971. Brick Development Association.
21. Heidebrecht A.C., and Stafford-Smith, B., "Approximate Analysis of Tall Wall-Frame Structures", Journal of the Structural Division, ASCE, Vol. 99, No. ST2, February, 1973, pp. 199-221.
22. Amrhein, J.E. Reinforced Masonry Engineering Handbook. Masonry Institute of American, Los Angeles, Cal., 1973.
23. Heidebrecht, A.C., Dynamic Analysis of Asymmetric Wall-Frame Buildings, ASCE National Structural Engineering Convention, April, 1975, New Orleans, Louisiana.
24. Johnson, Dr. Franklin, Editor. Proceedings of the International Conference on Masonry Structural Systems, Austin, Texas, 1969.

Some of the Suggested Topics for Research

1. Study of the mechanism of the failure of masonry buildings, subjected to earthquake forces.
2. Change in patterns of absorbed strain energy distribution in walls before and after cracking.
3. Evaluation of strength, stiffness and hysteretic characteristics of masonry structures studied on small scale models of masonry buildings.
4. Detailed research into the influence of perforation pattern (openings in walls) on the structural behaviour of bearing walls.
5. Experimental study of the masonry structures - natural periods of vibrations, modal shapes, and damping characteristics.

PROGRESSIVE COLLAPSE OF MASONRY STRUCTURES

By James E. Amrhein, S.E.*

ABSTRACT: The possibilities of progressive collapse and catastrophic failure has become an increasing concern to the engineer and government regulatory bodies. This paper outlines the various types of progressive collapse that could occur and provides some of the design parameters to be considered to prevent progressive collapse from occurring. It states some of the loading conditions that could be considered as well as the possible elements of failure. General recommendations are made for tying the structures together.

*Masonry Institute of America, Los Angeles, California

PROGRESSIVE COLLAPSE OF MASONRY STRUCTURES

James E. Amrhein, S.E.*

General

No owner, architect, engineer or builder wants to think that there could be a possibility of failure or collapse of his structure. However, under certain circumstances, either during construction or after the construction is completed, events may take place that cause certain elements to fail and the failure of these individual elements will cause additional elements to fail. This failure condition proceeds and then becomes known as a progressive collapse mechanism. Progressive collapse can be defined as a local failure, which precipitates additional failures of major areas or floors or frames of a structure. Although the initial failure may be relatively slight, the continuing or progressive failure can be catastrophic, causing major elements or the complete structure to collapse.



Figure 1. Ronan Point Apartment Building after the collapse, with a second identical building in the background. (Courtesy of London Express News and Feature Services)

*Masonry Institute of America - Los Angeles, California

The classic progressive collapse which has initiated concern in the engineering and building profession was the collapse of the 22-story precast concrete building called Ronan Point in London, England, in 1968.

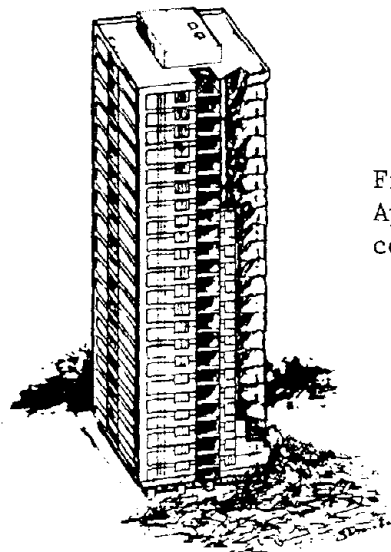


Figure 2. Ronan Point Apartment Building showing corner collapse.

A corner section of this building was completely destroyed when, on the 18th floor, several precast panels were blown out by a gas explosion. As a result of this tragic event, various agencies and engineers have been investigating the safety of buildings when certain elements no longer provide support in the structure.

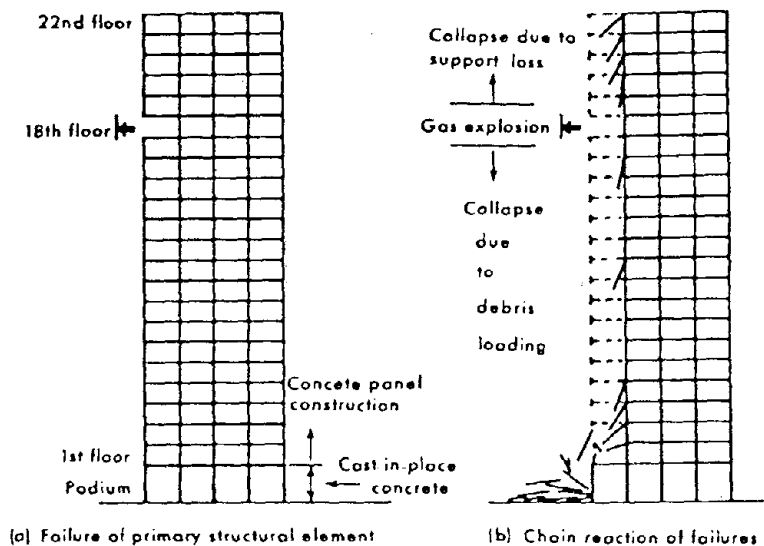


Figure 3. Development of the failure mechanism of the Ronan Point Collapse.

Standards concerning progressive collapse are still in the formation state, although the U.S. Department of Housing and Urban Development (HUD) has proposed some initial requirements. Engineers may develop their own assumptions and may determine what could possibly happen to their structures if various elements no longer provided support. This type of analysis should provide a concept of an alternate load and stress paths that may be taken within a structure. It should cause the engineer to consider redundant or alternate paths of load transfer.

Types of Progressive Collapse

1. Top Down. The "top down" type of progressive collapse would occur if an upper story was severely overloaded by stacking materials in a location that was not capable of supporting this overload, then the floor would collapse, dumping this extra material load onto the next floor which, by impact, would cause the floor to fall, and so on progress down the structure. This might also take place if shores were removed too early from an upper floor level and the floor had not gained sufficient strength to support the load and thus a failure would take place and a progressive collapse would occur.

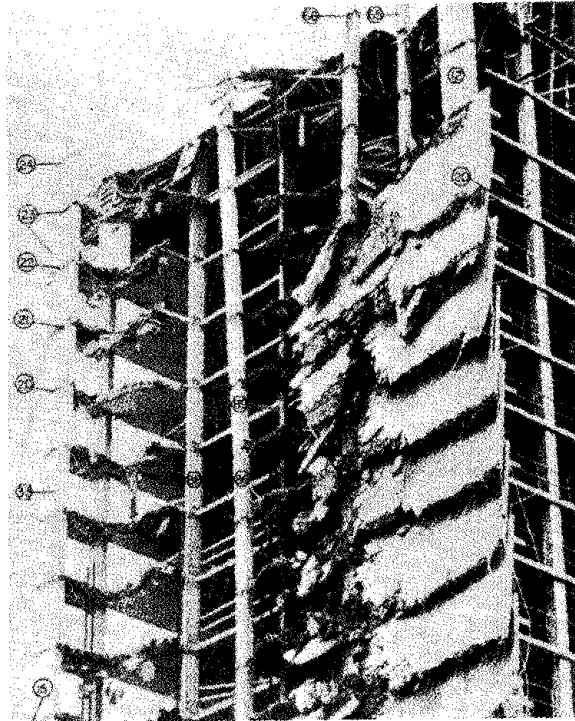


Figure 4. Progressive collapse from top down. Skyline Plaza collapse, Fairfax County, Virginia.

2. Bottom Up. This type of collapse, "bottom up", took place at Ronan Point in which support was lost when a gas explosion knocked out the precast wall panels, removing the support of the upper floor panels and floor systems, and they in turn collapsed due to lack of support. This can take place by loss of support from the bottom by either failure of a column, load bearing walls knocked out by explosions, walls or vertical support elements destroyed by means of impact such as trains, trucks or other items running into a building and thus knocking out its support mechanism.

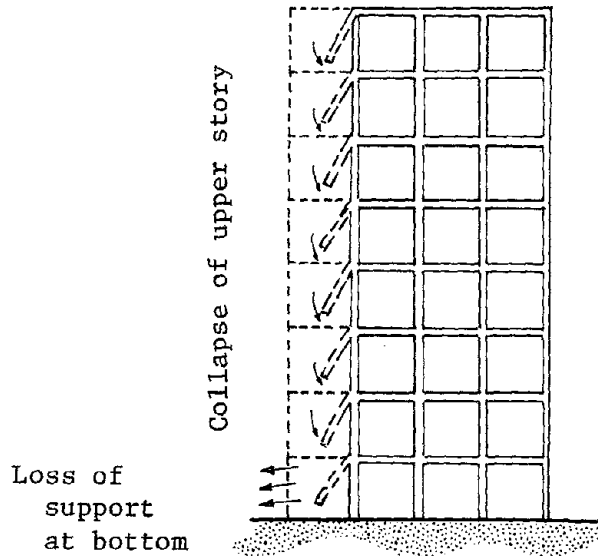


Figure 5. Loss of support at bottom causes upper floor to progressively collapse.

3. Domino Effect or Lateral Progressive Collapse. This collapse mechanism takes place when frames or walls which are erected collapse due to wind or seismic forces and one frame or wall falls over, hitting the next frame or wall, causing that frame or wall to fall over and hit the next frame or wall. This is a "domino effect", knocking down all the frames or walls of the structure.

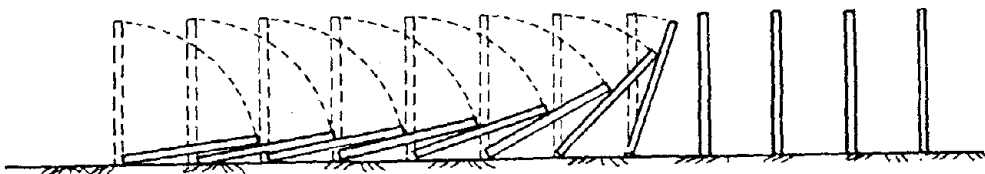


Figure 6. Progressive collapse of walls or frames by domino effect.

Criteria for Progressive Collapse

The governing agency, the owner, architect, engineer, or a combination of these, may have to decide to what extent progressive collapse should be considered. What criteria should be used to resist a progressive collapse condition. Should the failure of one column, one wall or one corner only be considered, or should the failure of several columns, walls or corners at the same time be considered? Possibly there should be consideration for the potential risk hazard that might occur. It would not seem reasonable that all four corners of a structure or a number of columns of a structure would all fail at the same time. Therefore, analyzing a structure in which many of the columns are no longer capable of supporting the loads or number of corners have completely given way causing the rest of the building to be seriously unstable may be far too conservative and create excessive cost to prevent such a collapse. Engineering judgement, along with a risk evaluation, should be made to determine what is a reasonable criteria for progressive collapse.

As a suggestion, perhaps one interior load bearing wall or one corner of a building could be considered to have failed or one frame or wall of a structure considered to have fallen over. These single events are more realistic and the potential of this happening is more within the realm of possibility than extrapolating this to simultaneous multiple failures.

The federal government, and in particular the Department of Housing and Urban Development (HUD), have considered the problems of progressive collapse and have prepared some preliminary documentation along these lines. They have stated that for probable extensive collapse, buildings shall be designed and constructed so that if any elements essential to the stability of the building fail, structural failure will be limited to three stories vertically and to 1,000 square feet or 25% of the horizontal area, whichever is less, of any story affected.

HUD further states that should any following structural element or combination of structural elements fail or lose their ability to carry load, the structure shall not collapse more than one story above or below the element under consideration, which might be:

- a) any single load bearing wall panel
- b) two adjacent wall panels forming an exterior corner of a building
- c) one or more floor elements
- d) one column
- e) any other one element of the structural sub system judged to be vital in the stability of the joining structural elements

Methods of Analysis to Prevent Progressive Collapse

The use of reinforced masonry systems is the key to resisting progressive collapse. In a single statement, "Tie the building together with reinforcing steel." This means that walls to walls, walls to floor, roof to walls, walls to foundations shall all be tied with reinforcing steel so that they act integrally as a unit. In addition, all wall elements should have boundary reinforcing steel across the top and bottom and down each side so that if support is lost underneath, these elements will act as cantilever elements pulling the load above back into other supporting elements. Reinforcing walls and connections will create redundant systems and multiple paths of load transfer so that in the event of loss of support of any particular element, the load will be moved to other systems and carried to the ground without collapse.

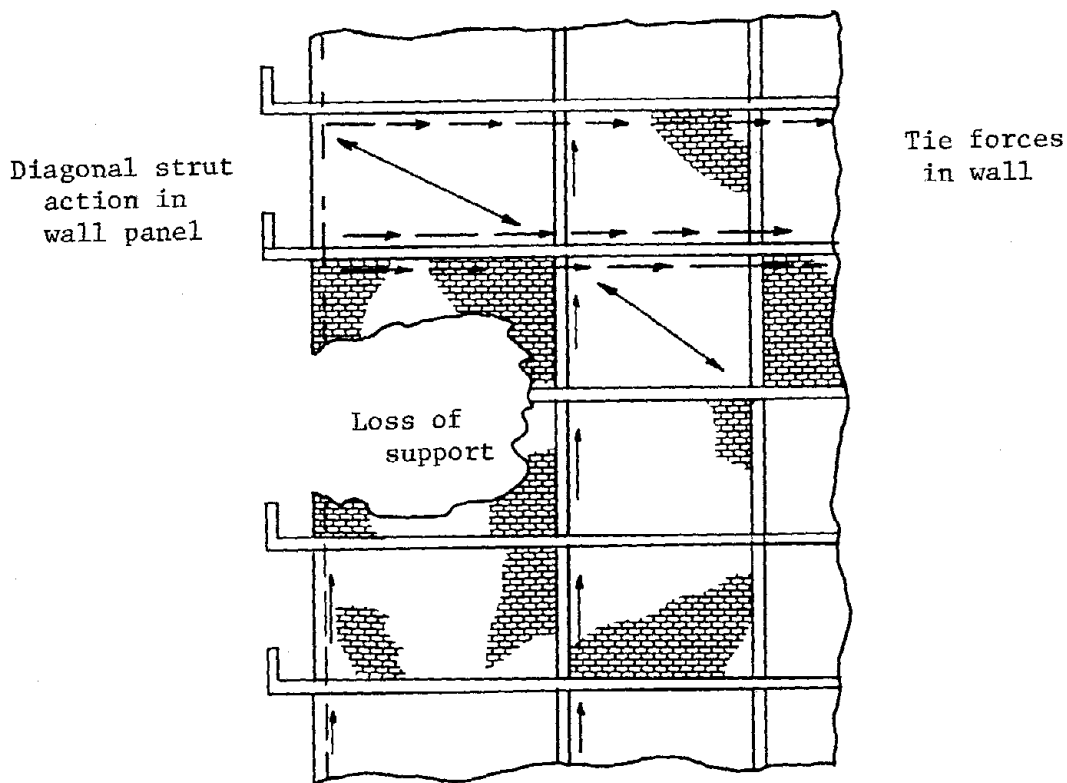


Figure 7. Tie walls and floors together to create redundant paths of resistance to prevent progressive collapse.

The method of analysis would be to assume the loss of support of any particular element and to then determine how the loads are transferred through the rest of the structure. For the analysis of progressive collapse, at least a third increase on the allowable stresses should be used. However, it is strongly recommended that yield stresses of steel be used and that ultimate stresses be used for the masonry systems. This concept, then, would consider yielding of the steel, catenary draping of floor systems, and even major displacements and deflections of other elements, but without collapse.

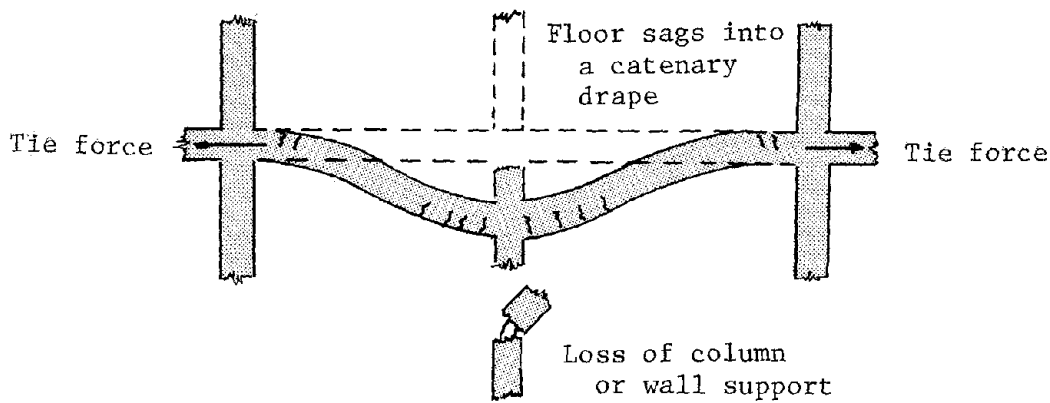


Figure 8. Development of catenary support which prevents collapse after loss of column or wall.

The Department of Housing and Urban Development recommends that if a structural component or portion thereof fails, the remaining structure shall support an assumed load of dead load plus one-third live load plus one-third wind load or earthquake force to permit evacuation, emergency operations and to allow for temporary support or repair to be made.

In the analysis of the system, in order to establish alternate paths around each critical structural member, the member shall be assumed to be removed. The remaining structure shall then be analyzed to redistribute and carry all forces or loads to the foundation.

It is reasonable to consider that when the loss of a column or load bearing wall occurs, the floor may develop catenary action and redistribute the loads to columns or load bearing walls. When walls are lost, it can be assumed that the reinforced masonry walls above will arch or cantilever and distribute loads to other load carrying elements.

It is necessary that the floor systems be tied to the walls so that if a load bearing wall underneath is lost, the floor will not drop down but will be supported by the wall above.

In the case of a frame or wall, the frames or walls must be adequately supported by guy wires, braces or other means so that if one falls over and hits the adjoining frame or wall, it will resist the loads imposed upon it.

In the consideration of explosion, an over pressure of 5 psi or 720 pounds per square foot has been used but is extremely high. It is far better to design the system as a reinforced load bearing masonry system of which all elements are tied together as stated above and in the event of loss of support from below, the elements can cantilever or arch and redistribute the loads to other elements.

Recommendations

In the consideration of progressive collapse, the minimum recommendation would be to adequately tie, as per UBC, all elements together and provide periferal reinforcing at the bottom, top and each side of the wall. This will strengthen the wall and carry the loads back to other resisting elements. It is important to develop continuity of reinforcing either by adequate laps or welding, particularly in horizontal bond beams, so that the walls themselves will act as horizontal beam elements between points of support.

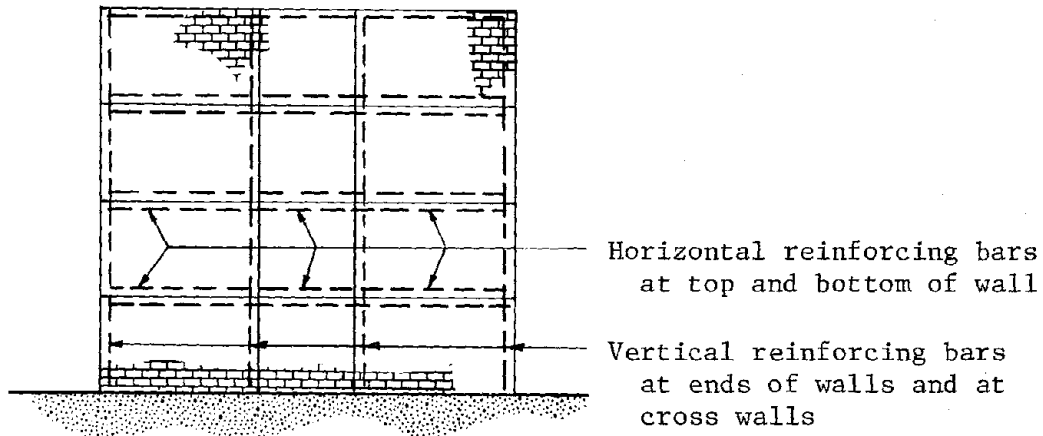


Figure 9. Minimum steel reinforcement layout to prevent sudden failure and progressive collapse.

Appendix I - References

- Amrhein, J.E., *Reinforced Masonry Engineering Handbook, 3rd Edition*, Masonry Institute of America, Los Angeles, California, 1978.
- Breen, J.E., *Progressive Collapse of Building Structures; Summary Report of Research Workshop*, November 1975.
- Harris, Harry G., and Muskivitch, John C., *Nature and Mechanism of Progressive Collapse in Industrialized Buildings*, Drexel University, Philadelphia, Pennsylvania, October 1977.
- HUD Staff, *Structural Design Requirements to Increase Resistance of Buildings to Progressive Collapse*, Proposed HUD Handbook, May 1974.
- Leyendecker, E.V., and Burnett, E.F.P., *The Incidence of Abnormal Loading in Residential Buildings*, NBS Building Science Series 89, Washington, D.C., December 1976.
- Leyendecker, E.V., and Ellingwood, B.R., *Design Methods for Reducing the Risk of Progressive Collapse in Buildings*, NBS Building Science Series 98, National Bureau of Standards, Washington, D.C., 1977.
- Leyendecker, E.V., and Fattal, S.G., *Investigation of the Skyline Plaza Collapse in Fairfax County, Virginia*, February 1977.

ENERGY SAVINGS WITH CONCRETE MASONRY CONSTRUCTION

By Eastman, E. G., Warren Insulated Bloc.

ABSTRACT: In today's energy problems a re-evaluation of the concrete and lightweight block production and marketing techniques must be initiated. With federal, state and local governmental agencies combining their efforts to limit heat loss in building walls the block producers must seek new ways to sell and promote masonry units. An examination of the block producers alternatives will be forthcoming from all fronts. Solar and underground buildings will be looked at as possible alternatives along with many other possibilities for the hollow core masonry units.

ENERGY SAVINGS WITH CONCRETE MASONRY CONSTRUCTION

By E. Gerry Eastman¹

THE JADED PAST

Not too many years ago a builder did a good job when he built a wall with a "U" value of say about a .25 (R=4). Building codes and officials were not so much interested in this design feature, energy, as they were insuring adequate fire resistance ratings. In those days of cheap and plentiful electricity, fuel oil and natural gas, in the United States there was little concern to fight wastefulness. Poor roof and wall designs gave the least possible insulation value, but it was OK as long as they would provide the right fire resistance rating. A building code was a document stipulating minimum construction practices for safety and the protection of human lives, not to conserve energy. These restrictions were to begin disappearing with the advent of the energy crunch circa 1973 which has now become a full blown crisis!

OVERKILL

At that critical point in our history the most obvious solution was to dictate stringent thermal insulation requirements via the building codes and standards. This would eliminate waste at least in new construction and hopefully instigate reinsulation in existing buildings and homes. Since residential building was one of the major, and is one of the major, segments of construction which could be readily made to comply with regulations aimed at eliminating energy use and abuse it was natural for a few of the highly regarded governmental and model code groups to attack this segment with vigor. The results? This resulted in overshooting what is realistically obtainable in one part of a building - the walls - without addressing the real problem areas, doors, windows, and mechanical systems and infiltration.

CAPACITY INSULATION

Publications published by the National Concrete Masonry Association, Portland Cement Association, Brick Institute of America, International Masonry Institute, International Union of Brick Layers and Allied Crafts-

¹Architectural Coordinator, Warren Insulated Bloc, Knoxville, TN

men, Laborers International Union in North America and Masonry Contractors Association of America. They were distributed to architects and engineers after a lot of research had been done by all of these organizations in hopes that they could talk the public into believing that masonry, be it brick, be it block, or be it poured concrete, was a thermal storage unit.

While the U.S. Government agencies were developing irrational thermal versions of what can be expected of building materials, the U.S. Bureau of National Standards was exploring its own intuitions. They followed along the same lines as expressed above, that there is more to evaluating insulating materials than simple steady-state tests could ever demonstrate.

So the National Bureau of Standards built and tested masonry construction inside an environmental chamber, one was virtually a little house. Subjecting it to varying cycles of temperatures enabled the investigators to verify what had been surmized by the more astute - there was definite advantage to increasing mass. The effects were to delay heat transfer and to minimize temperature differentials. This is considered heat storage capacity, or more simply, capacity insulation as distinguished from resistance insulation (steady-state).

ACCORDING TO NBS TESTS

Maximum rate of heat entry into exterior surfaces of a building varies with the time of day and orientation of the building. It will occur around 1 P.M. on a south wall, at 8 to 9 A.M. on an east wall and 4 P.M. on a west wall. The rate at which heat will continue to flow through the wall is governed mostly by the heat-storing capacity of the material. The rate of heat flow within the material will pulsate at varying intensities as the air temperature fluctuates. For example, it takes approximately 8 hours for the load received at 1 P.M. on a south wall made with 12" solid masonry to penetrate to the interior surface. Although this property may not be generally included in computing heat flow, it is recognized in the 1972 American Society of Heating, Refrigerating and Air Conditioning Engineers Handbook of fundamenatals.

NBS CONCLUSIONS

Results of the tests were very interesting. As predicted by the computer program, it was verified that placing insulation on the exterior was very effective in reducing and controlling variation of the indoor temperature. In this test series, when the indoor temperature was not controlled, that is, when allowed to float in response to changes in outdoor temperature, insulation placed inside compared with no insulation, was effective in cutting indoor temperature variation in half. Indoor temperature variation was further reduced by one-half when insulation was placed on the outside as compared with insulation on the inside.

Steady-state maximum calculated heat flow rates were 32, 63, 69, 67 and 29 percent higher than measured rates for the five tests where inside

temperature was controlled. The dynamic procedure predicted heat flow rates within 8 percent of measured rates. As discussed previously, the dynamic method takes into account the heat storage effects of the building and thus predicts maximum heating load to a more precise degree. Since concrete masonry possesses significant heat storage capacity, excluding this effect from the calculation, as is done with the steady-state method, can result in considerable oversizing of equipment needed to maintain a satisfactory indoor temperature.

The result is the mass factor we have heard so much about! The National Bureau of Standards, in Building Science Series 45, states that the heat flows calculated by the steady-state methods were 29 to 69% greater than those measured under dynamic conditions for masonry walls. Expressed another way, massive masonry walls perform 29 to 69% better than the steady-state values indicated by ASHRAE calculations. More research conducted by the Structural Clay Products Research Foundation, now a part of the Engineering and Research Division of the Brick Institute of America, indicates that the actual rate of heat transfer through typical building walls may be up to 20% less for masonry walls, up to 20% greater for wood frame walls and up to 60% greater for metal panel walls than the calculated rate based on published ASHRAE type "U" values.

National Concrete Masonry Association also ran some computer tests on mass vs. insulation.

COOLING LOAD VS. U-VALUES

For the first computer run, the walls of the model building were assumed to be composed of insulated wood frame walls having a weight of 8 pounds per square foot and a "U" value of 0.10. Results of the analysis indicated that maintaining 75°F. temperature would require air conditioning equipment capable of handling peak load of approximately 40,500 BTU per hour.

For the second computer run, the walls were changed from insulated wood frame to insulated concrete masonry. The "U" value for the masonry exterior walls was the same as for the frame, 0.10, but the weight increased to 40 pounds per square foot; masonry walls were assumed to be of 8 inch thick hollow lightweight block composed of concrete having a unit weight, or density equal to 100 pounds per cubic foot. The increased wall weight resulted in peak cooling load requirements of approximately 34,000 BTU per hour. The ability of the heavier walls to store and release heat in response to dynamic conditions accounted for a reduction in peak hourly cooling load requirements of approximately 6,500 BTU.

Subsequent computer runs in this series examined the effect of reduced insulation in the 40 pound per square foot block wall on peak hourly cooling requirements. The "U" value was increased in increments from 0.10 to a maximum of 0.38, at which value the masonry wall contained no insulation. The required cooling equipment capacity for the heavier masonry building is less than the insulated frame building until the "U" value of the masonry walls approaches 0.38 (no insulation).

COOLING LOAD VS. WEIGHT

The objective of the second series of tests was to examine in greater detail the influence of building weight on needed size, or capacity of equipment for air conditioning. As may be observed, the effect of wall, roof and floor weight on needed equipment size is dramatic. The masonry structure could be cooled with equipment 20 to 30% less in size than an insulated wood frame structure.

HEATING LOAD VS. WEIGHT

To study the influence of building weight on heating loads, several computer runs were made using the model building. Weight of the building elements was varied from 10 to 70 pounds per square foot, and the "U" value was held constant. There was a significant difference between peak heating load requirements as calculated by the two different methods, steady-state and dynamic.

NCMA CONCLUSIONS

The ability of concrete masonry walls to store heat is a definite benefit to the owner of a concrete masonry building. The capability to include "thermal inertia" in the heating and cooling load calculations now exists; when it can be included in the calculations the result is lower peak loads for heating and cooling. Peak loads determine the size and capacity of HVAC systems needed for a particular building; therefore selection of equipment for optimum efficiency and energy conservation depends upon a thorough and accurate thermal analysis.

"M" FACTOR

So why didn't we get the 29 to 69% credit? The "M" factor is being very much talked about by the masonry industry today and in what it will do for us in the future. I don't quite believe much in the "M" factor. For instance, in Knoxville, Tennessee, which has a 3,494 degree day rating, if we had a "U" value requirement of .12 and we went to the mass factor chart and looked up on the chart at our degree day, and came out with correction factor of .8495, our resulting "U" value would be .14. We've gone from .12 to .14.

Can we meet a .14 with a bare concrete block? I doubt it, as a matter of fact I know we can't. The lowest any of us can go with a bare concrete block is a .30 or so. But let's look at another factor in this mass factor madness. Throughout Tennessee the spread of degree days is varied. Knoxville is again 3,494 degree days, Nashville is 3,578 and Memphis is 3,232, the warmest place of all. Even disregarding the

elevations that exist, and the temperatures that exist across our state, our correction mass factors are all about the same, .8495, .8515, and .8425.

When applied to a required .12 factor, the resultant effective "U" factor is a .14 in any of these places. Doesn't that seem strange? In essence, this means that the same "U" value is used in Crossville, Tennessee where it is probably 10 degrees colder most every day of the year and in Memphis, Tennessee where it is probably 10 degrees warmer most every day of the year. What we have been given in this correction factor is almost nil, so if we are going to depend on this to make block producers money then we are going to have to wait a long while for it to pan out.

ARCHITECTURAL STUDY

Richard Stein, an architect in New York City, has been working on methods of BTU costing (energy) in construction vs. energy usage per wall value cost. Mr. Stein's calculation on construction of the same type office building (1) framed in steel, (2) in composite steel and (3) in reinforced concrete would result in a 42% energy savings if done in the concrete reinforced vs. steel frame. The steel frame building had an average heat loss of 293,000 BTU's per square foot, the composite steel building had a heat loss of 251,000 BTU's per square foot, and the reinforced concrete building had 172,000 BTU's per square foot heat loss.

It is his idea, that buildings should be considered as total energy depositories comprising of both the inherent energy of the structure and the energy of operation. It is his belief that proposed architects should evaluate on a project-by-project basis the most energy effective building envelope dependent upon location and building programs.

He also went on to state that maybe the client will never buy all this BTU costing, if his initial cost is higher, his mortgage payments being more significant and his building being funnier looking than before, but Mr. Stein's point of view was given a few more years those are the only kind of conditions under which clients will be able to afford construction of any kind.

I think it's fairly obvious to all, that more architects are taking this point of view and becoming more and more interested in the actual heating, ventilation, and air conditioning of a building and the amount of energy loss that building is going to have over its life expectancy. Any architect that is not taking this type of evaluation is not to be considered a competent architect in this day and age of energy crisis.

THINGS TO COME

As more or less "concrete people" we are going to have to become more familiar with many things that in the past were just the consideration of the architect - things like mass factors, aggregates and their heat loss coefficients, solar operation, insulated masonry, heat transfer tests, and their implications and even exterior coatings to cut down on air through the wall's surface.

Things like these and many others will become more and more a part of our vocabulary as the energy problem becomes more and more realized. I would be very misleading if I did not note our industry's belief in a promising future. There will be innovations in design, in materials and in masonry configurations which will further aid in establishing the concrete block as a building element for saving energy. This is the belief of our industry and this in my belief.

The benefits of thermal storage make masonry competitive with frame construction when solar systems are employed, thermal resistant aggregates will be developed and insulated masonry units of one design or another will be used a great deal throughout the country. For the past year we have all been working on finding the best energy related building block - energy wise, cost wise, and performance wise. What we have now is just the beginning.

ENERGY REGULATIONS

Now let's take a quick look at the National Energy Codes now standing as of September 1977. States that have adopted regulations include California, Connecticut, Michigan, Minnesota, Nevada, Nebraska, New Mexico, New York, North Carolina, Oregon, Virginia and Wisconsin. The Washington State Regulation relates only to electric resistance heating. Texas is developing recommended standards for voluntary adoption by cities. Colorado has adopted regulations relating to manufactured housing and multi-family dwellings in jurisdictions with no code enforcement.

Most states reported regulations for publicly owned buildings, some of these regulations are extremely sophisticated. Many states reported that they are waiting for a nationally recognized enforcement code that they can adopt by reference. This in essence is what Tennessee is doing.

Nevada and New Mexico have adopted a proposed Uniform Building Code, Chapter 53, Insulation Requirements, and the anticipation that this will become a portion of the UBC: Oregon reported that it may double its insulation requirements over that which were adopted prior to the organization of petroleum exporting companies' embargoes. Massachusetts has the authority to write its own code, but it is awaiting the Code Compatible Version of ASHRAE Standard 90-75 which has now been developed by the National Conference of States on Building Codes and Standards.

If Congress does not act, the Farmers Home Administration thermal code, as of March 15, 1978, will be requiring a .07 exterior opaque wall "U" factor. The Federal Housing Authority (FHA) has not at this time followed Farmers Home's lead, but it is expected that in the near future they will. There is no way on God's green earth that a concrete block by itself can be used to meet this type of "U" factor.

If concrete block were used to construct a building that had to meet a .07 "U" factor the building envelope would have to be wrapped with an average of 3" of polystyrene around the perimeter of the building. This done on either the interior or exterior of the concrete block, the concrete block would then need to be covered on the interior with a 15 minute fire barrier and on the exterior with some sort of moisture protection and something to block the ultra-violet rays that will be attacking the insulation. Without these types of protection the insulation would probably last less than a year.

HUD CODE DEVELOPMENT

As reported in the January 19th issue of The Engineering News Record, HUD by 1980 will have, not only a cash budget on every job, but also an energy budget. Buildings will have 16 classifications, 7 climatic regions and a measured BTU consumed per square foot budget demand.

As a result of these demands, the future buildings will start having very dramatic features, i.e., of solar collectors, massive windowless walls, buildings half underground and buildings all the way underground. Some subtle features that these buildings will have to initiate are extremely recessed windows, skylights to off-set luminars and computer control HVAC systems. Congress has already mandated performance over prescriptive standard in their Energy Conservation Standards for New Buildings Act of 1976 (Title III of BL940385). Therefore, the designer is responsible over the total thermal performance and structural performance of the building.

In response to this, ASHRAE developed 90-75 which blends forms (performance and prescriptive) by providing prescriptive goals for components "windows, doors, walls, roofs, etc." then giving a green light to alterations of these maximum prescriptive goals by designer preference for bettering energy uses, i.e. performance. This concept was not accepted by Congress or the AIA. The AIA claims it would stagnate design.

Joseph Sherman, Director of Hud's Division of Energy Building Technology and Standards, has taken the responsibilities of the code. He states that it will be an energy budget code with the maximum usage defined by existing federal buildings and the minimum usage established by field trials on new buildings, buildings constructed within this year. Trial energy budgets will be set this summer. Sherman feels "this will give me real information, not phony stuff on cost, impacts and problems about hundreds of buildings across the country."

The revised energy budgets will be published in the Federal Register

in August 1979. The final standards will be implemented by February of 1980.

BLOCK PRODUCERS ALTERNATIVES

Let's now take a look at the concrete block industry's alternatives to these very stringent thermal requirements placed on us:

1. To sell only foundations. With the success that we have had through the past years in selling all types of commercial and industrial businesses and other types of construction - to go back to just selling foundations is not a very appealing thought.

2. After-the-fact insulation systems. These after-the-fact systems are well known by us all. They are Perlite, Ureaformaldehyde, Zonolite and NCMA Stud Block. Most of us are doing these now, but only with more insulation will they meet the new thermal requirements set up by the different government agencies.

3. Insulated block systems. Most of us have heard of different types of insulated block systems such as the Warren Bloc System, Walton Block, Miracle Block, Gisoton Block, Waukesha Block, Korfil Block or the Formbloc. We have all looked at their pluses and minuses and we know approximately what kind of cost we are talking about. But what we don't know is whether or not they are going to meet our needs in the future.

4. The cladding systems. There are Fiberglas Clad System, Thermal Stud, Thermal Clad, Dryvit, Backbone, etc., and others I know nothing about.

5. To advocate and push solar concepts. The concrete block we have is in essence a solar storage panel. It has a contact surface, air behind that surface, and a structural form. This should be developed by our industry a great deal more than it has been considered. Presently The University of Tennessee, TVA, and HUD are talking about building a solar block house on the same sight now used for the Solar house and ACES house in Knoxville, Tennessee.

6. To advocate and push underground buildings. Underground buildings to the industry could mean a very large increase in the use of concrete block for all buildings. The reason for this is that the block could be poured full with grout and steel and be used as retaining walls and exterior walls for these buildings. At the same time it could be used for the interior wall partitions as supports of the concrete deck that will be supporting the upper floors of these types of buildings.

All of these alternatives deserve some of our time, but I will touch on only the ones I think most important and unknown to block producers - Solar Concepts (Alternative #5) and Underground Buildings (Alternative #6).

ALTERNATIVE # 5 - SOLAR CONCEPTS

PASSIVE SYSTEM CHARACTERISTICS

Passive solar buildings generally utilize considerable south facing windows and skylights to bring in the warmth of the sun. Passive buildings must be carefully oriented in response to the seasonal and daily movements of the sun to maximize solar heat gain in the winter and minimize solar heat gain in the summer. Moveable insulation is frequently used in passive systems to minimize heat outflow at night and on cloudy days, and to minimize undesirable heat gain in summer. One of the most significant characteristics of a passive solar building is the use of thermal mass: materials which have the ability to absorb and re-radiate large amounts of energy. Concrete masonry is an excellent material for use as thermal mass.

Passive design measures also include use of good insulation, earth berming, careful entrance location with regard to winter wind, use of air-lock vestibules, careful use of colors, careful consideration of natural ventilation and natural light, and use of natural vegetation for shading and windbreaks. It should also be noted that passive measures such as cross ventilation, exhaustion of hot air by convection, evaporation, and absorption of heat by thermal mass can provide up to 100% of the building's cooling needs in summer.

COST EFFECTIVE

Passive solar buildings have been able to provide 50 to 90% - even 100% of the building's heating and cooling needs in locations from New Hampshire to Oregon to New Mexico.

Thermal mass materials in general are particularly cost effective in that they simultaneously provide supporting structure, definition of spaces, acoustical separation, and thermal storage. What better definition of a concrete block?

THE KELLBAUGH HOUSE

72% of the heating needs of the Kellbaugh house in Princeton, New Jersey, are provided by a 15 inch thick vertical concrete wall facing south. Kellbaugh estimates that "... \$8,000 to \$10,000 of total cost of \$45,000 can be attributed to the passive solar heating and cooling system." Kellbaugh also points out that "...the initial cost could have been reduced significantly if concrete masonry block filled with concrete were used instead of poured-in-place concrete." Kellbaugh also developed a life cycle cost study. If natural gas escalates at an annual rate of 5%, the amortization period will be 17 years. The payback period will drop to 10 years if natural gas escalates at 15%.

The most effective use of massive construction materials is to store and re-radiate heat (or store "coolness") on the INSIDE. This means that contrary to standard practice INSULATION should be on the OUTSIDE. The problem of protecting exterior insulation can be easily solved with readily available material such as a thin coat of fiberglass reinforced stucco, vinyl, aluminum, asbestos, cement and other conventional siding materials.

DESIGN

There are four basic approaches for incorporating thermal mass in building design: (1) integrated mass, (2) vertical mass, (3) roof ponds and (4) rock storage. The first two concern the block producer most directly.

1. In this approach, thermal mass is used directly for wall, floor and in some cases ceiling construction. This approach can maximize performance of a passive solar system because it maximizes the surface area to volume of mass ratio. The new Pitkin County Air Terminal is an excellent example of this approach.

It stands at an elevation of 8,000 feet in 9,000 degree day climate. The floor is 5 inch concrete slab with perimeter insulation. North and east exterior walls are 8 inch concrete block; voids filled with concrete. All walls are insulated on the outside with rigid polystyrene. There is extensive use of berming. South facing vertical windows and skylights have moveable insulation. Solar energy provides 55 to 60% of the building's heating needs.

2. A vertical mass, covered with double glazing and painted black on its outer surface can double as a solar collector and heat storage container. This configuration is frequently referred to as the Trombe wall. The name is taken from the French professor, Felix Trombe who led studies of vertical mass walls. The Trombe wall has been used with considerable success. The Kellbaugh house discussed previously utilizes a 15 inch thick, two story high vertical mass to achieve 72% solar heating. The Los Alamos Scientific Laboratory has conducted extensive tests of the vertical mass concept. They have developed a computer model which simulates hour by hour performance of vertical mass walls using the climate and solar data for different locations. The model's accuracy has been verified by actual experiments. Consider the results of one series of tests. In these tests the parameters were mass wall one foot thick, glass to floor area ratio of 1/2, double glazing "U" factor of 0.5, infiltration rate of one per hour, maximum allowable temperature 75°F. (at which time excess heat was vented to the outside) and the minimum temperature 65°F. (at which time auxiliary heating activated). The results are as follows:

PERFORMANCE OF 12 IN. THICK SOLID CONCRETE MASONRY WALL

	<u>Degree Days</u>	<u>Solar Heating Fraction</u>
Los Alamos, NM	7350	63%
Albuquerque, NM	4269	93%
Madison, WS	7550	58%
Seattle, WA	5000	67%
Fresno, Ca	2880	80%
Bismark, ND	8220	51%
New York, NY	4860	63%

Keep in mind that one square foot of unshaded single pane glass adds about the same cooling load as 50 square feet of masonry wall.

ALTERNATIVE #6 - UNDERGROUND BUILDINGS

Many of us talk of building underground as if it were a new idea. We're not really being contradictory because, in a sense, it is a new concept.

We've built human spaces under earth or rock continually since primitive times. Desire for comfort and security prompted earlier peoples to live in caves or cliff dwellings. Settlers on the American prairies built hillside dugouts and sod houses for shelter from blizzards and the searing summer sun. Root and ground cellars are still in use today to store fruits and vegetables for longer keeping in summer and to prevent freezing in winter. Commercially steady temperature caves and cellars are used to age cheeses and wines and to store perishables.

ENERGY BENEFITS

Underground or earth-sheltered buildings conserve energy by utilizing the near constant temperatures of the earth a few feet below the surface. Exterior walls above ground face wide temperature swings -- from 100°F. to -30°F. in Minneapolis, for example, heating and cooling equipment inside must contend with the spread between desired interior comfort levels and the outside weather. On the extreme -30°F. night, insulation and the heating plant must fight a 100°F. difference.

However, going underground even a little bit with less than a foot

of soil overhead, shortened day-night temperature changes have almost no effect. And at about 20 feet underground the year around temperature of the earth varies only slightly --- from 47°F. to 50°F. in the Minneapolis area. That means having to deal with only about a 3°F. spread all year.

Therefore building underground obviously means less heating in winter and less cooling in summer. On a frigid -30°F. Minnesota winter day, for example, heat loss rate for an above ground wall with four inches of insulation is ten times greater than for an uninsulated wall underground. If wind chill factor is considered, the difference is even greater.

By going underground, the lower heating-cooling demand makes it feasible to design buildings that are totally independent of outside energy sources. Underground space can hoard heat energy produced by solar methods, for example, so that a modest surface area of collectors can provide all heating required, even where winters are severe. Capacities of such small solar units may not be enough to generate summer cooling by mechanical means, even with the lesser cooling load underground.

Such self-reliant buildings, combining energy saving efficiency of underground placement with developing technologies for solar and other methods of heating, cooling and electricity generation, may be common in the future. In the meantime, present technology makes earth protected homes, offices, schools and other buildings a practical, ready-to-go way to save energy resources.

MEETING ENERGY NEEDS

Buildings - commercial and residential - consume 29% of all energy in the United States. Almost half of all building space in use in 1985 will have been built since 1975. An earlier federal report suggests that if half the new buildings built each year had energy conserving designs which saved 40% of consumption, 15% of the present total U.S. energy consumed would be saved at the end of ten years. Underground buildings can easily produce that kind of savings. Engineering studies and data from existing project show that properly designed underground buildings may consume only 25 to 30% of the energy consumed by equivalent above ground spaces.

There are further advantages: underground space is quiet, even in a dense urban setting. The earth isolates noise and vibration. Avoidance of vibration, in fact, was what prompted the Brunson Instrument Co., Kansas City, to build its plant underground for manufacturing delicate precision instruments. The 140,000 square foot plant had a total heat and cooling bill of \$3200.00 in 1973. (The building is in an excavated limestone bluff about 100 feet below ground level.)

OLD/NEW TECHNOLOGY

In the same way, a new look is being taken at sub-surface moisture protection. "It's not necessarily a different technology, but it's a different question," say Ray Sterling of The Department of Civil and Mineral Engineering, University of Minnesota. "Until recently, for example, basement space has been a second class space and leaking and dampness has not been considered so important. Some houses being built still have leaky basements."

Sterling is project coordinator for the Earth Sheltered, Energy Independent Building Design Project (ESEI), a design study being prepared by the Civil and Mineral Engineering Department, University of Minnesota, for the state's Energy Agency. The study, due for release this month, is to provide practical information showing how earth-sheltered residential structures can be virtually independent of fossil fuels for heating and cooling.

Minnesota, incidentally, is becoming somewhat of a technology center for earth sheltered construction. The University's Department of Civil and Mineral Engineering has nationally recognized expertise in this area. In 1976 the Department issued a proposal that a University Engineering Building be designed as a demonstration underground facility. It is now receiving serious legislative consideration. The Department has a 50 by 100 foot mined demonstration space 80 feet below a campus soccer field. Besides showing the practicality of developing mined space in a congested urban setting, the project is used to measure the ground movement and roof deflection resulting from the excavation.

Minnesota's legislature has voted \$500,000 for demonstration underground houses. These homes will be instrumented ground homes. Last fall the legislature created a new Earth Sheltered and Underground Construction Institute, not yet given an official name. It will be housed at The University and serve as a technology and research clearing house.

THE UNDERGROUND MOVEMENT

Underground architecture has become a movement of sorts. Those architects, builders and owners who have become involved convey an evangelist's enthusiasm as they try to convert non-believers. Persons from a broad range of disciplines who have a professional interest have formed the American Underground Association to promote "recognition of the great potential of underground space," and to encourage research and information sharing on technical, environmental, legal, economic, social and political problems. The group publishes a quarterly journal, Underground Space.

Several areas in the past and present have constructed underground buildings. Some of the areas around the country are:

1. Malcolm Wells Architects Office in Cherry Hill, New Jersey.

2. An "Ecology House" in Marston Mills, Massachusetts.
3. Air Defense Radar Facilities.
4. 83,000 feet Williamson Hall at The University of Minnesota.
5. The 1859 Cooper Union Building had a 1200 person meeting hall underground.
6. Woolworth Building has a pool, gym and other facilities underground.
7. Winston House, Lyme, New Hampshire has 18 feet of earth cover.
8. Forth Worth is about to build its second underground school. The first school is 12 years old and is called Lake Worth Junior High. Built to protect it from noise of jets that fly over hourly.
9. Abo Elementary School in Artesia, New Mexico, built in 1962.
10. 39,000 square foot Student Center, Southwest Minnesota State University, built in 1974. The average earth cover is 3 feet.
11. Proposed 50,000 square feet research and administrative facility for historic Fort Snelling is designed to supply its own heating, cooling and electricity.

CONCLUSION

After reflecting on these alternatives one must think of more ways to sell and promote masonry in an energy conservative world. New avenues must be explored and exploited to the outer limits or the block business will meet an untimely death.

BIBLIOGRAPHY

A Comparison of Very Lightweight Walls of Wood, Metal and Glass Versus Concrete Masonry in Energy Conservation, National Concrete Masonry Association, 1976.

"Field Survey of Energy Use in Homes, Denver, Colorado," Applied Science and Engineering.

Georgia Information, Georgia Chapter American Institute of Architecture, Volume 78, Number 1, January 1978.

Heat Transmission Coefficients of Brick Masonry Walls, Technical Notes on Back Construction, August - September 1974.

HUD Hammers Out Energy Performance Codes for Buildings, Engineering News-Record, January 19, 1978.

Mass - Masonry - Energy, The Masonry Institute Committee.

NCMA's Interim Report on Energy Regulations, National Concrete Masonry Association, January 1978.

NCMA-TEK # 12, National Concrete Masonry Association, 1969.

NCMA-TEK # 26, National Concrete Masonry Association, 1971.

NCMA-TEK # 38, National Concrete Masonry Association, 1972.

NCMA-TEK # 58, National Concrete Masonry Association, 1974.

NCMA-TEK # 67, National Concrete Masonry Association, 1975.

NCMA-TEK # 68, National Concrete Masonry Association, 1975.

NCMA-TEK # 90, National Concrete Masonry Association, 1977.

Neal, Wallace. "Human Spaces Underground - An Old/New Technology," Construction Specifier, January 1978.

New Insight into Energy Use and Conservation in Structures, National Concrete Masonry Association, 1975.

Pictorial # 11, National Concrete Masonry Association, Volume 33, November 1977.

Redmond, Tom. Conserving Energy with Concrete Masonry Construction, National Concrete Masonry Association.

Statement to Farmers Home Administration, National Concrete Masonry Association, May 1977.

AVERAGE VS. PEAK THERMAL CHARACTERISTICS OF BUILDING SHELL ELEMENTS *

**

By Dexter, M., Bickle, L., McNamara, J., van der Meer, W.

ABSTRACT: A thermal network computer simulation code is described which uses first principles to calculate the thermal performance of walls under actual weather conditions. The hour-by-hour and integrated predictions show good comparison with experimental data. A technique is developed which uses the validated computer results to determine the efficiency with which a wall collects solar radiation.

AVERAGE VS PEAK THERMAL CHARACTERISTICS
OF BUILDING SHELL ELEMENTS

By Dexter, M., Bickle, L., **
McNamara, J., van der Meer, W.

INTRODUCTION

Two problems which inevitably occur in the design of solar buildings and systems are the necessity of calculating average loads and the need for solar load analysis. This paper describes a technique that can be applied to both these tasks. The key concept is the "Effective U-Factor" described by van der Meer⁽¹⁾. This characterizes the long-term average heat loss rather than the peak heat loss of building shell elements. Because it is a better indicator of average energy consumption, the Effective U-Factor has already been incorporated as a part of an effort by The State of New Mexico to implement Chapter 53^{***} of the Uniform Building Code (UBC). The result was a state-wide energy conservation standard that governs average rather than peak heating loads and takes into account both mass effects and incident solar energy.

This paper shows that the Effective U-Factor concept can be extended by considering the building shell elements as low-efficiency solar collectors. The theoretical computer code developed to generate Effective U-Factors is described here and compared with experimental data. The technique for determining the solar-collector efficiency of a wall from the Effective U-Factor data is described.

* This work supported by the New Mexico Energy Resources Board in cooperation with the New Mexico Energy Institute at the University of New Mexico.

** Dexter, M., Staff engineer Bickle Division/CM, Inc.
Bickle, L., President Bickle Division/CM, Inc.
McNamara, J., Research Assistant University of New Mexico
van der Meer, W., Professor of Architecture University of New Mexico.

*** Based on ASHRAE Standard 90-75

THEORY

Effective U-Factors

A one dimensional computer program was written to simulate the thermal performance of walls under actual weather conditions. The wall is modeled as shown in Figure 1. It is divided into a nodal network, and the finite difference forms of the governing equations are written and solved in implicit form on an hour-by-hour basis. The radiant heat transfer at the inside wall surface is modeled as a "gray" wall surface interacting with a "black" room (a deep cavity.) This heat transfer path is in parallel² with natural convection from the inside air to the vertical wall surface,

$$\bar{Nu} = 0.516 \cdot (Gr Pr)^{0.25}, \quad (1)$$

Where \bar{Nu} is the average Nusselt number, Gr is the Grashof number, and Pr is the Prandtl number. Radiation losses from the outside surface are modeled as a "gray" wall surrounded by a "black" body at a temperature equal to the average of the sky and the ground. The ground temperature is taken to³ be that of the ambient air, and the sky temperature (T_{sky}) is given by

$$T_{sky} = 0.0411 T_{air}^{1.5} \cdot \left[T_{air} \right] = \left[T_{sky} \right] \text{ (}^\circ\text{R)} \quad (2)$$

This radiation path is in parallel with a convection loss term for combined free and forced air flow. It is assumed that, in the absence of forced convection, natural convection will provide a heat transfer² coefficient of 1.0. The velocity corresponding to this natural flow² is vectorially added to the measured wind speed to determine the speed of the air flow over the wall. The convective heat transfer coefficient for combined² flow is determined from this speed using the modified Reynolds analogy.² Finally, an internal air space within the wall is modeled as a parallel radiation and convection path with the radiation interchange between two infinite, parallel, diffuse, gray⁴ bodies with uniform surface temperatures. The convection is modeled as⁴

$$\begin{aligned} \bar{Nu} &= C (Gr Pr)^m, \text{ where} \\ C &= 1.0, \quad m = 0.0 \quad \text{For } Gr < 2100 \\ C &= 0.13, \quad m = 0.33 \quad \text{For } Gr > 2100 \end{aligned} \quad (3)$$

Solar radiation incident on the outside surface of the wall is determined from measured total horizontal and direct normal solar radiation corrected to the orientation of the wall surface using the procedure in

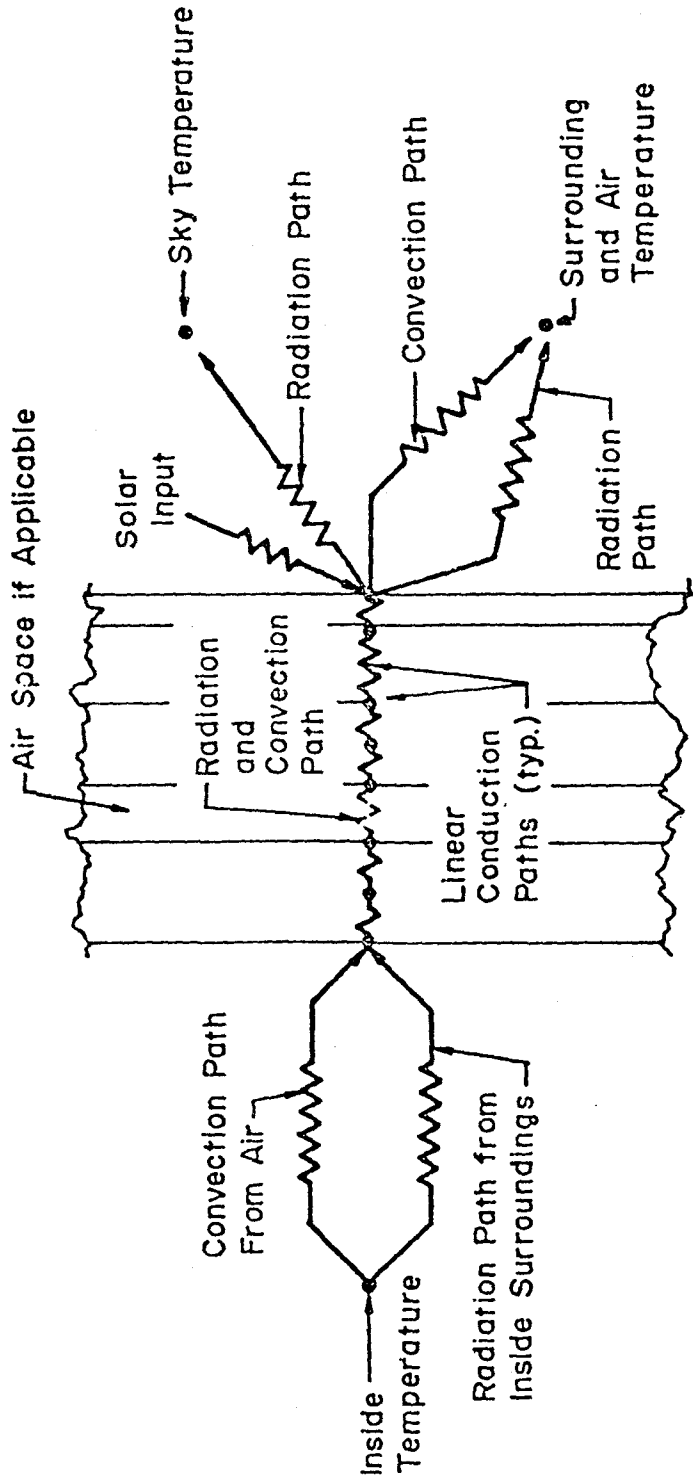


FIGURE 1
THERMAL NETWORK MODEL
FOR WALL

Chapter 59 of the ASHRAE 1974 Applications Handbook.

The actual measured weather data is used as an input to the model on an hour-by-hour basis. The governing equations and boundary conditions are written into a single matrix equation, which is solved, using a modified Gauss-Jordan solution technique⁵ for diagonally dominant tridiagonal matrices. The calculations are performed for a period of representative winter weather conditions (usually one to two weeks.) Each hour the net heat loss across the inside surface of the wall is summed, as is the inside-outside air temperature difference. At the end of the period of calculation, an Effective U-Factor (U_E) is determined by taking the ratio of the summed heat loss to the summed temperature difference,

$$U_E = \Sigma q / \Sigma \Delta T = \bar{q} / \bar{\Delta T} \quad (4)$$

Thus, the Effective U-Factor is related to the average rather than the peak heat loss of a wall section. As such, it should be used in energy studies and for predicting long-term average energy consumption, but not for sizing HVAC equipment which must meet peak loads.

Using the above analysis, Effective U-Factors were determined for 25 different wall configurations typical of construction in New Mexico. For each wall, calculations were made for four orientations (North, East, South, and West), three colors (solar absorptivity = 0.2, 0.5, and 0.8), and eleven climatic regions throughout New Mexico. The results were presented in tabular form convenient for use by building inspectors checking for compliance with Chapter 53, UBC. Two examples of these Tables are shown in Figure 2 and 3.

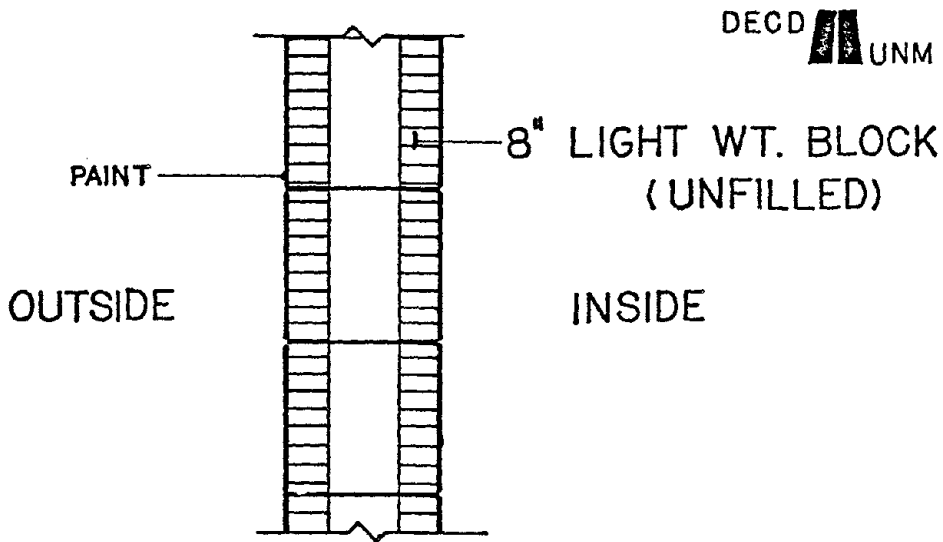
An Extension to Solar

The above data can be used to determine the solar performance of a wall as follows: It is hypothesized that the average heat loss of a wall (\bar{q}) can be given by a steady state loss term and a correction for solar gain,

$$\bar{q} = U_{ss} \bar{\Delta T} - \eta \bar{q}_s \quad (5)$$

Here U_{ss} is the steady-state U-value, $\bar{\Delta T}$ is the average inside-outside air temperature difference, \bar{q}_s is the average solar flux incident on the wall and η is the wall solar "collector" efficiency. Combining equations 4 and 5, the wall efficiency (η) as a solar collector is:

$$\eta = (U_{ss} - U_E) \bar{\Delta T} / \bar{q}_s \quad (6)$$



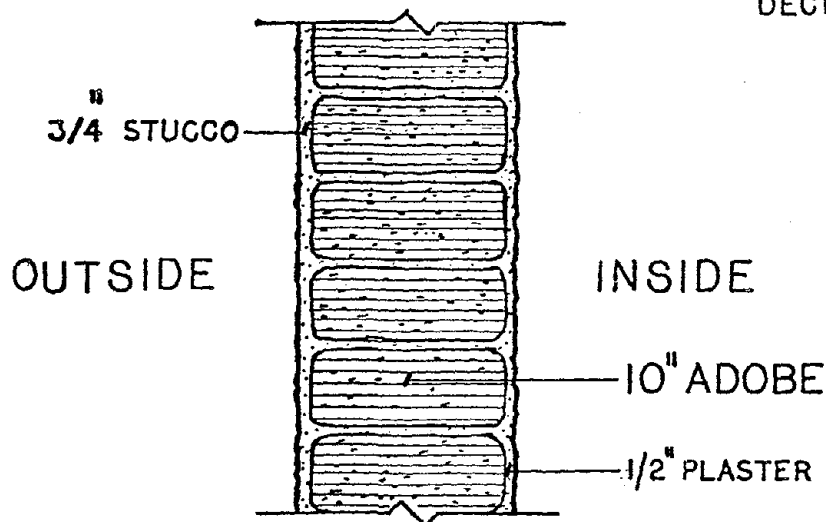
WALL TYPE 9: ASHRAE STEADY STATE U-VALUE 0.314 $\frac{\text{BTU}}{\text{SF-HR-}^\circ\text{F}}$

EFFECTIVE "U"-VALUE (U _E): HEATING												
N.M. CLIMATIC REGION	WALL ORIENTATION											
	NORTH			EAST			SOUTH			WEST		
	*L	M	D	L	M	D	L	M	D	L	M	D
1	.290	.234	.175	.277	.202	.119	.264	.158	.052	.279	.201	.124
2	.275	.245	.214	.266	.223	.179	.255	.194	.133	.268	.226	.185
3	.272	.247	.223	.263	.226	.190	.252	.198	.145	.265	.231	.197
4	.270	.250	.232	.260	.226	.195	.246	.195	.143	.262	.233	.204
5	.270	.251	.232	.259	.225	.193	.245	.191	.137	.262	.232	.203
6	.270	.251	.232	.258	.222	.188	.243	.185	.125	.262	.230	.199
7	.272	.251	.231	.258	.219	.181	.241	.176	.109	.262	.228	.193
8	.274	.250	.227	.258	.212	.168	.238	.162	.083	.263	.222	.181
9	.278	.249	.221	.259	.204	.150	.236	.145	.049	.264	.215	.165
10	.284	.247	.210	.260	.190	.119	.232	.115	-.008	.267	.203	.136
11	.284	.245	.201	.262	.181	.097	.231	.096	-.047	.269	.194	.117

*WALL COLORS: L=LIGHT
M=MEDIUM
D=DARK

NOTE: ALL ENTRIES IN THE TABLE ARE PRECEDED BY "0". THAT IS: .122 = 0.122; -.122 = -0.122

FIGURE 2



WALL TYPE 1: ASHRAE STEADY STATE U-VALUE 0.263 $\frac{\text{BTU}}{\text{SF-HR-}^\circ\text{F}}$

EFFECTIVE "U"-VALUE (U_E): HEATING

n.m. CLIMATIC REGION	WALL ORIENTATION											
	NORTH			EAST			SOUTH			WEST		
	*L	M	D	L	M	D	L	M	D	L	M	D
1	.260	.225	.191	.252	.205	.160	.244	.188	.138	.254	.210	.168
2	.237	.219	.200	.231	.205	.179	.225	.189	.155	.233	.208	.184
3	.232	.218	.203	.227	.204	.182	.220	.187	.156	.228	.208	.187
4	.230	.218	.207	.224	.203	.183	.215	.181	.149	.225	.206	.188
5	.230	.219	.207	.223	.202	.182	.214	.179	.145	.225	.206	.187
6	.231	.220	.208	.224	.202	.179	.214	.176	.139	.226	.206	.186
7	.234	.221	.209	.225	.201	.176	.214	.172	.131	.227	.205	.183
8	.238	.224	.209	.228	.199	.171	.215	.166	.119	.231	.205	.179
9	.244	.227	.209	.232	.198	.164	.217	.160	.105	.235	.204	.174
10	.255	.232	.209	.240	.195	.152	.221	.150	.082	.243	.204	.165
11	.262	.235	.208	.245	.194	.144	.224	.143	.067	.249	.203	.159

*WALL COLORS: L-LIGHT
M-MEDIUM
D-DARK

NOTE: ALL ENTRIES IN THIS TABLE ARE PRECEDED BY "0". THAT IS; .122 = 0.122; -.122 = -0.122

FIGURE 3

Theoretical Results

Using equation 6, the solar collector efficiency was determined for various typical wall sections from the Effective U-Factor project. Typical results are given in Figures 4 and 5. These results are for the two wall sections shown in Figures 2 and 3. The four wall orientations and the three surface colors are listed along the top. Three New Mexico locations are listed on the left side. The solar collector efficiency is listed for the two walls for each color and orientation.

From Figures 4 and 5, it is seen that the solar collector efficiency depends on construction and color of the wall, however, it is independent of wall orientation and of climate. These results hold for the different climates within the State of New Mexico. It is not currently known whether this independence with climate will hold for a climatic region radically different from New Mexico (such as Seattle, Washington). The results show quite clearly that the efficiency is a strong, linear function of the solar absorptivity of the wall. In many cases, average heat loss from a wall could be substantially reduced by simply making the outside surface a darker color. These savings in energy are often greater than the savings which would occur by adding a reasonable amount of extra insulation. Thus, substantial improvements in average thermal performance can be realized by simply making the wall a better solar collector.

The concept of a wall as a solar collector is important. In many ways, the collector efficiency (η), is a "correlation" factor, analogous to the mass factor. For light mass walls a "solar" factor can be developed. Unfortunately, solar effects and mass effects are closely coupled in masonry walls. Thus, the Effective U-Factor, which includes both effects, should be used for accurate estimates of long-term energy consumption. Masonry walls should still be treated as solar collectors and their collection efficiency maximized or minimized depending on whether heating or cooling is required.

Because of the potential implications of these results on the building code and because the magnitude of the results was somewhat unexpected, it was decided that an experimental verification project should be run to insure the validity of these results

LOCATION	NORTH			EAST			SOUTH			WEST		
	L	M	D	L	M	D	L	M	D	L	M	D
Los Alamos	2.2	5.0	7.7	2.2	5.1	8.0	2.0	5.0	8.1	2.0	4.8	7.8
Albuquerque	1.9	4.7	7.4	2.0	4.9	7.6	1.9	4.7	7.6	1.8	4.6	7.3
Las Cruces	1.7	4.8	7.5	2.0	5.2	8.1	2.1	5.1	8.2	1.9	4.8	7.7

FIGURE 4 solar collector efficiency for 8" C.M.U. WALL

LOCATION	NORTH			EAST			SOUTH			WEST		
	L	M	D	L	M	D	L	M	D	L	M	D
Los Alamos	0.9	2.6	4.4	1.1	3.0	4.7	1.2	2.9	4.7	1.1	2.8	4.5
Albuquerque	1.1	2.7	4.5	1.2	3.0	4.7	1.2	3.0	4.7	1.1	2.8	4.6
Las Cruces	1.1	2.9	4.6	1.2	3.2	5.1	1.3	3.3	5.2	1.2	3.1	4.9

FIGURE 5 solar collector efficiency for 10" ADOBE WALL

NOTE: L,M,D = Color of outside wall surface

EXPERIMENTAL SETUP

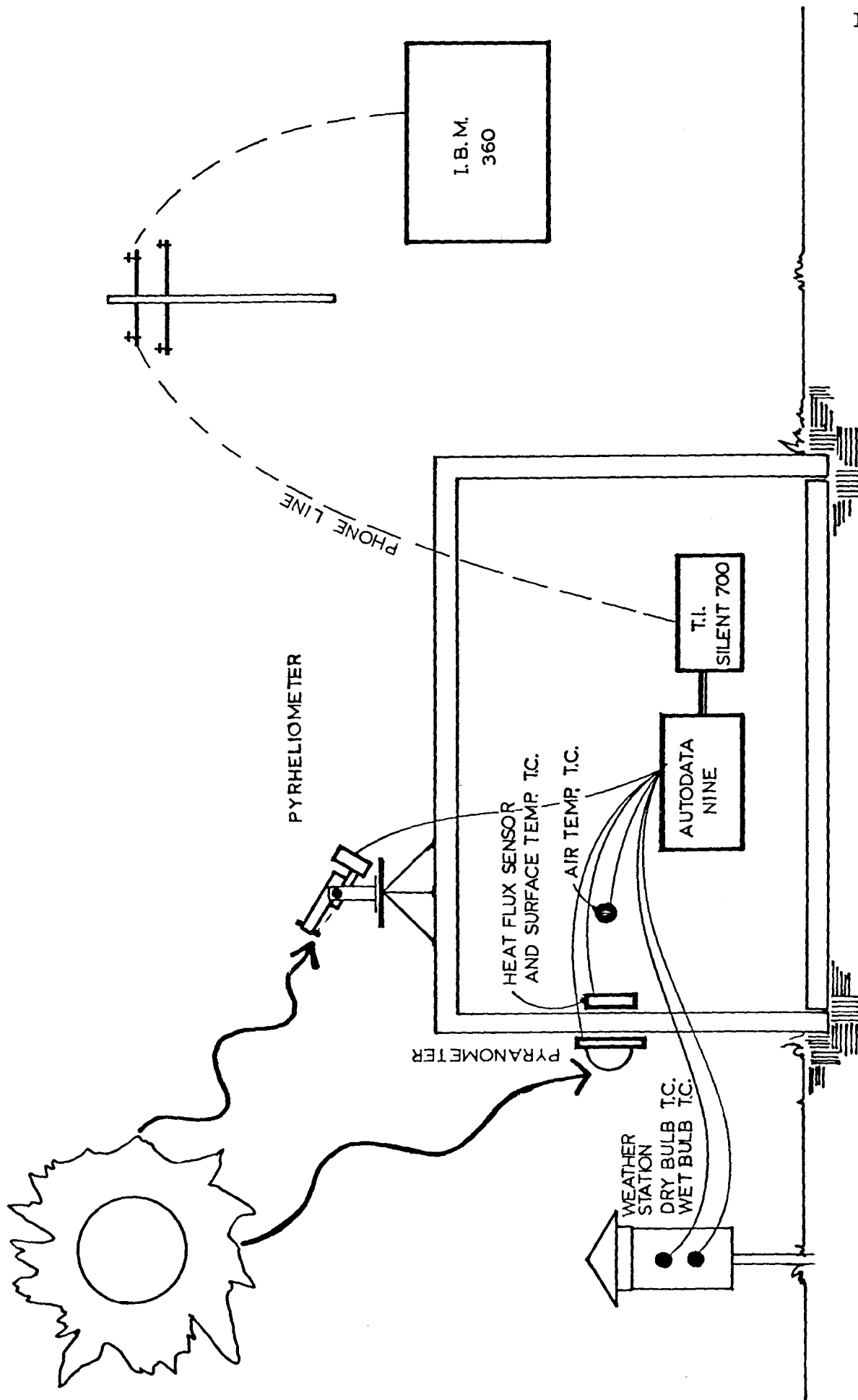
An experimental program was begun with the intention of measuring all data necessary to do a detailed verification of the theoretical computer code. A test plan was formulated involving tests on twelve separate wall sections. In each case, the information recorded included: outside ambient air temperature, inside air temperature, wind speed, total horizontal solar radiation, direct normal solar radiation, heat loss across the wall which is being tested, and in most cases, the solar insolation directly incident on the outside surface of the wall being tested. Data was taken every half hour, using the following sensors (Figure 6). Temperature measurements were made with type K thermocouples. Ambient wind speed was measured using a Kurz Model 435 temperature compensated, hot probe anemometer. Direct normal solar radiation was measured with an Eppley Model PSP Pytranometer. Heat flux across the inside surface of the wall was measured with a Hy/Cal Model BI-7x-K Bi-Directional thermopile-type heat flux sensor. The output of these sensors was scanned by an Acurex Autodata-9 Data Logger with an averaging option. The data taken were then stored on a TI Model 733-ASR stand-alone computer terminal for cassette storage of data in local mode. The sensors were scanned twenty times per minute by the Data Logger, and thirty minute running averages were made for all channels. At the end of each thirty minute period, the average value for each channel was written onto the TI Cassette Tape. Data was taken at each site for a period of five to six days. After this it was read into an IBM 360-67 Computer. All necessary data reduction for comparison with predictions of the computer code was done on a time-sharing system. This was done for data taken at ten separate houses with tests on twelve different walls selected to test the limits of the code with respect to mass, color, orientation, thermal insulation, and climatic region. Some typical results are given below.

EXPERIMENTAL RESULTS AND CORRELATION WITH THEORY

To verify the theoretical computer code, the experimental readings were compared with the theoretical predictions on an hourly basis as well as on an average basis. The computer code was run with the weather data measured at each site. Using this data the code determined the theoretical heat loss across the inside surface of the wall, and it determined the inside wall surface temperature. The calculated results were then plotted on an hourly basis against the measured values in each case. Two examples of results are given here.

The first example to be considered is a South-facing dark-colored light weight C.M.U. wall as shown in Figure 2. For this wall, the graph

TEST SITE INSTRUMENTATION



in Figure 7 gives the heat flux across the inside surface on the vertical axis with heat loss from the room as positive and heat gain into the room from the wall shown as negative. The horizontal axis gives the Julian Day with labels at the beginning of each day (hour Zero). The dots, which represent experimental data, show that generally a loss occurs at night with a sharp heat gain into the room during the day. Superimposed on the experimental data is the theoretical prediction of heat flux across the wall. It is seen that the correlation is quite close in magnitude to the measured data.

For this same wall configuration, the experimental and theoretical inside wall surface temperatures are plotted on Figure 7. The correlation is seen to be excellent.

A light-colored, North-facing, ten inch adobe as shown in Figure 3, was also tested. For this wall, the theoretical and experimental data of flux and temperature across the inside surface are shown in Figure 8. Again, agreement is quite good.

In addition to these, ten other walls were tested and the results were compared with theoretical predictions for each particular test. Hour-by-hour comparisons of theoretical and experimental data were plotted in each case and the results indicated good success from slightly better to slightly worse than the comparisons presented here. In all cases, it was determined that the computer code adequately described the physical system, and thus the validity of the hourly results of the theoretical program was established.

With the validity of the program established on an hourly basis, the measured and theoretical Effective U-Values were compared for each of the experimental sites to assure the accuracy of the integrated results. The differences in experimental and theoretical solar collector efficiency as defined in equation 6 above ranged from 2-9% for the wall sections studied. This is within the range of normal engineering accuracy for solar design and average load calculations. So, the validity of the code for estimating the solar collector efficiency of the wall has been demonstrated at the limits of the conditions likely to be encountered in normal construction. Therefore, the results of the theoretical computer code can be used to predict the solar performance of most walls encountered in normal construction.

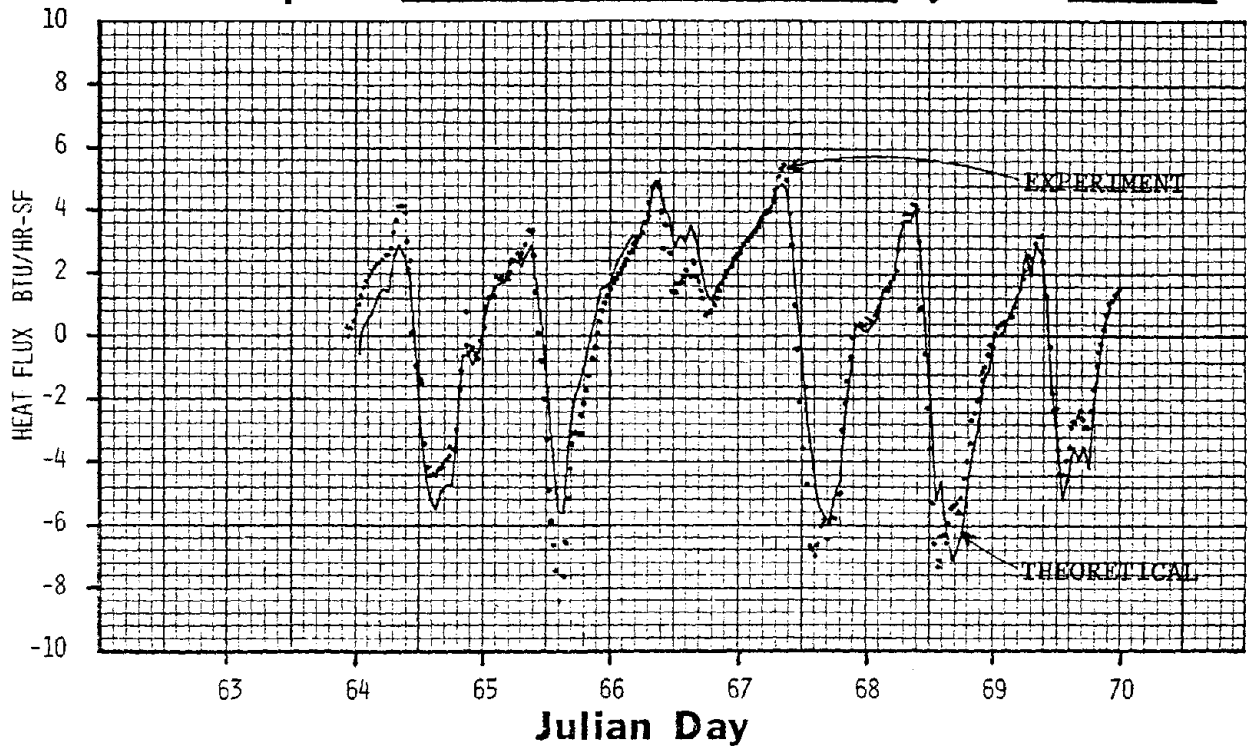
Site: G

Channel(s): 11 FLUX SENSOR B

Description: 8" CMU, SOUTH WALL HOLLOW PATH

y max. 10 BTU/HR-SF

y min. -10 BTU/HR-SF



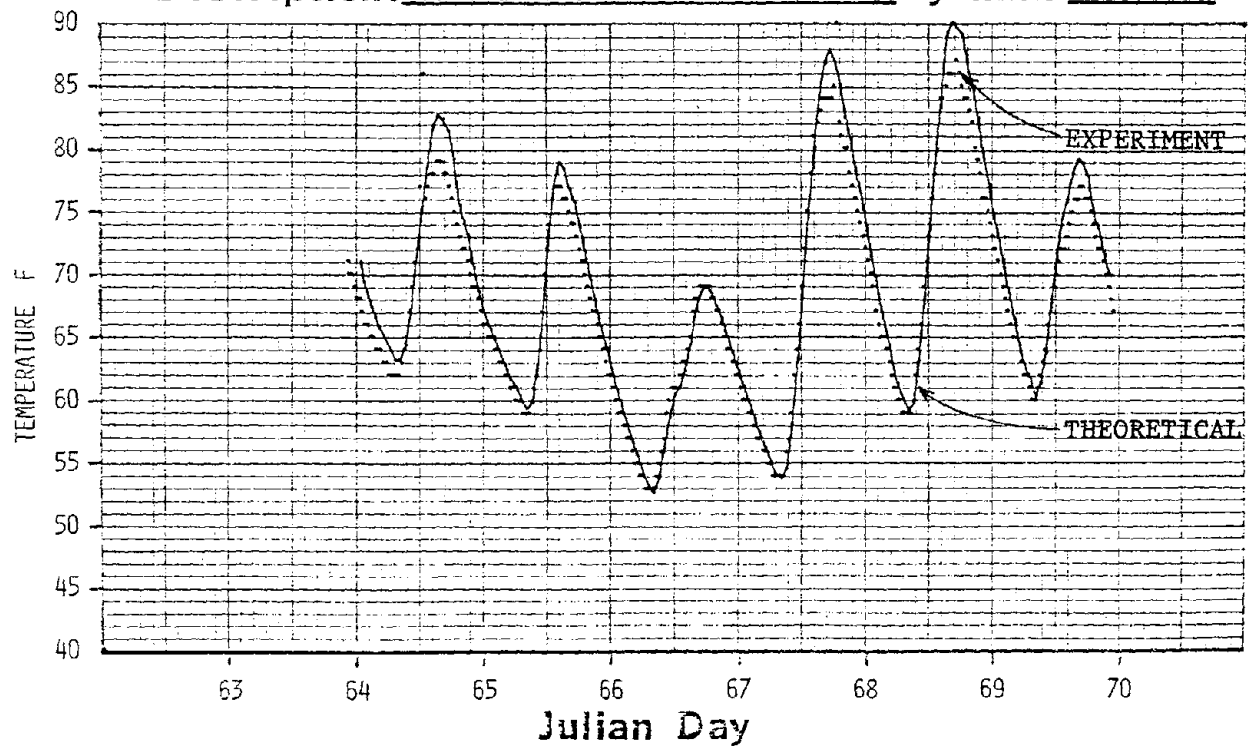
Site: G

Channel(s): 22 T.C. IN FLUX SENSOR A

Description: SURFACE TEMPERATURE SOUTH WALL

y max. 90 F

y min. 40 F



101-14

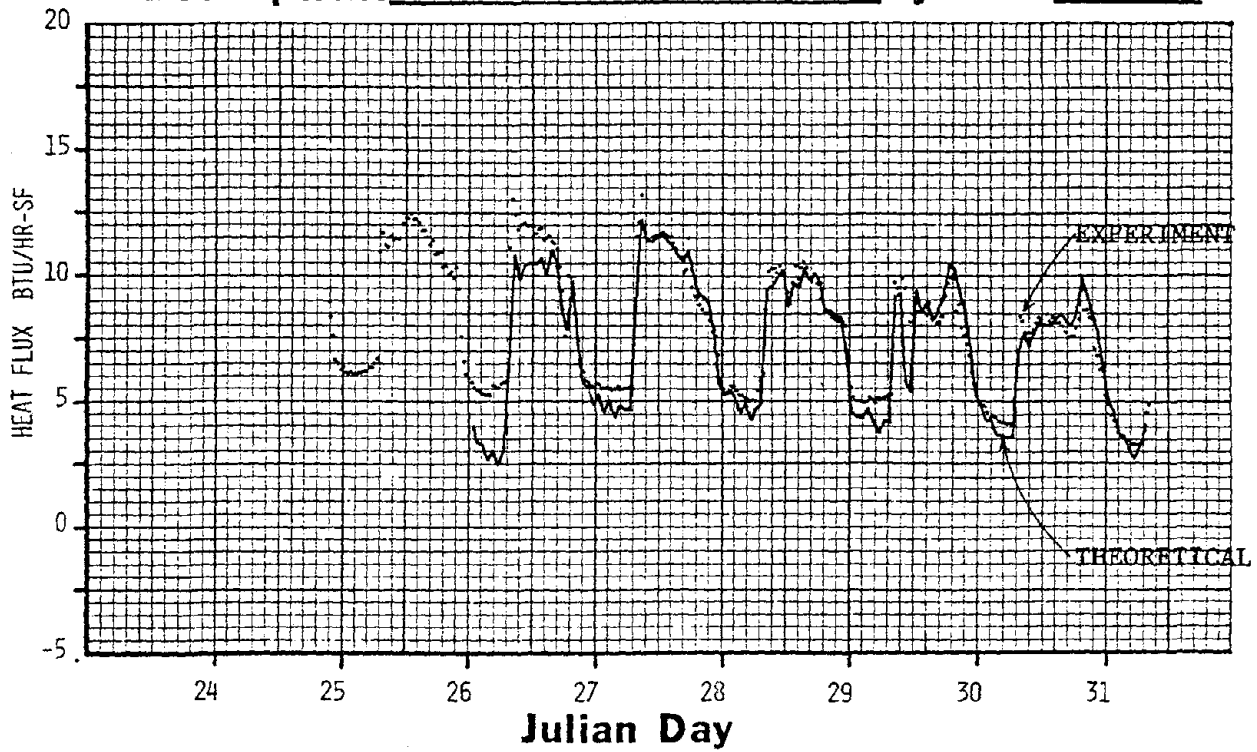
Site: D

Channel(s): 10 FLUX SENSOR A

Description: NORTH ADOBE WALL, LIGHT COLOR

y max. 20 BTU/HR-SF

y mim. -5 BTU/HR-SF



Site: D

Channel(s): 22 T.C. IN FLUX A

Description: SURFACE TEMP, NORTH ADOBE WALL

y max. 90 F

y mim. 40 F

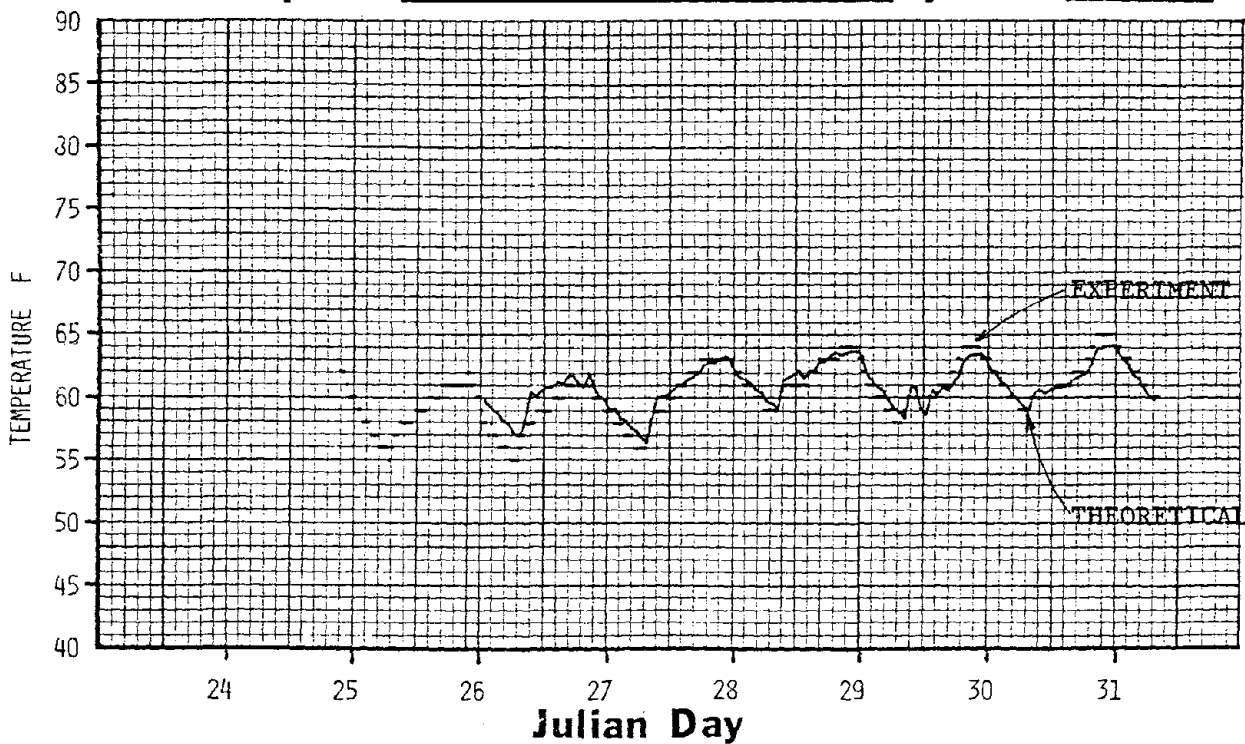


FIGURE 8

CONCLUSIONS

As a result of the theoretical computer code and the experimental field verification of this code, it was determined that a single number, the Effective U-Factor, can be used to describe the average thermal performance of a wall section. From this Effective U-Factor, the passive solar collector efficiency can be determined for a wall section. It was found that this collector efficiency is independent of wall orientation; is constant throughout New Mexico (and hopefully other climates); is linear with solar absorbtivity; and is different for different wall types. The solar collector efficiency can be used to predict the long-term thermal performance of a wall section.

These results are important because they show that the long-term average thermal performance of building shell elements can be significantly better than is predicted by steady-state analysis techniques. The Effective U-Factor concept provides a simple method of including both mass and solar effects in building energy conservation codes such as ASHRAE 90-75.

ACKNOWLEDGEMENTS

This work was done for the New Mexico Energy Resources Board and the New Mexico Energy Institute at the University of New Mexico. The work of Mr. Wybe J. van der Meer, Principal Investigator; the assistance of Dr. Jim Dritt, Project Coordinator and the support of Mr. Roger Easley are greatly appreciated.

REFERENCES

1. van der Meer, W.J., "Energy Conservative Housing for New Mexico," New Mexico Energy Institute, 1977.
2. Schlichting, H., "Boundary Layer Theory," McGraw-Hill, 1968.
3. Duffie, J., and Beckman, W., "Solar Energy Thermal Processes," Wylie & Sons, 1974.
4. McAdams, W., "Heat Transmission," McGraw-Hill, 1954.
5. Hornbeck, R., "Numerical Analysis," Quantum, 1975



ENERGY CONSERVATION IN THE MANUFACTURE AND USE OF BRICKS

By West, H.W.H. and Ford, R.W.

ABSTRACT: The conservation of energy has been a major recent concern both in the manufacture of bricks and in the use of brickwork. Energy audits have been carried out by BCRA on selected works and proposals made to minimise fuel usage in industry-wide surveys. A new method of building has been developed which enables masonry structures to be erected more economically and provides for greatly increased thermal insulation tailored to particular local or statutory requirements.

ENERGY CONSERVATION IN THE MANUFACTURE AND
USE OF BRICKS

by

H.W.H. WEST* AND R.W. FORD†

1. INTRODUCTION

The current so-called energy "crisis", that is expensive oil, followed more than a decade of cheap fuel in which prices for all energy sources had to be fixed in relation to the low prices obtaining for oil. What is now forgotten is that this was essentially an interlude, quite untypical of the trend of history which has inevitably meant the exploitation of progressively more difficult sources of fuel and hence progressively more expensive ones, until now we are faced - Middle East apart - with boring the sea-bed at depth under disturbingly hazardous conditions.

Much, therefore, of what needs to be done to conserve energy is already known from earlier times and particularly from the years of World War II when the whole of Europe at least was expert in the subject! Application of principles enunciated then and good management, together with relatively minor investment in instrumentation and insulation can lead to substantial savings.

2. FUEL SURVEYS

Recent British experience in this field goes back to 1942 when the fuel situation was becoming serious because of the demands of industry and reduced output from the coal mines. A fuel saving campaign was started and individual trade associations were encouraged to set up their own Fuel Efficiency Committees. For the refractories and heavy clay industries the British Refractories Research Association (the predecessor of BCRA) collected data on fuel consumption and production and made inspections of, and offered advice to, individual works, especially those which the returns showed had high fuel consumption.

* Head of the Heavy Clay Division and Officer-in-Charge
of the Mellor-Green Laboratory.

† Principal Scientific Officer

For the first time manufacturers had the yardstick of the industry average against which to measure their performance and what had previously been one of the costs which appeared in the accounts but about which little was done, now assumed a competitive importance especially when it was found that intermittent kilns used more than twice as much fuel as continuous ones. It is significant that these surveys ended in 1965 when the cheap fuel boom was well established.

During that twenty years the whole nature of the British brick industry had changed considerably. Works had been modernised, closed down, amalgamated, and new ones built. The use of boilers for steam and power production had given way to electricity and waste heat dryers had replaced steam-heated hot floors. Tunnel kilns were the preferred method of firing, chiefly to give improved working conditions and a higher proportion of first quality ware.

In the winter of 1973-74, however, a real fuel crisis occurred and BCRA again started a survey of the brick industry to provide basic data in communications with Government and to provide a start point for investigations to reduce fuel consumption. The data relate to 1973 and the following year the survey was repeated. Not all works were included but sufficient data are given in Table 2 to establish the important factors in process and product and to make comparison with the wartime surveys.

In 1942 the survey covered 326 works in refractories and all heavy clay products, - bricks, roofing tiles, land drains, floor quarries and clay sewer pipes. In recent surveys about 80% of the total productive capacity of the country has been covered. Fewer kilns were surveyed in 1974 when the total annual U.K. production had fallen from 6315 million clay bricks to 4975 million. The somewhat improved thermal input found no doubt owed a good deal to the closure of the more fuel intensive plants.

The enormous range of fuel consumption shown in Table 2 includes products as different as Fletton commons or Scottish composition bricks, both of which contain considerable inherent carbon, and Staffordshire blues fired under reducing conditions in intermittent kilns at a temperature more than 100 deg.C higher, but even within the same product and process differences can be found. The range of electricity consumption is also shown and these figures are net. If the electrical energy is recalculated to the basis of heat in fuel at the power station they need to be multiplied by a factor of approximately 4 to allow for the efficiency of generation. On transposing to thermal equivalents a factor of 0.143Th/kWh has been used.

Table 2
General Summary of Data Obtained from Energy Survey

Making Process	Type of Kiln	No. of Works	Total Therms/Ton Drying & Firing		Electricity Therms/Ton	
			Range	Mean	Range	Mean
Stiff Plastic Extrusion	Continuous	41	0.9-41.2	14.8	0.6-6.3	1.3
	Tunnel	13	15.2-44.3	26.8	0.32-3.03	1.5
Stiff Extrusion	Continuous	11	18.9-41.2	29.4	0.6-1.55	1.3
	Intermittent	2	49.2-55.8	52.5	2.4-2.9	2.65
	Tunnel	11	18.9-50.2	28.7	1.1-2.3	1.7
	Continuous	10	11.1-48.8	27.7	0.3-1.3	0.9
Hand Made and Soft Mud	Continuous	6	33.6-86.4	55.7	0.87-1.3	1.1
	Intermittent	2	39.6-53.2	46.4	1.5	1.5
Blue Engineering (Stiff Plastic or extruded)	Clamp	4	55.2-108.8	71.1	0.6-1.1	0.8
	Intermittent	5	51.6-69.3	63.1	-	-
Flettons Semi-dry pressed	Continuous	23	4.8-18.2	8.15	0.42-0.77	0.61

In Table 3 the same data are considered from the point of view of the raw material, account having been taken of inherent and added carbonaceous content. The importance of carbonaceous material, occurring in unique and readily available dispersed form in the Lower Oxford Clay, and, less helpfully, often as discrete pieces of coal, in the Carboniferous, is clearly seen. It is particularly interesting to note that a much lower percentage of this latter fuel form can be tolerated in facing and engineering bricks than is possible in black-hearted commons.

Some explanation should be given for the term "stock bricks". These are characterised by the high proportion of low grade fuel, coke breeze, coal slurry, town refuse etc. added to the bricks to give a distinctive appearance when fired in either continuous kilns or clamps. "London Stocks" also have a high proportion of chalk added in the form of a slurry. Stocks are made by the soft mud or hand-made process. Heat must be applied to a clamp to raise the temperature of the bricks sufficiently for the contained fuel to ignite. Traditionally this was accomplished by layers of large coke in the base, but of the 13 clamps in the 1974 survey, 2 are fired by oil and 5 by gas.

3. ENERGY AUDITS

The data given in these tables are useful and may seem extensive, but a much more intensive survey has been carried out by BCRA on behalf of the British Government on three building brick and four refractory works. These "energy audits" are carried out according to conventions agreed by the International Federation of Institutes of Advanced Study, and in essence require the calculation of all the energy which has gone into the product, including the raw materials, the energy cost of the metals in the machinery, even the energy cost of the bricks and mortar in the factory buildings! Strictly, the calculation of energy requirements should be taken right back to the point at which all the resources are in their natural state, but in this case information was only required back to the origin in U.K.

The results in Figures 1 and 2 show the importance of the energy content of the raw materials in the manufacture of some refractories and the over-riding importance of the firing process in building bricks. The Figures also show the primary fuel consumption expressed as a percentage of the total energy requirement. The primary fuel consumption includes the purchased electrical energy after allowing for the efficiency of generation (23.85%) and all other purchased fuels after correcting for the efficiency of the energy industries viz:-

North Sea Gas	90%
Oil	88.21%
Coal	96%

Table 3 Summary of Energy Consumption

Product	Clay	Output 1000T/yr	Therms per ton						Total A a+b+c+d	Total B b+c+d
			Inherent and Added a	Kiln and Dryer b	Power (1) c	Etc. (2) d	Total A a+b+c+d	Total B b+c+d		
<u>Continuous Kilns</u>										
Flettons (Commons & Facings)	Lower Oxford Clay	4664	25.0	8.9	1.9	0.5	36.2	11.2		
Commons	Carboniferous	913.4	20.9	7.6	3.8	0.4	32.7	11.8		
	Other	411.7	4.9	23.8	4.7	0.3	33.7	28.8		
	Total	1325.1	15.9	12.6	4.1	0.4	33.0	17.1		
Facings and Engineering	Carboniferous	1027.9	5.6	29.4	5.9	0.4	41.3	35.7		
	Keuper Marl	551.9	0.2	34.3	5.6	0.4	40.4	40.2		
	Etruria Marl	500.4	0.0	30.2	6.1	0.3	36.6	36.6		
	Boulder Clay	252.3	7.2	23.7	5.3	0.3	36.6	29.3		
	Weald Clay	151.2	0.0	36.6	5.6	0.4	42.7	42.7		
	Other	373.2	1.4	33.2	5.3	0.3	40.2	38.8		
Stocks	Various	187.6	23.6	31.9	5.5	0.6	61.6	38.0		
	Total	3044.5	4.1	30.9	5.7	0.4	41.1	37.0		
<u>Intermittent Kilns</u>										
Facings	Various	76.4	4.9	53.2	5.8	0.4	64.3	59.5		
Stocks	Various	123.4	22.0	28.1	3.1	0.6	53.8	31.8		
Blue	Various	115.3	0.0	67.2	8.2	0.5	75.8	75.8		

(1) Power is gross allowing for generation efficiency

(2) Mainly internal transport and clay winning

The electrical energy (again after allowing for the efficiency of generation) is expressed as a percentage of the gross energy requirement (GER) of the product.

4. ECONOMY IN PRODUCTION

The detailed breakdown of the data in energy audits enables management to minimise their energy costs at the various points of the process in exactly the same way as a breakdown of process costs enables money to be saved. At the more practical level the Department of Industry in U.K. has commissioned "Thrift" schemes in which consultants spend one day visiting a plant and making on the spot recommendations for economy. No measurements are taken, but it is surprising how many companies are wasting energy in ways which can be detected simply by inspection. Typically, the areas concerned are lighting, space heating, poorly insulated ducts and inefficiently operated boilers and compressors. In all 10% saving of energy is not unusual!

Less obvious energy wastage is detected only by more sophisticated and lengthy attention. BCRA provide a monitoring service for some of their member companies, by which regular visits are made to works and recommendations for improved operation made as a result of both observation and measurement. On subsequent visits the recommendations are checked to ensure that they have been implemented and the gain has been achieved. At one works, slight changes in the operation of an apparently efficient tunnel kiln and dryer resulted in a reduction of fuel consumption of over 10% and this has been maintained. Nevertheless, even on this works where monthly visits are made, the same failures to maintain plant, especially sand seals, are seen from time to time, and this emphasises that fuel economy is a management, not strictly a technical, problem.

One of the legacies of cheap fuel is that most works have inadequate instrumentation to monitor its use. Thus multiple kiln plants rarely have individual fuel meters on each kiln and it is instructive to see how much attention has been paid to this recently in U.S.A. Similarly, insulation is frequently neglected or inadequate, particularly on hot air ducts transferring waste heat from kilns to dryers. Without individual meters and instrumentation the effect of changes in firing methods cannot be measured and the value of the change in terms of overall cost determined. Sad to say, when new, and often patented, developments in burners or perhaps automatic re-circulation and fan control are carefully examined it is not infrequent to find that the claims are not borne out by objective data, and without such data, of course, the manager who ordered the new development is subjectively very prone to consider it a success - and say so loudly!

In any drying and firing operation some thermal losses are inevitable, but changes in the method of firing and type of kiln may enable quite startling improvements to be made. When clay sewer pipes were coal-fired in intermittent kilns and salt-glazed, as recently as 1961 they required 138Th/t for firing alone. When the change was made to unglazed pipes fired by oil or gas in tunnel kilns fuel consumption was reduced to less than 40Th/t for the process as a whole. This is higher than building bricks because of the typically higher firing temperatures and lower setting densities for pipes.

Similarly the choice of fuel itself is important. Oil and gas are "convenience fuels". Any change in fuel requires that the operation of the kiln should be reconsidered and this is to be expected to give improved thermal efficiency. In addition, however, greater control can be achieved with oil, and even more with gas, and more sophisticated automatic control systems may be used. Certainly the capital costs of the changeover would not have been accepted but for the lower labour charges and generally better quality ware leading to lower overall costs.

Increased outputs of up to one-third have been obtained at some works because gas enables stable flames to be achieved in the preheat section of the kiln at lower temperatures than is possible with coal or oil and this clearly has a big effect on profitability. Fuel consumptions are sometimes up to 10% higher and sometimes lower on changing to gas from solid or liquid fuel. Interestingly enough, General Shale Products Corporation in Tennessee report that changing their side-fired tunnel kilns from gas to powdered coal has resulted in a general reduction in fuel consumption.

This change, however, is very recent and the move away from solid fuel in Great Britain at least is shown in Figure 3. In Figure 4 the steady decline in total fuel consumption is directly related to the reduction in the number of intermittent kilns, especially coal-fired ones. In fact it is only the building brick industry in which coal has a major share of the total fuel used (43% in 1973), and this is because of the large number of Hoffmann and transverse arch kilns in use.

Clearly then all possible steps must be taken to minimise fuel consumption. The maximum use should be made of "waste" heat and BCRA are currently measuring the effect of thermal wheels installed to extract heat from exhaust gases, and also the direct use of exhaust gases for drying without affecting the colour of the goods by scumming.

5. SINGLE LEAF MASONRY

Besides fuel economy on the works forms of construction which provide a good thermal environment are to be encouraged, so that heating and cooling requirements are minimized.

In the United Kingdom the cavity wall is well established as the traditional method of meeting the requirements of external walling in dwellings. Originally in U.K. walls were solid brickwork, and in Scotland they still are - usually 215mm thick and rendered on the outside to resist rain. The possibility of replacing cavity construction by a superior form of wall using through the wall (T.T.W.) units is well known and various aspects have been discussed by Butterworth et al.¹ leading up to the concept of the V-brick. This was unfortunately not economically successful and any marketable form will have to use the superior properties of the product rather than rely upon thickness.

The simplest form of T.T.W. unit is the 'SCR brick' developed by the Structural Clay Products Research Foundation in Illinois². This was approximately 292 x 140 x 56 mm laid with 12 mm joints with the interior finish attached to furring on galvanized clips. T.T.W. units have been produced in Canada and a number of fine blocks of apartments can be seen constructed in this manner with insulation on the inside.

This single leaf masonry is not a new concept, but there are certain new elements in the BCRA programme:-

- (i) It is intended to be a coherent method of building but based on a design manual which clearly states the rules on which it is based.
- (ii) It uses the minimum thickness of brickwork required to guarantee the structural performance with a rudimentary cavity combined with proper d.p.c. details.
- (iii) When complete it will be a tested method in which by means of both laboratory and site tests the performance is known and the consequences of modification in plan form or details can be assessed.
- (iv) It is intended to be a brick method of construction, using the aesthetic excellence of facing bricks as well as their structural competence.

The concept optimises the use of clay products and completely eliminates concrete blocks from the periphery walls while permitting the maximum flexibility in providing enhanced thermal insulation at any desired level by the mere alteration of the thickness of the insulation material. In the standard form the wall is thus 102.5 mm

of facing brick, 50mm of Styrofoam insulation and 12½mm of plaster-board and finish. It gives a U value of 0.5 W/m²/°C well within the present Building Regulations and better than the likely future modification to 0.6 W/m²/°C. In fact it is the aspect of resistance to rain penetration that most people find immediately suspect in SLM and this was one compelling reason for building a real structure for occupation to demonstrate this and to enable measurements of thermal comfort and lack of condensation to be made. Before this, however, extensive laboratory testing had been carried out using the B.S. rain penetration apparatus which subjects the wall to a 64 mph gale of wind while saturating it from the top with 1 gal. of water every half an hour - a total rainfall of 2½ inches every 24 hours or 17½ inches over the 7 days of the test.

In brief single leaf walls with the inner face lined with dab-fixed boards of Styrofoam remained impermeable to water even after periods of testing of up to 14 days. Wall/floor, wall/wall and window/wall junctions have been successfully tested and specific designs for these details have been formulated. Similarly the effect of weepholes at ground and first floor level and the effect of fixing devices penetrating the brick leaf have all been tested and found satisfactory. Finally the single storey extension at Alsager has been tested insitu and the details proved successful.

In the single storey extension, apart from a small section of wall built as a thermal comparison in standard cavity construction with Thermalite block inner leaf, all external walls were constructed in 102.5 mm SLM using a 14 hole perforated wirecut facing brick. While calculations were provided for one wall there was no structural problem which could not be solved by existing design rules.

During construction thermocouples were inserted into the walls at various positions around the perimeter to measure the internal and external air and surface temperature and the temperature of the internal surface of the brickwork. Additional measurements of the effect of direct heat from the sun are made. All the data is recorded automatically at appropriate regular intervals on a data logger and processed by computer.

A demountable partition enables the test structure to be isolated from the main dwelling. Good agreement has been obtained between the calculated and actual heat requirements during winter. The application of thermal insulant on the inside surface of a single leaf of brickwork means that SLM behaves as a thermally light structure. It is generally believed that such structures are more economical to heat intermittently in winter but are more prone to summer overheating. Mathematical modelling assuming typical U.K. weather conditions has confirmed this³. Comparative analyses made on SLM structures with the thermal insulant applied either on the inside (lightweight) or on the outside (heavy weight) have indicated that heating requirements in the light weight house would be about 10% less in January if daytime heating only was used. Temperatures in excess of 25°C could occur during periods of high solar gain in

Summer in both types of structure, this effect being worse in the lightweight house. Under U.K. conditions this overheating problem can be largely overcome by increasing ventilation rates. In situations where air-conditioning was being used, the lightweight structure would make greater demands on the plant.

Practical tests have shown that under the rapid conditions of heating typical of switching on central heating in the evening there is little chance of condensation on the internal surface of the SLM wall, and under steady state conditions there is none. Similarly only under extreme conditions could condensation occur within the wall structure and then only at the brickwork/Styrofoam junction so that very little effect would be noted. Tests on an internal/external wall junction have indicated very little cold bridge effect in terms of surface condensation.

No special difficulties were found in fixing the radiators etc. in the single storey building, but loading tests have been carried out in the laboratory on Styrofoam/plasterboard assemblies with shelves and cupboards fixed in different ways. Various adhesives have been tested and with the best of these failure occurred at the umbrella type fixing rather than at the Styrofoam/plasterboard junction. A new type of fixing was developed but has now been superseded by a Fischer fixing which has been tested to sustain loads in excess of 300 kg. when supported at 4 points.

6. CONCLUSIONS

The most important aspect of economy in energy usage is: still good management. Managers need to check regularly that the measures they have adopted are the most efficient, and periodic visits by outsiders seem to be worthwhile in bringing to attention obvious areas of economy that tend to be overlooked. Proper metering of fuel and instrumentation of plant is essential, as is the accurate recording of data and the use of that data for control and as an input to future decision making on company fuel policy.

It may be necessary to revert to coal eventually with all the problems both in the works and in the wider environment that that entails. At least let that day be postponed for as long as possible by the sensible and effective use of the convenience fuels still available and by the construction of dwellings that minimize the need for space heating and air conditioning.

ACKNOWLEDGEMENTS

The authors thank Mr. A. Dinsdale, O.B.E., Director, British Ceramic Research Association, for permission to publish, and their colleagues of the Energy Research Group, A.E. Aldersley and C.N. Walley, who collected and analysed the data on which the first part of this paper is based.

APPENDIX I

1. BUTTERWORTH, B. and FOSTER, D: "The Development of the Fired-Earth Brick". Trans. Brit. Ceram. Soc. : Part I, 55, 457, 1956; Part II, 55, 481, 1956; Part III, 56, 529, 1957; Part IV, 57, 469, 1958; Part V, 58, 63, 1959.
2. Anon: "The SCR-brick Wall, Technical Notes on Brick and Tile Construction". Structural Clay Products Institute. Vol. 7, No. 7, 1956.
3. BASNETT, P., MOULD, A.E., and SIVIOUR, J.D.: "Some Effects of Ventilation Rate, Thermal Insulation and Mass on the Thermal Performace of Houses in Summer and Winter". Energy and Housing, Special Supplement to Building Science, Pergamon Press, 1975.

	<u>Electrical Energy</u>	<u>Primary Fuels</u>
Kiln furniture	9.1%	54.9%
Basic brick	13.5	54.6
Saggars	4.2	70.5
Steel		
Refractories	7.8	58.3
Firebricks	7.6	93.0

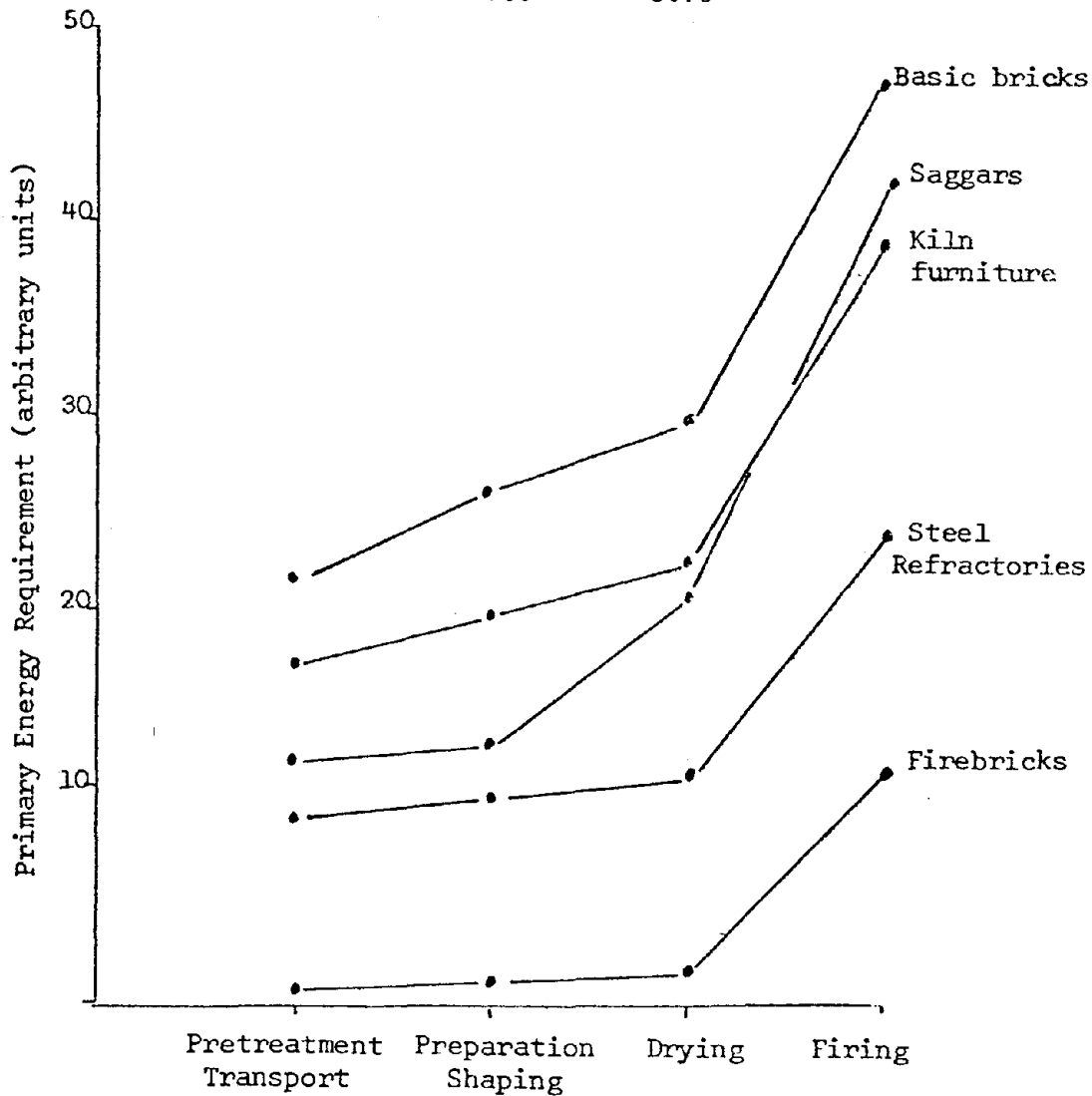


Figure 1 Cumulative Primary Energy Requirement Refractories

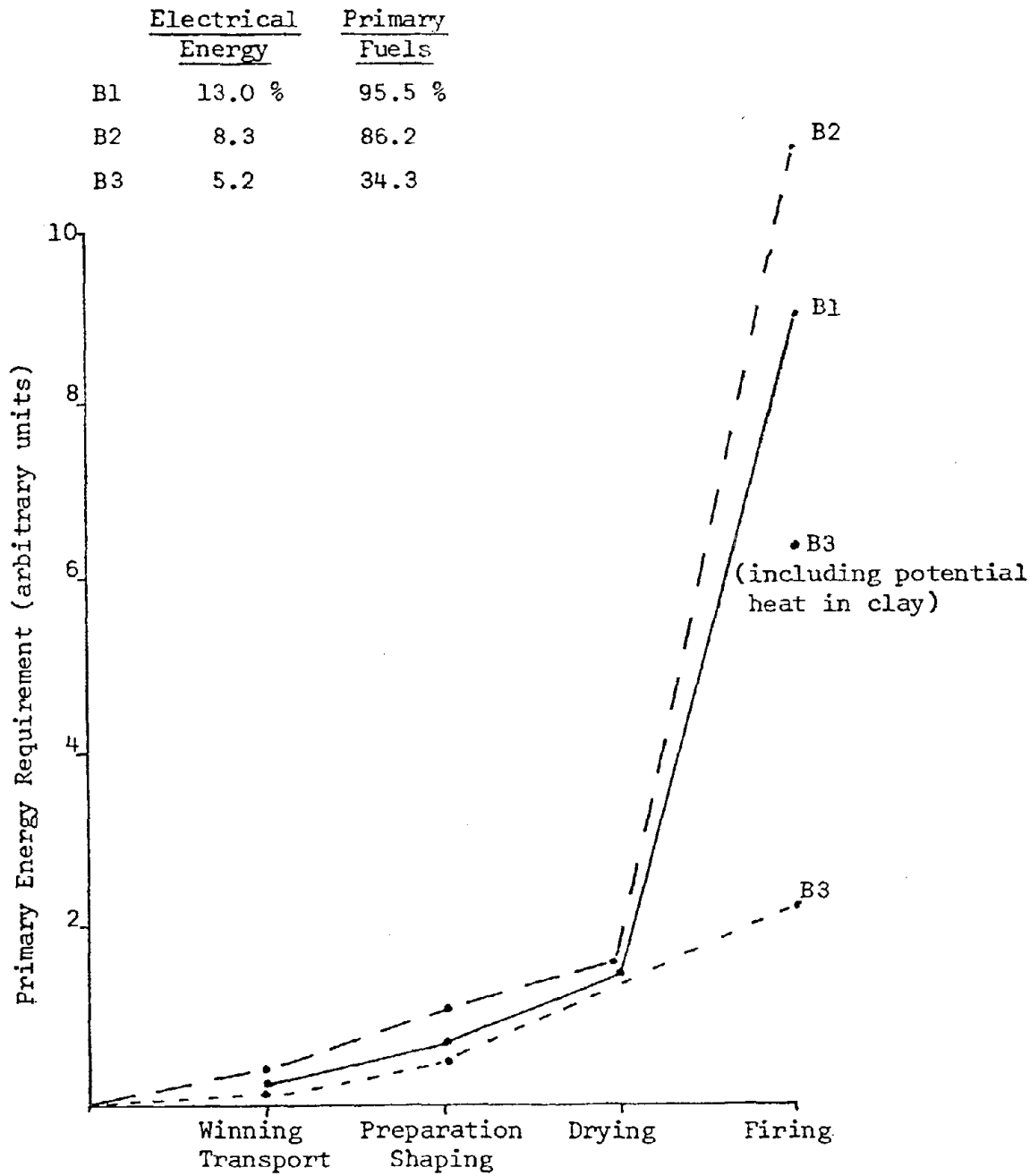


Figure 2 Cumulative Primary Energy Requirement Building Bricks

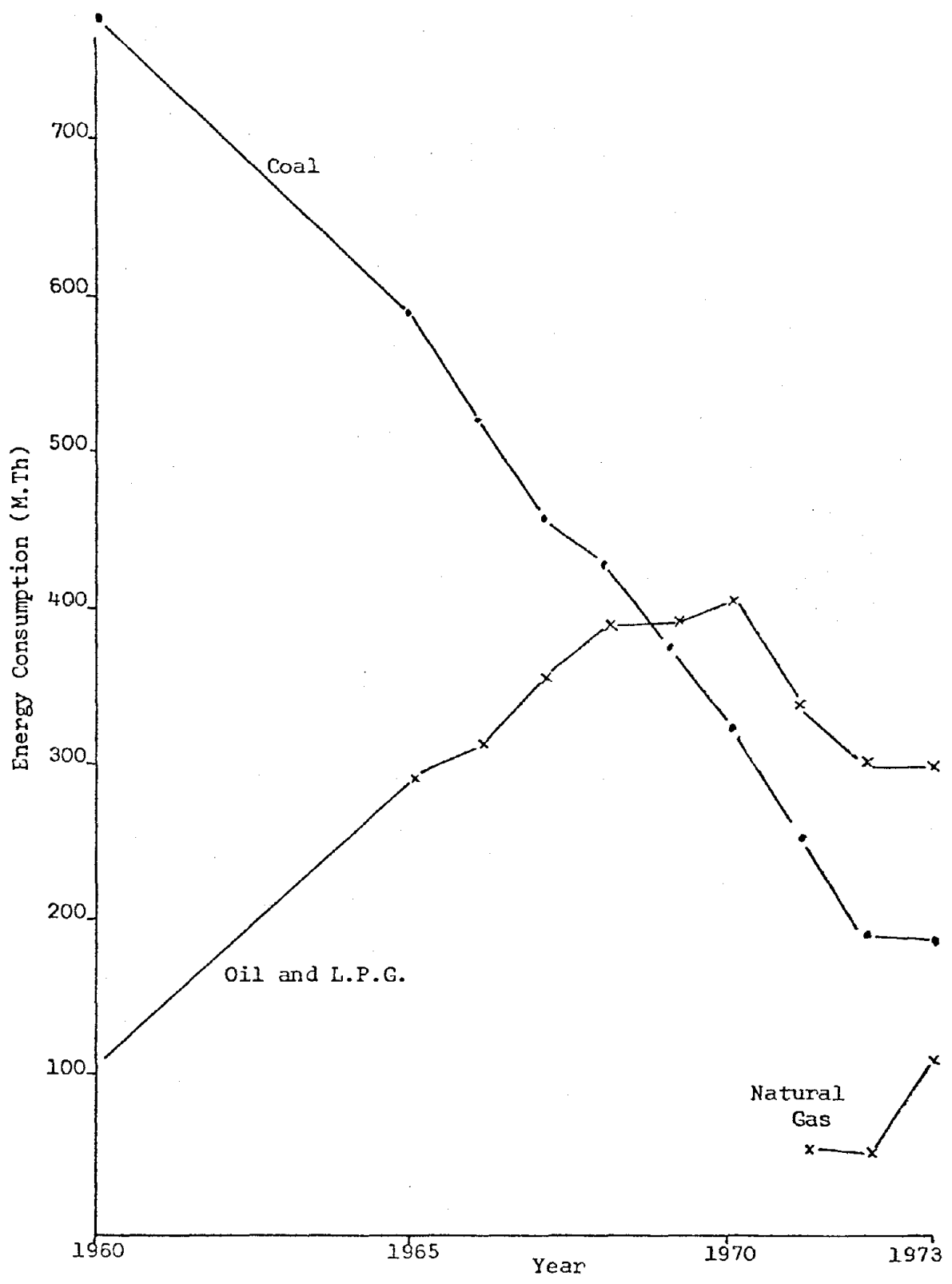
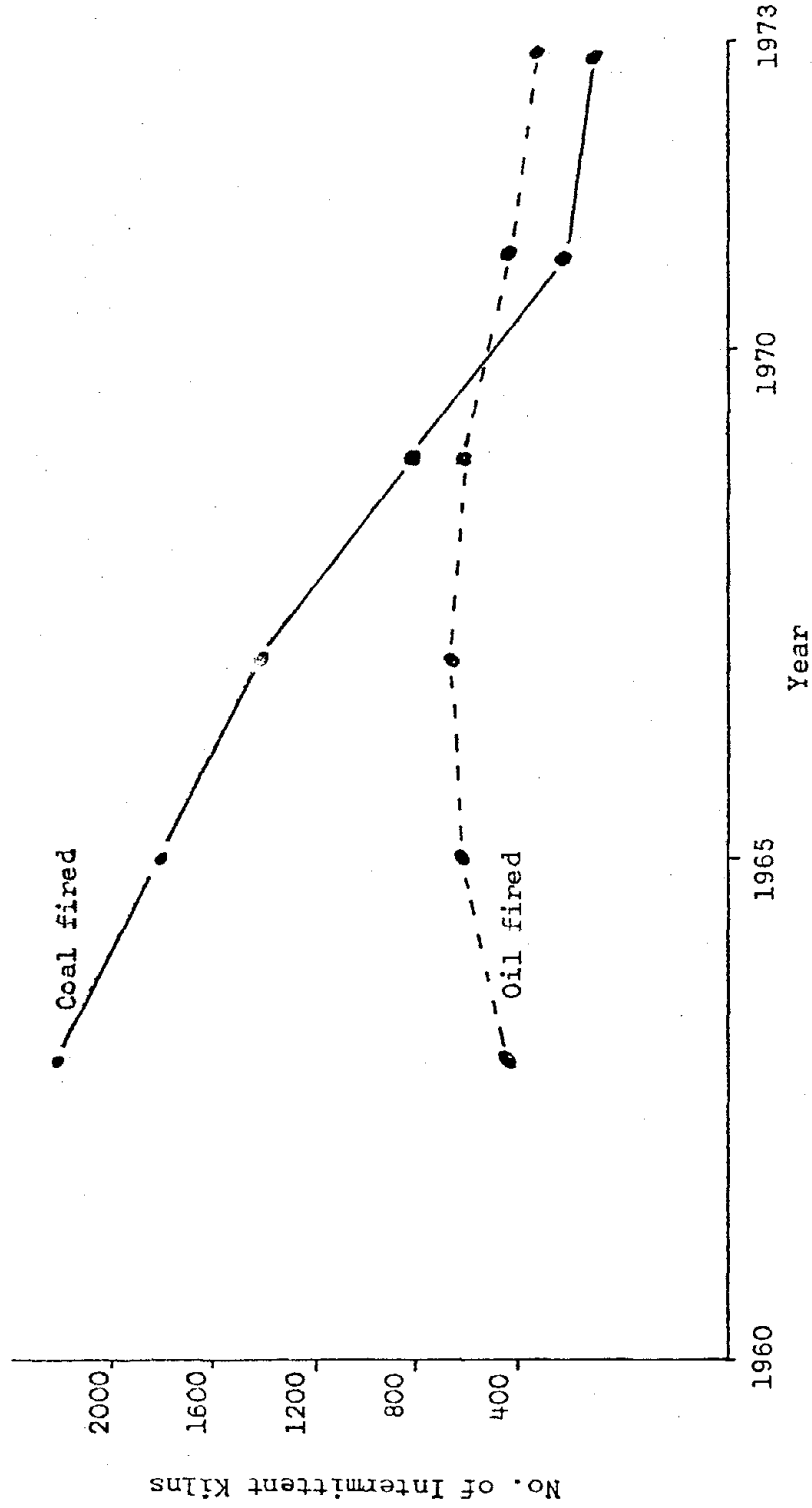


Figure 3 Consumption of Various Fuels in the Heavy Clay and Refractories Industries

Figure 4 Decline in Intermittent Firing in U.K.



EXPERIMENTAL AND THEORETICAL STUDY OF ENERGY CONSUMPTION
IN BUILDINGS

By Dr. Jay L. McGrew,¹ George P. Yeagle,²
and David P. McGrew³

ABSTRACT: Heat transfer experiments were conducted over the period March 28, 1978 through March 31, 1978 in the Chehalem Elementary School in Portland, Oregon. Heat flows, temperatures, sun flux, and wind speed were measured. The data was analyzed and monthly and yearly energy use projections were made.

Projections show that the addition of an additional pane of glass to the windows reduces heat flow through the windows and appears to be cost effective, but the actual projected yearly savings is only approximately \$200.00 per year at today's fuel costs.

The addition of insulation to the uninsulated brick walls will reduce heat flow through the walls over the year and results in a projected annual cost savings between \$400.00 and \$775.00 per year at current fuel costs. The cost of such additional insulation is estimated to be \$20,500.00 for the 11,752 square feet of wall. The annual rate of return on the investment is between 2.0% and 3.8%. The investment in insulation is thus not justified with current or any foreseeable future fuel costs.

Certain problems in the heating/air conditioning system were discovered. These problems will be corrected in a future project, and a significant savings in energy use and costs should be achieved.

¹ President, Applied Science and Engineering, Morrison, Colorado

² Research Scientist, Applied Science and Engineering, Morrison, Colorado

³ Research Scientist, Applied Science and Engineering, Morrison, Colorado

EXPERIMENTAL AND THEORETICAL STUDY
OF ENERGY CONSUMPTION IN BUILDINGS

By Dr. Jay L. McGrew,¹ George P. Yeagle,²
and David P. McGrew³

I. INTRODUCTION

The Beaverton School District accomplished a study of energy use in their 28 elementary schools, 6 intermediate schools, 3 high schools, and 3 support buildings for the period from July, 1976 through June, 1977. They found that energy use varied greatly between the various buildings and no clear reason for the variations could be established. One school, for example, used over three times the energy consumed in another school of similiar size. It was decided to accomplish a detailed experimental study in one of the schools to determine the reasons for high energy consumption. Chehalem Elementary School was selected for the detailed experimental study since it was one of the highest consumers of both natural gas and electricity.

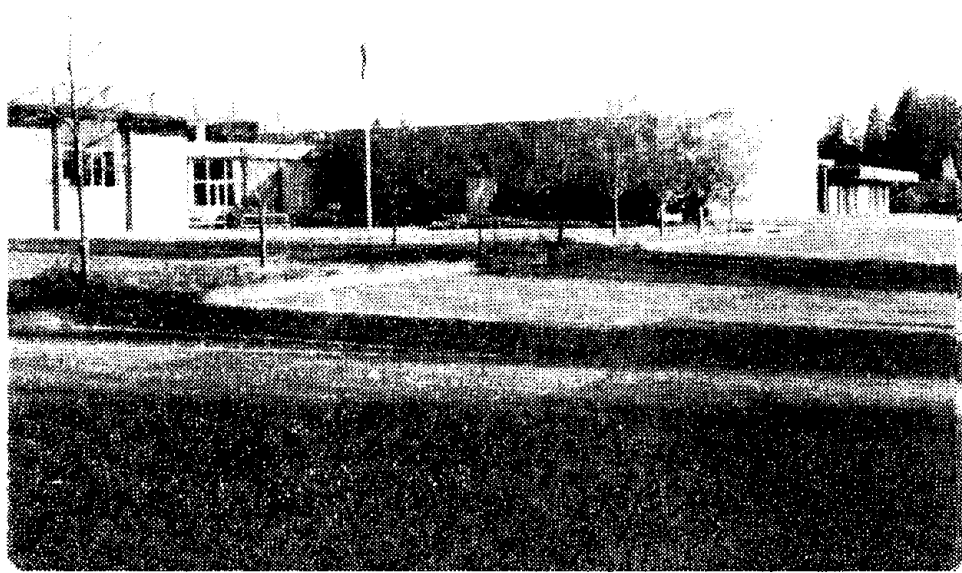
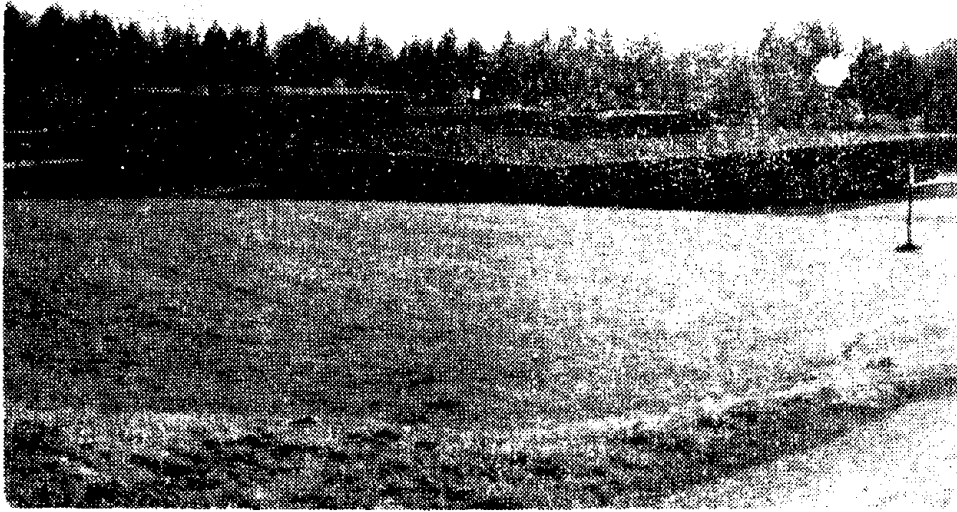
The objective of this phase of the study was to determine the yearly heat flow through the walls, ceiling, and windows, to identify major energy use problems in the school, and to determine the cost effectiveness of additional insulation and double glaze window treatments.

In this report we discuss the experimental apparatus and techniques used and present the results obtained in the tests, and also present analytical projections of the results to show monthly and yearly energy uses. We also present computed data on heat flow through north, south, east, and west facing windows using the ASE Window Computer Program. It should be noted that the window data presented is strictly computed and is not based upon actual measurements in the Chehalem School. The window computer program was developed by ASE in previous research and has been correlated with experimental data. The computer model considers sun positions and atmospheric absorption at each compute time (each hour), diffuse radiation due to earth and atmosphere, cloud cover, air temperature, and wind speed based on actual weather data in the Portland, Oregon area. The computer model calculates sun flux into the room through the window, and heat flow through the window due to long wave length radiation and convection mechanisms at each one hour time step. The daily total gain or loss through the window is computed and summed for each month.

¹President, Applied Science and Engineering, Morrison, Colorado

²Research Scientist, Applied Science and Engineering, Morrison, Colorado

³Research Scientist, Applied Science and Engineering, Morrison, Colorado



CHEHALEM ELEMENTARY SCHOOL

Finally the total heat flow through the window is computed for the so called "Winter" period. "Winter" is defined as that portion of the year during which significant space heating is used in the school.

Heat loss due to intentional air make-ups and unintentional infiltration was not measured in this study even though it is recognized that this is a major heat loss mechanism in the school.

With the data obtained we can compute the yearly cost due to heat flow through opaque walls, windows, and ceilings, and can then accurately estimate the potential annual energy and fuel cost savings by use of additional insulation and double panes.

II. EXPERIMENTAL TECHNIQUES AND APPARATUS

One section of the school was instrumented to determine heat flow through each of the four walls, heat flow through the ceiling, temperatures on the inside and outside surface of each wall, and ceiling and "attic" temperatures. In addition, inside and outside air temperatures were measured, as were sun flux and wind speed. The lights were instrumented to determine on and off periods, and the heating and air conditioning system was monitored to determine operating times.

Iron-constantan thermocouples were used to measure all temperatures. A pyranometer and precision cup anemometer were used for solar flux and wind speed respectively. Heat flows were measured by the use of heat meter calorimeters.

All data was recorded using a precision digital data logger with recording accuracies of 1 micro-volt on millivolt channels, and 0.1°F on temperature channels. Overall accuracy of the temperature measurements is approximately $\pm 0.5^{\circ}\text{F}$ while relative accuracies between any set of temperature channels is $\pm 0.1^{\circ}\text{F}$. The calorimeters are calibrated and overall recorded accuracy is $\pm 0.25\text{BTU}$

$$\frac{2}{\text{ft. hr.}}$$

It is noted that the instrumentation errors in the calorimeters is much smaller than the heat flow variations from point to point on the ceiling or a wall, and is also much smaller than the reproductibility of thermal conditions. The anemometer has a threshold wind speed of approximately 1/10 mph, and an accuracy of $\pm .17$ mph.

Wall heat flows and temperatures were measured at approximately the vertical mid point since this location would tend to yield average values which would then project to more realistic monthly and yearly heat flow values.

The list of instrumentation points is given below:

RECORDER CHANNEL #	MEASUREMENT
60	outside air temperature
61	inside air temperature
62	attic air temperature
63	ceiling temperature
64	outside surface temperature north wall
65	inside surface temperature north wall
66	outside surface temperature south wall
67	inside surface temperature south wall
68	outside surface temperature east wall
69	inside surface temperature east wall
71	inside surface temperature west wall
72	lights on/off
73	heating/air conditioner on/off
80	north wall heat flow
81	south wall heat flow
82	east wall heat flow
83	west wall heat flow
84	ceiling heat flow
90	solar flux
91	wind speed

III. BUILDING DESCRIPTION

The Chehalem Elementary School is located at 15555 SW Davis Road in Beaverton, Oregon which is a suburb of Portland. It is located on a 10 acre site and consists of 42,500 square feet on one level with 18 classrooms. The capacity of the school is 432 pupils.

The walls are uninsulated 8" through wall SCR treated brick of a light buff (tan) color. Total brick in the exterior walls is 11,700 square feet. The roof is 2 inch decking with rigid insulation and fire retardant gravel. The ceiling is "drop" construction with 32" space between roof and ceiling.

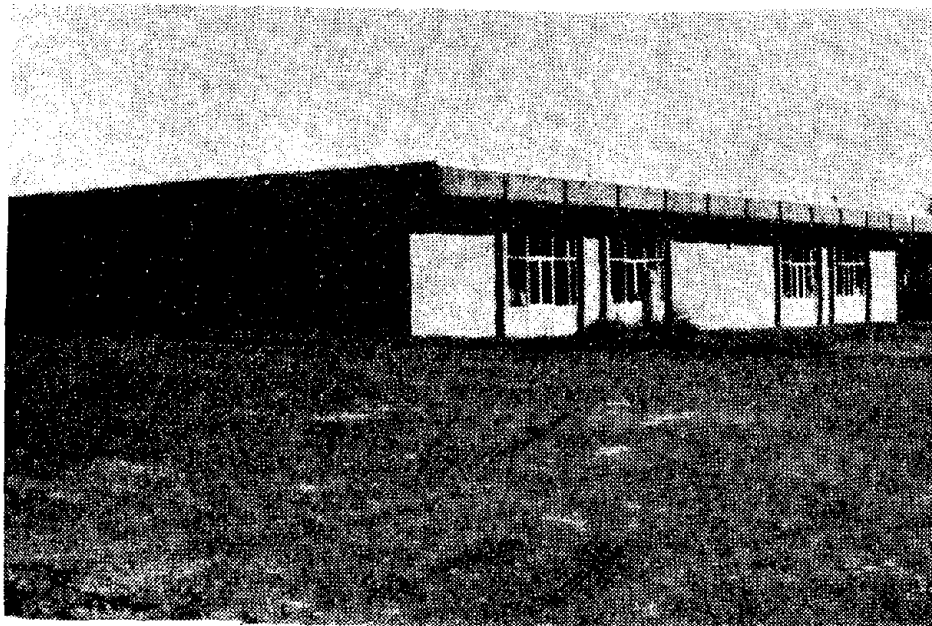
All windows are single glaze with opening sash in most areas. The total window area is 2,050 square feet.

One of the unusual features of the building is the use of a six foot eave overhang on all building faces except the gymnasium.

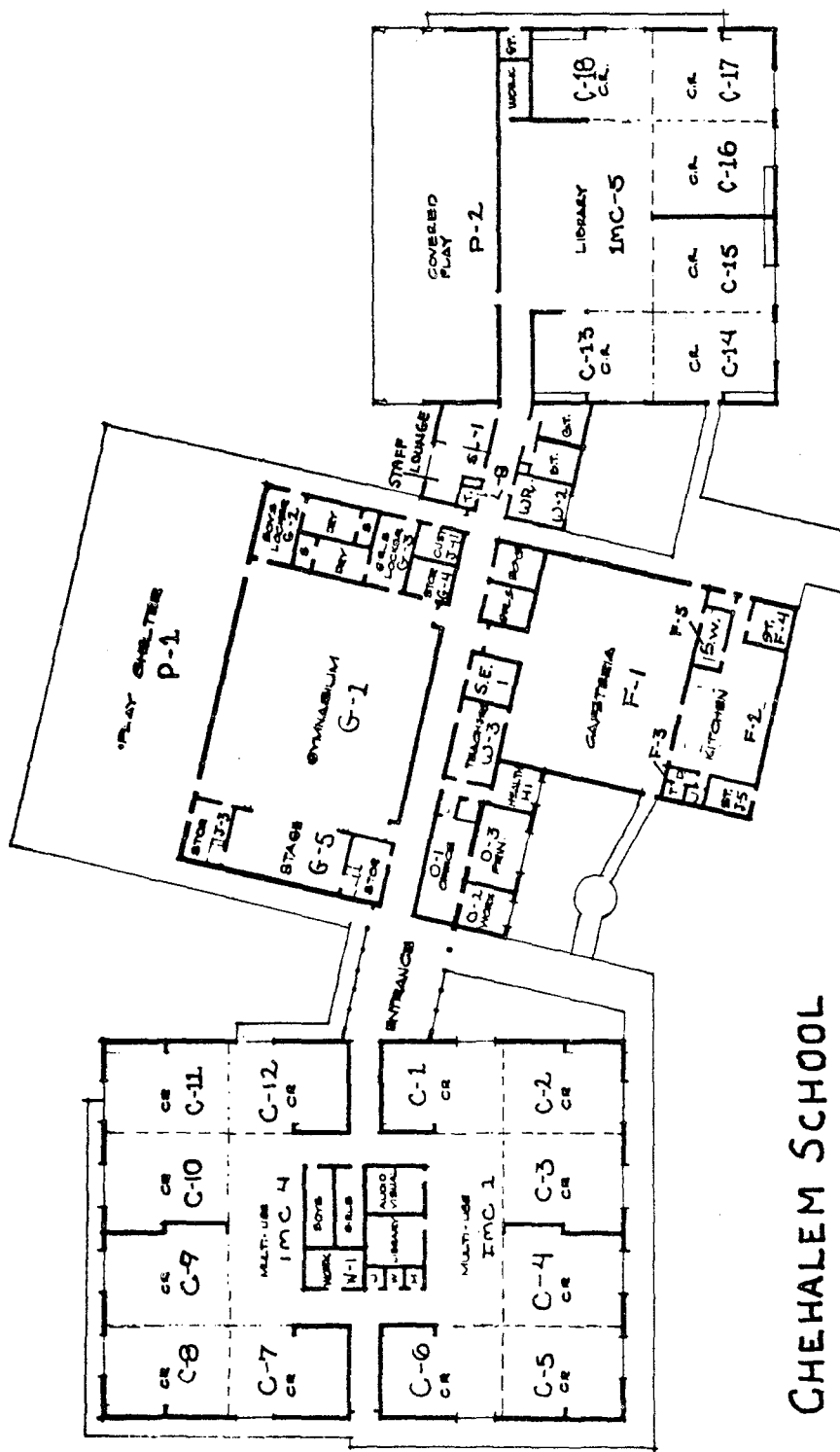
The building is heated and air conditioned with 6 roof mounted combination units. Heating is gas fired with multizone control in each unit. The total building light load during normal school hours is 74.6 KW fluorescent.

The floor plan for the school is shown in the accompanying diagrams. The northern segment of the building was used in the experiments and is shown in the accompanying photo.

This segment contains 6 classrooms and the library and is identical in construction and layout to the southern classrooms area but is only half the floor area. The north, east, and west walls are brick, but the west wall, adjacent to the covered play area is insulated frame with wood exterior covering. Wall heat flow and temperature sensors were placed on the walls in C-14, C-17, and on the west wall adjacent to the library. The photo of this north building segment was taken at approximately 7:00 a.m. on April 11, 1978, and shows the 6' eave overhang. The south facing wall receives no direct sunlight during the day at this time of year due to the overhang.

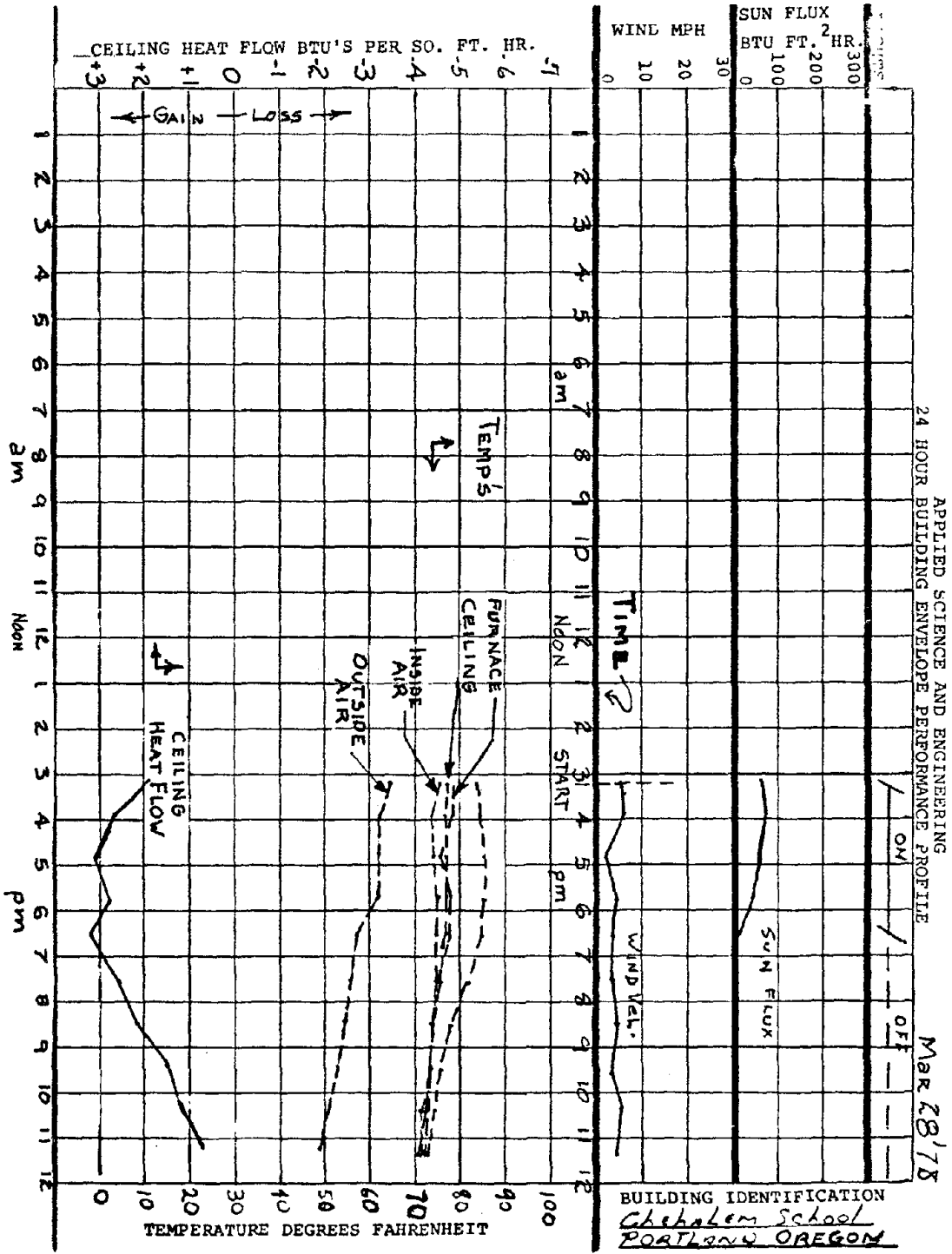


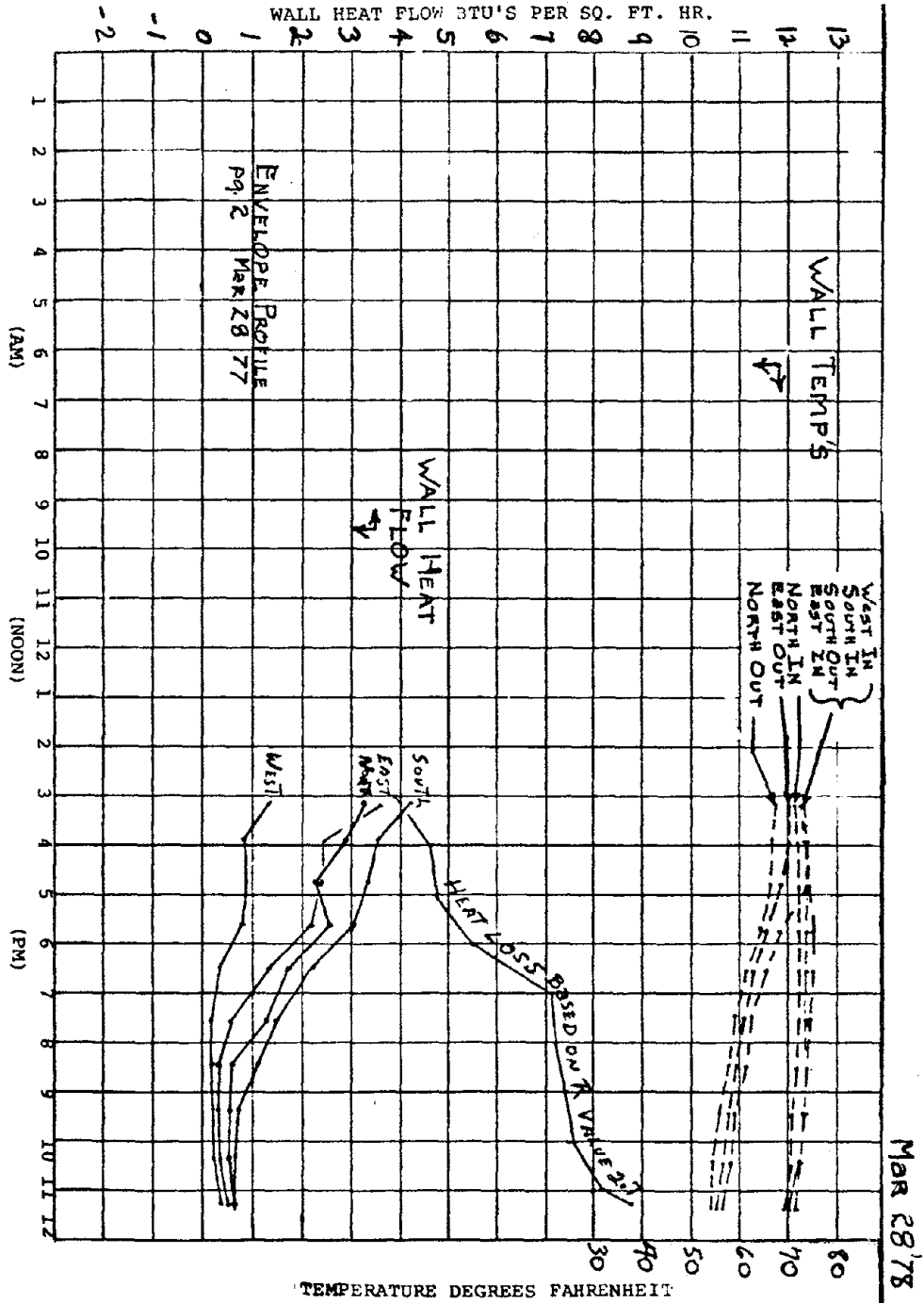
NORTH BUILDING SEGMENT
VIEW FROM SOUTH-EAST

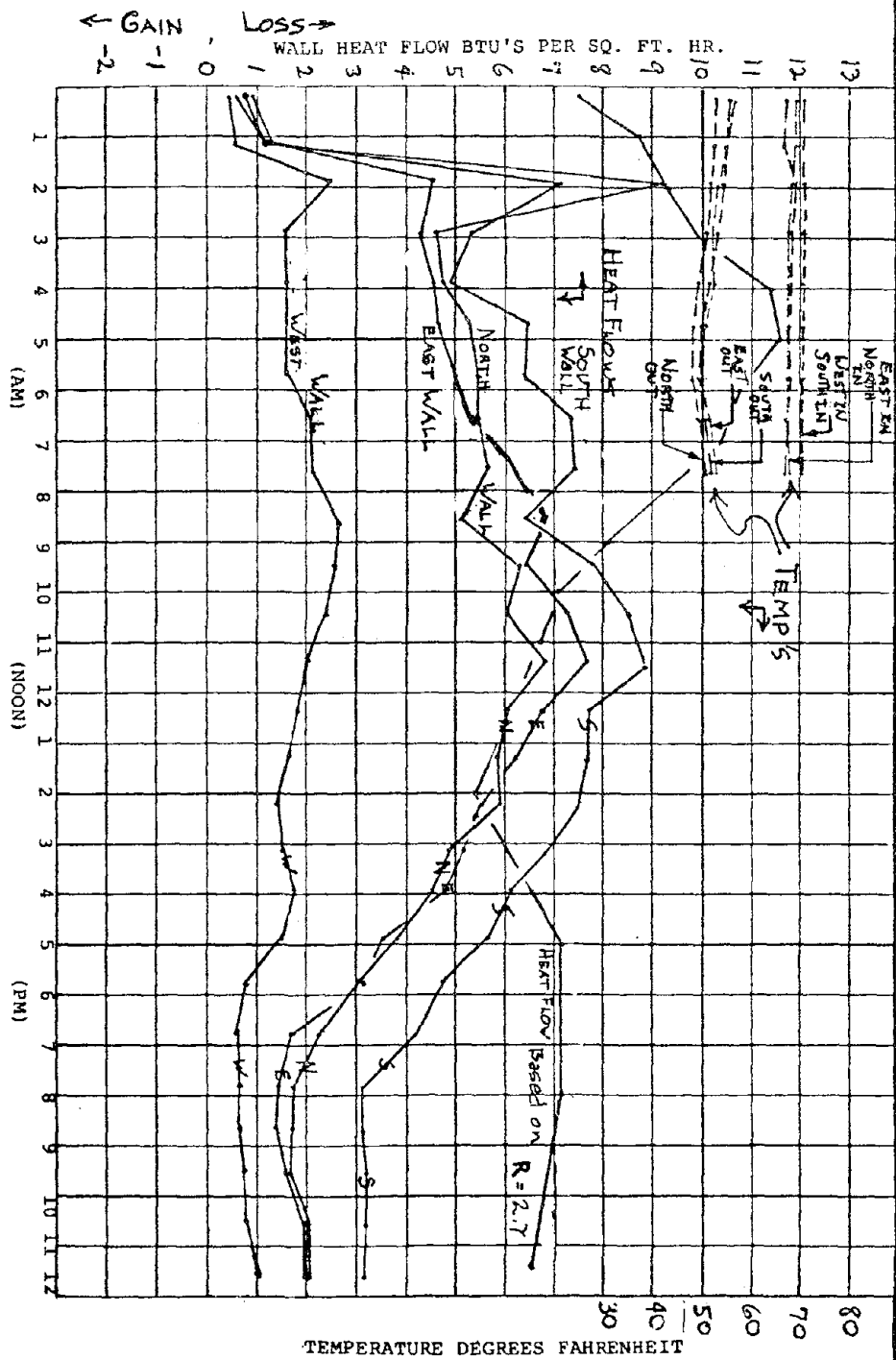


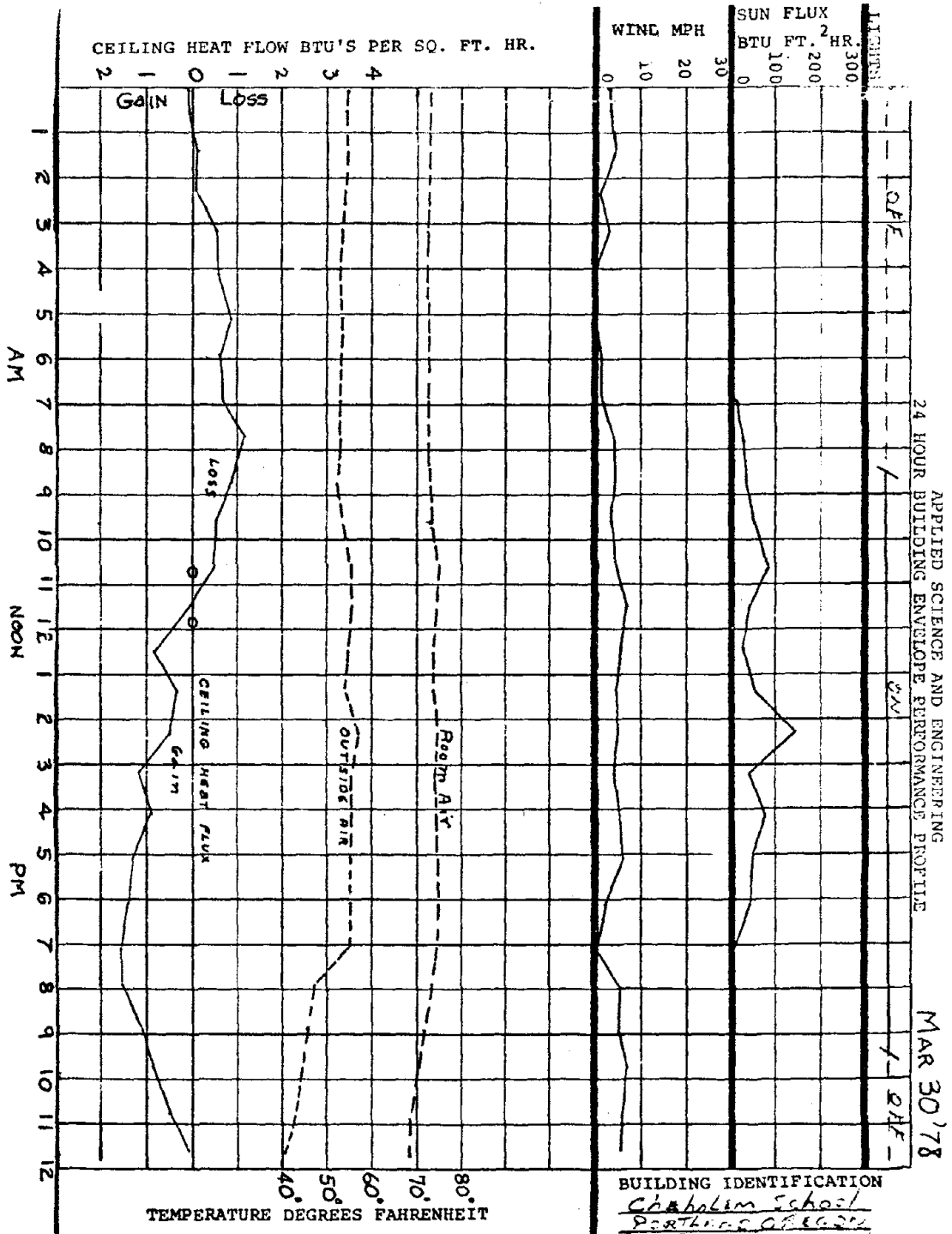
CHEHALEM SCHOOL

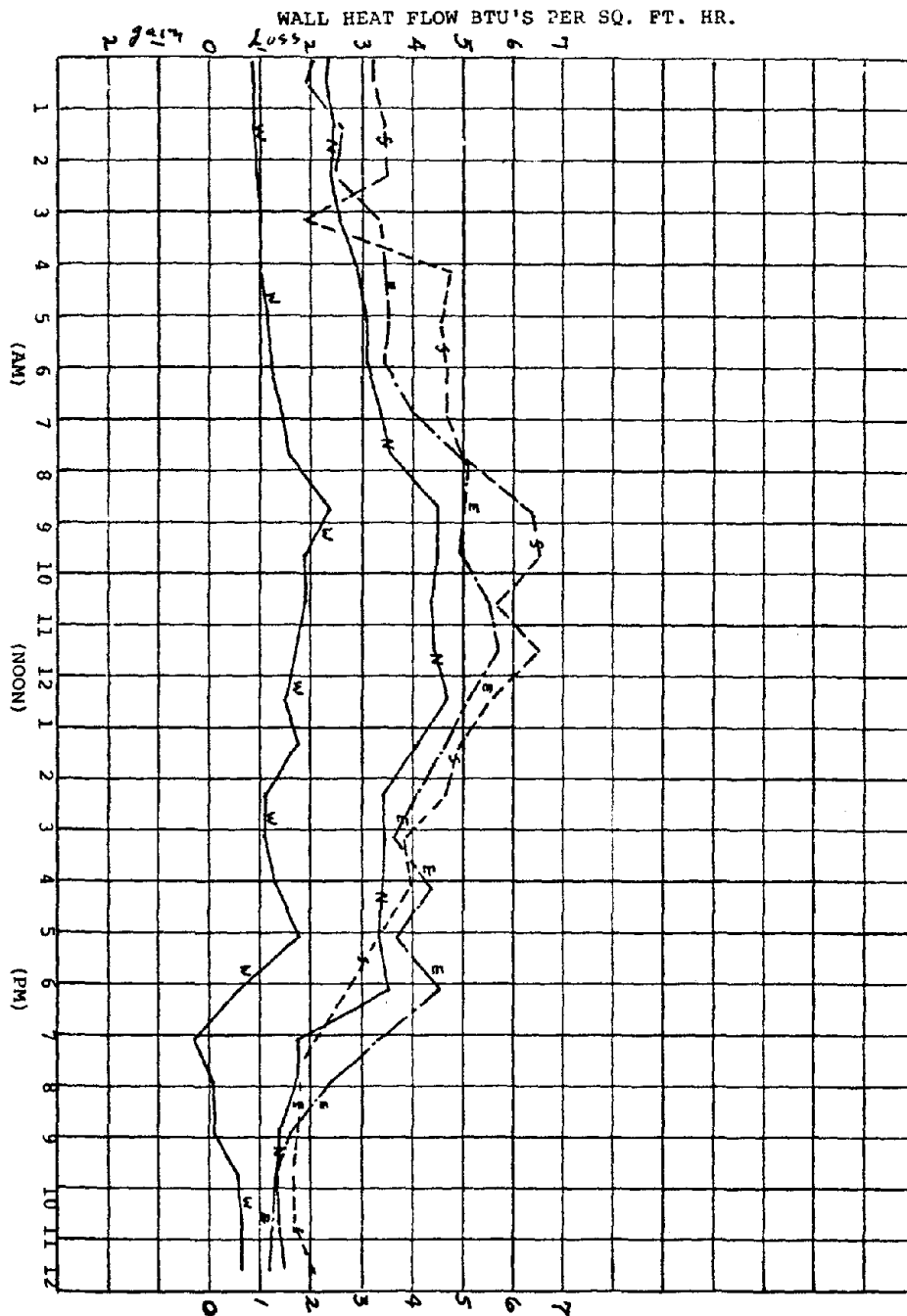
Approx. Area = 42,500 ft²



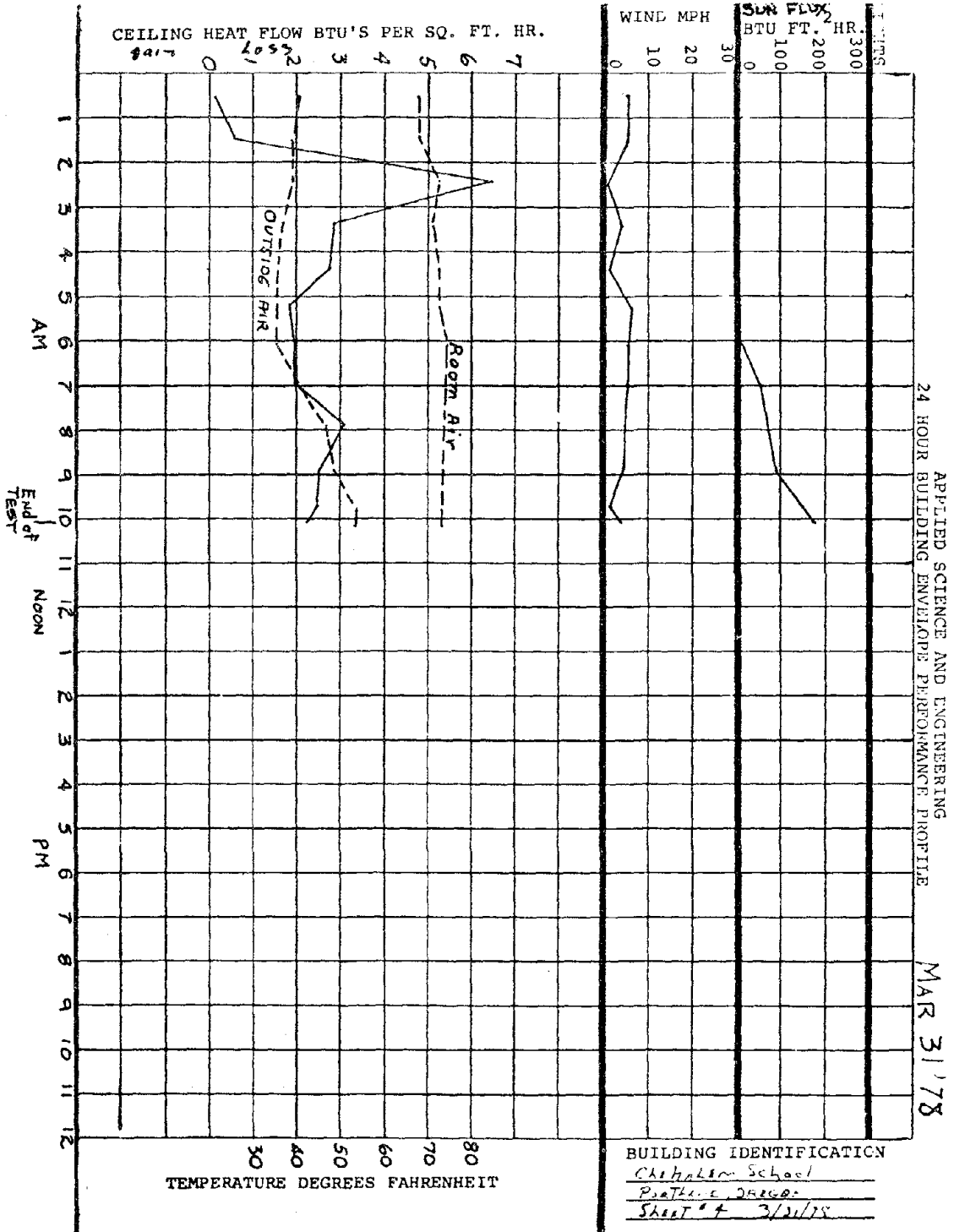


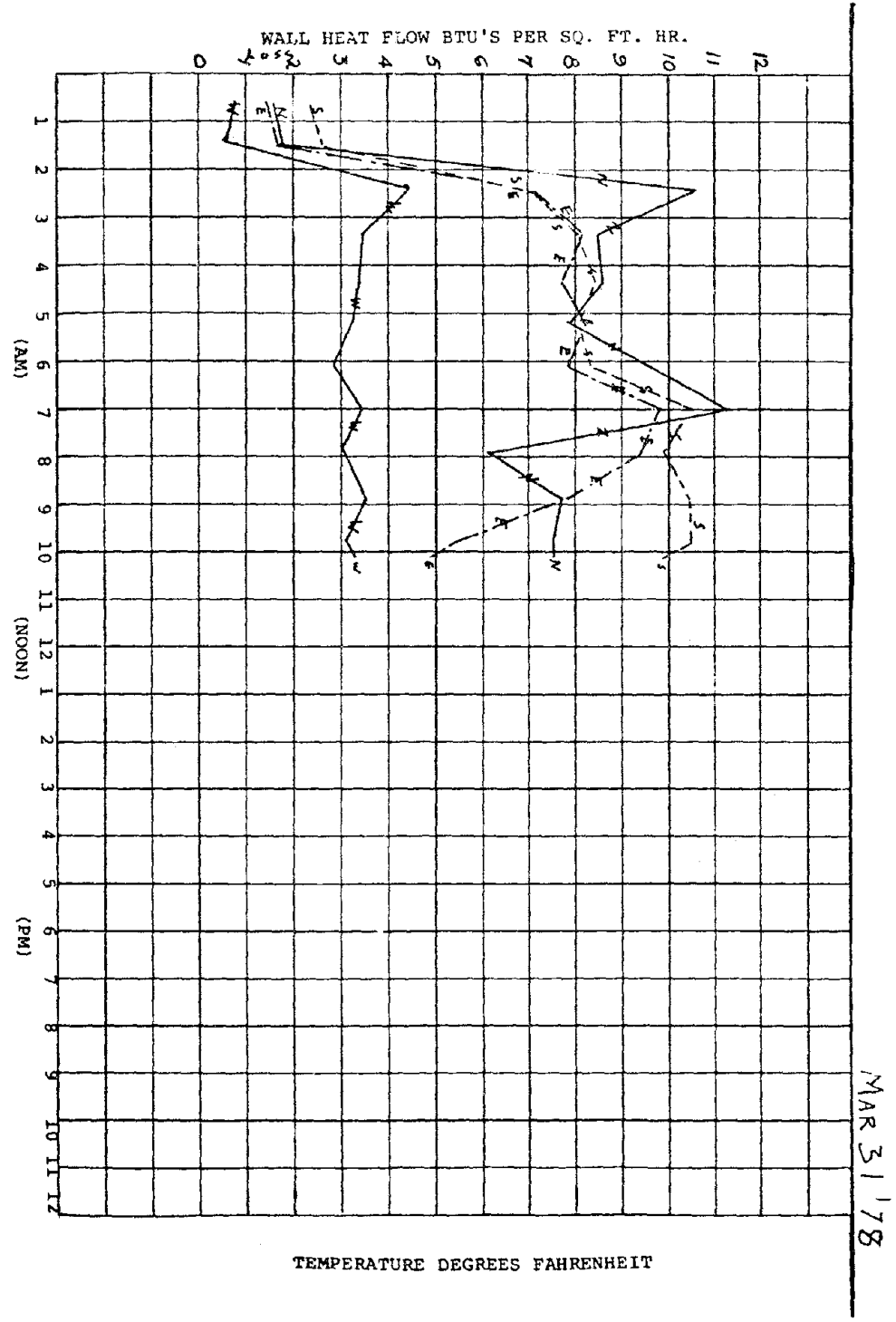






MAR 30 '78





IV. EXPERIMENTAL RESULTS

The energy use experiments were conducted in the Chehalem Elementary School building over the period March 28, 1978 through March 31, 1978. Measured wall and ceiling heat flow rates, lights, solar flux, wind speed, and selected temperatures are shown on the accompanying sheets. Much of the temperature data obtained is not plotted in order to improve the clarity of the more significant data. As a reference, heat loss is computed using the 'R' value method and actual measured inside and outside temperatures for 3/28 and 3/29. The daily heat loss computed by the 'R' value method is approximately 100% higher than the actual daily measured heat flow.

V. ANALYSES OF RESULTS

The data obtained in the previously discussed experiments has been analyzed to determine actual "in-situ" effective conductance and heat flow through the walls of the building. Fortunately, the north section of the school had three uninsulated brick walls and one insulated frame wall so a direct comparison of relative heat flow can be made.

1. Wall Heat Flow

The data obtained on March 29, 1978 is used for projection purposes since the overcast conditions, outside air temperatures, and wind closely approximate the long time average winter conditions in Portland. While not essential to our projection technique such close comparison between test and average winter conditioning is obviously desirable. The average outside temperature on March 29, 1978 was 52.2°F, while the long term October to May average Portland temperature is 46.7°F. It should be noted that our recorded outside temperature is measured near the outside building wall and thus tends to be from 2° to 6° warmer than the air as measured by a weather station. The integrated daily flux as measured by the pyranometer is 760 BTU/ft.² on the overcast March 29, 1978 test day. Over the heating period from October through May, more sun warming effect on the east and south walls would occur in an average year than is computed by projecting the March 29, 1978 test day sun effect, thus actual yearly heat flow through the south and east walls would be somewhat less than projected here. Unfortunately, our projection technique, which is based upon measuring the effective daily heat flow and projecting monthly and yearly flow with only outside average monthly temperatures are not capable of considering varying sun and wind effect. But since the sun flux and wind were representative of long term average winter conditions, the projected monthly and yearly heat flow values shown below are felt to be very representative of the actual values, though slightly high.

CHEHALEM SCHOOL
WALLS
MONTHLY HEAT FLOW* - BTU/MONTH

MONTH	SOUTH	EAST & WEST	WEST	NORTH	ALL WALLS
	(BRICK) 3,250 FT. ²	(BRICK) 4,670 FT. ²	(FRAME) 734 FT. ²	(BRICK) 3,100 FT. ²	11,752 FT. ²
OCT.	5.94	6.76	.35	4.13	17.18
NOV.	18.48	21.03	1.08	12.84	53.43
DEC.	22.23	25.30	1.29	15.44	64.26
JAN.	24.41	27.78	1.42	16.96	70.57
FEB.	18.60	21.17	1.08	12.94	53.79
MAR.	18.28	20.80	1.06	12.71	52.85
APR.	14.12	16.07	.82	9.81	40.82
MAY	9.96	11.33	.58	6.91	28.78
TOTAL YEARLY	132.0	150.0	7.09	91.0	381.0
AVERAGE BTU/FT. ²	40,615	32,120	9,659	29,354	

* ALL HEAT FLOWS ARE MILLIONS OF BTU'S

As can be seen the projected yearly average heat flow through the south wall is considerably larger than the heat flow through the east/west and north brick walls. This effect is due to the fact that the south classrooms are consistently used since they tend to be brighter and more cheery, and the students have a very significant heating effect. The south classroom tended to run in excess of 76°F during the day and also hotter at night than the other classrooms. The south classrooms are located immediately adjacent to the roof mounted furnace while the north classrooms have approximately 100 feet of air duct leading from the furnace. The furnace system has certain problems which are not delved into in this report, but which are the subject of future studies. The furnace system's problems result in the building undergoing heating at approximately 2:00 a.m. independent of the night set back time clock. This night-time heating problem results in a higher heat flow from the walls than would occur if the overheating did not persist.

With the data obtained for brick and insulated walls we can now directly project a potential energy and dollar savings by use of insulation as opposed to uninsulated brick in the exterior walls of the Chehalem School.

Savings with insulation:

Yearly average heat flow (all brick walls) =	34,030	$\frac{\text{BTU}}{\text{ft.}^2 \text{ Year}}$
Yearly average heat flow (insulated frame) =	9,659	$\frac{\text{BTU}}{\text{ft.}^2 \text{ Year}}$
<hr/>		
Yearly heat flow difference	= 24,371	$\frac{\text{BTU}}{\text{ft.}^2 \text{ Year}}$

At a current gas cost of 27¢ per therm (100,000 BTU) the maximum possible yearly savings by insulating the brick is:

$$\frac{24,371}{100,000} \times 27¢ = 6.58¢ \text{ per square foot-year and } 6.58¢ \times 11,752 = \\ \$773.30 \text{ savings for the} \\ \text{entire building per year}$$

The cost of insulating the brick including studs, insulation, wall board, and paint is estimated to be \$1.75 per square foot at current costs, or \$20,566 for all school walls. The return on investment is 3.8%. If the price of natural gas were to double to 54¢ per therm the return on investment would become 7.6% which would be a break even investment at 7.6% interest rate.

It should be pointed out that the actual savings to be achieved would be somewhat less than the projected savings because of the various factors previously discussed which tend to overstate potential savings.

In addition, we have assumed here that all heat loss through the walls is produced by the furnace and thus is a direct cost. In actuality much of the measured heat flow through the walls results from the students and teachers in the building, and overhead lights. Looking again at the wall heat flow data it is seen that each day the maximum heat flow rates and inside air temperatures occur during the occupied periods. The furnace system is off during this time since air temperature exceeds the thermostat temperature and no heat is called for.

A further factor to consider in properly evaluating the potential savings due to insulating the brick walls is the fact that less than half of the brick is actually exposed to the room, while more than half of the brick is covered with cabinets, closets, and other items.

Considering all factors, we estimate that the actual savings to be anticipated by use of insulation would be approximately half of projected maximum possible savings of \$773.30 at today's gas price, or approximately \$400.00 per year.

2. Window Heat Flow

The ASE window computer analysis was used to compute net heat flow (sun in and loss out) through the Chehalem School windows. The

analysis considers window orientation and size, eave overhang, geographical location, actual outside temperature and wind, and solar flux. As an example, computed heat flow through the south, east, west, and north windows have been plotted for one and two panes for the 24 hour day commencing at 12:00 midnight on January 1. Consider, for example, the south facing case. At midnight each window (1 or 2 panes) is undergoing a heat loss. At approximately 8:00 a.m., after sun up, net heat actually flows into the building, and continues to do so until about 4:00 p.m., at which time the windows again experience net heat loss. Over the 24 hour day the single pane window experiences a net daily loss of 136 BTU/ft.², while the double pane case actually experiences a net 78 BTU/ft.² gain. Heat flows are similarly computed on an hourly basis for the rest of the heating season and are plotted by month as shown. Heat flow in BTU per square foot of window is plotted versus month for north, south, east, and west cases. The net heat flows through east and west oriented windows are nearly identical and are plotted as one curve. Over the heating period for the school, the south window experiences a small net heat gain by the room, while the north, east, and west windows result in heat loss.

Monthly and seasonal heat flow through all school windows and window areas are listed below.

WINDOWS				
MONTHLY HEAT FLOW* - (10 ⁰ BTU/MONTH)				
	SOUTH	EAST AND WEST	NORTH	TOTAL ALL
MONTH	414 Sq. Ft.	1,440 Sq. Ft.	192 Sq. Ft.	2,046 Sq. Ft.
OCT.	+3.28	- 2.25	-1.41	- 0.36
NOV.	+ .08	-13.90	-2.70	-16.52
DEC.	-2.25	-21.00	-3.39	-26.64
JAN.	-2.07	-21.17	-3.46	-26.70
FEB.	- .77	-16.92	-3.23	-20.92
MAR.	+ .66	- 9.40	-2.61	-11.35
APR.	+1.01	+ 1.22	-1.48	+ .75
MAY	+1.33	+12.23	+ .15	+13.71
YEARLY	+1.27	-71.19	-18.13	-88.05
AVERAGE BTU/FT ²	+3,068	-49,437	-94,427	

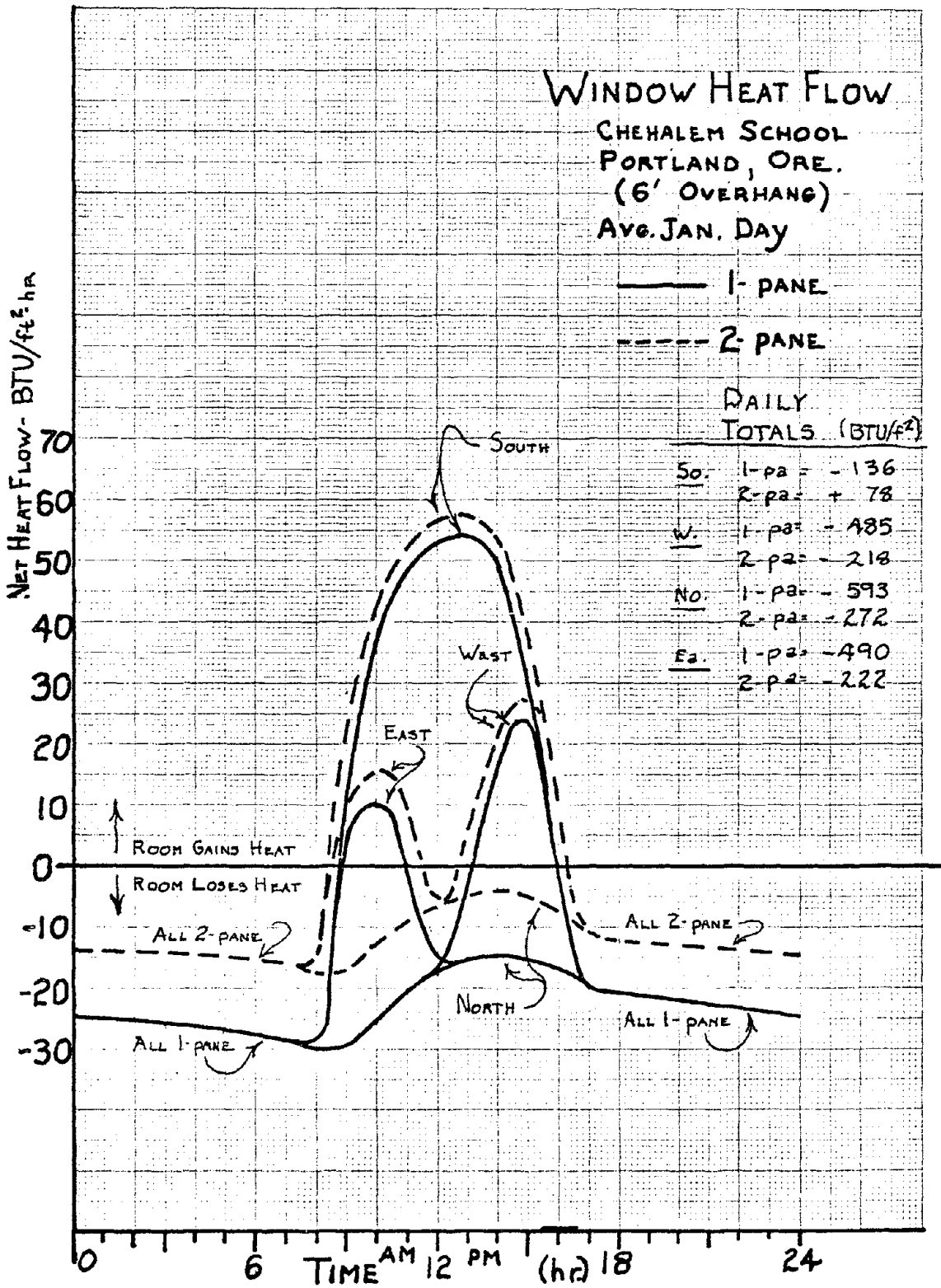
*all heat flows are millions of BTU's
 +indicates room gains heat
 -indicates room loses heat

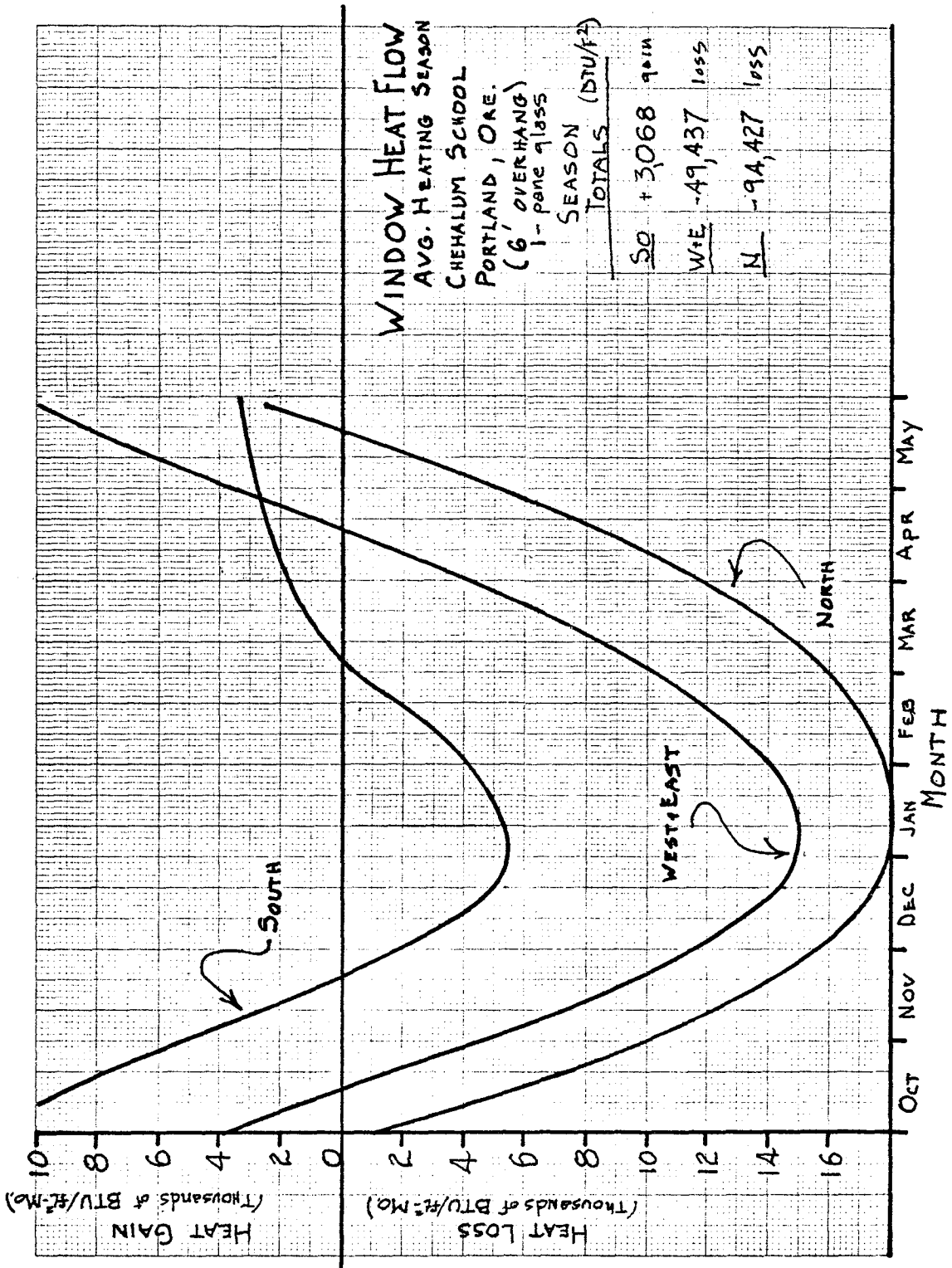
The effect of double pane window treatment is to increase gain through the south facing windows, and to reduce the loss through the east, west, and north facing windows.

HEATING SEASON LOSS THROUGH ONE SQUARE FOOT OF WINDOW

	NORTH ORIENTATION	EAST AND WEST
1 pane	94,427	49,400
2 panes	33,179	7,900
Season energy Savings @ 23¢/therm	61,248 BTU/FT ² 16.5¢	41,500 BTU/FT ² 11.2¢

All units are BTU/FT² year.





As can be seen, the yearly cost savings are 16.5¢/ft.² year and 11.2¢/ft.² year respectively for north and east/west windows. The double pane window treatment is cost effective on both north and east/west windows but unfortunately the absolute cost savings is rather small as follows:

YEARLY COST SAVINGS DUE TO DOUBLE PANE			
ORIENTATION	SAVINGS PER FT. ² YEAR	WINDOW AREA	YEARLY COST SAVINGS
NORTH	16.5¢	192 sq. ft.	31.68
EAST/WEST	11.2¢	1,440 sq. ft.	161.28
<u>TOTAL YEARLY SAVINGS \$192.96</u>			

A few additional cases were run to examine the effect of removing the overhang. The effect of the 6' overhang is drastic on the south, east, and west windows, and as might be anticipated is much less significant on the north windows. Without the overhang the single pane south window has a net heat gain on the first of January and a substantial heat gain over the year. The east and west windows lose heat on January 1, but about break even over the heating season, and the north window still loses heat each month and over the winter.

3. Ceiling Heat Flow

The space between the drop ceiling and the insulated roofing (attic) consistently ran at high temperatures. When the lights are on the "attic" ran in excess of 85°F and heat flowed into the room area below. At night the "attic" also ran warm due to the furnace system problems mentioned earlier. As a result of these problems the effect of roof insulation cannot be evaluated adequately at this point since a slight net heat gain by the room occurs over the day.

The effect of roof insulation can be further evaluated after the heating system problems are corrected.

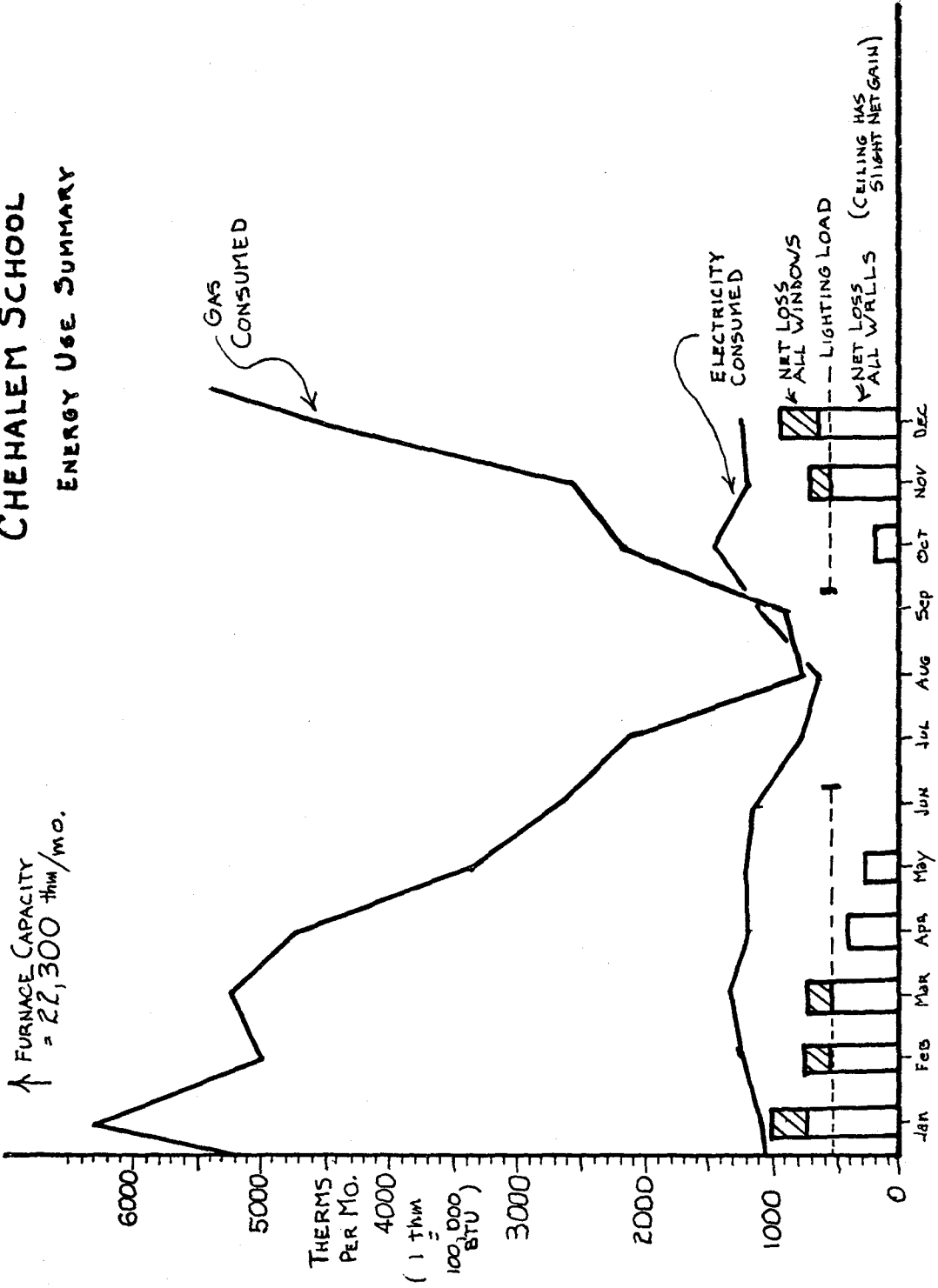
4. Total Building Energy Use

Using the data presented earlier, the fluorescent light electrical load, and the utility bills for a one year period, we now compute monthly energy use. The following figure shows gas and electricity consumed and the electrical energy used by the lights each month. Wall and window heat flows are also plotted. As can be seen the electrical energy use is a good deal higher than that consumed by the lights which are the only significant electrical energy consumers other than the air conditioning system. The lights consume 37.2% of the electricity consumed.

Gas consumption is extremely high as compared to heat flow through walls, windows, and ceiling. Heat flow through the walls is 7.1% of the total energy used, while window heat flow is 2.4% of the total energy consumed.

CHEHALEM SCHOOL

ENERGY USE SUMMARY



The combined furnace capacity is 22,320 therms per month which is greatly oversized for the maximum building heat load which is conservatively estimated to be 2,000 therms per month under the most extreme conditions.

VI. SUMMARY AND CONCLUSIONS

Summary - Heat transfer experiments were conducted over the period March 28, 1978 through March 31, 1978 in the Chehalem Elementary School in Portland, Oregon. Heat flows, temperatures, sun flux, and wind speed were measured. The data was analyzed and monthly and yearly energy use projections were made.

Projections show that the addition of an additional pane of glass to the windows reduces heat flow through the windows and appears to be cost effective, but the actual projected yearly savings is only approximately \$200.00 per year at today's fuel costs.

The addition of insulation to the uninsulated brick walls will reduce heat flow through the walls over the year and results in a projected annual cost savings between \$400.00 and \$775.00 per year at current fuel costs. The cost of such additional insulation is estimated to be \$20,500.00 for the 11,752 square feet of wall. The annual rate of return on the investment is between 2.0% and 3.8%. The investment in insulation is thus not justified with current or any foreseeable future fuel costs.

Certain problems in the heating/air conditioning system were discovered. These problems will be corrected in a future project, and a significant savings in energy use and costs should be achieved.

Conclusions - The following conclusions are drawn based upon the experimental data obtained and the results of the various theoretical efforts.

- 1) A problem exists with the heating/air conditioning system. The heating system is approximately 10 times oversized for the maximum anticipated building heat load and also appears to have serious control problems.
- 2) Heat flow through the uninsulated brick walls can be reduced significantly by the addition of insulation. A potential fuel cost savings between \$400.00 and \$775.00 per year can be achieved by the addition of insulation to the brick walls at today's fuel price. At an estimated \$20,500 labor and material cost (also today's prices) the return on investment is between 2% and 3.8% yearly and is thus not a valid expenditure.
- 3) Heat flow through windows can be reduced by use of double pane glass. A reasonable return on investment is achieved by use of double pane window treatment, but the total yearly savings of approximately \$200.00 at today's fuel costs is rather insignificant.

EXTERNALLY INSULATED MASONRY CONSTRUCTION CASE STUDY

By William C. Dries and Lawrence A. Soltis

ABSTRACT: The paper describes a case study of an energy efficient building constructed with a sprayed-on urethane insulation coated with a modified cement plaster.

Materials, insulating values, cost and payback time, and architectural and construction considerations are discussed.

EXTERNALLY INSULATED MASONRY CONSTRUCTION CASE STUDY

By William C. Dries¹ and Lawrence A. Soltis²

INTRODUCTION

Energy problems dictate new construction to be well insulated and otherwise energy efficient. Building codes are adopting various energy requirements; the Wisconsin Building Code requires heat loss calculations to ensure the heat loss not to exceed 13 Btu per square foot of building envelope (excluding infiltration and ventilation). It is difficult to obtain this through only filling masonry voids with insulating material. Thus additional insulation may be required on either the interior or exterior of the wall.

This paper describes a case study of insulating a 64000 square foot existing building and 24000 square foot addition using an externally sprayed-on urethane insulation coated with a modified cement plaster. Materials, specifications, insulating values, cost, payback time, architectural considerations, and construction problems will be discussed.

PROJECT DESCRIPTION

The existing building is a 64000 square foot one story (22'-0" high) steel framed manufacturing building with non-insulated precast wall panels and conventional built-up roofing with one inch rigid insulation. The 24000 square foot addition is steel framed with eight inch concrete block masonry walls and built-up roof.

Both existing building and new addition were coated with a two inch thick sprayed on urethane insulation and a modified cement plaster. Roof insulation for the new addition is two inch rigid.

The walls for the new addition are constructed of 8 x 8 x 16 hollow concrete masonry units conforming to ASTM C-90 with truss type wall reinforcement spaced sixteen inches on center vertically. Mortar was type M or S conforming to ASTM C-270. Walls were laterally supported at midheight and at top by the steel framing system.

The wall reinforcement had width to match ten inch wall thickness so as to project 1 3/4 inches on the exterior side of the wall to anchor the sprayed-on insulation. Mechanical fasteners (metal drive pins) spaced two foot on center vertically and horizontally were installed on the existing wall panels for insulation anchorage.

¹President, Dries, Jacques Associates, Inc., Middleton, Wisconsin

²Associate Professor, Department of Engineering, University of Wisconsin-Extension, Madison, Wisconsin

The existing precast wall was primed prior to spraying operations; the masonry wall was not primed. A two inch thick urethane foam insulation with in-place density of two pounds per cubic foot was sprayed on with a tolerance range of minus zero to plus one half inch. A 3 x 5 foot test panel was specified to establish the required texture and surface.

A proprietary modified white cement plaster finish coat three eights inch thick was sprayed on the insulation.

Masonry wall expansion joints were required by Code at thirty to forty foot intervals. Corresponding metal joints in the cement finish were specified. With externally applied insulation, the value of the expansion joints and spacing is questionable; however, no code variance was requested.

The insulation and cement finish cost about two dollars per square foot. The payback period, dependent on future utility cost assumptions, varies from four to eight years.

INSULATION AND MOISTURE PROTECTION

Thermal resistance (R) and transmittance (U) factors are shown in table 1 for insulated and non-insulated existing precast concrete walls and for concrete masonry walls.

TABLE 1 THERMAL RESISTANCE AND TRANSMITTANCE

<u>Existing Precast Walls Before Insulation</u>		<u>Insulated Existing Precast Wall</u>	
<u>Component</u>	<u>Resistance</u>	<u>Component</u>	<u>Resistance</u>
Outside Film	0.17	Outside Film	0.17
6' inch Precast	0.66	Cement Finish	0.10
Inside Film	<u>0.68</u>	2 inch Urethane	12.5
	R = 1.51	6 inch Precast	0.66
	U = 0.66	Inside Film	<u>0.68</u>
			R = 14.11
			U = 0.071
<u>Non-Insulated Masonry Walls</u>		<u>Insulated Masonry Walls</u>	
<u>Component</u>	<u>Resistance</u>	<u>Component</u>	<u>Resistance</u>
Outside Film	0.17	Outside Film	0.17
8 inch Concrete Block	1.04	Cement Finish	0.10
Inside Film	<u>0.68</u>	2 inch Urethane	12.50
	R = 1.89	8 inch Concrete Block	1.04
	U = 0.53	Inside Film	<u>0.68</u>
			R = 14.49
			U = 0.069

As shown the U-factor is reduced from 0.66 for the existing precast wall and 0.53 for the concrete masonry wall to 0.071 and 0.069 respectively.

Condensation control is no problem. The insulation does not allow the inside surface to be cooled below its dew point. The urethane is essentially a vapor barrier, thus no condensation occurs within the insulation.

ARCHITECTURAL AND CONSTRUCTION CONSIDERATIONS

Several problems regarding the architectural finish occurred during construction. The cement plaster finish is too thin to transmit movement to joints thirty to forty feet apart. Thus random cracking due to shrinkage/temperature effects occurs. Joints should either be more closely spaced or eliminated and the random cracks accepted.

The urethane and cement plaster finish were applied in accordance with manufacturers recommendations. It is difficult to achieve a completely smooth surface when spraying on the urethane. This unevenness is noticeable and cannot be corrected by varying the thickness of the cement plaster finish. This unevenness is not noticeable on a three by five foot test panel. Larger test panels would be desirable so that all parties can agree on the quality required of the finished wall.

Horizontal line discolorations sixteen inch on center corresponding to the extension of the wall reinforcement are noticeable.

Other areas of discoloration also occurred but their cause could not be ascertained. Possibilities include application of the cement plaster finish below 40°(F) producing improper curing; faulty materials; or improper mixing and application.

SUMMARY

An energy efficient building can be economically constructed by applying an external shell of urethane insulation and cement plaster finish to a concrete masonry building. Although some esthetic tradeoff is required, this is considered a good solution, particularly for industrial buildings, to our energy dilemma in building construction.

THE LOW-ENERGY FULL-BRICK HOUSE

by Cumming, S., and McNeilly, T.

ABSTRACT: The thermal performance of a test house, designed with due regard to thermal principles, is examined using a computer simulation technique based on real Melbourne climatic data. The performances of the house, when constructed with different wall and floor types, are simulated for both summer and winter seasons and the total energy requirements and temperature levels are compared. The benefit of massive construction is shown and the inadequacy is highlighted of an approach to the thermal performance of construction that is based on consideration of U-values alone.

THE LOW-ENERGY FULL-BRICK HOUSE

By Susan Cumming¹ and Tom McNeilly²

INTRODUCTION

This paper examines some aspects of the thermal performance of various typical Australian forms of construction used for the building of dwellings. Emphasis is placed on the comparative thermal performances of different brick and timber wall types.

A computer simulation technique is employed. It is based on actual climatic data for a typical Melbourne year and comparisons between constructions are made on the basis of the performances of a test house of these constructions over the entire year. Each such comparison is made in one of the following ways, depending on which is relevant to the situation:

- (1) by comparing the "comfort" levels achieved in the two houses when no heating or cooling is employed;
- (ii) by comparing the energy and plant requirements needed to achieve comfort conditions; or,
- (iii) by comparing the energy and plant requirements of the house in one construction with those needed to achieve the same level of comfort as prevails in the unconditioned house of the other construction.

TESTS AND FINDINGS

A. THE BDRI TEST HOUSE.

For the purpose of the tests a simple, conventional, rectangular model house was designed with its long axis running east to west. The house was divided into two zones and the adopted zone names are used throughout the paper; they are:

- (i) Living Zone. The living zone includes the living-room, kitchen and family-room, all of which were grouped to face north (the sunny aspect in Australia). Glazing of the north wall is 50% of the total wall area and it was provided with a controlled sunshading device. This sunshade takes the form of a timber pergola with a deciduous vine with sufficiently dense foliage, e.g. chinese gooseberry, to provide shade to the glass in summer, but give little obstruction to incident solar radiation in the winter.

¹Tutor in Architecture, University of Newcastle, N.S.W., Australia.

²Director, Brick Development Research Institute, Melbourne, Victoria, Australia.

Elevations

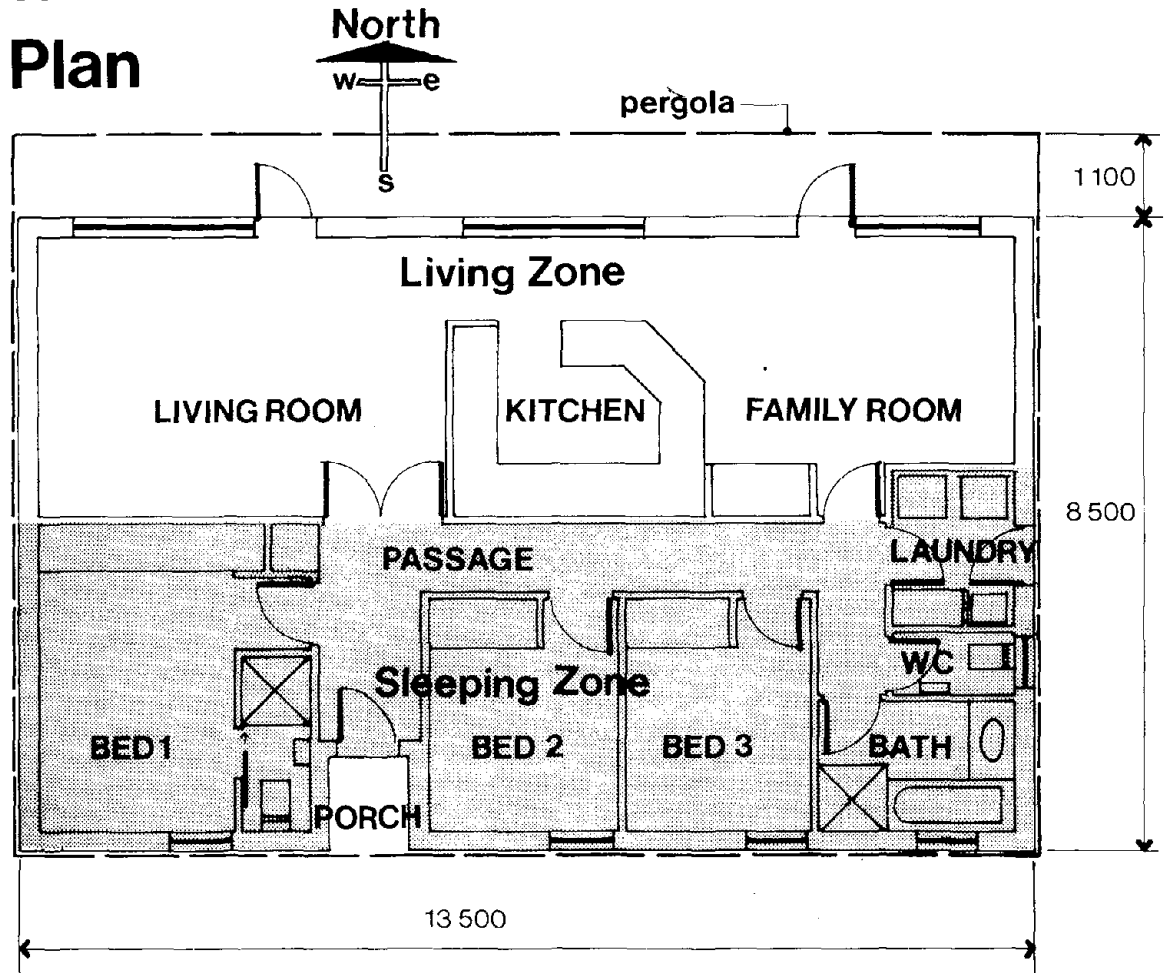
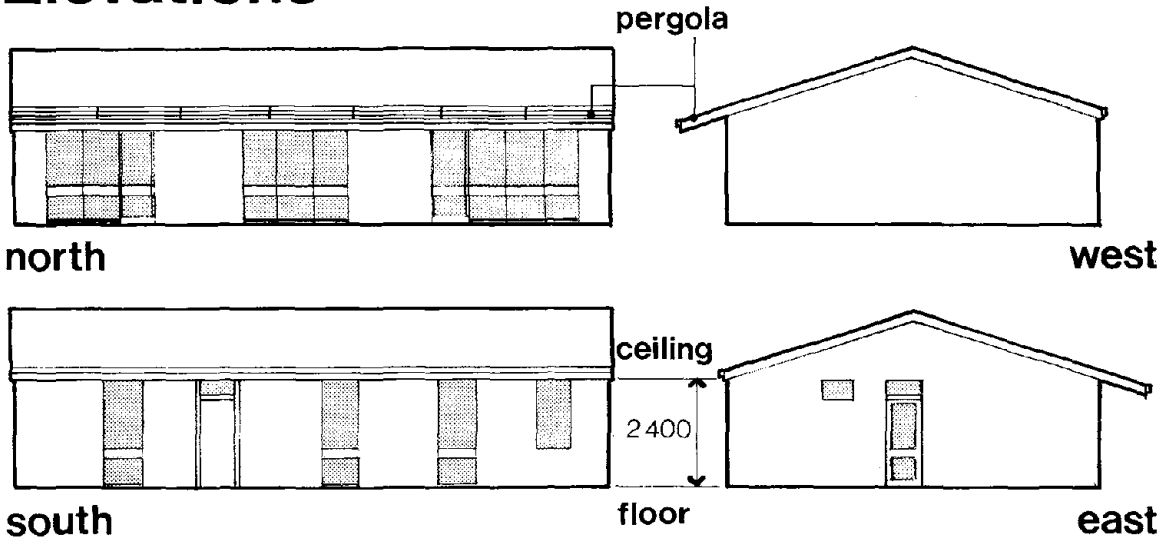


FIG.1 THE BDRI TEST HOUSE.

- (ii) Sleeping Zone. The sleeping zone includes the three bedrooms, plus entry, passage, laundry, bathroom and WC.

The test house is illustrated in Fig. 1.

The various construction methods for the house were as follows:

- Floor : concrete slab-on-ground or suspended timber (carpeted except for kitchen and bathroom).
- Roof : terra-cotta tiles with or without reflective foil sarking.
- Ceiling : 12 mm plasterboard with or without 50 mm bulk insulation.
- External Walls : specified for each test case.
- Internal Walls : 12 mm plasterboard on studs for brick-veneer or weatherboard; unplastered walls of approximate brick type for full-brick construction.

The basic wall constructions used in the tests (namely brick-cavity, brick-veneer and weatherboard) are detailed in Table 1 below.






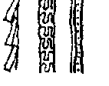
UNINSULATED WALLS		U'	INSULATED WALLS		U'		
BRICK CAVITY		110 extruded brick 50 airspace 110 extruded brick	1.67	BRICK CAVITY		110 extruded brick 70 urea formaldehyde 110 extruded brick	.38
BRICK VENEER		110 extruded brick 140 airspace (studs) 12 plasterboard	1.85	BRICK VENEER		110 extruded brick 50 airspace 50 bulk insulation 40 airspace reflective foil 12 plaster	.38
WEATHER BOARD		20 weatherboard 100 airspace 12 plasterboard	1.82	WEATHER BOARD		20 weatherboard 50 airspace 50 bulk insulation 40 airspace reflective foil 12 plasterboard	.38

TABLE 1 BASIC TEST WALL CONSTRUCTIONS & CORRESPONDING U-VALUES

U-values and other necessary thermal properties of brick building elements were calculated using the computer program "Heatran", developed by A.B. Coldicutt, with properties of bricks obtained from Handisyde et al⁽⁴⁾. Properties of all other building elements were taken from Coldicutt⁽³⁾.

For comparative purposes the three insulated walls were especially devised so that they would all have the same U-values. In order to achieve this value in the brick-veneer house it was assumed that normal Australian building practise was improved to give a still air-space in the cavity between the timber frame and the brick skin. It is therefore a better insulated wall than is normally provided.

B. THE SIMULATION METHODS.

The analysis technique involved use of the Tempal computer package developed by Coldicutt⁽²⁾ which gives predictions of the internal environment of the test building. Heat transfer through building elements is predicted by the advancing mean technique (developed by A.B. Coldicutt). This method has the following advantages over other modelling methods:

- i) it permits modelling of changes in air film and air space resistances and in infiltration and ventilation rates and it allows for the effect of the use of variable internal and external sun controls, such as blinds and the like; and,
- ii) it takes account of changes in shading throughout the year.

Runs of the program were made for 14-day periods, series of such periods or for a full year. When a full year run was made the year was, for convenience in assessment, divided into two distinct periods:

- (i) a 5 month "summer" period from November to March with the option of providing or not providing cooling; and,
- (ii) a 7 month "winter" (i.e. heating) period from April to October.

The user of the package specifies the test building and construction, the dates and city to which the climatic data is applicable, the ventilation conditions prevailing, the provisions for sun control and finally the heating or cooling requirements for the two separate zones, if any.

The output is given separately for the two zones of the house and those parts of it that are relevant to the present study are as follows. For unconditioned cases it is in the form of the hourly frequency of occurrence of specified ranges of interval environmental temperatures,* the frequency of these within specified hours and the number of days and hours when temperatures were above and below specified limits. In addition, when heating and cooling is specified, output is in the form of energy consumed (daily, fortnight periods and cumulative totals) and the hourly frequency of occurrence of loads required to maintain specified comfort conditions.

C. TESTS PERFORMED.

All tests employed recorded climatic data for Melbourne (lat.37° 49'S) for the year 1968 which was selected as a "typical" year. Average climatic data for Melbourne is given in Table 2.

* The internal environmental temperature is an effective air temperature, which expresses the combined effects of air temperature in a space and radiation from surfaces.

TABLE 2. MEANS OF CLIMATIC ELEMENTS: MELBOURNE

Meteorological Elements	Spring Sept-Nov	Summer Dec-Feb	Autumn March-May	Winter June-Aug
Atmospheric pressure (millibars)	1014.8	1013.2	1018.3	1018.7
Daily maximum temperature (°C)				
Mean	19.5	25.5	20.5	14.3
86 Percentile	25.1	33.7	25.3	16.7
14 Percentile	15.1	19.5	16.4	11.9
Daily minimum temperature (°C)				
Mean	9.8	14.5	11.1	7.0
86 Percentile	12.7	17.5	14.3	9.5
14 Percentile	6.8	11.5	8.0	3.7
Relative humidity 9 a.m. (Saturation = 100)	64	61	72	81
Global radiation (MJ/m ² .day)	18.1	23.0	12.3	10.4
Daily amount of cloudin- ess (scale 0 to 8)	4.8	4.2	4.7	5.1
Daily hours of sunshine	6.0	8.0	5.2	3.9

Notes to Table 2.

- 1) Daily maximum and minimum temperatures calculated from Table 086071, Climatic Averages Australia, Metric Edition. Department of Science and Consumer Affairs, Bureau of Meteorology. Aust. Govt. Publishing Service, Canberra, 1975.
- 2) Global radiation figures from Met. Bureau maps of average monthly global radiation.
- 3) All other figures from Victorian Year Book 1973. Commonwealth Bureau of Census and Statistics, p. 767.

A series of preliminary 14-day runs was first performed involving changes in various parameters. The results of these runs showed certain trends, some of which were further investigated in a second set of runs, over an entire year.

The details of these tests and of their outcomes will next be described.

i) 14-day Preliminary Runs

Various constructions were tested for three 14-day periods, of which one was a severe summer period, the second a severe winter, and the third a sunny winter fortnight.

Results of the summer run, in which no air-conditioning was used, indicated that significantly lower temperatures are maintained in the house of heavyweight construction (brick cavity) than in those of lightweight construction (brick-veneer or weatherboard), whether or not the latter constructions incorporated insulation. It appeared that insulation had little effect on the temperatures.

When brick types were compared, little difference was found between performances of brick cavity walls of perforated extruded or solid pressed bricks of the same thickness (i.e. 110 mm), but somewhat higher temperatures occurred when the brick cavity wall comprised narrower perforated extruded bricks of 76 mm thickness. The 76 mm brick is not in regular use in Australia and its effects were not studied beyond this preliminary stage. Roof and ceiling insulation did not appear to greatly affect summer temperatures, while floor type was seen to have a real effect, with higher temperatures occurring in the timber-floor house than the concrete-floor house. The use of an attic fan was examined which would provide a high ventilation rate when the internal temperature exceeded the external. It was found that, in the circumstances where the occupier of the house sensibly opens and closes windows, the installation of such a fan would result in temperatures which were only slightly lower than would be the case without the fan.

For the severe winter period heating was employed intermittently in both the day-time and the night-time zones. It was found that wall insulation reduced the required heating energy and that wall and ceiling insulation very greatly reduced such energy. Brick construction, using solid pressed bricks, appeared to require slightly more energy than did that of perforated extruded bricks. Regarding wall and floor type; the heavier-weight constructions required more heating energy than the lightweight, presumably because a greater mass was being heated daily, owing to the intermittent nature of the heating regime employed. This situation regarding the relative performances of the different wall types was reversed in the sunny winter period, with the brick cavity requiring slightly less energy than either of the two lightweight constructions. During this period the house was receiving substantial solar heat through the north glazing and the brick cavity construction was able to store much of this heat and re-radiate it later, thereby requiring less heating energy than the brick-veneer or weatherboard constructions which do not have nearly as great a heat storage capacity.

The results of these test runs raised a number of questions regarding the relative performances of the various walls. In a typical Melbourne winter, would solar radiation be such that the heavyweight construction would require less heating energy than the lightweight over the entire heating season? Over a full summer period, how great would be the difference in the frequency of occurrence of extreme temperatures in the heavyweight and lightweight unconditioned houses and would the provision of insulation in the walls have a significant effect on internal temperatures? Accordingly, full year runs were made.

ii) Full Year Runs

The continuous runs were made for the year April 1968 to March 1969, and will be described for the summer and winter periods separately.

(a) Summer Runs.

A series of summer runs was made using the basic wall types (brick cavity, brick-veneer and weatherboard), both insulated and uninsulated and with first timber and secondly concrete floors.

Additional relevant data:

- (i) Sun control. The dense foliage of the vine on the pergola provided shading of the north glass during the hottest periods. Further, at internal environmental temperatures greater than 25°C , but subject to the condition that transmitted radiation exceeds 100 Watt/m^2 , the user was assumed to draw white holland blinds.
- (ii) Natural cooling. As air-conditioning was not used, the occupant was assumed to have taken advantage of ventilation by opening windows when internal temperatures exceeded 23°C , provided conditions were favourable; i.e. external air temperatures not less than 18°C , but less than internal and wind speeds not greater than 4 m/s . At all other times the low ventilation rate resulting from good workmanship and well fitted closed windows and doors was assumed.

Results of these unconditioned cases are considered in terms of the internal environmental temperatures which occurred and the relationship of these to the temperature intervals suggested for comfort. The particular comfort intervals used are those described by Williamson et al⁽⁵⁾. They have been determined on the basis of several relevant parameters and, for summer in Melbourne, range from 20°C to 27°C in the living areas and from 13°C to 24°C in the sleeping quarters.

Details of the relative performances of the various methods of construction are given in histogram form in Figures 2 and 3. Figure 2 indicates the total number of days in the summer season on which temperatures in the particular zones exceeded the chosen comfort levels and the total number of hours of the occurrence of such temperatures is shown in Figure 3.

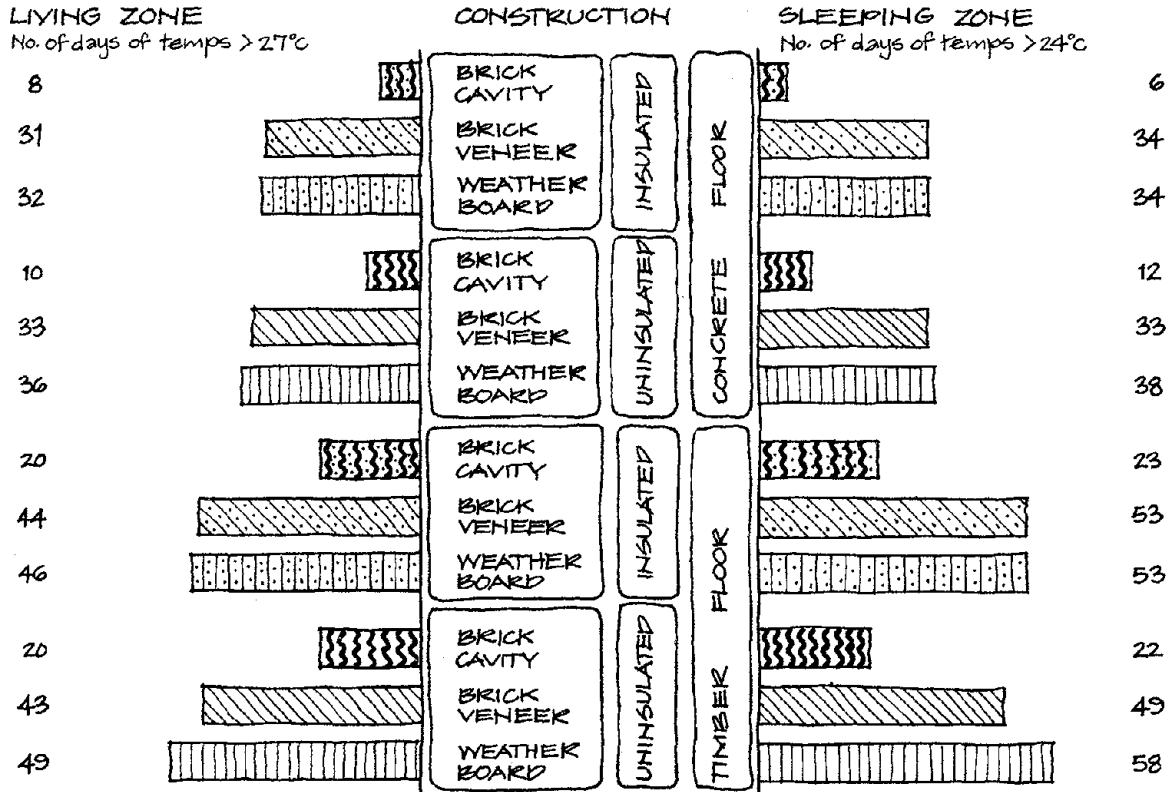


FIG.2 INCIDENCE (NOV-MAR) OF DAYS OF EXTREME TEMPERATURES (NO AIR-COND.)

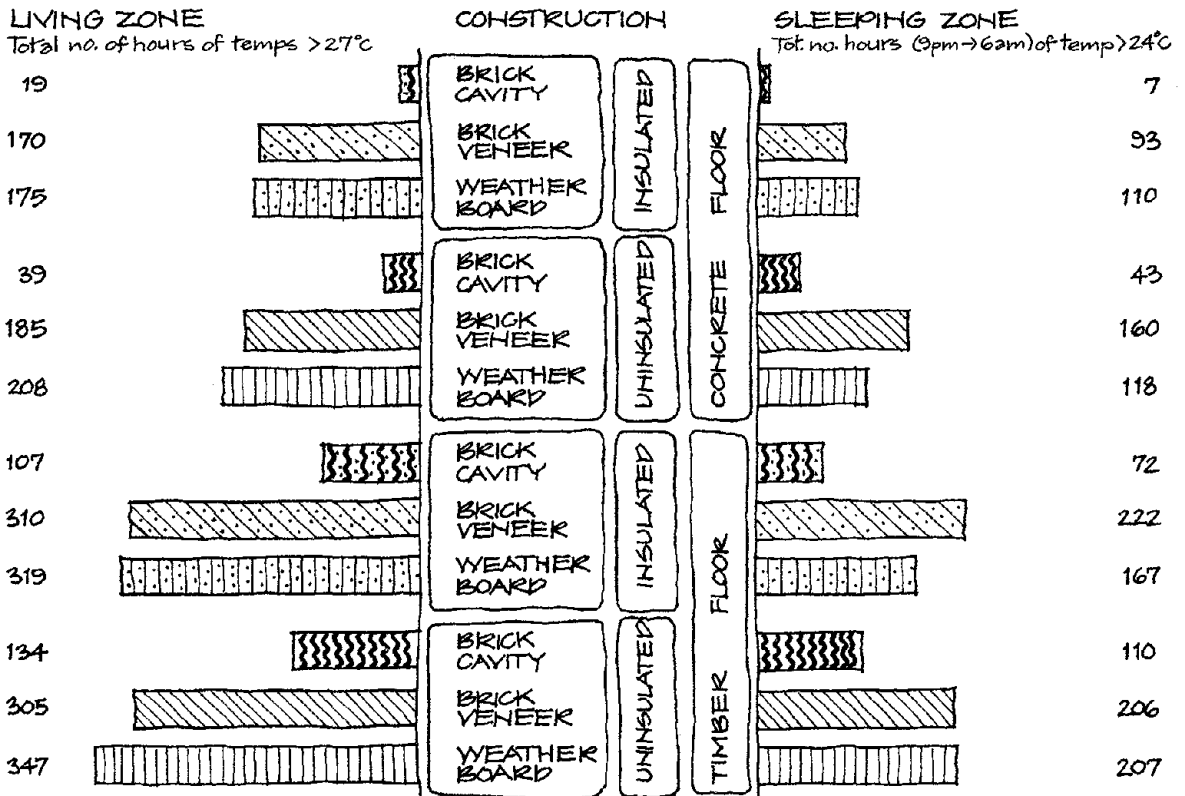


FIG.3 INCIDENCE (NOV-MAR) OF HOURS OF EXTREME TEMPERATURES (NO AIR-COND.)

Both measures of performance indicate the similarity of all the lightweight constructions and show the far greater occurrence of extreme temperatures in them than in the heavyweight brick cavity construction. The total number of days on which extreme temperatures occurred in the lightweight cases is from 2.3 to 5.7 times greater than that for the heavyweight construction of equivalent floor type, insulation, zone, etc., while the total number of hours of excessive temperatures in the brick-veneer or weatherboard house exceeds that of the equivalent brick cavity house by a factor of from 2.5 to 14.3. For the brick cavity construction with a concrete floor, particularly when it included insulation, it is interesting to note the small total numbers of houses of extreme and of days in which they occur in the two zones (19 hours total in the living zone and 7 night-time hours in the sleeping zone over the whole five month summer period).

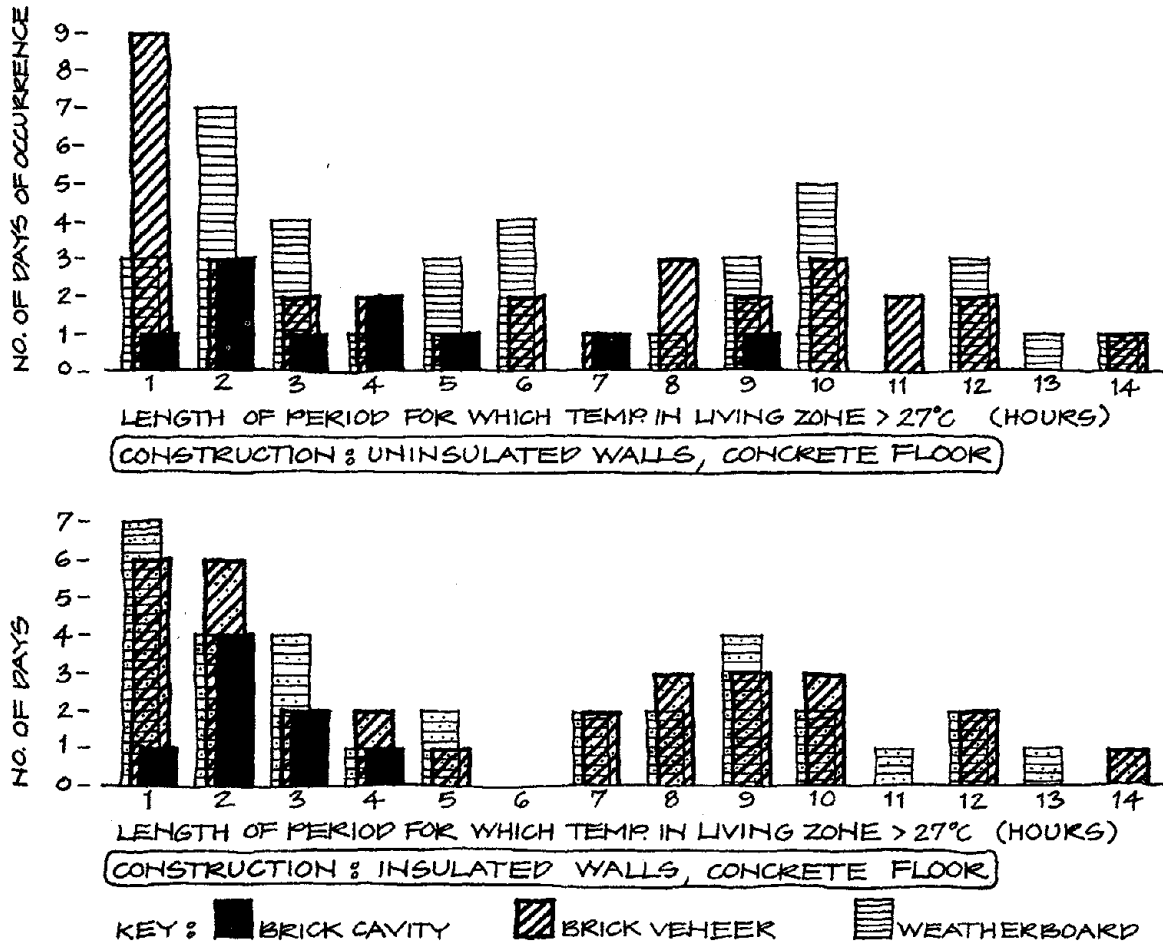


FIGURE 4 DISTRIBUTION OF PERIODS OF EXTREME TEMPS. (NOV-MAR).

The distribution of such hours of extreme temperatures should also be considered. Do they occur in long stretches, or are they sparsely scattered? Histograms showing the number of days on which extreme periods of various durations occurred are shown in Figure 4. It may be observed that such periods of discomfort tend to be not only fewer, but also far shorter in duration in the heavyweight construction than in the lightweight. Also relevant to the present discussion is the fact that, in the brick cavity house with concrete floor (whether the walls were insulated or uninsulated), the maximum temperature of the relevant comfort zone was never exceeded by more than 3°C (i.e. temperatures greater than 30°C in the living zone and 27°C in the sleeping zone did not occur), whereas in the houses of lightweight construction such excesses, shown in Figure 5, were found to occur. Temperatures which exceeded even 33°C were recorded in the living zone of some of such cases.

With respect to the comparison between the summer performances of the house when unconditioned, it may be concluded that, when outside air temperatures are high, lower temperatures are maintained in the heavyweight than in the lightweight constructions. This is a direct result of the fact that the brick cavity wall has a far greater heat capacity than either the brick-veneer or the weatherboard. Since the specific heat capacity of an element is the quantity of heat required to raise the temperature of a unit area of that element by a unit temperature increment, then a given heat input from outside a wall will cause a greater rise in temperature of this wall if it is of lightweight construction than if it is of heavyweight and hence give rise to higher internal air temperatures as the wall radiates heat. It was found (see Figure 5) that not only were excessively high temperatures less prevalent in the heavyweight construction but so also were those falling below the comfort levels; in other words, the mass has a stabilizing influence. The graphs of hourly temperatures for a three-day heat-wave period in February illustrate the points which have been made (Figure 6).

In considering the effect of insulation in walls on temperatures in summer, Figure 3, which shows total number of hours of extreme temperatures, may again be referred to. It is clear that in all the brick cavity cases insulation proved to be beneficial in that it caused a reduction in this number. However, for the brick-veneer and weatherboard cases the insulation in some instances gave rise to a greater occurrence of uncomfortably high temperatures, presumably because the large north glass area permitted solar heat gains and the insulation caused heat to be trapped. Evidently, the effect of wall insulation on comfort conditions in the unconditioned house in summer is minor in comparison to that of the mass of construction.

As the comfort conditions prevailing in the heavyweight and lightweight constructions were vastly different when no air-conditioning was employed, it was considered valid to compare the two forms of construction by looking at the plant and energy required by the brick-veneer and

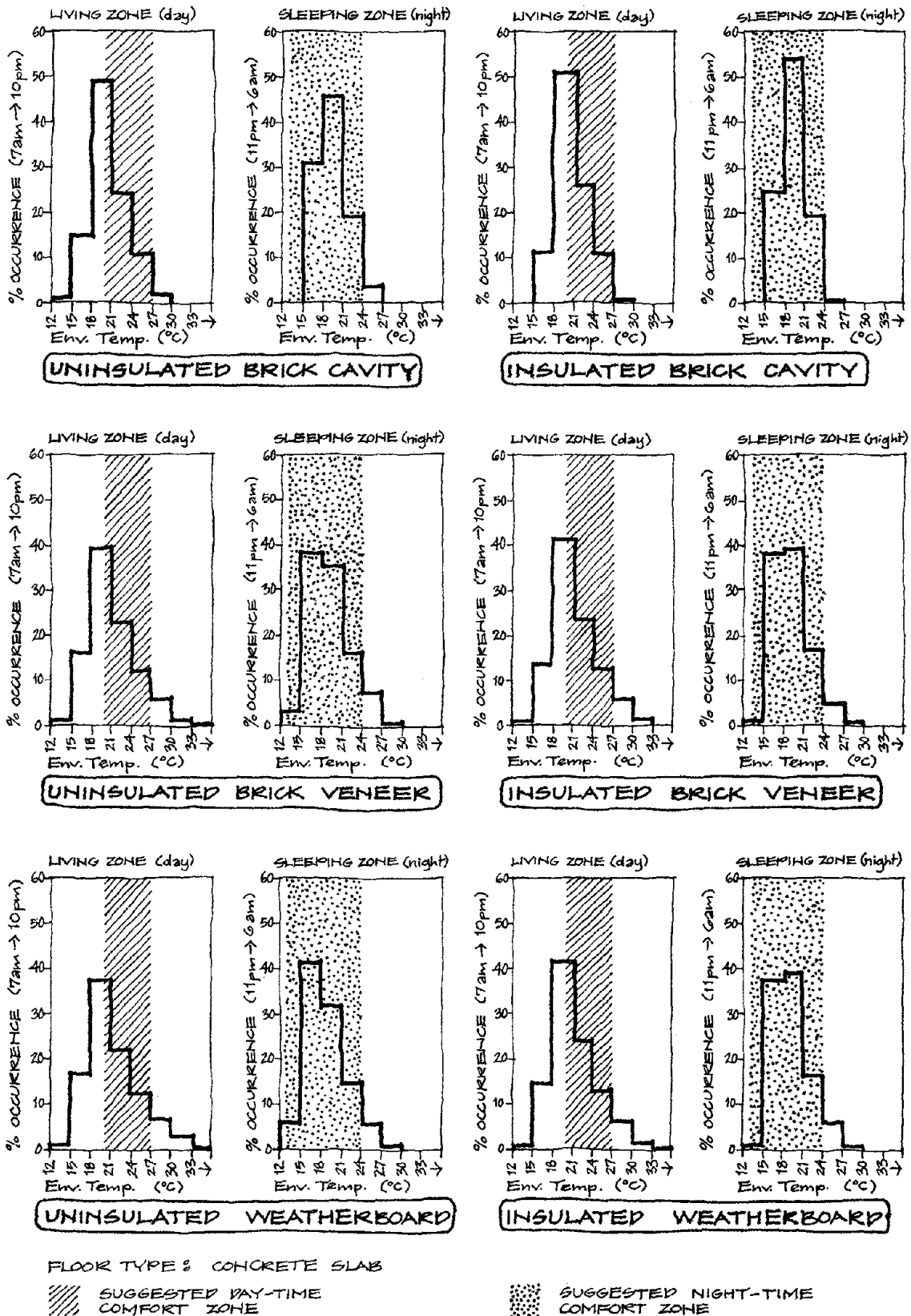


FIG. 5 FREQUENCY OF OCCURRENCE OF TEMPERATURES (NOV-MAR) WITHIN THE STATED RANGES EXPRESSED AS PERCENTAGE OF TOTAL DAY OR NIGHT HOURS

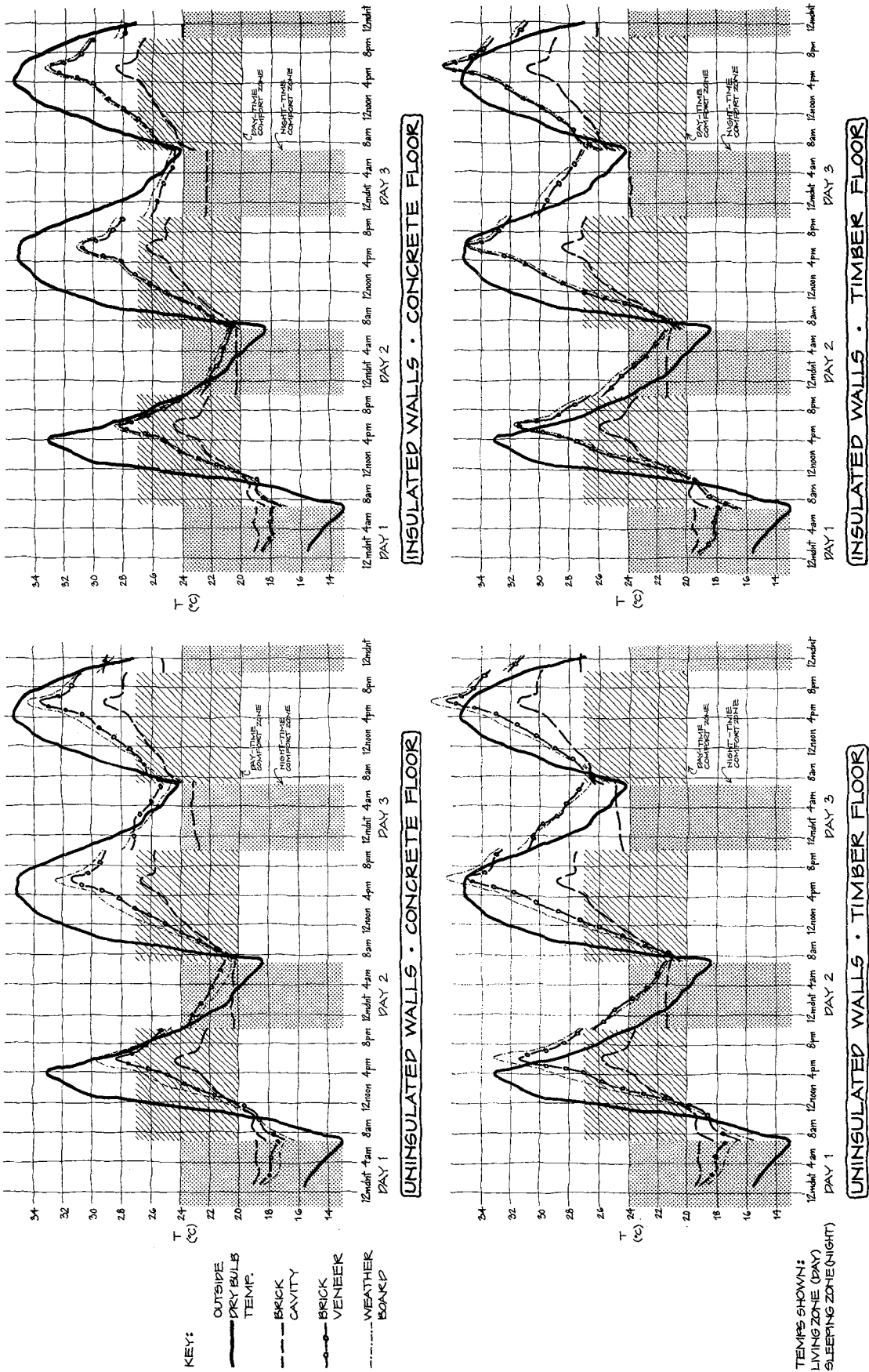


FIG. 6 GRAPHS OF HOURLY INTERNAL ENVIRONMENTAL TEMPERATURES IN UNCONDITIONED HOUSES FOR THREE DAYS IN FEB.

weatherboard houses to produce the comfort levels which occurred in the brick cavity house. Accordingly, runs of the computer program were made for some of the lightweight cases using the following cooling regime:

Living Zone : cooled to 26°C (+ 1 or - 2°C) from 7 a.m. to 11 p.m.
 Sleeping Zone : cooled to 22°C (+ 1 or - 2°C) from 7 p.m. to 6 a.m.

The results, in terms of cooling energy for the entire season and plant capacity required, are shown in Figure 7. The significant cost is that of the plant and its maintenance, the quantity of energy used being small.

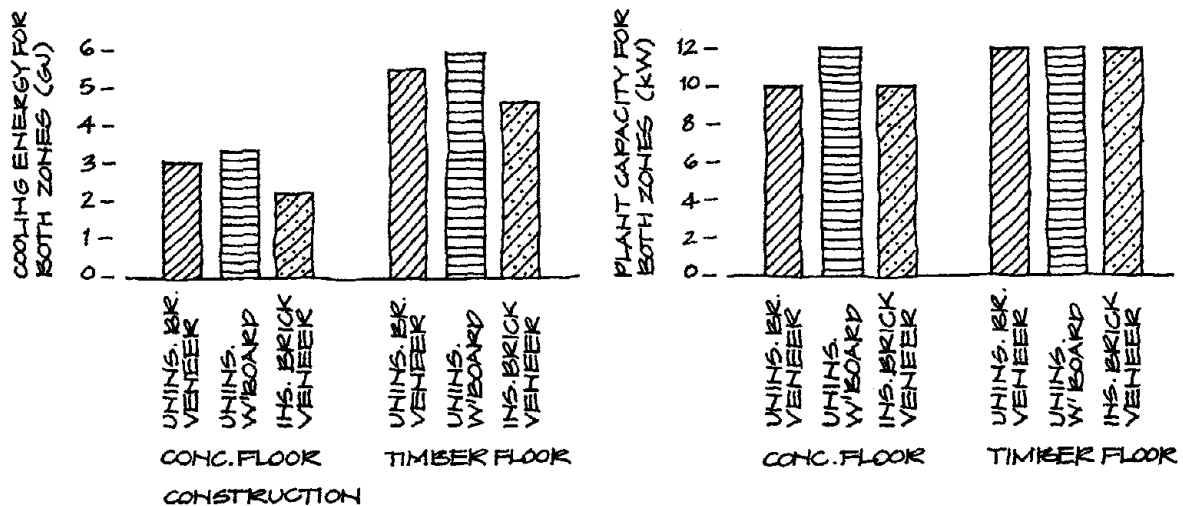


FIG. 7 SUMMER (NOV-MAR) COOLING ENERGY & PLANT CAPACITY REQUIRED BY LIGHTWEIGHT CONSTRUCTIONS FOR COMFORT LEVELS EQUIVALENT TO THOSE MAINTAINED IN THE UNCONDITIONED BRICK CAVITY HOUSE

Some concluding remarks concerning the outcomes of the full series of summer runs follow. Now, regarding performance of the various constructions, one cannot make an absolute statement of the acceptable frequency of occurrence of temperatures in excess of the comfort levels, as this is a subjective matter. One can simply say that if the levels in the brick cavity house are deemed acceptable (which is likely to be the case, especially for the insulated house with concrete floor), then cooling is not required in such a house, while to achieve equivalent comfort conditions in the brick-veneer or weatherboard house, a full air-conditioning system would be needed. On this basis of comparison the heavyweight construction is clearly far superior to the lightweight, as air-conditioning systems not only have high initial costs, but may also give rise to problems of maintenance, noise pollution, etc. If, however, the levels of extreme temperatures in the brick cavity house are deemed unacceptable (an unlikely conclusion) and cooling is insisted

upon to alleviate the total of 19 hours of extreme temperatures in the living zone and 7 night-time hours in the sleeping zone over the entire season (for the insulated case with concrete floor), then the inherent advantage of heavyweight construction over lightweight disappears.

The set of runs performed for the April to October (winter) period will now be considered.

(b) Winter Runs.

Two series of winter runs were carried out. Both zones were heated intermittently in one series and continuously in the other.

The heating regimes were as follows:

Intermittent Heating:

Living Zone : heated to 21°C (+ 2 or - 1°C) from 7 a.m. to 11 p.m.
 Sleeping Zone: heated to 15°C (+ 2 or - 1°C) from 9 p.m. to 6 a.m.

Continuous Heating:

Living Zone : heated to 21°C (+ 2 or - 1°C) for 24 hours each day
 Sleeping Zone: heated to 15°C (+ 2 or - 1°C) for 24 hours each day

Regarding sun control, the deciduous nature of the vine growing on the pergola meant that it caused minimal obstruction to the entry of solar radiation through the north glass during the winter season under consideration. An air infiltration rate was assumed that was consistent with closed windows except for those periods when, due to the entry of winter sun through the north facing glass, this would give rise to overheating of the space. At these times a higher rate was employed that was appropriate to open windows.

Results of the runs, in terms of total annual heating energy and required plant capacity, are shown in Figure 8. In fact some heating is needed during part of the summer period (November to March) in Melbourne and this portion of the total was estimated from the obtained April and October heating energies on the basis of the reasonable approximation that heating energy is proportional to number of heating degree days.

For the series of runs employing intermittent heating, the same heating energy was required for the three different wall types when they were insulated to the same degree. However, wall insulation caused a significant reduction in the quantity of energy used. Because of the greater mass which had to be heated up at the beginning of each heating period, the brick cavity house required a plant of slightly greater capacity than did the brick-veneer or weatherboard house.

For the cases in which the heating was run continuously in both zones, the brick cavity house required less energy than did either of the comparative lightweight constructions. Heat gained by means of the north glazing was being stored in the massive walls and re-radiated at a cooler time, thereby reducing the heat input required from the supplementary heating system. While this effect was also present in the runs using intermittent heating, it was cancelled out by the additional heating energy required each day to heat up the heavy-weight walls from an unheated state.

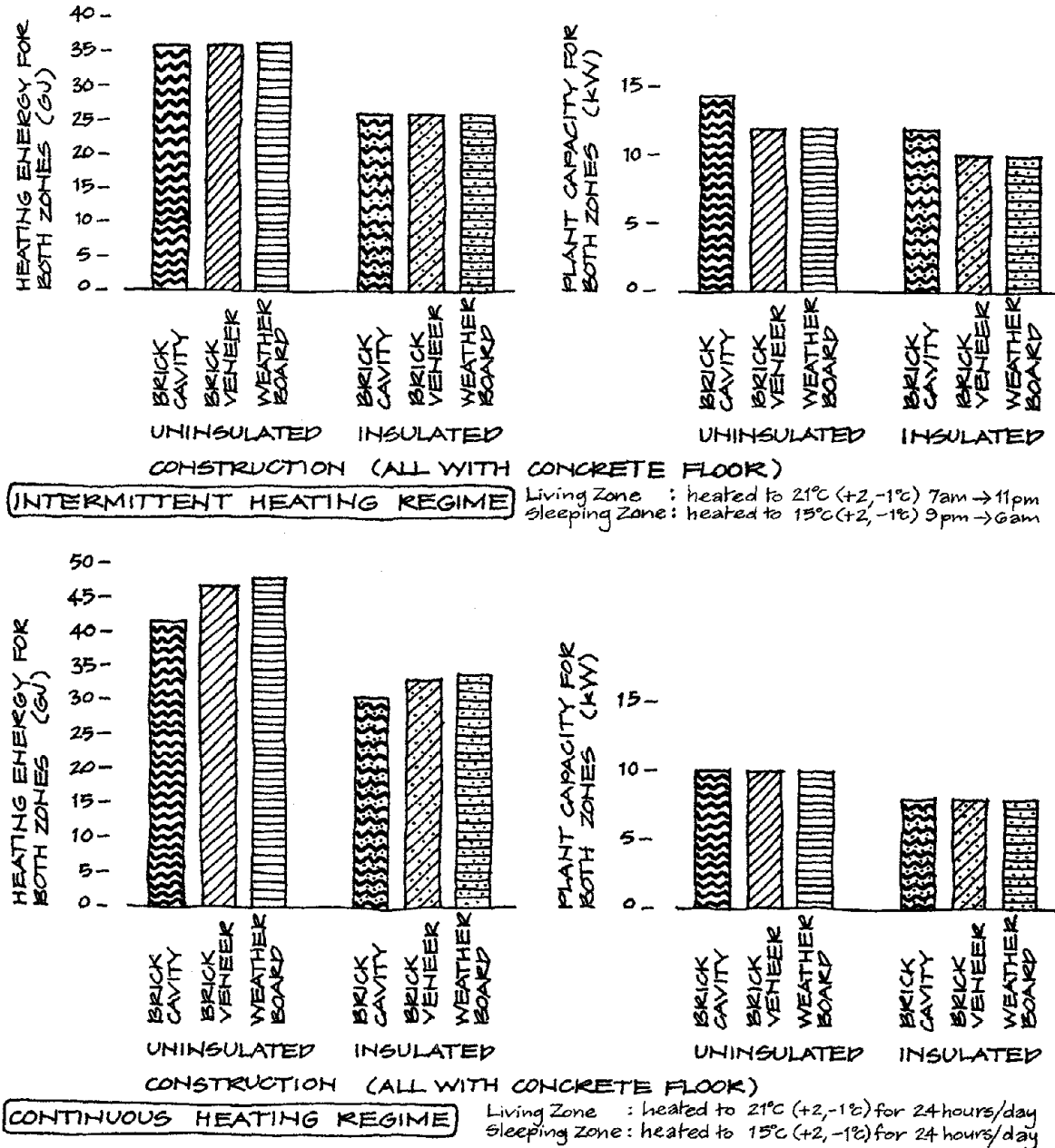


FIG.8 ANNUAL HEATING ENERGY & PLANT CAPACITY REQUIRED

While the mass of construction was seen to affect performance, U-value and hence insulation level, proved to be the dominant factor for the winter period. This contrasts with the summer period where the reverse situation is found to apply.

With regard to plant capacity required to heat the cavity-brick houses, it should be remembered that the test house had only 50% of its north wall area composed of glass. Coldicutt⁽¹⁾ has shown that in such a house, north facing glass can be substantially increased above this level and that this increase will be accompanied by a reduction in the mechanical heating load. To this extent the full potential brick-cavity construction could have for winter performance is not realised in this study.

CONCLUSIONS

Results of the tests described clearly show that an exclusive reliance in U-values is wrong and that the mass of construction is a highly significant factor regulating the thermal performance of a building. Considering the performance of the test building over the full year, the heavyweight (brick-cavity) construction was found to be superior to the lightweight (brick-veneer or weatherboard) construction, primarily in that an occupant would be highly likely to regard air-conditioning as unnecessary in the former but at least highly desirable in the latter. It must also be recognised that the heavyweight construction showed slightly superior performance in winter in some instances and it has been shown that this performance would have been improved had more glass been provided on the north wall.

It is recognised that the particular set of results described in this paper apply only to the specific set of conditions employed (weather pattern with high diurnal fluctuations, configuration of house, etc.), however, the value of heavyweight construction for its effect on thermal performance over the full year has been clearly shown.

ACKNOWLEDGEMENTS:

The principal author wishes to thank the Brick Development Research Institute for the financial assistance that enabled her to carry through the project on which this paper is based.

Both authors wish to thank Mr. Digby Hughes of the Brick Development Research Institute for his contribution towards the design of the test house and for his constructive criticism of the project at the various stages of its development.

Particular thanks are due to Mr. A.B. Coldicutt, Senior Lecturer, Department of Architecture & Building, University of Melbourne, for making his computer program available for use, for his constant advice and help and finally, for his editorial assistance in the concluding stages of the preparation of this paper.

APPENDIX 1 : REFERENCES

- (1) Coldicutt, A.B. Interactive systems for the reduction of heating and cooling loads in houses. Faculty paper; Faculty of Architecture, Building and Town and Regional Planning, University of Melbourne, Melbourne, Australia, 1978.
- (2) Coldicutt, A.B. Tempal - a design orientated thermal performance computer package. Faculty paper; Faculty of Architecture, Building and Town and Regional Planning, University of Melbourne, Melbourne, Australia, 1978.
- (3) Coldicutt, A.B. Thermal properties of construction. Faculty paper; Faculty of Architecture, Building and Town and Regional Planning, University of Melbourne, Melbourne, Australia, 1978.
- (4) Handisyde, C.C. and Melliush, D.J. Thermal Insulation of Buildings (Revised 1971, metric), HMSO, London, 1971.
- (5) Williamson, T and Coldicutt, A.B. Utilization of solar energy in dwellings. Paper to Symposium on Solar Utilization in Dwellings. Institution of Mechanical Engineers, Melbourne, Australia, 1974.

DEVELOPMENT OF SAND-LIME UNITS WITH HIGH THERMAL INSULATION

BY K. Wesche¹ and P. Schubert²

ABSTRACT: The considerable increase in energy cost in recent years has led to more severe requirements for a thermal protection of external units. These requirements can be generally met by masonry of lightweight units (for instance POROTON), of lightweight concrete blocks (with lightweight aggregates like natural pumice or expanded clay), and aerated concrete blocks at a justifiable wall thickness. Sand-lime units have, however, due to the composition and manufacturing process, a dense material of high thermal conductivity, that means, their thermal insulation is low. For this reason, possibilities have been studied to increase the properties of thermal insulation of sand-lime units. In general the following methods may be taken into consideration:

- (a) increasing the hollow parts in the stone,
- (b) reduction of the bulk density of the material,
- (c) a combination of (a) and (b).

Due to the present manufacturing processes, the bulk density of the material cannot be reduced or only in a small extent since a high compressive stress by the hydraulic press (generally $> 15 \text{ MN/m}^2$) is necessary for compacting the fresh unit for an immediate transport to the autoclave. Thereby, the holes in the stone will be limited to a maximum of about 50 % and the stone bulk density to a minimum of about 1000 kg/m^3 . For this bulk density the calculated value of the thermal conductivity of sand-lime masonry amounts to 0.50 W/(K.m) , whereas that of other masonry up to about 0.25 W/(K.m) only.

A considerable improvement of the thermal insulation of sand-lime units can only be achieved by a distinctly less bulk density of the material. Owing to the porosity connected with this fact, the compressive stress must be reduced considerably, that means, the transport stability of the fresh unit must be obtained exclusively or partly by other methods. This problem has been solved by an early strength development due to chemical processes, e.i. by using special binders and admixtures. Thereby, the raw material can be compacted at a very low stress (generally $< 1 \text{ MN/m}^2$). Units with a bulk density up to about 600 kg/m^3 at a minimum compressive strength of about 2.5 N/mm^2 can be produced, the thermal conductivity of which being below 0.25 W/(K.m) .

¹Prof. Dr.-Ing., Director of the Institut für Bauforschung der Rheinisch-Westfälischen Technischen Hochschule Aachen.

²Assistent of the Institut für Bauforschung der Rheinisch-Westfälischen Technischen Hochschule Aachen.

DEVELOPMENT OF SAND-LIME UNITS WITH HIGH THERMAL INSULATION

by K. Wesche¹ and P. Schubert²

1. INTRODUCTION AND FORMULATION OF PROBLEM

The extreme increase in energy costs in recent years has commanded severe requirements for thermal insulation of the external components in the Federal Republic of Germany. According to the thermal insulation regulation which became effective in November 1, 1977, different requirements for the thermal insulation are established according to the type of buildings and to the ratio building surface to building volume. The heat transfer coefficient k in $W/(K.m^2)$ is the characteristic value. It is required for the external wall surface (w_a) including windows (w_i) a mean value of $k_{m, w_a + w_i} \leq 1.85 W/(K.m^2)$ resulting from properties of thermal insulation of windows and walls and of their surface ratio. Thus, for the external wall section without windows it is deduced for common relations in the building of dwellings a k -value of about $\leq 1.2 W/(K.m^2)$. k -values between 0.9 and 0.7 $W/(K.m^2)$ are desirable. This results for a one-leaf external wall, being the most economic external wall construction, according to the wall thickness d_w (without plaster) in a calculated maximum "admissible" value of thermal conductivity of λ_R in $W/(K.m)$ which may be taken from Fig. 1. Thus, a λ_R -value of 0.20 up to 0.40 $W/(K.m)$ is desirable for this wall construction at a justifiable wall thickness. This value may be complied with lightweight and aerated concrete blocks as well as with lightweight fired clay units. For sand-lime units, however, the lowest λ_R -value is 0.50 $W/(K.m)$. The k -value of 0.9 $W/(K.m)$ is satisfied only with an external wall of 490 mm thickness.

Sand-lime units, belonging together with the aerated concrete blocks to the group of calcium silicate products, have many excellent properties as, for instance, high accuracy to size, high strength, a good weather resistance and a good acoustic insulation. Moreover, they are preferred as external wall material for architectural reasons, and they can be manufactured economically and energy-saving. In the first half year 1977, sand-lime units with a demand of about 40 % accounted to the most sold wall units in the Federal Republic of Germany. Therefore, it was only reasonable to comply with the limitations in

¹Prof. Dr.-Ing., Director of the Institut für Bauforschung der Rheinisch-Westfälischen Technischen Hochschule Aachen.

²Assistent of the Institut für Bauforschung der Rheinisch-Westfälischen Technischen Hochschule Aachen.

the application of severe regulations for the thermal insulation by a corresponding improvement of the properties which was the purpose of the investigations described below.

2. POSSIBLE IMPROVEMENT OF THE THERMAL INSULATION PROPERTIES

Of decisive influence on the thermal conductivity of the masonry unit is the thermal conductivity of the solid. It is with anorganic materials, in particular with crystals, on account of their atomic grid structure higher than with organic materials. According to J.S. Cammerer, the following λ -values in W/(K.m) may be taken for the various material groups:

Anorganic building materials in general	about 2.3 to 4.1
Anorganic building materials of amorphous character	about 0.9
Anorganic building materials of larger crystals, for instance, of quartz sand	about 5.8 to 7
Organic building materials	about 0.3 to 0.4

This list makes it clear that the sand-lime unit has most unfavourable properties of thermal insulation caused by the high proportion of quartz sand (about 90 % by volume).

The following three methods offer a key for their improvement:

- (a) Arrangement of as much holes as possible in the units,
- (b) Modified composition of the material, and
- (c) A combination of (a) and (b).

The present manufacturing process has been developed out of former requirements giving priority to the highest possible compressive strength of the unit. The moulding was in agreement with these requirements by the application of mechanical and hydraulic presses by which the raw material in the steel mould has been formed by compaction under high pressure - usually 15 MN/m^2 - to the fresh unit. By the high pressures it was possible on the one hand, to transport the fresh unit immediately to the autoclave and, on the other hand, to obtain due to its compacted structure a higher compressive strength after steam

curing in the autoclave. The thus produced solid unit had a λ_R -value of about 1.1 W/(K.m).

It has been tried several years ago to improve the thermal insulation according to the above mentioned methods (a) and (b). Since air with $\lambda \approx 0.02$ W/(K.m) is a poor heat conductor, holes in the unit by positioning steel cores on the pressure plate were arranged to compensate the good heat conduction of the material of the sand-lime unit. For technical reasons, usually only large circular holes could be made. This was disadvantageous in so far as a relatively high percentage of the heat was transferred by radiation and convection which disappear completely only with air voids of < 0.1 mm diameter. Only then, heat is completely transferred by the thermal conductivity of the air molecules. Slit-resembling cores lengthening the heat path, which are advantageous to thermal protection, could be manufactured only during the two last years, however, by sacrificing considerable costs: The slender cores had to sustain considerably higher stresses, the raw materials needed a special composition and the compaction had to be intensified so that the relatively small spaces between the holes would be sufficiently stable after pressing.

According to this method a unit bulk density of 1000 kg/m^3 can be obtained corresponding to a relatively high λ_R -value of 0.50 W/(K.m). In part, it is possible to produce units of 900 kg/m^3 . Since 50 % of the unit are holes and, thus, the critical thickness of the space between the holes is reached, these bulk densities of the unit must be regarded as limit values for this method. A considerable improvement of the λ_R -value can, therefore, not be expected.

But also the method (b) was not successful. The attempt to exchange quartz sand at least in part by other materials having a better thermal protection failed due to the uneconomical process and because this would have provided a slight improvement only, or the use of lightweight aggregate did not allow the necessary high amount of pressure to be applied to the fresh unit for a certain stability during transport to the autoclave since most of the light weight aggregates were destroyed and, thus, without any effect.

The experiments made so far, did not reveal an improvement of the properties for a thermal insulation of the sand-lime units. It can only consist in a considerable reduction of the bulk density of the fresh unit in combination with a high percentage of the holes. The reduction of the bulk density of the fresh unit is, however, opposed by the high amount of pressure applied to the unit which is required for an sufficient

stability of the fresh unit only. The aspect of a high compressive strength of the finished products is of minor importance here. A successful solution of the problem can only be obtained by a transport stability of the fresh unit without any remarkable mechanical effect.

3. DEVELOPED METHOD

The basic concept of the new method consists in the addition of an active component insuring the necessary early strength development of the fresh unit by a chemical process. For this purpose, a regulated-set-cement has been found applicable which has been developed in USA and which is also produced in the Federal Republic of Germany, for about five years. It is characterized by the klinker phase $C_{11} A_7 Ca F_2$ and has an initial setting time of approximately 5 to 10 min /1/. Thus, it was possible to reduce considerably the amount of pressure applied from about 15 MN/m^2 to below 1 MN/m^2 . That resulted in a completely new forming process, that is vibration.

On account of the very low mechanical stress of the raw material in the mould, practically any measures for a reduction of the bulk density can be applied. For economic reasons and for a thermal protection, the artificial production of a great number of small air voids proved to be most favourable. For this purpose, foam-forming admixtures were used being on the market in the Federal Republic of Germany for about five years. They are manufactured synthetically on the fatty alkyl sulfates base and produce stable micropores, usually 50 % by volume. Foam-forming may be carried out in a special device, the so-called foaming gun. Then, the "prefabricated" foam is mixed together with the raw material. Or foam-forming is effected in the raw material directly by pouring out the foam-forming admixture into the high-speed mixer where it is foam-forming. For the here developed process, the latter method has been adopted at first, in order to eliminate difficulties arising in proportioning for laboratory tests. The conditions for the effectiveness of the foam-forming admixture is not too stiff consistency of the raw material which should, preferably, be between soft and viscous so that by the proportions of foam-forming admixture and water content of the raw mixture a bulk density of the raw material up to about 1000 kg/m^3 can be obtained. To guarantee this very low bulk density, any compacting must be avoided, that means, the raw material only should be distributed uniformly in the mould, for instance, by a short vibration. This forming has also an important additional advantage: it allows a maximum of holes in the unit thus pro-

curing in the autoclave. The thus produced solid unit had a λ_R -value of about 1.1 W/(K.m).

It has been tried several years ago to improve the thermal insulation according to the above mentioned methods (a) and (b). Since air with $\lambda = 0.02$ W/(K.m) is a poor heat conductor, holes in the unit by positioning steel cores on the pressure plate were arranged to compensate the good heat conduction of the material of the sand-lime unit. For technical reasons, usually only large circular holes could be made. This was disadvantageous in so far as a relatively high percentage of the heat was transferred by radiation and convection which disappear completely only with air voids of < 0.1 mm diameter. Only then, heat is completely transferred by the thermal conductivity of the air molecules. Slit-resembling cores lengthening the heat path, which are advantageous to thermal protection, could be manufactured only during the two last years, however, by sacrificing considerable costs: The slender cores had to sustain considerably higher stresses, the raw materials needed a special composition and the compaction had to be intensified so that the relatively small spaces between the holes would be sufficiently stable after pressing.

According to this method a unit bulk density of 1000 kg/m^3 can be obtained corresponding to a relatively high λ_R -value of 0.50 W/(K.m). In part, it is possible to produce units of 900 kg/m^3 . Since 50 % of the unit are holes and, thus, the critical thickness of the space between the holes is reached, these bulk densities of the unit must be regarded as limit values for this method. A considerable improvement of the λ_R -value can, therefore, not be expected.

But also the method (b) was not successful. The attempt to exchange quartz sand at least in part by other materials having a better thermal protection failed due to the uneconomical process and because this would have provided a slight improvement only, or the use of lightweight aggregate did not allow the necessary high amount of pressure to be applied to the fresh unit for a certain stability during transport to the autoclave since most of the light weight aggregates were destroyed and, thus, without any effect.

The experiments made so far, did not reveal an improvement of the properties for a thermal insulation of the sand-lime units. It can only consist in a considerable reduction of the bulk density of the fresh unit in combination with a high percentage of the holes. The reduction of the bulk density of the fresh unit is, however, opposed by the high amount of pressure applied to the unit which is required for an sufficient

viding high thermal protection without any special technical problems and without any stresses of the cores.

Though the problem of a sufficient stability of the fresh unit is principally solved by the addition of a regulated-set-cement, there are, however, for the raw mixtures adjusted from soft to viscous states, too long waiting times of about 5 to 10 min with a proportion of regulated-set-cement in the mould which cannot be increased for economic reasons. The setting of this cement type had to be accelerated by additional measures in order to obtain economically interesting production cycles. This was achieved by the addition of a chloride-free accelerator for hardening, known for concrete, and/or by heating the mould walls and the cores.

The developed production method is shown in Fig. 2. Only the processing phases 5 and 6 had been modified compared with the hitherto existing method.

4. ADVANTAGES OF THE METHOD AND PROPERTIES OF THE DEVELOPED SICAPOR-SAND-LIME UNIT

4.1. Advantages of the method

By the developed method, the hitherto possible range of the bulk density of the unit, from 1000 up to 2000 kg/m³ is extended from 600 to 2000 kg/m³. The method provides the following decisive advantages:

- (a) Considerably improved thermal insulation property compared with other wall building materials at a sufficient compressive strength.
- (b) Due to the very low bulk density of the unit it is possible to use large units which results in considerable savings of wages at the construction site.
- (c) High reduction of capital costs for the forming machines (about 50 %), and lower wear costs at only unimportant higher material costs (10 to 20 %).

4.2. Properties of SICAPOR

In Fig. 3 results of the thermal conductivity measurements carried out on completely dry aerated concrete and sand-lime units obtained by Cammerer /2/ are represented. Test results from SICAPOR - determined on solid units - are entered into this figure. The comparison shows that the SICAPOR values are

equal to those of aerated concrete, they are, partly, even better. It is obvious that the expensive replacement of sand by lightweight aggregates (here expanded fly ash, FLUASINT) does not provide an improvement, this means, that the followed path of an artificial increasing by porosity for foam-forming admixtures has proved to be the right one.

In Fig. 4 the expected calculated values of the thermal conductivity λ_R of SICAPOR derived from available test results are compared with the available lowest λ_R -values of other types of masonry units and the presently manufactured sand-lime units. It is clearly noted the favourable behaviour of SICAPOR units which achieve approximately the λ_R -values of the aerated concrete blocks and that they decrease considerably those of the other masonry units. The improvement compared with the hitherto used sand-lime units is also significant. It may be due, besides the porosity of the solid material, to the best formed hole structure.

Fig. 5 shows the relation between bulk density of the material and the compressive strength of the material plotted according to the available test results of SICAPOR. The test values including all investigated substantial mix combinations prove so conclusively the ample adjustment range of bulk density and strength. Thereupon it will be possible to manufacture also units of the bulk density class of 600 kg/m^3 having a compressive strength of 2.5 N/mm^2 which will be sufficient in the main field of application for dwellings up to four storeys. For bulk density classes of 700 and 800 kg/m^3 , the compressive strength will be 2.5 to 5.0 N/mm^2 , and 7.5 N/mm^2 respectively.

Preliminary tests on SICAPOR have shown that other properties as frost resistance, shrinkage behaviour and weather resistance are, at least equal to those of the hitherto used sand-lime units.

Patents have been applied for the new method in 32 countries.

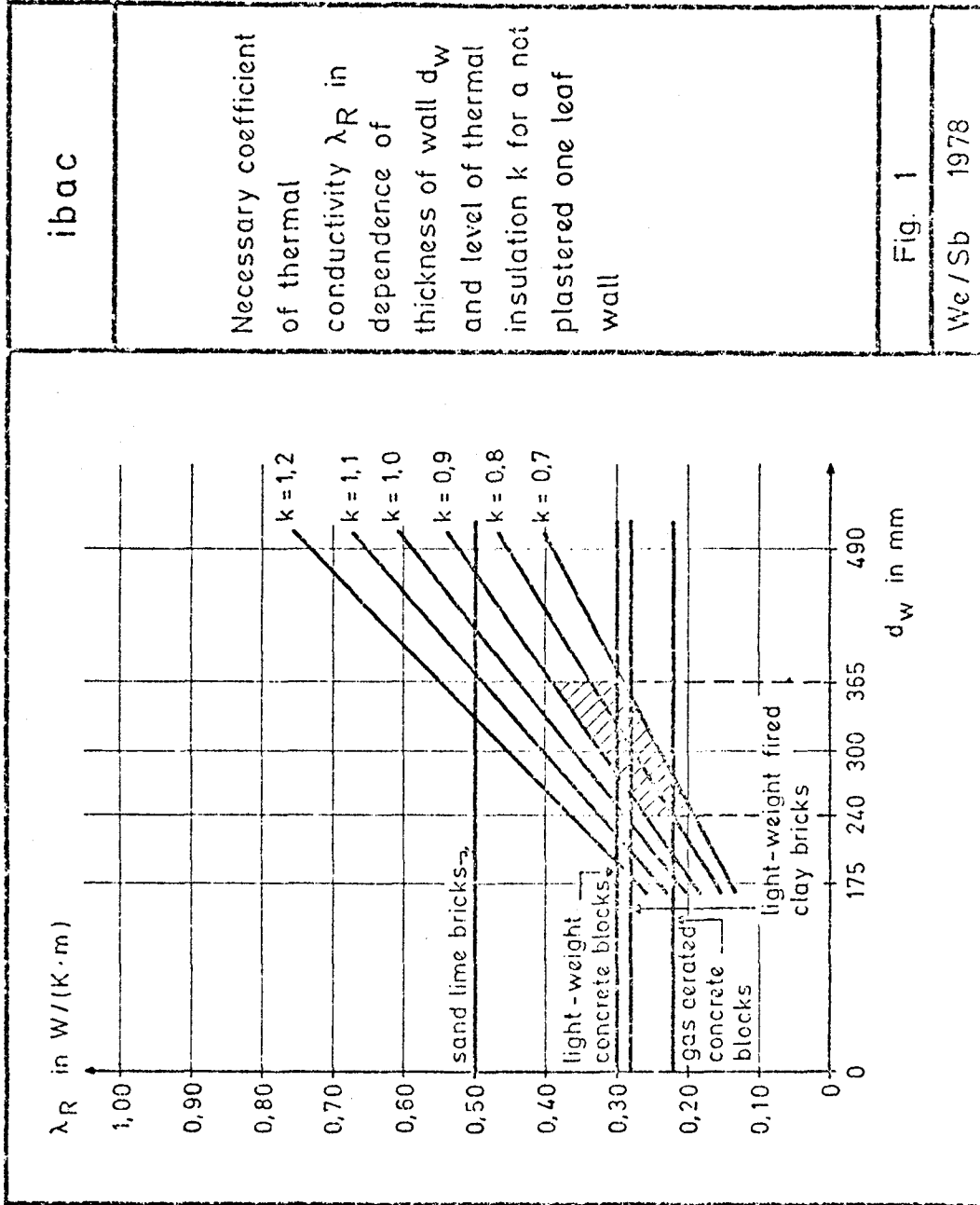
Fig. 6 shows a SICAPOR unit type 3DF having the dimensions of $240 \text{ mm} \cdot 175 \text{ mm} \cdot 113 \text{ mm}$.

5. SUMMARY

It is reported on a new method by which sand-lime units of a high thermal insulation can be manufactured. The method consists in that the required transport stability of the fresh units after demoulding is achieved by the addition of a rapidly hardening agent in combination with a setting accelerator and/or by heated moulds. Thus, the hitherto required high amount of pressure is no longer requested. This allows a high porosity of the material by foam-forming admixtures and, with regard to the thermal insulation, the best arrangement and forming of the holes in the unit. Thus, bulk densities of the units of about 600 kg/m^3 at calculated thermal conductivity values below 0.25 W/(K.m) and of a sufficient compressive strength of 2.5 N/mm^2 may be obtained. The already good thermal insulation of other types of masonry units is, in part, exceeded by these values. Patents have been applied for this economic method in 32 countries.

REFERENCES

- /1/ Efes, Y. und Schubert, P., Mörtel- und Betonversuche mit einem Schnellzement; Betonwerk + Festigkeit-Technik, Heft 11 und 12, 1976, p. 541 - 545 and p. 620 - 623.
- /2/ Cammerer, W.F., Wärmeleitfähigkeit von Calciumsilikatprodukten; 2. Internationales Symposium für dampfgehärtete Kalziumsilikat-Baustoffe, Hannover 1969, Lecture No. 13.



ibac

Necessary coefficient of thermal conductivity λ_R in dependence of thickness of wall d_w and level of thermal insulation k for a not plastered one leaf wall

Fig. 1

We/Sb 1978

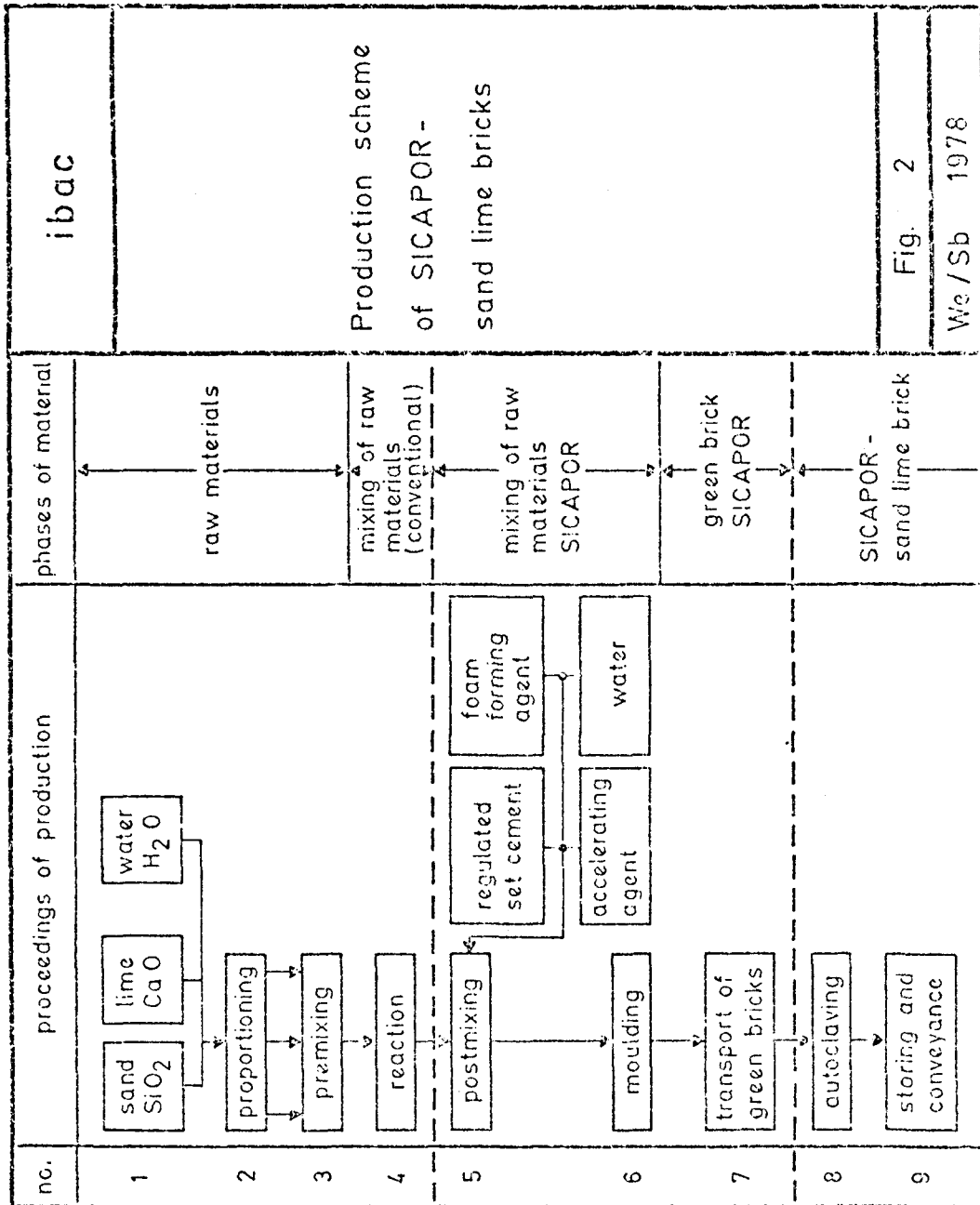


Fig. 2

We / Sb 1978

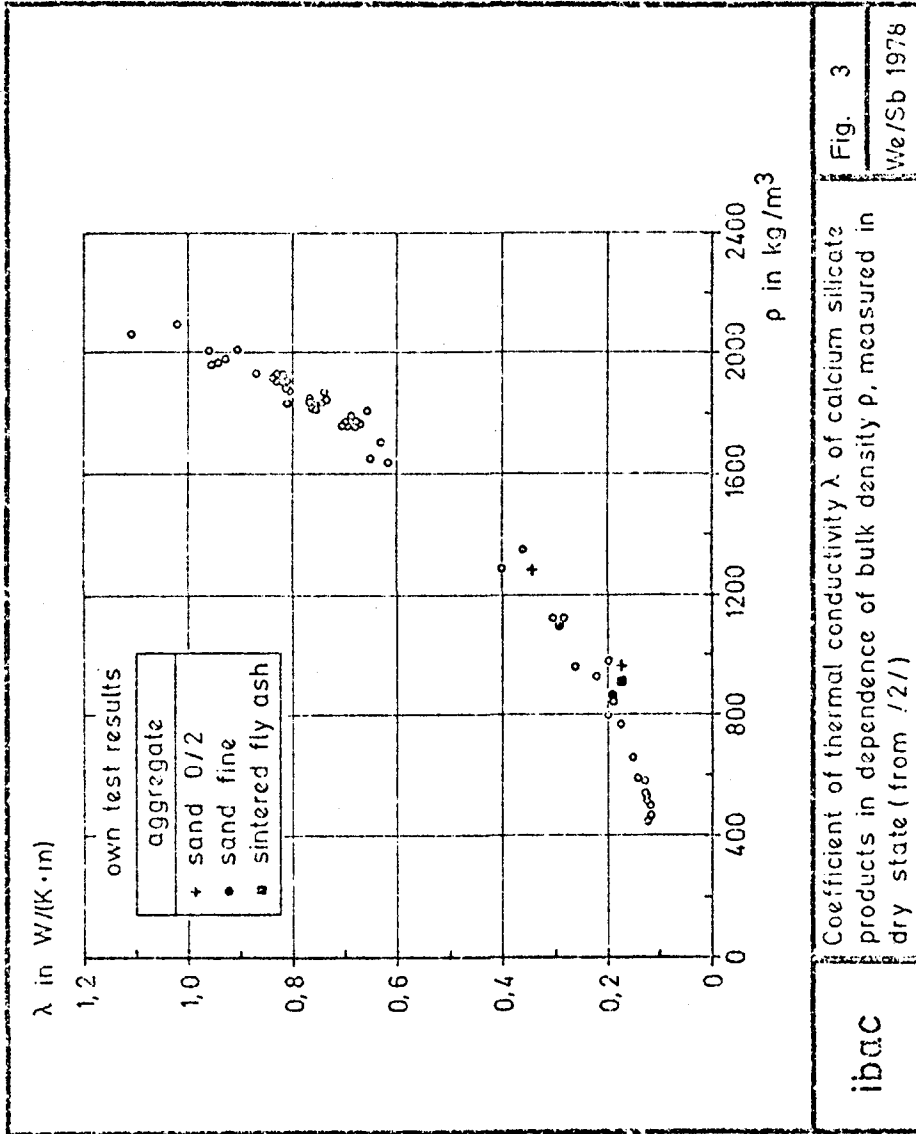
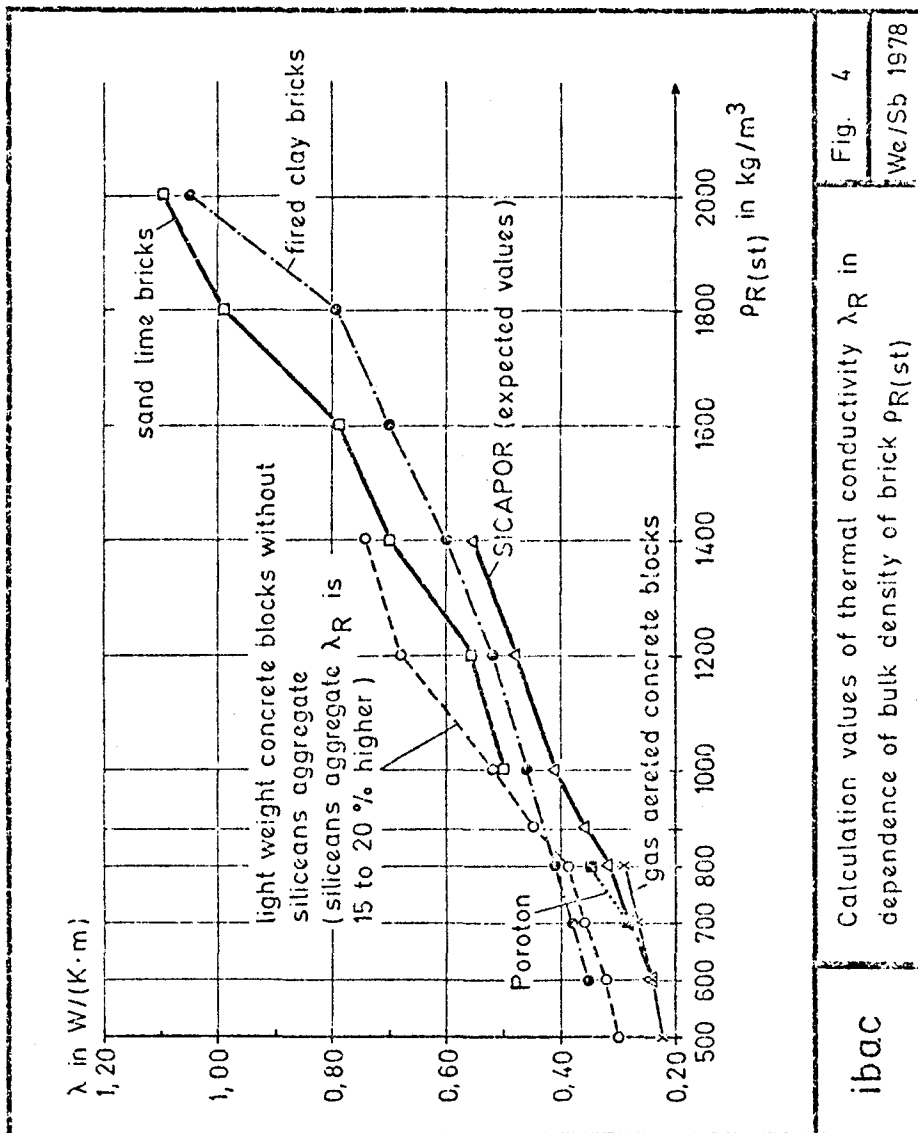


Fig. 3
We/Sb 1978

Coefficient of thermal conductivity λ of calcium silicate products in dependence of bulk density ρ , measured in dry state (from /2/)

ibac

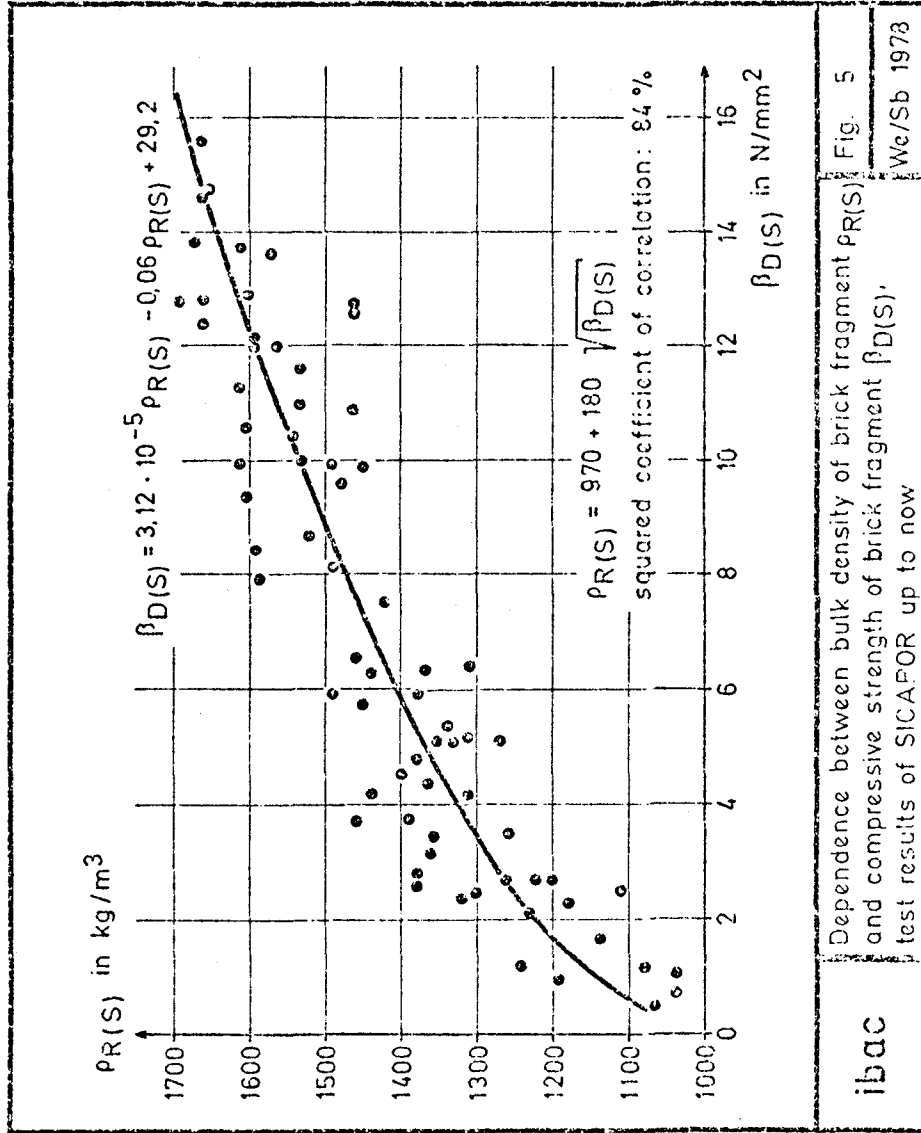


ibac

Calculation values of thermal conductivity λ_R in dependence of bulk density of brick ρ_R (st)

Fig. 4

We/Sb 1978



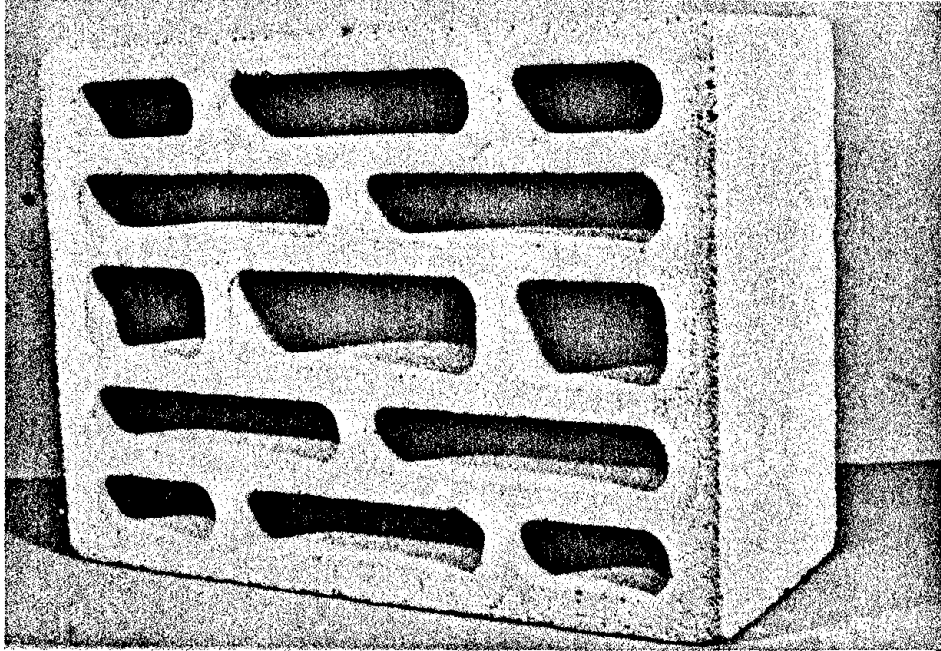


Fig. 6: SICAPOR mit (240 mm · 175 mm · 113 mm)

MODERN LOADBEARING MASONRY CONSTRUCTION IN THE WESTERN
UNITED STATES

By John R. Mock, Hendrick and Mock Architects, San Diego, CA

ABSTRACT: Explanation of the Concept and Development of the Use Standards Reinforced Concrete Masonry (Concrete block) in Modern Construction. Examples of construction projects in the western United States are used to illustrate the Basic Concepts of this new use of masonry. The paper reinforces the advantages of the system, which includes:

1. Quality control methods.
2. Speed and economy of construction.
3. High efficiency through repetitious construction and steady work.
4. Integral sound control and fireproofing.
5. Energy conservation in the combination of masonry with limited glass that together reduce the cost of building utility operations.
6. A real breakthrough for construction of most types to buildings in the four to seventeen story height range. (The current building codes limit height to 160 feet.)

MODERN LOADBEARING MASONRY CONSTRUCTION
IN THE WESTERN UNITED STATES

BY: John R. Mock, Architect¹

INTRODUCTION

The system of construction and case studies to be discussed represent only a few of the projects that have been constructed using reinforced loadbearing masonry walls since our firm, Hendrick and Mock Architects, designed the 8-story Hanalei Hotel in 1966. (This was the first application of this system over three stories in height in the United States).

In the time since the Hanalei construction was started 12 years ago, this system has become standard for military barracks and has remained the most economical for hotel construction. With the use of prestressed concrete planks or slabs, it has also been successfully adapted to apartment and condominium construction. Given a start and good promotion by the masonry industry the system is ready for competitive use for medium rise office buildings. Briefly, the possibilities of the system to be discussed are:

1. Quality control methods.
2. Speed and economy of construction.
3. High efficiency through repetitious construction and steady work.
4. Integral sound control and fireproofing.
5. Energy conservation in the combination of masonry with limited glass that together reduce the cost of building utility operations.
6. A real breakthrough for construction of most types of buildings in the four to seventeen story height range. (The current building codes limit height to 160 feet.)

NEW CONCEPT

The concept of a 8 inch thick concrete block walls holding up a building 12 stories high or even higher is quite an innovation that isn't easy to comprehend. As a comparison, the Swiss, who have been pioneers in loadbearing masonry construction, have built apartments with 15-1/4" thick outside walls to heights of 18 stories (way back in 1957).

¹John R. Mock, President of Hendrick and Mock Architects,
San Diego, California

In "modern masonry" the structural frame is eliminated completely and all structural loads are carried by the reinforced concrete block or brick masonry bearing walls and precast or cast-in-place concrete slabs. The masonry stiffens the steel and protects it from fire, while the steel adds resilience and toughness to the wall.

In concrete block construction, vertical steel is placed inside certain hollow cells of hi-stress concrete block and these cells are then filled with a rich soupy grout mixture of cement, sand and pea gravel. Horizontal steel is grouted in bond beams, which are masonry units depressed on the top to form a horizontal channel in the wall.

In areas of the country outside major seismic or earthquake zones, where wind loads govern design, the only difference in application would be to install steel of smaller diameter, further apart within cells of standard block to achieve the same structural results as we get in California, Hawaii and other seismic areas. Comparative costs also are less, due to lower labor factors and less reinforcing. This use of modern masonry has expanded rapidly since the first application in multi-story buildings by Hendrick and Mock. There are two main reasons for this popularity; the first being economy. The Hanalei was built at a cost of \$11.44 per square foot including elevators and 4-pipe air conditioning. This proved to be 20% less than similar projects employing other types of construction.

In recent projects the total cost per square foot has risen, due mainly to higher labor and material costs, but the relative economies remain. Even with overtime work authorized in the early stages of construction of the 10-story Town & Country Hotel Addition, and an expensive foundation using clusters of 60 ft. long piles, the cost was only \$16.30 per square foot. This was about equal to the cost of the average custom home build in California and far less than other Class A Structures. The Convention Center Ramada Inn 12-story hotel tower, which was completed in 1972 in Dallas, Texas, cost \$14.73 per square foot. This cost included a complete restaurant and meeting room complex on the top floor. For total project preliminary design budgets, we are currently using 30 to 32 dollars/square foot in California and 28 to 30 dollars/square foot in the southwest (Texas). East coast costs should run close to California and the mid-west should be slightly higher than the southwest.

The second reason is savings in construction time. The erection time for all walls, floors and the roof of the 207 room Hanalei, was 8 weeks. The total construction time from the start on February 11th, until the hotel was ready for occupancy four months later, was 141 days. The 324 room Town & Country Hotel which was completed in stages, took 208 total days for all work, not quite 7 months. Floor and roof

slabs for both projects were job cast on the ground and lifted into place by use of a truck crane.

In Texas we have been achieving similar results using flying forms since large truck cranes capable of lifting floor slabs that could weigh from 9 to 14 tons are not as available as climbing tower cranes and our sites have been quite tight. Construction of the 12-story Ramada Inn Convention Center Hotel in Dallas, was commenced on June 4, 1971. The hotel was substantially complete and opened for business on June 19, 1972. Masonry work began in October, 1971 and was complete on February 9, 1972. Total time for masonry work on the 12-story, 162,000 square foot hotel tower was just 64 working days! (18 Days were lost to bad weather and holidays).

To illustrate what an early opening means to a Owner, just consider the revenue produced by the advance opening of the 194 room center wing of the 324 room Town & Country in 148 days. The wing had a 100% occupancy during high tourist season from July 4th, until the 60 room west wing was opened August 29th, (after 208 days). This created 10,864 room day rentals at \$19.40 average per occupied room which is equal to \$215,107.00 or about \$40,000 plus gross profit. Obviously the 100% rental only occurs in the summer tourist season, but even maintaining occupancy on a 70% average for this period certainly wouldn't be hard to take.

INTRODUCTION TO CASE STUDIES

Although the case studies to be presented are constructed in Hawaii, California and Texas, the buildings actually represent enough variations to indicate what to expect of the system in any region of the country. All major building code requirements are quite similar regarding this type of construction.

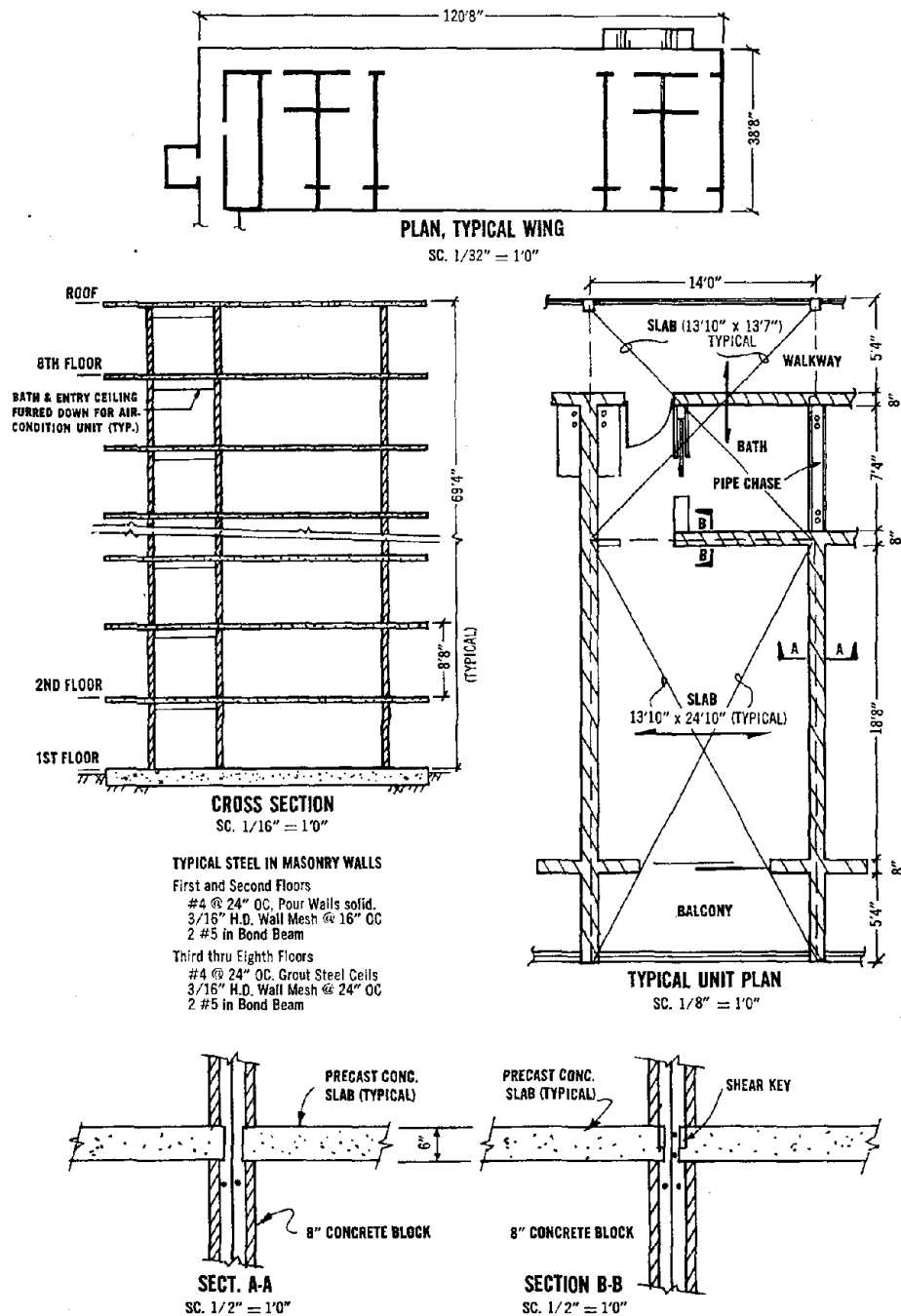
First of all, California and Hawaii are located in earthquake country. This state and Hawaii and the other western states, to a lesser degree, represent the most-restrictive structural requirements possible. This area also maintains a very high construction cost index. However, labor is quite productive and contractor's are quite competitive. They also are receptive to new systems. Hawaii is a special problem unto itself, but the relative cost savings still exist.

The Dallas-Fort Worth and Austin, Texas regions are representative of the growing south and southwestern parts of the country. Physically these areas look much like the mid-west and certain areas of the east.

Buildings must be designed for extreme temperature differences and rainfall is substantial. It is relatively hot much of the year, but snow and freezing also occur during the winter months. Actually a building designed for these parts of Texas could be relocated in any one of the more severe hot or cold weather climates of the country with few changes.

As with any area, most buildings and their Owner's requirements are also different.

With this, or any other building system, a little common sense goes a long way. Therefore, the information presented in the case studies should service as a starting point for designing and construction of this system.



Structural details of the masonry high rise Hanalei Hotel project.

HANALEI HOTEL, SAN DIEGO, CALIFORNIA

The Hanalei Hotel is roughly L-shaped with all rooms overlooking the central patio. The exterior is painted 8 x 8 x 16 concrete block scored to form a square grid pattern. Walls in motel units facing beds and patio are also concrete grid block, to create a warm interesting interior, something often lacking in many other high-rise structures. All block was manufactured by Hazard Products.

The use of 8 inch reinforced concrete block walls in the 8-story Hanalei project became possible because of major changes in the building codes. The 1964 Uniform Building Code permitted higher design stresses (over twice as high) in masonry than were previously allowed when the strength selected by the structural engineer is established by preliminary tests of masonry assemblies and the work is supervised by an inspector licensed by the City. This code change contributed savings in construction costs to the Owner, but more as a bonus, since both Owner and Architect were convinced that the use of masonry bearing walls combined with job cast pick-up concrete slabs was the most appropriate system of construction, even if lower floor walls might have to be of 12 inch block as required by previous codes. This conclusion came from previous design and cost studies for the Mission Valley Hills Complex of 3, 4, 6 and 12-story apartment buildings of masonry construction conducted for the Owner during 1965.

Manufacturers had long been able to make stronger blocks but prior to multi-story applications, there has never been any incentive.

Tests at the Hanalei Hotel showed that the lightweight expanded shale blocks average 3825 psi on the net section compared to the 3000 psi design stress required. All mortar and grout had a compressive strength of 3000 psi minimum. Blocks average 2000 psi on the gross area which would designate high stress block and at the time they were the first manufactured in the United States. All block used in the western states for high-rise construction is hi-stress, but this has proven unnecessary for other areas, such as Texas.

The first 3 weeks of construction were devoted to preparation of the mat foundation and the pouring and finishing of floor and roof slabs in piles adjacent to the building. The site areas used for casting beds and circulation of equipment was actually more area than all the hotel floors combined. The slabs were cast in stacks 8 to 11 high, with a maximum height of 5 feet. The last slab cast was the first slab placed.

The masonry contractor (Quality masonry and F.B. McCauley Joint Venture) started work on the 25th of February; from then on, the job proceeded at the rate of one floor finished each week

Progress pictures taken each Friday afternoon show the crane in approximately the same spot week after week, setting the precast floor slab.

One architectural advantage of using precast flab slabs is reduced floor to floor heights. In the Hanalei, we saved the cost of one story of concrete block by using 8'-8" floor to floor heights, eliminating suspended ceilings in motel rooms and applying ceiling finishes directly to the slab bottoms. We have continued to apply this method on subsequent projects. We have varied heights from 8 feet to as high as 9'-2" for 2nd floors and above and up to 13'-2" for first floors with public facilities.



SAN DIEGO HILTON ADDITION

The 8-story hotel addition to existing facilities is located on a 17 acre bench front site, contains 74,516 SF and 127 rooms with private balconies.

The structural system is similar to the Hanalei Hotel in that they both rest on a thick mat foundation over recompacted soil, due to poor soil conditions. All floor and roof slabs were job cast and lifted in place by use of a truck crane. The similarities end at that point of reference. The Hilton Inn has a double loaded corridor and a very tight site for casting beds. These two conditions and some rain during soils compaction operations and crane movement times added unexpected construction time. However, the block work progressed beautifully.

The double loaded corridor necessitated crane movement to two sides of the building to lift job-cast concrete slabs in place on masonry walls; where in the single loaded Hanalei the crane worked one side of the building between stacked concrete slabs, and each slab could be placed in less than 1 hour. Each room size slab varied in weight from 9 to 14 tons, sizes varied from 29'-1" by 20'4½" to 33'-8½" by 14'-1". Since all slabs were cast on one side of the building, some close and some in an adjacent parking area, many had to be moved twice - once onto a flat bed truck, and then from the truck by the crane into place. The double movement also was caused by the poor soils condition around the building. When the ground was dry the truck crane could pick up slabs and move them to required position with no trouble. After the rain the poor soil could not take the load of both a moving crane and a 14 ton slab.

Site tightness also made the spread out casting, so successful in the Hanalei, impossible. Since slabs can't be cast higher than the workman can easily place concrete in layers, some casting beds were also used twice. That is, after the original 8 to 10 slabs were placed, more were cast on the same bed. Due to these job conditions the construction time ran 216 calendar day time from ground breaking to first customer.

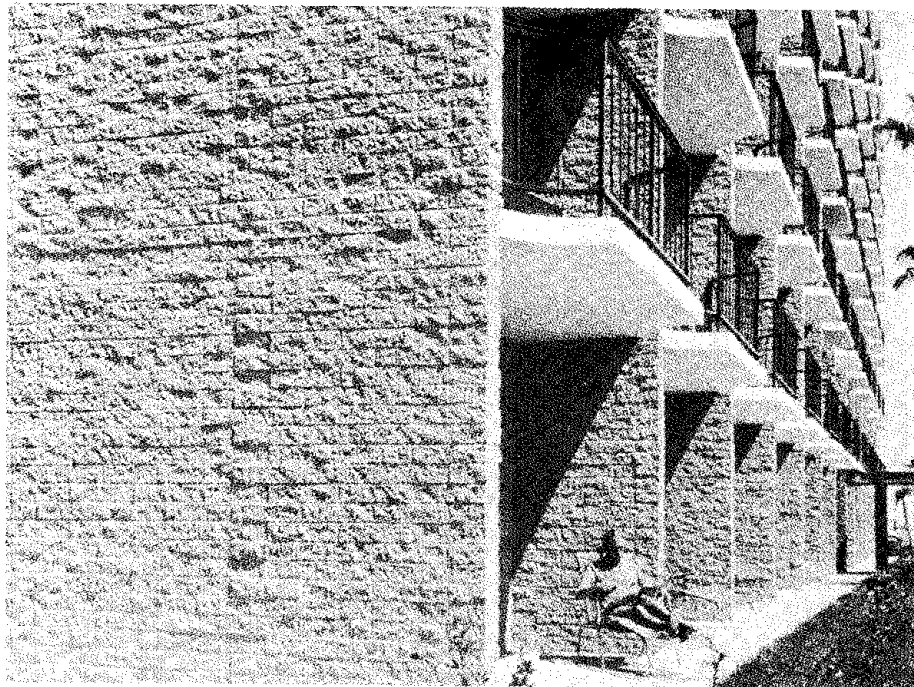
Production of "high stress" concrete block for the Hilton was relatively an easy and routine job for the block producers, Modern Block of Oceanside. Most of their regular production averages 2800 psi, so it was decided a unit that averaged 3600 to 3900 psi would be advisable to produce prisms of the required 3000 psi.

The use of texture (4" high split face) block on the exterior and regular 8" high precision block on the interior, created some material handling problems at the plant because of the 53 different sizes and shapes involved. To compound this, the mason contractor had found in their previous high rise construction experience that it was expedient to cut job labor by having pre-packaged material with all sizes and shapes to coincide with each individual wall section. Each floor required

16,053 concrete block units that were broken down into 79 packages which resulted in 153 cubes of block. The building was then divided into four quadrants and block was delivered with the appropriate number of packages for each section. This saved valuable space on an already limited job site. It enabled material to be placed close to the building, thus, saving rehandling on the part of the mason contractor (Custom Masonry) and it saved the manufacturer the pressure of delivering 12 loads of block at one time.



The 8-story San Diego Hilton which utilized 53 different sizes and shapes of concrete masonry units.



BARRACKS P-005, NAVAL AMPHIBIOUS BASE, CORONADO, CALIFORNIA

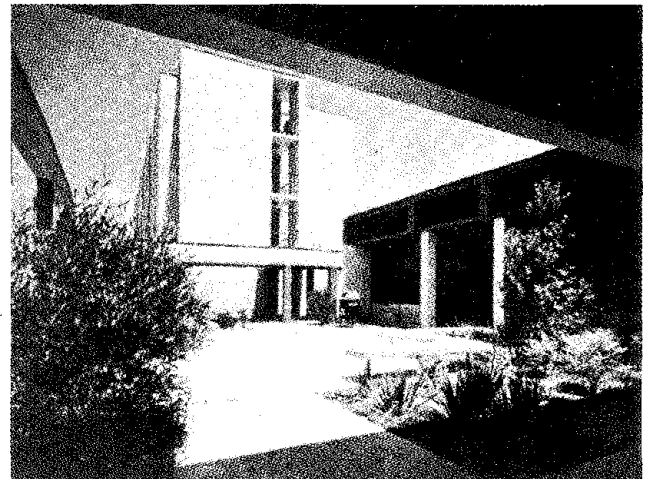
The barracks complex in Coronado, California, consists of four identical L-shaped four story towers, clustered around a landscaped central core area consisting of a one story central lounge building, mechanical equipment building and overhead pipe chase. The complex accommodates 1050 enlisted men in two and four men rooms.

Concrete blocks used in the wall system were high stress 4 x 8 x 16 units laid in common bond, (350,000 units were used). Floor slabs were precast on the site and then lifted into place as the masonry walls were laid up. This system of construction was adopted for the following reasons:

- a) Proven economy of construction.
- b) Proven ease of construction.
- c) Short construction period before occupancy for intended use.
- d) It provides an indigenous fireproofing system due to its noncombustible construction characteristics.
- e) Durable system for buildings, such as barracks, which are subject to constant use.
- f) Minimum maintenance even with considerable abuse.

The anticipated tenure of usage far exceeds the twenty-five year requirements of all government buildings with low maintenance costs during its life span. All interior and exterior masonry walls were left exposed with a paint finish.

Barracks, Naval Amphibious Base, Coronado, Calif.



The P-005, Naval Amphibious Base, Coronado, California accommodates 1,050 enlisted personnel.

ROADWAY INN, SAN DIEGO, CALIFORNIA

In loadbearing structures, the logical and most economical design solution is to carry all wall loads directly to the ground, without parking under the building. This observation also applies to other types of high rise construction. Structural spacings of columns for parking is never well suited to the column spacings necessary, or desirable, for tower type structures.

Total cost of construction in a combined parking and hotel building, for example, will increase. Naturally, when parking is necessary for the project and the site is small, the mix of tower and underground parking result. The car is king, and all tower walls or column spacings must work to drive aisle spaces, parking widths and ramp locations: or somewhere between the 1st or 2nd floor and the basement, large spandrel girders and beams of steel or concrete, must be used to carry the loads from bearing walls above to widely spaced columns below.

For example, the San Diego Roadway Inn was constructed on an approximately 200 foot square site, over a parking garage and an open first floor that contained lobby, restaurant and other public space. The fact that the garage was placed under the building, doubled the garage cost but provided the only parking solution. The concrete tower piers are spaced on a three car module of 27'-4" that is equal to the two room modules above. They support five stories of block bearing walls (80,000 units), from the 2nd through 6th floors, by extending from the basement to the underside of the 2nd floor slab.

At this point, concrete beams and slabs over the piers cantilever seven feet from each pier on two sides. Tower floors and roof, as well as all parking garage construction, were poured-in-place concrete due to the tight site. No real efficiencies resulted due to all the necessary forming. The only economies resulted from the use of masonry.

TOWN & COUNTRY HOTEL, SAN DIEGO, CALIFORNIA

The ten story, 324 room tower is the largest single concrete masonry building ever constructed in California. Each floor is over 20,000 square feet in area. The use of the pick-up floor and roof slab system is identical to the Hanalei except for the special balcony edge treatment.

The following points should be considered when designing for this pick-up type of slab construction:

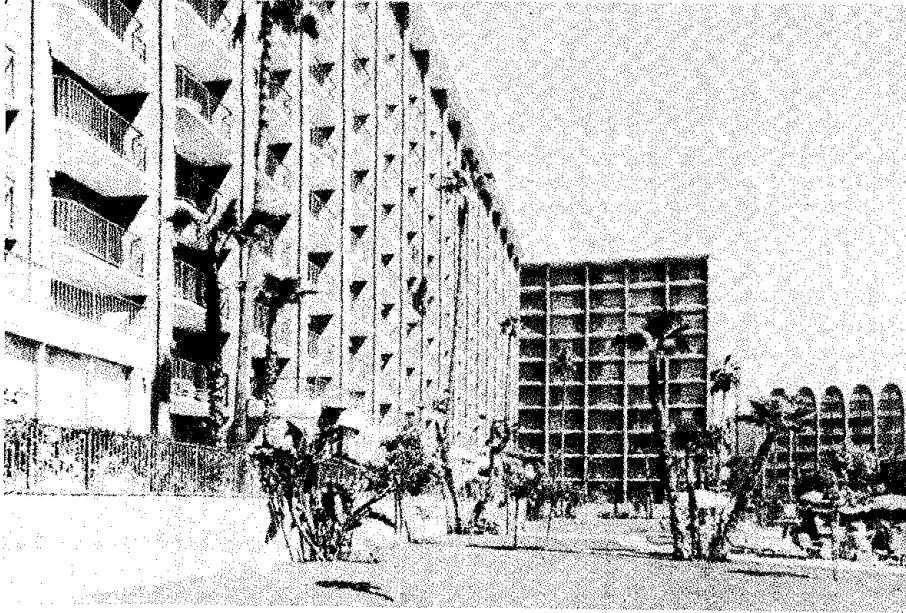
- 1) Sufficient spaces for casting beds.
- 2) Sufficient areas and access to the building for erection of slabs.
- 3) Repetition of units so that economical precasting of units can be made.
- 4) Availability of handling equipment.
- 5) Simple connections.
- 6) Sufficient slab thickness to control deflections.
- 7) Supervision, inspection and testing of all structural materials.

The tower contains 234,000 concrete blocks, mostly 8 x 8 x 16, but including several special shapes and textures manufactured for the first time. The 8 inch high combed face block used on the exterior and exposed on one wall in each hotel room was manufactured special for the project.

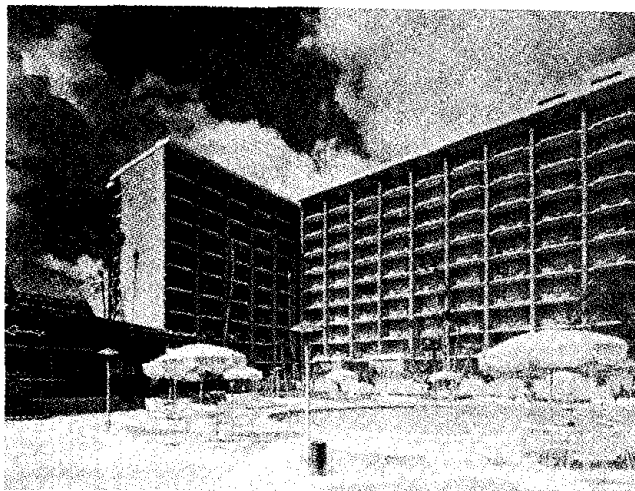
The block is now offered as a standard by Hazard Products. The combed face masonry units were designed to give the building a rich texture and contrast effectively with the smooth white finish of the precast concrete roof fascia and clean cut lines of the balcony slabs. A special hexagonal shaped concrete block (actually more shapes like a keyhole), is used as an architectural design element at the end of all balcony walls. It is also used for closely spaced columns at open walkways and at stair towers to provide both a visual and safety barrier for guests.

The building is one unit deep with an exterior corridor which gave rise to problems of height to width ratio, and in turn created critical stresses in the loadbearing block walls. The use of these decorative hexagonal pilaster and columns also allowed the structural engineer to increase the amount of grouted steel incorporated into the structure without bulky and unattractive square or rectangular projections within the bearing walls. When the hotel won a Portland Cement Association Design Award in 1970, it was the only privately funded project out of 10 winners. It also was the least expensive.

TOWN AND COUNTRY HOTEL - SAN DIEGO, CALIFORNIA



TOWN AND COUNTRY HOTEL, San Diego.



The 10-story Town & Country Hotel viewed from the swimming pool area.

RAMADA INN CONVENTION CENTER HOTEL, DALLAS, TEXAS

The hotel is located in downtown Dallas, just 223 steps away from the Convention Center. The most dramatic part of the facility is the roof-top restaurant, club and meeting rooms for which the entire skyline of downtown Dallas provides the setting.

The structural system consists of reinforced concrete block loadbearing walls and concrete floor slabs poured in place using flying forms.

Comparing earthquake (seismic) design requirements to those found in other parts of the country where wind governs, I can best illustrate the differences by comparing the masonry requirements we had in the Ramada Inn, to those of the west coast. In Texas, as in most of the country, high stress block units are not required. Grade A, standard 8 inch lightweight concrete piasler block normally produced in Dallas carry the loads for 12 stories. These average 2000 psi on the net section. In California these units could be used to 5 stories only. However, preliminary tests of prisms and prism tests as the building progressed were made for quality control purposes. Continuous special inspection and individual tests of 2000 psi grout, mortar and the block, were also made in accordance with the Dallas Code (1968 UBC).

Only part of the reduced requirements for higher stresses can be attributed to building shape; the rest by lighter loads due to wind. If one compares floor plans of the Town & Country and the Convention Center Ramada Inn, it can be seen that the Ramada Inn has a modified square plan, with rooms on each side of a central core and that the Ramada has three times the building depth in plan than the one room wide Town & Country. This produces a considerable amount of walls that serve to brace the building against the wind. Hotel room end walls of the Ramada are completely glass enclosed, which is quite a daring trick in California, although this type of plan is most conducive to this openness.

Other major differences in this and our other Texas projects are the exterior treatment, due to weather conditions, and the requirements for slight modification of normal Texas units to accommodate the reinforcing steel.

The standard 8 x 8 x 16 unit manufactured in California is even different; it is a square edge closed end one with two cells. This block has been used for years in California, rather than one with a slight recess on the ends (called Engineered Block), due to the steel and grouting required for seismic considerations. Also, Engineered Block cells do not line up vertically thus making it difficult to grout. To assume proper vertical joints and grouting continually, we used standard pilaster blocks in Dallas at no additional costs.

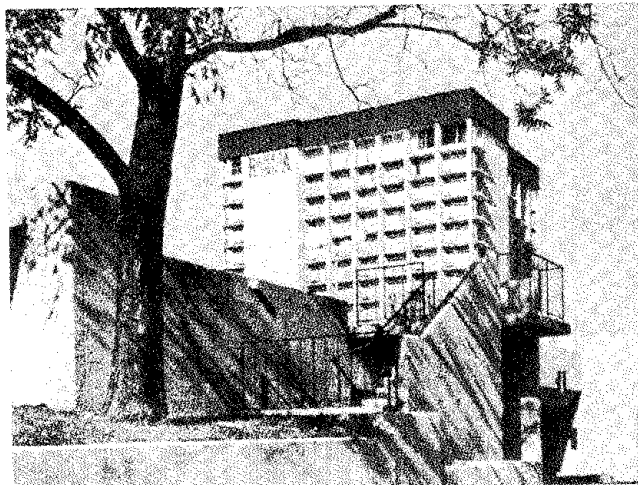
Other modifications were to have $1\frac{1}{2}$ inch depressions at the top of cells and ends to receive horizontal steel. We also have open end blocks (1 end open), double open end (H-block) and sometimes use U-blocks for exterior corners, in standard and bond beam shapes, developed so the mason can just slip the block around the vertical steel. In California these are all standard shapes. In Texas some of the units were manufactured for the job and others saw cut on the job by the mason. Holes for electrical outlets are either saw cut on the job or manufacturers make electrical units with blockouts to receive J-boxes. Where 3 hour walls are required, a thicker fact shell was manufactured.

To make it clear to the mason and block manufacturer, we provided isometrics of the block on the structural drawings as well as specified the shapes and standards for manufacture in order to make construction easier.

After much discussion with masons, manufacturers and observation of local projects, it was decided to have all exterior concrete block walls veneered with face brick as they are laid up, to act as waterproofing, decoration and added insulation. In Southern California and Hawaii we use a single wall of 8 inch thick concrete block exposed at exterior and interior sides in most projects due to the mild climate. Southern California has about 70% less rain than Dallas or Fort Worth, and then, only during one three month period.

The true fact is that when comparing California construction we have been talking about a structural system, that had to overcome the very high stresses that make up the seismic provisions of building codes and have been succeeding economically, whereas the system is actually more economically suited to other areas of the country.

Ramada Inn Convention Center Hotel, Dallas, Texas



Reinforced concrete block loadbearing walls and concrete floor slabs provide the structural system for the Ramada Inn Convention Center Hotel.

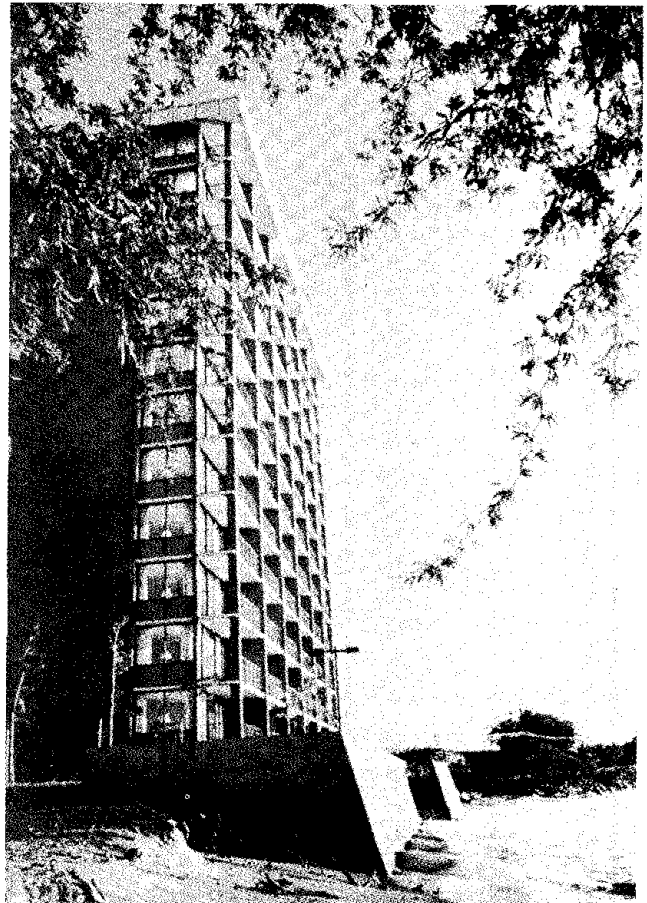
KAHANA BEACH RESORT CONDOMINIUMS, MAUI, HAWAII

Located on the west coast of the scenic island of Maui, Hawaii, this 12-story condominium features 72 studio units as well as 12 one bedroom units, all with balconies affording breathtaking views of the Pacific Ocean and the beautiful Hawaiian scenery.

The loadbearing concrete block walls are combed face high-stress units. Basic wall reinforcing is closely related to California construction. Few special shapes were manufactured due to the limited capacity of the local Maui block plant. However, the mason (Ken Suda) proved most resourceful on this first loadbearing project in the Islands.

Due to the extremely tight site all floors were cast-in-place concrete using standard forming systems. Since the allowable building area was controlled by the site area a double stair system was incorporated into the single stair tower in order to conserve valuable space and contribute to construction cost savings.

Kahana Beach Resort Condominiums, Maui, Hawaii



The first high-rise loadbearing structure in Hawaii, the Kahana Beach Condominiums, Maui.

FORT WORTH, TEXAS, HILTON INN

Downtown Fort Worth, Texas is the site of the 12-story convention-oriented Hilton Inn. The 2 acre private redevelopment project is just one block from the Tarrant County Convention Center and overlooking the Fort Worth Water Garden.

The project features a 12-story brick-faced loadbearing concrete masonry hotel tower with 275 guest rooms. Attached is a 2-story masonry and steel frame dining and convention facility which include the main hotel lobby, specialty shops, food and beverage facilities, and two story skylite atrium.

Although the building tower shape is quite different, the basic Texas system developed by the Convention Center Ramada Inn construction was followed. The basic masonry unit used was 8 x 8 x 16 "pilaster block" manufactured by Trinity Division, General Portland Cement Company of Dallas. Special shapes for the project were also manufactured by Trinity. Floors were cast-in-place using two sets of flying forms to maintain the floor a week construction schedule. Quality control was also maintained by bi-weekly thereafter above the 6th floor where wind and bearing stresses were lighter. The concrete block structure was veneered with denton (Texas) autumn gold blend brick, manufactured by Acme Brick Company, at the building exterior and interior. Mortar was made using natural warm tone cement found in the area. The brick facing added beauty and waterproofing.



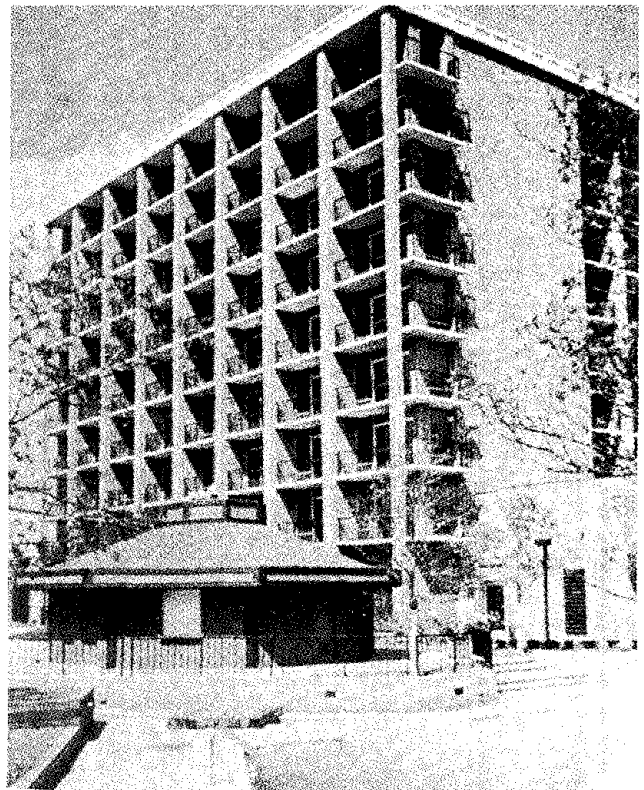
The Fort Worth Hilton complex which includes a 2-story dining and convention facility.

AUSTIN, TEXAS, HILTON INN

The project attempts to bring back the historic charm of Austin at the turn of the century, and features decor reminiscent of Austin's heritage and old fashioned hospitality. This was accomplished by the extensive use of antique modular clay brick veneer manufactured in Mineral Wells, Texas, as the major exposed material of the 9 story tower.

The tower plan and construction is similar to the Ramada Inn in Dallas, except for the following:

- 1) The contractor chose to use a conventional poured in place concrete floor system, using four pours per floor, since this method was as fast as flying forms due to the lower tower height, and its open courtyard within. Concrete and other materials were lifted in place by a truck crane.
- 2) The tower floor plan is rectangular with recessed balconies except at end units, rather than pin wheeled like the Ramada. The 22 rooms surround a central core containing stairs, services, elevators and a 3-story open atrium for each group of three floors. The elevator lobby extends under the atrium on the 1st, 4th and 7th floors while the upper 2 floors bridge the opening and one wall enhanced with historic artifacts extend 3-stories to an artificial skylite. The tower was constructed a floor each week and a half and was completed prior to delivery of steel which ordered for the long span meeting room space, prior to start of masonry construction.



The Highland Mall Hilton Inn, Austin, Texas.

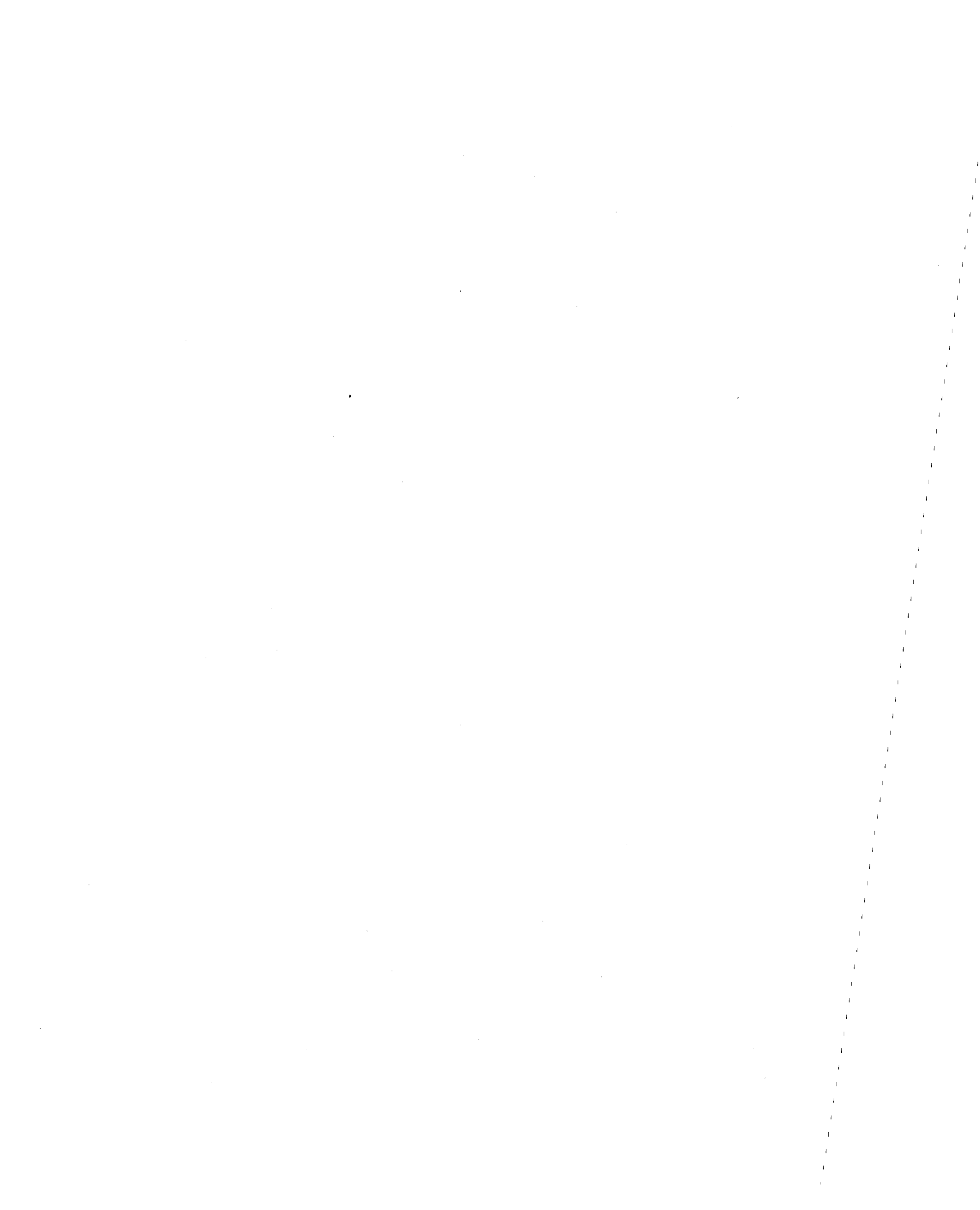
CONCLUSION

This is what each of these loadbearing masonry projects have in common:

Based upon an average floor area of 10 to 12,000 square feet, about 90% of the building walls and floors were erected without scaffolding more than 4 feet high or minimum shoring during each 5 to 6 work day period.

No other structural system can match this accomplishment! The actual appearance during construction was of buildings being assembled or manufactured in place rather than merely constructed. Most savings of time were directly related to the mason and his construction. Electrical conduits rose vertically with the walls. As each floor is placed, it serves as an instant work platform for all trades without down time for work stoppage. With this team work effort the "on and off" problem is eliminated, contractors profits increase and owners can occupy the buildings sooner. Each construction step was programmed in advance by the general contractor using controlled scheduling methods with the building team being lead by the general contractor and the mason contractor. When a trade starts on this type of project, it works steadily until its work is finished. Efficiency increases as the building moves to higher floors thus contributing to economy of construction.

After observing almost 100 stories of construction, refining our methods with practical experience, contractors suggestions, analyzing the production costs and efficiencies, as well as considering Owner's requirements we have concluded that "Modern Masonry" is a real breakthrough for construction of most type of buildings in the four to seventeen story height range. As lumber prices continue to rise, we also could include low rise structures if they have near to 80,000 square feet of total floor area.



A NONFERROUS REINFORCED CONCRETE
MASONRY STRUCTURE

Allan W. Flandro*

ABSTRACT: An investigation into the use of nonferrous alternate materials in lieu of conventional steel reinforcing bars in structural concrete masonry walls.

Materials studied were aluminum, copper, and fiber glass-resin rods.

Parameters considered were strengths, coefficients of expansion, resistances to alkalinity, availabilities, bonding characteristics, and costs.

Fiber glass-resin rods were selected as meeting all parameters satisfactorily and most parameters excellently. Adequate bonding to concrete was deemed questionable but placing a light sand upon the rod during fabrication while the resin is still wet was accepted to be an excellent method of producing a good bonding characteristic.

It was concluded that the use of fiber glass-resin rods will provide adequate reinforcing in concrete masonry walls at reasonable cost.

* Executive Secretary, Concrete Manufacturers Association of Utah, 2155 Regent Street #10, Salt Lake City, Utah 84115.

A NONFERROUS REINFORCED CONCRETE
MASONRY STRUCTURE

Introduction

The Hill Air Force Base near Ogden, Utah, has as its prime function the maintenance and support of the F-4 and F-16 fighter planes. In accomplishing this mission one of its responsibilities is to rebuild and recalibrate compasses. The engineering division at the base now plans to construct a single story building for this specific purpose and wants to have it built without any ferrous metal being used, an understandable requirement. All buildings at this base are designed under the supervision of the Sacramento District Corps of Engineers office which has a severe reinforcement requirement to meet possible wind and seismic stresses.

Definition of the Problem

The problem, then, was to find a satisfactory alternative to conventional steel reinforcement which would be nonferrous.

Analysis of the Problem

Early in the planning it was elected to use concrete masonry for the exterior and some interior walls, rising directly off the footings which will be placed 30 inches below grade so as to be unaffected by the frost. The roof is to be anchored to the bond beam at the top of the exterior walls and constructed of plywood sheathing on wooden trusses, all fastened together with nonferrous nails, either copper or aluminum.

Heating of the structure will be accomplished by forcing hot air from a remote heat source through plastic pipes under the concrete floor on grade to plastic heat registers. All electrical service will be provided with copper or aluminum wire to plastic fixtures. Such water as will be required will be piped through plastic and copper to porcelain or plastic fixtures and waste will be removed via plastic or clay pipe.

In reviewing the material requirements one sees that nearly all items, though not necessarily usual or common, are available at general building materials suppliers. The one item not falling in this category is an alternate for reinforcing steel and this was the problem presented to us by the in-house architect at Hill Air Force Base.

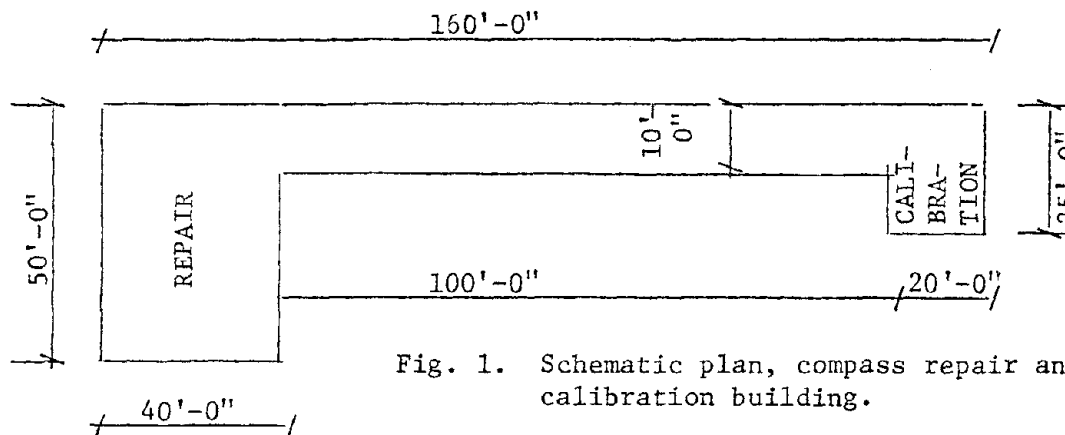


Fig. 1. Schematic plan, compass repair and calibration building.

A study was made of copper, aluminum, and fiber glass-resin rods or wire. Table 1 lists the physical characteristics and cost of each as well as those of steel for comparison. Note that aluminum has a high coefficient of expansion compared to that of concrete which is 5.5×10^{-6} in./in. Also the stock lengths of 12' would result in excessive waste and increased labor costs. Copper has a rather high coefficient of expansion, a "poor" rating of resistance to alkalinity, a high cost related to strength, and, as aluminum, comes in stock 12' lengths.

Fiber glass-resin rods present an interesting alternative. The coefficient of expansion at 3.5×10^{-6} in./in., though less than concrete, is close enough that no significant stresses should be produced in this structure due to temperature changes. Its cost when related to strength is about 1.6 times that of steel, it has a "fair" rating of resistance to alkalinity, and is furnished in continuous rolls.

All of these three alternates, being fabricated with a smooth surface, probably will have a poor bond with concrete. In the case of the fiber glass-resin rod two methods are suggested which should provide adequate bonding. First, the rods could be coated at the factory or at the construction site with polyester resin and while still wet have a thin layer of fine sand sprinkled on. The manufacturer advises that this procedure can be done at the factory at a very nominal cost. The extra coating of resin and sand would provide additional protection for the fibers against alkali attack. The second method would be to wind fiber glass roving around the rods at all intersections of the reinforcing and then swab the roving with polyester resin.

The first method would provide a more continuous type of anchorage similar to the conventional deformations on

Table 1
Physical Characteristics of
Various Materials

ITEM	DIA.	TENSILE STRENGTH in ksi		YIELD POINT	COEFFICIENT OF EXPANSION in./in.	RESISTANCE TO ALKALINITY	COST/FOOT		STOCK LENGTHS
		ULTIMATE					MATERIAL ONLY		
Reinforcing steel bars	1/2"	70	40	40	6.5×10^{-6}	Good	10¢	20, 40', 60'	
	3/4"	70	40	40	6.5×10^{-6}	Good	22¢	20, 40', 60'	
Aluminum rods 6061-T6	1/4"	42	35	35	13.1×10^{-6}	Good	10¢	12'	
	1/2"	42	35	35	13.1×10^{-6}	Good	27¢	12'	
Copper rods alloy 110	1/4"	48	40	40	9.8×10^{-6}	Poor	26¢	12'	
	1/2"	48	40	40	9.8×10^{-6}	Poor	85¢	12'	
Fiber glass- resin rods	1/4"	128	128	128	3.5×10^{-6}	Fair	10¢	In con- tinu- ous coils	
	3/8"	128	128	128	3.5×10^{-6}	Fair	16¢		
70% glass fibers	17/32"	128	128	128	3.5×10^{-6}	Fair	32¢		
	9/16"	128	128	128	3.5×10^{-6}	Fair	35¢		

reinforcing bars and would probably be less expensive. The second would provide a spot or local bond. Since the rods would have to be held in place and steel tie wire would not be allowed it may be that both methods would be used which should provide excellent bond.

Another problem is the alkalinity rating of "fair" for fiber glass-resin rods. The Owens-Corning authorities state that AR (alkali-resistant) fibers should be used, and a resin-rich surface be specified. If these two restrictions are followed no alkalinity problem should result. Those who are acquainted with the concrete masonry industry know that fiber glass fibers are used in concrete masonry surface bonding mixes that place the fibers in immediate contact with the alkalis of cement and lime, and when AR fibers are used no deleterious effect is experienced.

Some significant advantages of using fiber glass-resin over copper or aluminum are:

1. Its ultimate tensile strength is far in excess of either copper or aluminum and even steel, and its yield point strength is over three times that of any of the three because it is virtually the same as its ultimate strength.
2. It may be shipped in coils thus reducing splicing.
3. It weighs only about one-fourth as much as steel, reducing shipping costs and making it easy to handle.
4. It is more easily cut to length with a hacksaw or bolt cutter than steel.

In view of the above, fiber glass-resin rods were considered most advantageous and selected for further analysis. The structural strength integrity of fiber glass resin rods, when used as reinforcement in concrete, is confirmed in the experimental study made by Nawy, Neuwerth, and Phillips, "Behavior of Fiber Glass Reinforced Concrete Beams." They tested ten fiber glass reinforced beams and five steel reinforced beams. The report shows that the yield point is very close to the ultimate strength of fiber glass, the concrete failed before the fiber glass ruptured, the bond between concrete and fiber glass was not a cause of failure, and the product performed well in every respect. Although at ultimate loadings the deflections of fiber glass reinforced beams were three times as great as the comparable steel reinforced beams, at working loadings the deflections of steel reinforced and fiber glass reinforced beams were quite favorable, and upon release of the load all cracks were closed.

Full reinforcement design, as specified by the Sacramento District Corps of Engineers office would require two No. 4 steel bars running continuously in the footing, two No. 4 steel bars running continuously in each of three bond beams, and one No. 6 steel bar placed vertically from the footing to the top bond beam at 48" on centers. Also the concrete slab on grade would be reinforced with a 6" x 6" #10/#10 mesh for temperature stresses.

Calculation of the amount of fiber glass-resin rod replacement needed was made on the basis of comparative ultimate strengths. This is a more conservative approach than using yield strengths, and since fiber glass-resin rods are not commonly used as concrete reinforcement no working strength criteria are available.

Table 2

Comparison of Strengths

	DIAMETER in.	AREA sq. in.	ULTIMATE STRENGTH p.s.i.	CAPACITY lbs.
Conventional reinforcing steel bars:				
#4	.50	.196	70,000	13,720
#6	.75	.442	70,000	30,940
#10 wire		.014	70,000	980
Fiber glass-resin rods:				
1/4"	.250	.049	128,000	6,272
3/8"	.375	.110	128,000	14,137
17/32"	.531	.222	128,000	28,416
9/16"	.563	.249	128,000	31,808

Four standard sizes of fiber glass-resin rods were selected for this study-- $1/4"$, $3/8"$, $17/32"$, and $9/16"$. A comparison of their strengths and those of steel bars is shown in Table 2. It is quickly apparent that #4 steel bars may be replaced by $3/8"$ fiber glass-resin rods; #6 bars by $9/16"$ rods; and #10 wire by $1/4"$ rods at a ratio of 6 to 1. In other words, two $3/8"$ rods would be required in the footings running continuously, two $3/8"$ rods would be placed in each bond beam running continuously, and a $9/16"$ rod would run vertically from the footing to the top beam on 48" centers.

One-fourth-inch rods would be placed in the floor slab at 36" on center running both ways to provide temperature reinforcement. To make a good connection the rods should be extended beyond the perimeter of the floor into the masonry wall.

The arrangements of steel bar and fiber glass-resin reinforcement are shown in Figure 2. The fiber glass-resin reinforcement provides 3% greater strength than the steel based upon ultimate strength figures. If yield point strengths had been used the fiber glass-resin reinforcement would provide 78% more strength.

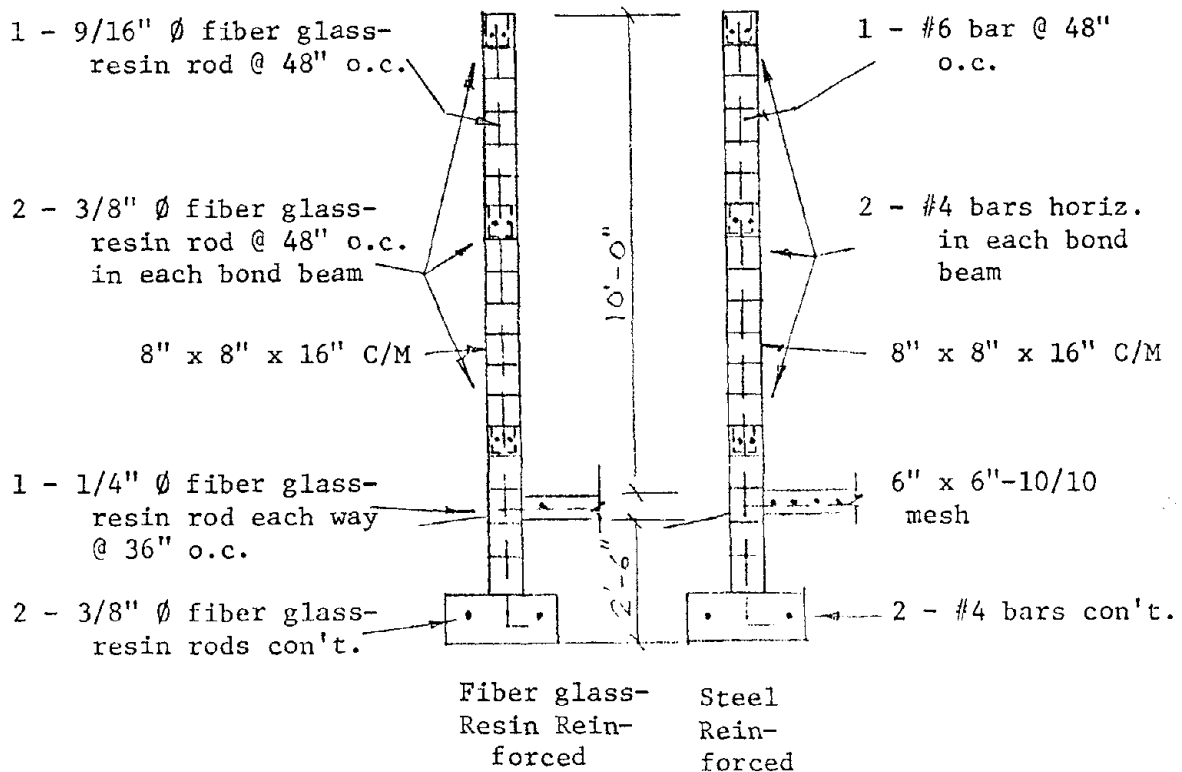


Fig. 2. Typical wall sections.

The entire fiber glass-resin reinforcement requirement could be shipped from the supplier to the job site in three coils, one for each size of rod, of about 8' in diameter and weighing a total of approximately 700 pounds. At \$8.19/cwt. the transportation cost would be \$56.00

A comparative cost of the two systems is shown below; materials only:

Cost of Steel Reinforcement Materials:

Footing	900' #4 bar @ 10¢	\$ 90
Bond beams	2700' #4 bar @ 10¢	270
Vertical bar	1460' #6 bar @ 22¢	321
Floor	3500 sq. ft. 6" x 6" #10/#10 @ 7¢	245
	Total, Delivered Locally	\$ 926

Cost of Fiber Glass-Resin Reinforcement Materials:

Footing	900' 3/8" \emptyset rod @ 16¢	\$ 144
Bond beams	2700' 3/8" \emptyset rod @ 16¢	432
Vertical rods	1460' 9/16" rod @ 35¢	511
Floor	2425' 1/4" rod @ 10¢	243
	Freight	56
	Total	\$1,386

Though the cost of fiber glass-resin reinforcement is 50% greater than that of steel it must be remembered that the comparison is based upon the ultimate strengths of the two materials, a very conservative approach. More familiarity with the use of this material in concrete may result in establishing a working strength criteria which very likely would be more favorable to it.

Since it is supplied in coils and being comparatively light in weight it should be easily handled by the workmen. Also the amount of splicing should be much less than when steel is used, which should result in a cost saving. However, even the 50% increase in material cost is not significant in a \$200,000 building when one considers the unique goal that has been attained.

Conclusion

The analysis is completely academic at the time of this writing inasmuch as no construction has been accomplished nor even final drawings completed. However, one can conclude that nonferrous reinforcement of a building can be accomplished with the use of fiber glass-resin rods which are available in the general marketplace. Further, the extra cost of using this material in lieu of steel is not a significant burden to the total building cost. Since the use of the fiber glass-resin rods in this function is an unusual concept, special care and attention should be taken to assure that proper bond and anchorage are obtained.

APPENDIX I - REFERENCES

Aluminum Association, "Aluminum Construction Manual."

Kaiser Aluminum Co., Manual No. D-3.

Nawy, Edward G., Neuwerth, Gary E., and Phillips, Charles J.,
"Behavior of Fiber Glass Reinforced Concrete Beams," Pro-
ceedings of the American Society of Civil Engineers, September
1971.

Owens-Corning Fiberglas Co., "An Introduction to Fiberglas-Reinforced
Plastics/Composites," No. 1-PL-6305.

MATERIAL SUPPLIER
SOURCES OF INFORMATION

Affiliated Metals, Inc.
2890 South 300 West
Salt Lake City, Utah 84115

Fiberchem, Inc.
3000 South 900 West
Salt Lake City, Utah 84119

Owens-Corning Fiberglas Corp.
840 West 2600 South
Salt Lake City, Utah 84119

The Polytrusion Co., Inc.
3050 Daimler St.
Santa Ana, California 92705

RELATIVE ECONOMIC PERFORMANCE OF BRICK MASONRY AND GLASS OFFICE BUILDINGS

By Grimm, Clayford T.

ABSTRACT: The Texas State Building Materials and Systems Testing Laboratory conducted a real estate investment analysis on a hypothetical, typical, high-rise office building to be occupied in the summer of 1975 in Dallas, Texas to determine the rate of return on the total investment as affected by ten alternative facade material combinations. The facades included two types of fenestration in three ratios of window area to gross facade area and three opaque wall materials.

In this typical office building, a comparison between a facade of 70% insulating reflective plate glass windows with 30% glass spandrels and a facade of 80% conventional brick masonry with 20% tinted plate glass windows indicates the following effects on the real estate investment. Use of the all-glass facade:

1. requires more than 9% higher initial building cost,
2. requires more than 8% higher total investment cost,
3. requires nearly 34% more cash equity,
4. requires more than 4% higher operating cost,
5. reduces the maximum internal rate of return on the investment by more than 22%, and
6. has no effect on rental income.

The principal cause of these relationships is the higher initial cost of the glass wall and the increased development and operating costs attributable to it, combined with no benefit of higher income. The report concludes that increasing fenestration above 20% of the facade area typically has no redeeming economic quality and that, if in any case increasing fenestration above 20% of the facade has any merit at all, the cost of achieving any such benefit should be made explicit.

RELATIVE ECONOMIC PERFORMANCE OF
BRICK MASONRY AND GLASS OFFICE BUILDINGS

By Clayford T. Grimm, P.E.¹

THE LABORATORY

The Texas State Building Materials and Systems Testing Laboratory (BMSTL) is an inter-university testing and evaluation facility created by an act of the 1971 session of the Texas Legislature to assist local governments, the construction industry, and the public through the evaluation of materials and methods in the building industry. The Laboratory is an operating Program of the Texas Department of Community Affairs and is managed by a Technical Testing and Evaluation Council, which consists of one representative appointed by the president of each of the following participating universities:

Lamar University	Texas Tech University
Prairie View A&M College	University of Houston
Texas A&I University	University of Texas at
Texas A&M University	Arlington
University of Texas at	University of Texas at
El Paso	Austin

At the request of the Acme Brick Co., the Texas Department of Community Affairs issued a report titled, Relative Thermal and Economic Performance of Masonry and Glass Building Enclosures, dated March 28, 1975. The report was unanimously approved by the Council governing the Laboratory. The report is based on research conducted by the Center for Building Research in The University of Texas at Austin. The report was written by Clayford T. Grimm, P.E., Associate Director of the Center; Dr. Jerold W. Jones, Assistant Professor of Mechanical Engineering; and Dr. Stephen A. Pyhrr, Assistant Professor of Real Estate and Finance.

This article summarizes that government report, copies of which are available from the Acme Brick Co., P.O. Box 425, Fort Worth, TX 76101.

OFFICE BUILDING DESCRIPTION

The report examined the economic performance of a hypothetical office building to be completed in Dallas, Texas during the summer of

¹Lecturer in Architectural Engineering, University of Texas at Austin, Austin, Texas.

1975. The effect of ten different exterior wall types on the internal rate of return on investment cost and the annual rate of return on equity was examined. Only three of the facades are discussed in this summary. They are listed in Table 1 and described in Section 4 of this summary.

The office building is rectangular, measuring 205 ft in length and 102 ft 6 in. in width with the major axis on an east-west orientation. It is a concrete-framed building having 15 stories above grade and one story below grade. Floor-to-floor height is 13 ft. The gross floor area is 336,200 ft² with a rentable floor area of 289,132 ft². There are five air-conditioning zones on each floor, i.e. one for each orientation and a core zone. The gross facade area is 119,925 ft².

The initial construction cost of the building, having a facade of 60% brick-block cavity walls and 40% tinted plate glass, is \$27.00 per gross ft² of building or \$9,077,400. Depreciable development costs for this building were estimated at 17% of building cost, and non-depreciable (i.e. expensed) development costs were estimated at 10% of building costs, providing a total development cost of \$2,450,898. Land for all buildings was assumed to cost \$1,452,384.

It was estimated that the average annual rental rate would be \$6.75 per ft² of rented area in each of the ten buildings. The effect of window area on rental rates is discussed in Section 6 of this summary. The first-year operating cost of the building with 40% fenestration (facade No. 3) was determined at 40% of the first-year gross effective income or \$749,430. The difference was determined between the first-year operating cost for that building and the same structure with the alternative facades. Operating cost differentials included the cost of operating the air-conditioning plant, cleaning windows and blinds, real estate taxes, glass-breakage insurance and interior wall painting as affected by each facade.

FACADE DESCRIPTION AND INITIAL COSTS

All glazing is in an inoperative anodized aluminum frame with sealant. Three types of glass considered were: (1) 0.25-in. polished tinted plate, (2) one-in. thick insulating glass having one light of 0.25-in. clear plate and one light of 0.25-in. tinted reflective plate, and (3) 0.25-in. standard color spandrel glass. Insulation behind spandrel glass was included. The estimated cost of windows with tinted glass includes stock venetian blinds having 2-in. steel slats. Such blinds are not included for windows having insulating reflective glass.

Conventional masonry construction was a 10-in. cavity wall, consisting of cleaned, standard, modular, face brick, 2-in. vermiculite insulation, and 4-in. x 8-in. x 16-in. lightweight concrete masonry units, metal ties, flashing, weepholes, 5/8-in. gypsum plaster, primed and painted two coats.

All construction costs were based on anticipated costs in Dallas, Texas during the spring of 1975, and include contractors' profit and overhead. The cost of masonry and windows were prorated in accordance with their relative proportions of the gross facade area to yield the unit facade costs shown in Table 2.

Initial cost estimates for facade No. 2 (70% insulating reflective glass and 30% spandrel glass) ranged from \$14.05 to \$15.65 per gross ft² of facade, exclusive of blinds. The average of four estimates was \$14.12, which figure was used in the analysis as shown in Table 2.

Initial cost estimates for tinted glass in anodized aluminum frame windows in facade Nos. 3 and 7 ranged from \$8.57 to \$10.51 per ft² of window. Of four estimates, the average was \$9.18. The average of the three lower prices was \$8.73 to which was added \$0.71 per ft² of window for venetian shades to yield \$9.44.

Initial cost estimates for the conventional masonry cavity wall ranged from \$5.27 to \$8.99 per ft² of wall. The average of seven estimates was \$6.63, which was used to estimate the cost of facade Nos. 3 and 7.

The weight of exterior walls can affect structural framing and foundation costs. Based on the wall weights shown in Table 1, item 1.5, foundation and framing cost differentials were computed for each facade as shown in Table 2, item 2.2.

In the absence of any documented evidence that speed of exterior wall erection affects building completion time, no consideration was given to speed of construction associated with the facade types.

Table 2 summarizes the initial costs for the same office building with 70%, 40% and 20% fenestration, i.e. facades 2, 3 and 7 respectively.

ENERGY REQUIREMENTS AND COSTS

The load and energy requirements for each of the buildings were determined by utilizing a computer-based building model developed by the National Bureau of Standards (NBS), using procedures recommended by the American Society for Heating, Refrigerating and Air Conditioning Engineers (ASHRAE) Task Group on Energy Requirements for Heating and Cooling in Buildings. Heating and cooling design loads were calculated for each case, and the annual energy requirements were then estimated based on Dallas weather records.

The lighting loads, ventilation rates and infiltration rates were held constant for all cases. The values used for these inputs were the same as those developed for an NBS study of similar-type general-use office space. Building load parameters such as lighting and ventilation were chosen on the basis of an energy-conservative design philosophy. This, coupled with the fact that the use of the NBS

computer simulation allows the HVAC equipment to be sized closely, results in both the initial cost and operating costs being somewhat lower than would usually be encountered with current design practice. Initial cost of the HVAC system for the building with 40% fenestration (facade No. 3) was assumed to be \$3.00 per gross ft² of floor area, while the first year HVAC operating cost was determined to be 13.3¢ per gross ft² of floor area for energy only exclusive of HVAC plant maintenance.

The HVAC plant capacity requirements for the building with alternative facades is shown in Table 2. Incremental changes in cooling plant capacity were priced at \$1,295 per ton. The incremental heating plant capacity requirement was priced at \$400 per therm of required plant capacity.

The operating cost of the cooling plant is priced at \$0.0134 per kilowatt-hr of electric energy requirement. The heating plant operating cost was priced at \$0.89 per 1000 ft³ of gas consumed.

The first-year annual energy cost for the 70%, 40% and 20% fenestrations on this building are shown in Table 3. The difference in first-year annual energy cost between the building with 70% fenestration and with 20% fenestration is enough to operate the HVAC system in the building having 20% fenestration for nearly six weeks. In other words, increasing fenestration from 20% tinted glass to 70% insulating reflective glass is equivalent to adding nearly six weeks of operation to the fuel cost each year.

OTHER OPERATING COSTS

First year building operating costs are summarized in Table 3.

Window and Blind Cleaning

The estimated cost of exterior and interior window-washing on the building having 20% fenestration was \$1,966. The cost of window-washing on the exterior and interior of the building having 100% glass exterior with 70% fenestration was estimated to be \$4,337. The cost of exterior and interior window washing on the building having 40% fenestration was estimated to be \$2,559.

In a typical clean environment, light transmission through glass is reduced 18% by dirt collection over a three-month period and 27% over six months. In Chicago, windows are typically washed monthly. However, in Los Angeles, quarterly washing is common. For the Dallas building, quarterly washing was assumed at an annual cost of \$7,864, \$10,236 and \$17,348 for the 20%, 40% and 70% fenestrations respectively.

The customary blind-cleaning service provides semiannual dusting and annual damp-cloth cleaning in place. The total annual blind-cleaning cost was estimated at \$24.22 per 1000 sq ft of shaded window

area. The average annual cost of blind cleaning with 20% and 40% fenestration was \$581 and \$1162 respectively. Interior venetian shades were not provided on windows having insulating reflective glass.

Real Estate Taxes

The nominal real estate tax rate (i.e. quotient of total annual tax bill divided by assessed value) in Dallas, Texas is 0.097. The ratio of assessed value to sales price is 0.169. The effective tax rate is 0.016393. The first-year real estate taxes were \$221,612, \$207,691 and \$204,987 for the building with 70%, 40% and 20% fenestration respectively.

Illumination Costs

A study was made of 166 offices in a typical multi-story multi-tenant office building in Austin, Texas to determine whether there is a reduction in artificial illumination as a function of fenestration. All lights were "on" in 164 or 98.8% of the offices. Apparently any natural illumination which may be available from time to time is used to augment the artificial illumination, not to replace it. This contention is supported by another case study. For these reasons, no differential illumination cost was applied to any of the facades in this report.

Fire Insurance

A study was made of a high-rise office building with a totally-reflective glass facade recently completed in Austin, Texas to determine the effect of the exterior facade on the fire-insurance rates on the building and its contents. Interviews were held with staff members in the rating section of the Texas Insurance Commission. The facade had no effect on the total insurance premium paid. In the absence of any documented evidence that insurance rates are affected by glass facades, no fire insurance cost differential was applied to the facades considered in this study.

Glass Breakage Insurance

Window breakage in New York City schools cost \$1.2 million in 1968. In Philadelphia schools in that year the cost was \$684,000 or \$2.28 per broken pane. Extended coverage insurance usually includes glass breakage due to windstorm, hail, explosion, riot, civil commotion, aircraft, vehicles, or smoke, but does not include accidents or vandalism. Although many building owners carry glass-breakage insurance, many are self-insured, in which case the cost of glass breakage should be considered a maintenance expenditure.

Glass insurance rates vary with time, location of building, location of window within the building, building occupancy, and glass type, thickness and size. An eight-story dormitory with stores at ground level located near The University of Texas at Austin has glass-

breakage insurance at an average annual cost of \$0.035 per ft² of glass. The annual rate on the glass windows on the first two floors is \$0.146 per ft², while the rate above the second floor is \$0.02 per ft² or about 1% of the glass-replacement cost.

An annual glass-breakage insurance rate of \$0.02 per ft² of glass is a conservatively low value for single-plate glass and about 25% higher for double-glazed windows in the upper floors of a high-rise office building.

Effect of Windows on Rental Rates

A survey was made in November 1974 by the Building Owners and Managers Association International of 81 office buildings in 43 cities, 37 in the U.S. and 6 in Canada, to determine the effect of fenestration on office rental rates. The age of all buildings was 10 years or less, and the average was 4.9 years. The buildings ranged in height from one to 60 stories, and the average height was 16.7 stories. The survey indicates that interior window shades are fully closed 27% of the time and partially closed 33% of the time. The windows are, therefore, less than 60% efficient as a see-through device.

In 78% of the buildings, rental rates were not related to the amount of glass in the facade. On the basis of these data, no differential rental income was attributed to the facades considered herein.

Effect of Wall Thickness on Rental Income

When lot area is larger than largest floor area and the building walls are not erected on the building restriction line, all of the floor area is provided which the real estate investment feasibility study indicates is economically justified, and the exterior walls are set outside that area. In this case wall thickness has no effect on amount of rented floor area. Thus, no consideration was given in this study to differential rental income as affected by wall thickness.

Wall Maintenance

The cost of interior wall painting was estimated at \$10.37 per 100 sq ft of wall surface area. Interior wall painting was estimated to occur at 3-year intervals. The first year annual interior painting of exterior opaque walls was, therefore, estimated at \$0.0346 per sq ft of wall. For the building having 40% fenestration (facade No. 3) this cost amounted to \$2,482. The first year annual interior painting of the exterior opaque walls for buildings with 20% fenestration was estimated at \$3,310. Other exterior wall maintenance and repair cost differentials, not mentioned above, were considered negligible.

REAL ESTATE INVESTMENT ANALYSIS

The technique of real estate investment analysis used to evaluate each of the buildings is fully described in Building Cost vs Operating Cost vs Rental Income, available from the Center for Building Research in the University of Texas at Austin. Input data on initial and operating costs were determined as described above. Input data on rental rates, rent loss, miscellaneous income, mortgage amount and terms, depreciation methods, income taxes, sales expense, and projected inflation rates for consumer prices, income, taxes, operating costs, building cost, development cost, land cost, and real estate value were determined by literature search and by in-depth interviews with Dallas real estate developers or property managers conducted during the fall of 1974. Projected inflation rates were based on price-change histories and expected changes in productivity, i.e. expected inflationary trends in rents, expenses and property value.

The rates of return for the building with three facades is shown in Table 4. Reducing glass area from 70% to 20% of the facade increases the maximum rate of return on equity from 8.8% to 12.6%, i.e. a 43% increase.

EVALUATION OF THE NEED FOR WINDOWS

Windows are sometimes thought to be psychologically necessary, but a literature search reveals no evidence to support that contention. A survey of office workers shows high preference for windows, but no factual basis to support a need for windows has been demonstrated. Considering the volume of research which has been done on the physical requirements for windows--daylight, glare, sound and heat transmission, ventilation, and infiltration--it is surprising to find virtually no evidence that visual contact with exterior is necessary or that the value received is justified by the cost.

A report on Effect of Windowless Classrooms on Elementary School Children by the University of Michigan indicates that windows are unnecessary in schools, prompting the use of windowless classrooms. Teachers with experience in windowless classrooms prefer them, and elementary school children with experience in both conventional and windowless classrooms show very little personal interest in whether their classrooms have windows or not. A study by the U.S. Public Health Service concludes that although windows should not be eliminated from long-term nursing areas of general hospitals, they serve no particular therapeutic purpose in diagnostic, treatment, intensive care, or nursing units. The Australian Commonwealth Experimental Building Station in a study of "Windows and the Indoor Environment," concludes that excessive (more than functionally necessary) use of glass can give rise to problems of heat, noise, and loss of privacy. Cooling systems cannot be economically contrived to provide comfort with any condition of glass-plus-sun in critical summer weather. It

is not just a matter of reducing the cooling load, which is important, but of avoiding uncomfortably hot solar-radiant areas next to glass. Glass should be avoided or minimized in the path of the sun's rays or the impact of solar energy should be absorbed on the outside of the building.

CONCLUSIONS

Table 5 summarizes the initial and operating costs attributable to windows and walls.

Insulating reflective glass is about 30% more expensive than tinted glass and nearly 85% more expensive than conventional brick masonry walls.

HVAC costs attributable to windows are 2.4 to 3.7 times greater than for masonry walls. The structural framing and foundation costs attributable to conventional masonry walls is about 11 times greater than for single glazed windows, but the cost difference is about \$1.00 per ft² of wall. Interior painting costs are higher for opaque walls.

The higher initial costs attributable to windows produces higher development costs, especially for construction financing and architectural fees.

The total investment cost in windows typically used in office buildings is about 70% greater than in conventional brick-block masonry cavity walls.

The higher the initial construction and development costs of a facade, the greater the equity requirement. Since the real estate resale value and rental income are not typically affected by the facade, the mortgage value of the property is unchanged, and the equity requirement is increased. Typically, a 50% increase in facade cost produces a 5% increase in office building cost and a 4.5% increase in investment cost. If the mortgage value is unchanged at 75% of original investment cost, the equity requirement increases by 18%.

Since rental rates and, therefore, mortgage values are typically not increased by greater window area, the increased investment costs associated with windows must be paid for entirely from increased equity. The annual rate of return on the incremental equity is typically zero, and the return on the entire investment is therefore reduced. This condition is further aggravated by the increased operating costs associated with windows, and therefore, reduced net spendable annual income.

The total annual operating cost attributable to tinted glass windows in this building is about 2.7 times greater than that attributable to the conventional brick-block cavity wall. First year annual operating costs attributable to the insulating reflective-glass

window are currently about 11% lower than that attributable to the tinted plate-glass window.

In the typical high-rise office building studied herein, the use of insulating reflective glass rather than tinted plate-glass in the facade is not economically justified. Higher initial construction cost, development cost, and real estate taxes associated with insulating reflective glass are not offset by reduced cost of the HVAC system and its operation.

In the case of this typical high-rise office building, increased facade window area with either of the two types of glass considered has the effects of increased development cost, increased construction cost, increased equity requirement, increased operating cost, and reduced return on investment.

TABLE 1. FACADE DESCRIPTION, PER CENT OF GROSS FACADE AREA

<u>Item No.</u>	<u>Facade Materials</u>	<u>Facade Number</u> (1)		
		<u>2</u>	<u>3</u>	<u>7</u>
1.1	Tinted plate glass, %	0	40	20
1.2	Insulating reflective plate glass, %	70	0	0
1.3	Spandrel glass, %	30	0	0
1.4	Masonry cavity wall, %	0	60	80
1.5	Facade weight, lb/ft ²	10.2	42	54

(1) Facade numbers are those used in the BMSTL Report, which includes data on ten facades, only three of which are shown here.

TABLE 2. INITIAL COSTS

Item No.	Cost Variable	Facade Number (1)		
		<u>2</u>	<u>3</u>	<u>7</u>
2.1	Facade, \$/ft ² of facade	14.12	7.76	7.19
2.1.1	Facade, \$	1,693,341	930,618	862,261
2.2	Foundation & framing, \$	145,220	208,780	232,765
2.3	HVAC, \$	1,020,350	1,008,600	915,150
2.3.1	HVAC Cooling capacity, tons/hr	590	580	510
2.3.2	HVAC Heating capacity, 10 ⁶ Btu/hr	4.4	4.7	4.0
2.4	Other building cost, \$	6,929,402	6,929,402	6,929,402
2.5	Building cost			
2.5.1	Total cost, \$	9,788,313	9,077,400	8,939,578
2.5.2	Relative bldg. cost	1.09	1.01	1.00
2.6	Development cost			
2.6.1	Depreciable dev. cost, \$	1,639,842	1,543,158	1,524,414
2.6.2	Non-depreciable dev. cost, \$	971,722	907,740	895,336
2.6.3	Total development cost, \$	2,611,564	2,450,898	2,419,750
2.6.4	Relative development cost	1.08	1.01	1.00
2.7	Total building & dev. cost, \$	12,399,877	11,528,298	11,359,328
2.8	Land	1,452,384	1,452,384	1,452,384
2.9	Total investment cost, \$	13,852,261	12,980,682	12,811,712
2.9.1	Rel. Inv. Cost	1.08	1.01	1.00
2.10	Mortgage, \$	9,735,510	9,735,510	9,735,510
2.11	Equity req., \$	4,116,751	3,245,172	3,076,202
2.12	Relative equity requirement	1.338	1.055	1.00

(1) Facade nos. are those used in the BMSTL report, which includes data on ten facades, only three of which are shown here.

TABLE 3. FIRST-YEAR OPERATING COST

<u>Item</u>	<u>Facade Number (1)</u>		
	<u>2</u>	<u>3</u>	<u>7</u>
3.1 HVAC plant operating cost, \$	45,060	44,700	40,614
3.2 Window cleaning, \$	17,348	10,236	7,864
3.3 Blind cleaning ⁽²⁾	0	1.162	581
3.4 Real estate taxes, \$	227,080	212,792	210,022
3.5 Glass breakage insurance, \$	2,819	959	480
3.6 Wall painting, \$	0	2,482	3,310
3.7 Other operating costs, \$	477,099	477,099	477,099
3.8 Total 1st-Yr operating costs, \$	769,406	749,430	739,970
3.9 Relative 1st-Yr operating cost, \$	1.039	1.013	1.00

(1) Facade nos. are those used in the BMSTL report, which includes data on ten facades, only three of which are shown here.

(2) Blinds not provided on insulating reflective glass windows but provided for tinted glass windows.

TABLE 4. RATE OF RETURN ON REAL ESTATE INVESTMENT

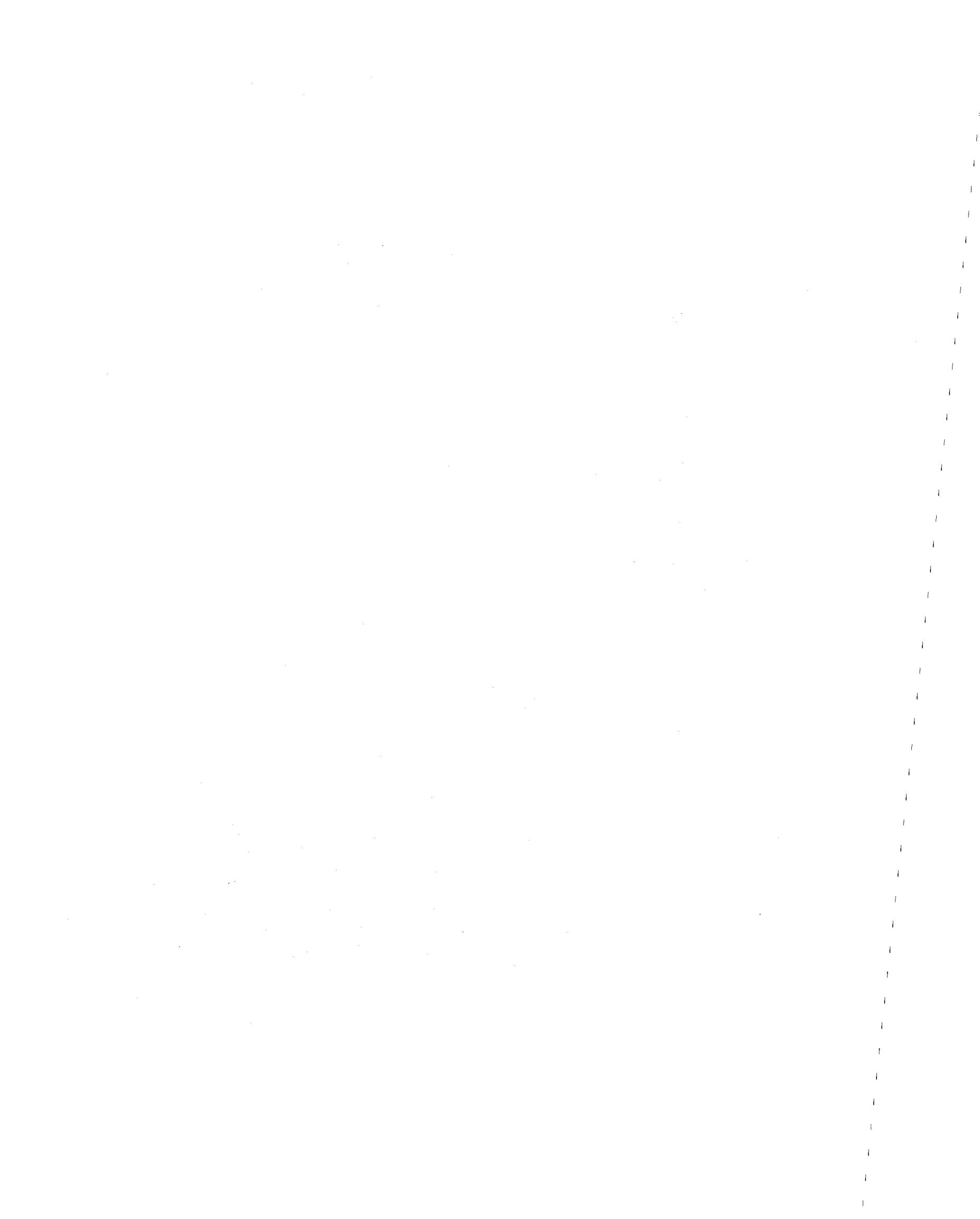
<u>Item No.</u>	<u>Rate of Return</u>	<u>Facade Number (1)</u>		
		<u>2</u>	<u>3</u>	<u>7</u>
4.1	<u>Max. internal rate of return on investment</u>			
4.1.1	Percent	12.6	15.4	16.2
4.1.2	Year	11	10	10
4.1.3	Relative	1.00	1.22	1.29
4.2	<u>Max. rate of return on equity including tax shelter</u>			
4.2.1	Percent	8.8	11.6	12.6
4.2.2	Year	20	20	19
4.2.3	Relative	1.00	1.32	1.43

(1) Facade nos. are those used in the BMSTL report, which includes data on ten facades, only three of which are shown here.

TABLE 5. RELATIVE INITIAL AND OPERATING COST ATTRIBUTABLE
TO WALLS, \$/FT² OF WALL

Item	Tinted Plate Glass Window Wall	Insulating Reflective Glass Window Wall	Conventional Brick-Block Cavity Wall
1.0 Initial Cost			
1.1 Wall Cost	9.44	12.14	6.63
1.2 HVAC	6.83	4.35	1.83
1.3 Frame and Foundation	0.10	0.20	1.10
1.4 Total Initial Cost	<u>16.37</u>	<u>16.69</u>	<u>9.56</u>
2.0 Development Cost (1)	4.42	4.51	2.58
3.0 Total Investment Cost	20.79	21.20	12.14
3.1 Relative Total Investment Cost	1.71	1.75	1.00
4.0 1st Year Operating Cost			
4.1 HVAC (2)	0.28	0.19	0.08
4.2 Window Cleaning	0.17	0.17	0.00
4.3 Blind Cleaning	0.02	0.00	0.00
4.4 Real Estate Taxes (3)	0.33	0.34	0.19
4.5 Glass Insurance	0.02	0.03	0.00
4.6 Wall Painting (4)	0.00	0.00	0.03
4.7 Total 1st yr Operating Cost	<u>0.82</u>	<u>0.73</u>	<u>0.30</u>
4.8 Relative 1st yr Operating Cost	2.73	2.43	1.00

- (1) 27% of initial cost
(2) Electricity at 1.34¢/kwh and gas at 89¢/mcf
(3) 1.6% of total investment cost
(4) At three-year intervals



PROBLEMS IN MASONRY WALLS - A Case History

By K.E. Fricke,¹ W.D. Jones,² J.E. Beavers³

ABSTRACT: Union Carbide Corporation - Nuclear Division, is an operating Contractor to the Department of Energy (DOE). The Union Carbide operated DOE facilities are the Oak Ridge Y-12 Plant, the Oak Ridge Gaseous Diffusion Plant (ORGDP), and the Oak Ridge National Laboratory (ORNL); and the Paducah Gaseous Diffusion Plant located at Paducah, Kentucky. Over the past 30 years many buildings have been constructed using conventional masonry construction techniques. During the past 10 years we have been experiencing several safety related problems with these buildings -- to the point of having to remove some of the existing exterior walls and rebuilding them. Our most recent experience was the removal and reconstruction of a brick veneer wall of a three-story building -- a building which was constructed less than 10 years ago. We are presently reviewing similar problems that exist throughout the three plants. The paper discusses the problems, their apparent causes, and possible solutions to such causes.

For the present, we intend to continue to build using masonry construction. However, as problems continue in this area, management will become more concerned and will begin to turn toward the use of steel buildings with metal panel walls.

¹Engineer, Struc. & Arch. Dept., Union Carbide Corp. - Nuclear Div., Oak Ridge, TN.

²Engineering Specialist, Struc. & Arch. Dept., Union Carbide Corp. - Nuclear Div., Oak Ridge, TN.

³Manager, Struc. & Arch. Dept., Union Carbide Corp. - Nuclear Div., Oak Ridge, TN.

PROBLEMS IN MASONRY WALLS

A CASE HISTORY

by

Kenneth E. Fricke¹, W. Dale Jones, P.E.² and James E. Beavers, P.E.³

INTRODUCTION

The use of brick or stone in construction has been with us since antiquity. Most of the ancient temples, pyramids, and the massive structures of medieval times, extending down through the Renaissance, were built of stone. Modern engineering practice employs an assembly of stone or brick bonded together with mortar or some other cementitious material. The long experience with masonry has not eliminated failures. Today, masonry failures are not only experienced after extended periods of time, but also during construction or even after a relatively short life. The fact that new types of construction are being used, combining brick with other materials, is leading to more frequent failures.

Union Carbide Corporation - Nuclear Division, is an operating contractor to the Department of Energy (DOE). The Union Carbide operated DOE facilities are the Oak Ridge Y-12 Plant, the Oak Ridge Gaseous Diffusion Plant (K-25), and the Oak Ridge National Laboratory (ORNL); and the Paducah Gaseous Diffusion Plant located at Paducah, Kentucky. Construction at the Oak Ridge sites began in 1943 and has continued, to meet expansion needs. During the past 35 years many of the buildings have been constructed using conventional masonry. The K-25 plant has close to 350 buildings of which 23 involve brick construction. At the ORNL, 10% of the 220 buildings are constructed with masonry walls, while at the Y-12 plant 50% of the buildings involve some form of masonry construction. There are approximately 310 buildings at the Y-12 plant, of which 108 are single-story, masonry bearing wall structures; in addition there are 35 multi-story buildings that use masonry walls in a non-structural capacity. As a result of the heavy use of brick

¹Engineer, Struc. & Arch. Dept., Union Carbide Corp. - Nuclear Div., Oak Ridge, TN

²Engineering Specialist, Struc. & Arch. Dept., Union Carbide Corp. - Nuclear Div., Oak Ridge, TN

³Manager, Struc. & Arch. Dept., Union Carbide Corp. - Nuclear Div., Oak Ridge, TN

construction several safety related problems have been experienced during the past 20 years, some to the point of necessitating the removal of all or parts of the walls and rebuilding them.

This paper briefly discusses the masonry wall failures encountered at these facilities, their probable causes, and their solutions. The main discussion focuses on two specific failures at the Y-12 plant. These failures involved substantial wall movements in two of the multi-story buildings (Fig. 1) that took place during the past three years. In the first case the entire curtain wall was removed and replaced, and in the second case only the brick veneer was replaced.

CASE I - WALL FAILURE

Building Description. The first building at the Y-12 plant whose wall failure required removal was the facility identified as 9204-2E (Fig. 1). The construction of this building was completed in January, 1970. It is a three story structure composed of a structural concrete frame with masonry filler walls and brick facing construction on the upper two stories. The first story construction, part of which lies below the grade level, consists of concrete columns poured integrally with an 8 in. wall, both being supported on a mat foundation.

The masonry walls are 12 in. thick, composed of 4 in. face brick and 8 in. filler. In the area of failure the filler wall is 8 in. clay tile on the first story wall and 8 in. hollow concrete block on the second story wall. Four inches of the filler is carried past the roof spandrel beam which is set in from the outside of the column line. The brick facing is supported on the outside of the concrete frame from a shelf in the foundation wall at an elevation 8 in. below the top of the second floor level, to the underside of the parapet coping. No shelf angles to help support the wall were included in the design. The distance from the top of the foundation wall to the third floor level is 30 ft and from there to the roof line an additional 18 feet. The parapet is 2 ft in height, capped with an 8 in. stone coping. The construction drawings showed the wythes of masonry being tied together with continuous joint reinforcement and the brick being tied to the columns and spandrel beams with dovetail anchors. Vertical expansion joints were shown through the two wythes of masonry on both sides of the columns.

Detection of Bulges. Soon after construction was completed bulges in the west wall were detected, although at that time no measurements were taken. The west elevation and a typical cross-section through it are shown in Figures 2 and 3. The bulge noted in 1970 is marked as area "A". Another inspection was made in August, 1973, and the conclusion then was that visually the walls had not moved appreciably over the three year span. However, because of visible cracks between

the interior cross-walls and the exterior wall, it was decided that for future reference, data points should be established at locations along the west wall.

In October, 1973 a survey was made from within the building. This survey showed a slight, but not alarming, increase in the bulge at "A". At the same time, no excessive movements were noted in other areas of the wall.

Rapid Wall Movement. In March, 1966, movements were again noted, and an inspection was made which resulted in observing a bulge at "B", that equaled or exceeded the displacement at area "A".

Between Friday, May 29, and the following Monday there was an apparent $1/4$ in. movement of the wall. As a result the west side of the building was roped off for safety reasons, and utility and electrical lines were removed from the entire west wall, 3rd floor, and north-center and south bays. A complete survey was made on both the interior and exterior of the wall.

The magnitude of the movement was most obvious at the cross-walls (column lines). An outward movement of as much as 2 in. was measured at the interior walls between column lines 1 and 2, 6 ft above the top of third floor level. Most locations showed an increase in the separation over the past three year span, with a maximum differential movement of $7/8$ in., in area "B". Fig. 4 shows the actual wall movements measured at various locations along the interior west wall.

Measurements taken on the outside of the wall also showed large displacements, with the maximum deflection measured at $2 \frac{5}{8}$ in. occurring in area "B", 4 ft above the third floor level. The maximum recorded deflection in area "A" was 2 in., and that between the second and third column lines was $1 \frac{5}{8}$ in., both occurring several feet above the third floor level. The deflections measured on the exterior of the wall correlated well with the deflections measured on the interior.

Apparent Causes. The conclusion was that the bulging was the result of normal thermal and moisture expansion coupled with design omissions. The causes of failure were reduced to two basic areas:

1. Contribution of the Structural Frame

During the various inspection tours of the building, there was no visual obvious contribution of the reinforced concrete structural frame to the bowing out of the masonry wall. Further examination of the structural drawings revealed nothing to cause one to suspect that the reinforced concrete frame was in any way inadequate, nor did a review of the design calculations. However, the concrete

block exterior wall bears directly against the spandrel beams at the third floor and roof levels and since the brick veneer is tied directly to the block, any expansion of the brick veneer is resisted by the bearing of the block walls against the spandrel beams, and a moment tending to cause the wall to bow out is introduced by the eccentricity of the bearing. Any deflection of the spandrel beam at the roof level would contribute to this bowing out. Results of the deflection calculations indicated that the total deflection of the roof spandrel beam -- dead + live + long term loads -- was on the order of L/900, less than that permitted by the ACT Building Code. Thus, the deflection of the roof spandrel beam was not excessive. The flexural strength of the beam was checked and also found to be adequate (2).

2. Thermal and Moisture Effects

As shown in the Technical Notes (4), a 50 ft high brick masonry wall subjected to a 100°F temperature increase would, on the average, expand approximately 1/4 inch. The moisture expansion of the same wall, using a moisture expansion coefficient of 0.0002, would approximately be 1/8 inch. If the wall were not allowed to move, these vertical deflections would more than cause the measured 2 in. bow. If curing shrinkage of the frame and deflection of the spandrel beams is added to this, the bow of course, would be even greater. No horizontal expansion joints for vertical expansion of the masonry were included in the design. It also became apparent that the vertical expansion joints did not function properly, as no closing of the joints was evident. This created additional bowing resulting from the resistance to horizontal movement of the masonry.

Summary. A description of what might have occurred at the wall follows (5). Initially the concrete masonry experienced a drying shrinkage which provided space for further movement. Drying shrinkage does not of course occur in clay tile. As the clay masonry expansion, and the frame shrinkage and deflection began to occur, the clay tile backup was clamped tighter within the frame, but the concrete backup, due to initial shrinkage, contained space for movement. This resulted in the concrete backup being essentially lifted off the third floor spandrel beam reducing its frictional resistance to movement. With the brick wall tied to the concrete backup, it merely pulled the block away from the building at the locations of least resistance.

The repair to this structure was to remove the existing brick and block wall and replace it with a new 12 in. block filler, facing the exterior with a metal siding. Since the building was not in a location within the plant where appearance was a concern, the use of the metal siding was acceptable.

CASE II - WALL FAILURE

Building Description. Failure occurred in a large addition to the Development Laboratory, building 9202 (Fig. 1), at the Y-12 plant. The addition, completed in 1964, is a three story steel frame structure with masonry walls composed of a 4 in. curtain wall and an 8 in. concrete block filler wall. The structure is supported by spread footings at the columns. The lower floor consists of a shipping and receiving area, and various laboratories. The second floor is office space and the third floor has laboratories.

Again, as was the case in Building 9204-2E failure occurred in the west wall (Fig. 5). The first story of the wall is composed of 3 3/4 in. brick, a 1 1/4 in. air gap, and an 8 in. poured concrete wall. The brick facing for the wall was carried by the poured concrete wall on a ledge (Fig. 6). In addition to the ledge, there are three shelf angles which help support the brick wall. Both upper story walls have the same composition, differing from the first story wall in that the air gap is increased to 2 1/4 in., and the filler wall is 8 in. concrete block (with the exception that at the floor levels the structural steel beams are protected by poured concrete which serves as the backup to the brick). There are three windows in the second story wall, reinforced by a composite W12 x 19 lintel beam and a 1/4 in. plate spanning the columns.

Detection of Bulges. In February, 1977, an exhaust duct was to have been attached to the west wall, however, bulging of the brick at various locations throughout the wall was noticed. Since the duct required bracing, the construction engineer decided the wall looked too unstable for such work and requested an inspection by the Structural and Architectural Design Department. Upon inspection, the interior walls revealed cracks in the concrete block starting approximately 9 ft above the third floor level at the columns and progressively widening to the roof beams as shown in Fig. 7. These cracks were most noticeable in the northwest corner of the building where the block separation was approximately 1/8 inch. It was also noticed that the lintel beams in the north wall over the third story windows were rotating about the corner edges of the windows.

An inspection of the outside of the building revealed that some settlement of the footing had occurred at the northwest corner. A shear crack in the brick veneer was clearly visible near the corner at the second story window on the north wall. Furthermore, the vertical

expansion joint on the west wall at the same corner was sheared over much of its length by the relative movement of the column and the west wall. However, it did not appear that this settlement was a principal factor in the bulging of the west wall and thus was not considered in the ensuing study.

A survey was made of the north and west walls, with a representation of the results for the west wall appearing in Fig. 8. The vertical solid line and the dashed line represent the location of the rear face of the brick and the leading edge of the shelf angles respectively. The distance between them is the amount of brick designed to be resting on the shelf angle. The irregular line represents the rear face of the brick as determined by the survey. Thus, either the distance the brick has moved or how much of it remained on the shelf angle can be obtained. The brick had moved a maximum of $1 \frac{3}{4}$ in. at the second story shelf angle (Elev. 977.75) in survey line 4, leaving less than one inch of brick sitting on the angle. The maximum movement obtained at the top shelf angle (Elev. 995.15) was approximately $1 \frac{1}{2}$ in. as measured in survey line 6. The brick did not move appreciably below the lintel beam (Elev. 974.65). Most of the movement took place in the area bounded by the lintel beam and column lines Zb and Zc (Fig. 5), with the displacements decreasing towards the corners of the building. From these results it became readily apparent that the upper part of the west wall was dangerously near failure. The results of the north wall survey indicated that there had been some movement. While the amount was not considered a safety hazard at this time, it has warranted continual monitoring.

Another survey was made of the building to measure the vibrational levels - due to the Exhaust Fan House and equipment on the roof - at the walls. Vibration levels were measured in the direction of the three axis along the top of the wall and in addition a horizontal east-west measurement was made at the third floor west wall. Similar measurements were made of the north wall. The results of this survey indicated the vibration levels to be insignificant.

Review of Wall Design. A review of the wall design revealed that the lintel beams in both the north and west walls were overstressed, that no horizontal expansion joints were included (except beneath the base plate of the lintel beams), and that the shelf angles in these walls were attached to the poured concrete overhangs at the upper floors rather than being attached to the steel frame as was done at the east wall. Furthermore, the lintel beam details appeared on the architectural drawings rather than on the structural drawings - an unusual practice.

The lintel beams have a column to column span of 20 ft and were considered to be simply-supported at each end. If the unbraced length is considered to be the full 20 ft the lintel beams in both walls do not meet the AISC specifications. If the beams are assumed to be braced at the window corners, the west wall beams barely meet the specifications, but the beams in the north wall are still inadequate. From the cross-section (Fig. 6) it will be noted that the lintel beams were supposed

to be completely encased by both the brick and the concrete block, in which case it might be argued that the beams be considered continuously supported. However, as the walls were non-structural walls, the beams should have been designed to support the loads on an unbraced length of 20 ft, thus resulting in the overstressed condition for the given design.

A vertical expansion joint was provided along each column line and a horizontal joint was provided below each of the lintel beams. As a result there were two horizontal joints provided in the north wall (where the brick movement had been less acute) and only one in the west wall. In the west wall the horizontal joint was only effective for the wall section below the joint - where, incidentally, the movement of the brick was virtually zero.

Demolition of the West Wall. After reviewing all of the available data, it was determined that the brick facade on the west wall should be replaced. For the purpose of obtaining more information regarding the actual wall installation, a step-by-step demolition sequence was prepared. The demolition called for the removal of all the brick above the windows. The two photographs in Fig. 9, taken during the demolition process, clearly show the brick bulging at the top shelf angle.

In addition, another abnormality was detected in the bolted connections of the shelf angle (Fig. 9b). The design provided for pre-drilled clearance holes in the angle where it was to be bolted to the concrete block wall. It was apparent that these holes were modified in the field with a cutting torch in order to compensate for a poor field fit. In addition many of the connecting bolts were loose, some to the point of being easily removable by hand. In spite of these irregularities, and also the fact that the angle was anchored into the block instead of the steel frame, the shelf angle appears to have performed satisfactorily. The second story shelf angle also performed as expected.

Wall ties were probably adequate in number throughout the wall sections between the floor levels, but again irregularities were visible. No ties had been placed in the vicinity of the poured concrete slab overhangs, between the top of the windows and the third floor level, nor in the area above the top shelf angles. Ties had been attached to the web of the lintel beam, but they were not long enough to reach to the brick wall, and instead of replacing them, they were pushed aside.

Reconstruction. Prior to erecting the new brick facing, stiffener plates were welded to each 20 ft span of lintel beam at the one-third points to provide intermediate bracing. A plate was welded to the top shelf angle at each location where the connection holes had been enlarged by burning, and each defective bolt was replaced. The new brick facing was tied to the existing concrete block wall with corrugated metal ties which were attached to the block through channel

slots anchored into the wall. In addition, ties were attached - where originally omitted - from the lintel beam to the brick wall. The ties were spaced 24 inches in the horizontal direction and as near to 16 in. in the vertical direction as was feasible. Where no ties had previously existed, between the top shelf angle and the parapet coping, one row of ties was placed. Expansion joints were placed at 1) the four column lines in the vertical direction, 2) between the shelf angles and the layer of brick immediately below, and 3) below the lintel beams.

Summary. The problems encountered in the west wall of this building were similar in nature to those found in the 9204-2E west wall. The movement in the wall was unquestionably due to thermal and moisture expansion effects. The lack of, or improper design of, expansion joints, inadequate tie spacing, plus some questionable construction practices were all factors contributing to the excessive wall displacements.

CONCLUDING REMARKS

The general problems that occur in all types of masonry construction are not new to the Oak Ridge facilities. In 1957 the main portal building at ORNL required repairs to two masonry walls which had cracked as a result of warping of a concrete canopy due to thermal stresses (3). In 1968, building 9203-A at Y-12 had sections of the north wall removed and replaced due to excessive movement of the brick veneer, and in the same building a small area of the west wall was taken down due to considerable cracking. At one of the facilities discussed in this paper, building 9202, further investigation, and additional repairs will be needed. At the second floor level of the south addition of that building the concrete block interior wall is separating from the rest of the structure, and repairs are recommended to the north wall of the north addition. Recently, a problem in the three story First Baptist Church educational building located in Oak Ridge necessitated replacement of the west wall brick due to extensive separation of the brick and block backup. Similar problems have plagued the industry at large throughout the United States and Great Britain as indicated by the numerous articles (1, 6, 7, 8) that have appeared in various publications in the last two years alone. The fact that failure occurs most often in west walls is not surprising due to exposure to the afternoon sun.

Masonry wall failures generally arise from 1) improper constraints which prevent the wall from freely expanding or contracting due to temperature fluctuation and moisture absorption and 2) external forces to the masonry wall. These technical aspects behind masonry failures have been well documented and will not be further entertained here. Rather, the questions - Why do these failures occur as frequently as they do, when the technical knowledge seems to be available and what can be done to prevent failures of this type in the future? - are

considered. The problems result from a combination of 1) inadequate design, 2) faulty construction practices, and 3) lack of adequate quality control.

Inadequate Design. Inadequate design practices can be traced to a lack of proper education. Very few engineers or architects have had more than a cursory introduction to the complexities of masonry construction in the university. Many must learn the technical aspects of the field either with on-the-job training and/or special seminars. The fact that brick is used in combination with other materials results in a behavior that is not well understood and hence, not properly anticipated and designed for. Many unsightly cracks can be avoided by understanding how the structural frame and the foundation of the building are expected to behave, and by providing proper expansion mechanisms to compensate for such behavior.

One of the contributory factors which may lead to masonry failures is an overreliance placed on the construction worker to incorporate the designer's intent. It is quite apparent that there exists a large gap between the designer at the drawing board and the man in the field, and unquestionably, both parties must share the blame.

Faulty Construction Practices. Due to the refinements being incorporated into today's designs, far greater attention to details is required at the construction site than was the case in the past. Hurried workmanship can lead to improper placing of wall ties, inferior fabrication of expansion joints (though, the design might also be at fault - using materials unsuitable for the purpose intended), poor brickwork, and inadequate waterproofing of the masonry. Loose connections between shelf angles and walls might permit the shelf angles to rotate enough to tip the masonry, or produce unsightly, and possibly hazardous bulging. All of these details are critical to the long-term stability of the walls and care should be taken to insure their proper construction.

Quality Control. Building failures, similar to those discussed herein, can be attributed in part to a lack of proper on-site inspection. Proper quality control at the construction site is an absolute requirement and when special quality control procedures are necessary the designer must specify them. The continued presence of a Quality Control inspector at a site would serve as a deterrent to some of the more questionable practices.

These are by no means the only problem areas that should be considered, but they provide a set of guidelines that would certainly improve the overall picture of masonry construction.

APPENDIX I

References

1. "Brick-Clad Concrete Proves Troublesome", Engineering News Record, p. 10, August 25, 1977.
2. Burdette, E.G.; Professor, University of Tennessee, Department of Civil Engineering, Knoxville, Tennessee; Letter to J. W. Gregory, June 30, 1976.
3. Carter, C. M.; "Report on Structural Study, Building 5000", ORNL Engineering Department, August, 1956.
4. "Differential Movement", Technical Notes on Brick and Tile Construction, Structural Clay Products Institute, 1963.
5. Grogan, J.C.; Executive Director, Brick Institute of America Region Nine, Atlanta, Georgia; Letter to J. W. Gregory, July 8 1976.
6. "Lack of Design Data, New Building Techniques Cause Facade Failures", Engineering News Record, p. 9, February 2, 1978.
7. "Spandrel Repairs Avert Collapse", Engineering News Record, p. 21, February 16, 1978.
8. "Two Buildings in City Lose Brick Facades", Engineering News Record, p. 45, May 19, 1977.

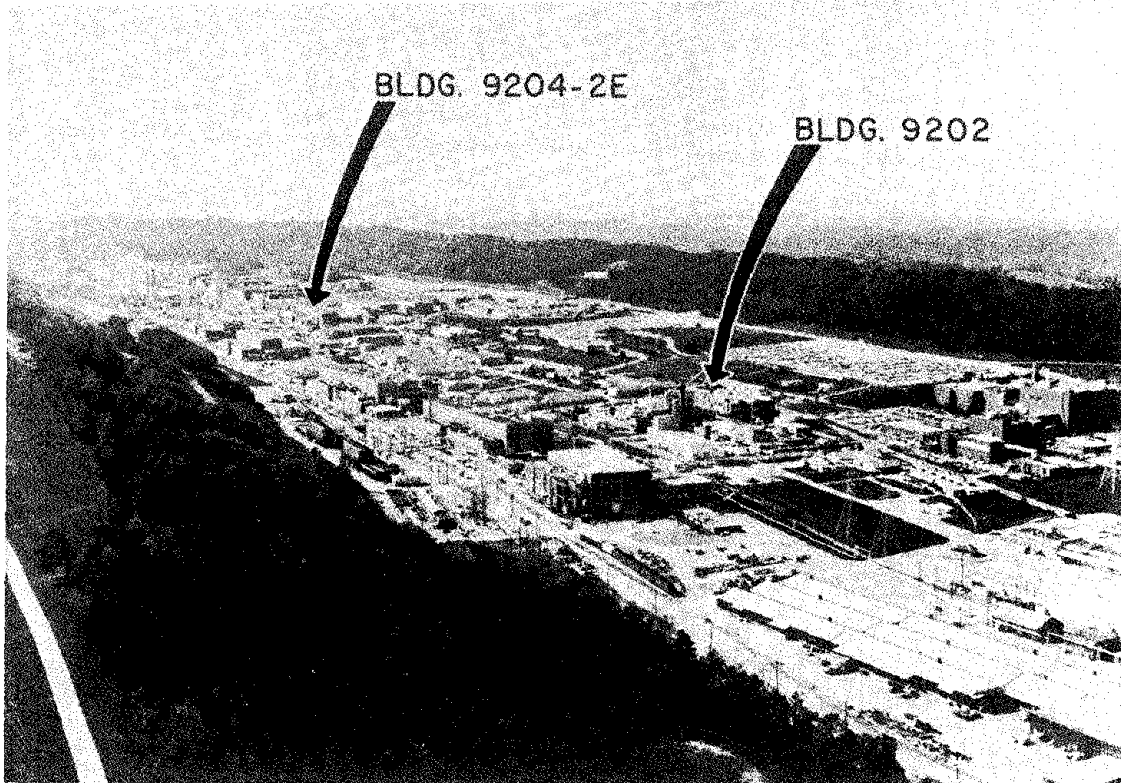


Figure 1: Aerial View Of The Y-12 Plant-Oak Ridge

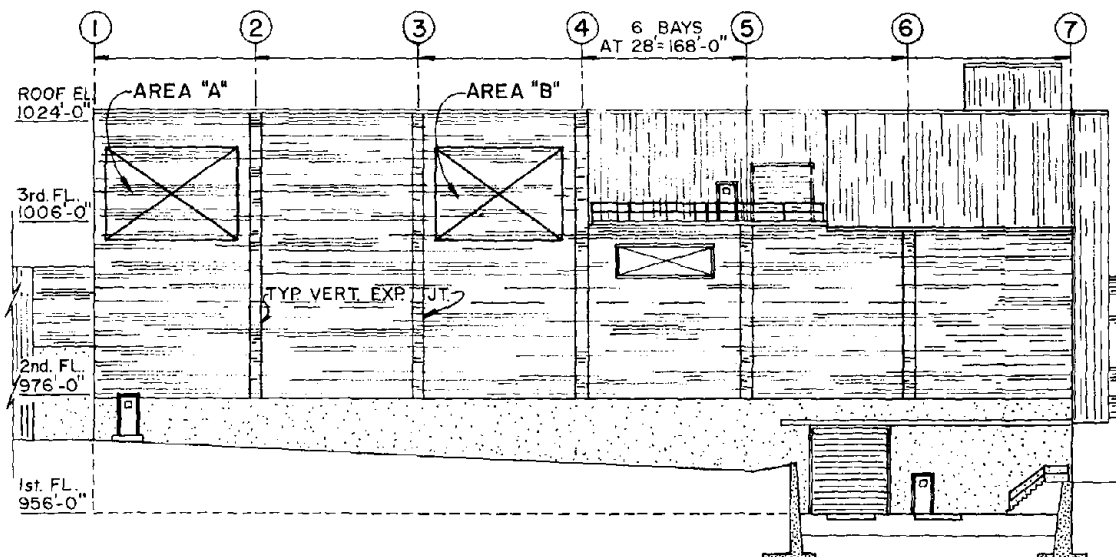


Figure 2: West Elevation Of Building 9204-2E

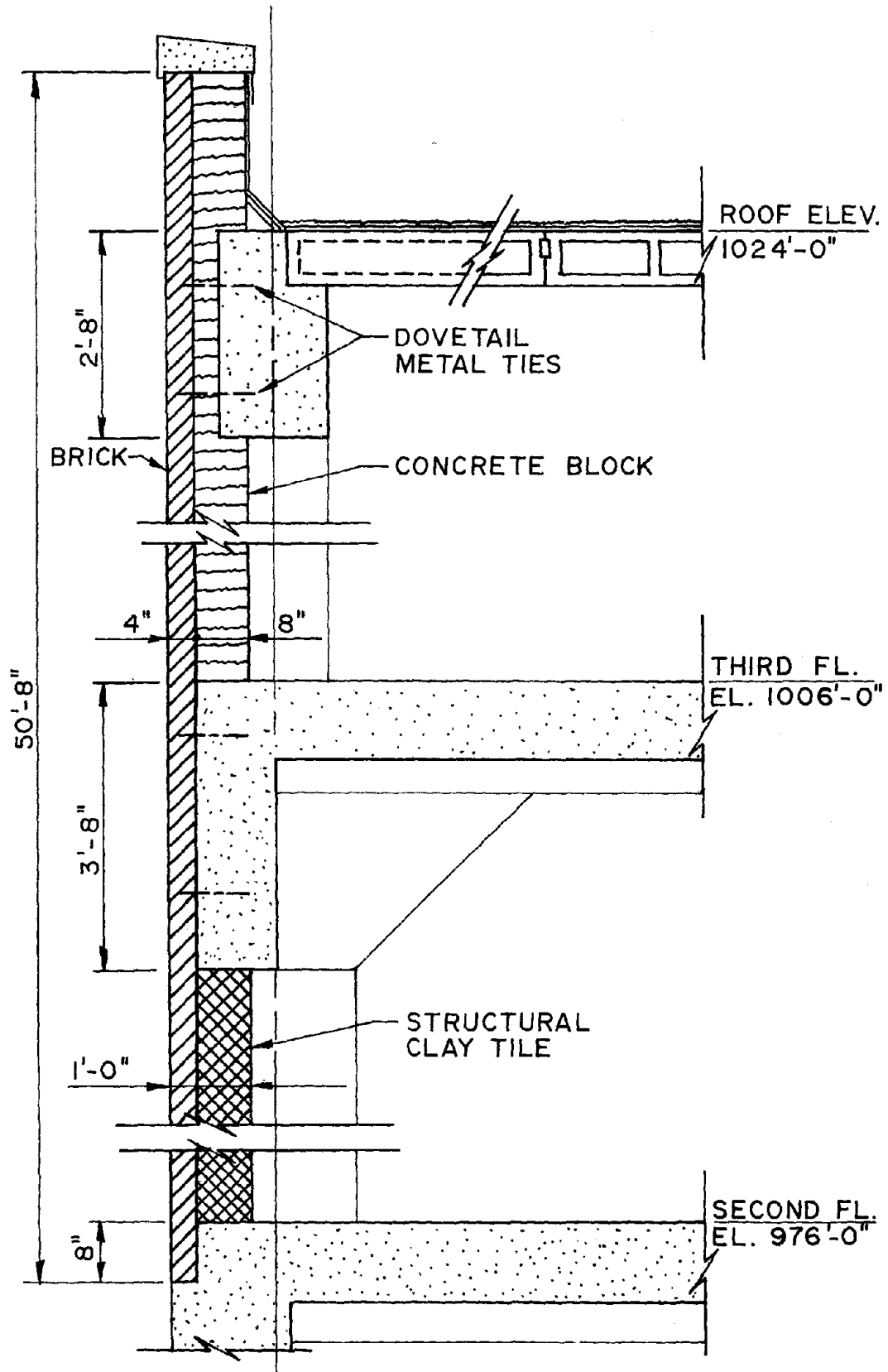


Figure 3: Cross-Section, West Wall, Building 9204-2E

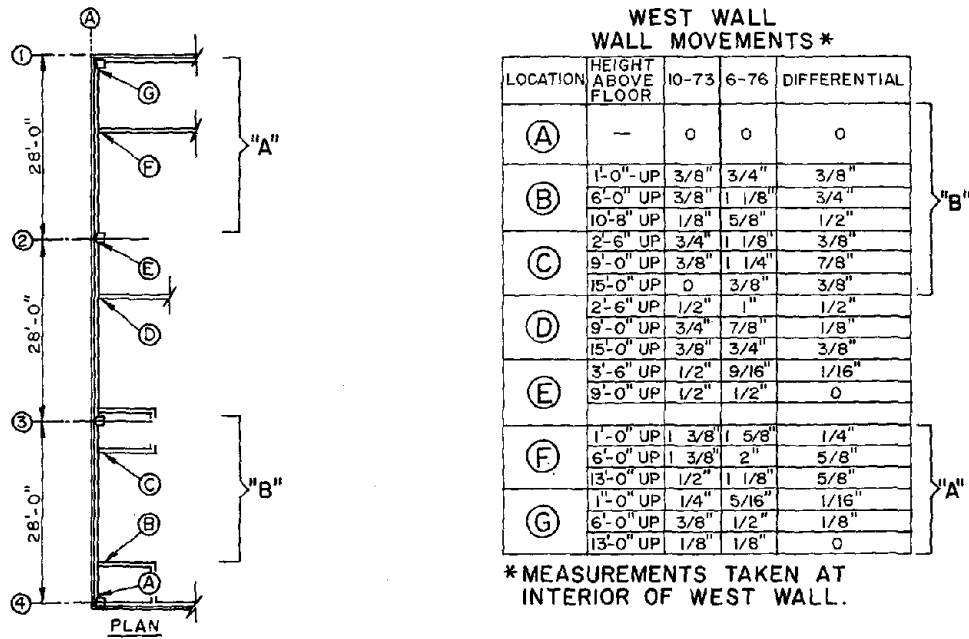


Fig. 4: Wall Measurements, West Wall, Bldg. 9204-2E

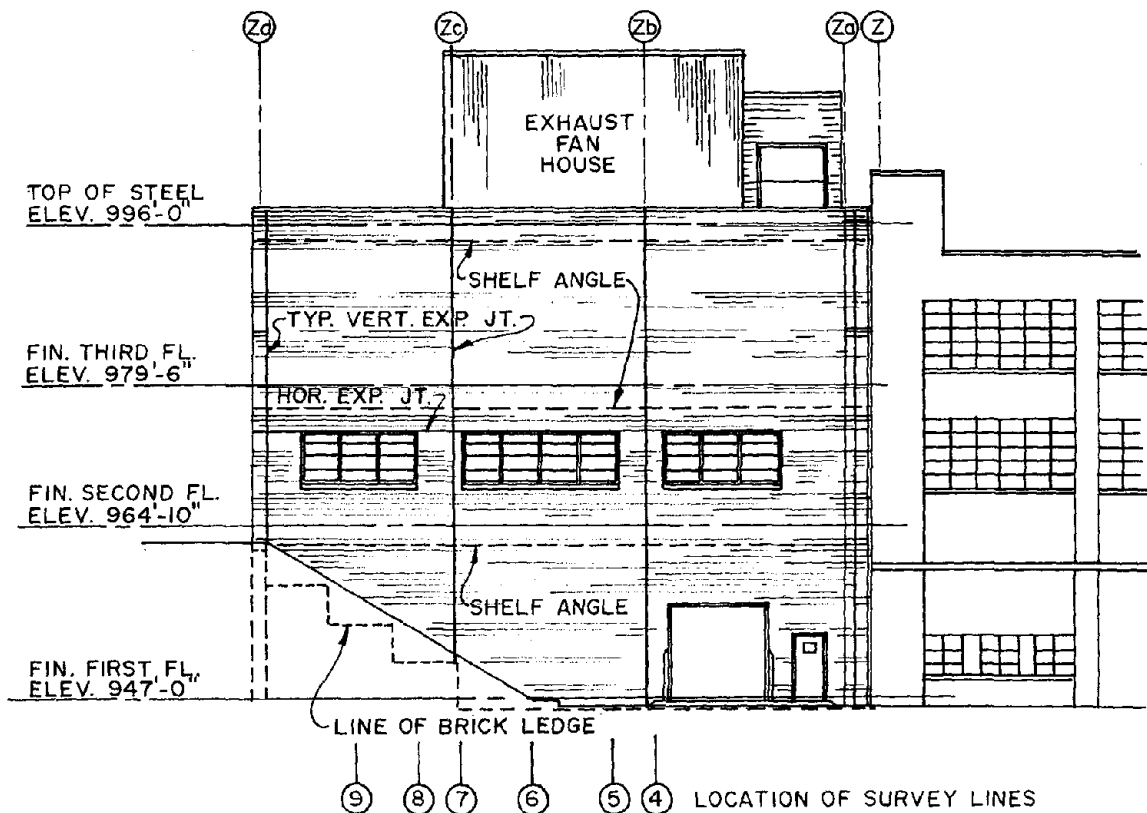


Figure 5: West Elev. Of North Addition, Bldg. 9202

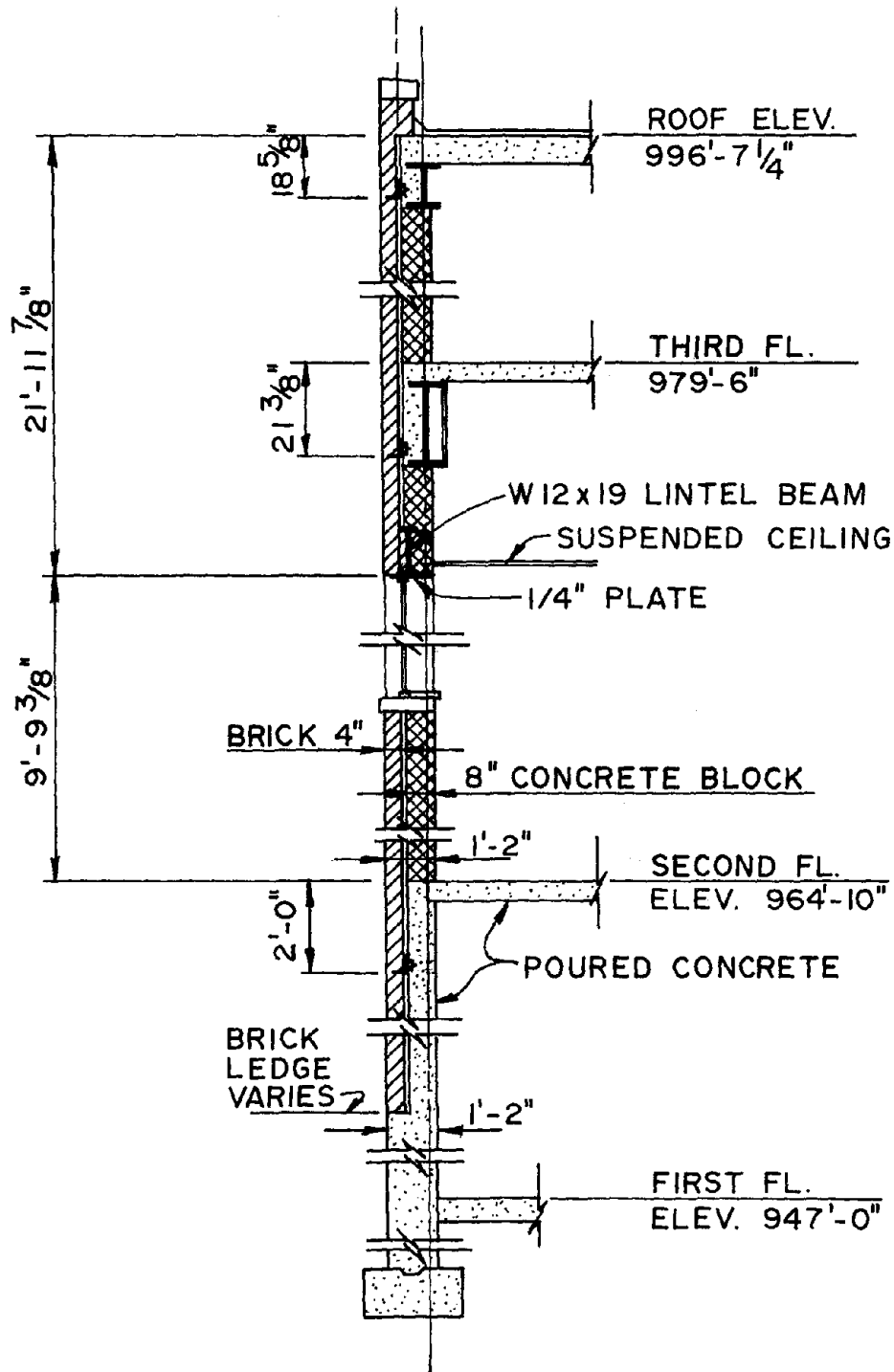
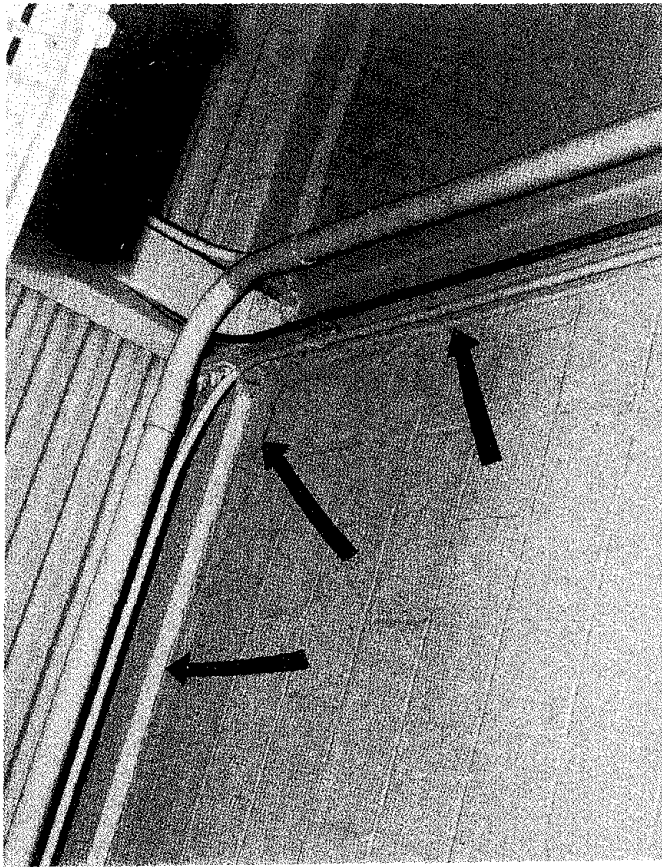
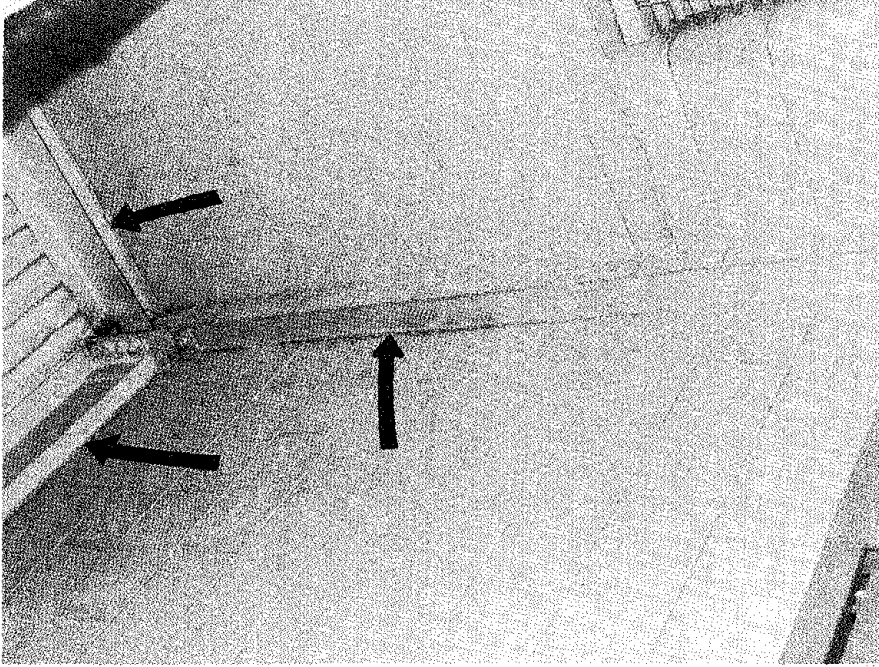


Figure 6: Cross-Section, West Wall, Building 9202



(a) WEST WALL



(b) NORTHWEST CORNER

Figure 7: Building 9202-Interior Wall Cracks

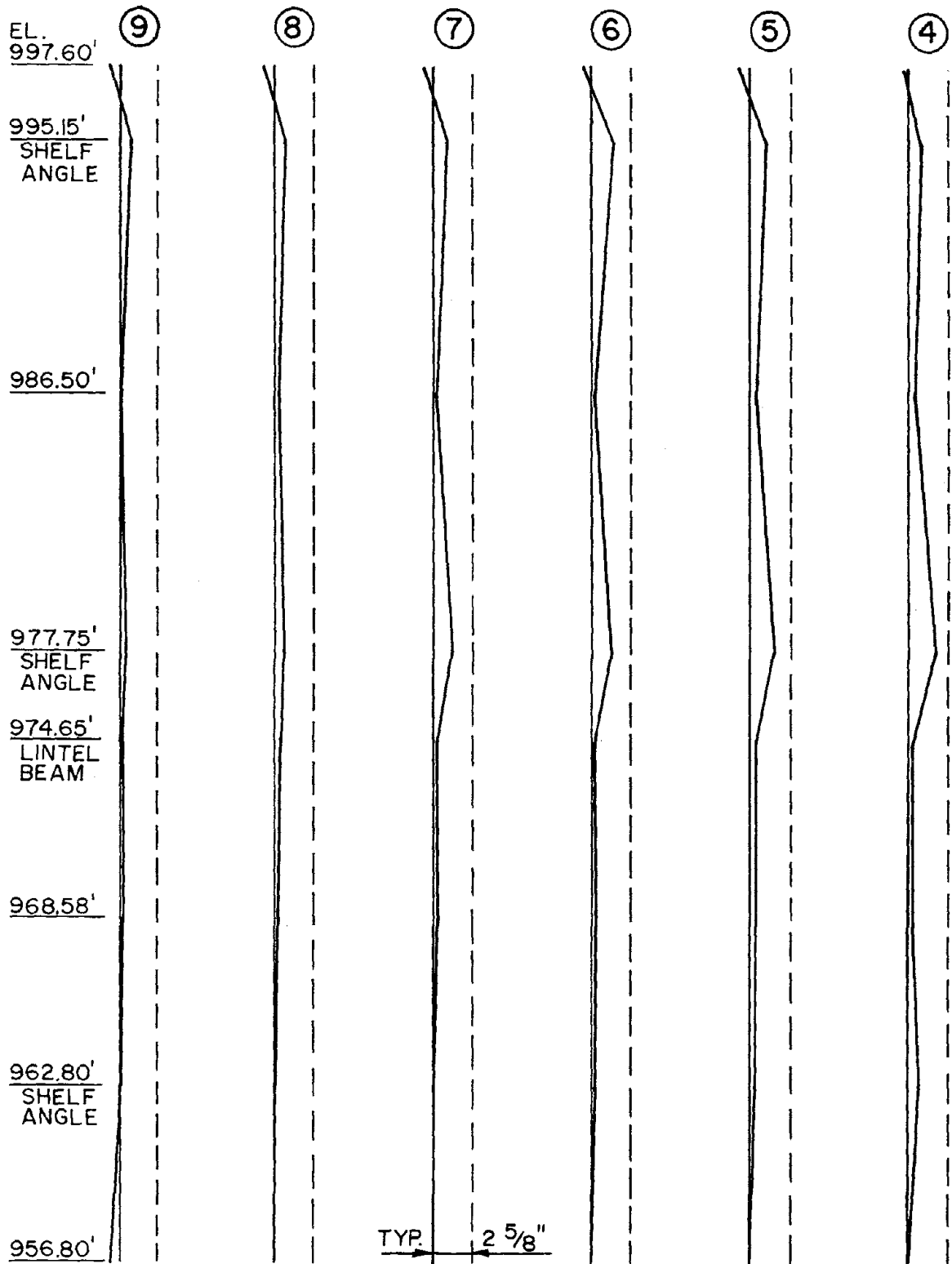
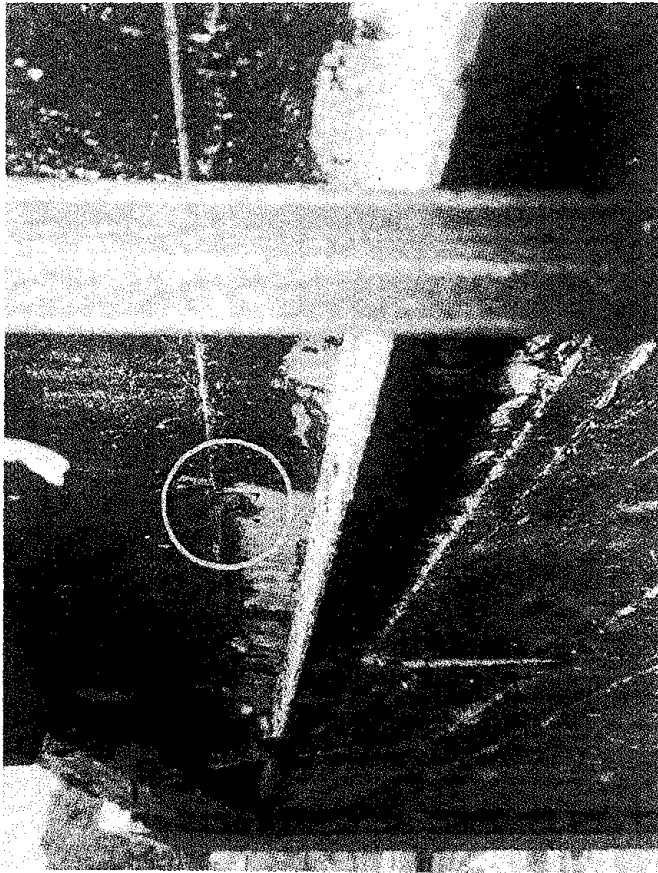


Figure 8: Example Of Survey Results, Building 9202

113-18



(a) WALL BULGE



(b) BOLTED CONNECTIONS

Figure 9: Building 9202- View Of The Top Shelf Angle

MASONRY PANELS: REVIEW, PRESENT USE AND DESIGN

By: Borchelt, J. Gregg, Masonry Institute of Houston-Galveston

Techniques used to fabricate masonry panels in the past and present are given. Factors influencing panel size, shape and layout are discussed. Techniques of achieving tensile stresses necessary for panelization are discussed and design information included. Curtain wall and loadbearing panels, connection details and quality control requirements are discussed.

MASONRY PANELS:
REVIEW, PRESENT USE AND DESIGN

J. Gregg Borchelt¹

INTRODUCTION

The design and construction of masonry panels has seen a number of changes in its relatively short history. At this time there are two methods of developing sufficiently high tensile stresses to allow preassembly of masonry. These are the use of high-bond mortar and reinforced masonry. Both rely on an engineering analysis for proper application. The manufacturing techniques to fabricate the panels has come full circle. The first masonry panels were hand built by masons. After a flurry of interest in various automated production methods, the majority of panels being built now are again hand crafted.

HISTORY

Although the use of panels is thought of as a relatively recent development in masonry construction, the use of prelaidd masonry can be traced to the late 1800's. Portions of masonry walls for buildings along the waterfront in Galveston, Texas were prelaidd and lowered into the seawater (2). Similar construction was undoubtedly used in other areas.

The first research in the United States into the application of masonry panels was done in the 1950's by the Structural Clay Products Research Foundation. This work was on reinforced masonry and led to the use of panels on a building in the Chicago area. Prebuilt, reinforced lintels were also the result of this research. In Europe the trend was to mechanize the brick and tile placement, using unskilled labor. So far the mechanized systems developed in other countries have not been successfully introduced into the United States.

The development of high-bond mortar additive in the mid 1960's increased the interest in and the use of masonry panels. The panels of this time were built by masons, working in special areas either at the jobsite or offsite. The interest in panels continued to grow and the proceedings of masonry conferences reflect this interest. The First International Brick Masonry Symposium held in 1969 contained 6 articles on panelization (7). The second of that series held at Stoke-on-Trent, Great Britain, in 1970, had 11 presentations on masonry panels (9).

¹Executive Director, Masonry Institute of Houston-Galveston, Houston, Texas.

During this time the trend in the United States was also to automate the bricklaying process. A variety of techniques utilizing rubber molds, steel grids, vacuum and pressure devices were tried, with unskilled labor operating the equipment. Mechanical bricklaying and blocklaying devices were developed along with specialized equipment to increase the productivity of skilled masons. Most of these efforts were by brick manufacturers or mason contractors. Of these techniques the author knows of only one that remains in operation, that is the blocklaying machine developed by Builders Equipment Company of Phoenix, Arizona. Masonry panels are again produced by hand, using skilled craftsmen. This change was noted by Grenley in the First Canadian Masonry Symposium in 1976 (6).

The high cost of developing and operating a capital intensive plant for panel production undoubtedly is instrumental in the decline of automated techniques. The extra price for this overhead, added to transportation and erection costs, priced the mass produced panels out of the market. Hand placed masonry units, on the wall or in panels, remain an extremely cost effective construction medium.

The interest from architects, contractors and suppliers in masonry panels keeps them as a part of the construction industry. However, it takes the active participation of a mason contractor to promote and sell large projects utilizing masonry panels. In order to best utilize masonry panels the project should be designed for that purpose. Then the most economical panel size, connection method and construction scheduling can be achieved. The more common application of panelized construction is in specialty uses: sloped sills, soffits, corbels, beams and unusual bond patterns (Figure 1). In most instances brick are used to assemble the panels, although reinforced block panels are occasionally built.

Thus we have come full circle in masonry panel construction. Skilled labor is again employed to construct panels which retain masonry's unique flexibility in layout, size, bond, coursing and color. The advantages which have made masonry a popular method of building for thousands of years are often achieved more economically with masonry panels.

AESTHETIC AND LAYOUT CONSIDERATIONS

Masonry panels are normally single wythe construction although there have been instances of double wythe panels for reinforced beams and columns and composite panels of brick and block construction. Panels are usually one story high with varying lengths. The most economical panels are longer than they are tall with a maximum length of about 25 feet although longer panels have been built. Transportation and erection restraints must be considered when determining maximum panel size.

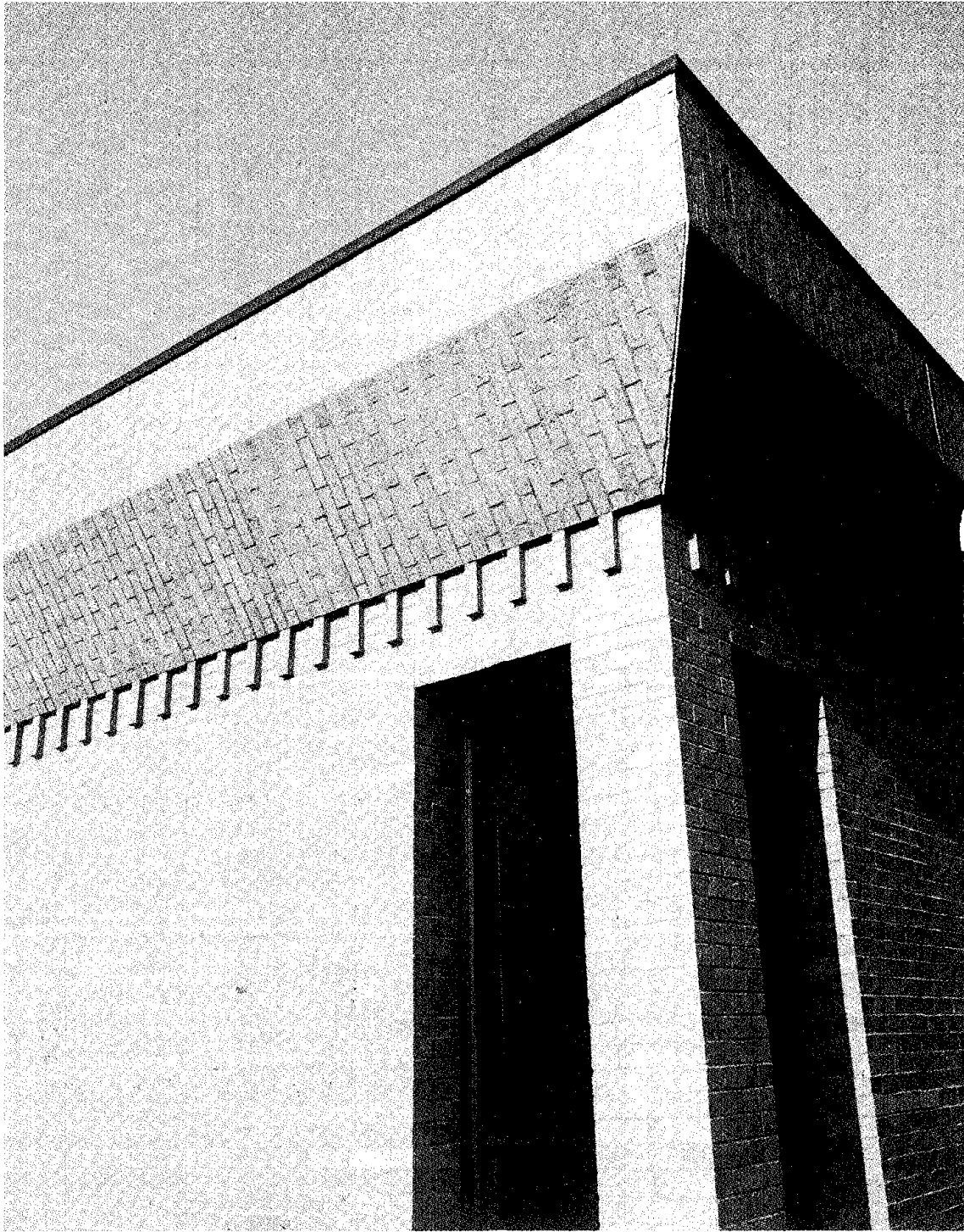


Figure 1. Typical Masonry Panel Project

Openings can easily be incorporated into masonry panels. It is best to have at least 2 feet of masonry on the perimeter of openings in order to allow proper stress distribution during placement and service. Projections, returns, arches and similar features can be achieved by combining small panels in a larger assembly.

Masonry elements of various shapes and configurations can be placed in any orientation to achieve individual design. Sloped and horizontal masonry can be economically attained. The masonry panels can be used in curtain wall or loadbearing applications. All types of structural frames and/or floor members work well with masonry panels. Welded, bolted or grouted connections are used to attach the panel to the other building components.

The joints between panels are best left as soft joints. This allows for differential movement between the building frame and panel, without transferring unwanted loads from panel to panel. Flashing and weepholes should be located at the horizontal joint between panels. A water tight joint is achieved with a sealant backer rod and a high quality caulk. Interior finishes and insulation are applied by laminating them directly to the inside surface of the panel or with non-structural furring studs.

The size, color and surface treatment of the masonry unit are normally determined by aesthetic requirements. Brick selected for use with high-bond mortar must be checked for proper strength development. Flexural test specimens must be made with the actual run of brick to be used in panel construction to verify the specified bond strength. This test method is described in the section on quality control. When reinforced brick panels are to be built it is common practice to use hollow brick meeting the requirements of ASTM C652, Standard Specifications for Hollow Brick (1). These units are cored in excess of 25% but less than 40% of the cross sectional area. The resulting cores are sufficiently large to receive vertical reinforcing bars and grout.

DESIGN INFORMATION

In recent years building standards containing engineered design of masonry structures have been recognized by the building codes and design professions (3,4,8). This approach is based on linear elastic behavior and working stress analysis. These principles of mechanics are also used in the design and analysis of masonry panels. The following assumptions are valid:

1. The masonry units and mortar work together as a homogeneous mass.
2. Stress is directly proportional to strain.

3. The moduli of elasticity of all materials remain constant.
4. Small deflection theory is applicable.
5. Sections plane before bending remain plane after bending.

All of the above assumptions apply to panels fabricated with high-bond mortar or conventional mortar and reinforcement. In addition, the following conditions are true for reinforced masonry panels:

6. Tensile forces are resisted only by the steel reinforcement.
7. Reinforcing is completely surrounded by and bonded to masonry material.
8. Reinforcing is stressed equally about the center of gravity of the bars.

Conventional practice with masonry construction allows higher design stresses when a competent inspector is present during construction. Design of masonry panels is based on these higher allowables since quality construction control is an integral part of the process. Material conformance to specifications, full bed and head joints with solid units and proper curing are all part of this inspection. Since fabrication usually takes place in a limited, accessible area, proper inspection is easier than it would be with in place construction.

High-Bond Mortars

Within recent years a number of companies have developed products which increase the bond strength of mortar to masonry units as well as the tensile and compressive strength of both the mortar and masonry. Design theory for masonry with high-bond mortar is based on an uncracked section, with higher allowable stresses. All pertinent design factors such as slenderness reduction and eccentricity of applied loads must be considered. In lieu of the high-bond mortar additive manufacturer's information on such matters, the practices of a recognized masonry design manual are acceptable (4,8).

While the actual design values established by the additive manufacturers may be different numerically, they are determined by product testing and factors of safety recognized by the masonry industry. Table I contains a list of allowable design stresses based on wall testing. This method should be used if there is no design data available from the manufacturer or governing building code. Care should be taken to assure that the brick used to build the panels develop the required design stress. It is not economical to use steel

reinforcement with high-bond mortar and this practice is not advised unless ductility is required.

Table I. Recommended Allowable Design Stresses (5)

<u>Stress</u>	<u>Symbol</u>	<u>Value</u> ^(a) pounds per square inch
Compressive		
Axial	F_a ^(b)	$0.25f'_m$ ^(c)
Flexural	F_b	$0.33f'_m$
Tensile		
Flexural	F_t	$0.30f'_t$ ^(d)
Shear	F_v	100
Bearing	F_m	$0.25f'_m$
Modulus of Elasticity	E_m	3,000,000

(a) Values may be increased by 1/3 when considering wind, blast or earthquake, provided the section thus formed is not less than that required by other factors.

(b) Effects of slenderness and eccentricity must be considered. See appropriate design literature.

(c) Testing procedure to determine f'_m shall be in accordance with ASTM E447, Standard Methods of Test for Compressive Strength of Masonry Assemblages, Method B (1).

(d) Testing procedure to determine f'_t shall be in accordance with ASTM E72, Standard Methods of Conducting Strength Tests of Panels for Building Construction, Uniform Transverse Load-Specimen Vertical (1).

Conventional Mortar and Reinforcement

Masonry panels fabricated with conventional mortar and steel reinforcement are designed in the same manner as laid in place masonry of the same materials. The following design criteria can be used for the materials indicated:

- a. solid brick masonry - Recommended Building Code Requirements for Engineered Brick Masonry (8).
- b. hollow clay masonry - Building Code Requirements for Reinforced Masonry (3).
- c. concrete masonry - "Concrete Masonry Structures - Design and Construction" (4).

The use of the partially reinforced provisions of each of these codes will provide the most economical steel schedule. All of these references include information on mortar and grout. The designer should call for the lowest strength mortar and the most fluid grout possible. Masonry's unique curing conditions result in optimum strength and these criteria keep wall costs low.

Curtain Wall Design

In curtain wall applications the masonry panels carry wind load, windows and their own weight. Most applications will have the panels spanning vertically from floor to floor although the panel can cantilever above and/or below the floor. It is also possible for a panel to span horizontally, with attachments to columns or pilasters. Wind loads are transferred to the structural framework with the use of connection devices. Normally the panel is analyzed as a simple beam strip with continuous support along the lines of connection. If the shape of the panel warrants, a plate analysis can be used. Maximum design stresses, must not be exceeded, these of course, include the load on the connection devices.

The weight of the masonry can be taken at each floor level by a series of shear connections or carried through the lower panels to the foundation. In the first instance, a soft joint exists between panels with one line of shear connectors, preferably near the bottom of the panel, carrying the panel weight. The top of the panel is stabilized by a series of lateral connections which allow for relative movement between the panel and the structural framework. This feature is extremely important to prevent indeterminant loads from being imparted to the masonry panel.

When the entire weight of the masonry is taken through the masonry to the foundation all of the connections provide lateral support only. Vertical weight transfer is achieved by placing shims in the joint between the panels. The joint thus formed can then either be tuck-pointed with nonshrink grout or filled with a sealant backer and caulking. Normal practice is to detail the inside surface of curtain-wall panels at least 1 inch from the structural framework.

In most curtain wall applications the flexural stresses, whether resisted by high-bond mortar or vertical reinforcement, required by wind load analysis are sufficient for prefabrication. Stresses due to

lifting, transportation and erection must be considered.

Loadbearing Panels

When masonry panels are used as loadbearing walls it is necessary to investigate several additional factors. Implicit among these is the vertical load imposed by the floor members. The actual mechanism employed to transfer this load to the masonry panels will be determined by the selection of the floor members, but sufficient bearing must be obtained. Three inch penetration into the bearing wall is generally accepted as a minimum regardless of the structural system. Increasing this value will obviously reduce the eccentricity of the applied load. In many instances with loadbearing panels it will be necessary to develop diaphragm action between the wall and floor. Perhaps the easiest method of achieving this feature is to have reinforcing bars embedded in the panel bent into a concrete topping cast onto the floor deck. In the absence of such a topping, weld plates or bolted shear connections can be used. Continuity between panels, of major importance when considering resistance to progressive structural collapse, is attained by using this same type of connection between adjoining panels. Both horizontal and vertical continuity can be realized in this manner. Complete design investigation should include building overturning as well as the above factors.

Several organizations now have computer programs available for a complete analysis of loadbearing masonry buildings. Check with local firms for further information.

Connection Details

Masonry panels are attached to other structural members in the same manner as other premanufactured building elements. Slight modifications in form, however, do exist with prelaid masonry panels. Connections of masonry panels must be adequately designed to transfer all of the applied loads. Design generally considers live, wind, seismic and dead loads. Although the use of the masonry panel, whether a curtain wall or loadbearing application, will determine the actual loads and thus connection spacing, it is customary to use a maximum spacing of 4 feet in order to maintain the effect of a continuous support. Connection spacing greater than twelve times the nominal wall thickness requires an analysis of bending between anchors. In order to develop the full design value of the various connection devices the minimum dimension as shown in Table II should be followed. All inserts in masonry shall be coated with a corrosion resistant metal such as copper, zinc or cadmium. The entire connection detail must be designed to have sufficient dimensional tolerance to allow for variations in the building frame, as well as the thermal and/or frame movement expected within the life of the building. Typically a minimum of 2 inches is detailed. Typical connection details are shown in Figure 2.

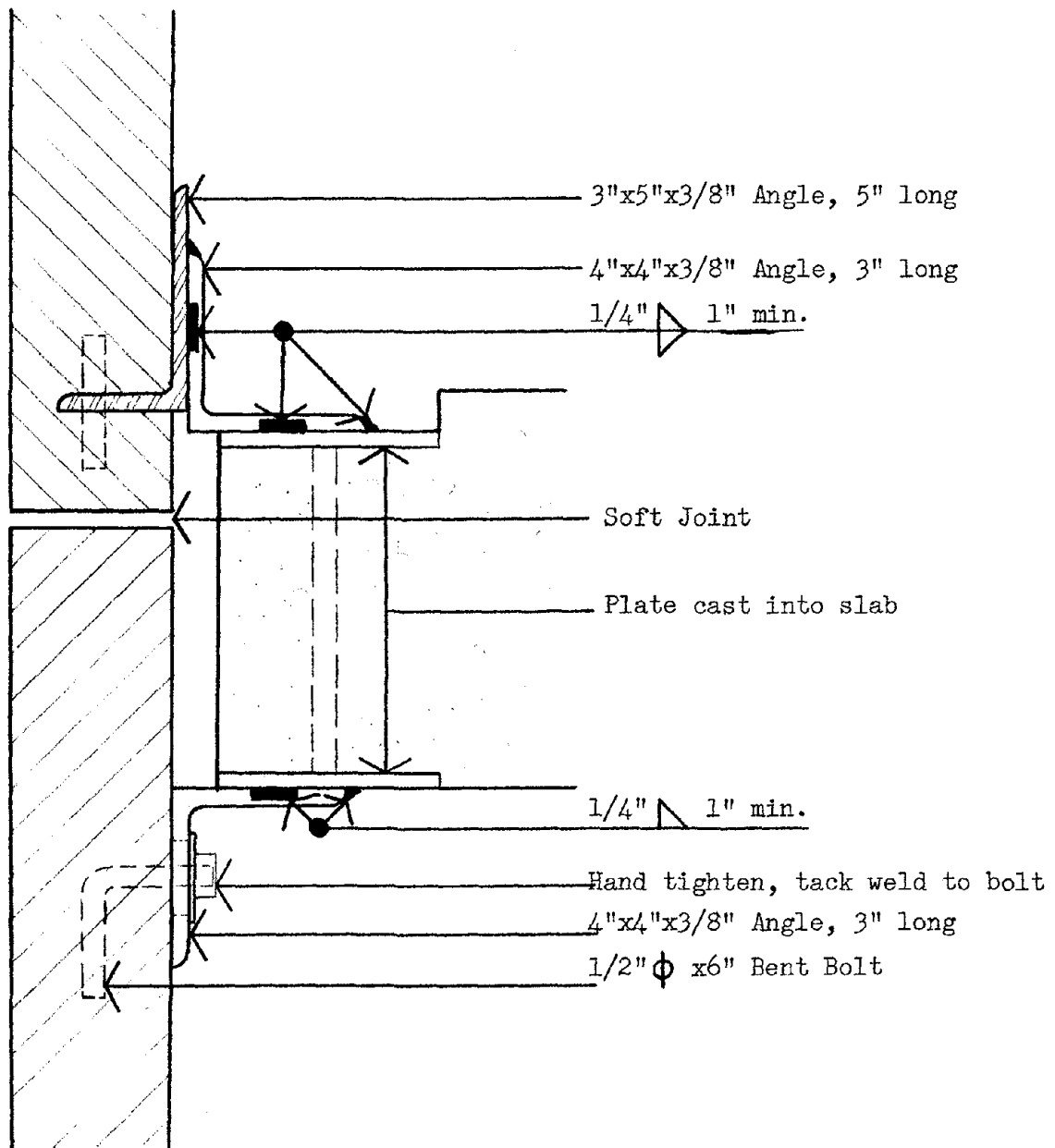


Figure 2. Typical Panel Connection Details

Table II. Minimum Dimensions for Connections to Develop Full Strength, in inches

<u>Location</u>	<u>Connection Load</u>	
	<u>Pullout</u>	<u>Shear</u> (direction of load)
Distance from edge	4	4 (parallel to edge) 8 (perpendicular to edge)
Distance between connections	12	12

There are three basic inserts which work well with masonry panels. The first is a 1/2 inch diameter bolt, 6 inches long, with a 90° bend. Two 3 inch legs or 2 and 4 inch legs are most common. The bolt is inserted into the mortar joint, the core of the brick or a notch in the brick. In all cases the bolt is completely surrounded with mortar, having a minimum of 4 inches embedment. The threaded leg of the bolt protrudes perpendicular to the masonry and provides a means of attaching a clip angle or ledger beam to the masonry. A typical clip angle is a 3 inch long piece of 4" x 3" x 3/8" or 4" x 4" x 3/8" angle, with a 9/16 inch by 2 inch vertical slot for the bolt to pass through. Connection bolts normally meet the requirements of ASTM A307. All loose steel items are ASTM A36 and should be primed and painted, coated with an impervious finish or corrosion resistant metal as circumstances dictate.

If a bolt/clip angle combination is used to transfer shear it is recommended that the nut be hand tightened and then welded to the clip angle. This will result in a positive transfer of load without the possibility of slipping between the masonry and clip angle. When a bolt/clip angle connection is used for pullout, that is lateral load only, it is advised that the nut be hand tightened and the nut tack welded to the bolt. This will allow a transfer of load perpendicular to the panel and relative movement between the panel and building frame in the direction of the slot. Such a lateral load connection attached to a steel frame is shown in Figure 3.

A weld plate in the plane of the masonry can be achieved by placing one leg of an angle into a bed joint of the masonry. A stud, normally 1/2 inch x 3 inches, is attached to this leg to provide pullout resistance. The remaining leg of the angle is placed tight



Figure 3. Lateral Load Connection

against the face of the masonry. Normally a 3" x 5" x 3/8" angle, 5 inches long, is used with the 3 inch leg embedded in the masonry. This type of detail can carry a greater shear load than a bolt because of the increased bearing surface. As indicated in Table III, the design value in shear is determined by the bearing area, A_b , and the ultimate compressive strength of the masonry, f'_m .

The third method of transferring loads from the masonry panel to other building components is to embed reinforcing bars into each. This technique relies on the development length of the particular bar diameter used to accomplish this transfer. Values of these lengths are readily available in the concrete design literature, as are the loads carried by the various bar sizes.

Table III. Design Values for Connection and Lifting Devices, in Pounds

Item	Mortar	Pullout	Shear
1/2" x 6" Connection Bolt	High-bond	750	1250
	Conventional	350	550
Connection Angle with 1/2" x 4" Stud	High-bond	750	$0.25f'_m A_b$
	Conventional	350	$0.25f'_m A_b$
1/2" x 10" Lifting Bolt	High-bond	2100	1250
	Conventional	550	550

Lifting Devices

Masonry panels are lifted by one of several methods. The most prevalent of these is to embed bolts or lift pins in the top courses and have them protrude from the top of the panel. When high-bond mortar is incorporated in the panel manufacturing, these items are embedded at least 8 inches into the masonry. Lifting forces are distributed to the entire panel when conventional mortar is used by tying the lifting item into the reinforcing steel. Several proprietary lifting devices are being successfully used with masonry panels. Design values for a typical lift bolt are found in Table III. It is necessary to consider any inclination of the lifting cables when determining the number of lifting items required.

Slings, straps or belts circling the panel allow it to be lifted from the bottom. Individual units or mortar joints are often omitted to provide a location for such devices.

FABRICATION REQUIREMENTS

Shop Drawings

There are two key features important in masonry panelization which are not included in conventional construction. First is the preparation of shop drawings. Prepared by the design or the panel fabricator, these drawings provide all the information necessary to manufacture and place the panels. Included are the location and designation of each panel on the project, the method, size and type of connections, insert placement on both the panel and structure and joint treatment. The detailed description of each panel contains all actual dimensions, opening size and location, inserts and location, bond, coursing, number of each required and weight. The approval of the shop drawings by the architect, engineer and general contractor is necessary prior to panel fabrication.

Quality Control

The second significant item is the quality control program. This is extremely important when high-bond mortar is used. Compatibility with the brick selected by the architect and manufactured for the project must be verified. Flexural prism tests made in accordance with ASTM E518, Flexural Bond Strength of Masonry, must achieve the minimum stresses specified by the engineer. A test of a seven brick high prism is shown in Figure 4. All materials should be tested to assure conformance with job specifications.

Job specifications should call for regular testing during the course of panel production. A minimum of three flexural specimens should be made on each shift. Mortar, grout and masonry compressive prisms should be sampled on loadbearing jobs. When a high-bond additive is used each batch of mortar should be sampled according to the manufacturer's recommendation. Accurate records must be maintained to assure the designer, builder and owner of proper performance of the masonry.

Transportation and Erection

The techniques used to handle and install masonry panels are similar to those used by other premanufactured building components. When built offsite, flat bed trucks are used to move the panels (Figure 5). Once at the site, each panel is lifted by a crane and installed in its proper location (Figure 6). Forklift trucks or special cradles have also been used to lift masonry panels.

The panels are usually placed on shims or wedges in their approximate position by the crane. They are temporarily secured to release the crane for the next panel. Final alignment is achieved and the permanent connections made. Lifting bolts are burned off to allow placement of adjacent components.

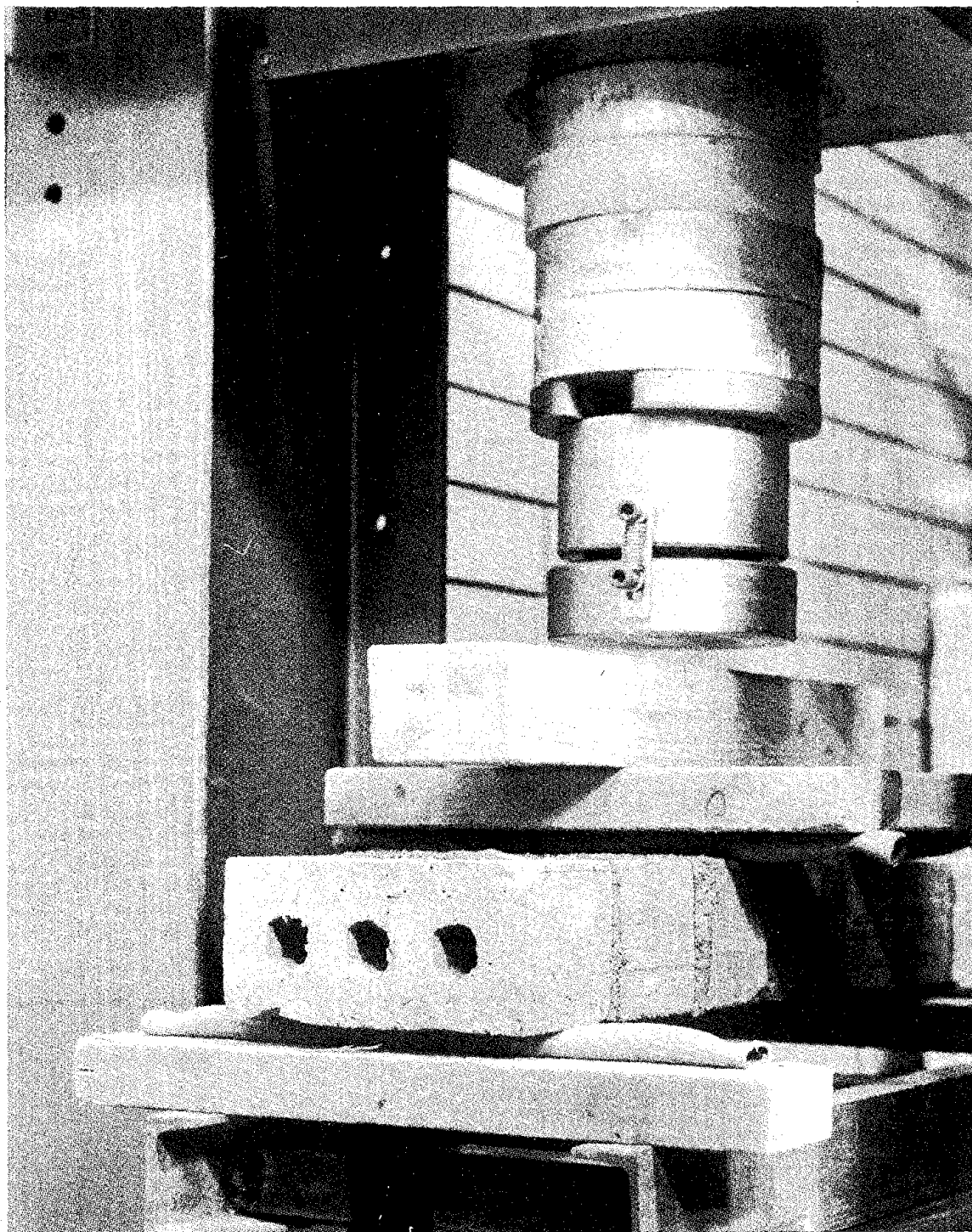


Figure 4. Flexural Prism Test

114-16

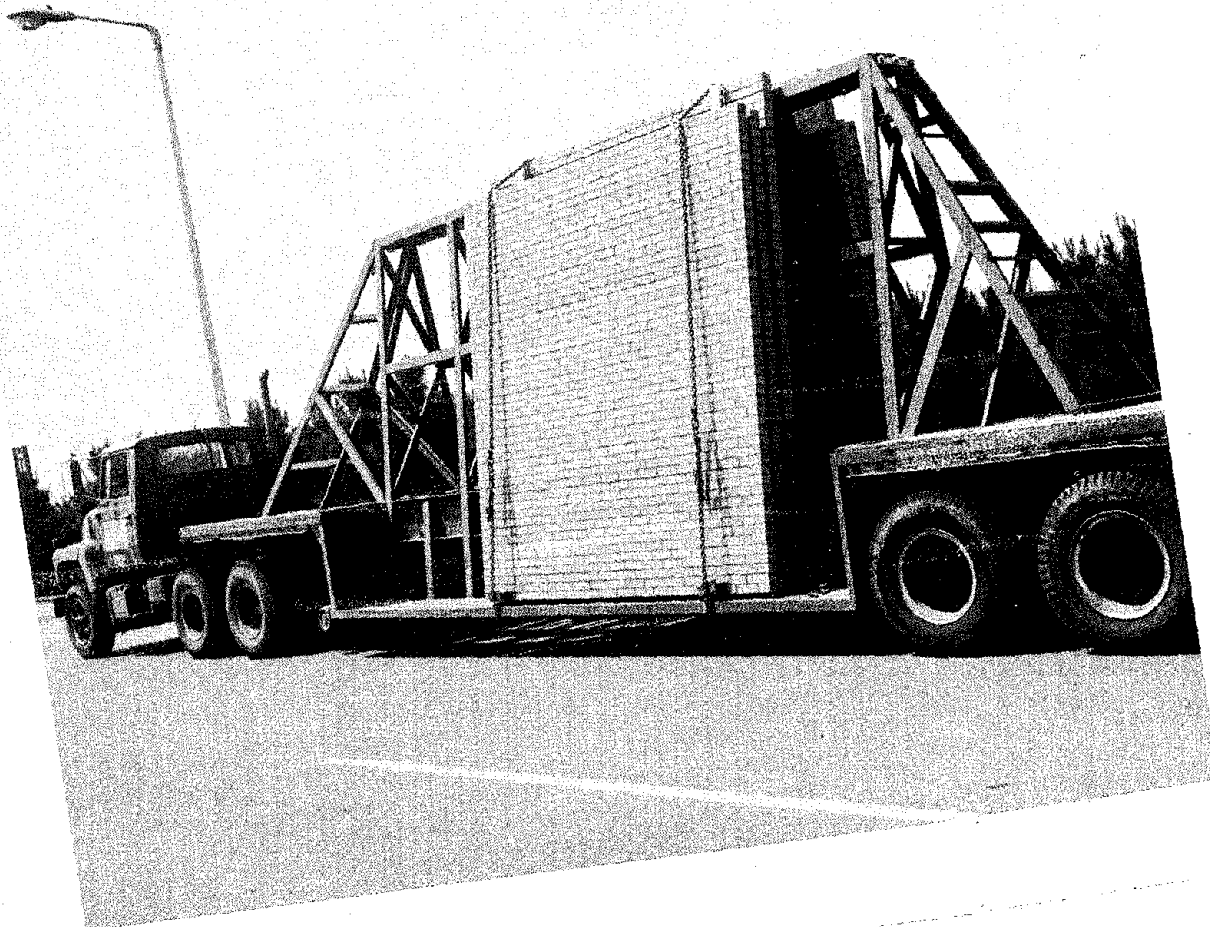


Figure 5. Shipping Masonry Panels

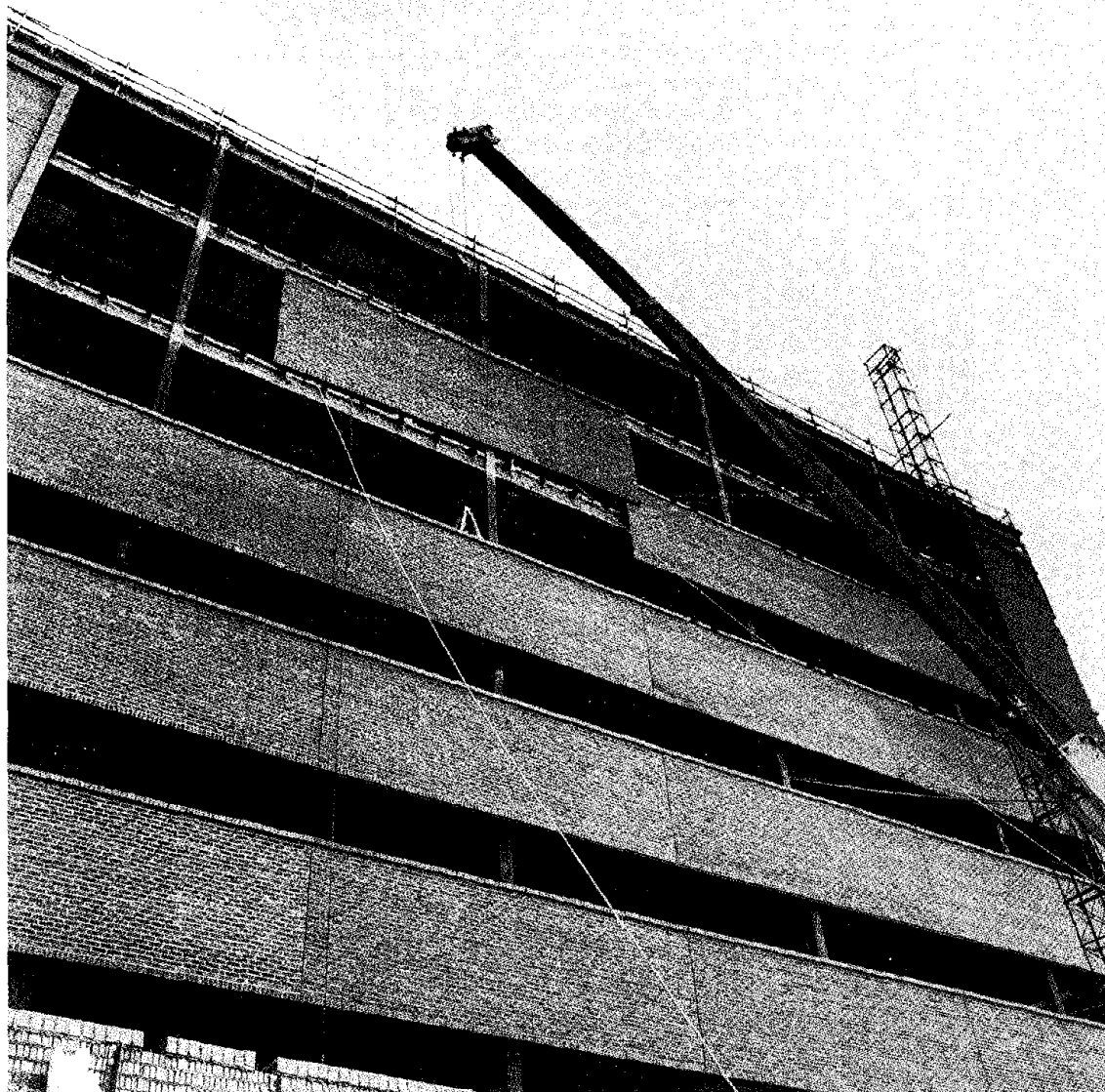


Figure 6. Masonry Panel Erection

SUMMARY

The design flexibility inherent with masonry construction has made hand built panels predominant. Returns, projections, corbels, special bonding arrangements and any sized panel can be incorporated since the panels are custom made. Fixed size, machine produced panels have not proven acceptable in the North American marketplace.

Either of two methods can be used to construct masonry panels. The difference is in the manner of resisting tensile forces. The first is to use a high-bond additive which imparts higher bond and tensile stresses to the masonry. A combination of conventional mortar, steel reinforcement and grout is the second. The reinforcement is placed vertically and/or horizontally as required.

Both techniques must have a proper analysis of imposed loads to provide structural integrity. Wind load, dead load, differential movement and connections must be given consideration. Shop drawings and a stringent quality control program are necessary.

APPENDIX I - REFERENCES

1. Annual ASTM Standards, Parts 16 & 18, American Society for Testing and Materials, Philadelphia, Pa., published annually.
2. Barnstone, H., The Galveston That Was, Macmillan Company, New York, N.Y., 1966, p. 122.
3. Building Code Requirements for Reinforced Masonry, American National Standards Institute, New York, N.Y., 1970.
4. "Concrete Masonry Structures - Design and Construction", Journal of the American Concrete Institute, Vol. 67, May, 1970, pp. 380-403, June, 1970, pp. 442-460.
5. D'Huy, G. J., "Design and Construction Practices for Preassembled Masonry Panels", presented at the April 14-18, 1975, ASCE National Structural Engineering Conference, New Orleans, La. (Preprint 2465).
6. Grenley, D. G., "Status of Masonry Prefabrication in North America", Proceedings of the First Canadian Masonry Symposium, University of Calgary, Calgary, Canada, June 1976, pp. 247-250.
7. Johnson, F. B., Designing, Engineering and Constructing with Masonry Products, Gulf Publishing Company, Houston, Tx., 1969.
8. Recommended Practice for Engineered Brick Masonry, Brick Institute of America, McLean, Va., 1969.
9. West, H. W. H. and Speed, K. H., Proceedings of the Second International Brick Masonry Conference, British Ceramic Research Association, Stoke-on-Trent, Great Britain, 1970.

APPENDIX II - NOTATION

<u>SYMBOL</u>	<u>MEANING</u>	<u>UNITS</u>
A_b	bearing area in contact with masonry	sq. in.
E_m	modulus of elasticity	lbs./sq. in.
F_a	allowable axial compressive stress	lbs./sq. in.
F_b	allowable flexural compressive stress	lbs./sq. in.
F_m	allowable bearing stress	lbs./sq. in.
F_t	allowable flexural tensile stress	lbs./sq. in.
F_v	allowable shear stress	lbs./sq. in.
f'_m	ultimate masonry compressive strength	lbs./sq. in.
f'_t	ultimate masonry flexural tensile strength	lbs./sq. in.

EFFECT OF MORTAR ON WATER PERMEANCE OF MASONRY

by Brown, Russell H.

ABSTRACT

Forty-eight walls were tested for water permeance according to ASTM E514-74 to determine the effect of mortar compositions and types. Wall construction was as near perfect as practicable. A single Portland cement/lime mortar and four different brands of masonry cement were tested. Each wall was a nominal eight inch thick composite parged wall built in the laboratory and cured in laboratory air. A comparison of the performance of walls in terms of Portland cement/lime versus masonry cement mortar was made. The effect of mortar type, retempering, mortar flow, air content, cube strength and water retention were evaluated. Conclusions based on these comparisons are stated, along with qualifications and limitations of the conclusions.

EFFECT OF MORTAR ON WATER PERMEANCE OF MASONRY

Russell H. Brown¹Introduction

Masonry has performed as a strong, durable, beautiful, and water-tight construction material for perhaps as many as ten thousand years. The recent development of rational structural design methods has revitalized interest in masonry among architects and engineers. The resulting thinner load-bearing walls can compete economically where they previously could not. A large percentage of masonry walls are not load-bearing, but are chosen primarily for their aesthetic and durability values. The vast majority of all such walls, whether load-bearing or not, have excellent performance records. However, when a wall fails to perform any of its required functions, it is damaging to the otherwise excellent reputation of the masonry industry. Water permeance of masonry walls is therefore a major concern of the masonry industry. The mason contractor is generally blamed for water permeance of walls due to poor workmanship, poor mortar quality, or improperly tooled joints. However, one-site inspection of walls that leak often reveals excellent workmanship and strict compliance with plans and specifications. A number of factors, in addition to workmanship, are thought to affect the water permeance of masonry walls; masonry design and detailing, compatibility of mortar with masonry units, initial rate of absorption of brick, the proper composition and proportion of masonry cement or Portland cement/lime mortars, and the compatibility of the brick and mortar selected.

In the Metropolitan Chicago area, calls on architects and engineers by local promotional personnel revealed dissatisfaction with the ability of masonry to keep water out of buildings. Similar calls on masonry contractors in the area revealed that many were involved in litigation, were being sued, or were having funds withheld on completed jobs, for reasons related solely to water penetration.

The Mason Contractors Association of DuPage County, Illinois and the Mason Contractors Association of Greater Chicago, Illinois, conducted a survey of masonry contracting firms to establish the frequency and characteristics of water permeable walls they had encountered. The most notable common denominator of problem walls reported appeared to be the use of masonry cement mortar. A research program was then undertaken to compare the permeance of walls made with several masonry cements to that of walls using Portland cement/lime mortars of different compositions, proportions and types. Using the services of an independent testing laboratory, forty-eight wall panels were tested for permeance according to ASTM E514-74 (1)². The results of the research program are presented and analyzed in this paper.

¹ Associate Professor of Civil Engineering and Engineering Mechanics, Clemson University, Clemson, South Carolina 29631.

² Numbers in parentheses refer to the Reference section of this paper.

Background

Several studies have been conducted to determine what factors affect water permeance of masonry. Fishburn (2) conducted tests on 140 walls using a test method which he developed which essentially led to ASTM E514-74. He considered fourteen kinds of workmanship, thirty-nine kinds of masonry units (many being proprietary), and ten kinds of mortar. He found that workmanship was very important in resistance to water penetration. Low brick suction and high water retentivity of mortar improved performance. Ritchie and Davidson (3) found that the factors which affected moisture penetration of brick masonry were initial rate of absorption of bricks, flow and water retention of mortar, thickness of mortar bed, time elapsed between spreading mortar and placing brick, and the energy used to bed the brick. Although their study included both masonry cement and Portland cement/lime mortars, no conclusions were stated concerning this comparison. Skeen (4) found that brick walls built of Type N Portland cement/lime mortar have considerably less water permeability than those built with masonry cement mortars. Fowler and Grimm (5) reported that good workmanship significantly improved resistance to permeability compared to that of walls of poor workmanship. They also found that the 4 inch nominal thickness brick walls leaked regardless of workmanship.

The Brick Institute of America (BIA) recommends that masonry cement mortar not be used unless its performance record is first established in laboratory tests of masonry assemblages (6). High air content and low Portland cement content of some masonry cements generally result in reduced bond according to the BIA. In contrast, the National Concrete Masonry Association (NCMA) recommends that either Portland cement/lime or masonry cement mortars are acceptable, the choice being a matter of economics and job size (7).

In summary, the literature shows that considerable attention has been given the problem of water permeance of masonry and implies that any masonry wall can leak regardless of design, materials and workmanship with the possible exception of the cavity wall. Factors which affect water permeance appear to be mortar type, flow, and water retentivity; brick initial rate of absorption; compatibility between brick and mortar; workmanship; and wall design. Recommendations from the BIA and the NCMA imply that masonry cement performs more favorably with concrete masonry units than with clay masonry units. The literature appears to be lacking in information concerning direct comparison between the performance of masonry cement mortars and Portland cement/lime mortars where water penetration is concerned.

Research Objectives and Scope

The objective of the research program reported herein was to determine the affect of mortar compositions and types on water permeance of masonry. The method selected for the evaluation was ASTM E514-74, "Water Permeance of Masonry." Four masonry cements were selected, each

from a different manufacturer. A single type of brick, concrete block and sand were used throughout the test program. Three replications of the water permeance test were performed on each of three mortar types (N, S, M) for each brand of masonry cement and Portland cement/lime mortar. An additional series of three tests was performed using Type O, Portland cement/lime mortar resulting in the testing of a total of forty-eight walls. The basic constituent materials, mortar, brick, sand and concrete block were tested for physical properties by applicable ASTM test methods.

Wall Construction

Walls were constructed on the site of the independent testing laboratory using experienced journeyman masons using workmanship which might be considered nearly "perfect". For every three masons there was a supervisor responsible for maintaining records and inspecting workmanship. All walls consisted of a nominal four inch wythe of brick, a nominal four inch wythe of concrete block, and a 3/8 inch parging (Fig. 1). Care was exercised to ensure full mortar bedding under the first course of brick and in all head and bed joints. Continuous galvanized joint reinforcement certified to be in compliance with ASTM A82 was placed in bed joints every 16 inches and completely embedded in mortar (Fig. 2). The portion of the upper and lower flashing within the wall was completely embedded in mortar (Fig. 3). Ends and tops of panels were filled with mortar. Mortar was proportioned by volume (Fig. 4) using sand, Portland cement, lime, and masonry cement in compliance with applicable ASTM Standards. Mortar was mixed in a 9 cubic foot mixer for five minutes after all ingredients were in the mixer. A new batch of mortar was mixed for each wall. Some mortars were retempered as required to maintain a workability acceptable to the mason. All mortar joints were tooled with a round jointer when thumbprint hard. Walls were washed according to the recommendation of BIA Technical Note 20 (6), Cleaning Dark Brick, Procedure B. Nominal dimensions of the wallettes were 49 inch lengths, 59 inch height and 8 inch thickness. Table 3 reports the amount of original mixing water used, mason comments and start and completion times of each wall. Time and quantity of retempering water is given in Table 4.

The author was not present during the construction of any of the wall specimens. However, the testing lab certified that the construction was in accordance to the methods described herein, and inspection of completed walls by the author confirmed much of the procedure.

Material Properties

Results of tests for brick and concrete block properties are presented in Tables 1 and 2. Mortar properties are presented in Tables 3 and 4 and results of permeance tests in Table 5. All tests were performed in strict compliance with ASTM standards. Mortar specimens were prepared and tested for compressive strength as follows: two inch cubes for all walls, three inch by six inch cylinders for thirty-four walls, and two inch by four inch cylinders for twelve walls.

Permeance Tests

All wall specimens were stored in laboratory air for at least

twenty-eight days prior to testing. Eight test chambers were constructed to facilitate a more rapid testing program (Fig. 5). Each wall was subjected to a twenty-four hour preconditioning period, a twenty-four hour minimum drying period, and a seventy-two hour test period. An estimate of the extent of damp wall area was made at the end of each twenty-four hour interval of the test period as well as after preconditioning. The volume of water in each flashing was measured separately at the end of each twenty-four hour interval of the test period (Fig. 6). Time for appearance of moisture through the wall, first visible water, and first leakage were recorded. As a result of the extensive familiarity with ASTM E514 which resulted from the test program, several modifications to the method will be recommended to ASTM Committee E6. The reproducibility or within-test variation was very high. However, the method was generally satisfactory and appeared to achieve its intended purpose of establishing a measuring device to measure the water permeance of walls.

Test Results and Analysis

Results of all measurements taken from permeance tests are shown in Table 5. Demonstration of correlation or lack of correlation between permeance and other parameters is shown in Figure 7 through Figure 14. Each parameter will be discussed herein.

Portland cement/lime vs. Masonry Cement Mortar - Figure 7 and 8 conclusively illustrate that walls constructed with Portland cement/lime (PCL) mortars are superior to masonry cement (MC) mortars (MCl-MC4) in resisting water permeance for the materials tested. The average of the total water accumulating on the lower flashing at the end of seventy-two hours (Fig. 7, dashed line) for PCL mortar was 812 ml, with five of nine walls without measurable leakage. If the Type 0 mortars are included in the group (PCL 10-12), the average is 815 ml, with seven of twelve without leakage. In contrast, walls of MCl through MC4 averaged 1964, 3977, 2291 and 3265 ml, respectively. Of the nine walls of each mortar type tested, only 3, 1, 1, and 0 respectively had no measurable leakage to the lower flashing at seventy-two hours. Equally conclusive observations can be made at the end of twenty-four hours or forty-eight hours.

Total water accumulating on the upper flashing was even more impressively in favor of PCL mortar. Average measured leakages for PCL, MCl-MC4 (Fig. 8 dashed line) were 270 (202 if Type 0 included), 2735, 1812, 5289 and 6774 ml, respectively. Only two of nine walls of PCL mortar leaked to the upper flashing compared to nineteen of thirty-six walls of MC mortar. If Type 0 mortars are included, only two of twelve walls of PCL mortar leaked to upper flashings.

Overall performance of walls can probably best be evaluated by the combined leakage accumulated in both the lower and upper flashing. Again PCL mortar walls were less permeable, with average total leakage of 1082 ml (1017 including Type 0) compared to 4700, 5790, 7580 and 10,040 ml, respectively for walls of MCl-MC4 mortars. In walls of PCL mortar, five of nine (seven of twelve including Type 0) did not leak measurably, whereas only five of thirty-six MC mortar walls did not leak.

The extent of damp area also illustrates a better performance of PCL mortar to MC mortars, but not as strikingly. At the end of seventy-two hours, walls of PCL mortar averaged 15% damp areas whereas the walls of MC1-MC4 averaged 23%, 31%, 26% and 26% respective damp area (Fig. 9). No dampness was observed in two of nine PCL mortar walls (two of twelve including Type 0) compared to two of thirty-six mortar walls.

Comparison between the four masonry cement mortar walls illustrates a wide variation in resistance to water permeance. Comparison of the total water in both the upper and lower flashing (the sum of the mean values in Fig. 7 and 8) reveals that walls of MC1 mortar were least permeable (4700 ml), followed by MC2 (5790 ml), MC3 (7580 ml), and MC4 (10,040 ml). Comparison of the number of walls that did not have measurable water permeance results in essentially the same ranking: MC1 had three; MC2 had one; MC3 had one; and MC4 had none. Of all the mortars considered, including both MC and PCL, only one had no measurable leakage to either flashing for the entire wall test series, MC1, Type M.

Effect of Mortar Type - Four types of mortar (N, S, M and O) were used in the test program. A comparison of wall performance on this basis is shown in Figs. 10, 11 and 12. Permeance of the brick wythe, as measured by water in lower flashing, was higher for Type N than for Type S and M mortars with average quantities of 4174, 1691 and 1520 ml (Fig. 10). The difference between walls of Type S and M mortars was not significant. No measurable water was detected in the lower flashing of two of fifteen walls of Type N mortar compared to three of fifteen for Type S and five of fifteen for Type M. Similar analysis of Fig. 11 shows that walls of Type S mortar are less permeable than M or N. Combining the upper and lower flashing water accumulation (Fig. 12) implies Type S is least permeable, followed by Type M and finally Type N. Type O mortar had no upper flashing water and less lower flashing water than the other types. However, the Type O data includes only PCL mortars and is not a fair comparison.

When the Portland cement/lime mortars are considered alone, Fig. 12 indicates that Type N and Type S mortars performed almost equally, and both performed better than Type M mortars.

Retempering - Eleven walls were made using mortar the mason chose to retemper (Table 4). Five of twelve walls of PCL mortar required retempering, and only six of thirty-six walls of MC mortar were retempered. Retempering had no apparent adverse effect on water permeance. The average total water in both flashings was less for retempered mortar (2731 ml) than for the entire group (5524 ml). The likelihood of zero leakage changed slightly due to retempering. Four of eleven retempered walls did not leak (36%) compared to twelve of forty-eight for the entire group (25%).

Mortar Flow - Initial flow of mortar was measured for every wall constructed. Inspection of the data reveals a decrease in total permeance water with increase in flow (Fig. 13). The trend was verified by a linear regression analysis which produced the expression for the straight line approximation shown on the figure. The author does not feel that the correlation coefficient for this expression (0.452) is

sufficiently high to justify adoption of the mathematical expression for other applications. The expression does, however, demonstrate a relationship between flow and water permeance.

Air Content - The air content of mortar can be divided essentially into two groups: PCL mortars with air ranging from 3.0 to 5.1% and MC mortar from 11.1 to 17%. Since there was no data for mortars between these ranges, it is difficult to reach any conclusions about air content. However, non-linear regression analysis produced the mathematical expression shown in Fig. 14. A correlation coefficient of 0.48 indicates the lack of a strong correlation between the data and the mathematical expression. However, both the data and the expression demonstrate an increase in water permeance with increased air content.

Cube Strength - Linear regression analysis of cube strength and total water permeance data indicated no apparent relationship. A correlation coefficient of under 0.10 shows virtually no dependence between the two variables.

Water Retention - There was no apparent relationship between water permeance and the water retention of the mortar. A correlation coefficient of 0.18 indicated a very weak dependence between the two quantities. If the water retention had varied over a wide range, a relationship would probably have been detected. However, the value of water retention was not systematically varied and a relationship was not established.

Mason Comments - Most walls were constructed of mortar considered satisfactory by the mason. Fourteen of forty-eight walls, however, were built of mortar which had some deficiency in the opinion of the mason (Table 3). The performance of this group of walls was not impaired appreciably when compared to the entire group. The average total leakage increased slightly (5848 ml compared to 5524 ml at 72 hours), but the 6% increase is not significant when compared to 134% coefficient of variation.

Rate of Permeance - Most of the walls with measurable leakage showed a reduced rate of leakage with time as illustrated by a reduction in slope with time (Fig. 15, 16 and 17). Several explanations for this phenomenon have been proposed. One explanation is the clogging of openings by fine particles carried by the water. During the preconditioning period, the leakage would probably exceed that of any other period; however, measurements were not taken. Another explanation is the additional curing afforded the mortar as testing progresses.

Water Permeance Ratings - Each wall was rated according to the criteria of ASTM E514, paragraph 8. Ratings are divided into five levels, the least permeable being Class E followed by Class G, F, P and L. Table 5 includes the water permeance rating.

Walls of PCL mortar had the most walls with the Class E rating (3), followed by MC1 and MC3 (each with two), and finally MC2 and MC4 (each with none). The worst rating observed in the program was Class P as

follows: PCL (2), MC1 (1), MC2 (3), MC3 (2), and MC4 (2). All remaining walls were rated Class F.

Comparison of the ratings in terms of mortar type shows Type N and Type M mortar each with three Grade E ratings and Type S with one. Grade P ratings were Type S (1), Type N (4), and Type M (5). The remaining walls were rated Class F.

The small sample of three walls of Type O mortar rated very high, two Grade E and one Grade F.

The author feels that the ratings systems were heavily affected by the subjective observation of time for appearance of first visible water. In almost every case, this single observation governed the wall rating.

Summary and Conclusions

Forty-eight walls were tested for water permeance according to ASTM E514-74 to determine the effect of mortar compositions and types. Test results led to the following conclusions for the materials tested:

- a) Walls constructed of Portland cement/lime mortars are more resistant to water permeance than those constructed of masonry cement mortars.
- b) For the masonry cement mortars tested, Type S mortar is slightly superior to Type M mortar and significantly superior to Type N mortar in resisting water penetration.
- c) For Portland cement/lime mortars tested, Type N and Type S mortars ranked approximately the same, both being superior to Type M mortar in resisting water permeance.
- d) Retempering of mortar has no adverse effect on water permeance.
- e) An increase in mortar flow improves the resistance to water permeance.
- f) Water permeance increases with air content of mortar.
- g) Even with excellent quality workmanship, some leakage should be expected in the type of walls tested.
- h) The rate of leakage reduces with time.
- i) Resistance to rain penetration varies significantly for different masonry cements tested.

Recommendations for Future Testing

The complexity and expense of performing the ASTM E514-74 tests limited the number of variables considered herein. Further studies should be performed with the following controlled variables:

- 1) Initial rate of absorption of brick.
- 2) Air content of mortar.
- 3) Initial flow of mortar.
- 4) Bond strength between mortar and masonry units.

Acknowledgements

The testing program was conceived by the Mason Contractors Association of DuPage County, Illinois, and joined and supported by the Chicago Masonry Institute Promotion Trust, the Masonry Advancement Cou-

cil of DuPage County, Illinois, Mason Contractors Association of Greater Chicago, and the Masonry Industry Fund of Northwest Indiana. The Fox Valley Mason Contractors Association of Illinois, the Mason Contractors Association of Lake County, Illinois, the Mason Contractors Association of Northwest Indiana, and the Masonry Promotion Fund of Lake County, Illinois, encouraged the testing program and provided their cooperation as needed. Frank Janko of the D. H. Johnson Company, mason contractors, Colin Munro, Executive Director of the Chicago Masonry Institute, and Robert and Richard Nelson, H. H. Holmes Testing Laboratory, provided considerable expertise and supervision of the testing program.

The efforts of all of these organizations and individuals are gratefully acknowledged.

References

1. "Standard Method of Test for Water Permeance of Masonry," Annual Book of ASTM Standards, Part 18, American Society for Testing and Materials, 1974.
2. Fishburn, Cyrus C., "Water Permeability of Walls Built of Masonry Units," Building Materials and Structures, Report BMS82, April 15, 1942, pp. 37.
3. Ritchie, T., and Davison, J. I., "Factors Affecting Bond Strength and Resistnace to Moisture Penetration of Brick Masonry," Symposium on Masonry Testing, ASTM STP 320, New York, 1962, pp. 16-30.
4. Skeen, J. W., "Experiments on the Rain Penetration of Brickwork," Transactions, British Ceramic Society, Vol. 70, No.1, 1971, pp. 27-30.
5. Fowler, D. W., and Grimm, C. T., "Effects of Sandblasting and Face Grouting on Water Permeance of Brick Masonry," Masonry: Past and Present, ASTM STP 589, 1975, pp. 255-271.
6. "Portland Cement-Lime Mortars for Brick Masonry," BIA Technical Notes on Brick Construction, #8, Brick Institute of America, Sept. 1972.
7. "Mortars for Concrete Masonry," NCMA-TEK 20, National Concrete Masonry Association, 1970.
8. "Cleaning Clay Products Masonry," BIA Technical Notes on Brick Construction, #20, Brick Institute of America, May, 1964.

Table 1
Analysis of Brick
by
ASTM C67-73

Sample	Absorption (%) 24 hr. Submersion	Absorption (%) 5 hr. Boiling	Saturation Coefficient	Initial Rate of Absorption grams/30 in ²	Compressive Strength psi
1	6.4	9.0	.71	12.7	7883
2	7.2	9.8	.73	15.3	8695
3	6.5	9.1	.71	14.6	8148
4	6.9	9.5	.72	14.6	7928
5	<u>7.2</u>	<u>9.8</u>	<u>.72</u>	<u>16.6</u>	<u>7519</u>
Average	6.84	9.44	.72	14.76	8035

Nominal Size: 8-9/16 x 3-7/8 x 2-3/4 in., 4 cores

Table 2
Analysis of Concrete Block
by
ASTM C140

Sample No.	Unit Wt. lbs/ft ³	Absorption %	Moisture Content (%)	Compressive Strength Gross Area	psi Net Area
1	113	13.5	37.6	1573	2458
2	112.8	11.8	44.7	1501	2346
3	113.7	12.1	34.8	1664	2600
4	113.8	12.5	35.3	1429	2233
5	<u>114.1</u>	<u>12.7</u>	<u>37.3</u>	<u>1467</u>	<u>2289</u>
Average	113.5	12.5	37.9	1526	2385

Nominal Size: 4 x 8 x 16 in., 3 cells

Table 3.

Sample	Mortar Type	Mixing Water Gal.	Retemp ¹	Mortar Properties									
				Time Start	Time Comp.	Mason ² Comments	Air Content %	Initial Flow %	Water Retention %	Cube ³ Strength psi	Cylinder 2 x 4 in. ⁴ psi	Strength 3 x 6 in. ⁵ psi	
PCL	1	N	11.88	No	1:45	3:10	-	4	109	87.9	802	-	765
	2	N	12.5	No	12:04	1:10	Sandy	-	120	-	1207	-	-
	3	N	11.25	Yes	2:25	4:20	-	-	119	-	1457	-	-
	4	S	15.25	No	1:00	2:05	-	4.1	120	89.2	2868	-	3135
	5	S	14.88	No	12:45	2:10	Too Rich	3.9	120	86.7	3070	-	3357
	6	S	18.75	Yes	1:22	3:40	Too Wet	-	114	-	2866	-	-
	7	M	12	No	11:35	2:00	Poor Work-ability	4.5	133	88.7	4192	-	4009
	8	M	12	Yes	11:17	1:45		5.1	132	89.4	3598	-	3272
	9	M	11	Yes	1:50	3:30		-	108	-	4750	-	-
	10	O	17	Yes	1:57	3:35	-	3.0	115	90.4	580	-	-
	11	O	16	No	2:05	3:20	-	3.7	117	91.0	617	-	723
	12	O	19	No	11:46	1:10	-	-	109	-	795	-	-
MC1	1	N	6.38	No	11:07	12:50	-	12.4	112	85.7	715	-	707
	2	N	8	No	8:47	10:25	-	-	109	-	990	-	-
	3	N	9	Yes	11:28	1:55	Poor work-ability	-	104	-	1072	-	-
	4	S	11	No	12:05	1:33	-	15.0	116	87.9	1752	1463	1511
	5	S	12.25	No	11:39	1:20	-	14.9	118	86.4	1683	1677	1632
	6	S	6.5	Yes	9:50	11:23	-	-	100	-	1827	-	-
	7	M	6.5	No	8:35	10:15	-	15.0	116	79.3	2130	2234	1906
	8	M	6.88	No	8:35	10:03	-	13.7	120	76.7	2123	2176	2008
	9	M	8.38	No	10:36	11:46	-	-	114	-	2360	-	-
MC2	1	N	7.25	No	10:36	11:56	-	14.0	108	89.0	875	-	938
	2	N	7.25	No	8:50	10:15	-	13.9	102	92.1	878	-	1044
	3	N	8.5	Yes	11:07	1:15	-	-	117	-	982	-	-
	4	S	8.25	No	1:29	2:43	-	15.1	120	90.0	1348	-	1440
	5	S	8.38	No	1:16	3:07	Fast Set	15.9	112	91.1	1645	-	1550
	6	S	8.06	No	12:58	2:17	-	17.0	108	87.0	1757	-	1436
	7	M	8.42	No	9:21	10:45	-	12.0	114	87.7	2720	2556	2187
	8	M	7.25	No	9:03	10:30	-	11.1	120	86.6	2695	2796	2540
	9	M	8	No	8:54	10:20	-	13.8	116	89.6	2628	2830	2790
MC3	1	N	6.25	No	10:06	11:13	-	14.0	100	86.0	960	-	3071
	2	N	6.88	No	9:33	11:00	Hi Shrink	14.9	102	86.3	903	-	818
	3	N	9.5	Yes	1:48	3:30	-	-	120	-	972	-	-
	4	S	10	No	2:21	3:29	-	12.9	120	90.0	1458	-	1508
	5	S	11	No	12:05	3:18	No Body	12.9	124	87.0	1260	-	1460
	6	S	11.67	No	1:50	2:59	-	12.8	114	93.0	1455	-	1420
	7	M	7.5	No	10:37	12:03	-	15.1	100	88.0	2952	2898	2705
	8	M	6.63	No	10:19	11:30	-	16.0	106	90.5	2415	2268	2193
	9	M	8	Yes	1:30	2:50	-	-	118	-	2140	-	-
MC4	1	N	7	No	9:21	11:10	Lumpy	13.4	111	81.0	1553	-	1520
	2	N	7.75	No	9:10	11:05	Too Rich	12.6	108	79.6	957	-	930
	3	N	8	Yes	11:44	-*	-	-	120	-	902	-	-
	4	S	7.88	No	8:36	9:48	-	14.2	104	82.3	1567	-	1329
	5	S	7.5	No	3:00	4:00	-	12.8	104	84.6	1238	-	1220
	6	S	6.97	No	2:40	4:00	Too Rich	11.8	112	89.3	1342	-	1201
	7	M	8.25	No	11:19	1:12	-	16.1	100	86.0	1532	1314	1297
	8	M	8.5	No	11:07	12:20	-	14.8	111	90.1	1478	1329	1444
	9	M	8	No	10:52	12:28	Poor Work-ability	15.4	105	91.4	1343	1539	1344

¹ Time and quantity of retempering in Table 4

² Mason comments generally satisfactory except as noted.

^{3,4,5} Average of 3 specimens.

* Insufficient mortar quantity - Panel completed 3 days later.

Table 4
Retempering of Mortar

Sample	Retemper Time	Retemper Water, oz.
PCL-3	2:53	6
	2:58	30
	3:18	6
	3:25	36
	3:40	6
PCL-6	Unknown	5 x 6
PCL-8	1:20	36
PCL-9	Unknown	3 x 6
PCL-10	2:55	6
	3:00	32
	3:23	18
MC1-3	11:45	4
	11:55	12
	12:12	12
	12:20	4
	1:00	36
	1:25	18
	1:45	18
MC1-6	Unknown	2 x 6
MC2-3	1:00	12
MC3-3	2:40	6
	2:50	6
	3:02	12
	3:05	30
MC3-9	2:20	6
MC4-3	1:00	36

Table 5.

Results of Water Permeance Tests

Sample	Mortar Type	Appearance of Moisture Hours	Visible Water Hours	Time to 1st. Leak Hours	Total Lower Flashing Water, ml				Total Upper Flashing Water, ml				PC*	Extent of Damp Area, %			Rating
					1	2	3	Total	1	2	3	Total		1	2	3	
PCL-1	N	2	46	-	-	-	-	-	-	-	-	-	7.1	6.5	6.7	7.2	E
2	N	-	-	-	-	-	-	-	-	-	-	-	-	-	-	-	E
3	N	< 1	1	-	617	456	247	1320	240	144	144	528	-	-	-	20.0	P
4	S	8	20	-	-	-	-	-	-	-	-	-	6.8	6.5	7.1	9.9	F
5	S	4.75	10	< 24	1290	400	80	1770	-	-	-	-	1.7	11.8	12.9	11.2	F
6	S	-	-	-	-	-	-	-	-	-	-	-	-	-	-	-	E
7	M	1	3	< 24	2200	1470	290	3960	20	1390	490	1900	22.2	22.8	31.9	29.6	F
8	M	< 1	6	-	210	25	25	260	-	-	-	-	64.0	64.7	42.2	55.6	F
9	M	< 1	< 1	-	-	-	-	-	-	-	-	-	-	-	-	3.0	P
10	O	2.5	6	-	-	-	-	-	-	-	-	-	8.0	8.2	14.0	14.0	F
11	O	2.25	-	-	-	-	-	-	-	-	-	-	.8	.8	5.6	6.3	E
12	O	6	-	-	1190	775	504	2469	-	-	-	-	-	-	-	11.5	E
MC1-1	N	< 1	< 1	-	530	300	345	1175	500	6070	7195	13765	22.7	34.0	41.1	41.5	P
2	N	< 1	6	< 24	890	490	257	1637	3041	1819	1584	6444	-	-	-	40.0	F
3	N	2	4	< 24	2688	2170	1829	6687	-	-	240	240	-	-	-	40.0	F
4	S	1	21	< 24	2225	1055	900	4180	-	-	-	-	-	30.2	30.3	30.8	F
5	S	3	8	-	815	1200	760	2775	175	610	600	1385	17.0	31.1	31.9	31.7	F
6	S	< 1	8	< 24	672	439	108	1219	1368	1097	324	2784	-	-	-	11.5	F
7	M	5	11.5	-	-	-	-	-	-	-	-	-	3.4	2.5	2.2	1.8	F
8	M	22	36	-	-	-	-	-	-	-	-	-	2.4	2.4	3.8	3.8	E
9	M	-	-	-	-	-	-	-	-	-	-	-	-	-	-	-	E
MC2-1	N	3	12	< 24	4290	1210	1110	6610	-	-	-	-	16.0	16.9	17.3	17.3	F
2	N	< 1	3	< 24	3645	3000	1600	8245	10	-	415	425	33.2	37.7	40.0	36.2	F
3	N	< 1	3	< 24	1920	1553	1344	4817	-	-	-	-	-	-	-	50.0	F
4	S	3.5	4.25	-	-	-	-	-	-	-	-	-	11.5	10.9	14.1	11.3	F
5	S	3.25	6.25	< 24	2415	2415	2995	7825	190	800	1275	2265	15.7	24.0	28.0	29.3	F
6	S	< 1	< 1	< 24	790	1015	600	2405	1550	1395	1235	4180	21.5	25.3	25.9	26.2	P
7	M	2	13	< 48	-	465	2405	2870	205	1810	1960	3975	26.3	16.3	36.3	37.1	F
8	M	< 1	1	< 24	100	70	15	185	2175	2070	1200	5445	-	56.8	59.1	61.9	P
9	M	1.5	2.75	< 24	1405	1225	205	2835	5	15	-	20	10.5	21.2	18.5	13.2	P
MC3-1	N	2.5	10	< 24	1300	2305	2600	6205	-	-	-	-	17.5	27.2	28.8	35.6	F
2	N	1.25	2	< 24	385	1800	1000	3185	4190	4700	3210	12100	30.7	39.1	38.7	39.0	P
3	N	24	-	-	924	473	293	1890	-	-	-	-	-	-	-	20.0	E
4	S	7	20	-	300	600	400	1300	-	-	-	-	-	17.2	28.3	30.5	F
5	S	2.25	3.25	-	25	100	80	205	-	-	-	-	20.5	21.1	23.5	21.0	F
6	S	3	7	-	-	110	280	390	-	-	-	-	21.5	25.5	24.5	23.4	F
7	M	< 1	< 1	< 24	2235	1785	1115	5135	14100	9605	8630	32335	33.3	38.2	38.2	38.0	P
8	M	< 1	15	< 24	5	1205	1100	2310	1380	1390	400	3170	-	35.7	36.3	28.5	F
9	M	-	-	-	-	-	-	-	-	-	-	-	-	-	-	-	E
MC4-1	N	< 1	6	< 24	2400	5205	2000	9605	10400	3200	1750	15350	-	18.4	22.6	22.2	F
2	N	< 1	2.75	< 48	25	585	325	935	50	4600	3950	8600	36.5	54.1	54.9	54.9	P
3	N	3	-	< 24	4265	3120	2921	10306	-	-	-	-	-	-	-	30.0	F
4	S	8	24	-	-	80	120	200	-	-	-	-	6.1	8.5	10.6	8.7	F
5	S	18	25	< 24	375	300	200	775	10420	10550	1300	22270	-	10.1	22.2	23.7	F
6	S	1.5	8	< 24	1215	640	465	2320	195	1065	1490	2750	32.5	30.2	36.9	36.9	F
7	M	< 1	2	< 24	50	-	-	50	4000	6000	2000	12000	-	21.7	19.0	27.4	P
8	M	< 1	3	< 48	800	1770	700	3270	-	-	-	-	11.5	14.8	16.6	14.3	F
9	M	< 1	4	-	635	790	500	1925	-	-	-	-	18.6	28.6	31.8	28.0	F

* Preconditioning period

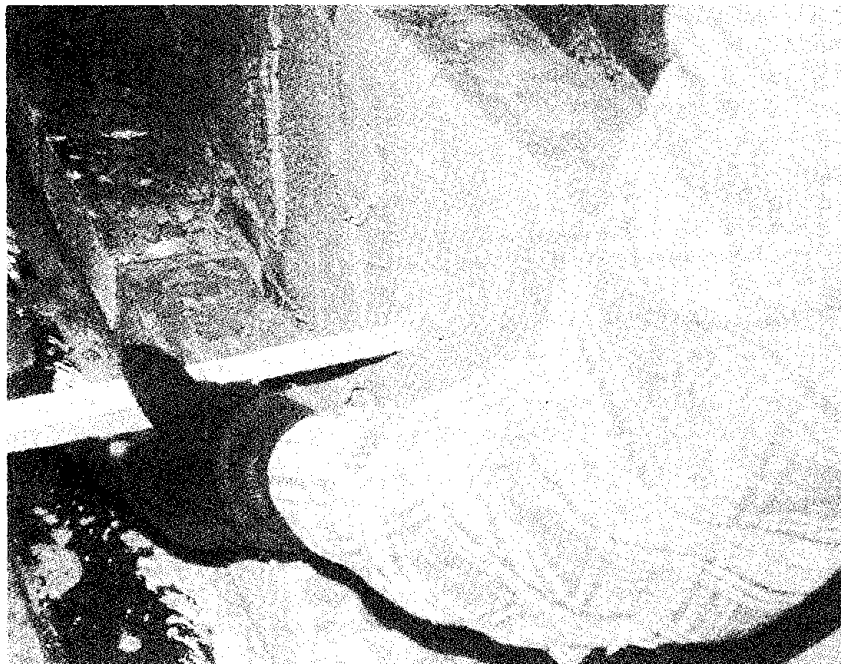


Fig. 1 - WALL SPECIMEN DURING CONSTRUCTION



Fig. 2 - REINFORCEMENT EMBEDDED IN MORTAR

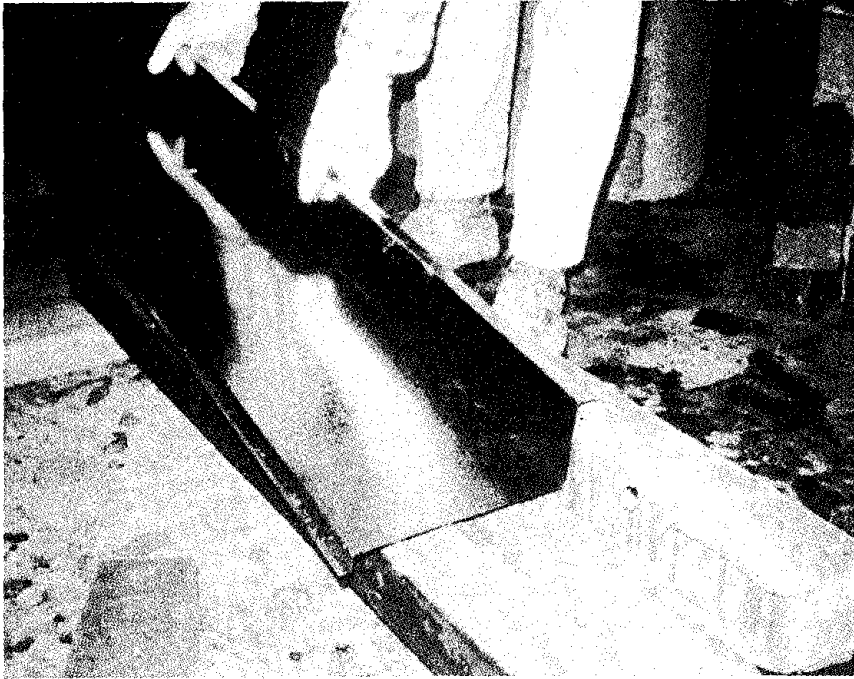


Fig. 3 - FLASHING FULLY EMBEDDED IN MORTAR

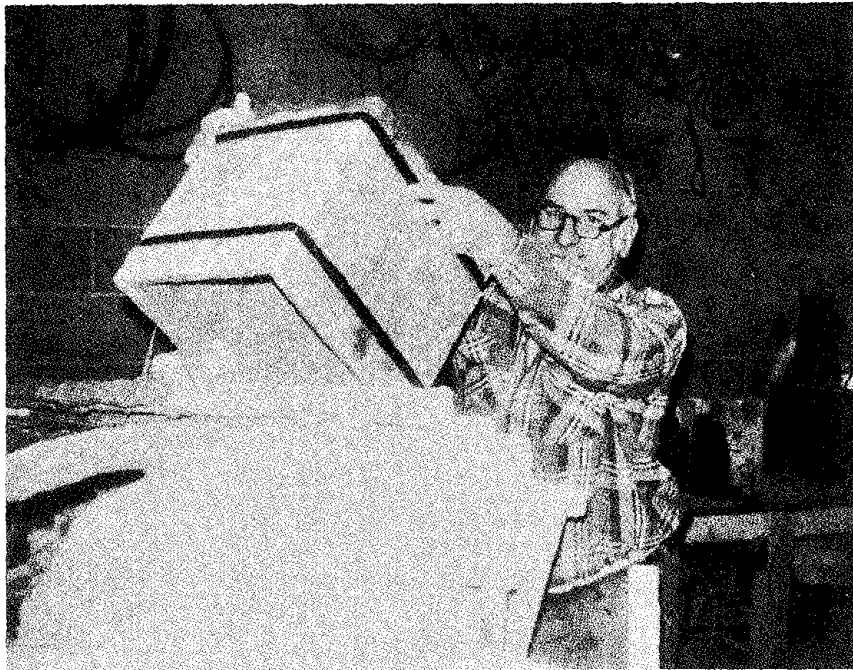


Fig. 4 - MORTAR PROPORTIONED BY VOLUME

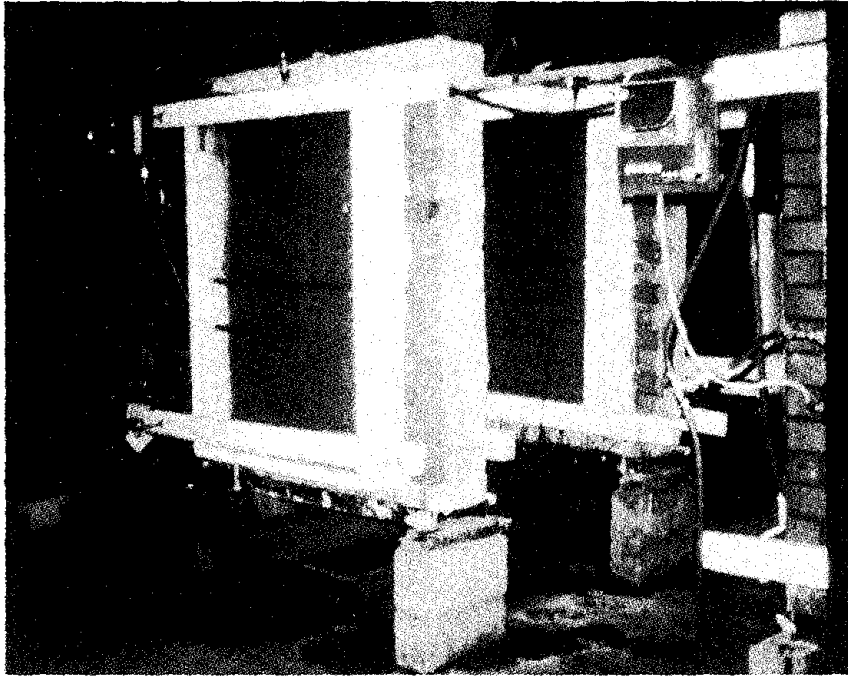


Fig. 5 - TEST CHAMBERS FOR ASTM E 514

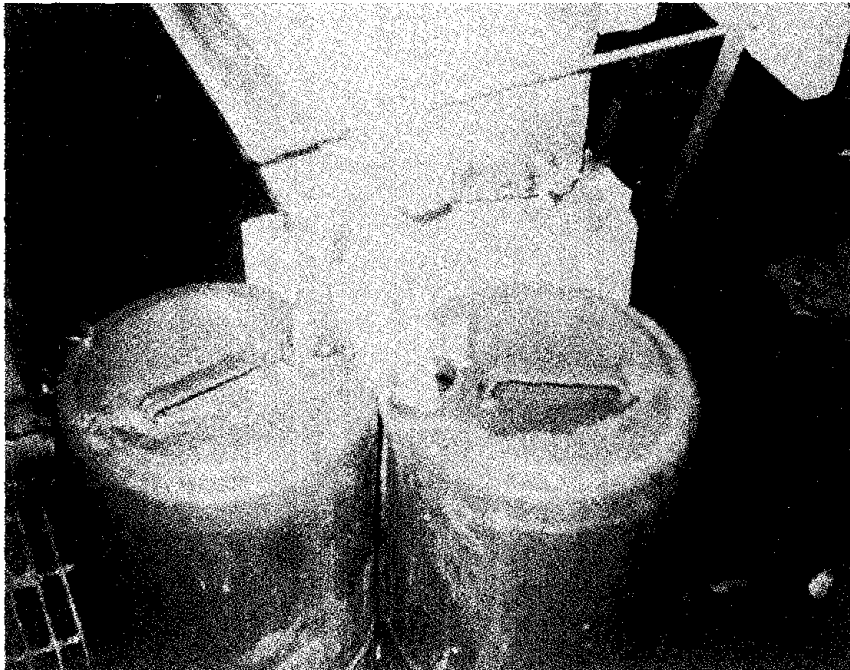


Fig. 6 - COLLECTION OF PERMEANCE WATER

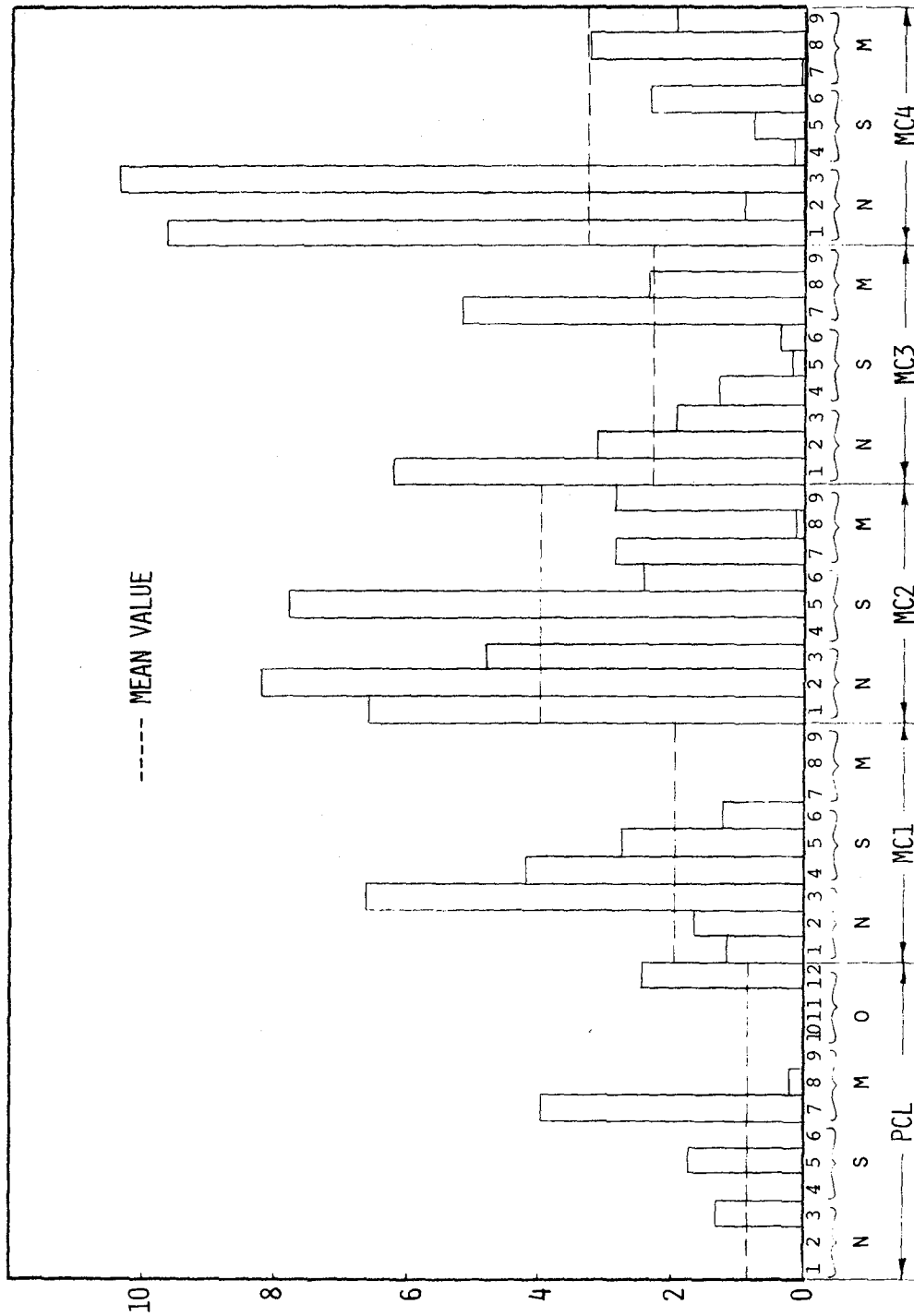


FIG. 7 - COMPARISON OF LOWER FLASHING WATER FOR WALLS OF DIFFERENT MORTARS

TOTAL WATER IN LOWER FLASHING AT 72 HR., LITERS

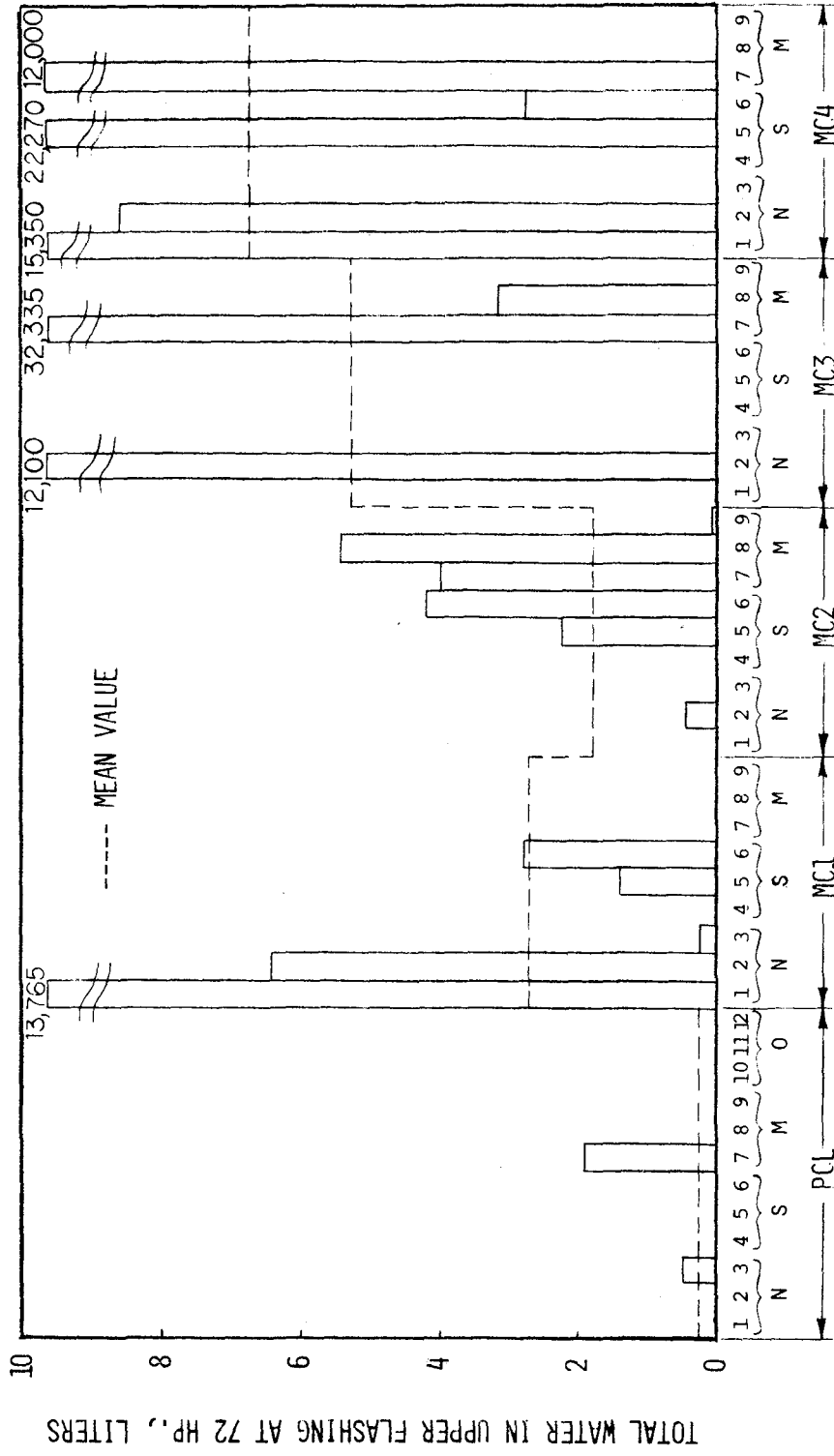


FIG. 8 - COMPARISON OF UPPER FLASHING WATER FOR WALLS OF DIFFERENT MORTARS

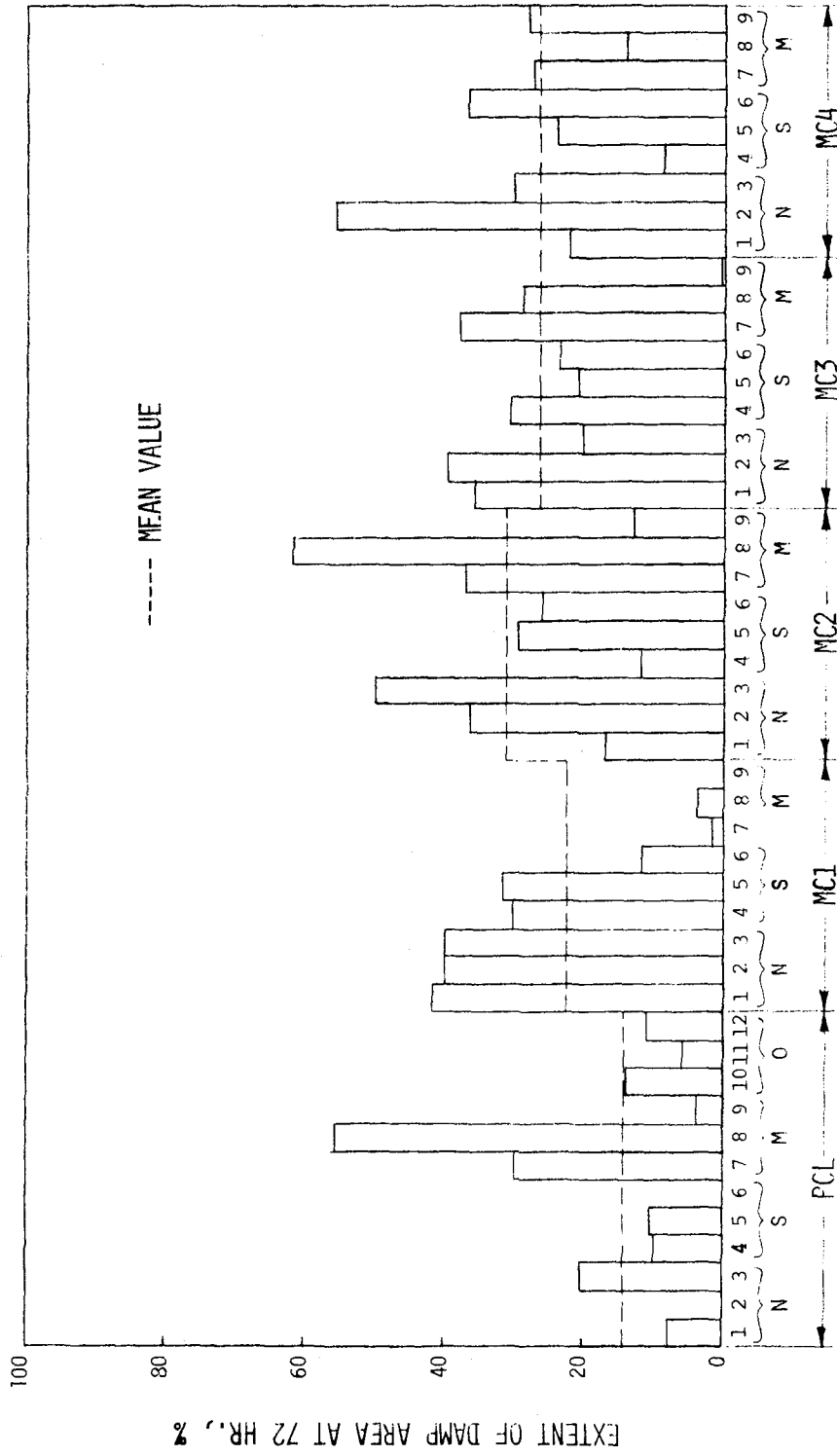


FIG. 9 - COMPARISON OF EXTENT OF DAMP AREA FOR WALLS OF DIFFERENT MORTARS

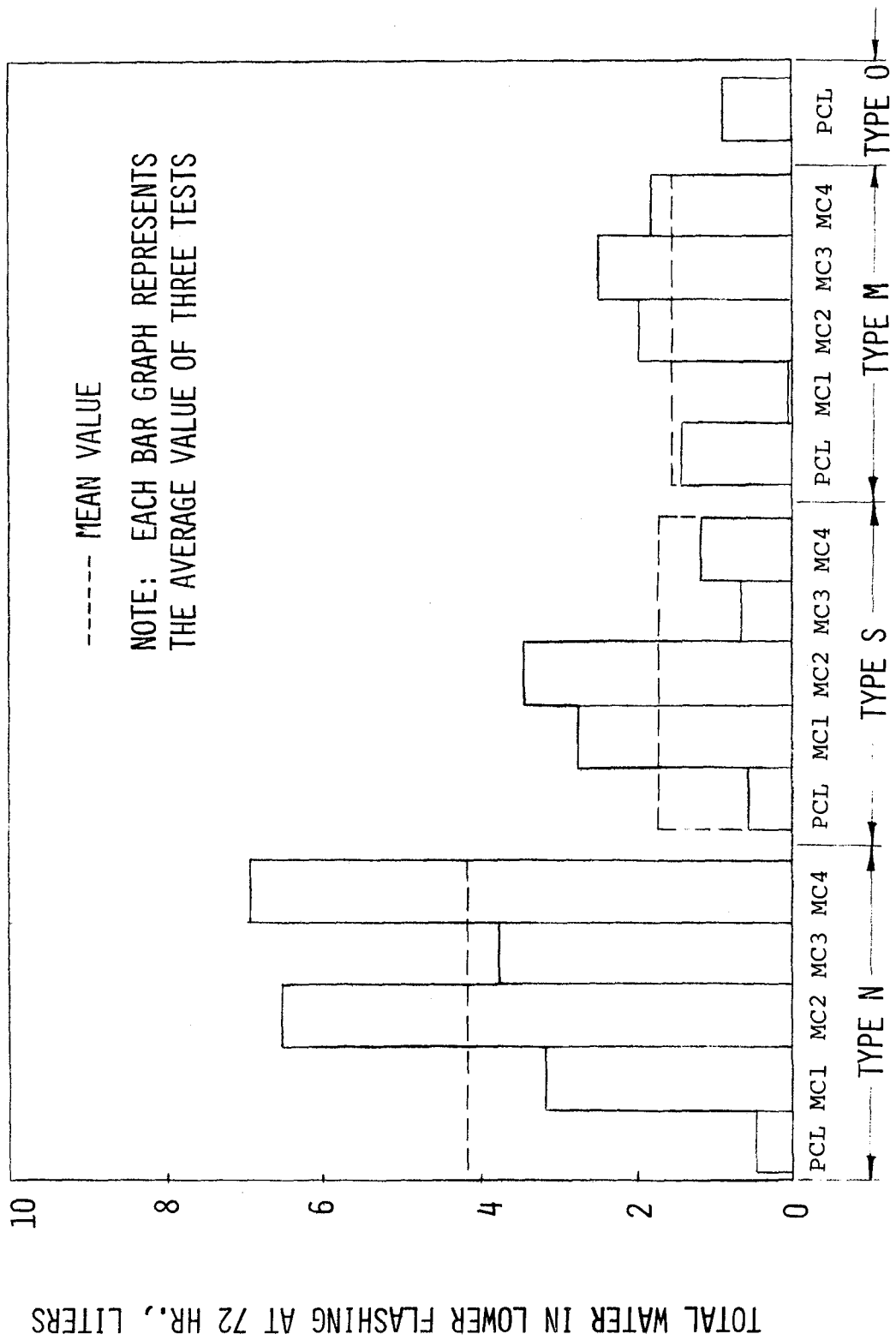


FIG. 10 - COMPARISON OF LOWER FLASHING WATER FOR VARIOUS MORTAR TYPES

TOTAL WATER IN LOWER FLASHING AT 72 HR., LITERS

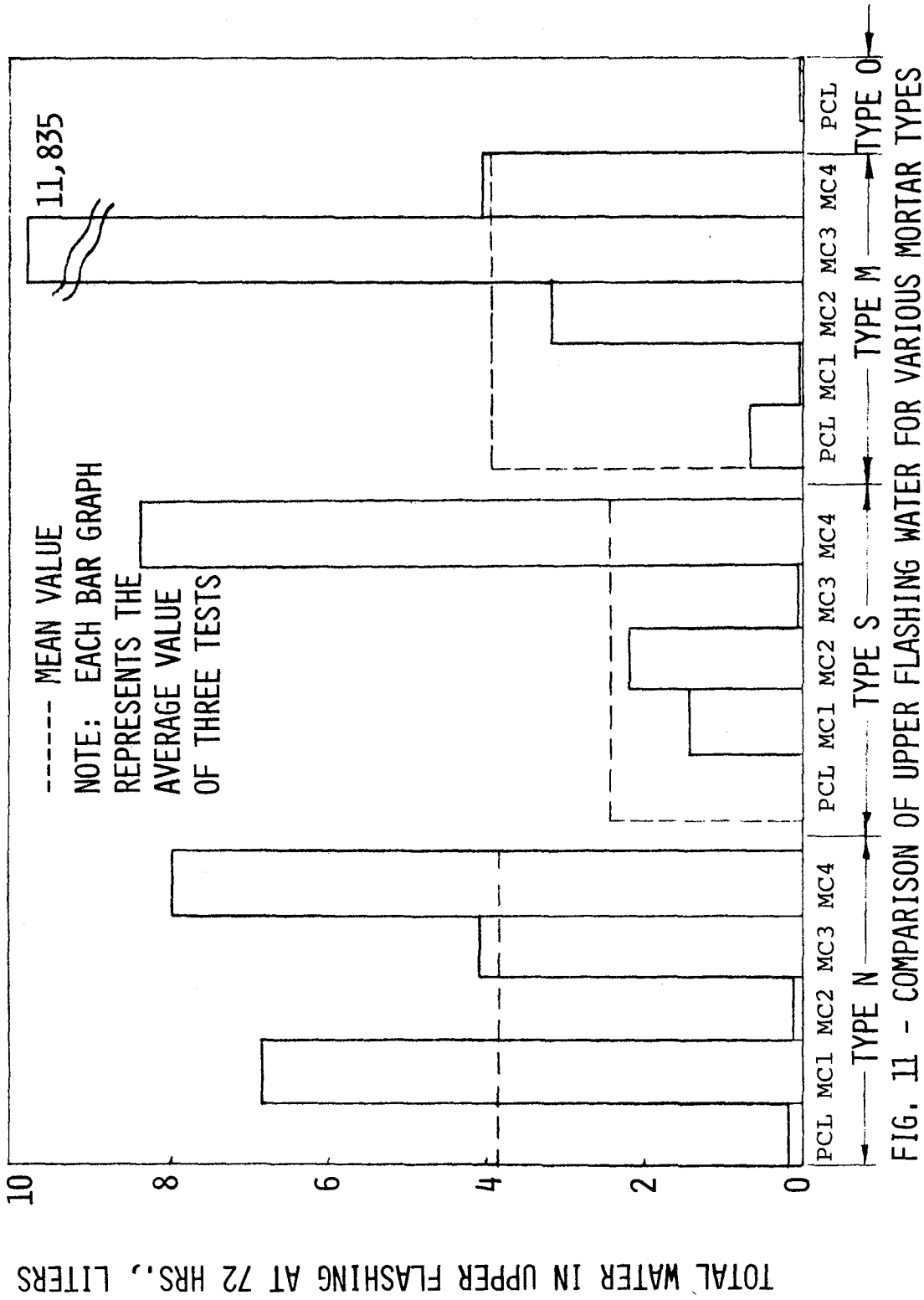


FIG. 11 - COMPARISON OF UPPER FLASHING WATER FOR VARIOUS MORTAR TYPES

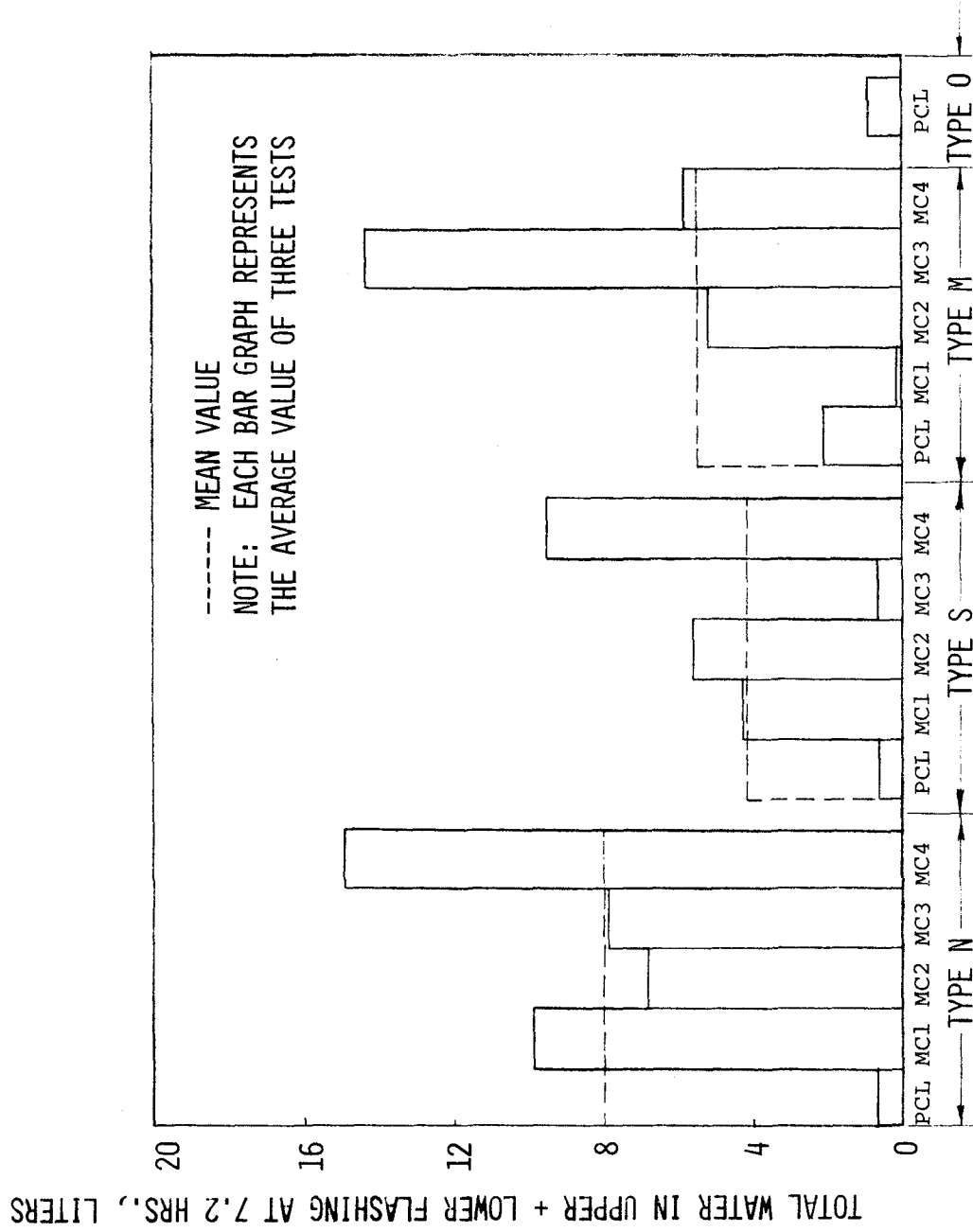


FIG. 12-COMPARISON OF TOTAL WATER FOR VARIOUS MORTAR TYPES

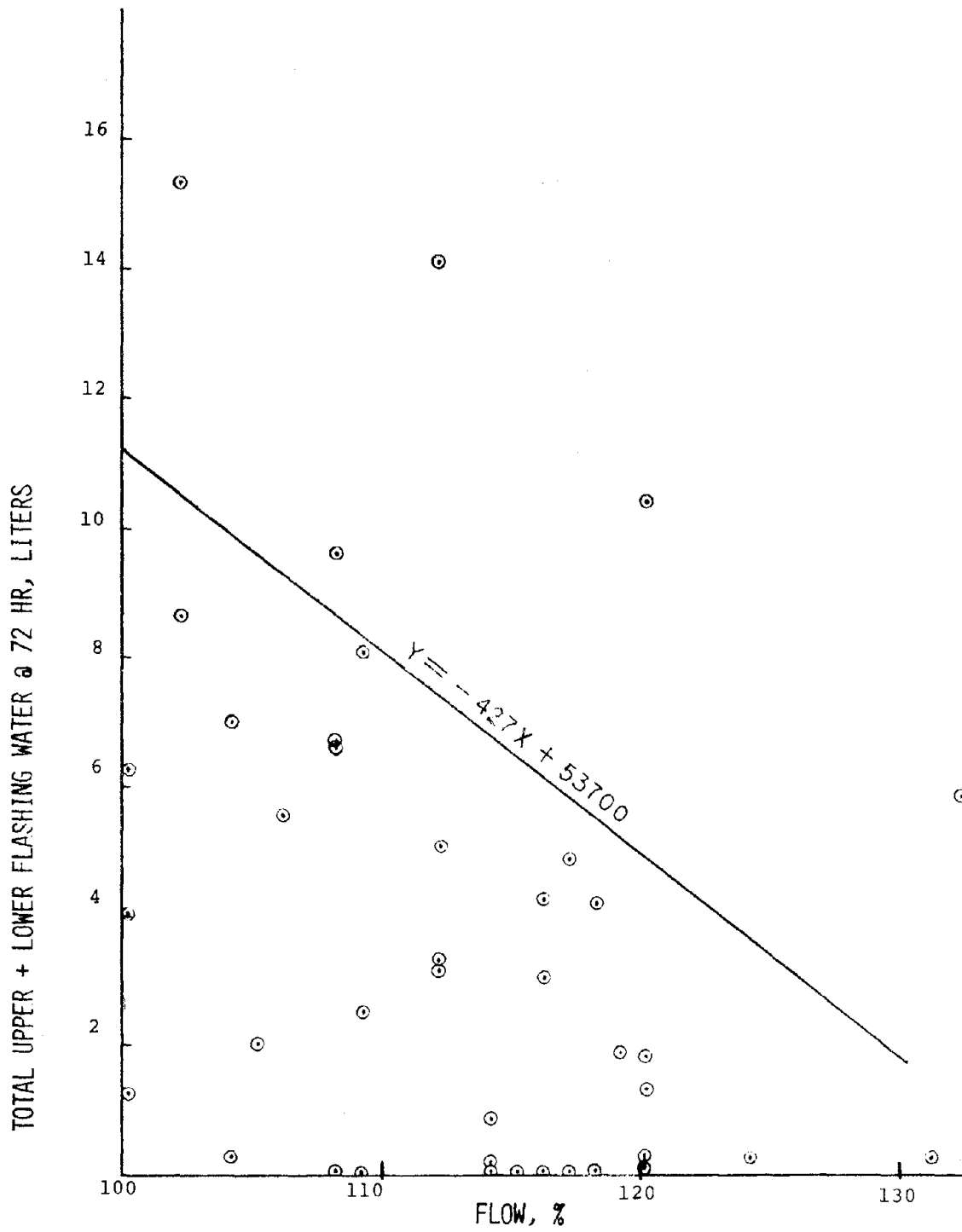


FIG. 13 - RELATIONSHIP BETWEEN MORTAR FLOW AND TOTAL PERMEANCE WATER

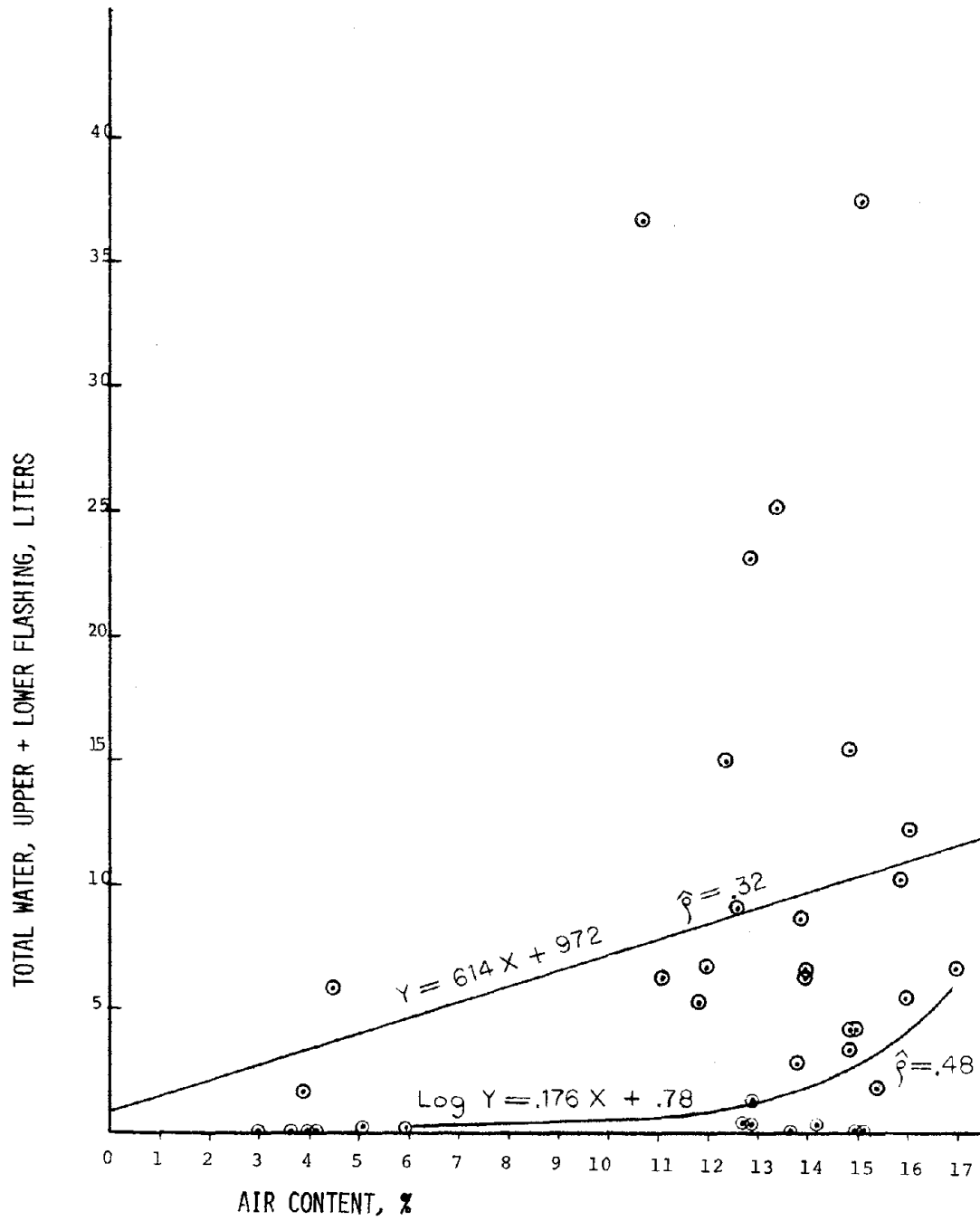


FIG. 14 - RELATIONSHIP BETWEEN AIR CONTENT AND TOTAL PERMEANCE WATER

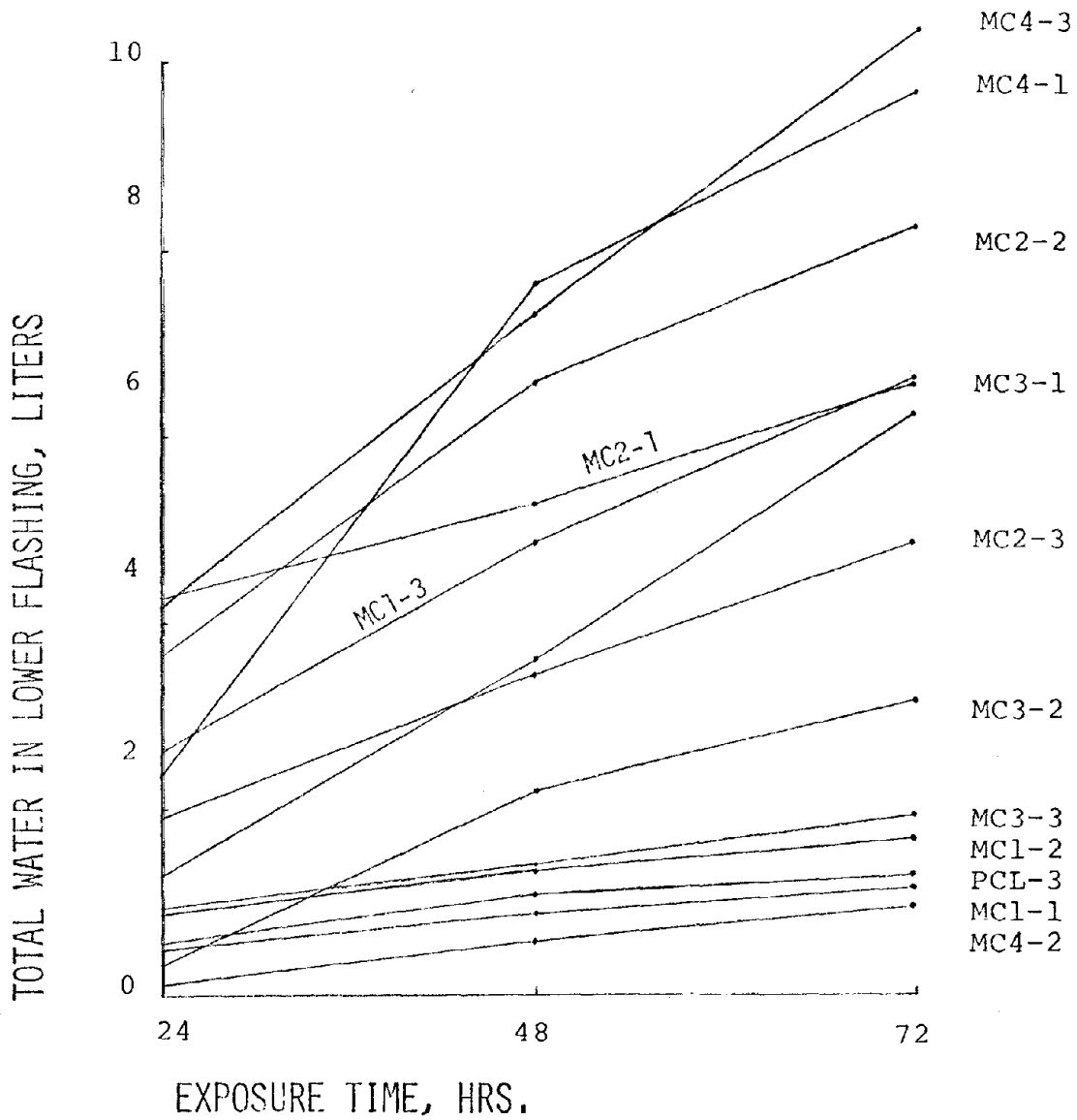


FIG. 15 - TIME RATE OF LEAKAGE, TYPE N MORTAR

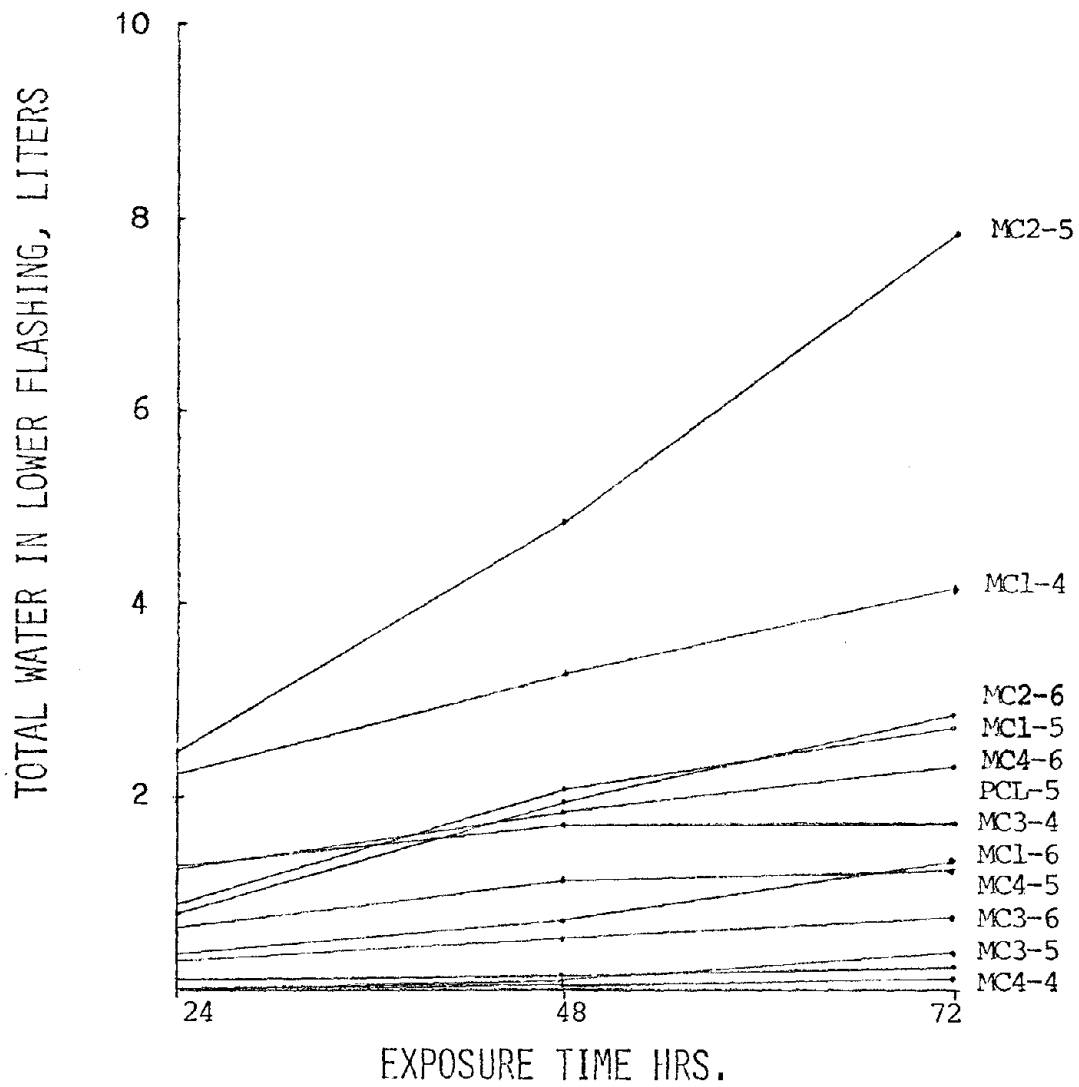
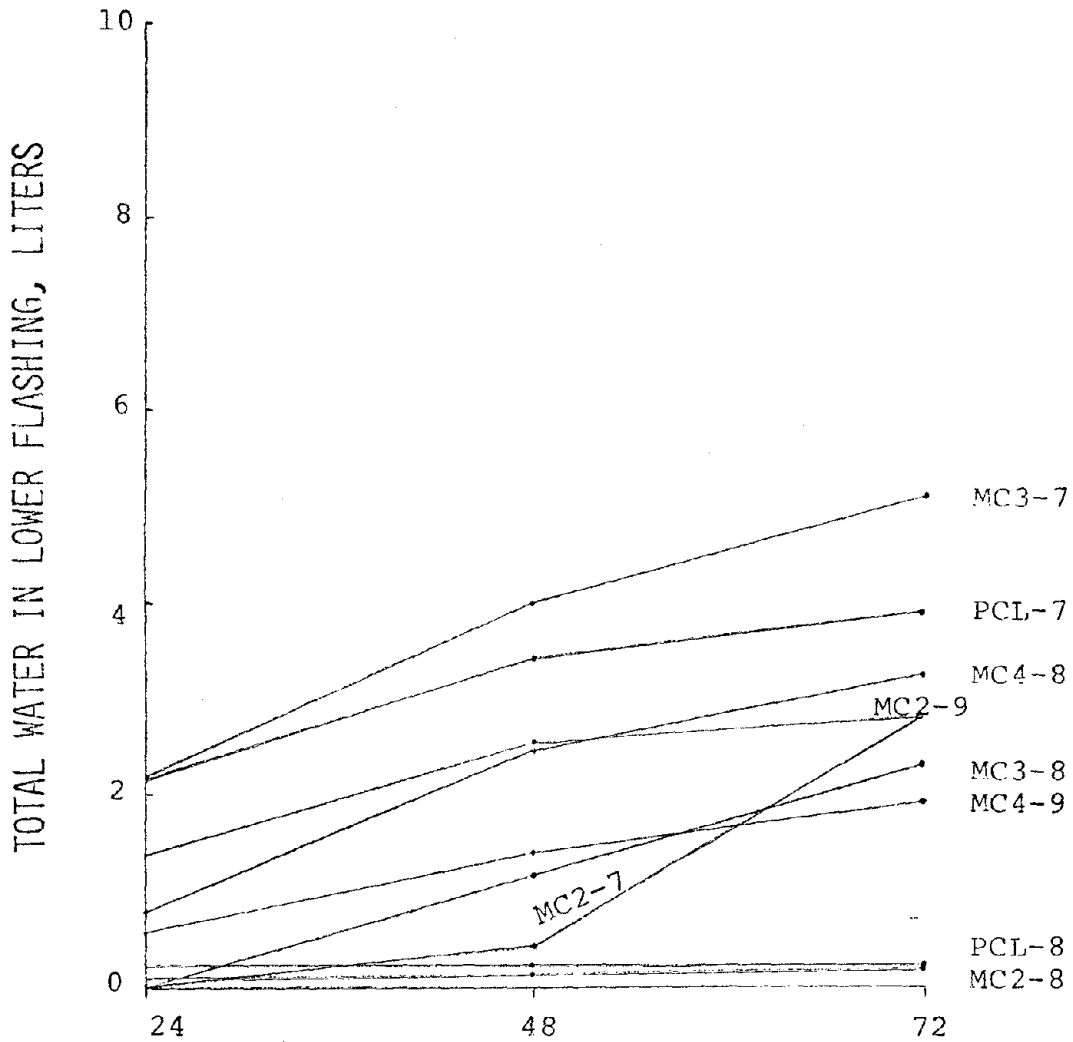


FIG. 16 - TIME RATE OF LEAKAGE, TYPE S MORTAR



EXPOSURE TIME, HRS.
FIG. 17 - TIME RATE OF LEAKAGE, TYPE M MOTOR

MEASURED STRESSES IN A CERAMIC VENEER
ON CONCRETE COLUMNS

W. G. Plewes¹

ABSTRACT: It has become recognized that compression stresses in masonry cladding resulting from differential elastic, shrinkage, creep, and thermal movements between it and the structural frame can produce spalling and buckling of facings.

Under the auspices of the Division of Building Research of the National Research Council of Canada, an investigation was made where the stresses in facing were measured. The measurements were made by the photoelastic method. Strips of photoelastic material were cemented adjacent to mortar joints in four clad columns. Cutting through the mortar joint relieved the existing stress in the veneer which produced colour changes in the photoelastic material. Stresses calculated confirmed that the veneer was, in fact, under a permanent state of stress.

¹Consultant, formerly Senior Research Officer, Division of Building Research, National Research Council of Canada.

MEASURED STRESSES IN A CERAMIC VENEER
ON CONCRETE COLUMNS

By W. G. Flewes¹

Loosening, displacement and damage to stone, tile, brick and other facings of buildings occur rather frequently due to a variety of causes. Frost action, thermal effects and settlement may be involved, but it has become more clearly recognized in recent years (1, 2, 3)² that compression stresses in cladding resulting from differential elastic, shrinkage, creep and thermal movements between it and the structural frame can produce spalling and buckling of facings.

The Division of Building Research of the National Research Council of Canada has investigated a number of cases involving brickwork and reports of such problems from other countries are numerous. In most of the buildings examined by the Division the cause of the problem was deduced from visible evidence and theoretical calculations. This paper reports one case where the stresses in a facing were measured.

Compressive loading of masonry enclosing a structural frame and ensuing problems is most likely to occur in high buildings where slender external wythes of veneer or cavity wall construction are continuous for the full height and unbroken by stress-relieving horizontal joints. In the present instance, however, the building was a modest four storeys, but undesirable behaviour arose from the transfer of load from large concrete columns to a thin ceramic veneer.

Description of Building

Figure 1 is a photograph of the building. The right hand end of the building of which two bays are visible is forty years younger than the remainder and of somewhat different construction. The new portion is where the trouble occurred. Its columns were of reinforced concrete supporting flat slab floors. Their cross-section was about 24 in. by 30 in. with the sides furred out with brickwork to form column-piers about 5 ft. wide (Fig. 2). The outside face of each pier was faced with ceramic veneer units 18" x 24" by 1 in. thick. The units were bedded in mortar and tied to the concrete and masonry pier with metal ties. The 2 in. space between the veneer and the back-up was solidly grouted

¹Consultant, formerly Senior Research Officer, Division of Building Research, National Research Council of Canada.

²Numerals in parentheses refer to corresponding items in Appendix I - References.

(Fig. 3). Face joints were raked out to a depth of about 1/4" and packed with a pointing mortar. It should be noted that where the veneer was backed up by the reinforced concrete column, the combination of the keys in the column face, the grout, and the scoring of the back face of the veneer provided a rigid positive shear connection between all three. The specified bedding mortar consisted of 1 cu ft Portland cement, 1/2 cu ft lime putty, 5 cu ft siliceous sand plus 2 quarts ammonium stearate paste. The pointing mortar was a mixture of 1 cu ft white cement, 3 cu ft siliceous sand plus 2 quarts of stearate paste. The grout contained 1 cu ft of Portland cement to 6 cu ft fine aggregate.

The Problem

About 5 years after construction it was noticed that the glazed veneer was spalled badly at the horizontal mortar joints, especially at the bottom storey (Fig. 4). A variety of causes were suggested, including building settlement, water penetration, frost action, workmanship, joint size, faulty glazing and type of mortar. None of these fitted the evidence. However, by making assumptions as to the probable magnitude of shrinkage (0.04 percent) and creep (100×10^{-8} in./in. per psi) in the concrete, calculations by ordinary methods (4, 5) indicated that shortening of the columns due to the loads, shrinkage and creep could cause stresses in the order of 3000 psi in the veneer because of the rigid connection between it and the columns.

Laboratory investigations indicated that the ceramic veneer had a crushing strength of about 6800 psi. Because the magnitude of the calculated stresses was only about half of the strength of the material and did not fully explain the spalling, it was decided to conduct a field investigation to determine if stresses did exist in the veneer and what other contributing factors might be present.

Field Investigation

To study the stress condition in the ceramic facing, strips of photoelastic plastic material called "Photo-stress" were cemented adjacent to mortar joints in four columns (Fig. 5). This plastic has the photoelastic property of changing colour under stress when viewed through a special analyzing viewer, and a calibration table can be used to evaluate a change in stress (6). A hacksaw blade was then used to cut through the mortar joint with the idea that cutting the joint would relieve any existing stress in the veneer and that such relief would be indicated by the change of colour of the Photo-stress.

It was found in cutting the joint that the 1/4" deep pointing mortar was very hard and that the bedding mortar was very soft and porous. Immediately the pointing mortar was cut through, colour changes occurred in the Photo-stress plastic corresponding to an indicated stress relief. A typical result is shown in Fig. 6, although the bands of colour were not quite so sharply defined as is indicated. At the four measuring points the following stresses were recorded:

<u>Gauge</u>	<u>Stress Relief</u> psi
A	1,850
B	1,850
C	3,100
D	1,590
E	1,850

It is possible that at other points, especially where the spalling had already occurred, the stress before spalling could have been higher.

Discussion

Although the accuracy of the method was not high (300 psi), it was concluded that the ceramic veneer was, in fact, under a permanent state of stress.

The results also showed that the use of a very hard pointing mortar over a soft bedding mortar was equally responsible for the spalling at the joints. If the average stress was in the order of 1500 - 3000 psi across the 1" thickness of ceramic veneer, then the stress would be up to four times as high locally where the force was carried across a joint almost entirely by the 1/4" strip of pointing mortar. Similar spalling effects were, in fact, reproduced in the laboratory by loading glazed tile specimens over a 1/4" width immediately behind the glazed face. Failure occurred at an average cross-sectional stress of only 2200 psi, but the local stress beneath the load was 8800 psi exceeding the strength of the material.

A uniformly soft or uniformly hard mortar across the thickness of the tile would have been a better situation. It should be noted that the specifications in the Architectural Terra Cotta Institute Catalogue 55-S (7) require the same mortar to be used for both setting and pointing - specifically 1 part Portland cement, 1/2 part high calcium lime putty and 4 1/2 parts sand.

Similar cases of deterioration have been observed on buildings with brick facings. It can occur even on steel frames, and in two instances spalling occurred at shelf angle levels due to the stress transfer across the pointing mortar at the toe of the angles.

Conclusion

Stresses in building slabs have seldom been measured. This paper offers confirmatory evidence from measurement that too rigidly attached facings can be stressed by load transfer from columns. Where spalling occurs at joints, uneven mortar resistance may be a factor.

ACKNOWLEDGMENT

Thanks is due to the Director of the Division of Building Research, National Research Council of Canada, for permission to publish this case record.

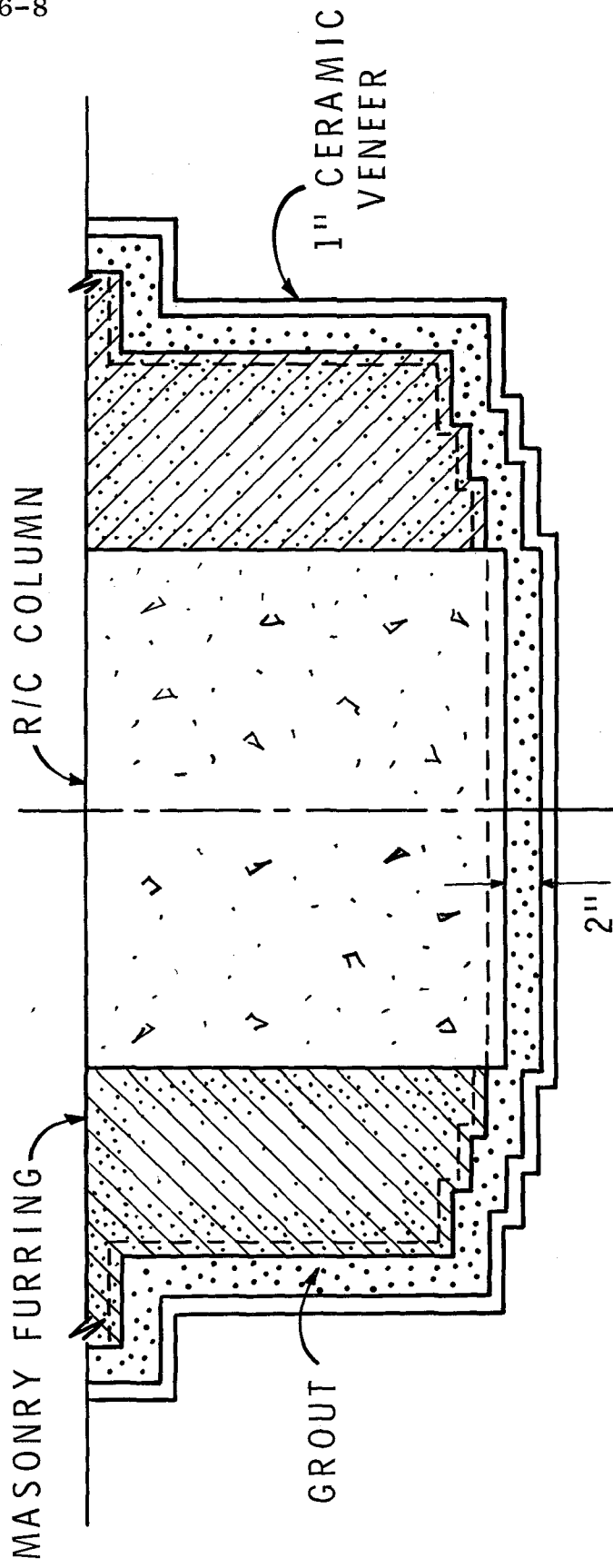
APPENDIX - REFERENCES

1. Flewes, W. G., Building Deformations - Vertical Movements, Record of the DBR Building Science Seminar, Autumn 1972, Cracks, Joints and Movements in Buildings, National Research Council of Canada, Division of Building Research, Proceedings No. 2, NRCC 15477, Ottawa 1976.
2. Flewes, W. G., Failure of Brick Facings on High-Rise Buildings, Canadian Building Digest, CBD 185, National Research Council of Canada, Division of Building Research, April 1977, pp. 4.
3. Grimm, C. T., Design for Differential Movement in Brick Walls, Journal of the Structural Division, Proceedings of the American Society of Civil Engineers, Vol. 101, No. ST11, November 1975, pp. 2385-2403.
4. Peabody, Dean, The Design of Reinforced Concrete Structures, 2nd Edition, John Wiley & Sons, Inc., New York, 1948.
5. Large, George Elwyn, Basic Reinforced Concrete Design - Elastic and Creep, 2nd Edition, The Ronald Press, New York, 1957.
6. Photoelastic Stress Analysis, Bulletin SFC200, Photoelastic Inc., Malvern, Pa.
7. Architectural Terra Cotta and Ceramic Veneer Catalogue 55-S of the Architectural Terra Cotta Institute affiliated with the Structural Clay Products Institute, Washington, D.C.



PHOTOGRAPH OF BUILDING

FIGURE 1



SCHEMATIC
CROSS-SECTION OF COLUMNS

FIGURE 2

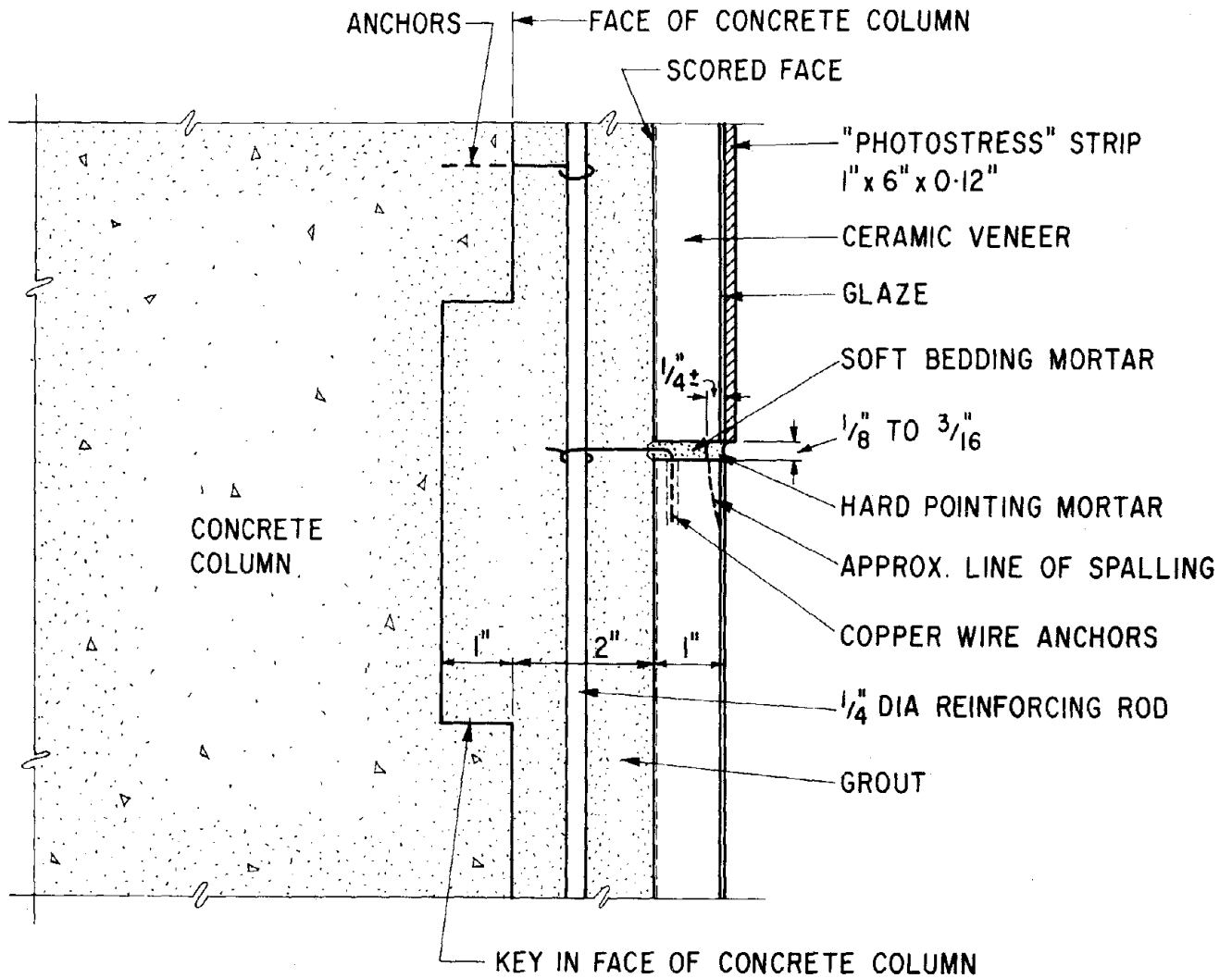
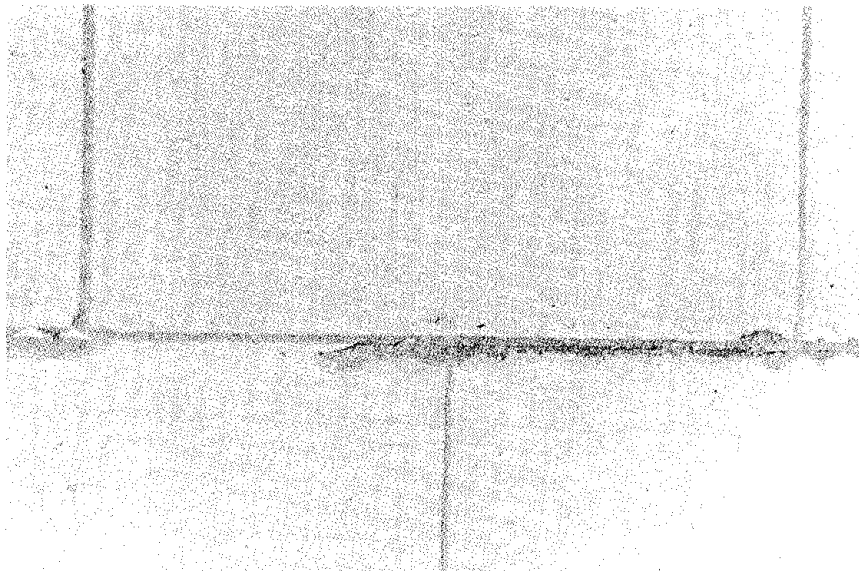
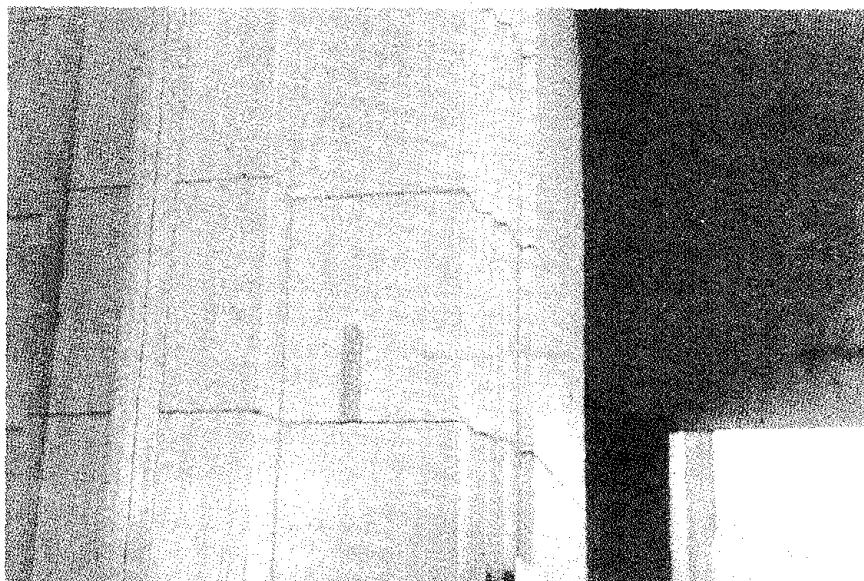


FIGURE 3

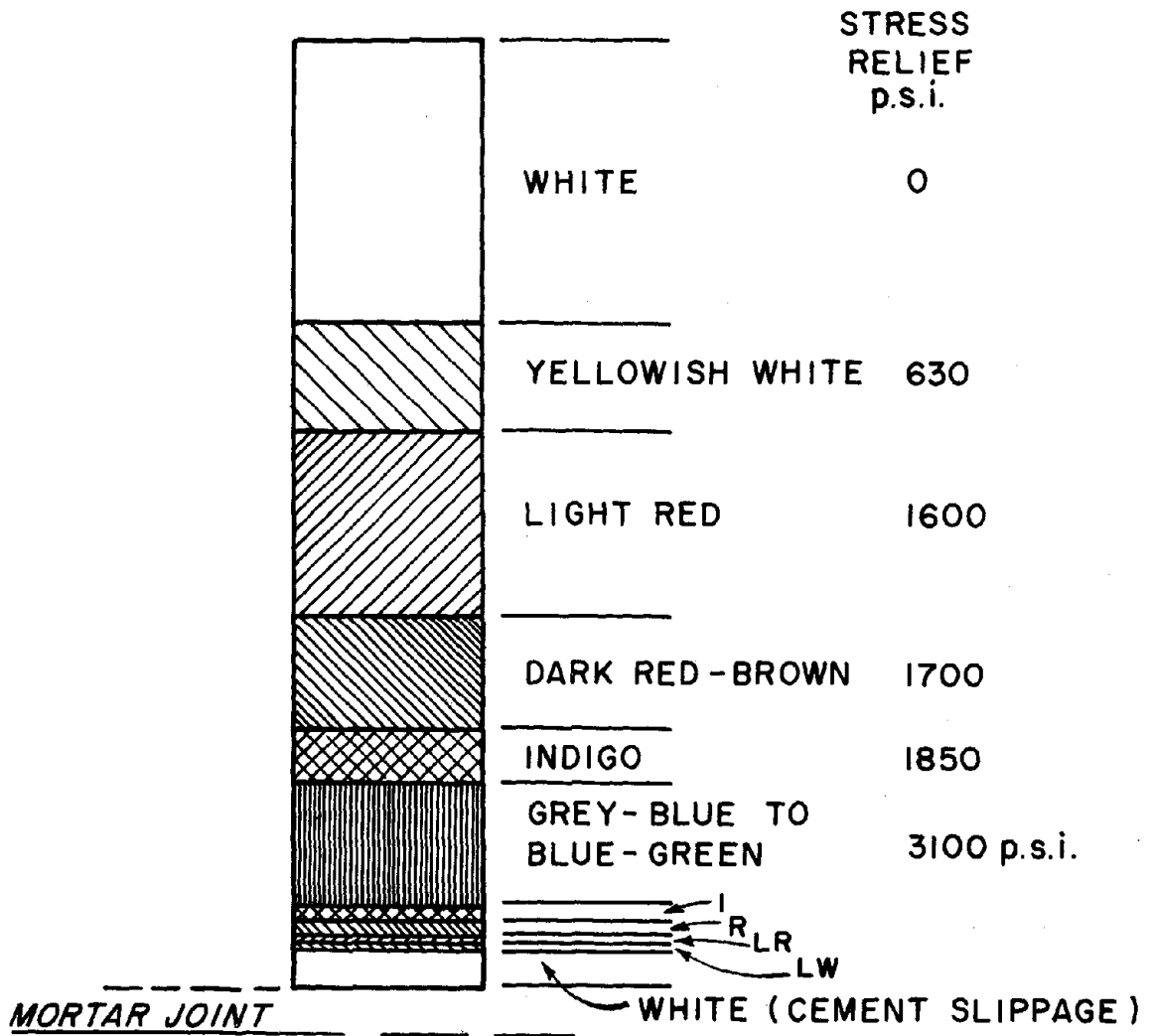
SKETCH SHOWING CONNECTION OF VENEER TO COLUMNS
 AND LOCATION OF "PHOTO-STRESS" AT A JOINT



SPALLING AT JOINTS
FIGURE 4

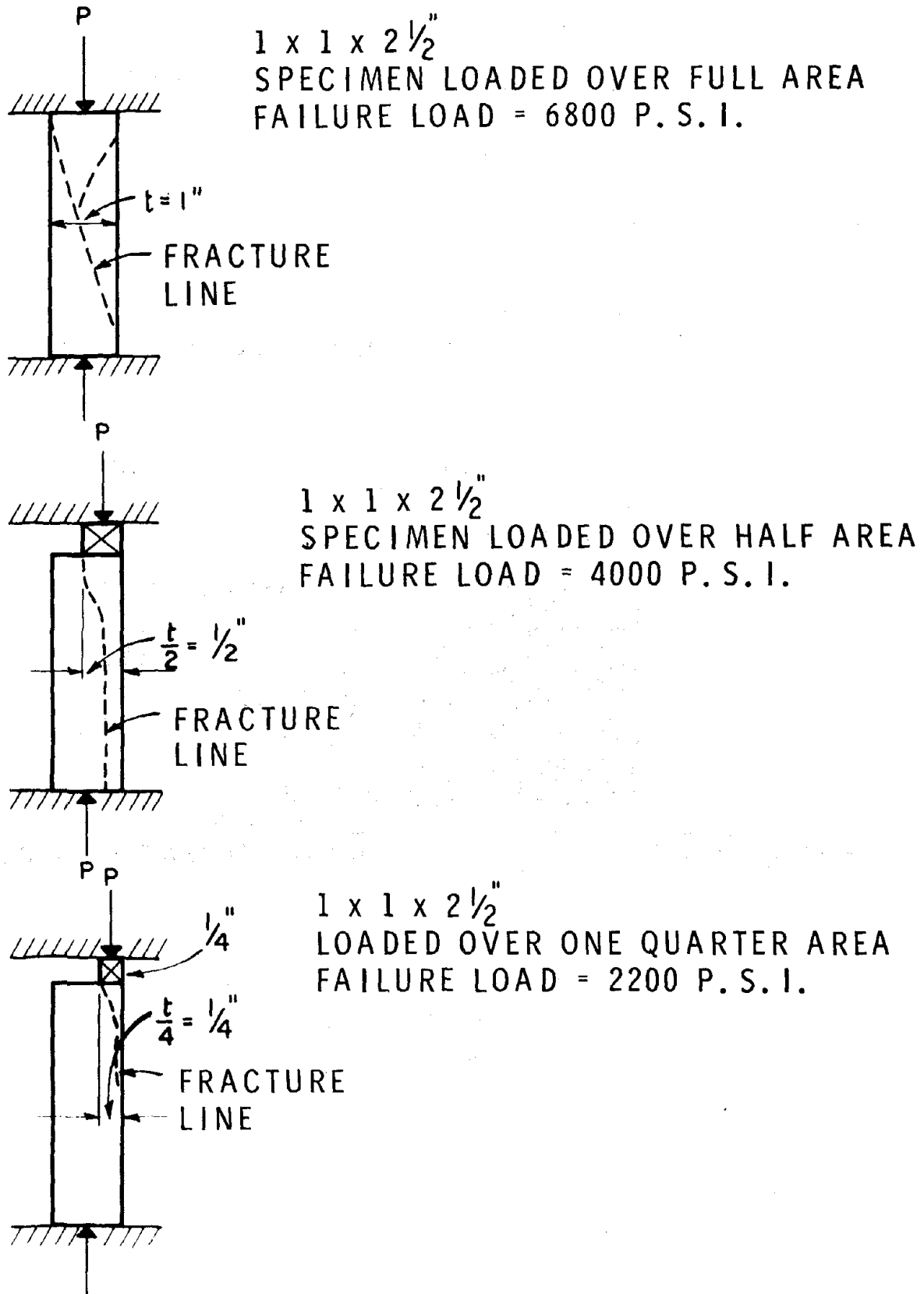


"PHOTO-STRESS" STRIP ON CERAMIC VENEER AT A JOINT
FIGURE 5



STRESS RELIEF INDICATED BY STRIP "C" AFTER CUTTING THE MORTAR JOINT

FIGURE 6



TESTS SHOWING EFFECT WHEN LOAD TRANSMITTED TO VENER SPECIMENS THROUGH LOADED AREAS OF VARIOUS WIDTHS

FIGURE 7

EDUCATION AND SCHOOLING - REINFORCED MASONRY DESIGN AND CONSTRUCTION

By Robert R. Schneider¹ and Walter L. Dickey²

ABSTRACT: The growth of the governing masonry code provisions of the State of California, Uniform Building Code, local codes from the early 1920's after the Santa Barbara and Japanese quakes and then the steady growth from 1934 to present.

Outline of Code requirements for design. The fallacies and validities of arbitrary code design provisions and proper consideration of compliance and deviation. Exceptions from Code provisions in the Research Recommendations and rulings.

Allowable or useable strengths for elastic design. Discussion of ultimate design.

Design principles and examples of simple flexural and shear members, i.e., beams, lintels and walls.

Design principles and examples of simple compression members, i.e., columns, piers and walls. Application of the principles to total building design.

Chronology of recent curriculum development in various programs with suggested recommendations for visual aids, texts and training guides available. New college and graduate level textbook available in about one year.

¹Prof. of Civ. Engrg., California State Polytechnic University, Pomona

²Consulting Structural Engineer, Higgins Brick Co., Redondo Beach, Calif.

EDUCATION IN REINFORCED MASONRY

By Robert R. Schneider¹ and Walter L. Dickey²

INTRODUCTION

One purpose of this paper is to emphasize the dire and growing need for schooling and education in the relatively new field of Reinforced Masonry Design and some of the reasons for the past lack of inclusion in curricula.

The major purpose is to warn of and clarify some of the items that might trip a professor in his first time through instruction of this subject.

Also to provide some guidelines through the codification of requirements that have such varying character, e.g., traditional, empirical, arbitrary, engineering, theoretical, practical, economic or whatever, and to suggest some aids for setting up a course for this heterogeneous subject, one of our major construction methods, but which perhaps has the least volume of research and academic background.

BACKGROUND

In the 50's and early 60's Robert Schneider was active in testing and engineering investigation of reinforced masonry construction, which added knowledge to the state of the art and which influenced him in later teaching, even leading to his setting up and nurturing full-fledged formal engineering classes in Reinforced Masonry Design at the University of California at Pomona.

W. L. Dickey's early contact with masonry (bricklayer in 1927 while still at the California Institute of Technology) and long subsequent structural engineering career including many large and excellent reinforced masonry structures, led to his specializing, in 1961, in masonry research, design and education with Masonry Research, which became Masonry Institute of America.

¹Prof. of Civ. Engrg., California State Polytechnic University, Pomona

²Consulting Structural Engineer, Higgins Brick Co., Redondo Beach, Calif.

Those two experiences both resulted in a strong awareness of the need for including reinforced masonry design as a subject in engineering curricula. There had been well developed courses and textbooks in strength of materials, in concrete, in prestressed concrete, in heavy steel, in light steel, in wood, in aluminum etc., but none comparably in masonry, either unreinforced or reinforced, although it is a major construction method.

Then when earthquake sensitivity of the 1930's forced some use, then total use, of reinforced masonry the need for education became greater. That growing need was not matched by comparable fulfillment. It became more acute as sophistication in seismic design increased, there was even more need for more information.

The above is not to say that reinforced masonry was developed for earthquake resistance only, but seismicity was a great stimulus. Reinforced masonry could be a very effective use of masonry, expanding masonry utilization from the older traditional, empirical or Master Mason application to more economical and cost effective solutions for our modern construction. As a consequence in 1954 and 1956 the San Francisco representative of "Clay Brick and Tile" arranged for a series of talks in St. Louis, Chicago and Kansas and other areas to present the economic advantages of reinforced masonry in competitive construction.

However, there was an obstacle in academia. The basis of reinforced masonry design was not developed by a large sponsor backing a comprehensive testing, research, and development program - such as Portland Cement Association and its superb concrete research program - or as was done in steel, or wood, or even aluminum. The subject was first and foremost a series of practical solutions, modified by scattered bits of research, and further modified by injection of hysterical reactions to catastrophic earthquakes (e.g., an arbitrary steel percentage requirement, a 4' maximum steel placement, an arbitrary column stirrup requirement and others which will be mentioned later).

The combination of empirical seismic resistance requirements, past rule of thumb provisions, with some recognition of "Strength of Materials" considerations made the teaching of "Reinforced Masonry Design" rather unpalatable to pure academia, with its desire for well ordered theory.

Perhaps another obstacle was the fact that there were not many theorists or engineers simultaneously with experience in use of this handcraft, (like Winston Churchill) or many bricklayers with adequate engineering who would initiate or conceive engineering courses for this hand laid material, and introduce it into engineering curricula. This was in spite of the need, and the implied responsibility of schooling to prepare the student for his role in the practitioner's office in as broad a manner as possible.

THE CODE

A common method of instruction in the subject of reinforced masonry design was frequently in answer to a neophyte engineer question such as, "Here is a masonry wall to design, how do I do it?"

The answer might be from his associate - "Well, on the last one we did it this way, and the Code says", with the implication that the Code was as if on stone tablets.

And Code was not all bad as a guide. It was based on the historical growth of venerable traditional design by master masons, with the addition of engineering generalizations and some test data. For average conditions it was sound. However, for special conditions and for engineering it was necessary to "interpret" the meaning and intent.

Also one very important item in design is the necessary continual awareness of the field placement problems, of how the masonry was actually built to provide for and accommodate the functional placement of steel and other engineering provisions.

The Code does contain definitive specifications of the various types of reinforced masonry construction. These are essentially assemblages of masonry units and mortar in which reinforcement is bonded by mortar or grout. They are included in a detailed specification manner, but deviations may be made, if proven by test and usage.

TRADITIONAL REQUIREMENTS

Some of the traditional, or arbitrary, or empirical, items that serve as guide or control are shown as follows, with comments as to validity. These comments and the discussions of design methods to follow are as currently pertinent to or expressed in the Uniform Building Code. This is because the UBC contains the result of continuous use and development of reinforced masonry from 1933 on and has frequently been the pattern for adoption in other areas, as well as being "THE CODE" governing jurisdictions under the International Conference of Building Officials.

The catastrophic Long Beach quake in 1933 inspired the initial introduction of masonry reinforcing into Code and those governing provisions have been used, refined, and up dated with each 3 year revision and reprinting.

The masonry wall types are defined and are traditionally limited in minimum thickness and in height or length to thickness ratios by Table 24-I of UBC.

TABLE NO. 24-I—MINIMUM THICKNESS OF MASONRY WALLS

TYPE OF MASONRY	MAXIMUM RATIO UNSUPPORTED HEIGHT OR LENGTH TO THICKNESS	NOMINAL MINIMUM THICKNESS (inches)
BEARING WALLS:		
1. Unburned Clay Masonry	10	16
2. Stone Masonry	14	16
3. Cavity Wall Masonry	18	8
4. Hollow Unit Masonry	18	8
5. Solid Masonry	20	8
6. Grouted Masonry	20	6
7. Reinforced Grouted Masonry	25	6
8. Reinforced Hollow Unit Masonry	25	6
NONBEARING WALLS:		
9. Exterior Unreinforced Walls	20	2
10. Exterior Reinforced Walls	30	2
11. Interior Partitions Unreinforced	36	2
12. Interior Partitions Reinforced	48	2

It is to be noted that the well preserved walls of the old walled city of Rothenberg were built in about the 1200's and would comply with these empirical limits.

The arbitrary limit on columns is "... No masonry column shall have an unsupported length greater than 20 times its least dimension". It is noted the 8-story high columns of the 2-mile-long Segovia aqueduct structure, built by the Romans in 100 BC would comply approximately with these limits so these seem to be conservative.

However, engineered provisions of end conditions and loading will have a great influence and this fact is an example of factors which are not thoroughly clarified by the Code. The above Table 24-1 includes "h" and "h/t".

One pertinent question a student might ask is, "which way is up, - how far is it?" since the terms "h" and "h/t" are used in limits and in the reduction factor for walls and columns which is

$$R = \left[1 - \left(\frac{h}{40t} \right)^3 \right]$$

In that expression t is the thickness in inches, and h is frequently subject to question.

For columns, h is simply

h = Clear height in inches.

For walls, in the past, " h " was called "height," but it was understood as a measure of either up or of sideways, dependent upon which way the wall spanned, that is, whether it spanned vertically from floor to floor or horizontally between pilaster to pilaster. This is now rather clearly stated in the UBC as

h = Clear unsupported distance in inches between supporting or enclosing members (vertical or horizontal stiffening elements).

This is the same meaning as the meaning in the early concrete design provisions from which this factor was borrowed.

To further clarify which way is up (h ?), we might clarify "How far is up?"

The definition states "clear distance." However, an exception states:

EXCEPTION: The height or length to thickness ratio may be increased and the minimum thickness may be decreased when data is submitted which justifies a reduction in the requirements specified in this Section.

One of the most sound techniques for utilizing that exception is the proper consideration of end restraint. If this can be defined correctly and determined correctly by structural calculations, which takes some doing, one may consider the clear distance as the clear distance between points of inflection, that is, as if there were pin joints at those points -- and there could be.

"How far" might, then, be defined as the distance between points of inflection. One approximation of this is shown in the following table:

Buckled shape of column is shown by dashed line	(a)	(b)	(c)	(d)	(e)	(f)
Theoretical K value	0.5	0.7	1.0	1.0	2.0	2.0
Recommended design value when ideal conditions are approximated	0.65	0.80	1.2	1.0	2.10	2.0
End condition code						
		Rotation fixed and translation fixed Rotation free and translation fixed Rotation fixed and translation free Rotation free and translation free				

It is hoped that the above discussion clarifies the questions propounded in the title, i.e., which way is up -- and how far is it.

Another code requirement with some confusion as to background is that the amount of steel required arbitrarily is .002 bt total, with not less than .0007 in each direction. This is not something related to shrinkage or weight or design. It is merely a requirement to improve the performance of masonry after failure. It does not include consideration of shrinkage, e.g., it does not make consideration of hollow units, only 30% solid, compared to solid walls, it does not consider whether the wall is of concrete units and rich grout which will shrink appreciably compared to clay units which will tend to expand etc. etc. It is "just because".

The spacing of steel is another similar item. It is arbitrarily not to exceed 4' oc in "Reinforced Masonry" or 8' in "Partially Reinforced Masonry". This is regardless of whether the wall thickness is 4", 8", or 16" or whatever. It is not related to weight or thickness, or to effective "d", i.e., whether the steel is at the center with a "d" of $1/2t$ or at one side with a "d" of $3/4t$. It is "just because", in order, hopefully, to provide for a so-called "basketing" and a better post failure performance under excessive seismic loading.

An instructor searching for an explanation of such arbitrary provisions would have a fruitless search.

STRESSES

The allowable masonry strengths to be used in design are determined in two basic methods. One is the assumption of a conservative value found by test and practice to be adequate for a particular assemblage.

Another is to make a sample of the masonry intended for the construction and test it for ultimate strength.

The allowable design stresses permitted are then assumed as fractions of the masonry strength, as shown in Table 24-H.

One unique feature of masonry is to be noted, namely, the limit to half stresses when there is not continuous inspection of the installation. If one does not observe the placement one can not be sure that the required provisions are included. That uncertainty would be in addition to the uncertainty due to scatter of strength and quality that is shown in field installations and tests.

Actually theory of probability might show that the statistically correct reduction factor should be $3/4$ instead of $1/2$ but it has been kept conservatively at $1/2$ because of the greater practical hazard in the structure. If a detail is a little wrong the structure may be 100% wrong. Also, the factor is compensated for slightly by the concurrent reduction in E_m . This results in a doubling of the n , or E_s/E_m , value, which has the effect of increasing the computed capacity of a section slightly by the elastic design equations.

The above are examples of minor items that may trip an instructor in this subject.

DESIGN

The design is based on the elastic performance assumptions that had been used in the past in early reinforced concrete design and is restated here since it has disappeared from the new concrete texts, being replaced by the "ultimate design" or by whatever other name it has assumed. The ultimate design has not been recommended for practical design of masonry because of the variability of performance of different assemblages, lack of knowledge of extensibility, and the hazard of introducing inappropriate complexities which might indicate unwarranted precision of results. It has been avoided also to avoid the swing to impractical type of items developed in ACI 318.

"At this point in time" it might be pointed out that the design values of Table 24-H are based on fractions of f'_m , the ultimate compressive strength of certain average conventional assemblages. For other assemblages of units or types of mortar or grout those design values may not be as nearly approximately correct. The use of such values must be used with caution in retrofit, in rehabilitation.

Also, at this point in time, it is to be noted that the E_m value has been stated to be $1000 f'_m$. In the past some academicians have taken the value as $1000.000 f'_m$. Actually it may be more correctly in the range of 600 to 700 f'_m , and some test results show a range of from 200 to 1500 f'_m . And yet some publications show groups of curves and tables and flexural coefficients, a dozen or so, falsely implying a high degree of precision and correctness. One such chart or table might suffice in practice, with less chance for error, and less wasted time searching for the right page.

Also the value of shear modulus is stated to be $400 f'_m$. It is actually not well known and definitely is not a precise number.

Also it has been the author's experience that the too early use of tables and other aids in lieu of basic "longhand" solutions is not healthy for the learning of the principles. Rather, the student should make some of his own curves, to get a better feel for what they mean in design.

ELASTIC DESIGN ASSUMPTIONS

The elastic design assumptions are basic and simple.

1. A section that is plane after bending. (i.e., stress proportional to strain)
2. Moduli of elasticity of the masonry and of the reinforcement remain constant (a fair approximation)

3. Tensile forces are resisted only by the tensile reinforcing. (a conservative assumption)
4. Reinforcement is completely surrounded by and bonded to masonry material so that they work together as a homogeneous material within the range of working stresses.
5. Stress in a bar is assumed uniform over its area.
6. The member is straight and of uniform cross-section
7. The span of the member is large compared to its depth

Those assumptions provide the basis for the simple derivations of the conventional flexural formulae used in design, i.e.,

$$p = \frac{A_s}{bd} \quad u = \frac{F_s}{E_m} \quad k = \sqrt{2np + (np)^2} - np \quad j = 1 - \frac{k}{3}$$

$$f_m = 2M'#/bd^2jk \quad f_s = M'#/A_sjd$$

$$A_s = M'#/f_sjd \quad u = V/\sum_o jd$$

$$v = V/bjd; \quad s = f_s A_v / 0.67vb \quad \text{or} \quad A_v = 0.67vb_s / f_s$$

In walls for T-beam design using net section

$$M_m = [(f_m jd)/(2kd)] [(bt)(2kd-t) + b'(kd-t)^2]$$

Where t = face shell thickness

$$f'_s = 2f'_c (kd - d') / (d - kd) \quad A'_s = \frac{M'_c}{f'_c (d-d') \left(\frac{n-1}{n}\right)}$$

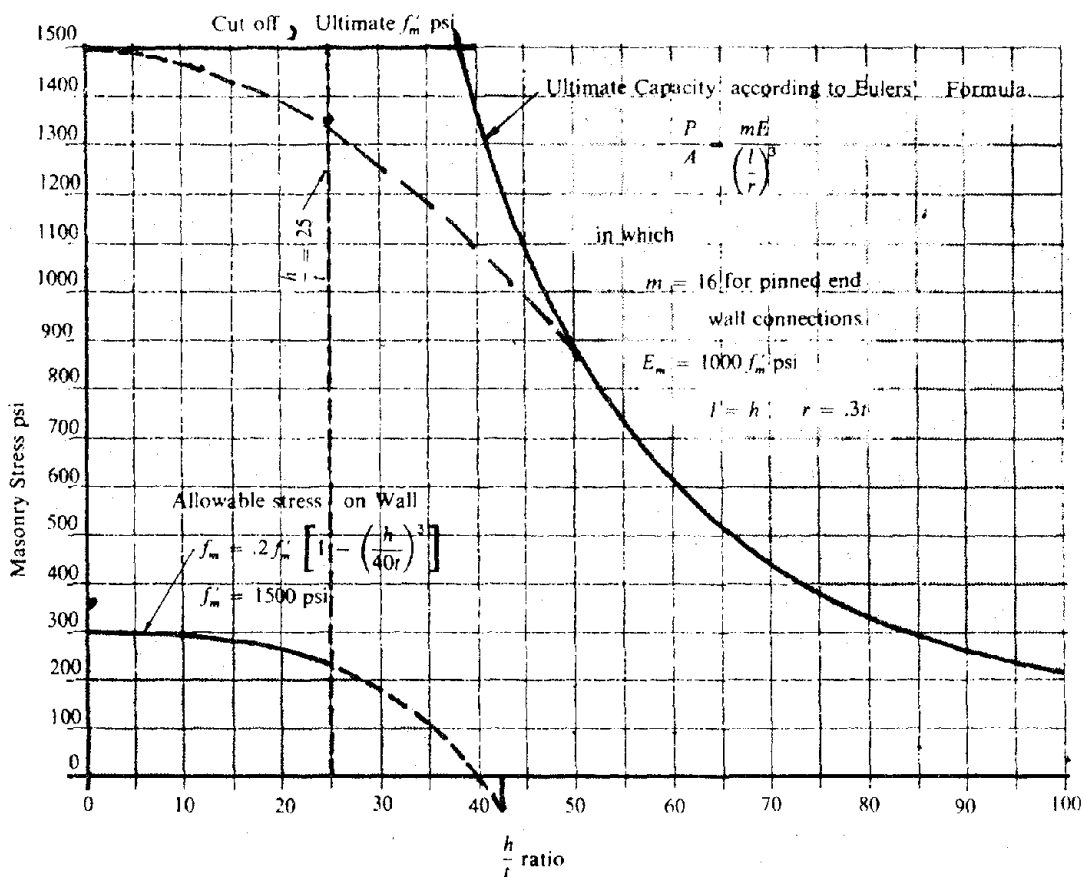
The derivation is simple and can be found in many of the old concrete design texts.

COMPRESSIVE MEMBERS

The design of Walls and Columns is based on a short member capacity, with a height reduction factor applied to that capacity.

The reduction formula $R = 1 - \left(\frac{h}{40t}\right)^3$ as given in the Uniform

Building Code is used to determine the allowable stress on walls and allowable loads on columns. This load or stress reduction equation is applied as a factor of safety against the possibility of buckling and there is a bearing wall limit of h/t of 25. The approximate reduction factor and the limits are not precise, nor valid. This can be shown by the following chart and discussion.



This plots the design curve for stress at the lower left, extended to minus value for *reducto ad absurdum*. It is plotted to the same scale as the ultimate cutoff of the material and to the comparable Eulers long column buckling factor, with a curved smooth transition between the two, a Johnson-Euler curve, which would be a reasonable shape of ultimate capacity.

Note the large factor of safety, which indicates that precise refinements of the design capacity curve may not be pertinent.

The shape of the code value curve is obviously incorrect since it comes to 0 at a value of h/t of 40, or a minus value at values above h/t of 40. The h/t limit of 25 is also not valid, e.g., if a wall has a good capacity at $h/t = 25$ it will still have almost as much capacity, instead of dropping to 0 capacity at h/t of 26. The above are obviously violations of natural laws of physics, which have not been repealed.

The capacity of columns is:

$$(.18 f_m' A_m + .65 f_s A_s) \text{ (times the same approximate reduction factor)}$$

The masonry stress times the area seems reasonable, but the .65 $f_s A_s$ will be difficult to explain to a student. For example if a masonry column of $f_m = 1350$ psi ($f_m = .18 \times 1350 = 244$, $E = 1,350,000$ and $n = 22$) is loaded with an axial stress of 244 psi, the steel shortens the same amount as the masonry and must then be stressed to a value of $244 \times 22 = 5,368$ psi. This is not the $.65 \times 20,000 = 13,500$ psi nor $.65 \times 24,000 = 15,600$ psi that would be used in design. The equation must be explained only as a reasonable approximation that shows empirical increase of column capacity when steel reinforcing is added.

Obviously charts and tables showing many significant digits as answers are not stating true representation of the truth and precision of those answers. They are merely academic manipulation of mathematical equations and numbers, mental gymnastics rather than engineering.

However, the equations are good approximations of safe performance and may be used accordingly.

INTERACTION

The clarification of interaction or capacity under combined bending and direct stress can be easily explained if kept simple.

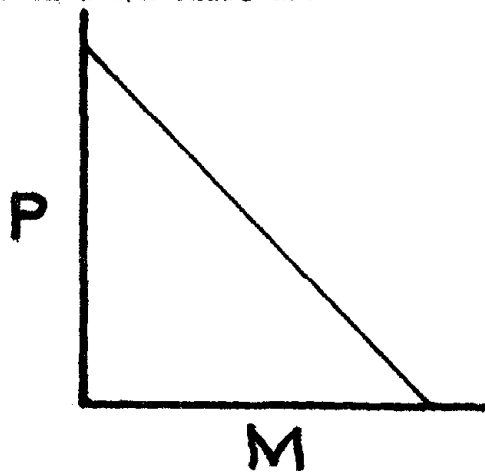
The simple interaction principle is that the fraction the element is developed in bending plus the fraction it is developed in compression shall not be more than 1 and is expressed by the equation:

$$\frac{f_a}{F_a} + \frac{f_b}{F_b} \text{ shall not exceed } 1$$

WHERE:

- f_a = Computed axial unit stress, determined from total axial load and effective area.
- F_a = Axial unit stress permitted by this Code at the point under consideration, if member were carrying axial load only, including any increase in stress allowed
- f_b = Computed flexural unit stress.
- F_b = Flexural unit stress permitted by this Code, if member were carrying bending load only, including any increase in stress allowed

That simple philosophical statement, expressed by the equation would plot in a simple curve on a P/M chart as:

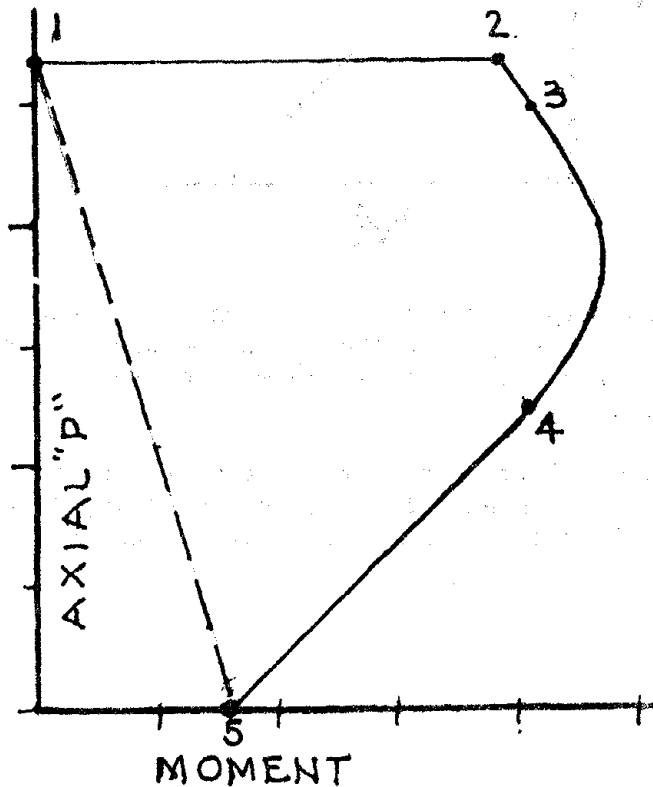


However if one explains the interaction by the use of mathematics based on the elastic assumptions there are immediate complications for the student, but refinements that may be more correct, and may warrant some higher capacities.

One may assume deformation of the plane of a section so that the stresses will be as shown and plot the corresponding load P and bending moment M and we will obtain values as shown in the following.

1. Assume a plane deformation of a section so the uniform stress is $F_a = .2 f'_m$, determine resulting $P = .2 f'_m bt$
2. Assume the plane deformation so stress at the centerline, the average stress, is F_a but so that the edge stress caused by bending is $F_b = .333 f'_m$ on one edge. The axial load P will remain the same while the M increases to a value of $(.333-.20) f'_m bt^2/6$
3. Continue assumed tilt of the plane till the stress is F_b on one side and 0 on the other. P will decrease and M will increase.
4. Continue deformation till stress is F_b on the one side and 0 at the center, where the steel is located. As P decreases M will increase then decrease.
5. Continue deformation with F_b at edge and with steel beginning to function in tension, until P is 0. The M value then will be that of the computed reinforced section with A_s and with d at $t/2$

This indicates that the student should receive some clarification of what might have happened to a wall under actual loading of various types, and a careful look at interaction and the connection of 1-5.



This phenomena is because when the section is fully under compression the full section modulus resists moment and full $P \times A$ functions, but when the plane distortion is such that tension will occur the masonry is not assumed to act in tension. In effect the actual assumption is that the full section acts, as unreinforced masonry with no steel functioning, until tension can be provided as the plane shifts to cause action as reinforced masonry at a d of $1/2xt$.

A plot of the P and M capacity of an 8" wall illustrates this for the assumption of vertical load and a wind load of 15 psf causing moment. This shows the small area in which reinforcing must be computed.

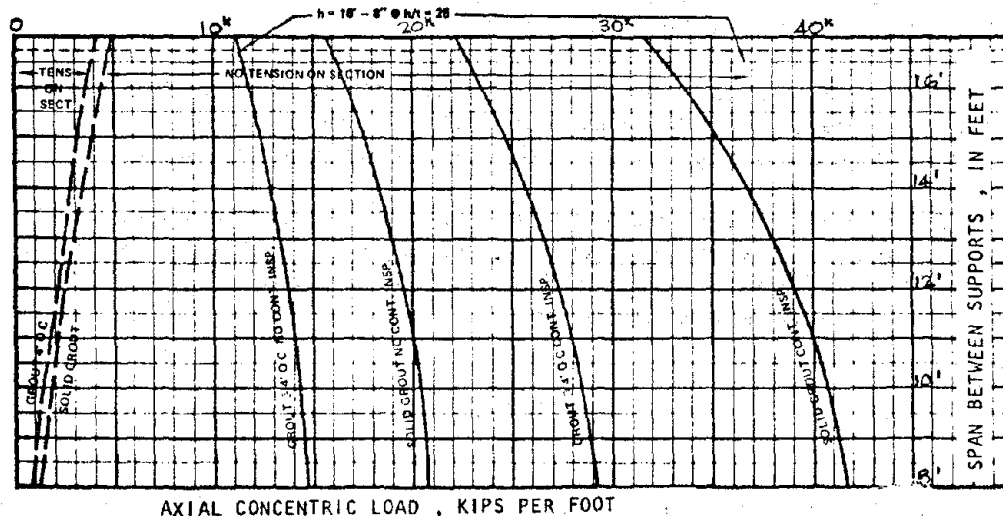
The curves below show maximum P , or axial concentric vertical load, that may be imposed on walls for various stress conditions.

The dashed boundary line shows where the tension stress due to bending force of wind is overcome by the compressive axial load stress, so there is no tension on wall.

Combinations of P & h to the right of the boundary are for compression over the entire section so no tension steel is required for moment, merely minimum arbitrary percentage of steel is required. The maximum load might be increased slightly by the use of transformed area of steel, but this factor is not included in this chart.

In the chart area where tension occurs, normal steel is adequate for most conditions and special calculation need be done for only a small area of combinations, i.e., for the chart area above the capacity indicated for arbitrary steel requirement of either .077 or .150 sq. in. per foot for hollow units, not continuously inspected.

The capacity is reduced according to the 1970 UBC reduction factor for height. Due to the fact that a 1/3 increase is applied to the permitted stresses for short time seismic or wind loads when combined with vertical load the calculated capacities are not reduced by the addition of such lateral loads. Therefore the capacity shown is for static, or dynamic conditions.



These methods could be refined and presented in various manners and explained so they will be suitable for practical engineering use. Many of the design items are to be clarified and to be used for designing parts of the structure, but keeping in mind that the practicing engineer must provide a total building design, not just beams, columns, walls, lintels etc. The total building design will consider the effect of all portions on the seismic input, the effect on total vertical load and total building performance and resistance.

This total building design concept has not, in the past been considered as fully as it should be in some concrete, wood or steel courses.

CURRICULUM DEVELOPMENT

The chronology of past curricula development is rather short, and will be mentioned only in part and partial.

In the late 50's Albyn Mackintosh prepared a handbook, then seminars on reinforced masonry, and some short courses at UCLA. Some partial term classes were put on by W. L. Dickey at UCLA, USC, University of Nevada and others, and he then collaborated with Professor Schneider, who initiated a full term course of reinforced masonry at Cal-Poly on a regular basis in about 1965. There were some classes at other universities in which reinforced masonry was included as part of reinforced concrete class, as by Amrhein at Long Beach State. There were some other short time classes and there was one recent full time class set up by Nolan at the University of Colorado.

There have been many other recent activities, and there is great promise of many more to come, to fulfill the responsibility of the teaching profession to engineering of this major construction system.

A course outline would be a variable depending on many factors, units required, extent of other classes, structural design classes, personality of the instructor, etc., so a specific one would be difficult to suggest in this presentation.

RECOMMENDATIONS

1. Liberal use of visual aids is suggested. There are good movies available for visual demonstration of successive steps of installation. There are some data sources such as Masonry Institute of America, and others similar, which have available items such as Masonry Design Manual containing design use information, Reinforced Masonry Engineering Handbook, which contains many design aids, charts and tables, and a long list of articles on various portions of the subject.

2. There will be a college and graduate level textbook published soon by Prentiss-Hall on "Reinforced Masonry Design." This will overcome one of the obstacles to providing design courses, i.e., the current lack of a textbook. Also, since there has been little past formal class schooling, the textbook will provide for graduate and extension courses for those engineers who have not had the benefit of undergraduate study in reinforced masonry.

It will also be a tool for "continuing education" of practicing engineers and others in the construction industry, a growing activity of academia.

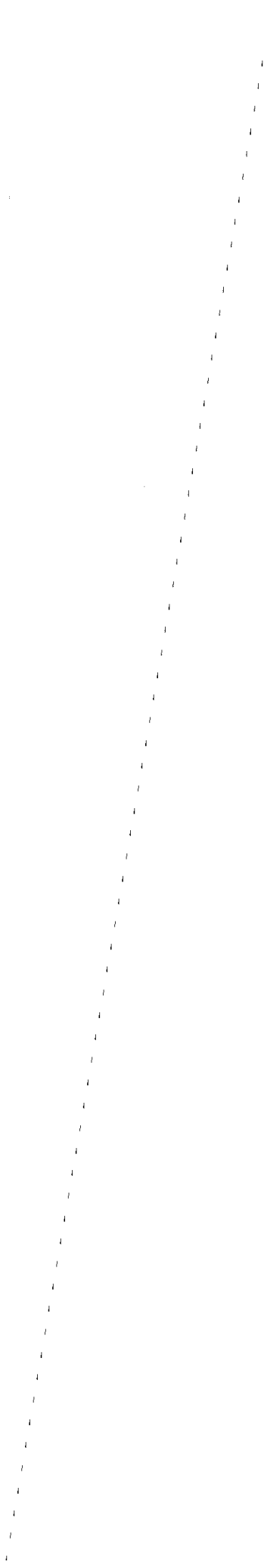
3. It is suggested that instructors' training include a session in actual mason apprentice training (and even some field experience) (close field observation would be a second option), from the mortar mixing, use, placement of units, mortar, steel and grout.

One good visual aid is a field trip to masonry under construction.

4. Another item is care in explaining items. Very few students will have had actual experience with masonry installation and details so pictorial description must be clear, lucid, and probably repetitive, more than in some other subjects.

5. Use long hand solution to the engineering problems rather completely before going to the short cuts of charts, tables and design aids. The actual design is quite simple.

Handwritten text, possibly bleed-through from the reverse side of the page. The text is extremely faint and illegible.



Effect of Sand on Water Permeance of Masonry

by

Kenneth Gillam¹

ABSTRACT

The paper details the results of sixty (60) E514 water permeability tests of masonry wall systems. The principle variable in the program was sand gradation and its effect on water transmission with different types of masonry mortar. The results tend to indicate that sand plays a major role in a wall system's overall effectiveness and that test method E514 is not highly reliable in producing meaningful results.

¹ Administrator Medusa Cement Company Technical Center,
Wampum, Pennsylvania 16157

by

Kenneth Gillam¹

INTRODUCTION

The use of masonry has historically produced a structure with extremely durable performance characteristics. One needs only consider the achievements of the Egyptians and Romans in masonry to reach this realization. Continuing architectural advances have furthered the use of masonry with thinner wall designs and structural qualities. These more recent structures still possess aesthetic appeal and are highly durable but an annoying problem of water transmission to the interior of the building will occasionally spoil the overall effect.

Three major factors are involved in constructing a building which does not transmit water to the interior. These are design, workmanship and compatibility of materials. The three intertwine, one with another and all must be considered when a leaking failure occurs.

Water transmission through masonry walls was first evaluated by Fishburn⁽¹⁾ during the 1930's and 1940's. His initial work resulted in a series of NBS reports (2,3,4,5,6,7,8,9) which concluded that workmanship is a principle factor in producing water impermeable walls. Palmer & Parsons⁽¹⁰⁾ determined that material's compatibility also played a major role in leak resistance of masonry structures.

Recently, under the auspices of Medusa Cement Company's Technical facility, a study was undertaken to update the level of understanding of the water permeability phenomenon utilizing currently available masonry materials. To that end a comprehensive program was outlined to investigate primarily material's compatibility with sand and ASTM test method E514 and its reliability in producing meaningful results.

The study has culminated with the construction and testing of sixty wall systems according to ASTM designation E514-74.⁽¹¹⁾ This report details the results of that study.

RESEARCH OBJECTIVES AND SCOPES

The objective of the research study was to determine the effect of two distinct sand compositions on water permeance of masonry with varying sources of masonry cements. The method selected for evaluation was ASTM E514-74. Four type "N" prepared

¹Administrator Medusa Cement Company Technical Center,
Wampum, Pennsylvania 16157

masonry cement mortars from different manufacturers, two Portland cement/lime type "N" mortars with the Portland cement being varied, two type "S" prepared masonry cement mortars from different manufacturers, and two type "M" prepared masonry cement mortars from different manufacturers were selected for the evaluation. A coarse and fine masonry sand, both of which were within ASTM C-144 gradation specifications, were selected as primary variables for the study. A single brick and concrete block type were used throughout the testing program. The basic constituent materials were tested for their physical properties by applicable ASTM methods.

WALL CONSTRUCTION

Walls were constructed at the Medusa Technical Center by a single experienced journeyman mason to help reduce the effects of workmanship in construction as a variable. All walls consisted of a four inch wythe of brick and a four inch wythe of concrete block. No back parging and no structural wire ties between the wythes was utilized. The cavity between the two wythes was kept as free of mortar droppings as possible and that opening was nominally $5/8$ of an inch. Extreme care was exercised to insure full bed and head joints throughout the wall construction process. The flashing was embedded in accordance with E514 criteria and the assemblage sealed as per test requirements. Mortar proportioning was accomplished by volume measure and held within compliance of ASTM C-270 specification. All mortar joints were tooled with a round jointer after sufficient time had elapsed to achieve the proper consistency for tooling.

The author was present during the construction and testing of all walls.

MATERIAL'S PROPERTIES

Results of tests for brick and concrete block properties are presented in Tables I and II. Mortar properties are presented in Table III with testing performed in accordance to ASTM C-91 requirements. Water permeability results are reported in Table IV with additional information relative to mixing water used and the air content of the mortar produced. The gradation for the two sands utilized is presented in Table V.

PERMEANCE TESTS

All wall specimens were stored in laboratory air for at least twenty-eight days prior to testing. It should be noted that only a six degree difference in temperature ($66-72^{\circ}$) was experienced and the relative humidity varied from 68 to 81 percent. To reduce additional variables five test chambers were constructed. Five test specimens were constructed each week and these specimens were tested at not less than thirty days or more than thirty-five days after construction.

Each wall underwent twenty-four hours of preconditioning and were then allowed to stand at least twenty-four hours or until all apparent moisture had disappeared from the block surface. The walls were then subjected to seventy-two hours of continuous testing in accordance with the test method. Results were tabulated in accordance with E514 requirements and are recorded in Table IV.

TEST RESULTS AND ANALYSES

Correlation of test results is extremely difficult due to the wide scatter noted within the testing. Also extreme caution must be exercised in making generalizations based on this data. The method is not precise and imposes boundary conditions which negates this type of extrapolation.

Effect Of Sand On Performance - The data indicates rather clearly that sand plays a significant role in the overall ability of the masonry system to resist water penetration. Note specifically: MC-II type "N", PCL-I, PCL-II, MC-II type "S", MC-I type "M" and MC-II type "M". It should be noted that the specific sand gradation may perform favorably with one given product and unfavorably with a second product. Therefore, any evaluation of water permeance must take into account this potential incompatibility.

A clear example of potential misinterpretation could result if MC-II and PCL-I with sand A were compared for product superiority. The obvious conclusion of that study would be that MC-II is highly superior to PCL-I. Overall indications are that MC-II is slightly superior to PCL-I but no clear verdict can be rendered. Therefore, any effort to establish product superiority where no significant variables are introduced can lead to false conclusions or even predetermined conclusions depending on which variables are excluded.

Effect Of Mortar Type - The results would tend to indicate that a type "S" mortar exhibits less probability of producing a system which leaks than does any other mortar type. In general type "N" prepared masonry cement mortar, Portland cement/lime type "N" mortar and type "S" prepared masonry cement mortar tend to perform better under the condition of test than does type "M" prepared masonry cement mortar.

Once again caution should be exercised in that the testing procedure requires movement of the panel between construction and testing. With the type "M" system being more rigid the movement may in effect damage the structural integrity of the wall system. Therefore, this method of test may unfairly penalize that mortar type. Once again no clear cut verdict can be reached.

Effect Of Air Content - The presence of greater or lesser amounts of air in the mortar does not appear to play a significant role in the ability of a wall system to resist water penetration. PCL-I and II contained significantly lower air content than did MC-I to IV but no apparent superiority exists within that group.

Also, in general, masonry sand B tends to entrain more air than masonry sand A and yet no apparent superiority tends to exist by grouping the data in this matter. Please note MC-II type "S" as an outstanding example of the opposite situation.

Overall Materials Compatibility - As indicated previously all materials (brick, sand and masonry cement type) play a role in the overall ability of a wall system to resist water penetration. Product superiority is not indicated by the data developed within this study. In certain instances one product appears to be slightly superior to another and yet with a variation in sand that apparent superiority is negated. All materials present in the construction of a masonry structure significantly affect the performance of that structure.

It must be restated that other factors, workmanship and design, also play an important role in water permeability. Materials compatibility is the variable most easily tested by E514 but may be less significant than other parameters. It is quite possible to have highly compatible materials for construction and produce a structure with serious leaks. Although materials compatibility is important, it represents only one third of the finished building's ability to resist water.

Effect Of E514 On Test Results - At best E514 is a semi-quantitative method for evaluating water permeance of a masonry wall system. The rating system places too much emphasis on observed phenomenon as opposed to measureable phenomenon. Appearance of first dampness and extent of dampness is a primary tool for determining the rating of a wall system. Rate of flow through the wall is much more readily determined but plays only a secondary role in performance rating.

The test method does not require that an exact flow rate be determined. Our data is reported within a flow range as required by the method. This flow range, not the normal E514 procedure, was used to determine the rating for the wall system.

Specific recommendations for improvements of test method E514 will be made to ASTM committee E-6 and C-15.

SUMMARY AND CONCLUSIONS

The following conclusions can be drawn from the data developed:

- a) Sand gradation plays a significant role in the overall ability of a wall system to resist water penetration.

- b) Type "S" mortar appears to perform more favorably under the condition of test than does any other mortar type.
- c) Air content does not appear to have a significant influence on a wall system's ability to resist water.
- d) The test method appears to introduce more variables that produce inconsistency than it does resolution to a difficult problem.
- e) All data was developed under highly defined boundary conditions and are applicable only under that set of conditions. Any attempt to generalize from this data or other data developed by test method E514 is highly suspect.

REFERENCES

1. Fishburn, Cyrus C., et. al., "Water Permeability of Masonry Walls," Building Materials and Structures, Report BMS7, July 12, 1938, 35pp.
2. Fishburn, Cyrus C., and Petersen, Perry H., "Effect of Heating and Cooling on the Permeability of Masonry Walls," Building Materials and Structures, Report BMS41, September 19, 1939, 6pp.
3. Fishburn, Cyrus C., "Effects of Wetting and Drying on the Permeability of Masonry Walls," Building Materials and Structures, Report BMS55, April 2, 1940, 6pp.
4. Woolley, Harold W., "Moisture Condensation in Building Walls," Building Materials and Structures, Report BMS63, August 9, 1940, 14pp.
5. Fishburn, Cyrus C., et. al., "Effect of Outdoor Exposure on the Water Permeability of Masonry Walls," Building Materials and Structures, Report BMS76, March 28, 1941, 21pp.
6. Whittlemore, Herbert L., et. al., "Structural, Heat-Transfer, and Water Permeability Properties of Five Earth-Wall Constructions," Building Materials and Structures, Report BMS78, June 11, 1941, 55pp.
7. Fishburn, Cyrus C., "Water Permeability of Walls Built of Masonry Units," Building Materials and Structures, Report BMS82, January 23, 1942, 37pp.
8. Fishburn, Cyrus C., "Water Permeability and Weathering Resistance of Stucco-Faced, Gunite Faced, and "Knap Concrete-Unit" Walls," Building Materials and Structures, Report BMS94, September 5, 1942, 20pp.
9. Fishburn, Cyrus C., and Parsons, Douglas E., "Tests of Cement-Water Paints and Other Waterproofings for Unit-Masonry Walls," Building Materials and Structures, Report BMS95, December 5, 1942, 37pp.
10. Palmer, L.A. and Parsons, D.A., "Permeability Tests of 8-Inch Brick WalleTTes," American Society for Testing Materials, Proceedings of the 37th Annual Meeting, Vol. 34, Part II, June 25-29, 1934, Technical Papers, pp419-431.
11. "Standard Method of Test for Water Permeance of Masonry" Annual Book of ASTM Standards, Part 18, American Society for Testing and Materials, 1974.

TABLE I - PHYSICAL PROPERTIES OF THE BRICKS USED

Properties of Bricks	Type Of Brick "A"
Average Dimensions (inches)	
Width	3½
Length	8
Depth	2¼
Average Dry Weight (lb)	3.92
Gross Area	27.30
Net Area	15.51
Absorption by Total Immersion (lb)	
24 Hour Cold	4.02
5 Hour Boil	4.04
Saturation Coefficient	0.77
Absorption by Partial Immersion (1 min. suction)	6.60g
Modulus of Rupture (lb/in ²)	700
Compressive Strength of (full-bricks (lb/in ²))	12,490

TABLE II - PHYSICAL PROPERTIES OF THE BLOCKS USED

<u>Block</u>	<u>Gross Area</u> (sq.in.)	<u>Wet Wt.</u> (lb)	<u>Dry Wt.</u> (lb)	<u>Svs. Wt.</u> (lb)	<u>Load Applied</u>	<u>Gross PSI</u>	<u>Absorption</u>	
							<u>Lbs/Ft.³</u>	<u>Percent</u>
Early Use	56.44	26.1	24.1	14.4	77,000	1,364	10.67	8.3
Later Use	56.44	26.5	24.5	14.8	142,059	2,517	10.47	7.9

TABLE III - C-91 PROPERTIES OF MORTARS USED

Cement Type	7 Day	28 Day	Flow %	Air Content %	Water Retention %	Blaine	Setting Times (hrs)	
							Gillmore Initial	Gillmore Final
MC-I "N"	1195	1430	110	21.0	78.6	4986	3:00	5:35
MC-II "N"	810	1218	114	20.7	79.4	7020	2:50	8:05
MC-III "N"	1433	1770	108	18.3	73.6	5988	3:30	8:00
MC-IV "N"	X - Not Available							
PCL-I 1:1:6	2123	2707	113	7.2	80.1	-	2:15	4:15
PCL-II 1:1:6	2537	2944	107	9.4	82.2	-	1:55	3:30
MC-I "S"	2398	2707	105	20.8	86.7	5833	2:40	5:00
MC-II "S"	1342	1872		22.5	81.7	5549	3:05	6:05
MC-I "M"	2470	3105	109	18.4	80.7	6548	2:30	5:10
MC-II "M"	3415	4122	109	17.3	78.0	6160	3:40	5:50

TABLE IV - RESULTS OF WATER PERMEANCE TESTS

Sample	Type	Sand	Mixing Water Gal/Ft. ³	Air Content %	Appear- (1)		Visible Water Hrs.Mins.	Time (2) 1st Leak Hrs.Mins.	Total (3) Water Flow ML/Hr.	Rating		
					ance Of Moisture Hrs.Mins.	Hrs.Mins.				1	2	3
MCI-1	N	A	1.24	12.6	5	-	-	0	1	1	1	E
2	N	A	--	--	3	12-44	5	50-1000	0	0	0	F
3	N	A	--	--	1	1:30	1:45	50-1000	0	0	0	F
MCI-1	N	B	1.14	15.5	0	12-44	12-24	50-1000	0	0	0	F
2	N	B	--	--	0	2:30	2:35	50-1000	0	0	0	F
3	N	B	--	--	0	3:10	3:35	50-1000	0	0	0	F
MCII-1	N	A	1.14	11.9	4:30	12-24	12-24	0-50	5	5	5	G
2	N	A	--	--	2:40	0	0	0	1	1	1	E
3	N	A	--	--	4:40	0	0	0	1	1	1	E
MCII-1	N	B	1.29	14.2	0	0	0	0	0	0	0	E
2	N	B	--	--	4	12-24	12-24	0-50	2	2	2	G
3	N	B	--	--	2	12-24	12-24	50-1000	1	1	1	F
MCIII-1	N	A	1.26	12.5	0	12-24	12-24	50-1000	0	0	0	G
2	N	A	--	--	0	12-24	12-24	0-50	0	0	0	F
3	N	A	--	--	Broken Specimen-----							
MCIV-1	N	B	1.20	15.5	2	12-24	12-24	50-1000	5	5	5	F
2	N	B	--	--	0	12-24	12-24	50-1000	0	0	0	F
3	N	B	--	--	8:20	12-24	12-24	50-1000	3	3	3	F

(1) Is only moisture above the upper flashing.
 (2) Based on first drop from flashing.
 (3) Exact leakage rates were not determined since ASTM only requires that ranges be determined.

TABLE IV - RESULTS OF WATER PERMEANCE TESTS

Sample	Type	Sand	Mixing Water Gal/Ft. ³	Air Content %	Appearance of Moisture Hrs.Mins.	Visible Water Hrs. Mins.	Time 1st Leak Hrs. Mins.	Ml/Hr.			Rating
								1	2	3	
MCV-1	N	A	1.26	11.7	0	0	0	0	0	0	E
	N	A	--	--	1:45	12-24	12-24	50-1000	3	3	F
	N	A	--	--	1:45	12-24	12-24	50-1000	5	5	F
MCV-1	N	B	1.14	15.2	0	12-24	12-24	50-1000	0	0	F
	N	B	--	--	24:10	12-24	12-24	50-1000	2	2	F
	N	B	--	--	6:55	12-24	12-24	50-1000	2	2	F
PCLI-1	N	A	1.63	2.5	1:40	3:30	3:30	1000-5000	10	10	P
	N	A	--	--	24	12-24	12-24	0-50	1	1	G
	N	A	--	--	0	12-24	12-24	0-50	0	0	G
PCLI-1	N	B	1.49	4.0	5	12-24	12-24	50-1000	5	5	F
	N	B	--	--	2:35	2:35	2:35	50-1000	1	1	F
	N	B	--	--	3:40	12-24	12-24	50-1000	1	1	F
PCLII-1	N	A	1.79	1.0	0	12-24	12-24	0-50	0	0	G
	N	A	--	--	0	12-24	12-24	0-50	0	0	G
	N	A	--	--	0	0	0	0	0	0	E
PCLII-1	N	B	1.72	1.7	0	12-24	12-24	0-50	0	0	G
	N	B	--	--	24-48	12-24	12-24	50-1000	0	2	F
	N	B	--	--	0	12-24	12-24	50-1000	0	0	F
MCI-1	S	A	1.42	9.8	0	12-24	12-24	0-50	0	0	G
	S	A	--	--	24	12-24	12-24	0-50	2	2	G
	S	A	--	--	30:50	24-48	+24	0-50	0	1	G

TABLE IV - RESULTS OF WATER PERMEANCE TESTS

Sample	Type	Sand	Mixing Water Gal/Ft. ³	Air Content %	Appear- ance Of Moisture Hrs.Mins.	Visible Water Hrs.Mins.	Time lst Leak Hrs.Mins.	Total Water Flow Ml/Hr.	Rating		
									1	2	3
MCI-1	S	B	1.34	11.0	0	0	0	0	0	0	E
	S	B	--	--	0	0	0	0	0	0	E
	S	B	--	--	0	12-24	50-1000	0	0	0	F
MCII-1	S	A	1.36	11.2	6:55	12-24	50-1000	7	7	7	F
	S	A	--	--	0	12-24	0-50	0	0	0	G
	S	A	--	--		12-24	50-1000	0	0	0	F
MCII-1	S	B	1.30	12.2	0	0	0	0	0	0	E
	S	B	--	--	4:25	0	0	0	1	1	E
	S	B	--	--	0	0	0	0	0	0	E
MCI-1	M	A	1.48	10.9	0	12-24	0-50	0	0	0	G
	M	A	--	--	2:40	12-24	50-1000	2	2	2	F
	M	A	--	--	2:40	12-24	0-50	3	3	3	G
MCI-1	M	B	1.26	11.5	30:50	0	24-48	0-50			G
	M	B	--	--	2:55	12-24	1000-5000	8	8	8	P
	M	B	--	--	0	12-24	50-1000	0	0	0	F
MCII-1	M	A	1.29	11.8	0	12-24	50-1000	0	0	0	F
	M	A	--	--	0	12-24	0-50	0	0	0	G
	M	A	--	--	2:55	12-24	50-1000	4	4	4	F
MCII-1	M	B	1.32	11.4	4:40	12-24	50-1000	3	3	3	F
	M	B	--	--	1:50	12-24	1000-5000	6	6	6	P
	M	B	--	--	0:50	12-24	50-1000	5	5	5	F

TABLE V - SAND SIEVE-ANALYSES

Sand Supplied By	Weight Percent Passing U.S. Standard Sieve No.				
	<u>8</u>	<u>16</u>	<u>30</u>	<u>50</u>	<u>100</u>
Masonry Sand A	99.9	98.2	89.2	30.4	1.5
Masonry Sand B	97.2	83.9	61.2	27.5	5.6
ASTM C-144 Sand Requirement	95-100	70-100	40-75	10-35	2-15

TECHNIQUES FOR EDUCATING THE STUDENT, INSPECTOR, ENGINEER AND ARCHITECT
IN THE DESIGN AND CONSTRUCTION OF MASONRY STRUCTURES

By James E. Amrhein, S.E.*

ABSTRACT: This paper provides information on the techniques of teaching masonry design and construction. The author has much experience in this area and points up some of the methods that can be utilized in the dissemination of knowledge and the training of personnel.

Included are course outlines that may be used in colleges and schools for the teaching of masonry, and also a list of publications and films that are available to assist those interested in teaching masonry or obtaining more information on masonry.

*Masonry Institute of America, Los Angeles, California
*California State University at Long Beach, California

TECHNIQUES FOR EDUCATING THE STUDENT, INSPECTOR, ENGINEER AND ARCHITECT
IN THE DESIGN AND CONSTRUCTION OF MASONRY STRUCTURES

by James E. Amrhein, S.E.*

For a material that has been used for 6000 years by man to construct walls for his shelter, there has been little formal training and information in the characteristics, qualities, design, construction and performance of masonry.

When we compare use of masonry, its history and the limited amount of published material available for training, education and learning to a relatively new material such as concrete, we should be appalled. Concrete, because it was a new material, sparked the imagination and curiosity of the researchers. Because masonry has been around for thousands of years, it has been assumed that masonry is designed and built by experience, by rule-of-thumb, for it was a low technological material and unsophisticated construction system. If it is built stout enough, it will perform; if one builds it and it falls down, it is to be built stronger. These have been the techniques by which we designed and built masonry structures. Teaching this approach and information in today's technological world is unsatisfactory. The demands for economy, the demands for guarantees and assurance that the building will not only be serviceable, but will perform in catastrophic circumstances and will be economical in competition with other materials requires a more sophisticated approach to design and construction of masonry structures.

The use of masonry, the characteristics of masonry, the technical design of masonry, the construction of masonry must all be described, explained and presented in such a manner to those interested that they will not only be able to use the material properly, but they will be able to recognize some of its deficiencies and thus open up areas for research to obtain answers to these deficiencies for an improvement of the material.

We seek avenues and opportunities whereby we can impart information and knowledge to those who are or wish to be involved in the masonry field. It is imperative that we conduct courses in masonry at all levels. Whether it is the apprentice learning to lay masonry units, whether it is the inspector insuring that the masonry units and walls are being properly built in accordance with plans and specifications and in accordance with accepted practice of construction, or whether it is the engineer designing a high rise masonry structure or the architect designing the overall concept of the building, they all must have correct information.

*Director of Engineering
Masonry Institute of America
Los Angeles, California

-- *Professor, Civil Engineering (Part Time)
California State University
Long Beach, California

How do we impart this information to the recipient? There are a number of techniques, and to state a few, there are:

- (1) lectures
- (2) seminars
- (3) courses
- (4) demonstrations and participation
- (5) laboratory training
- (6) field trips
- (7) audio-visual aids
- (8) publications

(1) Lectures. This is probably the easiest approach because it is a one-time opportunity. Even right now, I am presenting this paper in verbal form. We assemble a number of people at a coffee break, a lunch break, or after work, and present the latest information on any particular topic. Normally, a lecture is confined to one item so that it doesn't get either too long or too involved. Lectures are hard-hitting, pointed, and can answer immediate questions that do arise. They can spark and stimulate the opportunity for more detailed investigation and further lectures on the subject of masonry.

(2) Seminars. Seminars are classified as extended lectures. Perhaps you have a series of three, four or more hours making up a seminar. At the end of this conference, we have a series of seminars, which we call workshops, which are three hours of intense explanations and activities in a well-defined area. Seminars to inspectors may be on construction, grouting, masonry laying, and/or steel placement.

To laboratory personnel, seminars would be on masonry unit testing, prism testing, material testing for grout and reinforcing, and explanation of ASTM specifications and testing procedures.

Seminars to engineers would be on the mathematical design of masonry systems. Projects such as a retaining wall, an industrial building or a high rise building may be the subject of a seminar.

Seminars to architects can include specifications, waterproofing, details of assembly for masonry systems, connection details, modular layouts, color, texture and patterns of masonry systems.

(3) Courses. It is desirable not only to give lectures and seminars, but to obtain the recognition of universities that masonry is a major construction material that warrants a course in the engineering and/or architectural schools.

We have design courses in concrete, steel and wood; there should be a design course in masonry also. We have been fairly successful in having such courses introduced into a number of schools as teaching materials have become available. It is imperative to have the schools offer these courses and to have professors sympathetic to the use of masonry. One way of doing this is to have the school do some research in masonry. All schools look for grants; they look for technical problems to solve; they look for assistance in senior projects

and graduate projects for their students. Seed money, it need not be much, will help tremendously in getting engineering departments, architectural departments and professors interested in pursuing uses and research of masonry. Sparking their interest will create the opportunity for them to present lectures, seminars and full courses at their schools. As part of this paper, attached are a series of course outlines which have been used at many schools.

(4) Demonstrations and participation. I am a firm believer that not only talking is important, but seeing and doing are even more effective. I saw a sign in an apprenticeship school which I would like to share with you. It read, "1. hear and forget, 2. see and remember, 3. do and understand", and this is the progress that I like to encourage everyone to use in order to get across the message of masonry.

As part of the process of "do and understand", demonstrations and participation in the demonstration activity is of primary importance to get the proper feel of materials. Talking about mortar and talking about the various proportions of mortar is one thing - it is quite abstract and does not mean much - but if mortar is mixed up in the various proportions of Type M, S, N or O, and the participant will not only mix the mortar in those proportions but will then actually use the trowel to see how it spreads, he will get a very definite feel of the characteristics of each of those mortars. By taking a Type S mortar and varying the amount of sand, he will learn immediately the spreadability from a very harsh material to a very smooth material. The use of lime in the mortar from zero to an all lime mix will indicate how lime adds to the smoothness and spreadability of the mortar. Therefore, demonstration and participation in demonstration give first-hand knowledge as to the materials.

The use of demonstrations and participation may require a laboratory facility or some sort of facility where one can not only show the materials, but the people can participate. The area required need not be very large; even a patio would do. In fact, I have conducted demonstrations with participation outside the classroom in the patio area of the engineering building at Long Beach State University, and it worked very well. There is some planning to be done along these lines because equipment and materials are required; however, a hands-on activity teaches more than all the discussion in the world.

This type of participation is also reflected in a workshop activity, as will be carried on at the end of this seminar. I refer to workshops where those attending also do some of the work. It can be in design, by doing homework or actually solving problems in design, to get a gut feel of the techniques of design and what the answers mean. This, again, is participation in the process of learning masonry information.

(5) Laboratory training. As mentioned above, the use of demonstrations and participation is important. Laboratory personnel must be trained, particularly as new personnel keep coming onto the scene. They must be trained in making grout and mortar specimens, building prisms, etc. They must be trained in the proper use and operation of the testing equipment; therefore, seminars, laboratory demonstrations and teaching laboratory techniques are important in the dissemination of testing for masonry systems.

(6) Field trips. I believe we learn more on one field trip than from three lectures in a classroom. Field trips stimulate questions of Why do they do this?; What did that mean?; What is this equipment? Although we may talk grouting in a lecture, to see a grout pump and its operation is far more meaningful.

I recently had the good opportunity of being part of a delegation that went to Russia to exchange information on the seismic design of concrete and masonry structures. Although we had many technical conferences on their engineering and design, we learned far more by the field trips to the construction sites.

Field trips to construction sites not only reveal the types of construction and the structural systems being used, but also give immediate visualization of the quality of construction, the quality of the materials and the quality control that is being exercised on the job. My experience in the Soviet Union indicated that they are very competent in the field of design and engineering, but in the construction of their structures there is much to be desired. There was a tremendous gap between the office technology and the field construction and, after all, when an earthquake comes, it doesn't shake the paper that the building is designed on, it shakes the real building.

Taking a class to a construction site, explaining the modular layout of masonry units, the techniques of sawing masonry, the low lift and high lift grouting methods of construction, placement of steel and all the other details that make the structure will give realization to the lectures previously given on the subject.

(7) Audio-Visual aids. Many times it is very difficult to take large classes out into the field, or perhaps the scheduled time for the trip is not convenient for field construction; accordingly, we may substitute real field trips for a second best, which is audio-visual aids such as movie films and slides. The various masonry institutes, such as the National Concrete Masonry Association, the Brick Institute of America, my own organization, the Masonry Institute of America, have many films and slides that are available to use in presenting information and assisting in educational opportunities. These films are both entertaining and informational, as well as detailed in construction methods and research activities.

The use of audio-visual aids provides the "hear and see" which will help explain and understand the process of masonry construction and design.

(8) Publications. There are many publications available on the use of masonry, its layout and design. One of the areas that is really deficient is the availability of textbooks for schools and colleges. When we see the number of texts on reinforced concrete design, structural analysis, field design, etc., we recognize, then, that there is practically nothing on masonry design. If a course is to be taught on masonry, instructors have a hard time locating texts and materials that are adequate and will be aimed at the level that they wish to teach.

There are books on how to lay masonry for the bricklayer; there are publications on estimating masonry; but there are only a few publications on the design of masonry. There are technical notes from the Brick Institute of America and the National Concrete Masonry Association that give much information on the use of masonry, however, these are generally not available in book stores and they must be obtained from the various institutes.

There is one book out, that is the REINFORCED MASONRY ENGINEERING HANDBOOK, third edition, which is geared to engineering design of masonry systems. It is available and has been used by many colleges and professors. It is based on the 1976 Uniform Building Code with its latest revisions and includes both design techniques (design aids in the form of tables) and design examples to assist the architect and engineer. It has in it a course outline and homework problems. The course is geared for senior engineering, three units, 15 weeks for a 45-hour course. This can be cut down as needed based on time available and information wished to be covered.

The homework design problems are very important in the teaching of masonry design to architects and engineers because solving problems is their techniques of work, and the solving of homework problems is the first step in becoming competent in the field of masonry design.

The learning process is not easy. If it were easy, we would all be experts and geniuses. When I was a youngster, I would wish that I could put a book under my pillow, sleep on it, and during the night all the knowledge would go into my head. This, of course, never occurred because learning is a slow, arduous, difficult process, but by going through the process and taking advantage of the expertise of other people -- lectures, demonstrations, audio-visual tools, publications -- we can make the learning process a little bit easier and a little more interesting than trying to ferret everything out for ourselves.

Rather than provide in this lecture or paper a detailed explanation on grouting, testing masonry, inspection or design, I believe each one must gear their presentations for the audience that will be participating and to whom it is delivered.

I wish to impart the concept that education is the key upgrading masonry; it is the key to advancing the use and technology of masonry; it is the key that will bring masonry from the rule-of-thumb techniques, which I previously mentioned, to the sophisticated technological materials of today.

With the advancement of education of masonry systems to everyone involved in its use and design, it will raise masonry to a primary major construction material and system along with the other materials of construction.

CALIFORNIA STATE UNIVERSITY, LONG BEACH

CE 457 - Reinforced Masonry Design

Professor James E. Amrhein

<u>Lecture</u>	<u>Subject</u>
1	Introduction, Course Organization, Publications, History, Materials, Mortar; Types, Materials, Tests, ASTM Requirements FILM: MAN AND MASONRY - QUALITY CONTROL OF MASONRY, PART I High Strength Mortar, Sarabond, Threadline
2	Brick; ASTM Requirements, Face & Building Brick, Hollow Brick, Clay Block, C/B Ratio, I.R.A., Color, Tolerances, Types, Sizes, Texture, Manufacture, Bricklaying Film: QUALITY CONTROL OF MASONRY, PART II
3	Block; ASTM Requirements, Strength, Moisture Content Film: QUALITY CONTROL OF MASONRY, PART III Prisms; h/t correction, Effect of Joint Thickness, Grout; Requirements, Coarse and Fine Grout, Low and High Lift Construction, 4' Grout Film: MASONRY MEETS A CHALLENGE
4	Film: CONCRETE MASONRY TESTING Lab Tests; Mortar Mixing, Grout Mixing; Test Specimens Prisms; Reinforcing Steel; Joint Reinforcing, Minimum Size, Amount of Reinforcing, Expansion and Shrinkage Joints
5	TEST
6	Test Review: Structural Design, Code Requirements, Beams, $K = M/F$; np; Design, Shear Design, Bond, Tension Reinforcing
7	Retaining Wall Design, Stud Method, Earthquake Pressures
8	Wall Design, Load and Non-Load Bearing, h/t Limitations, Interaction Design; Deep Beams Film: MASONRY PREFAB-FABULOUS
9	Column Design, Projecting and Flush Pilasters, Combined Stresses, Minimum Dimensions, Reinforcing, Ties, h/t Limitations
10	Industrial Building Design, Walls, Lintels, Lateral Force Design, Shear Wall Analysis, Diaphragms, Flexible, Rigid, Connections
11	TEST
12	Test Review; Earthquake Forces, High Rise Design, Fixed and Cantilever Walls, Coupled Walls, Managua and San Fernando Earthquake Slides Film: EERC - EARTHQUAKE SHAKING TABLE TEST

CALIFORNIA STATE UNIVERSITY, LONG BEACH

CE 457 - Reinforced Masonry Design

Professor James E. Amrhein

Page 2

LectureSubject

- | | |
|----|--|
| 13 | Film: HIGH RISE, BEARING WALL CONCEPT
High Rise Design continued, Floor Systems; Connections;
Special Considerations |
| 14 | Fire Ratings
Film: INCENDIO - SAO PAULO
Veneer, Fireplaces and Chimneys
Special Products; Structural Coatings; Waterproofing;
Specifications; Review |
| 15 | FINAL EXAMINATION |

Text: REINFORCED MASONRY ENGINEERING HANDBOOK
by J.E. Amrhein

References:

1977 Masonry Code and Specifications
Handbook on Reinforced Grouted Brick Masonry Construction
Reinforced Grouted Brick Masonry, Field Inspectors Handbook
Reinforced Concrete Masonry Inspectors Manual
Brick Construction Specifications
Block Construction Specifications
NCMA and BIA TEK Notes
Numerous Publications by Masonry Institute of America

PORTLAND STATE UNIVERSITY

EAS 410/510M - Graduate Course
Design of Masonry Structures
By George Laszio, P.E.

Session

- 1 Introduction; masonry materials, bricks, hollow clay concrete blocks, etc. ASTM requirements and testing. U.B.C. requirements. Mortar, grout.
- 2 Flexural theory, development of flexure tables. Flexure design.
- 3 Design for shear; bond considerations.
Movie: "First Principles." Presentation by Mr. Ray Wimer, Executive Director, Masonry Institute of Oregon.
- 4 Compression members, theory.
Movie: "A Day in the Life of a Block Field Inspector and General Inspector."
- 5 Mid-term examination.
- 6 Design of compression members, development of tables; combined bending and axial load; walls, retaining walls, columns.
- 7 Introduction to lateral loads: seismic and wind, etc. U.B.C. requirements.
Movie: "Travelodge Building in Portland."
- 8 Design of one-story buildings - wall rigidities, connections, U.B.C. requirements.
- 9 Design of multi-story buildings.
- 10 Summary discussion.
- 11 Final examination.

Text Books Used: "Reinforced Masonry Engineering Handbook" by J.E. Amrhein
"U.B.C."; "U.B.C. Standards"
"1970 Masonry Codes and Specs"

UNIVERSITY OF COLORADO

ARCH. E. 431 Masonry Structure Design
 FACULTY: Professors Rathburn & Fang, Lecturer - Noland
 TIME : Wednesdays, 3:00 to 4:40 p.m.

Session

- 1 Course orientation: Definition of masonry, Types of units/mortar; Basic structural concept. History of masonry, masonry today.
- 2 Structural systems for masonry buildings. Design loads for buildings. Design projects.
- 3 The design process, codes, internal loads distribution of masonry buildings. Project.
- 4 Materials: mortar, grout, clay units, concrete units, reinforcement. Relevant standards and tests. Design project.
- 5 Topic of 9/22 continued.
- 6 Manufacture, dimensional tolerances, strength characteristics, etc. of clay and concrete units. Design project.
- 7 Allowable stresses in masonry. Design project.
- 8 Masonry Building Design - Case study. Design project.
- 9 One-hour exam. Design of structural elements. Design project.
- 10 Design of structural elements. Design project.
- 11 Design of structural elements. Design project.
- 12 Construction: methods and quality control. Design project.
- 13 Construction: Case study. Design project. Earthquake effects - San Fernando 1971
- 14 Special topics. Turn in projects.
- 15 Review
- 16 Final

Text: REINFORCED MASONRY
 ENGINEERING HANDBOOK
 by J.E. Amrhein

UNIVERSITY OF CALGARY - CALGARY, CANADA

Fall - September-December 1977

MASONRY BEHAVIOUR and DESIGN

Course Instructor: Dr. E. Jessop

OUTLINE

1. Masonry Materials and their Physical Properties
2. Materials Standards and Construction Specifications
3. Aspects of Construction Practice*
4. Structural Behaviour of Masonry Elements
5. Practical Design of Masonry Buildings
6. Design Theory
7. Structural Design of Masonry Elements
8. Prefabricated and Prestressed Masonry

*Includes a site visit

REFERENCE MATERIAL

1. Course Notes (to be handed out)
2. Structural Masonry, by Sven Sahlin
3. Reinforced Masonry Engineering Handbook, by James Amrhein
4. Masonry Design and Construction for Buildings, GSA 8304, 1977

UNIVERSITY OF TEXAS

Course No. ARE 377K, Masonry Engineering Lecture Schedule
 Monday, Wednesday, Friday: one hour each day
 By Clayford T. Grimm, P.E.

Session Number	Subject
1	Course Orientation
2	Masonry in Architectural History
3	Masonry in Architectural History
4	Quiz on Architectural History
5	Masonry Structural Systems
6	Aesthetic Theory
7	Visual Properties of Masonry
8	Color in Masonry
9	Aesthetics Quiz
10	Brick Manufacturer
11	Masonry Units Specifications ASTM C62, C216, C55, C145
12	Mortar
13	Auxiliary Materials
14	Materials Quiz
15	Strength of Brick Masonry
16	Strength of Brick Masonry
17	Strength of Concrete Masonry
18	Quiz on Masonry Strength
19	Dimensional Stability
20	Dimensional Stability
21	Dimensional Stability
22	Dimensional Stability Quiz
23	Masonry Construction
24	Masonry Construction Safety
25	Masonry Specifications
26	Masonry Specifications
27	Masonry Quality Control
28	Mason Productivity
29	Estimating Masonry
30	Masonry Construction Details
31	Masonry Construction Quiz
32	Water Permeance
33	Heat Loss
34	Heat Gain
35	Fire Resistance
36	Fire Resistance
37	Environmental Control Quiz
38	Curtain Walls
39	Bearing Walls
40	Bearing Walls
41	Reinforced Masonry
42	Masonry Shells
43	Masonry Arches
44	Structural Quiz

MASONRY INSTITUTE

55 New Montgomery St., San Francisco, CA 94105
(415) 781-7642

MASONRY INSTITUTE OF AMERICA

2550 Beverly Blvd., Los Angeles, CA 90057
(213) 388-0472

COUNTY OF ORANGE MASONRY PROMOTION

4050 Metropolitan Dr. #300, Orange, CA 92668
(714) 547-4451

MASONRY INSTITUTE OF THE INLAND EMPIRE

330 North D Street, San Bernardino, CA 92401
(714) 889-1101

MASONRY ADVISORY & TECHNICAL INSTITUTE

22300 Foothill Blvd., Hayward, CA 94541
(415) 538-7307

**UNIT MASONRY ASSOCIATION OF SAN DIEGO
AND IMPERIAL COUNTIES, INC.**

6150 Mission Gorge Rd., San Diego, CA 92120
(714) 280-1685

Directory of Masonry Publications and Films

Technical Information Engineering Assistance



The following publications and films cover materials, construction, inspection, design, engineering, code requirements and developments in the field of masonry. They are available from the organizations listed.

SUBJECT SERIES

- 100 BRICK MASONRY
- 200 CONCRETE UNIT MASONRY
- 300 GROUTING
- 400 MULTI-STORY LOAD BEARING
- 500 CODES & SPECIFICATIONS
- 600 TECHNICAL DATA
- 700 RESIDENTIAL MASONRY
- 800 GENERAL INFORMATION
- 900 VISUAL AIDS

100 BRICK MASONRY

101 Brick In Highway Structures

A report presenting photos of brick highway buildings, bridges, plazas, etc. \$.75

102 Reinforceable Hollow Brick

Describes hollow brick and includes information on fire ratings, design stresses and specifications. \$.15

103 Reinforceable Hollow Brick, ICBO RR No. 2730.

Approval of the use of hollow brick. \$.15

104 Specification for Hollow Brick

Standard Specification for Hollow Brick for reinforced brick masonry issued by Western States Clay Products Association. Covers physical requirements, dimensions, strength and tolerances. \$.15

105 Brick Ideas

A series of informational pamphlets. \$.40 each.

- Brick Retaining Walls
- Walls and Fences
- Entranceways
- Outdoor Brick Paving
- Outdoor Rooms

106 Brick In Community Design

Graphic examples of use of brick in civic construction. \$.45

107 Handbook on Reinforced Grouted Brick Masonry Construction

This Handbook explains reinforced grouted brick masonry construction and provides information for proper inspection of masonry. This publication includes information on brick veneers. \$2.50

(107A Northern California pocket edition. \$.75)

110 Tall-Thin Brick Walls

A 32-page booklet by Western States Clay Products Association describing the use and benefits of "Brick Masonry Deep Wall Beams", including examples and example calculations. \$2.00

200 CONCRETE UNIT MASONRY

202 How Big Is a Block

Three-page article by W. L. Dickey which discusses the nominal, actual and engineering sizes of various types of concrete block such as split, slump, scored and patterned units. \$.20

203 Concrete Masonry Structures—Design and Construction—Report of ACI Committee 531

Recommendations for design and construction of reinforced and non-reinforced concrete masonry structures including control joints, veneers and screen walls. Two hundred masonry terms are defined in the appendix. \$4.50

206 Reinforced Concrete Masonry Inspector's Manual

A pocket-size review of basic construction facts and inspection methods. By California Concrete Masonry Technical Committee. \$.75

208 Concrete Masonry Units

An article by James E. Amrhein and Raymond H. Cooley that discusses strength, web thickness and moisture content of masonry units as required by ASTM C90-70. \$.20

300 GROUTING**301 Filled Cell Concrete Masonry High Lift Grout Method**

Specification is reprinted from Schoolhouse Section of the California Office of Architecture and Construction, Circular No. 9. \$.20

302 High Lift Grout Method—Brick

Specification is reprinted from Schoolhouse Section of the California Office of Architecture and Construction, Circular No. 10. \$.20

303 High Lift Specifications—Block

A specification for high lift grouting of block construction developed by the California Concrete Masonry Technical Committee. \$.35

304 High Lift Specifications—Brick

A specification for high lift grouting of brick construction prepared by the Brick & Tile Association. \$.35

305 High Lift Grout for Block

A short but definitive explanation of high-lift grouting facts relating to block construction. By Walter L. Dickey \$.15

306 High Lift Grouting in Brick Masonry

A discussion of the procedures, advantages and limitations of masonry's new construction method. By Walter L. Dickey. \$.20

307 Grout, The Third Ingredient

Grout as a material, its makeup and how it is used in masonry walls. It presents code requirements, construction requirements and testing procedures. By James E. Amrhein, S.E. Price \$.20

308 Put Your Grout Where the Steel Is

This is a field research program in which it explains how grout can flow horizontally in a wall when the wall is grouted only where the steel is, as in partially grouted walls. This article describes the test program in San Diego and Los Angeles. By William McCullagh. Price \$.25

400 MULTI-STORY LOAD BEARING**401 Multi-Story Load Bearing Brick Walls**

Explanation of the benefits, advantages, and seismic design of load bearing brick buildings, from three to 18 stories high. \$3.00

403 A Look at Load-bearing Masonry Design

An article by James Kesler, Consulting Structural Engineer which expands and clarifies many of the design details, aspects of layout and improvement in the efficient application of this useful system. \$.20

404 Reinforced Masonry Bearing Walls in 13 Story Buildings

A reprint from ASCE Civil Engineering magazine by Robert Higgins which described the construction and cost of reinforced masonry for multi-story buildings. \$.20

405 Prestressed Hollow Core Plank and Masonry Load Bearing Walls for High Rise Buildings

A brochure outlining the use, design, construction and specification of prestressed concrete plant floors with concrete block walls for low rise and high rise buildings. Includes connection details. \$.35

500 CODES & SPECIFICATIONS**501 1977 Masonry Codes and Specifications**

Excerpts from the latest codes and standards such as ICBO, California State Code, ASTM, etc., that pertain to masonry. \$2.50

505 Masonry Veneer

This contains clarification of the 1973 U.B.C. requirements and the differences of other jurisdictions with aids for the design, detailing and use of masonry veneer. \$3.00

506 Specifying Glazed Structural Units

A Construction Specification Institute limited scope study covering the specification and use of Glazed Structural Clay Units, including details of special uses as approved by Los Angeles City. \$.75

507 Joint Reinforcement

Clarification of code requirements and types of joint reinforcing most appropriate to masonry construction in the West. Illustrated with typical design details. By Walter L. Dickey. \$.20

508 Composite Construction

Design details showing various combinations of common brick, glazed brick and glazed tile within different portions of structural walls. \$.20

509 Marble Veneer

A 16-page brochure containing information, details and code excerpts for the detailing and installation of marble veneer. \$2.00

510 Changes in the 1976 UBC Masonry

An article by James E. Amrhein, S.E., which explains and clarifies the changes in the 1976 edition of the Uniform Building Code that are pertinent to masonry. \$.20

512 Guidelines for Clear Waterproofing Masonry Walls

A 24-page guideline specification for masonry waterproofing and masonry caulking, including examples of details. \$1.00

513 Anchor Tied Masonry Veneer

A brief but detailed description of various anchors used in masonry. Specific references to 1976 UBC Section 3006 are cited and diagramed. \$.15

600 TECHNICAL DATA**601 Masonry Design Manual, 2nd Edition**

This 384-page manual covers the full subject of masonry, including brick, concrete block, glazed structural units, stone and veneer. \$14.00

602 Reinforced Masonry Engineering Handbook, 3rd Edition

A complete handbook on the engineering design of reinforced masonry structures conforming to the requirements of the 1976 UBC. Contains examples of retaining walls, industrial building and high rise building design, along with design tables and aids for many masonry strengths and two steel strengths. By James E. Amrhein, S.E. 340 pages. Price \$20.75

604 Shear Concrete Masonry Piers

A report on a block shear testing program conducted by Professor Robert S. Schneider at Cal-Poly College at Pomona, California for Masonry Institute of America. \$3.00

605 The Shear Truth About Brick Walls

A clearly illustrated report based on Blume & Assoc. test of the shear capacities. Written by R. Harrington and W. L. Dickey. \$1.00

606 Effective, "b" Test Report

Report of test made to determine the effect of spacing of reinforcement, i.e., the "b" or width of wall assumed to work with a bar. \$1.00

607 Masonry Wall Beams

A brochure describing the high test capacities, effect of openings and typical details of use. By Dr. R. Mayes, Chen Shy-Wen, and W. L. Dickey. \$.25

608 Noise Control

This brochure by John Van Houten, P.E., acoustical specialist, sets forth the California State standards for noise insulation and how masonry walls comply with the requirements. It includes definitions of terms, isolation vs insulation, sound transmission control and other subjects. \$2.00

609 Reinforcing Steel in Masonry

This 40-page handbook presents details, specifications and construction practice for the use of reinforcing steel in masonry structures. By James Amrhein, S.E. Price \$3.00

700 RESIDENTIAL MASONRY**701 Standard Details for One-Story Concrete Block Residences**

Standard designs and details for residential walls and beams showing reinforcing requirements, by R. H. Cooley, published by California Concrete Masonry Technical Committee. \$3.00

702 Fireplace and Chimney Handbook

A 96-page pocket handbook that includes design, specification, construction and code requirements for residential masonry fireplaces. \$1.50

703 Residential Fireplace and Chimney Details

A short form that can be filled in to obtain a building permit. Includes detail drawings, minimum code requirements and specifications. \$.25

704 Residential Garden Fence Design

ICBO approved designs for 4', 5', and 6' high garden fence of 4" thick and 6" thick block. Designed for 5 psf wind load. \$.25

705 Subterranean Garages

A brochure explaining the simplicity of design, economy and speed of construction of masonry basement garages. \$.50

706 Ideas in Residential Masonry Design

A 32-page well illustrated book that presents ideas and know-how on using masonry for the home, patio and garden. \$1.50

707 Great American Brick Fireplaces

A 12-page pictorial issued by the Brick Institute of America depicting several fireplace designs from Early America for contemporary living. Construction details included. \$.60

804 Masonry Stresses by Prism Testing

Technical article by W. L. Dickey on the techniques of establishing masonry strength, f'm, through the use of prisms. Sets forth procedure for testing and a relationship of the strength of component materials. \$.15

807 Why Reinforce Masonry Walls: Why This Amount of Steel?

This article by J.E. Amrhein and J.L. Noland explains why reinforcing is required in masonry and why the minimum amount is specified in the code. \$.15

808 Metric Conversion: The S.I. is Coming (systeme internationale)

This 4-page article by J.E. Amrhein explains the use of metric terms both common and technical. It provides an extensive table for conversion from the English system to the metric system and visa versa. \$.20

809 Glass Block

A 4-page article explaining the new uses and advantages of glass block in construction. \$.20

810 Cable Clamp Splice Connections for Reinforcing Steel

This two-page article describes the capability and capacity of cable clamps for short splices in reinforcing steel. By Dr. Robert Alexander and Robert Patterson. Price \$.15

811 Table of Allowable Stresses for Reinforced Solid and Hollow Masonry, 1976 UBC

Extended table of stresses for 16 masonry strengths. By James E. Amrhein, S.E. Price \$.15

800 GENERAL INFORMATION**801 Design Aids**

A series of single-sheet ideas on design and construction of masonry wall. \$1.25 per set.

900 VISUAL AIDS

901 Quality Control of Masonry—Part I

16 mm color-sound film is the first of series devoted to educate the masonry inspector and others concerned with improving construction quality. This part considers preparation, site, layout, and materials. (18 minutes) \$325.00

902 Quality Control of Masonry—Part II

Second film in series deals specifically with brick construction and inspection procedures. 16 mm color-sound film. (18 minutes) \$325.00

903 Quality Control of Masonry—Part III

Third film in series features block masonry construction and quality control methods. 16 mm color-sound (16 minutes) \$325.00

904 High Rise, Bearing Wall Concept
16mm color-sound film on speed and construction methods of multi-story earthquake resistant bearing walls. (16 minutes) \$300.00

905 Effective "b" Test

16 mm color-sound film showing a dramatic test for effectiveness of reinforcing spacing, and the flexibility of reinforced masonry. (10 minutes) \$250.00

906 Shear Test Program, Brick Walls

16 mm color-sound film showing test method and results of shear tests on brick masonry. (18 minutes) \$325.00

907 Concrete Masonry Shear

16 mm color-sound film on shear resistance of reinforced concrete masonry. (15 minutes) \$300.00

908 Friendly Enemies—Safety Film

16 mm color-sound film that shows how a useful, friendly tool or construction condition can be turned into a dangerous, hazardous enemy through improper or negligent use. (23 minutes) \$350.00

909 First Principles

16mm color sound film. Prof. Scully traces load bearing design from Hadrians Villa and Pantheon to modern examples such as Kahns Exeter and Dacca. By IMI. (17 minutes)

910 On a Bigger Scale

16 mm color movie of the masonry prefabrication of high rise buildings. Benefits described by BM & PIU President Murphy. (10 minutes)

911 Masonry Prefab-Fabulous

16 mm color-sound film showing examples of masonry prefabrication from seismic and non-seismic areas, with methods at site and off site, by hand and by machine, illustrating the coordination of designer and erector. (17 minutes) \$325.00

912 Concrete Masonry Test Lab Techniques

16 mm color-sound film showing proper methods of sampling, curing, handling, capping and testing mortar, grout, block and prisms. By California Concrete Masonry Technical Committee. (30 minutes) \$ 350.00

913 Man and Masonry

16 mm black-and-white sound film is devoted to the design and aesthetic qualities of masonry. For architects, designers and students. (15 minutes)

914 In the Wake of the Quake

16 mm black-and-white sound film of the devastation following the Alaska earthquake. Depicts the effects of construction failures. (22 minutes)

915 Masonry Meets a Challenge

16 mm color-sound film traces the development of High Lift Grouting. Primarily of interest to architects and engineers. (18 minutes) \$ 325.00

916 Three Little Pigs

16 mm color-sound correctly illustrating benefits of house of bricks compared musically with houses of straw and sticks.

917 Man From Monticello

16mm color-sound film describing Thomas Jefferson's influence on brick in architecture throughout history of the United States. Shows brick architecture at University of Virginia, Monticello and discusses Jefferson's role as an architect and planner (13 minutes).

918 Abstract Definitions

A 10-minute film depicting the play of light, shadows and color through glass block masonry units. Of interest to decorators, interior designers and architects.

Visual aids are for Masonry Industry use or purchase. Those showing prices can be purchased, others shown are for use or rent only.

Slide presentations available on request.